

AD-762 307

APPLIED GAS DYNAMICS, THIRD EDITION

G. N. Abramovich

Foreign Technology Division
Wright-Patterson Air Force Base, Ohio

21 May 1973

DISTRIBUTED BY:

NTIS

National Technical Information Service
U. S. DEPARTMENT OF COMMERCE
5285 Port Royal Road, Springfield Va. 22151

AD 762307

FOREIGN TECHNOLOGY DIVISION



APPLIED GAS DYNAMICS

by

G. N. Abramovich

AD D C
RECORDED
JUL 2 1973
R
C



Reproduced by
NATIONAL TECHNICAL
INFORMATION SERVICE
U S Department of Commerce
Springfield VA 22151

Approved for public release;
distribution unlimited.



BEST

AVAILABLE

COPY

EDITED MACHINE TRANSLATION

FTD-MT-24-0035-73

APPLIED GAS DYNAMICS

By: G. N. Abramovich

English pages: 1025

Source: Prikladnaya Gazovaya Dinamika, 3rd
Edition, 1969, pp. 1-437; 516-824.

Country of origin: USSR

Requester: FTD/POTA

This document is a SYSTRAN machine aided
translation, post-edited for technical accuracy
by: Kathleen L. Dion, Robert D. Hill,
Charles T. Ostertag, Jr. and Bernard L. Tauber.

Approved for public release;
distribution unlimited.

THIS TRANSLATION IS A RENDITION OF THE ORIGINAL FOREIGN TEXT WITHOUT ANY ANALYTICAL OR EDITORIAL COMMENT. STATEMENTS OR THEORIES ADVOCATED OR IMPLIED ARE THOSE OF THE SOURCE AND DO NOT NECESSARILY REFLECT THE POSITION OR OPINION OF THE FOREIGN TECHNOLOGY DIVISION.

PREPARED BY:

TRANSLATION DIVISION
FOREIGN TECHNOLOGY DIVISION
WP.AFB, OHIO.

UNCLASSIFIED

Security Classification

DOCUMENT CONTROL DATA - R & D

(Security classification of title, body or abstract and indexing annotation must be entered when the overall report is classified)

1. ORIGINATING ACTIVITY (Corporate author)		1a. REPORT SECURITY CLASSIFICATION	
Foreign Technology Division Air Force Systems Command U. S. Air Force		UNCLASSIFIED	
2. REPORT TITLE		1b. GROUP	
APPLIED GAS DYNAMICS			
3. DESCRIPTIVE NOTES (Type of report and inclusive dates)			
Translation			
4. AUTHOR(S) (Last name, middle initial, (not name)			
B. L. Abramovich			
5. REPORT DATE	7a. TOTAL NO. OF PAGES	7b. NO. OF REFS	
1960	1025	55	
6a. CONTRACT OR GRANT NO.		6b. ORIGINATOR'S REPORT NUMBER(S)	
a. PROJECT NO JMW3		FTD-WT-24-0035-73	
c.		6c. OTHER REPORT NO'S (Any other numbers that may be assigned this report)	
d. T71-04-03			
10. DISTRIBUTION STATEMENT			
Approved for public release; distribution unlimited.			
11. SUPPLEMENTARY NOTES		12. SPONSORING MILITARY ACTIVITY	
		Foreign Technology Division Wright-Patterson AFB, Ohio	
13. ABSTRACT			
01			

DD FORM 1473
(NOV 61)UNCLASSIFIED
Security Classification1473
IV

All figures, graphs, tables, equations, etc.
merged into this translation were extracted
from the best quality copy available.

3
FTD-MT-24-0035-73

III
C

Applied gas dynamics, Abramovich G. N., third revised edition. Main editorial staff for physical and mathematical literature of the "Nauka" publishing house, Moscow, 1969, 824 pages.

The bases of gas dynamics are set forth in application to the theory of jet engines and other gas machines and apparatuses. A detailed analysis is made of the theory of one-dimensional gas flows on which rest largely the contemporary methods of calculation of jet engines, vane machines, ejectors, wind tunnels, and test stands. Separate chapters are dedicated to the boundary-layer theory and theory of jets lying at the basis of the determination of the friction drag, velocity fields, and temperatures in nozzles, diffusers, combustion chambers, ejectors, etc. In connection with the rapid development of engines of new types - engines for high-altitude and extraterrestrial flight vehicles - the new edition of the book includes chapters on hypersonic flows, about the elements of hydrodynamics, and about the flows of rarefied gases.

Illust. 333, tables 12, references 157.

IV
E

TABLE OF CONTENTS

U. S. Board on Geographic Names Transliteration System	vii
Designations of the Trigonometric Functions	viii
Preface	ix
Chapter I. The Equations of Gas Dynamics for a Unit Stream	1
§ 1. The Equation of Continuity	1
§ 2. The Equation of Energy	4
§ 3. The Maximum Speed of Motion of a Gas. Mach Number	16
§ 4. The Mechanical Form of the Equation of Energy (Bernaulli Equation)	24
§ 5. The Equation of Momentum	38
§ 6. The Equation of Angular Momentum [Moment of Momentum]	52
§ 7. Entropy	58
§ 8. The Calculation of Reaction Force (Thrust)	61
§ 9. The Place of Application of the Reaction Force	73
Chapter II. Elements of Hydrodynamics	83
§ 1. The Motion of a Liquid Particle	83

§ 2.	The Equation of Continuity	87
§ 3.	About the Forces Which Act in a Liquid	89
§ 4.	The Connection Between Stresses and Strains	92
§ 5.	Navier-Stokes Equations	96
§ 6.	The Equation of Energy	98
§ 7.	Hydrodynamic Similarity	105
§ 8.	Laminar Flows	117
§ 9.	The Equations of Motion of an Ideal Fluid	121
§ 10.	Plane Steady Motions of an Ideal Compressible Liquid	128
§ 11.	Velocity Circulation	133
Chapter III. Shock Waves		147
§ 1.	Normal Shock Waves	147
§ 2.	Oblique Shock Waves	161
§ 3.	The Application of a Pneumatic Adapter in a Supersonic Flow	180
Chapter IV. The Acceleration of Gas Flow		183
§ 1.	Supersonic Nozzle	183
§ 2.	The Non-Calculated Conditions of Outflow from a Laval Nozzle	193
§ 3.	Supersonic Gas Flow with a Continuous Increase in Velocity (Prandtl-Mayer) Flow	199
§ 4.	Flow Around a Plane Wall	215
§ 5.	Flow Around a Convex Curvilinear Wall	217
§ 6.	Outflow from a Unit Two-Dimensional Nozzle with Oblique Section into Space with Reduced Pressure	220
Chapter V. One-Dimensional Gas Flows		224
§ 1.	Adiabatic Gas Flow with Friction. Critical Region of the Flow	224

§ 2.	Flow in a Tube of Constant Cross Section	228
§ 3.	Motion of Preheated Gas Along a Tube of Constant Cross Section	241
§ 4.	General Conditions of the Transition from Subsonic Flow to Supersonic Flow and Vice Versa	254
§ 5.	On the Propagation of Detonation and Burning in Gases	277
§ 6.	Calculation of Gas Flows by Means of Gas-Dynamic Functions	297
§ 7.	Gas Flow with Friction in the Cylindrical Tube with the Assigned Magnitude of the Ratio of Pressures at Inlet and Outlet	337
§ 8.	The Averaging of Parameters of Nonuniform Flow	348
Chapter VI. Boundary Layer Theory		359
§ 1.	Basic Concepts of a Boundary Layer	359
§ 2.	Laminar Boundary Layer	369
§ 3.	Transfer from Laminar to Turbulent Flow Conditions in a Boundary Layer	400
§ 4.	Turbulent Boundary Layer	409
§ 5.	Boundary-Layer Separation	429
§ 6.	Interaction of a Boundary Layer with Shock Waves	441
§ 7.	Flow of Fluid in Tubes	451
Chapter VII. Turbulent Jets		464
§ 1.	General Properties of Jets	464
§ 2.	Change in the Parameters Along the Length of a Jet	481
§ 3.	Subsonic Nonisothermal Jet of Simple Gas	491
§ 4.	Supersonic Isobaric Jet	501
§ 5.	Discharge of Supersonic Gas Jet from Nozzle in Off-Design Conditions	507

§ 6. The One-Dimensional Theory of the Initial ("Gas-Dynamic") Section of an Off-Design Supersonic Jet	518
Chapter VIII. Gas Flows in Nozzles and Diffusers	540
§ 1. The Resistance of a Nozzle	540
§ 2. The Forms of Nozzles	555
§ 3. The Resistance of a Subsonic Diffuser	566
§ 4. Supersonic Diffusers	580
Chapter X. The Elements of Gas Dynamics of the Airfoil and Rectilinear Airfoil Cascade	613
§ 1. The Basic Geometric Parameters of the Airfoil and Rectilinear Airfoil Cascade	613
§ 2. Zhukovskiy's (Joukowski's) Theorem on the Power Effect of a Potential Flow on the Airfoil in the Cascade	618
§ 3. Effect of Viscosity on the Power Influence of Flow	624
§ 4. Aerodynamic Coefficients	637
§ 5. Profile in a Plane Flow of Incompressible Fluid	641
§ 6. Streamlining of a Profile by a Subsonic Gas Flow	657
§ 7. Supersonic Streamlining of Airfoil	668
§ 8. Streamlining of Airfoil Cascade by the Flow of an Incompressible Fluid	678
§ 9. Streamlining of Airfoil Cascade by a Subsonic Flow of Gas	700
§ 10. Streamlining of a Supersonic Airfoil Cascade by a Gas Flow with Supersonic Axial Velocity Component	711
§ 11. Flow Around a Cascade of Supersonic Profiles by an Inviscid Flow of Gas with Subsonic Axial Velocity Component	732
§ 12. The Effect of Viscosity on Flow Around Supersonic Airfoil Cascades. A Solid Cascade of Plates	747

§ 13.	Construction of Purely Supersonic Cascades	759
§ 14.	Construction of Supersonic Cascades with Mixed Flow	769
§ 15.	Certain Findings Regarding Spatial Flow Around a Single Airfoil and a Cascade of Airfoils	788
Chapter XI. Hypersonic Gas Flows		801
§ 1.	Change in the Parameters of a Gas in an Isentropic Hypersonic Flow	801
§ 2.	Hypersonic Flow Around a Convex Obtuse Angle	803
§ 3.	Plane Shock Wave in a Hypersonic Flow	807
§ 4.	Hypersonic Flow Around a Flat Plate at a Small Angle of Incidence	813
§ 5.	Concerning the Hypersonic Flow Around Narrow Ogival Bodies	814
§ 6.	The Newton Law of Resistance	817
§ 7.	The Influence of Minor Blunting of the Front End of a Narrow Body on Flow Around It at Hypersonic Speeds	826
§ 8.	The Viscosity Effect in Hypersonic Flows	830
Chapter XII. Flows of Rarefied Gas		836
§ 1.	Different Types of the Flows of Rarefied Gases ..	836
§ 2.	Jumps of Velocity and Temperature at the Wall During Gas Flow with Slip	840
§ 3.	Gas Flow with Slip in the Tube	847
§ 4.	External Drag of Bodies in the Flow of Rarefied Gas in the Presence of Slip	854
§ 5.	Free Molecular Gas Flows and Elements of the Kinetic Theory of Gases	857
§ 6.	Pressure and Stress of Friction During the Free Molecular Flow Around a Solid	866

§ 7.	Calculation of Aerodynamic Forces with Free Molecular Flow Around Solids	880
§ 8.	The Free-Molecular Gas Flow in a Long Tube	888
§ 9.	The Molecular Outflow of Gas Through the Opening in the Wall and Through the Short Tube	896
Chapter XIII. Elements of Magnetic Gas Dynamics		899
§ 1.	Introduction	899
§ 2.	Elements of Electrostatics and Electrodynamics	901
§ 3.	Electromagnetic Fields	927
§ 4.	Equations of Magnetic Gas Dynamics	933
§ 5.	The Similarity Criteria in Hydromagnetics	942
§ 6.	Flow of Viscous Electroconductive Fluid Along a Plane Channel in a Transverse Magnetic Field	947
§ 7.	Magnetohydrodynamic Pumps, Accelerators, Chokes and Generators	957
§ 8.	The Entry of the Flow of an Electro- Conductive Fluid into a Magnetic Field and Discharge from It.....	961
§ 9.	The Equations of Magnetic Gas Dynamics for a Unit Stream	970
§ 10.	Magnetogasdynamic Shock Waves and Weak Disturbances	978
§ 11.	The Condition of Inversion of Effect During Gas Flow in an Electromagnetic Field	990
§ 12.	The Simplest Solutions of the Equations of a One-Dimensional Gas Flow in Lattice-Type Fields	996
Appendices I-V		1007
Bibliography		1024

U. S. BOARD ON GEOGRAPHIC NAMES transliteration SYSTEM

Block	Italic	Transliteration	Block	Italic	Transliteration
А а	<i>А а</i>	A, a	Р р	<i>Р р</i>	R, r
Б б	<i>Б б</i>	B, b	С с	<i>С с</i>	S, s
В в	<i>В в</i>	V, v	Т т	<i>Т т</i>	T, t
Г г	<i>Г г</i>	G, g	У у	<i>У у</i>	U, u
Д д	<i>Д д</i>	D, d	Ф ф	<i>Ф ф</i>	F, f
Е е	<i>Е е</i>	Ye, ye; E, e*	Х х	<i>Х х</i>	Kh, kh
Ж ж	<i>Ж ж</i>	Zh, zh	Ц ц	<i>Ц ц</i>	Ts, ts
З з	<i>З з</i>	Z, z	Ч ч	<i>Ч ч</i>	Ch, ch
И и	<i>И и</i>	I, i	Ш ш	<i>Ш ш</i>	Sh, sh
Я я	<i>Я я</i>	Y, y	Щ щ	<i>Щ щ</i>	Shch, shch
К к	<i>К к</i>	K, k	Ъ ъ	<i>Ъ ъ</i>	"
Л л	<i>Л л</i>	L, l	Ы ы	<i>Ы ы</i>	Y, y
М м	<i>М м</i>	M, m	Ь ь	<i>Ь ь</i>	'
Н н	<i>Н н</i>	N, n	Э э	<i>Э э</i>	E, e
О о	<i>О о</i>	O, o	Ю ю	<i>Ю ю</i>	Yu, yu
П п	<i>П п</i>	P, p	Я я	<i>Я я</i>	Ya, ya

* ye initially, after vowels, and after ъ, ь; e elsewhere.
When written as ѣ in Russian, transliterate as yѣ or ѣ.
The use of diacritical marks is preferred, but such marks
may be omitted when expediency dictates.

FOLLOWING ARE THE CORRESPONDING RUSSIAN AND ENGLISH
DESIGNATIONS OF THE TRIGONOMETRIC FUNCTIONS

Russian	English
sin	sin
cos	cos
tg	tan
ctg	cot
sec	sec
cosec	csc
sh	sinh
ch	cosh
th	tanh
cth	coth
sch	sech
csch	csch
arc sin	\sin^{-1}
arc cos	\cos^{-1}
arc tg	\tan^{-1}
arc ctg	\cot^{-1}
arc sec	\sec^{-1}
arc cosec	\csc^{-1}
arc sh	\sinh^{-1}
arc ch	\cosh^{-1}
arc th	\tanh^{-1}
arc cth	\coth^{-1}
arc sch	sech^{-1}
arc csch	csch^{-1}
<hr/>	
rot	curl
lg	log

Preface

In the book the bases of gas dynamics are set forth in application to the theory of jet engines and other machines and vehicles.

The third edition of the book is substantially revised and supplemented.

The contemporary methods of calculation of jet engines, vane machines, ejectors, wind tunnels, and test stands are based chiefly on the one-dimensional representations of gas hydrodynamics, therefore a considerable place in the book is assigned to one-dimensional flows.

At the same time many questions, for example the determining of the friction drag and velocity and temperature fields, the construction of the picture of flow in a combustion chamber, ejector and supersonic diffuser, the clarification of the power and thermal effect of the exhaust jet of a jet engine on the controls and other parts of a flight vehicle, and also on the walls of a test stand, etc., cannot be solved without the help of the differential equations of gas hydrodynamics or the equations of the boundary layer. In connection with this in the book considerable attention is allotted to the bases of hydrodynamics, the boundary-layer theory, and the theory of jets.

In the 15 years which passed since the publication of the previous edition great significance has been acquired by flight vehicles with jet engines of new types, providing flight at high supersonic (hypersonic) speed, entry into space, and re-entry. This led to the rapid development of the sections of gas dynamics in which the flows of rarefied gas, hypersonic flows, and motions of liquid and gas in electromagnetic fields are studied; in this third edition of the book the bases of these sections of contemporary gas dynamics are also presented.

A number of important questions (theory of supersonic nozzles, diffusers, ejectors and grids of wings, the use of gas-dynamic functions, etc.) is set forth in more detail than before in the new publication. The appearance of special texts and monographs on the theory of vane machines and the theory of jet engines made it possible to eliminate these sections from the book.

The book is compiled as a manual for the engine departments of aviation institutes according to the program confirmed by the Ministry of Higher and Secondary Special Education of the USSR and can be considered as a textbook also for machine construction and power institutes.

The author attempted to achieve the greatest possible clarity and the accessibility of presentation and in the illumination of every question sought the simplest means. Thus some tasks are examined twice: first in a simplified setting, and then more deeply in the special sections of the book. In order to make the book intelligible to the engineers and students who did not study the kinetic theory of gases and electrodynamics, brief information from these branches of physics is presented.

Several sections of this book were written by: N. M. Belyanin (Chapter VI), A. Ya. Cherkez (§§ 6-8, Chapter V, § 6 Chapter VII, and Chapter IX), S. I. Ginsburg (Chapter X).

The author expresses deep appreciation to S. G. Apel'taum, A. R. Bunimovich, A. B. Vatazhin, A. S. Ginevskiy, A. L. Gonor, I. P. Smirnovoy, and A. A. Stepchikov for the valuable observations made by them in the review of the separate chapters of the book.

G. N. Abramovich

CHAPTER I

THE EQUATIONS OF GAS DYNAMICS FOR A UNIT STREAM

§ 1. The Equation of Continuity

The fundamental equations of gas dynamics we will derive for an elementary stream of gas, the transverse dimensions of which are so low that in each of its cross sections it is possible to consider constant all the basic flow parameters: velocity, pressure, temperature, and gas density. Precisely in such a form the equations of gas dynamics are applied usually in the theory of jet engines. In those cases when within the limits of the cross section of a working jet the flow parameters are changed (for example the values of velocity or temperatures are dissimilar), the representation of the average cross-section values of these quantities is introduced, and then with the help of the appropriate, in the majority of cases insignificant, corrections it is possible to utilize all the equations obtained for an elementary stream. The method of an elementary stream is the basis of hydraulics, therefore the gas dynamics of an elementary (unit) stream are occasionally referred to as "gas hydraulics."

In order to obtain the equation of continuity, let us examine the stationary (steady-state) motion of the elementary stream of gas (Fig. 1.1). During stationary motion at any point of space the velocity of motion and the state of a liquid (density, pressure,

temperature) are retained constant in time. The particle trajectories during such motion are called the *flow lines*.¹ The lateral surface of the stream, which is called the *flow surface*, is impenetrable for a liquid (gas) (velocity vectors of flow are tangential to it); the flow surfaces forming are the flow lines.

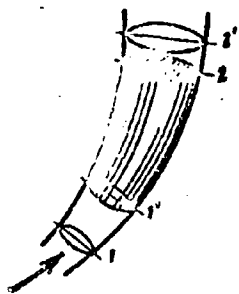


Fig. 1.1. Elementary stream.

Let us examine a certain section of the stream between two, normal to the flow surface, cross sections 1 and 2; let us note that in accordance with the direction of motion indicated in Fig. 1.1. in space 1-2 the inflow of gas is achieved only through cross section 1, and the gas discharge is achieved only through cross sections 2.

Beyond an infinitely small time interval dt the chosen part of the stream will be shifted into a new position 1'-2'. The displacement amounts to the fact that during the time dt the shaded space 1'-2 will contain the gas which is displaced from area 1-1', and a certain quantity of gas during the same time will flow out from this space and will fill the area 2-2'. The inflow of gas into space 1'-2 comprises

$$dO_1 = \gamma_1 F_1 dl_1 (kg) \quad (1)$$

where γ_1 - the specific gravity of gas in cross section 1, equal to the product of density ρ_1 by the acceleration of gravity g , F_1 - the cross-sectional area 1. The distance between cross sections 1 and 1' is equal to the product of the velocity of motion by the elementary time interval

¹During unsteady motion the flow lines are determined differently and do not coincide with the particle trajectories.

$$dl_1 = w_1 dz,$$

where w_1 is the velocity in cross section 1, from which

$$dQ_1 = \gamma_1 w_1 F_1 dz.$$

The discharge of gas from space 1'-2 is equal, obviously, to

$$dQ_2 = \gamma_2 w_2 F_2 dz.$$

During steady-state conditions and in the absence of breaks of continuity in a moving medium the inflow of gas should be equal to the discharge:

$$dQ_1 = dQ_2 = dQ.$$

Hence after the appropriate substitution we obtain the equation of continuity - the law of conservation of mass - for the unit stream of a compressible liquid (gas) during steady-state flow

$$\gamma_1 w_1 F_1 = \gamma_2 w_2 F_2. \quad (2)$$

In the case of a noncompressible liquid, i.e., with $\gamma = \text{const}$, equation (2) takes a simpler form:

$$w_1 F_1 = w_2 F_2. \quad (3)$$

which is used for gas flows when changes in the specific gravity of the gas can be disregarded.

On the basis of the equation of continuity (3) based on the arrangement of the flow lines in the incompressible medium it is possible to judge the velocity of motion. In places of thickening of the flow lines the velocity increases; if the flow lines are separating then the velocity drops. During the motion of gas it

is not always possible to determine directly by the arrangement of the flow lines the velocity change, since changes of density (specific gravity) of the gas can be considerable.

In a gas, as it is not difficult to see from the equation of continuity (2), the picture of the flow lines uniquely determines the change in the density of the flow:

$$I = \gamma w = \frac{G}{F},$$

representing the product of the specific gravity of the gas by the velocity, i.e., the mass flow rate of gas through a unit of area of cross section. In places of thickening of the flow lines the density of flow increases, while in places of divergence of flow lines it decreases.

The equation of constancy of gas discharge $G = \gamma w F = \text{const}$ also can be presented differentially

$$dG = \gamma w dF + w F d\gamma + \gamma F dw.$$

After dividing this relationship term by term by $\gamma w F$ we will obtain

$$\frac{dG}{G} = \frac{dw}{w} + \frac{d\gamma}{\gamma} + \frac{dF}{F}. \quad (4)$$

Here $\rho = \gamma/g$ - mass density of gas.

§ 2. The Equation of Energy

Following the first principle of thermodynamics (law of conservation of energy), let us put together the energy balance in the fixed coordinate system (Fig. 1.1), i.e., let us examine

the energy conversion in one and the same mass of gas, which at first filled the space 1-2 but in an infinitely small time interval dt is shifted into position 1'-2'.

An increase in any form of energy is equal to the difference in the quantities of this form of energy in positions 1'-2' and 1-2. In view of the fact that the shaded space 1'-2 is general for these two positions, the energy of the mass of the gas which fills space 1'-2 during subtraction is decreased,¹ and an increase in energy is measured by the difference in the energy content in infinitely small spaces 2-2' and 1-1'. Hence it follows that an increase in kinetic energy is equal to

$$dE_k = \frac{dG}{g} \frac{w_1^2 - w_2^2}{2};$$

here dG/g is the mass gas discharge through the cross section of the stream during the time dt . An increase in the potential energy (energy of position)

$$dE_p = dG(z_2 - z_1)$$

where z_2 and z_1 are the heights of the arrangement (leveling levels) of cross sections 2 and 1. An increase in the internal (thermal) energy

$$dE_t = \frac{dG}{A} (u_2 - u_1)$$

where $A = 1/427$ - the heat equivalent of mechanical work, $u = c_v T$ - thermal energy of a unit of weight of gas (product of heat capacity at a constant volume by the absolute temperature). If the heat

¹The motion of the gas is assumed to be as in the foregoing paragraph, steady-state.

capacity of the gas in cross sections 1 and 2 is identical, then the increase of internal energy is equal to

$$dE_1 = \frac{c_v dQ}{\lambda} (T_1 - T_0)$$

On the bases of the chosen part of the stream of gas the external forces of pressure p which are directed inside and along the normal to them act. With the displacement of the gas the external forces of pressure produce work. For example, the transfer of gas from cross section 1 into cross section 1' occurred as if under the action of a piston with an area F_1 with pressure p_1 . The work of the piston during time dt is equal to

$$p_1 F_1 w_1 dt = \frac{p_1}{T_1} dQ.$$

In exactly the same manner it is possible to visualize that pressure p_2 on cross section 2 is achieved by a piston with an area F_2 . During time dt the gas will move the piston into position 2, after carrying out the negative operation:

$$-p_2 F_2 w_2 dt = -\frac{p_2}{T_2} dQ.$$

The forces of pressure which act on the lateral surface of the stream (flow surface) do not produce any work since they are normal to the trajectories of the particle motion of the gas. Thus the energy introduced by the forces of pressure is equal to the difference between the operations of piston 1 and piston 2:

$$dE_1 = dQ \left(\frac{p_1}{T_1} - \frac{p_2}{T_2} \right).$$

To the gas stream in section 1-2 during time dt heat can be conducted in the amount of dW , in mechanical units equal to

$\frac{dW}{A}$. Further the gas stream during time dt can perform the technical work dL , for example, rotating a turbine wheel mounted between cross sections 1 and 2. Finally, one ought to consider the work being expended by the gas during the time dt for overcoming the forces of friction dL_{fp} .

According to the first principle of thermodynamics thermal energy and work of the forces of pressure conducted to the gas are expended on the completion of technical work, work of the forces of friction, and also on an increase in the reserves of the potential internal, and kinetic energy

$$\frac{dW}{A} + \left(\frac{p_1}{\gamma_1} - \frac{p_2}{\gamma_2} \right) dG = dL + dL_{fp} + (z_1 - z_2) dG + \frac{u_1^2 - u_2^2}{2A} dG + \frac{w_1^2 - w_2^2}{2g} dG.$$

After dividing all the terms of the resulting expression by value dG , we come to the equation of energy for a unit of weight (1 kgf) of the gas

$$\frac{Q}{A} + \frac{p_1}{\gamma_1} - \frac{p_2}{\gamma_2} = L + L_{fp} + z_1 - z_2 + \frac{u_1^2 - u_2^2}{2A} + \frac{w_1^2 - w_2^2}{2g}. \quad (5)$$

Here are introduced the designations: $Q = dW/dG$ - the heat supplied to 1 kgf of gas on section 1-2, $L = dL/dG$ - technical work being accomplished by 1 kgf of gas on the same section, $L_{fp} = dL_{fp}/dG$ - work of the forces of friction which is necessary for 1 kgf of gas.

The inflow of heat in general is achieved by two methods: from without (Q_{nap}) because of heat exchange through the lateral surface of the stream, and from within (Q_{en}) because of conversion into the heat of work of friction. Thus,

$$Q = Q_{nap} + Q_{en}. \quad (6)$$

The second part of the heat flux, obviously, is exactly equal to the thermal equivalent of the work of friction:

$$\frac{Q_{21}}{\lambda} = l_{12} \quad (7)$$

From thermodynamics the equation of state is known for a perfect gas

$$pv = RT, \quad (8)$$

where R - gas constant, and the specific volume of gas v is the value reverse to specific gravity $v = 1/\gamma$. Hence

$$\frac{p}{\gamma} = RT. \quad (9)$$

Furthermore a relationship is known which connects heat capacity at a constant volume (c_v) and heat capacity at a constant pressure (c_p):

$$c_p = c_v + AR. \quad (10)$$

Let us introduce into the examination the *heat content* (or *enthalpy*) of the gas, i.e., the product of heat capacity at a constant pressure by the absolute temperature

$$l = c_p T. \quad (11)$$

Then relationship (10) will take a somewhat different form:

$$l = n + ART \quad (12)$$

or on the basis of (9)

$$l = n + A \frac{p}{\gamma}. \quad (13)$$

Utilizing expressions (6), (7), and (13), it is possible to give the equation of energy the following form:

$$\frac{Q_{12}}{A} - L = z_2 - z_1 + \frac{w_2^2 - w_1^2}{2g} + \frac{i_2 - i_1}{A}. \quad (14)$$

The equation of energy (14) occasionally is also referred to as the equation of enthalpy. The fact that the equation of enthalpy does not contain the work due to friction is significant. In fact, since the work being expended for overcoming of friction or any other form of resistances is converted completely into heat, and the latter remains in the gas jet, the presence of the forces of friction cannot disturb the general energy balance, but only leads to the conversion of one form of energy into another.

Usually in technology it is necessary to deal with the particular forms of the equation of enthalpy. Thus in the majority of cases the change of potential energy is negligibly small in comparison with other parts of the equation of energy, and term $(z_2 - z_1)$ is disregarded. Then the equation of enthalpy takes the following form:

$$\frac{Q_{12}}{A} - L = \frac{w_2^2 - w_1^2}{2g} + \frac{i_2 - i_1}{A}. \quad (15)$$

In the absence of technical work and heat exchange with the surrounding medium, i.e., in the case of the energy isolated process in the gas, we have

$$A \frac{w_2^2 - w_1^2}{2g} = i_1 - i_2. \quad (16)$$

Specifically equation (16) determines the flow of gas along a tube, if there is no heat transfer through the walls. According to the aforesaid this equation is correct without depending on whether or not the forces of friction act. In other words, the change of enthalpy (temperature) in the isolated process is connected only with a velocity change. If the gas velocity is not changed, then the temperature remains constant.

The absence of the influence of the forces of friction can be explained by the following. Under the action of friction the pressure along the tube drops, i.e., the gas is expanded, and therefore the temperature should decrease. However, the work of the forces of friction is converted into heat; and since the work of the forces of friction is exactly equal to the mechanical equivalent of the heat generated because of this work, then preheating compensates for cooling.

Along a tube of constant cross-section under the influence of the forces of friction, the gas temperature in a subsonic flow even decreases. This occurs because the pressure drop is accompanied by a decrease in the specific gravity of the gas, and the current density remains constant: $j = G/F = \gamma w = \text{const.}$ Thus the gas velocity increases, and the temperature in accordance with equation (16) is reduced. At a low speed of motion the temperature changes only because of heat exchange either in those places where the gas passes through the turbine (expends the energy, $L_T > 0$) or through the compressor (derives energy $L_K < 0$).

If the change of velocity and heat exchange can be disregarded then the equation of enthalpy takes the following form:

$$i_2 - i_1 = -AL. \quad (17)$$

In other words, a change in the enthalpy of the gas in this case is equivalent to mechanical work. In the turbine wheel the gas temperature decreases

$$i_2 = i_1 - AL_T \quad (L_T > 0) \quad (18)$$

In the compressor impeller wheel the temperature increases

$$i_2 = i_1 - AL_K \quad (L_K < 0).$$

Let us recall that here we have in mind work L referred to 1 kgf of gas. Thus, following the equation of enthalpy, we obtain simple relationships for calculating temperature drops on the turbine and compressor during small changes in kinetic energy:

$$\Delta T = \frac{i_2 - i_1}{c_p} = - \frac{AL}{c_p}. \quad (19)$$

Here c_p is the mean value of heat capacity at a constant pressure in a given temperature range.

If the speed changes substantially, then the calculation will only be a little complicated. Precisely:

$$i_2 - i_1 + A \frac{w_1^2 - w_2^2}{2g} = -AL \quad (20)$$

Finally, during an isothermal process ($i_2 = i_1 = \text{const}$) the mechanical work is expended wholly for a change in kinetic energy

$$A \frac{w_1^2 - w_2^2}{2g} = -AL \quad (21)$$

A system close to isothermal can be obtained in a multistage compressor with the intermediate (between every pair of stages) cooling of gas.

$$Q_{\text{int}} = i_2 - i_1 + A \frac{w_1^2 - w_2^2}{2g}; \quad (22)$$

in such a form it is applied to heat exchange processes.

Let us return now to the energy isolated gas flows, when the conditions

$$Q_{\text{int}} = 0, \quad AL = 0, \quad (23)$$

are satisfied and the equation of enthalpy acquires the form (16). In this case it can be written in the following form:

$$i_1 + A \frac{w_1^2}{2g} = i_1 + A \frac{w_1^2}{2g} = i + A \frac{w^2}{2g} = \text{const} \quad (24)$$

Hence it is not difficult to see that if the gas jet is inhibited completely, then enthalpy of the gas reaches the maximum possible value:

$$i_0 = i + A \frac{w^2}{2g}. \quad (25)$$

The value of enthalpy i_0 obtained in this case we will call *full enthalpy*, and the corresponding absolute temperature

$$T_0 = \frac{i_0}{c_p} \quad (26)$$

- the *stagnation temperature*.

With the help of (25) from the equation of enthalpy (15) it is possible to eliminate velocity: we obtain the equation

$$Q_{np} - AL = i_0 - i_1. \quad (27)$$

Thus the gas temperature is obtained equal to the stagnation temperature when the rate of flow tails off to nothing itself in the absence of energy exchange with the surrounding medium. Using the mean value of heat capacity it is possible to calculate the stagnation temperature according to the following formula:

$$T_0 = T + A \frac{w^2}{2gc_p}. \quad (28)$$

For air ($c_p \sim 0.24$) we have approximately

$$T_0 \approx T + \frac{w^2}{2000}. \quad (29)$$

For example, in an air flow of normal temperature ($T = 300^\circ\text{K}$) at a rate of motion $w = 100; 350; 1000$ m/s the stagnation temperature $T_0 = 305, 360, 800^\circ\text{K}$ is obtained respectively.

One ought to emphasize that according to the equation of energy (24) in the energy isolated flow of an ideal gas there is a unique dependence between the gas temperature T (enthalpy i) and the rate of flow w . An increase in the velocity in such a flow is always accompanied by a reduction in temperature regardless of the change in other parameters of the gas. If in two cross sections of the energy isolated flow the rate of flow is identical, then in them the gas temperature will also be identical, whatever processes occurred in the flow between the cross sections in question. With a decrease in the velocity of flow down to zero the gas acquires the identical temperature T_0 regardless of the features of the slowing down process and the irreversible losses appearing in this case.

At the end of the inlet diffuser (Fig. 1.2) of the jet engine, usually without depending on the flying speed, a comparatively low flow velocity is established. Because of this the temperature of the air in the diffuser of the engine is close to the stagnation temperature. Assume the air speed at the end of diffuser $w_2 = 100$ m/s. Then the temperature here at the different flight speeds is obtained from the condition

$$T_1 \approx T_0 - \frac{w_2^2}{2000} \approx T_1 - \frac{w_1^2 - w_2^2}{2000}.$$

In our case ($w_2 = 100$ m/s, $T_1 = 300^\circ\text{K}$)

$$T_1 \approx 295 - \frac{w_1^2}{2000}. \quad (30)$$

The results of calculating the temperature T_2 according to formula (30) are tabulated in the following table:

Table.

w	100	350	1000 m/s
T_0	305	300	800°K
T_0	300	335	795°K

As we see, the heating of air obtained only because of braking at a high flow (flight) velocity is very considerable.

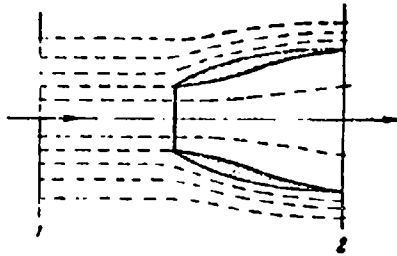


Fig. 1.2. The diffuser of a jet engine.

The equation of enthalpy explains the following, very interesting fact. During the flow of gas near a rigid surface without heat exchange the temperature of the latter is equal to the stagnation temperature in the gas. The fact is that in connection with the viscosity of the gas near a solid wall a fine boundary layer is always formed in which the gas velocity

relative to the wall is changed from the value equal to the ambient velocity of flow to zero (on the wall). But once the particles of gas directly near the wall are slowed down, then in the absence of heat exchange the temperature on the wall should be equal to the stagnation temperature. Thus, for instance, in the test section of a wind tunnel for supersonic speeds (Fig. 1.3), where the gas velocity is very great, its temperature $T_{p,q}$ should be considerably lower than in the precombustion chamber from which the quiescent gas (T_0) enters the tunnel. For example at a velocity in test section of $w_{p,q} = 600$ m/s and the stagnation temperature in the precombustion chamber $T_0 = 300^\circ\text{K}$ we obtain a temperature in the flow

$$T_{p,q} \approx T_0 - \frac{w_{p,q}^2}{2000} = 120^\circ\text{K}.$$

In spite of this, as experiments show, the wall temperature over the entire extent of the wind tunnel, including the test section,

remains constant and is approximately equal to the stagnation temperature: $T_{cr} = T_0 = \text{const.}$

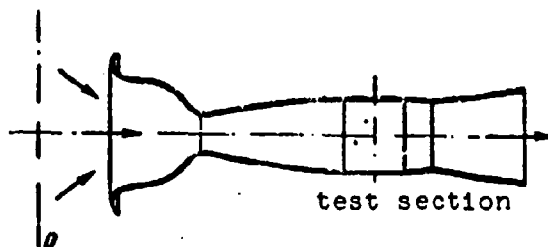


Fig. 1.3. The layout of a wind tunnel for supersonic speeds.

The temperature of a thermometer placed in the test section is also approximately equal to the stagnation temperature. This is explained by the formation at the walls of the tube and the thermometer of a boundary layer in which the circumfluent gas flow is completely retarded. Thus a fixed thermometer cannot measure the temperature in the flow of a gas. For these same reasons the surface of a body which is moving at a high speed in air is heated strongly. For example, the surface of a projectile which is leaving a gun at a velocity of $w = 1500$ m/s because of the formation of the air boundary layer in which the relative velocity is completely extinguished should have a temperature (T_0), exceeding by $T_0 - T = w^2/2000 = 1125^\circ\text{C}$ the temperature of the surrounding air. In actuality the temperature of projectile is less than that obtained here because of heat radiation in space. At a very high flying speed the icing of the surface of an aircraft is made impossible. For example, at a speed of $w = 900$ km/h (250 m/s) the stagnation temperature is higher by the value $\Delta T = 250^2/2000 = 31^\circ\text{C}$ than in the surrounding atmosphere. The surface temperature of the aircraft is close to the stagnation temperature, therefore in this example even with a frost of $20\text{--}25^\circ\text{C}$ icing will not result.

The actual temperature of a surface blown around by a gas usually differs from the stagnation temperature. For determining the surface temperature the following formula is used:

$$T_{\text{res}} = T + \gamma \frac{As^2}{2gc_p} \quad (31)$$

or for air

$$T_{\text{res}} \approx T + \gamma \frac{w^2}{2000} \quad (32)$$

Here ϕ is the correction factor which is determined for the most part experimentally and sometimes theoretically. With $\phi = 1$ expressions (31) and (32) are converted into the already known formulas for stagnation temperature. For a subsonic high-speed aircraft the approximate value of correction factor is equal to 0.9. For a supersonic high-altitude rocket the correction factor can decrease to the value $\phi \approx 0.5$.

Let us dwell on one more example from practice. During flow around a convex surface in a certain area outside the boundary layer the velocity is higher than in the incident flow, and therefore the temperature in such places is lower than in the incident flow. This explains one phenomenon which is sometimes observed by pilots during a dive. It amounts to the fact that at the moment of dive at a high speed part of the upper side of the wing is hidden from the pilot's eyes under a film of milky color. As soon as the pilot pulls out, i.e., speed is sharply lowered, the film disappears. Apparently, in this case in the air layers which have the increased velocity and low temperature moisture condensation occurs, which ceases on going to a lower speed, i.e., at a higher temperature.

§ 3. The Maximum Speed of Motion of a Gas. Mach Number.

In examining the outflow of gas in the absence of energy exchange, it is not difficult to be convinced of the fact that the discharge velocity under no conditions cannot be higher than a certain maximum value. In fact, from the relationship

$$I_0 = I + A \frac{w^2}{2g}$$

it follows that the maximum speed is reached when enthalpy in the flow is equal to zero, i.e., when the full enthalpy of the gas is wholly converted into kinetic energy

$$A \frac{w_{\max}^2}{2g} = I_0.$$

Hence we will obtain the formula for the maximum value of velocity in a gas

$$w_{\max} = \sqrt{\frac{2gI_0}{A}}. \quad (33)$$

The corresponding approximation formula for air, derived under the assumption of the constancy of heat capacity ($c_p \approx 0.24$), takes the following form:

$$w_{\max} \approx 44.8 \sqrt{T_0}$$

If the stagnation temperature of the air (temperature in the vessel from which the air escapes) is close to normal ($T_0 \approx 300^\circ\text{K}$), then the maximum possible discharge velocity $w_{\max} = 776 \text{ m/s}$.

An increase in the maximum value of velocity can be achieved only by way of an increase in the stagnation temperature (full enthalpy).

In order to transfer gas from the state of rest into motion with a speed w it is necessary to consume part of its enthalpy, equal to

$$A \frac{w^2}{2g} = I_0 - I.$$

After dividing both parts of this equality by full enthalpy we will obtain:

$$\frac{T_0 - T}{T_0} = \frac{Aw^2}{2RT_0}.$$

With a constant heat capacity this dimensionless expression takes the following form:

$$\frac{T_0 - T}{T_0} = \frac{Aw^2}{2gc_p T_0}.$$

Now if we multiply and divide the right side by the gas constant R, consider the relationship $AR = c_p - c_v$ and designate the relation of heat capacities by $k = c_p/c_v$, then we obtain

$$\frac{T_0 - T}{T_0} = \frac{w^2}{kgRT_0} \frac{k-1}{2}.$$

But, as is known from physics, the speed of sound in gas is equal to¹

$$a = \sqrt{kRT} = \sqrt{\frac{kp}{\rho}} = \sqrt{\frac{dp}{d\rho}}. \quad (34)$$

Thus the degree of utilization of gas enthalpy for obtaining the assigned value of the flow velocity is determined by the relation of the flow velocity to the speed of sound in a fixed gas:

$$\frac{T_0 - T}{T_0} = \frac{w^2}{a_0^2} \frac{k-1}{2}.$$

From here is derived the new expression for the maximum speed of outflow ($T = 0$):

¹This formula will be derived in § 1 Chapter III.

$$w_{\max} = a_0 \sqrt{\frac{2}{k-1}}. \quad (35)$$

For air ($k = 1.4$) we obtain

$$w_{\max} = 2.24 a_0$$

i.e., the maximum speed of outflow of air cannot exceed the speed of sound in stagnant air by more than 2.24 times; with $k = 1.2$ maximum gas velocity is higher:

$$w_{\max} = 3.16 a_0$$

Thermal drop cannot be broken down into full enthalpy, but into enthalpy in a flow, then we obtain

$$\frac{T_0 - T}{T} = \frac{w^2}{k R T} \frac{k-1}{2}.$$

In this case the flow velocity turns out to be referred to the speed of sound in a flow, and not in a fixed gas:

$$\frac{T_0 - T}{T} = \frac{w^2}{a^2} \frac{k-1}{2}. \quad (36)$$

The relation of the flow velocity to the speed of sound in a flow is accepted as the Mach number and designated by the letter M :

$$M = \frac{w}{a}. \quad (37)$$

The Mach number characterizes the degree of the conversion of enthalpy into the kinetic energy of flow

$$\frac{T_0 - T}{T} = \frac{k-1}{2} M^2.$$

The Mach number is the *basic similarity criterion* (see § 7, Chapter II) for *high-speed gas flows*.

If $M < 1$, then gas flow is called *subsonic*, with $M > 1$ - *supersonic*.

From the last expression it is possible to obtain a calculation formula for the relation of the stagnation temperature to the temperature in the flow as a function of the Mach number:

$$\frac{T_0}{T} = 1 + \frac{k-1}{2} M^2. \quad (38)$$

It is not difficult to see that the maximum value of Mach number (with $T = 0$) is equal to infinity. This fact is explained by the fact that upon reaching of maximum speed together with absolute temperature the speed of sound also becomes zero.

Since the flow velocity can be both higher and lower than the speed of sound, there is such a system when the flow velocity is equal to the speed of sound, i.e., $M = 1$. This system is called *critical*; to it corresponds the value of temperature in the flow:

$$T_{cr} = T_0 \frac{2}{k+1}. \quad (39)$$

In air ($k = 1.4$) the critical temperature obtained is 20% lower than the stagnation temperature. The value itself of the speed of sound for a critical system differs from the same for stagnant gas, but is also completely specific:

$$\frac{a_{cr}}{a_0} = \sqrt{\frac{T_{cr}}{T_0}}. \quad (40)$$

from which

$$a_{*p} = a_* \sqrt{\frac{2}{k+1}} = \sqrt{\frac{2k}{k+1} gRT_*}. \quad (41)$$

For air $R = 29.27$, therefore we have

$$a_* = 20.1 \sqrt{T_*} \quad a_{*p} = 18.3 \sqrt{T_*}$$

It is possible to characterize the degree of the conversion of enthalpy into kinetic energy in still one more way, after dividing the thermal drop into enthalpy in the case of a critical system:

$$\frac{T_* - T}{T_{*p}} \approx \frac{I_* - I}{I_{*p}} = \frac{w_*^2}{a_{*p}^2} \frac{k-1}{2}.$$

Hence with the help of equality (40) we obtain a new formula for the relation of the temperatures in the energy isolated gas flow:

$$\frac{T}{T_*} = 1 - \frac{k-1}{k+1} \lambda^2. \quad (42)$$

Here we accept the designation

$$\lambda = \frac{w}{a_{*p}}. \quad (43)$$

The value λ , which measures the relation of the flow velocity to critical speed, we will name the velocity coefficient. In a critical system ($w = w_{*p} = a_{*p}$) the velocity coefficient $\lambda_{*p} = M_{*p} = 1$. To the maximum flow velocity with $T = 0$ corresponds the specific maximum value of the velocity coefficient:

$$\lambda_{\max} = \sqrt{\frac{k+1}{k-1}}. \quad (44)$$

For air ($k = 1.4$) we have $\lambda_{\max} = 2.45$. For the case $k = 1.2$ correspondingly $\lambda_{\max} = 3.31$.

The velocity coefficient, as also the Mach number, can be considered the similarity criterion for gas flows which characterizes the degree of the conversion of enthalpy into kinetic energy.

To this value of Mach number corresponds the completely specific value of the velocity coefficient. Let us find a transfer equation from Mach number to the velocity coefficient:

$$M^2 = \frac{w^2}{a^2} = \frac{w^2}{a_{tp}^2} \frac{a_{tp}^2}{a^2} \frac{a^2}{a^2}.$$

from which on the basis of (39), (40), and (42) we obtain

$$M^2 = \frac{\frac{2}{k+1} \lambda^2}{1 - \frac{k-1}{k+1} \lambda^2}, \quad (45)$$

or

$$\lambda^2 = \frac{\frac{k+1}{2} M^2}{1 + \frac{k-1}{2} M^2}, \quad (46)$$

In gas dynamics and the theory of jet engines both pure numbers (λ : M) are applied. In some cases simpler relationships are obtained when using a velocity coefficient, while in others - the Mach number. Figure 1.4 depicts the curves $\lambda = f(M)$ for the cases $k = 1.4$ and $k = 1.2$.

Sometimes the maximum gas velocity w_{\max} serves as the scale of speeds. In these cases the dimensionless equation of enthalpy can be presented on the basis of (35) in the following form:

$$\frac{T_0 - T}{T_0} = \frac{w^2}{w_{\max}^2} = \Lambda^2.$$

The value

$$\Lambda = \frac{w}{w_{\max}} \quad (47)$$

is called the dimensionless gas velocity.

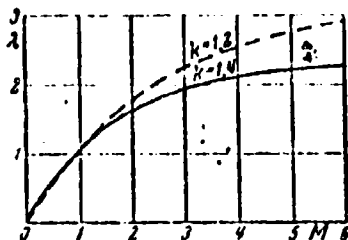


Fig. 1.4. The dependence of the velocity coefficient λ on Mach number.

The dependence of the relation of the temperature in the flow to the stagnation temperature on the dimensionless velocity appears thus:

$$\frac{T}{T_0} = 1 - \Lambda^2.$$

Let us show in conclusion that the equation of enthalpy for the energy

isolated stream can be given a purely kinematic form. For this let us write equation (24) in the form

$$c_p T + \Lambda \frac{w^2}{2g} = \Lambda \frac{w_{\max}^2}{2g}$$

and then multiply all its terms by the value gR/c_v

$$\frac{c_p}{c_v} gRT + \frac{AR}{c_v} \frac{w^2}{2} = \frac{AR}{c_v} \frac{w_{\max}^2}{2}.$$

Utilizing expressions $c_p = kc_v$, $AR = c_p - c_v$ and the formula for the speed of sound (34), we will obtain the relationship which relates the current value of the rate of flow and speed of sound with the maximum gas velocity:

$$\frac{2}{k-1} a^2 + w^2 = w_{\max}^2. \quad (48)$$

§ 4. The Mechanical Form of the Equation of Energy (Bernoulli Equation).

Above we examined in detail the equation of enthalpy. It related the gas temperature with the rate of motion taking into account energy effects (heat supply, technical work, and change of potential energy). Such factors as the pressure and the specific gravity of gas did not enter into the equation of enthalpy.

It is possible to obtain another (mechanical) form of the equation of energy, where, on the contrary, the gas temperature does not enter, but the rate of motion is connected with pressure and specific gravity. Differentially the equation of energy (5) can be written in the form

$$\frac{dQ}{\lambda} - d(pv) - dL - dL_p = \frac{du}{\lambda} + d\frac{w^2}{2g} + dz. \quad (49)$$

According to the first law of thermodynamics the heat applied to a gas can be expended only on an increase in internal energy and the work of expansion (deformation), i.e.

$$\frac{dQ}{\lambda} = \frac{du}{\lambda} + p dv. \quad (50)$$

Subtracting from equation (49) the equality (50), we will obtain

$$-dL - dL_p = d\frac{w^2}{2g} + dz + d(pv) - p dv. \quad (51)$$

Substituting in (51) the expression of specific volume ($v = 1/\gamma$), we obtain

$$-dL = d\frac{w^2}{2g} + dz + \frac{dp}{\gamma} + dL_p. \quad (52)$$

This is the mechanical form of the equation of energy, or, which is the same, the *equation of kinetic energies* for a unit stream.

After integration we will have

$$-L = \frac{w_2^2 - w_1^2}{2g} + (z_2 - z_1) + \int_1^2 \frac{dp}{\gamma} + L_{\text{fr}} \quad (53)$$

The derived equation is called the *generalized equation of Bernoulli*. It expresses the rate of motion as a function of pressure and specific gravity of the gas taking into account the technical work (L) produced by the gas, change in potential energy ($z_2 - z_1$) and work of the forces of friction (L_{fr}). In gas dynamics frequently they use the simplified form of the Bernoulli equation which corresponds to a system when technical work is absent ($L = 0$), there are no hydraulic losses ($dL_{\text{fr}} = 0$), and the reserve of potential energy does not change ($z_2 = z_1$). For this system the Bernoulli equation will be written in the following form:

$$\frac{w_2^2 - w_1^2}{2g} + \int_1^2 \frac{dp}{\gamma} = 0. \quad (54)$$

The Bernoulli equation is sometimes utilized in a somewhat different form. For this the integral is divided into two parts:

$$\int_1^2 \frac{dp}{\gamma} = \int_1^0 \frac{dp}{\gamma} + \int_0^2 \frac{dp}{\gamma} = \int_0^2 \frac{dp}{\gamma} - \int_1^0 \frac{dp}{\gamma}. \quad (55)$$

Then from (54) follows

$$\frac{w_1^2}{2g} + \int_1^0 \frac{dp}{\gamma} = \frac{w_2^2}{2g} + \int_0^2 \frac{dp}{\gamma} = \frac{w^2}{2g} + \int_0^2 \frac{dp}{\gamma} = \text{const.} \quad (56)$$

In this case the calculation of integrals is done each time from an absolute vacuum up to a pressure which corresponds to the assigned flow velocity. The constant of this equation can be obtained on the strength of the fact that during the expansion of a gas to an absolute vacuum the maximum flow velocity is reached.

Thus the Bernoulli equation can be given the following form:

$$\frac{w^2}{2g} + \int \frac{dp}{\gamma} = \frac{w_{max}^2}{2g}. \quad (57)$$

When the specific gravity of gas in section 1-2 of the elementary stream remains virtually constant, the integral in the Bernoulli equation is equal to

$$\int \frac{dp}{\gamma} = \frac{p_2 - p_1}{\gamma},$$

and the Bernoulli equation appears especially simply:

$$\frac{p_2 - p_1}{\gamma} + \frac{w_2^2 - w_1^2}{2g} = 0,$$

or

$$\frac{p_2}{\gamma} + \frac{w_2^2}{2g} = \frac{p_1}{\gamma} + \frac{w_1^2}{2g}. \quad (58)$$

In such a form it is applied in the hydraulics of an ideal non-compressible liquid. Sometimes the Bernoulli equation, for an ideal noncompressible liquid is written thus:

$$p_1 + \gamma \frac{w_1^2}{2g} = p_2 + \gamma \frac{w_2^2}{2g}. \quad (59)$$

In the first case it is formed for 1 kgf, and in the second - for 1 m³ of liquid. The kinetic energy of 1 kgf of liquid ($w_1^2/2g$) is called *velocity head*, while the kinetic energy of 1 m³ of liquid ($\gamma w^2/2g$) - *dynamic head*.

If it is not possible to disregard technical work, hydraulic losses, and change in potential energy, then the Bernoulli equation for 1 kgf of a noncompressible liquid takes this form:

$$-L = \frac{w_2^2 - w_1^2}{2g} + z_2 - z_1 + \frac{p_2 - p_1}{\gamma} + L_{\text{tr}} \quad (60)$$

By means of this equality it is possible to calculate, for example, the work which a liquid gives up to the turbine wheel ($L > 0$) which is standing between cross sections 1 and 2, if all the other terms of this equation are known.

In order to use the Bernoulli equation for a compressible gas it is necessary to know in advance the thermodynamic process of a change in the state of the gas, since without this the dependence of the specific gravity of gas on pressure is unknown and it is not possible to take integral $\int_1^2 \frac{dp}{\gamma}$, which expresses the work of extrusion. Let us compute this integral for the basic thermodynamic processes.

During an *isochoric process* (a constant volume, i.e., constant specific gravity), typical for the hydraulics of true liquids, as has already been indicated, this integral was equal to

$$\int_1^2 \frac{dp}{\gamma} = \frac{p_2 - p_1}{\gamma}. \quad (61)$$

In an *isobaric process* (constant pressure) the integral is equal to zero

$$\int_1^2 \frac{dp}{\gamma} = 0. \quad (62)$$

If an *isothermal process* (constant temperature) is achieved, then according to the equation of state of a gas (8) $p/\gamma = RT = \text{const.}$, i.e., pressure is directly proportional to the specific gravity of the gas $\gamma = \gamma_1 p/p_1$, from which is obtained the following expression for the integral:

$$\int_1^2 \frac{dp}{\gamma} = \frac{p_1}{\gamma_1} \int_1^2 \frac{dp}{p} = \frac{p_1}{\gamma_1} \ln \frac{p_2}{p_1}. \quad (63)$$

Let us assume now that the state of the gas changes on the *ideal adiabatic curve*

$$\frac{p}{\gamma^k} = \text{const.}$$

then

$$\gamma = \gamma_1 \left(\frac{p}{p_1} \right)^{\frac{1}{k}}.$$

and therefore the integral is equal to

$$\int_1^2 \frac{dp}{\gamma} = \frac{p_1^{\frac{1}{k}}}{\gamma_1^{\frac{1}{k}}} \int_1^2 \frac{dp}{p^{\frac{k+1}{k}}} = \frac{k}{k-1} \frac{p_1}{\gamma_1} \left[\left(\frac{p_2}{p_1} \right)^{\frac{k-1}{k}} - 1 \right]. \quad (64)$$

Finally, in a *polytropic process* with constant polytropic exponent ($n = \text{const.}$) $p/\gamma^n = \text{const}$ we will obtain the following expression for the integral:

$$\int_1^2 \frac{dp}{\rho} = \frac{n}{n-1} \frac{p_1}{\rho_1} \left[\left(\frac{p_2}{p_1} \right)^{\frac{n-1}{n}} - 1 \right]. \quad (65)$$

It should be noted that the heat applied to the gas is not reflected directly in the Bernoulli equation. However, it is considered during the calculation of the integral, since it influences the form of the function $\gamma = f(p)$, i.e., the nature of the process according to which the state of the gas changes.

The greatest value in gas dynamics belongs to an *ideal adiabatic* process which assumes the absence of a thermal effect and work of the forces of friction. Because of this, with an ideal adiabatic curve the entropy¹ of the gas remains constant, i.e., such a process is an ideal thermodynamic - *isentropic* - process. Let us recall that by no means is any adiabatic process ideal. For example, during the derivation of the equation of enthalpy we showed that the presence of friction does not disturb the adiabaticity of the process, but a process with friction no longer can be ideal, since it flows with an increase in entropy. In other words, the adiabaticity of the process required only zero heat transfer with the environment, and not a constancy of entropy. Thus adiabaticity is combined with the constancy of entropy only in an ideal process. If a change in the potential energy can be disregarded ($z_1 = z_2$) and there is no technical work ($L = 0$), and the process is ideally adiabatic, then the Bernoulli equation on the basis of (54) and (64) takes the following form:

$$\frac{n}{n-1} \frac{p_1}{\rho_1} \left[\left(\frac{p_2}{p_1} \right)^{\frac{n-1}{n}} - 1 \right] + \frac{w_1^2 - w_2^2}{2g} = 0. \quad (66)$$

Let us examine the case of the ideal deceleration of a gas jet, i.e., let us determine pressure $p_2 = p_0$, which will be obtained if

¹See below, § 7.

the rate of flow decreases by the isentropic route from $w_1 = w$ (with this $p_1 = p$, $\gamma_1 = \gamma$) to $w_2 = 0$. The Bernoulli equation in this case gives

$$\frac{k}{k-1} \frac{p}{\gamma} \left[\left(\frac{p_0}{p} \right)^{\frac{k-1}{k}} - 1 \right] = \frac{w^2}{2g}. \quad (67)$$

from which

$$\frac{p_0}{p} = \left(1 + \frac{k-1}{2} \frac{w^2}{k g \frac{p}{\gamma}} \right)^{\frac{k}{k-1}}.$$

Utilizing expression (34) which relates the speed of sound with the parameters of state of the gas,

$$a = \sqrt{\frac{k p}{\gamma}},$$

we will obtain for the calculation of pressure in an ideally decelerated gas flow, in the function of pressure (p) and Mach number before the deceleration:

$$\frac{p_0}{p} = \left(1 + \frac{k-1}{2} M^2 \right)^{\frac{k}{k-1}}. \quad (68)$$

Value p_0 is called the *total pressure*. Just as the stagnation temperature, the total pressure is a convenient characteristic of gas flow, since it immediately connects two factors: the rate and the pressure in the flow; the latter is usually called *static pressure*. Thus the ratio of the total pressure to static is a function of Mach number.

Formula (68) can be obtained directly from expression (40) for the stagnation temperature

$$\frac{T_0}{T} = 1 + \frac{k-1}{2} M^2.$$

using the relationships for the ideal adiabatic curve

$$\frac{p_0}{p} = \left(\frac{T_0}{T}\right)^{\frac{k}{k-1}}. \quad (69)$$

$$\frac{\rho_0}{\rho} = \left(\frac{T_0}{T}\right)^{\frac{1}{k-1}}. \quad (70)$$

Also obtained here is the formula for the calculation of density in an ideally decelerated gas jet

$$\frac{\rho_0}{\rho} = \left(1 + \frac{k-1}{2} M^2\right)^{\frac{1}{k-1}}. \quad (71)$$

With the help of function (42), which relates the stagnation temperature with the velocity coefficient, we find from relationship (69) the dependence of the total pressure on the velocity coefficient

$$\frac{p}{p_0} = \left(1 - \frac{k-1}{k+1} \lambda^2\right)^{\frac{k}{k-1}}. \quad (72)$$

For the density of an ideally decelerated gas we will obtain correspondingly

$$\frac{\rho}{\rho_0} = \left(1 - \frac{k-1}{k+1} \lambda^2\right)^{\frac{1}{k-1}}. \quad (73)$$

It is necessary to note that the true pressure which is obtained during the slowing down of a gas jet can differ significantly from the total pressure determined by formula (68). This is explained

by the fact that in actuality the slowing down of the jet frequently takes place not according to an ideal adiabatic curve, but with more or less essential hydraulic losses. For example, in a diffuser in the case of subsonic gas flow a decrease in velocity is usually accompanied by vortex formations which contribute considerable resistances into the gas flow. During the slowing down of supersonic flow shock waves which give the specific "wave" resistance are always formed. Thus real pressure in a decelerated gas jet is usually lower than the total pressure of the incoming jet.

Generally if losses are observed in the section of the jet 1-2, then this without fail leads to the fact that the total pressure in cross section 2 will be lower than the total pressure in cross section 1:

$$p_{02} < p_{01}.$$

If we introduce the dimensionless quantity which is called the *pressure coefficient*:

$$\sigma = \frac{p_{02}}{p_{01}}, \quad (74)$$

then the greater the losses the lower the value of the pressure coefficient and less the total pressure at the end of the section of the jet in question:

$$p_{02} = \sigma p_{01}. \quad (75)$$

It is possible to estimate losses also according to the difference in the total pressures:

$$\Delta p_0 = p_{01} - p_{02} = (1 - \sigma) p_{01}. \quad (76)$$

The application of the Bernoulli equation is the basis of the pneumatic method of determining the flow velocity, which consists of the fact that into the flow an adapter (Fig. 1.5) which consists of two tubes is introduced. The open orifice of one of these tubes (1) is placed in the nose of the adapter (towards the flow), and the openings of the second tube (2) are arranged in the lateral surface of the adapter (along the flow); at subsonic speed the deceleration of the gas jet from rendezvous with the adapter passes without any losses, since friction and vortex formation appear already on the lateral surface of the adapter, i.e., after the jet passes the area of its total stagnation, which is located before the spout of the adapter. Because of this in the first tube a pressure is created which is almost exactly equal to the total pressure of incoming flow; in the second tube, if its inlet is sufficiently moved away from spout, a pressure close to the static pressure of flow is established. Tubes 1 and 2 are connected with a manometer which measures pressure. The relation of the measured pressures

$$\frac{p_1}{p_2} = \frac{p_0}{p}$$

makes it possible according to formula (68) or (72) to calculate the values of the Mach number or the coefficient of flow velocity.

The calculations according to these formulas are sufficiently precise only for a subsonic flow. This is explained by the fact that during the stagnation of a supersonic flow a shock wave appears before the adapter; when these are intersected by the gas jets they undergo considerable hydraulic losses. Thus the pressure in tube 1 of the pneumatic adapter during supersonic flow differs significantly from the total pressure of incoming flow, which makes formulas (68) and (72) inapplicable in this case.

It is necessary to note that it is possible to use a pneumatic adapter also for the measurement of supersonic speed, but in this

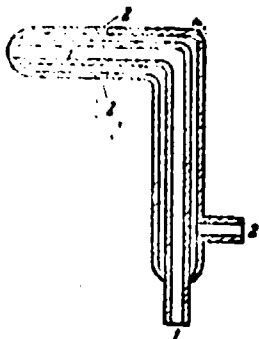


Fig. 1.5. Diagram of pneumatic adapter.

case one ought to apply special calculation equations which consider wave resistance. We will derive such formulas subsequently.

Thus the extreme value of velocity, above which it is not possible to apply formulas (68) and (72) in the stagnation of a gas flow, is equal to the sound $M = \lambda = 1$).

For the gas flow being accelerated these formulas can also be used at supersonic speeds, since an increase in velocity occurs usually without noticeable losses (isentropically) not only in area $M < 1$, but also in the area $M > 1$, i.e., the total pressure in the gas jet being accelerated barely changes. Specifically, from formulas (68) or (72) the *exhaust gas velocity* is calculated. In this case in the vessel where the gas rests the pressure is equal to the total pressure of the discharging jet p_0 , and in the outlet of the nozzle - to the static pressure p . From formula (68) we will obtain

$$M^2 = \left[\left(\frac{p_0}{p} \right)^{\frac{k-1}{k}} - 1 \right] \frac{2}{k-1}. \quad (77)$$

and from formula (72)

$$\lambda^2 = \left[1 - \left(\frac{p}{p_0} \right)^{\frac{k-1}{k}} \right] \frac{k+1}{k-1}. \quad (78)$$

From here we determine the discharge velocity w :

$$w = aM,$$

where

$$a = a_0 \sqrt{\frac{T}{T_0}} = a_0 \left(\frac{p}{p_0} \right)^{\frac{k-1}{2k}}. \quad (79)$$

or

$$w = a_{sp} \lambda,$$

where

$$a_{sp} = a_0 \sqrt{\frac{2}{k-1}}. \quad (80)$$

As it is not difficult to see, the calculation of the discharge velocity is done more conveniently according to the velocity coefficients than according to Mach numbers. The true values of the discharge velocity are somewhat lower than those determined according to formulas (77-80), since some losses of friction cannot be avoided, but the error for these formulas is usually no more than 1-5%.

Curves $\lambda = f(p_0/p)$ for cases $k = 1.4$ and $k = 1.2$ are shown in Fig. 1.6.

With the help of the Bernoulli equation we will investigate the technical work of a compressor and turbine. In the compressor the total pressure of gas increases: $p_{02} > p_{01}$, while in the gas turbine it drops: $p_{02} < p_{01}$. The pressure ratio p_{02}/p_{01} in the compressor is respectively more than a unit, and in the turbine - less than a unit. For greater clarity let us assume that the work due to friction and change in the potential energy are absent and the pressure change in the machine occurs over an isentropic law. In this case the Bernoulli equation will be written thus:

$$-L = \frac{w_2^2 - w_1^2}{2g} + \int_1^2 \frac{dp}{\gamma} = \frac{w_1^2 - w_2^2}{2g} + \frac{k}{k-1} \frac{p_1}{\gamma_1} \left[\left(\frac{p_2}{p_1} \right)^{\frac{k-1}{k}} - 1 \right]. \quad (81)$$

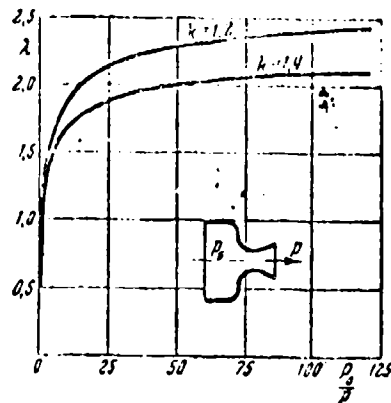


Fig. 1.6. The dependence of the velocity coefficient of outflow on the ratio of total pressure to static pressure in the nozzle exit section.

A compressor or turbine, working under such conditions, is called an *ideal compressor* or *ideal turbine*. Utilizing equality (67), let us introduce in expression (81) the total pressures before and after the machine, after eliminating from it the velocities:

$$\frac{k}{k-1} \left\{ \frac{p_2}{\gamma_2} \left[\left(\frac{p_{02}}{p_2} \right)^{\frac{k-1}{k}} - 1 \right] - \frac{p_1}{\gamma_1} \left[\left(\frac{p_{01}}{p_1} \right)^{\frac{k-1}{k}} - 1 \right] + \frac{p_1}{\gamma_1} \left[\left(\frac{p_2}{p_1} \right)^{\frac{k-1}{k}} - 1 \right] \right\} = -L,$$

from which

$$\frac{k}{k-1} \left\{ \frac{p_2^{1/k}}{\gamma_2} (p_{02})^{\frac{k-1}{k}} - \frac{p_1}{\gamma_1} - \frac{p_1^{1/k}}{\gamma_1} (p_{01})^{\frac{k-1}{k}} + \frac{p_2}{\gamma_1} + \frac{p_1^{1/k}}{\gamma_1} (p_1)^{\frac{k-1}{k}} - \frac{p_1}{\gamma_1} \right\} = -L;$$

but in an adiabatic process we have the equality

$$\frac{p_2^{1/k}}{\gamma_2} = \frac{p_1^{1/k}}{\gamma_1} = \frac{p_{01}^{1/k}}{\gamma_{01}} = \frac{p_{02}^{1/k}}{\gamma_{02}},$$

with the help of which after simple conversions we obtain

$$-L = \frac{k}{k-1} \frac{p_{01}}{\gamma_{01}} \left[\left(\frac{p_{02}}{p_{01}} \right)^{\frac{k-1}{k}} - 1 \right]. \quad (82)$$

Thus in the ideal case technical work can be determined by a change in the total pressures without allowing for the specific values of gas velocity before and after the machine. Work being transferred to the gas turbine is positive ($p_{02} < p_{01}$), and supplied by the compressor - negative ($p_{02} > p_{01}$).

Deviation from an ideal isentropic process in the machine is usually considered with the help of a cofactor which is the efficiency of the machine. In the case of the compressor we will obtain.

$$L_c = \frac{L}{\eta_c}. \quad (83)$$

In the case of the turbine

$$L_t = \eta_t L. \quad (84)$$

The relation of the values of the total pressure after and before the machine

$$\pi = \frac{p_{02}}{p_{01}} \quad (85)$$

we will call subsequently the *degree of pressure increase* (for a compressor) or the *degree of pressure decrease* (for a turbine). The equation of ideal technical work can also be written in the following form:

$$L = -\frac{k}{k-1} R T_{01} \left[\pi^{\frac{k-1}{k}} - 1 \right] \left[\frac{M g \cdot M}{k L_2} \right]. \quad (86)$$

The essential feature of technical work is the fact that its magnitude, as can be seen from expression (86), is directly proportional to the initial temperature of the gas. This property of technical work is the basis of the operating conditions of any thermal gas machine. For example, in the internal combustion engine the working medium is always compressed first, then is heated, and expands. In accordance with what was said, the work spent during the compression of a cold gas is less than work which it will produce after preheating during expansion up to initial pressure. From a difference in these works, strictly speaking, the effective work being accomplished by the internal combustion engine is obtained.

§ 5. The Equation of Momentum

According to Newton's second law the elementary change in momentum is equal to the elementary power pulse:

$$d(mw) = Pdz. \quad (87)$$

Here P is the sum of projections on any axis of all forces applied to the body of mass m , w is the projection of velocity on the same axis, dz is the action time of force P . In such a form Newton's law is utilized in the mechanics of solid states.

In connection with the flow of fluids and gases it is more convenient to have a somewhat different (hydrodynamic) form of equation for momentum. It was obtained for the first time by Euler. Let us derive the equation of momentum in a hydrodynamic form. For this let us isolate the elementary stream (Fig. 1.7) and draw two cross sections 1 and 2 normal to its axis. Let us break the entire mass of liquid included in volume 1-2 into a large number of parts so that within the limits of each of them, having the mass m , the velocity of motion could be considered constant, and let us establish a bond between the projections of forces and momentum

on the x-axis. According to equation (87) the sum of the projections of the pulses of all forces applied to the mass of liquid 1-2 is equal to the change in the projection of the total momentum:

$$P_x dt = d \sum m w_x \quad (88)$$

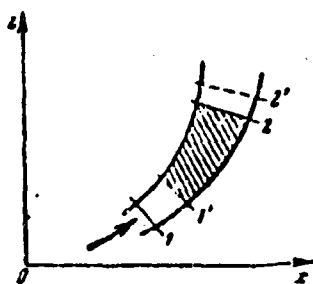


Fig. 1.7. Elementary stream.

Let us examine a change in the total momentum $d \sum m w_x$ during time dt , during which the chosen mass of liquid will move from position 1-2 into position 1'-2'. Let us suppose, as we did in the foregoing paragraphs, that the liquid is found in steady motion, then the momentum of mass 1'-2, which enters both into the initial and the final value of total momentum, remains constant and in the case of

subtraction is decreased. In other words the increase of the total momentum should be equal to the difference in the momentum taken respectively for masses 2-2' and 1-1' which in steady motion are identical:

$$d \sum m w_x = (w_{x2} - w_{x1}) dM.$$

Here dM is the mass of the liquid of element 1-1' (or 2-2'), w_{x2} , w_{x1} are projections of x-axis of the flow velocity in cross sections 2 and 1. Elementary mass dM is equal to the product of the per-second mass flow of liquid for the interval of time dt divided into the G force:

$$dM = \frac{G}{g} dt.$$

Hence

$$d \sum m w_x = (w_{x2} - w_{x1}) \frac{G}{g} dt.$$

Value Gw/g is called the *per-second momentum*.

Substituting the resulting expression into the initial equality (85) we come to the equation of momentum in hydrodynamic form (to the first equation of Euler), according to which the sum of the projections of all forces applied to the liquid jet in any section of it is equal to an increase in the projection of the per-second momentum in this section, or, what is the same, to the product of the mass flow per second by the increase in the projection of the velocity:

$$P_x = \frac{G}{g}(w_{x2} - w_{x1}) \quad (89)$$

Similar equations can be composed also for the other two axes.

Let us apply the equation of momentum to a rectilinear stream of constant section F . Let us draw the end parts of the control surface at right angles to the flow direction, whereupon let the generatrix of the lateral surface of the stream be parallel to the x -axis. The flow velocity w is directed to the side of the positive x -axis. Let us compose the equation of momentum in the flow direction. On the control surface the forces of pressure normal to it are acting. Thus projections on the x -axis of the forces of pressure applied to the lateral surface are equal to zero. Pressure change in the section between the end cross sections of the stream is proportional to the force which acts on the selected fluid element. This force, parallel to the x -axis, is equal to $(p_1 - p_2)F$. To the lateral surface is applied the force of friction directed parallel to the flow, against it: $-P_{\tau p}$. Furthermore, between the end cross sections of the stream any machine which receives technical work from a gas can be found. Let the projection on the direction of motion of the force, with which the machine acts on the gas, be equal to $-P$.¹ Thus the sum of the projections of all forces on the x -axis is equal to

¹The projection of the force applied by gas flow to the machine is considered positive.

$$P_s = (p_1 - p_2)F - P_{1p} - P_2$$

According to the equation of momentum this force should be equal to a change in the momentum:

$$(p_1 - p_2)F - P_{1p} - P_2 = \frac{Q}{g}(w_1 - w_2) \quad (90)$$

If the distance between cross sections 1 and 2 is infinitely small, then the equation of momentum must be written differentially:

$$\frac{Q}{g}dw + Fdp = -dP_{1p} - dP_2$$

After multiplying all the terms of this equation by the velocity of motion and after dividing by the mass flow rate of the gas, we will obtain the equation of work of all forces for a cylindrical stream referred to 1 kgf of gas:

$$\frac{wdw}{g} + \frac{dp}{\gamma} = -\frac{wdP_{1p}}{Q} - \frac{wdP_2}{Q}$$

Here the equation of expenditure in a cylindrical stream is used:

$$\gamma w = \frac{Q}{F} = \text{const.}$$

It is not difficult to see that the terms standing in the right side are the work of the forces of friction:

$$\frac{w}{Q}dP_{1p} = dL_{1p}$$

and technical work:

$$\frac{w}{Q}dP = dL$$

Thus the equation of momentum for a cylindrical stream of gas is easily converted into a Bernoulli equation:

$$-dL = d\left(\frac{w^2}{2g}\right) + \frac{dp}{\gamma} + dL_{fr} \quad (91)$$

Subsequently the equation of momentum for a cylindrical gas jet will be used in the following form:

$$dp + \rho w dw = -\frac{dP_{to}}{\rho} = -\frac{dP}{\rho}. \quad (92)$$

In the absence of the friction and power effect of gas on any machine the differential equation of momentum acquires a very simple form:

$$dp = -\rho w dw. \quad (93)$$

Equation (93) expresses an important property of gas flow. In the absence of applied forces and forces of friction an increase in the flow velocity can be caused only by a decrease in static pressure, and vice versa, the stagnation of flow in this case is always connected with an increase in pressure in it regardless of the nature of other processes which proceed in the flow and the change in the remaining parameters of the gas. In integral form the equation of momentum for a cylindrical stream will be written thus:

$$P_2 - P_1 + \rho_1 w_1 (w_2 - w_1) = -\frac{\rho_1}{\rho} P = -\frac{P}{\rho}.$$

or under condition $P_{tp} = 0$ and $P = 0$:

$$P_2 - P_1 = \rho_1 w_1 (w_2 - w_1). \quad (94)$$

or

$$p + \frac{\rho w^2}{2} = \text{const.}$$

Thus in a cylindrical stream pressure can be changed even when there is no friction and technical work. For this it is sufficient that the rate of flow would change, which can be achieved with the supply or removal of heat. For example, with the preheating of gas, in connection with a decrease in its density the velocity increases ($\rho_1 w_1 = \rho_2 w_2$), and pressure drops.

An important feature of the equation of momentum is that with its help the calculation of acting forces is conducted only on the state of flow on the control surface without penetration into the essence of processes which proceed inside this control surface. Thus the equation of momentum makes it possible in many instances to calculate sufficiently a hydrodynamic process without investigating the parts in it.

It should be noted that the effectiveness of the use of the equation of momentum depends basically on how successfully the control surface in the flow is selected.

Let us examine several examples of the application of equations of momentum and energy.

Example 1. Let us determine hydraulic losses in the flow of a noncompressible liquid during a sudden expansion of channel (Fig. 1.8). Experiment shows that in this case the jet coming out from the narrow section of the channel does not fill at first the entire cross section of the wide channel, but it spreads out gradually. In the corners between the surface of the jet and the walls the closed currents of liquid are formed, whereupon pressure on the end wall 1 according to experiments turns out to be nearly equal to static pressure at the outlet from the narrow section of the channel (p_1). During a sudden expansion of the channel considerable hydraulic resistance is observed, i.e., a decrease

occurs in the total pressure in the flow. If we place cross section 2 in such a place where the flow is already completely equalized, i.e., static pressure p_2 and flow velocity w_2 on the cross section are constant, then losses will be equal to the difference in the total pressures:

$$\Delta p_0 = p_{01} - p_{02}$$

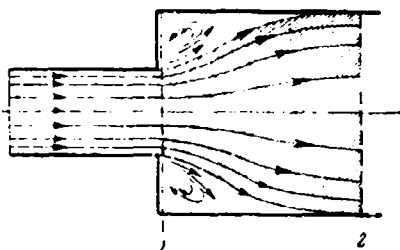


Fig. 1.8. The arrangement of flow during the sudden expansion of a channel.

The total pressure p_0 in the case of motion of a noncompressible liquid is determined in complete analogy with that as this was done for an ideal adiabatic process in § 4, i.e., as the pressure in a completely decelerated jet without losses and in the absence of technical work; with $z = \text{const}$ according to the Bernoulli equation for a noncompressible liquid we have

$$p_0 = p_1 + \frac{\rho w_1^2}{2}$$

Thus for a noncompressible liquid

$$\Delta p_0 = \left(p_1 + \frac{\rho w_1^2}{2} \right) - \left(p_2 + \frac{\rho w_2^2}{2} \right)$$

The velocities w_1 and w_2 can be connected with the equation of continuity

$$w_1 F_1 = w_2 F_2$$

the change in the static pressure ($p_1 - p_2$) is unknown in advance, i.e., one equation with two unknowns is obtained. Additionally it is possible to utilize the equation of momentum. Taking into account that the section of spreading of the jet 1-2 has too great a length, the force of friction is usually disregarded. Then the equation of momentum can be used in the simplest form (94):

$$p_1 - p_2 = \rho w_2 (w_1 - w_2)$$

Here the pressure constancy in cross section 1 is utilized. It is not self-evident, but as indicated above it is confirmed by experiments. Unlike the Bernoulli equation the equation of momentum makes it possible to determine immediately the difference in the values of static pressure which are obtained in a flow during a sudden expansion of the channel. If this result is substituted into the Bernoulli equation, then the total losses of pressure will be found during the sudden expansion of the channel:

$$\Delta p_0 = \rho \frac{(w_1 - w_2)^2}{2}$$

One ought to focus attention on the fact that the use of the equation of momentum brought success in this case because of the successful selection of control surface 1-2, on which the basic acting forces turned out to be known.

Example 2. Let us make the calculation of the simplest ejector which consists of nozzle A and a cylindrical mixing tube B, arranged in the space filled by a fixed liquid (Fig. 1.9). From the nozzle a jet is supplied which sucks the liquid from the surrounding space. Assume at the output from the mixing tube the velocity and specific gravity of the mixture are approximately constant. Let us construct the control surface from cross sections 1 and 2, which pass at right angles to flow on the nozzle section and the section of the mixing tube, and lateral surfaces directed parallel to flow. On the entire control surface one and the same pressure of the quiescent

liquid prevails, i.e., the main force vector of pressure is equal to zero.

If we disregard the force of friction on the walls of the mixing tube, then it will turn out that the sum of the projections on the x-axis of all the forces within the limits of the control surface 1-2 is equal to zero, and, consequently, there should be a change in momentum.

The change in momentum in an active jet in section 1-2.

$$\frac{G_1}{g} (w_2 - w_1).$$

The same for the liquid sucked in from the surrounding space, where it was found in rest ($w = 0$):

$$\frac{G_2 - G_1}{g} (w_1 - 0),$$

from which the total change in momentum

$$\frac{G_2 w_1}{g} - \frac{G_1 w_1}{g} = 0.$$

Here G_1 , G_2 are the per-second weight rates of the liquid respectively in the nozzle and at the exit from the mixing tube, w_1 and w_2 are the values of the discharge velocity from the nozzle and the mixing tube.

The result is that the fluid flow rates in the nozzle and at the outlet from the mixing tube are inversely proportional to the values of the corresponding velocities

$$\frac{G_2}{G_1} = \frac{w_1}{w_2}.$$

On the other hand it is obvious that

$$\frac{G_2}{G_1} = \frac{\gamma_2 w_2 F_2}{\gamma_1 w_1 F_1},$$

where γ is specific gravity, F - the cross-sectional area. Comparing the last two expressions, we arrive at the following calculation formula:

$$\frac{G_2}{G_1} = \sqrt{\frac{\gamma_2 F_2}{\gamma_1 F_1}}.$$

If the specific gravity of liquid in the active jet and in the surrounding space is identical, then the relation of the mass flows of the liquid is equal to the relation of the diameters of the mixing tube and nozzle:

$$\frac{G_2}{G_1} = \sqrt{\frac{F_2}{F_1}} = \frac{D_2}{D_1}.$$

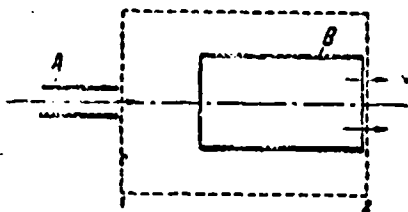


Fig. 1.9. The simplest ejector.

Example 3. Let us compute the force which acts on the walls of a diffuser (Fig. 1.10) in the absence of hydraulic flow losses of a noncompressible liquid. Let the pressure and the velocity in cross section 1 before the diffuser be constant and equal to p_1 , w_1 , and in cross section 2 after the

diffuser are also constant and equal to p_2 , w_2 . The Bernoulli equation, if there are no losses, gives

$$p_1 + \frac{\rho w_1^2}{2} = p_2 + \frac{\rho w_2^2}{2}.$$

from the equation of continuity we obtain

$$w_1 F_1 = w_2 F_2 = Q.$$

Let us draw the control surface from the cross sections of 1 and 2 and lateral surfaces located parallel to the flow and covering the diffuser. As a result of the slope of the walls of the diffuser the sum of projections on the x-axis of the forces of pressure applied from the walls to the liquid is not equal to zero ($P_d \neq 0$).

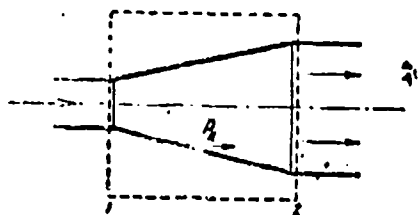


Fig. 1.10. For the calculation of the force of pressure in a diffuser.

The sum of the projections of all forces on the x-axis, which is obtained by means of the combination of forces P_d with the forces of pressure on the end cross sections, is equal to the change of momentum

$$P_2 + p_1 F_1 - p_2 F_2 = \frac{Q}{g} (w_2 - w_1).$$

Carrying out the replacement of values w_1 and p_2 with the help of the equations of continuity and Bernoulli, we come to the following expression for a projection on the direction of flow of the force which acts on the flow from the walls of the diffuser:

$$P_d = p_1 (F_2 - F_1) + \frac{Q w_2}{2g} \left(\frac{F_2 - F_1}{F_1} \right)^2.$$

Let the external pressure - p_u , then the projection on the x-axis of the force of external pressure on the diffuser

$$P_{уд} = p_u (F_2 - F_1).$$

In summation we obtain the following value of projection on the x-axis of the net force which acts on the walls of the diffuser:

$$-P = P_A - P_{\text{изп}} = (p_1 - p_A)(F_2 - F_1) + \frac{G w_1}{2g} \left(\frac{F_2 - F_1}{F_1} \right)^2.$$

In the particular case, when external pressure is equal with the pressure in the narrow cross section of the diffuser, this force is equal to

$$-P = \frac{G w_1}{2g} \left(\frac{F_2}{F_1} - 1 \right)^2 = \frac{\gamma w^2}{2g} F_1 \left(1 - \frac{F_1}{F_2} \right)^2.$$

The last expression is sometimes applied during the calculation of the force which acts on the inlet diffuser of a jet engine.

Example 4. Let us establish the interconnection between the flying speed and the discharge velocity from a ramjet engine, the layout of which is depicted in Fig. 1.11. In the intake of the engine the conversion of the dynamic head of incident flow into pressure occurs, i.e., dynamic air compression. In the combustion chamber heat will be supplied and the mixture of compressed air and the products of combustion which is formed is heated. In the exit nozzle the heated gases are expanded; here pressure is converted into dynamic head.

The bases of the theory of a ramjet engine were given for the first time by B. S. Stechkin in 1929.¹

The most ideal working cycle for a ramjet engine would be obtained in such a case when the air compression in section n - x (Fig. 1.11) is achieved on an ideal adiabatic curve and the flow velocity would be reduced to zero, the heat supply in the combustion chamber x - g would occur at constant pressure, whereupon the exhaust mixture would be expanded in the nozzle g - a up to atmospheric pressure also on an ideal adiabatic curve. A ramjet engine which works on the indicated ideal cycle is called ideal.

¹Stechkin, B. S., the Theory of the Jet Engine, Tekhnika Vozdushnogo Flota, No. 2, 1929.

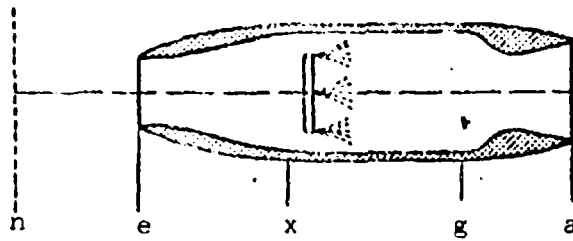


Fig. 1.11. The layout of a ramjet engine: e - entrance, x - the initial cross section of the combustion chamber, g - final cross section of combustion chamber, a - nozzle entry section.

The total pressure in the combustion chamber can be found from the Bernoulli equation which is integrated in this case with the help of the ideal adiabatic curve:

$$\frac{k}{k-1} \frac{p_n}{\rho_n} \left[\left(\frac{p_e}{p_n} \right)^{\frac{k-1}{k}} - 1 \right] = \frac{w_e^2}{2}.$$

The discharge velocity will be found from a similar expression with $p_n = p_a$

$$\frac{k}{k-1} \frac{p_n}{\rho_a} \left[\left(\frac{p_e}{p_n} \right)^{\frac{k-1}{k}} - 1 \right] = \frac{w_a^2}{2}.$$

From here we obtain the basic relationship

$$p_n \frac{w_n^2}{2} = p_a \frac{w_a^2}{2}.$$

Thus in an ideal ramjet engine the dynamic head of flow in the outlet is equal to the dynamic head of flight.

Utilizing this same equality, we will obtain for an ideal engine ($p_{0x} = p_{0r}$, $p_a = p_n$) one additional important result:

$$\lambda_a = \lambda_n.$$

i.e., the velocity coefficients in the outlet of an ideal engine and in the incoming undisturbed flow are equal. Hence ensues also the equality of the Mach numbers of flight and outflow:

$$M_a = M_n.$$

These relationships are valid for an ideal engine both at subsonic and at supersonic flying speed.

In an actual engine in connection with the losses of pressure in the inlet and outlet sections and in the combustion chamber the dynamic head on the exhaust is lower than the dynamic head of flight:

$$\rho_a \frac{w_a^2}{2} < \rho_n \frac{w_n^2}{2}.$$

For this reason the Mach number and the velocity coefficient in the outlet have smaller values than in the incident flow:

$$M_a < M_n, \quad \lambda_a < \lambda_n.$$

Thus an increase in the discharge velocity as compared with the flying speed is obtained not as a result of an increase in the dynamic head in the engine, but because of a decrease in the gas density following preheating.

The relationships obtained lead to a simple calculation formula for the discharge velocity in an ideal engine:

$$w_a = w_n \sqrt{\frac{\rho_n}{\rho_a}} = w_n \frac{a_{np.r}}{a_{np.x}},$$

where $a_{np.r}$, $a_{np.x}$ - the critical gas velocity respectively after and before preheating. From this formula it follows that the ratio of the discharge velocity to the flying speed for an ideal

engine is proportional to the square root from the relation of the stagnation temperatures taken at the end and the beginning of the combustion chamber:

$$\frac{w_e}{w_a} = \sqrt{\frac{T_{01}}{T_{02}}}$$

One ought to emphasize in this case that the stagnation temperature in the beginning of the combustion chamber can be calculated according to formula (42) as the function of temperature in the atmosphere and the velocity coefficient of flight

$$\frac{T_{01}}{T_{02}} = 1 - \frac{k-1}{k+1} \lambda_a^2$$

and the stagnation temperature at the end of the combustion chamber is determined by the fuel consumption in the engine and the rate of air flow.

§ 6. The Equation of Angular Momentum [Moment of Momentum]

As is known from mechanics, a change in the total moment of momentum relative to any axis, for example the y -axis, is equal to the sum of the moments of pulses of all forces applied to the body relative to the same axis (Fig. 1.12):

$$d \sum m (w_z z - w_x x) = M_y dt \quad (95)$$

Here mw_z , mw_x - the projections of the momentum of a certain elementary mass m on the axis z and x ; x , z - the corresponding coordinates, $m(w_x z - w_z x)$ - the moment of momentum of elementary mass m relative to the y -axis.

If the motion of the liquid is steady-state, then change in the total moment of momentum of the liquid which is moved during

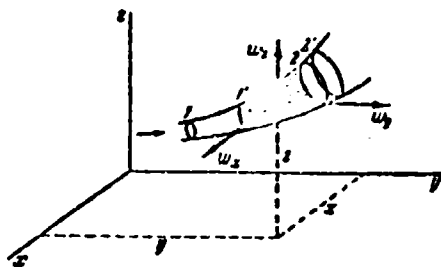


Fig. 1.12. For the derivation of the equation of angular momentum.

the time dt from space 1-2 into space 1'-2' is equal to a difference in the moment of momentum in volume elements 2-2' and 1-1':

$$d \sum m (w_x z - w_z x) = \frac{G}{g} [(w_{x1} z_1 - w_{z1} x_1) - (w_{x2} z_2 - w_{z2} x_2)] dt, \quad (96)$$

where G is the per-second fluid flow rate. This is explained by the fact that the moment of momentum of the shaded mass 1'-2 is decreased during subtraction, since the motion of liquid is assumed to be steady-state.

Substituting (96) into the left side of equality (95), we will obtain the second equation of Euler, i.e., the equation of angular momentum in a hydrodynamic form:

$$M_y = \frac{G}{g} [(w_{x1} z_1 - w_{z1} x_1) - (w_{x2} z_2 - w_{z2} x_2)]. \quad (97)$$

Similar equations can be formed for axes z and x . According to the second equation of Euler the sum of moments with respect to any axis of all forces applied to a liquid volume is equal to the difference in the moments with respect to the same axis of the per-second moments of the outgoing and incoming liquid.

The equation of angular momentum acquires a simpler form, if we introduce polar coordinates;¹ in this case the velocities are expanded to radial and circular components, whereupon the moments of radial components of moments are equal to zero. Equation (97) in this case takes the form

¹In this case motion is assumed to be plane-parallel, i.e., the particle trajectories are plane curves.

$$M = \frac{G}{g} (\omega_{2u} r_2 - \omega_{1u} r_1) \quad (98)$$

where M is the sum of the moments of all forces applied to any liquid volume relative to the origin of coordinates.

For the case of inertial motion ($M = 0$) we will obtain the known law of areas

$$\omega_r r = \text{const.} \quad (99)$$

Let us dwell on one example of the application of the equation of angular momentum.

Example. Let us explain the temperature effect of the gas before a compressor on the degree of increase in the pressure in it. Based on the equation of angular momentum (98) it is possible to find the moment of forces which appear on the compressor wheel. For this it is necessary to know the circular velocity component of the gas after (ω_{2u}) and before (ω_{1u}) the wheel, and also the distance from the axis of the outgoing (r_2) and incoming (r_1) mass of gas. Per-second shaft work of the wheel, as is known, is equal to the product of the moment of forces by angular velocity (ω), from which we obtain for 1 kgf of gas

$$-L = \frac{G}{g} (\omega_{1u} r_1 - \omega_{2u} r_2).$$

Thus the work of 1 kgf of gas on the wheel is determined by the kinematics of flow and the angular velocity of the wheel, but does not depend on the temperature and pressure of the gas (liquid) before the wheel. It was shown above that the work of the wheel is proportional to the difference in the full enthalpy after and before the wheel:

$$-L = \frac{h_2 - h_1}{A}.$$

Thus at constant values of the number of revolutions and volumetric gas flow rate, which determine the kinematics of flow, the drop in the enthalpy on the wheel does not change:

$$i_{02} - i_{01} = \text{const.}$$

Consequently, with heat capacity constant ($c_p = \text{const}$) the drop in the stagnation temperatures on the wheel also does not change:

$$\Delta T_0 = T_{02} - T_{01} = \text{const.}$$

Hence, using the equation of work of a compressor in the form (86), we note that the degree of pressure increase depends on the gas temperature before the wheel:

$$\Delta T_0 = \frac{T_{02}}{\tau_{02}} \left(\tau_{02}^{\frac{k-1}{k}} - 1 \right) = \frac{k-1}{kR} L_n = \text{const.}$$

Assume, for example, the degree of pressure increase in the compressor at the start ($T_{01} = T_{01H} = 288^\circ \text{ abs}$) is equal to $\pi_{0H, \text{cr}}$; with an increase in the velocity of flight, entailing an increase in the stagnation temperature before the wheel T_{01} , the degree of pressure increase in the compressor with a constant volume flow rate and number of revolutions can be calculated from the condition of constancy of work:

$$\tau_{02}^{\frac{k-1}{k}} - 1 = \frac{T_{02}}{T_{01H}} \left(\tau_{02H, \text{cr}}^{\frac{k-1}{k}} - 1 \right) \cdot \frac{T_{01H}}{T_{01}}.$$

If in the first approximation we disregard the dependence of the efficiency of compressor on inlet temperature, then we obtain

$$\tau_{02}^{\frac{k-1}{k}} - 1 = \frac{T_{02}}{T_{01H}} \left(\tau_{02H, \text{cr}}^{\frac{k-1}{k}} - 1 \right).$$

from which taking into account the equality

$$\frac{T_u}{T_{0u}} = 1 - \frac{k-1}{k+1} \lambda_u^2 = \frac{1}{1 + \frac{k-1}{2} M_u^2}$$

we have

$$\frac{k-1}{k} \pi_{0u} = 1 - \frac{\frac{k-1}{k} \pi_{0u} - 1}{1 + \frac{k-1}{2} M_u^2}$$

Thus in the last analysis from the equation of angular momentum it follows that the degree of pressure increase in the compressor of a turbojet engine drops with an increase in the velocity of flight. The results of the calculation according to this formula with a starting degree of pressure increase $\pi_{0 \text{ н.ст}} = 4$ and $k = 1.4$ are presented in the following table:

Table.

M_u	0	0.5	1	1.5	2	2.5	3
π_{0u}	4	3.8	3.2	2.75	2.3	2	1.75

The calculation carried out for value $\pi_{0 \text{ н}}$ is conditional, since it is based on the assumption of the independence of the work capacity on temperature even with a considerable change in it.

The basic purpose of a turbo-compressor device of a turbojet engine is to create in the exit nozzle (after the turbine) a greater total pressure than in the diffuser (before the compressor):

$$P_{0c} > P_{0d}$$

on the basis of this the following inequality should be fulfilled:

$$\pi_{0\kappa} \pi_{0\tau} \sigma_{\kappa,c} > 1.$$

Here $\sigma_{\kappa,c}$ - pressure coefficient which characterizes the total pressure losses in the combustion chamber (during the supply of heat).

In view of the fact that with an increase of flying speed the value $\pi_{0\kappa}$ decreases, and values $\pi_{0\tau}$ and $\sigma_{\kappa,c}$ remain virtually constant, at a certain value of flying speed the engine ceases to satisfy the last inequality.

In the case selected above ($\pi_{0\kappa,cr} = 4$) when $\pi_{0\tau} = 0.5$ and $\sigma_{\kappa,c} = 0.9$ this inequality is not fulfilled already at the values

$$M_u = 2.5 (\pi_{0\kappa} = 2, \pi_{0\kappa} \pi_{0\tau} \sigma_{\kappa,c} = 0.95)$$

and higher.

The increase of total pressure in the turbo-compressor device as a whole ($p_{0c} > p_{0d}$) depends also on the selected temperature before the turbine, with an increase in which the drop in pressure in the turbine decreases.

In other words, at a certain magnitude of flying speed the turbo-compressor device as a whole ceases to increase the pressure in the engine, i.e., becomes unsuitable. At these velocities of flight the work of a jet engine is ensured by air compression only because of the velocity of pressurization in consequence of which the turbojet engine loses its advantage over the ramjet.

At the subsonic, transonic and not very high supersonic flying speeds, when the compression of the gas in the compressor substantially predominates over expansion in the turbine, the turbojet engine retains all its advantages over the ramjet.

§ 7. Entropy

According to the second law of thermodynamics during real irreversible processes which flow in a final isolated system the entropy increases, and with reversible - remains constant.

Mathematically the increase of entropy dS is determined as:

$$dS = \frac{dQ}{T}.$$

here dQ is the full quantity of heat applied both from without and from within (for example, because of the work of the forces of friction), T is absolute temperature.

According to the first law of thermodynamics (50)

$$dQ = du + A p dv.$$

In the case of an ideal gas we have

$$du = c_v dT,$$

hence with the help of the equation of state ($p v = RT$) we obtain

$$dS = \frac{dQ}{T} = c_v \frac{dT}{T} + AR \frac{dv}{v},$$

from which after the replacement

$$AR = c_p - c_v = (k - 1) c_v$$

and integration we find

$$S_2 - S_1 = \int_1^2 \frac{dQ}{T} = c_v \ln \frac{T_2 v_2^k}{T_1 v_1^k} + \dots$$

or on the basis of the equation of state

$$S_2 - S_1 = c_p \ln \frac{p_2 v_2^k}{p_1 v_1^k}. \quad (100)$$

The change of entropy in an ideal adiabatic process which is reversible is equal to zero, since in this case

$$p_2 v_2^k = p_1 v_1^k = p v^k = \text{const.}$$

Any real process for an isolated final system flows in such a direction that the entropy increases:

$$S_2 - S_1 > 0.$$

In order to be convinced of this in the example of an ideal gas, let us pass in equality (100) from the flow parameters to the stagnation conditions, utilizing the obvious relationship

$$p v^k = p_0 v_0^k.$$

After expressing the specific volume by pressure and temperature

$$v_0 = \frac{RT_0}{p_0},$$

we will obtain

$$S_2 - S_1 = -c_p(k-1) \ln \frac{p_{02}}{p_{01}} \left(\frac{T_{01}}{T_{02}} \right)^{\frac{k}{k-1}}. \quad (101)$$

In an isolated system heat exchange with the surrounding medium is absent ($dQ_{\text{изв}} = 0$) and the stagnation temperature does not change:

$$T_{01} = T_{02}.$$

For such a system according to (101) the change in entropy

$$S_2 - S_1 = \int_1^2 \frac{dQ_{en}}{T} = AR \ln \frac{p_{02}}{p_{01}}. \quad (102)$$

Since the total pressure in a gas flow as a result of losses drops

$$p_{02} < p_{01}$$

and correspondingly the heat of friction always has a positive sign

$$dQ_{fr} > 0,$$

then entropy in an isolated system during an irreversible process always increases.

Introducing the pressure coefficient, which considers hydraulic losses

$$\sigma = \frac{p_{02}}{p_{01}},$$

we will obtain for an energy-isolated gas flow (without heat exchange and mechanical work) the direct connection between hydraulic losses and the increase of entropy:

$$S_2 - S_1 = -AR \ln \sigma. \quad (103)$$

In a heat-insulated gas flow ($dQ_{\text{heat}} = 0$) without losses ($dQ_{\text{fr}} = 0$) the entropy will remain constant also with the completion of mechanical work, in spite of the fact that the full enthalpy gas in this case changes:

$$-Al = I_{02} - I_{01} \neq 0.$$

This means that in an ideal compressor and in an ideal turbine

$$\frac{p_{02}}{p_{01}} = \left(\frac{T_{02}}{T_{01}} \right)^{\frac{k}{k-1}}.$$

In real machines the entropy of the working medium always changes.

Assume the difference in a real process from ideal is considered by a certain factor m

$$\frac{p_{02}}{p_{01}} = m \left(\frac{T_{02}}{T_{01}} \right)^{\frac{k}{k-1}}.$$

Then according to (101) a change in entropy

$$S_2 - S_1 = -c_p(k-1) \ln m. \quad (104)$$

Both in the compressor and in the turbine during a heat-insulated process ($dQ_{\text{нап}} = 0$) hydraulic losses are expressed in heat supply to the gas ($dQ_{\text{вн}} > 0$), i.e., in both cases $M < 1$.¹ Thus in real turbomachines entropy increases ($S_2 - S_1 > 0$).

§ 8. The Calculation of Reaction Force (Thrust)

The flight of a jet vehicle is achieved under the action of a reaction force, or, as it is frequently called, the reactive thrust which the jet of outgoing gases imparts to it. For the determination of the value of reaction force P there is no need to examine in detail pressure distribution on the internal and external walls of the jet vehicle. The reaction force can be determined in final form with the help of the equation of momentum.

¹Both in the compressor and in the turbine with an assigned drop in the temperatures and the initial pressure the final pressure is lower, the greater the hydraulic losses.

In accomplishing flight a body produces disturbances in the surrounding medium. It is always possible to separate a certain, sufficiently large, for example cylindrical, area whose boundaries go beyond the limits of the disturbed part of the flow (Fig. 1.13). On the lateral boundaries of this area the pressure and flow velocity (we consider the engine fixed, and the air - moving at the flying speed) are equal to their values on infinity before the engine.

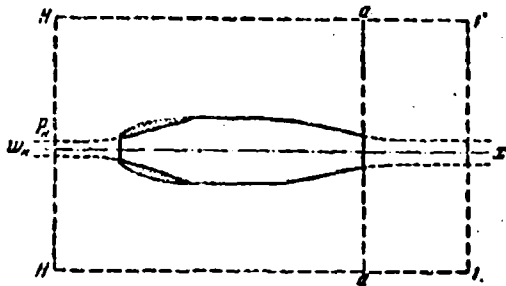


Fig. 1.13. Outline for determining reaction force.

Assume the x-axis coincides with the direction of flight and is the axis of symmetry of the engine; let us project on the x-axis the forces which act on the engine and on the surface of the selected outline. Since the forces of pressure in a liquid are normal to the

surface, the projections on the x-axis of the forces which act on the lateral surfaces of the outline become zero. Thus the equation of Euler [see (90)] will be written thus:

$$\int_0^{\infty} p_0 dF - \int_0^{\infty} p_1 dF + P = \int_0^{\infty} (w_1 - w_0) dm_0 + \int_0^{\infty} w_1 dm_r$$

Here the area on which the integrals are propagated and the range of integration of the first term of the right side are infinite. Force P is taken with sign + because during the solution of formula (90) it was assumed that the machine obtains work from the gas, and here the jet engine imparts work to the gas: $m_0 = G_0/g$ - the mass flow per second of air which flows into the outline through the cross section F ; $m_r = G_r/g$ - the supplementary mass flow per second of fuel which is supplied to the engine.

If we take the left face surface far in front of the engine, then pressure on it is constant and equal to atmospheric (p_∞), and the flow velocity is equal to the flying speed (w_∞). Furthermore, it is possible to assume that in a transverse direction already at a certain final distance from the surface of the engine the flow is not disturbed and area F , on which the integrals of the left side are propagated, is considered finite; in exactly the same manner the range of integration in the first term of the right side will be finite. Then one ought to write:

$$p_\infty F - \int_0^F p_1 dF + P = \int_0^{m_1} (w_1 - w_\infty) dm_1 + \int_0^{m_2} w_2 dm_2$$

In a large number of cases the disturbance which is caused by a flying body is so insignificant that in the nozzle-exit plane (outside the exhaust gas stream) the pressure of the circumfluent flow differs little from pressure on infinity (p_∞). Then the forces of pressure on the front and rear faces of the outline are balanced everywhere, besides the section which corresponds to the cross section of the exhaust jet (F_a). The velocities of flow in all the elementary streams, except those passing through the engine, are identical (here we disregard the influence of friction and vortex and wave losses on the external surface of the engine). Consequently a change in momentum is obtained only in a jet which flows through the engine. Then the equation of Euler takes the following form:

$$(p_1 - p_\infty) F_a + P = \frac{G_2}{g} (w_2 - w_\infty) + \frac{G_1}{g} w_\infty$$

from which the basic formula for reaction force is obtained

$$P = \frac{G_2}{g} (w_2 - w_\infty) + \frac{G_1}{g} w_\infty + (p_1 - p_\infty) F_a. \quad (105)$$

In these expressions G_g/g - the mass flow per second of the air being sucked into the engine w_a - the average speed of outflow.

One ought to emphasize that the relationship obtained is correct only in such a case when the velocity and the pressure in plane a (with the exception of the section of the working jet) are equal in accuracy to their values on infinity before the engine. Furthermore, here we disregard the external frontal engine drag which can always be taken into account separately.

Under the calculated conditions of work of a jet engine the pressure in the exhaust jet is equal to the pressure of surrounding air ($p_a = p_H$); in this case the reactive thrust is equal to the change in the momentum of the gas passed through the engine:

$$P = \frac{Q_a}{g}(w_a - w_H) + \frac{Q_t}{g}w_a. \quad (106)$$

In jet engines the second term of the right side is small and it is frequently disregarded,¹ i.e., for jet engines in the calculated case they accept²

$$P = \frac{Q_a}{g}(w_a - w_H). \quad (107)$$

The thrust of a liquid jet engine in which atmospheric air is not used is determined for the calculated conditions from the formula

$$P = \frac{Q_t + Q_a}{g}w_a. \quad (108)$$

¹Part by weight of fuel in the air passing through the engine does not exceed one-five percent: $G_f \sim (0.01-0.05) G_g$.

²One ought to emphasize that value w_H is the flying speed, and in no way the velocity in the inlet of the engine.

or in non-calculated conditions

$$P = \frac{G_r + G_o}{g} w_a + (p_a - p_n) F_a \quad (109)$$

Here G_o is the per-second mass flow of oxidizer.

Let us examine now the effect on the reaction force of the inconstancy of pressures in the plane of the output section of the engine. Let us construct the pressure and velocity curve for the nozzle edge (Fig. 1.14). For simplicity let us dwell on the case of subsonic outflow. It is possible, for example, to visualize such a flow about the engine at which the pressure near the output section is lowered, because of which the local velocity in the external flow increases. The pressure within the subsonic exhaust jet is approximately the same as on its boundary.

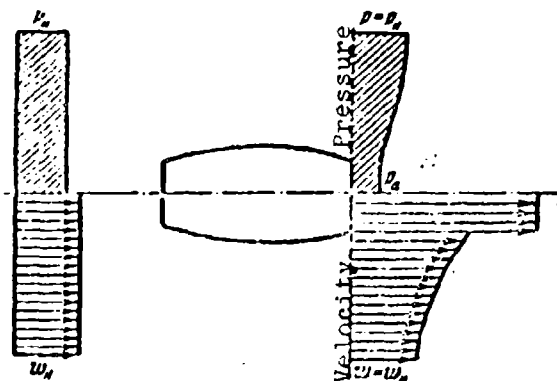


Fig. 1.14. The distribution of the pressure and flow velocity in the nozzle exit section.

For the calculation of reaction force let us make use of the basic property of nonuniform (in the values of total pressure) flows, which amounts to the fact that nonuniformity in the velocity distribution disappears very slowly, and pressure is equalized rapidly.

Thus, for instance, nonuniformity in the pressure field that appears during the rotation of a flow is equalized at a distance of 1.5-2 diameters of a straight tube after the place of rotation; the velocity is equalized at a distance of 20-30 diameters. This property can be used during the calculation of thrust. It is known from tests that if plane b is located away from the nozzle edge at a distance ab , greater than one diameter of a section (Fig. 1.15), then the pressure field already is uniform. Thus after moving away somewhat from the nozzle edge we enter a plane of constant pressure ($p_a = p_b$), in connection with which it is possible to determine reactive thrust by the formula

$$P = \frac{Q_s}{g}(w_b - w_a)$$

There remains only to find the velocity w_b , which the working jet in plane b has (Fig. 1.15). For this during subsonic outflow it is possible to make use of the Bernoulli equation without allowing for hydraulic and heat losses, since, as was noted, the section of the jet included between planes a and b is small.

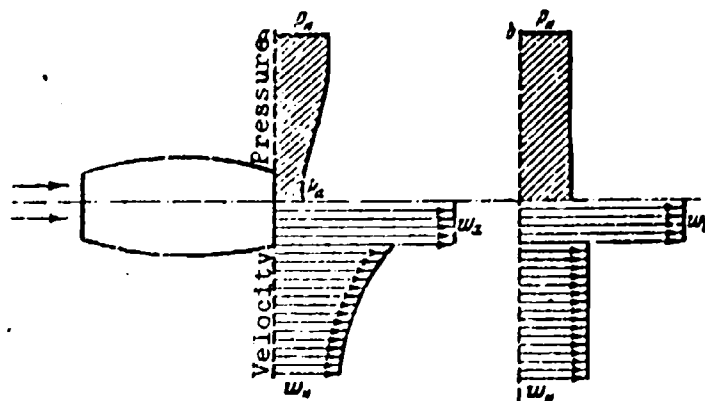


Fig. 1.15. The picture of the distribution of pressure and velocity beyond the engine.

Let us examine as an example the case of too great a subsonic speed ($M \ll 1$). Then according to the Bernoulli equation

$$p_a + \rho_a \frac{w_a^2}{2} = p_n + \rho_a \frac{w_b^2}{2}.$$

At such speed the pressure difference ($p_a - p_n$) is small, in consequence of which we accepted the gas density as constant.

Thus,

$$p_a - p_n = \rho_a \frac{w_b^2 - w_a^2}{2},$$

from which

$$w_b = w_a \sqrt{\frac{p_n - p_n}{\rho_a \frac{w_a^2}{2}} + 1}.$$

In the majority of cases at subsonic speed on the nozzle edge a pressure is established which is very close to atmospheric, and then $w_b = w_a$ is assumed. During the supersonic outflow between planes a and b shock waves can be formed. In this case the calculation of correction becomes somewhat complicated, but also is completely accessible.

One feature of a ramjet engine is interesting: if we retain the combustion-chamber temperature constant, then the value of reactive thrust (see § 6, Example 4)

$$P = \frac{Q}{g} (w_a - w_n) = \frac{Q}{g} w_n \left(\sqrt{\frac{T_{a,r}}{T_{n,1}}} - 1 \right)$$

at first increases with an increase in the velocity of flight, and then, in passing through a maximum, begins to decrease and with a certain value of velocity drops to zero. This is explained by the fact that an increase in the velocity of flight causes an

increase of stagnation temperature in the beginning of the chamber (T_{0x}), but in this case for the preservation of the stagnation temperature at the end of the chamber invariable it is necessary to decrease the heat supply. When the stagnation temperature in the incident flow becomes equal to the maximum permissible temperature in the engine ($T_{0x} = T_{0p}$), the supply of heat has to be discontinued. In this case the thrust level drops to zero. From formula (42) the following condition is obtained for the disappearance of thrust both for a subsonic and for a supersonic ideal engine:

$$\frac{T_u}{T_{0x}} = \frac{T_u}{T_{0p}} = 1 - \frac{k-1}{k+1} \gamma_{0x}^2$$

from which the velocity coefficient of flight at which an ideal engine ceases to develop thrust is equal to

$$\gamma_{0x} = \sqrt{\frac{k+1}{k-1} \left(1 - \frac{T_u}{T_{0p}} \right)}$$

A pressure increase in a ramjet engine is achieved because of the dynamic compression of air before the engine inlet and in its diffuser. Such an engine, as we saw, is effective only at a very high flying speed and is not able to develop thrust completely on the spot. For obtaining sufficient thrust in a jet engine on take-off and at moderate flying speed it is necessary to apply mechanical air compression. A jet engine with mechanical compression has already found wide application in contemporary aviation. The most common type of jet engine with mechanical compression is the turbojet engine (Fig. 1.16). In this engine¹ the air is sucked in by the compressor. After compression in the compressor the air enters the combustion chamber, from where the mixture of heated air and combustion products is directed to the turbine blades. Usually in

¹For a detailed presentation of the theory of a turbojet engine see the book: Inozemtsev, N. V., Aviation Gas-turbine Engines. Moscow, 1956.

a turbine only part of the energy of gases is utilized (for obtaining the mechanical work required for rotation of the compressor). The remaining (free) part of the energy of gases is converted into the kinetic energy of the discharging jet.



Fig. 1.16. Diagram of a turbojet engine: D - diffuser, K - compressor, T - gas turbine, A - combustion chamber, B - exit nozzle.

If the entire pressure excess which is found in the combustion chamber is utilized on the turbine wheel, the engine ceases to develop a reaction force, but in this case the power of the turbine exceeds the power being consumed by the compressor; the excess of power can be utilized, for example, for the rotation of a propeller or a dynamo.

The work being spent for compression of 1 kg of gas in the compressor, as is shown in § 4, is equal to

$$L_c = \frac{1}{\eta_c} \frac{\gamma}{\gamma - 1} \frac{p_{0x}}{p_{0d}} \left[\left(\frac{p_{0x}}{p_{0d}} \right)^{\frac{\gamma - 1}{\gamma}} - 1 \right].$$

Here p_{0x} , p_{0d} are the total pressures respectively after and before the compressor; η_c is the efficiency of the compressor; T_{0d} is the stagnation temperature before the compressor.

If we disregard the heat removal in the diffuser, then it is possible to consider that $T_{0d} = T_{0x}$. Let us agree, as before, that the degree of pressure increase in the compressor is understood as the ratio of the values of total pressure of the gas after and before the compressor:

$$\pi_{0.4} = \frac{p_{0.4}}{p_{0.3}}$$

By the degree of decrease in pressure in the turbine we will, as before, understand the ratio of the values of total pressure after and before the turbine:

$$\pi_{0.4} = \frac{p_{0.4}}{p_{0.3}}$$

Value $\pi_{0.4} = p_{0.4}/p_{0.3}$ characterizes the pressure excess in the nozzle.

Work being produced with 1 kg of gas in the turbine is equal

$$L_T = \frac{k}{k-1} R T_{0.4} \eta_T \left[\left(\frac{p_{0.3}}{p_{0.4}} \right)^{\frac{k-1}{k}} - 1 \right];$$

here $T_{0.4}$ - the stagnation temperature after the turbine, η_T - the efficiency of the turbine.

In a turbojet engine the work of the turbine is utilized virtually entirely for driving the compressor: $L_T = L_K$. If we disregard small changes in the gas constant and the adiabatic index, then we will have

$$T_{0.3} \left(\frac{p_{0.3}}{p_{0.4}} \right)^{\frac{k-1}{k}} = T_{0.4} \left(\frac{p_{0.4}}{p_{0.3}} \right)^{\frac{k-1}{k}} \eta_T \eta_K$$

from which

$$\frac{\frac{\frac{k-1}{k} \frac{T_{0c}}{T_{0n}} - 1}{\frac{k-1}{k}}}{\left(\frac{1}{\pi_{0n}}\right)^{\frac{k-1}{k}} - 1} = \frac{T_{0c}}{T_{0n}} \eta_{0n} \eta_{0c}$$

Usually the temperature of the stagnation gas in the exit nozzle is significantly higher than the temperature of the stagnation gas in the diffuser ($T_{0c} > T_{0n}$). Then from the equality of work of the compressor and the turbine it follows that the degree of an increase in air pressure in the compressor is higher than the degree of decrease in the pressure in the turbine ($\pi_{0n} > 1/\pi_{0c}$), i.e., there is excess pressure in the jet engine nozzle. This is necessary in order that the discharge velocity from the nozzle w_a and correspondingly the reactive thrust would be sufficiently great (both on the take-off and in flight). A turbojet engine usually develops considerable boost for take-off.

An essential feature of this engine model is also its insensitivity to a change of air density. The density of the air which enters the engine is noticeably increased with an increase in the velocity of flight, thanks to which the mass flow of air in the compressor increases.¹ The power being consumed by the compressor varies in proportion to the mass flow; however, the latter increases simultaneously also in the turbine. Consequently the power of the turbine increases proportionally to the power of the compressor, i.e., the balance of power is preserved.

Total work of gas in the engine is made up of the work of expansion in the turbine and in the nozzle:²

¹The compressor is a "volumetric" machine in which with a density change of gas the mass flow changes and volume flow rate remains constant.

²As shown above in a turbojet engine the equality $L_T = L_H$ is always fulfilled.

$$\Sigma L = L_t + L_{ct} \text{ or } \Sigma L = L_k + L_{ct}$$

Thus, as was already mentioned, after the using of a certain fraction of energy in the turbine wheel its remaining part (free) can be used in the exit nozzle.

The fraction of work of the compressor $\frac{L_k}{\Sigma L}$ is usually considerably more than half, therefore for the formation of free power in a turbojet engine a relatively small share of the available energy is expended.

The thrust of a turbojet engine is determined by the discharge velocity from the nozzle:

$$w_0 = \lambda_a a_{sp, c}$$

where

$$\lambda_a = f_1 \left(\frac{p_{t, c}}{p_n} \right), \quad a_{sp, c} = f_2 (T_{t, c}).$$

If the pressure after the turbine is higher than before the compressor, then the velocity coefficient of outflow under identical flight conditions for a turbojet engine is higher than for a ramjet engine. But higher temperatures are possible in the latter. Therefore the ramjet engine can develop larger specific thrusts even at less pressures in the jet nozzle. However, for a thrust augmentation in a turbojet engine it is possible to place behind the turbine a second combustion chamber (the so-called "afterburner") in which the gas can be heated additionally to the same temperature as in a ramjet engine. In this case the thrust of the turbojet engine substantially increases.

If we disregard the losses of pressure in the second combustion chamber, then the velocity coefficient of outflow (λ_a) will preserve the same value as without an afterburner, and the velocity will increase in proportion to the square root from the temperature.

§ 9. The Place of Application of the Reaction Force

Let us explain the question concerning in which point of the engine the reaction force is applied.

Let us examine first the simplest case - an ideal ramjet engine (Fig. 1.17). Let the velocity in the inlet be equal to the flying speed ($w_e = w_H$); then pressure in the inlet is equal to atmospheric ($p_e = p_H$); furthermore, let us suppose that the engine works under calculated conditions, i.e., the pressure in the outlet is also equal to atmospheric ($p_a = p_H$). At a low speed of movement of the gas in the combustion chamber the pressure in the latter can be considered constant ($p_d = p_r$).

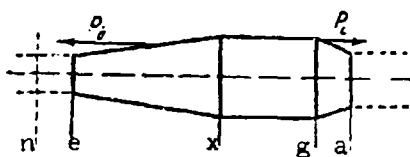


Fig. 1.17. Diagram of a ramjet engine (for determining the forces which act on an engine).

In the described ideal engine the drops in the pressures in the diffuser and nozzle are identical:

$$p_x - p_e = p_r - p_a.$$

However, in view of the fact that in the nozzle the air has a higher temperature than in the diffuser, the area of the outlet of engine should be greater than the area of the inlet. In fact, in an ideal engine the dynamic head in the outlet is equal to the dynamic head of incident flow, i.e., in the case in question to the dynamic head in the inlet:

$$\rho_a w_a^2 = \rho_e w_e^2.$$

Then from the equation of continuity (taking this equality into account) we obtain

$$\frac{F_a}{F_r} = \frac{\rho_a w_a}{\rho_r w_r} = \frac{\rho_a w_a^2}{\rho_r w_r^2} \frac{w_r}{w_a} = \frac{w_r}{w_a} = \sqrt{\frac{v_a}{v_r}}.$$

Consequently, during the supply of heat in the combustion chamber ($\rho_a = \rho_r$) we have

$$\frac{F_a}{F_r} > 1.$$

Thus the mean pressure which acts on the walls of the diffuser and nozzle is one and the same, but the projection of the wall of the diffuser on the plane perpendicular to the axis of the engine is greater than the corresponding projection of the nozzle wall. As a result of what was expounded the force of pressure from within on the diffuser (P_d) is greater than on the nozzle (P_c); the directions of these forces, as it appears from Fig. 1.17, are opposite.

If the external contours of the engine are very smooth, then air pressure on the external surface of the engine is very close to atmospheric, i.e., the force of pressure on the external surface can be disregarded. In the ideal case in question the reaction force which acts on the engine is reduced to the difference in the forces applied respectively to the diffuser and the nozzle:

$$P = P_d - P_c.$$

For the interpretation of this equality let us make use of the result obtained in § 5 (Example 3), according to which the magnitudes of forces which act on the diffuser and nozzle are respectively equal to

$$P_d = \frac{\gamma_a w_a^2}{2g} F_d \left(1 - \frac{F_c}{F_d}\right), \quad P_c = \frac{\gamma_r w_r^2}{2g} F_r \left(1 - \frac{F_d}{F_r}\right).$$

According to the conditions accepted above

$$P_A = P_C; \quad \gamma_n \omega_n^2 = \gamma_n \omega_n^2.$$

Then

$$P = P_A - P_C = \frac{\gamma_n \omega_n^2}{2g} P_A \left[\left(1 - \frac{F_C}{P_A}\right)^2 - \left(1 - \frac{F_n}{P_A}\right)^2 \right]$$

or

$$P = \frac{\gamma_n \omega_n^2}{2g} \left[2 - \frac{F_C + F_n}{P_A} \right] (P_A - F_C)$$

Let us examine an engine with low velocities in the combustion chamber, i.e., with the area of the chamber substantially larger than the area of the intake and outlets:

$$\frac{F_C}{P_A} \ll 1, \quad \frac{F_n}{P_A} \ll 1.$$

In this case we come to the following simple formula for the reaction force determined as a result of the subtraction of the force applied to the nozzle from the force applied to the diffuser:

$$P = \frac{\gamma_n \omega_n^2}{g} (P_A - F_n).$$

The same result can be obtained directly from the formula for reactive thrust

$$P = \frac{Q}{g} (\omega_a - \omega_n) = \frac{\gamma_n \omega_n^2 \cdot F_n}{g} \left(\frac{\omega_a}{\omega_n} - 1 \right).$$

or, taking into account the condition $\frac{w_a}{w_n} = \frac{F_a}{F_n}$, derived above

$$P = \frac{\gamma_n w_n^2}{g} (F_a - F_n)$$

Thus reactive thrust is obtained because the force of pressure on the diffuser is greater than on the nozzle. This is a consequence of the preheating of the gas, in connection with which the discharge area has to be made larger than the area of the cross section of the incoming jet.

In an actual engine, as was noted above, the values of velocity and pressure in the inlet usually differ from the same in an undisturbed incident flow, which impedes the determination of reaction force based directly on the difference in the forces applied to the diffuser and the nozzle; furthermore, in actuality the force which acts on the external surface of the engine is not usually equal to zero. However, in any event it is possible to demonstrate that in a ramjet engine the reaction force is the resultant of the forces of pressure applied to the walls of the internal and external bypasses of the engine.

Let us pause now on how extent of the inlet area of the engine influences reactive thrust. From the solution of the formula for reactive thrust given in § 8 it follows that the air speed upon entry into the engine does not influence the magnitude of reaction force; only the discharge velocity from the engine and the speed of the undisturbed incident flow play a role.

This fact has the following explanation. If the rate of entry of air into the engine is less than the approach stream velocity ($w_e < w_H$), then before the diffuser the slowing down of incident flow occurs (Fig. 1.18), whereupon the streams flow to the leading edge of the diffuser under a large angle of attack.

This leads to the fact that near the intake on the internal wall of the diffuser an area of increased static pressure appears (close in value to the total pressure of incoming flow), and on the external surface of diffuser - rarefaction; the larger the inlet of the diffuser, the higher the pressure on its internal surface and the greater the rarefaction on its external surface (angles of attack of the air streams increase). In other words, with a considerable slowing down of air before the diffuser the front wall of the latter behaves as wing at high angles of attack.¹

The indicated secondary force caused in this case ($w_e < w_H$) by the pressure difference on the front wall of the diffuser compensates exactly for the decrease in thrust which should be obtained because of contraction of the surface of the diffuser as compared with the case $w_e = w_H$. Let us note that in such systems a considerable share of the thrust falls on the fraction of rarefaction which appears on the external surface of the diffuser. If we completely *open up* the diffuser, i.e., make the intake area equal to the area of the combustion chamber (Fig. 1.19), then thrust will be produced only by rarefaction on the external surface of the diffuser (projection on the axis of the engine of the forces of pressure applied to the internal chamber walls and the diffuser in this case is equal to zero).

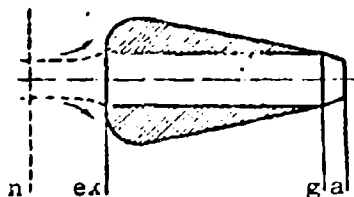


Fig. 1.18. Ramjet engine (VRD) [BPA] without an inlet diffuser.

¹The considerations given here are completely valid only with $M_H < 1$. The flow about the wing is examined in more detail in Chapter X.

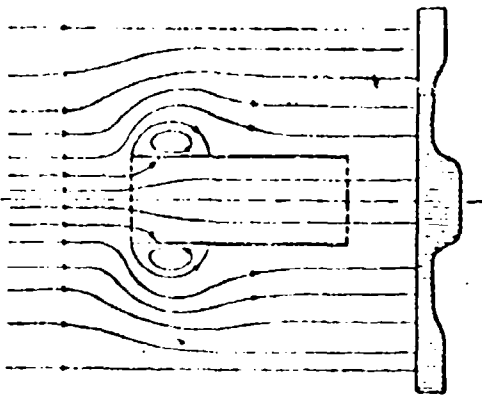


Fig. 1.19. The arrangement of the flow around a ramjet engine which has the form of a thin-walled tube.

If the rate of entry of air into the engine is greater than the flying speed ($w_e > w_H$), then flow before the diffuser is accelerated; in this case the streams flow to the leading edge of the diffuser at negative angles; in this case near the inlet on the external surface of the diffuser an increased pressure appears, and on internal surface - rarefaction. Such a pressure difference gives a secondary force which is di-

rected to the side opposite to the action of reaction force; this secondary force compensates for that increase in the reaction force which in the case $w_e > w_H$ would be possible to expect because of an increase in the surface of the diffuser (as compared with the case $w_e = w_H$). Thus the rate of entry of air into the engine should not be considered directly in the formula for the reaction force; however, it influences the thrust level indirectly, since it affects the resistance of the diffuser, with an increase of which the discharge velocity from the engine drops. So, with $w_e < w_H$ supplementary external drag appears, and with $w_e > w_H$ - supplementary hydraulic losses within the diffuser.

The ramjet engine, which has the form of a thin-walled tube (Fig. 1.19), does not develop thrust at all; the cylindrical form of an engine leads to the fact that the component of the force of pressure on the walls, parallel to the axes of the engine, is equal to zero. The essence of the matter lies in the fact that because of the disruption of the flow flowing around the tube from its front edge an external vortex drag appears which completely balances the reactive thrust; the velocity diagram in the wake after the tube in the area of external flow has depressions caused by vortex drag which compensate for the acceleration within the engine; in

other words the total momentum obtained in the flow after the engine is the same as before it.

In conclusion let us note that in a turbojet engine the reaction thrust consists not only of the result of the forces of pressure which acts directly on the walls of the engine, but also of the force applied to the turbo-compressor unit; this secondary force applied to the rotor is absorbed by the step bearing and is transferred through supports to the engine housing.

Formulas (105-109) derived above make it possible to determine the reaction force of an engine without allowing for the external drag which it creates when installed on a flight vehicle.

The useful part of reaction force, equal to the difference between the reaction force and the total external drag of the engine plant, is called the *effective thrust*:

$$P_{\text{eff}} = P - \sum X_{\text{ext}}$$

In certain cases the maximum value of effective thrust is reached under such conditions when reaction force is less than maximum possible, i.e., it can prove to be favorable to allow a certain decrease of reaction force, if in this case the gain in drag overlaps the loss in reaction force.

During a detailed study of the external frontal engine drag the latter is usually divided into several component parts (into engine components):

$$\sum X_{\text{ext}} = X_{\text{d}} + X_{\text{r}} + X_{\text{e}} \quad (111)$$

where X_{d} is the drag of the intake - diffuser; X_{r} is the drag of the engine nacelle, into which the engine is built (the principal

part of this term is usually made up of the force of friction on the external surface of the engine); X_c is the drag of the outlet (jet) nozzle. The terms of the external frontal engine drag (X_d , X_c) are examined in Chapter VIII, which deals with the gas dynamics of the engine components.

The reaction force of an engine, determined by formula (105), can be considered as the difference between the output pulse of the jet of gases which leave the nozzle:

$$I_c = -\frac{G_a + G_r}{g} w_a + (p_a - p_n) F_a \quad (112)$$

and the input pulse of the jet of the incoming undisturbed airflow being sucked into the engine:

$$I_{a1} = \frac{G_a}{g} w_r \quad (113)$$

In the case of a liquid-propellant rocket engine (ZhRD) [ЖРД] or a solid-propellant rocket engine the rate of air flow G_a in (112) is replaced by the oxidizer consumption (G_0), as this is done in formula (109). The total pulse of nozzle obtained during the full expansion of gas in the nozzle ($p_a = p_n$):

$$I_c = \frac{G}{g} w_r \quad (114)$$

Here and subsequently G - this is the total gas flow rate in the outlet of the nozzle ($G = G_a + G_r$ or $G = G_0 + G_r$). The outlet device of the engine, which includes the nozzle, possesses external drag, in connection with which a new concept is introduced - the *effective pulse of the nozzle*:

$$I_{\phi} = I_c - X_c \quad (115)$$

The ratio of the effective nozzle pulse to its pulse during ideal outflow (without losses) is called the *relative pulse of the nozzle*

$$\bar{\Gamma} = \frac{I_e}{I_{na}} \quad (116)$$

Then the relative effective pulse

$$\bar{\Gamma}_{\phi} = \frac{I_{\phi}}{I_{na}} = \bar{\Gamma} - \frac{X_e}{I_{na}} \quad (117)$$

The expression for the thrust of the engine in the absence of losses within the nozzle

$$P_{na} = I_{na} - I_{e1} \quad (118)$$

can be used with the help of (112), (113), and (117) for the representation of effective thrust depending on the relative effective pulse

$$P_{\phi} = \bar{\Gamma}_{\phi} P_{na} - (1 - \bar{\Gamma}_{\phi}) \frac{G_2}{g} w_2 - (X_a + X_r) \quad (119)$$

The last term of the right side in the sum of the external drag of the diffuser and engine nacelle:

$$X_a + X_r = \sum X_{nap} - X_e$$

i.e. the full external drag of the engine plant with the deduction of the external drag of its nozzle part.

In a rocket engine the second term of the rightside of (119) is equal to zero since air is not sucked into it ($G_2 = 0$).

The evaluation of the internal thrust of an engine (not allowing for external drag) is done with the help of relative pulse (116)

$$P = \bar{I} P_{ia} - (1 - \bar{I}) \frac{G_1}{g} w_a$$

or

$$P = (1 - \Delta \bar{I}) P_{ia} - \Delta \bar{I} \frac{G_1}{g} w_a. \quad (120)$$

The value

$$\Delta \bar{I} = 1 - \bar{I} \quad (121)$$

is called the *lost relative pulse of the nozzle*. The influence of losses in the engine components on the magnitude of thrust being developed by it is examined in detail in Chapter VIII.

CHAPTER II

ELEMENTS OF HYDRODYNAMICS

§ 1. The Motion of a Liquid Particle

Let us examine the motion of an infinitesimal liquid particle which has the initial form of a parallelepiped (Fig. 2.1). Unlike a solid, a liquid particle can be strongly transformed during its motion.

The faces of an infinitesimal particle of liquid which has the form of a right parallelepiped in the beginning of motion with ribs dx , dy , dz , can be beveled and extended in the course of time (Figs. 2.2 and 2.3).

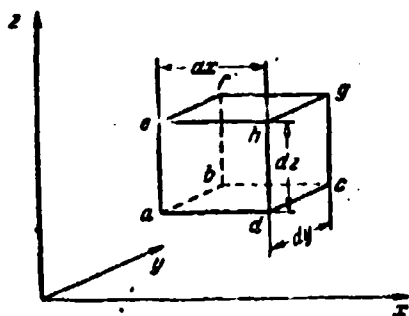


Fig. 2.1. Elementary parallelepiped in a fluid flow.

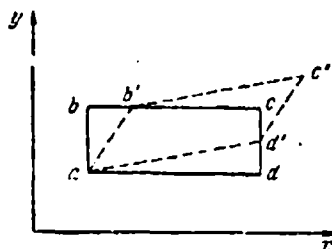


Fig. 2.2. Angular strain of faces.

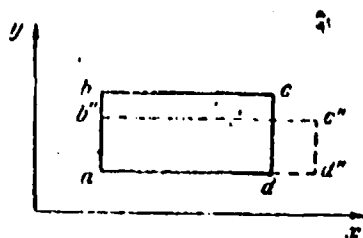


Fig. 2.3. Linear strain of faces.

Let the velocity component of particle motion at point a (Fig. 2.1) be u, v, w ; then the velocity components at point b are equal to

$$u + \frac{\partial u}{\partial y} dy, \quad v + \frac{\partial v}{\partial y} dy, \\ w + \frac{\partial w}{\partial y} dy,$$

at point d

$$u + \frac{\partial u}{\partial x} dx, \quad v + \frac{\partial v}{\partial x} dx, \\ w + \frac{\partial w}{\partial x} dx$$

and at point e

$$u + \frac{\partial u}{\partial z} dz, \quad v + \frac{\partial v}{\partial z} dz, \\ w + \frac{\partial w}{\partial z} dz.$$

The beveling of edge ab of a particle during an infinitesimal time dt , which is caused by a difference in the velocity component at points a and b (Fig. 2.2), is characterized by the displacement of point b, equal to

$$bb' = \frac{\partial u}{\partial y} dy dt.$$

The relative displacement or the angular strain

$$\frac{bb'}{ab} = \frac{\partial u}{\partial y} dt.$$

The beveling of the edge ad leads to angular strain

$$\frac{d\theta}{dt} = \frac{\partial v}{\partial x} dt.$$

In view of the fact that the angular strains during time dt are insignificant, the angle of slope of the face can be considered equal to the tangent of this angle. The full beveling of an initially right angle at point a in this case equals

$$\left(\frac{\partial u}{\partial y} + \frac{\partial v}{\partial x} \right) dt,$$

and the rate of the corresponding angular strain

$$\gamma_z = \frac{\partial u}{\partial y} + \frac{\partial v}{\partial x}. \quad (1a)$$

Index z indicates that the deformation of a particle is examined in plane xy perpendicular to the z -axis; in the remaining two planes, the rates of beveling of the quadrants obviously equal

$$\gamma_x = \frac{\partial v}{\partial z} + \frac{\partial w}{\partial y}, \quad (1b)$$

$$\gamma_y = \frac{\partial w}{\partial x} + \frac{\partial u}{\partial z}. \quad (1c)$$

Utilizing the same angular displacements of the faces of the particle, it is possible to determine the angular velocities of its rotation. Since the directions of rotation of the edges ab and ad are opposite, the mean angular velocity of rotation of the particle as a whole about the z -axis comprises

$$\omega_z = \frac{1}{2} \left(\frac{\partial v}{\partial x} - \frac{\partial u}{\partial y} \right). \quad (2a)$$

For the remaining two axes of rotation we have respectively

$$\omega_x = \frac{1}{2} \left(\frac{\partial w}{\partial y} - \frac{\partial v}{\partial z} \right), \quad \omega_y = \frac{1}{2} \left(\frac{\partial u}{\partial z} - \frac{\partial w}{\partial x} \right). \quad (2b)$$

The vector of the angular velocity of rotation ω whose components are ω_x , ω_y , and ω_z , is called *vorticity* and its value is determined, obviously, by the following equality:

$$w = \sqrt{w_x^2 + w_y^2 + w_z^2}. \quad (2c)$$

Let us dwell now on the linear deformations of the particle. The rates of motion of points a and d (Fig. 2.3) in the direction of the x-axis differ by the value

$$\left(u + \frac{\partial u}{\partial x} dx\right) - u = \frac{\partial u}{\partial x} dx. \quad (3)$$

In connection with this, the particle is lengthened during time dt to the value

$$dd'' = \frac{\partial u}{\partial x} dx dt.$$

The relative elongation of the particle

$$\frac{dd''}{dd} = \frac{\partial u}{\partial x} dt,$$

and the rate of the relative elongation of the particle in the direction of the x-axis is equal to

$$\epsilon_x = \frac{\partial u}{\partial x}. \quad (4a)$$

By analogy, the rates of relative elongation along other axes

$$\epsilon_y = \frac{\partial v}{\partial y}, \quad \epsilon_z = \frac{\partial w}{\partial z}. \quad (4b)$$

The elongation of the sides of a parallelepiped which depicts a liquid particle (Fig. 2.1) in general leads to a change in its volume; multiplying the difference in the rates of the forward motion of the opposite faces of parallelepiped determined according to formula (3), for the area of each of these faces we will obtain the rate of change in its volume because of linear strain in the direction of the horizontal axis; composing similar expressions for the rates of change in volume along the remaining two coordinate axes and totaling all three values, we find the full rate of change in the volume of the liquid particle:

$$\begin{aligned} \frac{dV}{dt} &= \frac{\partial u}{\partial x} dx dy dz + \frac{\partial v}{\partial y} dy dz dx + \\ &+ \frac{\partial w}{\partial z} dz dx dy = (\epsilon_x + \epsilon_y + \epsilon_z) dx dy dz. \end{aligned}$$

After the division of this expression into the initial volume of the liquid particle $V = dx dy dz$, we come to the value of the rate of a relative volume change in a liquid particle important in gas dynamics:

$$\epsilon = \frac{1}{V} \frac{dV}{dt} = \epsilon_x + \epsilon_y + \epsilon_z \quad (5)$$

on the basis of (4) we have finally

$$\epsilon = \frac{\partial u}{\partial x} + \frac{\partial v}{\partial y} + \frac{\partial w}{\partial z} \quad (6)$$

§ 2. The Equation of Continuity

The expression which stands in the right side of equality (6) is called in field theory the *divergence* (or *disagreement*) of the velocity vector and is designated thus:

$$\text{div } W = \frac{\partial u}{\partial x} + \frac{\partial v}{\partial y} + \frac{\partial w}{\partial z} = \epsilon \quad (7)$$

where W is the velocity vector.

In a continuous incompressible medium the volume of the particle does not change; consequently the equality

$$\text{div } W = \frac{\partial u}{\partial x} + \frac{\partial v}{\partial y} + \frac{\partial w}{\partial z} = 0 \quad (8)$$

is the equation of the continuity of a liquid.

Conditions of constancy of the mass of a liquid particle can be written in the following form:

$$M = \rho V = \text{const} \quad (9)$$

Here by liquid density ρ is understood the limit of the ratio of the mass of the particle to its volume

$$\rho = \lim_{\Delta V \rightarrow 0} \frac{\Delta M}{\Delta V} = \frac{dM}{dV} \quad (10)$$

whereupon it is assumed to be that, striving to zero, the volume ΔV is constricted toward a certain internal point.

Differentiating both parts of equality (9) for time and dividing the result by the value M , we will obtain

$$\frac{1}{\rho} \frac{d\rho}{dt} + \frac{1}{V} \frac{dV}{dt} = 0. \quad (11a)$$

Hence on the basis of (5) we come to the equation of continuity for a continuous compressible medium

$$\operatorname{div} W = -\frac{1}{\rho} \frac{d\rho}{dt}. \quad (11b)$$

Replacing the full density derivative of the liquid in terms of time by partial derivatives and utilizing (7), we obtain

$$-\rho \left(\frac{\partial u}{\partial x} + \frac{\partial v}{\partial y} + \frac{\partial w}{\partial z} \right) = \frac{d\rho}{dt} + u \frac{\partial \rho}{\partial x} + v \frac{\partial \rho}{\partial y} + w \frac{\partial \rho}{\partial z}.$$

In accordance with the rule of differentiation of products, this equation of continuity for a compressible medium (gas) leads to the form

$$\frac{\partial \rho}{\partial t} + \frac{\partial \rho u}{\partial x} + \frac{\partial \rho v}{\partial y} + \frac{\partial \rho w}{\partial z} = 0. \quad (12a)$$

The sum of the last three terms is the divergence of the vector of the current density ρW ; therefore the equation of continuity for a gas can also be written in the form

$$\frac{\partial \rho}{\partial t} + \operatorname{div}(\rho W) = 0. \quad (12b)$$

In the derivation of the differential equation of continuity the motion of a separate liquid particle was examined; Lagrange introduced such a method of study into hydrodynamics. Another method of study, developed for the first time by Euler, examines not the behavior of separate particles but the change in the parameters of a liquid in fixed points of space with time; Euler's method in many instances is more convenient than Lagrange's method - both in hydrodynamics and in gas dynamics it is used more frequently.

§ 3. About the Forces Which Act in a Liquid

Let us isolate a certain volume of liquid (Fig. 2.4) and let us examine it in isolation from the surrounding liquid medium.

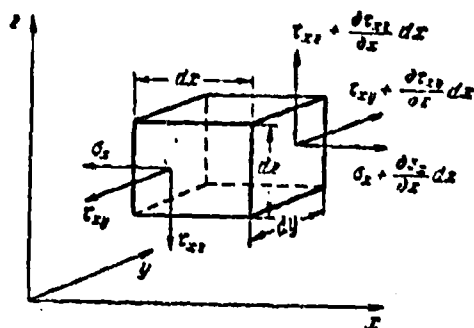


Fig. 2.4. Diagram of the forces which act on two faces of an elementary parallelepiped.

The forces which act on a given volume of liquid can be of two kinds: volume and surface. Volume forces are applied to all material particles constituting the volume. Pertaining to volume forces are: gravity, centrifugal force, magnetic forces and electrical. Surface forces are distributed over the surface of the isolated volume. They appear as a result of the effect of the environment on the given volume.

Surface forces, depending on how they are directed with respect to a given surface element, are subdivided into normal and tangential.

In order to characterize the change of a volume force ΔF or surface force ΔR from point to point the concept of stress, is introduced, implying by it the limit of the ratio of force to the volume ΔV (or respectively to the surface ΔS) which is reached with the contraction of the volume (or surface) to some internal point.

Thus, the stress of a volume force at a given point of the medium is

$$f = \lim_{\Delta V \rightarrow 0} \frac{\Delta F}{\Delta V} = \frac{dF}{dV}.$$

the surface stress

$$\sigma = \lim_{\Delta S \rightarrow 0} \frac{\Delta R}{\Delta S} = \frac{dR}{dS}.$$

Normal forces act both in a quiescent and in a moving liquid; tangential forces appear only during the motion of a liquid, and even then only when the liquid particles are strained.

For the majority of liquids, as experience shows, Newton's hypothesis is valid according to which the stresses are proportional to the rates of strain. The proportionality factor, which depends on the kind of liquid and its state, is called of the *coefficient of dynamic viscosity* or simply the viscosity.

Let us formulate equations of motion of a viscous compressible liquid for a elementary parallelepiped with sides dx , dy , dz .

Let us designate the components of volume stress f by X , Y , Z , the components of normal stress σ applied to the faces of the parallelepiped and parallel to the appropriate coordinate axes - σ_x , σ_y , σ_z , and the components of tangential stresses lying in the plane of each face - by letter τ with two indices (the first indicates the axis perpendicular to this face and the second - the axis parallel to the direction of the stress, for example τ_{xy} , τ_{xz} , τ_{yz}). Let us note, without the proof, that the equality of the moments of force relative to an arbitrary axis and the equality of tangential stresses with identical indices but arranged in reverse order follows from equilibrium conditions of a parallelepiped:

$$\tau_{xy} = \tau_{yx} \quad \tau_{xz} = \tau_{zx} \quad \tau_{yz} = \tau_{zy}. \quad (13a)$$

According to Newton's law the product of the mass of a parallelepiped times its acceleration is equal to the resultant of all forces applied to the parallelepiped.

Let us set up the appropriate equation for the projections of acceleration and resultant force on the x-axis. The normal stresses applied to the end faces give the force component:

$$\left[\left(\sigma_x + \frac{\partial \sigma_x}{\partial x} dx \right) - \sigma_x \right] dy dz = \frac{\partial \sigma_x}{\partial x} dx dy dz.$$

The force components from the tangential stresses which act on the lateral and upper faces:

$$\left[\left(\tau_{yx} + \frac{\partial \tau_{yx}}{\partial y} dy \right) - \tau_{yx} \right] dz dx = \frac{\partial \tau_{yx}}{\partial y} dx dy dz$$

and

$$\left[\left(\tau_{zx} + \frac{\partial \tau_{zx}}{\partial z} dz \right) - \tau_{zx} \right] dy dx = \frac{\partial \tau_{zx}}{\partial z} dx dy dz.$$

If we designate the components of the velocity vector along the axes x, y, z by u, v, w and consider that the mass of the particle $dM = \rho dx dy dz$, then the equation of motion along the x-axis for a unit of volume of liquid takes the form

$$\rho \frac{du}{dt} = X + \left(\frac{\partial \tau_x}{\partial x} + \frac{\partial \tau_{yx}}{\partial y} + \frac{\partial \tau_{zx}}{\partial z} \right). \quad (13b)$$

The full velocity derivative in equation (13b) can be expressed by partial derivatives:

$$\frac{du}{dt} = \frac{\partial u}{\partial t} + u \frac{\partial u}{\partial x} + v \frac{\partial u}{\partial y} + w \frac{\partial u}{\partial z}. \quad (13c)$$

Then the equation of motion along the x-axis can be presented in the form

$$\rho \frac{\partial u}{\partial t} + \rho u \frac{\partial u}{\partial x} + \rho v \frac{\partial u}{\partial y} + \rho w \frac{\partial u}{\partial z} = X + \left(\frac{\partial \tau_x}{\partial x} + \frac{\partial \tau_{yx}}{\partial y} + \frac{\partial \tau_{zx}}{\partial z} \right). \quad (14a)$$

Thus, it is possible to derive the equations of motion in the direction of the y and z axes:

$$\rho \frac{\partial v}{\partial t} + \rho u \frac{\partial v}{\partial x} + \rho v \frac{\partial v}{\partial y} + \rho w \frac{\partial v}{\partial z} = Y + \left(\frac{\partial \tau_{yx}}{\partial x} + \frac{\partial \tau_y}{\partial y} + \frac{\partial \tau_{zy}}{\partial z} \right), \quad (14b)$$

$$\rho \frac{\partial w}{\partial t} + \rho u \frac{\partial w}{\partial x} + \rho v \frac{\partial w}{\partial y} + \rho w \frac{\partial w}{\partial z} = Z + \left(\frac{\partial \tau_{zx}}{\partial x} + \frac{\partial \tau_{yz}}{\partial y} + \frac{\partial \tau_z}{\partial z} \right). \quad (14c)$$

The arithmetic mean of three normal stresses

$$\sigma = \frac{1}{3}(\sigma_x + \sigma_y + \sigma_z) \quad (15a)$$

does not change with the transformation of coordinates and for an inviscid liquid it is equal to the pressure taken with the reverse sign.

For future reference it is convenient to separate from the normal stresses the so-called "supplementary stresses" determined from the conditions

$$\left. \begin{aligned} \sigma'_x &= \sigma_x - \sigma, \\ \sigma'_y &= \sigma_y - \sigma, \\ \sigma'_z &= \sigma_z - \sigma. \end{aligned} \right\} \quad (15b)$$

Utilizing these relationships, the system of differential equations of motion can be presented in the form

$$\left. \begin{aligned} \rho \frac{du}{dt} &= X + \frac{\partial \sigma}{\partial x} + \left(\frac{\partial \sigma'_x}{\partial x} + \frac{\partial \sigma'_{yx}}{\partial y} + \frac{\partial \sigma'_{zx}}{\partial z} \right), \\ \rho \frac{dv}{dt} &= Y + \frac{\partial \sigma}{\partial y} + \left(\frac{\partial \sigma'_{yx}}{\partial x} + \frac{\partial \sigma'_y}{\partial y} + \frac{\partial \sigma'_{zy}}{\partial z} \right), \\ \rho \frac{dw}{dt} &= Z + \frac{\partial \sigma}{\partial z} + \left(\frac{\partial \sigma'_{zx}}{\partial x} + \frac{\partial \sigma'_{zy}}{\partial y} + \frac{\partial \sigma'_z}{\partial z} \right). \end{aligned} \right\} \quad (16)$$

It goes without saying that in each of these equations it is possible, in accordance with (13c), to replace the total derivative of the velocity component on the left side with its partial derivatives, and the tangential stresses with identical ones, but to consider transposed indices according to (13a) equal.

§ 4. The Connection between Stresses and Strains

The connection between the stresses which act on a parallelepiped (Fig. 2.4) and the rates of strain of the latter, as has already been indicated, is established by the Newton's law of viscosity.

Tangential stresses cause shearing strains (angular strains) whose definition was given in § 1 of this chapter. Since, in accordance with Newton's hypothesis, in a liquid the stresses are proportional to the rates of strain, in accordance with (1) we have

$$\tau_{xy} = \mu \left(\frac{\partial u}{\partial y} + \frac{\partial v}{\partial x} \right) = \mu \dot{\gamma}_{xy} \quad (17a)$$

where, as has already been indicated, the proportionality factor μ is the coefficient of dynamic viscosity depending on the kind of liquid and its state (temperature, pressure).

The tangential stresses in the other two coordinate planes are respectively

$$\tau_{yz} = \mu \left(\frac{\partial v}{\partial z} + \frac{\partial w}{\partial y} \right) = \mu \dot{\gamma}_{yz} \quad (17b)$$

$$\tau_{zx} = \mu \left(\frac{\partial w}{\partial x} + \frac{\partial u}{\partial z} \right) = \mu \dot{\gamma}_{zx} \quad (17c)$$

It is a more complex matter with normal stresses.

Extending Newton's hypothesis about the proportionality of stresses to the rates of strain to normal stresses and tensile strains (compression), it is necessary to keep in mind that the stretching of a liquid particle is accompanied by its lateral contraction, i.e., volume strain; in other words, strain in the direction of any axis is caused by stresses both parallel to this axis and perpendicular to it.

The detailed analysis of the fields of stresses and strains made by two different methods in hydrodynamics and in the Kinetic Theory of Gases,¹ made it possible to establish the tie between

¹Patterson G. N., The Molecular Flow of Gases. Fizmatgiz, M., 1960; Loytsyanskiy L. G., Fluid and Gas Mechanics. Fizmatgiz, M., 1957.

normal and tangential stresses from which it follows that the additional normal stress is equal to

$$\sigma_x' = \sigma_x - \sigma = 2\mu \left(\epsilon_x - \frac{1}{3} \epsilon \right). \quad (18)$$

where ϵ_x , ϵ are the relative linear and volume strains determined respectively from (4) and (6).

Furthermore, in the hydrodynamics of a viscous compressible liquid the second generalization of Newton's hypothesis is accepted according to which the mean normal stress is equal to the sum of two terms: the first term is the pressure taken with a negative sign which does not depend on the rate of volume strain, and the second term is proportional to the latter:

$$\sigma = -p + \eta \epsilon, \quad (19)$$

here η is the coefficient of the so-called second viscosity introduced into hydrodynamics for the first time by L. D. Landau. The minus sign with pressure considers that it is always directed inside the selected volume of liquid; value σ is customarily considered positive if it is directed outside.

Thus, according to (18) and (19) the components of normal stress are expressed in the following manner:

$$\left. \begin{aligned} \sigma_x &= -p + 2\mu \epsilon_x + \left(\eta - \frac{2}{3}\mu \right) \epsilon, \\ \sigma_y &= -p + 2\mu \epsilon_y + \left(\eta - \frac{2}{3}\mu \right) \epsilon, \\ \sigma_z &= -p + 2\mu \epsilon_z + \left(\eta - \frac{2}{3}\mu \right) \epsilon. \end{aligned} \right\} \quad (20)$$

In a noncompressible liquid $\epsilon = 0$, whence

$$\sigma_x = -p + 2\mu \epsilon_x, \quad \sigma_y = -p + 2\mu \epsilon_y, \quad \sigma_z = -p + 2\mu \epsilon_z. \quad (21)$$

L. D. Landau showed that in monatomic gases the second viscosity was equal to zero ($\eta = 0$), and with the majority of other homogeneous gases is very close to zero.

However, for some two-phase mixtures (for example, the mixture of a liquid and the gas) and thermodynamically nonequilibrium gas mixtures (for example, with the course of slow chemical reactions) the second viscosity becomes considerable.

Subsequently, we will assume $\eta = 0$, i.e., we will consider a gas without second viscosity; then the normal stresses are determined by the following expressions:

$$\left. \begin{aligned} \sigma_x &= -p + 2\mu \epsilon_x - \frac{2}{3} \mu e, \\ \sigma_y &= -p + 2\mu \epsilon_y - \frac{2}{3} \mu e, \\ \sigma_z &= -p + 2\mu \epsilon_z - \frac{2}{3} \mu e. \end{aligned} \right\} \quad (22)$$

From (18) it follows that the additional normal stresses appear only in viscous fluids, when $\mu \neq 0$.

Substituting in (18) the values ϵ_x and e from (4) and (6), we obtain

$$\sigma_x = 2\mu \frac{\partial u}{\partial x} - \frac{2}{3} \mu \left(\frac{\partial u}{\partial x} + \frac{\partial v}{\partial y} + \frac{\partial w}{\partial z} \right), \quad (23a)$$

and respectively for y and z-axes

$$\left. \begin{aligned} \sigma_y &= 2\mu \frac{\partial v}{\partial y} - \frac{2}{3} \mu \left(\frac{\partial u}{\partial x} + \frac{\partial v}{\partial y} + \frac{\partial w}{\partial z} \right), \\ \sigma_z &= 2\mu \frac{\partial w}{\partial z} - \frac{2}{3} \mu \left(\frac{\partial u}{\partial x} + \frac{\partial v}{\partial y} + \frac{\partial w}{\partial z} \right). \end{aligned} \right\} \quad (23b)$$

For a noncompressible liquid

$$\left. \begin{aligned} \sigma_x &= 2\mu \frac{\partial u}{\partial x} = 2\mu \epsilon_x, \\ \sigma_y &= 2\mu \frac{\partial v}{\partial y} = 2\mu \epsilon_y, \\ \sigma_z &= 2\mu \frac{\partial w}{\partial z} = 2\mu \epsilon_z. \end{aligned} \right\} \quad (24)$$

In a noncompressible liquid the additional normal stresses are connected with the rates of linear strain by exactly such relationships as tangential stresses with rates of angular strain.

It is not difficult to be convinced of this comparing equalities (24) and (17)

§ 5. Navier-Stokes Equations

Using formulas (17) and (23), in differential equations (14) it is possible to replace the stresses with rates of strain. In this case, we will obtain the so-called Navier-Stokes differential equations of motion of a viscous liquid.

For example, for motion parallel to the x-axis

$$\begin{aligned} \rho \frac{\partial u}{\partial t} + \rho u \frac{\partial u}{\partial x} + \rho v \frac{\partial u}{\partial y} + \rho w \frac{\partial u}{\partial z} = \\ = X - \frac{\partial p}{\partial x} + \frac{\partial}{\partial x} \left[2\mu \frac{\partial u}{\partial x} - \frac{2}{3}\mu \left(\frac{\partial u}{\partial x} + \frac{\partial v}{\partial y} + \frac{\partial w}{\partial z} \right) \right] + \\ + \frac{\partial}{\partial y} \left[\mu \left(\frac{\partial u}{\partial y} + \frac{\partial v}{\partial x} \right) \right] + \frac{\partial}{\partial z} \left[\mu \left(\frac{\partial u}{\partial z} + \frac{\partial w}{\partial x} \right) \right]. \end{aligned}$$

After simple conversions in the case of an invariable viscosity value in an entire zone of flow ($\mu = \text{const}$) we have

$$\begin{aligned} \rho \frac{\partial u}{\partial t} + \rho u \frac{\partial u}{\partial x} + \rho v \frac{\partial u}{\partial y} + \rho w \frac{\partial u}{\partial z} = X - \frac{\partial p}{\partial x} + \mu \left(\frac{\partial^2 u}{\partial x^2} + \frac{\partial^2 u}{\partial y^2} + \frac{\partial^2 u}{\partial z^2} \right) + \\ + \frac{1}{3}\mu \frac{\partial}{\partial x} \left(\frac{\partial u}{\partial x} + \frac{\partial v}{\partial y} + \frac{\partial w}{\partial z} \right). \end{aligned} \quad (25)$$

Utilizing designations for the Laplace operator

$$\Delta = \frac{\partial^2}{\partial x^2} + \frac{\partial^2}{\partial y^2} + \frac{\partial^2}{\partial z^2}$$

and the divergences of the velocity vector

$$\text{div } W = \frac{\partial u}{\partial x} + \frac{\partial v}{\partial y} + \frac{\partial w}{\partial z},$$

let us write equations (25) in a more concise form:

$$\begin{aligned} \rho \frac{\partial u}{\partial t} + \rho u \frac{\partial u}{\partial x} + \rho v \frac{\partial u}{\partial y} + \rho w \frac{\partial u}{\partial z} = \\ = X - \frac{\partial p}{\partial x} + \mu \Delta u + \frac{1}{3} \mu \frac{\partial}{\partial x} (\text{div } W), \end{aligned} \quad (26a)$$

and by analogy for motion in one direction of the y- and z-axes

$$\begin{aligned} \rho \frac{\partial v}{\partial t} + \rho u \frac{\partial v}{\partial x} + \rho v \frac{\partial v}{\partial y} + \rho w \frac{\partial v}{\partial z} = \\ = Y - \frac{\partial p}{\partial y} + \mu \Delta v + \frac{1}{3} \mu \frac{\partial}{\partial y} (\text{div } W), \end{aligned} \quad (26b)$$

$$\begin{aligned} \rho \frac{\partial w}{\partial t} + \rho u \frac{\partial w}{\partial x} + \rho v \frac{\partial w}{\partial y} + \rho w \frac{\partial w}{\partial z} = \\ = Z - \frac{\partial p}{\partial z} + \mu \Delta w + \frac{1}{3} \mu \frac{\partial}{\partial z} (\text{div } W). \end{aligned} \quad (26c)$$

Equations (26) are called the Navier-Stokes equations. In vector form the Navier-Stokes equations are reduced to one equation of the form

$$\rho \frac{dW}{dt} = R - \text{grad } p + \mu \Delta W + \frac{1}{3} \mu \text{grad}(\text{div } W), \quad (27)$$

where R is the vector of the stress of volume force.

In a viscous liquid the adhesion of particles of the liquid to the walls which limit flow occurs; therefore, with the integration of the differential equations of Navier-Stokes it is necessary to utilize as a boundary condition the equality to zero of the rate of flow at the wall ($W_w = 0$).

In the case of a noncompressible liquid ($\rho = \text{const}$) the last terms in the Navier-Stokes equations (26) and (27) are absent ($\text{div } W = 0$), in consequence of which these equations take a simpler form:

$$\left. \begin{aligned} \rho \frac{du}{dt} &= X - \frac{\partial p}{\partial x} + \mu \Delta u, \\ \rho \frac{dv}{dt} &= Y - \frac{\partial p}{\partial y} + \mu \Delta v, \\ \rho \frac{dw}{dt} &= Z - \frac{\partial p}{\partial z} + \mu \Delta w, \end{aligned} \right\} \quad (28)$$

$$\rho \frac{dW}{dt} = R - \text{grad } p + \mu \Delta W. \quad (29)$$

The solution of the Navier-Stokes equations, even for a noncompressible liquid, is a very complex problem.

Up to now it was possible to solve these equations accurately only in some very simple cases, for example, for the flow of a viscous fluid along a straight tube - Poiseuille's problem; for the flow between two parallel flat walls of which one is fixed and the other moves, i.e., Couette's problem; for a flow close to the critical point - the problem of Khiments [as transliterated] Howarth, et al.

The problems of the hydrodynamics of a viscous liquid are solved usually approximately by means of the rejection of some terms in the Navier-Stokes equations which, under various specific conditions, can be small in comparison with other terms.

§ 6. The Equation of Energy

Let us set up a differential equation of energy conservation for a moving particle of a compressible medium. According to the first law of thermodynamics the heat supplied to a body goes to increase its internal energy and to the accomplishment of the strain energy

$$dQ = d(c, T) + Ap dV. \quad (30)$$

Here $dQ = dQ_{\mu} + dQ_{\tau p}$ - the total quantity of heat conducted to 1 kgf of substance because of the heat exchange of the particle with the environment (dQ_{μ}) and the work of the friction forces ($dQ_{\tau p}$), $p dV$ - the compression work (strain).

For a particle with a volume of $V = dx dy dz$ and with weight $G = \rho g V$ the condition for energy conservation will be written in the following form:

$$dq = dq_{\mu} + dq_{\tau p} = G d(c, T) + Ap dV. \quad (31)$$

Here dq_{H} is the heat obtained by a particle from without, dq_{TP} - the heat of friction which is released on its faces.

Then the per-second heat flow per unit volume of the particle is equal to

$$\frac{1}{V} \frac{dq}{dt} = c_p \frac{dT}{dt} + \lambda p \frac{dV}{V dt}. \quad (32)$$

If the supply of heat from the environment is achieved only by way of thermal conductivity, then in a unit of time the heat flow passes across a unit of surface in accordance with the Fourier hypothesis:

$$\frac{dq_F}{F dt} = \lambda \frac{\partial T}{\partial n}. \quad (33)$$

Here λ is the coefficient of thermal conductivity depending on the properties of the liquid (temperature, pressure), $\frac{\partial T}{\partial n}$ - the temperature gradient along the normal to the surface, $\frac{dq_F}{dt}$ - the per-second heat flow, F - the surface of the particle.

Returning to the elementary parallelepiped dx, dy, dz (Fig. 2.4), let us write the per-second heat consumption across a face with area $dy dz$ in the direction of the x -axis

$$-\lambda \frac{\partial T}{\partial x} dy dz.$$

The per-second inflow of heat across the opposite face comprises

$$\left[\lambda \frac{\partial T}{\partial x} + \frac{\partial}{\partial x} \left(\lambda \frac{\partial T}{\partial x} \right) dx \right] dy dz.$$

Thus, an increase in the reserve of heat in volume $dx dy dz$ as a result of the inflow of heat through the indicated pair of faces during the time interval dt comprises

$$\frac{\partial}{\partial x} \left(\lambda \frac{\partial T}{\partial x} \right) dx dy dz dt.$$

Similarly, the inflow of heat in the direction of the y- and z-axes comprises respectively

$$\frac{\partial}{\partial y} \left(\lambda \frac{\partial T}{\partial y} \right) dy dz dx dt, \quad \frac{\partial}{\partial z} \left(\lambda \frac{\partial T}{\partial z} \right) dz dx dy dt.$$

The total amount of heat conducted to a particle by means of the heat exchange with the environment during time dt,

$$dq_n = \left[\frac{\partial}{\partial x} \left(\lambda \frac{\partial T}{\partial x} \right) + \frac{\partial}{\partial y} \left(\lambda \frac{\partial T}{\partial y} \right) + \frac{\partial}{\partial z} \left(\lambda \frac{\partial T}{\partial z} \right) \right] dx dy dz dt. \quad (34)$$

Let us now find the quantity of heat which enters volume dx dy dz as a result of the work of the friction forces.

The viscosity forces applied to the opposite faces of the parallelepiped have opposite direction. The per-second work is equal to the product of the force and the projection of the rate on the force direction. For example, the supplementary normal stresses σ_x , which act on faces with an area of dy dz, accomplish in one second the work (with consideration only of terms of the 1st order of smallness)

$$\begin{aligned} \left[-\sigma_x u + \left(\sigma_x + \frac{\partial \sigma_x}{\partial x} dx \right) \left(u + \frac{\partial u}{\partial x} dx \right) \right] dy dz = \\ = \left(\sigma_x \frac{\partial u}{\partial x} + u \frac{\partial \sigma_x}{\partial x} \right) dx dy dz = \frac{\partial (\sigma_x u)}{\partial x} dx dy dz. \end{aligned}$$

In the same manner the work is determined which is performed by tangential stresses τ_{xy} and τ_{xz} applied to the same faces in the direction of the two other velocity components (v and w):

$$\frac{\partial (\tau_{xy} v)}{\partial x} dx dy dz, \quad \frac{\partial (\tau_{xz} w)}{\partial x} dx dy dz.$$

The work of the normal and tangential stresses which act on the remaining two pairs of faces is calculated analogously. In summation, the following expression is obtained for the total per-second work of the friction forces which act on the surface of the parallelepiped:

$$\frac{dL_v}{dt} = \left[\frac{\partial}{\partial x} (\tau_{xx}u + \tau_{xy}v + \tau_{xz}w) + \frac{\partial}{\partial y} (\tau_{yx}u + \tau_{yy}v + \tau_{yz}w) + \right. \\ \left. + \frac{\partial}{\partial z} (\tau_{zx}u + \tau_{zy}v + \tau_{zz}w) \right] dx dy dz. \quad (35)$$

However not all work of viscous forces is converted into heat.

Part of this work, which corresponds to the resultant of viscous forces, which causes particle acceleration, is excluded on an increase in the mechanical energy of the particle.

The components of the resultant of the viscous forces in the direction of the x-y-and z-axes were determined in § 4 in the derivation of the equations of motions; the work being accomplished by these components of the resultant force in a unit of time, obviously, equals

$$\frac{dL_w}{dt} = \left[u \left(\frac{\partial \tau_{xx}}{\partial x} + \frac{\partial \tau_{xy}}{\partial y} + \frac{\partial \tau_{xz}}{\partial z} \right) + v \left(\frac{\partial \tau_{yx}}{\partial x} + \frac{\partial \tau_{yy}}{\partial y} + \frac{\partial \tau_{yz}}{\partial z} \right) + \right. \\ \left. + w \left(\frac{\partial \tau_{zx}}{\partial x} + \frac{\partial \tau_{zy}}{\partial y} + \frac{\partial \tau_{zz}}{\partial z} \right) \right] dx dy dz. \quad (36)$$

After deducting from the full work (35) the work of the displacement of the particle (36), we will obtain the unknown part of the per-second work of the viscous forces which is transformed into the heat:

$$\frac{dL_Q}{dt} = \left[\tau_{xx} \frac{\partial u}{\partial x} + \tau_{xy} \frac{\partial v}{\partial x} + \tau_{xz} \frac{\partial w}{\partial x} + \tau_{yx} \frac{\partial u}{\partial y} + \tau_{yy} \frac{\partial v}{\partial y} + \tau_{yz} \frac{\partial w}{\partial y} + \right. \\ \left. + \tau_{zx} \frac{\partial u}{\partial z} + \tau_{zy} \frac{\partial v}{\partial z} + \tau_{zz} \frac{\partial w}{\partial z} \right] dx dy dz = \frac{1}{A} \frac{dq_{vis}}{dt}. \quad (37)$$

If now in equation (32) we replace the value of the total per-second inflow of heat $dq = dq_{\mu} + dq_{rp}$ with the aid of (34) and (37), then we will obtain the equation of energy

$$\rho \frac{d(c_p T)}{dt} + \rho p \frac{1}{V} \frac{dV}{dt} = \left[\frac{\partial}{\partial x} \left(\lambda \frac{\partial T}{\partial x} \right) + \frac{\partial}{\partial y} \left(\lambda \frac{\partial T}{\partial y} \right) + \frac{\partial}{\partial z} \left(\lambda \frac{\partial T}{\partial z} \right) \right] + \\ + A \left[\tau_{xx} \frac{\partial u}{\partial x} + \tau_{xy} \frac{\partial v}{\partial x} + \tau_{xz} \frac{\partial w}{\partial x} + \tau_{yx} \frac{\partial u}{\partial y} + \tau_{yy} \frac{\partial v}{\partial y} + \tau_{yz} \frac{\partial w}{\partial y} + \right. \\ \left. + \tau_{zx} \frac{\partial u}{\partial z} + \tau_{zy} \frac{\partial v}{\partial z} + \tau_{zz} \frac{\partial w}{\partial z} \right]$$

After the replacement, in (37) of the viscous stresses by their values according to (17) and (24) we will obtain the heat of friction which is liberated in one second in elementary parallelepiped:

$$\frac{dq_{fr}}{dt} = A_{\mu} \Phi V, \quad (39)$$

where the multiplier

$$\begin{aligned} \Phi = & \frac{1}{\mu} \left[\tau_{xx} \frac{\partial u}{\partial x} + \tau_{xy} \frac{\partial v}{\partial x} + \tau_{xz} \frac{\partial w}{\partial x} + \left(\tau_{yx} \frac{\partial u}{\partial y} + \tau_{yy} \frac{\partial v}{\partial y} + \tau_{yz} \frac{\partial w}{\partial y} \right) + \right. \\ & \left. + \tau_{zx} \frac{\partial u}{\partial z} + \tau_{zy} \frac{\partial v}{\partial z} + \tau_{zz} \frac{\partial w}{\partial z} \right] = 2 \left[\left(\frac{\partial u}{\partial x} \right)^2 + \left(\frac{\partial v}{\partial y} \right)^2 + \left(\frac{\partial w}{\partial z} \right)^2 \right] + \\ & + \left(\frac{\partial u}{\partial y} + \frac{\partial v}{\partial x} \right)^2 + \left(\frac{\partial w}{\partial y} + \frac{\partial v}{\partial z} \right)^2 + \left(\frac{\partial u}{\partial z} + \frac{\partial w}{\partial x} \right)^2 - \\ & - \frac{2}{3} \left(\frac{\partial u}{\partial x} + \frac{\partial v}{\partial y} + \frac{\partial w}{\partial z} \right)^2 \end{aligned} \quad (40)$$

is called the dissipative function.

Utilizing the definition of the function Φ (39) and (40), we obtain the equation of energy conservation in the form

$$\rho g \frac{d(c_p T)}{dt} + \rho p \frac{dV}{dt} = \frac{\partial}{\partial x} \left(\lambda \frac{\partial T}{\partial x} \right) + \frac{\partial}{\partial y} \left(\lambda \frac{\partial T}{\partial y} \right) + \frac{\partial}{\partial z} \left(\lambda \frac{\partial T}{\partial z} \right) + A_{\mu} \Phi. \quad (41a)$$

We convert the second term of the left side of this equation with the aid of the condition for the conservation of mass (11a):

$$\rho \frac{dV}{dt} = - \frac{p}{\rho} \frac{d\rho}{dt} = - \left[\frac{dp}{dt} - \rho \frac{d(p/\rho)}{dt} \right].$$

Then the equation of energy can also be presented in the following form:

$$\begin{aligned} \rho g \frac{d}{dt} \left[c_p T + A \frac{p}{\rho g} \right] = & \lambda \frac{dp}{dt} + \frac{\partial}{\partial x} \left(\lambda \frac{\partial T}{\partial x} \right) + \\ & + \frac{\partial}{\partial y} \left(\lambda \frac{\partial T}{\partial y} \right) + \frac{\partial}{\partial z} \left(\lambda \frac{\partial T}{\partial z} \right) + A_{\mu} \Phi. \end{aligned} \quad (41b)$$

For the ideal gas which is subordinated to the equation of state $p/\rho g = RT$, the equation of energy is simplified, since

$$c_p T + A \frac{p}{\rho g} = (c_p + AR) T = c_p T = i.$$

Hence

$$\rho g \frac{dl}{dt} = A \frac{dp}{dt} + \frac{\partial}{\partial x} \left(\lambda \frac{\partial T}{\partial x} \right) + \frac{\partial}{\partial y} \left(\lambda \frac{\partial T}{\partial y} \right) + \frac{\partial}{\partial z} \left(\lambda \frac{\partial T}{\partial z} \right) + A \mu \Phi. \quad (41c)$$

If the coefficients of thermal conductivity and heat capacity do not change in the entire zone of flow, then we have the equation of energy in the following form:

$$\rho g \frac{dl}{dt} = \rho g c_p \frac{dT}{dt} = A \frac{dp}{dt} + \lambda \Delta T + A \mu \Phi. \quad (42)$$

In a noncompressible liquid, the second term of the left side of equation of energy (41a) is equal to zero and, furthermore, $c_p = c_v = c$; therefore, the equation of energy is obtained in the following form:

$$\rho g c \frac{dT}{dt} = A \frac{dp}{dt} + \lambda \Delta T + A \mu \Phi. \quad (43)$$

The dissipative function of Φ in this case also takes a simpler form since the last term of the right side of (40) is equal to zero.

For a stationary two-dimensional (plane-parallel) flow the equation of energies (42) takes the following form:

$$\rho g c_p \left(u \frac{\partial T}{\partial x} + v \frac{\partial T}{\partial y} \right) = A \left(u \frac{\partial p}{\partial x} + v \frac{\partial p}{\partial y} \right) + \lambda \left(\frac{\partial^2 T}{\partial x^2} + \frac{\partial^2 T}{\partial y^2} \right) + A \mu \left\{ 2 \left[\left(\frac{\partial u}{\partial x} \right)^2 + \left(\frac{\partial v}{\partial y} \right)^2 \right] + \left(\frac{\partial u}{\partial y} + \frac{\partial v}{\partial x} \right)^2 - \frac{2}{3} \left(\frac{\partial u}{\partial x} + \frac{\partial v}{\partial y} \right)^2 \right\}. \quad (44)$$

In certain cases in gas dynamics it is more convenient to use another form of the equation of energy which can be obtained with the aid of the Navier-Stokes equations.

Let us multiply the first of the Navier-Stokes equations (16) by the velocity component u , the second - by v , the third - by w and let us add all three equations term by term.

Then we will have

$$\rho \frac{d}{dt} \left(\frac{W^2}{2g} \right) = \rho \left(\frac{dp}{dt} - \frac{\partial p}{\partial t} \right) + \rho \left(u \left(\frac{\partial v}{\partial x} + \frac{\partial v}{\partial y} + \frac{\partial v}{\partial z} \right) + \right. \\ \left. + v \left(\frac{\partial u}{\partial x} + \frac{\partial u}{\partial y} + \frac{\partial u}{\partial z} \right) + w \left(\frac{\partial u}{\partial x} + \frac{\partial v}{\partial y} + \frac{\partial w}{\partial z} \right) \right). \quad (45)$$

Here for simplicity the work of the volume forces is rejected as not playing a role in gas dynamics and the mean normal stress is replaced by the pressure ($\sigma = -p$).

Adding equation (45) which reflects a change in kinetic energy with equation (42) which considers a change in the enthalpy, and utilizing expression (40), after some conversions we obtain

$$\rho \frac{d}{dt} \left[1 + A \frac{W^2}{2g} \right] = \rho \frac{\partial p}{\partial t} + \lambda \Delta T + A \left[\frac{\partial}{\partial x} (\tau_{xx}u + \tau_{xy}v + \tau_{xz}w) + \right. \\ \left. + \frac{\partial}{\partial y} (\tau_{yx}u + \tau_{yy}v + \tau_{yz}w) + \frac{\partial}{\partial z} (\tau_{zx}u + \tau_{zy}v + \tau_{zz}w) \right]. \quad (46)$$

As is known from § 2, Chapter I, the sum of the enthalpy and heat equivalent of kinetic energy is called total enthalpy (full heat content)

$$1 + A \frac{W^2}{2g} = h. \quad (47)$$

Substituting (47) into the left side of equation (46) and replacing the stresses by the strain rates with the aid of (8), (17) and (24), after the conversions we obtain the equation of energies in this form:

$$\rho \frac{dh}{dt} = A \frac{\partial p}{\partial t} + \lambda \Delta T + A \mu \lambda \left(\frac{W^2}{2} \right) + \frac{A}{3} \mu (W \times \nabla) \operatorname{div} W, \quad (48)$$

where

$$\nabla \operatorname{div} W = \frac{\partial}{\partial x} (\operatorname{div} W) + \frac{\partial}{\partial y} (\operatorname{div} W) + \frac{\partial}{\partial z} (\operatorname{div} W).$$

In gas dynamics great significance is had (see the following paragraph) by the dimensionless quantity

$$\frac{\lambda}{c_p \mu} = \operatorname{Pr},$$

called the Prandtl number. Let us introduce this number into the right side of equation (48). For this let us add and subtract the term

$$\frac{\lambda}{c_p} \Delta \left(A \frac{W^2}{2g} \right).$$

utilize (47), and consider that with $c_p = \text{const}$

$$\lambda \Delta T = \frac{\lambda}{c_p} \Delta L$$

Thus, we have

$$\rho g \frac{dl_0}{dt} = A \frac{\partial p}{\partial t} + \frac{\lambda}{c_p} \Delta l_0 + \mu (1 - \text{Pr}) \Delta \left(\frac{A W^2}{2g} \right) + \frac{A}{3} \mu (W \times \nabla) \text{div } W. \quad (49)$$

For gases the Prandtl number is close to unity (for example, for air $\text{Pr} = 0.72$). With $\text{Pr} = 1$, the third term of the right side is equal to zero and the equation of energy is simplified:

$$\rho g \frac{dl_0}{dt} = A \frac{\partial p}{\partial t} + \frac{\lambda}{c_p} \Delta l_0 + \frac{A}{3} \mu (W \times \nabla) \text{div } W. \quad (50)$$

§ 7. Hydrodynamic Similarity

In view of the impossibility of obtaining the exact solution of the Navier-Stokes equations and equation of energy for the overwhelming majority of tasks of hydrodynamics and gas dynamics, resort is had either to approximate solutions or to experiments on models. In the latter case, the question arises concerning the conditions of similarity for the flow around of a full-scale object and its model.

The first condition in such similarity is the geometric similarity which is accomplished if the dimensions of all compatible elements of the model and nature differ the very same number of times and, furthermore, if the compatible elements are arranged at identical angles to the velocity vector of the incident flow.

Let any characteristic dimensions of the model r_m differ from the corresponding characteristic dimension of nature r_n by k_2 times. Then the value

$$\frac{r_m}{r_n} = k_2 \quad (51)$$

is the linear scale of modeling (Fig. 2.5). The kinematic similarity of flows near the model and nature is achieved if at compatible points whose coordinates are proportional:

$$\frac{x_m}{x_n} = \frac{y_m}{y_n} = \frac{z_m}{z_n} = \frac{r_m}{r_n} = k_2 \quad (52)$$

the components of the velocity vectors satisfy the condition

$$\frac{u_m}{u_n} = \frac{v_m}{v_n} = \frac{w_m}{w_n} = \frac{u_{\infty m}}{u_{\infty n}} = k_u \quad (53)$$

where $u_{\infty m}$, $u_{\infty n}$ are the velocities of the undisturbed incident flow respectively of the model and in nature at a great distance ("at infinity") from the body. The value k_u is called the kinematic scale of modeling.

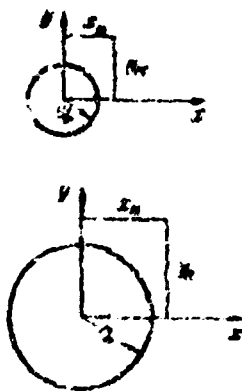


Fig. 2.5. Illustration of geometric similarity.

From condition (52) it follows that compatible points of the two flows can be determined in the following manner:

$$\frac{x_m}{r_m} = \frac{x_n}{r_n}; \quad \frac{y_m}{r_m} = \frac{y_n}{r_n}; \quad \frac{z_m}{r_m} = \frac{z_n}{r_n} \quad (54)$$

i.e., as points with identical relative values of coordinates.

In exactly the same manner, from condition (53) we obtain that at the compatible points of two kinematically similar flows, without depending on the kinematic scale of modeling, the dimensionless values of the corresponding velocity components are identical:

$$\frac{u_n}{u_{\infty n}} = \frac{u_n}{u_{\infty n}}; \quad \frac{v_n}{v_{\infty n}} = \frac{v_n}{v_{\infty n}}; \quad \frac{w_n}{w_{\infty n}} = \frac{w_n}{w_{\infty n}}. \quad (55)$$

The condition of dynamic similarity of two flows, obviously, is satisfied when values of the corresponding forces applied to the model and nature differ the very same number of times:

$$\left. \begin{aligned} \frac{\rho_n \frac{du_n}{dt}}{\rho_n \frac{du_n}{dt}} &= \frac{\rho_n \frac{dv_n}{dt}}{\rho_n \frac{dv_n}{dt}} = \frac{\rho_n \frac{dw_n}{dt}}{\rho_n \frac{dw_n}{dt}} = k_R \\ \frac{X_n}{X_n} &= \frac{Y_n}{Y_n} = \frac{Z_n}{Z_n} = k_R \\ \frac{P_{xn}}{P_{xn}} &= \frac{P_{yn}}{P_{yn}} = \frac{P_{zn}}{P_{zn}} = k_R \\ \frac{R_{xn}}{R_{xn}} &= \frac{R_{yn}}{R_{yn}} = \frac{R_{zn}}{R_{zn}} = k_R \end{aligned} \right\} \quad (56)$$

The first of the presented equalities contains the projections of inertia force which stand on the left side of the Navier-Stokes equations, the second - volume forces, the third - the forces of hydrodynamic pressure, and the fourth - the forces of friction grouped in the right side of the Navier-Stokes equations.

The coefficient k_R characterizes the dynamic scale of modeling. From equalities (56) it is evident that without depending on the value of the scale k_R the dynamic similarity occurs if the dimensionless values of the corresponding forces applied to the model and full-scale object are identical:

$$\begin{aligned}\frac{X_n}{\rho_n \frac{du_n}{dt}} &= \frac{X_n}{\rho_n \frac{du_n}{dt}}; & \frac{Y_n}{\rho_n \frac{du_n}{dt}} &= \frac{Y_n}{\rho_n \frac{du_n}{dt}} \quad \text{etc.} \\ \frac{P_{xn}}{\rho_n \frac{du_n}{dt}} &= \frac{P_{xn}}{\rho_n \frac{du_n}{dt}} \quad \text{etc.} \\ \frac{R_{xn}}{\rho_n \frac{du_n}{dt}} &= \frac{R_{xn}}{\rho_n \frac{du_n}{dt}} \quad \text{etc.}\end{aligned}$$

Hydrodynamically similar are the flows in which conditions of geometric, kinematic and dynamic similarity are satisfied simultaneously.

If we write the Navier-Stokes equations in a dimensionless form, then for two hydrodynamically similar flows these equations will turn out to be completely identical.

Let us reduce the Navier-Stokes equation to the dimensionless form (25), for which first we express all values which enter the equations in fractions of the corresponding values for an undisturbed flow far from the body (u_∞ , ρ_∞ , μ_∞ , p_∞) and also characteristic values of time (t_0) and dimension (l):

$$\begin{aligned}\frac{u_\infty}{t_0} \frac{\partial \frac{u}{u_\infty}}{\partial \frac{t}{t_0}} + \frac{u_\infty}{l} \left(\frac{u}{u_\infty} \frac{\partial \frac{u}{u_\infty}}{\partial \frac{x}{l}} + \frac{v}{u_\infty} \frac{\partial \frac{u}{u_\infty}}{\partial \frac{y}{l}} + \frac{w}{u_\infty} \frac{\partial \frac{u}{u_\infty}}{\partial \frac{z}{l}} \right) = \\ = \frac{X}{\rho} - \frac{p_\infty \rho_\infty}{\rho_\infty \rho} \frac{\partial \frac{p}{p_\infty}}{\partial \frac{x}{l}} + \frac{\mu_\infty u_\infty \rho_\infty}{\rho_\infty \mu} \frac{\mu}{\mu_\infty} \left\{ \left[\frac{\partial^2 \frac{u}{u_\infty}}{\partial \left(\frac{x}{l} \right)^2} + \frac{\partial^2 \frac{u}{u_\infty}}{\partial \left(\frac{y}{l} \right)^2} + \frac{\partial^2 \frac{u}{u_\infty}}{\partial \left(\frac{z}{l} \right)^2} \right] + \right. \\ \left. + \frac{1}{3} \frac{\partial}{\partial \frac{x}{l}} \left(\frac{\partial \frac{u}{u_\infty}}{\partial \frac{x}{l}} + \frac{\partial \frac{v}{u_\infty}}{\partial \frac{y}{l}} + \frac{\partial \frac{w}{u_\infty}}{\partial \frac{z}{l}} \right) \right\}, \quad (57)\end{aligned}$$

and then let us divide by the value u_∞^2/l , proportional to the force of inertia for a unit of mass:

$$\begin{aligned}
& \frac{l}{\rho_{\infty} u_{\infty}} \frac{\partial^2 u}{\partial t^2} + \frac{u}{u_{\infty}} \frac{\partial^2 u}{\partial x^2} + \frac{v}{u_{\infty}} \frac{\partial^2 u}{\partial y^2} + \frac{w}{u_{\infty}} \frac{\partial^2 u}{\partial z^2} = \\
& = \frac{gl}{u_{\infty}^2} - \frac{\rho_{\infty}}{\rho} \frac{\partial p}{\partial x} \frac{1}{u_{\infty}^2} + \frac{\mu_{\infty}}{\mu} \frac{\partial^2 u}{\partial x^2} \frac{1}{u_{\infty}^2} \left[\left(\frac{\partial^2 u}{\partial x^2} + \frac{\partial^2 u}{\partial y^2} + \frac{\partial^2 u}{\partial z^2} \right) + \right. \\
& \quad \left. + \frac{1}{3} \frac{\partial}{\partial x} \left(\frac{\partial u}{\partial x} + \frac{\partial v}{\partial y} + \frac{\partial w}{\partial z} \right) \right]. \quad (58)
\end{aligned}$$

Here it is accepted that mass force X is the force of the earth's gravity, i.e., $X/\rho = g$.

The dimensionless Navier-Stokes equation (58) contains the following dimensionless complexes:

$$\frac{l}{\rho_{\infty} u_{\infty}}, \quad \frac{gl}{u_{\infty}^2}, \quad \frac{\rho_{\infty}}{\rho_{\infty} u_{\infty}^2}, \quad \frac{\mu_{\infty}}{\rho_{\infty} u_{\infty}}.$$

It is obvious that for geometrically and kinematically similar flows the dimensionless equations of motion (58) will be identical in the case where each of these complexes has the very same value for a full-scale object and models and if at the compatible points of these flows the relative values of the density and viscosity are identical ($\rho/\rho_{\infty} = \text{idem}$, $\mu/\mu_{\infty} = \text{idem}$)

$$\left. \begin{aligned} \frac{l_u}{\rho_{\infty} u_{\infty}} &= \frac{l_m}{\rho_{\infty} u_{\infty}} = Sh, & \frac{gl_u}{u_{\infty}^2} &= \frac{gl_m}{u_{\infty}^2} = Fr, \\ \frac{\rho_{\infty}}{\rho_{\infty} u_{\infty}^2} &= \frac{\rho_{\infty}}{\rho_{\infty} u_{\infty}^2} = Eu, & \frac{\mu_{\infty}}{\rho_{\infty} u_{\infty}} &= \frac{\mu_{\infty}}{\rho_{\infty} u_{\infty}} = R. \end{aligned} \right\} \quad (59)$$

Dimensionless complexes (59) are thus the criteria of dynamic similarity for geometrically and kinematically similar systems.

Awarded to these similarity criteria are the following designations and names:

$$\left. \begin{aligned} \frac{l}{ut} &= Sh - \text{Strouhal number,} \\ \frac{u'}{g l} &= Fr - \text{Froude number,} \\ \frac{p}{\rho u^2} &= Eu - \text{Euler number,} \\ \frac{\mu}{\rho u l} &= R - \text{Reynolds number.} \end{aligned} \right\} \quad (60)$$

In expressions (60) the indices are omitted since in them one ought to substitute some characteristic values of the parameters which do not mandatorily correspond to their values at "infinity."

Let us recall that each of the criteria of dynamic similarity was formed by the division of the corresponding force into a value proportional to the force of inertia; therefore the Froude number in essence determines the ratio of the gravitational force (volume force) to the force of inertia, the Reynolds number - the ratio of the viscosity force to the force of inertia, the Strouhal number - the ratio of the supplementary (local) force caused by the unsteady nature of the motion to the force of inertia, and the Euler number - the ratio of the force of hydrodynamic pressure to the force of inertia.

In a noncompressible liquid Euler's criterion is not determinant since it is possible to take the dynamic pressure $\rho u^2/2$ as a characteristic pressure p and then Eu is a constant number.

In a compressible medium Eu criterion can be presented with the use of the known expression for the speed of sound $a^2 = kp/\rho$ in the form

$$Eu = \frac{1}{\gamma M^2};$$

this means that in the case of gas flows two supplementary similarity criteria appear:

Poisson's number

$$k = \frac{\nu}{c_p}$$

and the Mach number

$$M = \frac{u}{c}$$

the values of which with the similarity of flows near the model and nature should be respectively identical

$$k_n = k_n, \quad M_n = M_n$$

Let us now move on to an examination of the equation of energy. To reduce the equation of energy (42) to dimensionless form let us refer, as formerly, all values of velocities to the velocity of the undisturbed incident flow u_∞ , all linear values - to the characteristic linear dimension of the object l , all pressures - to the pressure in the incident flow p_∞ , and all temperatures - to a difference in the temperatures of the incident flow (far from the body) and the wall of body $\Delta T_0 = T_\infty - T_w$. For simplicity let us investigate the equation of energy for steady flow conditions (it is not difficult to show that consideration of unsteady terms in the equation of energy leads to a Strouhal number, i.e., to the criterion obtained earlier from the Navier-Stokes equations).

Then from (43) and (40) we have

$$\begin{aligned} \frac{\rho R T_\infty u_\infty}{l} \left[\frac{u}{u_\infty} \frac{\partial \frac{\Delta T}{\Delta T_0}}{\partial \frac{x}{l}} + \frac{v}{u_\infty} \frac{\partial \frac{\Delta T}{\Delta T_0}}{\partial \frac{y}{l}} + \frac{w}{u_\infty} \frac{\partial \frac{\Delta T}{\Delta T_0}}{\partial \frac{z}{l}} \right] = \\ = \frac{\Delta u_\infty p_\infty}{l} \left[\frac{u}{u_\infty} \frac{\partial \frac{p}{p_\infty}}{\partial \frac{x}{l}} + \frac{v}{u_\infty} \frac{\partial \frac{p}{p_\infty}}{\partial \frac{y}{l}} + \frac{w}{u_\infty} \frac{\partial \frac{p}{p_\infty}}{\partial \frac{z}{l}} \right] + \\ + \frac{\lambda \Delta T_0}{l} \left[\frac{\partial^2 \frac{\Delta T}{\Delta T_0}}{\partial (\frac{x}{l})^2} + \frac{\partial^2 \frac{\Delta T}{\Delta T_0}}{\partial (\frac{y}{l})^2} + \frac{\partial^2 \frac{\Delta T}{\Delta T_0}}{\partial (\frac{z}{l})^2} \right] + \end{aligned}$$

$$+ A \mu \frac{u_{\infty}^3}{l^3} \left\{ 2 \left[\left(\frac{\partial \frac{u}{u_{\infty}}}{\partial \frac{x}{l}} \right)^2 + \left(\frac{\partial \frac{v}{u_{\infty}}}{\partial \frac{y}{l}} \right)^2 + \left(\frac{\partial \frac{w}{u_{\infty}}}{\partial \frac{z}{l}} \right)^2 \right] + \left(\frac{\partial \frac{u}{u_{\infty}}}{\partial \frac{y}{l}} + \frac{\partial \frac{v}{u_{\infty}}}{\partial \frac{x}{l}} \right)^2 + \right. \\ \left. + \left(\frac{\partial \frac{w}{u_{\infty}}}{\partial \frac{y}{l}} + \frac{\partial \frac{v}{u_{\infty}}}{\partial \frac{z}{l}} \right)^2 + \left(\frac{\partial \frac{u}{u_{\infty}}}{\partial \frac{z}{l}} + \frac{\partial \frac{w}{u_{\infty}}}{\partial \frac{x}{l}} \right)^2 - 2 \left(\frac{\partial \frac{u}{u_{\infty}}}{\partial \frac{x}{l}} + \frac{\partial \frac{v}{u_{\infty}}}{\partial \frac{y}{l}} + \frac{\partial \frac{w}{u_{\infty}}}{\partial \frac{z}{l}} \right) \right\}$$

and further, after the division of all terms by the common factor of the left side:

$$\frac{u}{u_{\infty}} \frac{\partial \frac{\Delta T}{\Delta T_0}}{\partial \frac{x}{l}} + \frac{v}{u_{\infty}} \frac{\partial \frac{\Delta T}{\Delta T_0}}{\partial \frac{y}{l}} + \frac{w}{u_{\infty}} \frac{\partial \frac{\Delta T}{\Delta T_0}}{\partial \frac{z}{l}} = \frac{\rho_{\infty} \rho_{\infty} A u_{\infty}^3}{\rho_{\infty} u_{\infty}^3 \rho \kappa c_p \Delta T_0} \left[\frac{u}{u_{\infty}} \frac{\partial \frac{p}{p_{\infty}}}{\partial \frac{x}{l}} + \right. \\ \left. + \frac{v}{u_{\infty}} \frac{\partial \frac{p}{p_{\infty}}}{\partial \frac{y}{l}} + \frac{w}{u_{\infty}} \frac{\partial \frac{p}{p_{\infty}}}{\partial \frac{z}{l}} \right] + \frac{\lambda}{\rho g c_p u_{\infty} l} \left[\frac{\partial^2 \frac{\Delta T}{\Delta T_0}}{\partial \left(\frac{x}{l} \right)^2} + \frac{\partial^2 \frac{\Delta T}{\Delta T_0}}{\partial \left(\frac{y}{l} \right)^2} + \frac{\partial^2 \frac{\Delta T}{\Delta T_0}}{\partial \left(\frac{z}{l} \right)^2} \right] + \\ + A \frac{u_{\infty}^3}{\rho g c_p \Delta T_0} \left\{ 2 \left[\left(\frac{\partial \frac{u}{u_{\infty}}}{\partial \frac{x}{l}} \right)^2 + \left(\frac{\partial \frac{v}{u_{\infty}}}{\partial \frac{y}{l}} \right)^2 + \left(\frac{\partial \frac{w}{u_{\infty}}}{\partial \frac{z}{l}} \right)^2 \right] + \right. \\ \left. + \left(\frac{\partial \frac{u}{u_{\infty}}}{\partial \frac{y}{l}} + \frac{\partial \frac{v}{u_{\infty}}}{\partial \frac{x}{l}} \right)^2 + \left(\frac{\partial \frac{w}{u_{\infty}}}{\partial \frac{y}{l}} + \frac{\partial \frac{v}{u_{\infty}}}{\partial \frac{z}{l}} \right)^2 + \left(\frac{\partial \frac{u}{u_{\infty}}}{\partial \frac{z}{l}} + \frac{\partial \frac{w}{u_{\infty}}}{\partial \frac{x}{l}} \right)^2 - \right. \\ \left. - 2 \left(\frac{\partial \frac{u}{u_{\infty}}}{\partial \frac{x}{l}} + \frac{\partial \frac{v}{u_{\infty}}}{\partial \frac{y}{l}} + \frac{\partial \frac{w}{u_{\infty}}}{\partial \frac{z}{l}} \right) \right\}. \quad (61)$$

Here $\Delta T = T - T_w$ is the excess local temperature (in comparison with the wall temperature), whereupon $dT = d(\Delta T)$. The left side of the equation of energy reflects the convective heat transfer; therefore, the division of all terms by the dimensional factor of the left side means that all forms of heat fluxes are expressed in fractions of the convective.

The thermal similarity of the two processes is achieved when they are both described by the very same dimensionless equation of energy. This condition is satisfied with the observance of:

1) hydrodynamic similarity;

2) the similarity of the temperature fields, i.e., the equality of dimensionless values of the excess temperature in compatible points of two flows $\Delta T/\Delta T_\infty = \text{idem}$ with $x/l = \text{idem}$, $y/l = \text{idem}$, $z/l = \text{idem}$.

3) equality, in both flows, of values of each of the following dimensionless complexes of equation (61):

$$\frac{P_\infty}{\rho u_\infty^2} \frac{Au_\infty^3}{g c_p \Delta T_0}; \quad \frac{\lambda}{\rho g c_p u_\infty}; \quad \frac{Au_\infty}{\rho g c_p \Delta T_0}.$$

It is expedient to transform these complexes somewhat. So, the first of them is the product of the already known Euler criterion times the so-called temperature criterion

$$\theta = \frac{Au_\infty^3}{g c_p \Delta T_0} = \frac{k A R T_\infty}{c_p \Delta T_0} \frac{u_\infty^3}{k g R T_\infty}.$$

Since $AR = c_p - c_v$; $k = c_p/c_v$; $k g R T_\infty = a_\infty^2$ then

$$\theta = \frac{Au_\infty^3}{g c_p \Delta T_0} = (k-1) \frac{T_\infty}{\Delta T_0} M_\infty^3. \quad (62)$$

Consequently, the temperature criterion which considers the relation of the compression work being achieved by dynamic pressure to the convective heat flux is proportional to the square of the Mach number and to the ratio of the full temperature of the incident flow to its excess temperature. The value

$$\frac{Au^3}{2 g c_p} = T^* - T = \Delta T^*$$

is a temperature increase with the adiabatic stagnation of flow; therefore we also have

$$\theta = 2 \frac{\Delta T^*}{\Delta T_0} = 2 \frac{T_\infty^* - T_\infty}{T_\infty - T_0}. \quad (63)$$

Thus, the temperature criterion is equal to the doubled ratio of the temperature increase with the stagnation of flow to the excess gas temperature; hence, it is clear that this criterion has significance only with large flow rates.

We convert the factor with the second term of the right side of equation (61), which expresses the ratio of the heat being transferred by heat conductivity, to the convective heat flux thus:

$$\frac{\lambda}{gc_p u \rho u_\infty l} = \frac{1}{Pr R}. \quad (63a)$$

One of its dimensionless cofactors is the reciprocal value of the Reynolds number known to us; the second dimensionless factor, inversely proportional to the value called the Prandtl number

$$Pr = \frac{c_p \mu}{\lambda} = \frac{\gamma}{\gamma_0}, \quad (64)$$

depends only on the physical properties of the medium. The value $\gamma_0 = \frac{\lambda}{\rho g c_p}$, which is called the coefficient of temperature conductivity, has a dimensionality of the kinematic viscosity coefficient ν .

The product of the Prandtl and Reynolds numbers is called Peclet's criterion or number

$$Pe = \frac{u l}{\gamma_0} = Pr R. \quad (65)$$

This criterion is widely utilized in modeling the processes of heat exchange. The factor with the third term of the right side of equation (61), which is the ratio of the heat being scattered to the convective heat flux, does not lead to new criteria since it equals the ratio of the temperature criterion to the Reynolds number:

$$\frac{A u_\infty}{gc_p \Delta T_0 l} = \frac{A u_\infty^2}{gc_p \Delta T_0} \frac{\rho}{\rho u_\infty} = \frac{\theta}{R}. \quad (66)$$

To the aforesaid it should be added that for a medium of variable density we should include in the Navier-Stokes equations the volume forces of Archimedes, since according to Archimedes' law "a particle surrounded by a liquid of different density loses in its weight as much as the volume of liquid it displaces weighs." Thus, the Archimedes force applied to a particle which has volume V , is equal to

$$(1 - \gamma_\infty) V = g(\rho - \rho_\infty) V.$$

The projections of the Archimedes force referred to a unit of volume which should be substituted into the Navier-Stokes equations can be presented in the form

$$X = g_x(\rho - \rho_\infty) \quad Y = g_y(\rho - \rho_\infty) \quad Z = g_z(\rho - \rho_\infty)$$

where g_x , g_y , g_z are the projections of the gravity acceleration to the coordinate axes.

The ratio of Archimedes' force to inertial force, which should stand in this case in the right side of the Navier-Stokes equation for the x-axis, will be written in the form

$$\frac{Xl}{\rho u_\infty^2} = \frac{g_x(\rho - \rho_\infty)l}{\rho u_\infty^2}.$$

The relative change in volume, and consequently also in the density, is proportional to the temperature change:

$$\frac{\Delta V}{V} = \frac{\rho - \rho_\infty}{\rho} = \beta(T_\infty - T),$$

where β is the volume expansion coefficient.

In an ideal gas with constant pressure $\frac{\rho}{\rho_\infty} = T_\infty/T$, i.e., $\beta = 1/T_\infty$ therefore

$$\frac{Xl}{\rho u_\infty^2} = \frac{g_x l}{u_\infty^2} \frac{\Delta T}{T_\infty} \frac{\Delta T}{\Delta T_0} = \frac{\Delta T}{T_\infty} \frac{1}{Fr} \frac{\Delta T}{\Delta T_0}.$$

The dimensionless factor

$$Ar = \frac{\Delta T_0}{T_\infty} \frac{1}{Fr} \quad (67)$$

is called Archimedes' number; it is important for hydrodynamic similarity when the temperature drops in a gas flow are great and the velocities are low.

As we see, Archimedes' criterion is obtained from the division of the relative temperature drop by Froude's number.

In the general case ($\beta \neq 1/T_\infty$)

$$Ar = \frac{g l}{u_\infty^2} \beta \Delta T_0 = \frac{g \beta \Delta T_0 l^3}{\nu^2} \frac{\nu}{u_\infty l} = \frac{Gr}{Re^2}. \quad (68)$$

The dimensionless quantity

$$Gr = \frac{g l^3 \beta \Delta T}{\nu^2}, \quad (69)$$

which expresses the ratio of Archimedes' force to the viscosity force, is called Grashof's number.

Thus, for the satisfaction of the conditions of hydrodynamic and thermal similarity it is necessary that in the model of the value of the similarity criteria:

$$\left. \begin{array}{ll} \text{Reynolds number:} & R = \frac{u_\infty l}{\nu}, \\ \text{Prandtl's number:} & Pr = \frac{\nu}{\chi} = \frac{u_\infty l}{\alpha}, \\ \text{Grashof's number:} & Gr = \frac{g l^3 \beta \Delta T_0}{\nu^2}, \\ \text{temperature} & \theta = \frac{u_\infty^2}{g l \beta \Delta T_0}, \\ \text{criterion:} & \end{array} \right\} \quad (70)$$

be the same as in a full-scale object.

For gases, the equality of the Mach number

$$M = \frac{u_\infty}{a_\infty}$$

and the relation of heat capacities

$$\lambda = \frac{c_p}{c_v}$$

should also be observed.

§ 8. Laminar Flows

We come to one of the simple special cases of the exact solution of the Navier-Stokes' equation in the case of the so-called "laminar flows," when only one velocity component is retained, and the other two are equal to zero everywhere:

$$u = u(x, y, z, t), \quad v = 0, \quad w = 0.$$

If the mass forces are negligible, then in this case the equations of motion take the following form:

$$\begin{aligned} \frac{\partial u}{\partial t} + u \frac{\partial u}{\partial x} &= -\frac{1}{\rho} \frac{\partial p}{\partial x} + \nu \left(\frac{\partial^2 u}{\partial x^2} + \frac{\partial^2 u}{\partial y^2} + \frac{\partial^2 u}{\partial z^2} \right) + \frac{1}{3} \nu \frac{\partial}{\partial x} \left(\frac{\partial u}{\partial x} \right), \\ 0 &= -\frac{1}{\rho} \frac{\partial p}{\partial y} + \frac{1}{3} \nu \frac{\partial}{\partial y} \left(\frac{\partial u}{\partial x} \right), \quad 0 = -\frac{1}{\rho} \frac{\partial p}{\partial z} + \frac{1}{3} \nu \frac{\partial}{\partial z} \left(\frac{\partial u}{\partial x} \right), \end{aligned}$$

and the equation of continuity

$$\frac{\partial \rho}{\partial t} + \frac{\partial (\rho u)}{\partial x} = 0.$$

If, furthermore, we are restricted to the case of the steady flow of a noncompressible liquid ($\frac{\partial u}{\partial t} = 0$, $\rho = \text{const}$), then from the equation of continuity ensues the invariability of the velocity in the direction of flow $\partial u / \partial x = 0$, and from the latter two equations of motion - the pressure constancy in the transverse directions: $\partial p / \partial y = 0$, $\partial p / \partial z = 0$. Then from the first equation of motion we will obtain

$$\frac{dp}{dx} = \mu \left(\frac{\partial^2 u}{\partial y^2} + \frac{\partial^2 u}{\partial z^2} \right).$$

Let the laminar flow of a viscous noncompressible liquid be plane-parallel, whereupon the rates of flow in the direction of the z-axis

do not change $\partial u / \partial z = 0$. Then in the first equation of motion only tangential viscous stresses which act in plane (x, y) will be preserved:

$$\dot{\epsilon}_x = 0, \quad \tau_{xx} = 0 \quad \text{and} \quad \tau_{yx} = \mu \frac{du}{dy}. \quad (71)$$

Relationship (71) expresses Newton's law of viscous friction in the simplest form; differentiating (71), we obtain

$$\frac{\partial \tau_{yx}}{\partial y} = \mu \frac{d^2 u}{dy^2} = \mu \frac{d^2 u}{dy^2}.$$

Then the first of the equations of motion takes the form

$$\frac{dp}{dx} = \mu \frac{d^2 u}{dy^2}. \quad (72a)$$

Let us examine the plane-parallel laminar flow of a viscous noncompressible liquid in a channel formed by two infinite parallel plates.

If the distance between the plates is equal to $2b$ and the origin of the coordinates lies on the axis of the channel (Fig. 2.6), then as a boundary condition of the task it is possible to accept the condition of the adhesion of the liquid to the wall:

$$u = 0 \quad \text{with} \quad y = \pm b. \quad (72b)$$

Integrating differential equation (72a), we have

$$\frac{dp}{dx} y + C_1 = \mu \frac{du}{dy}. \quad (72c)$$

From the symmetry condition it follows that in the median plane

$(y = 0) \frac{du}{dy} = 0$, and this means $C_1 = 0$.

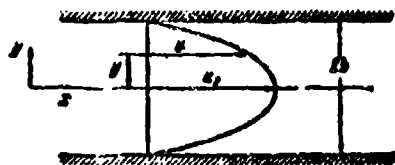


Fig. 2.6. Plane-parallel flow in a channel.

Now integrating equation (72c), we obtain

$$\frac{1}{2} \frac{dp}{dx} y^2 + C_1 = \mu u,$$

whence on the basis of (72b) we have

$$C_1 = -\frac{1}{2} \frac{dp}{dx} b^2,$$

and consequently,

$$u = \frac{1}{2} \frac{1}{\mu} \frac{dp}{dx} (y^2 - b^2) \quad (72d)$$

The rate of flow on the axis of the channel (with $y = 0$)

$$u_0 = -\frac{1}{2\mu} \frac{dp}{dx} b^2. \quad (72e)$$

After dividing term by term equality (72d) by (72e), we obtain

$$\frac{u}{u_0} = 1 - \frac{y^2}{b^2}. \quad (73a)$$

From (73a) it follows that the dimensionless velocity profile with the laminar motion of a liquid in a flat channel does not depend either on the value of the viscosity or on the value of the longitudinal pressure gradient and is a quadratic parabola.

Using the condition of the constancy of the fluid flow rate it is possible, on the strength of (73a), to determine the so-called "mean rate of flow" in the channel

$$u_0 = \frac{\int_0^b u dy}{b} = u_0 \int_0^1 \frac{u}{u_0} d\left(\frac{y}{b}\right) = u_0 \int_0^1 \left(1 - \frac{y^2}{b^2}\right) d\frac{y}{b} = \frac{2}{3} u_0. \quad (73b)$$

We compute the pressure gradient along the channel. For this, we determine from (73a) the second derivative of the rate in the transverse direction

$$\frac{d^2 u}{dy^2} = -\frac{2u_0}{b^2}$$

and we substitute this value in (72a)

$$\frac{dp}{dx} = -\frac{2\mu u_p}{b^3}.$$

Thus, the losses of pressure with a laminar flow of a liquid in a flat channel are proportional to the rate and inversely proportional to the square of the height of the channel. The pressure change on a section of finite length $x = l$ equals

$$\Delta p = -\frac{2\mu u_p l}{b^3}, \quad (74)$$

or in dimensionless form

$$\frac{\Delta p}{\rho \frac{u_p^2}{2}} = -\frac{16\mu}{\rho u_p h} \frac{l}{h}.$$

Here $h = 2b$ is the full height of the channel. Replacing maximum speed by the average with the aid of (73b), we obtain of known Hardy formula

$$\Delta p = -\lambda \frac{l}{h} \rho \frac{u_{cp}^2}{2}, \quad (75)$$

in which the loss factor for friction

$$\lambda = \frac{24}{R_h} \quad (76)$$

is expressed as a Reynolds number determined for the average rate and height of the channel

$$R_h = \frac{\rho u_{cp} h}{\mu}. \quad (77)$$

The minus sign in formula (75) indicates that the pressure along the channel decreases.

After calculating the value of the transverse gradient of the rate at the wall ($y = b$), with the aid of (73a) we find from (71) the friction stress at the wall

$$\tau_w = -\frac{2\mu u_0}{h} = -\frac{6\mu u_0 c_f}{h} \quad (78)$$

or in dimensionless form

$$c_f = \frac{\tau_w}{\frac{\rho u_0^2}{2}} = -\frac{12\mu}{\rho u_0 h} = -\frac{12}{Re} \quad (79)$$

The value c_f is called the *surface friction coefficient*. Values τ_w and c_f can also be determined directly from (75) if one considers that the force of the difference in pressures which acts on a column of liquid with a height h and length l , should be balanced by the force of friction applied to walls):¹

$$\tau_w 2l = \Delta p h.$$

Hence

$$\tau_w = \frac{1}{2} \Delta p \frac{h}{l} = -\frac{\lambda}{2} \rho \frac{u_0^2}{2}. \quad (80)$$

i.e.,

$$c_f = \frac{\lambda}{2}.$$

Differential equation (72a) also describes the laminar flow between two parallel walls of which one moves in its plane at a rate of U , and the other is fixed (Couette flow).

§ 9. The Equations of Motion of an Ideal Fluid

The analysis of the Navier-Stokes equations of motion conducted by Prandtl back in 1904 showed that in the case of a liquid of

¹The velocity profile in the transverse cross section is stable and the liquid density is invariable and, consequently, the total momentum along the slot is constant.

low viscosity (water, air, etc.) with sufficiently large values of Reynolds number the influence of viscosity is felt only in a thin layer adjacent to the surface of the body being flowed around - the boundary layer).¹ Outside this layer the role of the viscous forces turns out to be so small that the corresponding terms in the Navier-Stokes equations (26) or (27) can be disregarded.

In that case we obtain the equations of motion of an ideal compressible liquid

$$\rho \frac{dw}{dt} = X - \frac{\partial p}{\partial x}, \quad \rho \frac{dv}{dt} = Y - \frac{\partial p}{\partial y}, \quad \rho \frac{dw}{dt} = Z - \frac{\partial p}{\partial z}, \quad (81)$$

or

$$\rho \frac{dW}{dt} = R - \text{grad } p. \quad (82)$$

Since in many instances under these conditions heat-transfer is also substantially exhibited only in the boundary layer, in the remaining part of the gas flow according to the equation of energy (50)

$$\rho g \frac{dl_0}{dt} = A \frac{\partial p}{\partial x} \quad (83)$$

and, in particular, with steady motion

$$l_0 = \text{const.} \quad (84)$$

But in the absence of friction and heat exchange in gas an ideal adiabatic process is achieved, in connection with which instead of the equation of energies it is possible to utilize the equation of the ideal adiabatic curve

$$\frac{p}{\rho^\gamma} = \text{const.} \quad (85)$$

¹For more detail about the boundary layer, see Chapter VI.

In the case where the liquid is ideal and incompressible ($\rho = \text{const}$), the task of the integration of the equations of motion (81) is greatly simplified. This was also indicated for the first time by Euler, whose name the equations of motion bear (81). The analytical methods for the solution of the equations of motion of an ideal fluid received great development, and at present a great number of cases of flow around bodies have been studied (wings, wing trusses, bodies of axisymmetric form, all possible channels, etc.). From the aggregate of the works in this direction an important direction of contemporary mechanics was formed - classical hydrodynamics.

In conjunction with the boundary-layer theory, the hydrodynamics of an ideal fluid became a powerful means for the solution of problems of the aerodynamics of aircraft, hydrodynamics of a ship, mechanics of the motion of a liquid along tubes, and many others.

For example in the case of the flow around a body of smooth form with large values of Reynolds number, the boundary layer is so thin that the pressure distribution over the body surface is determined in the first approximation from the equations of motion of an ideal fluid. Further, as will be shown in Chapter VI, from the known distribution of pressures it is possible to calculate the boundary layer and to find the friction stresses at the surface. If necessary it is possible, in the second approximation, to calculate the boundary layer effect on the external flow around the body (beyond the limits of a layer) and then to determine the friction stress more accurately. But frequently they do not resort to the calculation of the second approximation, since the first approximation gives satisfactory results.

The solution of the equations of motion (81) has an especially simple form in the case of the vortex-free motion of an ideal fluid when vorticity is equal to zero (see expressions (2)), i.e.,

$$\left. \begin{aligned} \omega_x &= \frac{1}{2} \left(\frac{\partial w}{\partial y} - \frac{\partial v}{\partial z} \right) = 0, \\ \omega_y &= \frac{1}{2} \left(\frac{\partial u}{\partial z} - \frac{\partial w}{\partial x} \right) = 0, \\ \omega_z &= \frac{1}{2} \left(\frac{\partial v}{\partial x} - \frac{\partial u}{\partial y} \right) = 0. \end{aligned} \right\} \quad (86)$$

From conditions (86) it follows that some function ϕ exists whose partial derivatives in terms of coordinates x, y, z are equal to the corresponding velocity components, i.e.,

$$u = \frac{\partial \phi}{\partial x}, \quad v = \frac{\partial \phi}{\partial y}, \quad w = \frac{\partial \phi}{\partial z}.$$

Actually, substituting these values in (86), we obtain the identities

$$\frac{\partial w}{\partial y} - \frac{\partial v}{\partial z} = \frac{\partial^2 \phi}{\partial z \partial y} - \frac{\partial^2 \phi}{\partial y \partial z} = 0 \quad \text{etc.}$$

Function ϕ is customarily called the *velocity potential*, and vortex-free motion - *potential*.

Let us replace on the left side of the first of equations (81) the full velocity derivative by the sum of its partial derivatives and let us add to it the sum equal to zero

$$v \frac{\partial v}{\partial x} + w \frac{\partial w}{\partial x} - v \frac{\partial v}{\partial x} - w \frac{\partial w}{\partial x}.$$

Then this equation is reduced to the form

$$\frac{\partial u}{\partial x} + \frac{1}{2} \frac{\partial W^2}{\partial x} - 2(v\omega_x - w\omega_x) = X - \frac{1}{\rho} \frac{\partial p}{\partial x}, \quad (87a)$$

where $W = \sqrt{u^2 + v^2 + w^2}$ is the full rate of flow of the liquid.

In a similar manner, it is possible to transform the equations of motion along the remaining two coordinate axes:

$$\left. \begin{aligned} \frac{\partial v}{\partial x} + \frac{1}{2} \frac{\partial W^2}{\partial y} - 2(w\omega_x - u\omega_x) &= Y - \frac{1}{\rho} \frac{\partial p}{\partial y}, \\ \frac{\partial w}{\partial x} + \frac{1}{2} \frac{\partial W^2}{\partial z} - 2(u\omega_y - v\omega_x) &= Z - \frac{1}{\rho} \frac{\partial p}{\partial z}. \end{aligned} \right\} \quad (87b)$$

System of equations (87) is called the Lamb-Gromeko equations.
If the velocity potential ϕ , the potential of volume forces θ

$$\begin{aligned} \frac{\partial \phi}{\partial x} &= u, & \frac{\partial \phi}{\partial y} &= v, & \frac{\partial \phi}{\partial z} &= w, \\ \frac{\partial \theta}{\partial x} &= X, & \frac{\partial \theta}{\partial y} &= Y, & \frac{\partial \theta}{\partial z} &= Z \end{aligned}$$

and also some function $P(x, y, z, t)$ that satisfies the conditions

$$\frac{\partial P}{\partial t} = \frac{1}{\rho} \frac{\partial p}{\partial x}, \quad \frac{\partial P}{\partial y} = \frac{1}{\rho} \frac{\partial p}{\partial y}, \quad \frac{\partial P}{\partial z} = \frac{1}{\rho} \frac{\partial p}{\partial z};$$

exist, then equations (87) are written as follows:

$$\left. \begin{aligned} \frac{\partial}{\partial x} \left(\frac{\partial \phi}{\partial t} \right) + \frac{1}{2} \frac{\partial W^2}{\partial x} &= \frac{\partial \theta}{\partial x} - \frac{\partial P}{\partial x}, \\ \frac{\partial}{\partial y} \left(\frac{\partial \phi}{\partial t} \right) + \frac{1}{2} \frac{\partial W^2}{\partial y} &= \frac{\partial \theta}{\partial y} - \frac{\partial P}{\partial y}, \\ \frac{\partial}{\partial z} \left(\frac{\partial \phi}{\partial t} \right) + \frac{1}{2} \frac{\partial W^2}{\partial z} &= \frac{\partial \theta}{\partial z} - \frac{\partial P}{\partial z}. \end{aligned} \right\} \quad (88)$$

Used here is the condition of the independence of a mixed derivative of the order of differentiation

$$\frac{\partial u}{\partial t} = \frac{\partial}{\partial t} \left(\frac{\partial \phi}{\partial x} \right) = \frac{\partial}{\partial x} \left(\frac{\partial \phi}{\partial t} \right) \quad \text{etc.}$$

If we multiply the first of equations (88) by dx , the second - by dy , the third - by dz and then add them term by term, then we will obtain

$$\begin{aligned} & \left[\frac{\partial}{\partial x} \left(\frac{\partial \phi}{\partial t} \right) dx + \frac{\partial}{\partial y} \left(\frac{\partial \phi}{\partial t} \right) dy + \frac{\partial}{\partial z} \left(\frac{\partial \phi}{\partial t} \right) dz \right] + \frac{1}{2} \left[\frac{\partial W^2}{\partial x} dx + \frac{\partial W^2}{\partial y} dy + \frac{\partial W^2}{\partial z} dz \right] = \\ & = \left[\frac{\partial \theta}{\partial x} dx + \frac{\partial \theta}{\partial y} dy + \frac{\partial \theta}{\partial z} dz \right] - \left[\frac{\partial P}{\partial x} dx + \frac{\partial P}{\partial y} dy + \frac{\partial P}{\partial z} dz \right]. \end{aligned} \quad (89)$$

Each of the brackets in this expression is a total differential; therefore, instead of (89) we have

$$d \left(\frac{\partial \phi}{\partial t} \right) + d \left(\frac{W^2}{2} \right) + dP = d\theta. \quad (90)$$

This brings us to the so-called Lagrange integral:

$$P + \frac{w^2}{2} + \frac{\partial \varphi}{\partial t} = 0 + C(t), \quad (90a)$$

where $C(t)$ is the arbitrary function of time.

Since by definition

$$P = \int \frac{dp}{\rho}, \quad (90b)$$

the Lagrange integral can be presented in the following form:

$$\int \frac{dp}{\rho} + \frac{w^2}{2} + \frac{\partial \varphi}{\partial t} = 0 + C(t), \quad (90c)$$

In the case of steady motion ($\frac{\partial \varphi}{\partial t} = 0$, $C(t) = \text{const}$) we have

$$\int \frac{dp}{\rho} + \frac{w^2}{2} = 0 + \text{const.}$$

If the liquid is barotropic, i.e., the density is a one-valued function of pressure, then integral (90c) can always be calculated; with steady motion of a noncompressible liquid ($\rho = \text{const}$), Lagrange's integral appears thus;

$$\frac{p}{\rho} + \frac{w^2}{2} = 0 + \text{const.}$$

An important feature of Lagrange's integral is the fact that it is valid in the entire space filled by the liquid.

If a velocity potential does not exist, i.e., the motion is vortical, then the equations of motion of an ideal fluid (81) also can be integrated, but only along the flow line and under the condition of steady motion.

With steady motion, the elementary displacement of a particle along the flow line $ds = w dt$ or in projections to coordinate axes x -, y -, z

$$dx = u dt, \quad dy = v dt, \quad dz = w dt.$$

Let us now multiply each of equations (81) by the corresponding projection of elementary displacement along the flow line and let us add these three equations:

$$ndu + vdv + wdw = Xdx + Ydy + Zdz - \left(\frac{1}{\rho} \frac{\partial p}{\partial x} dx + \frac{1}{\rho} \frac{\partial p}{\partial y} dy + \frac{1}{\rho} \frac{\partial p}{\partial z} dz \right).$$

The left side of this equation is the total differential from $(W^2/2)$. If there is a potential of the force function ($d\phi = Xdx + Ydy + Zdz$) and the liquid is barotropic ($\frac{dp}{\rho} = dP$), then this equation can be written in the form

$$d\left(\frac{W^2}{2}\right) = d\phi - dP.$$

Integrating, we come to Bernoulli's known integral:

$$P + \frac{W^2}{2} = \phi + \text{const}$$

or

$$\int \frac{dp}{\rho} + \frac{W^2}{2} - \phi = \text{const.}$$

If the force field is caused only by the earth's gravity and the z-axis is directed vertically upward, then the projections of the force which acts on the unit of mass

$$X=0, \quad Y=0, \quad Z=-g=\frac{d\phi}{dz}.$$

In such a case Bernoulli's integral takes the form already known from Chapter I

$$\int \frac{dp}{\rho} + \frac{W^2}{2} + gz = \text{const} \quad (91)$$

or for a noncompressible liquid

$$\frac{p}{\rho} + \frac{W^2}{2} + gz = \text{const.} \quad (91a)$$

Let us recall again that unlike the Lagrange integral, Bernoulli's integral is valid only along the flow line, i.e., the value of the constant in right side of (91) for different flow lines is dissimilar. Only in the case of a *steady potential* flow does Bernoulli's integral convert to a Lagrange integral and is made suitable for any point of space.

§ 10. Plane Steady Motions of an Ideal Compressible Liquid

The plane (two-dimensional) steady motions of an ideal compressible liquid are described by the following system of differential equations:

by the equations of motion

$$\left. \begin{aligned} \rho u \frac{\partial u}{\partial x} + \rho v \frac{\partial u}{\partial y} &= -\frac{\partial p}{\partial x}, \\ \rho u \frac{\partial v}{\partial x} + \rho v \frac{\partial v}{\partial y} &= -\frac{\partial p}{\partial y} \end{aligned} \right\} \quad (92)$$

(here volume forces are omitted).

By the equation of continuity

$$\frac{\partial(\rho u)}{\partial x} + \frac{\partial(\rho v)}{\partial y} = 0. \quad (93)$$

By the equation of the ideal adiabatic process (instead of the equation of energy)

$$\frac{p}{\rho^\gamma} = \text{const.} \quad (94)$$

In a noncompressible liquid ($\rho = \text{const}$) equation (94) drops out and the equation of continuity is simplified:

$$\frac{\partial u}{\partial x} + \frac{\partial v}{\partial y} = 0. \quad (95)$$

If there is a velocity potential ϕ , then

$$\frac{\partial \phi}{\partial x} = u, \quad \frac{\partial \phi}{\partial y} = v \quad (95a)$$

Substituting (95a) in (95), we obtain for the velocity potential the Laplace equation:

$$\frac{\partial^2 \phi}{\partial x^2} + \frac{\partial^2 \phi}{\partial y^2} = 0. \quad (95b)$$

to the solution of which the task of the construction of the plane-parallel potential flow of an ideal noncompressible liquid is also reduced. In this case, the boundary condition of impenetrability is utilized for the liquid of the firm limit of the body being flowed around $W_{nw} = 0$, i.e., the equality to zero of the component of the velocity vector normal to it near the wall.

With motion along the flow line, the particle of liquid during time dt covers the path $dS = W dt$ or, in projections to coordinate axes, $dx = u dt$, $dy = v dt$. Excluding the time from this, we obtain the equation of the flow line

$$\frac{dx}{u} = \frac{dy}{v}$$

or

$$u dy - v dx = 0. \quad (96)$$

As is known from mathematics, if the following equality is satisfied

$$\frac{\partial v}{\partial y} = -\frac{\partial u}{\partial x},$$

then the left side of equation (96) is a total differential of some function $\Psi(x, y)$. For the potential flows of a noncompressible liquid, this condition, as follows from the equation of continuity (95), is always satisfied.

Thus, the differential equation of the flow line can be written in the following manner:

$$d\psi = u dy - v dx = 0$$

or

$$\psi(x, y) = \text{const.} \quad (96a)$$

Function ψ whose value along the flow line is kept constant is called the stream function.

In accordance with (96a), the velocity component can be expressed as partial derivatives of the stream function

$$u = \frac{\partial \psi}{\partial y}, \quad v = -\frac{\partial \psi}{\partial x}. \quad (97)$$

If we substitute (97) into the equation of continuity (95), then it will become the identity:

$$\frac{\partial^2 \psi}{\partial x \partial y} - \frac{\partial^2 \psi}{\partial y \partial x} = 0.$$

The physical sense of the stream function is very simple. Let us draw two close flow lines in the flow through arbitrary points 1 and 2 (Fig. 2.7). It is not difficult to see that the volume fluid flow rate in the plane flow between the adjacent flow lines is equal to

$$dV = u dx - v dy = d\psi.$$

Thus,

$$V = \int_1^2 (u dy - v dx) = \psi(x_2, y_2) - \psi(x_1, y_1)$$

i.e., the per-second volume fluid flow rate which flows between flow lines 1 and 2 is equal to the difference in values of the stream function on these lines.

In view of the impenetrability of the flow lines for a liquid, the value of the stream function on each flow line is constant.

Comparing (97) and (95a), we see that the families of the flow lines ($\Phi = \text{const}$) and the lines of equal value of velocity potential ($\phi = \text{const}$) form the orthogonal grid of the curves.

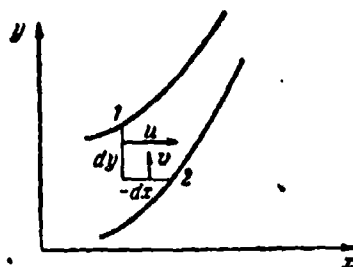


Fig. 2.7. For determining of the fluid flow rate between adjacent flow lines.

If any two plane-parallel steady flows of an ideal noncompressible liquid are known, i.e., for each of these flows the value and the direction of velocity at each point of the plane are known, then it is possible to construct the new resulting flow which will arise as a result of the *superposition* of these two known flows. For this, at each point of the plane it is necessary to construct the velocity vectors of each of the two known flows. The sum of these vectors is the velocity vector of the resulting flow.

Let us give a simple method for the graphic determination of flow lines of the resulting flow from the flow lines of the superimposed flows. For this, let us draw on the drawing the flow line any two plane flows (Fig. 2.8). The intersection of these flow lines forms a grid. The flow lines should be drawn so that the sides of the cells of this grid depict in a specific scale the velocity vectors of the superimposed flows at a particular point.¹

¹It is easy to show that for the satisfaction of this condition it suffices to draw the flow lines so that the flow rate between any two adjacent flow lines for both flows would be identical.

Then for obtaining the flow lines of the resulting flow it suffices to connect the consecutive points of intersection of the flow lines of the superimposed flows with each other, i.e., to draw a *diagonal* in each cell of the grid. These diagonals depict, in the same scale, the velocity vectors of the resulting flow at the corresponding points (Fig. 2.8).

In the case of the compressible liquid (gas) it is convenient to convert equations (92)-(94), introducing in them the speed of sound $a = \sqrt{dp/d\rho}$. For this let us present the equation of continuity (93) in the form

$$u \frac{\partial \rho}{\partial x} + v \frac{\partial \rho}{\partial y} + \rho \left(\frac{\partial u}{\partial x} + \frac{\partial v}{\partial y} \right) = 0 \quad (98)$$

and let us express the density gradients through the pressure gradients and the speed of sound:

$$\begin{aligned} \frac{\partial \rho}{\partial x} &= \frac{d\rho}{dp} \frac{\partial p}{\partial x} = \frac{1}{a^2} \frac{\partial p}{\partial x}, \\ \frac{\partial \rho}{\partial y} &= \frac{d\rho}{dp} \frac{\partial p}{\partial y} = \frac{1}{a^2} \frac{\partial p}{\partial y}. \end{aligned} \quad (99)$$

Expressing the pressure gradients in (92b) with the aid of (92) through the velocities, we obtain

$$\begin{aligned} \frac{\partial p}{\partial x} &= -\frac{\rho}{a^2} \left(u \frac{\partial u}{\partial x} + v \frac{\partial u}{\partial y} \right), \\ \frac{\partial p}{\partial y} &= -\frac{\rho}{a^2} \left(u \frac{\partial v}{\partial x} + v \frac{\partial v}{\partial y} \right). \end{aligned} \quad (99a)$$

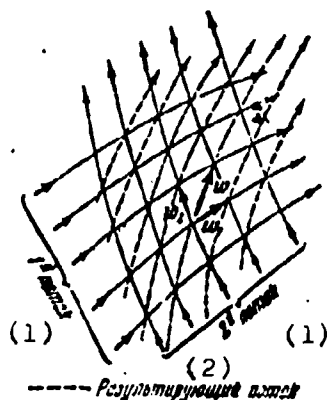


Fig. 2.8. The graphic addition of flows.
KEY: (1) Flow; (2) Resulting flow.

Substituting (99a) and (95a) into the equation of continuity (93), we have

$$(a^2 - u^2) \frac{\partial^2 \varphi}{\partial x^2} - 2uv \frac{\partial^2 \varphi}{\partial x \partial y} + (a^2 - v^2) \frac{\partial^2 \varphi}{\partial y^2} = 0. \quad (100)$$

We derived the fundamental differential equation of gas dynamics for a plane potential steady flow.

In the particular case of low rates of flow of gas ($u \ll a$, $v \ll a$) equation (100) converts to the Laplace equation (95b) which determines the motion of a noncompressible liquid.

For the construction of a velocity field in a supersonic flow, equation (100) is usually solved by the method of characteristics.

In the study of flow around thin bodies at low angles of attack both in a subsonic and supersonic flow, equation (100) is solved by the method of slight disturbances (linearization method).

§ 11. Velocity Circulation

In a steady plane of motion the particle speed w is the function of two coordinates

$$\mathbf{w} = \mathbf{w}(x, y)$$

This vector function determines the *velocity field*.

In the study of different cases of gas flows, in particular of the flow around wings and other bodies, it is useful to introduce some value connected with the velocity field of the flow in question and called the *velocity circulation*.

By the velocity circulation Γ over a closed loop L we understand the integral

$$\oint_L \mathbf{w} \cos(\mathbf{w}, \mathbf{n}) dL \quad (101)$$

where w is the value of the velocity vector, (w, \hat{l}) - the angle between the velocity vector and the direction of the loop at a given point, dl - the element of length of the arc of the loop. The sign L shows that the integral is taken on a closed loop.

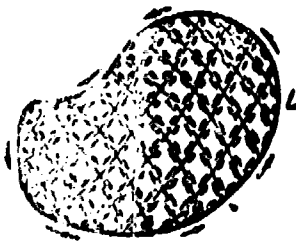


Fig. 2.9. For the summation of circulation.

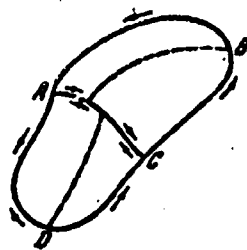


Fig. 2.10. For the summation of circulation.

Thus, the velocity circulation is the limit of the sum of the products of the velocity projection tangential to the outline times the corresponding element of length of the loop. We will consider the counterclockwise direction of the circuit the positive direction of the circuit on the loop.¹

From the very definition of circulation it follows that the circulation through any loop L can be expressed in the form of the sum of the circulations through the separate cells of an arbitrary grid which covers the area limited by the loop L (Fig. 2.9). In fact, let us examine some closed loop $ADCBA$. Let arbitrary arc AC divide the area limited by this loop into two cells: $ACBA$ and $ABCA$ (Fig. 2.10). We express the circulation for each cell. For the first cell

$$\Gamma_{ACBA} = \oint_{ACBA} w \cos(w, \hat{l}) dl$$

¹Sometimes it is more convenient to consider the opposite direction positive.

In this case the integral of loop ACBA can be divided into two integrals: an integral of arc CBA and of arc AC. For the second cell

$$\Gamma_{ADCA} = \oint_{ADCA} w \cos(\widehat{w, \vec{l}}) dL$$

The integral of this loop is composed of the integrals of arc ADC and of arc CA. The sum of circulations for loops ACBA and ADCA is equal to the sum of four integrals, whereupon the integral of arc AC which enters the first circulation and the integral of arc CA which enters the second circulation cancel each other out since they represent the integral of the very same arc passable in opposite directions the (integrand in both integrals is one and the same). Thus the sum of circulations for loops ACBA and ADCA equals the sum of the integrals of arcs CBA and ADC, i.e., the integral of loop ADCBA. Thus,

$$\Gamma_{ACBA} + \Gamma_{ADCA} = \Gamma_{ADCBA}$$

Thus, the sum of the circulations for the loops of two adjacent cells is equal to the circulation for the entire loop L. If each of the cells ABCA and ACDA is divided into two more cells, then for each of them it is possible to completely repeat the above given consideration. Continuing the process of division further and repeating the same considerations each time, we come to the above-expressed position about the summation of circulations (see Fig. 2.9).

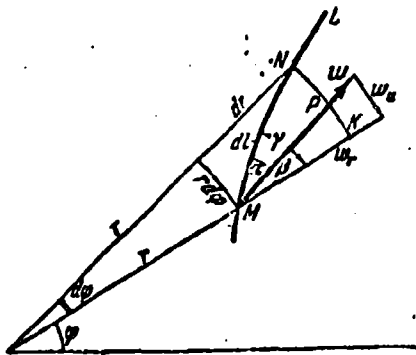


Fig. 2.11. For determining the connection between vortex and circulation.

Now we express the expression under the integral sign in formula (101) with the use of polar coordinates (r, ϕ) . For this let, us examine Fig. 2.11. Let $M(r, \phi)$ be a point of an arbitrary loop L , $dl = MN$ - an element of the arc of this loop, w - the velocity vector at point M with projections w_r and w_ϕ . Let us designate angle $(w, \widehat{L}) = \angle NMP = \alpha$, $\angle PMK = \beta$, $\angle NMPK = \gamma$. From the figure one can see that

$$\alpha = \gamma - \beta$$

Therefore

$$\cos(\widehat{w, L}) = \cos \alpha = \cos(\gamma - \beta) = \cos \gamma \cos \beta + \sin \gamma \sin \beta$$

But from the small curvilinear right triangle MNK we obtain

$$\begin{aligned} \cos \gamma &= \frac{MK}{MN} = \frac{dr}{dl}, \\ \sin \gamma &= \frac{NK}{MN} = r \frac{d\gamma}{dl}. \end{aligned}$$

Further, it is obvious, that

$$\cos \beta = \frac{w_r}{w}, \quad \sin \beta = \frac{w_\phi}{w}.$$

Substituting these values in the expression for $\cos(\widehat{w, L})$, we find

$$\cos(\widehat{w, L}) = \frac{dr}{dl} \frac{w_r}{w} + \frac{r}{dl} \frac{d\gamma}{dl} \frac{w_\phi}{w}.$$

Then the expression under the integral sign in formula (101) assumes the form

$$w \cos(\widehat{w, L}) dl = w dl \frac{w_r dr + w_\phi r d\gamma}{w dl} = w_r dr + w_\phi r d\gamma.$$

Thus, in polar coordinates we obtain the following formula for the velocity circulation

$$\Gamma = \oint w_r dr + w_\theta r d\varphi. \quad (102)$$

The elementary displacement of a particle of liquid or gas in general, as noted, consists of three parts: forward displacement, rotation, and deformation of the particle. The motions in which the rotation of particles is absent are called vortex-free and motion with rotation - vortical.

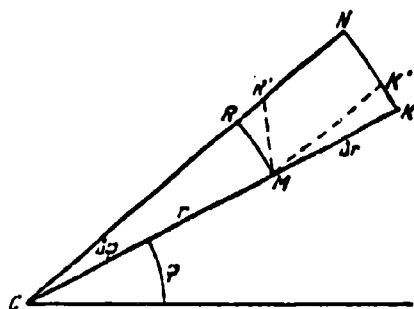


Fig. 2.12. For the determination of vorticity in polar coordinates.

With the motion of a liquid particle MKNR (Fig. 2.12) with rotation, its form changes in general. Suppose that after a small time interval dt faces MR and MK occupy position MR' and MK'. The displacement of the particle as a whole, determined by the forward velocity, is not important in this question. We determine the angular velocities of the rotation of points R and K relative to point M. If the velocity component at point M is designated by w_r and w_θ , then velocity components at point K are equal to

$$w_r + \frac{\partial w_r}{\partial r} \Delta r \quad \text{and} \quad w_\theta + \frac{\partial w_\theta}{\partial r} \Delta r,$$

and the components of relative velocity of point K (relative to point M) $\frac{\partial w_r}{\partial r} \Delta r$ and $\frac{\partial w_\theta}{\partial r} \Delta r$. It is obvious that the rotation of point K relative to point M creates only the second of these components

since the first is perpendicular to the direction of rotation (is directed along MK). Thus, the circular velocity of rotation of point K relative to M due to which path KK' is made equals $\frac{\partial w_\theta}{\partial r} \Delta r$, and the relative angular velocity of rotation of point K near the center M is equal to

$$\omega_K = \frac{\frac{\partial w_\theta}{\partial r} \Delta r}{\Delta r} = \frac{\partial w_\theta}{\partial r}.$$

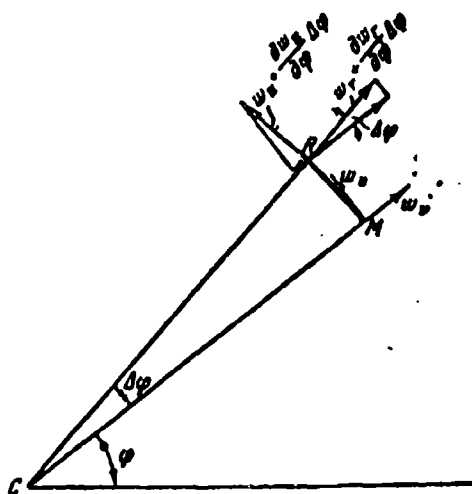


Fig. 2.13. For the determination of increases in velocity in polar coordinates.

The velocity components at point R equal (Fig. 2.13)

$$w_r + \frac{\partial w_r}{\partial r} \Delta r \quad \text{and} \quad w_\theta + \frac{\partial w_\theta}{\partial r} \Delta r.$$

The rotation of point R relative to M occurs in a direction perpendicular to chord MR. By virtue of the smallness of angle $\Delta\phi$ it is possible to consider chord MR perpendicular to radius CM, and the chord length MR ~ equal to the arc length MR. Then the direction of rotation of point R relative to M is parallel to radius CM. We find the projections of both velocity components of point R for the direction of rotation. Figure 2.13 shows that these projections are respectively equal to

$$-\left(w_r + \frac{\partial w_r}{\partial r} \Delta r\right) \cos \Delta\phi \quad \text{and} \quad \left(w_\theta + \frac{\partial w_\theta}{\partial r} \Delta r\right) \sin \Delta\phi.$$

The minus sign at the first projection is accepted because this projection creates clockwise rotation, and counterclockwise rotation is considered positive. Considering approximately $\Delta\phi \approx 1$ and $\sin \Delta\phi \approx \Delta\phi$ and rejecting the term of the second order of smallness which has $(\Delta\phi)^2$, as a factor we obtain the following values of the projections in question:

$$-(w_r + \frac{\partial w_r}{\partial \varphi} \Delta\varphi) \text{ and } w_u \Delta\varphi.$$

In order to obtain the circular rotational velocity of point R relative to M, from the obtained expressions, obviously, it is necessary to subtract the projections of the velocity components at the very point M to the same direction CM. But projection of w_r to CM equals the value w_r itself and the projection of w_u to CM is equal to zero. Thus, the circular velocity of point R relative to M, which causes displacement RR' (Fig. 2.12), is expressed thus:

$$w_u \Delta\varphi - (w_r + \frac{\partial w_r}{\partial \varphi} \Delta\varphi - w_r).$$

Then the relative angular velocity of rotation of point R near center M equals

$$\omega_R = \frac{w_u \Delta\varphi - \frac{\partial w_r}{\partial \varphi} \Delta\varphi}{MR} = \frac{w_u}{r} - \frac{1}{r} \frac{\partial w_r}{\partial \varphi},$$

since

$$MR \approx r \Delta\varphi.$$

As the mean angular velocity of a particle relative to point M we take the arithmetic mean of the angular velocities of the extreme points R and K:

$$\omega_{cp} = \frac{\omega_R + \omega_K}{2} = \frac{1}{2} \left(\frac{\partial w_u}{\partial r} + \frac{w_u}{r} - \frac{1}{r} \frac{\partial w_r}{\partial \varphi} \right).$$

It is convenient to convert this expression to the form

$$\omega_z = \frac{1}{2r} \left(r \frac{\partial w_\theta}{\partial r} + w_\theta - \frac{\partial x_r}{\partial \varphi} \right) = \frac{1}{2r} \left[\frac{\partial (w_\theta r)}{\partial r} - \frac{\partial w_r}{\partial \varphi} \right]. \quad (103)$$

Formula (103) determines the value of the *vorticity* (see § 1) in *polar coordinates*.

In hydrodynamics it is proved that the motions of an ideal fluid, having been vortex-free at some point in time, always remain vortex-free. But if motion was vortical at some moment, it will be always vortical. The arising of vortices should be caused by special reasons, for example, by the viscosity of a gas or liquid.

A condition for the absence of vortices is

$$\omega_z = 0 \quad (104)$$

or in polar coordinates

$$\frac{\partial (w_\theta r)}{\partial r} - \frac{\partial w_r}{\partial \varphi} = 0. \quad (105)$$

In order to explain the connection between the concepts of vortex and circulation, we transform the integrand in formula (102). Let us examine surface element MKNR bounded by coordinate lines MK, MR and RN, KN (Fig. 2.14).

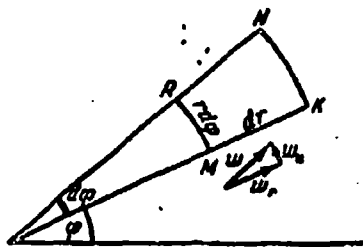


Fig. 2.14. For the determination of circulation in polar coordinates.

Let us compose the expression under the integral sign for circulation over the loop MKNR. It is obvious that we will obtain

$$d\Gamma = w_r dr + \left(w_\theta + \frac{\partial w_\theta}{\partial r} dr \right) (r + dr) d\varphi - \left(w_r + \frac{\partial w_r}{\partial \varphi} d\varphi \right) dr - w_\theta r d\varphi.$$

Here w_r is the tangential projection of the velocity on segment $MK = dr$, $w_\theta + \frac{\partial w_\theta}{\partial r} dr$ - the tangential projection of the velocity on arc $KN = (r + dr) d\varphi$, $w_r + \frac{\partial w_r}{\partial \varphi} d\varphi$ - the tangential projection of the velocity on segment $NR = dr$ and w_θ - the tangential projection of the velocity on arc $RM = r d\varphi$.

With the last two terms, the minus sign is taken because the positive direction of the velocity on segment NR and on arc RM is opposite to the direction of the circuit over loop $MKNR$. Performing calculations and rejecting the term of the third order of smallness $\frac{\partial w_\theta}{\partial r} (dr)^2 d\varphi$ we obtain

$$d\Gamma = \left(r \frac{\partial w_\theta}{\partial r} + w_\theta - \frac{\partial w_r}{\partial \varphi} \right) dr d\varphi = \frac{1}{r} \left[\frac{\partial (r w_\theta)}{\partial r} - \frac{\partial w_r}{\partial \varphi} \right] r d\varphi dr.$$

Comparing this expression with expression (103) for vorticity ω and noting that the product $r d\varphi dr$ is the elementary area dF encompassed by loop $MKNR$, let us write the last expression in this form:

$$d\Gamma = 2\omega dF.$$

If we now divide the area included by arbitrary loop L into small elementary areas formed by the grid of coordinate lines (Fig. 2.15) and utilize the rule for the summation of circulations, then we obtain

$$\Gamma_L = \sum d\Gamma_i = \sum 2\omega_i dF_i$$

or, if we pass from sums to integrals:

$$\Gamma = \oint_L w_r dr + w_\theta r d\varphi = 2 \int_V \omega dF. \quad (106)$$

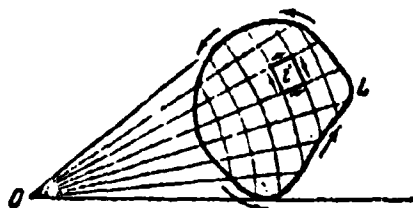


Fig. 2.15. For the summation of circulation and vorticity.

The obtained result expresses the unknown connection between vorticity and circulation.¹ If the value of the vortex is identical in all points: $\omega = \omega_0 = \text{const}$, then

$$\Gamma = 2\omega_0 \int_{\Omega} dF = 2\omega_0 F,$$

i.e., in this case the value of the circulation over some loop is equal to double the product of the value of the vortex times the area being included by the loop.

Let us examine the steady motion of a liquid. Circulation Γ with steady motion retains constant value over any fixed closed loop.²

Let us assume further that the motion is steady and vortex-free ($\omega = 0$). In this case, the circulation over any fixed loop is equal to zero. The latter conclusion, however, is correct only in the case when within a fixed loop only particles of liquid which accomplish vortex-free motion are found. Circulation over a fixed closed loop is different from zero if the loop encompasses a area within which is found, for example, a single vortex³ or the streamlined body.⁴

¹Formula (106) expresses the Stokes theorem for plane motion (see, for example, N. Ya. Fabrikant, Aerodynamics. "Science," M., 1964).

²In hydrodynamics it is proved for a very broad class of practically important motions that, as in the case of unsteady motion, the circulation along a closed loop is constant; however, in this case the so-called liquid loop is examined, i.e., the loop which consists of the same particles. The latter statement is called *Thompson's theorem*. From this theorem it follows that if a certain mass of liquid at zero time had vortex-free motion or rested, then also henceforth in this part of the liquid vortices will not arise, which was already mentioned above (see also the textbook by N. Ya. Fabrikant cited above in the first footnote).

³About a single vortex, see below - Example 2.

⁴As will be shown below, with the flow of a viscous liquid around a body vortices are formed in the flow.

Thus, we see that the arising of circulation is always connected with the formation of vortices in the flow of a liquid or gas.

Let us now examine some very simple examples of the motion of a liquid which make it possible to explain the physical sense of the concepts of vortex and circulation.

Example 1. The rotation of the liquid as a solid. Let the liquid rotate as a solid around the origin of coordinates with constant angular velocity ω . Then the value of the velocity at each point $w = \omega r$, where r is the distance of the point from the coordinate origin. We find the radial and circular velocity components. It is clear that in this case

$$w_r = 0, \quad w_\theta = w = \omega r.$$

Let us compose the expression for vorticity. According to formula (103)

$$\omega = \frac{1}{2r} \left[\frac{\partial(rw_\theta)}{\partial r} - \frac{\partial w_r}{\partial \theta} \right] = \frac{1}{2r} \frac{\partial}{\partial r} (r^2 \omega) = \omega.$$

The value of the vorticity in all points is identical and equal to the constant angular velocity of the rotation of the particles of liquid. This result was evident earlier since it follows directly from the very definition of a vortex.

Let us now find the value of circulation over a loop which encircles the origin of the coordinates. Let us take as such a loop a circle of radius r . From formula (102) we obtain

$$\Gamma = \oint w_r dr + w_\theta r d\theta = \int_0^{2\pi} \omega r^2 d\theta = 2\pi \omega r^2.$$

The value of the circulation is proportional to the square of the radius. Dividing it by the area of a circle F , we find

$$\frac{\Gamma}{F} = \frac{2\pi \omega r^2}{\pi r^2} = 2\omega = 2\omega$$

or

$$\Gamma = 2\pi R.$$

This equality illustrates the Stokes theorem (106); in this case, the value of circulation along the circumference is equal to twice the product of the constant value of the vortex ω times the area of the circle.

Example 2. Vortex-free circulating motion. As the second example, let us examine the plane motion of a liquid where the particles of liquid move along concentric circumferences around the coordinate origin at velocities inversely proportional to the distances of the particles from the coordinate origin so that the velocity at every point $w = c/r$, where c is constant. Here the radial and circular velocity components equal $w_u = w = c/r$. We find the value of the vortex:

$$\omega = \frac{1}{2r} \left[\frac{\partial}{\partial r} (r w_u) - \frac{\partial w_r}{\partial \varphi} \right] = \frac{1}{2r} \frac{\partial}{\partial r} \left(r \frac{c}{r} \right) = 0.$$

Thus, the value of the vortex at all points except the coordinate origin is equal to zero. In the coordinate origin ($r = 0$) the velocity is equal to infinity, i.e., the coordinate origin is mathematically a singular point. Physically, such motion is possible only outside some nucleus of finite radius r_0 . The nucleus can consist of a solid or of a liquid of the same or another density. Outside the nucleus the flow is vortex-free. On the surface of the nucleus the velocity has some finite quantity $w_0 = c/r_0$.

Let us find the value of circulation over a circumference with the center at the coordinate origin:

$$\Gamma = \oint_C \frac{c}{r} r d\varphi = \int_0^{2\pi} c d\varphi = \text{const};$$

in this case circulation over any circumference is a constant value. Since $w = c/r$, it is possible to write

$$\Gamma = \oint c \, dr = 2\pi r_0 w_0 = \text{const} = \Gamma_0, \text{ etc.}$$

where r_0 is the radius of the nucleus and w_0 is the velocity on its surface.¹ Thus, the velocity at any point

$$w = \frac{\Gamma_0}{2\pi r} = \frac{\Gamma}{2\pi r}.$$

The examined motion of a liquid is called *vortex-free circulating motion*, and the velocity field corresponding to it is called the *velocity field of a plane isolated vortex*. If we consider the fluid incompressible, then pressure

$$p = \text{const} - \frac{\rho w^2}{2} = \text{const} - \frac{\rho \Gamma^2}{8\pi^2 r^2}$$

decreases with a decrease in the distance from the coordinates origin, i.e., from the center of the vortex.

With $r_0 \rightarrow 0$ the nucleus converts to a point. This point is called *point isolated vortex*. Therefore, vortex-free circulating motion can be connected with a point vortex; the latter induces at each point of a plane a velocity perpendicular to the segment which connects this point with the vortex and equal in magnitude to $\Gamma/2\pi r$, where r is the length of the indicated segment, i.e., it induces vortex-free circulating motion with circulation Γ .



Fig. 2.16. Diagram of the flow around rounded and acute edges.

¹As it is not difficult to show, circulation over any closed loop which does not embrace the nucleus is equal to zero, i.e., the nucleus plays the role of a vortex.

Let us now note one important phenomenon which pertains to the flow around bodies by the flow of an ideal fluid. If the outline of the body being flowed around has a section which is an arc with a small radius of curvature (Fig. 2.16a), then part of the flow near this arc resembles circulating motion: the velocity increases in proportion to the approach to the outline of the arc and with sufficiently small radii of curvature can become very large. With some (sufficiently small) radius of curvature the velocity should be so great that the pressure (computed according to the Bernoulli equation for a noncompressible liquid) should become negative, which is impossible. When the radius of curvature is equal to zero, i.e., when liquid flows around an acute edge (the point of inflection of the outline, Fig. 2.16b), the velocity becomes infinite exactly as in the center of the vortex, which induces circulating motion. But an infinite velocity requires unreal infinite negative pressure. Therefore, infinite velocity is impossible, consequently, the nonseparated flow around acute edges is impossible and the separation of the jets occurs.¹ The only possible case of the nonseparated flow around a body with an acute edge (winged shape) by a flow of an ideal noncompressible liquid is the case depicted on Fig. 2.16c: here the acute edge lies on the dividing line of the flows which flow around the upper and lower sides of the shape, and the liquid jets smoothly converge from the outline of the body.

In a real liquid which possesses viscosity, with the separation of the jets from the eddying particles of the boundary layer a vortex is formed which seemingly "rounds" the acute edge, and the liquid jets no longer flow around the acute edge, but around this vortex.

¹Subsequently it will be shown that in the supersonic flow of a gas the nonseparated flow around an acute edge is possible; in this case, velocity does not become infinite.

CHAPTER III

SHOCK WAVES

§ 1. Normal Shock Waves

In the case of the flight of a body at supersonic speed ($w_H > a_H$) a shock wave (compression shock) which produces considerable resistance develops in front of it.

If the body in question is a flight vehicle equipped with a jet engine, then in the supersonic air jet which is slowed down when it flows into the engine a shock wave also occurs. It is possible to visualize fundamentally the smooth transition of supersonic flow into subsonic, being achieved by means of a special inverse nozzle mounted at the engine inlet. In this case total pressure losses would not take place. However, the deceleration of a supersonic flow in such a manner cannot be carried out entirely, by virtue of which it is necessary to reconcile with the existence of shock waves and the presence of the corresponding wave resistance.

Numerous tests show that any pressure increase which arises in any place of a gaseous medium is propagated in it at a high speed in different directions in the form of pressure waves. The weak pressure waves travel at the speed of sound; their study is covered in acoustics. The strong pressure waves, as can be seen from the tests, are propagated at velocities considerably greater

that the speed of sound. The basic feature of the strong pressure wave lies in the fact that the wave front is very narrow, in connection with which the state of the gas (pressure, density, temperature) changes with a jump.¹

It is possible to give the following qualitative explanation of this fact. Assume in a certain area (Fig. 3.1) a pressure change occurred and the first wave obtained a smooth form 1AB2. On separate infinitely narrow sections of the wave the magnitude of pressure increases insignificantly, therefore the propagation of such a wave occurs at the speed of sound. In the area of high compressions (A) naturally higher temperatures are observed than in the area of low compressions (B), by virtue of which the "top" of the pressure wave moves faster than its "foot." To the side of less pressures (to the right) the wave is propagated as a compression wave, to the side of high pressures (to the left) - as a rarefaction wave. Thus, even if at first the compression wave is flat, then in the course of time it is made steeper and steeper; this process will stop and the wave will acquire a stable form only from the moment when the wave front becomes entirely plane (1'-2'). Thus the compression waves are propagated as pressure jumps (explosions), in connection with which they are called shock waves.

For those same reasons, i.e., as a result of the fact that at point A the rarefaction wave moves faster than at point B, the wave front of the rarefaction wave is spread with time. In other words, the development of a rarefaction wave should not lead to expansion shocks.

¹The approximate theory says that the thickness of the area in which a strong pressure wave diminishes should be of the order of the free-path length of molecules.

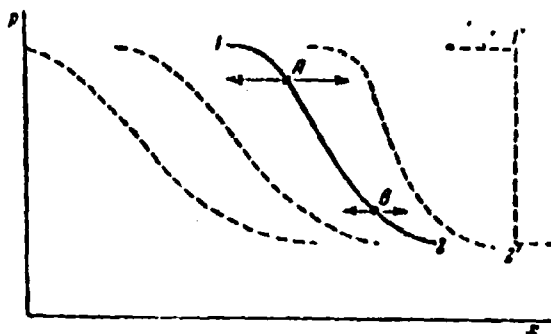


Fig. 3.1. Diagram of the development of compression and rarefaction waves.

It will be shown below that in adiabatic (without heat supply) compression shocks an increase in the entropy of the gas occurs and in adiabatic expansion shocks, if they existed, entropy should decrease. By this is proved the legitimacy of the existence of adiabatic pressure jumps and simultaneously the impossibility of the emergence of adiabatic expansion shocks (as is known from thermodynamics, in a finite closed system entropy cannot decrease). In full conformity with this is found that known fact, that the expansion shocks (condensation shock, flame front) observed sometimes in actuality are obtained only during the supply of heat into the area of shock, i.e., under such conditions, when with an expansion shock the entropy of the gas increases. It is necessary to note that the emergence of expansion shocks during the supply of heat to a gas does not contradict in any way the process depicted in Fig. 3.1. In fact, if in the area of reduced pressures B because of the supply of heat a temperature is obtained which is higher than in the high-pressure area A, then the speed of sound at the foot of the wave is higher than at the top; in connection with this in the course of time the steepness of the rarefaction wave front should be intensified, which gives rise to the formation of a thermal expansion shock.

Let us pause now on the theory of shock waves. Let us visualize, for example, that under the influence of the sharp displacement of the piston (Fig. 3.2) in the tube a strong compressive wave developed and is propagated from left to right.

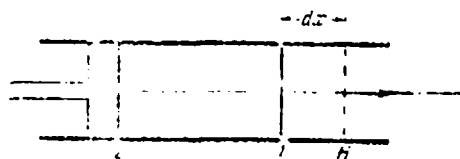


Fig. 3.2. Diagram of shock wave propagation.

Assume during an infinitesimal time interval the wave front moved the distance dx . This means that in the area 1-H during time dt there was a pressure increase from value p_H (pressure of the undisturbed gas) to value p_1 (pressure behind the front of the compression wave), in accordance with which in area 1-H an increase should be observed in the gas density by the value

$$\Delta \rho = \rho_1 - \rho_H.$$

However this can occur only in the case when a certain quantity of gas, equal to

$$dQ = (\rho_1 - \rho_H) g F dx,$$

will overflow from volume 1-2 into volume H-1 (here F - the cross-sectional area). Thus during the propagation of a strong compression wave the gas behind the wave front should be in motion, following in the same direction as the wave. From the equation of continuity it is possible to determine the speed of the gas flow (w_H):

$$dQ = \rho_1 g F w_H dt,$$

from which

$$w_H = \frac{\rho_1 - \rho_H}{\rho_1} \frac{dx}{dt}. \quad (1)$$

But the derivative of the path in time is nothing else but the velocity of motion of the wave:

$$w_s = \frac{dx}{dt}. \quad (2)$$

Hence we obtain the equality which relates the *velocity of propagation of the wave with the velocity of the gas which is moving behind the wave front in the same direction*:

$$w_s = w_n \frac{p_1}{p_1 - p_n}. \quad (3)$$

Applying the equation of momentum to the area H-1 it is possible to obtain another relationship between the same values. In fact, during the time dt the mass of the gas which filled the volume H-1, $\Delta M_H = \rho_H F dx$ will pass from the state of rest into motion at a rate of w_n . The corresponding change in momentum should be equal to the power pulse caused by the difference of pressures which act in cross sections 1 and H:

$$(p_1 - p_n) F dt = \rho_H F (w_n - 0) dx,$$

from which the wave velocity is equal to

$$w_s = \frac{dx}{dt} = \frac{p_1 - p_n}{\rho_H w_n}. \quad (4)$$

After substituting the expression for gas velocity (3) into equation (4), we will obtain the velocity of propagation of the compression wave as the function of the increase of pressure and increase of density

$$w_s = \sqrt{\frac{p_1 - p_n}{\rho_H \frac{p_1}{p_1 - p_n}}}. \quad (5)$$

In the case of a *weak wave*, when the increase of pressure (and density) obtained is insignificant: $\rho_1 \approx \rho_H$, $p_1 \approx p_H$, we have

$$w_s = a = \sqrt{\frac{dp}{d\rho}}. \quad (6)$$

A *weak wave* is none other than an *acoustic wave*, therefore expression (6) is the determining of the *speed of sound*.

From a comparison of equalities (5) and (6) it is evident that the *velocity of propagation of a strong compression wave is always greater than the speed of sound*. Usually sound propagation is accompanied by such an insignificant change in the state of the gas that entropy can be considered virtually constant, i.e., it is assumed that in this case an ideal adiabatic process $p/\rho^k = \text{const}$ takes place. But in this case

$$\frac{dp}{d\rho} = k \frac{p}{\rho}$$

or on the basis of the equation of state for an ideal gas

$$\frac{dp}{d\rho} = k_s RT.$$

From here we obtain the formula already applied above [(34) in Chapter I] for the speed of sound in an ideal gas

$$a = \sqrt{\frac{k p}{\rho}} = \sqrt{k_s RT}.$$

Substituting expression (5) into equality (3), we find the formula for the speed of gas flow behind the front of the compression wave

$$w_n = \sqrt{\frac{(p_1 - p_n)(\rho_1 - \rho_n)}{\rho_1 \rho_n}}. \quad (7)$$

It is not difficult to see that with the weakening of the compression wave the speed of the gas flow drops. In the case of a weak sound wave the gas behind its front is fixed, since according to equality (7) with $p_1 \approx p_n$ and $\rho_1 \approx \rho_n$ we obtain $w_n \approx 0$. In actuality, as is known, a sound wave consists of the correctly alternating areas of compression and rarefaction, whereupon the gas beyond its front is found in a very weak oscillatory motion; the average forward velocity of gas particles is equal to zero.

Let us note now that as a result of the outflow of gas from area 1-2 (Fig. 3.2), which is disposed behind the front of a strong compression wave, the pressure in this area decreases in the course of time. For this reason the shock wave which developed in the fixed gas under the effect of unit compression (for example, an explosion or displacement of the piston) always attenuates more or less rapidly. And only when the disturbing source does not cease its action it is possible to obtain an undamped shock wave. The property, discovered above, of shock waves to be propagated at a velocity greater than the speed of sound leads to the fact that undamped shock waves are formed before the body

only when motion occurs at supersonic speed. For example, during motion in a gas with a constant supersonic speed of the solid before the latter a shock wave of constant intensity is formed which moves at the same speed as the body.

We will investigate in more detail the change in the state of the gas which is obtained during the passage of a stationary shock wave in it. We will turn first to the simplest arrangement, when the wave front makes a right angle with the direction of propagation. Such a wave is called a *normal shock wave*.

For the convenience of calculation it is advantageous to turn the motion, i.e., to stop the wave front, after directing a flow towards the wave at a velocity equal to the velocity of propagation of the wave (Fig. 3.3):

$$w_s = -w_s$$

then the relative gas velocity behind the wave front

$$w_1 = w_s - w_s \quad (8)$$

After stopping the shock wave by the counterflow of gas, we obtained a certain fixed surface, intersecting which all the elementary streams of gas simultaneously undergo abrupt changes in the velocity of motion, density, pressure, and temperature. Because of this a shock wave is also called a *compression shock*. Shock waves are conveniently observed in supersonic wind tunnels during the flow of air about fixed solids.

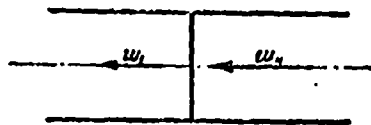


Fig. 3.3. Diagram of a normal shock wave.

Let us accept the cross-sectional area of a jet equal to a unit ($F = 1 \text{ m}^2$) and, using the known equations of gas dynamics, find the connection between the values of gas velocity before and after the shock wave (Fig. 3.3). The equation of continuity gives

$$\rho_1 w_1 = \rho_2 w_2.$$

Disregarding the force of friction in view of the thinness of the shock wave, from the equation of momentum we will obtain

$$p_1 - p_2 = \rho_2 w_2 (w_2 - w_1).$$

Comparing these equations we find

$$p_1 - p_2 = \rho_2 w_2^2 - \rho_1 w_1^2 = w_1 w_2 (p_1 - p_2) \quad (9)$$

from which

$$\frac{p_1 - p_2}{\rho_1 - \rho_2} = w_1 w_2 \quad (10)$$

If heat is not given from without, then the full enthalpy of the gas remains constant. Thermal outputs can be disregarded since the lateral surfaces of the jet in the area of shock are negligibly small. Thus from the equation of enthalpy follows

$$i_0 = c_p T_0 = c_p T_1 + A \frac{w_1^2}{2g} = c_p T_2 + A \frac{w_2^2}{2g} = \text{const};$$

here T_0 - the stagnation temperature. From this equation we have

$$T_2 = T_0 - \frac{A}{2gc_p} w_2^2$$

According to the equation of state of the gas

$$\frac{p_1}{\rho_1 T_1} = \frac{p_2}{\rho_2 T_2} = gR,$$

consequently,

$$T_0 = \frac{p_{01}}{gR\rho_{01}} = \frac{p_{02}}{gR\rho_{02}};$$

here p_{01} , p_{02} - the total pressure respectively after and before the shock wave, ρ_{01} , ρ_{02} - the gas density which corresponds to total stagnation in the same cross sections. Consequently,

$$p_2 = p_1 \left(\frac{\rho_{02}}{\rho_{01}} - \frac{A R w_2^2}{2c_p} \right).$$

From thermodynamics we have the known relationship

$$AR = c_p \frac{k-1}{k},$$

therefore

$$p_2 = p_1 \left(\frac{\rho_{02}}{\rho_{01}} - \frac{k-1}{2k} w_2^2 \right). \quad (11)$$

By analogy we obtain

$$p_1 = p_2 \left(\frac{\rho_{01}}{\rho_{02}} - \frac{k-1}{2k} w_1^2 \right). \quad (12)$$

After subtracting equality (11) from equality (12) we have

$$p_1 - p_2 = (p_1 - p_2) \frac{p_{01}}{p_{02}} + \frac{k-1}{2k} (\rho_1 w_1^2 - \rho_2 w_2^2)$$

from which on the basis of (9) is derived

$$\frac{p_1 - p_2}{p_1 - p_2} = \frac{2k}{k+1} \frac{p_{01}}{p_{02}} \quad (13)$$

Utilizing expression [(41) Chapter I] for the critical speed

$$a_{kp}^2 = \frac{2k}{k+1} gRT_0 = \frac{2k}{k+1} \frac{p_{01}}{\rho_{01}}$$

we find

$$\frac{p_1 - p_2}{p_1 - p_2} = \frac{2k}{k+1} gRT_0 = a_{kp}^2 \quad (14)$$

Finally, comparing equalities (10) and (14), we come to the following simple relationship between the velocities of gas before and after a normal shock:

$$w_2 w_1 = a_{kp}^2 \quad (15)$$

This kinematic relationship can be reduced to a dimensionless form by introducing the velocity coefficients ($\lambda = w/a_{kp}$):

$$\frac{w_2}{a_{kp}} \frac{w_1}{a_{kp}} = 1$$

or

$$\lambda_2 \lambda_1 = 1, \quad (16)$$

from which it is clear that in a normal shock wave the supersonic gas velocity always converts to subsonic, since if $w_1 > a_{kp}$, then $w_2 < a_{kp}$. Simultaneously it is possible to note that the greater the value of the velocity coefficients before the shock, the less its value after the shock, i.e., the higher the initial velocity w_1 the stronger the shock wave obtained. With a decrease in the initial velocity the shock declines and disappears entirely with $w_1 \approx w_2 \approx a$.

Let us establish now the connection between pressure and gas density in a shock wave. For this let us add equalities (11) and (12):

$$p_1 + p_2 = (p_1 + p_2) \frac{p_{01}}{p_{02}} + \frac{k-1}{2k} (\rho_1 w_1^2 + \rho_2 w_2^2)$$

From the equation of continuity it follows that

$$\rho_n w_n \cdot (\rho_1 w_1) = w_n w_1 (\rho_1 - \rho_n)$$

Substituting this result into the foregoing expression, we have

$$\frac{\rho_1 + \rho_n}{\rho_1 - \rho_n} = \frac{\rho_{0n}}{\rho_{01}} - \frac{k-1}{2k} w_n w_1$$

from which on the basis of (10) and (13) we obtain the basic dynamic relationship

$$\frac{\rho_1 - \rho_n}{\rho_1 + \rho_n} = k \frac{\rho_1 + \rho_n}{\rho_1 - \rho_n}, \quad (17)$$

according to which the ratio of the increase of pressure to the increase of density in the shock wave is proportional to the ratio of the mean pressure to the average density. Hence, by the way, follows the result, already known to us, that with an infinitesimal shock wave ($p_1 \approx p_n$, $\rho_1 \approx \rho_n$) the result is

$$\frac{dp}{d\rho} = k \frac{p}{\rho}.$$

This confirms the assumption made above that an *ideal adiabatic process answers to a shock wave*.

Let us examine in more detail the thermodynamic process of a change in the state of the gas in a shock wave. For this let us present the dynamic relationship (17) in a somewhat different form:

$$\frac{\rho_1 + \rho_n}{\rho_1 - \rho_n} = k \frac{\rho_1 + \rho_n}{\rho_1 - \rho_n}.$$

Let us divide the numerator and denominator in the left side of this equality by the value ρ_n , and in the right by ρ_1 :

$$\frac{\frac{\rho_1}{\rho_n} + 1}{\frac{\rho_1}{\rho_n} - 1} = k \frac{1 + \frac{\rho_n}{\rho_1}}{1 - \frac{\rho_n}{\rho_1}}.$$

Hence after the simple conversions the dependence is obtained of relation ρ_1/ρ_n on the relation p_1/p_n in the shock wave, which is called the *shock adiabatic curve*:

$$\frac{\rho_1}{\rho_n} = \frac{\frac{k+1}{k-1} + \frac{p_n}{p_1}}{1 + \frac{k+1}{k-1} \frac{p_n}{p_1}}. \quad (18)$$

The essential feature of a shock adiabatic curve is the fact that during an unlimited pressure rise in a shock wave ($p_1 \rightarrow \infty$) the increase in density has a definite limit which, as this is evident from equation (18), is equal to

$$\left| \frac{\rho_1}{\rho_0} \right|_{\max} = \frac{k+1}{k-1}. \quad (19)$$

For example for air ($k = 1.4$) an increase in density in the shock wave cannot be more than six-fold:

$$\left| \frac{\rho_1}{\rho_0} \right|_{\max} = 6.$$

During a shock wave in a gas with a smaller value of index k a stronger, but also more limited increase in density can be observed; for example, with $k = 1.2$

$$\left| \frac{\rho_1}{\rho_0} \right|_{\max} = 11.$$

One ought to emphasize that unlike the shock adiabatic curve, in the case of an ideal adiabatic process in which takes place the dependence

$$\frac{\rho_1}{\rho_0} = \left(\frac{p_1}{p_0} \right)^{1/k},$$

the increase in density with an increase of pressure is not limited ($\rho_1 \rightarrow \infty$ with $p_1 \rightarrow \infty$).

The comparison of shock and ideal adiabatic curves is made in Fig. 3.4.

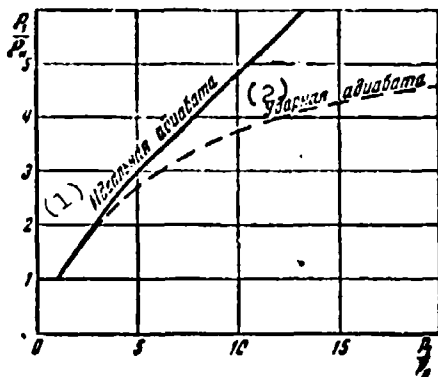


Fig. 3.4. Comparison of shock and ideal adiabatic curves.
KEY: (1) Ideal adiabatic curve;
(2) Shock adiabatic curve.

A change in the pressure and gas density in a direct shock wave can be presented in the function of Mach number before the jump. From the equation of momentum taking into account the formula for the speed of sound [(34) Chapter I] and the equation of continuity we find

$$\frac{p_1}{p_2} - 1 = k M_1^2 \left(1 - \frac{\rho_1}{\rho_2} \right).$$

If with the help of the shock adiabatic curve we replace the relation ρ_2/ρ_1 with its expression through relation p_1/p_2 , then after several conversions we will obtain

$$\frac{p_1}{p_2} = \frac{2k}{k+1} M_1^2 - \frac{k-1}{k+1}. \quad (20)$$

Specifically for air ($k = 1.4$)

$$\frac{p_1}{p_2} = \frac{7}{6} M_1^2 - \frac{1}{6}.$$

It is possible to express the pressure ratio in a direct shock wave and in the function of the velocity coefficient before the shock λ_1 ; for this one ought to replace in equality (20) the variables according to formula (45) from Chapter I:

$$\frac{p_1}{p_2} = \frac{\lambda_1^2 - \frac{k-1}{k+1}}{1 - \frac{k-1}{k+1} \lambda_1^2}. \quad (21)$$

With a decrease in the velocity of incident flow down to a critical value ($M_1 = 1$) the shock wave degenerates ($p_1 = p_2$). In a subsonic flow, as has already been indicated above, shock waves are impossible. In a normal shock wave the pressure increase depends only on the value of Mach number in the incident flow, whereupon with an increase of M the pressure increases unlimitedly ($p_1 \rightarrow \infty$ with $M_1 \rightarrow \infty$). After substituting the results of (20) into equation (18) it is not difficult to derive the dependence of density after the normal shock wave directly from the Mach number or with the help of (45) of Chapter I on the velocity coefficient λ_1 in the incident flow:

$$\frac{p_1}{p_2} = \frac{\rho_1}{\rho_2} = \frac{\frac{k+1}{k-1}}{1 + \frac{1}{M_1^2} \frac{k+1}{k-1}} = \lambda_1^2 \quad (22)$$

From equality (22) again we conclude that even at an infinite value of Mach number the gas density increases in the shock by not more than $k + 1/k - 1$ times.

Let us determine the losses of total pressure in a normal shock wave.

The total pressure in the jet after the shock obviously is equal to

$$p_{02} = \frac{p_1}{\left(1 - \frac{k-1}{k+1} \lambda_1^2\right)^{\frac{k}{k-1}}} = \frac{p_1}{\left(1 - \frac{k-1}{k+1} \frac{1}{\lambda_2^2}\right)^{\frac{k}{k-1}}} \quad (23)$$

The total pressure before the shock is equal to

$$p_{01} = \frac{p_1}{\left(1 - \frac{k-1}{k+1} \lambda_1^2\right)^{\frac{k}{k-1}}}$$

therefore the pressure coefficient which considers wave resistance (losses in normal shock) can be presented, if we utilize expression (21), in the following manner:

$$\sigma_n = \frac{p_{01}}{p_{02}} = \lambda_2^2 \left[\frac{1 - \frac{k-1}{k+1} \lambda_1^2}{1 - \frac{k-1}{k+1} \frac{1}{\lambda_2^2}} \right]^{\frac{1}{k-1}} \quad (24)$$

At a flying speed equal to or less than the speed of sound ($\lambda_H \leq 1$), wave resistance disappears

$$\sigma_n = 1;$$

formula (24) is valid only with $\lambda_H \geq 1$. At an infinitely high flying speed ($\lambda_H^2 = \frac{k+1}{k-1}$) $\sigma = 0$ is obtained, however, in this case losses will not absorb the entire initial reserve of the total pressure, since the other factor (p_{0H}) approaches infinity. The

dependence curve $\sigma_n = f(\lambda_n)$ for air ($k = 1.4$) is given in Fig. 3.5.

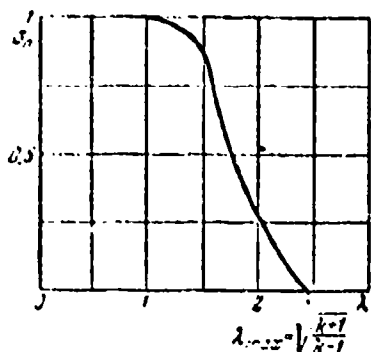


Fig. 3.5. The dependence of pressure coefficient after a normal shock wave on the velocity coefficient.

From equalities (71) of Chapter I and (22) it is possible to obtain a formula for determining the density of the decelerated gas after a normal shock wave

$$\frac{\rho_{01}}{\rho_n} = \frac{\lambda_n^2}{\left(1 - \frac{k-1}{k+1} \lambda_n^2\right)^{\frac{1}{k-1}}}. \quad (25)$$

In conclusion let us note that equality (10) derived above and the equation of continuity make it possible to present the flow velocity before the shock as the following function of an increase in pressure and density:

$$w_n = \sqrt{\frac{p_1 - p_n}{\rho_1 - \rho_n} \frac{\rho_1}{\rho_n}}.$$

But there is an expression (5) already known for the velocity of propagation of a direct shock wave in stagnant air. Such a result is completely natural, since in order to stop a shock wave it is necessary to direct the gas flow towards the wave and to impart to it a velocity equal to the wave velocity.

Substituting expression (22) into relationship (15), we obtain a new formula for the relative gas velocity behind the front of the shock

$$w_1 = a_1 \sqrt{\frac{\rho_1}{\rho_2}}$$

Hence with the help of (19) it is revealed that the coefficient of relative gas velocity after the shock cannot be less than a certain specific value:

$$|\lambda_{\min}| = \sqrt{\frac{k-1}{k+1}}. \quad (26)$$

If we pass from a fixed shock wave to a shock which is propagated in a fixed gas at a rate of $w_{\Pi} = -w_H$, then with the help of the equalities obtained it is possible to determine the absolute velocity which the gas acquires in the wake of the shock:

$$w_H = w_H - w_1 = a_1 \left(\sqrt{\frac{\rho_1}{\rho_2}} - \sqrt{\frac{\rho_2}{\rho_1}} \right) \quad (27)$$

or on the basis of (22)

$$w_H = w_H \left(1 - \frac{1}{\lambda_1^2} \right) \quad (28)$$

and in a dimensionless form

$$\lambda_2 = \lambda_1 - \frac{1}{\lambda_1}. \quad (29)$$

According to law (16) behind a shock wave the gas velocity relative to the wave front is obtained always less than sonic ($\lambda_1 < 1$); on the basis of this it becomes clear why any pressure change which proceeds behind the wave and is propagated at the speed of sound can overtake the wave front. Precisely because of this the pressure drop described above (Fig. 3.2) in the wake behind a shock wave which originated in a fixed gas leads to a weakening of the drop in pressure on the wave front and causes its attenuation.

§ 2. Oblique Shock Waves

The characteristic feature of a normal shock wave, as it was possible to note, is the fact that, intersecting its front, the gas flow does not change its direction, whereupon the front of the

normal shock is arranged at right angles to the flow direction. Besides normal shock waves, the so-called *oblique shock waves* are also encountered. The front of an oblique shock is situated inclined toward the flow direction (Fig. 3.6). An oblique

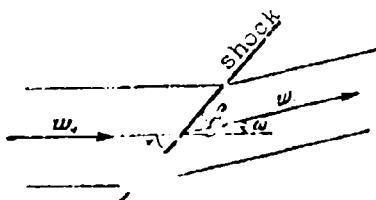


Fig. 3.6. Diagram of an oblique shock wave.

shock is obtained when, intersecting the front of the shock, the gas flow should change its direction. For example during the supersonic flow of gas about a tapered body (Fig. 3.7a), which deflects the flow from the initial direction by angle ω , before the body oblique shock waves are formed which converge on its

spout (Fig. 3.8). An oblique shock wave is formed during flow around a cone (Fig. 3.7b). The discontinuity surface in this case will be a cone with a vertex in the spout of the streamlined body. Thus, if up to the encounter of the jet with the front of an oblique shock the velocity vector w_1 formed with it an angle α (Fig. 3.6), then after the intersection of the front the jet is deflected by angle ω , and the angle between the vector of velocity and the shock front becomes equal to

$$\beta = \alpha - \omega. \quad (30)$$

Let us separate the velocity vector into two components, of which one is normal (w_n), and the other is parallel (w_t) to the front of the shock (Fig. 3.9). It is not difficult to show that during the intersection between the jet of the front and the oblique shock the normal component of the velocity decreases:

$$w_{n1} < w_{n2} \quad (31)$$

and the tangential component remains constant:

$$w_t = \text{const.} \quad (32)$$

We will turn for this to Fig. 3.10, in which is depicted a rectangular outline HHH which covers part of the front of the oblique shock. The lateral sections of the outline (H-1) are

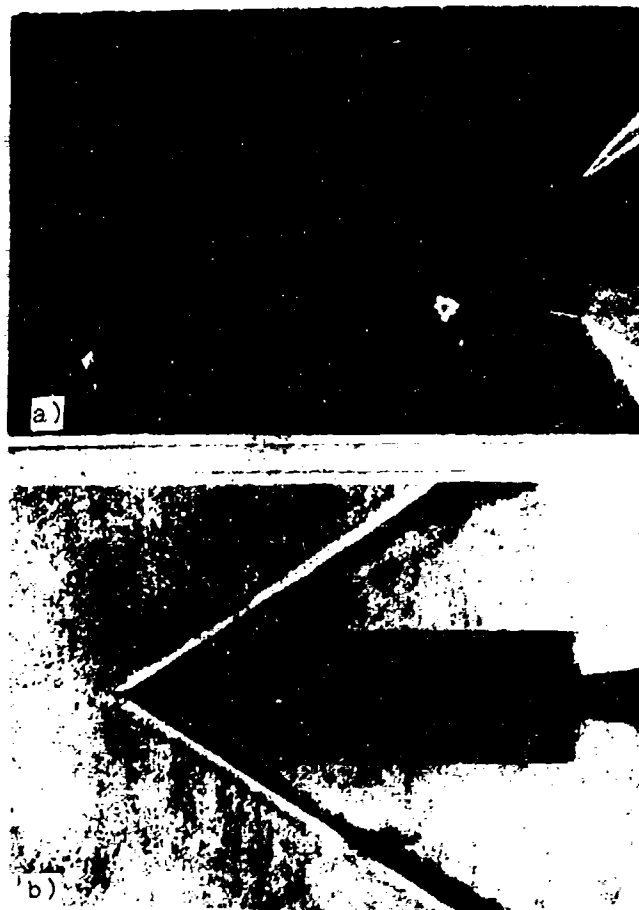


Fig. 3.7. Shadow photographs of oblique shock waves during supersonic flow around a wedge a) and a cone b).

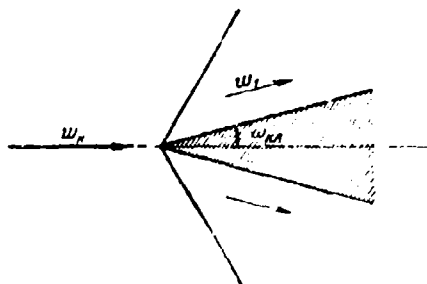


Fig. 3.8. The formation of an oblique shock wave during flow around a wedge.

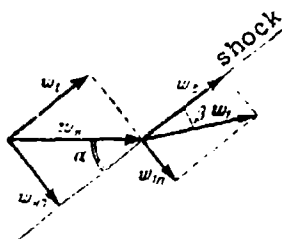


Fig. 3.9.

Fig. 3.9. The kinematics of flow with an oblique shock wave.

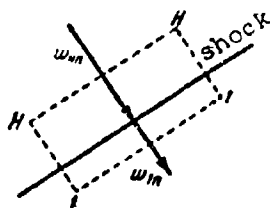


Fig. 3.10.

Fig. 3.10. Calculation diagram of an oblique shock wave.

conducted at right angles to the front, and the end (H-H and l-l) - are parallel to it. Let us compile the balance of the momentum for this outline first in projection on the direction of the front. In view of the fact that the forces of pressure on both lateral surfaces (H-l) are identical, the corresponding projection of the momentum remains constant, from which ensues condition (32), which indicates the constancy of the tangential component of velocity. If now we make up the equation of momentum in the direction H-l perpendicular to the front, then in view of the fact that on surfaces H-H and l-l substantially different pressures act, the result will be¹

$$p_1 - p_2 = \rho_2 w_{2n} (w_{1n} - w_{2n})$$

The pressure in the shock wave increases ($p_1 > p_2$), from which follows condition (31) according to which the normal component of velocity in the shock decreases.

The given considerations show that an oblique shock wave is reduced to a normal shock, which is carried together with the flow of gas sideways at a velocity w_t . Unlike the normal shock in

¹During the compilation of this equation we took into consideration the continuity condition

$$\rho_1 w_{1n} = \rho_2 w_{2n}$$

an oblique shock not the full speed of gas flow undergoes disruption (abrupt decrease), but only its component normal to the front of the shock. In fact, according to the equation of continuity

$$\rho_1 w_{1n} = \rho_2 w_{2n}$$

The equation of enthalpy in an adiabatic case (there is no heat exchange) gives

$$T_0 = T_n + \frac{A}{2gc_p} w_n^2 = T_1 + \frac{A}{2gc_p} w_1^2$$

Further we have $w_n^2 = w_{1n}^2 + w_1^2$, $w_1^2 = w_{1n}^2 + w_1^2$, from which

$$c_p T_0 - \frac{A}{2g} w_1^2 = c_p T_n + \frac{A}{2g} w_{1n}^2 = c_p T_1 + \frac{A}{2g} w_{1n}^2$$

Let us introduce into the examination the *temperature of partial stagnation*, understanding by this the following value:

$$T_n = T_n + \frac{A}{2gc_p} w_{1n}^2 = T_1 + \frac{A}{2gc_p} w_{1n}^2 = T_0 - \frac{A}{2g} w_1^2$$

i.e., the temperature which will be obtained not during the total stagnation of flow, but only with damping of components of velocity which are normal to the shock front. As this equality shows, the temperature of partial stagnation has one and the same value before and behind the shock front, which ensues from the condition $w_t = \text{const.}$ If we add to these equations also the equation of state

$$\frac{p_1}{\rho_1 T_1} = \frac{p_n}{\rho_n T_n}$$

then it will turn out, as one would expect, that an oblique shock wave is described precisely by the same relationships as the direct shock wave (see page 154), with the only difference that in the first case instead of the full speed its components normal to the shock front are figured, and instead of the total stagnation temperature T_0 they figure the temperature of partial stagnation T_n .

Because of this, without repeating all the computations which were given in detail in the theory of normal shock, we can write immediately a number of prepared expressions. For example instead of equality (10) we have

$$\frac{\rho_1 - \rho_n}{\rho_1 - \rho_n} = w_{1n} w_{nn} \quad (33)$$

Correspondingly instead of equality (14) we will obtain

$$\frac{\rho_1 - \rho_n}{\rho_1 - \rho_n} = \frac{2k}{k+1} gRT_n = a_{np}^2 \quad (34)$$

Here a_{np} - the conditional critical speed, which corresponds to the temperature of partial stagnation T_n . The basic kinematic relationship for an oblique shock takes the following form:

$$w_{1n} w_{nn} = a_{np}^2 \quad (35)$$

Equality (34) makes it possible to connect total critical speed with the conditional critical speed:

$$a_{np}^2 = \frac{2k}{k+1} gRT_n = a_{np}^2 + \frac{k-1}{k+1} w^2 \quad (36)$$

Using this expression it is possible to obtain the second frequently encountered form of the basic kinematic relationship for an oblique shock wave:

$$w_{1n} w_{nn} + \frac{k-1}{k+1} w^2 = a_{np}^2 \quad (37)$$

In the particular case, when an oblique shock converts into normal ($\alpha = 90^\circ$, $w_t = 0$, $w_{nn} = w_n$, $w_{1n} = w_1$), from relationships (35) and (37) we obtain the already known relationship (15). Converting to the velocity coefficients $\lambda_{1n} = w_{1n}/a_{np}$, $\lambda_{nn} = w_{nn}/a_{np}$, we will obtain in the case of an oblique shock the dimensionless kinematic relationship

$$\lambda_{1n} \lambda_{nn} = 1 \quad (38)$$

which corresponds to equality (16) for a normal shock. It is natural that dynamic relationship (17) is useful for an oblique shock wave without any changes, and the shock adiabatic curve is applicable to the oblique shock wave precisely in the same form (18) as to a normal shock.

Changes in the static and total pressures in an oblique shock are found respectively from dependences (21) and (24), if we insert into these formulas instead of λ_n the value λ_{nn} :

$$\frac{p_1}{p_n} = \frac{\lambda_{nn}^2 - \frac{k-1}{k+1}}{1 - \frac{k-1}{k+1} \lambda_{nn}^2}, \quad (39)$$

$$\frac{p_{01}}{p_{0n}} = \lambda_{nn}^2 \left[\frac{1 - \frac{k-1}{k+1} \lambda_{nn}^2}{1 - \frac{k-1}{k+1} \lambda_{nn}^2} \right]^{\frac{1}{k-1}}. \quad (40)$$

whereupon the velocity coefficient λ_{nn} is calculated here on the normal component of velocity and the conditional critical velocity:

$$\lambda_{nn} = \frac{w_{nn}}{a_{spn}}.$$

It is possible, it goes without saying, to obtain such formulas which relate the pressure change in an oblique shock directly with the absolute velocity of incident flow.

According to the momentum equation the increase of static pressure in an oblique shock is equal to

$$p_1 - p_n = \rho_n w_{nn} (w_{nn} - w_{1n}).$$

Substituting equation (37) into this momentum equation and converting to coefficients λ , we will obtain

$$p_1 - p_n = \rho_n a_{sp}^2 \left(\lambda_n^2 \sin^2 \alpha - 1 + \frac{k-1}{k+1} \lambda_n^2 \cos^2 \alpha \right).$$

However, from (42) and (41) of Chapter I it follows that

$$\frac{p_n}{p_n} = \frac{\frac{2k}{k+1}}{1 - \frac{k-1}{k+1} \lambda_n^2} \frac{1}{a_{sp}^2}.$$

Hence the relation of values of static pressure after and before oblique shock waves is equal to

$$\frac{p_1}{p_n} = \frac{\lambda_n^2 \left[1 - \frac{4k}{(k+1)^2} \cos^2 \alpha \right] - \frac{k-1}{k+1}}{1 - \frac{k-1}{k+1} \lambda_n^2}. \quad (41)$$

Expression (41) with an increase in the angle of oblique shock up to a value $\alpha = 90^\circ$ converts to the known expression (21), obtained above for a normal shock. Let us compute the value p_1/p_H for air ($k = 1.4$):

$$\frac{p_1}{p_H} = \frac{\lambda_H^2 (1 - 0.972 \cos^2 \alpha) - 0.167}{1 - 0.167 \lambda_H^2}.$$

The relation of values of total pressure after and before an oblique shock is a function of the velocity coefficients and can be determined in the following manner:

$$\sigma_k = \frac{p_{01}}{p_{02}} = \frac{p_{01}}{p_1} \frac{p_1}{p_H} \frac{p_H}{p_{02}}, \quad (42)$$

where

$$\frac{p_H}{p_{02}} = \left(1 - \frac{k-1}{k+1} \lambda_H^2\right)^{\frac{k}{k-1}}, \quad \frac{p_1}{p_{01}} = \left(1 - \frac{k-1}{k+1} \lambda_1^2\right)^{\frac{k}{k-1}}$$

and the relation of values of static pressure p_1/p_H is taken according to formula (41).

Thus for determining the total pressure σ_k in an oblique shock wave it is necessary to know the velocity coefficient λ_1 . From the velocity triangles after and before the oblique shock (Fig. 3.9) it follows that

$$w_1^2 = w_{1n}^2 + w_t^2, \quad w_{1n} = w_2 \sin \alpha, \quad w_t = w_2 \cos \alpha. \quad (43)$$

Utilizing these relationships, and also (37), let us derive calculation equations for the velocity coefficient after an oblique shock wave:

$$\lambda_1^2 = \frac{w_1^2}{a_{1p}^2} = \frac{w_{1n}^2}{a_{1p}^2} + \frac{w_t^2}{a_{1p}^2},$$

$$w_{1n} = \frac{a_{1p}^2 - \frac{k-1}{k+1} w_t^2}{w_{2n}} = \frac{a_{1p}^2 - \frac{k-1}{k+1} w_2^2 \cos^2 \alpha}{w_2 \sin \alpha}.$$

Inserting values w_{1n} and w_t in the expression for λ_1 , we will obtain

$$\lambda_1^2 = \lambda_H^2 \cos^2 \alpha = \frac{\left(1 - \frac{k-1}{k+1} \lambda_H^2 \cos^2 \alpha\right)^2}{\lambda_H^2 (1 - \cos^2 \alpha)}. \quad (44)$$

An increase in the angle of shock to normal ($\alpha = 90^\circ$) leads to the known relationship (16) for a normal shock.

An increase in the pressure in an oblique shock wave can also be presented in the function of Mach number of incident flow and angle α , which forms the velocity vector w_{1n} with the shock front. Let us substitute into the momentum equation

$$p_1 - p_2 = w_{1n} \rho_1 (w_{1n} - w_{2n})$$

the value w_{1n} from (43) and divide both parts of the latter by the value p_1 . Then, utilizing the equation of continuity and the formula for the speed of sound [(34) Chapter I], we will obtain

$$\frac{p_1}{p_2} = 1 + k M_1^2 \sin^2 \alpha \left(1 - \frac{p_2}{p_1} \right).$$

After expressing with the help of the equation of shock adiabatic curve (18) the density ratio ρ_2/ρ_1 by the pressure ratio, and after substituting it in the last equation, we come to the unknown dependence:

$$\frac{p_1}{p_2} = \frac{2k}{k+1} M_1^2 \sin^2 \alpha - \frac{k-1}{k+1}. \quad (45)$$

With the same velocity of incident flow an oblique shock, as this follows from (45), is always weaker than a normal shock.

The intensity of an oblique shock wave changes with a change in the slope angle of its front to the direction of incident flow. In the extreme case, when an oblique shock converts into normal ($\alpha = 90^\circ$), the increase in pressure obtained is maximum. In this case equality (45) converts to equality (20), known from the theory of a normal shock wave.

In another maximum case, when the angle of inclination of the jump to the direction of flow before it is determined by the condition

$$\sin \alpha_0 = \frac{1}{M_1}. \quad (46)$$

the oblique shock degenerates into an infinitely weak wave ($p_1 \approx p_2$). Let us explain this fact in somewhat more detail. Assume at a certain point O of a supersonic gas flow an infinitesimal disturbance (Fig. 3.11) of pressure developed. The weak compression wave (or rarefaction) will break into a run from the center of the disturbance in all directions at the speed of sound a . In a unit of time ($\tau = 1$ s) the wave front will be a sphere of radius $r = a$. However, the entire mass of the gas in which the wave arose is carried along the flow at supersonic speed $w_\infty > a$. Because of this the weak pressure waves will never exceed the limits of the cone, the surface of which is the envelope for spherical waves. The generatrix of such a cone is called the *Mach wave* or *characteristics*. Angle α_0 between the generatrix and the axis is called the *Mach angle* or the *angle of propagation of weak disturbances*. This angle, as can be seen from Fig. 3.11, is determined by the equality

$$\sin \alpha_0 = \frac{a}{w_\infty} = \frac{1}{M_\infty}.$$

Thus the front of a very weak oblique shock wave is disposed with respect to incident flow at an angle α_0 which is determined by equality (46). Strong disturbances, as it was shown above, are propagated at supersonic speed, in connection with which the front of a strong shock forms with the incident flow a larger angle than the characteristic: $\alpha > \alpha_0$.

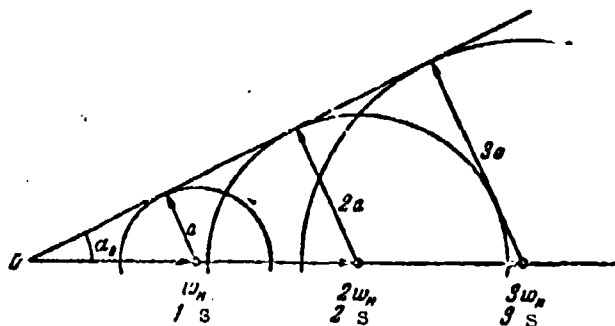


Fig. 3.11. The development of a wave of weak disturbances.

Thus the range of change in angle α for an oblique shock wave is determined by the following limits:

$$90^\circ \geq \alpha \geq \alpha_0.$$

After substituting expression (45) into the equation of shock adiabatic curve (18), we will obtain the equality which relates relation ρ_1/ρ_u in the case of an oblique shock wave with the Mach number of incident flow and the angle of inclination of the shock:

$$\frac{p_1}{p_u} = \frac{\frac{k+1}{k-1}}{1 + \frac{1}{M_u^2 \sin^2 \alpha} \frac{2}{k-1}} = \lambda_{us}^2. \quad (47)$$

This equality with $M \approx 1/\sin \alpha$ gives $\rho_1 \approx \rho_u$, and in the case $\alpha = 90^\circ$ converts to corresponding equality (22) for a normal shock wave.

Knowing the density ratio of the gas after and before the oblique shock, it is possible to calculate the angle ω , by which the flow in the shock (Fig. 3.6) is deflected. From the equation of continuity we have

$$\frac{w_{1n}}{w_{un}} = \frac{p_u}{p_1}.$$

At the same time from the velocity triangles (Fig. 3.9) it follows that

$$\frac{w_{1n}}{w_{un}} = \frac{\operatorname{tg} \beta}{\operatorname{tg} \alpha}. \quad (48)$$

Hence we obtain

$$\operatorname{tg} \beta = \frac{p_u}{p_1} \operatorname{tg} \alpha \quad (49)$$

or on the basis of equalities (47) and (38)

$$\begin{aligned} \operatorname{tg} \beta &= \lambda_{us}^2 \operatorname{tg} \alpha = \\ &= \frac{1 + \frac{k-1}{2} M_u^2 \sin^2 \alpha}{\frac{k+1}{2} M_u^2 \sin^2 \alpha} \operatorname{tg} \alpha = \frac{k-1}{k+1} \left(1 + \frac{2}{k-1} \frac{1}{M_u^2 \sin^2 \alpha} \right) \operatorname{tg} \alpha. \end{aligned} \quad (50)$$

But if the angle β between the velocity vector behind the shock and the front of the latter is known, then the angle of flow deflection is determined by relationship (30).

We indicated the method of determining the angle by which the flow in a shock is deflected when the position of the front is known. If, on the contrary, the specific deviation in the supersonic flow is assigned, then when as a result of deviation the velocity should decrease (for example during supersonic flow around the wedge depicted in Fig. 3.7a), an oblique shock wave develops; in this case according to formulas (30) and (50) the angle α at which the shock front will be arranged with respect to the flow can be calculated.

In Fig. 3.12 are represented the curves $\alpha = f(\omega)$, corresponding to different values of Mach number of incident flow and constructed for air ($k = 1.4$). As we see, for every value of Mach number there is a certain maximum deviation in the flow ($\omega = \omega_{\max}$). So with $M = 2$ flow can be deflected by no more than an angle $\omega_{\max} = 23^\circ$, with $M = 3 - \omega_{\max} = 34^\circ$, with $M = 4 - \omega_{\max} = 39^\circ$. Even at the infinite speed ($M = \infty$) flow can be deflected a maximum by the angle $\omega_{\max} = 46^\circ$. The presence of such a limitation in the deviation of flow after a shock wave is a completely natural fact, since as with an infinitely weak shock, i.e., when angle α is equal to the angle of propagation of weak disturbances, and the generatrix of the Mach cone is characteristic, so also with the strongest - a normal shock, the angle of flow deflection becomes equal to zero, therefore the curves $\omega = f(\alpha)$ have maximums.

On the curves in Fig. 3.12 it is also evident that for the same deviation in the flow there are two positions of the shock front. Experiments show that of the two possible positions of jump the stabler is that in which the angle between the flow direction and the shock front is less. Thus in Fig. 3.12 more important are the lower branches of the curves lying under the points of the maxima. The lower intersection of each of the curves $\alpha = f(\omega)$ with the vertical axis corresponds to the regeneration of the jump into a weak wave, and the angle α_0 obtained in this case represents the angle of weak disturbances.

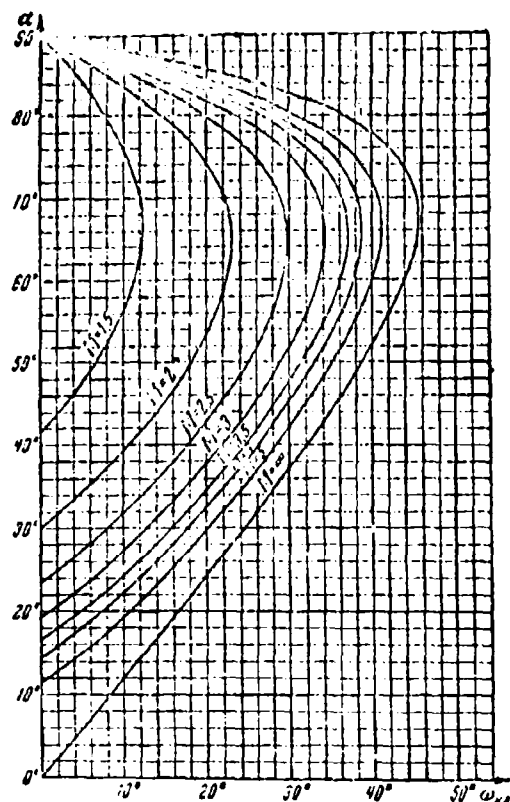


Fig. 3.12. The dependence of the direction of an oblique shock on the angle of deflection of flow.

During supersonic flow around a wedge, in which the angle with the vertex is greater than is assumed in Fig. 3.12 the formation of a flat oblique shock wave is impossible. Experience shows that in this case a shock wave with a curvilinear front is formed (Fig. 3.13), whereupon the surface of the shock is placed in front, without being in contact with the spout of the wedge. In its central part the shock obtained is normal, but with removal from the axis of symmetry converts into an oblique shock which at great distances degenerates into a weak wave. The same shock configuration is observed during supersonic flow around a body which has a rounded nose (Fig. 3.14).

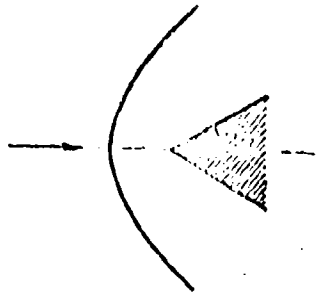


Fig. 3.13. The shock wave during supersonic flow around a wedge with too great an angle with a vertex ($\omega_{\text{pr}} > \omega_{\text{max}}$).



Fig. 3.14. Shadow photographs of shock waves during supersonic flow around a) a rotating body; b) a winged shape.

It is sometimes necessary to calculate the flow velocity after an oblique shock wave. It is simplest to do this using the velocity triangles (Fig. 3.9), from which it follows that

$$w_1 = \frac{w_2}{\cos \beta}, \quad w_2 = w_1 \cos \alpha.$$

Hence we obtain

$$w_1 = w_2 \frac{\cos \alpha}{\cos \beta} \quad (51)$$

or in dimensionless designations

$$\lambda_1 = \lambda_2 \frac{\cos \alpha}{\cos \beta}. \quad (52)$$

Utilizing formula (45) in Chapter I it is possible to find the appropriate value of the Mach number behind the oblique shock:

$$M_1^2 = \frac{2}{k-1} \frac{1}{1 - \frac{k-1}{k+1} \lambda_1^2}.$$

In Fig. 3.15 are given the dependence curves of M_1 number after the shock wave on the position of the front $M_1 = f(\alpha)$ for three values of Mach number in an incident flow ($M = 2, 3, 4$). As we see, in all three cases at the slope angles of front $\alpha \leq 60^\circ$ the flow velocity after the oblique shock wave turns out to be supersonic. The extreme left point of every curve answers to the conditions of the transfer of the oblique shock wave into a weak wave, the extreme right point - into a normal shock wave.

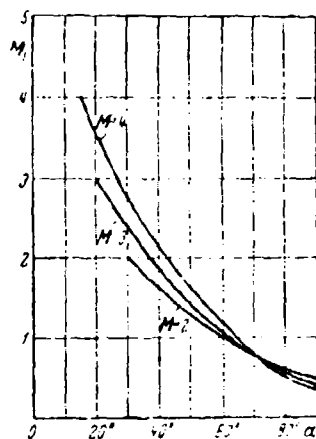


Fig. 3.15 The dependence of M_1 number after a shock wave on the slope angle of the jump.

The case where a normal shock is formed is the simplest, since in this case subsonic flow is obtained immediately. After an oblique shock the flow slows down, but, as we saw, it can remain supersonic. In that case the subsequent slowing down should be accompanied by a second shock, which can be both normal and oblique. In the latter case one additional shock can be required. Thus the total stagnation of supersonic flow requires either one normal shock or a system of several oblique shocks, usually completed by weak normal shock. It is possible to visualize such a system of shocks in which the losses are less than in one normal shock.

Let us pause now on the supersonic flow around a cone. During the symmetric supersonic flow around a cone (Fig. 3.16) before the latter a conical shock wave is established (Fig. 3.7b), whereupon the apexes of the cone and shock wave (surface of shock) virtually coincide. In view of the fact that the thickness of the shock is always very low, the formulas given above for calculating a plane-parallel oblique shock are also applicable to an axisymmetric shock. Specifically if the angle between the front and the flow direction α and the speed before the shock are known (Fig. 3.16), then according to formulas (50) and (30) it is possible to find the flow direction $\omega_{\kappa\lambda}$, according to formula (51) - the velocity, and according to formula (45) - static pressure directly after the shock. However, unlike the plane in an axisymmetric flow the direction of the gas jet directly behind the shock ($\omega_{\kappa\lambda}$) is not parallel to the body surface ($\omega_{\kappa\lambda} \neq \omega_{\text{нон}}$). In connection with this the angle of deflection of jets behind the shock is tapered, approaching asymptotically a half angle at the vertex of the cone. Directly after the shock the angle of deflection has the smallest value $\omega_{\kappa\lambda} < \omega_{\text{нон}}$ and, as it was mentioned, is obtained the same as for a plane flow, i.e., it can be determined with the help of Fig. 3.12.

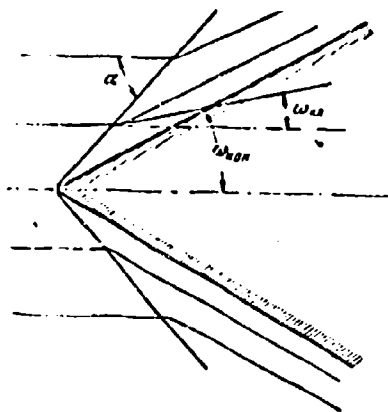


Fig. 3.16. The layout of supersonic flow around a cone.

The dependence of angle α between the front of the shock and the flow direction from the half angle in the apex of the cone (ω_{HON}) for the case $\lambda_H = 2$ ($M_H = 3.16$) is given in Fig. 3.17 (solid line).¹ Here is plotted the curve $\alpha = f(\omega_{\text{HON}})$, which gives the angles of deflection of flow directly after the shock (dotted line), i.e., corresponding to plane flow (flow around a wedge). As we see, at the identical angles of a cone and wedge on the cone the shock obtained is weaker (more inclined).

It was shown above that the changes of the direction of flow, velocity, and state of the gas in the shock itself do not depend on the surface form of the shock; at the assigned flow velocity (λ_H) and angle of shock α these changes are obtained identically in plane-parallel and axisymmetric flows. The distinction in these two cases consists only of the fact that the same angle of shock is not obtained at the identical cone and wedge apex angles. In other words, during a comparison of axisymmetric and plane oblique shocks it is advantageous to express all the factors in the function of the angle of shock, but not the apex

¹Petrov G. I. and Ukhov Ye. P., The calculation of the recovery of pressure upon transition from supersonic flow to subsonic in different systems of flat shock waves, M., 1947.

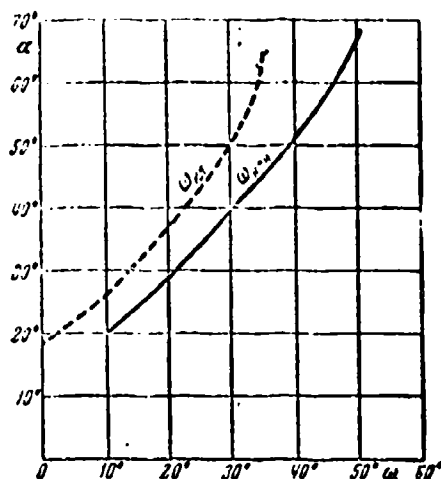


Fig. 3.17. Comparison of the angles of oblique shock on a cone and on a wedge (dotted line) with the velocity coefficient $\lambda_H = 2$ ($M_H = 3.16$).

angle of an aerodynamic body. In this case the results obtained in the calculation of an axisymmetric and plane shocks will be identical.

The gas flow after a shock in the axisymmetric case differs from plane; the flow velocity, static pressure, and gas density have close, but dissimilar values, and the angles of rotation of flow in a shock (wedge angle) and on infinity (angle of cone) are substantially different. Figure 3.18 gives the curves $\omega_{\text{KOH}} = f(\omega_{\text{KL}})$ for different values of Mach numbers. In Fig. 3.19 are depicted the curves of values of M_1 numbers after the shock (dotted line) and M_2 on the surface of a cone (solid line) in the function of the angle of shock at the different values of velocity. As we see, the decrease obtained in the velocity between the area lying directly after the shock (it corresponds to plane flow) and the surface of the cone is insignificant; since the Mach numbers after the shock and on the surface of the cone are close, then the corresponding λ numbers are close. For practical calculations the velocity after a conical shock can be accepted equal to the arithmetic mean value

$$\lambda_1 \approx \frac{\lambda_{1\text{пл}} + \lambda_{1\text{кон}}}{2} \quad (53)$$

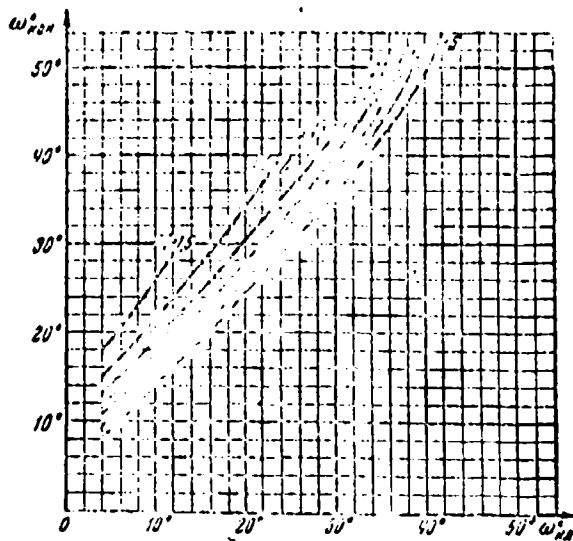


Fig. 3.18. The dependence of semiapex angle of a cone on the angle of rotation of flow in a shock for different flow velocities.

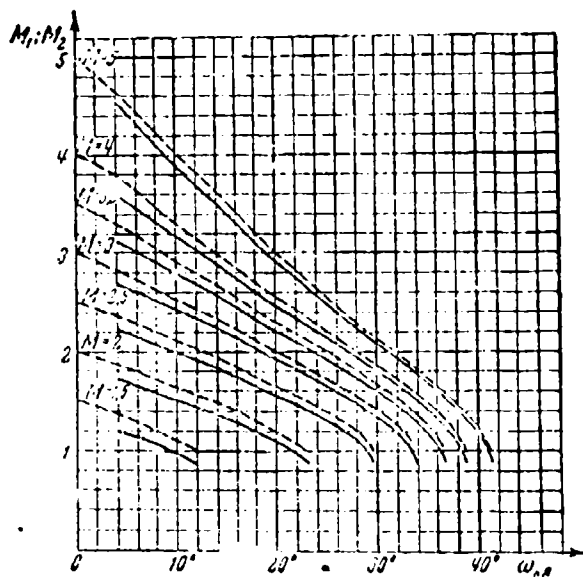


Fig. 3.19. Values of M numbers after a shock (dotted line) and on the surface of a cone depending on the angle of shock.

or even the velocity after the plane shock

$$\lambda_1 \approx \lambda_{1pr} \quad (54)$$

In this case for axisymmetric flow the formulas obtained above for a plane-parallel flow turn out to be suitable, with the only difference that different apex angles of the body correspond to the same angles of shock (Fig. 3.17).

§ 3. The Application of a Pneumatic Adapter in a Supersonic Flow

For velocity measurement of a supersonic gas flow it is possible to use an ordinary pneumatic adapter (Fig. 3.20). It is only necessary to consider that during supersonic flow around the adapter the shock wave appears before it. If the axis of symmetry of the adapter is parallel to the flow direction, then the central gas stream which undergoes total stagnation at first passes through the direct part of the shock wave, where its velocity becomes subsonic, then with approach to opening 1 the velocity decreases smoothly to zero.

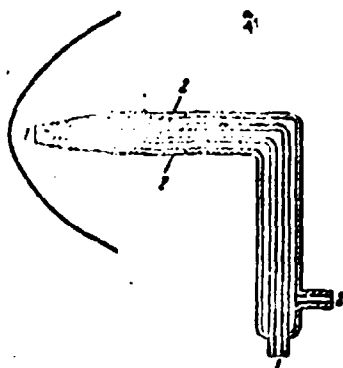


Fig. 3.20. Pneumatic adapter in a supersonic flow.

The pressure in tube 1 (p_{01}) can be calculated by the following method. From expression (68) of Chapter I we have

$$\frac{p_{01}}{p_1} = \left(1 + \frac{k-1}{2} M_1^2\right)^{\frac{k}{k-1}};$$

where p_1 and M_1 - static pressure and Mach number directly behind the shock wave. Utilizing formulas (45), (46) of Chapter I and formula (16) in this chapter, we pass to the Mach number in the incident flow:

$$M_1^2 = \frac{\frac{2}{k+1} \lambda_1}{1 - \frac{k-1}{k+1} \lambda_1} = \frac{\frac{2}{k+1} \lambda_2'}{1 - \frac{k-1}{k+1} \lambda_2'} = \frac{1 + \frac{k-1}{2} M_2^2}{k M_2^2 - \frac{k-1}{2}}$$

$$1 + \frac{k-1}{2} M_1^2 = \frac{\left(\frac{k+1}{2}\right)^k M_1^2}{\frac{k-1}{2} \left(\frac{2k}{k-1} M_1^2 - 1\right)}.$$

Hence on the basis of equality (20) we obtain the well-known formula which expresses the ratio of pressure p_{01} in tube 1 to the static pressure in the incident flow (p_μ) as the function of Mach number in the incident flow:

$$\frac{p_{01}}{p_\mu} = \left(\frac{k+1}{2}\right)^{\frac{k+1}{k-1}} \left(\frac{2}{k-1}\right)^{\frac{1}{k-1}} \frac{M_\mu^{\frac{2k}{k-1}}}{\left(\frac{2k}{k-1} M_\mu^2 - 1\right)^{\frac{1}{k-1}}}. \quad (55)$$

For air ($k = 1.4$) this formula is reduced to the following form:

$$\frac{p_{01}}{p_\mu} = \frac{166.7 M_\mu^2}{(7 M_\mu^2 - 1)^{2.5}}. \quad (56)$$

If the lateral openings 2 are found at a distance equal to not less than 4-6 diameters of the adapter from its leading edge, then, as experience shows, the pressure in tube 2 is equal to the static pressure of incident flow (p_μ). Thus values p_{01} and p_μ are measured directly on manometers connected respectively to tubes 1 and 2 of the adapter.

For the calculation of the flow velocity according to formulas (55) or (56) it is necessary to also know the speed of sound, or, which is the same, the temperature of the incident flow:

$$w_\mu = M_\mu a_\mu, \quad a_\mu = \sqrt{k g R T_\mu}.$$

In certain cases it is more convenient to use the formula which expresses the pressure ratio in the tubes of the adapter in the function of the velocity coefficient of incident flow (λ_μ). This formula can be obtained from expressions (21) and (23) of this chapter:

$$\frac{p_{01}}{p_n} = \frac{1}{\left(\frac{1}{\lambda_n^2} - \frac{k-1}{k+1}\right) \left(1 - \frac{k-1}{k+1} \frac{1}{\lambda_n^2}\right)^{\frac{1}{k-1}}}. \quad (57)$$

For air ($k = 1.4$)

$$\frac{p_{01}}{p_n} = \frac{1}{\left(\frac{1}{\lambda_n^2} - 0.167\right) \left(1 - \frac{0.167}{\lambda_n^2}\right)^{2.5}}. \quad (58)$$

The calculation of the velocity of incident flow according to formula (57) can be fulfilled, if the value of the critical velocity is known:

$$w_n = \lambda_n a_{np}$$

where

$$a_{np} = \sqrt{\frac{2k}{k+1} g R T_{0n}}$$

whereupon

$$T_{0n} = \frac{T_n}{1 - \frac{k-1}{k+1} \frac{1}{\lambda_n^2}}.$$

Let us note, for example, that in wind tunnels namely the stagnation temperature is always known, i.e., the temperature of the air being sucked into the tube.

CHAPTER IV

THE ACCELERATION OF GAS FLOW

§ 1. Supersonic Nozzle

In a supersonic nozzle, called the *Laval nozzle*, gas flow is converted in such a way that the discharge velocity becomes greater than the speed of sound:

$$M > 1, \quad w_a > a.$$

Let us examine the case of a one-dimensional flow of gas in a supersonic nozzle. The equation of continuity gives

$$\frac{G}{g} = \rho w F = \text{const.}$$

The gas moves along the nozzle with acceleration, therefore at low speed, when gas density can be considered constant, it is necessary to decrease the cross sections. This is caused by the contraction of the initial part of the nozzle. During the further expansion of gas an increase in velocity is accompanied by a noticeable decrease in the pressure, and therefore gas density, which partially compensates for the increase of velocity, and therefore it is no longer necessary to narrow the cross section of channel so rapidly. Finally, the process passes through such a stage, when the density of the expanding gas decreases inversely proportional to the velocity. As is known, in this cross section of the channel the flow velocity is equal to the speed of sound. A further increase in velocity is accompanied by an even more

rapid increase in density, as a result of which, as this follows from the equation of continuity, the cross section of the nozzle should be increased.

Thus, the supersonic nozzle intended for the obtaining of a supersonic flow should consist of narrowing (subsonic) and widening (supersonic) parts (Fig. 4.1). In the narrowest cross section of the supersonic nozzle (critical cross section) the flow velocity is equal to sound.

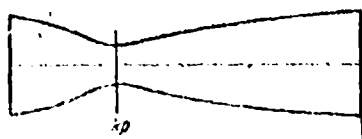


Fig. 4.1. The Laval nozzle.

Let us examine together the equations of continuity and Bernoulli (not allowing for friction) differentially:

$$d(\rho w F) = 0, \quad d\left(\frac{\rho}{2} w^2 + \int p d\alpha\right) = 0.$$

Let us divide the second equation by ρw^2 and multiply and divide its first term by $d\alpha$. Then we will obtain

$$\frac{1}{w^2} \frac{d\rho}{\rho} \frac{dw}{w} + \frac{dw}{w} = 0.$$

From the first equation we have

$$F w d\rho + F \rho dw + \rho w dF = 0$$

or after division by $\rho w F$

$$\frac{d\rho}{\rho} = -\frac{dF}{F} - \frac{dw}{w}.$$

Substituting this result in the second equation and taking into account that according to equality (34) of Chapter I the pressure derivative in terms of density in an ideal adiabatic process is equal to the square of the speed of sound in a gas, we will obtain

$$\left(\frac{w^2}{a^2} - 1\right) \frac{dw}{w} = \frac{dF}{F}. \quad (1)$$

Analyzing this equality, it is possible to note that during the expansion (acceleration) of gas, when $dw/w > 0$, the cross section of nozzle should change in the manner that was indicated above, namely:

if $w < a$, then $\frac{dF}{F} < 0$ (contraction),
 if $w = a$, then $\frac{dF}{F} = 0$ (critical region),
 if $w > a$, then $\frac{dF}{F} > 0$ (expansion).

Thus three conditions are observed: *subsonic* $w < a_{kp}$, *critical* $w = a_{kp}$, *supersonic* $w > a_{kp}$.

It should be noted that near the critical cross section the flow is very sensitive to a change in the cross section of the channel. Thus, for instance, for a change in Mach number by 10% (from $M = 0.9$ to $M = 1$) it is sufficient to change the cross-sectional area by 1%, and for transfer from $M = 0.95$ to $M = 1$ - by 0.25%. Because of this it is not possible to maintain critical conditions on a sufficiently extended section of a straight tube (boundary layer, formed due to slowing down of gas at the walls, as it narrows the cross section of the jet).

Density, as was already mentioned, with an increase of velocity decreases. In the nozzle throat $dF/F = 0$, this means that the cross-sectional area passes through the extremum (minimum). From the relationship (1) it follows that precisely in the narrow cross section of the Laval nozzle is a flow velocity obtained which is equal to the local speed of sound.

Let us examine the dependence of the velocity on the cross-sectional area of the nozzle. For this, using the equation of continuity, let us connect the arbitrary cross section of the supersonic nozzle with its minimum cross section:

$$\rho w F = \rho_{kp} w_{kp} F_{kp}$$

hence

$$\frac{F}{F_{kp}} = \frac{\rho_{kp} w_{kp}}{\rho w}$$

However $w = aM$ and $M_{kp} = 1$, therefore

$$\frac{F}{F_{kp}} = \frac{\rho_{kp} a_{kp}}{\rho a M}$$

But, as is known,

$$\frac{a_{kp}}{a} = \left(\frac{T_{kp}}{T} \right)^{\frac{1}{2}}$$

and during an ideal process

$$\frac{p_{kp}}{p} = \left(\frac{T_{kp}}{T} \right)^{\frac{k}{k-1}},$$

consequently,

$$\frac{P}{P_{kp}} = \left(\frac{T_{kp}}{T} \right)^{\frac{k+1}{2(k-1)}} \frac{1}{M^2}$$

on the basis of equations (32) and (39) of Chapter I we have

$$\frac{T_{kp}}{T} = \frac{1 + \frac{k-1}{2} M^2}{1 + \frac{k-1}{2}}.$$

Then, substituting in (2)

$$\frac{P}{P_{kp}} = \frac{\left(1 + \frac{k-1}{2} M^2 \right)^{\frac{k+1}{2(k-1)}}}{M^2 \left(\frac{k+1}{2} \right)^{\frac{k+1}{2(k-1)}}}. \quad (2)$$

For air $k = 1.4$, therefore we have

$$\frac{P}{P_{kp}} = \frac{(1 + 0.2 M^2)^3}{1.73 M^5}. \quad (3)$$

From these formulas it is evident that the dimensionless value of the cross-sectional area of a nozzle is a function only of Mach number. One ought to emphasize that all the resulting expressions are valid in the absence of thermal and hydraulic losses, i.e., during a change in the state of the gas over an ideal adiabatic curve.

If the configuration of the supersonic nozzle is assigned, then it is possible to determine which Mach number is obtained in any cross section. To each value of Mach number corresponds a specific magnitude of the relation P/P_{kp} . Curve $P/P_{kp} = f(M)$, constructed according to formula (3), is given in Fig. 4.2. In this case, as can be seen from the curve, equation (3), and

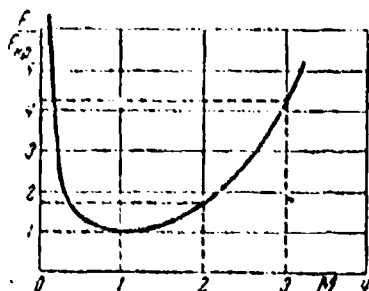


Fig. 4.2. The dependence of the dimensionless area of a Laval nozzle on Mach number ($k = 1.4$).

this means equation (2), has two solutions; to one and the same F/F_{kp} answer two values of Mach number: one at subsonic speed and another at supersonic speed. For the nozzle inlet which precedes the critical cross section all the subsonic solutions are suitable while for the output part all supersonic are suitable. A unique solution is obtained only in the critical cross section ($F/F_{kp} = 1$).

The pressure and gas density during an ideal process depend unambiguously on Mach number and are determined by formulas (68) and (71) of Chapter I. Hence it follows that after selecting an arbitrary cross section we will obtain in this cross section the specific value of Mach number to which correspond the specific values of temperature, pressure, and gas density (with an accuracy up to the boundary layer effect).

The velocity in this cross section of the supersonic nozzle depends only on the stagnation temperature T_0 . A change in total pressure p_0 does not influence velocity since local pressure p changes proportionally to it and their relation remains constant; also remaining constant is the relation of the temperatures

$$\frac{T}{T_0} = \left(\frac{p}{p_0} \right)^{\frac{k-1}{k}}.$$

For obtaining a specific value of Mach number on a section of the supersonic nozzle it is necessary in the appropriate manner to select the cross-sectional area and, furthermore, it is necessary to have a sufficient reserve of pressure in the chamber

before the nozzle. In other words, for achievement of the required Mach number in a nozzle section the pressure in the chamber should exceed the ambient pressure by a certain number of times.

Let us assume that the pressure in the chamber p_0 increased, then in the nozzle section the pressure also increases and the gas escapes with an excess pressure. Somewhere after the nozzle section the pressure will be made even with atmospheric, the pressure excess will be consumed in the jet for an increase in velocity, and since for a supersonic flow an increase in the velocity requires an increase in the transverse jet cross-sectional area, then the jet seemingly forms in space an expanding supersonic nozzle. But if the pressure in the chamber for any reason is lowered, then in the section lowering of pressure will occur, whereupon the pressure obtained in certain cases can be lower than atmospheric; the discharge velocity in this case will not be changed, since it is the function only of the area ratio of the exit section and the nozzle throat. A pressure change in the atmosphere does not show up in outflow from the nozzle, since the pressure wave, which is propagated at the speed of sound, is carried by the supersonic gas flow. Based on the exit of the gas jet from the nozzle the pressure in it finally should be equal to atmospheric, i.e., to be raised because of the stagnation of supersonic flow; this process is accompanied by the emergence of shock waves and will be lower, the more detailed it is analyzed.

This pressure in a section of this supersonic nozzle is not connected with the pressure of the atmosphere, but depends only on the pressure in the chamber and the nozzle configuration.

Only in the case of the so-called calculated conditions the pressure in the nozzle section is equal to atmospheric pressure: $p_n = p_a$. Under non-calculated conditions, when pressure in the section is greater or less than atmospheric, a pressure change should occur in the jet outside the nozzle.

It has already been noted that the process of the conversion of pressure into velocity in supersonic and subsonic flows proceeds without essential losses, i.e., approximately with a constant entropy, and therefore is very close to an ideal adiabatic curve. Precisely therefore the calculation formulas given above for an ideal supersonic nozzle give good results for real nozzles.

In many instances the calculation equations are simplified if the variables of the gas state are determined in a function not of Mach number, but of the velocity coefficient. The convenience of operation with the velocity coefficient is connected with the fact that its denominator (critical velocity) depends only on the stagnation temperature, which is constant for any section of flow with an isolated process. The laws of change of temperature, pressure, and gas density in the function of coefficient λ are expressed by formulas (42), (72), and (73) of Chapter I.

Let us derive the expression which relates the cross-sectional area of a supersonic nozzle with the velocity coefficient. We will turn to the equation of continuity

$$\frac{F}{F_{kp}} = \frac{\rho_{kp} a_{kp}}{\rho \omega}.$$

Substituting here

$$\omega = \lambda a_{kp}, \quad \frac{\rho_{kp}}{\rho} = \left(\frac{T_{kp}}{T} \right)^{\frac{1}{k-1}},$$

we will obtain

$$f_u = \frac{F}{F_{kp}} = \frac{1}{\lambda} \left[\frac{\frac{2}{k-1}}{1 - \frac{k-1}{k+1} \lambda^2} \right]^{\frac{1}{k-1}}. \quad (4)$$

In conclusion we will derive the formula for calculating the gas flow rate per second in a supersonic nozzle. It is convenient to find the gas flow rate through the nozzle throat:

$$Q = \rho_{kp} a_{kp} F_{kp}. \quad (5)$$

since from expressions (42), (72), (73) of Chapter I it is simplest to determine the state of the gas in the critical cross section ($\lambda = 1$):

$$\left. \begin{aligned} \frac{T_0}{T_{*p}} &= \frac{k+1}{2}, & \frac{\rho_0}{\rho_{*p}} &= \left(\frac{k+1}{2}\right)^{\frac{1}{k-1}}, \\ \frac{p_0}{p_{*p}} &= \left(\frac{k+1}{2}\right)^{\frac{k}{k-1}}, & \frac{a_0}{a_{*p}} &= \left(\frac{T_0}{T_{*p}}\right)^{\frac{1}{2}} = \left(\frac{k+1}{2}\right)^{\frac{1}{2}}. \end{aligned} \right\} \quad (6)$$

Specifically for air ($k = 1.4$) we have

$$T_0 = 1.2 T_{*p}, \quad \rho_0 = 1.58 \rho_{*p}, \quad p_0 = 1.89 p_{*p}, \quad a_0 = 1.1 a_{*p} \quad (7)$$

Replacing with the help of relationships (6) the critical values of density and speed of sound in expression (5) by the values which correspond to the state of stagnation, i.e., to the state in the chamber before the nozzle, we will obtain

$$Q = \rho_0 a_0 F_{*p} \left(\frac{2}{k+1}\right)^{\frac{k+1}{2(k-1)}}.$$

or, utilizing the equation of state and formula (34) in Chapter I:

$$Q = \frac{\rho_0 F_{*p}}{\sqrt{T_0}} \left(\frac{2}{k+1}\right)^{\frac{k+1}{2(k-1)}} \left(\frac{kg}{R}\right)^{\frac{1}{2}}. \quad (8)$$

Thus the gas flow rate through the supersonic nozzle depends only on the state of the gas in the chamber before the nozzle. For air ($k = 1.4$, $R = 29.27$) we have the following simplified consumption formula:

$$Q = 0.4 \frac{\rho_0 F_{*p}}{\sqrt{T_0}} [\text{kgf/s}]. \quad (8a)$$

According to formulas (8) they determine the dimensions of the supersonic nozzle throat for the assigned consumption and the known state of the gas before the nozzle.

When the discharge velocity is less than critical, a simple convergent adapter - a convergent channel - is used as the nozzle. The state of the gas and the rate of flow in different cross

sections of the convergent channel can be determined by those same formulas as in the case of a supersonic nozzle. However, flow in convergent channel has a number of features which must be considered.

It is most important that with a subsonic system of outflow the pressure in the jet on the nozzle section p_a is virtually equal to the pressure in the surrounding medium p_H , since under these conditions any pressure change in the atmosphere in the form of a pressure wave penetrates inside the nozzle, producing a change in the pressure before the nozzle and the corresponding change in the discharge velocity; the rearrangement of flow is continued until the pressure in the jet on the nozzle section is equal to atmospheric. Thus unlike the supersonic nozzle, in a simple convergent channel the discharge velocity is determined not by its form, but only by the pressure in the chamber before the convergent channel. Thus if the pressure in the chamber p_0 is known, then at the assigned pressure in the plane of the output section p_H the velocity coefficient of outflow is found directly through formula (78) in Chapter 1:

$$\lambda_a = \frac{k+1}{k-1} \left[1 - \left(\frac{p_H}{p_0} \right)^{\frac{k-1}{k}} \right]. \quad (9)$$

The velocity of outflow is equal to $w_a = \lambda_a a_{ap}$, where the critical speed depends, according to (41) of Chapter I, only on temperature in the chamber before the nozzle (stagnation temperature):

$$a_{ap} = a_0 \sqrt{\frac{2}{k+1}} = \sqrt{\frac{2}{k+1} k R T_0}.$$

The gas flow rate in a convergent channel we will find from the equation of continuity, after applying it to the exit section:

$$G = \rho_a w_a F_a.$$

If we utilize the already known dependences

$$\frac{\rho_a}{\rho_0} = \left(\frac{p_H}{p_0} \right)^{\frac{1}{k}}, \quad \frac{w_a}{a_0} = \frac{2}{k+1} \sqrt{\frac{k-1}{k}},$$

then the result is

$$G = g_{cr} \lambda_a F_a \left(1 - \frac{k-1}{k+1} \lambda_a^2 \right)^{\frac{1}{k-1}} \left(\frac{k+1}{k-1} \lambda_a^2 \right)^{\frac{1}{k-1}}$$

or

$$G = \frac{F_a F_{kp}}{F_{kp}} \lambda_a \left(1 - \frac{k-1}{k+1} \lambda_a^2 \right)^{\frac{1}{k-1}} \left(\frac{k+1}{k-1} \lambda_a^2 \right)^{\frac{1}{k-1}} \quad (10)$$

Formula (10) can also be used for determining the gas flow rate in a supersonic nozzle under calculated conditions of outflow, when the nozzle exit pressure F_a is equal to the pressure in the surrounding medium $p_a = p_H$. It is necessary, however, to have in mind that with $F_a = \text{const}$ and $p_0 = \text{const}$ from formula (10) it follows that with a lowering of pressure $p_a = p_H$, i.e., with an increase of the discharge velocity λ_a in the range of values $\lambda_a > 1$, the gas flow rate through the nozzle decreases $G \rightarrow 0$. This is explained by the fact that simultaneously with an increase of λ_a there should be an increase in the ratio of area F_a to the throat area F_{kp} , the value of which does not depend on $p_a = p_H$.

In Fig. 4.3 is represented the plotted function

$$\begin{aligned} \bar{G}_a = \frac{G_a}{G_{kp}} &= \lambda_a \left(1 - \frac{k-1}{k+1} \lambda_a^2 \right)^{\frac{1}{k-1}} \left(\frac{k+1}{k-1} \lambda_a^2 \right)^{\frac{1}{k-1}} = \\ &= \left(\frac{k+1}{2} \right)^{\frac{1}{k-1}} \sqrt{\left(\frac{k+1}{k-1} \right) \left[1 - \left(\frac{p_a}{p_0} \right)^{\frac{k-1}{k}} \right] \left(\frac{p_0}{p_a} \right)^{\frac{1}{k}}}. \end{aligned}$$

which describes the change of the ratio of the gas flow rate through the cross section of the calculated nozzle to the gas flow rate through the critical cross section of the same area depending on a jump in pressures p_0/p_H . As we see, with $p_0/p_H \rightarrow \infty$ the gas flow rate in the exit section $\bar{G}_a \rightarrow 0$. This means that to obtain the assigned final gas flow rate G in this case is possible only by means of increasing the discharge area up to $F_a \rightarrow \infty$ (with $F_{kp} = \text{const}$).

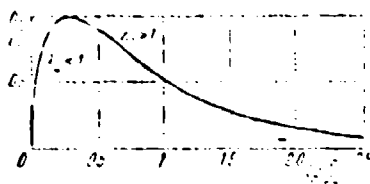


Fig. 4.3. Dependence of gas consumption on the ratio of pressures in the chamber and the surrounding medium.

§ 2. The Non-Calculated Conditions of Outflow from a Laval Nozzle

Let us examine supersonic non-calculated outflow from a Laval nozzle when $p_a > p_u$. At a considerable distance from the nozzle the pressure in the jet and in the atmosphere should be equalized. In connection with this the pressure in the jet in proportion to distance from the outlet decreases gradually, the gas velocity increases, and the cross section of supersonic jet increases (Fig. 4.4). Experience shows that in this case the overexpansion of the jet occurs, i.e., in a certain widest jet cross-sectional area (a_1) a subatmospheric pressure $p_{a1} < p_u$ is established. After this the jet begins to narrow, since pressure should approach atmospheric, and the velocity correspondingly decreases. The stagnation of supersonic flow naturally leads to the emergence of shock waves. As a result of this in a certain part of the jet cross-sectional area b_1 the velocity becomes subsonic, and the pressure higher than atmospheric. Then the pressure again decreases, drawing close to atmospheric; the corresponding increase of subsonic velocity leads to jet contraction. With a sufficiently large pressure excess the velocity again reaches critical, and then even a supersonic value, i.e., a second supersonic section appears, on which the jet is expanded. As a result of the second overexpansion ($p_{a2} < p_u$) and the subsequent increase in pressure a second group of shock waves b_2 appears. It is natural that as a result of losses in the first shock the second overexpansion of the jet and the second group of shock waves are weaker than the first. Thus gradually the jet scatters its energy (for more detail about this see § 6, Chapter VII). With a small pressure excess in the nozzle section the fluctuations of velocity and

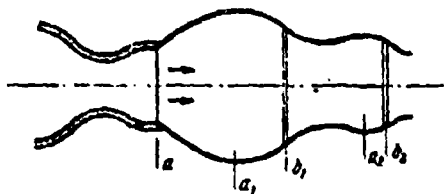


Fig. 4.4. Supersonic outflow with an excess of pressure.

pressure are also obtained along the axis of the jet, but without shock waves.

Supersonic outflow from a nozzle when in the section a pressure less than the surrounding predominates is achieved by means of a complex system of jumps. Let us examine, for example, a plane-parallel gas jet,¹ flowing out into a medium of greater pressure (Fig. 4.5). From the edge of the nozzle the oblique shock waves which are encountered on the axis of the jet at point O will move away. The elementary streams of gas, intersecting the front of an oblique shock (a-O), convert to the area of atmospheric pressure $p_{\text{atm}} > p_a$. The deviation of streams from the initial direction, which takes place during a shock, should lead to their collision on the axis of symmetry. In actuality a second rotation of streams occurs which returns them to the initial direction, but this leads to the emergence of the second group of shocks (Ob). It is natural that if in the areas aOb atmospheric pressure predominates, then more to the right of lines O-b (Fig. 4.5) a pressure greater than atmospheric will be obtained. Thus after the second group of shocks the same conditions are established as during outflow with a pressure excess ($p_a > p_{\text{atm}}$). The less the pressure p_a in the nozzle section, the greater the angle obtained between the front of oblique shock and the flow direction; in this case the angle by which the flow should turn in the second group of shocks Ob increases. Simultaneously the flow velocity after

¹The discussion concerns a nozzle, the cross section of which has the form of an elongated rectangle. Supersonic outflow from an axisymmetric nozzle has been studied less, and we will not examine it here.

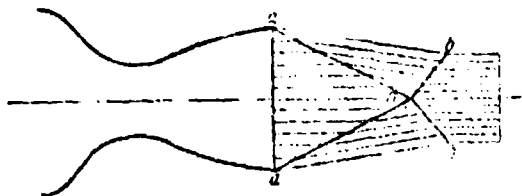


Fig. 4.5. The diagram of outflow from a plane-parallel Laval nozzle under the conditions of overexpansion.

the first group of shocks (in the area aOb) decreases therefore finally such a system begins during which the necessary angle of rotation (ω) of flow cannot be realized in shocks Ob , i.e., $\omega > \omega_{max}$. From this point on, in the center section of the jet a shock wave is formed and the entire arrangement of shocks takes on the bridge-type form (Fig. 4.6). With an increase in the counterpressure the section of shock wave $c-c$ increases. In the case of great counterpressure the supersonic outflow turns out to be impossible, and the pressure jumps are shifted inside the nozzle, i.e., they are achieved in a smaller cross section, the lower the speed for this supersonic flow. In that case the nozzle exit behind the front of the shock works as a usual subsonic diffuser. If within the nozzle the separation of flow from the walls develops, which is accompanied by a usually complex system of shocks (§ 6, Chapter VI), then outflow into the atmosphere occurs at a supersonic velocity less than under calculated conditions.

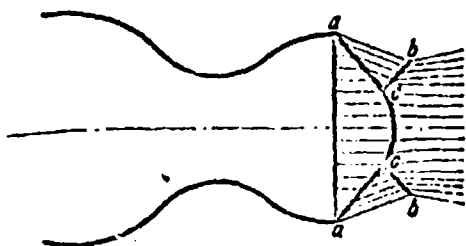


Fig. 4.6. Bridge-type shock during non-calculated outflow from a Laval nozzle.

With a pressure drop in the chamber the shock will approach all the closer to the critical cross section, simultaneously becoming weaker. After approaching close to the critical cross section, the shock will disappear, the supersonic nozzle in this case will be converted into a venturi tube (Fig. 4.7).

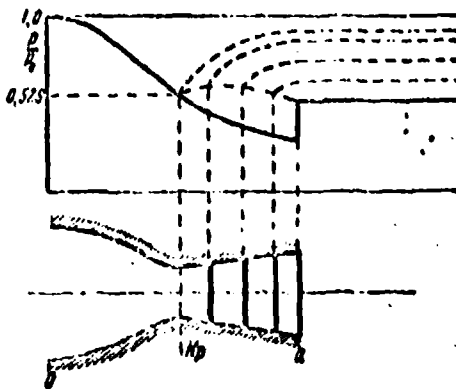


Fig. 4.7. Pressure curves with a shock wave within a Laval nozzle.

The location of the plane of the shock is determined by the ratio of pressure in the chamber (before the nozzle) to the pressure in that medium into which the gas escapes. It should be noted that systems during which shocks are obtained within a supersonic nozzle are encountered in engines rarely. Usually the gas is expanded before the nozzle exit section and escapes at supersonic speed.

A more detailed examination of the supersonic jet which escapes from the nozzle under non-calculated conditions is given in Chapter VII, and the question concerning outflow with the formation of shocks within a nozzle is given in Chapter VIII.

Let us pause on engine operation under non-calculated conditions of the outflow of gas from the nozzle.

In engine operation under calculated conditions the pressure in the plane of the nozzle exit section both in the working jet and in the external flow is equal to atmospheric. However, such a condition is satisfied only at one value of pressure ratio p_a/p_0 .

With a change in the flying speed the pressure in the nozzle section in a jet engine changes. Because of this the invariable exit cross section becomes non-corresponding to calculated conditions: the first - with insufficient, the second - too great a discharge opening area of the nozzle.

In the first case in the Laval section nozzle a constant pressure is maintained whose value is higher than atmospheric, since the exit section is less than calculated, as a result of which the gas in the nozzle is not completely expanded. The value of pressure in the section is equal to

$$p_a = p_v \left(1 - \frac{k-1}{k+1} \lambda_a^2 \right)^{\frac{k}{k-1}}.$$

The less the dimensionless area of the discharge opening (f_a), the lower the velocity coefficient (λ_a), and therefore the higher the pressure in the section (p_a). Emerging from the nozzle, the jet continues to be expanded in the atmosphere and the flow velocity increases. Figure 4.8 shows the boundaries of the region in the jet within which the mean pressure remains excess.

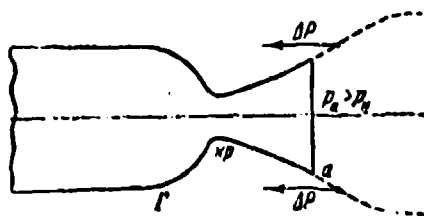


Fig. 4.8. Discharge from a nozzle with a pressure excess.

If we construct the nozzle to the calculated dimensions, then because within the supplementary part of the nozzle increased pressure predominates a thrust increase ΔP will be obtained. Consequently, *in the case of an insufficient discharge area the thrust of the engine is less than under calculated conditions.*

Another area of work of the Laval nozzle answers to that case where the discharge opening area exceeds calculated, i.e., when the value of the total pressure is not sufficient for obtaining atmospheric pressure at the output. Under these conditions the Laval nozzle is filled by supersonic flow up to the section itself, but the pressure obtained in the section is lower than atmospheric, i.e., the nozzle works with overexpansion. When the jet leaves into the atmosphere in it a complex system of shock waves is established which maintains the rarefaction in the nozzle section.

Work under the conditions of overexpansion is possible only up to pressures $p_a \geq p_{a \text{ min}}$. In another case, as was noted, the shock wave will move inside the Laval nozzle, pressure in the section will be equaled with atmospheric, and the discharge velocity will become subsonic. These operating conditions, as it was already mentioned, are almost never encountered in engines and do not have a practical value.

In other words, with too wide a nozzle the outlet velocity usually is the same as under calculated conditions, but pressure here according to the given formula is lower than atmospheric; in this case in the exit section of a Laval nozzle a section of overexpansion is obtained in which to the walls the force ΔP , directed along the flow, is applied (Fig. 4.9). Thus, *in the system of overexpansion reactive thrust is lower than calculated*. For a thrust augmentation it is profitable to *discard* the section of overexpansion after shortening the nozzle to the calculated dimensions.

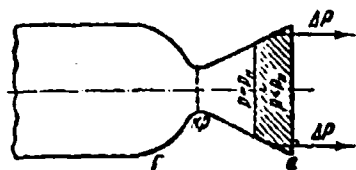


Fig. 4.9. Discharge from a nozzle with overexpansion.

Thus, in all cases of deviation from calculated conditions of outflow with $p_0 = \text{const}$ the reaction force is less than under calculated conditions. Actually, as it follows from formula (105) in Chapter I, the reactive thrust

$$P = \frac{G_a}{g} (w_a - w_n) + \frac{G_r}{g} w_n + (p_a - p_n) F_n$$

Under the conditions of overexpansion the third term in the right side of this equality is negative ($p_a < p_n$), but the first two terms are greater than under calculated conditions (due to increase in w_a); under the conditions of pressure excess ($p_a > p_n$) the third term is positive, and the first two terms as a result of decrease in w_a are less than under calculated conditions.

Calculations show that a certain departure from calculated conditions will not entail a considerable decrease in the reactive thrust. This is obtained because the change of the third term in the thrust formula is compensated for largely by the change of the first two terms. Because of this when the nozzle exit section is greater than the cross section of the combustion chamber, for purposes of reducing head resistance it is possible without special damage for thrust to shorten the nozzle, after accepting $F_a = F_r$, i.e., working under non-calculated conditions. It is possible to demonstrate theoretically, on which we are not dwelling here, that in a jet engine value P/F_a reaches a maximum when the discharge velocity is precisely equal to the flying speed ($w_a = w_H$), and the pressure in the output section is significantly higher than calculated ($p_a > p_H$). In such a system the thrust is formed only as a result of the pressure excess in the nozzle section:

$$P = (p_a - p_H)P_\sigma$$

It was established above that at constant values of total pressure and stagnation temperature in an engine the greatest thrust is obtained in the calculated system of outflow.

It is natural that in the case of an uncontrolled exhaust nozzle, i.e., a nozzle with constant sections, thrust increases with an increase in the total pressure, since in this case pressure in the nozzle section increases, but the velocity coefficient of outflow does not change.

§ 3. Supersonic Gas Flow with a Continuous Increase in Velocity (Prandtl-Mayer) Flow

Let us examine first the simplest form of supersonic gas flow - a forward steady flow. During such a flow all the gas particles move along parallel trajectories at a constant velocity. The particle trajectories are simultaneously the flow lines which are impenetrable for a gas.

If the flow encounters no obstructions in the form of solids or boundaries (walls), then the gas experiences no disturbances. The simplest boundary which is capable of changing the nature of the uniform forward gas flow is a rectilinear solid wall. Let us examine first the case where such a wall is arranged parallel to the direction of flow, i.e., it coincides with one of the flow lines. If the moving gas occupies the entire infinite area above the wall and the wall itself is also infinite in length, then it is clear that in this case the wall will have no effect on the gas flow.¹ Let us note that this position is correct in general also for curved lines of flow: if the wall coincides with the flow line, then it does not exert an influence on the moving gas.

If at certain point A of the wall (Fig. 4.10) there was some obstruction, then it would cause a weak disturbance of the steady flow. Such a disturbance would be extended in a uniform supersonic flow on a straight line - a characteristic constituting with the direction of velocity the angle α_0 , determined from the condition

$$\sin \alpha_0 = \frac{1}{M}.$$

This angle, as it is already known to us, is called the angle of propagation of weak disturbances.

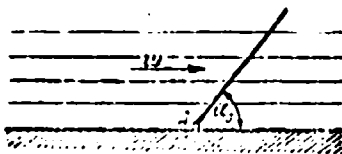


Fig. 4.10. The parallel uniform flow above a plane wall.

Now we can give the flow pattern of an external obtuse angle. Assume at a certain point C the wall turns, forming with the initial direction the angle δ (Fig. 4.11). During the supersonic flow around the external obtuse angle ACB the gas is expanded,

¹The viscosity effect of gas here can be disregarded.

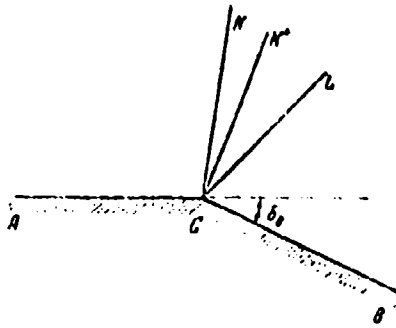


Fig. 4.11. The rotation of the supersonic flow of gas during flow around the angle ACB.

since the area occupied by the gas increases; during expansion the gas is accelerated. Along the section of wall AC the gas velocity is constant. The corner point C during the flow of gas around it is an obstruction which serves as the source of the emergence of weak disturbances in the gas flow. These disturbances, as it was shown, are propagated in a steady flow on straight line - characteristic CK, which separates the undisturbed gas flow from disturbed. Along the section of wall CB the gas velocity again takes a constant value, greater than in the initial flow along AC. This means that the disturbance which arose as a result of the flow around the corner point C terminated on another characteristic CL, which is also rectilinear. Thus the rotation of flow to the new direction is achieved within angle KCL between two rectilinear characteristics. For greater clarity let us break down the section of the continuous expansion of gas within the angle KCL into a large number of sections with insignificant, but discontinuous changes in parameters.

The first low jump in velocity and pressure will occur on the plane, the trace of which is the straight line CK; since pressure in this case drops, then according to the theory of jumps the velocity component normal to plane CK increases; in view of the invariability of the tangential component of velocity the flow changes its direction little, differing from the plane of the expansion shock to the side opposite to that into which it would be deflected in a compression shock. Thus, after plane CK of the weak expansion shock the flow obtained a somewhat greater

... reflects a little in the appropriate direction, density, density and temperature of the gas are slightly ... The disturbance which is propagated from the area of ... already now should be limited by the new characteristic CK', which as a result of deviation in the flow and increase in Mach number is located more to the right of the ... characteristic CK. Left of characteristic CK' no disturbances penetrate, therefore along the line CK', just as before this along the line CK, the parameters of the gas and the speed of motion are invariable.

... flow velocity, which increased somewhat in the first ... is designed on directions which are normal and tangential to the second characteristic CK', then it will turn out that the normal component of velocity here is less ($w'_u < w_u$), and radial - ... ($w'_p > w_p$) than on line CK.

The second weak expansion shock, which we combine with plane CK', causes a new deviation in flow to the side CB and the further expansion of gas which is accompanied by an increase in velocity.

The rotation of flow obviously will be completed if the stream adjacent to the wall becomes parallel to direction CB (Fig. 4.11). Consequently at the wall itself the velocity vector is parallel to CB.

But on the strength of the fact that all characteristics outgoing from point C are rectilinear, i.e., the velocity (and the remaining parameters of gas) along them does not change, then also along the last characteristic CL the velocity vector retains a constant (in value and direction) value w_k .¹ Thus after the

Point C is a *singular point*, since at this point converge the rays, for each of which the values of velocity and pressure are constant. These constant values of velocity and pressure are different for different rays.

last characteristic CL the flow again becomes forward. But after point C the flow does not experience more disturbances. Consequently, after rotation about the angle the flow above wall CB will be the same as was the flow above wall AC, i.e., a uniform and parallel flow at constant velocity $w_H > w_h$. The last characteristic CL, on which is completed the rotation of the gas flow about point C, is located at an angle α_k to the wall CB, which corresponds to the equality

$$\sin \alpha_k = \frac{1}{M_h}.$$

whereas the first characteristic is located at an angle α_H to the wall AC in accordance with the equality

$$\sin \alpha_H = \frac{1}{M_H};$$

here M_H, M_k are values of M numbers before and after the rotation of flow.

As is known, finite adiabatic expansion shocks are impossible. However if we break down angle KCL into an infinite number of infinitesimal angles, then we pass from the conditional diagram with small expansion shocks examined above to the continuous expansion of gas; instead of a finite number of weak shocks we obtain an infinite number of characteristics - a beam of characteristics.

Thus the rotation of a flow around an obtuse angle and the expansion of gas (decrease in the pressure) connected with this can be considered as a sequence of weak disturbances, the source of which is the vertex of the angle; these disturbances are propagated in the flow according to rectilinear characteristics outgoing from the vertex.

The considerations given show that during the rotation of a supersonic gas flow about an external obtuse angle the values of velocity, pressure, and density remain constant along the rays outgoing from the point of inflection and are characteristics.

Thus during the analytical study of the flow about an obtuse angle it is convenient to make use of polar coordinates, having placed the origin of the coordinates at this point of inflection. The coordinate lines are then the rays outgoing from the point of inflection and concentric circumferences with a center in this point of inflection. Coordinates of the points on a plane are the radius-vector r of this point and the angle ϕ , made up by the radius-vector with the ray which has the fixed direction, which we will determine later. All the parameters of gas we will consider as functions of r and ϕ : $w = w(r, \phi)$, $p = p(r, \phi)$, $\rho = \rho(r, \phi)$. On the strength of the fact that the parameters of gas along the rays in our problem are retained constant, the partial derivatives of w , p and ρ in terms of r are equal to zero (during movement along the ray changes do not occur in the parameters of the gas). Thus,

$$\frac{\partial w}{\partial r} = 0, \quad \frac{\partial p}{\partial r} = 0, \quad \frac{\partial \rho}{\partial r} = 0. \quad (11)$$

Velocity component on the radius-vector and in the direction perpendicular to it we designate respectively by w_r and w_n . Then the velocity $w = \sqrt{w_r^2 + w_n^2}$. On the strength of the fact that $\partial w / \partial r = 0$, we also have

$$\frac{\partial w_r}{\partial r} = 0 \quad \text{and} \quad \frac{\partial w_n}{\partial r} = 0. \quad (12)$$

The basic property of the characteristic, as it is already known, consists of the fact that the velocity component normal to it is equal to the speed of sound a , but the characteristic coincides with the radius-vector, therefore in the polar coordinate system selected by us the normal component of the velocity can be found from the condition

$$w_n = a. \quad (13)$$

The gas flow around the external obtuse angle is smooth and accelerated, therefore it is possible to consider it vortex-free. But then circulation on any closed loop is equal to zero. Let us compose the expression for circulation on the loop MRNK,

limited by the segments of two radius-vectors carried out from the vertex of the angle and two arcs, going around this loop clockwise (Fig. 4.12):

$$\Delta \Gamma = w_a r \Delta \varphi + \left(w_r + \frac{\partial w_r}{\partial \varphi} \Delta \varphi \right) \Delta r - \left(w_a + \frac{\partial w_a}{\partial r} \Delta r \right) (r + \Delta r) \Delta \varphi - w_r \Delta r = 0;$$

taking into account the constancy of the velocity on the radius-vector which is a characteristic, we have

$$\frac{\partial w_r}{\partial \varphi} - w_a = 0. \quad (14)$$

This is a condition of the absence of eddying in a supersonic gas flow which flows around an external obtuse angle. It could also be obtained directly from expression (103) of Chapter II. Every stream of the flow in question can be considered energy isolated, whereupon the equation of energy it is advantageous to utilize in a kinematic form (48) from Chapter I:

$$\frac{2}{k-1} a^2 + w^2 = w_{\max}^2. \quad (15)$$

In a smoothly accelerated gas flow, which we are examining in this case, the losses of total pressure are usually insignificant, therefore the thermodynamic process of flow about the angle we will consider isentropic, i.e., being subordinated to the equation for an ideal adiabatic curve:

$$p = \text{const.} \quad (16)$$

four equations (13)-(16) compose the system, to the solution of which the problem of the flow of a supersonic flow of gas about an external obtuse angle is reduced.

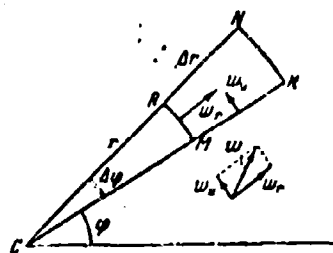


Fig. 4.12. To the derivation of the condition of absence of eddying.

From equations (13) and (15) it follows that

$$\frac{w_n^2}{k-1} + \frac{w_r^2 + w_n^2}{2} = \frac{w_{max}^2}{2},$$

or

$$w_n^2 + \frac{k-1}{k+1} w_r^2 = \frac{k-1}{k+1} w_{max}^2 \quad (17)$$

Now utilizing equation (14), we come to the following differential¹ equation:

$$\left(\frac{dw_r}{d\varphi}\right)^2 + \frac{k-1}{k+1} w_r^2 = \frac{k-1}{k+1} w_{max}^2 \quad (18)$$

Dividing in this equation the variables w_r and ϕ we will obtain

$$\frac{dw_r}{\sqrt{\frac{k-1}{k+1} w_{max}^2 - w_r^2}} = d\varphi$$

or

$$\sqrt{\frac{k+1}{k-1}} \frac{d\left(\frac{w_r}{w_{max}}\right)}{\sqrt{1 - \left(\frac{w_r}{w_{max}}\right)^2}} = d\varphi.$$

By integration we obtain

$$\sqrt{\frac{k+1}{k-1}} \arcsin \frac{w_r}{w_{max}} = \varphi + c_1,$$

where c_1 - the integration constant. Solving this expression relative to the unknown value w_r , we find

$$w_r = w_{max} \sin \left[\sqrt{\frac{k-1}{k+1}} (\varphi + c_1) \right].$$

Then from equation (14) it immediately follows that

$$w_n = w_{max} \sqrt{\frac{k-1}{k+1}} \cos \left[\sqrt{\frac{k-1}{k+1}} (\varphi + c_1) \right].$$

Let us determine now the integration constant c_1 . Let us examine the case where the velocity of undisturbed flow (before rotation)

¹Since the parameters of the gas along lines $\phi = \text{const}$ during the flow about an external angle do not change, they are the functions only of one variable - polar angle ϕ . Thus in equation (18) and further the partial derivatives in terms of ϕ are replaced by full.

is equal to the speed of sound ($M_H = 1$). This means that the initial characteristic KC (Fig. 4.11) is perpendicular to wall AC, since

$$\sin \alpha_H = \frac{1}{M_H} = 1,$$

i.e., polar angles ϕ must be counted off from the perpendicular to the direction of the velocity of undisturbed flow. Then with $\phi = 0$, we have $w_r = 0$, $w_u = w$, and the expression for w_r is converted into the equation for determining c_1 :

$$0 = w_{max} \sin \left[\sqrt{\frac{k-1}{k+1}} (0 + c_1) \right].$$

Hence it is clear that $c_1 = 0$. Thus we obtain the following expressions for the velocity components w_r and w_u :

$$\begin{aligned} w_r &= w_{max} \sin \left(\sqrt{\frac{k-1}{k+1}} \tau \right), \\ w_u &= w_{max} \sqrt{\frac{k-1}{k+1}} \cos \left(\sqrt{\frac{k-1}{k+1}} \tau \right). \end{aligned}$$

Using expressions (35) and (41) of Chapter I, it is possible to pass from the maximum gas velocity to critical

$$w_{max} = a_{*p} \sqrt{\frac{k+1}{k-1}}$$

and to write the expressions for w_r and w_u in the following form:

$$w_r = a_{*p} \sqrt{\frac{k-1}{k+1}} \sin \left(\sqrt{\frac{k-1}{k+1}} \tau \right), \quad (19)$$

$$w_u = a_{*p} \cos \left(\sqrt{\frac{k-1}{k+1}} \tau \right). \quad (20)$$

With $\phi = 0$ we will obtain $w_r = 0$, $w_u = w = a_{*p}$, i.e., the speed of undisturbed flow is equal to the critical speed of sound.

Now let us find the value of full velocity for each of the rays: $w = \sqrt{w_r^2 + w_u^2}$. From equations (19) and (20) we will obtain

$$\begin{aligned} w^2 &= a_{*p}^2 \left[\frac{k-1}{k+1} \sin^2 \left(\sqrt{\frac{k-1}{k+1}} \tau \right) + \cos^2 \left(\sqrt{\frac{k-1}{k+1}} \tau \right) \right] = \\ &= a_{*p}^2 \left[1 - \frac{1}{k+1} \sin^2 \left(\sqrt{\frac{k-1}{k+1}} \tau \right) \right]. \end{aligned}$$

From here we determine the velocity coefficient

$$\lambda^2 = \frac{w^2}{a_0^2} = 1 - \frac{2}{k+1} \sin^2 \left(\sqrt{\frac{k-1}{k+1}} \varphi \right). \quad (21)$$

All the remaining gas parameters are expressed as the velocity coefficient according to the formulas obtained in Chapter I:

$$\frac{p}{p_0} = \left(1 - \frac{k-1}{k+1} \lambda^2 \right)^{\frac{k}{k-1}}. \quad (22)$$

$$\frac{\rho}{\rho_0} = \left(1 - \frac{k-1}{k+1} \lambda^2 \right)^{\frac{1}{k-1}}. \quad (23)$$

$$\frac{T}{T_0} = 1 - \frac{k-1}{k+1} \lambda^2. \quad (24)$$

$$M = \sqrt{\frac{\frac{2}{k+1} \lambda^2}{1 - \frac{k-1}{k+1} \lambda^2}}. \quad (25)$$

Thus after determining by formula (21) the value λ^2 for the corresponding values of ϕ , we will be able from formulas (22)-(25) to calculate completely the state of the gas for each of the rays passing through the vertex of the angle. With $\phi = 0$ $\lambda = 1$ is obtained, with $\phi > 0$ we have $\lambda > 1$. In proportion to the increase in the polar angle the gas velocity increases, and the pressure, density, and temperature decrease.

As can be seen from expression (21), with a certain value of the polar angle the velocity coefficient can achieve the maximum value

$$\lambda_{\max}^2 = \frac{k+1}{k-1},$$

when the pressure, temperature, and gas density are equal to zero. It is obvious that a further increase in velocity is impossible, and, consequently, the rotation of flow will be discontinued. In other words, there is an extreme value of polar angle determined from the condition

$$\sin^2 \left(\sqrt{\frac{k-1}{k+1}} \varphi_{\max} \right) = 1.$$

Hence it follows that

$$\varphi_{\max} = \frac{\pi}{2} \sqrt{\frac{k+1}{k-1}}. \quad (26)$$

Let us note that the solution obtained is useful for all values of velocity of a supersonic undisturbed flow, and not only in the case $\lambda_H = 1$. If the velocity of undisturbed flow is greater than the speed of sound, then computation according to formula (21) should be begun not from the zero polar angle ($\phi = 0$), but from that value of angle (ϕ_H) which corresponds to the given velocity of the undisturbed flow (λ_H). From formula (21) it follows that

$$\varphi_H = \sqrt{\frac{k+1}{k-1}} \arcsin \sqrt{\frac{k-1}{k} (\lambda_H^2 - 1)}. \quad (27)$$

The suitability of the solution obtained for any value of velocity is based on the fact that in this problem along any characteristic the velocity and the remaining parameters of the gas do not change, i.e., on any characteristic the flow is uniform and parallel. And therefore for the rotation of the flow, which proceeds to the right of this characteristic, the prehistory of the flow cannot be important, i.e., this value of λ_H is achieved as a result of the acceleration of gas during preliminary rotation from $\lambda = 1$ and $\phi = 0$ to $\lambda = \lambda_H$ and $\phi = \phi_H$ or rotation begins immediately at the value of the velocity coefficient $\lambda = \lambda_H$. Thus, in the case $\lambda_H > 1$ with $\phi \leq \phi_H$ flow remains undisturbed, i.e., all the parameters of the gas retain their value. With $\phi > \phi_H$ the parameters of the gas are calculated from the formulas (22)-(25) obtained above. It is necessary only to remember that at a velocity of undisturbed flow greater than the speed of sound angles ϕ must be counted off not from the perpendicular to the direction of undisturbed flow, but from the straight line making up angle $\phi_H + \alpha_H$ with the direction of undisturbed flow, where $\alpha_H = \arcsin \frac{1}{M_H}$.

Fig. 4.13. Diagram of the computation of angles ϕ with $w_n > a_{np}$.

$$\frac{BC}{AB} = \frac{dr}{r d\theta}.$$
$$\frac{dr}{r d\varphi} = \frac{w_r}{w_\varphi}, \quad (28)$$

210

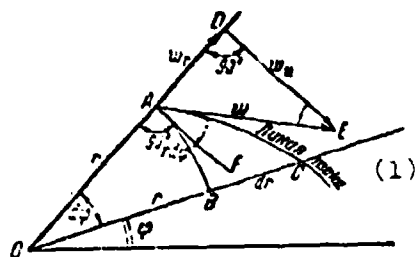


Fig. 4.14. For determining the flow line during flow around an external obtuse angle.

KEY: (1) Flow line.

In the case of flow around the angle w_r and w_u are determined by formula (19) and (20), therefore differential equation (28) takes the form

$$\frac{dr}{r} = \sqrt{\frac{k+1}{k-1}} \frac{\sin\left(\sqrt{\frac{k-1}{k+1}}\varphi\right)}{\cos\left(\sqrt{\frac{k-1}{k+1}}\varphi\right)} d\varphi.$$

It can also be rewritten in this form:

$$\frac{dr}{r} = -\frac{\sqrt{\frac{k+1}{k-1}} d\left[\cos\left(\sqrt{\frac{k-1}{k+1}}\varphi\right)\right]}{\cos\left(\sqrt{\frac{k-1}{k+1}}\varphi\right)}.$$

Integrating this differential equation, we find

$$\ln r = -\frac{k+1}{k-1} \ln \cos\left(\sqrt{\frac{k-1}{k+1}}\varphi\right) + \ln r_0$$

where through $\ln r_0$ is designated the arbitrary integration constant. After involution we will obtain

$$r = r_0 \left[\cos\left(\sqrt{\frac{k-1}{k+1}}\varphi\right) \right]^{-\frac{k+1}{k-1}}. \quad (29)$$

Equation (29) is the equation of flow lines in polar coordinates. Here r_0 is the length of the radius vector of the flow line of the flow line with $\varphi = 0$, i.e., in an undisturbed flow. From equation (29) it is evident that all the flow lines are similar curves with the center of similitude in the vertex of the angle. Distance along the normal between two adjacent flow lines increases in the direction of flow.

Now let us find angle δ , between the tangent to the flow line and the direction of undisturbed flow which moves at the speed of sound, i.e., the angle to which the flow is turned after reaching the appropriate ray, constituting the angle ϕ with a perpendicular to the direction of the velocity of undisturbed flow (with $\lambda_M = 1$). For this let us examine Fig. 4.15. Here w is the velocity vector at point B directed tangentially to the flow line. Angle α is the local angle of the propagation of weak disturbances. This angle is equal, as is known, to the angle between the direction of velocity w and characteristic BE at the particular point. Angle δ is the unknown angle of rotation of flow. From the figure it is clear that $\angle ABD = \delta$, and angle $ABC = \alpha$. Then from triangles ABC and ABD we have

$$\angle A = \pi - \varphi - \alpha \text{ and } \angle A = \frac{\pi}{2} - \delta$$

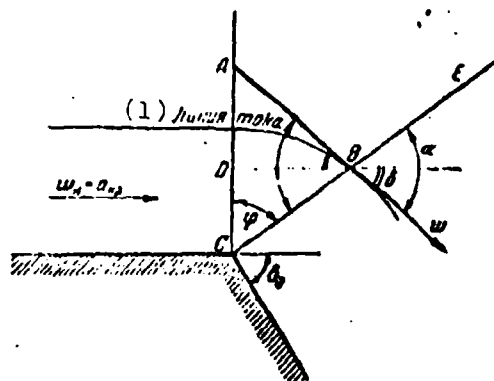


Fig. 4.15. The connection between angles α , ϕ , and δ during flow around an obtuse angle.
KEY: (1) Flow line.

Thus

or

$$\pi - \varphi - \alpha = \frac{\pi}{2} - \delta$$

$$\delta = \alpha + \varphi - \frac{\pi}{2}. \quad (30)$$

The angle of propagation of weak disturbances

$$\alpha = \arcsin \frac{1}{M}. \quad (31)$$

Thus for the calculation of the angle of rotation of flow δ , which corresponds to the assigned value of angle ϕ , it is necessary to perform the following operations:

- 1) determine by formula (21) the velocity coefficient λ for the assigned value of ϕ ,
- 2) by formula (25) determine the Mach number,
- 3) by formula (31) determine the angle α , and, finally,
- 4) calculate angle δ according to formula (30) for the assigned value of ϕ . Thus we will obtain the angle of rotation of flow δ as a function of the polar angle ϕ .

Up to now the independent variable was the polar angle ϕ and all the gas parameters were calculated as a function of this angle. In actuality the value of the circumfluous obtuse angle, i.e., the value of the angle of rotation of flow δ_0 , and the value of the velocity of incident flow are usually known. According to these data it is necessary to determine all parameters of the gas (velocity, pressure, temperature, etc.) after the rotation of flow around the assigned obtuse angle. Thus for practical calculations it is convenient to compile a table, where as the basic parameter the angle of rotation of flow δ is accepted, and all the remaining parameters of the gas are calculated in the function of this angle. Such a table, calculated from formulas (21)-(25), (30) and (31), is given in the appendix to the book on pages 1007-1009. It is necessary to use this table in the following manner: from the given speed of undisturbed flow w_∞ the velocity coefficient λ_∞ is determined. Further the *fictitious* angle of rotation of flow δ_∞ which corresponds to value λ_∞ is sought (angle to which the flow which flows at the speed of sound should turn in order to achieve the assigned velocity w_∞). Then angle $\delta_\infty = \delta_\infty + \delta_0$ is found, where δ_0 is the assigned angle of rotation of flow (Fig. 4.16). For a value δ_∞ from the table values $\lambda_\infty, \frac{\rho_\infty}{\rho_0}, \frac{p_\infty}{p_0}, \frac{T_\infty}{T_0}$ and M_∞ are extracted; they determine respectively the velocity coefficient, pressure, density, temperature, and Mach number after the rotation of flow around the assigned obtuse angle. Curves $\phi(\delta)$, $M(\delta)$, and $\alpha(\delta)$ and $\frac{p}{p_0} = f(\delta)$ are depicted in Fig. 4.17.

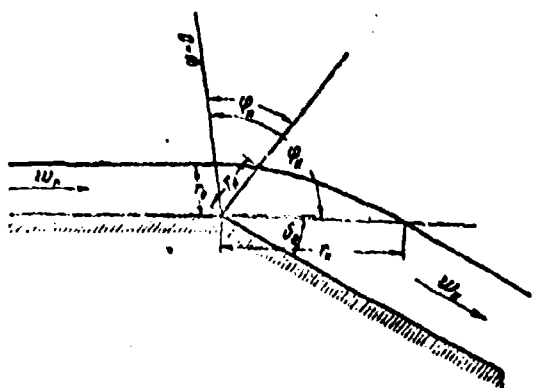


Fig. 4.16. The flow line of a supersonic flow which flows around an external obtuse angle.

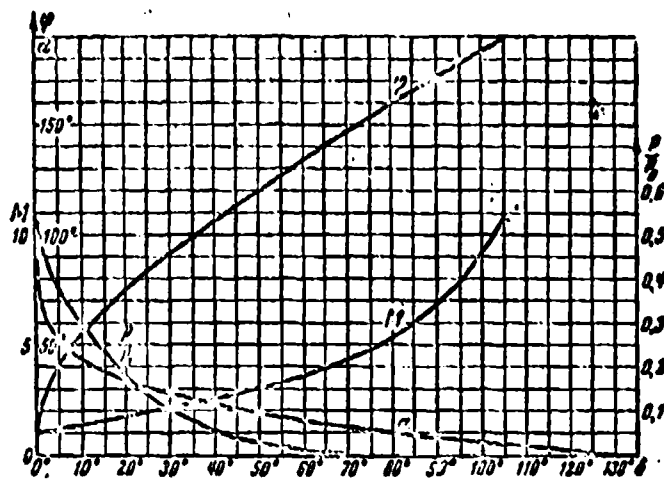


Fig. 4.17. Auxiliary curves for the calculation of supersonic flow around an external obtuse angle ($k = 1.4$).

If desired it is possible to determine the form of the flow line according to formula (29), after assigning value r_0 and a series of values ϕ from $\phi = \phi_H$ to $\phi = \phi_M$ (Fig. 4.16).

For determining the angle of rotation of flow δ_0 depending on the initial and final velocity it is possible to use the simple formula proposed by A. Ya. Cherkez which approximates well the precise relationships and the tabulated data with $k = 1.4$:

$$\delta_0 = 7.8 (\lambda_0^2 - \lambda_\infty^2) \quad (32)$$

Here λ_1 and λ_2 respectively are the velocity coefficients of flow before and after rotation. With $\lambda < 2.3$ ($\frac{p}{p_0} > 0.0005$) the error for the determination of angle δ_0 from this formula does not usually exceed 1°.

The given theory of flow of a supersonic flow of gas around an external obtuse angle is applied for the solution of a large number of specific problems of gas dynamics; some of them we will examine below.

§ 4. Flow Around a Plane Wall

Assume the supersonic flow of gas flows at an assigned velocity over a plane fixed wall. At point C (Fig. 4.18) the wall is broken, but the pressure in space after point C is less than the pressure in the undisturbed flow along the wall. Then exactly as in the case of the flow about an external obtuse angle, point C will be the disturbance source. Flow, flowing around point C, will turn itself on a certain angle δ . Its velocity will increase, and the pressure in the flow will drop to the value of the pressure which exists in space beyond point C. The picture of flow in this case is completely similar to the flow around the external obtuse angle. The only difference is that in the case of the flow around the obtuse angle the angle of rotation of flow δ is assigned and it is required to find all parameters of the gas after rotation, and in the case of the flow around a half-infinite plane wall being examined by us the pressure in the flow after rotation is assigned and it is required to find the angle of rotation of flow and all the remaining parameters of the gas. The angle δ defines the boundaries which separate the deviated flow of gas from the fixed gas under the wall (dotted line in Fig. 4.18).

For calculating the flow around a plane half-infinite wall it is possible to use Table I on pages 1007-1009. Through the assigned

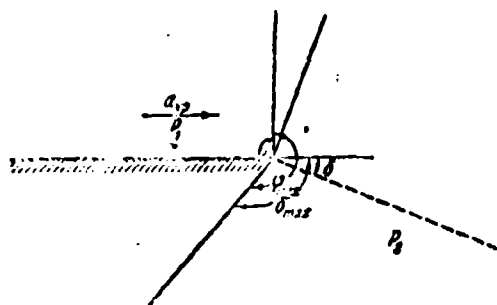


Fig. 4.18. Diagram of the supersonic flow around a wall.

magnitude of pressure the angle of rotation of flow and all the remaining parameters of the gas are found.

It is easy to calculate the *maximum angle δ_{\max} to which the gas flow which descends from a plane wall can turn*. This angle is the angle of rotation of flow, the initial velocity of which is equal to the speed of sound during outflow into a vacuum.

Let us assume in formula (22) $p = 0$. Then

$$\lambda^2 = \frac{k+1}{k-1} = \lambda_{\max}^2.$$

Substituting $\lambda = \lambda_{\max}$ into formula (27), we find

$$\varphi_{\max} = \frac{\pi}{2} \sqrt{\frac{k+1}{k-1}}.$$

Since with $\lambda = \lambda_{\max}$ from (25) we have $M = \infty$, then $\alpha = \arcsin \frac{1}{M} = 0$. Then from formula (30) we obtain

$$\delta_{\max} = \left(\sqrt{\frac{k+1}{k-1}} - 1 \right) \frac{\pi}{2}.$$

With $k = 1.4$ values ϕ_{\max} and δ_{\max} will be $\phi_{\max} = 220^\circ 27'$, $\delta_{\max} = 130^\circ 27'$. Hence it follows that the flow which flows from a plane wall into a vacuum does not fill the entire free space under the wall. Ray $\phi = \phi_{\max}$ separates this flow from the void under the wall. It is clear that this position is correct not only for the case $\lambda_H = 1$, but also with $\lambda_H > 1$. The angle of rotation of such a flow during outflow into a vacuum is equal to $\delta_{\max} - \delta_H$, where δ_H is the fictitious angle of rotation of flow which corresponds to the assigned value λ_H . This critical angle, by which the supersonic flow of assigned velocity can turn, let us designate δ_{np} . Thus,

$$\delta_{np} = \delta_{max} - \delta_n.$$

The dependence of δ_{np} on Mach number of undisturbed flow (with $k = 1.4$) is presented in the chart of Fig. 4.19. With $M = 1$ we have $\delta_n = 0$ and $\delta_{np} = \delta_{max}$. With $M = \infty$

$$\delta_n = \delta_{max} \text{ and } \delta_{np} = 0.$$

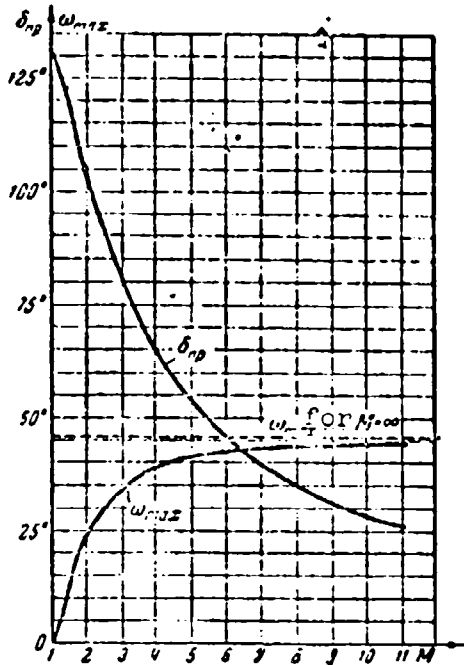


Fig. 4.19. The critical angles of rotation of flow in a shock wave and during the flow around an external obtuse angle.

If the supersonic flow should flow around an obtuse angle for which $\delta > \delta_{np}$, then after the rotation of flow around the vertex of the angle the flow blows away and follows not on wall, but on the ray which corresponds to $\delta = \delta_{np}$; between the ray and the wall a vacuum is formed. This phenomenon can be called the *separation of supersonic flow*.

§ 5. Flow Around a Convex Curvilinear Wall

In order to compose a representation of the picture which appears during flow around a convex curvilinear wall let us

examine first one of the flow lines obtained during flow around an obtuse angle and accept it for the projection of a solid wall (Fig. 4.20). Above this wall the flow parameters are known, since they will remain the same as they were above the corresponding (now *solidified*) flow line during flow around an angle.

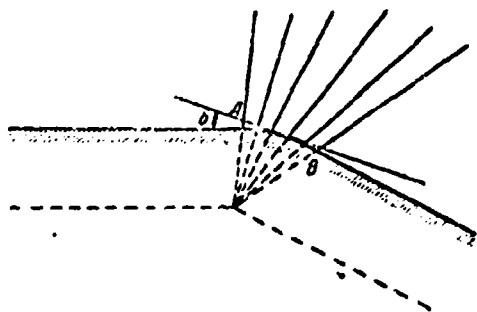


Fig. 4.20. Diagram of supersonic flow around a convex curve.

Past every point of the streamlined curved line passes a rectilinear characteristic, along which all the gas parameters remain constant. The state of the gas on every characteristic is determined from the angle of rotation of flow δ , which corresponds to this characteristic and is equal to the angle between the characteristic which is tangential to the wall at the *initial point* and the direction of undisturbed flow. During the calculation of the gas parameters it is necessary to make use of the previously derived formulas or the table of Appendix I to the book on pages 1007-1009.

Let us note that the *same accurately qualitative picture takes place during the flow around a convex curvilinear wall of any form*. It is necessary only that the convexity of the wall be directed always to the side of the gas. In order to show this, let us replace the arbitrary curved wall by an inscribed broken line which consists of a succession of rectilinear segments (Fig. 4.21a). Flow around such a broken line is reduced to flow around a succession of external obtuse angles, and therefore can be calculated completely. The flow pattern is shown in Fig. 4.21b. If now we increase infinitely the number of vertexes of the broken

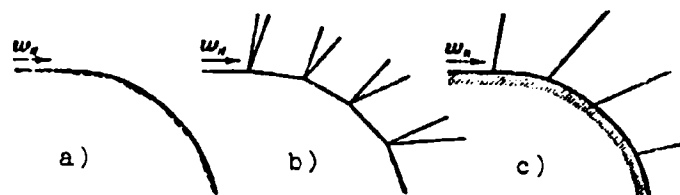


Fig. 4.21. Transfer from flow around a broken wall to the flow around a convex curve.

line inscribed into this curve, then in the end we will obtain flow around a curve, whereupon it is clear that through every point of curve passes the rectilinear characteristic, along which the gas parameters are not changed (Fig. 4.21c).

In order to calculate the flow around an arbitrary curve of a convex wall it is necessary to know only the angle of rotation, i.e., the direction of the tangent for every point of the wall. If, for example, the form of the wall is assigned by an equation in the form $y = y(x)$ (x -axis is directed along the velocity vector of undisturbed flow), then, differentiating this equation, we will find the tangent angle with the x -axis for every value of abscissa x , equal to the angle of rotation of flow δ .

Thus

$$\delta = \arctg |y'(x)|$$

Knowing δ , it is easy to determine all the gas parameters, acting exactly the same as in the case of flow around an obtuse angle. Specifically it is possible to find the distribution of velocity and pressures along the wall. During flow around a curved convex wall, just as during flow around an angle, the gas is accelerated. The gas velocity increases continuously and the pressure drops.

If it turns out that at any point of the wall

$$\delta > \delta_{np}$$

then flow separation will occur.

The determination of the form of the flow lines during flow around a convex wall of arbitrary form is a more difficult task, and we will not examine it here. The strict theory of flow around a curved wall was developed by I. A. Kibel and S. A. Khristianovich.

§ 6. Outflow from a Unit Two-Dimensional Nozzle with Oblique Section into Space with Reduced Pressure

Let us examine the outflow of a supersonic flow of gas from a two-dimensional nozzle. Let the nozzle provide a constant velocity in its section and the pressure in the free space into which the gas escapes is less than the pressure in the nozzle-section plane. The theory of flow around a plane wall given above makes it possible to determine the direction of the jet boundaries directly after the nozzle section.

The behavior of the gas near the edges of the nozzle A and B (Fig. 4.22) is precisely the same as during flow around one plane wall. Near each of the edges the flow will turn by such an angle δ that the pressure in the flow will become equal to the assigned pressure in free space. Consequently the jet as a whole is expanded during outflow. The angle of rotation of flow δ around each of the edges can be found from the assigned magnitudes of velocity and pressure in the nozzle section and the pressure in free space just as during the flow around one plane wall. This angle δ determines the direction of the jet boundaries behind the nozzle section. Along the entire free boundary of the jet there is a constant value of velocity which corresponds to external pressure and can be calculated easily according to the formulas and table given above.

The beams of the rectilinear characteristics outgoing from points A and B intersect as is shown in the figure. After the

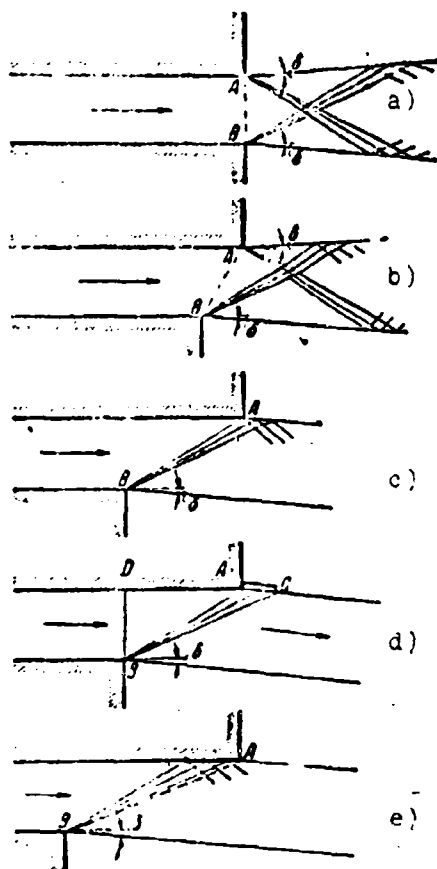


Fig. 4.22. The different systems of outflow from a nozzle with an oblique section.

intersection of characteristics the flow velocity changes, and, as this follows from § 2 of Chapter III, the characteristics cease to be rectilinear. This fact considerably complicates the calculation of further sections of the jet.

If the nozzle-section plane is not perpendicular to the axis of flow, then such a nozzle is called a *nozzle with an oblique section*. The presence of an oblique section disturbs the symmetry of flow and considerably complicates the calculation of the flow appearing in this case. The study of outflow from channels with an oblique section has important practical value, since such an outflow takes place during the operation of steam and gas turbines, where usually the nozzle vehicles are channels with an oblique section.

Let us examine the supersonic outflow of gas from a two-dimensional nozzle with an oblique section into space in which the pressure is less than the pressure in the flow within the nozzle. The oblique edge is formed during the displacement of edge B of the nozzle relative to edge A backwards, against the flow. In the case of minor displacement of edge B, i.e., with a small slant of the section plane AB (Fig. 4.22b), obviously an unsymmetric free jet will be obtained. In this case the area of intersection of the beams of the characteristics outgoing from edges A and B is moved to point A.

Consequently the rectilinear characteristics outgoing from edge A begin to be bent earlier than in the case of a direct section. Behind the section plane AB the jet is expanded. The angles of rotation of flow near each of the edges A and B obviously are the same as in the case of a direct section.

The extreme position of edge B for a flow of such a form is that position of it in which the "first" characteristic, carried out from edge B, passes accurately past edge A. Such a case is depicted in Fig. 4.22c. The picture of flow near edge B is similar as before to the flow around one plane wall. Thus the direction of the jet boundary behind edge B is retained as previous and it can be determined easily. The characteristics outgoing from edge A will begin to be bent immediately after point A. This complicates the determination of the second jet boundary behind point A.

If after edge A we make a directing deflector, realized on the flow line which corresponds to the rotation of flow around edge B (Fig. 4.22d), then flow can be calculated completely. The flow around edge B at the assigned external pressure is analogous to the flow around an external obtuse angle. Thus the form of the flow line can be determined by formula (29).

Thus we obtain the shape of directing deflector AC. Pressure on ray BC is equal to the assigned external pressure, as a result of which behind ray BC the jet again becomes parallel and uniform. The velocity in this jet is greater than the velocity within the nozzle in cross section BD. The jet is deflected from the nozzle axis by the angle δ , determined by the ratio of external pressure to the pressure within the nozzle in cross section BD.

Displacing edge B still further back, we will obtain the case of outflow from an oblique section as depicted in Fig. 4.22e. Here the "first" characteristic outgoing from edge B comes to the

opposite wall within the nozzle at a certain point left of A. Precise calculation of flow near the section of the wall between the indicated point and point A and the determination of the jet boundary behind edge A is a sufficiently complex problem. If as in the preceding case we make a directing deflector, having placed its beginning in the point of encounter of the first characteristic with the wall A, then we will reduce the case in question to the preceding one.

The effectively applicable cases of outflow from an oblique section are the cases b, d, and e. In cases c and d the approximate computation, defining the discharge velocity and the angle of rotation of the jet as a whole just as in the case d, is used, i.e., the small change in the flow parameters connected with the disturbance of the picture of flow near edge A accepted during the calculation is disregarded.

Let us emphasize again that in all practically applicable cases of outflow from a plane channel with an oblique section into space with reduced pressure the flow in the oblique section undergoes expansion, and the jet obtains an additional deviation; in this case the discharge velocity increases as compared with the velocity which can be provided by the same nozzle with a direct section.

CHAPTER V

ONE-DIMENSIONAL GAS FLOWS

§ 1. Adiabatic Gas Flow with Friction. Critical Region of the Flow

Let us examine the steady flow of gas in a tube of constant cross section in the presence of friction but without heat exchange with environment.

The equation of continuity in this case ($G = \text{const}$, $F = \text{const}$) takes the following form:

$$\rho w = \text{const},$$

or in differential form

$$\frac{dp}{\rho} = -\frac{dw}{w}. \quad (1)$$

The differential equation of state

$$dp = gR(\rho dT + T d\rho). \quad (2)$$

From equations (1) and (2) we obtain

$$\frac{dp}{\rho} = gR dT - gRT \frac{dw}{w}. \quad (3)$$

Using the Bernoulli equation in differential form

$$\frac{dp}{\rho} + w^2 \frac{dw}{w} + g dL_{TP} = 0$$

and the known expression for the speed of sound

$$a^2 = kgRT,$$

we convert expression (3) to the new form

$$gRdT + \left(w^2 - \frac{a^2}{k}\right) \frac{dw}{w} + g dL_{TP} = 0. \quad (4)$$

In view of the fact that the process in question is energy isolated, the stagnation temperature along the tube does not change $T_0 = \text{const}$. This is equivalent to the condition

$$dT_0 = dT + \frac{Aw^2}{gc_p} \frac{dw}{w} = 0,$$

or, taking into account the known equalities $AR = c_p - c_v$, $c_p = kc_v$,

$$gRdT = -\frac{k-1}{k} w^2 \frac{dw}{w}. \quad (5)$$

Substituting (5) into (4), we arrive at the relation which connects the velocity change along the tube of constant cross section with the work of forces of friction:

$$(M^2 - 1) \frac{dw}{w} = -\frac{k}{a^2} g dL_{TP} \quad (6)$$

It is important that the friction is a one-sided action: the work of the forces of friction is always positive ($dL_{TP} > 0$). Therefore, according to the relation (6) *under the effect of friction the subsonic flow ($M < 1$) is accelerated ($dw > 0$), and the supersonic flow ($M > 1$) is slowed down ($dw < 0$)*. The continuous transition through the speed of sound under the action only by friction is impossible.

Let us derive the formulas which determine the change in the parameters of gas along the insulated tube in the presence of friction.

In view of the fact that the process in the gas is energy isolated, the stagnation temperature is not changed:

$$T_{01} = T_{02} = \text{const.} \quad (7)$$

The thermodynamic temperature, if we use equations (42) of Chapter I and (7), is determined from the relation

$$\frac{T_2}{T_1} = \frac{1 - \frac{k-1}{k+1} \lambda_2^2}{1 - \frac{k-1}{k+1} \lambda_1^2}. \quad (8)$$

As a result of the constancy of stagnation temperature, the critical velocity along the tube also does not change; hence the ratio of the coefficients of velocity is equal to the ratio of the velocities on the basis of the equation of the continuity - the inverse density ratio

$$\frac{\lambda_2}{\lambda_1} = \frac{w_2}{w_1} = \frac{\rho_1}{\rho_2}. \quad (9)$$

After substituting equalities (8) and (9) into the equation of state, we obtain the dependence of the pressure on the velocity coefficient:

$$\frac{p_2}{p_1} = \frac{\lambda_1}{\lambda_2} \frac{1 - \frac{k-1}{k+1} \lambda_2^2}{1 - \frac{k-1}{k+1} \lambda_1^2}. \quad (10)$$

In view of the constancy of stagnation temperature, the total pressure is proportional to the density of the stagnated gas¹

¹This results from the equation of state and formula (72) in Chapter I.

$$\frac{p_{01}}{p_{02}} = \frac{p_{01}}{p_{02}} = \frac{p_1}{p_2} \left(\frac{1 - \frac{k-1}{k+1} \lambda_1}{1 - \frac{k-1}{k+1} \lambda_2} \right)^{\frac{1}{k-1}}.$$

Hence on the basis of (10) we obtain

$$\frac{p_{01}}{p_{02}} = \frac{p_{01}}{p_{02}} = \frac{p_1}{p_2} \left(\frac{1 - \frac{k-1}{k+1} \lambda_1}{1 - \frac{k-1}{k+1} \lambda_2} \right)^{\frac{1}{k-1}}. \quad (11)$$

Let us give λ_1 any constant value, and we will consider λ_2 as a variable and parameters T_1 , p_2 , p_2 , p_{02} , p_{02} as functions of the variable λ_2 . It was established above, on the basis of relation (6), that the friction accelerates the subsonic and slows down the supersonic flow. Then it is necessary to consider λ_2 as increasing with subsonic and decreasing with supersonic flow. Therefore, according to dependences (8), (9) and (10), the thermodynamic temperature, density and static pressure along the insulated tube under the effect of friction decrease in subsonic and increase in supersonic flow. From equality (11) it follows that in the critical cross section when $\lambda_2 = 1$ the total pressure p_{02} has a minimum value,¹ but then from expression (102) of Chapter I it follows that in the critical cross section the entropy reaches a maximum value. The total pressure and the density of the stagnated gas, in accordance with equality (11), both in subsonic and supersonic flow along the tube decrease, and only one parameter - the stagnation temperature - is not changed.

¹It is possible to be convinced of this by differentiating the equality (11) with respect to λ_2 . By substituting one into the expression of the derivative instead of λ_2 , we obtain

$$\frac{d}{d\lambda_2} \left(\frac{p_{01}}{p_{02}} \right)_{\lambda_2=1} = 0.$$

The second derivative is positive when $\lambda_2 = 1$.

The fact that the entropy reaches a maximum in the critical cross section causes the existence of the critical region of the flow in the insulated tube, which makes the smooth transition through the speed of sound under the effect of friction impossible; with such a transition the entropy should decrease, and this contradicts the second law of thermodynamics.

Figure 5.1 depicts curves of temperature, density, pressure, stagnation temperature, and total pressure in the insulated tube as a function of the velocity coefficient λ_2 when $\lambda_1 = 0.1$ for subsonic flow, $\lambda_1 = 2.3$ for supersonic flow, and $k = 1.4$. The arrows at the figures indicate the direction of the course of the process.

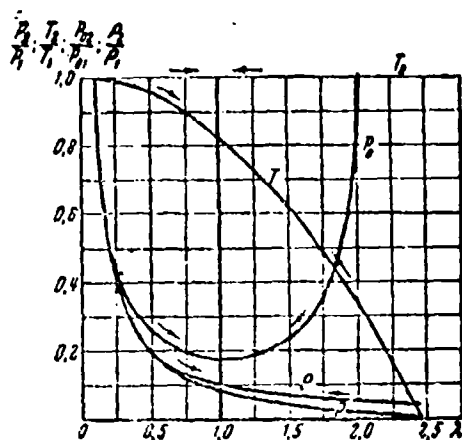


Fig. 5.1. Dependence of gas parameters on the velocity coefficient in a tube of constant cross section.

5.2. Flow in a Tube of Constant Cross Section

Let us investigate the effect of friction on the change in parameters of the turbulent gas flow in tubes of constant diameter. For this let us replace work of the force of friction in relation (6) with the expression conventional in hydraulics

$$dL_{fr} = \zeta \frac{w^2}{2g} \frac{dx}{D}; \quad (12)$$

here ζ is the coefficient of friction in the tube, D - diameter of the tube, dx - length of the infinitesimal section of the tube. Then we obtain

$$(M^2 - 1) \frac{dw}{w} = -\zeta k \frac{M^2 dx}{2D}.$$

By using expression (45) of Chapter I and the constancy of critical velocity in the tube, from which follows the equality

$$\frac{dw}{w} = \frac{d\lambda}{\lambda}.$$

let us turn in relation (6) from the M number to the coefficient of critical velocity λ :

$$\left(\frac{1}{\lambda^2} - 1\right) \frac{d\lambda}{\lambda} = \frac{k}{k+1} \zeta \frac{dx}{D}. \quad (13)$$

Let us allow in the first approximation that the coefficient of friction in the tube, both in subsonic and supersonic flows, does not depend on the M number and, consequently, on the velocity coefficient λ .

In rough tubes the value ζ for incompressible fluid does not depend on the Reynolds number R and is determined from formula¹

$$\zeta = \frac{1}{\left(1.74 + 21k \frac{1}{\epsilon}\right)^2}, \quad (14)$$

where $\epsilon = 2h/D = h/r$ is the relative roughness of the tube (h - the height of the projections of the roughness).

¹See "Problems of turbulence," page 29, ONTI, 1936.

Let us examine, further, the friction in the so-called technically smooth tubes. The technically smooth tube is characterized by the fact that the projections of roughness in it are covered with a laminar sublayer.¹ The thickness of the sublayer decreases with an increase in the R number; therefore, the same tube with low R is smooth but with large R is rough (Fig. 5.2).

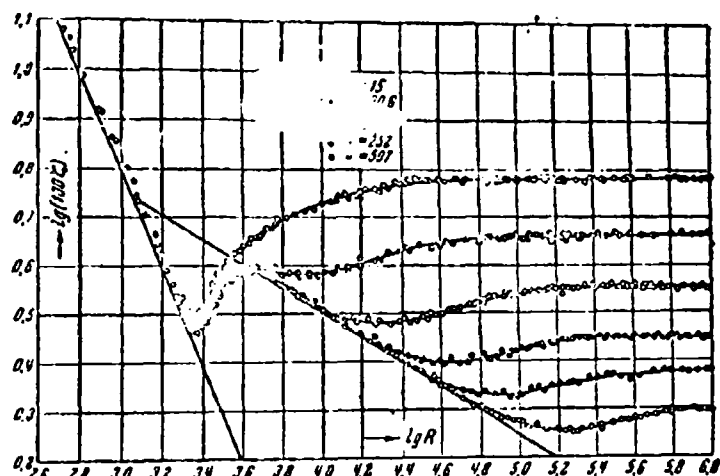


Fig. 5.2. Dependence of the coefficient of friction ζ on R in tubes with different roughness according to experiments of Nikuradze.

In technically smooth tubes, for the turbulent flow of incompressible fluid the coefficient of friction depends on the R number and can be determined by the formula

$$\zeta = 0.0032 + \frac{0.221}{R^{0.237}} \quad (15)$$

where $R = \rho w D / \mu$.

¹For more detail about the laminar sublayer see Chapter VI.

Since in the tube of constant cross section, according to the equation of continuity $\rho w = \text{const}$, then the R number along the length of the tube changes insignificantly (only because of a viscosity change).

Thus, we approximately assume the coefficient of friction in the tube to be a constant value:

$$\zeta \approx \text{const.}$$

In this case equation (13) is easily integrated:

$$\frac{1}{\lambda_1^2} - \frac{1}{\lambda_2^2} - \ln \frac{\lambda_2^2}{\lambda_1^2} = \frac{2k}{k+1} \zeta \frac{x}{D}; \quad (16)$$

here λ_1 is the value of the velocity coefficient at the beginning of the tube $x = 0$, and λ_2 is the value of the velocity coefficient in an arbitrary cross section of the tube at a distance of $x = x_2$ from the beginning. With the aid of expression (16) it is possible to determine the value of the velocity coefficient in the arbitrary cross section of the tube if the velocity coefficient at the beginning of the tubes λ_1 , the diameter of the tube D , the coefficient of friction ζ , and the index of ideal adiabatic curve k are known.

Let us introduce the function $\phi(\lambda) = 1/\lambda^2 + 2 \ln \lambda$ and call the dimensionless quantity which is on the right side of equation (16)

$$\frac{2k}{k+1} \zeta \frac{x}{D} = \chi$$

the normalized length of the tube. Then equation (16) can be presented in the form

$$\varphi(\lambda_1) - \varphi(\lambda_2) = \chi. \quad (17)$$

Thus, a change in the flow velocity between the two cross sections of the tube is such that a difference of the functions $\phi(\lambda)$ in them is equal to the normalized length of this section of the tube. By using the graph of function $\phi(\lambda)$ (Fig. 5.3), it is possible to determine the change in the coefficient of the flow velocity along the length of the tube depending on values λ and ξ . Function $\phi(\lambda)$ when $\lambda = 1$ has a minimum equal to $\phi(\lambda) = 1$. Therefore, at the rated value λ_1 the value of the difference on the left side of equation (17) and, consequently, also the normalized length of the tubes χ cannot be more than a certain critical value determined from condition $\lambda_2 = 1$:

$$\chi_{cr} = \varphi(\lambda_1) - 1. \quad (18)$$

Actually, let us equate to zero the derivative of the normalized length χ with respect to λ_2 when $\lambda_1 = \text{const}$:

$$\frac{d\chi}{d\lambda_2} = -\frac{d}{d\lambda_2} \varphi(\lambda_2) = \frac{2}{\lambda_1^2} - \frac{2}{\lambda_2^3} = 0.$$

Hence we find

$$\lambda_2 = 1.$$

Since when $\lambda_2 = 1$

$$\frac{d^2\chi}{d\lambda_2^2} = -\frac{6}{\lambda_1^2} + \frac{2}{\lambda_2^4} = -4.$$

Then condition $\lambda_2 = 1$ determines the maximum of the value of the normalized length of the tube for the assigned value of the velocity coefficient at the inlet into the tube λ_1 . Since equation (17) is correct not only for the entire tube, but also for any section of it, it follows from it that the velocity equal to the speed of sound can be achieved only in the outlet section of the tube. Actually, if we assume that the velocity coefficient λ is

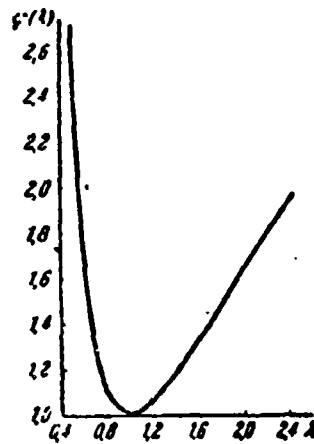


Fig. 5.3. Graph of function

$$\varphi(\lambda) = \frac{1}{\lambda^2} + 2 \ln \lambda$$

equal to unity in any intermediate cross section of the cylindrical tube, then from equation (17), recorded for the subsequent section of the tube, we obtain

$$\varphi(\lambda) = 1 - \chi < 1.$$

Since, by definition, function $\phi(\lambda) \geq 1$ (Fig. 5.3), then this case is not real.

It was shown above that with flow in the cylindrical tube with friction, the subsonic flow is accelerated and the supersonic - braked, and the maximally possible state in both cases with a continuous change in the parameters is the critical regime, i.e., the achievement by the flow of the speed of sound in the outlet section of the tube. Equation (17) makes it possible to establish the quantitative connection between the change in velocity and the normalized length of the tube χ . If at the inlet into the tube the flow is subsonic and the velocity coefficient of it is equal to λ_1 , and if the normalized length of the tube is less than the critical value determined by formula (18), then at outlet from the tube the flow will be also subsonic, whereupon from equation (17)

It follows that the velocity coefficient $\lambda_2 > \lambda_1$. If flow at the inlet is subsonic and the normalized length of the tube is equal to the critical (maximum) value for the given λ_1 , then at the outlet from the tube the flow velocity is equal to the speed of sound and $\lambda_2 = 1$.

If finally the normalized length of the tube is greater than maximum determined from formula (18), then equation (17) does not have a solution for λ_2 ($\phi(\lambda_2) < 1$). This means that the taken initial value of the velocity coefficient λ_1 cannot be realized. At the beginning of the tube with assigned normalized length χ , the flow velocity cannot exceed the value obtained from formula

$$\varphi(0) = \chi + 1, \quad (19)$$

since in this case the velocity at the outlet from the tube is equal to the critical velocity, and through the tube the maximally possible gas flow rate per second occurs.

Figure 5.4 depicts the dependence of the maximum value of the velocity coefficient at the inlet into the tube λ_{np} on the dimensionless length of the tube x/D for the subsonic flow when $\xi = 0.015$ and $k = 1.4$. At these values of ξ and k

$$\frac{x}{D} = \frac{k+1}{2k} \frac{1}{\epsilon} \chi \approx 57\chi.$$

It should be noted that the obtained change in the velocity coefficient (formula (16)), both when $\lambda_1 < 1$ and $\lambda_1 > 1$, corresponds to the completely definite change in the total and static pressure of the gas (see formulas (10) and (11) § 1). Everywhere above we assumed that such a pressure change can always be realized: this was the condition in the retention of the constant value λ_1 with a change in the normalized length of the tube up to the obtaining of $\lambda_2 = 1$. If for some reason or other the indicated change in pressure is impossible, for example, at the assigned

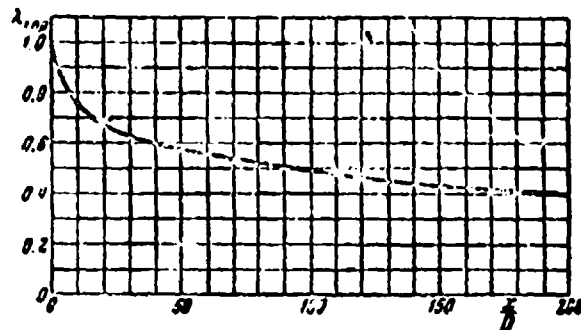


Fig. 5.4. Dependence of the maximum value of the velocity coefficient at the beginning of the tube on its length.

magnitude of a drop in pressures at the inlet and outlet, then the flow in question with the assigned initial velocity coefficient can prove to be unreal. This question is examined in more detail below in § 7.

With supersonic flow, for which formula (16) is also suitable, the following systems are possible. If with the assigned initial velocity λ_1 the normalized length is less the maximum ($\chi < \chi_{\text{кр}}$), then at the end of the tube supersonic flow ($\lambda_2 > 1$) is obtained. If the normalized length is equal to the maximum ($\chi = \chi_{\text{кр}}$), then the velocity at the end of the tube is equal to the critical velocity ($\lambda_2 = 1$). If the normalized length calculated according to formula (17) is more than the maximum, determined according to formula (18) at the assigned value of the velocity coefficient at the beginning of the tube λ_1 , then the smooth braking of supersonic flow for the extent of the entire tube is impossible; in a certain cross section of the tube a shock wave occurs, after which the accelerated subsonic flow is established.

Determining the position of this shock wave can be carried out in the following manner. Let the supersonic velocity at the beginning of the tube λ_1 , the length of tube x , diameter of the tube D , coefficient of friction ζ and the index of ideal adiabatic curve k be assigned. We compute according to formula (17) the

normalized length of the tube χ . According to formula (18) we determine the maximum normalized length $\chi_{\text{кр}}$ and are convinced of the fact that the true normalized length is greater than the maximum ($\chi > \chi_{\text{кр}}$). In this case, as was shown, in a certain cross section at a distance of $\chi_{\text{ск}}$ from the beginning of the tube a shock wave appears. For simplicity we assume that the shock wave is normal, and then the velocity coefficients before the shock (λ') and after the shock (λ'') are connected by relation (16) of Chapter III

$$\lambda \lambda'' = 1.$$

The velocity coefficient before the shock (λ') can be found from formula (16):

$$\frac{1}{\lambda'^2} - \frac{1}{\lambda'^2} - \ln \frac{\lambda'^2}{\lambda'^2} = \frac{2k}{k+1} \zeta \frac{x_{\text{ск}}}{D} = \chi_{\text{ск}} \quad (20)$$

The velocity coefficient after the shock, where the accelerated subsonic flow ($\lambda'' < 1$) is established, is connected with the length of the subsonic section of the tube at the end of a stall ($\lambda_2 = 1$) which takes by formula (18):

$$\frac{1}{\lambda''^2} - 1 - \ln \frac{1}{\lambda''^2} = \frac{2k}{k+1} \zeta \frac{x - x_{\text{ск}}}{D} = \chi - \chi_{\text{ск}}$$

whence

$$\lambda'' - 1 - \ln \lambda'' = \chi - \chi_{\text{ск}} \quad (21)$$

By solving together the two equations (20) and (21) with two unknowns ($\chi_{\text{ск}}$, λ'), we arrive at the equation with one unknown, according to which the velocity before the shock is calculated:

$$\lambda'^2 + \frac{1}{\lambda'^2} - 1 - \ln \frac{1}{\lambda'^2} = \chi \quad (22)$$

after which according to formula (21) the location of the shock is determined.

Formulas (20), (21), and (22) for determining the location of the shock wave are inconvenient, since according to them it is necessary to conduct the calculations by the method of successive approximations. It is possible to recommend auxiliary graphs (Fig. 5.5), which substantially simplify the calculations. Curve (1) corresponds to the auxiliary dependence

$$\varphi(\lambda) = \frac{1}{\lambda^2} + \ln \lambda^2. \quad (23)$$

Curve (2) represents function (21):

$$\chi - \chi_{cr} = \lambda^2 - 1 - \ln \lambda^2.$$

Curve (3) corresponds to function (18):

$$\chi_{sp} = \frac{1}{\lambda_1^2} - 1 - \ln \frac{1}{\lambda_1^2}.$$

Let us explain the method of the use of these curves in a concrete example. Let a tube with the normalized length $\chi = 0.6$ be given. According to curve (3) it is evident that in this tube there will be the critical regime ($\lambda_2 = 1$) at the value of the velocity coefficient at the inlet $\lambda_1 = 1.95$. Let us check first the flow pattern in the tube in the case of $\lambda_1 > 1.95$, for example, for $\lambda_1 = 2.2$. According to formula (16) it is possible to calculate the velocity at the end of the tube

$$\frac{1}{\lambda_2^2} + \ln \lambda_2^2 = \frac{1}{\lambda_1^2} + \ln \lambda_1^2 - \chi$$

or, in accordance with notation (23)

$$\varphi_2 = \varphi_1 - \chi. \quad (24)$$

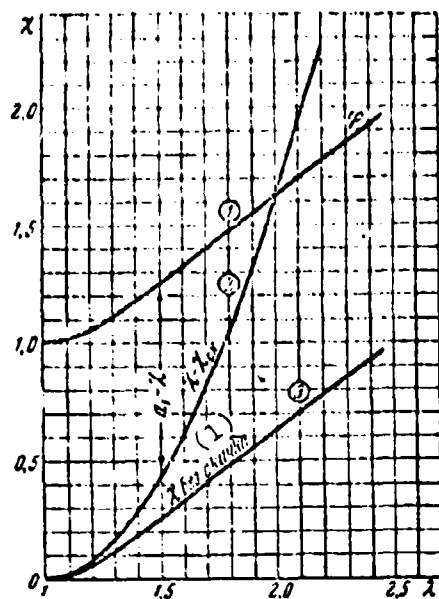


Fig. 5.5. Auxiliary curves for calculating supersonic flow in a tube of constant cross section.
KEY: (1) without a shock.

On curve (1) when $\lambda_1 = 2.2$ we find point $\phi_1 = 1.78$, whence

$$\phi_2 = 1.78 - 0.60 = 1.18,$$

which on curve (1) corresponds to the value of the velocity coefficient at the end of the tube $\lambda_2 = 1.4$. Thus, in the tube which has the normalized length $\chi = 0.6$, at the initial value of the velocity coefficient $\lambda_1 = 2.2$ there occurs smooth braking of the supersonic flow up to the value of the velocity coefficient $\lambda_2 = 1.4$.

Let us now assume that the tube has a normalized length greater than maximum ($\chi > \chi_{kp}$), i.e., in this example $\lambda_1 < 1.95$. Let us assume that $\lambda_1 = 1.8$. Then according to curve (3)

$$\chi_{kp} = 0.48, \text{ i.e., } \chi_{kp} < \chi.$$

In this case in the tube a shock wave appears, as a result of which in the section of the tube with a length of $\chi - \chi_{CH}$ subsonic flow is established, whereupon, as can be seen from the comparison of curves (2) and (3), the critical length of the tube is substantially increased. To search for the location of the shock wave, we transform formula (20) with the aid of notations (23). Then the distance from the beginning of the tube to the cross section in which there occurs the shock wave is equal to

$$\chi_{CH} = \varphi_1 - \varphi' \quad (25)$$

But, on the other hand,

$$\chi = (\chi - \chi_{CH}) + \chi_{CH}$$

By replacing the last term on the right side of this formula according to (25), we obtain

$$\varphi_1 - \chi = \varphi' - (\chi - \chi_{CH}) \quad (26)$$

Now, using the curves of Fig. 5.5, let us determine the location of the shock wave in the tube when $\lambda_1 = 1.8$. According to curve (1), we find

$$\varphi_1 = 1.48,$$

whence

$$\varphi_1 - \chi = 1.48 - 0.60 = 0.88.$$

It remains to find the value λ' at which the distance between curves (1) and (2) is equal according to (26)

$$\varphi' - (\chi - \chi_{CH}) = 0.88.$$

According to Fig. 5.5 we obtain

$$\lambda' = 1.4, \quad \varphi' = 1.18,$$

which corresponds according to formula (24) to the normalized distance from the beginning of the tube to the shock wave:

$$\chi_{\text{sh}} = \varphi_1 - \varphi' = 0.3.$$

Calculated and plotted on Fig. 5.6 by the described method according to curves of Fig. 5.5 are curves of the change in the velocity coefficient $\lambda = f(\chi)$ in a tube with normalized length $\chi = 0.6$, which are obtained at different values of the velocity coefficient λ_1 at the beginning of the tube (when $\chi = 0$). As we see, the shock wave is located nearer to the beginning of the tube, the less the initial supersonic gas velocity. Values of subsonic velocity after the shock wave lie in all cases on the universal curve which corresponds to formula

$$\chi = \frac{1}{\lambda_1^2} - 1 - \ln \frac{1}{\lambda_1^2}.$$

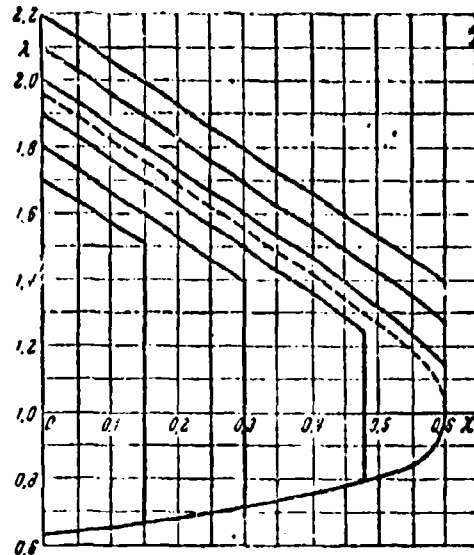


Fig. 5.6. Curves of distribution of values of the velocity coefficient in a tube with normalized length $\chi = 0.6$ at different initial velocities and $\lambda_2 \geq 1$.

When $\lambda_1 = 1.6$ the shock is located at the beginning of the tube ($\lambda_1 = \lambda'$), i.e., the section of the supersonic flow is completely eliminated. The gas flow in the tube with the assigned drop in the pressures is examined in § 7.

§ 3. Motion of Preheated Gas Along a Tube of Constant Cross Section¹

The process of the heat feed introduces a special form of resistance: with the preheating of the moving gas the total pressure drops.

We will examine the motion of gas in the tube depicted on Fig. 5.7. Let us designate λ_x and λ_r as the velocity coefficients in the corresponding cross sections. Let the velocity in the tube be low:

$$\lambda_x < 1 \text{ and } \lambda_r < 1.$$

Let us resort to the following idealized diagram. Gas enters into the tube X-Γ from the channel with a large cross section I (Fig. 5.7). On section I-X the flow without losses and heat exchange is realized. The heat feed is achieved only in the cylindrical tube X-Γ. After this the gas, without losses and heat exchange, escapes into the wide channel II. Despite the fact that in channels I and II the velocity is low, and hydraulic losses can be disregarded, values of the total pressure in cross sections I and II are dissimilar; as we will now show, as a result of preheating the total pressure in the second channel is less.

¹See Abramovich, C. N., on a thermal critical region in gas flow, Rep rts of the Academy of Sciences of the USSR, No. 7, Vol. 54, 1946.

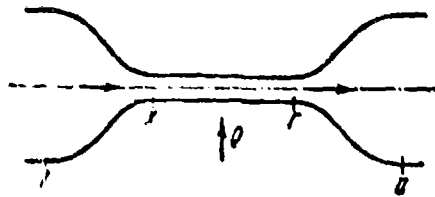


Fig. 5.7. On the determining of thermal resistance.

According to the Bernoulli equation

$$p_1 = p_0 - \rho_1 \frac{w_1^2}{2}, \quad p_2 = p_0 - \rho_2 \frac{w_2^2}{2}.$$

Hence a change in the total pressure

$$p_0 - p_0 = (p_1 - p_2) + \left(\rho_1 \frac{w_1^2}{2} - \rho_2 \frac{w_2^2}{2} \right). \quad (27)$$

From the equation of continuity $\rho_x w_x = \rho_r w_r$ it follows that if as a result of preheating the gas density decreases, then its velocity increases, and, therefore, the static pressure drops.

From the momentum equation it is possible to determine the drop in static pressure with preheating in the section X-Γ (disregarding the friction):

$$p_1 - p_2 = \rho_1 w_1 (w_1 - w_2)$$

or

$$p_1 - p_2 = 2 \left(\rho_1 \frac{w_1^2}{2} - \rho_2 \frac{w_2^2}{2} \right).$$

After substituting this difference into equation (27), we have

$$p_0 - p_0 = \rho_1 \frac{w_1^2}{2} - \rho_2 \frac{w_2^2}{2}. \quad (28)$$

Hence it is apparent that with the preheating of the slowly moving

gas, the magnitude of the losses is low. At a considerable velocity they cannot be disregarded.

It is not difficult to explain the discovered "thermal" resistance from the viewpoint of thermodynamics. In the example examined the expansion of gas in the converging nozzle section, then its preheating at reduced pressure, and finally compression in the diffuser occur. But such a cycle is contrary to the usual cycle of the thermal machine in which the heat feed proceeds at increased pressure. Because of this the process in question is connected with the absorption and not the release of energy.

It is possible to propose another method of the thermodynamic interpretation of "thermal resistance." As is known, an increase in entropy in the gas depends both on the quantity of the supplied heat and on the temperature level:

$$\Delta S_{1-2} = \int_1^2 \frac{dQ}{T}.$$

With the same quantity of heat the increase in entropy, consequently, the more the losses, the lower the mean temperature of the process, i.e., the higher the flow velocity.

Let us estimate the effect of the heat feed on the gas flow rate in the tube. Let us assume that the outflow of gas occurs through the tube of constant cross section (Fig. 5.8) in which the gas temperature increases from the value of T_x to T_r . Being limited by the case of low speeds ($\lambda_r \ll 1$) at which the absolute value of pressure is changed insignificantly, we will obtain

$$\frac{w_x}{w_r} = \frac{\rho_r}{\rho_x} \approx \frac{T_x}{T_r} \approx \frac{T_{0,x}}{T_{0,r}}.$$

From the momentum equation, disregarding the friction resistance, we have

$$p_x - p_r = \rho_x w_x^2 \left[\frac{T_r}{T_x} - 1 \right]$$

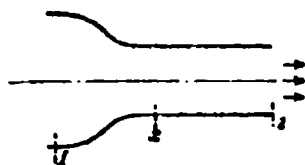


Fig. 5.8. Taking the effect of preheating on the gas flow rate in a tube into consideration.

and by definition

$$p_{0x} - p_x = \frac{1}{2} \rho_x w_x^2.$$

Then

$$p_{0x} - p_r = (p_x - p_r) + (p_{0x} - p_x) = \frac{1}{2} \rho_x w_x^2 \left[2 \frac{T_r}{T_x} - 1 \right]. \quad (29)$$

Here $p_{0x} = p_0$ is the total pressure in the vessel of which the gas escapes, and $p_r = p_H$ is the static pressure in the outlet section of the tube.

The mass flow rate of the gas with the assigned drop in pressures $H = (p_0 - p_H)$ is equal to

$$G = \rho_x w_x G F,$$

where F is the cross section of the tube. Since from (29) it follows that

$$w_x = \sqrt{\frac{2H}{\rho_x \left(2 \frac{T_r}{T_x} - 1 \right)}},$$

then the ratio of the gas flow rates in the absence and the presence of preheating in the tube

$$\frac{G_x}{G_r} = \sqrt{2 \frac{T_r}{T_x} - 1}. \quad (30)$$

As we see, the heat feed with the assigned drop in pressures leads to a decrease in the mass flow rate of gas with a simultaneous increase in the discharge velocity.

Let us investigate now the pressure drop across section X-Γ of the tube at high subsonic speed of the gas flow.

At the considerable rates of flow the gas density with preheating decreases not only due to an increase in the temperature, but also as a result of a decrease in the static pressure. In connection with this the gas velocity increases along the tube more rapidly than the temperature does. The speed of sound, which is proportional to the square root of the absolute temperature, increases along the tube considerably more slowly than does the flow velocity. Because of this $M = w/a$ along the length of the tube increases.

The flow, which has any initial velocity, is possible because of the corresponding preheating up to the critical velocity ($M_r = 1$). At the high initial value of the M number insignificant preheating is required. The lower the speed, the greater the *critical* preheating is necessary. But it is not possible to transfer the flow in the cylindrical tube into the supersonic region by any preheating. This phenomenon is called *thermal critical region*.¹

It is natural that after the critical region is achieved at the end of the tubes, the flow velocity at the beginning of the tube cannot be increased by any methods. If upon achieving the critical region the preheating of the gas is continued, then the value of the critical speed at the end of the tube increases, and the velocity at the beginning of the tube decreases. In other

¹The basis of the phenomenon of thermal critical region is given in more detail in the following paragraph.

words, the assigned quantity of heat corresponds to a completely defined limiting value of the M number at the beginning of the tube.

The enthalpy of the stagnated gas is comprised of the enthalpy in the flow and heat equivalent of the kinetic energy:

$$h_1 = h_0 + A \frac{w_1^2}{2g}, \quad h_2 = h_0 + A \frac{w_2^2}{2g}.$$

As a result of the heat feed, the enthalpy at the end of the tube is more than that at the beginning by the value of the supplied quantity of heat

$$Q = h_2 - h_1$$

Hence we obtain

$$Q = c_p(T_2 - T_1) = c_p(T_2 - T_1) + \frac{A}{2g}(w_2^2 - w_1^2) \quad (31)$$

Equation (31), together with the equations of continuity, momentum and state, forms a system sufficient for determining four unknown parameters of gas - p_2 , ρ_2 , T_2 , w_2 - at the end of the tube.

From the momentum equation we have

$$\rho_2 \left(\frac{p_2}{\rho_2} - 1 \right) = \rho_1 w_1 (w_1 - w_2)$$

Inserting in this equation values p_x and p_1 from the equation of state

$$\frac{p_2}{\rho_2} \frac{T_2}{T_1} - 1 = \frac{p_1}{\rho_1} w_1^2 \left(1 - \frac{p_2}{p_1} \right)$$

and taking into account that according to formula (34) of Chapter I $kp_1/\rho_1 = a_1^2$, we will obtain

$$\frac{p_x}{p_r} \frac{T_x}{T_r} - 1 = k M_x^2 \left(1 - \frac{p_x}{p_r} \right). \quad (32)$$

The ratio of temperatures T_x and T_r can be presented in the form

$$\frac{T_x}{T_r} = \frac{T_{0x} - \frac{A w_x^2}{c_p^2 g}}{T_{0r} - \frac{A w_r^2}{c_p^2 g}} = \frac{T_{0x} - \frac{A w_x^2}{c_p^2 g T_{0r}}}{1 - \frac{A w_r^2}{c_p^2 g T_{0r}}}.$$

Introducing the critical velocity $a_{kp,r}$, we obtain

$$\frac{T_x}{T_r} = \frac{\frac{T_{0x}}{T_{0r}} - \frac{k-1}{k+1} \left(\frac{p_r}{p_x} \right)^{\frac{1}{k}} \lambda_x^2}{1 - \frac{k-1}{k+1} \lambda_r^2}.$$

Inserting into (32) this expression for T_x/T_r and replacing M_r^2 according to formula (45) of Chapter I, we arrive at the quadratic equation

$$\left(\frac{p_r}{p_x} \right)^{\frac{1}{k}} \frac{\lambda_x^2}{1 + \lambda_x^2} - \frac{p_r}{p_x} + \frac{T_{0x}}{T_{0r}} \frac{1}{1 + \lambda_x^2} = 0. \quad (33)$$

and solving which, we find¹

$$\frac{p_r}{p_x} = \frac{1 + \lambda_x^2}{2 \lambda_x^2} \left[1 \pm \sqrt{1 - \frac{4 \lambda_x^2}{(1 + \lambda_x^2)^2} \frac{T_{0x}}{T_{0r}}} \right] \quad (34)$$

or

$$\frac{p_x}{p_r} = \frac{1 + \lambda_x^2}{2 \lambda_x^2} \left[1 \pm \sqrt{1 - \frac{4 \lambda_x^2}{(1 + \lambda_x^2)^2} \frac{T_{0r}}{T_{0x}}} \right]. \quad (35)$$

¹One of the roots of the equation, which corresponds to the subsonic flow velocity, is obtained with the - sign, and the second root (with the + sign) gives the solution for the supersonic flow velocity.

Equation (35) is used when the state of the gas at the beginning of the tube is known. If the gas velocity at the end of the tube is reduced to the critical, then it is convenient to use equation (34).

In the absence of preheating ($T_{0x} = T_{0r}$) $\rho_r = \rho_x$.

If at the end of the tube the thermal critical region ($\lambda_r = 1$) occurs, then equation (34) takes the following form:

$$\frac{p_x}{p_r} = \frac{w_x}{w_r} = 1 \pm \sqrt{1 - \frac{T_{0x}}{T_{0r}}}. \quad (36)$$

In this case

$$w_r = a_{spr} = \sqrt{\frac{2k}{k+1} g R T_{0r}}.$$

The limiting value of the velocity at the beginning of the tube in this case is equal to

$$|w_x|_{op} = a_{spr} \left(1 \pm \sqrt{1 - \frac{T_{0x}}{T_{0r}}} \right). \quad (37)$$

Having divided both parts of equality (37) by a_{spr} , we can turn to the velocity coefficient:

$$|\lambda_x|_{op} = \frac{a_{spr}}{a_{sprx}} \left(1 \pm \sqrt{1 - \frac{T_{0x}}{T_{0r}}} \right).$$

Since

$$\frac{a_{spr}}{a_{sprx}} = \sqrt{\frac{T_{0r}}{T_{0x}}},$$

then

$$|\lambda_x|_{op} = \sqrt{\frac{T_{0r}}{T_{0x}}} \pm \sqrt{\frac{T_{0r}}{T_{0x}} - 1}. \quad (38)$$

Data on the change of the maximum subsonic velocity at the inlet into the tube with the variation of preheating are given in the following table:

T_{0x}/T_{0x0}	1	2	4	6	φ
$ \lambda_x _{mp}$	1	0,41	0,27	0,22	0,17

A decrease in the velocity at the beginning of the tube (when $\lambda_x < 1$) with the intensification of preheating in conditions of the thermal critical region is explained by a decrease in the gas flow rate. In fact, with the thermal critical region the gas velocity increases in proportion to the square root of the temperature:

$$w_x = a_x \sim \sqrt{T_x}$$

and the gas density decreases more rapidly than does the value $1/T_x$ (in view of a decrease in the pressure):

$$\rho_x \sim \frac{p_x}{T_x}$$

and therefore the gas flow rate

$$G = \rho_x w_x F \sim \frac{p_x}{\sqrt{T_x}}$$

Since density at the beginning of the tube does not depend on the preheating, then the drop in the gas flow rate leads to a decrease in the velocity at the beginning of the tube. Small values of the velocity coefficient at the inlet of the combustion chamber, which are obtained with great preheating, lead to the large overall dimensions of the engine. With an increase in the velocity of flight the initial temperature T_{0x} and limiting value of the velocity at the inlet into the combustion chamber are increased.

According to the momentum equation, a drop in pressure in the tube is equal to

$$\frac{p_x}{p_r} - 1 = \frac{p_r w_r^2}{p_r} \left(1 - \frac{w_x}{w_r} \right).$$

On the basis of formulas (34) and (45) of Chapter I, we have

$$k \frac{p_x}{p_r} = a_r^2 = \frac{1 - \frac{k-1}{k+1} \lambda_r^2}{\frac{2}{k+1}} a_{i.p.r}^2$$

and therefore

$$\frac{p_x}{p_r} = 1 + \frac{\frac{2k}{k+1} \lambda_r^2}{1 - \frac{k-1}{k+1} \lambda_r^2} \left(1 - \frac{w_x}{w_r} \right). \quad (39)$$

A maximum pressure change is obtained upon reaching the thermal critical region ($\lambda_r = 1$). In this case on the basis of (36)

$$\left| \frac{p_x}{p_r} \right|_{np} = 1 \pm k \sqrt{1 - \frac{T_{0x}}{T_{0r}}}. \quad (40)$$

Here the - sign corresponds to $\lambda_x > 1$, and the + sign corresponds to $\lambda_x < 1$. By achieving when $\lambda_x < 1$ ¹ a very great preheating ($T_{0x}/T_{0r} \rightarrow 0$), it is possible to reduce the pressure to the following value:

$$\left| \frac{p_x}{p_r} \right|_{np} = k + 1$$

or when $k = 1.4$

$$\left| \frac{p_x}{p_r} \right|_{np} = 2.4.$$

¹The case $\lambda_x > 1$ will be discussed below.

Let us recall that the pressure drop necessary for obtaining the critical velocity in the nozzle is

$$\frac{p_0}{p_{*p}} = \left(\frac{k+1}{2} \right)^{\frac{k}{k-1}},$$

i.e., when $k = 1.4$

$$\frac{p_0}{p_{*p}} = 1.89.$$

Let us determine now the drop in total pressure in the cylindrical tube. At the beginning and end of the tube we have, respectively,

$$\frac{p_a}{p_{*a}} = \left(1 - \frac{k-1}{k+1} \lambda_a^2 \right)^{\frac{k}{k-1}}, \quad \frac{p_r}{p_{*r}} = \left(1 - \frac{k-1}{k+1} \lambda_r^2 \right)^{\frac{k}{k-1}}.$$

Having divided the first equation by the second, we will obtain

$$\frac{p_a}{p_{*a}} \frac{p_{*r}}{p_r} = \left(\frac{1 - \frac{k-1}{k+1} \lambda_a^2}{1 - \frac{k-1}{k+1} \lambda_r^2} \right)^{\frac{k}{k-1}}.$$

Hence the coefficient of total pressure in the tube is equal to

$$\sigma_v = \frac{p_{*r}}{p_{*a}} = \frac{p_r}{p_a} \left(\frac{1 - \frac{k-1}{k+1} \lambda_a^2}{1 - \frac{k-1}{k+1} \lambda_r^2} \right)^{\frac{k}{k-1}}. \quad (41)$$

The greatest drop in total pressure is obtained with the thermal critical region. By substituting expressions (38) and (40) into equality (41), we obtain for these flow conditions

$$\sigma_{*p} = \frac{\left[k - (k-1) \left(1 \pm \sqrt{1 - \frac{T_{*a}}{T_{*r}}} \right) \frac{T_{*r}}{T_{*a}} \right]^{\frac{k}{k-1}}}{1 \mp k \sqrt{1 - \frac{T_{*a}}{T_{*r}}}}. \quad (42)$$

Here the upper signs correspond to the regime $\lambda_x > 1$. The dependence of the change in total pressure with the thermal critical region in the tube on the ratio of stagnation temperatures, calculated for $\lambda_x < 1$ according to formula (42), is represented in the following table ($k = 1.4$):

T_{0r}/T_{0x}	1	1.5	2	4	6	8	∞
σ_{np}	1	0.89	0.86	0.82	0.81	0.80	0.70

As we see, when $\lambda_x < 1$ the losses in total pressure with real preheating ($T_{0r}/T_{0x} \approx 4-8$) are obtained of the same order as those with infinitely great preheating.

Thus, when $\lambda_x < 1$ and $k = 1.4$ the total pressure at the end of the preheating is not less than 80% of the total pressure at the beginning of the preheating.

For greater clarity of the results, let us transform expression (42) somewhat. For this from (38) we will obtain the connection between the critical preheating of the gas ($\lambda_r = 1$) and the corresponding value of the initial velocity up to the preheating:

$$\left(\frac{T_{0r}}{T_{0x}}\right)_{np} = \frac{(1 + \lambda_x^2)^2}{4\lambda_x^2}. \quad (42a)$$

Hence it follows that at the maximally possible gas velocity up to preheating ($\lambda_x^2 = k + 1/k - 1$), the critical preheating does not exceed values

$$\left(\frac{T_{0r}}{T_{0x}}\right)_{np, \max} = \frac{k^2}{(k-1)(k+1)},$$

which when $k = 1.4$ gives $(T_{0r}/T_{0x})_{np, \max} = 2.04$.

By substituting (42a) into (42) and selecting the signs according to the physical sense of the problem, we have

$$\sigma_{np} = \frac{1 + \lambda_x^2}{2} \left(\frac{k+1}{2} \right)^{\frac{1}{k-1}} \left(1 - \frac{k-1}{k+1} \lambda_x^2 \right)^{\frac{1}{k-1}}. \quad (42b)$$

Hence it follows that when $\lambda_x = 0$, i.e., $\frac{T_{0r}}{T_{0x}} = \infty$, $\sigma_{np} = \frac{1}{2} \left(\frac{k+1}{2} \right)^{\frac{1}{k-1}}$; when $\lambda_x = 1$, i.e., $T_{0r}/T_{0x} = 1$, $\sigma_{np} = 1$, and when $\lambda_x^2 = k + 1/k - 1$, i.e., $T_{0r}/T_{0x} = k^2/k^2 - 1$, $\sigma_{np} = 0$.

Curves $\sigma_{np}(\lambda_x)$ and $(T_{0r}/T_{0x})_{np} = f(\lambda_x)$, obtained with the aid of formulas (42a) and (42b), are plotted on Fig. 5.9.

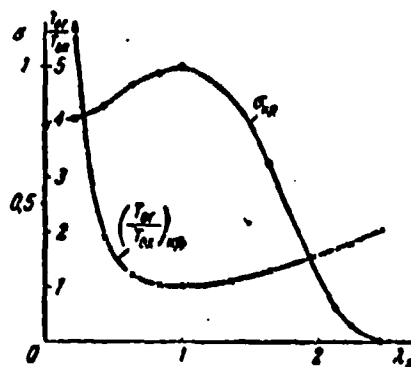


Fig. 5.9. Dependence of the degree of preheating and coefficient of total pressure on the flow velocity at critical region ($\lambda_r = 1$).

It was shown above that at the low rates of the gas flow along the tube with the heat feed in the case of a constant drop in pressures, the intensification of preheating leads to a reduction in the gas flow rate.

In § 6 it will be shown that with a constant drop in pressures the preheating causes a decrease in the gas flow rate at high flow rates.

§ 4. General Conditions of the Transition from Subsonic Flow to Supersonic Flow and Vice Versa

In the previous paragraphs it was shown that with the heat feed or the accomplishment of work due to friction in the gas moving along the cylindrical tube at subsonic velocity an increase in Mach number occurs; the same phenomenon is observed in subsonic flow during flow without a heat exchange and friction in the converging tube.

It will be proved below that the change in M number in the gas flow occurs not only under the effect of friction and thermal and geometric effects, but also with the change in the gas flow rate in the channel and upon the completion of mechanical work. The indicated effects produce a change in the M number both in the subsonic and in supersonic flow of gas.

Let us examine in general the effect of these effects on the flow velocity of the gas. For simplicity we will consider the gas to be ideal. The mass flow rate of the gas is equal to $G = g\rho wF$.

Hence after differentiation and term-by-term division by G , we have

$$\frac{dG}{G} = \frac{d\rho}{\rho} + \frac{dw}{w} + \frac{dF}{F}. \quad (43)$$

Differentiating the equation of state for an ideal gas ($p = g\rho RT$), we obtain

$$dp = gR(dT + T \frac{d\rho}{\rho})$$

or

$$\frac{dp}{p} = gR \left(dT + T \frac{d\rho}{\rho} \right). \quad (44)$$

A comparison of expressions (43) and (44) gives

$$\frac{dp}{\rho} = gRdT + gRT \left(\frac{dQ}{Q} - \frac{dP}{P} - \frac{dw}{w} \right). \quad (45)$$

On the other hand, from the Bernoulli equation in differential form (formula (91) in Chapter I), we have

$$\frac{dp}{\rho} = -w dw - g dL - g dL_{fr} \quad (46)$$

where L is the technical work, and L_{fr} is the work due to friction. Comparing (45) and (46), and eliminating terms which contain density and pressure, we obtain

$$gRdT + \frac{a^2}{k} \left(\frac{dQ}{Q} - \frac{dP}{P} \right) + \left(w^2 - \frac{a^2}{k} \right) \frac{dw}{w} + g dL + g dL_{fr} = 0. \quad (47)$$

Used here is expression for speed of sound ($a^2 = kgRT$). It is possible to get rid of the term which contains temperature ($gRdT$) with the aid of the differential equation of energy

$$dQ_{app} = dI + Ad \left(\frac{w^2}{2g} \right) + dL = \frac{Ak}{g(k-1)} gRdT + \frac{A}{g} w dw + AdL, \quad (48)$$

where Q_{app} is the heat applied to the gas from without, and $dI = c_p dT = AR \frac{k}{k-1} dT$ - the increase in enthalpy. Substituting (48) into (47) and producing the elementary conversions, we arrive at the relation which connects speed change in the gas flow rate with the external actions (geometric, flow rate, mechanical, thermal and friction):

$$(M^2 - 1) \frac{dw}{w} = \frac{dP}{P} - \frac{dQ}{Q} - \frac{g}{a^2} dL - \frac{k-1}{k} \frac{g}{a^2} dQ_{app} - \frac{kg}{a^2} dL_{fr} \quad (49)$$

This relation was established by L. A. Vulis¹ and was called the condition of the inversion of effect. The feature of this relation consists in the fact that the sign of its left side changes upon the transition of the value of velocity through the critical. Therefore, the nature of the effect of separate physical effects on the gas flow is the opposite with subsonic and supersonic regimes. The effects which produce acceleration in the subsonic flow (narrowing of the channel, the feed of the additional mass of gas, the accomplishment of work by gas, friction and heat feed, $dF < 0$, $dG > 0$, $dL > 0$, $dQ_{\text{Hap}} > 0$), lead to a slowing down of the supersonic flow; the effect of the opposite sign (expansion of the channel, the suction of the gas, imparting of mechanical energy to the gas and heat removal, $dF > 0$, $dG < 0$, $dL < 0$, $dQ_{\text{Hap}} < 0$), lead to a slowing down of the subsonic and acceleration of the supersonic flow. Hence there follows the important derivation that under the effect of one-way action the velocity of the gas flow can be reduced to the critical but cannot be transferred through it. For example, by means of the heat feed it is possible to accelerate the subsonic flow but only until $M = 1$ is obtained. In order to transfer the subsonic flow into the supersonic, it is necessary to change the effect sign, i.e., in zone $M = 1$ begin to remove the heat. Such is the substantiation of the phenomenon of the thermal critical region in the combustion chamber described in the foregoing paragraph. The preheating of the gas in supersonic flow and further braking will become possible only in such a case when, beginning with $M = 1$, we switch over to the cooling of the gas.

Let us examine each of four effects separately.

In this case we will obtain in addition to the known Laval nozzle (geometric effect) three additional methods indicated by

¹Vulis, L. A. Reports of the Academy of Sciences of the USSR, No. 8, Vol. 54, 1946; Vulis, L. A. Thermodynamics of gas flows. Energiizdat, 1950.

L. A. Vulis of the transition through the speed of sound, i.e., flow, mechanical and thermal nozzles.

The *geometric nozzle*, i.e., the known *Laval nozzle*, is the channel in which only because of the imparting to it of the corresponding shape it is possible to carry out a transition from subsonic velocity to supersonic. In this special case of a *strictly geometric effect on flow* ($dF \neq 0$) other effects are absent, i.e., the gas flow rate ($dG = 0$) is not changed, there is no exchange of heat and work with the environment ($dQ_{\text{nap}} = 0$, $dL = 0$), and there is no friction ($dL_{\text{tp}} = 0$).

But then the relation (49) turns into the previously obtained equality (1) of Chapter IV:

$$(M^2 - 1) \frac{d\omega}{\omega} = \frac{dF}{F}.$$

Without discussing for a second time the study of the flow in the Laval nozzle, let us recall only that the acceleration of flow in the subsonic part of the Laval nozzle ($M < 1$) is obtained by means of the narrowing of the channel ($dF < 0$), but, beginning from the critical cross section ($M = 1$), for obtaining the supersonic flow and its further acceleration, it is necessary to change the effect sign, i.e., expand the channel ($dF > 0$).

The flow of an ideal gas in a geometric nozzle (Fig. 4.1) in the absence of friction is isentropic. In the critical cross section ($M = 1$) of the nozzle the effect passes through the minimum ($dF = 0$).

The *flow nozzle* makes it possible to obtain a transition through the speed of sound because of a change in the gas flow rate in the tube of constant cross section ($dF = 0$) in the absence of an exchange with the environment of work ($dL = 0$) and heat ($dQ_{\text{nap}} = 0$) and without friction ($dL_{\text{tp}} = 0$). In this case relation (49) takes the following form:

$$(M^2 - 1) \frac{dw}{w} = - \frac{dQ}{Q}.$$

The acceleration of motion ($dw > 0$) is reached here because of the feed of the additional mass of gas in the subsonic part of the channel and suction of the gas in its supersonic part. In the critical cross section ($M = 1$) the gas flow rate and, therefore, the current density pass through the maximum.

The flow nozzle in principle is similar to the geometric nozzle. If we divide the flow in the flow nozzle into separate streams of constant flow rate, then each of them is a geometric nozzle with the narrowest cross section in the area of the critical region ($M = 1$); however, the narrowing of the elementary streams in it is achieved by means of the narrowing of the overall channel and because of the feed and removal of additional quantities of gas (Fig. 5.10).

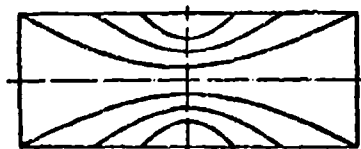


Fig. 5.10. Diagram of flow in a flow nozzle.

It is natural that the change of state of an ideal gas in the flow nozzle (without friction) occurs according to the isentropic law.

The *mechanical nozzle* gives one additional principally possible means of the transition through the speed of sound: because of the technical work in the absence of other effects ($dF = 0$, $dG = 0$, $dQ_{\text{nap}} = 0$, $dL_{\text{TP}} = 0$).

In this case the fundamental relation (49) appears thus:

$$(M^2 - 1) \frac{dw}{w} = - \frac{g}{a^2} dL.$$

from which it follows that if the gas flow accomplishes work ($dL > 0$), for example, on the turbine wheel, then in the subsonic regime ($M < 1$) it is accelerated ($dw > 0$) and in the supersonic ($M > 1$) decelerated ($dw < 0$). With the supply of work to the gas ($dL < 0$), i.e., on the compressor blades, in the subsonic flow deceleration is observed, and in supersonic flow acceleration is observed.

The continuous transition through the speed of sound in the mechanical nozzle is obtained with a change in the effect sign in the critical cross section. In principle, by passing the subsonic flow of the gas through the turbine, it is possible to accelerate it up to the critical velocity; after this it is necessary to release it through the compressor, and then the accelerating supersonic flow will be obtained (Fig. 5.11).

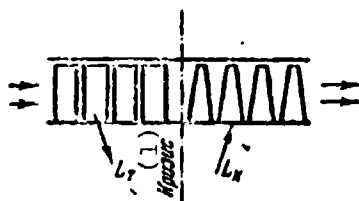


Fig. 5.11. Diagram of a mechanical nozzle.
KEY: (1) Critical region.

Thus, supersonic mechanical nozzle should consist of a series-connected turbine (in the region $M < 1$) and compressor (in the region $M > 1$), between which the critical cross section ($M = 1$) is located.

A feature of the mechanical nozzle is the fact that the stagnation parameters pass in its critical cross section through the minimum. In fact, the enthalpy equation for the mechanical nozzle can be written in the following way:

$$h_0 = h_0^* + AL.$$

Here i_{0H} and i_0 are values of total enthalpy of the gas in the initial and arbitrary cross sections of the nozzle, respectively, and L is the technical work by the ideal gas between the initial and arbitrary cross sections of the nozzle. Therefore, in the subsonic part of the mechanical nozzle, where the gas accomplishes work (on the turbine), i.e., $L > 0$, the total enthalpy (the stagnation temperature) decreases $i_0 < i_{0H}$.

In the supersonic area, where mechanical energy is fed to the gas ($L < 0$), there occurs an increase in the total enthalpy in comparison with its value in the critical cross section:

$$i_0 > i_{0cr} \text{ or } T_0 > T_{0cr}$$

It is possible to be convinced by a different method in the fact that the total pressure and density of the stagnation gas pass together with the stagnation temperature in the critical cross section of the mechanical nozzle past the minimums. For two arbitrary cross sections of the ideal mechanical nozzle, which is, by definition, the channel of constant cross section, we have

$$\frac{M_1}{M_2} = \frac{w_1 a_1}{w_2 a_2} = \frac{\rho_1 a_1}{\rho_2 a_2}.$$

In view of the absence of friction and thermal conductivity, the parameters of gas in such a nozzle are changed as with the ideal adiabatic process:

$$\frac{\rho_1}{\rho_2} = \left(\frac{p_1}{p_2}\right)^{\frac{1}{\gamma}} = \left(\frac{T_1}{T_2}\right)^{\frac{1}{\gamma-1}}.$$

Taking into account that the ratio of values of the speed of sound

$$\frac{a_1}{a_2} = \left(\frac{T_1}{T_2}\right)^{\frac{1}{2}},$$

we obtain the following simple dependences between the value of the M number and parameters of the gas in the ideal mechanical nozzle:

$$\frac{M_2}{M_1} = \left(\frac{T_1}{T_2} \right)^{\frac{k+1}{2(k-1)}} = \left(\frac{p_1}{p_2} \right)^{\frac{k+1}{2k}} = \left(\frac{\rho_1}{\rho_2} \right)^{\frac{k+1}{k}}. \quad (50)$$

Thus, a monotonic increase in the value of the M number in the mechanical nozzle is accompanied by a monotonic drop in temperature, pressure and density.

Curves of the change in the parameters of flow and braking in the supersonic mechanical nozzle when $M_1 = 0.1$ are represented on Figs. 5.12 and 5.13.

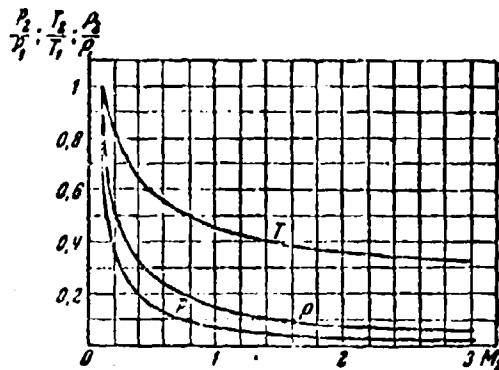


Fig. 5.12

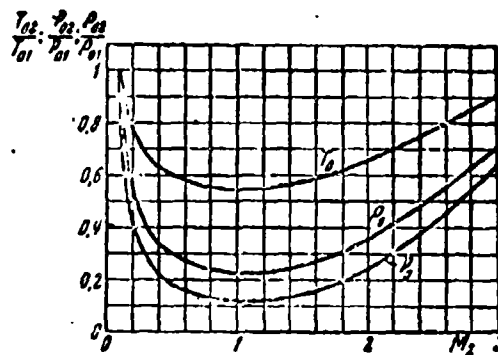


Fig. 5.13.

Fig. 5.12. Dependence of gas parameters on M_2 number in the mechanical nozzle when $M_1 = 0.1$; $k = 1.4$.

Fig. 5.13. Dependence of the stagnation conditions on the M_2 number in the mechanical nozzle when $M_1 = 0.1$; $k = 1.4$.

From expression (50) it follows that the maximum velocity of outflow from the mechanical nozzle is not at all limited

$$\frac{w_2}{w_1} = \frac{p_1}{p_2} = \left(\frac{M_2}{M_1} \right)^{\frac{2}{k+1}},$$

since when $M_2 \rightarrow \infty$ we have $w_2 \rightarrow \infty$. This result should not be of a surprise, since in the supersonic section of the mechanical nozzle energy will be fed to the gas ($dL < 0$).

The thermal nozzle, still not realized, gives the possibility in principle of the transition of the gas flow through the speed of sound because of one additional - purely thermal - effect in the absence of other effects, i.e., in a cylindrical tube ($dF = 0$), with the constant gas flow rate ($dG = 0$), without the accomplishment of mechanical work ($dL = 0$) and without friction ($dL_{rp} = 0$). The fundamental relation (49) in connection with the thermal nozzle takes the following form:

$$(M^2 - 1) \frac{dw}{w} = - \frac{k(k-1)}{Aa^2} dQ_{nap}$$

The acceleration of gas ($dw > 0$) in subsonic flow ($M < 1$) is here connected with the heat feed ($dQ_{nap} > 0$) and in supersonic flow - with its removal ($dQ_{nap} < 0$). The heat feed with the supersonic regime and the heat removal with the subsonic regime produce the slowing down of the flow ($dw < 0$). Thus in order to convert subsonic flow in supersonic by means of a thermal nozzle, in the subsonic section of the latter it is necessary to increase the enthalpy of the gas, and in supersonic - reduce it, i.e., in the critical cross section of the thermal nozzle, where the quantity of heat fed to the gas passes through the maximum ($dQ_{nap,kr} = 0$), it follows to change the effect sign.

The stagnation temperature in the critical cross section of the thermal nozzle (in the opposite case of the mechanical nozzle) reaches a maximum value; this ensues from the equation of enthalpy, which in connection with the thermal nozzle takes the following form:

$$I_{0n} = I_0 - Q_{nap}$$

From the foregoing paragraph, which contains the theory of thermal resistance, it follows that with the heat feed to the gas flow the total pressure in it drops, and with the heat removal - it increases. Formulas of thermal resistance were derived in

connection with the case of the flow of gas without friction along a tube of constant cross section, i.e., precisely to the case of the thermal nozzle.

From this theory it follows that the total pressure in the critical cross section of the thermal nozzle, just as in the mechanical nozzle, passes through the minimum. The density of the stagnated gas, directly proportional to the total pressure and inversely proportional to the stagnation temperature, reaches a minimum value in the critical cross section.

In the ideal nozzles examined above, geometric, flow and mechanical, a change in the state of the gas was isentropic, i.e., it was described by the equation of the ideal adiabatic curve $p/\rho^k = \text{const.}$

In the thermal nozzle in connection with the feed and heat removal the entropy changes.

Let us investigate the thermodynamic process which takes in the thermal nozzle.¹ The differential form of the equation of momentum, in connection with the cylindrical tube in the absence of friction, takes the following form:

$$dp = -\rho w dw.$$

The continuity equation in this case ($dF = 0$, $dG = 0$) gives

$$\frac{dp}{\rho} = -\frac{dw}{w};$$

¹See Vulis L. A. On the transition through the speed of sound in gas flow. Reports of the Academy of Sciences of the USSR, No. 8, Vol. 54, 1946.

hence

$$\frac{dp}{dp} = w^2. \quad (51)$$

For the polytropic process with the constant polytropic exponent $p/p^n = \text{const}$, after differentiation¹ we have

$$\frac{dp}{dp} = n \frac{p}{p} = n \frac{a^2}{k}, \quad (52)$$

since the speed of sound in the gas $a^2 = kp/\rho$. Equating the right sides of expressions (51) and (52), we note that the polytropic exponent in the thermal nozzle is a substantially variable value

$$n = kM^2. \quad (53)$$

Formula (53) shows the presence of two characteristic cross sections in the thermal nozzle.

In the cross section where $M = 1/\sqrt{k}$, the local importance of the polytropic exponent is equal to unity: $n = 1$, i.e., the elementary thermodynamic process in this cross section is isothermal ($dT = 0$), and, therefore, the gas temperature here passes through the maximum.

In the critical cross section of the thermal nozzle, i.e., when $M = 1$, the polytropic exponent on the basis of formula (53) is equal to the index of the ideal adiabatic curve: $n = k$, i.e., here there occurs the elementary isentropic process during which, as has already been indicated above, the quantity of heat supplied to the gas and the stagnation temperature pass through the maximum ($dQ_{\text{nap}} = 0$, $dT_0 = 0$).

¹With the explicit nature of the thermodynamic process in any section of the small change in parameters of state it is possible to assume that the local value of the index n is constant, although as a whole the process is connected with a change in the polytropic exponent.

From the isothermal to the critical cross sections of the thermal nozzle an interesting phenomenon is observed: a temperature decrease of the gas ($dT < 0$) with the heat feed ($dQ_{\text{нар}} > 0$). In this section of the nozzle the increase in kinetic energy of the gas is greater than the increase in total enthalpy.

To search for the dependence of the gas pressure on M number in the thermal nozzle without friction we utilize the equation of momentum in the following form:

$$p_1 + \rho_1 w_1^2 = p_2 + \rho_2 w_2^2 \quad (54)$$

hence

$$p_1 (1 + \kappa M_1^2) = p_2 (1 + \kappa M_2^2)$$

or

$$\frac{p_2}{p_1} = \frac{1 + \kappa M_1^2}{1 + \kappa M_2^2} \quad (55)$$

In other words, the gas pressure in the thermal nozzle with an increase in M number monotonically decreases despite the increase in total pressure in the supersonic part.

The dependence of the gas density and rate of flow in the thermal nozzle on M number can be found by the following method:

$$\frac{M_2^2}{M_1^2} = \frac{w_2^2}{w_1^2} \frac{a_1^2}{a_2^2} = \frac{w_2^2}{w_1^2} \frac{T_1}{T_2}$$

but from the equations of state and continuity we have

$$\frac{T_2}{T_1} = \frac{p_2 \rho_2}{p_1 \rho_1}, \quad \frac{p_2}{p_1} = \frac{w_1}{w_2}$$

and therefore

$$\frac{M_2^2}{M_1^2} = \frac{w_1}{w_2} \frac{2_1}{2_2}$$

Using dependence (55), we obtain

$$\frac{p_2}{p_1} = \frac{w_1}{w_2} = \frac{M_1}{M_2} \frac{1 + kM_1^2}{1 + kM_2^2}, \quad (56)$$

from which it is clear that gas density along the thermal nozzle monotonically decreases with an increase in M number.

The gas temperature in the thermal nozzle as a function of M number can be obtained by the division of equality (55) into equality (56):

$$\frac{T_2}{T_1} = \frac{M_1^2}{M_2^2} \left[\frac{1 + kM_1^2}{1 + kM_2^2} \right]^2. \quad (57)$$

As it is not difficult to be convinced from expression (57), the temperature curve has a maximum at point¹

$$M_2' = \frac{1}{k}.$$

In any two cross sections of the thermal nozzle with an identical temperature ($T_2 = T_1$) values of the M numbers, as this appears from expression (57), are connected by the following dependence:

$$M_2 M_1 = \frac{1}{k}.$$

Let us derive the formulas for the stagnation parameters in the thermal nozzle. These formulas acquire a simpler form if in them the M number is replaced with the velocity coefficient λ , for which it is possible to use the known relation (46) of Chapter I.

Let us find the stagnation temperature, using formula (42) of Chapter I, from the equality

In order in equality (57) we will consider M_1 and T_1 as constant values. Putting derivative dT_2/dM_2 to zero, we find $M_2 = 1/\sqrt{k}$.

$$\frac{T_{01}}{T_{02}} = \frac{T_2}{T_1} \frac{1 - \frac{k-1}{k+1} \lambda_1}{1 - \frac{k-1}{k+1} \lambda_2};$$

after substituting (57) here, after preliminarily replacing M by λ according to formula (45) of Chapter I, we obtain

$$\frac{T_{01}}{T_{02}} = \frac{\lambda_2}{\lambda_1} \left(\frac{1 + \lambda_1^2}{1 + \lambda_2^2} \right)^k. \quad (58)$$

The total pressure in the thermal nozzle can be obtained with the aid of formula (72) of Chapter I from the expression

$$\frac{p_{01}}{p_{02}} = \frac{p_2}{p_1} \left[\frac{1 - \frac{k-1}{k+1} \lambda_1}{1 - \frac{k-1}{k+1} \lambda_2} \right]^{\frac{k}{k-1}};$$

hence, by using equality (55), we come to the following dependence:

$$\frac{p_{01}}{p_{02}} = \frac{1 + \lambda_1}{1 + \lambda_2} \left[\frac{1 - \frac{k-1}{k+1} \lambda_1}{1 - \frac{k-1}{k+1} \lambda_2} \right]^{\frac{1}{k-1}}. \quad (59)$$

The density of the stagnated gas in the thermal nozzle can be determined by means of the division of expression (59) into expression (58):

$$\frac{\rho_{01}}{\rho_{02}} = \frac{\lambda_1}{\lambda_2} \frac{1 + \lambda_2}{1 + \lambda_1} \left[\frac{1 - \frac{k-1}{k+1} \lambda_1}{1 - \frac{k-1}{k+1} \lambda_2} \right]^{\frac{1}{k-1}}. \quad (60)$$

Curves of the change in flow parameters in the thermal nozzle, depending on number M_2 when $M_1 = 0.1$, are given on Figs. 5.14 and 5.15.

Let us determine the quantity of heat (Q) which must be fed in the thermal nozzle in order to change the gas velocity from any

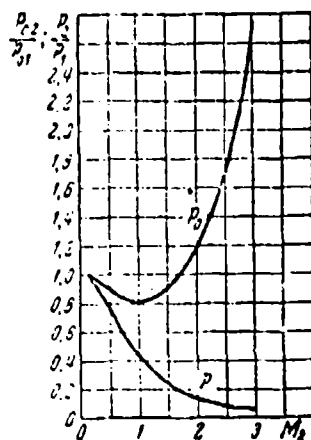


Fig. 5.14.

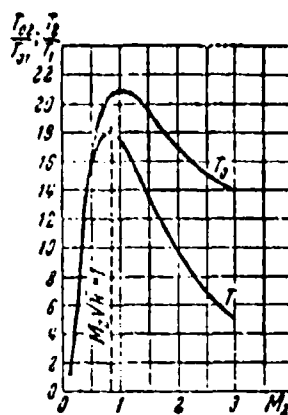


Fig. 5.15.

Fig. 5.14. Dependence of the static and total pressures on the M_2 number in the thermal nozzle when $M_1 = 0.1$; $k = 1.4$.

Fig. 5.15. Dependence of the flow temperatures and braking on the M_2 number in the thermal nozzle when $M = 0.1$; $k = 1.4$.

one value (λ_1) to another (λ_2). With constant heat capacity we have

$$Q = c_p(T_{01} - T_{02})$$

or in a dimensionless form

$$q = \frac{Q}{c_p T_{01}} = \frac{T_{01}}{T_{01}} - 1;$$

substituting here the relation of the stagnation temperatures from equality (58), we find

$$q = \frac{0.1 - \lambda(1 - \lambda)}{1 + \lambda^2}.$$

The maximum quantity of heat which corresponds to the critical preheating (to $\lambda_c = 1$) is equal to

$$q_{max} = \left(\frac{1 - \lambda_1}{2\lambda_1} \right)^2. \quad (61)$$

It sharply decreases with an increase in the initial gas velocity (λ_1), which is indicated on the graph of Fig. 5.16. The maximally possible discharge velocity from the thermal nozzle (when $M_2 = \infty$), according to equality (56), depends on the initial value of the M_1 number

$$\frac{w_{max}}{w_1} = 1 + \frac{1}{\lambda M_1^2}.$$

Specifically, if we take a reading from the critical cross section, i.e., assume that¹

$$M_1 = 1, w_1 = a_{*p},$$

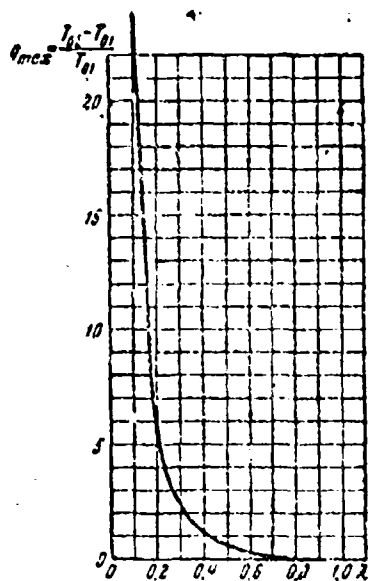


Fig. 5.16. Dependence of critical preheating in a tube of constant cross section on the initial value of the velocity coefficient.

¹It should be considered that in connection with the heat feed the value of the critical velocity along the length of the nozzle is changed.

then we will obtain

$$\frac{w_{max}}{a_{sp}} = \frac{k+1}{k}.$$

Besides the four described "pure" designs of supersonic nozzles, combined configurations are fundamentally possible. The most real combined nozzle is the so-called "semi-thermal nozzle," in which the subsonic section is thermal and supersonic geometric (Fig. 5.17). In such a nozzle the gas is accelerated from a certain initial subsonic value of velocity up to the critical velocity in the cylindrical tube 1-2 because of the heat feed, and the transition to supersonic speed and further acceleration of flow are achieved without heat exchange in the expanding tube 2-3. The calculation of the subsonic section of the semi-thermal nozzle is conducted according to formulas of the thermal nozzle, while that of the supersonic section is conducted according to formulas in the geometric nozzle.

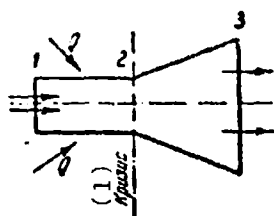


Fig. 5.17. Diagram of a semi-thermal nozzle.
KEY: (1) Critical region.

Let us compare the semi-thermal nozzle with the geometric at the identical finite value of total enthalpy (i_{03}), having in mind that in the semi-thermal nozzle the preheating of the gas is accomplished in the cylindrical tube 1-2, and in the geometric nozzle the same quantity of heat is fed to the gas up to its nozzle inlet. Values of the discharge velocity from both nozzles are identical, since in critical cross sections the value of the stagnation temperature is the same. The total pressure at the outlet of the semi-thermal nozzle is lower in connection with the presence of thermal resistance in its subsonic section, and

therefore the static pressure at the outlet from the semi-thermal nozzle is lower.

Let us examine the example of the semi-thermal nozzle with the initial gas velocity, which corresponds to the value of the velocity coefficient $\lambda_1 = 0.2$. In this case the dimensionless quantity of the preheating of the gas in the subsonic section of the nozzle, according to expression (61), should be equal to

$$q_{\text{max}} = \left(\frac{1 - \lambda_1^2}{2\lambda_1} \right)^2 = 5.75.$$

The losses of total pressure in the semi-thermal nozzle ($\lambda_2 = 1$) can be calculated according to formula (59):

$$\left(\frac{p_{01}}{p_{01, \text{nr}}} \right) = \left(\frac{p_{01}}{p_{01, \text{nr}}} \right) = \frac{1 + \lambda_1^2}{2} \left[\frac{1 - \frac{k-1}{k+1} \lambda_1^2}{\frac{2}{k+1}} \right]^{\frac{1}{k-1}}.$$

When $\lambda_1 = 0.2$ and $k = 1.4$ we have

$$\left(\frac{p_{01}}{p_{01, \text{nr}}} \right) = z_{\text{nr}} = 0.82.$$

The total pressure in the geometric nozzle maintains a constant value:

$$\left(\frac{p_{01}}{p_{01, \text{r}}} \right) = 1.$$

Therefore, the static pressure at the outlet from the semi-thermal nozzle with the same discharge velocity differs z_{nr} times from static pressure at the outlet from the geometric nozzle:

$$p_{\text{out}} = z_{\text{nr}} p_{01, \text{r}}.$$

further,

$$\left(\frac{p_{01}}{p_{01, \text{r}}} \right) = \frac{p_{01} p_{01, \text{r}}}{p_{01, \text{r}} p_{01}} = z_{\text{nr}} \left(1 - \frac{k-1}{k+1} \lambda_1^2 \right)^{\frac{k}{k-1}}.$$

where λ_2 is the velocity coefficient of the outflow from the nozzle, and p_{01} is the total pressure in the initial cross section of the nozzle. With equal drops in the pressure

$$\left(\frac{p_1}{p_{01}}\right)_{\text{st}} = \left(\frac{p_1}{p_{01}}\right)_r$$

the velocity of discharge from the semi-thermal nozzle is less than that from the geometric nozzle ($\lambda_{3\text{nr}} < \lambda_{3r}$); this results from equality

$$\sigma_{\text{nr}} \left(1 - \frac{k-1}{k+1} \lambda_{3\text{nr}}^2\right)^{\frac{k}{k-1}} = \left(1 - \frac{k-1}{k+1} \lambda_{3r}^2\right)^{\frac{k}{k-1}},$$

which connects the ratio of the static pressure to the total pressure with the velocity coefficient. For example, when $\sigma_{\text{nr}} = 0.82$ and $\lambda_{3r} = 2$ the velocity coefficient of outflow from the semi-thermal nozzle $\lambda_{3\text{nr}} = 1.97$, i.e., 1.5% less than the velocity coefficient of outflow from the geometric nozzle.

In examining the different types of the nozzles intended for transition through the speed of sound, in all cases we had in mind the transition from subsonic to supersonic velocity. The obtained formulas are suitable principally for the reverse case, i.e., the smooth conversion of supersonic flow into subsonic; however, with the braking of supersonic flow there can arise shock waves, which complicate the phenomenon.

Let us discuss now briefly the joint development of two or several effects. As a first example let us analyze the case of the geometric nozzle with friction. The fundamental relation (49) in this case takes the form

$$(M^2 - 1) \frac{dw}{w} = \frac{dF}{F} - \frac{k}{a^2} dL_{\text{fr}}.$$

The most interesting feature of this nozzle is the fact that the critical velocity is obtained in its divergent part, since when $M = 1$

$$\frac{dF}{F} = \frac{gk}{a^2} dL_{np} > 0,$$

and in the narrow cross section ($dF = 0$ when $dw > 0$) the subsonic velocity and $M < 1$ occur.

Let us now explain the chief characteristics of the geometric nozzle with heat exchange. From the fundamental relation (49) in this case we have

$$(M^2 - 1) \frac{dw}{w} = \frac{dF}{F} - \frac{g}{a^2} \frac{k-1}{\lambda} dQ_{np}$$

The location of the critical cross section ($M = 1$) is determined by the equality

$$\frac{dF}{F} = \frac{g}{a^2} \frac{k-1}{\lambda} dQ_{np}$$

With the heat feed ($dQ_{np} > 0$) - for example, with the afterburning of gases in the nozzle - the critical velocity is reached in the divergent part of the nozzle ($dF > 0$), and with the heat removal ($dQ_{np} < 0$), i.e., the heat transfer through the nozzle walls, the critical velocity is reached in the convergent section of the nozzle ($dF < 0$). In the first case in the narrow cross section of the nozzle ($dF = 0$), there occurs subsonic velocity and in the second case - supersonic velocity.

By the same means it is possible to investigate the joint effect in the gas flow of any other actions. In this case it is important to emphasize that in accordance with equation (49) the transition from $M < 1$ to $M > 1$ requires in any event a sign change of the total action.

In conclusion let us note one fact which sometimes leads to misunderstandings in the qualitative analysis of laws governing some flows. In connection with this let us again return to equation (49).

Above in the analysis of the equation of momentum (92) of Chapter I, we noted that independently of the processes occurring in the flow, a change in the rate of flow is always caused by the action of the force of friction, applied forces, and also the difference in forces of pressure on the chosen element of gas flow. The different forms of the external action in different ways affect the static pressure in the flow. The meaning of the joint solution of equations (43)-(47), as a result of which relation (49) was obtained, was reduced so that the value of the pressure gradient in flow is expressed by external actions; the value dp in this case was excluded from the momentum equation or the Bernoulli equation (46).

In the analysis of equation (49) it is revealed that: a) a change in the gas velocity is caused by such factors which are not connected with direct force action on the flow (for example, the heat feed), b) the total effect in a number of cases turns out to be opposite to that which can be expected on the basis of the analysis of the action of applied forces. Actually, for example, the force of friction which always acts opposite to the direction of motion in subsonic flow leads not to braking but acceleration of the flow. The latter means that in flow with friction there occurs such a reduction in the static pressure that the force of pressure acting in the flow exceeds the force of friction.

In exactly the same manner as with the feed of mechanical energy to the subsonic gas flow, its pressure is increased so that the force of pressure acting counter to flow exceeds the applied force which caused it. As a result the flow, to which the applied force is applied in the direction of motion when $M < 1$, is not accelerated but braked.

Thus, above, in the analysis of external actions on the gas flow, it was assumed everywhere that in the flow there appear appropriate pressure gradients, which as a final result determine

the change in the rate of the flow. Thus, for instance, for the acceleration of the subsonic gas flow in the thermal nozzle (i.e., when $F = \text{const}$) the pressure at the inlet into the nozzle should exceed the outlet pressure by the value which is determined by the initial and final M numbers (see formula (55)).

Having the same meaning are above obtained relationships between static pressures of the gas in flow with friction (50), flow with the feed of mechanical energy, and so on. In many instances, however, it is known in advance that in the flow in question there is no longitudinal pressure gradient. The change in the gas velocity in this case ($dp = 0$) is completely determined by the equation of momentum in the form

$$\rho x dx = -\frac{1}{F} (dP + dP_{rp}),$$

where dP_{rp} is the force of friction, and dP is the applied force. Hence it follows that in isobaric flow both at subsonic and supersonic velocities the friction leads to a decrease in the velocity; the applied forces which act on the flow or the applied external mechanical energy ($dP < 0$) always accelerate the gas flow; the heat feed when $dp = 0$ does not at all change the velocity of the directed motion of gas, since in this case there are no applied forces.

An example of isobaric flow can be, in particular, supersonic flow in a solid wall. The boundary layer near such a wall is formed as a result of the continuous braking of the flow by forces of external action (friction). In summation, the velocity of the flow in it decreases when $p = \text{const}$ from the supersonic to the small subsonic value.

In exactly the same manner the isobaric supersonic jet, being mixed with the fixed atmospheric air, accelerates its particles to the supersonic velocity by means of a one-sided mechanical

action - the feed of the momentum in the collision of particles of gas and air.

With further flow in any stream filament within the isobaric supersonic jet there occurs continuous braking - with the transition through the speed of sound - down to low speeds, and also because of one-sided external action - the transfer of momentum into the environment.

These examples do not contradict the laws established above and the equation of the transformation of actions (49). The fact is that in the presence of any external action the condition in isobaricity ($p = \text{const}$) can be fulfilled only with a completely defined change in the *cross-sectional area* F .

Thus, for instance, at subsonic flow in a cylindrical tube with friction the velocity of the gas increases, and the static pressure drops. In order that the pressure in the flow is constant, the channel must be made divergent, i.e., the geometric effect $dF > 0$ must be added to the effect of friction. Since independently of the shape of the channel with flow with friction the total pressure is lowered, then in such an isobaric flow the gas velocity is decreased.

§ 5. On the Propagation of
Detonation and Burning in Gases¹

The creator of the theory of the propagation of detonation in gases is the well-known Russian physicist V. A. Mikhel'son who devoted in 1889 the work "On the normal ignition speed of fulminating gas mixtures" to this problem.²

The outstanding theoretical and experimental studies in the field of burning and detonation belong to N. N. Semenov, Ya. B. Zel'dovich, D. A. Frank-Kamenetsiy, K. I. Shchelkin and other Soviet scientists.³

The propagation of the flame in a combustible gas mixture, without depending on the mechanism of ignition (by thermal conductivity with slow burning or by a shock wave with detonation), is subordinated to the fundamental laws of gas dynamics and, therefore, can be described by equations of the conservation of mass, momentum and energy.

The flame front is a thin layer of gas of virtually constant cross section, on both sides of which values of the velocity of motion (relative to the wave front), temperature, pressure and other parameters are different. In accordance with this, the flame front can be treated as a surface of nonremovable discontinuity (thermal shock).

¹In this section an expanded presentation of the following work is given: Abramovich, G. N. and Vulis, L. A., On the mechanics of the propagation of detonation and burning. Reports of the Academy of Sciences of the USSR, Vol. 55, Issue 2, 1947.

²Mikhel'son, V. A., Complete collected works, Vol. 1, M., 1930.

³See, for example, Zel'dovich, Ya. B., Theory of the burning and detonation of gases. Publishing House of the Academy of Sciences of the USSR, 1944.

In the contemporary concept the detonation wave, which is propagated in the combustible gaseous medium, is two-layered. The first layer is an adiabatic shock wave, with the passage through which the gas is greatly heated. In chemically active gas this heating, if it is sufficiently intensive, can cause ignition. In connection with the fact that the shock wave thickness is negligible (order of the mean free path of the molecule), within limits its process of burning, apparently, is developed not in the state. Therefore, the area in which there occurs burning forms a second, more extended, but virtually also very thin layer which adjoins directly to the shock wave (Fig. 5.18).

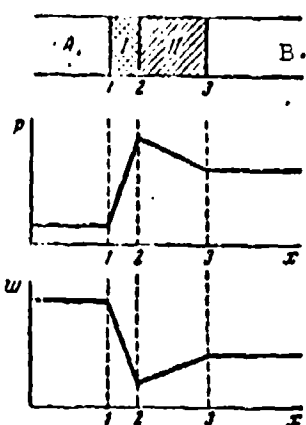


Fig. 5.18. Diagram of the detonation wave: A - fresh mixture, B - products of combustion; I. shock wave, II. combustion zone.

The heating of the gas with its passage through the shock wave in detonation burning in essence replaces the preheating with its thermal conductivity in normal burning.

Let us examine the phenomenon of detonation in conditions of a one-dimensional problem. In the case for a plane shock wave according to the known relation (15) of Chapter III, the product of the gas velocity relative to the wave front (taken, respectively, in front of and behind the front) is equal to the square of the critical velocity:

$$w_1 w_2 = a_{kp}^2$$

The value w_1 is the velocity of the propagation of the shock wave (in our case, the detonation wave in a fixed gas). For the study of the process it is convenient to consider that the gas flows at a rate of w_1 to the region of detonation, and the wave front is fixed. This inverted scheme of the phenomenon is accepted by us in the subsequent presentation.

Shock wave (pressure shock), as is known, is propagated at a hypercritical velocity ($w_1 > a_{kp}$), and therefore the gas velocity behind the wave front is always lower than the critical velocity ($w_2 < a_{kp}$). In other words, the process of burning with detonation, as with slow burning, occurs in the subsonic part of the gas flow.

At the end of the second layer of the detonation wave, as a result of the heat feed with burning, the gas velocity is higher than at first, and the pressure is respectively lower. Thus, the first layer of the detonation wave is a compression shock, and the second layer, where burning occurs, is the expansion shock. The approximate nature of the distribution of the pressure and gas velocity in the detonation wave is shown on Fig. 5.18.

Let us turn to the calculation of the shock wave.

In the calculation of the change in the state of the gas in the first layer of the plane detonation wave, we can use relations for the normal shock wave.

For the case in question it is important that in the first layer of the detonation wave (adiabatic shock wave) the stagnation temperature remains constant $T_{01} = T_{02}$. Consequently, the critical velocity in the first layer does not change $a_{1kp} = a_{2kp}$, whereas in the products of combustion its value is increased $T_{03} > T_{01}$ and, respectively, $a_{3kp} > a_{1kp}$. This circumstance

must be considered subsequently in the calculation of the velocity coefficients:

$$\lambda_1 = \frac{w_1}{a_{1kp}}, \quad \lambda_2 = \frac{w_2}{a_{2kp}}, \quad \lambda_3 = \frac{w_3}{a_{3kp}}.$$

From the continuity equation $\rho_1 w_1 = \rho_2 w_2$ and expression (16) of Chapter III, let us find for a change in density and velocity the relation

$$\frac{\rho_2}{\rho_1} = \frac{w_1}{w_2} = \lambda_1^2. \quad (62)$$

The law of pressure change in the normal shock wave can be obtained from the momentum equation in the form of the known equality (21) of Chapter III

$$\frac{p_2}{p_1} = \frac{\lambda_1^2 - \frac{k-1}{k+1}}{1 - \frac{k-1}{k+1} \lambda_1^2}. \quad (63)$$

From (62) and (63) it follows that the change in gas temperature in the shock wave

$$\frac{T_2}{T_1} = \frac{1 - \frac{k-1}{k+1} \lambda_1^2}{1 - \frac{k-1}{k+1} \lambda_1^2}. \quad (64)$$

For example, at the velocity of propagation of the shock wave $w_1 = 2000$ m/s, the initial temperature of the gas $T_1 = 400^\circ\text{K}$, $R = 30$ kgm/kg·deg and $k = 1.4$ we have $T_{01} \approx 2400^\circ\text{K}$, $a_{1kp} \approx 900$ m/s, $\lambda_1 \approx 2.2$, $\lambda_2 \approx 0.45$, to which corresponds $T_2 \approx 2300^\circ\text{K}$.

There are no doubts that in this case the shock wave can cause the ignition of the combustible gas mixture.

Let us now study the calculation of the combustion zone.

It is natural that all formulas derived in §§ 3 and 4 for the case of the preheating of gas in a cylindrical tube are also

suitable for calculating the second (thermal) layer of the detonation wave, since in the derivation of the indicated formulas the length of the tube was not important (the friction and thermal conductivity through the side surface were disregarded).

For calculating the state of the gas in the second (subsonic) layer of the detonation wave - in the region of burning - it is most simple to resort to the relation (58) between the stagnation temperature and the velocity coefficient

$$\frac{T_{01}}{T_{02}} = \frac{\lambda_1(1+\lambda_1)^2}{\lambda_2(1+\lambda_2)^2} = \frac{\lambda_1(1+\lambda_1)^2}{\lambda_1(1+\lambda_1)^2}, \quad (65)$$

whence after the solution of biquadratic equation, we obtain the following expression:

$$\lambda_2 = \frac{1}{\lambda_1} = \frac{1+\lambda_1}{2\lambda_1} \left[1 - \sqrt{1 - \frac{0.1}{(1+\lambda_1)^2} \frac{T_{01}}{T_{02}}} \right] \sqrt{\frac{T_{01}}{T_{02}}}, \quad (66)$$

or

$$\lambda_2 = \frac{1+\lambda_1}{2\lambda_1} \left[1 - \sqrt{1 - \frac{0.1}{(1+\lambda_1)^2} \frac{T_{01}}{T_{02}}} \right] \sqrt{\frac{T_{01}}{T_{02}}}. \quad (67)$$

Rejected here are the roots which give the supersonic solutions, since the combustion zone where the relative velocities are lower than the speed of sound ($\lambda_2 < 1$) is examined; furthermore, we assume that $T_{01} = T_{02}$. The velocity coefficient λ_2 - directly after the shock wave - is usually considerably less than unity; if in this case the relative temperature increment of braking in the region of burning is small ($T_{03}/T_{01} \approx 1$), then formula (67) can be substantially simplified:

$$\lambda_2 \approx \frac{\lambda_1}{1+\lambda_1} \sqrt{\frac{T_{01}}{T_{02}}} \approx \lambda_1 \sqrt{\frac{T_{01}}{T_{02}}}$$

(since under the assumptions made $\lambda_2^2 \ll 1$). Thus,

$$\lambda_2 \approx \lambda_1 \sqrt{1 + \frac{\Delta T_0}{T_{01}}}, \quad (68)$$

where $\Delta T_0 = Q/c_p$, if Q is the quantity of heat which is liberated

with the combustion of a unit weight of mixture. From formula (65) it is evident that with weak heating ($\Delta T_0/T_{01} \approx 0$) the velocity coefficient for the products of combustion is close to the velocity coefficient after the shock wave.

With the intensifying of the shock wave, i.e., with an increase in the velocity of propagation of the shock wave, the stagnation temperature of the initial mixture $T_{01} = T_{02}$ sharply increases according to the known equality (42) of Chapter I

$$T_{01} = \frac{T_1}{1 - \frac{k-1}{k+1} \lambda_1^2}; \quad (69)$$

In this case the temperature in the flow in front of the region of burning T_2 sharply increases. In the limit when $M_1 = \infty$ and $\lambda_1 = \sqrt{\frac{k+1}{k-1}}$ we have $T_{01} = T_{02} = \infty$ and $T_2 = \infty$. With an increase in temperature T_2 , in connection with the increasing role of thermal dissociation,¹ the absolute difference in the stagnation temperatures somewhat decreases:

$$\Delta T_0 = T_{02} - T_{01}$$

Consequently, with the intensification of the shock wave both the relative heating of the gas $\Delta T_0/T_{01}$ and the velocity coefficient of the combustion products λ_3 decreases.

This is evident most distinctly if into formula (68), instead of the variable stagnation temperature we introduce the constant temperature of the cold gas:

$$\lambda_3 \approx \frac{1}{\lambda_1} \sqrt{1 + \frac{\Delta T_0}{T_1} \left(1 - \frac{k-1}{k+1} \lambda_1^2\right)}. \quad (70)$$

¹The thermal dissociation is the phenomenon of partial decomposition of the products of burning observed at high temperatures and also at low pressures; a reaction occurs in the opposite direction and is accompanied by an absorption of heat.

The burning which occurs behind the front of a very powerful shock wave begins at such a high thermal level that it can cause only a relatively small increase in stagnation temperature. Therefore, in the limit

$$(\rho_2)_{\text{cr}} \sim \lambda_1 = \frac{1}{\lambda_1},$$

i.e., the detonation wave approaches with the usual shock wave.

Let us study the steady-state condition of detonation.

The considerations given make it possible to imagine the process of the formation of the stationary wave of detonation in the following form. Usually the detonation wave appears as the result of local explosion in the combustible mixture. In the region of the explosion very high pressures are developed and directed from it is a very powerful shock wave. In transit through the cold combustible mixture, this wave, as was noted above, causes considerable heating of the gas and can lead it up to ignition. Precisely in this case, behind the shock-wave front there follows the region of burning which forms the wave detonation in totality with the shock wave. Since near the explosion center the propagation velocity of the wave and its intensity are very great, the relative gas velocities at the beginning of the region of burning and at the end of it are close to each other and substantially lower than the critical velocity:

$$\lambda_2 \approx \lambda_3 \ll 1.$$

However, with distance from the blast center the detonation wave is attenuated, and the propagation velocity of it λ_1 decreases. In connection with this there occurs a reduction in the stagnation temperature at the beginning of the region of burning (T_{02}) and an increase in the velocity coefficient of the gas (λ_2). In this case the relative heating of gas ($\Delta T_0/T_{01}$) and the velocity of motion (68) of the combustion products (λ_3) increase. It is obvious that when the detonation

wave is attenuated so much that λ_3 will be raised up to the critical value ($\lambda_{3kp} = 1$), a further deceleration of detonation will prove to be impossible¹).

Consequently, the detonation process, which began from the explosion, continuously weakens, until the propagation velocity is lowered to a minimum value which corresponds to the onset of the thermal critical region in the combustion zone. From this point on, the propagation of the detonation wave acquires a stable stationary nature.

As was shown in 1.4, further acceleration and transition to the stationary region are possible solely with a change in the sign of the effect - in this case upon the transition from the mass liberation in the combustion zone to its removal, beginning from the critical cross section (thermal nozzle). Thus, the onset of the thermal critical region in the zone of combustion leads to the establishment of stationary values λ_1 , λ_2 , and λ_3 .

We can determine the coefficient of the propagation velocity of the steady-state detonation wave, after substituting value $\lambda_3 = 1$ into equation (60). In this case

$$\lambda_1 = \lambda_2 = \sqrt{\frac{T_{01}}{T_{02}}} = \sqrt{\frac{T_{01}}{T_{02}} - 1} \quad (71)$$

or after release from the radicals

$$\frac{T_{01}}{T_{02}} = \left(\frac{1 + \lambda_1^2}{2\lambda_1^2} \right)^2 = \left(\frac{1 + \lambda_1^2}{2\lambda_1^2} \right)^2. \quad (72)$$

For $\lambda_{03} = T_{01} + \Delta T_{01}$, we also obtain

$$\frac{\Delta T_{01}}{T_{01}} = \left(\frac{2(1 - \lambda_1^2)}{\lambda_1^2} \right)^2 = \left(\frac{1 - \lambda_1^2}{\lambda_1^2} \right)^2. \quad (73)$$

Unlike this the simple shock wave, formed as a result of the explosion and being propagated in the inert medium, with distance from the blast center completely degenerates into an ordinary wave.

The last two expressions, just as equation (65), retain identical form with the substitution in them of velocity coefficients λ_1 and λ_2 . Thereby a change in the stagnation temperature is connected here either with the propagation velocity of detonation (λ_1) or with the maximum propagation velocity of the combustion zone (λ_2). It is important that the maximum value λ_2 is retained without depending on the mechanism of ignition, i.e., it is related both to the detonation and the steady-state flame propagation.

Let us turn to the calculation of the propagation velocity of the wave.

Let us designate for brevity the thermal characteristic of the combustible mixture Φ^1 :

$$\frac{T_{02} - T_{01}}{T_1} = \frac{\Delta T_0}{T_1} = \Phi.$$

From formulas (69) and (72) we have

$$\Phi \left(1 - \frac{k-1}{k+1} \lambda_1^2\right) = \left(\frac{k-1}{2\lambda_1}\right)^2,$$

whence the square of the velocity coefficient of the wave propagation is equal to

$$\lambda_1^2 = \frac{1 + 2\Phi}{1 + \Phi \frac{k-1}{k+1}} \left[1 \pm \sqrt{1 - \frac{1 + \Phi \frac{k-1}{k+1}}{(1 + 2\Phi)^2}} \right]. \quad (74)$$

In equation (74) both signs before the radical correspond to the real values of the velocity coefficient. The positive sign

¹In meaning this value is equal to the ratio of the quantity of liberated heat to the initial gas enthalpy $\Phi = Q/c_p T_1$. For example, for a cold ($T_1 \approx 300^\circ \text{ abc}$) mixture of gasoline with air (when $\alpha \approx 1$) $\Phi \approx 6.5$.

corresponds to detonation burning ($\lambda_1 > 1$), i.e., the propagation velocity of the shock wave. The negative sign corresponds to the propagation of the slow burning. It should be noted that formula (74) also with a negative sign is suitable for detonation. In this case it connects the velocity coefficient directly behind the shock front λ_2 (instead of λ_1) with value $\Phi' = \Delta T_0/T_2$ (instead of $\Phi = \Delta T_0/T_1$).

In practically interesting cases where $\Phi > 1$, instead of expression (74), it is possible with an error of less than 2% to accept approximately:

a) for the propagation velocity of the stationary wave of detonation

$$\lambda_1 = \frac{2 + 4\Phi}{1 + 4\Phi \frac{k-1}{k+1}}; \quad (75)$$

b) for the maximum propagation velocity of the wave of burning

$$\lambda_1 = \frac{1}{2 + 4\Phi}. \quad (76)$$

Using the known connection between the velocity coefficient and the M number, it is possible to obtain also similar dependences of the M number for waves of detonation and burning on the thermal characteristic of the gas mixture.

Figure 5.19a and 5.19b show graphs of the dependence

$$\lambda_1 = f(\Phi) \quad \text{and} \quad M_1 = F(\Phi)$$

for the gas mixture (when $k = 1.4$). The upper branches of both curves (in the supersonic region of motion $\lambda_1 > 1$, $M_1 > 1$) correspond to the steady minimum propagation velocity of detonation and the lower branches (in the subsonic region $\lambda_1 < 1$, $M_1 < 1$) - the maximum rate of combustion, i.e., the maximally possible velocity of the normal propagation of the flame.

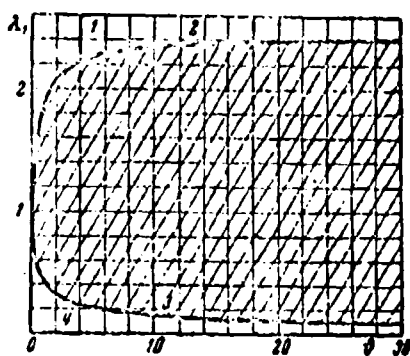


Fig. 5.19a.

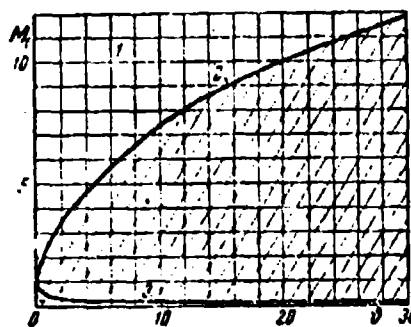


Fig. 5.19b.

Figure 5.19a. Dependence of the extreme value of the coefficient of the propagation velocity of the wave of burning on the thermal characteristic of the mixture: 1 - region of unsteady detonation; 2 - steady-state regime of detonation; 3 - maximum rate of combustion; 4 - region of normal burning.

Figure 5.19b. Dependence of the extreme value of the M number for the wave propagation of burning on the thermal characteristic of the mixture: 1 - region of unsteady detonation; 2 - steady-state regime of detonation; 3 - maximum rate of combustion; 4 - region of normal burning.

We arrive at the single concept of the propagation velocity of burning. In this case in the supersonic region (above the curve) the values which correspond to the nonstationary state of detonation lie, whereas in the subsonic region (below the curve) there is a countless multitude of values which correspond to the stationary normal propagation of burning at the low speeds of flow of the gas. Finally, the conditions which correspond to the shaded area (Figs. 5.19a and 5.19b) cannot be realized in connection with the phenomenon of the thermal critical region (i.e., the impossibility to transfer to the speed of sound during the heat feed).

By precisely this, apparently, one should explain the fact that the transition from slow burning to detonation, as experiments in the tubes show, is always achieved intermittently.

One should note one interesting feature of the curves obtained. As can be seen from the graphs, the most insignificant thermal effect suffices in order that the maximum rate of combustion becomes substantially lower and the detonation velocity substantially higher than the sonic.

Let us give the calculation of pressures with detonation and burning.

The calculation of the maximum expansion shock in the flame front attained with the thermal critical region can be produced by means of the momentum equation. In the case of $\lambda_3 = M_3 = 1$ we have¹

$$\frac{p_2}{p_1} = 1 + k \left(1 - \frac{w_2}{w_1} \right),$$

but in these conditions

$$\frac{w_2}{w_1} = \lambda_1 \sqrt{\frac{T_{01}}{T_{02}}},$$

whence, on the basis of dependence (71), we obtain

$$\frac{w_2}{w_1} = 1 - \sqrt{1 - \frac{T_{01}}{T_{02}}}. \quad (77)$$

Thus, the maximum pressure drop in the gas flow in the region of burning is equal to

$$\frac{p_2}{p_1} = 1 + k \sqrt{1 - \frac{T_{01}}{T_{02}}}. \quad (78)$$

¹In order to obtain this expression, let us write the momentum equation (94) of Chapter I for our case:

$$p_2 - p_1 = \rho_1 w_1 (w_1 - w_2)$$

or

$$\frac{p_2}{p_1} - 1 = k \frac{\rho_1 w_1}{k p_1} \left(1 - \frac{w_2}{w_1} \right),$$

but

$$\frac{\rho_1 w_1^2}{k p_1} = \frac{w_1^2}{a_1^2} = M_1^2 = 1.$$

or on the basis of expression (72)

$$\frac{p_2}{p_1} = 1 + k \frac{1 - \lambda_1^2}{1 + \lambda_1^2} = 1 + k \frac{\lambda_1^2 - 1}{\lambda_1^2 + 1}. \quad (79)$$

In this case the value of the velocity coefficient both in detonation and in the extreme case of normal burning is taken from the relation (74).

If we use equality (75), then the following approximation formula of the pressure drop in the second region of the wave of detonation (for $\lambda > 1$) is found:

$$\frac{p_2}{p_1} \approx 1 + \frac{1 + 8\lambda + \frac{1}{\lambda}}{1 + 8\lambda + \frac{1}{\lambda}}. \quad (80)$$

Correspondingly, equality (76) leads to the approximation expression of a drop in pressures for the maximum rate of the normal burning:

$$\frac{p_2}{p_1} \approx 1 + k \frac{1 + \frac{4\lambda}{3}}{3 + 4\lambda}. \quad (81)$$

The pressure change in transit through the entire region of detonation, which consists of an adiabatic shock wave and combustion zone, will be obtained in the division of equality (63) into (79):

$$\frac{p_2}{p_1} = \frac{p_2}{p_1} \frac{p_1}{p_1} = \frac{\lambda_1^2 + 1}{k + 1 - (k - 1)\lambda_1^2}. \quad (82)$$

Very simple dependences are obtained for a density change of the gas. At the maximum speed of normal burning, on the basis of the equation of continuity and expressions (77) and (72), we obtain

$$\frac{p_2}{p_1} = \frac{w_1}{w_2} = \frac{2}{\lambda_1 + 1} = \frac{2\lambda_1}{1 + \lambda_1^2}. \quad (83)$$

With the steady-state condition of detonation burning, using equalities (16) of Chapter III and (62), we have

$$\frac{p_2}{p_1} = \frac{\rho_2}{\rho_1} \frac{p_2}{p_1} = \frac{2\lambda}{\lambda+1}. \quad (84)$$

Let us discuss in more detail some general properties of the one-dimensional nonadiabatic waves, and let us give, in particular, the calculating equations for determining the absolute velocity of propagation of the wave. From the momentum and continuity equations it follows that in any case of the shock wave (in disregarding forces of friction) the following relation is correct:

$$\frac{p_2 - p_1}{\rho_2 - \rho_1} = u_1 w_2. \quad (85)$$

On the other hand, the equation of enthalpy, taking into account the equation of state of an ideal gas, gives for the pressure jump with any feed (or removal) of heat¹

$$\frac{p_2 - p_1}{\rho_2 - \rho_1} = a_{1,p}^2 + \frac{p_1}{\rho_2 - \rho_1} (a_{2,p}^2 - a_{1,p}^2) \quad (86)$$

¹Let us write the equation of enthalpy (25) of Chapter I for gas before and after the shock wave

$$c_p (T_{02} - T_1) = A \frac{w_1^2}{2g}, \quad c_p (T_{01} - T_2) = A \frac{w_2^2}{2g},$$

or, by replacing from the equation of state $T = \frac{p}{Rg\rho}$

$$p_1 = \rho_1 g R T_{01} - \frac{AR}{2c_p} \rho_1 w_1^2, \quad p_2 = \rho_2 g R T_{02} - \frac{AR}{2c_p} \rho_2 w_2^2$$

By subtracting from the second equation the first, taking into account the equalities

$$\frac{AR}{2c_p} = \frac{k-1}{2k}, \quad a_{1,p}^2 = \frac{2k}{k+1} g R T_1$$

and the law of the momenta, we obtain (86).

From equations (85), (86) and continuity, it is not difficult to derive the relation between velocities for the arbitrary pressure jump:

$$w_1 w_3 (w_1 - w_3) = a_{1np}^2 w_1 - a_{1np}^2 w_3 \quad (87)$$

In the particular case when the heat feed is absent and $a_{1np}^2 = a_{3np}^2$, we again obtain the relation (16) of Chapter III for the adiabatic shock wave.

In the case of interest to us of the steady-state detonation (or the propagation of burning at the maximum rate), when the thermal critical region begins, i.e., $\lambda_3 = 1$ and $w_3 = a_{3np}$, equation (87) assumes the form

$$(w_1 - a_{1np})^2 = a_{1np}^2 - a_{1np}^2 \quad (88)$$

whereupon for the detonation

$$w_1 > a_{1np}$$

for the slow burning

$$w_1 < a_{1np}$$

Just as in the dimensionless equations given previously, we have here two solutions:

$$w_1 = a_{1np} \pm \sqrt{a_{1np}^2 - a_{1np}^2} \quad (89)$$

which correspond to the minimum rate of the propagation of detonation (with the + sign) and the maximum speed of slow burning (with the - sign).

The obtained general relations are used for any nonadiabatic pressure jumps without depending on the mechanism of heat liberation. We saw that in the two cases examined above of the propagation of the flame front immediately the thermal shock

(i.e., the combustion zone) represented both with detonation and with normal burning the expansion shock in the subsonic flow. It is not difficult to indicate the case of the thermal compression shock in the supersonic flow. We have in mind the well-known condensation shocks, which are accompanied by the transition from a higher supersonic velocity to a lower but still supersonic velocity. And in this case the equations and derivations given above remain valid.

In conclusion let us investigate the flow of gases behind the wave front.

Obtained above were the fundamental principles characterizing the gas flow passing through the region of the shock of detonation or flame with a fixed front, i.e., in a reversed scheme. Let us examine now which form all relations will acquire, if we pass to the normal scheme when the gas is fixed, and in it the wave of detonation or burning at the rate w_1 is propagated. In this case behind the shock-wave front there follow the still not ignited particles of gas with the velocity

$$w_x = w_1 - w_p$$

and moving behind the region of burning are products of burning with the velocity

$$w_r = w_1 - w_p$$

where we understand w_x and w_r as absolute velocities. It is not difficult to see that in the case of the detonation

$$w_1 > w_x > w_p$$

i.e., the flame front and products of burning move in the same direction as does the shock-wave front, but only the particle velocity in the flame front is higher than in the products of burning:

$$w_1 > w_r$$

In the case of normal burning, when

$$w_1 = w_x < w_p$$

the value w_r is negative, i.e., the directions of motion of the products of burning and flame front are opposite.

As it was established, with the steady-state condition of detonation and with the maximum rate of normal burning, there occurs

$$w_1 = a_{1kp} \text{ or } \lambda_1 = 1,$$

in consequence of which in these conditions the rate of the motion of products of burning is equal to

$$w_r = w_1 - a_{1kp},$$

where according to dependence (89) obtained above

$$w_1 = a_{1kp} \pm \sqrt{a_{1kp}^2 - a_{1kp}^2}.$$

Hence we arrive at the following expression for the propagation velocity of products of burning in cases of stationary detonation and the maximum state of the normal burning:

$$w_r = \pm \sqrt{a_{1kp}^2 - a_{1kp}^2}. \quad (90)$$

The plus sign corresponds to detonation, and the minus sign - to normal burning.

Let us now find the values of velocity coefficients. For the shock-wave front we obtain $\lambda_1 = w_1/a_{1kp}$. For particles following directly after the shock-wave front,

$$\lambda_1 = \frac{w_1}{a_{1kp}} = \lambda_1 - \lambda_2 = \lambda_1 - \frac{1}{\lambda_1}, \quad (91)$$

since $a_{1kp} = a_{2kp}$. Finally, for products of burning according to (90) we have

$$\lambda_r = \frac{w_r}{a_{1kp}} = \pm \sqrt{1 - \frac{1}{\lambda_1^2}}.$$

Hence by means of (72) we find

$$\lambda_r = \frac{\lambda_1^2 - 1}{\lambda_1^2 + 1}. \quad (92)$$

Positive values of λ_r are obtained with detonation ($\lambda_1 > 1$), and negative values are obtained with normal burning ($\lambda_1 < 1$). In the case of $\lambda_1 = 1$ we have $\lambda_r = 0$, i.e., with the motion of the wave at the speed of sound the gas remains fixed, which completely corresponds to the physical nature of the phenomenon¹.

The greatest value of the rate of products of normal burning $\lambda_r = -1$ is obtained, naturally, in the fixed mixture of infinite caloricity [$Q = \infty$, i.e., $\lambda_1 = 0$, see (76)].

The maximum of the rate of products of detonation is reached also with infinite caloricity [with (75) $Q = \infty$, $\lambda_1 = \frac{k+1}{k-1}$], but in this case, as it is not difficult to see from (92), it is equal to

$$\lambda_r = \frac{1}{k}.$$

Thus, *the absolute velocity of the motion of the burned particles is always less than the speed of sound*. This result is valid both during normal burning and detonation.

Meanwhile as it is not difficult to see from (91), the velocity of unburned particles (at the beginning of the combustion zone) in the case of detonation can be more than sonic; this is obtained in the state

$$\lambda_1 = \lambda_1 - \frac{1}{\lambda_1} > 1, \text{ i.e., when } \lambda_1^2 - \lambda_1 - 1 > 0.$$

Solving this inequality, we obtain

$$\lambda_1 > \frac{1 + \sqrt{5}}{2} = 1.62 \quad \text{and} \quad M_1 > 2.$$

¹Above [see (74)] it was shown that $\lambda_1 = 1$ is obtained only with zero caloricity of the mixture, when the detonation and burning degenerate into the usual shock waves.

The maximum value of this velocity, obviously, is obtained in the state $M_1 = \infty$ and $\lambda_1^2 = \frac{k+1}{k-1}$, and it is equal to

$$\lambda_{1, \max} = \sqrt{\frac{k+1}{k-1}} - \sqrt{\frac{k-1}{k+1}}.$$

if $k = 1.4$, then $\lambda_{x, \max} = 2.04$ and $M_{x, \max} = 3.4$.

An interesting result will be obtained if we connect the absolute gas velocity at the beginning and end of the zone of the detonation burning:

$$\frac{w_2}{w_1} = \frac{\lambda_2 a_{1,up}}{\lambda_1 a_{2,up}}.$$

Hence, by using dependences (91), (92) and (72), we find the following simple relation:

$$w_2 = 2w_1 \quad (93)$$

i.e., with detonation the particle speed before the flame front is always twice higher than the velocity of the burned particles.

The pressures both behind the shock-wave from (p_2) and at the end of the combustion zone (p_3), obviously, are not changed from the fact that we changed the motion, i.e., they can be determined by formulas (63) and (79). It is possible, however, by means of (92) to give to formula (79) the following very simple form:

$$\frac{p_2}{p_1} = 1 \pm k\lambda_r \quad (94)$$

Here the minus sign is taken during normal burning and the plus sign during detonation. In the limiting cases of normal burning ($\lambda_r = -1$) and detonation ($\lambda_r = \frac{1}{k}$), we obtain, respectively, for the maximum rate of normal burning

$$\frac{p_2}{p_1} = 1 \pm k \quad (95)$$

and for the minimum rate of detonation

$$\frac{p_2}{p_1} = 2. \quad (96)$$

With the encounter of products of burning with a poorly streamlined body, there will occur a pressure increase up to value p_{03} , which for both these states is found from the same expression, which corresponds to the isentropic process of compression:

$$\frac{p_2}{p_{02}} = \left(1 - \frac{k-1}{k+1} \lambda_2^2\right)^{\frac{k}{k-1}}. \quad (97)$$

The more considerable increase in pressure occurs with a cessation of the particles of the still unignited gas moving at the rate of w_x . In the state of $\lambda_x < 1$ the same isentropic dependence acts:

$$\frac{p_2}{p_{02}} = \left(1 - \frac{k-1}{k+1} \lambda_2^2\right)^{\frac{k}{k-1}}. \quad (98)$$

For supersonic conditions ($\lambda_x > 1$), when braking begins from the normal shock wave, which converts the flow to subsonic velocity $\lambda_x = \frac{1}{\lambda_x}$ and the pressure determined by formula (63)

$$\frac{p_2}{p_1} = \frac{1 - \frac{k-1}{k+1} \lambda_2^2}{1 - \frac{k-1}{k+1} \lambda_1^2}. \quad (99)$$

we have with the total stagnation

$$\frac{p_2}{p_{02}} = \left(1 - \frac{k-1}{k+1} \lambda_2^2\right)^{\frac{k}{k-1}} \quad (100)$$

or finally

$$\frac{p_2}{p_{02}} = \frac{1}{\lambda_2^2} \left(1 - \frac{k-1}{k+1} \lambda_2^2\right) \left(1 - \frac{k-1}{k+1} \lambda_1^2\right)^{\frac{1}{k-1}}.$$

In the extreme case $\lambda_1^2 = \frac{k+1}{k-1}$, i.e., $\lambda_x = 2.04$ (when $k = 1.4$), we obtained the maximum pressure increase with braking

$$\frac{p_{01}}{p_1} \approx 18,$$

or in comparison with the pressure in products of burning

$$\frac{p_{01}}{p_1} \approx 30.$$

With the encounter of the gases following directly behind the detonation, with a sharp-nosed obstruction an oblique shock wave can arise instead of a normal wave. In the latter case a pressure increase with the braking of the gases proves to be less.

§ 6. Calculation of Gas Flows by Means of Gas-Dynamic Functions

Established above were the numerical relationships between the pressure, density, temperature and velocity coefficient of the gas flow and also the stagnation parameters for some cases of the gas flows. These equations contain the parameters of the gas, in particular, the velocity coefficient λ , in high and fractional powers, and therefore their conversion, the obtaining of explicit dependences between the parameters in general, and the solution of the numerical problems frequently represent considerable difficulties. At the same time, in examining the different equations of gas flow, derived, for example, in § 4 of Chapter I and § 4 of Chapter V, it is possible to note that the value of the velocity coefficient λ enters into them in the form of several frequently encountered combinations or expressions which were called *gas-dynamic functions*. Given to these functions are abbreviated notations, and their values, depending on value λ and the adiabatic index k , are calculated and reduced to tables.

The gas-flow calculation by means of tables of gas-dynamic functions received widespread acceptance and is at present conventional. Besides the reduction in the calculating work, the advantage of the calculation with the use of gas-dynamic functions

is the considerable simplification in the conversions in the joint solution of the fundamental equations, which makes it possible to obtain, in general, the solutions, of very complex problems. With such calculation the basic qualitative laws governing the flow and the relation between parameters of the gas flow are more clearly revealed. As it will be possible to see below, the use of gas-dynamic functions makes it possible to conduct the calculation of one-dimensional gas flows, taking into account the compressibility virtually as simple as the calculation of flows of an incompressible fluid is conducted.

Let us examine the basic gas-dynamic functions from those being used at present and in a number of examples illustrate their use for the solution of different problems.

The first and simplest group of gas-dynamic functions is introduced for the sake of simplicity in the recording of relationships between the parameters in the flow, the stagnation parameters and the velocity coefficient of the gas. In § 3 of Chapter I, by means of the transformation of the equation of energy, we obtained formula (42)

$$\frac{T}{T_0} = 1 - \frac{k-1}{k+1} \lambda^2,$$

which connects the stagnation temperature T_0 with the temperature in the flow T and the velocity coefficient λ . Let us denote

$$1 - \frac{k-1}{k+1} \lambda^2 = \tau(\lambda). \quad (101)$$

In § 4 of Chapter I expressions (72) and (73) were obtained for ratio of pressure and density in the flow to the total pressure and density of the isentropically stagnant gas. Let us introduce for them the notations

$$\pi(\lambda) = \frac{p}{p_0} = \left(1 - \frac{k-1}{k+1} \lambda^2\right)^{\frac{k}{k-1}}, \quad (102)$$

$$\epsilon(\lambda) = \frac{p}{p_0} = \left(1 - \frac{k-1}{k+1} \lambda^2\right)^{\frac{1}{k-1}}. \quad (103)$$

The connection between gas-dynamic functions $\tau(\lambda)$, $\pi(\lambda)$ and $\epsilon(\lambda)$ results from the obvious relationship between values ρ , p and T :

$$\epsilon(\lambda) = \frac{\pi(\lambda)}{\tau(\lambda)}. \quad (104)$$

It should be noted that equations (101), (102) and (103) connect the parameters of the gas *in the same cross section of the flow* and are valid independently of the flow pattern and processes occurring in the gas: the transition from parameters in the flow to parameters of the stagnated gas by definition occurs on the ideal adiabatic curve. The nature of the change in the gas-dynamic functions $\tau(\lambda)$, $\pi(\lambda)$ and $\epsilon(\lambda)$, depending on λ , is shown on Fig. 5.20: with an increase in λ from zero to the maximum value $\lambda_{\max} = \sqrt{\frac{k+1}{k-1}}$ functions $\tau(\lambda)$, $\pi(\lambda)$ and $\epsilon(\lambda)$ monotonically decrease from unity to zero. This completely corresponds to their physical meaning: at very low velocities ($\lambda \rightarrow 0$) the parameters in the flow virtually do not differ from the parameters of the completely stagnant gas; with an increase in the velocity up to the limiting value ($M \rightarrow \infty$, $\lambda \rightarrow \lambda_{\max}$), the temperature, pressure and density of the gas at the finite value of the stagnation parameters tend to zero.

Having available graphs or tables in which for each value of λ values of functions $\pi(\lambda)$, $\epsilon(\lambda)$, and $\tau(\lambda)$ are given, it is possible to determine rapidly the stagnation parameters according to parameters in the flow and vice versa. Such tables for values $k = 1.40$ and 1.33 are given at the end of the book. Given there are auxiliary graphs, which can be used, instead of the tables, if high accuracy of the calculations is not required.

Example 1. In section 1 of the subsonic part of an ideal Laval nozzle the following are known: pressure in the flow $p_1 = 16 \text{ kg/cm}^2$, stagnation temperature $T_{01} = 400^\circ\text{K}$, and velocity

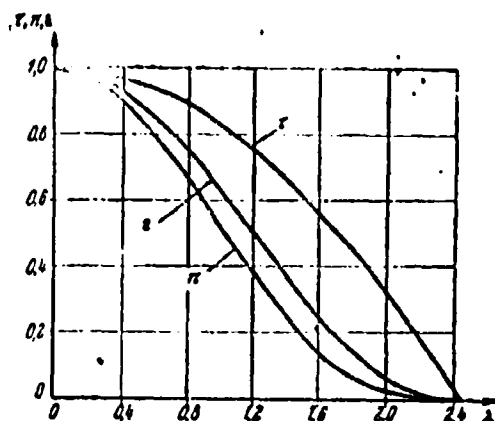


Fig. 5.20. Graphs of gas-dynamic functions $\tau(\lambda)$, $\epsilon(\lambda)$, and $\pi(\lambda)$ when $k = 1.4$.

coefficient $\lambda_1 = 0.6$. It is required to determine the velocity coefficient λ_2 and gas pressure in section 2, where the temperature T_2 is equal to 273°K.

Since the stagnation temperature and total pressure of the gas in the ideal nozzle in question are not changed, $T_{02} = T_{01}$ and $p_{02} = p_{01}$. Using the first equality and relation (101),

we write

$$\tau(\lambda_2) = \frac{T_2}{T_m} = \frac{T_2}{T_{01}}.$$

After substituting the assigned values T_2 and T_{01} , we find $\tau(\lambda_2) = 0.6825$ and from the tables determine (when $k = 1.40$) $\lambda_2 = 1.38$. Thus, the unknown section is located in the supersonic part of the nozzle. We further use the condition of constancy of the total nozzle pressure. By expressing the total pressure in terms of the pressure in the flow and function $\pi(\lambda)$ according to (102), we obtain

$$\frac{p_1}{\pi(\lambda_1)} = \frac{p_2}{\pi(\lambda_2)} \quad \text{or} \quad p_2 = p_1 \frac{\pi(\lambda_1)}{\pi(\lambda_2)}.$$

For $\lambda_1 = 0.6$ and $\lambda_2 = 1.38$ in the tables, we find the values of functions $\pi(\lambda)$ and determine

$$p_2 = 10 \frac{0.2628}{0.0053} = 5.23 \text{ kg/cm}^2.$$

Let us find now at the same initial data what the gas temperature will be in the section 3 of the nozzle, where the gas pressure is equal to the atmospheric $p_3 = 1.033 \text{ kg/cm}^2$. Let us write

$$\pi(\lambda_3) = \frac{p_3}{p_{03}} = \frac{p_3}{p_{01}} \quad \text{or} \quad \pi(\lambda_3) = p_3 \frac{\pi(\lambda_1)}{p_1}.$$

Hence we find

$$\kappa(\lambda_3) = \frac{1.033}{16} 0.8053 = 0.052,$$

and then from the tables we determine the value $\lambda_3 = 1.85$. This value of the velocity coefficient in the table corresponds to $\tau(\lambda_3) = 0.4296$. Further, we easily find the gas temperature in section 3

$$T_3 = T_{0,1}(\lambda_3) = 400 \cdot 0.4296 = 171.5^\circ \text{K}.$$

Thus other problems connected with the determination of the dependence between the gas parameters in different cross sections of the flow are solved.

Let us examine further the two gas-dynamic functions which are used in the *equation of the gas flow rate*. Let us substitute into the expression of the gas flow rate per second, in terms of the cross section of the area $F G = \gamma w F$, the relations which express the specific weight of the gas γ and flow velocity w in terms of stagnation parameters p_0 and T_0 and the velocity coefficient λ :

$$\gamma = \rho \left(1 - \frac{k-1}{k+1} \lambda^2\right)^{\frac{1}{k-1}} = \frac{p_0}{RT_0} \left(1 - \frac{k-1}{k+1} \lambda^2\right)^{\frac{1}{k-1}},$$

$$w = \lambda a_{*p} = \lambda \sqrt{2g \frac{k}{k+1} RT_0}.$$

Then we will obtain

$$G = \frac{p_0}{RT_0} F \lambda \left(1 - \frac{k-1}{k+1} \lambda^2\right)^{\frac{1}{k-1}} \sqrt{2g \frac{k}{k+1} RT_0}. \quad (105)$$

After multiplying both sides of this equation by $a_{*p} = \sqrt{2g \frac{k}{k+1} RT_0}$ after cancellations we have

$$\frac{G}{g} a_{*p} = \frac{2k}{k+1} p_0 F \lambda \left(1 - \frac{k-1}{k+1} \lambda^2\right)^{\frac{1}{k-1}}. \quad (106)$$

This equation expresses the gas flow rate in this cross section in terms of the total pressure, the critical speed of sound and the

certain function of the velocity coefficient

$$\lambda \left(1 - \frac{k-1}{k+1} \lambda^2\right)^{\frac{1}{k-1}} = \lambda \epsilon(\lambda)$$

where $\epsilon(\lambda)$ is the gas-dynamic function (103) introduced above.

The new gas-dynamic function $q(\lambda)$ is defined as the value proportional to the product $\lambda \epsilon(\lambda)$:

$$q(\lambda) = \left(\frac{k+1}{2}\right)^{\frac{1}{k-1}} \lambda \left(1 - \frac{k-1}{k+1} \lambda^2\right)^{\frac{1}{k-1}}. \quad (107)$$

The proportionality factor is selected so that when $\lambda = 1$ we have $q(\lambda) = 1$. Because of this the gas-dynamic function $q(\lambda)$ acquires the physical meaning of the dimensionless current density:

$$q(\lambda) = \frac{\rho w}{(\rho w)_{\text{sp}}},$$

where $(\rho w)_{\text{sp}}$ is the maximum value of the current density (with the assigned stagnation parameters), which corresponds to the flow at the speed of sound. Actually,

$$\frac{\rho w}{(\rho w)_{\text{sp}}} = \frac{\rho}{\rho_0} \frac{p_0}{p_{\text{sp}}} \frac{w}{w_{\text{sp}}} = \frac{q(\lambda)}{q(1)} \lambda = \left(\frac{k+1}{2}\right)^{\frac{1}{k-1}} \lambda \epsilon(\lambda).$$

The graph of function $q(\lambda)$ is given on Fig. 5.21. With an increase in the velocity coefficient λ from zero to unit, the value $q(\lambda)$ increases from zero to its maximum value $q(\lambda) = 1$ and further is again lowered to zero at value $\lambda = \lambda_{\text{max}}$. Thus, the current density is maximum when $q(\lambda) = 1$ and is decreased both with a decrease and an increase in the velocity in comparison with the critical value. The same value of function $q(\lambda)$ corresponds to two possible values of the velocity coefficient, one of which is more and the other less than unity.

Substituting function $q(\lambda)$ into expression (106), we have

$$\frac{d}{dx} a_{\text{sp}} = \frac{2k}{k-1} \left(\frac{2}{k+1}\right)^{\frac{1}{k-1}} \rho_0 q(\lambda) \quad (108)$$

By replacing in (108) quantity a_{kp} by its value, we obtain the following formula for the calculation of the gas flow rate (see also § 1 of Chapter IV):

$$Q = m \frac{C_p F q(\lambda)}{\sqrt{R}}, \quad (109)$$

where

$$m = \sqrt{k \left(\frac{2}{k+1} \right)^{\frac{k+1}{k-1}}} \sqrt{\frac{R}{R^*}} = N \sqrt{\frac{R}{R^*}}.$$

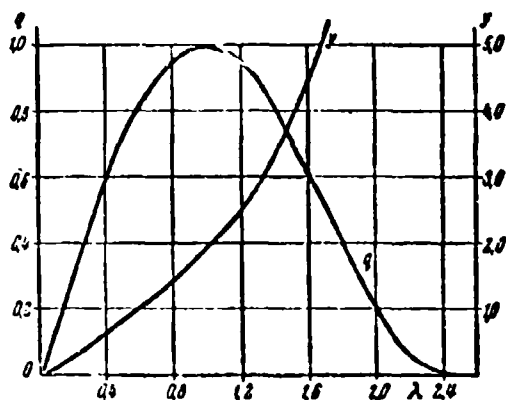


Fig. 5.21. Graphs of gas-dynamic functions $q(\lambda)$, $y(\lambda)$ when $k = 1.4$.

In the following table values of N for different values of k are given:

k	1.67	1.4	1.35	1.33	1.30	1.25	1.10
N	0.723	0.685	0.676	0.673	0.667	0.658	0.628

For air ($k = 1.4$, $R = 29.27$ kg-m/kg-deg) the numerical coefficient in equation (109) $m = 0.3965$ [deg^{0.5}·s⁻¹]. For exhaust gases in turbojet engines ($k = 1.33$, $R = 29.4$ kg-m/kg-deg) $m = 0.389$. For powder gases, on the average it is possible to consider that $m = 0.343$. With flow at the speed

of sound $q(\lambda) = 1$, equation (109) is reduced to expression (8) obtained in Chapter IV for the calculation of the gas flow rate through the Laval nozzle according to the parameters of gas in the nozzle throat area.

In the solution of a number of problems, it is required to connect the gas flow rate not with the total but with the static pressure in the flow. It is easy to obtain such a connection from expressions (108) or (109) if we replace in their right sides the value of total pressure

$$p_0 = \frac{p}{\pi(\lambda)} = \frac{p}{\left(1 - \frac{k-1}{k+1}\lambda^2\right)^{\frac{k+1}{2}}}$$

Then we obtain the relations

$$q_{\lambda p} = \frac{2k}{k+1} \left(\frac{2}{k+1}\right)^{\frac{1}{k-1}} p F y(\lambda) \quad (110)$$

and

$$Q = m \frac{p F y(\lambda)}{\sqrt{T_0}} \quad (111)$$

where the function

$$y(\lambda) = \frac{q(\lambda)}{\pi(\lambda)} = \left(\frac{k+1}{2}\right)^{\frac{1}{k-1}} \frac{\lambda}{1 - \frac{k-1}{k+1}\lambda^2} \quad (112)$$

is the second gas-dynamic function with the aid of which it is possible to calculate the gas flow rate (see Fig. 5.21). Its values, just as the values of function $q(\lambda)$, for different values of k are given in tables and on auxiliary graphs at the end of the book. With an increase in λ function $y(\lambda)$ monotonically increases, whereupon when $\lambda \rightarrow \lambda_{\max}$, $y(\lambda) \rightarrow \infty$. Both formula (109) and formula (111) express the gas flow rate by means of parameters of its state in the cross section of the flow in question, and that is why they are valid independently of the nature of the processes occurring in the flow of gas. Formulas (109) and (111) are conveniently used in the compilation of equations of continuity for the gas flow, whereupon for each cross section there can be selected that formula which corresponds better to the assigned or unknown values.

Expressions (109), (111) and the equations of continuity compiled with their aid directly lead to a number of dependences derived earlier by a more complex means and also make it possible to solve various problems quite simply. Let us give several examples of the calculation.

Example 2. Determine the dependence between the area of any cross section of an ideal Laval nozzle and the velocity coefficient of the flow in this cross section, i.e., find the law of a change in the area in the Laval nozzle. Since for any cross section of an ideal nozzle, the flow rate, total pressure and stagnation temperature are identical, then from (109) it follows that $Fq(\lambda) = \text{const.}$ Since for critical cross sections $q(\lambda)_{\text{кр}} = 1$, then $Fq(\lambda) = F_{\text{кр}}$ or $\frac{F}{F_{\text{кр}}} = \frac{1}{q(\lambda)}$, i.e., the cross-sectional area of the nozzle varies indirectly proportional to the value of function $q(\lambda)$. In accordance with the graph of function $q(\lambda)$, this means that with an increase in the velocity the area decreases at subsonic velocities and increases at supersonic velocities, having a minimum when $\lambda = 1$.

Example 3. In the section of the cylindrical tube between the two cross sections 1 and 2 as a result of hydraulic losses (friction, local resistances) the total pressure of the moving gas is lowered. The losses of total pressure between cross sections 1 and 2 are estimated by the value of the coefficient of total pressure $\sigma = p_{02}/p_{01} < 1$. Determine the nature of the change in the velocity and static pressure of the gas in the tube in the absence of heat exchange with the environment. Let us write, after making use of formula (109), the condition of the equality of the gas flow rates in cross sections 1 and 2:

$$\frac{p_{01} F_1 q(\lambda_1)}{\sqrt{T_{01}}} = \frac{p_{02} F_2 q(\lambda_2)}{\sqrt{T_{02}}}.$$

Since in this case $F_1 = F_2$ and $T_{01} = T_{02}$, then

$$q(\lambda_2) = \frac{p_{01}}{p_{02}} q(\lambda_1) \quad \text{or} \quad q(\lambda_2) = \frac{1}{\sigma} q(\lambda_1).$$

Hence according to the assigned values of λ_1 and σ , it is possible with the aid of tables of gas-dynamic functions to determine λ_2 . The obtained result is valid both for subsonic

and supersonic flow velocities. Since $\sigma < 1$, then $q(\lambda_2) > q(\lambda_1)$.

From this inequality it follows (see the plotted function $q(\lambda)$ on Fig. 5.21) that in the presence of flow friction (when $G = \text{const}$, $F = \text{const}$, $T_0 = \text{const}$) the velocity of the subsonic flow along the length of the tube increases, and the velocity of the supersonic flow decreases.

In order to determine the change in static pressure, it is possible to compare with each other values $p_1 = p_{01}\pi(\lambda_1)$ and $p_2 = p_{02}\pi(\lambda_2)$. However, a more clearly unknown result can be obtained from the condition of the equality of the gas flow rates if we use in this case expression (111)

$$\frac{p_1 F_1 y(\lambda_1)}{\sqrt{T_{01}}} = \frac{p_2 F_2 y(\lambda_2)}{\sqrt{T_{02}}} \quad \text{or} \quad \frac{p_1}{p_2} = \frac{y(\lambda_1)}{y(\lambda_2)}.$$

Since function $y(\lambda)$ is increasing, then hence we conclude that in the presence of resistance, in accordance with the change in the velocity coefficient found above, the static pressure will decrease if the flow velocity is subsonic and increase if the velocity is supersonic.

Example 4. Determine the velocity coefficient λ_2 and static pressure of the air p_2 at outlet from the diffuser, if it is known that at the inlet to the diffuser the total pressure $p_{01} = 3 \text{ kg/cm}^2$, the velocity coefficient $\lambda_1 = 0.85$, the area ratio of the outlet and inlet sections $F_2/F_1 = 2.5$ and the coefficient of total pressure $\sigma = p_{02}/p_{01} = 0.94$. To solve the problem we write the equation of continuity, using formula (109)

$$\frac{p_{01} F_1 q(\lambda_1)}{\sqrt{T_{01}}} = \frac{p_{02} F_2 q(\lambda_2)}{\sqrt{T_{02}}}.$$

Disregarding the heat exchange through walls of the diffuser, we have $T_{02} = T_{01}$, and therefore, $q(\lambda_2) = \frac{1}{\sigma} \frac{F_1}{F_2} q(\lambda_1)$. According to

tables for $\lambda_1 = 0.85$ we find $q(\lambda_1) = 0.9729$. Then $q(\lambda_2) = 0.425 \cdot 0.9729 = 0.413$, to which corresponds $\lambda_2 = 0.27$ and $\pi(\lambda_2) = 0.9581$. From the relation (102) we have $p_2 = p_{02} \pi(\lambda_2) = \sigma p_{01} \pi(\lambda_2)$ or $p_2 = 0.94 \cdot 3 \cdot 0.9581 = 2.7 \text{ kg/cm}^2$.

Example 5. With the compressor testing, in its outlet cross section, the area of which $F = 0.1 \text{ m}^2$ the static pressure $p = 4.2 \text{ kg/cm}^2$ and the stagnation temperature of the air $T_0 = 480^\circ\text{K}$ are measured. Determine the total pressure of the air if its flow rate $G = 50 \text{ kg/s}$.

From the equation of flow rate (m) we determine the function $y(\lambda)$ in terms of the known value of the static pressure of the air:

$$y(\lambda) = \frac{G \sqrt{T_0}}{\pi p F} = \frac{50 \sqrt{480}}{\pi \cdot 4.2 \cdot 0.1 \cdot 10^4} = 0.406.$$

From the tables of gas-dynamic functions, we find that the values $\lambda = 0.406$ and $\pi(\lambda) = 0.907$ correspond to this value $y(\lambda)$. Hence the total air pressure $p_0 = p/\pi(\lambda) = 4.2/0.907 = 4.63 \text{ kg/cm}^2$.

If we do not use gas-dynamic functions, then the similar calculations which are frequently made in the processing of experimental data must be carried out by a more complex method, by means of successive approximation.

Let us examine the gas-dynamic functions which are used in the *equation of the momentum of gas*. The sum of the per-second momentum and force of pressure of the gas in the cross section of the flow in question can be called the total momentum of flow I

$$I = \frac{G}{g} w + pF = \frac{G}{g} \left(w + \frac{p}{\rho w} \right). \quad (113)$$

If in (113) we substitute the relations

$$w = \lambda a_{sp}; \quad \frac{p}{\rho} = gRT = gRT_0 \left(1 - \frac{k-1}{k+1} \lambda^2\right) = \frac{k+1}{2k} a_{sp}^2 \left(1 - \frac{k-1}{k+1} \lambda^2\right),$$

then we obtain

$$\frac{Q}{g} w + pF = \frac{Q}{g} \left[\lambda a_{sp} + \frac{k+1}{2k} \frac{a_{sp}}{\lambda} \left(1 - \frac{k-1}{k+1} \lambda^2\right) \right]. \quad (114)$$

After the opening of the brackets and simplifications, we reduce expression (114) to the form

$$\frac{Q}{g} w + pF = \frac{k+1}{2k} \frac{Q}{g} a_{sp} z(\lambda) \quad (115)$$

where

$$z(\lambda) = \lambda + \frac{1}{\lambda}. \quad (116)$$

The graph of the gas-dynamic function $z(\lambda)$ is given in Fig. 5.22. The minimum value of function $z(\lambda) = 2$ corresponds to the critical rate of flow ($\lambda = 1$). Both in subsonic and supersonic flows $z(\lambda) > 2$; any real flow conditions do not correspond to values $z(\lambda) < 2$. It is easy to see that with the replacement of value λ by the value opposite to it $\lambda' = 1/\lambda$ the value of function $z(\lambda)$ does not change. Thus, one value of $z(\lambda)$ can correspond to *two mutually opposite values of the velocity coefficient* λ - one of them determines the subsonic and the other the supersonic gas flow. Let us note also that function $z(\lambda)$, unlike all remaining gas-dynamic functions, does not depend on the value of the adiabatic index k .

Expression (115) for the momentum of flow considerably simplifies recording and transformation of the equation of the momentum of gas. It proves to be extremely useful in the solution of a wide range of problems of gas dynamics as, for example, in the calculation of flows with shock waves, heat feed and cooling, flows with friction and with a shock during sudden expansion of the channel, in the calculation of the process of the mixing of flows, in the determination of forces which act on

walls of the channel, in the calculation of reactive thrust, and so on.

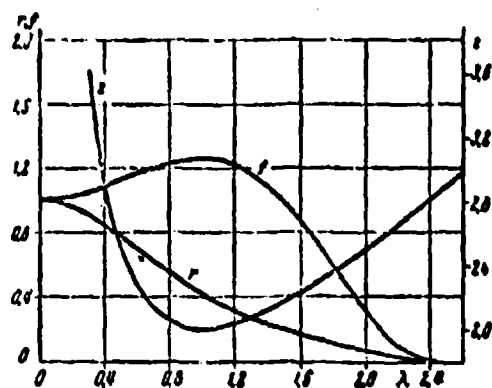


Fig. 5.22. Graphs of gas-dynamic functions $z(\lambda)$, $f(\lambda)$, $r(\lambda)$ when $k = 1.4$.

The following two examples make it possible to show visually how the solving of problems is simplified when using relation (115). In the first of them the previously solved problems (Chapter III § 1) of the normal shock wave is examined, and in the second - the problem of the flow of the preheated gas in the cylindrical tube.

Example 6. Determine the relationships between the gas parameters before and after the normal shock wave.

The relationship between the gas parameters in the shock wave was established above by us on the basis of the fact that with transition through the normal shock the total energy, flow rate and momentum of flow are maintained constant. Let us write the same equations with the use of gas-dynamic functions.

The equation of momentum or the momentum of the flow

$$\frac{G}{g} \cdot w_1 + p_1 F_1 = \frac{G}{g} \cdot w_2 + p_2 F_2$$

taking into account expression (115), assumes the form

$$G_1 a_{k,p_1} z(\lambda_1) = G_2 a_{k,p_2} z(\lambda_2)$$

From equations of the conservation of flow rate and total energy, we have

$$G_1 = G_2 \quad T_{01} = T_{02} \quad \text{or} \quad a_{k,p_1} = a_{k,p_2}$$

Taking this into account and reducing the corresponding values of flow rate and speed of sound in the momentum equation, we obtain

$$z(\lambda_1) = z(\lambda_2).$$

This equation has two solutions: either $\lambda_2 = \lambda_1$, which corresponds to the shock-free flow with the constant gas parameters, or

$$\lambda_2 = \frac{1}{\lambda_1},$$

which corresponds to the normal shock. The same expression - the basic kinematic relation of the theory of shock waves - was obtained above, see formula (16) in Chapter III.

According to the known value of the velocity coefficient, with the aid of the equation of continuity, a change in the total and static pressures in the shock wave is easily determined. Since $F_2 = F_1$ and $T_{02} = T_{01}$, then by using formulas (109) and (111), it is possible to present the equation of continuity for the flow of gas before and after the shock in the form

$$p_{01} q(\lambda_1) = p_{02} q(\lambda_2) \quad \text{or} \quad p_{02} q(\lambda_2) = p_{01} q(\lambda_1).$$

Hence, taking into account that $\lambda_2 = \frac{1}{\lambda_1}$, it follows that

$p_{02}/p_{01} = q(\lambda_1)/q\left(\frac{1}{\lambda_1}\right)$; $p_2/p_1 = y(\lambda_1)/y\left(\frac{1}{\lambda_1}\right)$. These relations are equivalent to equations (24) and (21) of Chapter III but are obtained by a considerably simpler means.

Example 7. The gas which moves in the cylindrical tube is heated by means of heat exchange through the walls of the tube. As a result of the heat feed the stagnation temperature of the gas is increased from 400°K at the inlet into the tube to 800°K at the outlet from it. The velocity coefficient of flow at the inlet into the tube $\lambda_1 = 0.4$. It is required to determine, disregarding friction, the coefficient of flow velocity after preheating and also the change in the total and static pressures in the flow.

The fundamental relation which determines the laws governing the gas flow in the cylindrical tube with the heat feed will be obtained from the equation of momentum. In this case it takes the form of

$$\frac{G}{\rho} w_1 + \rho_1 F = \frac{G}{\rho} w_2 + \rho_2 F,$$

since the heat feed is not connected with the force effect on the flow, and the forces of pressure in the initial and final cross section are the only forces which produce a change in the momentum of the gas. After replacing expressions for the momenta of the flow of gas according to relation (115) and considering that the heat capacity of the gas and the adiabatic index with preheating do not change, we will obtain

$$a_{sp_1} z(\lambda_1) = a_{sp_2} z(\lambda_2) \quad \text{or} \quad z(\lambda_2) = z(\lambda_1) \sqrt{\frac{T_{01}}{T_{02}}}.$$

Since when $\lambda_1 = 0.4$ we have $z(\lambda_1) = 2.9$, then

$$z(\lambda_2) = 2.9 \sqrt{\frac{100}{800}} = 2.05$$

With the aid of the tables of function $z(\lambda)$ or the direct calculation from the quadratic equation $\lambda_2 + 1/\lambda_2 = 2.05$, we determine the two possible values of the velocity coefficient at the outlet: $\lambda_2' = 0.8$, $\lambda_2'' = 1/\lambda_2' = 1.25$. The real solution will be only the first solution, since by preheating it is not possible to transfer the subsonic flow into supersonic (see § 4)

By knowing the coefficient of flow velocity $\lambda_2 = 0.8$, it is easy to determine the change in the total and static pressures in the process of preheating. To do this, just as in the foregoing example, it is possible to use the equation of continuity from which for the given case ($G = \text{const}$, $F = \text{const}$) it follows that

$$\begin{aligned} \frac{p_{02}}{p_{01}} &= \frac{y(\lambda_1)}{y(\lambda_2)} \sqrt{\frac{T_{01}}{T_{02}}} = \frac{0.597}{0.518} \sqrt{\frac{100}{800}} = 0.875, \\ \frac{p_2}{p_1} &= \frac{y(\lambda_1)}{y(\lambda_2)} \sqrt{\frac{T_{01}}{T_{02}}} = \frac{0.6182}{1.125} \sqrt{\frac{100}{800}} = 0.618. \end{aligned}$$

lines both the total and static pressures, as a result of the preheating of the gas, decrease. The obtained value $p_2/p_1 = 0.648$ and is that relationship of the static pressures of the gas in the initial and final cross sections of the section of the tube in question which must be created in order to maintain at this preheating the assigned magnitude of the velocity coefficient at the inlet $\lambda = 0.8$.

The equation of the conservation of momentum makes it possible to establish some general laws governing the flow in a cylindrical tube with preheating or cooling. Thus, for instance, it is easy to see that with an increase in the ratio T_{02}/T_{01} the value of function $z(\lambda_2)$ (when $z(\lambda_1) = \text{const}$) always decreases. In accordance with the nature of the course of function $z(\lambda)$ (Fig. 1, b), this means that with an increase in preheating in the subsonic flow the velocity coefficient increases, while in supersonic flow it decreases. In both cases the flow velocity will approach the critical value $\lambda_2 = 1$ at which function $z(\lambda)$ takes on its smallest possible value $z(\lambda_2) = 2$. This causes the value of the maximally possible preheating for the assigned initial velocity $(T_{02}/T_{01})_{\text{max}} = z^2(\lambda_1)/4$. For the values of the parameters taken in this example the maximum value of the preheating corresponds to $T_{02} = 840^\circ\text{K}$. From the equations of flow rate it is possible to determine the pressure ratio p_2/p_1 necessary for the realization of such conditions while maintaining $\lambda_1 = \text{const}$. With an increase in the preheating above the indicated value, we will obtain $z(\lambda_2) < 2$, which indicates the physical impossibility of such preheating at the assigned rate of flow at the inlet.

After replacing in relation (115) the product $\frac{Q}{g} a_{\text{av}}$ with its value according to (108) or (110), we obtain the expression for the momentum of the gas flow in the first case in terms of the total pressure and in the second case in terms of the static pressure:

$$\frac{Q}{g} w + pF = \left(\frac{2}{k+1} \right)^{\frac{1}{k-1}} p_0 F q(\lambda) z(\lambda)$$

and

$$\frac{G}{g} w + pF = \left(\frac{2}{k+1}\right)^{\frac{1}{k-1}} pF y(\lambda) z(\lambda)$$

Let us introduce the notations for the two new functions of the velocity coefficient λ which enter into the right sides of these expressions:

$$f(\lambda) = \left(\frac{2}{k+1}\right)^{\frac{1}{k-1}} q(\lambda) z(\lambda) = (k+1) \left(1 - \frac{k-1}{k+1} \lambda^2\right)^{\frac{1}{k-1}}, \quad (117)$$

$$r(\lambda) = \left(\frac{k+1}{2}\right)^{\frac{1}{k-1}} \frac{1}{y(\lambda) z(\lambda)} = \frac{1 - \frac{k-1}{k+1} \lambda^2}{1 + \lambda^2}. \quad (118)$$

By substituting these notations, we finally obtain

$$\frac{G}{g} w + pF = pF f(\lambda) \quad (119)$$

$$\frac{G}{g} w + pF = \frac{pP}{r(\lambda)}. \quad (120)$$

Function $r(\lambda)$ is introduced as the value opposite to the product $y(\lambda) z(\lambda)$ in order to facilitate the use of the tables (product $y(\lambda) z(\lambda)$ rapidly increases with an increase in λ , approaching infinity at $\lambda \rightarrow \lambda_{\max}$; value $r(\lambda)$ changes within the limits of unity to zero). The graphs of functions $f(\lambda)$ and $r(\lambda)$ are given on Fig. 5.22)

Equations (119) and (120) show the number of properties of the momentum of gas flow. Let us focus attention on the fact that on the right side of these equations there are no values of gas flow rates and temperature or critical velocity. Hence it follows that if at the assigned cross-sectional area F and velocity coefficient λ the total or static pressure in the flow is constant, then the momentum retains a constant value independently of the temperature and gas flow rate.

The physical meaning of this consists in the fact that with a change in temperature (or stagnation temperature) in the gas when $\lambda = \text{const}$ the velocity of flow varies directly proportional and the flow rate inversely proportional to the square of the temperature so that the product Gw remains constant. Let us note that function $f(\lambda)$ in the region of the subsonic and low supersonic velocities changes very little (approximately 10% in the interval $\lambda = 0.55-1.35$). Hence, according to (119), it follows that the momentum of the gas flow at constant total pressure and cross-sectional area weakly depends on value λ over a wide range of its change and is determined basically by the value of product $p_0 F$.

Expressions (119) and (120) for the momentum of gas are very convenient in the solution of problems connected with the determination of forces which act on the part of the gas on walls of the channel, which is necessary, in particular, in the calculation of the reactive thrust of different engine installations.

For the reactive thrust of rocket engine, above (§ 8 of Chapter I) we obtain the expression

$$P = \frac{G}{g} w_e + (p_e - p_a) F_e$$

This formula determines the thrust of a jet engine of any type when operating at the place where the initial momentum of the air which enters into the engine is equal to zero. We convert this formula with the aid of the relations obtained above, for which on its right side we replace the expression of the momentum of gas in the nozzle exit section according to formulas (119) and (120). In the first case we obtain

$$P = p_a F_e \lambda^2 (\lambda^2 - 1) \text{ or } P = p_a F_e \lambda^2 (\Pi_0 - 1) \quad (121)$$

where $\Pi_0 = p_{0a}/p_a$ is the available pressure ratio in the nozzle.

In exactly the same manner it is possible to obtain the second expression

$$P = p_a F_n \left[\frac{p_a}{p_n} \frac{1}{r(\lambda_a)} - 1 \right] \text{ or } P = p_n F_n \left[\frac{n}{r(\lambda_a)} - 1 \right], \quad (122)$$

where $n = p_a/p_n$ is the so-called *off-design ratio of the nozzle*, i.e., the ratio of the static pressure of the gas in the nozzle edge to the atmospheric pressure.

Formula (121) is very convenient for the calculation of reactive thrust and is widely applied in the calculation of engines. The velocity coefficient λ_a is determined by the type of the jet nozzle and by the available pressure ratio. If the nozzle is made nonexpanding and the pressure ratio exceeds the critical value, then $\lambda_a = 1$; for a supersonic nozzle $\lambda_a = \lambda_{\text{pacy}}$ at all values of Π_0 greater than the computed value and in the considerable part of the range $\Pi_0 < \Pi_{\text{pacy}}$. Hence it follows that over a wide range of conditions of contemporary engines $\lambda_a = \text{const}$, and by formula (121) the linear dependence of the reactive thrust on the value of the available pressure ratio Π_0 is defined, since $f(\lambda_a) = \text{const}$. Let us recall that also when $\lambda_a \neq \text{const}$ the value of function $f(\lambda)$ is very little affected in the considerable region of the subsonic and supersonic velocities.

Formula (122) is convenient for the calculation of thrust in conditions when the static pressure in the nozzle edge is equal to the atmospheric pressure and $n = 1$. Such conditions exist, in particular, at the subsonic speed of the outflow of gas from the nozzle, and also in the operation of supersonic nozzles in design conditions.

Let us note that for the calculation of reactive thrust, according to (121) and (122) it is not required to know the gas flow rate and its temperature. The temperature change, as can be seen from (121) and (122), when $p_n = \text{const}$, $p_0 = \text{const}$ and $F = \text{const}$ does not at all affect the thrust level, which is

connected with the mutually inverse dependence of the discharge velocity and gas flow rate on temperature.

Expressions (121) and (122) can be used also for the calculation of the thrust of jet engines in flight; in this case on the right side it is necessary to subtract the so-called input momentum of the airflow $G_B w_H / g$, where G_B is the rate of air flow and w_H - the flight velocity (see § 8 of Chapter I).

Let us examine the examples of the use of given expressions of reactive thrust.

Example 8. Determine how the value of reactive thrust depends on the velocity coefficient of the gas at nozzle exit when $\Pi_0 = \text{const.}$

From formula (121) it directly follows that if $F_a = \text{const}$ and $\Pi_0 = \text{const}$, then the dependence of the thrust on the velocity coefficient λ_a is determined by a change in function $f(\lambda)$. Under these conditions, however, with a change in λ , the gas flow rate changes.

There is great practical interest in another case of the change in the velocity coefficient λ_a , when the flow rate per second and the initial parameters of the gas are maintained constant. This condition can be realized if in the constant throat area of the supersonic nozzle F_{HP} we change the discharge area F_a . The nature of the dependence of thrust on value λ_a in this case will make it possible to determine the rational expansion ratio of the nozzle for an engine with the assigned parameters and gas flow rate. Equations (120) and (121) are not completely convenient for such a calculation, since they include the two variables λ_a and F_a . Therefore, let us transform the equation F_a by means of the equation of the flow rate

$$F_a = \frac{G \sqrt{T_{0g}}}{\pi p_{0g} q(\lambda_a)} = \frac{F_{HP}}{q(\lambda_a)}.$$

Taking into account the relationship between functions $f(\lambda)$, $q(\lambda)$ and $z(\lambda)$, we obtain

$$P = p_{0a} F_{\kappa p} \left[\left(\frac{2}{k+1} \right)^{\frac{1}{k-1}} z(\lambda) - \frac{1}{\Pi_0 \cdot q(\lambda_a)} \right].$$

In the design conditions of the outflow of gas, i.e., with expansion up to atmospheric pressure, the velocity coefficient is determined from the relation

$$\pi(\lambda_a) = \frac{1}{\Pi_0}.$$

In terms of this value λ_a the design expansion ratio of the nozzle $F_a/F_{\kappa p} = 1/q(\lambda_a)$ and the value of reactive thrust in design conditions are sought. In this calculation the losses in total pressure between cross sections $F_{\kappa p}$ and F_a are not considered.

Let us assume that $k = 1.33$ and $\Pi_0 = 25$; then in the design operating mode of the nozzle

$$\pi(\lambda_a) = \frac{1}{25} = 0.04, \lambda_a = 1.97, q(\lambda_a) = 0.279, \\ z(\lambda_a) = 2.477.$$

The discharge area of such a nozzle is equal to $F_{\kappa p}/q(\lambda_a) = 3.58 F_{\kappa p}$, and the thrust $P = 1.417 p_{0a} F_{\kappa p}$. The values of P at other values of λ_a , i.e., other values of F_a , are determined with the aid of tables. Results of such calculations are given on Fig. 5.23. Shown there are values $F_a/F_{\kappa p}$ for each value of λ_a . From the graph it is evident that the greatest thrust value is obtained with the total nozzle expansion, i.e., with the design conditions of the outflow. However, the nature of the functional dependence of thrust on the velocity coefficient is such that even with a noticeable reduction in the value λ_a and $F_a/F_{\kappa p}$ in comparison with their values in design conditions, the magnitude of the thrust decreases insignificantly. This makes it possible in certain cases to use nozzles with an incomplete expansion of

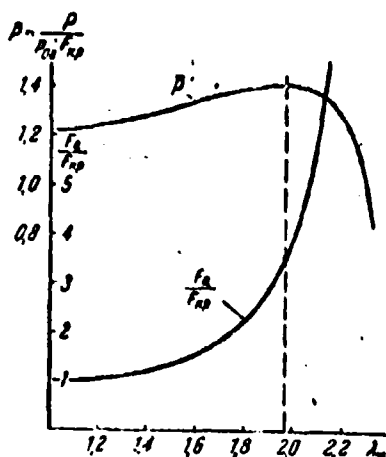


Fig. 5.23. Change in thrust with the assigned initial parameters and gas flow rate depending on the velocity coefficient at the nozzle exit (Example 8).

the gas and with the low supercritical pressure ratios p_0/p_H to use even the simple nonexpanding nozzles in which $\lambda_a = 1.0$. If one considers that in a nozzle with incomplete expansion there will be less losses of friction, then the reduction in thrust in comparison with the design conditions will be even less.

At the same time, as can be seen from Fig. 5.23, when $\lambda_a > \lambda_{pac}$, the thrust sharply decreases, i.e., it is inexpedient to use the nozzle with the overexpansions of the gas, even if one does not consider the increased losses of friction in it and the possibility of the formation of shock waves.

With the outflow of gas into a vacuum ($p_H = 0$) the thrust value varies in proportion to the value of the function $z(\lambda)$, i.e., monotonically increases with an increase in $\lambda_a > 1$. Actually, in this case the design conditions are

$$z(0_a) = \frac{p_a}{p_{0a}} = 0; \quad \lambda_a = \lambda_{min}; \quad \frac{F_a}{F_{ap}} = \frac{1}{q(0_a)} = \infty.$$

Since the nozzle of the outlet area cannot be made infinite, such design conditions cannot be realized. At any final value F_a/F_{ap} the thrust of the engine, which operates in a vacuum, will be less than a theoretically possible value. However, from graphs of functions $z(\lambda)$ and $q(\lambda)$ it is evident that with a considerable decrease in F_a/F_{ap} the reduction in the thrust is not very large. Thus, if instead of $F_a/F_{ap} = \infty$ we take (when $k = 1.33$) $F_a/F_{ap} = 10$, $q(\lambda_a) = 0.1$, $\lambda_a = 2.208$, then the thrust value with respect to the maximum theoretical value (when $\lambda_a = \lambda_{max} = 2.657$) will be

$$\frac{P}{P_{\max}} = \frac{z(\lambda_a)}{z(\lambda_{\max})} = \frac{2.661}{3.033} = 0.88;$$

when $F_a/F_{\max} = 20$, i.e., when $q(\lambda_a) = 0.05$ and $\lambda_a = 2.313$, $P/P_{\max} = 2.745/3.033 = 0.905$.

Examined in the following example is the problem of the flow of compressible gas with the sudden expansion of the channel, which is encountered in a number of practical problems. Above (§ 5 of Chapter I) we solved this problem for flow at low velocities, when it was possible to disregard the density change of the gas.

Example 9. For the measurement of the rate of air flow in the pipeline, installed on its straight section is a metering nozzle with the flow passage cross-sectional area F_2 equal to 0.45 of the area of the pipeline $F_1 = F_3$ (Fig. 5.24). It is required to determine the losses of total pressure which appear in the flow behind the nozzle as a result of a sudden expansion of the channel and also the velocity coefficient λ_3 after the alignment of the velocity field, if according to results of pressure measurements p_1 and Δp the velocity coefficient of the flow in the nozzle $\lambda_2 = 0.52$ is known. Determine also the reduction in static pressure in pipeline caused by the installation of nozzle.

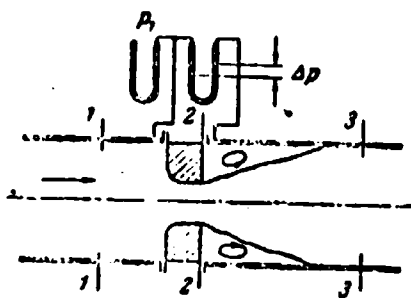


Fig. 5.24. Diagram of the installation of the nozzle for the measurement of the gas flow rate (Example 9).

Let us write the equation of the momentum for the section of the flow between cross sections 1 and 3, disregarding the wall friction and taking into account that at the subsonic velocities of the air in the nozzle the static pressure is constant in the whole cross section 2:

$$\frac{Q}{g} (w_3 - w_1) = p_1 F_1 - p_3 F_3$$

or

$$\frac{Q}{g} \omega_1 + p_1 F_1 = \frac{Q}{g} \omega_2 + p_2 F_2 = p_2 (F_2 - F_3).$$

Let us now replace the expressions of momenta according to (115), and let us express the static pressure p_2 by means of the equation of the flow rate (110). The equation of the momentum takes the form

$$\frac{k+1}{2k} \frac{Q}{g} a_{sp} [z(\lambda_1) - z(\lambda_2)] = \frac{k+1}{2k} \left(\frac{k+1}{2} \right)^{\frac{1}{k-1}} \frac{Q}{g} a_{sp} \frac{1}{y(\lambda_2)} \left(\frac{p_2}{p_1} - 1 \right).$$

After cancellation we obtain

$$z(\lambda_2) = z(\lambda_1) + \left(\frac{k+1}{2} \right)^{\frac{1}{k-1}} \frac{1}{y(\lambda_2)} \left(\frac{p_2}{p_1} - 1 \right).$$

From this equation according to values λ_2 and F_3/F_2 the velocity coefficient λ_3 after the expansion of the tube is determined. Let us note that the result does not depend on values of the pressure and gas temperature and is changed little depending on the adiabatic index k . After substituting into the latter equation the assigned values $\lambda_2 = 0.52$, $z(\lambda_2) = 2.44$, $y(\lambda_2) = 0.859$, $\frac{F_2}{F_3} = 0.45$, we obtain $z(\lambda_3) = 2.44 + 1.577 \frac{1}{0.859} 1.22 = 4.68$; hence, according to tables we find $\lambda_3 = 0.225$, $q(\lambda_3) = 0.3475$, $y(\lambda_3) = 0.358$.

The losses of total pressure of the air between cross sections 2 and 3 is determined from the equation of continuity

$$\frac{p_{02} F_2 q(\lambda_2)}{\sqrt{T_{02}}} = \frac{p_{03} F_3 q(\lambda_3)}{\sqrt{T_{03}}}.$$

With the help of tables, hence we find

$$\epsilon = \frac{p_{03}}{p_{02}} = \frac{F_2 q(\lambda_2)}{F_3 q(\lambda_3)} = \frac{0.45 \cdot 0.7302}{0.3475} = 0.948.$$

In order to determine the change in the static pressure, it is necessary preliminarily to find the value of the velocity coefficient of the flow in the tube in front of the nozzle. Let us write the equation of the equality of the rate of air flow in cross sections 1 and 2, whereupon, taking into account that the length of section 1-2 is small, the contours of the nozzle are smooth and the flow is with acceleration, we consider the total pressure of the air in cross sections 1 and 2 to be identical. In this case the equation of continuity takes the form $F_1 q(\lambda_1) = F_2 q(\lambda_2)$. Hence we find $q(\lambda_1) = 0.45 \cdot 0.7309 = 0.329$, $\lambda_1 = 0.213$, $y(\lambda_1) = 0.338$. It is easy to see that similarly there can be obtained the result if between cross sections 1 and 2 there are losses of total pressure, being evaluated by the coefficient $\sigma = p_{02}/p_{01}$, the value of which is known. In this case we obtain

$$q(\lambda_1) = \frac{p_2}{p_1} q(\lambda_2).$$

A change in the static pressure on the entire section between cross sections 1 and 3 can be determined from the equation of continuity

$$\frac{\rho_1 F_1 y(\lambda_1)}{1 T_{01}} = \frac{\rho_3 F_3 y(\lambda_3)}{1 T_{03}}.$$

Since $T_{01} = T_{03}$ and $F_1 = F_3$, we have $p_3/p_1 = y(\lambda_1)/y(\lambda_3) = 0.338/0.358 = 0.944$.

Such a result can be obtained also from the relation

$$\frac{p_3}{p_1} = \frac{\rho_3}{\rho_1} \frac{\pi(\lambda_1)}{\pi(\lambda_3)} = \frac{\pi(\lambda_1)}{\pi(\lambda_3)}.$$

Since $\lambda_3 > \lambda_1$, i.e., $\pi(\lambda_3) < \pi(\lambda_1)$, hence it is apparent that as a result of an increase in the flow velocity in the tube a reduction in the static pressure here, as in other local resistances when $\lambda < 1$ and $F_3 = F_1$, is somewhat larger than a reduction in the total pressure. In this case, in view of the smallness of the velocity coefficients in the tube λ_1 and λ_3 , this distinction is small.

In the following example we will again return to the examination of the flow of the gas being preheated in the cylindrical channel. Unlike the analysis carried out in § 3 of Chapter V and in Example 7 of this section, we will examine the case where a *drop in pressures in the flow is assigned*. This determines a number of features of the flows which could not be revealed above, when it was assumed to be that a drop in the pressures is always sufficient for the maintaining of the assigned velocity coefficients at the beginning and end of the tube.

Example 10. The afterburner of a turbojet engine is a cylindrical tube installed after the turbine with a nozzle of variable area at the outlet (5.25). In the chamber there occurs the burning of the additionally injected fuel, in consequence of which the gas temperature is increased. Let the flow parameters of the gas at the inlet into the chamber be $p_{01} = 1.98 \text{ kg/cm}^2$, $T_{01} = 880^\circ \text{K}$, and $\lambda_1 = 0.4$. These values should be maintained constant independently of the value of preheating of the gas, otherwise the operating mode of the turbine and compressor will be changed.

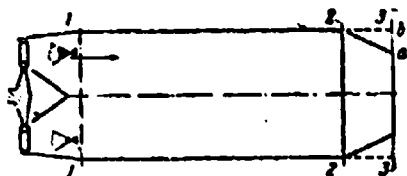


Fig. 5.25. Diagram of an afterburner of a turbojet engine: a - initial position of the nozzle, b - opened nozzle (Example 10).

Let us determine a maximally possible increase in gas temperature and the magnitude of losses of total pressure in the chamber in these conditions.

The assigned initial flow parameters determine the gas flow rate. As can be seen from the expression of the flow rate (109),

the more the stagnation temperature at chamber outlet, the larger, other conditions being equal, the cross-sectional area of the nozzle should be. Therefore, maximally possible preheating of the gas corresponds to the total opening of the nozzle.

Let us allow that the nozzle is made in such a way that with full expansion the area of its outlet section is equal to the area of the chamber, i.e., $F_3 = F_2 = F_1$ (position b on Fig. 5.25). The ratio of the total pressure at the inlet into the chamber to atmospheric pressure at the earth $\Pi_0 = p_{01}/p_H = 1.98/1.033 = 1.92$. This value somewhat exceeds the critical value (when $k = 1.33$), $\left(\frac{k+1}{2}\right)^{\frac{k}{k-1}} = 1.85$. Therefore, if the total pressure of the flow with preheating of the gas was maintained constant, then in the outlet section the rate of flow was equal to the speed of sound and $\lambda_3 = 1$. However, as we saw above (see Example 7), with the heat feed to the flow its total pressure is lowered, and therefore in this case it can be found that $p_{03}/p_H < 1.85$, and the discharge velocity will be subsonic.

In order to explain this, let us write the equation of the momentum of flow, expressing the momentum in cross section 1 in terms of the known total pressure p_{01} according to formula (119) and in cross section 3 - in terms of the static pressure p_3 (120), whereupon for the present we assume that the pressure p_3 is equal to the atmospheric pressure p_H , i.e., conditions of the outflow are subsonic. The wall friction and change in the adiabatic index are disregarded:

$$p_{01} F_1 f(\lambda_1) = p_H F_3 \frac{1}{f(\lambda_3)}.$$

Hence (when $k = 1.33$) we find

$$f(\lambda_1) = \frac{p_{01}}{p_H} = \frac{1.92}{1.98 \cdot 1.7822} = 0.583,$$

and, further, according to the tables $\lambda_3 = 0.91$, i.e., $\pi(\lambda_2) = 0.6048$, $f(\lambda_3) = 1.2525$, $z(\lambda_3) = 2.01$

Conditions of the outflow of gas will actually be subsonic, no matter how great the preheating in the chamber was: the assigned total pressure of the gas which is being lowered in the process of the heat feed is insufficient for the producing

of sonic velocity of outflow into the atmosphere. If the total pressure p_{01} was high, for example, $p_{01} = 2.4 \text{ kg/cm}^2$, then from the latter formula it would follow that $r(\lambda_3) = 0.398$; this value is less than the critical, since $r(1) = 0.429$. Consequently, at such a pressure the outflow conditions would be critical and $\lambda_2 = 1.0$.

The value found of the velocity coefficient of flow at nozzle outlet ($\lambda_2 < 1$ or $\lambda_3 = 1$) makes it possible to find all the flow parameters. For determining the gas temperature it is convenient to use, for example, the momentum equation (115), from which it follows that

$$T_{01} = T_{01} \left[\frac{r(\lambda_3)}{r(1)} \right]^2 = 890 \left(\frac{2.9}{2.01} \right)^2 = 1835 \text{ }^\circ\text{K}.$$

This is the limiting value of the stagnation temperature at the nozzle outlet. If we increase the preheating of the gas above this value, then the flow velocity at the inlet into the chamber will be lowered.

In order to determine the total pressure of the gas in the outlet section, in this case, it is possible to use the relation $p_{03} = p_H / \pi(\lambda_3) = 1.033 / 0.6048 = 1.71 \text{ kg/cm}^2$, which is correct when $\lambda_2 < 1$, i.e., when $p_3 = p_H$. By knowing p_{03} , we compute the coefficient of total pressure $\sigma = p_{03} / p_{01} = 1.71 / 1.98 = 0.865$.

To determine the changes in the total and static pressures in the process of preheating, it is possible to obtain simple relations, if we write the equality of the momenta of gas in the initial and final cross section in the form of

$$p_{01} F_1 f(\lambda_1) = p_{02} F_2 f(\lambda_2) \text{ and } p_1 F_1 \frac{1}{r(\lambda_1)} = p_2 F_2 \frac{1}{r(\lambda_2)}.$$

Hence we obtain

$$\sigma = \frac{p_{02}}{p_{01}} = \frac{f(\lambda_1)}{f(\lambda_2)}, \quad \frac{p_2}{p_1} = \frac{r(\lambda_1)}{r(\lambda_2)}.$$

These relations are valid in any flow conditions of the gas. Specifically, for conditions in this example we determine $\sigma = 1.0822/1.2525 = 0.865$.

The expressions obtained for σ and p_3/p_1 are convenient for the analysis of the nature of pressure change, determination of the maximum losses of total pressure and for obtaining certain other results found by a more complex means in § 3 of Chapter V.

Thus, for instance, from the equation for determining σ it follows that the preheating of the gas leads to a reduction in the total pressure both in subsonic and supersonic flows. Actually, since with preheating the value of the velocity coefficient always approaches unity (it increases when $\lambda < 1$ and decreases when $\lambda > 1$), then according to Fig. 5.22 the value of function $f(\lambda)$ in the process of preheating always increases, $f(\lambda_3) > f(\lambda_1)$ and $\sigma < 1$. Since in the region of subsonic velocities the limits of the change in value $f(\lambda)$ are small ($\sim 25\%$), then the coefficient of total pressure σ when $\lambda < 1$ cannot be lower than the certain limiting value

$$\sigma_{\min} = \frac{f(0)}{f(1)} = \frac{1.00}{1.2591} = 0.793 \quad (k = 1.33).$$

In supersonic flow, according to Fig. 5.22, any values of the coefficient of total pressure ($0 < \sigma < 1$) are possible.

On the other hand, with respect to a change in function value $r(\lambda)$, it is possible to establish the nature of a change in the static pressure in the flow of the preheated gas. At the subsonic velocity, when the velocity coefficient with the preheating of the gas increases, we have (see Fig. 5.22) $r(\lambda_3) < r(\lambda_1)$ or $p_3 < p_1$, i.e., the static pressure in the flow decreases. A maximum change in the static pressure, obviously, is equal to

$$\frac{r(1)}{r(0)} = \frac{1}{k+1}.$$

In supersonic flow, when $\lambda_3 < \lambda_1$, we have $r(\lambda_3) > r(\lambda_1)$ or $p_{03} > p_{01}$.

Thus, with the preheating of the supersonic flow, in place of the reduction in total pressure, the static pressure increases as a result of a decrease in the velocity coefficient of the flow.

What will occur, if while maintaining the assigned pressure ratio p_{01}/p_{02} , we increase the gas temperature above the value obtained above $T_{02} = 1835^\circ$, i.e., increase the preheating?

Being diverted from the examination of the acting drop in pressure, on the basis of the formula derived in Example 7, it would be possible to arrive at the conclusion that since $\lambda_1 < 1$ and $\lambda_2 < 1$, then with an increase in the preheating the velocity coefficient λ_2 will increase, approaching $\lambda = 1$. However, this will be incorrect, since when using this formula always it is necessary to keep in mind that the results obtained from it are valid only under the condition of the sufficiency of the pressure drops acting on the flow; the more the preheating, the greater the pressure ratio p_{01}/p_{02} should be. This was repeatedly indicated above in solving the problems.

Actually, in this case when $p_{01} = \text{const}$ with an increase in preheating the losses of total pressure of gas increase and the total pressure of the gas in the outlet section of the tube is lowered, in consequence of which there is a decrease in the velocity coefficient λ_3 , which depends only on the ratio of the total and static pressures in the flow:

$$\lambda^2(\lambda) = p_t/p_{0t} = p_{0t}/p_{01}.$$

Thus, if $p_{01}/p_{02} = \text{const}$, then with an increase in the preheating, when value λ is lowered, the value of the velocity coefficient at the outlet (tube) does not increase but decreases. The velocity coefficient of the flow at the inlet into the tube simultaneously decreases.

In order to determine the actual values of the velocity coefficients at the inlet and outlet with the assigned magnitudes of preheating T_{03}/T_{01} and drop in pressures between the inlet and output section, it is necessary to find the *joint solutions* of the equation (see Example 7)

$$z(0) = z(1) \sqrt{\frac{T_{01}}{T_{02}}}$$

from one of the following equations which express the constancy of the assigned drop in pressures, for example:

$$\frac{p_{01}}{p_{02}} = \frac{f(0)}{f(1)} = \text{const} \quad \text{or} \quad \frac{p_{01}}{p_{02}} = \frac{q(0)}{q(1)} \sqrt{\frac{T_{01}}{T_{02}}} = \text{const},$$

if the ratio of total pressures is assigned;

$$\frac{p_1}{p_2} = \frac{r(0)}{r(1)} = \text{const} \quad \text{or} \quad \frac{p_1}{p_2} = \frac{y(0)}{y(1)} \sqrt{\frac{T_{01}}{T_{02}}} = \text{const},$$

if the ratio of static pressures is assigned;

$$\frac{p_{01}}{p_1} = \frac{1}{r(0) \cdot f(0)} = \text{const} \quad \text{or} \quad \frac{p_{01}}{p_1} = \frac{y(0)}{q(0)} \sqrt{\frac{T_{01}}{T_{02}}} = \text{const},$$

if the ratio of the total pressure at the inlet to the static pressure at the outlet from the tube (available pressure ratio) is assigned. The latter case is encountered most frequently. The joint solution of the equations is most conveniently conducted by the graphic method with the aid of tables of gas-dynamic functions.

Common in the examples examined above of the gas flow was the fact that the flow velocity was directed along the axis of the channel.

In a number of problems of applied gas dynamics it is necessary to calculate such flows in which the *vector of absolute gas velocity comprises a certain angle with the axis of the flow*. Besides the axial velocity w_a , which determines the gas flow rate

and momentum along the axis of the flow, here there are velocity components in the plane perpendicular to the axis - radial w_r or circular w_t velocity of the particles of gas. Serving as an example can be the flow of twisted gas in the annular channel, which is encountered in different vortex apparatuses (circular component), or the expansion of the supersonic gas jet escaping into the atmosphere with a large excess pressure (radial component).

If the gas parameters in the flow cross section can be assumed to be constant, then for calculating such flows methods and formulas given in this section can be used.

At first glance it can be shown that for this it suffices in all the derived relations to take only the axial component of velocity into consideration. This, however, is not so, since at the assigned stagnation conditions the value of the temperature, static pressure, and gas density will also depend on the value of the circular (radial) velocity component; changes in the latter will affect the rate of discharge and momentum of flow. The fact is that according to the equation of energy and the relations (101), (102) and (103) obtained from it, the connection between the parameters in the flow and stagnation parameters is determined by a change in the absolute velocity (or the velocity coefficient calculated according to the absolute velocity and total stagnation temperature), independently of the angle being composed by the velocity vector with the axis.

Let us show how to generalize the relations obtained above for the case of motion from the tangential (radial) velocity component. Let us examine the one-dimensional flow of gas with the stagnation parameters p_0 and T_0 and the absolute velocity w making up the angle α with the axis of the flow. The gas flow rate per second through the cross section of area F , perpendicular to the axis, is equal to

$$Q = \gamma F w_\alpha = \gamma F w \cos \alpha.$$

where w_a is the axial component of the gas velocity. In the same way as in the derivation of formula (109), hence it is possible to obtain

$$Q = \frac{p_0}{kT_0} \left(1 - \frac{k-1}{k+1} \lambda^2\right)^{\frac{1}{k-1}} F \lambda a_{*p} \cos \alpha = m \frac{p_0 F q(\lambda)}{\sqrt{T_0}} \cos \alpha,$$

where

$$\lambda = \frac{w}{a_{*p}} = \frac{w}{\sqrt{2g \frac{k}{k+1} RT_0}}.$$

The latter relation can be rewritten in the form

$$Q = m \frac{p_0 F q(\lambda, \alpha)}{\sqrt{T_0}}, \quad (123)$$

where

$$q(\lambda, \alpha) = q(\lambda) \cos \alpha \quad (124)$$

is the gas-dynamic function $q(\lambda)$, generalized for the case of the flow of gas with the velocity component in the plane perpendicular to the axis. In exactly the same manner it is possible to obtain the formula similar to (111)

$$Q = m \frac{p_0 F y(\lambda, \alpha)}{\sqrt{T_0}}, \quad (125)$$

where

$$y(\lambda, \alpha) = y(\lambda) \cos \alpha \quad (126)$$

Thus, if angle α is assigned, then for the calculation of the gas flow rate and compilation of the equations of continuity, the same formulas as when $\alpha = 0$ are used, since the generalized functions $q(\lambda, \alpha)$ and $y(\lambda, \alpha)$ are determined from angle α and from values $q(\lambda)$ and $y(\lambda)$ for the velocity coefficient in the absolute flow of the gas.

The momentum of the flow of gas in the direction of the axis

$$I = \frac{Q}{g} w_a + pF = \frac{Q}{g} w \cos \alpha + pF.$$

By converting this expression similar to the way in which this was done in the solution of formula (115), we have

$$I = \frac{G}{g} \left(\omega \cos \alpha + \frac{p g}{\gamma \omega \cos \alpha} \right) = \frac{G}{g} \left[\lambda a_{sp} \cos \alpha + \frac{RT_0 g}{\lambda a_{sp} \cos \alpha} \left(1 - \frac{k-1}{k+1} \lambda^2 \right) \right]$$

or after the simplifications

$$I = \frac{k+1}{2k} \frac{G}{g} a_{sp} z(\lambda, \alpha), \quad (127)$$

where

$$z(\lambda, \alpha) = \frac{1}{\cos \alpha} \left[\left(\frac{2k}{k+1} \cos^2 \alpha - \frac{k-1}{k+1} \right) \lambda + \frac{1}{\lambda} \right]. \quad (128)$$

Expression (127) is similar to the expression obtained when $\alpha = 0$ but contains instead of $z(\lambda)$ the generalized function $z(\lambda, \alpha)$, the graph of which is given on Fig. 5.26. When $\alpha = 0$ function $z(\lambda, \alpha)$ is reduced to $z(\lambda) = \lambda + 1/\lambda$; the minimum value of it $z(\lambda) = 2$ corresponds $\lambda = 1$. When $\alpha \neq 0$ the minimum values of function $z(\lambda, \alpha)$ are less than two, whereupon with an increase in angle α the minimums of the curves are displaced into the region of supersonic velocity.

For the conducting of numerical calculations, it is possible to compile tables of function $z(\lambda, \alpha)$ or a grid of curves more detailed than on Fig. 5.26, at different values of α (see the graph in the appendix).

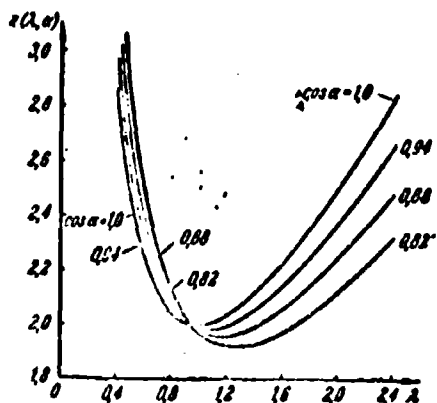


Fig. 5.26. Graph function $z(\lambda, \alpha)$.

Formulas (123) and (127) make it possible to establish the nature of a density change of the current, cross-sectional area, specific impulse and other values which characterize the gas flow, depending on the velocity coefficient λ and angle α between the velocity vector and the axis. However, here we will not discuss this.

When using generalized functions $q(\lambda, \alpha)$, $y(\lambda, \alpha)$, $z(\lambda, \alpha)$ and their combinations, all the equations obtained in this section can be used for calculating flows with a circular or radial component of velocity.

Example 11. The twisted flow of gas moves in the annular channel between two cylindrical surfaces (Fig. 5.27). The velocity coefficient of the flow at the channel inlet $\lambda_1 = 0.85$, and the direction of absolute velocity is assigned by angle $\alpha_1 = 30^\circ$ to the axis of the channel. With channel flow the stagnation temperature of the gas is reduced from 900° to 700°K as a result of the thermal conductivity through the walls into the environment. Disregarding the friction and also a change in the parameters on the radius of the channel, determine the parameters of the gas at outlet from the channel. The adiabatic index $k = 1.40$.

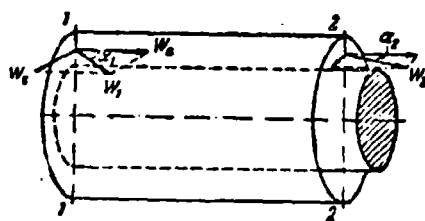


Fig. 5.27. Twisted gas flow in the annular channel (Example 11).

As above, in the examination of flow in the cylindrical channel with the heat feed, we obtain the fundamental equation from the condition of the constancy of the momentum of gas in cross sections of the channel. In this case this condition takes the form

$$\frac{Q}{g} \rho_{sp, 1} z(\lambda_1, \alpha_1) = \frac{Q}{g} \rho_{sp, 2} z(\lambda_2, \alpha_2)$$

or

$$z(\lambda_2, \alpha_2) = z(\lambda_1, \alpha_1) \sqrt{\frac{T_{01}}{T_{02}}}$$

By substituting the assigned values of the stagnation temperatures and the value of function $z(\lambda_1, \alpha_1) = 2.055$ (see Fig. 5.26), we obtain

$$z(\lambda_2, \alpha_2) = 2.33$$

This value of the function can correspond, generally speaking, to different combinations of values λ_2 and α_2 , and therefore for determining these values we use the condition of the constancy of the moment of momentum (see § 6 of Chapter 1). Since the mean radius of the channel does not change and there are no moments of applied forces, then in the flow, independently of the occurring processes, the circular velocity component should be constant. Therefore,

$$w_{\theta 1} = w_{\theta 2} \quad \text{or} \quad \lambda_2 \sigma_{sp2} \sin \alpha_2 = \lambda_1 \sigma_{sp1} \sin \alpha_1$$

Hence we determine

$$\lambda_2 \sin \alpha_2 = \lambda_1 \sin \alpha_1 \sqrt{\frac{T_{01}}{T_{02}}} = 0.85 \cdot 0.5 \sqrt{\frac{800}{700}} = 0.482$$

The joint solution of the two obtained equations is most conveniently carried out graphically. Being given a number of values of angle α_2 , we find the values of the velocity coefficient $\lambda_2 = 0.482 / \sin \alpha_2$ corresponding to them; substituting these values α_2 and λ_2 into $z(\lambda, \alpha)$, we plot the graph of this function. The point of curve where $z(\lambda, \alpha) = 2.33$ corresponds to values of parameters in the outlet section of the channel, and in this case we find $\lambda_2 = 0.72$, $\alpha_2 = 42^\circ$. In the calculations it is possible also to use an auxiliary graph or tables of function $z(\lambda, \alpha)$.

The condition of the retention of the gas flow rate in cross sections 1 and 2, when using expression (123), makes it possible to determine the ratio of total pressures of the gas - the coefficient of total pressure:

$$\sigma = \frac{p_{02}}{p_{01}} = \frac{q(\lambda_1) \cos \alpha_1}{q(\lambda_2) \cos \alpha_2} \sqrt{\frac{T_{01}}{T_{02}}} = \frac{0.9729 \cdot 0.865}{0.9061 \cdot 0.743} \sqrt{\frac{800}{700}} = 1.10$$

(cooling of the flow is accompanied by an increase in the total pressure).

A change in the static pressure is easy to determine from the relation

$$\frac{p_1}{p_0} = \frac{p_{01} \pi(\lambda_1)}{p_{01} \pi(\lambda_0)} = 1,10 \cdot \frac{0,7289}{0,6382} = 1,233$$

or from the equation of the equality of the flow rates recorded in form (125).

In conclusion let us list the introduced gas-dynamic functions and the relationships between them:

1. The simplest functions which express the relationship between the gas parameters in the flow and stagnation parameters:

$$\begin{aligned} \tau(\lambda) &= 1 - \frac{k-1}{k+1} \lambda^2; & \pi(\lambda) &= \left(1 - \frac{k-1}{k+1} \lambda^2\right)^{\frac{k}{k-1}}; \\ s(\lambda) &= \left(1 - \frac{k-1}{k+1} \lambda^2\right)^{\frac{1}{k-1}}; \end{aligned}$$

in this case

$$\pi(\lambda) = \tau(\lambda) s(\lambda)$$

2. The functions which make it possible to express the gas flow rate by the total pressure

$$q(\lambda) = C \lambda s(\lambda)$$

or by the static pressure

$$y(\lambda) = \frac{q(\lambda)}{\tau(\lambda)} = C \frac{\lambda}{\tau(\lambda)}.$$

By means of these functions we obtain the two expressions for the gas flow rate

$$G = m \frac{p_0 F y(\lambda)}{\sqrt{T_0}} = m \frac{p F q(\lambda)}{\sqrt{T_0}};$$

3. The function

$$z(\lambda) = \lambda + \frac{1}{\lambda},$$

with the aid of which the momentum of the gas flow can be represented in the form of the product of the stagnation temperature (critical speed of sound) by the gas flow rate

$$I = \frac{Q}{g} w + pF = \frac{k+1}{2k} \frac{Q}{g} a_{cr} z(\lambda).$$

4. Functions $f(\lambda)$, $r(\lambda)$, with the aid of which the momentum of the gas flow is expressed in terms of the total or static pressure:

$$f(\lambda) = \frac{1}{C} q(\lambda) z(\lambda), \quad r(\lambda) = C \frac{1}{y(\lambda) z(\lambda)}.$$

Correspondingly we obtain two expressions for the momentum of the gas flow:

$$I = p_0 F f(\lambda) = \frac{p_0 F}{r(\lambda)}.$$

The constant which enters into the expressions for functions $q(\lambda)$, $y(\lambda)$, $f(\lambda)$, and $r(\lambda)$

$$C = \frac{1}{\sqrt{11}} = \left(\frac{k+1}{2} \right)^{\frac{1}{k-1}}.$$

is equal to 1.577 for $k = 1.4$ and 1.588 for $k = 1.33$.

5. Functions $q(\lambda, \alpha)$, $y(\lambda, \alpha)$ and $z(\lambda, \alpha)$, which make it possible to propagate the methods examined above and design formulas for the case of gas flow from the circular or radial component velocity.

6. In the solution of some problems derivatives of different gas-dynamic functions are also used. By means of differentiation and simple transformations, it is possible to obtain their expressions in terms of initial functions.

For example,

$$\frac{dz(l)}{d\lambda} = -k \left(\frac{2}{k+1} \right)^{\frac{k}{k-1}} q(l),$$

$$\frac{dq(l)}{d\lambda} = q(l) \left[\frac{1}{\lambda} - \left(\frac{2}{k+1} \right)^{\frac{k}{k-1}} j(l) \right] \text{ and so on.}$$

What is the meaning of simplifications being obtained in the recording of fundamental equations with the aid of gas-dynamic functions?

As can be seen from the examples given above, the major advantage of the expressions obtained here is that they contain such flow parameters the nature of change in which can be easily established from conditions of the problem, for example, the constancy of stagnation temperature T_0 in adiabatic flows and an increase in T_0 with the heat feed, the retention of total pressure p_0 in the isentropic flow and a drop p_0 in the presence of losses, and so on. By the selection of the corresponding expression for the flow rate or momentum, it is possible to reduce to a minimum a number of unknown parameters in the fundamental equations. In this case it is frequently possible to find the unknown values directly from the initial equations, avoiding the bulky transformations.

Let us note some general rules which are useful in the solution of equations in general form and calculations with the aid of tables of gas-dynamic functions.

In all cases when the general or numerical expression of the value of the velocity coefficient λ or any one of its functions are obtained, it is possible to consider that all the gas-dynamic functions and coefficient λ (from the tables or graphs) are known. This is the basic condition in the simplification of the calculations, since it eliminates the need for obtaining in explicit form the dependences between λ and its functions. In the numerical calculations one should consider that functions $\tau(\lambda)$,

$\pi(\lambda)$ and $\varepsilon(\lambda)$ in the region of low velocities and function $q(\lambda)$, $z(\lambda)$ and $f(\lambda)$ at sonic speeds are changed very little with a change in value λ . Therefore, in the indicated regions an insignificant error in the value of the functions, can lead to a great error in the calculation of the velocity coefficient λ . Such calculations should be avoided, and as far as possible, in these cases, other equations which include, for example, functions, $y(\lambda)$ and $r(\lambda)$ should be used. If this for any reason is impossible, then it is necessary to conduct all preliminary calculations with a high degree of accuracy. It is understandable that in these regions it is not recommended to determine λ according to the indicated functions by means of graphs. In particular, this is related to function $z(\lambda)$, which over wide limits of the change in λ (from 0.65 to 1.55) varies in value by a total of 10%. Therefore, for the determination of λ in terms of the value of function $z(\lambda)$ in the region of sonic speeds, it is possible to calculate the possible values of λ directly from the equation

$$\lambda + \frac{1}{\lambda} = z(\lambda)$$

whence

$$\lambda = \frac{z(0) \pm \sqrt{z^2(0) - 4}}{2} = \frac{2}{z(0) \mp \sqrt{z^2(0) - 4}}.$$

In order to avoid the error connected with the subtraction of close values, the supersonic solution is located by the first and the subsonic solution by the second of these expressions.

From the examples examined in this section, it is possible to see the efficiency of the method of calculation with the use of gas-dynamic functions in the solution of sufficiently complex problems which are of practical use.

§ 7. Gas Flow with Friction in the Cylindrical Tube with the Assigned Magnitude of the Ratio of Pressures at Inlet and Outlet

Using the relations derived in the foregoing section let additionally explain some laws governing the one-dimensional gas flow in a cylindrical tube with friction. In §§ 1 and 2 it was established that the friction leads to an increase in the velocity of subsonic flow and a decrease in the velocity of supersonic flow, whereupon in both cases the maximum conditions correspond to the critical velocity in the outlet section of the tube.

The results obtained in § 2 are valid, however, only when the velocity coefficient at the inlet into the tube λ_1 is maintained constant, which requires the creation of a *quite definite drop in the pressures in the flow* for each mode and each value of the normalized length of the tube. In actuality, most frequently it is the opposite: the assigned value is the drop in pressures between the inlet and outlet sections of the tube, and values of the velocity, flow rate and other flow parameters are determined by the acting drop in pressures and by the resistance in the section of the tube in question. For flow in the inlet of the tube the most characteristic value, which is usually known or can be easily determined, is the total pressure p_{01} ; for the characteristic of flow at the outlet from the tube, it is important to know the static pressure in the environment or reservoir where the gas escapes from the tube p_H . If the flow velocity in the outlet section is less than the speed of sound, then static pressure of the flow, as is known, is equal to the external pressure, i.e., $p_2 = p_H$. If $\lambda_2 = 1$, then in the outlet section of the tube $p_2 \geq p_H$. Finally, when $\lambda_2 > 1$ also conditions when $p_2 < p_H$ are possible.

Let us call the value $\Pi_0 = p_{01}/p_H$ the available pressure ratio. The flow parameters in the cylindrical tube defined basically by

the value of the available pressure ratio Π_0 : the process is actually as though it were an outflow of gas from the vessel with pressure p_{01} into a medium with pressure p_H through the channel with the assigned resistance. Therefore, in the examination of the law governing flow with friction, it is necessary to consider the value of the available pressure ratio in the flow; without this the obtained results can prove to be unreal.

Let us assume, for example, that at subsonic velocity at the inlet into the tube the available pressure ratio Π_0 is less than the critical pressure ratio

$$\Pi_{cr} = \frac{1}{\pi(\lambda)} = \left(\frac{\lambda+1}{2}\right)^{\frac{\lambda}{\lambda-1}};$$

for air $\Pi_{cr} = 1.893$. Due to friction the total pressure of the flow along the length of the tube is decreased, and therefore in the outlet section of the tube $p_{02}/p_H < p_{01}/p_H < 1.893$. This means that the flow escapes from the tube under the action of the subcritical pressure ratio, and, consequently, the velocity of such a flow will always be subsonic. No matter how much it is possible to increase the normalized length of the tube it is impossible to obtain value $\lambda_2 = 1$: the drop in the pressures acting in the flow is insufficient for producing the sonic speed of outflow at the outlet from the tube.

Thus, the conclusion obtained previously that with an increase in the normalized length of the tube up to the maximum (critical) value, the flow velocity at outlet from the tube reaches the speed of sound and is valid only in such a case when a sufficient (depending on values λ_1 and χ) pressure ratio Π_0 is provided.

Let us show how the calculation of flow parameters with flow in the tube with friction is produced if $\lambda_1 < 1$ and the value of the available pressure ratio is assigned.

Let us write the equation of continuity for flow in the tube, whereupon flow rate in the inlet section is expressed with the aid of formula (109) in terms of the total pressure, and the flow rate in the exit section is expressed by the static pressure with the aid of formula (111)

$$\frac{p_{01} F_1 q(\lambda_1)}{\sqrt{T_{01}}} = \frac{p_2 F_2 y(\lambda_2)}{\sqrt{T_{01}}}.$$

Since for the adiabatic flow in a cylindrical tube $T_{02} = T_{01}$ and $F_2 = F_1$, then hence it follows that

$$y(\lambda_2) = \frac{p_{01}}{p_2} q(\lambda_1).$$

If $\lambda_2 < 1$, then, as was noted, $p_2 = p_H$ or

$$y(\lambda_2) = \Pi_0 q(\lambda_1) \quad (129)$$

Equation (129), which mutually connects values of the velocity coefficients in the inlet and outlet sections of the tube at the assigned value Π_0 and $\lambda_1 < 1$, is correct without depending on the flow pattern and length of the tube. On the other hand, the change in parameters of the gas in the tube is determined by the value of the coefficient of friction and by the length of the tube. Earlier in § 2 the formula describing the change in the flow parameters as a result of the friction was obtained:

$$\gamma(\lambda_1) - \gamma(\lambda_2) = \chi, \quad (130)$$

where $\chi = \frac{2k}{k+1} \epsilon \frac{x}{D}$ is the normalized length of the tube. Equation (130) establishes the dependence between the velocity coefficients λ_1 and λ_2 of the assigned value χ . Equations (129) and (130) can be considered as the system of two equations with two unknowns, the roots of which determine values λ_1 and λ_2 as a function of the assigned values Π_0 and χ . By these values of the velocity coefficients is determined the real flow conditions of the gas through the tube with the assigned normalized length χ under the action of the available end pressures Π_0 .

Let us examine some of the following properties of the flow at subsonic speed of the flow at the inlet into the tube. In the first place let us compare the one-dimensional subsonic gas flow in the tube in the presence of friction with an ideal flow with the identical available pressure ratio Π_0 . A change in the gas parameters along the length of the tube is connected with friction, and therefore in an ideal flow, when $p_{02} = p_{01}$, the gas parameters are constant in all the cross sections of the tube. The velocity coefficient in the outlet section $\lambda_2 = \lambda_1 < 1$, which in an ideal case is determined by the value of the available pressure ratio $\pi(\lambda_2) = 1/\Pi_0$ is more than that during flow with friction, when $p_{02} < p_{01}$, and $\pi(\lambda_2) = 1/\sigma\Pi_0$. The more the normalized length of the tube, the larger will be the total losses of pressure and the less will be the flow velocity at the outlet from the tube as compared with the velocity in the ideal case of the flow. Thus, it is necessary to keep in mind that, although with flow in the tube with friction *the velocity of the flow along the length of the tube increases*, its greatest value, the outlet velocity, always *remains less than that with the same pressure ratio Π_0 in the case of the flow without friction* (for example, a very short tube, when $\chi \approx 0$). The more the normalized length of the tube, the less (at given Π_0) the flow velocity both at the outlet and inlet.

It is interesting to note that if $\Pi_0 = \text{const}$, then when $\lambda_2 < 1$ the change in the normalized length of the tube χ always leads to a change in the inlet velocity of the tube, independently of the larger or smaller value χ of its critical value for the given $\lambda_1 < 1$. The retention of $\lambda_1 = \text{const}$ with a change in the normalized length of the tube and $\lambda_2 < 1$ requires a corresponding change in value in the available pressure ratio: the longer the tube, the larger the value Π_0 necessary for maintaining the assigned conditions at the inlet, i.e., the retention of the gas flow rate.

On the other hand, if at the assigned length of the tube ($\chi = \text{const}$) we increase the pressure ratio Π_0 , then the velocities at both the inlet and at outlet will increase until the value λ_2 reaches the critical value $\lambda_2 = 1$. A further increase in Π_0 changes neither λ_1 nor λ_2 ; however, in the outlet section of the tube a surplus pressure in comparison with the environment (reservoir) will be established. For these conditions equation (129) is incorrect, since with its derivation it was assumed that $p_2 = p_H$; the relation between the flow parameters is determined only by equation (130). From the continuity condition it is possible only to find the minimum required value Π_0 at which the mode with $\lambda_2 = 1$ and assigned value λ_1 is established, since according to equation (129)

$$\Pi_{0, \min} = \frac{q(\lambda_1)}{q(\lambda_2)} = \left(\frac{\lambda_1 + 1}{2}\right)^{\frac{k}{k-1}} \frac{1}{q(\lambda_1)} = \frac{\Pi_{kp}}{q(\lambda_1)}.$$

Since $q(\lambda_1) < 1$, from the latter relation it is evident that with flow in the tube with friction the critical outlet velocity is established with the pressure ratio of $\Pi_0 > \Pi_{kp}$, where the Π_{kp} is the pressure ratio necessary for obtaining $\lambda = 1$ during flow without friction. The conditions $\lambda_2 = 1$ for this value λ_1 begins with an increase in the normalized length χ up to the value

$$\chi = \chi_{kp} = \varphi(\lambda_1) - 1, \quad (131)$$

and in this case condition $\Pi_0 \geq \Pi_{0, \min}$ should be observed.

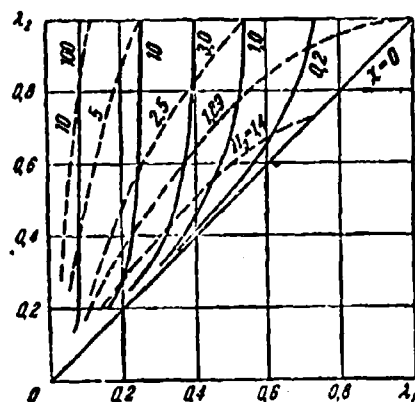


Fig. 5.28. Relationship between parameters of subsonic flow at the inlet and outlet sections of the cylindrical tube in the presence of friction.

Figure 5.28 gives results of the calculations of subsonic flow in the tube with friction. The graph illustrates the basic regularities of the flow given above and, in particular, shows that

a) when $\lambda_1 = \text{const}$ with an increase in the normalized length χ value λ_2 increases, whereupon always $\lambda_1 < \lambda_2 \leq 1$;

b) at a constant available pressure ratio Π_0 , with an increase in χ , value λ_1 is always decreased; λ_2 is decreased also, if $\lambda_2 < 1$;

c) for each value of the normalized length χ there is a completely defined value of the pressure ratio $p_{01}/p_H = \Pi_0$, which corresponds to the assigned flow velocity at the outlet and inlet into tube, respectively;

d) the limiting value λ_1 , which corresponds to $\lambda_2 = 1$, for each value χ is established with the defined value, which is increased with an increase in χ of the value of the pressure ratio and does not increase with a further increase in Π_0 .

Let us now examine the features of flow with friction with supersonic velocity at the inlet into the tube. From formula (130) it follows that if the normalized length of the tube is less than the critical value, determined for the given value of $\lambda_1 > 1$ by formula (131), then along the length of the tube the flow velocity will decrease, remaining supersonic. At the outlet from the tube with continuous braking of the flow, $\lambda_2 > 1$ will be obtained. At a certain value of the normalized length of the tube, called the critical from equation (130), it follows that $\phi(\lambda_2) = 1$, i.e., $\lambda_2 = 1$. This length corresponds to the maximally possible flow conditions with a continuous change in velocity from the assigned value $\lambda_1 > 1$ to $\lambda_2 = 1$. If $\chi > \chi_{HP}$, then the continuous braking of flow in the tube is impossible. In this case equation (130), which describes the flow with a continuous

velocity change, does not have solutions for λ_2 , since from it $\phi(\lambda_2) < 1$ follows. In actuality, here in the initial section of the tube the supersonic flow is braked to a certain value $\lambda' > 1$, and then in the tube there appears a shock wave, behind which subsonic flow is established with an increase in the velocity along the length of the tube from value λ'' (after the shock) to $\lambda_2 \leq 1$, as was noted above.

The location of the shock and relative length of the supersonic and subsonic sections of the flow, depending on the assigned parameters, can be determined in the following manner. Let us designate the normalized length of the tube from its beginning up to the shock wave (supersonic section of the flow)

$$\chi_1 = \frac{2\lambda}{\lambda + 1} \zeta \frac{r_1}{D}.$$

Let us write equation (130) for sections with a continuous velocity change, i.e., separately for the supersonic and subsonic sections:

$$\zeta(\lambda_1) - \zeta(\lambda') = \chi_1, \quad (132)$$

$$\zeta(\lambda'') - \zeta(\lambda_2) = \chi - \chi_1. \quad (133)$$

Let us make a term-by-term summation of equations (132) and (133), assuming in this case that the shock wave is normal, and therefore the relation $\lambda'' = 1/\lambda'$ is correct. As a result we obtain

$$\zeta(\lambda_1) - \zeta(\lambda_2) + \zeta\left(\frac{1}{\lambda'}\right) - \zeta(\lambda) = \chi.$$

Let us denote

$$\Phi(\lambda) = \zeta\left(\frac{1}{\lambda}\right) - \zeta(\lambda) = \lambda^2 - \frac{1}{\lambda^2} - 4 \ln \lambda. \quad (134)$$

Then the latter equation can be written in the form

$$\Phi(\lambda) = \chi - \zeta(\lambda_1) + \zeta(\lambda_2). \quad (135)$$

Figure 5.29 gives auxiliary graph for determining the function $\Phi(\lambda)$ from value λ . Relation (135) establishes the relationship

between the parameters of flow, which moves with friction in the tube with normalized length χ when in the tube a normal shock wave appears.

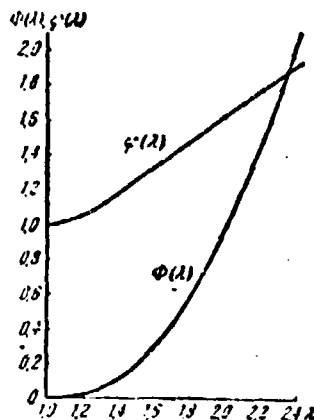


Fig. 5.29. Auxiliary graphs of functions $\phi(\lambda)$ and $\phi(\lambda')$ in the region of supersonic flow velocities

$$\begin{aligned}\phi(\lambda) &= \frac{1}{\lambda^2} + 2 \ln \lambda, \quad \phi(\lambda') = \\ &= \lambda'^2 - \frac{1}{\lambda'^2} - 4 \ln \lambda.\end{aligned}$$

Entering into formula (135), besides the known values of χ and λ_1 , is also the thus far unknown value of the velocity coefficient at the outlet from the tube λ_2 . Since after the shock the flow is subsonic, then for determining λ_2 let us use the equation of continuity

$$y(\lambda_2) = \pi_0 q(\lambda_2)$$

which is correct both when $\lambda_1 < 1$ and when $\lambda_1 > 1$. If from this equation it follows that $y(\lambda_2) \geq y(1)$, then $\lambda_2 = 1$ at $y(\lambda_2) < y(1)$ and $\lambda_2 < 1$. Substituting value $\lambda_2 \leq 1$ thus found into equation (135), let us determine $\phi(\lambda')$. Further according to the graph (Fig. 5.29) we find values λ' and $\phi(\lambda')$, and, after using equation (132), we compute the value χ_1 - the normalized length of the tube necessary for the shock-free supersonic flow from λ_1 to λ' . The value χ_1 determines the location of the shock along the length of the tube, since when $\zeta = \text{const}$ we have $\chi_1/\chi = \chi_1/\chi$.

With the critical flow conditions at the outlet from the tube, when $\lambda_2 = 1$, the result of the calculation, as it is easy to see,

does not depend on Π_0 : a shock appears in the definite cross section of the tube independently of the value of the available pressure ratio. The calculation according to formulas (129), (132) and (135) shows that when $\lambda_2 < 1$ the shock wave with a decrease in Π_0 will be moved from its end position, which corresponds to $\lambda_2 = 1$, to the inlet section of the tube. The minimum value of the available pressure ratio, at which the flow with the assigned initial velocity coefficient $\lambda_1 > 1$ is possible, is determined by the fact that the shock wave, in moving upstream, will approach directly to the inlet section.

Let us give an example of the calculation of flow with a shock wave within the tube. Let us assume that the velocity coefficient at the inlet into the tube $\lambda_1 = 1.8$ and the total normalized length of the tube $\chi = 0.6$ are assigned (at standard values of the coefficient of friction this corresponds approximately to 30 calibers of the tube). The available ratio of total pressure of the flow at the inlet into the tube to the static pressure in the reservoir, where the gas escapes from the tube, is $\Pi_0 = 3.0$.

The critical value of the normalized length of the tube for the assigned value λ_1 is determined:

$$\chi_{cr} = \varphi(\lambda_1) = 1.1 = 0.485$$

(we find value $\varphi(\lambda_1)$ from the auxiliary graph of Fig. 5.29). Since the assigned normalized length of the tube $\chi = 0.6$ is more than the critical value, then, as was noted, the continuous braking of the flow is impossible, and a shock wave appears in the tube.

Let us determine the velocity coefficient of the flow at the outlet from the tube with the aid of equation (129):

$$y(\lambda_2) = \Pi_0 q(\lambda_2) = 3.0, 0.075 = 1.222 \quad \text{or} \quad \lambda_2 = 0.71.$$

Further we substitute the obtained values of λ_2 and the assigned values of λ_1 and χ into equation (135), which determines the velocity

coefficient of the flow in front of the shock $\phi(\lambda') = 0.6 + 1.25 - 1.485 = 0.365$. From the graph on Fig. 5.29 we find that this value $\phi(\lambda')$ corresponds to $\lambda' = 1.66$ and $\phi(\lambda') = 1.375$. We determine the normalized length of the supersonic section of flow according to formula (132)

$$\lambda_1 = \tau(\lambda_1) - \tau(\lambda') = 1.485 - 1.375 = 0.11$$

and find the distance from the inlet into the tube in front of the cross section where the shock wave appears (when $\zeta = \text{const}$):

$$\frac{x_1}{x} = \frac{\lambda_1}{\lambda} = \frac{0.11}{0.6} = 0.184.$$

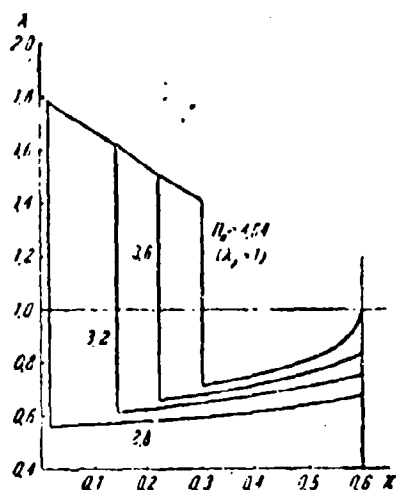


Fig. 5.30. The possible conditions of supersonic flow in a cylindrical tube with friction with the length of the tube greater than the critical value. $\lambda_1 = 1.8$; $\lambda = 0.6$ (example of the calculation)

Thus, at a length of approximately 18% of the total length of the tube, the supersonic flow under the action of friction is slowed down from $\lambda_1 = 1.8$ to $\lambda' = 1.66$, and then in the shock the velocity falls to $\lambda'' = 0.6$; in the remaining part of the tube the subsonic flow is accelerated to $\lambda_2 = 0.71$ and escapes from the tube, having a static pressure equal to the pressure in the reservoir p_H .

At other values of the available pressure ratio, the position of the shock will be different. Figure 5.30 gives results of the calculation according to the given method at different values of Π_0 . The

maximally possible conditions are determined, on one hand, by the achievement of critical velocity at the outlet from the tube (during the calculation we assume that $\lambda_2 = 1$ and find the most remote shock-wave position) from the inlet, and on the other hand,

by the emergence of a shock wave directly behind the inlet section of the tube. In this case ($\lambda_1 = 1.8$, $\chi = 0.6$) the critical flow conditions at the outlet is obtained when $\Pi_0 = y(1)/q(\lambda_1) = 1.893/0.4075 = 4.64$.

According to formulas (135) and (132), by means of the graph on Fig. 5.29, we find $\phi(\lambda') = 0.6 + 1 - 1.485 = 0.115$, $\lambda' = 1.41$, and $\phi(\lambda') = 1.185$. We further have $x_1 - 1.485 - 1.185 = 0.3$, and, therefore, $x_1/x = 0.3/0.6 = 0.5$.

The minimum value of Π_0 , at which supersonic flow at the inlet into the tube is possible, corresponds to $\tau(1) = \tau(\frac{1}{\lambda_1}) - 0.5 = 2.07 - 0.6 = 1.47$ or $\lambda_2 = 0.66$. Therefore, we have

$$\Pi_0 = \frac{y(\lambda_1)}{q(\lambda_1)} = \frac{1.117}{0.4075} = 2.74$$

For determining the total and static pressure from the value of the velocity coefficients at the inlet and outlet, it is sufficient to write conditions of the equality of flow rates of gas in the inlet and outlet sections, having used expressions (109) or (111).

It was indicated above that if the normalized length of the tube is less than the critical for this value λ_1 , then the laws governing the flow with friction allow the existence of the flow with a continuous change (reduction) in the supersonic velocity on the entire length. It is possible to show, however, that together with the completely supersonic flow, here the shocked flow within the tube and the subsonic speed at outlet is also possible. Such flow conditions in the case $\chi < \chi_{kp}$ can exist only in the defined interval of values $p_{01}/p_{\infty} = \Pi_0$ which is found from the condition that in the exit section of the tube the static pressure of subsonic flow should be equal to the pressure of the environment.

§ 3. The Averaging of Parameters of Nonuniform Flow

In practice it is frequently necessary to calculate gas flows with parameters variable in cross section. In a number of cases, however, these flows can be considered as one-dimensional, with some mean values of the parameters in each cross section. In this case the problem of the averaging of gas parameters in the cross section of the nonuniform flow appears.

Sometimes as the mean values of the parameters we take the mean values in area, velocity, pressure, temperature, and so on. It is possible to show however, that such simple averaging is, generally speaking, incorrect and can lead to erroneous results: the ratio of the mean values of total and static pressures will not correspond to the mean value of the velocity coefficient, and the gas flow rate calculated according to the mean parameters will be more or less real and so on. If the initial nonuniformity of flow is small, then quantitatively these errors are insignificant; with great nonuniformity of the parameters the error can be significant. Therefore, the solution of the stated mission in general will be approached by other means.

The assigned nonuniform flow is characterized by a number of total (integral) values, that is, by the gas flow rate, energy, momentum, enthalpy, entropy, and so on. Replacing this flow by the one-dimensional flow - the averaged - one should try to maintain the total characteristics (properties) of the flow constant. Since the state of the one-dimensional gas flow is determined by three independent parameters (for example, the total pressure \bar{p}_0 , stagnation temperature \bar{T}_0 and velocity coefficient $\bar{\lambda}$), then in averaging, it is simultaneously possible to maintain only the three total physical characteristics of the initial flow constant.

The most widespread is the method of the determination of mean values of parameters p_0 , T_0 and $\bar{\lambda}$ while maintaining in the initial and averaged flows values of the flow rate of the gas G , total energy E and momentum I identical. Conditions $G = \text{const}$, $E = \text{const}$ and $I = \text{const}$ give the three equations with three unknowns necessary for the solution of the problem. Let us assume that in the cross section of the initial nonuniform flow the temperature field and full and static pressure fields are known (assigned or measured). Then it is possible to consider at each point of the cross section the values of total pressure p_0 , stagnation temperature T_0 and velocity coefficient λ are known. According to value λ , for each point of the cross section gas-dynamic functions $q(\lambda)$, $z(\lambda)$, etc., can be found. For the flow, as a whole, the values of flow rate, momentum and energy are determined by means of integration of the corresponding elementary expressions over the entire cross section. Thus, for instance, the gas flow rate is equal to

$$G = \int_{F_1} dQ = \int_{F_1} m \frac{p_0 q(\lambda)}{T_0} dF. \quad (136)$$

If the velocity field is assigned in the form of a graph or table, the gas flow rate can be calculated according to methods of graphic or numerical integration.

The total values of energy E and momentum I are determined similarly.

Let us turn to the solution of the problem of the averaging of parameters p_0 , T_0 and λ . Let us equate the values of total energy of the gas calculated in one case according to the true and in another case according to the mean values of the gas parameters:

$$G c_p T_0 = \int_{F_1} c_p T_0 dQ = E \quad (137)$$

We consider the heat capacity of gas c_p to be constant over the entire cross section. Let us substitute into this equation the expression for the elementary gas flow rate and the expression written above for the total gas flow rate in the flow. Hence we obtain the first unknown value - the mean stagnation temperature of the gas:

$$\bar{T}_0 = \frac{E}{c_p G} = \frac{\int_0^1 p_0 f(\lambda) T_0 dF}{\int_0^1 \frac{p_0 f(\lambda)}{T_0} dF}. \quad (138)$$

From formula (138) it is evident that \bar{T}_0 is the averaged-mass value of the stagnation temperature. Let us use the obtained average value of the stagnation temperature for calculation of the mean value of the critical speed of sound

$$a_{*p} = \sqrt{2g \frac{k}{k+1} R \bar{T}_0}.$$

Let us find the mean value of the velocity coefficient of flow $\bar{\lambda}$ from the condition of the equality of the effective momentum of flow and the momentum calculated according to the mean values of the parameters. For the sake of simplicity of the calculation, let us express the total momentum by means of formula (115) in terms of function $z(\lambda)$, and let us present the elementary momentum according to formula (119) in terms of the total pressure and function $f(\lambda)$. As a result we will obtain

$$\frac{k+1}{2k} \frac{Q}{g} a_{*p} z(\bar{\lambda}) = \int_0^1 p_0 f(\lambda) dF,$$

whence

$$z(\bar{\lambda}) = \frac{2gk}{k+1} \frac{l}{G a_{*p}} = \frac{2gk}{k+1} \frac{1}{G a_{*p}} \int_0^1 p_0 f(\lambda) dF. \quad (139)$$

In accordance with the assigned flow conditions of the gas from two values of the velocity coefficient $\bar{\lambda}$ determined by function $z(\bar{\lambda})$, we select the real value $\lambda > 1$ or $\lambda < 1$. The reason for the ambiguity of solving the problem in this case is quite obvious:

the assigned condition of the retention of flow rate, momentum and total energy will not be disturbed, if in the averaged flow the shock wave arises; the velocity coefficient in this case acquires a new value opposite in magnitude so that function $z(\lambda)$ will be a constant value (see § 6, Example 6).

After determining the stagnation temperature and the velocity coefficient in the averaged flow, we find the average value of total pressure \bar{p}_0 from the expression for the gas flow rate:

$$p_0 = \frac{\sigma V \bar{T}_0}{m F q(\lambda)}. \quad (140)$$

An interesting relation can be obtained if we use the momentum equation for determining the average total pressure:

$$p_0 f(\bar{\lambda}) = \int_0^1 p_0 f(\lambda) dF.$$

Hence we have

$$p_0 = \frac{\int_0^1 p_0 f(\lambda) dF}{f(\bar{\lambda})}.$$

Value $f(\bar{\lambda})$ is the value of function $f(\lambda)$ for the value of the velocity coefficient $\bar{\lambda}$ averaged over the cross section found above. On the basis of the theorem of the mean known from integral calculus, the latter relation can be presented in the form

$$p_0 = \frac{f(\lambda)}{f(\bar{\lambda})} \frac{\int_0^1 p_0 dF}{F}.$$

Here $f(\lambda)$ is the value of function $f(\lambda)$ at a certain point of the range of integration, i.e., at a certain point of the cross section F . As has already been indicated, the value of function $f(\lambda)$ changes very little over wide limits of the change in λ (at subsonic and small supersonic velocities). Therefore, the two values of function $f(\lambda)$ in the given cross section of the flow $f(\lambda)$ and $f(\bar{\lambda})$ will be close in value. Hence, it follows that

$$p_0 \approx \frac{\int p_0 dF}{F} \quad (141)$$

The obtained relation means that the value of total pressure \bar{p}_0 differs little from the *total pressure average in area value*. Calculations show that if the velocity coefficient λ on the cross section changes within limits of 0.4-1.0 or 1-1.4, then the error of the calculation \bar{p}_0 in the formula (141) usually does not exceed 2-3%.

From found values \bar{T}_0 , $\bar{\lambda}$ and \bar{p}_0 all the remaining parameters of the averaged flow, speed \bar{w} , density $\bar{\rho}$ and so on, are unambiguously determined. Let us note that the mean values of the parameters, which satisfy the conditions stated in the problem, are obtained quite definite independently of the method and order of the solution of the fundamental equations, although in this case expressions different in appearance can be obtained.

Let us discuss the physical meaning of the obtained averaged flow parameters. It is easy to see that values of parameters \bar{T}_0 , \bar{p}_0 and $\bar{\lambda}$ and others are equal to the appropriate parameters of such a gas flow which can be formed during the alignment (for example, because of turbulent mixing) of the initial nonuniform flow in the heat-insulated tube of constant cross section without friction against the walls; in this case the flow rate, momentum and total energy of the gas will also maintain constant values. In other words, the found equivalent (averaged) flow can be actually obtained during the flow of the initial gas without external actions. If we calculate and compare the entropy of the gas in the nonuniform and averaged flow, then it will appear that the averaged parameters correspond to the larger value of entropy. This is explained by the fact that with the mixing of the gas particles at different velocities losses to shock appear, the total kinetic energy decreases, and the thermal energy increases.

In connection with this, the given method of averaging in certain cases can prove to be unacceptable. Thus, for instance, if according to the mean values of flow parameters in the outlet section of the compressor found by such method, we calculate its efficiency, then the value less than real will be obtained, since to the real losses (increase in entropy) in the process of the compression of gas will be added the theoretical losses, which appear as a result of the aforementioned replacement of the real flow parameters by the mean values. Therefore, when according to the meaning of the problem it is required to evaluate the work capacity of the initial flow of gas, it is advantageous, as L. I. Sedov and G. G. Chernyy indicated, to carry out averaging in order to maintain the total quantity of the entropy of gas constant¹.

For determining the three parameters of the averaged flow, besides the condition of the retention of entropy, we also use equations of the constancy of flow rate and total energy.

The mean values of the parameters we compute by the following way. From equation (136) we find the total gas flow rate. Further, as above, from the equation of energy (138) we determine the stagnation temperature \bar{T}_0 . The condition of the constancy of entropy (see § 7, Chapter 1) in the averaged and real flow is written in the form

$$GAR \ln \frac{(T_0)^{\frac{k}{k-1}}}{p_0} = AR \int_{d\Omega} \ln \frac{(T_0)^{\frac{k}{k-1}}}{p_0} d\Omega$$

This equation includes only one unknown parameter - the average total pressure \bar{p}_0 . For determining \bar{p}_0 , for dG we substitute its value obtained above and then convert the equation to the form

¹Sedov, L. I., Chernyy, G. G., On the averaging of nonuniform flows of gas in channels. Theoretical hydromechanics, Collection of articles, No. 12, Issue 4. Oborongiz, 1954.

$$\ln p_0 = \frac{m}{G} \int \left(\ln p_0 - \frac{k}{k-1} \ln \frac{T_0}{T_1} \right) \frac{\rho_0 q(\lambda)}{V T_0} dF. \quad (142)$$

Frequently the stagnation temperature T_0 can be considered identical in all points of the cross section, i.e., we assume $\bar{T}_0 = T_0$. In this case equation (142) takes the form

$$\ln p_0 = \frac{1}{G} \int_0^Q \ln p_0 dQ. \quad (143)$$

Consequently, the average value of total pressure is found by the averaging of the logarithm of total pressure in the initial flow with respect to the flow rate. The integrals of the right side of equations (142) and (143) are calculated usually by means of graphic or numerical integration. If the velocity in the initial flow is variable over the cross section, then values of \bar{p}_0 calculated according to formulas (142) and (143) will always be more than values of \bar{p}_0 determined for the same conditions according to formula (140) (when $I = \text{const}$).

We find the velocity coefficient of flow from the equation of the flow rate

$$q(\lambda) = \frac{G V T_0}{m \bar{p}_0 F}. \quad (144)$$

In connection with the indicated increase in total pressure \bar{p}_0 , this value of $q(\lambda)$ proves to be less in value than that found earlier. This means that the average velocity in the subsonic flow will be less and in supersonic larger than the corresponding values obtained with the first method of averaging. In both cases this means that the momentum of flow averaged over entropy, proportional to the value of function $z(\lambda)$, will be greater than the total momentum of the initial nonuniform flow.

Other methods of the averaging of parameters of nonuniform flow are possible. However, it is obvious that with any method of the averaging of parameters of nonuniform flow, only part of its total characteristics is retained, and some properties of flow

are unavoidably lost. We saw that in the first case with averaging the entropy and in the second case the momentum of flow were changed. It is possible to indicate other conditionalities connected with the process of the averaging of parameters. So, let us assume that in the initial flow the static pressure p is equal over the entire cross section. After the replacement of the real parameters by average ones, the static pressure \bar{p} calculated according to \bar{p}_0 and $\bar{\lambda}$ will prove to be different than that in the initial flow. The same is possible in the relation to the value of the velocity coefficient, total pressure, etc., if they are constant on the cross section of the initial flow. Hence it follows that in each real case it is necessary to select such a method of averaging which would most fully reflect the features of the assigned problem. Thus, for instance, in the calculation of losses of efficiency it is rational to use the averaging of the flow parameters with which the condition of the retention of entropy is satisfied. With the averaging of the parameters of flow which escape from the jet nozzle, such a method will be unacceptable, since in this case the most significant is the retention of the real value of the momentum of flow, which characterizes the reactive thrust.

Let us note further one feature of the determination of the average parameters of gas in the supersonic flow.

Let us assume that at all points of the cross section of the supersonic flow the value of the stagnation temperature T_0 is constant. Let us determine the mean values of the parameters in such a flow, using the second of the methods of the averaging examined above with which in the averaged flow the actual values of total energy, entropy and flow rate of the gas are retained. From the equation of energy we obtain the obvious result of $\bar{T}_0 = T_0$. From equation (143) we find the value \bar{p}_0 . The third parameter - the mean velocity coefficient $\bar{\lambda}$ - is found from the equation of the flow rate

$$q(\lambda) = \frac{1}{\rho_0 F_0} \int_{F_0} \frac{\rho \lambda^2 dF}{1 F_0};$$

hence when $T_0 = \bar{T}_0$ we have

$$q(\bar{\lambda}) = \frac{1}{\rho_0 F} \int_{F_0} p_0 q(\bar{\lambda}) dF. \quad (145)$$

The total momentum of the initial nonuniform flow, according to (119), is equal to

$$\int_{F_0} p_0 f(\bar{\lambda}) dF.$$

In order that the averaged flow at the value of total pressure \bar{p}_0 found above would have the same momentum, the velocity coefficient in it should satisfy the relation $\bar{\lambda}$

$$f(\bar{\lambda}) = \frac{1}{\rho_0 F} \int_{F_0} p_0 f(\bar{\lambda}) dF. \quad (146)$$

In general the value $\bar{\lambda}$ will differ from $\bar{\lambda}$. Actually, the condition of the conservation of momentum is given by the fourth equation for determining the three unknown values; such a system of equations will be inconsistent. However, in the given case of averaging there are some features. Let us replace in expression (146) the value of function $f(\lambda)$ in terms of (117) and, after using the theorem of the mean, carry out beyond the integral sign a certain mean value of function $\bar{z}(\lambda)$. As a result we will obtain

$$p_0 F \bar{z}(\bar{\lambda}) q(\bar{\lambda}) = \bar{z}(\bar{\lambda}) \int_{F_0} p_0 q(\bar{\lambda}) dF$$

or

$$q(\bar{\lambda}) = \frac{\bar{z}(\bar{\lambda})}{z(\bar{\lambda})} \cdot \frac{1}{\rho_0 F} \int_{F_0} p_0 q(\bar{\lambda}) dF.$$

By comparing this expression with equation (145), we note that they differ only by the factor on the right side, and therefore

$$q(\bar{\lambda}) = \frac{\bar{z}(\bar{\lambda})}{z(\bar{\lambda})} q(\bar{\lambda}). \quad (147)$$

In the region of supersonic velocity function $z(\lambda)$ (Fig. 5.22) changes very little: with an increase in the velocity from sonic to the maximum (from $\lambda = 1$ to $\lambda = \lambda_{\max}$) the value $z(\lambda)$ increases a total by $\sim 40\%$ ($k = 1.40$), and in this case the value of the pressure ratio p/p_0 drops from 0.528 to zero. If we examine the degree of irregularity of flows really being encountered, then value $z(\lambda)$ within the limits of the cross section usually changes by not more than 15-20%. Therefore, the two mean values of the function in this interval $z(\lambda)$ and $\bar{z}(\lambda)$ will differ little from each other.

The calculations carried out for supersonic flows of different laws of the change in the velocity coefficient in the cross section show that even with a very great nonuniformity of flow - for example, during a change in the total pressure p_0 of 5-10 times when $p = \text{const}$ - the factor of the right side of equation (147) differs from unity by a total of 0.5-1.5%. Therefore, it is possible to consider that $q(\lambda) \sim q(\bar{\lambda})$, i.e., the results of the determination of the mean velocity coefficient from the equation of the flow rate and momentum equation virtually coincide. The accuracy of this approximate relationship is higher, the more values of λ in the flow; however, also at moderate supersonic velocities ($\lambda > 1.2-1.3$) the distinction between values λ and $\bar{\lambda}$ consists of fractions of a percent¹.

Thus, with averaging by the indicated method of flow parameters at high supersonic velocities and stagnation temperature constant in cross section, *simultaneously with a high degree of accuracy four integral relationships are satisfied*, and these express the equality of total energy, flow rate, momentum and entropy in the initial and averaged flow. The condition $T_0 = \text{const}$

¹See Cherkez, A. Ya., On certain features of the averaging of parameters in supersonic gas flow. *Izvestiya of the Academy of Sciences of the USSR, OTN*, No. 4, 1962.

is in this case very significant, since otherwise the value $q(\bar{\lambda})$, obtained from the equation of flow rate, will depend on the distribution law of the stagnation temperature and can differ as much as possible from value $q(\lambda)$, found from the momentum equation, which does not include the value T_0 . The physical meaning of the obtained result consists in the fact that at high supersonic speed and $T_0 = \text{const}$, substantial changes in the pressures, densities and other flow parameters insignificantly change the velocity magnitude. Changed even less, in proportion to the value of function $z(\lambda)$, is the value of the momentum of the gas with its assigned flow rate: an increase in the momentum to a considerable degree is compensated by a reduction in the static pressure so that

$$\frac{d}{d\lambda} w + pF = \frac{k+1}{2k} \frac{d}{d\lambda} a_{sp} z(\lambda) \approx \text{const} \cdot Q$$

The indicated property of supersonic flows means the possibility of a one-dimensional examination and the use of methods given in this chapter for calculating flows with very great nonuniformity.

Thus, for instance, shown in Chapter VII is the high accuracy of such a calculation in connection with the flow in cross section of which the static pressure changes 10-20 times (initial section of the supersonic jet).

CHAPTER VI

BOUNDARY LAYER THEORY

§ 1. Basic Concepts of a Boundary Layer

The widely developed theory of motion of an ideal fluid usually gives a completely satisfactory picture of real flows, with the exception of the areas in immediate proximity to the surface of a streamlined body. In these areas, the forces of internal friction or viscosity forces which are decisive in the emergence of resistance of bodies during motion in liquid acquire vital importance. Disregard of these forces leads to the fact that the resistance of a body, uniformly moving in unlimited space turns out to be equal to zero, which contradicts experimental data.

The amount of friction force acting on a unit of area, i.e., the stress of friction is designated usually as τ . The stress of friction in the boundary layer according to Newton's hypothesis is proportional to the velocity gradient in a direction normal to the body surface (§ 4 Chapter II), i.e.,

$$\tau = \mu \frac{\partial u}{\partial y}; \quad (1)$$

the proportionality factor μ characterizes the viscous properties of the liquid and is called the *coefficient of dynamic viscosity*.

Theoretical interpretation of Newton's law (1) can be obtained for gases on the basis of the kinetic theory. According to the assumption lying as the basis of the kinetic theory, molecules of gas are found in continuous but random movement, so that gas as a whole remains stationary. The kinetic energy of this random movement of molecules represents the thermal energy of the gas. Let us assume now that along with the random movement of molecules there is regulated movement of finite (very large in comparison with the separate molecules) masses of the gas parallel to a certain plane S_0 , whereby the speed of this motion u is proportional to distance y from the plane in question (Fig. 6.1). At arbitrary distance y_1 let us conduct plane S_1 parallel to S_0 , and let us examine the transfer of momentum because of the random movement of the molecules through this plane. The molecules which pass through the plane from the bottom upwards possess less momentum in the direction of velocity u than the molecules which pass downward, and because of this the velocity of a layer of gas lying higher than plane S_1 will decrease, while the velocity of a layer of gas lying lower than plane S_1 , - will increase. To obtain the quantitative characteristic of this interaction, let us perform the following simplified calculations. Let us assume that in a unit of volume on the average there are found N molecules which have an average velocity of random movement c . In the direction perpendicular to plane S_1 it moves $N/3$ molecules, whereby, of them, $N/6$ move from the top downward and just as many move from the bottom upward. During time dt through area dS on plane S_1 in each direction there pass $1/6 N c dS dt$ molecules. Let us introduce yet another concept of the mean free path. Under mean free path λ is implied that average distance which the molecules cover between collisions with each other. The molecule which was found at a distance λ lower than plane S_1 possessed momentum

$$m(u_1 - \frac{\partial u}{\partial y} \lambda)$$

(m - the mass of the molecules, u_1 - the velocity of the regulated motion in plane S_1). Since on the mean free path the momentum is retained, then the molecules moving from the bottom upwards transfer a momentum equal to

$$\frac{1}{6} Ncm \left(u_1 - \frac{\partial u}{\partial y} l \right) dS dt.$$

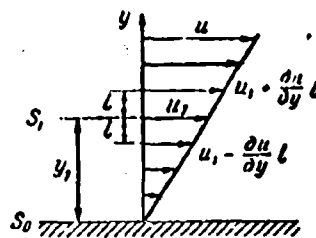


Fig. 6.1. Interpretation of Newton's law on the basis of kinetic theory.

Correspondingly, there is transferred downward the momentum

$$\frac{1}{6} Ncm \left(u_1 + \frac{\partial u}{\partial y} l \right) dS dt.$$

This transfer of momentum gives rise to the appearance of tangential stress τ along plane S_1 . Since the change in momentum is equal to the impulse of the acting force

$$\tau dS dt = \frac{1}{6} Ncm \left(u_1 + \frac{\partial u}{\partial y} l \right) dS dt - \frac{1}{6} Ncm \left(u_1 - \frac{\partial u}{\partial y} l \right) dS dt,$$

then for the tangential stress we obtain the expression

$$\tau = \frac{1}{3} \rho c l \frac{\partial u}{\partial y}. \quad (2)$$

which is nothing but Newton's law, whereby, $\mu = 1/3 \rho c l$.

The more precise calculations made by Enskog and Chapman, considering the effect of velocity u on the velocity distribution of the molecules give a somewhat different numerical factor $\mu = 0.499\text{pcl}$.

In accordance with kinetic theory, the coefficient of dynamic viscosity of gases should not depend on pressure - its value should vary in proportion to the square root from absolute temperature (since $\rho \sim p/T$, $c \sim \sqrt{T}$, $l \sim T/p$). The first conclusion is approximately validated by experiment within sufficiently wide limits. As concerns the increase in values of μ with an increase in the temperature, it occurs more rapidly than follows from the kinetic theory. A more precise calculation, taking into account the molecular attracting and repulsion forces, leads to formula which satisfactorily agrees with the experimental data

$$\frac{\mu}{\mu_0} = \left(\frac{T}{273} \right)^{3/2} \frac{273 + C}{T + C} \quad (3)$$

where T is expressed in $^{\circ}\text{K}$.

Values of μ_0 and C for various gases are given in Table 1.

Table 1.

Gas	$^{\circ}\text{C}$	$\mu_0 10^6$ $\frac{\text{kgf}\cdot\text{s}}{\text{m}^2}$	Gas	$^{\circ}\text{C}$	$\mu_0 10^6$ $\frac{\text{kgf}\cdot\text{s}}{\text{m}^2}$
Air	122	1.75	Hydrogen	83	0.85
Nitrogen	107	1.70	Helium	80	1.88
Oxygen	138	1.96	Ammonia	626	0.96

In practical calculations, however, it is more convenient to use the exponential dependence of μ on temperature

$$\frac{\mu}{\mu_0} = \left(\frac{T}{T_0} \right)^{\omega} \quad (4)$$

The results of calculating the coefficient of viscosity of air in formulas (3) and (4) (where $\omega = 0.75$) in the range of temperatures from 100 to 1000°K are given in Fig. 6.2. The solid curve corresponds to Sutherland's formula, while the broken line corresponds to the exponential formula. In this figure, the experimental values of μ are shown by the dots.

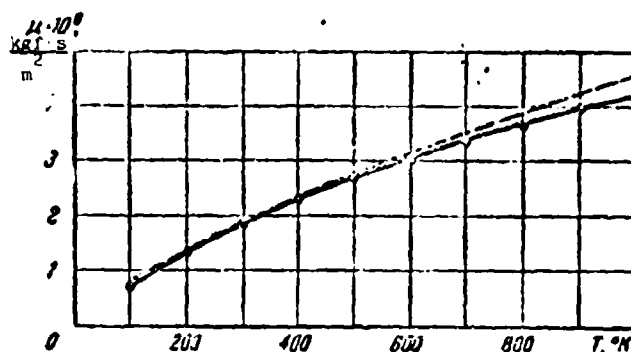


Fig. 6.2. Dependence of the coefficient of dynamic viscosity of air on temperature.

The coefficient of dynamic viscosity for liquid bodies depends very slightly on pressure and decreases rather rapidly with an increase in temperature. Since in a liquid body the mean free path of a molecule is commensurable with the molecular dimension, the kinetic theory in this case is unsuitable. The cohesive forces of the molecules under these conditions acquire great significance. In view of the complexity of the interaction of separate molecules in a liquid body at present there is no complete liquid theory, and therefore, there is no viscosity theory.

Let us consider the laminar layer motion of a viscous liquid near a solid wall. Under the action of viscosity forces, layers of liquid in proportion to their proximity to the wall are gradually slowed down and, at the wall itself adhere to it. This zone of flow of a viscous liquid located about a streamlined body is called the *boundary layer*. Outside the boundary layer the effect of viscosity is usually exhibited weakly and the picture of flow is close to that which the ideal fluid theory gives. Thus for an analytical investigation of the flow of viscous fluids, the whole field of flow can be broken into two areas: into the area of the boundary layer near the wall, where it is necessary to consider the forces of friction, and into the zone of flow outside the boundary layer in which it is possible to disregard the forces of friction and therefore to apply the laws governing the theory of an ideal fluid. Consequently, the boundary layer is that zone of flow of a viscous liquid in which the values of the forces of friction and inertia have an identical order. On the basis of this, it is possible to estimate the boundary layer thickness.

For simplicity, let us examine the flow of a liquid along a flat plate. The x-axis is directed along the plate, the y-axis - at right angles to it. For the motion which proceeds basically in the direction of the x-axis, the force of inertia pertaining to the elementary volume $dx dy dz$ is equal to $\rho \frac{du}{dt} dx dy dz$, where u is the velocity of motion of the liquid in the direction of the x-axis. For steady motion:

$$\frac{du}{dt} = \frac{\partial u}{\partial x} \frac{dx}{dt} = u \frac{\partial u}{\partial x}.$$

consequently, the force of inertia is equal to $\rho u \frac{\partial u}{\partial x} dx dy dz$.

The resultant force of friction parallel to the direction of motion, as can easily be seen from Fig. 6.3, is equal to

$$\left(\tau + \frac{\partial \tau}{\partial y} dy \right) dx dz - \tau dx dz = \frac{\partial \tau}{\partial y} dx dy dz.$$

Equating the force of inertia to the force of friction, we obtain the relationship

$$\rho u \frac{\partial u}{\partial x} \sim \frac{\partial \tau}{\partial y},$$

or, utilizing Newton's law (1),

$$\rho u \frac{\partial u}{\partial x} \sim \mu \frac{\partial^2 u}{\partial y^2}. \quad (5)$$

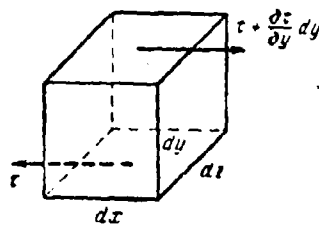


Fig. 6.3. Forces of friction applied to an elementary volume.

For a plate of length l , the value of $\partial u / \partial x$ is proportional to u_0 / l , where u_0 is the velocity of external flow. Consequently, the force of inertia has a value on the order of $\rho u_0^2 / l$. The velocity gradient in the direction perpendicular to wall, i.e., the value of $\partial u / \partial y$ is on the order of u_0 / δ , where δ is the boundary layer thickness. Thus the force of friction is proportional to $\mu u_0 / \delta^2$. Substituting these values of forces in relationship (5), we obtain for the boundary layer thickness the expression

$$\delta \sim \sqrt{\frac{\mu l}{\rho u_0}}, \text{ or } \frac{\delta}{l} \sim \frac{1}{\sqrt{\frac{\rho u_0 l}{\mu}}} = \frac{1}{\sqrt{R_l}}. \quad (6)$$

The dimensionless quantity $\rho u_0 l / \mu = R_l$ is the Reynolds number calculated along the length of the plate.

Analogously, it is possible to estimate the amount of friction stress at the wall $\tau_w = \mu (\partial u / \partial y)_w$. Utilizing the values $(\partial u / \partial y)_w \sim u_0 / \delta$, $\delta \sim \sqrt{\mu l / \rho u_0}$, obtained above, we find the expression for the amount of friction stress:

$$\tau_w \sim \mu \frac{u_0}{\delta} \sim \sqrt{\frac{\mu \rho u_0^3}{l}}.$$

Dividing the stress of friction τ_w by ρu_0^2 , we obtain the connection between the dimensionless quantity $\tau_w / \rho u_0^2$ and the Reynolds number

$$\frac{\tau_w}{\rho u_0^2} \sim \frac{1}{\sqrt{R_l}}. \quad (7)$$

Relationships (6) and (7) show that Reynolds number is the fundamental characteristic of a laminar boundary layer. Both the boundary layer thickness, i.e., the dimensions of the area where the forces of friction have an essential effect and also the value itself of these forces of friction are determined basically by the value of the Reynolds number. A similar result can also be obtained from the dimensional theory.

For gases, the coefficients of dynamic viscosity are low (Fig. 6.2), therefore the Reynolds numbers will be rather large even at relatively low values of the rate of flow. As follows from relationship (6), the thickness of the boundary layer because of this is low in relation to the length of the plate,

i.e., all the effect of viscosity is concentrated in a thin layer close to the streamlined surface. This conclusion is in good agreement with the results of experiments in the study of low-viscous flows.

Let us explain these qualitative considerations by a numerical example. Let us estimate the order of thickness of the boundary-layer at the end of the plate as a length of $l = 0.1$ m, the air flowing past at a temperature of $T = 300^\circ\text{K}$ at a rate of $u_0 = 15$ m/s. The air density at this temperature and atmospheric pressure equal $\rho = 0.120$ kgf·s²/m⁴, while the coefficient of viscosity $\mu = 1.85 \cdot 10^{-6}$ kgf·s/m² (Fig. 6.2). To these parameters there corresponds a Reynolds number $R_l = \rho u_0 l / \mu \approx 10^5$. According to formula (6), the relative thickness of the boundary-layer is on the order of $\delta/l \sim 1/300$.

The Reynolds number is the determining parameter not only for the quantitative characteristics of the boundary layer, but also for the character of flow itself. With small Reynolds numbers, the motion of the gas particles has a regulated laminar nature, such a flow is called *laminar*. With large Reynolds numbers the motion of the gas particles becomes irregular, uneven velocity pulsations appear, such a flow is called *turbulent*. The transition of laminar flow into turbulent occurs at a specified value of the Reynolds number called the *critical*. The critical Reynolds number is not constant and depends to a very great degree on the value of the initial disturbances, i.e., on the intensity of turbulence of the incident flow.

Experimental studies of the transition of a laminar boundary layer to a turbulent on a flat plate showed that the critical value of the Reynolds number

where λ_2 is the velocity coefficient of the outflow from the nozzle, and p_{01} is the total pressure in the initial cross section of the nozzle. With equal drops in the pressure

$$\left(\frac{p_1}{p_{01}}\right)_{\text{nr}} = \left(\frac{p_1}{p_{01}}\right)_e$$

the velocity of discharge from the semi-thermal nozzle is less than that from the geometric nozzle ($\lambda_{3\text{nr}} < \lambda_{3r}$); this results from equality

$$\sigma_{\text{nr}} \left(1 - \frac{k-1}{k+1} \lambda_{3\text{nr}}^2\right)^{\frac{k}{k-1}} = \left(1 - \frac{k-1}{k+1} \lambda_{3r}^2\right)^{\frac{k}{k-1}},$$

which connects the ratio of the static pressure to the total pressure with the velocity coefficient. For example, when $\sigma_{\text{nr}} = 0.82$ and $\lambda_{3r} = 2$ the velocity coefficient of outflow from the semi-thermal nozzle $\lambda_{3\text{nr}} = 1.97$, i.e., 1.5% less than the velocity coefficient of outflow from the geometric nozzle.

In examining the different types of the nozzles intended for transition through the speed of sound, in all cases we had in mind the transition from subsonic to supersonic velocity. The obtained formulas are suitable principally for the reverse case, i.e., the smooth conversion of supersonic flow into subsonic; however, with the braking of supersonic flow there can arise shock waves, which complicate the phenomenon.

Let us discuss now briefly the joint development of two or several effects. As a first example let us analyze the case of the geometric nozzle with friction. The fundamental relation (49) in this case takes the form

$$(M^2 - 1) \frac{dw}{w} = \frac{dF}{F} - \frac{gk}{a^2} dL_{\text{fr}}.$$

The most interesting feature of this nozzle is the fact that the critical velocity is obtained in its divergent part, since when $M = 1$

$$\frac{dF}{F} = \frac{gk}{a^2} dL_{np} > 0,$$

and in the narrow cross section ($dF = 0$ when $dw > 0$) the subsonic velocity and $M < 1$ occur.

Let us now explain the chief characteristics of the geometric nozzle with heat exchange. From the fundamental relation (49) in this case we have

$$(M^2 - 1) \frac{dw}{w} = \frac{dF}{F} - \frac{g}{a^2} \frac{k-1}{\lambda} dQ_{np}.$$

The location of the critical cross section ($M = 1$) is determined by the equality

$$\frac{dF}{F} = \frac{g}{a^2} \frac{k-1}{\lambda} dQ_{np}.$$

With the heat feed ($dQ_{np} > 0$) - for example, with the afterburning of gases in the nozzle - the critical velocity is reached in the divergent part of the nozzle ($dF > 0$), and with the heat removal ($dQ_{np} < 0$), i.e., the heat transfer through the nozzle walls, the critical velocity is reached in the convergent section of the nozzle ($dF < 0$). In the first case in the narrow cross section of the nozzle ($dF = 0$), there occurs subsonic velocity and in the second case - supersonic velocity.

By the same means it is possible to investigate the joint effect in the gas flow of any other actions. In this case it is important to emphasize that in accordance with equation (49) the transition from $M < 1$ to $M > 1$ requires in any event a sign change of the total action.

In conclusion let us note one fact which sometimes leads to misunderstandings in the qualitative analysis of laws governing some flows. In connection with this let us again return to equation (49).

Above in the analysis of the equation of momentum (92) of Chapter I, we noted that independently of the processes occurring in the flow, a change in the rate of flow is always caused by the action of the force of friction, applied forces, and also the difference in forces of pressure on the chosen element of gas flow. The different forms of the external action in different ways affect the static pressure in the flow. The meaning of the joint solution of equations (43)-(47), as a result of which relation (49) was obtained, was reduced so that the value of the pressure gradient in flow is expressed by external actions; the value dp in this case was excluded from the momentum equation or the Bernoulli equation (46).

In the analysis of equation (49) it is revealed that: a) a change in the gas velocity is caused by such factors which are not connected with direct force action on the flow (for example, the heat feed), b) the total effect in a number of cases turns out to be opposite to that which can be expected on the basis of the analysis of the action of applied forces. Actually, for example, the force of friction which always acts opposite to the direction of motion in subsonic flow leads not to braking but acceleration of the flow. The latter means that in flow with friction there occurs such a reduction in the static pressure that the force of pressure acting in the flow exceeds the force of friction.

In exactly the same manner as with the feed of mechanical energy to the subsonic gas flow, its pressure is increased so that the force of pressure acting counter to flow exceeds the applied force which caused it. As a result the flow, to which the applied force is applied in the direction of motion when $M < 1$, is not accelerated but braked.

Thus, above, in the analysis of external actions on the gas flow, it was assumed everywhere that in the flow there appear appropriate pressure gradients, which as a final result determine

the change in the rate of the flow. Thus, for instance, for the acceleration of the subsonic gas flow in the thermal nozzle (i.e., when $F = \text{const}$) the pressure at the inlet into the nozzle should exceed the outlet pressure by the value which is determined by the initial and final M numbers (see formula (55)).

Having the same meaning are above obtained relationships between static pressures of the gas in flow with friction (50), flow with the feed of mechanical energy, and so on. In many instances, however, it is known in advance that in the flow in question there is no longitudinal pressure gradient. The change in the gas velocity in this case ($dp = 0$) is completely determined by the equation of momentum in the form

$$\rho w dw = -\frac{1}{F} (dP + dP_{\tau p}),$$

where $dP_{\tau p}$ is the force of friction, and dP is the applied force. Hence it follows that in isobaric flow both at subsonic and supersonic velocities the friction leads to a decrease in the velocity; the applied forces which act on the flow or the applied external mechanical energy ($dP < 0$) always accelerate the gas flow; the heat feed when $dp = 0$ does not at all change the velocity of the directed motion of gas, since in this case there are no applied forces.

An example of isobaric flow can be, in particular, supersonic flow in a solid wall. The boundary layer near such a wall is formed as a result of the continuous braking of the flow by forces of external action (friction). In summation, the velocity of the flow in it decreases when $p = \text{const}$ from the supersonic to the small subsonic value.

In exactly the same manner the isobaric supersonic jet, being mixed with the fixed atmospheric air, accelerates its particles to the supersonic velocity by means of a one-sided mechanical

action - the feed of the momentum in the collision of particles of gas and air.

With further flow in any stream filament within the isobaric supersonic jet there occurs continuous braking - with the transition through the speed of sound - down to low speeds, and also because of one-sided external action - the transfer of momentum into the environment.

These examples do not contradict the laws established above and the equation of the transformation of actions (49). The fact is that in the presence of any external action the condition in isobaricity ($p = \text{const}$) can be fulfilled only with a completely defined change in the *cross-sectional area* F .

Thus, for instance, at subsonic flow in a cylindrical tube with friction the velocity of the gas increases, and the static pressure drops. In order that the pressure in the flow is constant, the channel must be made divergent, i.e., the geometric effect $dF > 0$ must be added to the effect of friction. Since independently of the shape of the channel with flow with friction the total pressure is lowered, then in such an isobaric flow the gas velocity is decreased.

§ 5. On the Propagation of Detonation and Burning in Gases¹

The creator of the theory of the propagation of detonation in gases is the well-known Russian physicist V. A. Mikhel'son who devoted in 1889 the work "On the normal ignition speed of fulminating gas mixtures" to this problem.²

The outstanding theoretical and experimental studies in the field of burning and detonation belong to N. N. Semenov, Ya. B. Zel'dovich, D. A. Frank-Kamenetsiy, K. I. Shchelkin and other Soviet scientists.³

The propagation of the flame in a combustible gas mixture, without depending on the mechanism of ignition (by thermal conductivity with slow burning or by a shock wave with detonation), is subordinated to the fundamental laws of gas dynamics and, therefore, can be described by equations of the conservation of mass, momentum and energy.

The flame front is a thin layer of gas of virtually constant cross section, on both sides of which values of the velocity of motion (relative to the wave front), temperature, pressure and other parameters are different. In accordance with this, the flame front can be treated as a surface of nonremovable discontinuity (thermal shock).

¹In this section an expanded presentation of the following work is given: Abramovich, G. N. and Vulis, L. A., On the mechanics of the propagation of detonation and burning. Reports of the Academy of Sciences of the USSR, Vol. 55, Issue 2, 1947.

²Mikhel'son, V. A., Complete collected works, Vol. 1, M., 1930.

³See, for example, Zel'dovich, Ya. B., Theory of the burning and detonation of gases. Publishing House of the Academy of Sciences of the USSR, 1944.

In the contemporary concept the detonation wave, which is propagated in the combustible gaseous medium, is two-layered. The first layer is an adiabatic shock wave, with the passage through which the gas is greatly heated. In chemically active gas this heating, if it is sufficiently intensive, can cause ignition. In connection with the fact that the shock wave thickness is negligible (order of the mean free path of the molecule), within limits its process of burning, apparently, is developed not in the state. Therefore, the area in which there occurs burning forms a second, more extended, but virtually also very thin layer which adjoins directly to the shock wave (Fig. 5.18).

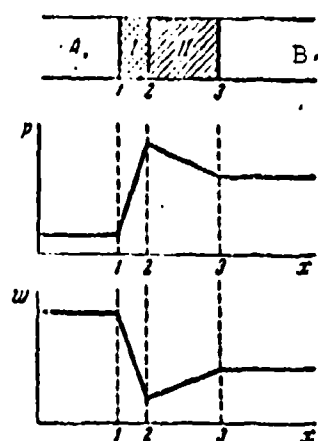


Fig. 5.18. Diagram of the detonation wave: A - fresh mixture, B - products of combustion; I. shock wave, II. combustion zone.

The heating of the gas with its passage through the shock wave in detonation burning in essence replaces the preheating with its thermal conductivity in normal burning.

Let us examine the phenomenon of detonation in conditions of a one-dimensional problem. In the case for a plane shock wave according to the known relation (15) of Chapter III, the product of the gas velocity relative to the wave front (taken, respectively, in front of and behind the front) is equal to the square of the critical velocity:

$$w_1 w_2 = a_{cr}^2$$

The value w_1 is the velocity of the propagation of the shock wave (in our case, the detonation wave in a fixed gas). For the study of the process it is convenient to consider that the gas flows at a rate of w_1 to the region of detonation, and the wave front is fixed. This inverted scheme of the phenomenon is accepted by us in the subsequent presentation.

Shock wave (pressure shock), as is known, is propagated at a hypercritical velocity ($w_1 > a_{kp}$), and therefore the gas velocity behind the wave front is always lower than the critical velocity ($w_2 < a_{kp}$). In other words, the process of burning with detonation, as with slow burning, occurs in the subsonic part of the gas flow.

At the end of the second layer of the detonation wave, as a result of the heat feed with burning, the gas velocity is higher than at first, and the pressure is respectively lower. Thus, the first layer of the detonation wave is a compression shock, and the second layer, where burning occurs, is the expansion shock. The approximate nature of the distribution of the pressure and gas velocity in the detonation wave is shown on Fig. 5.18.

Let us turn to the calculation of the shock wave.

In the calculation of the change in the state of the gas in the first layer of the plane detonation wave, we can use relations for the normal shock wave.

For the case in question it is important that in the first layer of the detonation wave (adiabatic shock wave) the stagnation temperature remains constant $T_{01} = T_{02}$. Consequently, the critical velocity in the first layer does not change $a_{1kp} = a_{2kp}$, whereas in the products of combustion its value is increased $T_{03} > T_{01}$ and, respectively, $a_{3kp} > a_{1kp}$. This circumstance

must be considered subsequently in the calculation of the velocity coefficients:

$$\lambda_1 = \frac{w_1}{a_{1kp}}, \quad \lambda_2 = \frac{w_2}{a_{2kp}}, \quad \lambda_3 = \frac{w_3}{a_{3kp}}.$$

From the continuity equation $\rho_1 w_1 = \rho_2 w_2$ and expression (16) of Chapter III, let us find for a change in density and velocity the relation

$$\frac{\rho_2}{\rho_1} = \frac{w_1}{w_2} = \lambda_1^2. \quad (62)$$

The law of pressure change in the normal shock wave can be obtained from the momentum equation in the form of the known equality (21) of Chapter III

$$\frac{p_2}{p_1} = \frac{\lambda_1^2 - \frac{k-1}{k+1}}{1 - \frac{k-1}{k+1} \lambda_1^2}. \quad (63)$$

From (62) and (63) it follows that the change in gas temperature in the shock wave

$$\frac{T_2}{T_1} = \frac{1 - \frac{k-1}{k+1} \lambda_1^2}{1 - \frac{k-1}{k+1} \lambda_1^2}. \quad (64)$$

For example, at the velocity of propagation of the shock wave $w_1 = 2000$ m/s, the initial temperature of the gas $T_1 = 400^\circ\text{K}$, $R = 30$ kgm/kg·deg and $k = 1.4$ we have $T_{01} \approx 2400^\circ\text{K}$, $a_{1kp} \approx 900$ m/s, $\lambda_1 \approx 2.2$, $\lambda_2 \approx 0.45$, to which corresponds $T_2 \approx 2300^\circ\text{K}$.

There are no doubts that in this case the shock wave can cause the ignition of the combustible gas mixture.

Let us now study the calculation of the combustion zone.

It is natural that all formulas derived in §§ 3 and 4 for the case of the preheating of gas in a cylindrical tube are also

suitable for calculating the second (thermal) layer of the detonation wave, since in the derivation of the indicated formulas the length of the tube was not important (the friction and thermal conductivity through the side surface were disregarded).

For calculating the state of the gas in the second (subsonic) layer of the detonation wave - in the region of burning - it is most simple to resort to the relation (58) between the stagnation temperature and the velocity coefficient

$$\frac{T_{02}}{T_{01}} = \frac{\lambda_1(1+\lambda_1)^2}{\lambda_2(1+\lambda_2)^2} = \frac{\lambda_1(1+\lambda_1)^2}{\lambda_2(1+\lambda_2)^2}. \quad (65)$$

whence after the solution of biquadratic equation, we obtain the following expression:

$$\lambda_2 = \frac{1}{\lambda_1} - \frac{1+\lambda_1}{2\lambda_1} \left[1 - \sqrt{1 - \frac{4\lambda_1}{(1+\lambda_1)^2} \frac{T_{01}}{T_{02}}} \right] \sqrt{\frac{T_{01}}{T_{02}}}, \quad (66)$$

or

$$\lambda_2 = \frac{1+\lambda_1}{2\lambda_1} \left[1 - \sqrt{1 - \frac{4\lambda_1}{(1+\lambda_1)^2} \frac{T_{01}}{T_{02}}} \right] \sqrt{\frac{T_{01}}{T_{02}}}. \quad (67)$$

Rejected here are the roots which give the supersonic solutions, since the combustion zone where the relative velocities are lower than the speed of sound ($\lambda_2 < 1$) is examined; furthermore, we assume that $T_{01} = T_{02}$. The velocity coefficient λ_2 - directly after the shock wave - is usually considerably less than unity; if in this case the relative temperature increment of braking in the region of burning is small ($T_{03}/T_{01} \approx 1$), then formula (67) can be substantially simplified:

$$\lambda_2 \approx \frac{\lambda_1}{1+\lambda_1} \sqrt{\frac{T_{01}}{T_{02}}} \approx \lambda_1 \sqrt{\frac{T_{01}}{T_{02}}}$$

(since under the assumptions made $\lambda_2^2 \ll 1$). Thus,

$$\lambda_2 \approx \lambda_1 \sqrt{1 + \frac{\Delta T_0}{T_{01}}}, \quad (68)$$

where $\Delta T_0 = Q/c_p$, if Q is the quantity of heat which is liberated

with the combustion of a unit weight of mixture. From formula (68) it is evident that with weak heating ($\Delta T_0/T_{01} \approx 0$) the velocity coefficient for the products of combustion is close to the velocity coefficient after the shock wave.

With the intensifying of the shock wave, i.e., with an increase in the velocity of propagation of the shock wave, the stagnation temperature of the initial mixture $T_{01} = T_{02}$ sharply increases according to the known equality (42) of Chapter I

$$T_0 = \frac{T_1}{1 - \frac{k-1}{k+1} M_1^2}; \quad (69)$$

In this case the temperature in the flow in front of the region of burning T_2 sharply increases. In the limit when $M_1 = \infty$ and $\lambda_1 = \sqrt{\frac{k+1}{k-1}}$ we have $T_{01} = T_{02} = \infty$ and $T_2 = \infty$. With an increase in temperature T_2 , in connection with the increasing role of thermal dissociation,¹ the absolute difference in the stagnation temperatures somewhat decreases:

$$\Delta T_0 = T_{02} - T_{01}.$$

Consequently, with the intensification of the shock wave both the relative heating of the gas $\Delta T_0/T_{01}$ and the velocity coefficient of the combustion products λ_3 decreases.

This is evident most distinctly if into formula (68), instead of the variable stagnation temperature we introduce the constant temperature of the cold gas:

$$\lambda_3 \approx \frac{1}{\lambda_1} \sqrt{1 + \frac{\Delta T_0}{T_1} \left(1 - \frac{k-1}{k+1} M_1^2\right)}. \quad (70)$$

¹The thermal dissociation is the phenomenon of partial decomposition of the products of burning observed at high temperatures and also at low pressures; a reaction occurs in the opposite direction and is accompanied by an absorption of heat.

The burning which occurs behind the front of a very powerful shock wave begins at such a high thermal level that it can cause only a relatively small increase in stagnation temperature. Therefore, in the limit

$$(\rho_2)_{np} \approx \lambda_2 = \frac{1}{\lambda_1},$$

i.e., the detonation wave approaches with the usual shock wave.

Let us study the steady-state condition of detonation.

The considerations given make it possible to imagine the process of the formation of the stationary wave of detonation in the following form. Usually the detonation wave appears as the result of local explosion in the combustible mixture. In the region of the explosion very high pressures are developed and directed from it is a very powerful shock wave. In transit through the cold combustible mixture, this wave, as was noted above, causes considerable heating of the gas and can lead it up to ignition. Precisely in this case, behind the shock-wave front there follows the region of burning which forms the wave detonation in totality with the shock wave. Since near the explosion center the propagation velocity of the wave and its intensity are very great, the relative gas velocities at the beginning of the region of burning and at the end of it are close to each other and substantially lower than the critical velocity:

$$\lambda_2 \approx \lambda_3 \ll 1.$$

However, with distance from the blast center the detonation wave is attenuated, and the propagation velocity of it λ_1 decreases. In connection with this there occurs a reduction in the stagnation temperature at the beginning of the region of burning (T_{02}) and an increase in the velocity coefficient of the gas (λ_2). In this case the relative heating of gas ($\Delta T_0/T_{01}$) and the velocity of motion (68) of the combustion products (λ_3) increase. It is obvious that when the detonation

wave is attenuated so much that λ_3 will be raised up to the critical value ($\lambda_{3kp} = 1$), a further deceleration of detonation will prove to be impossible¹).

Consequently, the detonation process, which began from the explosion, continuously weakens, until the propagation velocity is lowered to a minimum value which corresponds to the onset of the thermal critical region in the combustion zone. From this point on, the propagation of the detonation wave acquires a stable stationary nature.

As was shown in § 4, further acceleration and transition to the supercritical region are possible solely with a change in the sign of the effect - in this case upon the transition from the heat liberation in the combustion zone to its removal, beginning from the critical cross section (thermal nozzle). Thus, the onset of the thermal critical region in the zone of combustion leads to the establishment of stationary values λ_1 , λ_2 , and λ_3 .

We can determine the coefficient of the propagation velocity of the steady-state detonation wave, after substituting value $\lambda_3 = 1$ into equation (66). In this case

$$\lambda_1 = \lambda_2 = \sqrt{\frac{T_{01}}{T_{02}}} = \sqrt{\frac{T_{01}}{T_{02}} - 1} \quad (71)$$

or after release from the radicals

$$\frac{T_{01}}{T_{02}} = \left(\frac{21 + 1}{2\lambda_1} \right)^2 = \left(\frac{1 + 21}{2\lambda_1} \right)^2. \quad (72)$$

Substituting $T_{03} = T_{01} + \Delta T_0$, we also obtain

$$\frac{\Delta T_0}{T_{01}} = \left(\frac{21 - 1}{2\lambda_1} \right)^2 = \left(\frac{1 - 21}{2\lambda_1} \right)^2. \quad (73)$$

Unlike this the simple shock wave, formed as a result of the explosion and being propagated in the inert medium, with distance from the blast center completely degenerates into an

The last two expressions, just as equation (65), retain identical form with the substitution in them of velocity coefficients λ_1 and λ_2 . Thereby a change in the stagnation temperature is connected here either with the propagation velocity of detonation (λ_1) or with the maximum propagation velocity of the combustion zone (λ_2). It is important that the maximum value λ_2 is retained without depending on the mechanism of ignition, i.e., it is related both to the detonation and the steady-state flame propagation.

Let us turn to the calculation of the propagation velocity of the wave.

Let us designate for brevity the thermal characteristic of the combustible mixture Φ^1 :

$$\frac{T_{02} - T_{01}}{T_1} = \frac{\Delta T_0}{T_1} = \Phi.$$

From formulas (69) and (72) we have

$$\Phi \left(1 - \frac{k-1}{k+1} \lambda_1^2\right) = \left(\frac{\lambda_1^2 - 1}{2\lambda_1}\right)^2,$$

whence the square of the velocity coefficient of the wave propagation is equal to

$$\lambda_1^2 = \frac{1+2\Phi}{1+\Phi \frac{k-1}{k+1}} \left[1 \pm \sqrt{1 - \frac{1+\Phi \frac{k-1}{k+1}}{(1+2\Phi)^2}}\right]. \quad (74)$$

In equation (74) both signs before the radical correspond to the real values of the velocity coefficient. The positive sign

¹In meaning this value is equal to the ratio of the quantity of liberated heat to the initial gas enthalpy $\Phi = Q/c_p T_1$. For example, for a cold ($T_1 \approx 300^\circ \text{ abc}$) mixture of gasoline with air (when $\alpha \approx 1$) $\Phi \approx 6.5$.

corresponds to detonation burning ($\lambda_1 > 1$), i.e., the propagation velocity of the shock wave. The negative sign corresponds to the propagation of the slow burning. It should be noted that formula (74) also with a negative sign is suitable for detonation. In this case it connects the velocity coefficient directly behind the shock front λ_2 (instead of λ_1) with value $\Phi' = \Delta T_0/T_2$ (instead of $\Phi = \Delta T_0/T_1$).

In practically interesting cases where $\Phi > 1$, instead of expression (74), it is possible with an error of less than 2% to accept approximately:

a) for the propagation velocity of the stationary wave of detonation

$$\lambda_1^2 = \frac{2 + 4\Phi}{1 + 4\Phi \frac{k-1}{k+1}}; \quad (75)$$

b) for the maximum propagation velocity of the wave of burning

$$\lambda_1^2 = \frac{1}{2 + 4\Phi}. \quad (76)$$

Using the known connection between the velocity coefficient and the M number, it is possible to obtain also similar dependences of the M number for cases of detonation and burning on the thermal characteristic of the gas mixture.

Figure 5.19a and 5.19b show graphs of the dependence

$$\lambda_1 = f(\Phi) \quad \text{and} \quad M_1 = F(\Phi)$$

for the gas mixture (when $k = 1.4$). The upper branches of both curves (in the supersonic region of motion $\lambda_1 > 1$, $M_1 > 1$) correspond to the steady minimum propagation velocity of detonation and the lower branches (in the subsonic region $\lambda_1 < 1$, $M_1 < 1$) - the maximum rate of combustion, i.e., the maximally possible velocity of the normal propagation of the flame.



Fig. 5.19a.

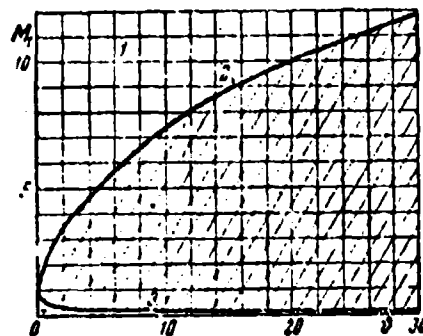


Fig. 5.19b.

Figure 5.19a. Dependence of the extreme value of the coefficient of the propagation velocity of the wave of burning on the thermal characteristic of the mixture: 1 - region of unsteady detonation; 2 - steady-state regime of detonation; 3 - maximum rate of combustion; 4 - region of normal burning.

Figure 5.19b. Dependence of the extreme value of the M number for the wave propagation of burning on the thermal characteristic of the mixture: 1 - region of unsteady detonation; 2 - steady-state regime of detonation; 3 - maximum rate of combustion; 4 - region of normal burning.

We arrive at the single concept of the propagation velocity of burning. In this case in the supersonic region (above the curve) the values which correspond to the nonstationary state of detonation lie, whereas in the subsonic region (below the curve) there is a countless multitude of values which correspond to the stationary normal propagation of burning at the low speeds of flow of the gas. Finally, the conditions which correspond to the shaded area (Figs. 5.19a and 5.19b) cannot be realized in connection with the phenomenon of the thermal critical region (i.e., the impossibility to transfer to the speed of sound during the heat feed).

By precisely this, apparently, one should explain the fact that the transition from slow burning to detonation, as experiments in the tubes show, is always achieved intermittently.

One should note one interesting feature of the curves obtained. As can be seen from the graphs, the most insignificant thermal effect suffices in order that the maximum rate of combustion becomes substantially lower and the detonation velocity substantially higher than the sonic.

Let us give the calculation of pressures with detonation and burning.

The calculation of the maximum expansion shock in the flame front attained with the thermal critical region can be produced by means of the momentum equation. In the case of $\lambda_3 = M_3 = 1$ we have¹

$$\frac{p_2}{p_1} = 1 + k \left(1 - \frac{w_2}{w_1} \right),$$

but in these conditions

$$\frac{w_2}{w_1} = \lambda_1 \sqrt{\frac{T_{01}}{T_{02}}},$$

whence, on the basis of dependence (71), we obtain

$$\frac{w_2}{w_1} = 1 - \sqrt{1 - \frac{T_{01}}{T_{02}}}. \quad (77)$$

Thus, the maximum pressure drop in the gas flow in the region of burning is equal to

$$\frac{p_2}{p_1} = 1 + k \sqrt{1 - \frac{T_{01}}{T_{02}}}. \quad (78)$$

¹In order to obtain this expression, let us write the momentum equation (94) of Chapter I for our case:

$$p_2 - p_1 = \rho_1 w_1 (w_1 - w_2)$$

or

$$\frac{p_2}{p_1} - 1 = k \frac{\rho_1 w_1^2}{\rho_1 p_1} \left(1 - \frac{w_2}{w_1} \right),$$

but

$$\frac{\rho_1 w_1^2}{k p_1} = \frac{w_1^2}{a_1^2} = M_1^2 = 1.$$

or on the basis of expression (72)

$$\frac{p_2}{p_1} = 1 + k \frac{1 - \lambda_1^2}{1 + \lambda_1^2} = 1 + k \frac{\lambda_1^2 - 1}{\lambda_1^2 + 1}. \quad (79)$$

In this case the value of the velocity coefficient both in detonation and in the extreme case of normal burning is taken from the relation (74).

If we use equality (75), then the following approximation formula of the pressure drop in the second region of the wave of detonation (for $\lambda > 1$) is found:

$$\frac{p_2}{p_1} \approx 1 + \frac{1 + 8\lambda + \frac{1}{\lambda}}{1 + 8\lambda + \frac{1}{\lambda}}. \quad (80)$$

Correspondingly, equality (76) leads to the approximation expression of a drop in pressures for the maximum rate of the normal burning:

$$\frac{p_2}{p_1} \approx 1 + k \frac{1 + 4\lambda}{3 + 4\lambda}. \quad (81)$$

The pressure change in transit through the entire region of detonation, which consists of an adiabatic shock wave and combustion zone, will be obtained in the division of equality (63) into (79):

$$\frac{p_2}{p_1} = \frac{p_2}{p_1} \frac{p_1}{p_1} = \frac{\lambda_1^2 + 1}{k + 1 - (k - 1)\lambda_1^2}. \quad (82)$$

Very simple dependences are obtained for a density change of the gas. At the maximum speed of normal burning, on the basis of the equation of continuity and expressions (77) and (72), we obtain

$$\frac{\rho_2}{\rho_1} = \frac{w_1}{w_2} = \frac{2}{\lambda_1^2 + 1} = \frac{2\lambda_1}{1 + \lambda_1^2}. \quad (83)$$

With the steady-state condition of detonation burning, using equalities (16) of Chapter III and (62), we have

$$\frac{p_1}{p_2} = \frac{\rho_2}{\rho_1} \frac{p_2}{p_1} = \frac{2\lambda}{\lambda + 1}. \quad (84)$$

Let us discuss in more detail some general properties of the one-dimensional nonadiabatic waves, and let us give, in particular, the calculating equations for determining the absolute velocity of propagation of the wave. From the momentum and continuity equations it follows that in any case of the shock wave (in disregarding forces of friction) the following relation is correct:

$$\frac{p_2 - p_1}{\rho_2 - \rho_1} = w_1 w_2. \quad (85)$$

On the other hand, the equation of enthalpy, taking into account the equation of state of an ideal gas, gives for the pressure jump with any feed (or removal) of heat¹

$$\frac{p_2 - p_1}{\rho_2 - \rho_1} = a_{2,p}^2 + \frac{p_1}{\rho_2 - \rho_1} (a_{2,p}^2 - a_{1,p}^2). \quad (86)$$

¹Let us write the equation of enthalpy (25) of Chapter I for gas before and after the shock wave

$$c_p (T_2 - T_1) = A \frac{w_1^2}{2g}, \quad c_p (T_2 - T_1) = A \frac{w_2^2}{2g},$$

or, by replacing from the equation of state $T = \frac{p}{Rg\rho}$

$$p_1 = \rho_1 g R T_{01} - \frac{AR}{2c_p} \rho_1 w_1^2, \quad p_2 = \rho_2 g R T_{02} - \frac{AR}{2c_p} \rho_2 w_2^2$$

By subtracting from the second equation the first, taking into account the equalities

$$\frac{AR}{2c_p} = \frac{k-1}{2k}, \quad a_{i,p}^2 = \frac{2k}{k+1} g R T_i$$

and the law of the momenta, we obtain (86).

From equations (85), (86) and continuity, it is not difficult to derive the relation between velocities for the arbitrary pressure jump:

$$w_1 w_2 (w_1 - w_2) = a_{1sp}^2 w_1 - a_{1sp}^2 w_2 \quad (87)$$

In the particular case when the heat feed is absent and $a_{1kp}^2 = a_{3kp}^2$, we again obtain the relation (16) of Chapter III for the adiabatic shock wave.

In the case of interest to us of the steady-state detonation (or the propagation of burning at the maximum rate), when the thermal critical region begins, i.e., $\lambda_3 = 1$ and $w_3 = a_{3kp}$, equation (87) assumes the form

$$(w_1 - a_{3sp})^2 = a_{1sp}^2 - a_{1sp}^2 \quad (88)$$

whereupon for the detonation

$$w_1 > a_{3sp}$$

for the slow burning

$$w_1 < a_{3sp}$$

Just as in the dimensionless equations given previously, we have here two solutions:

$$w_1 = a_{3sp} \pm \sqrt{a_{1sp}^2 - a_{1sp}^2} \quad (89)$$

which correspond to the minimum rate of the propagation of detonation (with the + sign) and the maximum speed of slow burning (with the - sign).

The obtained general relations are used for any nonadiabatic pressure jumps without depending on the mechanism of heat liberation. We saw that in the two cases examined above of the propagation of the flame front immediately the thermal shock

(i.e., the combustion zone) represented both with detonation and with normal burning the expansion shock in the subsonic flow. It is not difficult to indicate the case of the thermal compression shock in the supersonic flow. We have in mind the well-known condensation shocks, which are accompanied by the transition from a higher supersonic velocity to a lower but still supersonic velocity. And in this case the equations and derivations given above remain valid.

In conclusion let us investigate the flow of gases behind the wave front.

Obtained above were the fundamental principles characterizing the gas flow passing through the region of the shock of detonation or flame with a fixed front, i.e., in a reversed scheme. Let us examine now which form all relations will acquire, if we pass to the normal scheme when the gas is fixed, and in it the wave of detonation or burning at the rate w_1 is propagated. In this case behind the shock-wave front there follow the still not ignited particles of gas with the velocity

$$w_1 = w_1 - w_p$$

and moving behind the region of burning are products of burning with the velocity

$$w_r = w_1 - w_p$$

where we understand w_x and w_r as absolute velocities. It is not difficult to see that in the case of the detonation

$$w_1 > w_2 > w_r$$

i.e., the flame front and products of burning move in the same direction as does the shock-wave front, but only the particle velocity in the flame front is higher than in the products of burning:

$$w_1 > w_r$$

In the case of normal burning, when

$$w_1 = w_1 < w_p$$

the value w_r is negative, i.e., the directions of motion of the products of burning and flame front are opposite.

As it was established, with the steady-state condition of detonation and with the maximum rate of normal burning, there occurs

$$w_2 = a_{2kp} \text{ or } \lambda_2 = 1,$$

in consequence of which in these conditions the rate of the motion of products of burning is equal to

$$w_r = w_1 - a_{1kp},$$

where according to dependence (89) obtained above

$$w_1 = a_{1kp} \pm \sqrt{a_{1kp}^2 - a_{1kp}^2}.$$

Hence we arrive at the following expression for the propagation velocity of products of burning in cases of stationary detonation and the maximum state of the normal burning:

$$w_r = \pm \sqrt{a_{1kp}^2 - a_{1kp}^2}. \quad (90)$$

The plus sign corresponds to detonation, and the minus sign - to normal burning.

Let us now find the values of velocity coefficients. For the shock-wave front we obtain $\lambda_1 = w_1/a_{1kp}$. For particles following directly after the shock-wave front,

$$\lambda_1 = \frac{w_1}{a_{1kp}} = \lambda_1 - \lambda_1 = \lambda_1 - \frac{1}{\lambda_1}, \quad (91)$$

since $a_{1kp} = a_{2kp}$. Finally, for products of burning according to (90) we have

$$\lambda_r = \frac{w_r}{a_{1kp}} = \pm \sqrt{1 - \frac{T_{01}}{T_{02}}}.$$

Hence by means of (72) we find

$$\lambda_r = \frac{\lambda_1 - 1}{\lambda_1 + 1}. \quad (92)$$

Positive values of λ_r are obtained with detonation ($\lambda_1 > 1$), and negative values are obtained with normal burning ($\lambda_1 < 1$). In the case of $\lambda_1 = 1$ we have $\lambda_r = 0$, i.e., with the motion of the wave at the speed of sound the gas remains fixed, which completely corresponds to the physical nature of the phenomenon¹.

The greatest value of the rate of products of normal burning $\lambda_r = -1$ is obtained, naturally, in the fixed mixture of infinite caloricity [$q = \infty$, i.e., $\lambda_1 = 0$, see (76)].

The maximum of the rate of products of detonation is reached also with infinite caloricity [with (75) $q = \infty$, $\lambda_1 = \frac{k+1}{k-1}$], but in this case, as it is not difficult to see from (92), it is equal to

$$\lambda_r = \frac{1}{k}.$$

Thus, *the absolute velocity of the motion of the burned particles is always less than the speed of sound*. This result is valid both during normal burning and detonation.

Meanwhile as it is not difficult to see from (91), the velocity of unburned particles (at the beginning of the combustion zone) in the case of detonation can be more than sonic; this is obtained in the state

$$\lambda_1 = \lambda_1 - \frac{1}{\lambda_1} > 1, \text{ i.e., when } \lambda_1^2 - \lambda_1 - 1 > 0.$$

Solving this inequality, we obtain

$$\lambda_1 > \frac{1 + \sqrt{5}}{2} = 1.62 \quad \text{and} \quad M_1 > 2.$$

¹Above [see (74)] it was shown that $\lambda_1 = 1$ is obtained only with zero caloricity of the mixture, when the detonation and burning degenerate into the usual shock waves.

The maximum value of this velocity, obviously, is obtained in the state $M_1 = \infty$ and $\lambda_1^2 = \frac{k+1}{k-1}$, and it is equal to

$$\lambda_{1 \max} = \sqrt{\frac{k+1}{k-1}} - \sqrt{\frac{k-1}{k+1}}.$$

if $k = 1.4$, then $\lambda_{x \max} = 2.04$ and $M_{x \max} = 3.4$.

An interesting result will be obtained if we connect the absolute gas velocity at the beginning and end of the zone of the detonation burning:

$$\frac{w_1}{w_r} = \frac{\lambda_1 a_{1sp}}{\lambda_r a_{rsp}}.$$

Hence, by using dependences (91), (92) and (72), we find the following simple relation:

$$w_1 = 2w_r \quad (93)$$

i.e., with detonation the particle speed before the flame front is always twice higher than the velocity of the burned particles.

The pressures both behind the shock-wave from (p_2) and at the end of the combustion zone (p_3), obviously, are not changed from the fact that we changed the motion, i.e., they can be determined by formulas (63) and (79). It is possible, however, by means of (92) to give to formula (79) the following very simple form:

$$\frac{p_3}{p_1} = 1 \pm k\lambda_r \quad (94)$$

Here the minus sign is taken during normal burning and the plus sign during detonation. In the limiting cases of normal burning ($\lambda_r = -1$) and detonation ($\lambda_r = \frac{1}{k}$), we obtain, respectively, for the maximum rate of normal burning

$$\frac{p_3}{p_1} = 1 + k \quad (95)$$

and for the minimum rate of detonation

$$\frac{p_1}{p_0} = 2. \quad (96)$$

With the encounter of products of burning with a poorly streamlined body, there will occur a pressure increase up to value p_{03} , which for both these states is found from the same expression, which corresponds to the isentropic process of compression:

$$\frac{p_1}{p_{01}} = \left(1 - \frac{k-1}{k+1} \lambda_1^2\right)^{\frac{k}{k-1}}. \quad (97)$$

The more considerable increase in pressure occurs with a cessation of the particles of the still unignited gas moving at the rate of w_x . In the state of $\lambda_x < 1$ the same isentropic dependence acts:

$$\frac{p_1}{p_{01}} = \left(1 - \frac{k-1}{k+1} \lambda_1^2\right)^{\frac{k}{k-1}}. \quad (98)$$

For supersonic conditions ($\lambda_x > 1$), when braking begins from the normal shock wave, which converts the flow to subsonic velocity $\lambda_x = \frac{1}{\lambda_x}$ and the pressure determined by formula (63)

$$\frac{p_1}{p_0} = \frac{1 - \frac{k-1}{k+1} \lambda_1^2}{1 - \frac{k-1}{k+1} \lambda_1^2}. \quad (99)$$

we have with the total stagnation

$$\frac{p_1}{p_{01}} = \left(1 - \frac{k-1}{k+1} \lambda_1^2\right)^{\frac{k}{k-1}} \quad (100)$$

or finally

$$\frac{p_1}{p_{01}} = \frac{1}{\lambda_1^2} \left(1 - \frac{k-1}{k+1} \lambda_1^2\right) \left(1 - \frac{k-1}{k+1} \frac{1}{\lambda_1^2}\right)^{\frac{1}{k-1}}.$$

In the extreme case $\lambda_1^2 = \frac{k+1}{k-1}$, i.e., $\lambda_x = 2.04$ (when $k = 1.4$), we obtained the maximum pressure increase with braking

$$\frac{P_{01}}{P_1} \sim 15,$$

or in comparison with the pressure in products of burning

$$\frac{P_{01}}{P_1} \sim 30.$$

With the encounter of the gases following directly behind the detonation, with a sharp-nosed obstruction an oblique shock wave can arise instead of a normal wave. In the latter case a pressure increase with the braking of the gases proves to be less.

§ 6. Calculation of Gas Flows by Means of Gas-Dynamic Functions

Established above were the numerical relationships between the pressure, density, temperature and velocity coefficient of the gas flow and also the stagnation parameters for some cases of the gas flows. These equations contain the parameters of the gas, in particular, the velocity coefficient λ , in high and fractional powers, and therefore their conversion, the obtaining of explicit dependences between the parameters in general, and the solution of the numerical problems frequently represent considerable difficulties. At the same time, in examining the different equations of gas flow, derived, for example, in § 4 of Chapter I and § 4 of Chapter V, it is possible to note that the value of the velocity coefficient λ enters into them in the form of several frequently encountered combinations or expressions which were called *gas-dynamic functions*. Given to these functions are abbreviated notations, and their values, depending on value λ and the adiabatic index k , are calculated and reduced to tables.

The gas-flow calculation by means of tables of gas-dynamic functions received widespread acceptance and is at present conventional. Besides the reduction in the calculating work, the advantage of the calculation with the use of gas-dynamic functions

is the considerable simplification in the conversions in the final solution of the fundamental equations, which makes it possible to obtain, in general, the solutions, of very complex problems. When such calculation the basic qualitative laws governing the flow and the relation between parameters of the gas flow are more clearly revealed. As it will be possible to see below, the use of gas-dynamic functions makes it possible to conduct the calculation of one-dimensional gas flows, taking into account the compressibility virtually as simple as the calculation of flows of an incompressible fluid is conducted.

Let us examine the basic gas-dynamic functions from those being used at present and in a number of examples illustrate their use for the solution of different problems.

The first and simplest group of gas-dynamic functions is introduced for the sake of simplicity in the recording of relationships between the parameters in the flow, the stagnation parameters and the velocity coefficient of the gas. In § 3 of Chapter I, by means of the transformation of the equation of enthalpy, we obtained formula (42)

$$\frac{T}{T_0} = 1 - \frac{k-1}{k+1} \lambda^2,$$

which connects the stagnation temperature T_0 with the temperature in the flow T and the velocity coefficient λ . Let us denote

$$1 - \frac{k-1}{k+1} \lambda^2 = \tau(\lambda). \quad (101)$$

In § 4 of Chapter I expressions (72) and (73) were obtained for ratio of pressure and density in the flow to the total pressure and density of the isentropically stagnant gas. Let us introduce for them the notations

$$\pi(\lambda) = \frac{p}{p_0} = \left(1 - \frac{k-1}{k+1} \lambda^2\right)^{\frac{k}{k-1}}, \quad (102)$$

$$\epsilon(\lambda) = \frac{p}{p_0} = \left(1 - \frac{k-1}{k+1} \lambda^2\right)^{\frac{1}{k-1}}. \quad (103)$$

The connection between gas-dynamic functions $\tau(\lambda)$, $\pi(\lambda)$ and $\epsilon(\lambda)$ results from the obvious relationship between values ρ , p and T :

$$\epsilon(\lambda) = \frac{\pi(\lambda)}{\tau(\lambda)}. \quad (104)$$

It should be noted that equations (101), (102) and (103) connect the parameters of the gas in the same cross section of the flow and are valid independently of the flow pattern and processes occurring in the gas: the transition from parameters in the flow to parameters of the stagnated gas by definition occurs on the ideal adiabatic curve. The nature of the change in the gas-dynamic functions $\tau(\lambda)$, $\pi(\lambda)$ and $\epsilon(\lambda)$, depending on λ , is shown on Fig. 5.20: with an increase in λ from zero to the maximum value $\lambda_{\max} = \sqrt{\frac{k+1}{k-1}}$ functions $\tau(\lambda)$, $\pi(\lambda)$ and $\epsilon(\lambda)$ monotonically decrease from unity to zero. This completely corresponds to their physical meaning: at very low velocities ($\lambda \rightarrow 0$) the parameters in the flow virtually do not differ from the parameters of the completely stagnant gas; with an increase in the velocity up to the limiting value ($M \rightarrow \infty$, $\lambda \rightarrow \lambda_{\max}$), the temperature, pressure and density of the gas at the finite value of the stagnation parameters tend to zero.

Having available graphs or tables in which for each value of λ values of functions $\pi(\lambda)$, $\epsilon(\lambda)$, and $\tau(\lambda)$ are given, it is possible to determine rapidly the stagnation parameters according to parameters in the flow and vice versa. Such tables for values $k = 1.40$ and 1.33 are given at the end of the book. Given there are auxiliary graphs, which can be used, instead of the tables, if high accuracy of the calculations is not required.

Example 1. In section 1 of the subsonic part of an ideal Laval nozzle the following are known: pressure in the flow $p_1 = 16 \text{ kg/cm}^2$, stagnation temperature $T_{01} = 400^\circ\text{K}$, and velocity

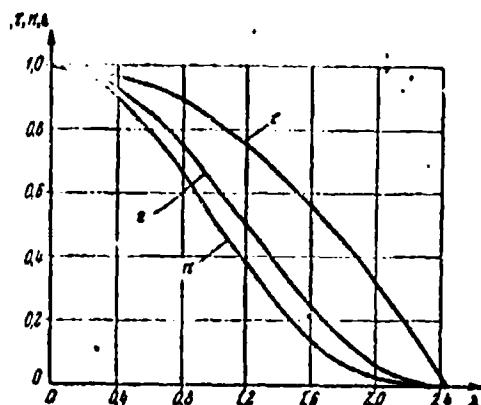


Fig. 5.20. Graphs of gas-dynamic functions $\tau(\lambda)$, $\epsilon(\lambda)$, and $\pi(\lambda)$ when $k = 1.4$.

coefficient $\lambda_1 = 0.6$. It is required to determine the velocity coefficient λ_2 and gas pressure in section 2, where the temperature T_2 is equal to 273°K.

Since the stagnation temperature and total pressure of the gas in the ideal nozzle in question are not changed, $T_{02} = T_{01}$ and $P_{02} = P_{01}$. Using the first equality and relation (101),

we write

$$\tau(\lambda_1) = \frac{T_1}{T_{01}} = \frac{T_2}{T_{01}}.$$

After substituting the assigned values T_2 and T_{01} , we find $\tau(\lambda_2) = 0.6825$ and from the tables determine (when $k = 1.40$) $\lambda_2 = 1.38$. Thus, the unknown section is located in the supersonic part of the nozzle. We further use the condition of constancy of the total nozzle pressure. By expressing the total pressure in terms of the pressure in the flow and function $\pi(\lambda)$ according to (102), we obtain

$$\frac{P_1}{\pi(\lambda_1)} = \frac{P_2}{\pi(\lambda_2)} \quad \text{or} \quad P_2 = P_1 \frac{\pi(\lambda_2)}{\pi(\lambda_1)}.$$

For $\lambda_1 = 0.6$ and $\lambda_2 = 1.38$ in the tables, we find the values of functions $\pi(\lambda)$ and determine

$$P_2 = 16 \frac{0.2628}{0.0053} = 5.23 \text{ kg/cm}^2.$$

Let us find now at the same initial data what the gas temperature will be in the section 3 of the nozzle, where the gas pressure is equal to the atmospheric $p_3 = 1.033 \text{ kg/cm}^2$. Let us write

$$\pi(\lambda_1) = \frac{P_1}{P_{01}} = \frac{P_2}{P_{02}} \quad \text{or} \quad \pi(\lambda_2) = P_2 \frac{\pi(\lambda_1)}{P_{01}}.$$

Hence we find

$$\pi(\lambda_3) = \frac{1.033}{16} 0.8053 = 0.052,$$

and then from the tables we determine the value $\lambda_3 = 1.85$. This value of the velocity coefficient in the table corresponds to $\tau(\lambda_3) = 0.4296$. Further, we easily find the gas temperature in section 3

$$T_3 = T_0 \tau(\lambda_3) = 400 \cdot 0.4296 = 171.5^\circ \text{K}.$$

Thus other problems connected with the determination of the dependence between the gas parameters in different cross sections of the flow are solved.

Let us examine further the two gas-dynamic functions which are used in the equation of the gas flow rate. Let us substitute into the expression of the gas flow rate per second, in terms of the cross section of the area F $G = \gamma w F$, the relations which express the specific weight of the gas γ and flow velocity w in terms of stagnation parameters p_0 and T_0 and the velocity coefficient λ :

$$\gamma = \gamma_0 \left(1 - \frac{k-1}{k+1} \lambda^2\right)^{\frac{1}{k-1}} = \frac{p_0}{RT_0} \left(1 - \frac{k-1}{k+1} \lambda^2\right)^{\frac{1}{k-1}},$$

$$w = \lambda a_{*p} = \lambda \sqrt{2g \frac{k}{k-1} RT_0}.$$

Then we will obtain

$$G = \frac{p_0}{RT_0} F \lambda \left(1 - \frac{k-1}{k+1} \lambda^2\right)^{\frac{1}{k-1}} \sqrt{2g \frac{k}{k-1} RT_0}. \quad (105)$$

After multiplying both sides of this equation by $a_{*p} = \sqrt{2g \frac{k}{k-1} RT_0}$ after cancellations we have

$$\frac{G}{g} a_{*p} = \frac{2k}{k+1} p_0 F \lambda \left(1 - \frac{k-1}{k+1} \lambda^2\right)^{\frac{1}{k-1}}. \quad (106)$$

This equation expresses the gas flow rate in this cross section in terms of the total pressure, the critical speed of sound and the

certain function of the velocity coefficient

$$\lambda \left(1 - \frac{k-1}{k+1} \lambda^2\right)^{\frac{1}{k-1}} = \lambda_*(\lambda)$$

where $\epsilon(\lambda)$ is the gas-dynamic function (103) introduced above. The new gas-dynamic function $q(\lambda)$ is defined as the value proportional to the product $\lambda \epsilon(\lambda)$:

$$q(\lambda) = \left(\frac{k+1}{2}\right)^{\frac{1}{k-1}} \lambda \left(1 - \frac{k-1}{k+1} \lambda^2\right)^{\frac{1}{k-1}}. \quad (107)$$

The proportionality factor is selected so that when $\lambda = 1$ we have $q(\lambda) = 1$. Because of this the gas-dynamic function $q(\lambda)$ acquires the physical meaning of the dimensionless current density:

$$q(\lambda) = \frac{\rho w}{(\rho w)_{kp}}.$$

where $(\rho w)_{kp}$ is the maximum value of the current density (with the assigned stagnation parameters), which corresponds to the flow at the speed of sound. Actually,

$$\frac{\rho w}{(\rho w)_{kp}} = \frac{\rho}{\rho_0} \frac{p_0}{p_{kp}} \frac{w}{w_{kp}} = \frac{\epsilon(\lambda)}{\epsilon(1)} \lambda = \left(\frac{k+1}{2}\right)^{\frac{1}{k-1}} \lambda_*(\lambda).$$

The graph of function $q(\lambda)$ is given on Fig. 5.21. With an increase in the velocity coefficient λ from zero to unit, the value $q(\lambda)$ increases from zero to its maximum value $q(\lambda) = 1$ and further is again lowered to zero at value $\lambda = \lambda_{\max}$. Thus, the current density is maximum when $q(\lambda) = 1$ and is decreased both with a decrease and an increase in the velocity in comparison with the critical value. The same value of function $q(\lambda)$ corresponds to two possible values of the velocity coefficient, one of which is more and the other less than unity.

Substituting function $q(\lambda)$ into expression (106), we have

$$\frac{Q}{K} a_{*p} = \frac{2k}{k+1} \left(\frac{2}{k+1}\right)^{\frac{1}{k-1}} p_0 q(\lambda) \quad (108)$$

By replacing in (108) quantity a_{np} by its value, we obtain the following formula for the calculation of the gas flow rate (see also § 1 of Chapter IV):

$$G = m \frac{p_0 F q(\lambda)}{\sqrt{T_0}} \quad (109)$$

where

$$m = \sqrt{k \left(\frac{2}{k+1} \right)^{\frac{k+1}{k-1}}} \sqrt{\frac{p_0}{R}} = N \sqrt{\frac{p_0}{R}}.$$

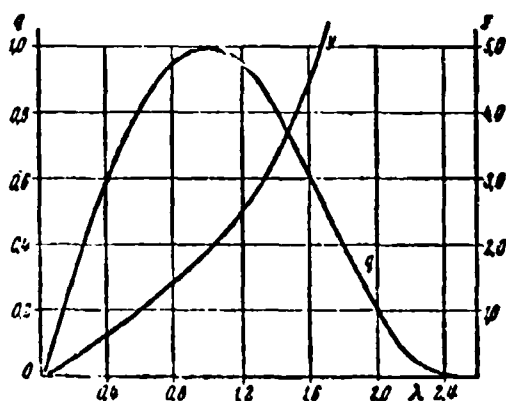


Fig. 5.21. Graphs of gas-dynamic functions $q(\lambda)$, $y(\lambda)$ when $k = 1.4$.

In the following table values of N for different values of k are given:

k	1.67	1.4	1.35	1.33	1.30	1.25	1.10
N	0.723	0.685	0.670	0.673	0.667	0.658	0.628

For air ($k = 1.4$, $R = 29.27$ kg-m/kg-deg) the numerical coefficient in equation (109) $m = 0.3965$

[deg^{0.5}.s⁻¹]. For exhaust gases

in turbojet engines ($k = 1.33$, $R = 29.4$ kg-m/kg-deg) $m = 0.389$.

For powder gases, on the average it is possible to consider that

$m = 0.343$. With flow at the speed

of sound $q(\lambda) = 1$, equation (109) is reduced to expression (8) obtained in Chapter IV for the calculation of the gas flow rate through the Laval nozzle according to the parameters of gas in the nozzle throat area.

In the solution of a number of problems, it is required to connect the gas flow rate not with the total but with the static pressure in the flow. It is easy to obtain such a connection from expressions (108) or (109) if we replace in their right sides the value of total pressure

$$p_s = \frac{p}{\pi(\lambda)} = \frac{p}{\left(1 - \frac{k-1}{k+1} \lambda^2\right)^{\frac{k+1}{k-1}}}.$$

Then we obtain the relations

$$\frac{G}{G_{cr}} = \frac{2k}{k+1} \left(\frac{2}{k+1}\right)^{\frac{1}{k-1}} p F y(\lambda) \quad (110)$$

and

$$G = m \frac{p F y(\lambda)}{\sqrt{T_0}} \quad (111)$$

where the function

$$y(\lambda) = \frac{q(\lambda)}{\pi(\lambda)} = \left(\frac{k+1}{2}\right)^{\frac{1}{k-1}} \frac{\lambda}{1 - \frac{k-1}{k+1} \lambda^2} \quad (112)$$

is the second gas-dynamic function with the aid of which it is possible to calculate the gas flow rate (see Fig. 5.21). Its values, just as the values of function $q(\lambda)$, for different values of k are given in tables and on auxiliary graphs at the end of the book. With an increase in λ function $y(\lambda)$ monotonically increases, whereupon when $\lambda \rightarrow \lambda_{\max}$, $y(\lambda) \rightarrow \infty$. Both formula (109) and formula (111) express the gas flow rate by means of parameters of its state in the cross section of the flow in question, and that is why they are valid independently of the nature of the processes occurring in the flow of gas. Formulas (109) and (111) are conveniently used in the compilation of equations of continuity for the gas flow, whereupon for each cross section there can be selected that formula which corresponds better to the assigned or unknown values.

Expressions (109), (111) and the equations of continuity compiled with their aid directly lead to a number of dependences derived earlier by a more complex means and also make it possible to solve various problems quite simply. Let us give several examples of the calculation.

Example 2. Determine the dependence between the area of any cross section of an ideal Laval nozzle and the velocity coefficient of the flow in this cross section, i.e., find the law of a change in the area in the Laval nozzle. Since for any cross section of an ideal nozzle, the flow rate, total pressure and stagnation temperature are identical, then from (109) it follows that $Fq(\lambda) = \text{const.}$ Since for critical cross sections $q(\lambda)_{\text{kp}} = 1$, then $Fq(\lambda) = F_{\text{kp}}$ or $\frac{F}{F_{\text{kp}}} = \frac{1}{q(\lambda)}$, i.e., the cross-sectional area of the nozzle varies indirectly proportional to the value of function $q(\lambda)$. In accordance with the graph of function $q(\lambda)$, this means that with an increase in the velocity the area decreases at subsonic velocities and increases at supersonic velocities, having a minimum when $\lambda = 1$.

Example 3. In the section of the cylindrical tube between the two cross sections 1 and 2 as a result of hydraulic losses (friction, local resistances) the total pressure of the moving gas is lowered. The losses of total pressure between cross sections 1 and 2 are estimated by the value of the coefficient of total pressure $\sigma = p_{02}/p_{01} < 1$. Determine the nature of the change in the velocity and static pressure of the gas in the tube in the absence of heat exchange with the environment. Let us write, after making use of formula (109), the condition of the equality of the gas flow rates in cross sections 1 and 2:

$$\frac{p_{01} F_1 q(\lambda_1)}{\sqrt{T_{01}}} = \frac{p_{02} F_2 q(\lambda_2)}{\sqrt{T_{02}}}.$$

Since in this case $F_1 = F_2$ and $T_{01} = T_{02}$, then

$$q(\lambda_2) = \frac{p_{01}}{p_{02}} q(\lambda_1) \quad \text{or} \quad q(\lambda_2) = \frac{1}{\sigma} q(\lambda_1).$$

Hence according to the assigned values of λ_1 and σ , it is possible with the aid of tables of gas-dynamic functions to determine λ_2 . The obtained result is valid both for subsonic

and supersonic flow velocities. Since $\sigma < 1$, then $q(\lambda_2) > q(\lambda_1)$.

From this inequality it follows (see the plotted function $q(\lambda)$ on Fig. 5.21) that in the presence of flow friction (when $G = \text{const}$, $F = \text{const}$, $T_0 = \text{const}$) the velocity of the subsonic flow along the length of the tube increases, and the velocity of the supersonic flow decreases.

In order to determine the change in static pressure, it is possible to compare with each other values $p_1 = p_{01}\pi(\lambda_1)$ and $p_2 = p_{02}\pi(\lambda_2)$. However, a more clearly unknown result can be obtained from the condition of the equality of the gas flow rates if we use in this case expression (111)

$$\frac{p_1 F_1 y(\lambda_1)}{\sqrt{T_{01}}} = \frac{p_2 F_2 y(\lambda_2)}{\sqrt{T_{02}}} \quad \text{or} \quad \frac{p_1}{p_2} = \frac{y(\lambda_1)}{y(\lambda_2)}.$$

Since function $y(\lambda)$ is increasing, then hence we conclude that in the presence of resistance, in accordance with the change in the velocity coefficient found above, the static pressure will decrease if the flow velocity is subsonic and increase if the velocity is supersonic.

Example 4. Determine the velocity coefficient λ_2 and static pressure of the air p_2 at outlet from the diffuser, if it is known that at the inlet to the diffuser the total pressure $p_{01} = 3 \text{ kg/cm}^2$, the velocity coefficient $\lambda_1 = 0.85$, the area ratio of the outlet and inlet sections $F_2/F_1 = 2.5$ and the coefficient of total pressure $\sigma = p_{02}/p_{01} = 0.94$. To solve the problem we write the equation of continuity, using formula (109)

$$\frac{p_{01} F_1 q(\lambda_1)}{\sqrt{T_{01}}} = \frac{p_{02} F_2 q(\lambda_2)}{\sqrt{T_{02}}}.$$

Disregarding the heat exchange through walls of the diffuser, we have $T_{02} = T_{01}$, and therefore, $q(\lambda_2) = \frac{1}{\sigma} \frac{F_1}{F_2} q(\lambda_1)$. According to

tables for $\lambda_1 = 0.85$ we find $q(\lambda_1) = 0.9729$. Then $q(\lambda_2) = 0.425 \cdot 0.9729 = 0.413$, to which corresponds $\lambda_2 = 0.27$ and $\pi(\lambda_2) = 0.9581$. From the relation (102) we have $p_2 = p_{02}\pi(\lambda_2) = \sigma p_{01}\pi(\lambda_2)$ or $p_2 = 0.94 \cdot 3 \cdot 0.9581 = 2.7 \text{ kg/cm}^2$.

Example 5. With the compressor testing, in its outlet cross section, the area of which $F = 0.1 \text{ m}^2$ the static pressure $p = 4.2 \text{ kg/cm}^2$ and the stagnation temperature of the air $T_0 = 480^\circ\text{K}$ are measured. Determine the total pressure of the air if its flow rate $G = 50 \text{ kg/s}$.

From the equation of flow rate (m) we determine the function $y(\lambda)$ in terms of the known value of the static pressure of the air:

$$y(\lambda) = \frac{G \sqrt{T_0}}{m p \lambda} = \frac{50 \sqrt{480}}{0.3595 \cdot 4.2 \cdot 0.1 \cdot 10^5} = 0.678.$$

From the tables of gas-dynamic functions, we find that the values $\lambda = 0.406$ and $\pi(\lambda) = 0.907$ correspond to this value $y(\lambda)$. Hence the total air pressure $p_0 = p/\pi(\lambda) = 4.2/0.907 = 4.63 \text{ kg/cm}^2$.

If we do not use gas-dynamic functions, then the similar calculations which are frequently made in the processing of experimental data must be carried out by a more complex method, by means of successive approximation.

Let us examine the gas-dynamic functions which are used in the equation of the momentum of gas. The sum of the per-second momentum and force of pressure of the gas in the cross section of the flow in question can be called the total momentum of flow I

$$I = \frac{G}{g} w + pF = \frac{G}{g} \left(w + \frac{p}{\rho} \right). \quad (113)$$

If in (113) we substitute the relations

$$w = \lambda a_{sp}; \quad \frac{p}{\rho} = gRT = gRT_0 \left(1 - \frac{k-1}{k+1} \lambda^2\right) = \frac{k+1}{2k} a_{sp}^2 \left(1 - \frac{k-1}{k+1} \lambda^2\right),$$

then we obtain

$$\frac{Q}{g} w + pF = \frac{Q}{g} \left[\lambda a_{sp} + \frac{k+1}{2k} \frac{a_{sp}^2}{\lambda} \left(1 - \frac{k-1}{k+1} \lambda^2\right) \right]. \quad (114)$$

After the opening of the brackets and simplifications, we reduce expression (114) to the form

$$\frac{Q}{g} w + pF = \frac{k+1}{2k} \frac{Q}{g} a_{sp} z(\lambda) \quad (115)$$

where

$$z(\lambda) = \lambda + \frac{1}{\lambda}. \quad (116)$$

The graph of the gas-dynamic function $z(\lambda)$ is given in Fig. 5.22. The minimum value of function $z(\lambda) = 2$ corresponds to the critical rate of flow ($\lambda = 1$). Both in subsonic and supersonic flows $z(\lambda) > 2$; any real flow conditions do not correspond to values $z(\lambda) < 2$. It is easy to see that with the replacement of value λ by the value opposite to it $\lambda' = 1/\lambda$ the value of function $z(\lambda)$ does not change. Thus, one value of $z(\lambda)$ can correspond to *two mutually opposite values of the velocity coefficient* λ - one of them determines the subsonic and the other the supersonic gas flow. Let us note also that function $z(\lambda)$, unlike all remaining gas-dynamic functions, does not depend on the value of the adiabatic index k .

Expression (115) for the momentum of flow considerably simplifies recording and transformation of the equation of the momentum of gas. It proves to be extremely useful in the solution of a wide range of problems of gas dynamics as, for example, in the calculation of flows with shock waves, heat feed and cooling, flows with friction and with a shock during sudden expansion of the channel, in the calculation of the process of the mixing of flows, in the determination of forces which act on

walls of the channel, in the calculation of reactive thrust, and so on.

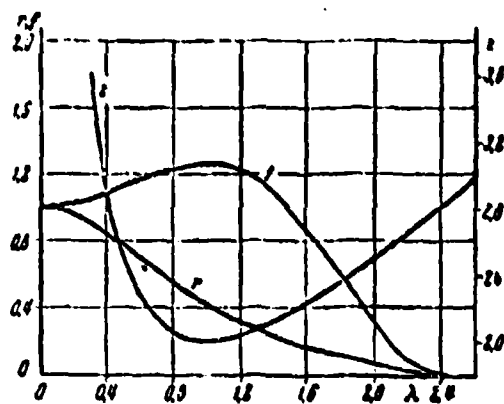


Fig. 5.22. Graphs of gas-dynamic functions $z(\lambda)$, $f(\lambda)$, $r(\lambda)$ when $k = 1.4$.

The following two examples make it possible to show visually how the solving of problems is simplified when using relation (115). In the first of them the previously solved problems (Chapter III § 1) of the normal shock wave is examined, and in the second - the problem of the flow of the preheated gas in the cylindrical tube.

Example 6. Determine the relationships between the gas parameters before and after the normal shock wave.

The relationship between the gas parameters in the shock wave was established above by us on the basis of the fact that with transition through the normal shock the total energy, flow rate and momentum of flow are maintained constant. Let us write the same equations with the use of gas-dynamic functions.

The equation of momentum or the momentum of the flow

$$\frac{G_1}{g} \cdot w_1 + p_1 F_1 = \frac{G_2}{g} \cdot w_2 + p_2 F_2$$

taking into account expression (115), assumes the form

$$G_1 a_{kp1} z(\lambda_1) = G_2 a_{kp2} z(\lambda_2)$$

From equations of the conservation of flow rate and total energy, we have

$$G_1 = G_2 \quad T_{01} = T_{02} \quad \text{or} \quad a_{kp1} = a_{kp2}$$

Taking this into account and reducing the corresponding values of flow rate and speed of sound in the momentum equation, we obtain

$$z(\lambda_1) = z(\lambda_2).$$

This equation has two solutions: either $\lambda_2 = \lambda_1$, which corresponds to the shock-free flow with the constant gas parameters, or

$$\lambda_2 = \frac{1}{\lambda_1},$$

which corresponds to the normal shock. The same expression - the basic kinematic relation of the theory of shock waves - was obtained above, see formula (16) in Chapter III.

According to the known value of the velocity coefficient, with the aid of the equation of continuity, a change in the total and static pressures in the shock wave is easily determined. Since $F_2 = F_1$ and $T_{02} = T_{01}$, then by using formulas (109) and (111), it is possible to present the equation of continuity for the flow of gas before and after the shock in the form

$$\rho_0 q(\lambda) = \rho_0 q(\lambda) \quad \text{or} \quad \rho_0 y(\lambda) = \rho_0 y(\lambda).$$

Hence, taking into account that $\lambda_2 = \frac{1}{\lambda_1}$, it follows that

$p_{02}/p_{01} = q(\lambda_1)/q\left(\frac{1}{\lambda_1}\right)$; $p_2/p_1 = y(\lambda_1)/y\left(\frac{1}{\lambda_1}\right)$. These relations are equivalent to equations (24) and (21) of Chapter III but are obtained by a considerably simpler means.

Example 7. The gas which moves in the cylindrical tube is heated by means of heat exchange through the walls of the tube. As a result of the heat feed the stagnation temperature of the gas is increased from 400°K at the inlet into the tube to 800°K at the outlet from it. The velocity coefficient of flow at the inlet into the tube $\lambda_1 = 0.4$. It is required to determine, disregarding friction, the coefficient of flow velocity after preheating and also the change in the total and static pressures in the flow.

The fundamental relation which determines the laws governing the gas flow in the cylindrical tube with the heat feed will be obtained from the equation of momentum. In this case it takes the form of

$$\frac{G}{g} w_1 + p_1 F = \frac{G}{g} w_2 + p_2 F,$$

since the heat feed is not connected with the force effect on the flow, and the forces of pressure in the initial and final cross section are the only forces which produce a change in the momentum of the gas. After replacing expressions for the momenta of the flow of gas according to relation (115) and considering that the heat capacity of the gas and the adiabatic index with preheating do not change, we will obtain

$$a_{sp_1} z(\lambda_1) = a_{sp_2} z(\lambda_2) \text{ or } z(\lambda_2) = z(\lambda_1) \sqrt{\frac{T_{01}}{T_{02}}}.$$

Since when $\lambda_1 = 0.4$ we have $z(\lambda_1) = 2.9$, then

$$z(\lambda_2) = 2.9 \sqrt{\frac{100}{800}} = 2.05$$

With the aid of the tables of function $z(\lambda)$ or the direct calculation from the quadratic equation $\lambda_2 + 1/\lambda_2 = 2.05$, we determine the two possible values of the velocity coefficient at the outlet: $\lambda_2' = 0.8$, $\lambda_2'' = 1/\lambda_2' = 1.25$. The real solution will be only the first solution, since by preheating it is not possible to transfer the subsonic flow into supersonic (see § 4)

By knowing the coefficient of flow velocity $\lambda_2 = 0.8$, it is easy to determine the change in the total and static pressures in the process of preheating. To do this, just as in the foregoing example, it is possible to use the equation of continuity from which for the given case ($G = \text{const}$, $F = \text{const}$) it follows that

$$\frac{p_{02}}{p_{01}} = \frac{q(\lambda_2)}{q(\lambda_1)} \sqrt{\frac{T_{01}}{T_{02}}} = \frac{0.7597}{0.7518} \sqrt{\frac{800}{100}} = 0.875,$$

$$\frac{p_2}{p_1} = \frac{q(\lambda_2)}{q(\lambda_1)} \sqrt{\frac{T_{01}}{T_{02}}} = \frac{0.6182}{1.1125} \sqrt{\frac{800}{100}} = 0.618.$$

then both the total and static pressures, as a result of the preheating of the gas, decrease. The obtained value $p_2/p_1 = 0.648$ and is that relationship of the static pressures of the gas in the initial and final cross sections of the section of the tube in question which must be created in order to maintain at this preheating the assigned magnitude of the velocity coefficient at the inlet $\lambda = 0.8$.

The equation of the conservation of momentum makes it possible to establish some general laws governing the flow in a cylindrical tube with preheating or cooling. Thus, for instance, it is easy to see that with an increase in the ratio T_{02}/T_{01} the value of the function $z(\lambda_1)$ (when $z(\lambda_1) = \text{const}$) always decreases. In accordance with the nature of the course of function $z(\lambda)$ (Fig. 4.25), this means that with an increase in preheating in the subsonic flow the velocity coefficient increases, while in supersonic flow it decreases. In both cases the flow velocity will approach the critical value $\lambda_2 = 1$ at which function $z(\lambda)$ takes smallest possible value $z(\lambda_2) = 2$. This causes the value of the maximally possible preheating for the assigned initial velocity $(T_{02}/T_{01})_{\text{max}} = z^2(\lambda_1)/4$. For the values of the parameters taken in this example the maximum value of the preheating corresponds to $T_{02} = 840^\circ\text{K}$. From the equations of flow rate it is possible to determine the pressure ratio p_2/p_1 necessary for the realization of such conditions while maintaining $\lambda_1 = \text{const}$. With an increase in the preheating above the indicated value, we will obtain $z(\lambda_1) < 2$, which indicates the physical impossibility of such preheating at the assigned rate of flow at the inlet.

After replacing in relation (115) the product $\frac{G}{\rho} a_{*1}$ with its value according to (108) or (110), we obtain the expression for the momentum of the gas flow in the first case in terms of the total pressure and in the second case in terms of the static pressure:

$$\frac{G}{\rho} w + pF = \left(\frac{2}{k+1} \right)^{\frac{1}{k-1}} p_0 F q(\lambda) z(\lambda)$$

and

$$\frac{q}{g} w + pF = \left(\frac{2}{k+1}\right)^{\frac{1}{k-1}} pF y(\lambda) z(\lambda)$$

Let us introduce the notations for the two new functions of the velocity coefficient λ which enter into the right sides of these expressions:

$$f(\lambda) = \left(\frac{2}{k+1}\right)^{\frac{1}{k-1}} q(\lambda) z(\lambda) = (k+1) \left(1 - \frac{k-1}{k+1} \lambda^2\right)^{\frac{1}{k-1}}, \quad (117)$$

$$r(\lambda) = \left(\frac{k+1}{2}\right)^{\frac{1}{k-1}} \frac{1}{y(\lambda) z(\lambda)} = \frac{1 - \frac{k-1}{k+1} \lambda^2}{1 + \lambda^2}. \quad (118)$$

By substituting these notations, we finally obtain

$$\frac{q}{g} w + pF = pJ f(\lambda) \quad (119)$$

$$\frac{q}{g} w + pF = \frac{pF}{r(\lambda)}. \quad (120)$$

Function $r(\lambda)$ is introduced as the value opposite to the product $y(\lambda) z(\lambda)$ in order to facilitate the use of the tables (product $y(\lambda) z(\lambda)$ rapidly increases with an increase in λ , approaching infinity at $\lambda \rightarrow \lambda_{\max}$; value $r(\lambda)$ changes within the limits of unity to zero). The graphs of functions $f(\lambda)$ and $r(\lambda)$ are given on Fig. 5.22)

Equations (119) and (120) show the number of properties of the momentum of gas flow. Let us focus attention on the fact that on the right side of these equations there are no values of gas flow rates and temperature or critical velocity. Hence it follows that if at the assigned cross-sectional area F and velocity coefficient λ the total or static pressure in the flow is constant, then the momentum retains a constant value independently of the temperature and gas flow rate.

The physical meaning of this consists in the fact that with a change in temperature (or stagnation temperature) in the gas when $\lambda = \text{const}$ the velocity of flow varies directly proportional and the flow rate inversely proportional to the square of the temperature so that the product Gw remains constant. Let us note that function $f(\lambda)$ in the region of the subsonic and low supersonic velocities changes very little (approximately 10% in the interval $\lambda = 0.55-1.35$). Hence, according to (119), it follows that the momentum of the gas flow at constant total pressure and cross-sectional area weakly depends on value λ over a wide range of its change and is determined basically by the value of product $p_0 F$.

Expressions (119) and (120) for the momentum of gas are very convenient in the solution of problems connected with the determination of forces which act on the part of the gas on walls of the channel, which is necessary, in particular, in the calculation of the reactive thrust of different engine installations.

For the reactive thrust of rocket engine, above (§ 8 of Chapter I) we obtain the expression

$$P = \frac{G}{g} w_a + (p_a - p_a) F_a$$

This formula determines the thrust of a jet engine of any type when operating at the place where the initial momentum of the air which enters into the engine is equal to zero. We convert this formula with the aid of the relations obtained above, for which on its right side we replace the expression of the momentum of gas in the nozzle exit section according to formulas (119) and (120). In the first case we obtain

$$P = p_a F_a \left(\frac{1}{\lambda_a} \right) - p_a F_a \quad \text{or} \quad P = p_a F_a \left(\Pi_0 / \lambda_a - 1 \right), \quad (121)$$

where $\Pi_0 = p_{0a} / p_a$ is the available pressure ratio in the nozzle.

In exactly the same manner it is possible to obtain the second expression

$$P = p_n F_n \left[\frac{p_n}{p_n} \cdot \frac{1}{r(\lambda_a)} - 1 \right] \text{ or } P = p_n F_n \left[\frac{n}{r(\lambda_a)} - 1 \right], \quad (122)$$

where $n = p_a/p_n$ is the so-called *off-design ratio of the nozzle*, i.e., the ratio of the static pressure of the gas in the nozzle edge to the atmospheric pressure.

Formula (121) is very convenient for the calculation of reactive thrust and is widely applied in the calculation of engines. The velocity coefficient λ_a is determined by the type of the jet nozzle and by the available pressure ratio. If the nozzle is made nonexpanding and the pressure ratio exceeds the critical value, then $\lambda_a = 1$; for a supersonic nozzle $\lambda_a = \lambda_{pac}$ at all values of Π_0 greater than the computed value and in the considerable part of the range $\Pi_0 < \Pi_{pac}$. Hence it follows that over a wide range of conditions of contemporary engines $\lambda_a = \text{const}$, and by formula (121) the linear dependence of the reactive thrust on the value of the available pressure ratio Π_0 is defined, since $f(\lambda_a) = \text{const}$. Let us recall that also when $\lambda_a \neq \text{const}$ the value of function $f(\lambda)$ is very little affected in the considerable region of the subsonic and supersonic velocities.

Formula (122) is convenient for the calculation of thrust in conditions when the static pressure in the nozzle edge is equal to the atmospheric pressure and $n = 1$. Such conditions exist, in particular, at the subsonic speed of the outflow of gas from the nozzle, and also in the operation of supersonic nozzles in design conditions.

Let us note that for the calculation of reactive thrust, according to (121) and (122) it is not required to know the gas flow rate and its temperature. The temperature change, as can be seen from (121) and (122), when $p_n = \text{const}$, $p_0 = \text{const}$ and $F = \text{const}$ does not at all affect the thrust level, which is

connected with the mutually inverse dependence of the discharge velocity and gas flow rate on temperature.

Expressions (121) and (122) can be used also for the calculation of the thrust of jet engines in flight; in this case on the right side it is necessary to subtract the so-called input momentum of the airflow $G_a w_H / g$, where G_a is the rate of air flow and w_H - the flight velocity (see § 8 of Chapter I).

Let us examine the examples of the use of given expressions of reactive thrust.

Example 8. Determine how the value of reactive thrust depends on the velocity coefficient of the gas at nozzle exit when $\Pi_0 = \text{const.}$

From formula (121) it directly follows that if $F_a = \text{const}$ and $\Pi_0 = \text{const.}$, then the dependence of the thrust on the velocity coefficient λ_a is determined by a change in function $f(\lambda)$. Under these conditions, however, with a change in λ , the gas flow rate changes.

There is great practical interest in another case of the change in the velocity coefficient λ_a , when the flow rate per second and the initial parameters of the gas are maintained constant. This condition can be realized if in the constant throat area of the supersonic nozzle F_{np} we change the discharge area F_a . The nature of the dependence of thrust on value λ_a in this case will make it possible to determine the rational expansion ratio of the nozzle for an engine with the assigned parameters and gas flow rate. Equations (120) and (121) are not completely convenient for such a calculation, since they include the two variables λ_a and F_a . Therefore, let us transform the equation F_a by means of the equation of the flow rate

$$F_a = \frac{G \sqrt{T_{0a}}}{m p_{0a} q(\lambda_a)} = \frac{F_{np}}{q(\lambda_a)}.$$

Taking into account the relationship between functions $f(\lambda)$, $q(\lambda)$ and $z(\lambda)$, we obtain

$$P = p_{0a} F_{\kappa p} \left[\left(\frac{2}{k+1} \right)^{\frac{1}{k-1}} z(\lambda) - \frac{1}{\Pi_0 q(\lambda)} \right].$$

In the design conditions of the outflow of gas, i.e., with expansion up to atmospheric pressure, the velocity coefficient is determined from the relation

$$\kappa(\lambda_a) = \frac{1}{\Pi_0}.$$

In terms of this value λ_a the design expansion ratio of the nozzle $F_a/F_{\kappa p} = 1/q(\lambda_a)$ and the value of reactive thrust in design conditions are sought. In this calculation the losses in total pressure between cross sections $F_{\kappa p}$ and F_a are not considered.

Let us assume that $k = 1.33$ and $\Pi_0 = 25$; then in the design operating mode of the nozzle

$$\kappa(\lambda_a) = \frac{1}{25} = 0.04, \lambda_a = 1.97, q(\lambda_a) = 0.279, \\ z(\lambda_a) = 2.477.$$

The discharge area of such a nozzle is equal to $F_{\kappa p}/q(\lambda_a) = 3.58 F_{\kappa p}$, and the thrust $P = 1.417 p_{0a} F_{\kappa p}$. The values of P at other values of λ_a , i.e., other values of F_a , are determined with the aid of tables. Results of such calculations are given on Fig. 5.23. Shown there are values $F_a/F_{\kappa p}$ for each value of λ_a . From the graph it is evident that the greatest thrust value is obtained with the total nozzle expansion, i.e., with the design conditions of the outflow. However, the nature of the functional dependence of thrust on the velocity coefficient is such that even with a noticeable reduction in the value λ_a and $F_a/F_{\kappa p}$ in comparison with their values in design conditions, the magnitude of the thrust decreases insignificantly. This makes it possible in certain cases to use nozzles with an incomplete expansion of

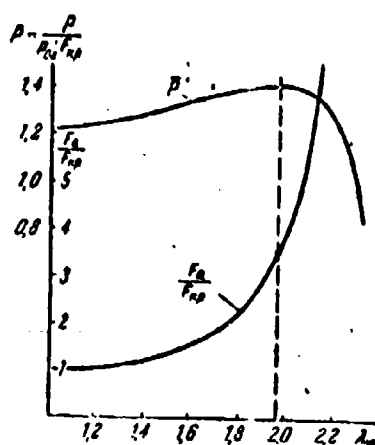


Fig. 5.23. Change in thrust with the assigned initial parameters and gas flow rate depending on the velocity coefficient at the nozzle exit (Example 8).

the gas and with the low supercritical pressure ratios p_0/p_H to use even the simple nonexpanding nozzles in which $\lambda_a = 1.0$. If one considers that in a nozzle with incomplete expansion there will be less losses of friction, then the reduction in thrust in comparison with the design conditions will be even less.

At the same time, as can be seen from Fig. 5.23, when $\lambda_a > \lambda_{\text{расч}}$, the thrust sharply decreases, i.e., it is inexpedient to use the nozzle with the overexpansions of the gas, even if one does not consider the increased losses of friction in it and the possibility of the formation of shock waves.

With the outflow of gas into a vacuum ($p_H = 0$) the thrust value varies in proportion to the value of the function $z(\lambda)$, i.e., monotonically increases with an increase in $\lambda_a > 1$. Actually, in this case the design conditions are

$$z(\lambda_a) = \frac{p_a}{p_{0a}} = 0; \quad \lambda_a = \lambda_{\text{max}}; \quad \frac{F_a}{F_{\text{ap}}} = \frac{1}{q(\lambda_a)} = \infty.$$

Since the nozzle of the outlet area cannot be made infinite, such design conditions cannot be realized. At any final value F_a/F_{ap} the thrust of the engine, which operates in a vacuum, will be less than a theoretically possible value. However, from graphs of functions $z(\lambda)$ and $q(\lambda)$ it is evident that with a considerable decrease in F_a/F_{ap} the reduction in the thrust is not very large. Thus, if instead of $F_a/F_{\text{ap}} = \infty$ we take (when $k = 1.33$) $F_a/F_{\text{ap}} = 10$, $q(\lambda_a) = 0.1$, $\lambda_a = 2.208$, then the thrust value with respect to the maximum theoretical value (when $\lambda_a = \lambda_{\text{max}} = 2.657$) will be

$$\frac{P}{P_{\max}} = \frac{z(\lambda_a)}{z(\lambda_{\max})} = \frac{2.661}{3.033} = 0.88;$$

when $F_a/F_{\max} = 20$, i.e., when $q(\lambda_a) = 0.05$ and $\lambda_a = 2.313$, $P/P_{\max} = 2.745/3.033 = 0.905$.

Examined in the following example is the problem of the flow of compressible gas with the sudden expansion of the channel, which is encountered in a number of practical problems. Above (§ 5 of Chapter I) we solved this problem for flow at low velocities, when it was possible to disregard the density change of the gas.

Example 9. For the measurement of the rate of air flow in the pipeline, installed on its straight section is a metering nozzle with the flow passage cross-sectional area F_2 equal to 0.45 of the area of the pipeline $F_1 = F_3$ (Fig. 5.24). It is required to determine the losses of total pressure which appear in the flow behind the nozzle as a result of a sudden expansion of the channel and also the velocity coefficient λ_3 after the alignment of the velocity field, if according to results of pressure measurements p_1 and Δp the velocity coefficient of the flow in the nozzle $\lambda_2 = 0.52$ is known. Determine also the reduction in static pressure in pipeline caused by the installation of nozzle.

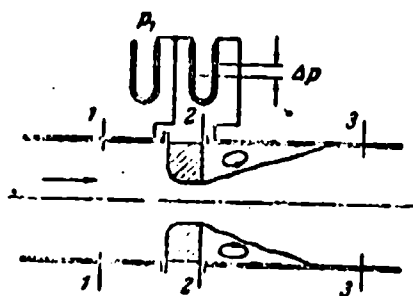


Fig. 5.24. Diagram of the installation of the nozzle for the measurement of the gas flow rate (Example 9).

Let us write the equation of the momentum for the section of the flow between cross sections 1 and 3, disregarding the wall friction and taking into account that at the subsonic velocities of the air in the nozzle the static pressure is constant in the whole cross section 2:

$$\frac{\rho}{g} (w_1 - w_3) = p_1 F_1 - p_3 F_3$$

or

$$\frac{Q}{k} \omega_1 + p_1 F_1 - \frac{Q}{k} \omega_2 - p_2 F_2 = p_1 (F_1 - F_2).$$

Let us now replace the expressions of momenta according to (115), and let us express the static pressure p_2 by means of the equation of the flow rate (110). The equation of the momentum takes the form

$$\frac{k+1}{2k} \frac{Q}{k} a_{sp} [z(\lambda_2) - z(\lambda_1)] = \frac{k+1}{2k} \left(\frac{k+1}{2} \right)^{\frac{1}{k-1}} \frac{Q}{k} a_{sp} \frac{1}{y(\lambda_1)} \left(\frac{p_2}{p_1} - 1 \right).$$

After cancellation we obtain

$$z(\lambda_2) = z(\lambda_1) + \left(\frac{k+1}{2} \right)^{\frac{1}{k-1}} \frac{1}{y(\lambda_1)} \left(\frac{p_2}{p_1} - 1 \right).$$

From this equation according to values λ_2 and F_3/F_2 the velocity coefficient λ_3 after the expansion of the tube is determined.

Let us note that the result does not depend on values of the pressure and gas temperature and is changed little depending on the adiabatic index k . After substituting into the latter equation the assigned values $\lambda_2 = 0.52$, $z(\lambda_2) = 2.44$, $y(\lambda_2) = 0.859$,

$$\frac{F_2}{F_3} = 0.45, \text{ we obtain } z(\lambda_3) = 2.44 + 1.577 \frac{1}{0.859} 1.22 = 4.68;$$

hence, according to tables we find $\lambda_3 = 0.225$, $q(\lambda_3) = 0.3475$, $y(\lambda_3) = 0.358$.

The losses of total pressure of the air between cross sections 2 and 3 is determined from the equation of continuity

$$\frac{p_{01} F_2 q(\lambda_2)}{\sqrt{T_{01}}} = \frac{p_{02} F_3 q(\lambda_3)}{\sqrt{T_{02}}}.$$

With the help of tables, hence we find

$$\epsilon = \frac{p_{02}}{p_{01}} = \frac{F_2 q(\lambda_2)}{F_3 q(\lambda_3)} = \frac{0.45 \cdot 0.7309}{0.3475} = 0.948.$$

In order to determine the change in the static pressure, it is necessary preliminarily to find the value of the velocity coefficient of the flow in the tube in front of the nozzle. Let us write the equation of the equality of the rate of air flow in cross sections 1 and 2, whereupon, taking into account that the length of section 1-2 is small, the contours of the nozzle are smooth and the flow is with acceleration, we consider the total pressure of the air in cross sections 1 and 2 to be identical. In this case the equation of continuity takes the form $F_1 q(\lambda_1) = F_2 q(\lambda_2)$. Hence we find $q(\lambda_1) = 0.45 \cdot 0.7309 = 0.329$, $\lambda_1 = 0.213$, $y(\lambda_1) = 0.338$. It is easy to see that similarly there can be obtained the result if between cross sections 1 and 2 there are losses of total pressure, being evaluated by the coefficient $\sigma = p_{02}/p_{01}$, the value of which is known. In this case we obtain

$$q(\lambda_1) = \frac{F_2}{F_1} q(\lambda_2).$$

A change in the static pressure on the entire section between cross sections 1 and 3 can be determined from the equation of continuity

$$\frac{p_1 F_1 y(\lambda_1)}{\sqrt{T_{01}}} = \frac{p_3 F_3 y(\lambda_3)}{\sqrt{T_{03}}}.$$

Since $T_{01} = T_{03}$ and $F_1 = F_3$, we have $p_3/p_1 = y(\lambda_1)/y(\lambda_3) = 0.338/0.358 = 0.944$.

Such a result can be obtained also from the relation

$$\frac{p_3}{p_1} = \frac{p_{03} \pi(\lambda_3)}{p_{01} \pi(\lambda_1)} = \frac{\pi(\lambda_1)}{\pi(\lambda_3)}.$$

Since $\lambda_3 > \lambda_1$, i.e., $\pi(\lambda_3) < \pi(\lambda_1)$, hence it is apparent that as a result of an increase in the flow velocity in the tube a reduction in the static pressure here, as in other local resistances when $\lambda < 1$ and $F_3 = F_1$, is somewhat larger than a reduction in the total pressure. In this case, in view of the smallness of the velocity coefficients in the tube λ_1 and λ_3 , this distinction is small.

In the following example we will again return to the examination of the flow of the gas being preheated in the cylindrical channel. Unlike the analysis carried out in § 3 of Chapter V and in Example 7 of this section, we will examine the case where a drop in pressures in the flow is assigned. This determines a number of features of the flows which could not be revealed above, when it was assumed to be that a drop in the pressures is always sufficient for the maintaining of the assigned velocity coefficients at the beginning and end of the tube.

Example 10. The afterburner of a turbojet engine is a cylindrical tube installed after the turbine with a nozzle of variable area at the outlet (5.25). In the chamber there occurs the burning of the additionally injected fuel, in consequence of which the gas temperature is increased. Let the flow parameters of the gas at the inlet into the chamber be $p_{01} = 1.98 \text{ kg/cm}^2$, $T_{01} = 880^\circ \text{K}$, and $\lambda_1 = 0.4$. These values should be maintained constant independently of the value of preheating of the gas, otherwise the operating mode of the turbine and compressor will be changed.

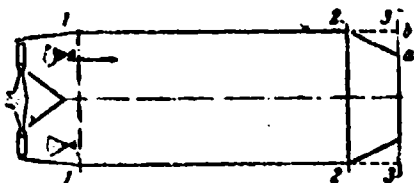


Fig. 5.25. Diagram of an afterburner of a turbojet engine: a - initial position of the nozzle, b - opened nozzle (Example 10).

Let us determine a maximally possible increase in gas temperature and the magnitude of losses of total pressure in the chamber in these conditions.

The assigned initial flow parameters determine the gas flow rate. As can be seen from the expression of the flow rate (109),

the more the stagnation temperature at chamber outlet, the larger, other conditions being equal, the cross-sectional area of the nozzle should be. Therefore, maximally possible preheating of the gas corresponds to the total opening of the nozzle.

Let us allow that the nozzle is made in such a way that with full expansion the area of its outlet section is equal to the area of the chamber, i.e., $F_3 = F_2 = F_1$ (position b on Fig. 5.25). The ratio of the total pressure at the inlet into the chamber to atmospheric pressure at the earth $\Pi_0 = p_{01}/p_H = 1.98/1.033 = 1.92$. This value somewhat exceeds the critical value (when $k = 1.33$), $\left(\frac{k+1}{2}\right)^{\frac{k}{k-1}} = 1.85$. Therefore, if the total pressure of the flow with preheating of the gas was maintained constant, then in the outlet section the rate of flow was equal to the speed of sound and $\lambda_3 = 1$. However, as we saw above (see Example 7), with the heat feed to the flow its total pressure is lowered, and therefore in this case it can be found that $p_{03}/p_H < 1.85$, and the discharge velocity will be subsonic.

In order to explain this, let us write the equation of the momentum of flow, expressing the momentum in cross section 1 in terms of the known total pressure p_{01} according to formula (119) and in cross section 3 - in terms of the static pressure p_3 (120), whereupon for the present we assume that the pressure p_3 is equal to the atmospheric pressure p_H , i.e., conditions of the outflow are subsonic. The wall friction and change in the adiabatic index are disregarded:

$$p_{01} F_1 f(\lambda_1) = p_3 F_3 \frac{1}{f(\lambda_3)}.$$

Hence (when $k = 1.33$) we find

$$f(\lambda_1) = \frac{p_{01}}{p_3 f(\lambda_3)} = \frac{1.92}{1.033 \cdot 1.7822} = 0.181,$$

and, further, according to the tables $\lambda_3 = 0.91$, i.e., $\pi(\lambda_2) = 0.6048$, $f(\lambda_3) = 1.2525$, $z(\lambda_3) = 2.01$

Conditions of the outflow of gas will actually be subsonic, no matter how great the preheating in the chamber was: the assigned total pressure of the gas which is being lowered in the process of the heat feed is insufficient for the producing

of sonic velocity of outflow into the atmosphere. If the total pressure p_{01} was high, for example, $p_{01} = 2.4 \text{ kg/cm}^2$, then from the latter formula it would follow that $r(\lambda_3) = 0.398$; this value is less than the critical, since $r(1) = 0.429$. Consequently, at such a pressure the outflow conditions would be critical and $\lambda_2 = 1.0$.

The value found of the velocity coefficient of flow at nozzle outlet ($\lambda_2 < 1$ or $\lambda_3 = 1$) makes it possible to find all the flow parameters. For determining the gas temperature it is convenient to use, for example, the momentum equation (115), from which it follows that

$$T_{01} = T_{01} \left[\frac{r(\lambda_2)}{r(\lambda_3)} \right]^2 = 880 \left(\frac{2.9}{2.01} \right)^2 = 1835 \text{ }^\circ\text{K}.$$

This is the limiting value of the stagnation temperature at the nozzle outlet. If we increase the preheating of the gas above this value, then the flow velocity at the inlet into the chamber will be lowered.

In order to determine the total pressure of the gas in the outlet section, in this case, it is possible to use the relation $p_{03} = p_H / \pi(\lambda_3) = 1.033 / 0.6048 = 1.71 \text{ kg/cm}^2$, which is correct when $\lambda_2 < 1$, i.e., when $p_3 = p_H$. By knowing p_{03} , we compute the coefficient of total pressure $\sigma = p_{03} / p_{01} = 1.71 / 1.98 = 0.865$.

To determine the changes in the total and static pressures in the process of preheating, it is possible to obtain simple relations, if we write the equality of the momenta of gas in the initial and final cross section in the form of

$$p_{01} F_1 f(\lambda_1) = p_{02} F_2 f(\lambda_2) \text{ and } p_1 F_1 \frac{1}{r(\lambda_1)} = p_2 F_2 \frac{1}{r(\lambda_2)}.$$

Hence we obtain

$$\sigma = \frac{p_{02}}{p_{01}} = \frac{f(\lambda_1)}{f(\lambda_2)}, \quad \frac{p_2}{p_1} = \frac{r(\lambda_1)}{r(\lambda_2)}.$$

These relations are valid in any flow conditions of the gas. Specifically, for conditions in this example we determine $\sigma = 1.0822/1.2525 = 0.865$.

The expressions obtained for σ and P_3/P_1 are convenient for the analysis of the nature of pressure change, determination of the maximum losses of total pressure and for obtaining certain other results found by a more complex means in § 3 of Chapter V.

Thus, for instance, from the equation for determining σ it follows that the preheating of the gas leads to a reduction in the total pressure both in subsonic and supersonic flows. Actually, since with preheating the value of the velocity coefficient always approaches unity (it increases when $\lambda < 1$ and decreases when $\lambda > 1$), then according to Fig. 5.22 the value of function $f(\lambda)$ in the process of preheating always increases, $f(\lambda_3) > f(\lambda_1)$ and $\sigma < 1$. Since in the region of subsonic velocities the limits of the change in value $f(\lambda)$ are small ($\sim 25\%$), then the coefficient of total pressure σ when $\lambda < 1$ cannot be lower than the certain limiting value

$$\sigma_{\min} = \frac{f(0)}{f(1)} = \frac{1.00}{1.2591} = 0.793 \quad (k = 1.33).$$

In supersonic flow, according to Fig. 5.22, any values of the coefficient of total pressure ($0 < \sigma < 1$) are possible.

On the other hand, with respect to a change in function value $r(\lambda)$, it is possible to establish the nature of a change in the static pressure in the flow of the preheated gas. At the subsonic velocity, when the velocity coefficient with the preheating of the gas increases, we have (see Fig. 5.22) $r(\lambda_3) < r(\lambda_1)$ or $P_3 < P_1$, i.e., the static pressure in the flow decreases. A maximum change in the static pressure, obviously, is equal to

$$\frac{r(1)}{r(0)} = \frac{1}{k+1}.$$

In supersonic flow, when $\lambda_3 < \lambda_1$, we have $r(\lambda_3) > r(\lambda_1)$ or $\lambda_3 > \lambda_1$.

Thus, with the preheating of the supersonic flow, despite of the reduction in total pressure, the static pressure increases as a result of a decrease in the velocity coefficient of the flow.

What will occur, if while maintaining the assigned pressure ratio p_{01}/p_{02} , we increase the gas temperature above the value obtained above $T_{02} = 1835^\circ$, i.e., increase the preheating?

Being diverted from the examination of the acting drop in pressures, on the basis of the formula derived in Example 7, it would be possible to arrive at the conclusion that since $\lambda_1 < 1$ and $\lambda_2 < 1$, then with an increase in the preheating the velocity coefficient λ_3 will increase, approaching $\lambda = 1$. However, this will be incorrect, since when using this formula always it is necessary to keep in mind that the results obtained from it are valid only under the condition of the sufficiency of the pressure drop acting on the flow; the more the preheating, the greater the pressure ratio p_{01}/p_{02} should be. This was repeatedly indicated above in solving the problems.

Actually, in this case when $p_{01} = \text{const}$ with an increase in preheating the losses of total pressure of gas increase and the total pressure of the gas in the outlet section of the tube is lowered, in consequence of which there is a decrease in the velocity coefficient λ_3 , which depends only on the ratio of the total and static pressures in the flow:

$$\lambda^2(\lambda) = p_0/p_{01} = p_{01}/p_{02}.$$

Thus, if $p_{01}/p_{02} = \text{const}$, then with an increase in the preheating, when p_{01} is lowered, the value of the velocity coefficient at the outlet (tube) does not increase but decreases. The velocity coefficient of the flow at the inlet into the tube also correspondingly decreases.

In order to determine the actual values of the velocity coefficients at the inlet and outlet with the assigned magnitudes of preheating T_{03}/T_{01} and drop in pressures between the inlet and output section, it is necessary to find the *joint solutions* of the equation (see Example 7)

$$z(0.1) = z(0.2) \sqrt{\frac{T_{01}}{T_{02}}}$$

from one of the following equations which express the constancy of the assigned drop in pressures, for example:

$$\frac{p_{01}}{p_{02}} = \frac{f(0.1)}{f(0.2)} = \text{const} \quad \text{or} \quad \frac{p_{01}}{p_{02}} = \frac{q(0.1)}{q(0.2)} \sqrt{\frac{T_{01}}{T_{02}}} = \text{const},$$

if the ratio of total pressures is assigned;

$$\frac{p_1}{p_2} = \frac{r(0.1)}{r(0.2)} = \text{const} \quad \text{or} \quad \frac{p_1}{p_2} = \frac{y(0.1)}{y(0.2)} \sqrt{\frac{T_{01}}{T_{02}}} = \text{const},$$

if the ratio of static pressures is assigned;

$$\frac{p_{01}}{p_1} = \frac{1}{r(0.1) \cdot f(0.1)} = \text{const} \quad \text{or} \quad \frac{p_{01}}{p_1} = \frac{y(0.1)}{q(0.1)} \sqrt{\frac{T_{01}}{T_{02}}} = \text{const},$$

if the ratio of the total pressure at the inlet to the static pressure at the outlet from the tube (available pressure ratio) is assigned. The latter case is encountered most frequently. The joint solution of the equations is most conveniently conducted by the graphic method with the aid of tables of gas-dynamic functions.

Common in the examples examined above of the gas flow was the fact that the flow velocity was directed along the axis of the channel.

In a number of problems of applied gas dynamics it is necessary to calculate such flows in which the *vector of absolute gas velocity comprises a certain angle with the axis of the flow*. Besides the axial velocity w_a , which determines the gas flow rate

and momentum along the axis of the flow, here there are velocity components in the plane perpendicular to the axis - radial w_r or circular w_t velocity of the particles of gas. Serving as an example can be the flow of twisted gas in the annular channel, which is encountered in different vortex apparatuses (circular component), or the expansion of the supersonic gas jet escaping into the atmosphere with a large excess pressure (radial component).

If the gas parameters in the flow cross section can be assumed to be constant, then for calculating such flows methods and formulas given in this section can be used.

At first glance it can be shown that for this it suffices in all the derived relations to take only the axial component of velocity into consideration. This, however, is not so, since at the assigned stagnation conditions the value of the temperature, static pressure, and gas density will also depend on the value of the circular (radial) velocity component; changes in the latter will affect the rate of discharge and momentum of flow. The fact is that according to the equation of energy and the relations (101), (102) and (103) obtained from it, the connection between the parameters in the flow and stagnation parameters is determined by a change in the absolute velocity (or the velocity coefficient calculated according to the absolute velocity and total stagnation temperature), independently of the angle being composed by the velocity vector with the axis.

Let us show how to generalize the relations obtained above for the case of motion from the tangential (radial) velocity component. Let us examine the one-dimensional flow of gas with the stagnation parameters p_0 and T_0 and the absolute velocity w making up the angle α with the axis of the flow. The gas flow rate per second through the cross section of area F , perpendicular to the axis, is equal to

$$Q = \gamma F w_a = \gamma F w \cos \alpha$$

where w_a is the axial component of the gas velocity. In the same way as in the derivation of formula (109), hence it is possible to obtain

$$Q = \frac{p_0}{kT_0} \left(1 - \frac{k-1}{k+1} \lambda^2\right)^{\frac{1}{k-1}} F \lambda a_{*p} \cos \alpha = m \frac{p_0 F q(\lambda)}{\sqrt{T_0}} \cos \alpha,$$

where

$$\lambda = \frac{w}{a_{*p}} = \frac{w}{\sqrt{2g \frac{k}{k+1} RT_0}}.$$

The latter relation can be rewritten in the form

$$Q = m \frac{p_0 F q(\lambda, \alpha)}{\sqrt{T_0}}, \quad (123)$$

where

$$q(\lambda, \alpha) = q(\lambda) \cos \alpha \quad (124)$$

is the gas-dynamic function $q(\lambda)$, generalized for the case of the flow of gas with the velocity component in the plane perpendicular to the axis. In exactly the same manner it is possible to obtain the formula similar to (111)

$$Q = m \frac{p_0 F y(\lambda, \alpha)}{\sqrt{T_0}}, \quad (125)$$

where

$$y(\lambda, \alpha) = y(\lambda) \cos \alpha \quad (126)$$

Thus, if angle α is assigned, then for the calculation of the gas flow rate and compilation of the equations of continuity, the same formulas as when $\alpha = 0$ are used, since the generalized functions $q(\lambda, \alpha)$ and $y(\lambda, \alpha)$ are determined from angle α and from values $q(\lambda)$ and $y(\lambda)$ for the velocity coefficient in the absolute flow of the gas.

The momentum of the flow of gas in the direction of the axis

$$I = \frac{Q}{g} w_a + pF = \frac{Q}{g} w \cos \alpha + pF.$$

By converting this expression similar to the way in which this was done in the solution of formula (115), we have

$$I = \frac{G}{g} \left(\omega \cos \alpha + \frac{pg}{\gamma \omega \cos \alpha} \right) = \frac{G}{g} \left[\lambda a_{sp} \cos \alpha + \frac{RT_0 g}{\lambda a_{sp} \cos \alpha} \left(1 - \frac{k-1}{k+1} \lambda^2 \right) \right]$$

or after the simplifications

$$I = \frac{k+1}{2k} \frac{G}{g} a_{sp} z(\lambda, \alpha), \quad (127)$$

where

$$z(\lambda, \alpha) = \frac{1}{\cos^2 \alpha} \left[\left(\frac{2k}{k+1} \cos^2 \alpha - \frac{k-1}{k+1} \right) \lambda + \frac{1}{\lambda} \right]. \quad (128)$$

Expression (127) is similar to the expression obtained when $\alpha = 0$ but contains instead of $z(\lambda)$ the generalized function $z(\lambda, \alpha)$, the graph of which is given on Fig. 5.26. When $\alpha = 0$ function $z(\lambda, \alpha)$ is reduced to $z(\lambda) = \lambda + 1/\lambda$; the minimum value of it $z(\lambda) = 2$ corresponds $\lambda = 1$. When $\alpha \neq 0$ the minimum values of function $z(\lambda, \alpha)$ are less than two, whereupon with an increase in angle α the minimums of the curves are displaced into the region of supersonic velocity.

For the conducting of numerical calculations, it is possible to compile tables of function $z(\lambda, \alpha)$ or a grid of curves more detailed than on Fig. 5.26, at different values of α (see the graph in the appendix).

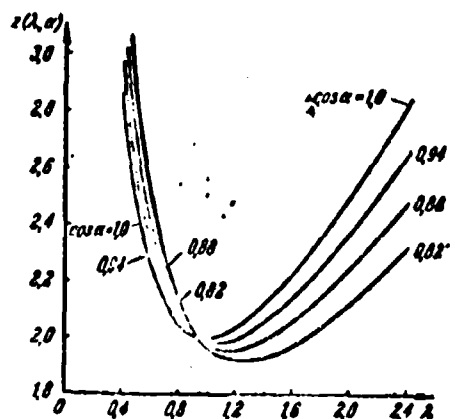


Fig. 5.26. Graph function $z(\lambda, \alpha)$.

Formulas (123) and (127) make it possible to establish the nature of a density change of the current, cross-sectional area, specific impulse and other values which characterize the gas flow, depending on the velocity coefficient λ and angle α between the velocity vector and the axis. However, here we will not discuss this.

When using generalized functions $q(\lambda, \alpha)$, $y(\lambda, \alpha)$, $z(\lambda, \alpha)$ and their combinations, all the equations obtained in this section can be used for calculating flows with a circular or radial component of velocity.

Example 11. The twisted flow of gas moves in the annular channel between two cylindrical surfaces (Fig. 5.27). The velocity coefficient of the flow at the channel inlet $\lambda_1 = 0.85$, and the direction of absolute velocity is assigned by angle $\alpha_1 = 30^\circ$ to the axis of the channel. With channel flow the stagnation temperature of the gas is reduced from 900° to 700°K as a result of the thermal conductivity through the walls into the environment. Disregarding the friction and also a change in the parameters on the radius of the channel, determine the parameters of the gas at outlet from the channel. The adiabatic index $k = 1.40$.

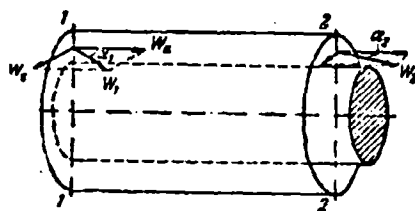


Fig. 5.27. Twisted gas flow in the annular channel (Example 11).

As above, in the examination of flow in the cylindrical channel with the heat feed, we obtain the fundamental equation from the condition of the constancy of the momentum of gas in cross sections of the channel. In this case this condition takes the form

$$\frac{Q}{g} \rho_1 z(\lambda_1, \alpha_1) = \frac{Q}{g} \rho_2 z(\lambda_2, \alpha_2)$$

or

$$z(\lambda_2, \alpha_2) = z(\lambda_1, \alpha_1) \sqrt{\frac{T_{01}}{T_{02}}}$$

By substituting the assigned values of the stagnation temperatures and the value of function $z(\lambda_1, \alpha_1) = 2.055$ (see Fig. 5.26), we obtain

$$z(\lambda_2, \alpha_2) = 2.33$$

This value of the function can correspond, generally speaking, to different combinations of values λ_2 and α_2 , and therefore for determining these values we use the condition of the constancy of the moment of momentum (see § 6 of Chapter 1). Since the mean radius of the channel does not change and there are no moments of applied forces, then in the flow, independently of the occurring processes, the circular velocity component should be constant. Therefore,

$$w_{1\tau} = w_{2\tau} \quad \text{or} \quad \lambda_1 a_{*1} \sin \alpha_1 = \lambda_2 a_{*2} \sin \alpha_2$$

Hence we determine

$$\lambda_2 \sin \alpha_2 = \lambda_1 \sin \alpha_1 \sqrt{\frac{T_{*1}}{T_{*2}}} = 0.85 \cdot 0.5 \sqrt{\frac{800}{700}} = 0.482$$

The joint solution of the two obtained equations is most conveniently carried out graphically. Being given a number of values of angle α_2 , we find the values of the velocity coefficient $\lambda_2 = 0.482 / \sin \alpha_2$ corresponding to them; substituting these values α_2 and λ_2 into $z(\lambda, \alpha)$, we plot the graph of this function. The point of curve where $z(\lambda, \alpha) = 2.33$ corresponds to values of parameters in the outlet section of the channel, and in this case we find $\lambda_2 = 0.72$, $\alpha_2 = 42^\circ$. In the calculations it is possible also to use an auxiliary graph or tables of function $z(\lambda, \alpha)$.

The condition of the retention of the gas flow rate in cross sections 1 and 2, when using expression (123), makes it possible to determine the ratio of total pressures of the gas - the coefficient of total pressure:

$$\sigma = \frac{p_{02}}{p_{01}} = \frac{q(\lambda_1) \cos \alpha_1}{q(\lambda_2) \cos \alpha_2} \sqrt{\frac{T_{*1}}{T_{*2}}} = \frac{0.9729 \cdot 0.865}{0.9061 \cdot 0.743} \sqrt{\frac{800}{700}} = 1.10$$

(cooling of the flow is accompanied by an increase in the total pressure).

A change in the static pressure is easy to determine from the relation

$$\frac{p_2}{p_1} = \frac{p_{02}}{p_{01}} \frac{\pi(\lambda_2)}{\pi(\lambda_1)} = 1,10 \cdot \frac{0,7289}{0,6387} = 1,233$$

or from the equation of the equality of the flow rates recorded in form (125).

In conclusion let us list the introduced gas-dynamic functions and the relationships between them:

1. The simplest functions which express the relationship between the gas parameters in the flow and stagnation parameters:

$$\tau(\lambda) = 1 - \frac{k-1}{k+1} \lambda^2, \quad \pi(\lambda) = \left(1 - \frac{k-1}{k+1} \lambda^2\right)^{\frac{k}{k-1}};$$

$$\epsilon(\lambda) = \left(1 - \frac{k-1}{k+1} \lambda^2\right)^{\frac{1}{k-1}};$$

in this case

$$\pi(\lambda) = \tau(\lambda) \epsilon(\lambda).$$

2. The functions which make it possible to express the gas flow rate by the total pressure

$$q(\lambda) = C \lambda \epsilon(\lambda)$$

or by the static pressure

$$y(\lambda) = \frac{q(\lambda)}{\pi(\lambda)} = C \frac{\lambda}{\tau(\lambda)}.$$

By means of these functions we obtain the two expressions for the gas flow rate

$$Q = m \frac{p_0 F y(\lambda)}{\sqrt{T_0}} = m \frac{p F q(\lambda)}{\sqrt{T_0}};$$

3. The function

$$z(\lambda) = \lambda + \frac{1}{\lambda},$$

with the aid of which the momentum of the gas flow can be represented in the form of the product of the stagnation temperature (critical speed of sound) by the gas flow rate

$$I = \frac{Q}{k} w + pF = \frac{k+1}{2k} \frac{Q}{g} a_{*p} z(\lambda).$$

4. Functions $f(\lambda)$, $r(\lambda)$, with the aid of which the momentum of the gas flow is expressed in terms of the total or static pressure:

$$f(\lambda) = \frac{1}{C} q(\lambda) z(\lambda), \quad r(\lambda) = C \frac{1}{y(\lambda) z(\lambda)}.$$

Correspondingly we obtain two expressions for the momentum of the gas flow:

$$I = p_0 F f(\lambda) = \frac{pF}{r(\lambda)}.$$

The constant which enters into the expressions for functions $q(\lambda)$, $y(\lambda)$, $f(\lambda)$, and $r(\lambda)$

$$C = \frac{1}{r(1)} = \left(\frac{k+1}{2} \right)^{\frac{1}{k-1}},$$

is equal to 1.577 for $k = 1.4$ and 1.588 for $k = 1.33$.

5. Functions $q(\lambda, \alpha)$, $y(\lambda, \alpha)$ and $z(\lambda, \alpha)$, which make it possible to propagate the methods examined above and design formulas for the case of gas flow from the circular or radial component velocity.

6. In the solution of some problems derivatives of different gas-dynamic functions are also used. By means of differentiation and simple transformations, it is possible to obtain their expressions in terms of initial functions.

For example,

$$\frac{dn(\lambda)}{d\lambda} = -\lambda \left(\frac{2}{k+1} \right)^{\frac{k}{k-1}} q(\lambda),$$

$$\frac{dq(\lambda)}{d\lambda} = q(\lambda) \left[\frac{1}{\lambda} - \left(\frac{2}{k+1} \right)^{\frac{k}{k-1}} y(\lambda) \right] \text{ and so on.}$$

What is the meaning of simplifications being obtained in the recording of fundamental equations with the aid of gas-dynamic functions?

As can be seen from the examples given above, the major advantage of the expressions obtained here is that they contain such flow parameters the nature of change in which can be easily established from conditions of the problem, for example, the constancy of stagnation temperature T_0 in adiabatic flows and an increase in T_0 with the heat feed, the retention of total pressure p_0 in the isentropic flow and a drop p_0 in the presence of losses, and so on. By the selection of the corresponding expression for the flow rate or momentum, it is possible to reduce to a minimum a number of unknown parameters in the fundamental equations. In this case it is frequently possible to find the unknown values directly from the initial equations, avoiding the bulky transformations.

Let us note some general rules which are useful in the solution of equations in general form and calculations with the aid of tables of gas-dynamic functions.

In all cases when the general or numerical expression of the value of the velocity coefficient λ or any one of its functions are obtained, it is possible to consider that all the gas-dynamic functions and coefficient λ (from the tables or graphs) are known. This is the basic condition in the simplification of the calculations, since it eliminates the need for obtaining in explicit form the dependences between λ and its functions. In the numerical calculations one should consider that functions $\tau(\lambda)$,

$\pi(\lambda)$ and $\varepsilon(\lambda)$ in the region of low velocities and function $q(\lambda)$, $z(\lambda)$ and $f(\lambda)$ at sonic speeds are changed very little with a change in value λ . Therefore, in the indicated regions an insignificant error in the value of the functions, can lead to a great error in the calculation of the velocity coefficient λ . Such calculations should be avoided, and as far as possible, in these cases, other equations which include, for example, functions, $y(\lambda)$ and $r(\lambda)$ should be used. If this for any reason is impossible, then it is necessary to conduct all preliminary calculations with a high degree of accuracy. It is understandable that in these regions it is not recommended to determine λ according to the indicated functions by means of graphs. In particular, this is related to function $z(\lambda)$, which over wide limits of the change in λ (from 0.65 to 1.55) varies in value by a total of 10%. Therefore, for the determination of λ in terms of the value of function $z(\lambda)$ in the region of sonic speeds, it is possible to calculate the possible values of λ directly from the equation

$$\lambda + \frac{1}{\lambda} = z(\lambda)$$

whence

$$\lambda = \frac{z(\lambda) \pm \sqrt{z^2(\lambda) - 4}}{2} = \frac{2}{z(\lambda) \mp \sqrt{z^2(\lambda) - 4}}.$$

In order to avoid the error connected with the subtraction of close values, the supersonic solution is located by the first and the subsonic solution by the second of these expressions.

From the examples examined in this section, it is possible to see the efficiency of the method of calculation with the use of gas-dynamic functions in the solution of sufficiently complex problems which are of practical use.

§ 7. Gas Flow with Friction in the Cylindrical Tube with the Assigned Magnitude of the Ratio of Pressures at Inlet and Outlet

Using the relations derived in the foregoing section let additionally explain some laws governing the one-dimensional gas flow in a cylindrical tube with friction. In § § 1 and 2 it was established that the friction leads to an increase in the velocity of subsonic flow and a decrease in the velocity of supersonic flow, whereupon in both cases the maximum conditions correspond to the critical velocity in the outlet section of the tube.

The results obtained in § 2 are valid, however, only when the velocity coefficient at the inlet into the tube λ_1 is maintained constant, which requires the creation of a *quite definite drop in the pressures in the flow* for each mode and each value of the normalized length of the tube. In actuality, most frequently it is the opposite: the assigned value is the drop in pressures between the inlet and outlet sections of the tube, and values of the velocity, flow rate and other flow parameters are determined by the acting drop in pressures and by the resistance in the section of the tube in question. For flow in the inlet of the tube the most characteristic value, which is usually known or can be easily determined, is the total pressure p_{01} ; for the characteristic of flow at the outlet from the tube, it is important to know the static pressure in the environment or reservoir where the gas escapes from the tube p_H . If the flow velocity in the outlet section is less than the speed of sound, then static pressure of the flow, as is known, is equal to the external pressure, i.e., $p_2 = p_H$. If $\lambda_2 = 1$, then in the outlet section of the tube $p_2 \geq p_H$. Finally, when $\lambda_2 > 1$ also conditions when $p_2 < p_H$ are possible.

Let us call the value $\Pi_0 = p_{01}/p_H$ the available pressure ratio. The flow parameters in the cylindrical tube defined basically by

the value of the available pressure ratio Π_0 : the process is actually as though it were an outflow of gas from the vessel with pressure p_{01} into a medium with pressure p_H through the channel with the assigned resistance. Therefore, in the examination of the law governing flow with friction, it is necessary to consider the value of the available pressure ratio in the flow; without this the obtained results can prove to be unreal.

Let us assume, for example, that at subsonic velocity at the inlet into the tube the available pressure ratio Π_0 is less than the critical pressure ratio

$$\Pi_{cr} = \frac{1}{\pi(1)} = \left(\frac{\lambda+1}{2}\right)^{\frac{\lambda}{\lambda-1}};$$

for air $\Pi_{cr} = 1.893$. Due to friction the total pressure of the flow along the length of the tube is decreased, and therefore in the outlet section of the tube $p_{02}/p_H < p_{01}/p_H < 1.893$. This means that the flow escapes from the tube under the action of the subcritical pressure ratio, and, consequently, the velocity of such a flow will always be subsonic. No matter how much it is possible to increase the normalized length of the tube it is impossible to obtain value $\lambda_2 = 1$: the drop in the pressures acting in the flow is insufficient for producing the sonic speed of outflow at the outlet from the tube.

Thus, the conclusion obtained previously that with an increase in the normalized length of the tube up to the maximum (critical) value, the flow velocity at outlet from the tube reaches the speed of sound and is valid only in such a case when a sufficient (depending on values λ_1 and χ) pressure ratio Π_0 is provided.

Let us show how the calculation of flow parameters with flow in the tube with friction is produced if $\lambda_1 < 1$ and the value of the available pressure ratio is assigned.

Let us write the equation of continuity for flow in the tube, whereupon flow rate in the inlet section is expressed with the aid of formula (109) in terms of the total pressure, and the flow rate in the exit section is expressed by the static pressure with the aid of formula (111)

$$\frac{p_{01} F_1 q(\lambda_1)}{\sqrt{T_{01}}} = \frac{p_1 F_2 y(\lambda_2)}{\sqrt{T_{01}}}.$$

Since for the adiabatic flow in a cylindrical tube $T_{02} = T_{01}$ and $F_2 = F_1$, then hence it follows that

$$y(\lambda_2) = \frac{p_{01}}{p_1} q(\lambda_1)$$

If $\lambda_2 < 1$, then, as was noted, $p_2 = p_H$ or

$$y(\lambda_2) = \Pi_0 q(\lambda_1) \quad (129)$$

Equation (129), which mutually connects values of the velocity coefficients in the inlet and outlet sections of the tube at the assigned value Π_0 and $\lambda_1 < 1$, is correct without depending on the flow pattern and length of the tube. On the other hand, the change in parameters of the gas in the tube is determined by the value of the coefficient of friction and by the length of the tube. Earlier in § 2 the formula describing the change in the flow parameters as a result of the friction was obtained:

$$\tau(\xi) - \tau(0) = \chi \quad (130)$$

where $\chi = \frac{2k}{k+1} \xi \frac{\pi}{D}$ is the normalized length of the tube. Equation (130) establishes the dependence between the velocity coefficients λ_1 and λ_2 of the assigned value χ . Equations (129) and (130) can be considered as the system of two equations with two unknowns, the roots of which determine values λ_1 and λ_2 as a function of the assigned values Π_0 and χ . By these values of the velocity coefficients is determined the real flow conditions of the gas through the tube with the assigned resistance (normalized length) under the action of the available drop in pressures Π_0 .

Let us examine some of the following properties of the flow at subsonic speed of the flow at the inlet into the tube. In the first place let us compare the one-dimensional subsonic gas flow in the tube in the presence of friction with an ideal flow with the identical available pressure ratio Π_0 . A change in the gas parameters along the length of the tube is connected with friction, and therefore in an ideal flow, when $p_{02} = p_{01}$, the gas parameters are constant in all the cross sections of the tube. The velocity coefficient in the outlet section $\lambda_2 = \lambda_1 < 1$, which in an ideal case is determined by the value of the available pressure ratio $\pi(\lambda_2) = 1/\Pi_0$ is more than that during flow with friction, when $p_{02} < p_{01}$, and $\pi(\lambda_2) = 1/\sigma\Pi_0$. The more the normalized length of the tube, the larger will be the total losses of pressure and the less will be the flow velocity at the outlet from the tube as compared with the velocity in the ideal case of the flow. Thus, it is necessary to keep in mind that, although with flow in the tube with friction *the velocity of the flow along the length of the tube increases*, its greatest value, the outlet velocity, always *remains less than that with the same pressure ratio Π_0 in the case of the flow without friction* (for example, a very short tube, when $x \approx 0$). The more the normalized length of the tube, the less (at given Π_0) the flow velocity both at the outlet and inlet.

It is interesting to note that if $\Pi_0 = \text{const}$, then when $\lambda_2 < 1$ the change in the normalized length of the tube x always leads to a change in the inlet velocity of the tube, independently of the larger or smaller value x of its critical value for the given $\lambda_1 < 1$. The retention of $\lambda_1 = \text{const}$ with a change in the normalized length of the tube and $\lambda_2 < 1$ requires a corresponding change in value in the available pressure ratio: the longer the tube, the larger the value Π_0 necessary for maintaining the assigned conditions at the inlet, i.e., the retention of the gas flow rate.

On the other hand, if at the assigned length of the tube ($\chi = \text{const}$) we increase the pressure ratio Π_0 , then the velocities at both the inlet and at outlet will increase until the value λ_2 reaches the critical value $\lambda_2 = 1$. A further increase in Π_0 changes neither λ_1 nor λ_2 ; however, in the outlet section of the tube a surplus pressure in comparison with the environment (reservoir) will be established. For these conditions equation (129) is incorrect, since with its derivation it was assumed that $p_2 = p_H$; the relation between the flow parameters is determined only by equation (130). From the continuity condition it is possible only to find the minimum required value Π_0 at which the mode with $\lambda_2 = 1$ and assigned value λ_1 is established, since according to equation (129)

$$\Pi_{0 \min} = \frac{y(\lambda_1)}{q(\lambda_1)} = \left(\frac{k+1}{2} \right)^{\frac{k}{k-1}} \frac{1}{q(\lambda_1)} = \frac{\Pi_{0*}}{q(\lambda_1)}.$$

Since $q(\lambda_1) < 1$, from the latter relation it is evident that with flow in the tube with friction the critical outlet velocity is established with the pressure ratio of $\Pi_0 > \Pi_{0*}$, where the Π_{0*} is the pressure ratio necessary for obtaining $\lambda = 1$ during flow without friction. The conditions $\lambda_2 = 1$ for this value λ_1 begins with an increase in the normalized length χ up to the value

$$\chi = \chi_{sp} = \tau(\lambda_1) - 1, \quad (131)$$

and in this case condition $\Pi_0 \geq \Pi_{0 \min}$ should be observed.

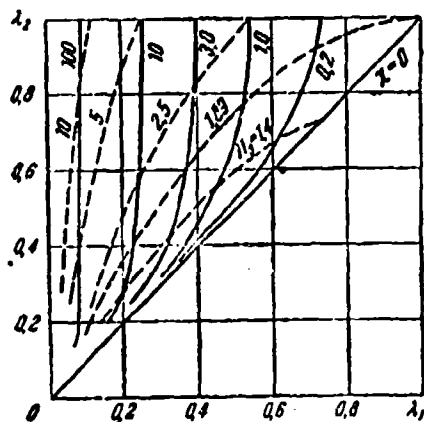


Fig. 5.28. Relationship between parameters of subsonic flow at the inlet and outlet sections of the cylindrical tube in the presence of friction.

Figure 5.28 gives results of the calculations of subsonic flow in the tube with friction. The graph illustrates the basic regularities of the flow given above and, in particular, shows that

a) when $\lambda_1 = \text{const}$ with an increase in the normalized length χ value λ_2 increases, whereupon always $\lambda_1 < \lambda_2 \leq 1$;

b) at a constant available pressure ratio Π_0 , with an increase in χ , value λ_1 is always decreased; λ_2 is decreased also, if $\lambda_2 < 1$;

c) for each value of the normalized length χ there is a completely defined value of the pressure ratio $p_{01}/p_H = \Pi_0$, which corresponds to the assigned flow velocity at the outlet and inlet into tube, respectively;

d) the limiting value λ_1 , which corresponds to $\lambda_2 = 1$, for each value χ is established with the defined value, which is increased with an increase in χ of the value of the pressure ratio and does not increase with a further increase in Π_0 .

Let us now examine the features of flow with friction with supersonic velocity at the inlet into the tube. From formula (130) it follows that if the normalized length of the tube is less than the critical value, determined for the given value of $\lambda_1 > 1$ by formula (131), then along the length of the tube the flow velocity will decrease, remaining supersonic. At the outlet from the tube with continuous braking of the flow, $\lambda_2 > 1$ will be obtained. At a certain value of the normalized length of the tube, called the critical from equation (130), it follows that $\phi(\lambda_2) = 1$, i.e., $\lambda_2 = 1$. This length corresponds to the maximally possible flow conditions with a continuous change in velocity from the assigned value $\lambda_1 > 1$ to $\lambda_2 = 1$. If $\chi > \chi_{kp}$, then the continuous braking of flow in the tube is impossible. In this case equation (130), which describes the flow with a continuous

velocity change, does not have solutions for λ_2 , since from it $\phi(\lambda_2) < 1$ follows. In actuality, here in the initial section of the tube the supersonic flow is braked to a certain value $\lambda' > 1$, and then in the tube there appears a shock wave, behind which subsonic flow is established with an increase in the velocity along the length of the tube from value λ'' (after the shock) to $\lambda_2 \leq 1$, as was noted above.

The location of the shock and relative length of the supersonic and subsonic sections of the flow, depending on the assigned parameters, can be determined in the following manner. Let us designate the normalized length of the tube from its beginning up to the shock wave (supersonic section of the flow)

$$\chi_1 = \frac{2k}{k+1} \ln \frac{\lambda_1}{\lambda'}$$

Let us write equation (130) for sections with a continuous velocity change, i.e., separately for the supersonic and subsonic sections:

$$\tau(\lambda_1) - \tau(\lambda') = \chi_1 \quad (132)$$

$$\tau(\lambda'') - \tau(\lambda_1) = \chi - \chi_1 \quad (133)$$

Let us make a term-by-term summation of equations (132) and (133), assuming in this case that the shock wave is normal, and therefore the relation $\lambda'' = 1/\lambda'$ is correct. As a result we obtain

$$\tau(\lambda_1) - \tau(\lambda_1) + \tau\left(\frac{1}{\lambda'}\right) - \tau(\lambda') = \chi$$

Let us denote

$$\Phi(\lambda) = \tau\left(\frac{1}{\lambda}\right) - \tau(\lambda) = \lambda^2 - \frac{1}{\lambda^2} - 4 \ln \lambda \quad (134)$$

Then the latter equation can be written in the form

$$\Phi(\lambda') = \chi - \tau(\lambda_1) + \tau(\lambda_1) \quad (135)$$

Figure 5.29 gives auxiliary graph for determining the function $\Phi(\lambda)$ from value λ . Relation (135) establishes the relationship

between the parameters of flow, which moves with friction in the tube with normalized length χ when in the tube a normal shock wave appears.

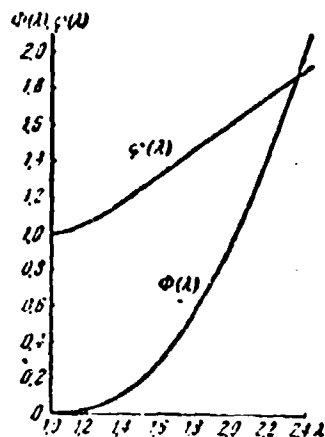


Fig. 5.29. Auxiliary graphs of functions $\phi(\lambda)$ and $\phi'(\lambda)$ in the region of supersonic flow velocities

$$\phi'(\lambda) = \frac{1}{\lambda^2} + 2 \ln \lambda, \quad \phi(\lambda) = \lambda^2 - \frac{1}{\lambda^2} - 4 \ln \lambda.$$

Entering into formula (135), besides the known values of χ and λ_1 , is also the thus far unknown value of the velocity coefficient at the outlet from the tube λ_2 . Since after the shock the flow is subsonic, then for determining λ_2 let us use the equation of continuity

$$y(\lambda_2) = \Pi_0 q(\lambda_2)$$

which is correct both when $\lambda_1 < 1$ and when $\lambda_1 > 1$. If from this equation it follows that $y(\lambda_2) \geq y(1)$, then $\lambda_2 = 1$ at $y(\lambda_2) < y(1)$ and $\lambda_2 < 1$. Substituting value $\lambda_2 \leq 1$ thus found into equation (135), let us determine $\phi(\lambda')$. Further according to the graph (Fig. 5.29) we find values λ' and $\phi(\lambda')$, and, after using equation (132), we compute the value χ_1 - the normalized length of the tube necessary for the shock-free supersonic flow from λ_1 to λ' . The value χ_1 determines the location of the shock along the length of the tube, since when $\zeta = \text{const}$ we have $x_1/x = \chi_1/\chi$.

With the critical flow conditions at the outlet from the tube, when $\lambda_2 = 1$, the result of the calculation, as it is easy to see,

does not depend on Π_0 : a shock appears in the definite cross section of the tube independently of the value of the available pressure ratio. The calculation according to formulas (129), (132) and (135) shows that when $\lambda_2 < 1$ the shock wave with a decrease in Π_0 will be moved from its end position, which corresponds to $\lambda_2 = 1$, to the inlet section of the tube. The minimum value of the available pressure ratio, at which the flow with the assigned initial velocity coefficient $\lambda_1 > 1$ is possible, is determined by the fact that the shock wave, in moving upstream, will approach directly to the inlet section.

Let us give an example of the calculation of flow with a shock wave within the tube. Let us assume that the velocity coefficient at the inlet into the tube $\lambda_1 = 1.8$ and the total normalized length of the tube $\chi = 0.6$ are assigned (at standard values of the coefficient of friction this corresponds approximately to 30 calibers of the tube). The available ratio of total pressure of the flow at the inlet into the tube to the static pressure in the reservoir, where the gas escapes from the tube, is $\Pi_0 = 3.0$.

The critical value of the normalized length of the tube for the assigned value λ_1 is determined:

$$\chi_{cr} = \chi(\lambda_1) = 1 : 0.485$$

(we find value $\chi(\lambda_1)$ from the auxiliary graph of Fig. 5.29). Since the assigned normalized length of the tube $\chi = 0.6$ is more than the critical value, then, as was noted, the continuous braking of the flow is impossible, and a shock wave appears in the tube.

Let us determine the velocity coefficient of the flow at the outlet from the tube with the aid of equation (129):

$$y(\lambda_1) = 11.7(\lambda_1) = 3.0, 1075 = 1.222 \quad \text{or} \quad \lambda_2 = 0.71.$$

Further we substitute the obtained values of λ_2 and the assigned values of λ_1 and χ into equation (135), which determines the velocity

coefficient of the flow in front of the shock $\phi(\lambda') = 0.6 + 1.25 - 1.485 = 0.365$. From the graph on Fig. 5.29 we find that this value $\phi(\lambda')$ corresponds to $\lambda' = 1.66$ and $\phi(\lambda') = 1.375$. We determine the normalized length of the supersonic section of flow according to formula (132)

$$\lambda_1 = \tau(\lambda_1) - \tau(\lambda') = 1.485 - 1.375 = 0.11$$

and find the distance from the inlet into the tube in front of the cross section where the shock wave appears (when $\zeta = \text{const}$):

$$\frac{x_1}{x} = \frac{\lambda_1}{\lambda} = \frac{0.11}{0.6} = 0.184.$$

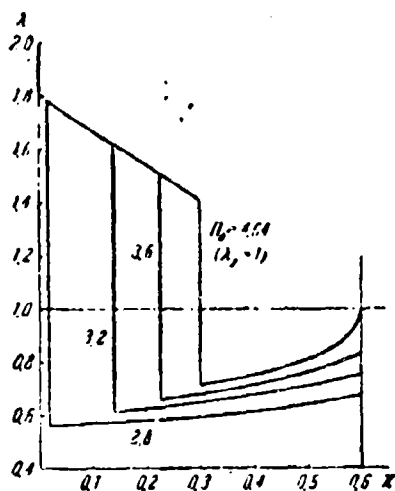


Fig. 5.30. The possible conditions of supersonic flow in a cylindrical tube with friction with the length of the tube greater than the critical value. $\lambda_1 = 1.8$; $x = 0.6$ (example of the calculation)

Thus, at a length of approximately 18% of the total length of the tube, the supersonic flow under the action of friction is slowed down from $\lambda_1 = 1.8$ to $\lambda' = 1.66$, and then in the shock the velocity falls to $\lambda'' = 0.6$; in the remaining part of the tube the subsonic flow is accelerated to $\lambda_2 = 0.71$ and escapes from the tube, having a static pressure equal to the pressure in the reservoir p_H .

At other values of the available pressure ratio, the position of the shock will be different. Figure 5.30 gives results of the calculation according to the given method at different values of Π_0 . The

maximally possible conditions are determined, on one hand, by the achievement of critical velocity at the outlet from the tube (during the calculation we assume that $\lambda_2 = 1$ and find the most remote shock-wave position) from the inlet, and on the other hand,

by the emergence of a shock wave directly behind the inlet section of the tube. In this case ($\lambda_1 = 1.8$, $\chi = 0.6$) the critical flow conditions at the outlet is obtained when $\Pi_0 = \gamma(1)/q(\lambda_1) = 1.893/0.4075 = 4.64$.

According to formulas (135) and (132), by means of the graph on Fig. 5.29, we find $\phi(\lambda') = 0.6 + 1 - 1.485 = 0.115$, $\lambda' = 1.41$, and $\phi(\lambda') = 1.185$. We further have $\chi_1 - 1.485 - 1.185 = 0.3$, and, therefore, $\chi_1/\chi = 0.3/0.6 = 0.5$.

The minimum value of Π_0 , at which supersonic flow at the inlet into the tube is possible, corresponds to $\gamma(0) = \gamma(\frac{1}{\lambda_1}) - 0.6 = 2.97 - 0.6 = 1.47$ or $\lambda_2 = 0.66$. Therefore, we have

$$\Pi_0 = \frac{\gamma(\lambda_2)}{q(\lambda_2)} = \frac{1.117}{0.1073} = 2.74$$

For determining the total and static pressure from the value of the velocity coefficients at the inlet and outlet, it is sufficient to write conditions of the equality of flow rates of gas in the inlet and outlet sections, having used expressions (109) or (111).

It was indicated above that if the normalized length of the tube is less than the critical for this value λ_1 , then the laws governing the flow with friction allow the existence of the flow with a continuous change (reduction) in the supersonic velocity on the entire length. It is possible to show, however, that together with the completely supersonic flow, here the shocked flow within the tube and the subsonic speed at outlet is also possible. Such flow conditions in the case $\chi < \chi_{KP}$ can exist only in the defined interval of values $p_{01}/p_H = \Pi_0$ which is found from the condition that in the exit section of the tube the static pressure of subsonic flow should be equal to the pressure of the environment.

§ 3. The Averaging of Parameters of Nonuniform Flow

In practice it is frequently necessary to calculate gas flows with parameters variable in cross section. In a number of cases, however, these flows can be considered as one-dimensional, with some mean values of the parameters in each cross section. In this case the problem of the averaging of gas parameters in the cross section of the nonuniform flow appears.

Sometimes as the mean values of the parameters we take the mean values in area, velocity, pressure, temperature, and so on. It is possible to show however, that such simple averaging is, generally speaking, incorrect and can lead to erroneous results: the ratio of the mean values of total and static pressures will not correspond to the mean value of the velocity coefficient, and the gas flow rate calculated according to the mean parameters will be more or less real and so on. If the initial nonuniformity of flow is small, then quantitatively these errors are insignificant; with great nonuniformity of the parameters the error can be significant. Therefore, the solution of the stated mission in general will be approached by other means.

The assigned nonuniform flow is characterized by a number of total (integral) values, that is, by the gas flow rate, energy, momentum, enthalpy, entropy, and so on. Replacing this flow by the one-dimensional flow - the averaged - one should try to maintain the total characteristics (properties) of the flow constant. Since the state of the one-dimensional gas flow is determined by three independent parameters (for example, the total pressure \bar{p}_0 , stagnation temperature \bar{T}_0 and velocity coefficient $\bar{\lambda}$), then in averaging, it is simultaneously possible to maintain only the three total physical characteristics of the initial flow constant.

The most widespread is the method of the determination of mean values of parameters p_0 , T_0 and λ while maintaining in the initial and averaged flows values of the flow rate of the gas G , total energy E and momentum I identical. Conditions $G = \text{const}$, $E = \text{const}$ and $I = \text{const}$ give the three equations with three unknowns necessary for the solution of the problem. Let us assume that in the cross section of the initial nonuniform flow the temperature field and full and static pressure fields are known (assigned or measured). Then it is possible to consider at each point of the cross section the values of total pressure p_0 , stagnation temperature T_0 and velocity coefficient λ are known. According to value λ , for each point of the cross section gas-dynamic functions $q(\lambda)$, $z(\lambda)$, etc., can be found. For the flow, as a whole, the values of flow rate, momentum and energy are determined by means of integration of the corresponding elementary expressions over the entire cross section. Thus, for instance, the gas flow rate is equal to

$$G = \int_{F_1} dG = \int_{F_1} m \frac{p_0 q(\lambda)}{\sqrt{T_0}} dF. \quad (136)$$

If the velocity field is assigned in the form of a graph or table, the gas flow rate can be calculated according to methods of graphic or numerical integration.

The total values of energy E and momentum I are determined similarly.

Let us turn to the solution of the problem of the averaging of parameters p_0 , T_0 and λ . Let us equate the values of total energy of the gas calculated in one case according to the true and in another case according to the mean values of the gas parameters:

$$G c_p T_0 = \int_{F_1} c_p T_0 dG = E \quad (137)$$

We consider the heat capacity of gas c_p to be constant over the entire cross section. Let us substitute into this equation the expression for the elementary gas flow rate and the expression written above for the total gas flow rate in the flow. Hence we obtain the first unknown value - the mean stagnation temperature of the gas:

$$\bar{T}_0 = \frac{E}{c_p G} = \frac{\int_0^1 \rho_0 q_0 F T_0 dF}{\int_0^1 \frac{\rho_0 q_0}{T_0} dF}. \quad (138)$$

From formula (138) it is evident that \bar{T}_0 is the averaged-mass value of the stagnation temperature. Let us use the obtained average value of the stagnation temperature for calculation of the mean value of the critical speed of sound

$$a_{*p} = \sqrt{2g \frac{k}{k+1} R \bar{T}_0}.$$

Let us find the mean value of the velocity coefficient of flow $\bar{\lambda}$ from the condition of the equality of the effective momentum of flow and the momentum calculated according to the mean values of the parameters. For the sake of simplicity of the calculation, let us express the total momentum by means of formula (115) in terms of function $z(\lambda)$, and let us present the elementary momentum according to formula (119) in terms of the total pressure and function $f(\lambda)$. As a result we will obtain

$$\frac{k+1}{2k} \frac{Q}{g} a_{*p} z(\bar{\lambda}) = \int_0^1 p_0 f(\lambda) dF,$$

whence

$$z(\bar{\lambda}) = \frac{2gk}{k+1} \frac{I}{Q a_{*p}} = \frac{2gk}{k+1} \frac{1}{Q a_{*p}} \int_0^1 p_0 f(\lambda) dF. \quad (139)$$

In accordance with the assigned flow conditions of the gas from two values of the velocity coefficient $\bar{\lambda}$ determined by function $z(\bar{\lambda})$, we select the real value $\lambda > 1$ or $\lambda < 1$. The reason for the ambiguity of solving the problem in this case is quite obvious:

the assigned condition of the retention of flow rate, momentum and total energy will not be disturbed, if in the averaged flow the shock wave arises; the velocity coefficient in this case acquires a new value opposite in magnitude so that function $z(\lambda)$ will be a constant value (see § 6, Example 6).

After determining the stagnation temperature and the velocity coefficient in the averaged flow, we find the average value of total pressure \bar{p}_0 from the expression for the gas flow rate:

$$p_0 = \frac{GV\bar{f}_0}{mFq(\bar{\lambda})}. \quad (140)$$

An interesting relation can be obtained if we use the momentum equation for determining the average total pressure:

$$p_0 F f(\bar{\lambda}) = \int_F p f(\lambda) dF.$$

Hence we have

$$p_0 = \frac{\int_F p f(\lambda) dF}{F f(\bar{\lambda})}.$$

Value $f(\bar{\lambda})$ is the value of function $f(\lambda)$ for the value of the velocity coefficient $\bar{\lambda}$ averaged over the cross section found above. On the basis of the theorem of the mean known from integral calculus, the latter relation can be presented in the form

$$p_0 = \frac{f(\bar{\lambda})}{f(\bar{\lambda})} \frac{\int_F p dF}{F}.$$

Here $\bar{f}(\lambda)$ is the value of function $f(\lambda)$ at a certain point of the range of integration, i.e., at a certain point of the cross section F . As has already been indicated, the value of function $f(\lambda)$ changes very little over wide limits of the change in λ (at subsonic and small supersonic velocities). Therefore, the two values of function $f(\lambda)$ in the given cross section of the flow $f(\lambda)$ and $\bar{f}(\lambda)$ will be close in value. Hence, it follows that

$$p_0 \approx \frac{\int p_0 dP}{F} \quad (141)$$

The obtained relation means that the value of total pressure \bar{p}_0 differs little from the *total pressure average in area value*. Calculations show that if the velocity coefficient λ on the cross section changes within limits of 0.4-1.0 or 1-1.4, then the error of the calculation \bar{p}_0 in the formula (141) usually does not exceed 2-3%.

From found values \bar{T}_0 , $\bar{\lambda}$ and \bar{p}_0 all the remaining parameters of the averaged flow, speed \bar{w} , density $\bar{\rho}$ and so on, are unambiguously determined. Let us note that the mean values of the parameters, which satisfy the conditions stated in the problem, are obtained quite definite independently of the method and order of the solution of the fundamental equations, although in this case expressions different in appearance can be obtained.

Let us discuss the physical meaning of the obtained averaged flow parameters. It is easy to see that values of parameters \bar{T}_0 , \bar{p}_0 and $\bar{\lambda}$ and others are equal to the appropriate parameters of such a gas flow which can be formed during the alignment (for example, because of turbulent mixing) of the initial nonuniform flow in the heat-insulated tube of constant cross section without friction against the walls; in this case the flow rate, momentum and total energy of the gas will also maintain constant values. In other words, the found equivalent (averaged) flow can be actually obtained during the flow of the initial gas without external actions. If we calculate and compare the entropy of the gas in the nonuniform and averaged flow, then it will appear that the averaged parameters correspond to the larger value of entropy. This is explained by the fact that with the mixing of the gas particles at different velocities losses to shock appear, the total kinetic energy decreases, and the thermal energy increases.

In connection with this, the given method of averaging in certain cases can prove to be unacceptable. Thus, for instance, if according to the mean values of flow parameters in the outlet section of the compressor found by such method, we calculate its efficiency, then the value less than real will be obtained, since to the real losses (increase in entropy) in the process of the compression of gas will be added the theoretical losses, which appear as a result of the aforementioned replacement of the real flow parameters by the mean values. Therefore, when according to the meaning of the problem it is required to evaluate the work capacity of the initial flow of gas, it is advantageous, as L. I. Sedov and G. G. Chernyy indicated, to carry out averaging in order to maintain the total quantity of the entropy of gas constant¹.

For determining the three parameters of the averaged flow, besides the condition of the retention of entropy, we also use equations of the constancy of flow rate and total energy.

The mean values of the parameters we compute by the following way. From equation (136) we find the total gas flow rate. Further, as above, from the equation of energy (138) we determine the stagnation temperature \bar{T}_0 . The condition of the constancy of entropy (see § 7, Chapter 1) in the averaged and real flow is written in the form

$$0.4R \ln \frac{(\bar{T}_0)^{\frac{\gamma}{\gamma-1}}}{\bar{p}_0} = AR \int_{\Omega} \ln \frac{(T_0)^{\frac{\gamma}{\gamma-1}}}{p_0} d\Omega$$

This equation includes only one unknown parameter - the average total pressure \bar{p}_0 . For determining \bar{p}_0 , for dG we substitute its value obtained above and then convert the equation to the form

¹Sedov, L. I., Chernyy, G. G., On the averaging of nonuniform flows of gas in channels. Theoretical hydromechanics, Collection of articles, No. 12, Issue 4. Oborongiz, 1954.

$$\ln p_0 = \frac{m}{G} \int \left(\ln p_0 - \frac{k}{k-1} \ln \frac{T_0}{T_0} \right) \frac{\rho_0 q(\lambda)}{V T_0} dF. \quad (142)$$

Frequently the stagnation temperature T_0 can be considered identical in all points of the cross section, i.e., we assume $\bar{T}_0 = T_0$. In this case equation (142) takes the form

$$\ln p_0 = \frac{1}{G} \int \ln p_0 dQ. \quad (143)$$

Consequently, the average value of total pressure is found by the averaging of the logarithm of total pressure in the initial flow with respect to the flow rate. The integrals of the right side of equations (142) and (143) are calculated usually by means of graphic or numerical integration. If the velocity in the initial flow is variable over the cross section, then values of \bar{p}_0 calculated according to formulas (142) and (143) will always be more than values of \bar{p}_0 determined for the same conditions according to formula (140) (when $I = \text{const}$).

We find the velocity coefficient of flow from the equation of the flow rate

$$q(\lambda) = \frac{GV\bar{T}_0}{m\bar{p}_0 F}. \quad (144)$$

In connection with the indicated increase in total pressure \bar{p}_0 , this value of $q(\lambda)$ proves to be less in value than that found earlier. This means that the average velocity in the subsonic flow will be less and in supersonic larger than the corresponding values obtained with the first method of averaging. In both cases this means that the momentum of flow averaged over entropy, proportional to the value of function $z(\lambda)$, will be greater than the total momentum of the initial nonuniform flow.

Other methods of the averaging of parameters of nonuniform flow are possible. However, it is obvious that with any method of the averaging of parameters of nonuniform flow, only part of its total characteristics is retained, and some properties of flow

are unavoidably lost. We saw that in the first case with averaging the entropy and in the second case the momentum of flow were changed. It is possible to indicate other conditionalities connected with the process of the averaging of parameters. So, let us assume that in the initial flow the static pressure p is equal over the entire cross section. After the replacement of the real parameters by average ones, the static pressure \bar{p} calculated according to \bar{p}_0 and $\bar{\lambda}$ will prove to be different than that in the initial flow. The same is possible in the relation to the value of the velocity coefficient, total pressure, etc., if they are constant on the cross section of the initial flow. Hence it follows that in each real case it is necessary to select such a method of averaging which would most fully reflect the features of the assigned problem. Thus, for instance, in the calculation of losses of efficiency it is rational to use the averaging of the flow parameters with which the condition of the retention of entropy is satisfied. With the averaging of the parameters of flow which escape from the jet nozzle, such a method will be unacceptable, since in this case the most significant is the retention of the real value of the momentum of flow, which characterizes the reactive thrust.

Let us note further one feature of the determination of the average parameters of gas in the supersonic flow.

Let us assume that at all points of the cross section of the supersonic flow the value of the stagnation temperature T_0 is constant. Let us determine the mean values of the parameters in such a flow, using the second of the methods of the averaging examined above with which in the averaged flow the actual values of total energy, entropy and flow rate of the gas are retained. From the equation of energy we obtain the obvious result of $\bar{T}_0 = T_0$. From equation (143) we find the value \bar{p}_0 . The third parameter - the mean velocity coefficient $\bar{\lambda}$ - is found from the equation of the flow rate

$$q(\bar{\lambda}) = \frac{V \bar{F}_0}{\rho_0 F_0} \int_{F_0} \frac{\rho q(\lambda) dF}{V \bar{F}_0};$$

hence when $T_0 = \bar{T}_0$ we have

$$q(\bar{\lambda}) = \frac{1}{\rho_0 F} \int_{\sigma_0} p_0 q(\lambda) dF. \quad (145)$$

The total momentum of the initial nonuniform flow, according to (119), is equal to

$$\int_{\sigma_0} p_0 q(\lambda) dF.$$

In order that the averaged flow at the value of total pressure \bar{p}_0 found above would have the same momentum, the velocity coefficient in it should satisfy the relation λ

$$f(\bar{\lambda}) = \frac{1}{\rho_0 F} \int_{\sigma_0} p_0 f(\lambda) dF. \quad (146)$$

In general the value $\bar{\lambda}$ will differ from $\bar{\lambda}$. Actually, the condition of the conservation of momentum is given by the fourth equation for determining the three unknown values; such a system of equations will be inconsistent. However, in the given case of averaging there are some features. Let us replace in expression (146) the value of function $f(\lambda)$ in terms of (117) and, after using the theorem of the mean, carry out beyond the integral sign a certain mean value of function $\bar{z}(\lambda)$. As a result we will obtain

$$\rho_0 F \bar{z}(\bar{\lambda}) q(\bar{\lambda}) = \bar{z}(\lambda) \int_{\sigma_0} p_0 q(\lambda) dF$$

or

$$q(\bar{\lambda}) = \frac{\bar{z}(\lambda)}{\bar{z}(\bar{\lambda})} \cdot \frac{1}{\rho_0 F} \int_{\sigma_0} p_0 q(\lambda) dF.$$

By comparing this expression with equation (145), we note that they differ only by the factor on the right side, and therefore

$$q(\bar{\lambda}) = \frac{\bar{z}(\lambda)}{\bar{z}(\bar{\lambda})} q(\bar{\lambda}). \quad (147)$$

In the region of supersonic velocity function $z(\lambda)$ (Fig. 5.22) changes very little: with an increase in the velocity from sonic to the maximum (from $\lambda = 1$ to $\lambda = \lambda_{\max}$) the value $z(\lambda)$ increases a total by ~40% ($k = 1.40$), and in this case the value of the pressure ratio p/p_0 drops from 0.528 to zero. If we examine the degree of irregularity of flows really being encountered, then value $z(\lambda)$ within the limits of the cross section usually changes by not more than 15-20%. Therefore, the two mean values of the function in this interval $z(\lambda)$ and $\bar{z}(\lambda)$ will differ little from each other.

The calculations carried out for supersonic flows of different laws of the change in the velocity coefficient in the cross section show that even with a very great nonuniformity of flow - for example, during a change in the total pressure p_0 of 5-10 times when $p = \text{const}$ - the factor of the right side of equation (147) differs from unity by a total of 0.5-1.5%. Therefore, it is possible to consider that $q(\lambda) \approx q(\bar{\lambda})$, i.e., the results of the determination of the mean velocity coefficient from the equation of the flow rate and momentum equation virtually coincide. The accuracy of this approximate relationship is higher, the more values of λ in the flow; however, also at moderate supersonic velocities ($\lambda > 1.2-1.3$) the distinction between values λ and $\bar{\lambda}$ consists of fractions of a percent¹.

Thus, with averaging by the indicated method of flow parameters at high supersonic velocities and stagnation temperature constant in cross section, *simultaneously with a high degree of accuracy four integral relationships are satisfied*, and these express the equality of total energy, flow rate, momentum and entropy in the initial and averaged flow. The condition $T_0 = \text{const}$

¹See Cherkez, A. Ya., On certain features of the averaging of parameters in supersonic gas flow. *Izvestiya of the Academy of Sciences of the USSR, OTN*, No. 4, 1962.

is in this case very significant, since otherwise the value $q(\bar{\lambda})$, obtained from the equation of flow rate, will depend on the distribution law of the stagnation temperature and can differ as much as possible from value $q(\lambda)$, found from the momentum equation, which does not include the value T_0 . The physical meaning of the obtained result consists in the fact that at high supersonic speed and $T_0 = \text{const}$, substantial changes in the pressures, densities and other flow parameters insignificantly change the velocity magnitude. Changed even less, in proportion to the value of function $z(\lambda)$, is the value of the momentum of the gas with its assigned flow rate: an increase in the momentum to a considerable degree is compensated by a reduction in the static pressure so that

$$\frac{Q}{g} w + pF = \frac{k+1}{2k} \frac{Q}{g} a_{*p} z(\lambda) \approx \text{const} \cdot Q$$

The indicated property of supersonic flows means the possibility of a one-dimensional examination and the use of methods given in this chapter for calculating flows with very great nonuniformity.

Thus, for instance, shown in Chapter VII is the high accuracy of such a calculation in connection with the flow in cross section of which the static pressure changes 10-20 times (initial section of the supersonic jet).

CHAPTER VI

BOUNDARY LAYER THEORY

§ 1. Basic Concepts of a Boundary Layer

The widely developed theory of motion of an ideal fluid usually gives a completely satisfactory picture of real flows, with the exception of the areas in immediate proximity to the surface of a streamlined body. In these areas, the forces of internal friction or viscosity forces which are decisive in the emergence of resistance of bodies during motion in liquid acquire vital importance. Disregard of these forces leads to the fact that the resistance of a body, uniformly moving in unlimited space turns out to be equal to zero, which contradicts experimental data.

The amount of friction force acting on a unit of area, i.e., the stress of friction is designated usually as τ . The stress of friction in the boundary layer according to Newton's hypothesis is proportional to the velocity gradient in a direction normal to the body surface (§ 4 Chapter II), i.e.,

$$\tau = \mu \frac{\partial u}{\partial y}; \quad (1)$$

the proportionality factor μ characterizes the viscous properties of the liquid and is called the *coefficient of dynamic viscosity*.

Theoretical interpretation of Newton's law (1) can be obtained for gases on the basis of the kinetic theory. According to the assumption lying as the basis of the kinetic theory, molecules of gas are found in continuous but random movement, so that gas as a whole remains stationary. The kinetic energy of this random movement of molecules represents the thermal energy of the gas. Let us assume now that along with the random movement of molecules there is regulated movement of finite (very large in comparison with the separate molecules) masses of the gas parallel to a certain plane S_0 , whereby the speed of this motion u is proportional to distance y from the plane in question (Fig. 6.1). At arbitrary distance y_1 let us conduct plane S_1 parallel to S_0 , and let us examine the transfer of momentum because of the random movement of the molecules through this plane. The molecules which pass through the plane from the bottom upwards possess less momentum in the direction of velocity u than the molecules which pass downward, and because of this the velocity of a layer of gas lying higher than plane S_1 will decrease, while the velocity of a layer of gas lying lower than plane S_1 , - will increase. To obtain the quantitative characteristic of this interaction, let us perform the following simplified calculations. Let us assume that in a unit of volume on the average there are found N molecules which have an average velocity of random movement c . In the direction perpendicular to plane S_1 it moves $N/3$ molecules, whereby, of them, $N/6$ move from the top downward and just as many move from the bottom upward. During time dt through area dS on plane S_1 in each direction there pass $1/6 N c dS dt$ molecules. Let us introduce yet another concept of the mean free path. Under mean free path l is implied that average distance which the molecules cover between collisions with each other. The molecule which was found at a distance l lower than plane S_1 possessed momentum

$$m \left(u - \frac{\partial u}{\partial y} l \right)$$

(m - the mass of the molecules, u_1 - the velocity of the regulated motion in plane S_1). Since on the mean free path the momentum is retained, then the molecules moving from the bottom upwards transfer a momentum equal to

$$\frac{1}{6} Ncm \left(u_1 - \frac{\partial u}{\partial y} l \right) dS dt.$$

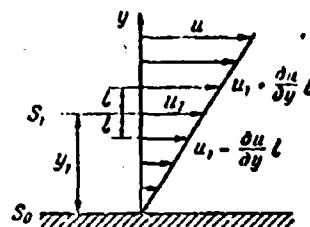


Fig. 6.1. Interpretation of Newton's law on the basis of kinetic theory.

Correspondingly, there is transferred downward the momentum

$$\frac{1}{6} Ncm \left(u_1 + \frac{\partial u}{\partial y} l \right) dS dt.$$

This transfer of momentum gives rise to the appearance of tangential stress τ along plane S_1 . Since the change in momentum is equal to the impulse of the acting force

$$\tau dS dt = \frac{1}{6} Ncm \left(u_1 + \frac{\partial u}{\partial y} l \right) dS dt - \frac{1}{6} Ncm \left(u_1 - \frac{\partial u}{\partial y} l \right) dS dt,$$

then for the tangential stress we obtain the expression

$$\tau = \frac{1}{3} \rho c l \frac{\partial u}{\partial y}, \quad (2)$$

which is nothing but Newton's law, whereby, $\mu = 1/3 \rho c l$.

The more precise calculations made by Enskog and Chapman, considering the effect of velocity u on the velocity distribution of the molecules give a somewhat different numerical factor $\mu = 0.499\rho c l$.

In accordance with kinetic theory, the coefficient of dynamic viscosity of gases should not depend on pressure - its value should vary in proportion to the square root from absolute temperature (since $\rho \sim p/T$, $c \sim \sqrt{T}$, $l \sim T/p$). The first conclusion is approximately validated by experiment within sufficiently wide limits. As concerns the increase in values of μ with an increase in the temperature, it occurs more rapidly than follows from the kinetic theory. A more precise calculation, taking into account the molecular attracting and repulsion forces, leads to formula which satisfactorily agrees with the experimental data

$$\frac{\mu}{\mu_0} = \left(\frac{T}{273} \right)^{3/2} \frac{273 + C}{T + C}, \quad (3)$$

where T is expressed in $^{\circ}\text{K}$.

Values of μ_0 and C for various gases are given in Table 1.

Table 1.

Gas	C°	$\mu_0 10^6$ $\frac{\text{kgf}\cdot\text{s}}{\text{m}^2}$	Gas	C°	$\mu_0 10^6$ $\frac{\text{kgf}\cdot\text{s}}{\text{m}^2}$
Air	122	1.75	Hydrogen	83	0.85
Nitrogen	107	1.70	Helium	80	1.88
Oxygen	138	1.96	Ammonia	626	0.96

In practical calculations, however, it is more convenient to use the exponential dependence of μ on temperature

$$\frac{\mu}{\mu_0} = \left(\frac{T}{T_0} \right)^{\omega} \quad (4)$$

The results of calculating the coefficient of viscosity of air in formulas (3) and (4) (where $\omega = 0.75$) in the range of temperatures from 100 to 1000°K are given in Fig. 6.2. The solid curve corresponds to Sutherland's formula, while the broken line corresponds to the exponential formula. In this figure, the experimental values of μ are shown by the dots.

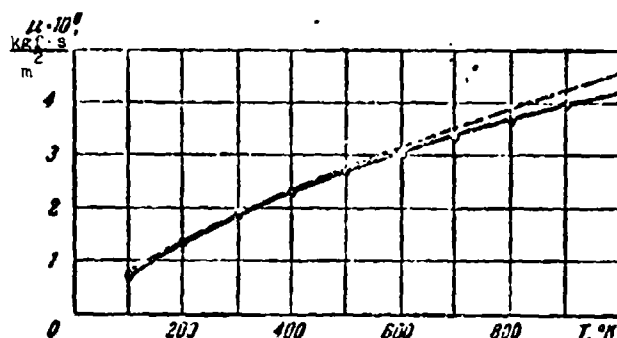


Fig. 6.2. Dependence of the coefficient of dynamic viscosity of air on temperature.

The coefficient of dynamic viscosity for liquid bodies depends very slightly on pressure and decreases rather rapidly with an increase in temperature. Since in a liquid body the mean free path of a molecule is commensurable with the molecular dimension, the kinetic theory in this case is unsuitable. The cohesive forces of the molecules under these conditions acquire great significance. In view of the complexity of the interaction of separate molecules in a liquid body at present there is no complete liquid theory, and therefore, there is no viscosity theory.

Let us consider the laminar layer motion of a viscous liquid near a solid wall. Under the action of viscosity forces, layers of liquid in proportion to their proximity to the wall are gradually slowed down and, at the wall itself adhere to it. This zone of flow of a viscous liquid located about a streamlined body is called the *boundary layer*. Outside the boundary layer the effect of viscosity is usually exhibited weakly and the picture of flow is close to that which the ideal fluid theory gives. Thus for an analytical investigation of the flow of viscous fluids, the whole field of flow can be broken into two areas: into the area of the boundary layer near the wall, where it is necessary to consider the forces of friction, and into the zone of flow outside the boundary layer in which it is possible to disregard the forces of friction and therefore to apply the laws governing the theory of an ideal fluid. Consequently, the boundary layer is that zone of flow of a viscous liquid in which the values of the forces of friction and inertia have an identical order. On the basis of this, it is possible to estimate the boundary layer thickness.

For simplicity, let us examine the flow of a liquid along a flat plate. The x-axis is directed along the plate, the y-axis - at right angles to it. For the motion which proceeds basically in the direction of the x-axis, the force of inertia pertaining to the elementary volume $dx dy dz$ is equal to $\rho \frac{du}{dt} dx dy dz$, where u is the velocity of motion of the liquid in the direction of the x-axis. For steady motion:

$$\frac{du}{dt} = \frac{\partial u}{\partial x} \frac{dx}{dt} = u \frac{\partial u}{\partial x}.$$

consequently, the force of inertia is equal to $\rho u \frac{\partial u}{\partial x} dx dy dz$.

The resultant force of friction parallel to the direction of motion, as can easily be seen from Fig. 6.3, is equal to

$$\left(\tau \cdot \frac{\partial z}{\partial y} dy \right) dx dz = \tau dx dz = \frac{\partial z}{\partial y} dx dy dz.$$

Equating the force of inertia to the force of friction, we obtain the relationship

$$\mu \frac{\partial u}{\partial x} \sim \frac{\partial z}{\partial y},$$

or, utilizing Newton's law (1),

$$\mu \frac{\partial u}{\partial x} \sim \mu \frac{\partial^2 u}{\partial y^2}. \quad (5)$$

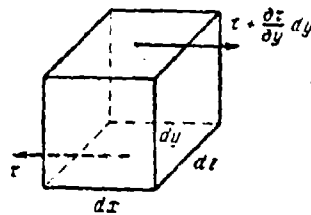


Fig. 6.3. Forces of friction applied to an elementary volume.

For a plate of length l , the value of $\partial u / \partial x$ is proportional to u_0 / l , where u_0 is the velocity of external flow. Consequently, the force of inertia has a value on the order of $\rho u_0^2 / l$. The velocity gradient in the direction perpendicular to wall, i.e., the value of $\partial u / \partial y$ is on the order of u_0 / δ , where δ is the boundary layer thickness. Thus the force of friction is proportional to $\mu u_0 / \delta^2$. Substituting these values of forces in relationship (5), we obtain for the boundary layer thickness the expression

$$\delta \sim \sqrt{\frac{\mu l}{\rho u_0}}, \text{ or } \frac{\delta}{l} \sim \frac{1}{\sqrt{\frac{\rho u_0 l}{\mu}}} = \frac{1}{\sqrt{R_l}}. \quad (6)$$

The dimensionless quantity $\rho u_0 l / \mu = R_l$ is the Reynolds number calculated along the length of the plate.

Analogously, it is possible to estimate the amount of friction stress at the wall $\tau_w = \mu (\partial u / \partial y)_w$. Utilizing the values $(\partial u / \partial y)_w \sim u_0 / \delta$, $\delta \sim \sqrt{\mu l / \rho u_0}$, obtained above, we find the expression for the amount of friction stress:

$$\tau_w \sim \mu \frac{u_0}{\delta} \sim \sqrt{\frac{\mu \rho u_0^3 l}{1}}.$$

Dividing the stress of friction τ_w by ρu_0^2 , we obtain the connection between the dimensionless quantity $\tau_w / \rho u_0^2$ and the Reynolds number

$$\frac{\tau_w}{\rho u_0^2} \sim \frac{1}{\sqrt{R_l}}. \quad (7)$$

Relationships (6) and (7) show that Reynolds number is the fundamental characteristic of a laminar boundary layer. Both the boundary layer thickness, i.e., the dimensions of the area where the forces of friction have an essential effect and also the value itself of these forces of friction are determined basically by the value of the Reynolds number. A similar result can also be obtained from the dimensional theory.

For gases, the coefficients of dynamic viscosity are low (Fig. 6.2), therefore the Reynolds numbers will be rather large even at relatively low values of the rate of flow. As follows from relationship (6), the thickness of the boundary layer because of this is low in relation to the length of the plate,

i.e., all the effect of viscosity is concentrated in a thin layer close to the streamlined surface. This conclusion is in good agreement with the results of experiments in the study of low-viscous flows.

Let us explain these qualitative considerations by a numerical example. Let us estimate the order of thickness of the boundary-layer at the end of the plate as a length of $l = 0.1$ m, the air flowing past at a temperature of $T = 300^\circ\text{K}$ at a rate of $u_0 = 15$ m/s. The air density at this temperature and atmospheric pressure equal $\rho = 0.120$ kgf·s²/m⁴, while the coefficient of viscosity $\mu = 1.85 \cdot 10^{-6}$ kgf·s/m² (Fig. 6.2). To these parameters there corresponds a Reynolds number $R_l = \rho u_0 l / \mu \approx 10^5$. According to formula (6), the relative thickness of the boundary-layer is on the order of $\delta/l \sim 1/300$.

The Reynolds number is the determining parameter not only for the quantitative characteristics of the boundary layer, but also for the character of flow itself. With small Reynolds numbers, the motion of the gas particles has a regulated laminar nature, such a flow is called *laminar*. With large Reynolds numbers the motion of the gas particles becomes irregular, uneven velocity pulsations appear, such a flow is called *turbulent*. The transition of laminar flow into turbulent occurs at a specified value of the Reynolds number called the *critical*. The critical Reynolds number is not constant and depends to a very great degree on the value of the initial disturbances, i.e., on the intensity of turbulence of the incident flow.

Experimental studies of the transition of a laminar boundary layer to a turbulent on a flat plate showed that the critical value of the Reynolds number

$$R_{\text{kp}} = \left(\frac{\rho u_{\text{cp}} x}{\mu} \right)_{\text{kp}} = 10^3 + 10^4.$$

(Here x is the distance from the leading edge of the plate). The most characteristic sign of such transition on the plate is a sharp increase in the boundary layer thickness and in the stress of friction on the wall. One of the features of the boundary layer on the plate is the fact that near leading edge it is always laminar and only at a certain distance x_{kp} does the transition to turbulent flow conditions begin. In view of the complexity of motion in the transition region and its small extent, usually the finite dimensions of this area are disregarded i.e., it is considered that the transition of the laminar boundary layer to turbulent occurs abruptly with $x = x_{\text{kp}}$.

Studies of flows in a circular tube with sharp edges of the entrance section showed that the critical value of the Reynolds number

$$R_{\text{kp}} = \left(\frac{\rho u_{\text{cp}} d}{\mu} \right)_{\text{kp}} \approx 2300. \quad (8)$$

(Here u_{cp} is the average velocity, d is the diameter of the tube). This value is the lower limit of the critical Reynolds number. At smaller values of R the turbulent flow cannot exist even during strong initial disturbances. If we insure entry of liquid into the tube with low initial disturbances, then the critical Reynolds number can exceed a value of 100,000.

The liquid decelerated in the boundary layer in certain cases does not lie close over the entire streamlined surface of the body in the form of a fine layer. Such a special case is the motion of a viscous liquid along the wall against growing pressure in external flow (flow in a diffuser). As the results of numerous experiments and theoretical evaluation show (§ 2),

the pressure remains constant across the boundary layer, therefore, the longitudinal pressure gradient which is present in the external flow, affects the entire boundary layer. If the positive pressure gradient is sufficiently great, then the layers of liquid directly adjacent to the surface of the body and possessing insignificant momentum can stop and even begin to move in the opposite direction. This phenomenon, which is called boundary layer separation, is schematically represented on Fig. 6.4. In the zone of flow with breakaway, the basic boundary layer concepts do not hold true.

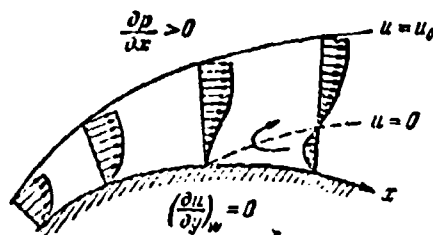


Fig. 6.4. Diagram of the formation of boundary-layer separation.

§ 2. Laminar Boundary Layer

There are two methods of calculating the parameters of a liquid in a boundary layer. The first method consists in the solution of a system of differential equations in partial derivatives which describe boundary layer flow and which were first obtained by Prandtl. Such an approach is connected with very great mathematical difficulties even with the use of computers. It is also necessary to bear in mind that in this case the results are obtained in the form of tables, and therefore their generalization is difficult. The second method consists of finding methods of approximate computation which would make it possible to rapidly determine the necessary

parameters. Such simple approximation methods can be obtained if we forego the determination of solutions which satisfy the differential equations for each particle, and instead of this restrict ourselves to the search for solutions which satisfy certain basic equations for the entire boundary layer and certain most important boundary conditions on the wall and on the edge of the boundary layer. The fundamental equations which are usually utilized in these methods are the equations of the momentum and energy for the entire boundary layer. In this case, however, it is still necessary to be given the velocity and temperature profiles. On how successfully the form of these shapes is selected, to a considerable degree, depends on the accuracy of the results obtained. Thus recently there has been wide acceptance of the methods of calculation of the parameters of a boundary layer in which to obtain the form of the velocity and temperature the differential Prandtl equations or their particular solutions are utilized; further calculation is performed with the aid of an integral equation of momentum.

Let us derive the differential equations for a laminar boundary layer during a steady plane-parallel flow of a viscous compressible ideal gas. In this case of a Navier-Stokes equation, the equation of energy and the equation of continuity take the form (§§ 5 and 6 Chapter II):

$$\mu \frac{\partial u}{\partial x} + \nu \frac{\partial u}{\partial y} = -\frac{\partial p}{\partial x} + \frac{\partial}{\partial x} \left[\mu \left(\frac{4}{3} \frac{\partial u}{\partial x} - \frac{2}{3} \frac{\partial v}{\partial y} \right) \right] + \frac{\partial}{\partial y} \left[\mu \left(\frac{\partial u}{\partial y} + \frac{\partial v}{\partial x} \right) \right], \quad (9)$$

$$\mu \frac{\partial v}{\partial x} + \nu \frac{\partial v}{\partial y} = -\frac{\partial p}{\partial y} + \frac{\partial}{\partial x} \left[\mu \left(\frac{4}{3} \frac{\partial v}{\partial x} - \frac{2}{3} \frac{\partial u}{\partial y} \right) \right] + \frac{\partial}{\partial y} \left[\mu \left(\frac{\partial u}{\partial y} + \frac{\partial v}{\partial x} \right) \right], \quad (10)$$

$$\delta \nu u \frac{\partial}{\partial x} (c_p T) + \delta \nu v \frac{\partial}{\partial y} (c_p T) =$$

$$= A u \frac{\partial p}{\partial x} + A v \frac{\partial p}{\partial y} + \frac{\partial}{\partial x} \left[\lambda \frac{\partial T}{\partial x} \right] + \frac{\partial}{\partial y} \left[\lambda \frac{\partial T}{\partial y} \right] + A \mu \left[2 \left(\frac{\partial u}{\partial x} \right)^2 + 2 \left(\frac{\partial v}{\partial y} \right)^2 + \frac{\partial v}{\partial x} \frac{\partial u}{\partial y} + \frac{\partial u}{\partial x} \frac{\partial v}{\partial y} - \frac{2}{3} \left(\frac{\partial u}{\partial x} + \frac{\partial v}{\partial y} \right)^2 \right], \quad (11)$$

$$\frac{\partial (\rho u)}{\partial x} + \frac{\partial (\rho v)}{\partial y} = 0, \quad (12)$$

where the axis x is directed along the aerodynamic body and axis y - at right angles to it; u, v are projections of the velocity vector on axes x and y ; T, ρ, p are temperature, density, and pressure; μ, λ, c_p are the coefficients of viscosity and thermal conductivity and specific heat under constant pressure, A - the thermal equivalent of work.

Simplification of these equations is based on the use of the previously noted fact that for low-viscosity liquids (with the large Reynolds numbers) the effect of viscosity and thermal conductivity is concentrated in a thin layer close to the streamlined surface, i.e.,

$$\frac{\delta}{l} \ll 1, \quad \frac{\delta_T}{l} \ll 1,$$

where l is the characteristic length of the streamlined surface, δ is the thickness of the dynamic boundary layer, δ_T is the thickness of thermal boundary layer.

Let us reduce equations (9)-(12) to dimensionless form, introducing dimensionless quantities in the following manner:

$$\bar{u} = \frac{u}{u_0}, \quad \bar{v} = \frac{v}{u_0}, \quad \bar{x} = \frac{x}{l}, \quad \bar{y} = \frac{y}{l}, \quad \bar{\delta} = \frac{\delta}{l}, \quad \bar{\delta}_T = \frac{\delta_T}{l}, \\ \bar{\rho} = \frac{\rho}{\rho_0}, \quad \bar{p} = \frac{p}{p_0}, \quad \bar{T} = \frac{T}{T_0}, \quad \bar{\mu} = \frac{\mu}{\mu_0}, \quad \bar{\lambda} = \frac{\lambda}{\lambda_0}, \quad \bar{c}_p = \frac{c_p}{c_{p0}}.$$

Here the values with subscript 0 are the flow parameters outside the boundary layer. Then we obtain

$$\bar{\rho} \bar{u} \frac{\partial \bar{a}}{\partial \bar{x}} + \bar{\rho} \bar{v} \frac{\partial \bar{a}}{\partial \bar{y}} = - \frac{\bar{p}_0}{\bar{\rho}_0 \bar{u}_0} \frac{\partial \bar{p}}{\partial \bar{x}} + \\ + \frac{\bar{\mu}_0}{\bar{\rho}_0 \bar{u}_0 l} \left\{ \frac{\partial}{\partial \bar{x}} \left[\bar{\mu} \left(\frac{4}{3} \frac{\partial \bar{a}}{\partial \bar{x}} - \frac{2}{3} \frac{\partial \bar{v}}{\partial \bar{y}} \right) \right] + \frac{\partial}{\partial \bar{y}} \left[\bar{\mu} \left(\frac{\partial \bar{a}}{\partial \bar{y}} + \frac{\partial \bar{v}}{\partial \bar{x}} \right) \right] \right\}, \\ \bar{\rho} \bar{u} \frac{\partial \bar{\theta}}{\partial \bar{x}} + \bar{\rho} \bar{v} \frac{\partial \bar{\theta}}{\partial \bar{y}} = \\ = - \frac{\bar{p}_0}{\bar{\rho}_0 \bar{u}_0} \frac{\partial \bar{p}}{\partial \bar{y}} + \frac{\bar{\mu}_0}{\bar{\rho}_0 \bar{u}_0 l} \left\{ \frac{\partial}{\partial \bar{y}} \left[\bar{\mu} \left(\frac{4}{3} \frac{\partial \bar{\theta}}{\partial \bar{y}} - \frac{2}{3} \frac{\partial \bar{u}}{\partial \bar{x}} \right) \right] + \frac{\partial}{\partial \bar{x}} \left[\bar{\mu} \left(\frac{\partial \bar{\theta}}{\partial \bar{y}} + \frac{\partial \bar{u}}{\partial \bar{x}} \right) \right] \right\}.$$

$$\begin{aligned} \bar{u} \frac{\partial}{\partial \bar{x}} (\bar{c}_p \bar{T}) + \bar{v} \frac{\partial}{\partial \bar{y}} (\bar{c}_p \bar{T}) &= \frac{\lambda \rho_0}{g \rho_0 c_{p0} T_0} \left(\bar{u} \frac{\partial \bar{p}}{\partial \bar{x}} + \bar{v} \frac{\partial \bar{p}}{\partial \bar{y}} \right) + \\ &+ \frac{\lambda_0}{g \rho_0 u_0 c_{p0} T_0} \left[\frac{\partial}{\partial \bar{x}} \left(\bar{\lambda} \frac{\partial \bar{T}}{\partial \bar{x}} \right) + \left(\bar{\lambda} \frac{\partial \bar{T}}{\partial \bar{y}} \right) \right] + \\ &+ \frac{A \mu_0 u_0}{g \rho_0 c_{p0} T_0} \bar{u} \left[2 \left(\frac{\partial \bar{u}}{\partial \bar{x}} \right)^2 + 2 \left(\frac{\partial \bar{v}}{\partial \bar{y}} \right)^2 + \left(\frac{\partial \bar{u}}{\partial \bar{x}} + \frac{\partial \bar{v}}{\partial \bar{y}} \right)^2 - \frac{2}{3} \left(\frac{\partial \bar{u}}{\partial \bar{x}} + \frac{\partial \bar{v}}{\partial \bar{y}} \right)^2 \right], \\ \frac{\partial (\bar{\rho} \bar{u})}{\partial \bar{x}} + \frac{\partial (\bar{\rho} \bar{v})}{\partial \bar{y}} &= 0. \end{aligned}$$

The dimensionless quantities

$$\frac{\rho_0}{\rho_0 u_0} = \frac{1}{k M_0^2}, \quad \frac{\lambda \rho_0}{g \rho_0 c_{p0} T_0} = \frac{k-1}{k}$$

do not depend on the Reynolds number, whereas the others are inversely proportional to Reynolds number R_0 :

$$\begin{aligned} \frac{\mu_0}{\rho_0 u_0} &= \frac{1}{R_0}, \quad \frac{\lambda_0}{g \rho_0 u_0 c_{p0} T_0} = \frac{\lambda_0}{g c_{p0} u_0} \frac{\mu_0}{\rho_0 u_0} = \frac{1}{Pr} \frac{1}{R_0}, \\ \frac{A \mu_0 u_0}{g \rho_0 c_{p0} T_0} &= \frac{\mu_0}{\rho_0 u_0} \frac{A u_0^2}{g c_{p0} T_0} = \frac{(k-1) M_0^2}{R_0}. \end{aligned}$$

Here k is the ratio of heat capacities; M_0 is Mach number of the external flow; Pr is the Prandtl number calculated from the parameters outside the boundary layer.

Let us now approach an evaluation of the separate terms of the equations. Values \bar{u} , $\bar{\rho}$, \bar{p} , \bar{T} , $\bar{\mu}$, $\bar{\lambda}$, \bar{c}_p are on the order of unity. With a change of \bar{x} from 0 to 1, the values of \bar{u} , $\bar{\rho}$, \bar{T} can change to a value on the order of unity, therefore the derivatives $\partial \bar{u} / \partial \bar{x}$, $\partial \bar{\rho} / \partial \bar{x}$, $\partial \bar{T} / \partial \bar{x}$ are also on the order of unity. From the equation of continuity it follows that, since the value of $\partial \bar{u} / \partial \bar{x}$ is on the order of unity, the value of $\partial \bar{v} / \partial \bar{y}$ has that same order. Since with $\bar{y} = 0$, $\bar{v} = 0$, then \bar{v} will be on the order of δ . The value of $\partial \bar{v} / \partial \bar{x}$ has that same order of δ . With $\bar{y} = 0$, $\bar{u} = 0$, while with $\bar{y} = \delta$, $\bar{u} = 1$, consequently $\partial \bar{u} / \partial \bar{y} = 1/\delta$. Then

$$\frac{\partial}{\partial x} \left[\mu \left(\frac{4}{3} \frac{\partial n}{\partial x} - \frac{2}{3} \frac{\partial \theta}{\partial y} \right) \right] + \frac{\partial}{\partial y} \left(\mu \frac{\partial \theta}{\partial x} \right) \sim 1,$$

$$\frac{\partial}{\partial y} \left(\mu \frac{\partial n}{\partial y} \right) \sim \frac{1}{\delta^2}, \quad \bar{\mu} n \frac{\partial n}{\partial x} \sim 1, \quad \bar{\mu} \bar{v} \frac{\partial n}{\partial y} \sim 1.$$

Since in the boundary layer the terms which depend on the viscosity have an identical order with the inertia terms, then from the first equation of motion it follows that

$$\frac{1}{R_0 \delta} \sim 1, \text{ or } \delta \sim \frac{1}{\sqrt{R_0}}. \quad (13)$$

This evaluation of the thickness of the boundary layer confirms the rougher calculation made in § 1. Retaining in the first equation of motion only the terms which are on the order of unity we obtain

$$\bar{\mu} n \frac{\partial n}{\partial x} + \bar{\mu} \bar{v} \frac{\partial n}{\partial y} = - \frac{1}{R_0 M_0^2} \frac{\partial p}{\partial x} + \frac{1}{R_0} \frac{\partial}{\partial y} \left(\mu \frac{\partial n}{\partial y} \right). \quad (14)$$

In the second equation of motion, the terms which depend on the viscosity and inertia terms are on the order of δ , therefore, $\partial \bar{p} / \partial y \sim \delta$. The total change in pressure for the extent of the boundary layer thickness normal to the wall can be calculated by means of integration of this relationship and is on the order of δ^2 , i.e., it is very small. Thus it is possible to consider that the pressure in the cross section of the boundary layer remains virtually constant and equal to the pressure in the external flow. Thus, the second equation of motion can be written in the form

$$\frac{\partial p}{\partial y} = 0. \quad (15)$$

Let us make a similar evaluation for the separate terms of the equation of energy. Since the Prandtl number for gases is close to unity, and for true liquids is on the order of 10-1000,

then the factor $1/PrR_0$ which stands before the members and which depend on thermal conductivity will be low with large Reynolds numbers. Consequently, the terms which depend on thermal conductivity will have an identical order with the terms which depend on the heat convection only in that case when the temperature gradient $\partial \bar{T}/\partial \bar{y}$ is great, i.e., near the streamlined surface is a thin layer of liquid in which an abrupt change occurs in the temperature in the direction perpendicular to the wall. Let the thickness of this thermal boundary layer be δ_T , then

$$\frac{\partial}{\partial y} \left(\lambda \frac{\partial T}{\partial y} \right) \sim \frac{1}{\delta_T^3}.$$

In order that the heat transfer as a result of thermal conductivity would be of the same order as the heat transfer as a result of convection, the thickness of thermal boundary layer should satisfy the relationship

$$\frac{1}{PrR_0 \delta_T^3} \sim 1, \text{ or } \delta_T \sim \frac{1}{\sqrt{PrR_0}}. \quad (16)$$

Taking into account the evaluation for δ (13), we obtain the relationship

$$\frac{\delta_T}{\delta} \sim \frac{1}{\sqrt{Pr}}. \quad (17)$$

which shows that with $Pr \sim 1$, i.e., for gases, the thickness of the dynamic boundary layer will be of the same order as the thickness of thermal boundary layer. Since

$$\begin{aligned} \bar{u} \frac{\partial \bar{p}}{\partial x} \sim 1, \quad \bar{v} \frac{\partial \bar{p}}{\partial y} \sim \bar{v}, \quad \frac{\partial}{\partial x} \left(\lambda \frac{\partial T}{\partial x} \right) \sim 1, \\ \frac{\partial}{\partial y} \left(\lambda \frac{\partial T}{\partial y} \right) \sim \frac{1}{\delta^3}, \quad \left[2 \left(\frac{\partial \bar{u}}{\partial x} \right)^2 + 2 \left(\frac{\partial \bar{v}}{\partial y} \right)^2 - \frac{2}{3} \left(\frac{\partial \bar{u}}{\partial x} + \frac{\partial \bar{v}}{\partial y} \right)^2 \right] \sim 1, \\ \left(\frac{\partial \bar{u}}{\partial x} \right)^2 \sim \bar{v}, \quad 2 \frac{\partial \bar{u}}{\partial x} \frac{\partial \bar{v}}{\partial y} \sim 1, \quad \left(\frac{\partial \bar{u}}{\partial y} \right)^2 \sim \frac{1}{\delta^3}. \end{aligned}$$

leaving in the equation of energy the terms on the order of unity, we obtain

$$\begin{aligned} \bar{\rho} \bar{u} \frac{\partial}{\partial x} (\bar{c}_p \bar{T}) + \bar{\rho} \bar{v} \frac{\partial}{\partial y} (\bar{c}_p \bar{T}) = \\ = \frac{1}{\lambda M} \bar{u} \frac{\partial \bar{p}}{\partial x} + \frac{1}{\bar{\rho} R} \frac{\partial}{\partial y} \left(\lambda \frac{\partial \bar{T}}{\partial y} \right) + \frac{1}{R_0} (k-1) M_{\infty}^2 \bar{u} \left(\frac{\partial \bar{u}}{\partial y} \right)^2. \end{aligned} \quad (18)$$

Returning in equations (14), (15), and (18) to dimensional variables and connecting the equation of continuity (12), we obtain the differential equations of a laminar boundary layer for a steady plane-parallel flow of a compressible ideal gas:

$$\rho u \frac{\partial u}{\partial x} + \rho v \frac{\partial u}{\partial y} = - \frac{\partial p}{\partial x} + \frac{\partial}{\partial y} \left(\mu \frac{\partial u}{\partial y} \right), \quad (19)$$

$$\frac{\partial p}{\partial y} = 0, \quad (20)$$

$$g \rho u \frac{\partial}{\partial x} (c_p T) + g \rho v \frac{\partial}{\partial y} (c_p T) = A u \frac{\partial p}{\partial x} + \frac{\partial}{\partial y} \left(\lambda \frac{\partial T}{\partial y} \right) + A \mu \left(\frac{\partial u}{\partial y} \right)^2, \quad (21)$$

$$\frac{\partial (\rho u)}{\partial x} + \frac{\partial (\rho v)}{\partial y} = 0. \quad (22)$$

In order to close this system, to equations (19)-(22) it is necessary to connect the equation of state

$$p = \rho g R T, \quad (23)$$

and also to determine the dependence of the coefficients of viscosity and thermal conductivity on temperature.

It is still necessary to formulate the boundary conditions. For an impenetrable wall, the velocity should satisfy the condition $u = v = 0$ with $y = 0$.

For a penetrable wall, during the supplying of gas normal to the surface with velocity v_w , boundary conditions are written in the form $u = 0$, $v = v_w$ with $y = 0$. The temperature can satisfy a condition of absence of thermal conductivity on

the wall (flow around a heat insulated surface) - this case $\partial T / \partial y = 0$ with $y = 0$; in another case the wall temperature T_w can be assigned. Other boundary conditions are possible for example, there can be assigned heat flow on the wall.

With $y = \infty$ there are assigned values $u = u_0$, $T = T_0$, where u_0 and T_0 are the velocity and the temperature of external flow, and also conditions of smooth transition from boundary layer to external flow $\partial u / \partial y = 0$, $\partial T / \partial y = 0$.

Since the thickness of the boundary layer is low, even at a short distance from the streamlined surface, the flow parameters virtually coincide with the parameters when $y = \infty$. Thus boundary conditions can be assigned not with $y = \infty$, but with $y = \delta$, where δ is the boundary layer thickness, i.e., such a distance from wall at which, for example, the velocity differs from the velocity with $y = \infty$ by less than 1%.

The equation of energy (21) with $c_p = \text{const.}$ can be conveniently converted by introducing, instead of temperature T , the stagnation temperature $T^* = T + Au^2 / 2gc_p$. To do this, let us multiply the equation of motion (19) by Au and add with equation (21):

$$gc_p u \frac{\partial T^*}{\partial x} + gc_p v \frac{\partial T^*}{\partial y} = \frac{\partial}{\partial y} \left(\lambda \frac{\partial T}{\partial y} \right) + A \frac{\partial}{\partial y} \left[\mu \frac{\partial}{\partial y} \left(\frac{u^2}{2} \right) \right]. \quad (24)$$

Adding and deducting in the right side of this relationship the term $gc_p \frac{\partial}{\partial y} (u \partial T / \partial y)$ and dividing both parts of the equality by gc_p , we obtain

$$u \frac{\partial T^*}{\partial x} + v \frac{\partial T^*}{\partial y} = \frac{\partial}{\partial y} \left[\left(\frac{1}{Pr} - 1 \right) \mu \frac{\partial T}{\partial y} \right] + \frac{\partial}{\partial y} \left(\mu \frac{\partial}{\partial y} \left(\frac{u^2}{2} \right) \right),$$

where Pr - the Prandtl number which characterizes the relationship of the heat which is isolated because of friction to the heat being transferred because of thermal conductivity. The Prandtl number for gases usually differs insignificantly

from one. Thus, with $T = 300^\circ\text{K}$ for helium $Pr = 0.68$, for argon $Pr = 0.66$, for air $Pr = 0.70$, for carbon dioxide $Pr = 0.77$, and for hydrogen $Pr = 0.69$. Temperature and pressure weakly affect the value of the Prandtl number. Therefore very frequently in constructing the method of calculation of the parameters of a boundary layer it is assumed that $Pr = 1$. This leads to simplification in the equation of energy, since the first term in the right side disappears.

Let us examine longitudinal flow around a *flat heat-insulated plate* of a compressible gas with $Pr = 1$. In this case, $\partial p / \partial x = 0$ and the equations for the boundary layer can be written in the following form:

$$\mu u \frac{\partial u}{\partial x} + \mu v \frac{\partial u}{\partial y} = \frac{\partial}{\partial y} \left(\mu \frac{\partial u}{\partial y} \right), \quad (25)$$

$$\mu u \frac{\partial T^*}{\partial x} + \mu v \frac{\partial T^*}{\partial y} = \frac{\partial}{\partial y} \left(\mu \frac{\partial T^*}{\partial y} \right), \quad (26)$$

$$\frac{\partial(\rho u)}{\partial x} + \frac{\partial(\rho v)}{\partial y} = 0. \quad (27)$$

Boundary conditions for the problem in question:

$$u = v = 0, \quad \frac{\partial T}{\partial y} = 0 \quad \text{with } y = 0, \quad (28)$$

$$u = u_\infty, \quad T = T_\infty \quad \text{with } y = \infty.$$

Comparing equations (25) and (26), we see that the equation of energy has a solution of the form

$$T^* = au + b,$$

whereby the unknown coefficients a and b can be determined from the boundary conditions. With $y = 0$

$$\frac{\partial T}{\partial y} = \frac{dT}{du} \frac{\partial u}{\partial y} = \left(\frac{dT^*}{du} - A \frac{u}{g c_p} \right) \frac{\partial u}{\partial y} = a \frac{\partial u}{\partial y} = 0,$$

i.e., $a = 0$. With $y = \infty$

$$T^* = b = T_0 + A \frac{u_0^2}{2gc_p} = T_0^*$$

Consequently, the stagnation temperature in this case remains constant in the cross section of the boundary layer

$$T^* = T + A \frac{u^2}{2gc_p} = T_0^* \quad (29)$$

and the wall temperature T_w is equal to the stagnation temperature of the external flow

$$T_w = T_0^* = T_0 \left(1 + \frac{k-1}{2} M_0^2 \right), \quad (30)$$

where M_0 is the Mach number of the external flow.

For determining the velocity profile and stress of friction on the wall it is necessary to solve equations (25) and (27) together relative to u and v , utilizing for the temperature expression (29), and for the density - the equation of state (23). The simplest method of solving these equations is that proposed by A. A. Dorodnitsyn. By means of special substitution the obtained system of equations is reduced to a form similar to that which takes place in an incompressible liquid. Dorodnitsyn's substitution consists of the introduction, instead of coordinate y , of a new variable η

$$\eta = \int_0^y \frac{\rho}{\rho_0} dy, \quad (31)$$

and instead of coordinate x - the value $\xi = x$. Since

$$\frac{\partial}{\partial y} = \frac{\rho}{\rho_0} \frac{\partial}{\partial \eta}, \quad \frac{\partial}{\partial x} = \frac{\partial}{\partial \xi} + \frac{\partial \eta}{\partial \xi} \frac{\partial}{\partial \eta},$$

then equation (25) now takes the form

$$\mu \left(\frac{\partial u}{\partial \xi} + \frac{\partial u}{\partial \eta} \frac{\partial \eta}{\partial \xi} \right) + \rho v \frac{\rho}{\rho_0} \frac{\partial u}{\partial \eta} = \frac{\rho}{\rho_0} \frac{\partial}{\partial \eta} \left(\mu \frac{\rho}{\rho_0} \frac{\partial u}{\partial \eta} \right).$$

Dividing both parts of this relationship by ρ , utilizing the exponential law for the coefficient of viscosity (4) and the equation of state (23) under the condition $p = p_0$, we obtain

$$u \frac{\partial u}{\partial \xi} + v \frac{\partial u}{\partial \eta} = \frac{\mu}{\rho_0} \frac{\partial}{\partial \eta} \left[\left(\frac{T}{T_0} \right)^{n-1} \frac{\partial u}{\partial \eta} \right]. \quad (32)$$

Moreover, here there is introduced the designation

$$V = u \frac{\partial \eta}{\partial x} + v \frac{\partial \eta}{\partial y}. \quad (33)$$

We now convert the equation of continuity (27), for which we present it first in the form

$$\rho \frac{\partial u}{\partial x} + u \frac{\partial \rho}{\partial x} + \frac{\partial (\rho v)}{\partial y} = 0. \quad (34)$$

We differentiate relationship (31), first with respect to x (with constant value of y)

$$\frac{\partial \eta}{\partial x} = \int_y^{\eta} \frac{1}{\rho_0} \frac{\partial \rho}{\partial x} dy,$$

and then with respect to η

$$\frac{\partial}{\partial \eta} \left(\frac{\partial \eta}{\partial x} \right) = \frac{\rho_0}{\rho} \frac{\partial}{\partial y} \left(\frac{\partial \eta}{\partial x} \right) = \frac{1}{\rho} \frac{\partial \rho}{\partial x}.$$

Substituting the obtained expression for $\partial \rho / \partial x$ in relationship (34) and converting to the new variable ξ, η , we find

$$\rho \frac{\partial u}{\partial \xi} + \rho \frac{\partial u}{\partial \eta} \frac{\partial \eta}{\partial x} + \rho u \frac{\partial}{\partial \eta} \left(\frac{\partial \eta}{\partial x} \right) + \frac{\rho}{\rho_0} \frac{\partial (\rho v)}{\partial \eta} = 0.$$

After dividing by ρ we obtain the equation of continuity

$$\frac{\partial u}{\partial \xi} + \frac{\partial V}{\partial \eta} = 0. \quad (35)$$

where V corresponds to the introduced designation (33).

Boundary conditions (28) in Dorodnitsyn's variables take the following form:

$$\left. \begin{aligned} u=0, v=0 & \text{ with } \eta=0, \\ u=u_0 & \text{ with } \eta=\infty. \end{aligned} \right\} \quad (36)$$

For the classical case of an incompressible liquid with constant coefficient of viscosity, equations (25) and (27) take the form

$$u \frac{\partial u}{\partial x} + v \frac{\partial u}{\partial y} = \frac{\nu_0}{\rho_0} \frac{\partial^2 u}{\partial y^2}, \quad (37)$$

$$\frac{\partial u}{\partial x} + \frac{\partial v}{\partial y} = 0, \quad (38)$$

boundary conditions for longitudinal flow about the plate will be

$$\left. \begin{aligned} u=v=0 & \text{ with } y=0, \\ u=u_0 & \text{ with } y=\infty. \end{aligned} \right\} \quad (39)$$

Thus, in Dorodnitsyn's variables the equations which describe flow in the boundary layer of a compressible gas differ from the equations which take place for an incompressible liquid only by the presence of the factor $(T/T_0)^{\omega-1}$ in relationship (32). If we take $\omega = 1$, then this distinction disappears.

Therefore, for the solution of the system of equations (32) and (35) with boundary conditions (36) it is possible to utilize the method proposed by Blasius for the boundary layer of an incompressible liquid.

Let us introduce in accordance with the equalities

$$u = \frac{\partial \psi}{\partial \eta}, \quad v = -\frac{\partial \psi}{\partial \xi} \quad (40)$$

the flow function ψ which satisfies equation of continuity (35). Equation of motion (32) in this case assumes the form

$$\frac{\partial \psi}{\partial \eta} \frac{\partial^2 \psi}{\partial \xi^2 \partial \eta} - \frac{\partial \psi}{\partial \xi} \frac{\partial^2 \psi}{\partial \eta^2} = \frac{\mu_0}{\rho_0} \frac{\partial}{\partial \eta} \left[\left(\frac{T}{T_0} \right)^{-1} \frac{\partial^2 \psi}{\partial \eta^2} \right],$$

and boundary conditions (36)

$$\begin{aligned} \psi &= 0, \quad \frac{\partial \psi}{\partial \eta} = 0 \quad \text{with } \eta = 0, \\ \frac{\partial \psi}{\partial \eta} &= u_0 \quad \text{with } \eta = \infty. \end{aligned}$$

Let us introduce the dimensionless flow function

$$\psi = \sqrt{\frac{\mu_0 u_0}{\rho_0}} \xi f$$

and a new dimensionless coordinate

$$\zeta = \eta \sqrt{\frac{\rho_0 u_0}{\mu_0 \xi}},$$

whereby we will assume that f depends only on ζ . Then for the flow derivatives we have

$$\left. \begin{aligned} \frac{\partial \psi}{\partial \eta} &= u = \sqrt{\frac{\mu_0 u_0}{\rho_0}} \xi \frac{df}{d\zeta} \sqrt{\frac{\rho_0 u_0}{\mu_0 \xi}} = u_0 f', \\ \frac{\partial \psi}{\partial \xi} &= -v = \frac{1}{2} \sqrt{\frac{\mu_0 u_0}{\rho_0 \xi}} f - \sqrt{\frac{\mu_0 u_0}{\rho_0}} \xi f' \frac{1}{2} \eta \sqrt{\frac{\rho_0 u_0}{\mu_0 \xi}} = \\ &= \frac{1}{2} \sqrt{\frac{\mu_0 u_0}{\rho_0 \xi}} (f - \zeta f'), \\ \frac{\partial^2 \psi}{\partial \eta^2} &= \sqrt{\frac{\mu_0 u_0}{\rho_0}} \xi f'' \frac{\rho_0 u_0}{\mu_0 \xi} = u_0 \sqrt{\frac{\rho_0 u_0}{\mu_0 \xi}} f'', \\ \frac{\partial^2 \psi}{\partial \xi \partial \eta} &= -\frac{1}{2} u_0 f'' \eta \sqrt{\frac{\rho_0 u_0}{\mu_0 \xi}}. \end{aligned} \right\} \quad (41)$$

Substituting these values in the equation of motion, we obtain

$$-\frac{1}{2} \frac{u_0}{\xi} f' f'' - \frac{1}{2} \frac{u_0}{\xi} f'' (f - \zeta f') = \frac{u_0}{\xi} \frac{d}{d\zeta} \left[\left(\frac{T}{T_0} \right)^{-1} f'' \right].$$

or after simplification

$$ff'' + 2 \frac{d}{d\zeta} \left[\left(\frac{T}{T_0} \right)^{n-1} f' \right] = 0. \quad (42)$$

From relationship (29) the temperature can be expressed as the velocity

$$\begin{aligned} T &= T_0 - A \frac{u^2}{2gc_p} = T_0 - T_0 \frac{k-1}{2} M_0^2 \left(\frac{u}{u_0} \right)^2 = \\ &= T_0 \left[1 + \frac{k-1}{2} M_0^2 (1 - f'^2) \right]. \end{aligned} \quad (43)$$

Substituting (43) in (42), we obtain the usual differential equation of the third order

$$ff'' + 2 \frac{d}{d\zeta} \left[\left(1 + \frac{k-1}{2} M_0^2 (1 - f'^2) \right)^{n-1} f' \right] = 0 \quad (44)$$

with boundary conditions

$$\begin{aligned} f &= 0, f' = 0 \text{ with } \zeta = 0, \\ f' &= 1 \text{ with } \zeta = \infty. \end{aligned}$$

The solution of this equation can be obtained only by numerical methods. After the dependence of f on ζ is found it is possible to determine the velocity profile in Dorodnitsyn's variables

$$\frac{u}{u_0} = f' \left(\eta \sqrt{\frac{\rho_0 u_0}{\mu_0 \zeta}} \right),$$

and consequently, the distribution of temperatures (43) and the density distribution

$$\frac{\rho}{\rho_0} = \frac{T_0}{T} = \frac{1}{\left[1 + \frac{k-1}{2} M_0^2 (1 - f'^2) \right]}.$$

Transition to the physical coordinate system is made from the formula

$$y = \int_0^x \left[1 + \frac{k-1}{2} M_0^2 (1 - \eta^2) \right] d\eta, \quad x = \xi$$

Let us find the stress of friction on the wall

$$\begin{aligned} \tau_w &= \mu_w \left(\frac{\partial u}{\partial y} \right)_w = \mu_w \frac{\rho_w}{\rho_0} \left(\frac{\partial u}{\partial \eta} \right)_{\eta=0} \\ \text{Since } \frac{\partial u}{\partial \eta} &= \frac{\partial^2 \psi}{\partial \eta^2} = u_0 \sqrt{\frac{\rho_0 u_0}{\mu_0 k}} f'', \text{ then} \\ \tau_w &= \mu_w \frac{\rho_w}{\rho_0} u_0 \sqrt{\frac{\rho_0 u_0}{\mu_0 k}} f''(0) \end{aligned} \quad (45)$$

Then for the coefficient of friction c_f we have

$$c_f = \frac{\tau_w}{\frac{\rho_w u_w^2}{2}} = 2 \frac{\mu_w \rho_w}{\rho_0 \mu_0} \sqrt{\frac{\rho_0}{\rho_0 u_0 k}} f''(0) = \frac{2}{\sqrt{R_x}} \left(\frac{T_w}{T_0} \right)^{-1} f''(0) \quad (46a)$$

Expressing the temperature ratio T_w/T_0 with the aid of relationship (30), we finally obtain

$$c_f = \frac{2}{\sqrt{R_x}} \left(1 + \frac{k-1}{2} M_0^2 \right)^{-1} f''(0) \quad (46b)$$

For an incompressible liquid ($M_0 = 0$) the solution of equation (44) was first found by Blasius. In this case $f''(0) = 0.332$, and therefore the coefficient of friction in an incompressible liquid c_{f_H} is equal to

$$c_{f_H} = \frac{0.664}{\sqrt{R_x}} \quad (46c)$$

The resistance of a plate with a width of b and length of l about which an incompressible gas flows only on one side, is equal to

$$W = b \int_0^l \tau_w dx.$$

Expressing τ_w in terms of the coefficient of friction (46c) and integrating, we obtain

$$w = \frac{\rho_0 u_0^2}{2} b l \frac{1.328}{\sqrt{R_l}}.$$

Consequently, the drag coefficient of such a plate will be equal to

$$C_{w_2} = \frac{2w}{\frac{\rho_0 u_0^2}{2} b l} = \frac{1.328}{\sqrt{R_l}}. \quad (47)$$

For a compressible gas the value of $f''(0)$ depends on M_0 . Calculation of the profiles of velocity and temperature, and also the stress frictions on the wall for a compressible gas with $\omega = 0.76$ were performed by Kármán and Tsien. The results of this calculation are represented in Figs. 6.5, 6.6 and in Fig. 6.7 (solid line).

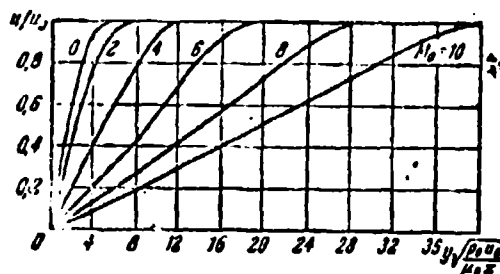


Fig. 6.5. Velocity distribution in laminar boundary layer on heat-insulated plate with $Pr = 1$, $\omega = 0.76$, $k = 1.4$.

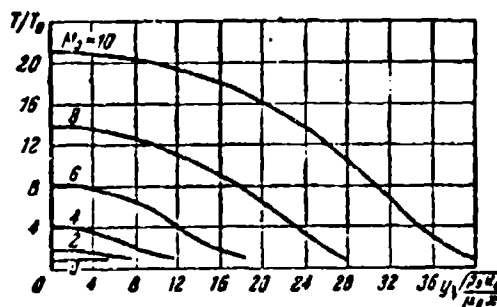


Fig. 6.6. Distribution of temperatures in laminar boundary layer on heat-insulated plate with $Pr = 1$, $\omega = 0.76$, $k = 1.4$.

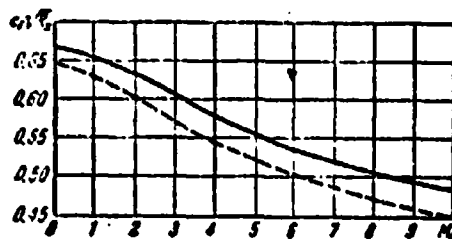


Fig. 6.7. Coefficient of friction for a laminar boundary layer on a heat-insulated plate with $Pr = 1$, $\omega = 0.76$, $k = 1.4$.

Let us now examine the laminar boundary layer of a compressible gas on a flat plate in the presence of thermal conductivity. As before, we will be restricted to the case of $Pr = 1$. Equations (25), (26) and (27) and boundary conditions (28) in this case are retained, with the exception of the condition for temperature on the surface of the plate, which in this case should be written in the form

$$T = T_w \text{ with } y=0.$$

Just as earlier, the equation of energy has a solution of the form

$$T^* = au + b.$$

With $y = 0$ we have $T^* = b = T_w$. For determining the unknown coefficient a we utilize the condition $T_0^* = au_0 + T_w$ with $y = \infty$. Hence we obtain $a = (T_0^* - T_w)/u_0$. Consequently, the distribution of the stagnation temperature in this case is described by the formula

$$T^* = (T_0^* - T_w) \frac{u}{u_0} + T_w \quad (48)$$

Then,

$$\frac{T}{T_0} = \left(1 + \frac{k-1}{2} M_0^2 - \frac{T_w}{T_0} \frac{u}{u_0} + \frac{T_w}{T_0} - \frac{k-1}{2} M_0^2 \left(\frac{u}{u_0}\right)^2\right),$$

and instead of equation (44) we obtain a new equation

$$ff'' + 2 \frac{d}{dx} \left\{ \left(1 + \frac{k-1}{2} M_0^2 - \frac{T_w}{T_0} \frac{u}{u_0} + \frac{T_w}{T_0} - \frac{k-1}{2} M_0^2 \left(\frac{u}{u_0}\right)^2\right) f' + \frac{T_w}{T_0} - \frac{k-1}{2} M_0^2 f'^2 \right\} = 0. \quad (49)$$

The boundary conditions for equation (44) in this case also remain valid for (49).

Calculation of the velocity and temperature profile according to equation (49) for different numbers of M_0 with $\omega = 0.76$ and $T_w/T_0 = 0.25$ was also performed by Kármán and Tsien. The results of the calculation are shown in Figs. 6.8 and 6.9.

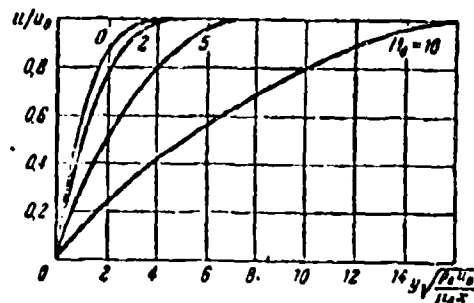


Fig. 6.8. Velocity distribution in laminar boundary layer on a plate in the presence of thermal conductivity ($T_w/T_0 = 0.25$), $Pr = 1$, $\omega = 0.76$, $k = 1.4$.

The coefficient of friction can be calculated according to formula (46a), whereby the value of $f''(0)$ will be in this case, as noted, the function of two parameters M_0 and T_w/T_0 .

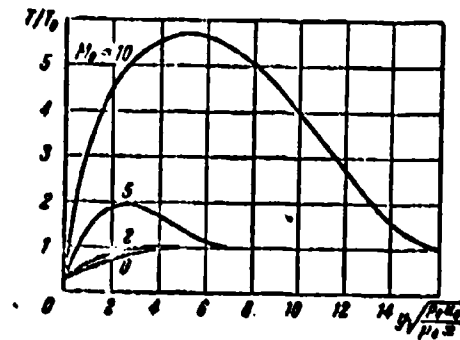


Fig. 6.9. Distribution of temperatures in a laminar boundary layer on a plate in the presence of thermal conductivity ($T_w/T_0 = 0.25$), $Pr = 1$, $\omega = 0.76$, $k = 1.4$.

For determining specific heat flow q_w (i.e., the heat flow in a unit of time through a unit of surface of the plate) we utilize relationship (29) from which it follows that

$$\frac{\partial T}{\partial y} = \frac{\partial T^*}{\partial y} - A \frac{u}{g c_p} \frac{\partial u}{\partial y}.$$

Since with $y = 0$, $u = 0$, when $(\partial T / \partial y)_w = (\partial T^* / \partial y)_w$. But from equation (48) we have

$$\left(\frac{\partial T^*}{\partial y} \right)_w = \frac{(T_s^* - T_w)}{u_s} \left(\frac{\partial u}{\partial y} \right)_w.$$

therefore,

$$q_w = \lambda_w \left(\frac{\partial T}{\partial y} \right)_w = \lambda_w \frac{T_s^* - T_w}{u_s} \left(\frac{\partial u}{\partial y} \right)_w = \lambda_w \frac{T_s^* - T_w}{u_s} \tau_w \quad (50)$$

Introducing the dimensionless heat-transfer coefficient (Stanton number) and replacing τ_w in (46a) we obtain

$$St = \frac{q_w}{g \rho u c_p (T_s^* - T_w)} = \frac{c_p}{2} \quad (51)$$

Here it is taken into account that $\frac{R^{*}u_{\infty}^2}{\lambda_w} = Pr_w = 1$. Thus, if the coefficient of friction c_f is found, then the Stanton number is easily determined.

With number $Pr \neq 1$ calculations were also performed for a laminar boundary layer of a compressible liquid (Brainerd and Emmons, Crocco, Kop and Hartree). In this case it turned out that the temperature of the heat-insulated surface T_{w0} was not equal to the stagnation temperature of the external flow, but is determined from the relationship

$$T_{w0} = T_0 \left(1 + \frac{k-1}{2} M_0^2 Pr \right). \quad (52)$$

The results of calculating the stress of friction on a flat plate in general ($Pr \neq 1$, $\omega \neq 1$) are well described by Yang's approximation formula.

$$c_f \sqrt{Re} = 0.664 \left[0.45 + 0.55 \frac{T_w}{T_0} + 0.09(k-1) M_0^2 Pr \right]^{\frac{n-1}{2}}. \quad (53)$$

A formula for the Stanton number was obtained which is a generalization of relationship (51) with $Pr \neq 1$:

$$St = \frac{q_w}{St_{0, \omega, Pr} (T_{w0} - T_w)} = \frac{c_f}{2} Pr^{-\frac{1}{2}}. \quad (54)$$

The methods described for the solution of the differential equations of a laminar boundary layer pertain to the simplest case of flow along a plate. With a more intricate shape of aerodynamic surface, i.e., in the presence of a pressure gradient in the external flow, the task of determining the parameters of the boundary layer becomes immeasurably more difficult. Therefore attempts were made to create a method of calculation based on the solution of integral equations composed for the entire boundary layer. Let us now pass to the derivation of these equations and an examination of the methods of their solution.

Let us compose the integral equation of impulses during steady-state flow in the boundary layer of a compressible liquid. Applying the equation of momentum to the element of the boundary layer with length dx and unit width, we obtain
(§ 5 Chapter 1)

$$P_x = \Delta(\Sigma mu),$$

where $\Delta(\Sigma mu)$ is the change in projection on axis x of the momentum of a liquid which flows for a unit of time through the surface which limits the volume in question (Fig. 6.10), and P_x - the projection on axis x of the resultant of all forces applied to the selected volume. First let us calculate the change in momentum. Through the element of area dy in cross section 1 there flows in a unit of time a mass of liquid $\rho u dy$ which transfers the momentum $\rho u^2 dy$. Thus the momentum being transferred by the liquid which flows through cross section 1 is equal to

$$(\Sigma mu)_1 = \int \rho u^2 dy.$$

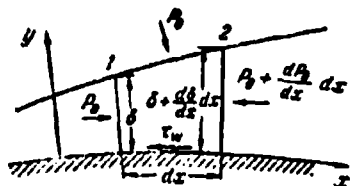


Fig. 6.10. Forces applied to an element of a boundary layer.

The momentum of the liquid flowing through cross section 2:

$$(\Sigma mu)_2 = \int \rho u^2 dy + \left(\frac{d}{dx} \int \rho u^2 dy \right) dx.$$

The mass of the liquid flowing through the boundary of the boundary layer in Section 1-2 is equal to the difference in the flow rates through cross sections 2 and 1, i.e.,

$$(\Sigma m)_{1-1} = \frac{d}{dx} \left(\int_0^\delta \rho u dy \right) dx.$$

Since the velocity on the boundary of boundary layer is equal to the velocity of external flow u_0 , then the momentum being introduced by this mass of liquid into the volume in question will be

$$(\Sigma mu)_{1-1} = u_0 \frac{d}{dx} \left(\int_0^\delta \rho u dy \right) dx.$$

Consequently, a change in projection on axis x of the momentum is equal to

$$\begin{aligned} \Delta(\Sigma mu) &= (\Sigma mu)_1 - (\Sigma mu)_1 - (\Sigma mu)_{1-1} = \\ &= \left(\frac{d}{dx} \int_0^\delta \rho u^2 dy - u_0 \frac{d}{dx} \int_0^\delta \rho u dy \right) dx. \end{aligned}$$

Let us now find the resultant of all forces applied to the volume in question. In this case, the mass forces can be disregarded. The forces of friction in cross sections 1 and 2 do not give a component to axis x . The force of friction on the boundary of boundary layer is equal to zero, since $\partial u / \partial y = 0$ with $y = \delta$. The force of friction acting on the side of the wall for the volume in question is equal to $P_{xw} = -\tau_w dx$.

The projections of the forces of pressure on axis x are equal to: in cross section 1, $P_{x1} = p_0 \delta$, in cross section 2, $P_{x2} = -\left[p_0 \delta + \frac{d(p_0 \delta)}{dx} dx \right]$, on the boundary of the boundary layer

$P_{x1,2} = p_0 \frac{d\delta}{dx} dx$. The sum of the projections of the forces of pressure

$$P_{x1} + P_{x2} + P_{x1,2} = p_0 \delta - p_0 \delta - \frac{d(p_0 \delta)}{dx} dx + p_0 \frac{d\delta}{dx} dx = -\delta \frac{dp_0}{dx}.$$

Then the projection of the resultant of all forces applied to the selected volume will be

$$P_x = -\left(\lambda \frac{dP_2}{dx} + \tau_w\right) dx.$$

Substituting the found values of $\Delta(\Sigma mu)$ and P_x in the equation of momentum, we obtain the integral relationship of impulses in the boundary layer

$$-\frac{d}{dx} \int \rho u^2 dy + u_0 \frac{d}{dx} \int \rho u dy = \lambda \frac{dP_2}{dx} + \tau_w \quad (55)$$

In this equation u_0 and p_0 are known functions of x and are determined during the calculation of external flow. If external flow is isentropic, then from the equation of motion it follows that

$$\frac{dP_2}{dx} = -\rho u_0 \frac{du_0}{dx}.$$

After also writing the obvious equality

$$u_0 \frac{d}{dx} \int \rho u dy = \frac{d}{dx} \int \rho u u_0 dy - \frac{du_0}{dx} \int \rho u dy,$$

let us substitute these expressions in relationship (55). As a result we have

$$\frac{d}{dx} \int \rho u (u_0 - u) dy + \frac{du_0}{dx} \int (\rho u u_0 - \rho u) dy = \tau_w \quad (56)$$

This equation can also be obtained directly from the differential equations of a boundary layer. To do this it is necessary to add term-by-term the equation of motion (19) with the equation of continuity (22), multiplied by $(u - u_0)$, and then to add and to deduct $\rho u \partial u_0 / \partial x$ in the right side of the obtained relationship

$$\frac{\partial}{\partial x} [\rho u (u - u_0)] + \rho u \frac{\partial u_0}{\partial x} + \frac{\partial}{\partial y} [\rho v (u - u_0)] = \rho u_0 \frac{du_0}{dx} + \frac{\partial}{\partial y} \left(\mu \frac{\partial u}{\partial y} \right)$$

and to integrate within the limits of boundary layer from 0 to δ taking into account the boundary conditions.

Let us introduce now the concepts regarding the displacement thickness δ^* and the momentum thickness δ^{**} which are determined respectively by the following expressions:

$$\delta^* = \frac{\int_0^\delta (\rho_0 u_0 - \rho u) dy}{\rho_0 u_0} = \int_0^\delta \left(1 - \frac{\rho u}{\rho_0 u_0}\right) dy, \quad (57)$$

$$\delta^{**} = \frac{\int_0^\delta \rho u (u_0 - u) dy}{\rho_0 u_0^2} = \int_0^\delta \left(1 - \frac{u}{u_0}\right) \frac{\rho u}{\rho_0 u_0} dy. \quad (58)$$

These values have a specific physical sense. The displacement thickness is the distance to which the flow lines of external flow are moved aside from the body as a result of a decrease in the velocity and a change in density in the boundary layer. The momentum thickness is the thickness of the gas layer with constant parameters and momentum equal to the difference in the momenta of the flow of gas with nonuniform current density but with constant velocity u_0 and flow with variable values of velocity and density.

Utilizing the introduced values δ^* and δ^{**} , the integral relationship of momentum (56) can be presented in the form

$$\frac{d}{dx} (\rho_0 u_0^2 \delta^{**}) + \rho_0 u_0 \delta^* \frac{du_0}{dx} = \tau_w,$$

or

$$\frac{d\delta^{**}}{dx} + \delta^{**} \left[\frac{1}{\rho_0 u_0^2} \frac{d(\rho_0 u_0^2)}{dx} + \frac{H}{u_0} \frac{du_0}{dx} \right] = \frac{\tau_w}{\rho_0 u_0^2}, \quad (59)$$

where $H = \delta^*/\delta^{**}$. If we assign the velocity laws of distribution and temperature, then stress of friction will be expressed as the momentum thickness δ^{**} . Then relationship (59) which is

the ordinary differential equation can be used for determination of the distribution of the value of δ^{**} along the streamlined surface.

As shown above, the differential equations of the boundary layer of a compressible gas in Dorodnitsyn's variables have very nearly the same form as for the boundary layer of an incompressible liquid. Therefore, it should be expected that the boundary layer velocity profile of a compressible gas in Dorodnitsyn's variables will be close to the velocity profile in an incompressible liquid. The results of precise calculations confirm this assumption.

For the laminar boundary layer of an incompressible liquid the distribution of velocities is usually assigned in the form of a polynomial

$$\frac{u}{u_0} = \sum_{k=0}^n A_k \left(\frac{y}{\delta}\right)^k,$$

whereby the values of coefficients A_k are determined from boundary conditions on the wall and on the boundary of the boundary layer. Usually in the solution they are limited to polynomials of the third or fourth degree. For the boundary layer of a compressible gas the velocity profile, therefore, can be assigned in the form

$$\frac{u}{u_0} = \sum_{k=0}^n A_k \left(\frac{\eta}{\Delta}\right)^k, \quad \Delta = \int_0^\delta \frac{1}{\rho} dy, \quad (30)$$

whereby η is the Dorodnitsyn variable (31).

Let us examine the flow of a compressible gas around a flat plate.

The integral equation of impulses (59) in the absence of a pressure gradient in external flow assumes the form

$$\frac{d\psi}{dx} = \frac{\tau_w}{\rho u_0^2} \quad (61)$$

We approximate the velocity profile for an incompressible liquid by a polynomial of the third degree. For a search of coefficients A_k we utilize the following boundary conditions:

$$u = 0 \text{ with } y = 0; u = u_0, \frac{\partial u}{\partial y} = 0 \text{ with } y = \delta.$$

The second condition on the wall can be obtained from the differential equation of motion (25) which for an incompressible liquid assumes the form

$$\rho u \frac{\partial u}{\partial x} + \rho v \frac{\partial u}{\partial y} = \mu \frac{\partial^2 u}{\partial y^2};$$

since $u = v = 0$ with $y = 0$, then from this equation we have $\partial^2 u / \partial y^2 = 0$.

By definition (31), $\rho dy = \rho_0 d\eta$, therefore in Dorodnitsyn's variables these boundary conditions will be written in the form

$$\begin{aligned} u=0, \quad \frac{\partial^2 u}{\partial \eta^2} &= 0 \text{ with } \eta=0, \\ u=u_0, \quad \frac{\partial u}{\partial \eta} &= 0 \text{ with } \eta=\Delta. \end{aligned}$$

Utilizing these conditions from (60) we obtain the system of equations

$$\begin{aligned} A_0 &= 0, \quad A_2 = 0, \quad A_0 + A_1 + A_2 + A_3 = 1, \\ A_1 + 2A_2 + 3A_3 &= 0. \end{aligned}$$

Hence $A_0 = 0$, $A_1 = \frac{3}{2}$, $A_2 = 0$, $A_3 = -1/2$, and therefore, for the velocity profile we obtain

$$\frac{u}{u_0} = \frac{3}{2} \frac{\eta}{\Delta} - \frac{1}{2} \left(\frac{\eta}{\Delta} \right)^3. \quad (62)$$

Utilizing (62) and (31), we find the stress of friction on the
11

$$\tau_w = \mu_w \left(\frac{\partial u}{\partial y} \right)_w = \mu_w \left(\frac{\partial u}{\partial \eta} \right)_{\eta=0} \frac{\rho_w}{\rho_0} = \dots = \frac{\rho_w}{\rho_0} \frac{u_0}{\Delta},$$

and the momentum thickness

$$\delta^{**} = \int_0^{\delta} \left(1 - \frac{u}{u_0} \right) \frac{\rho u}{\rho_0 u_0} dy = \int_0^{\delta} \left(1 - \frac{u}{u_0} \right) \frac{u}{u_0} d\eta = N\Delta.$$

Here

$$N = \int_0^1 \left(1 - \frac{u}{u_0} \right) \frac{u}{u_0} d \frac{\eta}{\Delta} = \frac{39}{280}.$$

The obtained expressions make it possible to establish the
connection between τ_w and δ^{**} :

$$\tau_w = A_1 N \frac{\rho_w}{\rho_0} \frac{u_0}{\Delta} \quad (63)$$

Substituting the expression for τ_w from (63) in the integral
relationship of momentum (61) and integrating, we obtain the
distribution of the momentum thickness along the plate

$$\delta^{**} = \sqrt{2 A_1 N \frac{\rho_w}{\rho_0} \frac{u_0 x}{u_0}} \quad \text{or} \quad \frac{\delta^{**}}{x} = \sqrt{2 A_1 N \frac{\rho_w}{\rho_0} \frac{u_0}{u_0}} \frac{1}{\sqrt{R_x}}, \quad (64)$$

where

$$R_x = \frac{\rho_0 u_0 x}{\mu_0}.$$

Replacing in relationship (63) the value of δ^{**} according to
expression (64) we obtain the formula for the coefficient of
the friction

$$c_f = \frac{\tau_w}{\rho_e u_e^2} = \sqrt{2 A_1 N \frac{\rho_w \mu_w}{\rho_e \mu_e} \frac{1}{\sqrt{R_x}}}. \quad (65)$$

Substituting numerical values of coefficients A_1 and N and utilizing a power law for the viscosity-temperature dependence (4), we finally obtain

$$c_f = \frac{\tau_w}{\rho_e u_e^2} = \frac{0.617}{\sqrt{R_x}} \left(\frac{T_w}{T_e} \right)^{\frac{n-1}{2}}. \quad (66)$$

For determining the velocity profile in physical coordinates x , y , and the calculation of the boundary layer thickness δ and a displacement thickness δ^* it is necessary to know the distribution of temperatures. If we are restricted to the case $Pr = 1$, then the stagnation temperature according to (48) will be proportional to the velocity. Then

$$\begin{aligned} \frac{p_e}{p} = \frac{T}{T_e} &= \left(1 + \frac{k-1}{2} M_e^2 - \frac{T_w}{T_e} \right) \frac{u}{u_e} + \frac{T_w}{T_e} - \frac{k-1}{2} M_e^2 \left(\frac{u}{u_e} \right)^2 = \\ &= \left(1 + \frac{k-1}{2} M_e^2 - \frac{T_w}{T_e} \right) \left[\frac{3}{2} \frac{\eta}{\Delta} - \frac{1}{2} \left(\frac{\eta}{\Delta} \right)^2 \right] + \frac{T_w}{T_e} - \\ &\quad - \frac{k-1}{2} M_e^2 \left[\frac{3}{2} \frac{\eta}{\Delta} - \frac{1}{2} \left(\frac{\eta}{\Delta} \right)^2 \right]^2, \end{aligned}$$

and therefore

$$\begin{aligned} y = \int_0^{\eta} \frac{p_e}{p} d\eta &= \Delta \int_0^{\frac{\eta}{\Delta}} \frac{p_e}{p} d\left(\frac{\eta}{\Delta}\right) = \\ &= \Delta \left\{ \frac{T_w}{T_e} \frac{\eta}{\Delta} + \left(1 + \frac{k-1}{2} M_e^2 - \frac{T_w}{T_e} \right) \left[\frac{3}{4} \left(\frac{\eta}{\Delta} \right)^2 - \frac{1}{8} \left(\frac{\eta}{\Delta} \right)^4 \right] - \right. \\ &\quad \left. - \frac{k-1}{2} M_e^2 \left[\frac{3}{4} \left(\frac{\eta}{\Delta} \right)^3 - \frac{3}{10} \left(\frac{\eta}{\Delta} \right)^5 + \frac{1}{28} \left(\frac{\eta}{\Delta} \right)^7 \right] \right\}. \end{aligned}$$

Since $y = \delta$ with $\eta = \Delta$, then

$$\delta = \Delta \left[\frac{T_w}{T_e} + \frac{5}{8} \left(1 + \frac{k-1}{2} M_e^2 - \frac{T_w}{T_e} \right) - \frac{17k-1}{33} \frac{1}{2} M_e^2 \right].$$

Now it is easy to find the connection between y/δ and η/Δ

$$\frac{\eta}{\delta} = \frac{\frac{T_w}{T_0} \left[\frac{3}{4} \left(\frac{\eta}{\Delta} \right)^4 - \frac{1}{8} \left(\frac{\eta}{\Delta} \right)^4 \right]}{\frac{T_w}{T_0} + \frac{5}{8} \left(1 + \frac{k-1}{2} M_0^2 - \frac{T_w}{T_0} \right) - \frac{17}{35} \frac{k-1}{2} M_0^2} - \frac{\frac{k-1}{2} M_0^2 \left[\frac{3}{4} \left(\frac{\eta}{\Delta} \right)^4 - \frac{3}{10} \left(\frac{\eta}{\Delta} \right)^4 + \frac{1}{28} \left(\frac{\eta}{\Delta} \right)^4 \right]}{\frac{T_w}{T_0} + \frac{5}{8} \left(1 + \frac{k-1}{2} M_0^2 - \frac{T_w}{T_0} \right) - \frac{17}{35} \frac{k-1}{2} M_0^2}. \quad (67)$$

Relationships (62) and (67) give in parametrical form the velocity distribution in the boundary layer on a flat plate.

Since $\Delta = \delta^{**}/N$ and δ^{**} is connected with the Reynolds number by formula (66), for the boundary layer thickness we obtain the expression

$$\frac{\delta}{x} = \frac{4.64}{\sqrt{R_x}} \left(\frac{T_w}{T_0} \right)^{\frac{n-1}{2}} \left[\frac{T_w}{T_0} + \frac{5}{8} \left(1 + \frac{k-1}{2} M_0^2 - \frac{T_w}{T_0} \right) - \frac{17}{35} \frac{k-1}{2} M_0^2 \right]. \quad (68)$$

Performing simple calculations, let us find for the displacement thickness

$$\delta^* = \int_0^{\delta} \left(1 - \frac{\rho}{\rho_0} \right) dy = \delta \left(1 - \frac{5}{8} \frac{\Delta}{\delta} \right)$$

or after the substitution of values Δ/δ and δ/x

$$\frac{\delta^*}{x} = \frac{1.74}{\sqrt{R_x}} \left(\frac{T_w}{T_0} \right)^{\frac{n-1}{2}} \left(\frac{T_w}{T_0} + \frac{13}{35} \frac{k-1}{2} M_0^2 \right). \quad (69)$$

In the absence of thermal conductivity $T_w = T_0 \left(1 + \frac{k-1}{2} M_0^2 \right)$ as follows from the equation of energy (30). Then

$$\frac{\delta^*}{x} = \frac{\delta^{**}}{x} = \frac{0.647}{\sqrt{R_x}} \left(1 + \frac{k-1}{2} M_0^2 \right)^{\frac{n-1}{2}}. \quad (70)$$

$$\frac{\delta}{x} = \frac{4.64}{\sqrt{R_x}} \left(1 + \frac{18}{35} \frac{k-1}{2} M_0^2 \right) \left(1 + \frac{k-1}{2} M_0^2 \right)^{\frac{n-1}{2}}. \quad (71)$$

$$\frac{\delta^*}{x} = \frac{1.74}{\sqrt{R_x}} \left(1 + \frac{14}{35} \frac{k-1}{2} M_0^2 \right) \left(1 + \frac{k-1}{2} M_0^2 \right)^{\frac{n-1}{2}}. \quad (72)$$

For an incompressible liquid ($M_0 = 0$) the approximate value of the coefficient of friction

$$c_f = \frac{0.647}{\sqrt{R_x}} \quad (73)$$

is close to the value found during integration of the differential equations of the boundary layer (46c).

Values of the boundary layer thickness δ , the displacement thickness δ^* and the momentum thickness δ^{**} for an incompressible liquid also can be found from relationships (70), (71), (72):

$$\frac{\delta}{x} = \frac{4.64}{\sqrt{R_x}}, \quad \frac{\delta^*}{x} = \frac{1.74}{\sqrt{R_x}}, \quad \frac{\delta^{**}}{x} = \frac{0.647}{\sqrt{R_x}}.$$

Figure 6.11 shows the boundary layer velocity profiles on a flat plate with $M_0 = 10$, $k = 1.4$, $\omega = 0.76$, calculated according to formulas (62) and (67) for two values of the ratios of temperatures $T_w/T_0 = 0.25$, $T_w/T_0 = 21$ (dotted curve). Thus are given the velocity distributions obtained by Kármán and Tsien by integration of the boundary layer equations (unbroken curve). The results of calculating the coefficient of friction on a heat-insulated plate for a compressible gas in formula (70) with $\omega = 0.76$ are shown in Fig. 6.7 by dotted lines. The solid line corresponds to precise values.

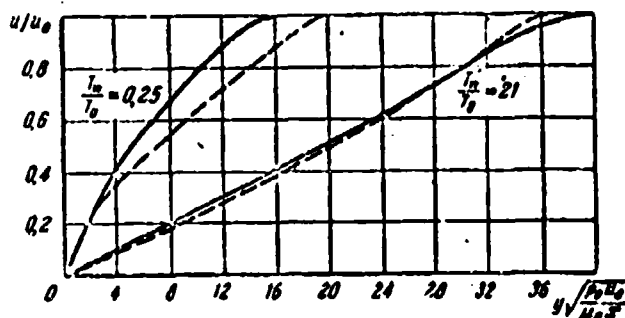


Fig. 6.11. Velocity distribution in a boundary layer on a flat plate; according to the approximation formula (dotted curve), precise values (unbroken curve) ($M_0 = 10$, $\omega = 0.76$, $k = 1.4$).

Thus, the simple method of calculation based on the solution of the integral equation of momentum when using a velocity profile in the form of a polynomial makes it possible to determine the parameters of the boundary layer with sufficient practical accuracy.

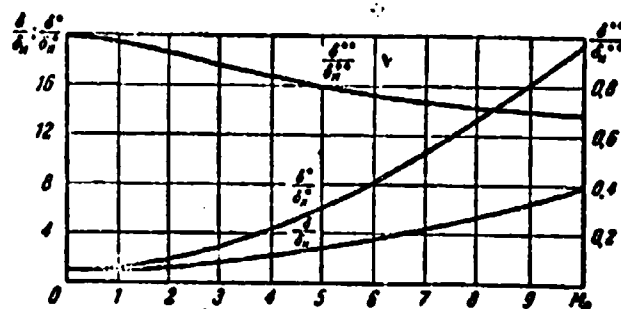


Fig. 6.12. Dependence of thickness of boundary layer displacement thickness, and thickness of pulse loss on a flat insulated plate on M_0 ($Pr = 1$, $\omega = 0.76$, $k = 1.4$).

As an example, Fig. 6.12 gives the values of the boundary layer thickness, displacement thickness, and momentum thickness on a flat heat-insulated plate for different M_0 numbers with $\omega = 0.76$, $k = 1.4$. Values δ_H , δ_H^* and δ_H^{**} are characteristic thicknesses in an incompressible liquid calculated with the same Reynolds number as for a compressible gas. The value of the number M_0 substantially affects the characteristic boundary layer thicknesses; so, with $M_0 = 10$ the boundary layer thickness increases 8 times, and the displacement thickness increases 20 times in comparison with their values in an incompressible liquid.

§ 3. Transfer from Laminar to Turbulent Flow Conditions in a Boundary Layer

Laminar flow, as experiment shows, is stable only under certain conditions determined by the value of the critical Reynolds number. With Reynolds numbers of large critical value, laminar flow becomes unstable and converts to turbulent. This transition is connected with the emergence in the flow of undamped disturbances. If the velocity and pressure disturbances forming as a result of any external reasons in the course of time attenuate, then the main stream is considered stable, but if in the course of time they build up, then this testifies to the instability of the main stream and possible transition of laminar conditions to turbulent. On the strength of such an assumption about the nature of the transition it is possible to attempt to determine the value of the critical Reynolds number with the aid of the stability theory.

Let us examine the plane-parallel flow of an incompressible liquid, whereby we will for simplicity consider that the velocity component U depends only on coordinate y , while the velocity component V is everywhere equal to zero. The pressure of the liquid P in the basic motion is a function of coordinates x and y . Boundary layer flow can be approximately considered precisely such a flow, since the change in longitudinal component U in the direction of coordinate x is considerably weaker than in the direction of coordinate y , and transverse component V is low in comparison with the value of U .

Let us apply on this main stream a two-dimensional perturbation motion, the velocities and the pressure in which depend on time t :

$$u'(x, y, z), \quad v'(x, y, z), \quad p'(x, y, z).$$

Then the pressure and the velocities of the resulting motion will be equal to

$$p = P + p', \quad u = U + u', \quad v = v'. \quad (74)$$

The basic laminar flow should satisfy a Navier-Stokes equation. We will assume that the resulting motion also satisfies a Navier-Stokes equation, while the applied disturbances are small so that it is possible to disregard the squares of the perturbation velocities. Depending on whether the perturbation motion attenuates or builds up in the course of time, the main stream will be either stable or unstable. Substituting the values in (74) in the Navier-Stokes equations and rejecting the squares of low values, we obtain

$$\begin{aligned} \frac{\partial u'}{\partial t} + U \frac{\partial u'}{\partial x} + v' \frac{dU}{dy} + \frac{1}{\rho} \frac{\partial p'}{\partial x} + \frac{1}{\rho} \frac{\partial p'}{\partial x} &= \nu \left(\frac{\partial^2 u'}{\partial y^2} + \frac{\partial^2 u'}{\partial x^2} + \frac{\partial^2 u'}{\partial y^2} \right), \\ \frac{\partial v'}{\partial t} + U \frac{\partial v'}{\partial x} + \frac{1}{\rho} \frac{\partial p'}{\partial y} + \frac{1}{\rho} \frac{\partial p'}{\partial y} &= \nu \left(\frac{\partial^2 v'}{\partial x^2} + \frac{\partial^2 v'}{\partial y^2} \right), \\ \frac{\partial u'}{\partial x} + \frac{\partial v'}{\partial y} &= 0, \quad \nu = \frac{\mu}{\rho}. \end{aligned} \quad (75)$$

Taking into account that the basic motion is subordinated to the Navier-Stokes equations which for the case in question take the form

$$\frac{1}{\rho} \frac{\partial P}{\partial x} = \nu \frac{d^2 U}{dy^2}, \quad \frac{1}{\rho} \frac{\partial P}{\partial y} = 0, \quad (76)$$

we obtain for the perturbation motion the following system of equations:

$$\begin{aligned} \frac{\partial u'}{\partial t} + U \frac{\partial u'}{\partial x} + v' \frac{dU}{dy} + \frac{1}{\rho} \frac{\partial p'}{\partial x} &= \nu \left(\frac{\partial^2 u'}{\partial x^2} + \frac{\partial^2 u'}{\partial y^2} \right), \\ \frac{\partial v'}{\partial t} + U \frac{\partial v'}{\partial x} + \frac{1}{\rho} \frac{\partial p'}{\partial y} &= \nu \left(\frac{\partial^2 v'}{\partial x^2} + \frac{\partial^2 v'}{\partial y^2} \right), \\ \frac{\partial u'}{\partial x} + \frac{\partial v'}{\partial y} &= 0. \end{aligned} \quad (77)$$

Differentiating the first equation of system (77) for v , and the second equation - for x and eliminating from the thus

obtained relationships the value $\partial^2 p' / \partial x \partial y$, i.e., pressure, we will obtain the equation which connects the velocity component of the perturbation motion u' and v' . This equation of motion, together with the equation of continuity serves for determining u' and v' . The boundary conditions for boundary layer flow consist of the fact that the velocities of the perturbation motion u' and v' should be equal to zero at the wall and at a great distance from wall, i.e.,

$$u' = v' = 0 \text{ with } y = 0; u' = v' = 0 \text{ with } y = \infty. \quad (78)$$

Let us assume that on the laminar flow there is applied a disturbance which consists of separate vibrations, each of which is a wave which is propagated in direction x . Let us introduce a stream function for separate vibration in the form of the following complex expression:

$$\psi(x, y, t) = \varphi(y) e^{i(\alpha x - ct)}. \quad (79)$$

where $\varphi = \varphi_r + i\varphi_i$ is the complex amplitude, α - the actual value connected with the wavelength of the disturbance with relationship $\lambda = 2\pi/\alpha$. The complex quantity $c = c_r + ic_i$, whereby c_r is a velocity of propagation of the waves in direction x , and c_i is the coefficient of build-up, on the sign of which depends whether the vibrations build up or attenuate. If $c_i < 0$, then the vibrations attenuate and the laminar flow is stable, but if $c_i > 0$, then the vibrations build up and the laminar flow is not stable.

There is a physical sense, of course, only to the real part of the stream function, i.e., the value

$$\text{Re}(\psi) = e^{c_i t} [\varphi_r \cos \alpha(x - c_r t) - \varphi_i \sin \alpha(x - c_r t)].$$

Composing derivatives of the stream function, let us find for velocity components of the perturbation motion the values

$$\begin{aligned} u' &= \frac{\partial y}{\partial y} = \tau'(y) e^{i\alpha(x-\alpha)}, \\ v' &= -\frac{\partial y}{\partial x} = -i\alpha \tau(y) e^{i\alpha(x-\alpha)}. \end{aligned} \quad (80)$$

The equation of continuity in this case will be satisfied, and the equation of motion which is obtained after elimination of pressure assumes the form

$$(U - c)(\tau'' - \alpha^2 \tau) - U'' \tau = -\frac{\mu}{\rho} (\tau^{IV} - 2\alpha^2 \tau'' + \alpha^4 \tau).$$

Let us pass over in this equation to dimensionless quantities, for which let us divide all velocities by the velocity outside the boundary layer u_0 , and all the lengths - by the momentum thickness δ^{**}

$$\bar{U} = \frac{U}{u_0}, \quad \bar{c} = \frac{c}{u_0}, \quad \bar{x} = x \delta^{**}, \quad \bar{\tau} = \frac{\tau}{u_0 \delta^{**}}.$$

Then we obtain

$$(\bar{U} - \bar{c})(\bar{\tau}'' - \bar{\alpha}^2 \bar{\tau}) - \bar{U}'' \bar{\tau} = \frac{1}{R} (\bar{\tau}^{IV} - 2\bar{\alpha}^2 \bar{\tau}'' + \bar{\alpha}^4 \bar{\tau}), \quad (81)$$

where $R = U \delta^{**} / \nu$ the Reynolds number for the basic laminar flow, and differentiation is made in terms of the variable (y/δ^{**}) .

Equation (81) is called the differential equation of perturbation motion. The stability analysis of the solution of this equation is a problem of the eigenvalues of differential equation (81) under boundary conditions (78). Let us assume that the main stream is assigned, i.e., the velocity distribution in the laminar boundary layer $U(y)$ is known. Then equation (81) will contain four parameters: R , $\bar{\alpha}$, \bar{c}_r , \bar{c}_i . For each selected paired R and $\bar{\alpha}$ it is possible to find the eigen

function Φ and the complex eigenvalue $\bar{\sigma} = \bar{\sigma}_r + i\bar{\sigma}_i$, whereby, here $\bar{\sigma}_r$ is the dimensionless velocity of propagation of perturbations, and $\bar{\sigma}_i$ is the dimensionless coefficient of the build-up:

$$c_r = c_r(\alpha, R), \quad c_i = c_i(\alpha, R)$$

With $\bar{\sigma}_i < 0$, the motion in question is stable with respect to the perturbations of the wavelength in question, and with $\bar{\sigma}_i > 0$ - is unstable.

The case $\bar{\sigma}_i = 0$ corresponds to neutral vibrations the curve $\bar{\sigma}_i(\bar{\alpha}, R) = 0$ in plane $\bar{\alpha}, R$ separates the unstable region of the laminar boundary layer from the stability region. This curve is called neutral. The smallest Reynolds number on the neutral curve is the critical Reynolds number for this flow. With Reynolds numbers less than critical, the perturbations of any wavelength attenuate. With Reynolds numbers greater than critical there are perturbations with a determined wavelength which build up.

The calculation of the neutral curve for the case of flow around a flat heat-insulated plate by an incompressible flow was performed by V. Tollmien and verified by K. K. Lin. In the calculations it was accepted that the velocity distribution in laminar boundary layer is described by Blasius's law.

A similar method of small disturbances was used by K. K. Lin and P. Lis during the stability analysis of laminar boundary layer on a flat plate flowed past with a flow of a compressible gas. In this case, the neutral curve equation can be written in the form

$$c_i(\alpha, R, M_\infty, \frac{T_\infty}{T_w}) = 0. \quad (82)$$

The results of calculating neutral curves are represented in Figs. 6.13 and 6.14.

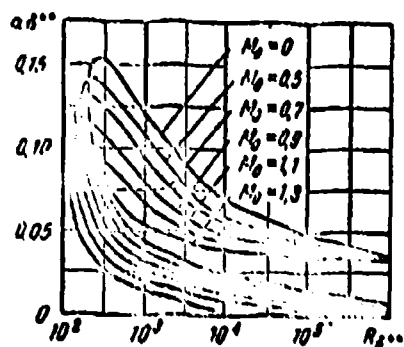


Fig. 6.13. Neutral curves for a flow around a flat heat-insulated plate.

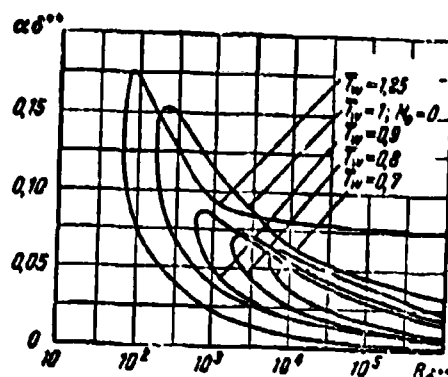


Fig. 6.14. Neutral curves for the flow around a flat plate by a flow of gas, $M_0 = 0.7$.

These calculations showed that the critical Reynolds number decreases with an increase in the M_0 number of external flow in the absence of thermal conductivity from the plate. Cooling of the plate leads to an increase in critical Reynolds number at a constant value of M_0 number, i.e., it has an effect on the boundary layer.

Thus, with the aid of the method of slight disturbances it is possible to obtain the value of the critical Reynolds number. Beginning from that place on the plate where the Reynolds number reaches its critical value, begin to build up disturbances with a determined wavelength. Further downstream disturbances with other wavelengths also become unstable. Finally, at a certain distance from the beginning of the loss of stability, the laminar flow changes to turbulent. The critical Reynolds number determined by experimental method from observation of the transition of the laminar flow conditions to turbulent corresponds to that place on the plate where the flow turbulence leads to rearrangement of the entire flow. Critical Reynolds numbers thus found from experiments usually exceed in value their theoretical values.

Thus, the method of slight disturbances makes it possible to determine only the lower boundary of values of critical Reynolds numbers, i.e., it gives those values of Reynolds numbers less than R_{kp} with which the laminar flow always is stable. Furthermore, with the aid of this method it is possible to explain the effect on the stability of the laminar boundary layer of such parameters as M_0 and T_w/T_0^* .

The second important problem connected with the transition of laminar boundary layer to turbulent is the calculation of the basic flow parameters in the transition region. At present there is no strict theory of transition region by virtue of the complexity of the processes taking place, therefore, in conducting quantitative estimates in the transition region it is necessary to utilize different empirical and semi-empirical methods.

Let us examine one semi-empirical approach to parameter determining in transition region proposed recently by L. A. Vulis. This method is based on the following diagram of the transient process. With an increase in the characteristic coordinate of the state - the Reynolds number - and the achievement of critical value, the laminar flow becomes unstable. With a further increase in the Reynolds number there occurs a gradual transition into the new steady state which corresponds to stable turbulent flow. The reading of the Reynolds number as the coordinates of state in the transition region should be made from its critical value, i.e., a coordinate of state χ will be equal to

$$\chi = R - R_{cr} \quad (83)$$

Let $L(\chi)$ - a certain characteristic of flow which unambiguously depends on the Reynolds number whereby $L_1(\chi)$ - a function of the R number for a laminar condition, $L_2(\chi)$ - for turbulent, $L(\chi)$ - for the transition region. Then the measure of the disorder of the turbulent system should be the name given to the relation

$$\omega = \frac{L_1(x) - L(x)}{L_1(x) - L_1(0)}, \quad (84)$$

which is a relation principally possible, but still not realized with a given x of value of change in L and to its full change with the final rearrangement of the flow conditions. For laminar flow $\omega = 1$, since $L(x) = L_1(x)$, while for turbulent $L(x) = L_2(x)$ and $\omega = 0$.

The basic assumption made by L. A. Vulis consists of the fact that the relative change in the measure of disorder is proportional to the increases of the coordinates:

$$\frac{d\omega}{dx} = -\omega^2 dx, \quad (85)$$

Actually, the greater the value of disorder ω , the more intensively should ordering occur, i.e., the greater should be the derivative $d\omega/dx$. Such a quantitative expression is typical for the different processes of establishment and relaxation.

Integrating relationship (85) under the initial condition $x = 0$, $\omega = 1$, we obtain

$$\omega = e^{-x},$$

or, substituting for ω expression (84):

$$L(x) = L_1(x) - [L_1(x) - L_2(x)]e^{-x}, \quad (86)$$

It should be noted that $L(x) \rightarrow L_2(x)$ with $x \rightarrow \infty$, i.e., with an increase in Reynolds number, the flow parameters approach the parameters of a turbulent condition whereby this approach occurs rather rapidly (exponentially). It is still necessary to explain the nature of joining curve $L(x)$ with curves $L_1(x)$ and $L_2(x)$.

Differentiating relationship (86) with respect to χ , we have

$$\frac{dL(\chi)}{d\chi} = \frac{dL_2(\chi)}{d\chi} - \left[\frac{dL_2(\chi)}{d\chi} - \frac{dL_1(\chi)}{d\chi} \right] e^{-\alpha^2 \chi} + \alpha^2 [L_2(\chi) - L_1(\chi)] e^{-\alpha^2 \chi}$$

whence with $\chi = 0$ (at the point of joining with the curve for a laminar condition)

$$\left[\frac{dL(\chi)}{d\chi} \right]_{\chi=0} = \left[\frac{dL_1(\chi)}{d\chi} \right]_{\chi=0} + \alpha^2 [L_2(0) - L_1(0)]$$

and therefore, in general

$$\left[\frac{dL(\chi)}{d\chi} \right]_{\chi=0} \neq \left[\frac{dL_1(\chi)}{d\chi} \right]_{\chi=0}.$$

With $\chi \rightarrow \infty$

$$\left[\frac{dL(\chi)}{d\chi} \right]_{\chi=\infty} = \left[\frac{dL_2(\chi)}{d\chi} \right]_{\chi=\infty}.$$

i.e., there occurs a smooth transition to the developed turbulent system.

As an example, let us examine the resistance of a flat plate flowed around by a flow of an incompressible liquid. As shown above, during laminar flow the drag coefficient is equal to (47)

$$C_w = \frac{1,328}{\sqrt{R}}.$$

During turbulent flow conditions, as will be shown further, the drag coefficient is expressed by the following formula:

$$C_w = \frac{0,073}{R^{0,5}}.$$

Accepting that $R_{\text{HP}} = 5 \cdot 10^5$, $\alpha^2 = 10^{-6}$, we obtain the expression for the drag coefficient of the plate in the transition region

$$C_W = \frac{0.073}{R^{0.5}} - \left(\frac{0.073}{R^{0.5}} - \frac{1.328}{\sqrt{R}} \right) e^{-(R-5 \cdot 10^5) 10^{-6}}. \quad (87)$$

Values of C_W , calculated from this formula are given in Fig. 6.15 (curve 2). This figure shows values of C_W for laminar flow conditions in the boundary layer (curve 1), for turbulent (curve 3) and experimental data obtained for a transition region by Hebers.

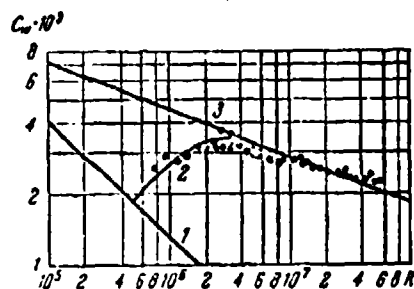


Fig. 6.15. Drag coefficient of a flat plate in the transition region.

In this case it is necessary to keep in mind that the value of α^2 , just as R_{HP} , depends on the initial turbulence of the main flow and can be determined at present only experimentally.

§ 4. Turbulent Boundary Layer

The equations of motion, energy, and continuity for a turbulent boundary layer can be obtained by means of averaging over time the initial boundary layer equations (19) - (22). For simplicity, let us examine first an incompressible liquid. Let us break down the turbulent flow into averaged motion and pulsating motion. After designating the averaged over time value of the velocity component u as \bar{u} , and the pulsating velocity - as u' , etc., we obtain the following equations for the velocity components, for the pressure and for the temperature:

$$u = \bar{u} + u', \quad v = \bar{v} + v', \quad p = \bar{p} + p', \quad T = \bar{T} + T'. \quad (88)$$

Under the mean value here and throughout we have in mind the mean values over time at a fixed point of space, for example:

$$\bar{u} = \frac{1}{t} \int_0^t u dt. \quad (89)$$

For averaging, it is necessary to take such a large time interval t so that the averaged value would not depend on time. Then the averaged over time values of pulsating quantities will be equal to zero:

$$\bar{u}' = \bar{v}' = \bar{p}' = \bar{T}' = 0.$$

From determination (89) there ensue the following rules of averaging:

a) $\overline{u+v} = \bar{u} + \bar{v}$ (90)
Actually

b) $\overline{u+v} = \frac{1}{t} \int_0^t (u+v) dt = \frac{1}{t} \int_0^t u dt + \frac{1}{t} \int_0^t v dt = \bar{u} + \bar{v}$ (91)
 $\bar{u} = \bar{u}$

Actually

$$\bar{u} = \frac{1}{t} \int_0^t u dt = \bar{u}$$

since, by definition, \bar{u} does not depend on time.

c) $\overline{uv} = \bar{u}\bar{v}$ (92)

Actually,

$$\bar{u} = \frac{1}{t} \int_0^t u \, dt = \frac{1}{t} \int_0^t v \, dt = \bar{v}.$$

$$\frac{\partial \bar{u}}{\partial x} = \frac{\partial \bar{v}}{\partial x}.$$

d) (93)

Actually,

$$\frac{\partial \bar{u}}{\partial x} = \frac{1}{t} \int_0^t \frac{\partial u}{\partial x} \, dt = \frac{\partial}{\partial x} \left(\frac{1}{t} \int_0^t u \, dt \right) = \frac{\partial \bar{u}}{\partial x}.$$

since the limits of integration do not depend on x .

Let us now pass to the derivation of the equations of a turbulent boundary layer. For the case of an incompressible liquid with constant physical properties, equations (19), (20), (22), and (24) take the form

$$\rho u \frac{\partial u}{\partial x} + \rho v \frac{\partial u}{\partial y} = -\frac{\partial p}{\partial x} + \rho \frac{\partial^2 u}{\partial y^2}. \quad (94)$$

$$\frac{\partial p}{\partial y} = 0. \quad (95)$$

$$g \rho u \frac{\partial T}{\partial x} + g \rho v \frac{\partial T}{\partial y} = \lambda \frac{\partial^2 T}{\partial y^2} + A \mu \frac{\partial^2}{\partial y^2} \left(\frac{u^2}{2} \right). \quad (96)$$

$$\frac{\partial u}{\partial x} + \frac{\partial v}{\partial y} = 0. \quad (97)$$

Let us multiply both parts of the equation of continuity (97) by ρu and let us add it term by term with the equation of motion (94)

$$\rho \frac{\partial (uv)}{\partial x} + \rho \frac{\partial (uv)}{\partial y} = -\frac{\partial p}{\partial x} + \rho \frac{\partial^2 u}{\partial y^2}. \quad (98)$$

Multiplying both parts of the equation of continuity by $g \rho T$ and adding it up term by term with the equation of energy, we have

$$gcp \frac{\partial (uT^*)}{\partial x} + gcp \frac{\partial (vT^*)}{\partial y} = \lambda \frac{\partial T}{\partial x} + A\mu \frac{\partial}{\partial y} \left(\frac{u^2}{T} \right). \quad (99)$$

Let us substitute in equations (95), (97), (98), and (99) instead of u , v , p , T , their values from (88) and produce averaging over time. Utilizing the rule of averaging (93), from (95) we obtain

$$\frac{dp}{dy} = 0. \quad (100)$$

Utilizing the rules of averaging (90) and (93), we convert the equation of continuity (97) to the form

$$\frac{\partial u}{\partial x} + \frac{\partial v}{\partial y} = 0. \quad (101)$$

Let us pass to averaging of the converted equation of motion (98). On the basis of the rules of averaging (90) and (93) we obtain

$$\begin{aligned} \frac{\partial (u^2)}{\partial x} &= \frac{\partial}{\partial x} (u^2 + 2u\bar{u}' + u'^2) = \frac{\partial (u^2)}{\partial x} + \frac{\partial \bar{u}'^2}{\partial x}, \\ \frac{\partial (uv)}{\partial y} &= \frac{\partial}{\partial y} (uv + u\bar{v}' + u'\bar{v} + u'v') = \frac{\partial (uv)}{\partial y} + \frac{\partial \bar{u}'\bar{v}'}{\partial y}, \\ \frac{\partial^2 u}{\partial y^2} &= \frac{\partial^2 \bar{u}}{\partial y^2} + \frac{\partial^2 \bar{u}'}{\partial y^2} = \frac{\partial^2 \bar{u}}{\partial y^2}, \quad \frac{\partial^2 p}{\partial x^2} = \frac{\partial^2 p}{\partial x^2}. \end{aligned}$$

therefore the equation of motion (98) after averaging assumes the form

$$\rho \frac{\partial (u^2)}{\partial x} + \rho \frac{\partial (uv)}{\partial y} = -\frac{\partial p}{\partial x} - \rho \frac{\partial \bar{u}'^2}{\partial x} - \rho \frac{\partial \bar{u}'\bar{v}'}{\partial y} + \rho \frac{\partial^2 \bar{u}}{\partial y^2}.$$

Deducting term by term from this relationship the equation of continuity (101), multiplied by $\rho \bar{u}$, and disregarding the derivative in terms of x of the pulsating components in comparison with the derivative in terms of y , as is done during the derivation of the boundary layer equations, we finally obtain the differential equation of motion for a turbulent boundary layer

$$\rho u \frac{\partial u}{\partial x} + \rho v \frac{\partial u}{\partial y} = -\frac{\partial p}{\partial x} + \frac{\partial}{\partial y} \left(\mu \frac{\partial u}{\partial y} - \rho \overline{uv} \right). \quad (102)$$

Let us make similar conversions with the equation of energy (99). Since

$$\frac{\partial(\rho T^*)}{\partial x} = \frac{\partial(\rho T^*)}{\partial x} + \frac{\partial \overline{\rho T^*}}{\partial x}, \quad \frac{\partial(\rho T^*)}{\partial y} = \frac{\partial(\rho T^*)}{\partial y} + \frac{\partial \overline{\rho T^*}}{\partial y}, \quad \frac{\partial T^*}{\partial y} = \frac{\partial T}{\partial y},$$

$$\overline{u^2} < u^2, \quad \frac{\partial \overline{u^2}}{\partial x} < \frac{\partial u^2}{\partial x}, \quad T^* = T + A \frac{\partial u}{\partial y},$$

then the equation of energy (99) after term-by-term subtraction of relationship (101), multiplied by $gc_p \overline{T^*}$, assumes the form

$$gc_p \rho u \frac{\partial T^*}{\partial x} + gc_p \rho v \frac{\partial T^*}{\partial y} = \frac{\partial}{\partial y} \left(\lambda \frac{\partial T}{\partial y} - gc_p \overline{vT} \right) + A \frac{\partial}{\partial y} \left(\mu \frac{\partial u}{\partial y} - \rho \overline{uv} \right). \quad (103)$$

whereby

$$\overline{T^*} = \overline{T} + A \frac{\partial u}{\partial y}.$$

Comparing the equations for a turbulent boundary layer (100)-(103) with equations for a laminar boundary layer (94)-(97) it is possible to note the following. The equation of continuity and the second equation of motion take identical form. The first equation of motion and the equation of energy for the averaged parameters of the turbulent boundary layer differ from the corresponding equations for a laminar boundary layer by the presence of supplementary tangential stresses and supplementary heat flows.

A simple interpretation of these supplementary terms was given by Prandtl. For a presentation of Prandtl's idea, let us examine a plane-parallel flow whose velocity coincides in direction with axis x , while the value of the velocity depends only on coordinate y . Consequently, $\bar{u} = \bar{u}(y)$, $\bar{v} = 0$, whereupon let $\frac{d\bar{u}}{dy} > 0$.

The mechanism of turbulent flow can be presented in the following simplified manner. In the process of turbulent flow there appear liquid volumes, each of which at a certain distance moves in any direction as a whole at a determined velocity. Let us assume that such a liquid volume which arose in a layer with coordinate $y_1 - l$ and which possesses velocity $\bar{u}(y_1 - l)$ moves a distance l as a whole in the direction of axis y . When this liquid volume enters a layer with coordinate y_1 , then the velocity in this layer will be changed by the value

$$u' = u(y_1 - l) - u(l) = -\left(\frac{du}{dy}\right)_l l$$

which is its pulsating component. In this case $v' > 0$. Analogously, the liquid volume which enters layer y_1 from layer $y_1 + l$ has a higher velocity than its surrounding medium. Consequently, pulsating component u' will be equal to

$$u' = u(y_1 + l) - u(y_1) = \left(\frac{du}{dy}\right)_l l$$

in this case $v' < 0$.

The mixing length l , to known degree, is similar to the length of the mean free path of molecules in the kinetic theory of gases, the only difference being that there occur microscopic motions of the molecules, and here - macroscopic motions of turbulent volumes. In general, the length of mixing depends on time and can take positive or negative values. Thus, the pulsating component also depends on time

$$u' = l \frac{du}{dy}. \quad (104)$$

The emergence of pulsations of velocity in transverse direction can be presented in the following. In a layer with

coordinate y_1 for some reason there occurs an increase in the velocity, i.e., there appears a positive pulsating component $u' > 0$. The liquid volume which has this velocity $\bar{u}(y_1) + u'$ contends with the volume located in front which has velocity $\bar{u}(y_1)$ and therefore a transverse motion appears directed to both sides from layer y_1 . If in the layer with coordinate y_1 a decrease occurs in the velocity ($u' < 0$), then the liquid volume which has this velocity lags behind the volume which has velocity $\bar{u}(y_1)$ and a transverse motion directed from both sides to layer y_1 appears. On the basis of these considerations it is possible to draw the conclusion that the value of transverse pulsating velocity v' has the same order as the value of the longitudinal pulsating velocity u' . As shown above, the volume of liquid coming into layer y_1 with positive value of v' usually produces the negative pulsating velocity u' . The volume of liquid coming into layer y_1 with negative value of v' usually produces the positive pulsating velocity u' , i.e.,

$$v' = -ku', \quad (105)$$

where k is the proportionality factor which is on the order of unity.

Then the product of $u'v'$ will usually be negative, and therefore the averaged over time value $\overline{u'v'}$ will be different from zero and negative.

$$\overline{u'v'} = -k\overline{u'^2} = -k\overline{u'^2} \left(\frac{du}{dy} \right)^2.$$

In view of a certain uncertainty of the mixing length, it is possible to include coefficient k in this value. Then we obtain

$$\overline{u'v'} = -l^2 \left(\frac{du}{dy} \right)^2, \text{ where } l^2 = k\overline{u'^2}. \quad (106)$$

It should be noted that all the considerations carried out above applied to the case of a positive value of the derivative $d\bar{u}/dy$. Similar considerations for $d\bar{u}/dy < 0$ show that in this case the product of $u'v'$ is usually positive. Then

$$\overline{u'v'} = \mu' \left(\frac{d\bar{u}}{dy} \right)^2. \quad (107)$$

Formulas (106) and (107) can, therefore, be presented in one formula

$$\overline{u'v'} = -\mu' \left| \frac{d\bar{u}}{dy} \right| \frac{d\bar{u}}{dy}. \quad (108)$$

It is also entirely possible to derive a formula for the averaged value of the product $\overline{v'T'}$, if one assumes that the mechanism of heat transfer is similar to the mechanism of the transfer of momentum. In this case, $T' = \lambda' d\bar{T}/dy$, and therefore

$$\overline{v'T'} = -\lambda' \left| \frac{d\bar{u}}{dy} \right| \frac{d\bar{T}}{dy}. \quad (109)$$

Expressions (108) and (109) are obtained for the special case of flow when $\bar{u} = \bar{u}(y)$; however, they can also be applied in the general case of velocity distribution in a boundary layer.

Utilizing relationships (108) and (109), the equation of motion (102), and the equation of energy (103), we convert to the form

$$\rho u \frac{\partial \bar{u}}{\partial x} + \rho v \frac{\partial \bar{u}}{\partial y} = -\frac{\partial \bar{p}}{\partial x} + \frac{\partial}{\partial y} \left[(\mu + \mu') \frac{\partial \bar{u}}{\partial y} \right], \quad (110)$$

$$g' \mu u \frac{\partial \bar{T}}{\partial x} + g' \rho v \frac{\partial \bar{T}}{\partial y} = A u \frac{\partial \bar{p}}{\partial x} + \frac{\partial}{\partial y} \left[(\lambda + \lambda') \frac{\partial \bar{T}}{\partial y} \right] + A (\mu + \mu') \left(\frac{\partial \bar{u}}{\partial y} \right)^2. \quad (111)$$

where $\mu' = \rho \mu' \left(\frac{\partial \bar{u}}{\partial y} \right)$ is a coefficient of eddy viscosity, $\lambda' = g' \rho \lambda' \left(\frac{\partial \bar{u}}{\partial y} \right)$ - the coefficient of eddy conductivity. Here and throughout, the line above the averaged parameters is omitted.

Prandtl's hypothesis about the mixing length turned out to be very fruitful, since it opened up real possibilities for calculating turbulent flow. Although the mixing length is not a physical constant for each liquid unlike the molecular coefficients of viscosity and thermal conductivity, however, as experimental data show, it does not depend on the flow parameters. The mixing length basically is a function of coordinate y . Since during flow along a smooth wall in immediate proximity to its surface, the velocity pulsations are equal to zero, then $l = 0$ with $y = 0$. Accepting the simplest hypothesis that near the wall the mixing length is proportional to the distance from the wall

$$l = Ay, \quad (112)$$

it is possible to obtain, following Prandtl, the velocity profile in a turbulent boundary layer during the flow of an incompressible liquid along a flat plate ($\partial p / \partial x = 0$). In this case, from equation (110) it follows that with $y = 0$, when $u = v = 0$,

$$\frac{\partial}{\partial y} \left[(\mu + \mu_t) \frac{\partial u}{\partial y} \right] = \frac{\partial \tau}{\partial y} = 0.$$

Differentiating equation (110) with respect to y and taking into account the equation of continuity (101), we obtain $\frac{\partial \tau}{\partial y} = 0$ with $y = 0$, i.e., near the wall the stress of friction remains constant

$$\tau = \tau_w \quad (113)$$

Disregarding the coefficient of molecular viscosity μ in comparison with the coefficient of eddy viscosity μ_t and substituting for μ_t its expression in terms of the path length of mixing, we obtain the relationship

$$\tau = \rho l^3 \left(\frac{\partial u}{\partial y} \right)^2,$$

which during the replacement of value l by expression (112) assumes the form

$$\tau = \rho k^2 y^3 \left(\frac{\partial u}{\partial y} \right)^2.$$

After integrating this equation, taking into account equality (113), we obtain

$$u = \frac{1}{k} \sqrt{\frac{\tau_w}{\rho}} \ln y + C \quad (114)$$

This relationship can be written in the following dimensionless form:

$$\frac{u}{v_*} = \frac{1}{k} \ln \frac{y}{y_*} + C_1, \quad (115)$$

where $v_* = \sqrt{\tau_w/\rho}$, $y_* = \rho/\rho_*$.

The value of k , according to the results of measurements, is a universal constant of turbulent flow and is equal to 0.4. The second constant C_1 depends on the properties of the surface being flowed around. The universal velocity distribution law (115) derived for flow along a flat wall turns out to be valid also during the flow of a liquid in a circular tube. Figure 6.16 provides a comparison of the results of calculation according to formula (115) with $C_1 = 5.5$ with the experimental data for tubes obtained by Nikuradze with different Reynolds numbers.

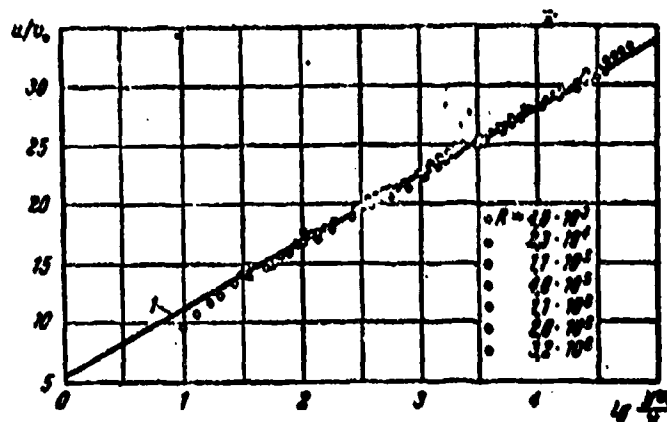


Fig. 6.16. Velocity distribution in a smooth pipe. Curve 1 corresponds to universal logarithmic law.

It should be noted that the universal velocity distribution law is derived on the assumption that in the major portion of the turbulent boundary layer the coefficient of molecular viscosity is low in comparison with the turbulent coefficient of viscosity. Such an assumption is justified only with the very large Reynolds numbers, therefore the universal velocity distribution law should be considered as an asymptotic law for very large Reynolds numbers. Experiments carried out during the flow of an incompressible flow about a flat plate show that with moderate Reynolds numbers the velocity distribution is described well by the power law

$$\frac{u}{u_0} = \left(\frac{y}{\delta}\right)^{1/n}, \quad (116)$$

whereby the value of n depends slightly on the Reynolds number. With $R_x = 10^6 - 10^8$ it is possible to take $n = 7$.

The equations of motion, energy, and continuity for a turbulent boundary layer of a compressible gas can also be

obtained by means of averaging over time in the initial boundary layer equations (19)-(23). For the averaged parameters these equations take the form (with constant heat capacity)

$$\mu \frac{\partial u}{\partial x} + \mu \frac{\partial u}{\partial y} = - \frac{\partial p}{\partial x} + \frac{\partial}{\partial y} \left[(\mu + \mu_t) \frac{\partial u}{\partial y} \right], \quad (117)$$

$$\frac{\partial p}{\partial y} = 0, \quad (118)$$

$$sc_p u \frac{\partial T}{\partial x} + sc_p v \frac{\partial T}{\partial y} = \lambda \frac{\partial T}{\partial x} + \frac{\partial}{\partial y} \left[(\lambda + \lambda_t) \frac{\partial T}{\partial y} \right] + \frac{A (\mu + \mu_t) \left(\frac{\partial u}{\partial y} \right)^2}, \quad (119)$$

$$\frac{\partial (\rho u)}{\partial x} + \frac{\partial (\rho v)}{\partial y} = 0. \quad (120)$$

Here μ_t and λ_t are coefficients of eddy viscosity and eddy conductivity which characterize the transfer of momentum and heat because of transverse pulsations of velocity.

Boundary conditions in this system of equations take the same form as for a laminar boundary layer:

$$\left. \begin{aligned} u = v = 0, \quad T = T_w \quad \text{with } y = 0, \\ u = u_\infty, \quad T = T_\infty \quad \text{with } y = \delta. \end{aligned} \right\} \quad (121)$$

For the solution of equations (117)-(120), besides the equation of state and dependences of coefficients μ and λ on temperature, it is necessary to know the value of the coefficients of turbulent transfer μ_t and λ_t . In view of the absence at the present time of a final theory of turbulence, the determining of these coefficients bears a semi-empirical nature and is based on a number of hypotheses.

Therefore, during the calculation of a turbulent boundary layer they usually utilize the approximation method based on the solution of the integral equation of momentum (59). In this

case, it is necessary to assign the velocity distribution and temperatures in the boundary layer.

Let us examine the case of flow about a flat plate with Prandtl number equal to one. We first convert the equation of energy. Multiplying (117) by Au , adding with (119) and introducing the stagnation temperature:

$$T^* = T + A \frac{u^2}{2g_p}$$

we obtain

$$\rho u \frac{\partial T^*}{\partial x} + \rho v \frac{\partial T^*}{\partial y} = \frac{\partial}{\partial y} \left[(\mu + \mu_t) \frac{\partial T^*}{\partial y} \right] + \frac{\partial}{\partial y} \left[\left(\frac{1}{Pr_t} - 1 \right) \mu \frac{\partial T^*}{\partial y} \right] + \frac{\partial}{\partial y} \left[\left(\frac{1}{Pr_t} - 1 \right) \mu_t \frac{\partial T^*}{\partial y} \right]. \quad (122a)$$

Value $Pr = (gc_p \mu_t) / \lambda_t$ is the Prandtl number for the turbulent parameters. According to data available at present, the number Pr_t is close to one. Therefore,, subsequently we will take $Pr_t = 1$. With $Pr = Pr_t = 1$, relationship (121) is simplified and assumes the form

$$\rho u \frac{\partial T^*}{\partial x} + \rho v \frac{\partial T^*}{\partial y} = \frac{\partial}{\partial y} \left[(\mu + \mu_t) \frac{\partial T^*}{\partial y} \right]. \quad (122b)$$

Since during the longitudinal flow about a flat plate $\partial p / \partial x = 0$, then from equation (117) we obtain

$$\rho u \frac{\partial u}{\partial x} + \rho v \frac{\partial u}{\partial y} = \frac{\partial}{\partial y} \left[(\mu + \mu_t) \frac{\partial u}{\partial y} \right]. \quad (123)$$

As a result of the similarity of equations (122b) and (123), the solution of the equation of energy (122b) can be presented in the form

$$T^* = ax + b,$$

where the unknown coefficients a and b are determined from boundary conditions (121):

$$u=0, T^*=T_w=b; u=u_0, T^*=T_0^*=au_0+T_w, a=(T_0^*-T_w)/u_0.$$

Consequently,

$$T^*=(T_0^*-T_w)\frac{u}{u_0}+T_w. \quad (124)$$

Before going over to finding the velocity profile, it is necessary to note the following fact. Near the streamlined body the Reynolds number determined from the local parameters of the liquid can be arbitrarily small. Therefore, in this area there should exist laminar flow where the friction and the heat exchange are determined by molecular transfer, i.e., $\mu \gg \mu_T$, $\lambda \gg \lambda_T$. This part of the boundary layer is called the *laminar sublayer*. In the remaining, basic part of the boundary layer, the determining role is played by transfer, by means of turbulent pulsations, i.e., $\mu \ll \mu_T$, $\lambda \ll \lambda_T$. We will consider that the Reynolds number on the boundary of the laminar sublayer does not depend on the Mach number M_0 and the intensity of the heat exchange

$$\frac{\rho_0 u_0 \delta_1}{\mu_1} = \alpha; \quad (125)$$

according to experimental data, the coefficient $\alpha = 12.5$.

The velocity distribution in the laminar sublayer can be considered linear

$$\frac{u}{u_1} = \frac{y}{\delta_1}. \quad (126)$$

The velocity distribution law in the major portion of the turbulent boundary layer can be obtained on the basis of analysis of the experimental data.

The results of experimental research of velocity profiles in the major portion of the turbulent boundary layer of a

compressible gas on a plate are represented in Fig. 6.17. It turns out that the Mach number M_0 and the temperature factor $\bar{T}_w = T_w/T_0^*$ have little effect on the form of the velocity distribution. Therefore, we will consider power law (116) valid also for a compressible gas.

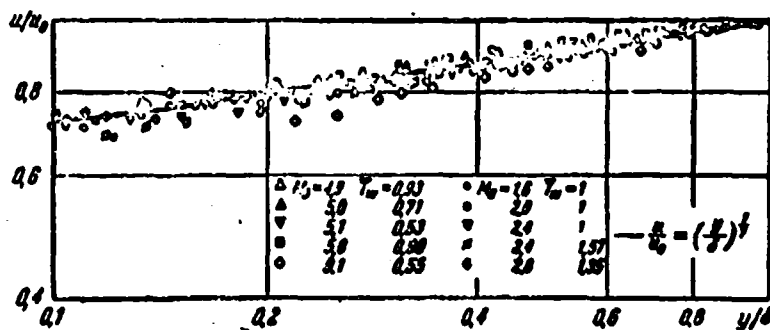


Fig. 6.17. Velocity profile in a turbulent boundary layer of compressible gas on a flat plate.

Let us find the expression for the stress of friction on the wall, utilizing (126):

$$\tau_w = \mu_0 \left(\frac{\partial u}{\partial y} \right)_w = \mu_0 \frac{u_n}{\delta_n}. \quad (127)$$

Since, on the boundary of the laminar sublayer, the values of the velocity calculated according to formulas (126) and (116) should coincide, $u_n/u_0 = (\delta_n/\delta)^{1/n}$. Taking for the dependence of the coefficient of viscosity on temperature, power law (4), we obtain

$$\tau_w = \frac{\rho_0 u_0^2}{R_\delta} \left(\frac{u_n}{u_0} \right)^{1-n} \left(\frac{T_w}{T_0} \right)^n. \quad (128)$$

Here $R_\delta = \rho_0 u_0 \delta / \mu_0$ - the Reynolds number calculated according to the boundary layer thickness, while the value u_n/u_0 should be determined from condition (125).

Solving relationship (125) relative to δ_n , we obtain

$$\frac{\delta_n}{\delta} = \frac{\sigma^2}{R_0^2} \left(\frac{T_0}{T_n} \right)^{1+\sigma} \frac{u_n}{u_0}.$$

On the other hand, $\delta_n/\delta = (u_n/u_0)^n$, therefore

$$\left(\frac{u_n}{u_0} \right)^{n+1} = \frac{\sigma^2}{R_0^2} \left(\frac{T_0}{T_n} \right)^{1+\sigma}.$$

Utilizing the connection between the stagnation temperature and velocity (124), let us find the following algebraic equation for determining relative speed on the boundary of the laminar sublayer:

$$\begin{aligned} \left(\frac{u_n}{u_0} \right)^{n+1} = \frac{\sigma^2}{R_0^2} & \left\{ 1 + \frac{k-1}{2} M_0^2 \left[1 - \left(\frac{u_n}{u_0} \right)^2 \right] \right\}^{1+\sigma} \times \\ & \times \left\{ 1 + (\bar{T}_w - 1) \frac{\left(1 + \frac{k-1}{2} M_0^2 \right) \left(1 - \frac{u_n}{u_0} \right)}{1 + \frac{k-1}{2} M_0^2 \left[1 - \left(\frac{u_n}{u_0} \right)^2 \right]} \right\}^{1+\sigma}. \end{aligned} \quad (129)$$

This equation must be solved by the method of successive approximations, i.e., to assign arbitrarily the value u_n/u_0 , to substitute this value in the right side of relationship (129), to find a new value of u_n/u_0 , etc. Since the value of u_n/u_0 is usually equal to 0.3-0.7, then as a first approximation let us take $u_n/u_0 = 0.5$. Then in the second approximation we obtain

$$\left(\frac{u_n}{u_0} \right)^{n+1} = \frac{\sigma^2}{R_0^2} \left(1 + 0.75 \frac{k-1}{2} M_0^2 \right)^{1+\sigma} \left[1 + \frac{\bar{T}_w - 1}{2} \frac{1 + \frac{k-1}{2} M_0^2}{1 + 0.75 \frac{k-1}{2} M_0^2} \right]^{1+\sigma}.$$

The value standing in brackets changes slightly during a change in number M_0 . So, with $\bar{T}_w = 0.5$, it changes from 0.750 to 0.672 during a change in the Mach number from 0 to 10. Limiting ourselves to the first two approximations, we finally obtain

$$\frac{u_s}{u_*} = \left(\frac{u_*}{R_s}\right)^{\frac{1}{n+1}} \left(1 + 0.75 \frac{k-1}{2} M_s^2\right)^{\frac{1+\omega}{n+1}} \left(\frac{1+\tau_w}{2}\right)^{\frac{1+\omega}{n+1}}. \quad (130)$$

Then the expression for the stress of friction (128) with $n = 7$, $\omega = 0.75$ assumes the form

$$\frac{\tau_w}{\rho_* u_*^2} = \frac{0.0226}{R_s^{1/4}} \frac{\left(1 + \frac{k-1}{2} M_s^2\right)^{1.11}}{\left(1 + 0.75 \frac{k-1}{2} M_s^2\right)^{1.11}} \bar{\tau}_w^{0.75} \left(\frac{2}{1+\tau_w}\right)^{1.11}. \quad (131)$$

Before turning to the integration of the equation of momentum (59), which in the case of a plate appears thus:

$$\frac{d\delta^{**}}{dx} = \frac{\tau_w}{\rho_* u_*^2}, \quad (132)$$

it is still necessary to find the connection between δ^{**} and δ . Utilizing velocity profile (116) and temperature profile (124), we obtain

$$\frac{\delta^{**}}{\delta} = 1 - \frac{\tau_w}{T_w} - n \int_0^1 \frac{z^{n+1} dz}{\left(1 + \frac{k-1}{2} M_s^2\right) \left((1 - \tau_w)z + \tau_w\right) - \frac{k-1}{2} M_s^2 z^2},$$

$$\frac{\tau_w}{T_w} = 1 - n \int_0^1 \frac{z^n dz}{\left(1 + \frac{k-1}{2} M_s^2\right) \left((1 - \tau_w)z + \tau_w\right) - \frac{k-1}{2} M_s^2 z^2}.$$

The results of calculating the values of δ^*/δ and δ^{**}/δ for $n = 7$, $k = 1.4$ are given in Figs. 6.18 and 6.19.

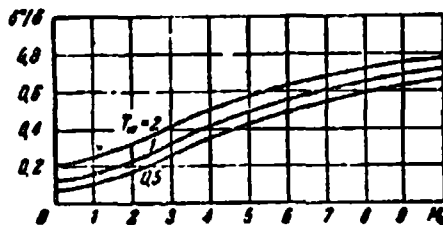


Fig. 6.18. Relative displacement thickness for a turbulent boundary layer.

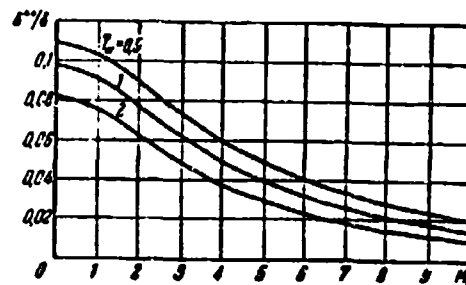


Fig. 6.19. Relative momentum thickness for a turbulent boundary layer.

For an incompressible liquid (with $M_0 = 0$, $\bar{T}_w = 1$)

$$\frac{\delta^{**}}{\delta} = \frac{n}{(n+1)(n+2)}, \quad \frac{\delta^*}{\delta} = \frac{1}{n+1}.$$

Integrating relationship (132) with the initial condition $\delta = 0$ with $x = 0$, we obtain the distribution of the boundary layer thickness along the plate

$$\frac{\delta}{x} = \frac{0.0375}{R_x^{1/2}} \left(\frac{\delta^{**}}{\delta} \right)^{n+1} \frac{\left(1 + \frac{k-1}{2} M_0^2 \right)^{n+1}}{\left(1 + 0.75 \frac{k-1}{2} M_0^2 \right)^{1.25}} \bar{T}_w^{n+1} \left(\frac{2}{1 + \bar{T}_w} \right)^{1.25}. \quad (133)$$

Substituting the found value of δ from (133) in (131), we obtain the expression for the coefficient of friction

$$c_f = \frac{\tau_w}{\frac{\rho_\infty u_\infty^2}{2}} = \frac{0.0922}{R_x^{1/2}} \left(\frac{\delta^{**}}{\delta} \right)^{n+1} \frac{\left(1 + \frac{k-1}{2} M_0^2 \right)^{n+1}}{\left(1 + 0.75 \frac{k-1}{2} M_0^2 \right)^{1.25}} \bar{T}_w^{n+1} \left(\frac{2}{1 + \bar{T}_w} \right)^{1.25}. \quad (134)$$

After the boundary layer thickness is found, the displacement thickness and the momentum thickness are found according to known ratios δ^*/δ and δ^{**}/δ .

The drag coefficient of a plate of length l and width b is equal to

$$C_w = \frac{\int_0^l \tau_w dx}{\frac{\rho_\infty u_\infty^2}{2} M}.$$

After substitution of the value τ_w from relationship (134) and after integration, we obtain

$$C_w = \frac{0.116}{R_l^{1/2}} \left(\frac{\delta^{**}}{\delta} \right)^{n+1} \frac{\left(1 + \frac{k-1}{2} M_0^2 \right)^{n+1}}{\left(1 + 0.75 \frac{k-1}{2} M_0^2 \right)^{1.25}} \bar{T}_w^{n+1} \left(\frac{2}{1 + \bar{T}_w} \right)^{1.25}. \quad (135)$$

The results of calculating the drag coefficient in formula (135) for the case $\bar{T}_w = 1$ (absence of thermal conductivity) are represented in Fig. 6.20.

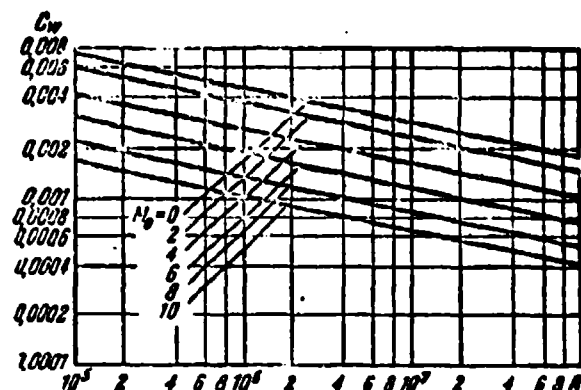


Fig. 6.20. Drag coefficient of the plate with $\bar{T}_w = 1$.

For an incompressible liquid at $M_0 = 0$, $\bar{T}_w = 1$, the value of $\delta^{**}/\delta = 7/72$, and therefore

$$\frac{\delta^*}{x} = \frac{0.37}{Re_x^{1/2}}, \quad c_f = \frac{0.058}{Re_x^{1/2}}, \quad C_{D,x} = \frac{0.073}{Re_x^{1/2}}.$$

For determining heat flow let us make use of integral (124) of the equation of energy

$$q_w = \lambda_w \left(\frac{\partial T}{\partial y} \right)_w = \frac{\lambda_w}{\mu_w} \frac{T_f - T_w}{u_w} \tau_w.$$

This expression coincides with formula (50) for a laminar boundary layer. Therefore, for a dimensionless heat flow we have (with $Pr_w = 1$)

$$St = \frac{q_w}{\rho_c \rho_w u_w (T_f - T_w)} = \frac{c_f}{2}. \quad (136)$$

Relationship (136) is the consequence of the assumption regarding the presence of analogy between the processes of the transfer of momentum and heat with $Pr = Pr_T = 1$ (Reynolds' analogy).

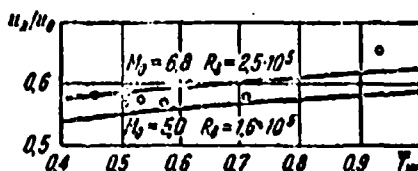


Fig. 6.21. Relative velocity on the boundary of a laminar sublayer.

The method presented for calculation of a turbulent boundary layer of a compressible gas is confirmed by the results of experimental research. Figure 6.21 gives the computed values of relative velocity on the boundary of a laminar sublayer (according to formula (130)) and the experimental values of Lobb, Winckler and Perch. A comparison of the experimental and calculated coefficients of friction for a flat plate is shown in Fig. 6.22. The unbroken curve is the calculated ratio c_f/c_{fH} calculated with identical Reynolds numbers referred to the momentum thickness. The black dots designate experimental values of this ratio. The dotted curve corresponds to the ratio c_f/c_{fH} calculated with identical R_x . Experimental values for this case are shown by the open dots.

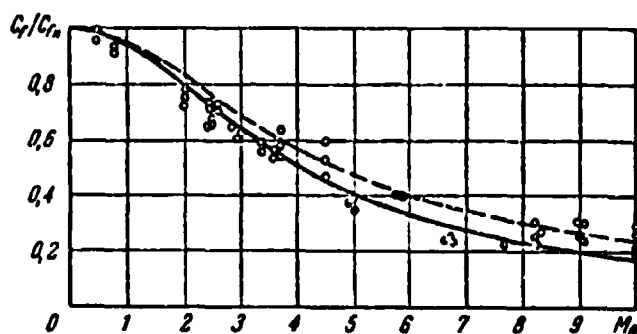


Fig. 6.22. Coefficient of friction for a turbulent boundary layer of a compressible gas.

§ 5. Boundary-Layer Separation

In the presence of a pressure gradient in external flow the boundary-layer flow becomes more complex than during flow about a flat plate. Since pressure remains constant across the boundary layer, the effect of the pressure gradient in external flow extends to the entire boundary layer. This effect basically is reduced to a change of the boundary layer velocity profile.

The reason for such a change of the velocity profile can be understood if we examine the following simplified diagram of flow. Let there be in a certain cross section of a boundary layer the velocity profile $u(y)$, where on the edge of the boundary $u(\delta) = u_0$. At a certain small distance Δx from this cross section the pressure in the external flow, and, consequently, throughout the boundary layer, will change by Δp . Disregarding the forces of friction and considering that flow occurs parallel to the wall, for every stream of liquid it is possible to write the Bernoulli equation

$$\rho u \Delta u = -\Delta p \quad \text{or} \quad \frac{\Delta u}{u} = -\frac{\Delta p}{\rho u^2}.$$

Consequently, in the section lying a distance Δx from the initial section, the velocity u_1 will be equal to

$$u_1 = u + \Delta u = u \left(1 + \frac{\Delta u}{u} \right) = u \left(1 - \frac{\Delta p}{\rho u^2} \right).$$

Respectively in the external flow

$$u_{01} = u_0 \left(1 - \frac{\Delta p}{\rho u_0^2} \right).$$

Then we finally have

$$\frac{u_1}{u_{01}} = \frac{u}{u_0} \cdot \frac{\left(1 - \frac{\Delta p}{\rho u^2} \right)}{\left(1 - \frac{\Delta p}{\rho u_0^2} \right)}.$$

If flow occurs against building pressure, then $\Delta p > 0$, and when $u < u_0$ the term in parentheses will be less than unity. Consequently, the velocity profile in this case becomes less full. If pressure along the flow decreases, then $\Delta p < 0$, and when $u < u_0$ the term in parentheses will be more than unity. In this case the velocity profile becomes fuller. The results of experimental study of a boundary layer in the presence of pressure gradient in the external flow qualitatively confirm the obtained conclusions. Figure 6.23 gives the velocity profile in the turbulent boundary layer of a noncompressible liquid when both a positive and negative pressure gradient are present. Experiments were carried out in narrowing flat ducts (flow with accelerating pressure gradient) and in expanding ducts (flow with negative pressure gradient). Half the expansion angle α characterized the amount of pressure gradient.

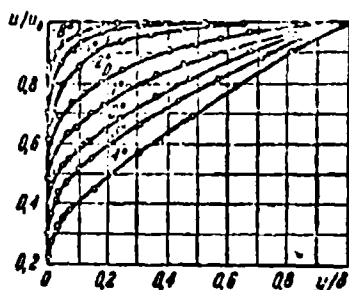


Fig. 6.23.

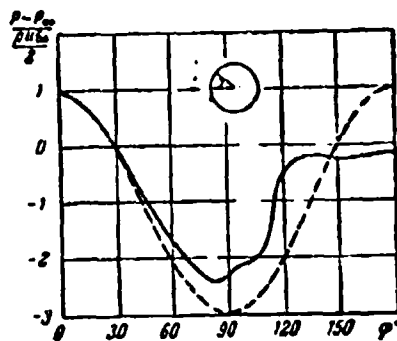


Fig. 6.24

Fig. 6.23. Velocity profile when pressure gradient is present, (according to experiments of Nikuradze).

Fig. 6.24. Pressure distribution on a circular cylinder.

With a sufficiently large positive pressure gradient in the external flow the layers of liquid near the wall can stop and even begin to move in the opposite direction, i.e., boundary-layer separation occurs (Fig. 6.4). The cross section of the

boundary layer beginning with which back flow of liquid occurs is called the point of boundary layer separation. At this point the following relationship holds:

$$\left(\frac{\partial u}{\partial y}\right)_w = 0, \text{ i.e., } \tau_w = 0. \quad (137)$$

The boundary-layer separation is always connected with the formation of vortices which penetrate the external flow and substantially distort the picture of flow obtained from the ideal fluid theory, even far from the body. For an explanation let us give some information about the flow of noncompressible liquid about a circular cylinder. Figure 6.24 shows two curves of pressure distributions along the circumference of a cylinder; the dotted curve follows the ideal fluid theory, and the unbroken curve was obtained experimentally by Flaksbart with Reynolds number

$$R = \frac{\rho_{\infty} u_{\infty} d}{\mu_{\infty}} = 6.7 \cdot 10^4,$$

i.e., with turbulent boundary layer. The subscript here designates the parameters in undisturbed flow. On the front side of the cylinder the measured pressure distribution more or less coincides with theoretical distribution for ideal fluid. On the rear side of the cylinder measured values of pressure differ significantly from the theoretical. This is explained by the fact that at $\phi = 125^\circ$ boundary-layer separation occurs. As a result of distinction in the distribution of pressure from the theoretical, pressure drag appears. A similar pattern is observed during flow about wing profiles. Thus, the boundary-layer separation exerts a substantial influence on the flow pattern of different bodies and, consequently also on such fundamental characteristics as resistance and lift. In connection with this the need for knowing how to calculate the position of the separation point of a boundary layer becomes obvious. In the most general form the conditions of boundary-layer separation were obtained by G. M. Bam-Zelkovich on the basis of the dimensional theory.

Flow in an arbitrary cross section of a boundary layer will be determined, if we assign:

- a) velocity profile in a certain initial cross section of the boundary layer;
- b) pressure distribution on the edge of the boundary layer;
- c) the value of velocity u_0 and density ρ_0 of external flow at any one point;
- d) characteristic linear dimensions which correspond to the cross section in question (for example, distance x of this cross section from the initial).

Pressure distribution on the edge of a boundary layer can be assigned by the value of pressure itself p_0 and all its derivatives (p'_0 , p''_0 , etc) in the cross section in question.

The basic assumption on which are based all further conclusions is the following: for flow in a certain cross section of a boundary layer the essential effect comes from external flow only in the close vicinity of this cross section.

This assumption is confirmed by the following experimental facts. First, the boundary layer velocity profile on the walls of the straight portions of cylindrical pipes is the same as the vicinity profile on a flat plate regardless of whatever flow (accelerated or slowed) preceded flow about the straight portion of the tube. In the second place, the velocity profile above the separation point in the turbulent boundary layer of non-compressible liquid does not depend on the flow parameters in external flow before the separation point. The universality of

the separation profile with a different flow pattern before the section of breakaway also testifies to fact that it is possible to disregard the effect of external flow outside the small vicinity of the considered section. Finally, experiments in the study of the interaction of a shock wave on a boundary layer directly show that the noticeable changes in the boundary layer occur only at a distance equal to several boundary layer thicknesses. Consequently, even very strong pressure change in external flow caused by a shock wave affects the flow pattern in the boundary layer in front of the shock wave only in a small neighborhood.

Thus, experiments show that flow in a certain cross section of a boundary layer is affected only by the parameters of external flow near this cross section. Hence it follows that the effect of the velocity profile in the initial cross section can be disregarded. Because of this for characteristic linear dimensions it is advantageous to use not distance x from the initial cross section, but any linear characteristic z of the boundary layer in the cross section in question (for example the displacement thickness δ^* or the depth of loss of momentum δ^{**}). From the basic assumption it follows also that if in external flow all pressure derivatives p_0 in x at a particular point are finite, then in the expansion of pressure p_0 in x it is possible to be restricted to the first derivative of p_0 .

Under these assumptions we obtain the following parameter system, determining flow in an arbitrary cross section of a laminar or turbulent boundary layer:

u_0 - velocity, ρ_0 - density, p_0 - pressure of external flow in the section in question, p'_0 - first derivative of pressure in x , z - characteristic dimension of boundary layer, μ_0 - coefficient of dynamic viscosity, λ_0 - coefficient of thermal conductivity, k - ratio of heat capacities.

According to the fundamental theory of the dimensional theory any dimensionless complex is a function only of dimensionless combinations of the determining parameters.

Then, for example, for the dimensionless stress of friction on the wall we have

$$\frac{\tau_w}{\rho_0 u_0^2} = \Phi_1 \left(M_0, \frac{\rho_0 z}{\rho_0 u_0^2}, \frac{\rho_0 u_0^2}{\mu_0} \right). \quad (138)$$

where M_0 are the Mach numbers of the external flow.

Function Φ_1 should obviously depend even on Pr and k numbers, but these arguments are omitted, since for this gas they can be considered as constants.

At the separation point of boundary layer $\tau_w = 0$. Solving equation (138) relative to $(\rho_0 z)/(\rho_0 u_0^2)$ and expanding in series in powers of $\mu_0/(\rho_0 u_0^2)$, we obtain

$$\frac{\rho_0 z}{\rho_0 u_0^2} = \Psi_1 \left(M_0, \frac{\mu_0}{\rho_0 u_0^2} \right) = \tau_2(M_0) + \tau_1(M_0) \frac{\mu_0}{\rho_0 u_0^2} + \dots \quad (139)$$

Let us complete now in equality (139) the same passage to the limit which is made during the derivation of the boundary layer equations, i.e., let us assume that viscosity vanishes ($\mu_0 \rightarrow 0$).

In laminar boundary layer when the coefficient of viscosity vanishes (Reynolds number $R \rightarrow \infty$) the characteristic dimension of the boundary layer also vanishes ($z/l \sim 1/\sqrt{R} \rightarrow 0$, where l is the characteristic dimension of the streamlined body). Consequently, $(\rho_0 z)/(\rho_0 u_0^2)$ vanishes as $1/\sqrt{R}$.

Furthermore, we have

$$\frac{p'_0}{\rho_0 u_0^2} = \frac{p'_0}{\rho_0 u_0^2} \frac{1}{z} = \frac{1}{R} \frac{1}{z}.$$

We find, hence, that $\mu_0/(\rho_0 u_0 z)$ vanishes (when $u_0 \rightarrow 0$) just as $1/\sqrt{R}$. Because of this in formula (139) the terms proportional to $(\mu_0/\rho_0 u_0 z)^n (n \geq 0)$, vanish as $1/\sqrt{R}$. Since $\phi_0(M_0)$ does not vanish (at $\mu_0 \rightarrow 0$), for a laminar boundary layer $\phi_0(M_0)$ should be identically zero. Multiplying both sides of (139) by $(\rho_0 u_0 z)/\mu_0$, and passing to the limit as $R \rightarrow \infty$, we find that at the separation point of the laminar boundary layer the following relationship is valid:

$$\frac{p'_0}{\rho_0 u_0^2} = \eta_1(M_0) \quad (140)$$

In the case of a turbulent boundary layer the characteristic dimension of the boundary layer at $\mu_0 \rightarrow 0$ does not vanish, since the boundary layer thickness is determined by turbulent mixing. Consequently $p'_0 z / \rho_0 u_0^2$ does not vanish. In this case $\phi_0(M_0) \neq 0$, all the remaining terms in (139) vanish at $\mu_0 \rightarrow 0$. Thus, for a turbulent boundary layer at the separation point the following relationship should be made:

$$\frac{p'_0 z}{\rho_0 u_0^2} = \varphi_0(M_0) \quad (141)$$

Function $\phi_0(M_0)$ and $\phi_1(M_0)$ can be determined theoretically and experimentally. Their values, of course, depend on which of the parameters is accepted as the characteristic dimension of the boundary layer z . For a turbulent boundary layer in non-compressible liquid ($M_0 = 0$) the quantity $\phi_0(0)$ is equal approximately to 0.015, if as the characteristic dimension z we take the displacement thickness δ^* . If for characteristic dimension we take the depth of momentum loss δ^{**} , then $\phi_0(0) = 0.005$.

For a turbulent boundary layer at $M_0 \neq 0$ quantity $\phi_0(M_0)$ can be determined as follows. We will search for the stress distribution of friction across a boundary layer at the separation point in the form of a polynomial from y/δ

$$\frac{\tau}{\rho_0 u_1^2} = a_0 + a_1 \frac{y}{\delta} + a_2 \left(\frac{y}{\delta}\right)^2 + a_3 \left(\frac{y}{\delta}\right)^3, \quad (142)$$

where for determination of coefficients a_0, a_1, a_2, a_3 we utilize the following conditions:

$$y = 0, \tau_w = 0 \text{ (at the separation point),}$$

$$y = 0, \left(\frac{d\tau}{dy}\right)_w = \frac{d\rho_0}{dx} \text{ (follows from the equation of motion (117))}$$

$$y = \delta, \tau = 0 \text{ (on the limit of the boundary layer).}$$

One additional necessary condition can be obtained by differentiating with respect to y the equation of motion (117):

$$\rho u \frac{\partial^2 u}{\partial y \partial x} + u \frac{\partial^2 u}{\partial y^2} + \rho \frac{\partial u}{\partial y} \frac{\partial u}{\partial x} + \rho v \frac{\partial^2 u}{\partial y^2} + \rho \frac{\partial v}{\partial y} \frac{\partial u}{\partial y} + v \frac{\partial^2 u}{\partial y^2} = \frac{\partial^2 \tau}{\partial y^2}.$$

Hence at $y = 0$ we have ($u = v = 0, \partial u / \partial y = 0$) $\partial^2 \tau / \partial y^2 = 0$. Then, for the coefficients of the polynomial (142) we obtain

$$a_0 = a_1 = 0, \quad a_2 = -a_3 = \frac{1}{\rho_0 u_1^2} \frac{d\rho_0}{dx}.$$

and relationship (142) assumes the form

$$\frac{\tau}{\rho_0 u_1^2} = \left[\frac{y}{\delta} - \left(\frac{y}{\delta}\right)^3 \right] \frac{1}{\rho_0 u_1^2} \frac{d\rho_0}{dx}. \quad (143)$$

The stress of friction in the turbulent boundary layer can be represented in the form of the sum

$$\tau = \tau_m + \tau_r$$

where $\tau_m = \mu \partial u / \partial y$ - stress of friction caused by molecular transfer and τ_r is the tangential stress caused by turbulent pulsations.

In accordance with the hypothesis of Prandtl

$$\tau_r = \rho l^2 \left(\frac{\partial u}{\partial y} \right)^2$$

where l - mixing path length. Thus, relationship (143) can be rewritten in the form

$$\mu \frac{\partial u}{\partial y} + \rho l^2 \left(\frac{\partial u}{\partial y} \right)^2 = \frac{d p_0}{d x} \left[\frac{y}{\delta} - \left(\frac{y}{\delta} \right)^2 \right]. \quad (144)$$

Far from the separation point the stress of viscous friction is negligibly small in comparison with the stress of eddy viscosity for all distances from wall which exceed a certain determined value, which is called the thickness of the laminar sublayer. Within this sublayer the stress of viscous friction reaches large values, since $\partial u / \partial y$ is great here. However, at the separation point $(\partial u / \partial y)_w = 0$ (at $y = 0$) and the stress of viscous friction will be low even at the wall. Thus viscous friction can be disregarded throughout the cross section. Then from (144) we will obtain

$$\rho l^2 \left(\frac{\partial u}{\partial y} \right)^2 = \frac{d p_0}{d x} \left[\frac{y}{\delta} - \left(\frac{y}{\delta} \right)^2 \right]. \quad (145)$$

This equation can serve for determining the velocity profile in the separation point.

Since beginning with the separation point flow behaves approximately as a free turbulent jet, it is possible to assume that the mixing length in the breakaway section is constant and equal in magnitude to the mixing length for free turbulent jets. As is known, from the theory of jets (§ 1 Chapter VII) the ratio of mixing length to the width of the jet, which in our case is equivalent to boundary thickness δ , is a constant value, i.e., $l = l/\delta = \text{const}$. Introducing the dimensionless quantities $\bar{\rho} = \rho/\rho_0$, $\bar{u} = u/u_0$, $\bar{y} = y/\delta$, from relationship (145) we will obtain

$$\mu^{1/2} \left(\frac{du}{dy} \right)^2 = \frac{1}{\rho_0 u_0^2} \frac{d\rho_0}{dx} (y - y^2) \quad (146)$$

In the case of zero heat transfer and $Pr = 1$ the stagnation temperature is constant, and therefore

$$\bar{t} = \frac{1}{1 + \frac{k-1}{2} M_0^2 (1 - u^2)}.$$

Integrating equation (146) over the boundary layer from $\bar{y} = 0$ to \bar{y} , we will obtain

$$\frac{1}{\sqrt{\frac{k-1}{2} M_0^2}} \arcsin \frac{u}{\sqrt{1 + \frac{k-1}{2} M_0^2}} = \frac{1}{l} \sqrt{\frac{1}{\rho_0 u_0^2} \frac{d\rho_0}{dx}} \int_0^{\bar{y}} \sqrt{y - y^2} dy.$$

or

$$u = \sqrt{1 + \frac{k-1}{2} M_0^2} \sin \left(\frac{1}{l} \sqrt{\frac{k-1}{2} M_0^2} \frac{1}{\rho_0 u_0^2} \frac{d\rho_0}{dx} \int_0^{\bar{y}} \sqrt{y - y^2} dy \right). \quad (147)$$

When $\bar{y} = 1$ $\bar{u} = 1$, therefore from relationship (147) it follows that

$$\frac{1}{\rho_0 u_0^2} \frac{d\rho_0}{dx} = \frac{2}{k-1} \frac{1}{M_0^2} \left(\frac{l}{A} \arcsin \frac{1}{\sqrt{1 + \frac{k-1}{2} M_0^2}} \right)^2. \quad (148)$$

where

$$A = \int_0^1 \sqrt{1-y^2} dy = 0.473.$$

Substituting (148) into (147), we will obtain finally for the velocity distribution at the separation point

$$u = \sqrt{1 + \frac{2}{k-1} M_\infty^2} \sin \left(\frac{1}{A} \arcsin \frac{1}{\sqrt{1 + \frac{2}{k-1} M_\infty^2}} \int_0^{\eta} \sqrt{1-y^2} dy \right). \quad (149)$$

From (141) and (148) it follows that if for the characteristic dimension we take the displacement thickness δ^* , then

$$\varphi_0(M_\infty) = \frac{2}{k-1} \frac{1}{M_\infty^2} \left(\frac{1}{A} \arcsin \frac{1}{\sqrt{1 + \frac{2}{k-1} M_\infty^2}} \right)^{\frac{2}{k-1}}.$$

For a noncompressible liquid ($M_\infty = 0$) we have

$$\varphi_0(0) = \left(\frac{2}{k-1} \right) \left(\frac{1}{A} \right)^{\frac{2}{k-1}}.$$

Eliminating from these two relationships the unknown τ , we will finally obtain

$$\varphi_0(M_\infty) = \frac{2}{k-1} \frac{1}{M_\infty^2} \left(\frac{\delta^*}{\delta} \right)^{\frac{2}{k-1}} \varphi_0(0) \left(\arcsin \frac{1}{\sqrt{1 + \frac{2}{k-1} M_\infty^2}} \right)^{\frac{2}{k-1}}. \quad (150)$$

The ratio δ^*/δ is defined by expression (57), since the velocity profile and temperature profile in the boundary layer are known.

The change in $\phi_0(M_0)$ depending on M_0 , calculated according to formula (150), is shown on Fig. 6.25 by the unbroken curve. The results of the experiments are plotted there. The open circles correspond to nonseparable flow, and the solid circles correspond to flow with boundary-layer separation.

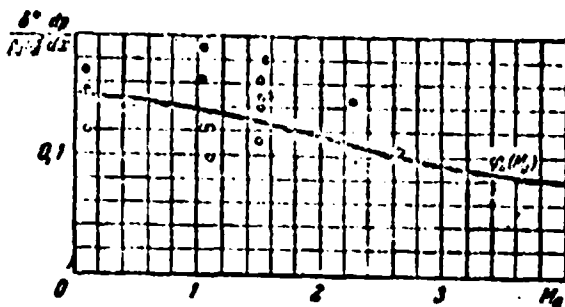


Fig. 6.25. Parameter of breakaway of turbulent boundary layer as a function of Mach number M_0 .

Thus, boundary-layer separation appears when the parameter

$$\xi = \frac{\delta^*}{\rho_0 u} \frac{d\rho_0}{dx}$$

reaches a certain critical value which depends on M_0 and is determined by formula (150). Thus to provide for nonseparable flow during the slowing of a flow of gas ($d\rho_0/dx > 0$) it is necessary to achieve the slowing in such a way that parameter ξ nowhere reaches its critical value.

For determining parameter distribution ξ along the streamlined surface, besides the parameters of external flow, it is necessary to know the characteristic dimension of the boundary layer (for example, the displacement thickness). The boundary-layer calculation in the presence of pressure gradient in external flow is a rather complex problem, since in this case the velocity profile (and temperature profile) will depend on the pressure gradient and change from one cross section to the next.

For a laminar boundary layer of both noncompressible liquid and compressible gas at variable pressure in the external flow there are different methods of calculation. The most precise methods are based on numerical integration of differential equations and require the use of a computer. For a turbulent boundary layer of noncompressible liquid approximate, semi-empirical methods of calculation have been developed. In the case of small pressure gradient in the external flow the turbulent boundary layer of compressible liquid can be calculated when the effect of the pressure gradient is considered only in the integral relationship of momentum (59). In this case it is considered that the velocity profile and temperature profile, and also the dependence of the stress of friction on the characteristic boundary layer thickness take the same form as in the case of flow about a flat plate.

§ 6. Interaction of a Boundary Layer with Shock Waves

The build-up of a boundary layer on a streamlined surface always affects the external flow. In the absence of shock waves this effect is reduced to the following. The boundary layer growth in the direction of flow is connected with an increase in the displacement thickness δ^* , which leads to deviation in the flow lines of the external flow. Thus, flow in the external flow will be the same as during flow about a fictitious outline displaced with respect to the real one by the displacement thickness. Consequently, during the calculation of flow it is necessary to apply the method of successive approximations: first calculated is the flow about a body by an ideal fluid, then according to the found pressure distribution along the body surface are found the parameters of the boundary layer (including displacement thickness); the flow about the fictitious body whose contour is shifted by δ^* is further calculated, etc. However, usually the

displacement thickness is low in comparison with the dimensions of the body and therefore it is possible to be restricted to the first approximation.

When shock waves are present, the boundary layer usually has a stronger effect on external flow, in certain cases substantially changing the picture of the entire flow. The fact is that the shock wave changes in the velocity and temperature in the direction normal to the front of the wave, which usually differs little from the flow direction, are great in comparison with changes in these values along the wave. In the boundary layer changes in the velocity and the temperatures in the flow direction are usually insignificant, while the changes of these values across the boundary layer are great. Consequently, in the interaction region of the shock wave with the boundary layer the velocity and the temperature substantially change both lengthwise and across the flow. Consequently, the basic assumptions of the boundary-layer theory and theory of shock waves in this case cease to be valid. Thus, theoretical study of the interaction region shock waves with a boundary layer should represent an extremely complex problem. Experimental study of this zone of flow is also not a simple matter. However, available data make it possible to present the picture of interaction as the following. The presence of a shock wave leads to a sharp increase in pressure on the wall. The pressure increase is transferred towards the flow in the subsonic part of boundary layer, which produces a thickening or even a boundary-layer separation. In this place the flow line in the external flow differs from wall, which affects the form and shock-wave intensity. The picture of interaction depends substantially on the flow conditions in the boundary layer.

Let us examine the interaction of the shock wave with a laminar boundary layer. Basic data on this question have been

obtained during flow about wing profiles at high subsonic speed. In the forming local supersonic zones appear normal shock waves. If the Mach number M_0 in the supersonic zone only a little exceeds unity (i.e., the drop in pressure in the shock is low), then the boundary layer either does not separate at all or after the separation adheres again to the wall, remaining laminar or changing to turbulent (Fig. 6.26). Immediately after the shock wave appear rarefaction waves as during flow about an external obtuse angle. At the place of attachment the flow is at a certain angle to the wall; therefore a new shock wave appears which can cause a new boundary-layer separation. Thus, several constructive shock waves can appear, which is observed in practice. With an increase in M_0 , i.e., with an increase in the shock-wave intensity, considerable boundary layer growth occurs, and pronounced boundary-layer separation appears (Fig. 6.27). At the place of boundary-layer thickening are formed compressible waves as during flow about a concave wall. At a certain distance from the wall the compressive waves become one or several oblique shocks. Figure 6.28 gives pressure distributions in the interaction region of the shock wave with the laminar boundary layer at different distances from the wall and at $M_0 = 1.225$ (according to experiments of Ackert, Feldman and Rotta). These data show that near the wall the pressure increases gradually, and not abruptly. Considerable pressure change across the boundary layer is observed also. Thus, the zone of interaction is characterized by the presence of longitudinal and transverse gradients of pressure. Consequently, the shock wave and boundary layer lose some distinguishing features, which it is necessary to consider during practical problems.



Fig. 6.26. Schlieren photograph of flow about a profile with $M_\infty = 0.843$, $R = 8.45 \cdot 10^5$ (Lipman).



Fig. 6.27.

Fig. 6.27. Schlieren photograph of flow about a profile with $M_\infty = 0.895$, $R = 8.77 \cdot 10^5$ (Lipman).

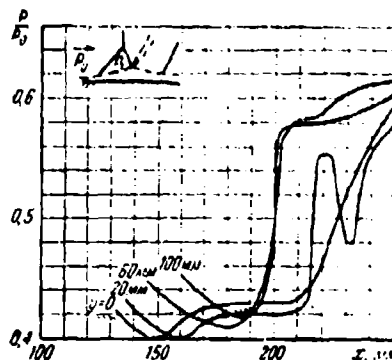


Fig. 6.28.

Fig. 6.28. Pressure distribution in the interaction region of shock wave with laminar boundary layer.

Similar features of flow are observed during the interaction of a boundary layer with an oblique shock wave falling from outside or with a shock formed during flow about an internal obtuse angle.

One of the basic quantitative characteristics of such interaction is the pressure ratio on the wall at the separation point p_1 to pressure in undisturbed flow p_0 . According to Guesde's theory this value does not depend on the type of interaction and shock-wave intensity in the external flow, but is determined by M_0 and by the Reynolds number

$$\frac{p_1}{p_0} = 1 + 0.565 \frac{AM_0^2}{[(M_0^2 - 1) R_x]^{1/4}}, \quad (151)$$

$M_0 > 1.2.$

This ratio is called the *critical drop*.

The values of p_1/p_0 with $M_0 = 2$, calculated from formula (151) (unbroken curve) and obtained experimentally by different authors during study of flow about an internal obtuse angle and during study of the reflection of an oblique shock from a flat wall, are given on Fig. 6.29.

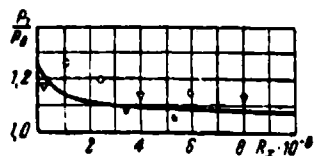


Fig. 6.29. Dependence of critical pressure drop as the ratio of oblique shock to Reynolds number with a laminar boundary layer.

Taking into account the complexity of the measurements, and therefore, their low accuracy, one ought to consider the agreement of the calculated and experimental results as satisfactory. As follows from formula (151), pressure ratio p_1/p_0 increases with a decrease in R_x or increase in M_0 . Physically this means that the less R_x is, the more the viscosity force preventing separation near the wall. An increase in M_0 leads to an increase in the momentum of the mass of gas in the boundary layer, which also impedes separation. Knowing M_0 and the drop in pressures on the first oblique shock, it is possible to determine the angle of inclination of this shock relative to the incident flow.

For the full construction of the picture of flow it is necessary to know how to determine the distance b by which the oblique shock wave will move away towards the flow. According to experimental data available at present, this distance is proportional to the displacement thickness of the undisturbed boundary layer and increases with an increase in the shock-wave intensity in the external flow. The values of b found by G. I. Petrov and his colleagues during study of flow about the internal blunt angle with $M_0 = 2.0$, depending on the intensity of the basic shock are given on Fig. 6.30. The small open circles correspond to $R_x = 3.5 \cdot 10^5$, and the solid to $R_x = 5.3 \cdot 10^5$.

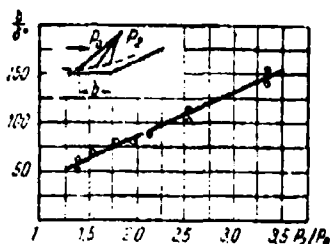


Fig. 6.30. Separation of oblique shock depending on intensity of the basic shock with laminar boundary layer.

The amount of experimental research devoted to study of the interaction of the shock wave with turbulent boundary layer is considerably larger. This is explained by the fact that the theoretical examination of this question is extremely difficult as a result of the complexity of the phenomenon and absence of a final theory of turbulence; at the same time in practice this case is encountered very frequently. As an example let us examine the interaction of an oblique shock wave falling from outside with a turbulent boundary layer on a flat plate. With low intensity of the falling shock the picture of flow differs little from the picture given by the ideal fluid theory (Fig. 6.31a). The difference is in the small bending of the falling and the reflected shock waves, and a certain increase in the boundary layer thickness. With larger intensity of the falling shock wave occurs boundary-layer separation and a system of shocks appears (Fig. 6.31b). With further increase of the intensity of the shock at the point of intersection of the falling and the first oblique shocks a normal shock wave is formed (Fig. 6.31c). A similar pattern of interaction takes place during flow about an internal obtuse angle, with the emergence of shock waves in the local supersonic zone, during flow about winged profiles during off-design outflow from the nozzle. Figure 6.32 depicts the photograph of flow about a winged profile with $M_\infty = 0.843$, $R_L = 1.69 \cdot 10^6$. The boundary layer before the shock is turbulent; the intensity of the shock is small and breakaway does not occur. With $M_\infty = 0.895$, $R_L = 1.75 \cdot 10^6$. The

shock-wave intensity increases and the boundary layer separates from the wall (Fig. 6.33). The cause of the reflected oblique shock is the same as during the interaction of the shock wave with a laminar boundary layer: the transfer of pressure increase towards the flow and the boundary layer growth. Figure 6.34 gives pressure distributions in the interaction region of a shock wave with a turbulent boundary layer on winged profile. The broken line shows change in the displacement thickness. These data show that in the interaction region there are considerable longitudinal and transverse gradients of pressure, as with a laminar boundary layer. The quantitative characteristics of the interaction of shock waves with a laminar and with a turbulent boundary layer, however, are different, since the fullness of the velocity profile is not identical.

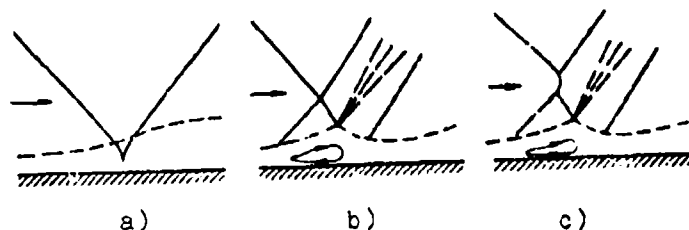


Fig. 6.31. Diagrams of interaction of shock wave with turbulent boundary layer on flat plate.



Fig. 6.32. Schlieren photographs of flow about a profile with $M_\infty = 0.843$, $R_L = 1.69 \cdot 10^6$ (Lipman).



Fig. 6.33. Schlieren photographs of flow about a profile with $M_\infty = 0.895$, $R_L = 1.75 \cdot 10^6$ (Lipman).

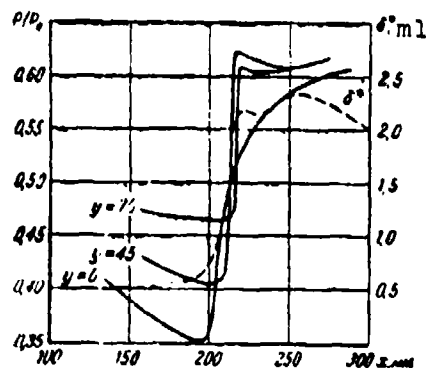


Fig. 6.34. Pressure distribution in the interaction region of shock wave with turbulent boundary layer.

The experimental data show that the pressure ratio in the first oblique shock (critical drop) does not depend on the method of realization and intensity of the basic shock wave or on the Reynolds number (i.e., the parameters of the boundary layer), but is determined by the value M_0 of the external flow. Figure 6.35 gives the results of study of the pressure ratio p_1/p_0 in the first oblique shock, obtained by I. P. Nekrasov with different Reynolds numbers and $M_0 = 2.0$. Figure 6.36 shows the values of p_1/p_0 depending on M_0 at different cases of interaction, indicated in the figure. This figure plots the computed value of this ratio, calculated according to an empirical formula of I. P. Nekrasov

$$\lg \frac{p_1}{p_0} = 0,16M - 0,072 \quad (152)$$

(solid curve) and according to Guesde's formula

$$\frac{p_1}{p_0} = \left(\frac{1 + 0,2M_0^2}{1 + 0,128M_0^2} \right)^{1,5} \quad (153)$$

(broken curve).

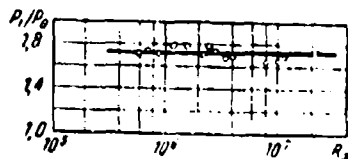


Fig. 6.35. Dependence of a critical drop in pressure in detached oblique shock on Reynolds number with turbulent boundary layer.

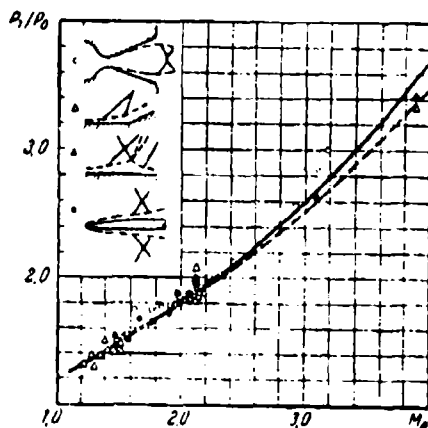


Fig. 6.36. Dependence of critical drop in pressures in a detached oblique shock on the number M_0 during the interaction of the shock wave with a turbulent boundary layer.

The amount of separation of the oblique shock from the point of intersection of the falling shock with the wall depends on the intensity of the falling shock on M_0 and on the local parameters of the boundary layer. Figure 6.37 gives the results of experimental determination of this linear dimension. The quantity δ^* is the displacement thickness of the boundary layer in the absence of a shock wave in the external flow.

It is necessary to keep in mind that the presence of shock waves in the external flow affects the velocity distribution and pressure in the boundary layer. With low intensity of the falling shock this effect leads to a certain boundary layer growth; the velocity profile in this case is affected little. With high intensity of the falling shock wave boundary-layer separation appears and a vortex zone is formed. Downstream from the separation point begins the mixing of the detached stream and the build-up of a new wall boundary layer. Because of the pressure transfer along the subsonic part of the boundary layer upstream the pressure ceases to be constant across the boundary layer, i.e., $\partial p / \partial y \neq 0$. Thus, all methods of calculation developed under the assumption of constant static pressure in the cross section of the boundary layer can be used only a sufficient distance from the place of interaction. Comparison of the above data shows that the breakaway of the laminar boundary layer appears with small shock-wave intensity, while during turbulent flow conditions the amount of the critical drop is considerably more. Moreover, at $M_0 < 1.3$ value of the critical drop for a turbulent boundary layer is more than the pressure ratio in the normal shock wave. Consequently, at $M_0 < 1.3$ the breakaway of the turbulent boundary layer cannot occur. This is explained by the fact that the velocity profile during turbulent flow conditions in the boundary layer is considerably more full than with laminar conditions, i.e., corresponds to larger momentum. Thus, separation of the turbulent boundary layer requires a more intense shock wave than for separation of a laminar layer. For this reason the pressure increase near the wall caused by a shock wave of identical intensity shifts towards the flow in the turbulent boundary layer a shorter distance than in a laminar boundary layer. Because of this the value of the separation of the first oblique shock wave in turbulent flow conditions is less than with laminar conditions (Figs. 6.30, 6.37).

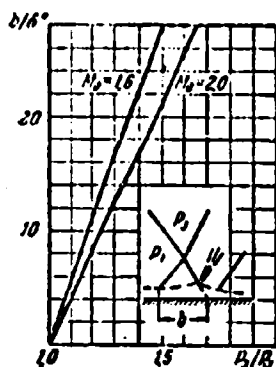


Fig. 6.37. Separation of oblique shock during interaction of shock wave with turbulent boundary layer.

§ 7. Flow of Fluid in Tubes

The flow of a fluid in channels of different cross section is very frequently encountered in practice. In this case usually the speed of motion in the channel is considerably less than the speed of sound, and therefore the fluid can be considered incompressible. Let us examine first a steady laminar axisymmetric flow in a circular cylinder pipe. Assume that the liquid flows into the tube at a constant speed. On walls is formed a boundary layer whose thickness increases along the tube. Since the density and flow rate through every cross section remain constant, an average speed is maintained. Thus the decrease in velocity near the wall caused by the presence of friction leads to an increase in the velocity outside the boundary layer (in the flow core). This zone of flow is called the *initial section*. At a certain distance from the entry the boundary layer thickness becomes equal to the radius of the tube, i.e., boundary layers meet. This zone of flow is called the *principal section* and is characterized by an invariable velocity profile. The length of the initial section can be determined approximately by the formula

$$l_0 = 0.034R, \quad (154)$$

which was obtained theoretically by Shiller. So, at $R = 1000$ and $R = 5000$ the quantity L_H is 30 and 150 tube diameters respectively. Subsequently we will examine only flow in the principal section. The x-axis is directed along the axis of the tube, and the y coordinate is read from the axis of the tube. Considering that the flow in all cross sections is identical the (velocity component in the axial direction does not depend on x), from the equation of continuity in cylindrical coordinates we will obtain

$$\frac{d(yv)}{dy} = 0, \text{ or } yv = \text{const},$$

where v is the velocity component in the radial direction. Since $v = 0$, at $y = r$, consequently, $v = 0$ throughout the flow. Then the equation of Navier-Stokes in cylindrical coordinates assumes the form

$$r^2 \frac{d^2 u}{dy^2} + \frac{1}{y} \frac{du}{dy} = \frac{dp}{dx}, \quad \frac{dp}{dy} = 0, \quad (155)$$

whereupon the boundary condition is $u = 0$ at $y = r$. Integrating equation (155), we will obtain the velocity distribution in the cross section of the tube

$$u = -\frac{1}{4r^2} \frac{dp}{dx} (r^2 - y^2). \quad (156)$$

Maximum velocity is reached on the axis of the tube at $y = 0$

$$u_m = \frac{r^2}{4r^2} \left(-\frac{dp}{dx} \right). \quad (157)$$

The amount of pressure gradient dp/dx is connected with the fluid flow rate through the tube. Actually,

$$Q = 2\pi \int_0^r u dy = \frac{\pi r^4}{8r^2} \left(-\frac{dp}{dx} \right). \quad (158)$$

whence the average rate of flow will be

$$u_{cp} = \frac{r^2}{8\eta} \left(-\frac{dp}{dx} \right). \quad (159)$$

In technical computations it is accepted to introduce resistance coefficient ζ

$$-\frac{dp}{dx} = \zeta \frac{\rho u_{cp}^2}{d}, \quad (160)$$

where d is the diameter of the tube. Substituting into relationship (160) the value of dp/dx from equality (159), we will obtain

$$\zeta = \frac{2d}{\rho u_{cp}^2} \frac{\rho u_{cp}^2}{r^2} = \frac{32\eta}{\rho u_{cp} d}. \quad (161)$$

If we introduce Reynolds number $R = \frac{\rho u_{cp} d}{\eta}$, then the law of resistance in a circular tube during laminar flow will take the form

$$\zeta = \frac{64}{R}. \quad (162)$$

This law is well confirmed by the results of experimental research (Fig. 6.38). The solid curve is computed according to formula (162), and the points correspond to the experimental data obtained by Gagen.

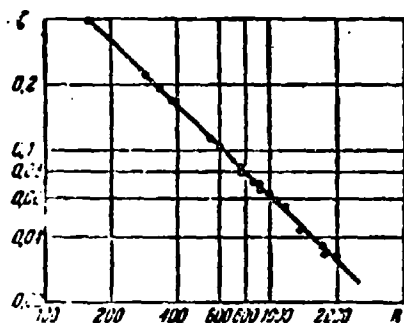


Fig. 6.38. Resistance coefficient for smooth circular tubes during laminar flow.

Laminar flow conditions occur only with Reynolds numbers less than its critical value. According to experiments in tubes, the critical Reynolds number is approximately equal to $R_{kp} = 2300$. However, it is necessary to have in mind that value R_{kp} largely depends on conditions in the flow, in the first place on the initial turbulence of the moving flow. In special experiments, where the turbulence of the external flow was insignificant, it was possible to keep the laminar flow conditions at significantly greater values than the critical value of the Reynolds number.

In general at $R > R_{kp}$ the turbulent flow conditions develop in the boundary layer, whereupon just as during laminar conditions, flow in the tube can be subdivided into the initial entrance section and the principal section. The length of the initial section, according to measurements of Kirsten, comprises from 50 to 100 tube diameters, and according to experiments of Nikuradze comprises from 25 to 40 diameters.

Let us examine flow in the principal section of a cylindrical circular tube. Let us isolate in the fluid a cylinder which has length l and radius y . In the principal section of the tube the velocity distributions in different cross sections are identical, therefore forces of inertia are absent and the cylinder will be in equilibrium under the tangential stresses on its lateral surface and the pressure difference $p_1 - p_2$ on its bases, i.e.

$$\tau = \frac{p_1 - p_2}{l} y. \quad (163)$$

According to this formula the tangential stress is proportional to the distance from the axis of the tube and reaches its greatest value on the wall

$$\tau_w = \frac{p_1 - p_2}{l} \frac{r}{2}. \quad (164)$$

The resistance coefficient ζ , determined by relationship (160), upon replacement of the pressure gradient by its value from formula (164), will be

$$\zeta = 4 \frac{u_0}{u_{cp}^2} \quad (165)$$

Unlike laminar flow, for which the connection between resistance coefficient (or pressure drop) and fluid flow rate is determined theoretically from the solution of the equations of Navier-Stokes, in a turbulent system such a connection can be found only when the velocity profile is known from experiment. As has already been indicated in § 4, the boundary layer velocity profile on a flat plate at $R_x = 10^5 - 10^8$ ($R_\delta = 2 \cdot 10^4 - 10^6$) is well described by the exponential formula with exponent 1/7, which in the selected coordinate system takes the form

$$\frac{u}{u_0} = \left(\frac{r-y}{r} \right)^{1/7}$$

The expression for the resistance coefficient ζ can be immediately obtained from relationship (131) at $T_w = 1$, $M_0 = 0$ and by replacing R_δ by $R = (\rho u_{cp} d / \mu)$ (considering $\delta = r$), and u_0 by u_{cp} :

$$u_{cp} = \frac{2\pi \int_0^r u_y dy}{\pi r} = 2u_0 \int_0^1 \left(1 - \frac{y}{r} \right)^{1/7} \frac{y}{r} d\left(\frac{y}{r}\right) = 0.517 u_0$$

$$R_\delta = \frac{\rho u_{cp}^3}{\mu} = \frac{1}{2} \frac{u_0}{u_{cp}} R$$

Then according to (165) we have

$$\zeta = 8 \frac{u_0}{\rho u_{cp}^2} = 8 \frac{u_0}{\rho u_0^2} \left(\frac{u_0}{u_{cp}} \right)^2 = 8 \frac{0.1226}{R^{0.25}} 2^{0.25} \left(\frac{u_0}{u_{cp}} \right)^{1.75} = \frac{0.708}{R^{0.25}} \quad (166)$$

This formula is close to the Blasius formula

$$\zeta = \frac{0.116}{R^{0.5}}$$

obtained on the basis of vast experimental material for $R = 4 \cdot 10^3 - 10^5$.

For large Reynolds numbers the experimental values of coefficient ζ prove to be higher than those calculated from the Blasius formula or according to formula (166).

To eliminate this disagreement we use (during the calculation of the resistance coefficient) the logarithmic velocity profile, which is asymptotic as $R \rightarrow \infty$, since during the derivation of this profile, molecular viscosity is disregarded as compared with turbulent (§ 4). For the selected coordinate system the logarithmic velocity distribution law (1.5) takes the form

$$\frac{u}{u_0} = 2.5 \ln \frac{r}{r_0} + 5.5 \quad (167)$$

and is well confirmed by experimental data of Nikuradse for large Reynolds numbers (Fig. 6.16). On the axis of the tube $y = 0$, therefore from (167) we have

$$\frac{u_z}{u_0} = 2.5 \ln \frac{r}{r_0} + 5.5 \quad (168)$$

Knowing the velocity profile (167), it is easy to find the mean rate of flow over the cross section of the tube

$$\frac{u_m}{u_0} = 2.5 \ln \frac{r}{r_0} + 1.75 \quad (169)$$

We express ζ through v_0 and u_{cp} , substituting into equality (165) the value $\tau_w = \rho v_0^2$ (according to determination (115)):

$$\zeta = 8 \left(\frac{v_0}{u_{cp}} \right)^4 \text{ or } \frac{v_0}{u_{cp}} = \frac{1}{2} \sqrt[4]{\zeta}. \quad (170)$$

Furthermore, we transform the quantity $v_0 R / v$:

$$\frac{v_0}{v} = \frac{1}{2} \sqrt[4]{\zeta} \frac{u_{cp}}{v} = \frac{1}{4} \sqrt[4]{\zeta} R \sqrt{\zeta}$$

Then relationship (169) can be written in the form

$$\frac{21.3}{\sqrt[4]{\zeta}} = 2.3 \lg \left(\frac{1}{4} \sqrt[4]{\zeta} R \sqrt{\zeta} \right) + 1.75$$

or

$$\frac{1}{\sqrt[4]{\zeta}} = 2.3 \lg (R) - 0.91. \quad (171)$$

This formula qualitatively describes well the change in resistance coefficient for smooth pipes with large Reynolds numbers. Best quantitative agreement is obtained, however, if we change somewhat the theoretical numerical factors and accept

$$\frac{1}{\sqrt[4]{\zeta}} = 2.15 \lg R - 0.8 \quad (172)$$

Figure 6.39 compares the values of ζ calculated according to Blasius's formula (solid curve) and according to formula (172) (broken curve), with experimental values of the resistance coefficient of tubes as obtained by different authors. As we see, for determining the resistance coefficient of smooth circular tubes at $R = 4 \cdot 10^3 - 10^5$ it is possible to utilize formula (166), and when $R > 10^5$, formula (172).

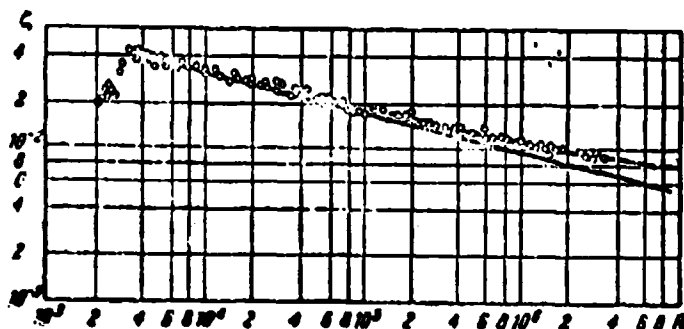


Fig. 6.39. Resistance coefficient for smooth circular tubes during turbulent flow.

Studies of the flow of a fluid in tubes with noncircular cross section showed that the laws of resistance for both laminar and turbulent systems take the same form as for circular tubes, if instead of the diameter we use the hydraulic diameter, equal to the ratio of four times the cross-sectional area to the perimeter. Figure 6.40 gives the results of measurements of ζ made by Shiller and Nikuradze, and values of ζ calculated from formulas (163) (curve 1) and (172) (curve 2). Here the characteristic dimension is the hydraulic diameter.

Finally, let us examine the motion of an ideal gas with constant thermal capacity in a channel of constant cross section in the presence of friction and heat exchange. The temperature of the walls we will consider constant. The equations of continuity, momentum and energy for the average parameters take the form

$$\rho u S = \frac{G}{g}, \quad S \frac{d}{dx} (\rho u^2) = -U \tau_w, \quad c_p S \frac{d}{dx} (\rho u T) = -U q_w, \quad (173)$$

where S is the cross-sectional area of the channel, U - its perimeter, G - the mass flow rate of gas.

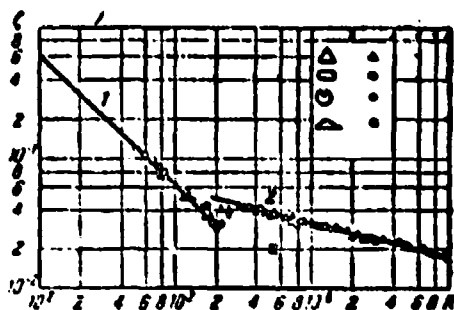


Fig. 6.40. Resistance coefficient for tubes with non-circular cross section.

Introducing the dimensionless coefficients of friction c_f and thermal conductivity St into the last two equations, and taking into account that $\rho u = \text{const}$, as follows from the equation of continuity (173), we will obtain

$$S \frac{d}{dx} (\rho u^2 \cdot \lambda \cdot p) = -U c_f \frac{\rho u^2}{2} \quad (174)$$

$$S \frac{dT_p}{dx} = -U St (T_p - T_w) \quad (175)$$

while c_f and St depend on the flow conditions (laminar or turbulent) and on the following dimensionless parameters:

$$c_f = c_f \left(Re, \lambda, \frac{T_w}{T_p} \right) \quad (176)$$

$$St = St \left(Re, Pr, \lambda, \frac{T_w}{T_p} \right) \quad (177)$$

where λ is the velocity coefficient, which is the ratio of the rate of flow to the critical speed of sound.

At small rates of flow ($\lambda \ll 1$) the quantity λ is not the determining parameter. In this case the heat-transfer coefficient will change only because of a change in the gas temperature

along the channel. Then the equation of energy (175) is integrated and the distribution of the stagnation temperature along the channel is determined. The velocity distribution is found from the equation of momentum (174). Precisely such an approach is usually utilized in the examination of the motion of a noncompressible fluid in a channel of constant cross section. During study of the motion of compressible gas, separate integration of the equations of energy and momentum is impossible, since the heat-transfer coefficient in this case depends on the gas velocity. Introducing gas-dynamic functions and the dimensionless stagnation temperature $\theta = T^*/T_w$, we will obtain

$$\rho = m \frac{p^* S q(\theta)}{\sqrt{1-\theta}}, \quad m = \text{const}, \quad (178)$$

$$\frac{k+1}{2k} \frac{d}{dx} [V^2 \theta(x)] = -\frac{\eta}{S} \frac{q}{2} \sqrt{\theta} \lambda, \quad (179)$$

$$\frac{d\theta}{dx} = -\frac{\eta}{S} \text{St}(\theta - 1), \quad (180)$$

Dividing (179) term-by-term by (180), we eliminate the variable x

$$\frac{k+1}{k} \frac{d[V^2 \theta(x)]}{d\theta} = \frac{q}{2 \text{St}(\theta - 1)} \sqrt{\theta}.$$

Differentiating in the left side, we will obtain a differential first-order equation connecting dimensionless stagnation temperature θ and the velocity coefficient λ :

$$\left(1 - \frac{1}{k}\right) \frac{d\lambda}{d\theta} = \frac{q}{2 \text{St}(\theta - 1)} \frac{\lambda}{\theta - 1} - \frac{1}{2\theta} \left(\lambda + \frac{1}{k}\right). \quad (181)$$

For simplicity of further computations we assume that a Reynold's analogy holds both during laminar and during turbulent flow conditions, i.e., $c_f = 2\text{St}$. Then equation (181) takes the form

$$\left(1 - \frac{1}{\lambda^2}\right) \frac{d\lambda}{d\theta} = \frac{2\lambda}{\lambda^2 - 1} - \frac{1}{\lambda^2} \left(1 - \frac{1}{\lambda^2}\right) \quad (182)$$

The integral curves of this equation are shown on Fig. 6.41 for $k = 1.4$. To determine the direction of the process during gas flow in the channel we utilize the equation of energy (180). If the channel is entered by a gas whose stagnation temperature is lower than the wall temperature ($\theta < 1$), then the gas will be heated ($d\theta/dx > 0$) and $\theta \rightarrow 1$. If the channel is entered by gas whose stagnation temperature is higher than the wall temperature ($\theta > 1$), then the gas will be cooled ($d\theta/dx < 0$) and $\theta \rightarrow 1$. Consequently, to the gas flow in the channel corresponds motion along integral curves to $\theta = 1$. In the area $\theta < 1$ both effects (heat supply and friction) act in one direction: during subsonic flow ($\lambda < 1$) occurs flow acceleration, and at supersonic flow a slowing down occurs. In the area $\theta > 1$ the joint effect of heat removal and friction is more complicated, since friction exerts an accelerating action, and heat removal a slowing action.

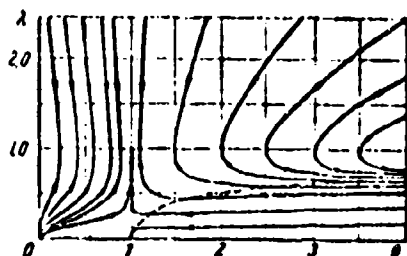


Fig. 6.41. Integral curves of the differential equation describing a flow of compressible gas in a channel of constant cross section with friction and heat exchange at $k = 1.4$. The broken line is $d\lambda/d\theta = 0$.

Let us first examine subsonic flow ($\lambda < 1$). With large differences in the gas and wall temperatures (large θ) and low speeds (low λ) the effect of heat exchange turns out to be more essential and a slowing of the flow occurs ($d\lambda/d\theta > 0$). With large λ and low θ the friction effect predominates and flow is accelerated ($d\lambda/d\theta < 0$). Along the line of the transition from slowing to acceleration $d\lambda/d\theta = 0$. Then from equation (182) we will obtain the equation of this line in the following form:

$$\lambda = \sqrt{\frac{\theta - 1}{\frac{k-1}{k+1}\theta + 1}}.$$

This curve is shown on Fig. 6.41 by broken lines. During supersonic flow of heated gas ($\theta > 1$, $\lambda > 1$) the predominant effect comes from friction and flow is slowed.

After the dependence of λ on θ is found, it is possible to determine the remaining flow parameters. From the equation of continuity (178) follows

$$\frac{\rho^*}{\rho_n^*} = \sqrt{\frac{\theta}{\theta_n}} \frac{\lambda_n \left(1 - \frac{k-1}{k+1} \lambda_n^2\right)^{\frac{1}{k-1}}}{\left(1 - \frac{k-1}{k+1} \lambda^2\right)^{\frac{1}{k-1}}};$$

the subscript "n" designates parameters in the beginning of the channel.

Utilizing fundamental relationships between the stagnation conditions and static parameters, we will obtain

$$\frac{p}{p_n} = \sqrt{\frac{\theta}{\theta_n}} \frac{\lambda_n \left(1 - \frac{k-1}{k+1} \lambda_n^2\right)^{\frac{1}{k-1}}}{\left(1 - \frac{k-1}{k+1} \lambda^2\right)^{\frac{1}{k-1}}},$$

$$\frac{T}{T_n} = \frac{\theta}{\theta_n} \frac{1 - \frac{k-1}{k+1} \lambda_n^2}{1 - \frac{k-1}{k+1} \lambda^2}.$$

Since $u = a\lambda$,

$$\frac{u}{u_n} = \frac{p_n}{p} = \frac{\lambda}{\lambda_n} \sqrt{\frac{\theta}{\theta_n}}.$$

Finally, integrating relationship (180), we find the connection between x and θ

$$x = \frac{s}{U} \int_0^1 \frac{d\theta}{St(\frac{\theta}{\pi} - 1)}.$$

since the dependence of λ on θ is already known, therefore, dependence of St on θ is known.

CHAPTER VII

TURBULENT JETS

§ 1. General Properties of Jets

In many instances of the motion of liquid and gas in the flow appear so-called surfaces of tangential discontinuity; the flows of liquid on both sides of such a surface are called jet streams. Depending on the relative direction of motion of the jets they can be cocurrent or counter. The characteristic feature of jet streams is the fact that the tangential discontinuity on the interface undergo such quantities, for example, as rate of flow, temperature, admixture concentration, whereas the static pressure distribution turns out to be continuous.

On the surface of tangential discontinuity (in connection with its instability) appear the vortices, which in disordered fashion move along and across the flow; because of this between adjacent jets occurs an exchange of finite masses (moles) of substance, i.e., transverse transfer of momentum, heat and admixtures. As a result on the boundary of two jets is formed an area of finite thickness with continuous velocity and temperature distribution and admixture concentration; this area is called the *jet turbulent boundary layer*. At very low values of the Reynolds number the jet boundary layer can be laminar, but we will not deal with this comparatively rare flow event.

The simplest case of a jet boundary layer occurs during the discharge of a fluid with regular initial velocity field (u_0) into a substance moving at constant velocity (u_∞), since in this case in the initial jet cross-sectional area the boundary layer thickness is equal to zero. The thickening of the jet boundary layer, which consists of increased particles of the surrounding substance and stagnation particles of the jet itself leads, on one hand, to an increase in the cross section, and on the other hand, to the gradual "eating" of the potential nucleus of the jet - an area lying between the internal boundaries of the boundary layer. The schematic diagram of such a jet stream is depicted on Fig. 7.1. The part of the jet in which there is a potential flow nucleus is called the *initial* section.

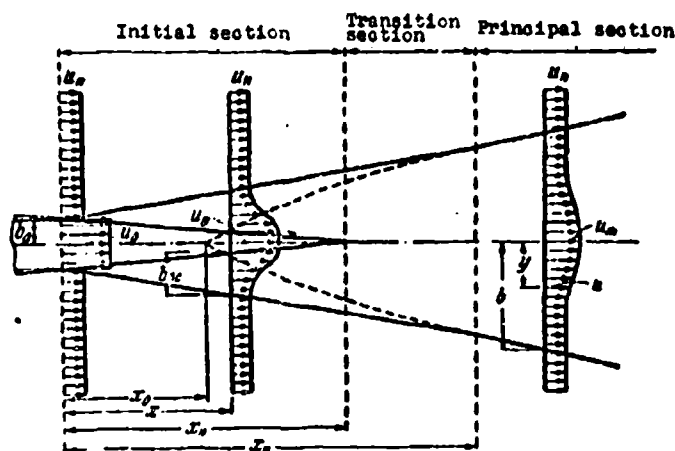


Fig. 7.1. The diagram of flow in a jet.

As numerous experiments show, one of the basic properties of such a jet is the constancy of static pressure in the entire flow zone¹ as a consequence of which the speed in the potential core

¹In certain cases (during the interaction of a jet with any obstruction) the condition of pressure constancy can be disturbed, but these special cases will be dealt with separately.

of the jet remains constant. Washout of the jet behind the limits of the initial section is expressed not only by its thickening, but also a change of velocity along its axis.

At a certain distance from the end of the initial section the jet stream acquires the same form as a flow of fluid from a source of infinitesimal thickness (in the axisymmetric case the source is a point, and the plane-parallel case it is a straight line perpendicular to the plane of spreading out of the jet): the corresponding section of the jet is called the *principal section*. Between the *principal* and *initial* sections of the jet is the so-called transition section.

Frequently a simplified diagram of a jet is used, and the length of the transition section is assumed to be zero; in this case the cross section in which the *principal* and *initial* sections meet is called transition jet cross-sectional area. If calculations consider the transition section, then the transition cross section is considered as coinciding with the beginning of the principal section.

The most studied form of a turbulent jet stream is the jet which spreads in a quiescent medium; such a jet is called *submerged*.

In the described diagram of a jet it is assumed that the boundary layer has finite thickness; some theories of the submerged jet accept a boundary layer of infinite thickness with asymptotic profiles of velocity, temperature and other quantities. Both these representations of a boundary layer are virtually possible to reconcile between one another, since an asymptotic

boundary layer can be always approximately replaced with a layer of finite thickness.¹

The characteristic feature of turbulent jet, as shown by theory and numerous experiments, is the smallness of the transverse components of velocity in any jet cross-sectional area in comparison with the longitudinal velocity. Consequently, if the X-axis is combined with the axis of symmetry of the jet, the velocity components along the y-axis will turn out to be so low that in engineering applications of jet theory they can be disregarded.

Experiments show that profiles of excess values of velocity, temperature and admixture concentration both in a submerged turbulent jet and in a jet spreading in cocurrent flow have an identical universal form. Figure 7.2 gives the universal velocity profile obtained in the experiments of Forstall and Shapiro² in the principal section of an axisymmetric air jet moving into an air flow of the same direction and same temperature, while the dimensionless excess values of velocity $\Delta u / \Delta u_m$ are constructed as a function of dimensionless ordinates y/y_c :

$$\frac{\Delta u}{\Delta u_m} = \frac{u - u_a}{u_m - u_a} = f\left(\frac{y}{y_c}\right). \quad (1)$$

¹In this case the "boundaries" of an asymptotic layer are considered to be the surfaces on which the values of velocity (or, for example, temperature) differ from the boundary values by a certain preassigned low value, for example by 1%.

²Almost all literature sources utilized in this chapter are contained in the bibliography to the monograph of the author (G. N. Abramovich, *Teoriya turbulentnykh struy*. Fizmatgiz, M., 1960). References only to later sources are given.

Here u - velocity at a distance y from the axis of the jet, u_m - velocity on the axis of the jet, u_H - velocity of cocurrent flow, y_c - distance from axis of jet to place in which excess velocity is half its maximum value: $u_c - u_H = 0.5 (u_m - u_H)$.

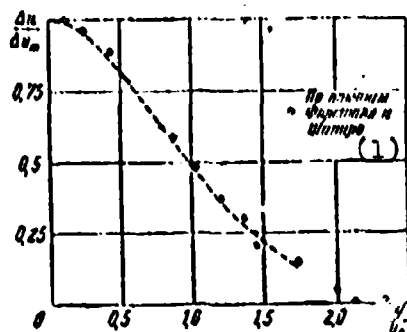


Fig. 7.2. Dimensionless excess velocity profile in principal section of an axisymmetric air jet spreading in a cocurrent airflow.

KEY: (1) According to experiments of Forstal and Shapiro.

These experiments were carried out with different ratios of the speed of cocurrent flow to the discharge velocity: $m = u_H/u_0 = 0.2; 0.25; 0.46$. Figure 7.2 depicts also the velocity profile in the submerged jet (dotted line), taken from experiments of Tryupel'; the universal velocity profile with and without cocurrent flow turned out to be virtually identical.

According to the experiments of Weinstein, Osterle and Forstal, and also Fertman dimensionless excess velocity profiles in flat cocurrent and submerged jets are described by the same universal relationship as in axially symmetrical jets.

Investigated in the works of B. A. Zhestkov, V. V. Glazkov and M. D. Gusev, velocity fields in the mixing zone of two plane-parallel turbulent jets of one direction with different velocities relationships ($m = 0, 0.23, 0.43, 0.64$) are represented on Fig. 7.3 in the following dimensionless coordinates:

$$\frac{\Delta u}{\Delta u_0} = f\left(\frac{y}{y_0}\right). \quad (2)$$

here $\Delta u = u - u_\mu$ excess velocity in jet, $\Delta u_0 = u_0 - u_\mu$ - initial difference in the jet velocities, $\Delta y_c = y - y_{0.5}$ - transverse distance from measurement point to point at which velocity $\Delta u_c = 0.5 \Delta u_0$, $\Delta y_b = y_{0.9} - y_{0.1}$ - distance between the points at which excess values of velocity are equal respectively to $\Delta u_1 = 0.9 \Delta u_0$ and $\Delta u_2 = 0.1 \Delta u_0$.

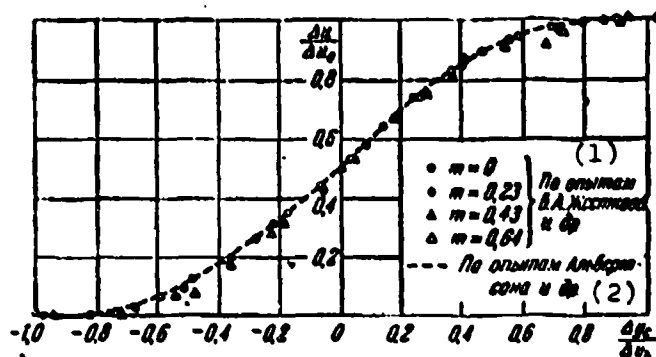


Fig. 7.3. Dimensionless excess velocity profile in the boundary layer of two flat plane cocurrent air jets (initial section). KEY: (1) According to experiments of B. A. Zhestkov, et al.; (2) According to experiments of Albertson, et al.

The same figure graphs the velocity curve in the boundary layer of the initial section of a submerged flat jet, obtained in experiments of Albertson, et al. In this case also the velocity profile is universal, but differs somewhat from the same for the principal section.

Measurements made by the author in conjunction with F. M. Vafin in the initial zone of flow astern of a poorly streamlined body located on the axis of a channel of constant cross section (in the flat and axisymmetric cases) showed that, in spite of the existence of a zone of return currents. The dimensionless velocity profiles (2), in the construction of which it was taken

into consideration that the velocity of the return current ($u_{\text{H}} < 0$) changes with distance from the stern of the body, turned out to be the same as in the boundary layer of an ordinary jet.

Similar results are obtained in the combustion chamber of a gas-turbine engine. In the beginning of the chamber a large area of return currents is usually created, meeting on the axis of symmetry. Typical profiles of the axial components of velocity in the different cross sections of such a chamber, obtained during "cold blow-through" (without combustion) in A. I. Mikhaylov's work, are plotted on Fig. 7.4. These profiles, but in dimensionless coordinates of type (2), coincide with those given on Fig. 7.3.

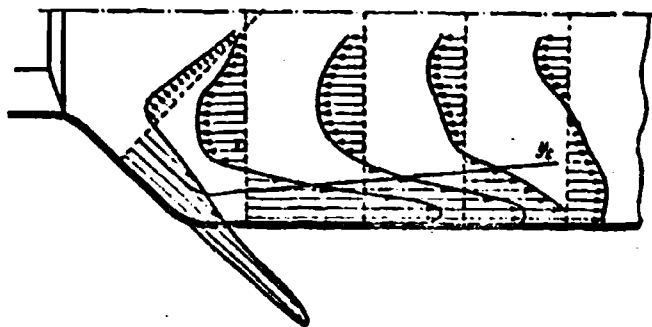


Fig. 7.4. Velocity profile in the combustion chamber of a turbojet engine (cold blow-through) according to experimental data of A. I. Mikhaylov.

The experiments of L. A. Vulis, Ye. V. Ivanov and other researchers show that the profiles of dimensionless excess values of velocity in a jet held by a counterflow are also universal and close to the same for a submerged jet.

Approximate analytical dependences can be selected to describe a universal velocity profile.

Subsequently for a description of the velocity profile in the principal section of a jet of any form we will use function $f(\eta)$, which was first theoretically obtained by Schlichting:

$$\frac{u - u_0}{u_m - u_0} = f(\eta) = (1 - \eta^2)^2. \quad (3)$$

Here $\eta = y/b$ - distance from point with velocity u to axis of jet, expressed in fractions of half-thickness (or radius) of a given jet cross-sectional area.

The relative distance to the point at which the excess velocity is half that on the axis of the jet ($\frac{u - u_0}{u_m - u_0} = 0.5$), is easily determined from (3):

$$\eta_{0.5} = \eta_0 = 0.441. \quad (4)$$

The velocity profiles calculated from formula (3) agree well with the experimental velocity profile.

In the initial section of the jet ($u_m = u_0$) the curve of the universal velocity

$$\frac{u_0 - u}{u_0 - u_0} = f(\eta_m) = (1 - \eta_m^2)^2. \quad (5)$$

matches well with experimental data (Fig. 7.3), where dimensionless ordinate η_m is read from the external jet boundary (Fig. 7.5):

$$\eta_m = \frac{y - y_1}{b} = \frac{y - y_1}{y_2 - y_1}. \quad (6)$$

Curve (5) as a result of a change in the beginning of the reading differs from curve (3). The coordinates of points $y_{0.5}$, $y_{0.9}$, $y_{0.1}$, which we used for comparison of the calculated curve with experimental data, were found from (5) with the determination of (6).

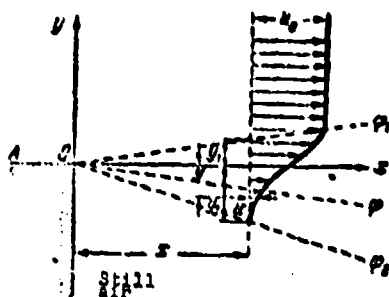


Fig. 7.5. Diagram of boundary layer of submerged jet.

The described results were obtained at moderate jet velocities ($M_0 \ll 1$) and slightly different density values of the substance of the jet ρ_0 and the surrounding medium ρ_∞ , i.e., at $n = \rho_\infty/\rho_0 \approx 1$. Experiments, however, show that the universality of the velocity profile is not disturbed even with a considerable change in the density ratio ($0.25 \leq n \leq 4$).

If the parameter of compressibility n differs from unity by not more than a factor of 4, the temperature profiles in the jets are also universal, while for the initial section it is possible to use the linear dependence

$$\frac{T - T_\infty}{T_0 - T_\infty} = \eta_n \quad \text{or} \quad \frac{T_0 - T}{T_0 - T_\infty} = 1 - \eta_n. \quad (7)$$

where η_n is determined in accordance with (6), and the indices on the values of temperature are the same as in (5) on the values of velocity. Dependence (7) is comparable with the experimental data on Fig. 7.6.

In the cross sections of the principal section the following dependence of excess temperature on the excess velocity is valid:

$$\frac{T - T_\infty}{T_0 - T_\infty} = \left(\frac{u - u_\infty}{u_0 - u_\infty} \right)^{Pr_0}. \quad (8)$$

Here Pr_T is Prandtl's "turbulent" number, proportional to the ratio of heat emitted as a result of eddy viscosity to heat removed by turbulent mixing.

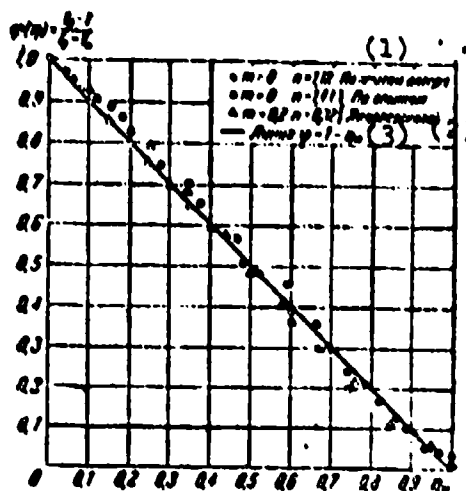


Fig. 7.6. Temperature profile in boundary layer of jet.
KEY: (1) According to author's experiments; (2) According to experiments of Yakovlevskiy; (3) Line.

Experiments carried out for $n = 0.03-300$ show that for axially symmetrical jets it is possible to take $Pr_T = 0.8$, and for flat jets $Pr_T = 0.5$.

Comparison of the temperature profile (8) in the principal section with the experimental data is demonstrated on Fig. 7.7.

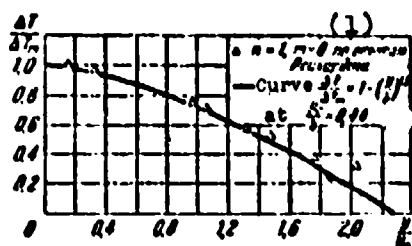


Fig. 7.7. Profile of excess temperature in the principal section of a flat jet ($Pr = 0.5$).
KEY: (1) According to Reichardt's experiments.

According to the experimental data of B. A. Zhestkov, M. M. Maximov, et al. dependences (7) and (8) are valid also for jets with high initial discharge velocity ($M_0 > 1$). However, in this case instead of the thermodynamic temperatures these dependences should include the stagnation temperatures.

The distribution of admixture in the cross sections of a turbulent jet, if the admixture concentration is not too great, in order to influence substantially the density field obeys the same law as the distribution of temperature:

$$\frac{T - T_a}{T_m - T_a} = \frac{r - r_a}{r_m - r_a}. \quad (8a)$$

Here $\alpha = \frac{G_a}{G + G_a}$ is the weight concentration of admixture, which is the ratio of the weight of admixture to the weight of the entire mixture in the same volume.

The validity of equality (8a) is confirmed by numerous experimental data

Let us examine the expansion of the boundaries of a turbulent jet. Let us assume that the rate of buildup of the boundary layer thickness is proportional to the pulsation component of the transverse velocity

$$\frac{db}{dt} \sim v.$$

which in turn, is proportional to the transverse gradient of the longitudinal (main) flow velocity:

$$v \sim l \frac{du}{dy}.$$

Here l is the turbulent mixing path.

In view of the similarity of the velocity profiles in different sections of the boundary layer, the transverse gradient of

longitudinal velocity is proportional to the difference in the velocities on the boundaries

$$\frac{dn}{dy} \sim \frac{n_1 - n_2}{\delta}.$$

Because of this we have

$$v' \sim \frac{l}{\delta} (n_1 - n_2).$$

From the similarity of profiles it follows also that the ratio of characteristic linear dimensions is a constant value

$$\frac{l}{\delta} = \text{const},$$

therefore the pulsation component of transverse velocity is proportional to the difference in the velocities on the boundaries of the layer

$$v' \sim (n_1 - n_2).$$

Since, by hypothesis,

$$v' \sim \frac{db}{dt} = \frac{db}{dx} \frac{dx}{dt} = \frac{db}{dx} v.$$

the law governing build-up of boundary layer thickness along the length of the jet can be presented in the following form:

$$\frac{db}{dx} \sim \frac{|v'|}{u} \sim \frac{|n_1 - n_2|}{|n|}. \quad (9)$$

The quantity $\epsilon = |v'|/|u|$, called the turbulence level of a flow, is always positive, since it is calculated from the mean absolute values of transverse pulsation velocity $|v'|$ and the longitudinal flow velocity $|u|$, which means that in all cases $db/dx > 0$. It remains to explain which value of forward velocity should be substituted into the denominator of expression (9).

The characteristic value of average speed can be determined by different methods. Averaging, however, should be over the depth (and not the cross-sectional area) of the jet; this follows from the experimental fact that the laws governing build-up of thickness in flat and axially symmetrical jets are approximately identical. Judging from the experimental data, it is advantageous to use the value of mean mass flow rate:

$$u = \frac{\int_1^2 \rho u dy}{\int_1^2 \rho dy} \quad (10)$$

which in the case of a noncompressible fluid is close to the arithmetic mean¹ of its absolute values on the boundaries of the layer:

$$u = \frac{\int_1^2 u dy}{b} \approx 0.5 (|u_1| + |u_2|) \quad (11)$$

In that case we will obtain the following law governing increase in boundary layer thickness:

$$\frac{db}{dx} \sim \frac{|u_1 - u_2|}{|u_1| + |u_2|} \quad (12)$$

Expression (12) leads to interesting conclusions. In the boundary layer which appears on the edge of two boundless jets ($u_1 = \text{const}$, $u_2 = \text{const}$) the thickness is proportional to the distance from the beginning of the displacement

$$\frac{db}{dx} = \text{const}, \quad \text{or} \quad b = \text{const} \cdot x,$$

¹For velocity profile (3).

where

$$\text{const} = c \frac{|u_1 - u_2|}{|u_1| + |u_2|}. \quad (13)$$

The value of the coefficient c should be determined experimentally, for example by the results of study of a jet spreading in a motionless medium ($u_2 = 0$), when the following equality holds:

$$b_s = cx. \quad (14)$$

In general ($u_2 \neq 0$) the boundary layer thickness is found on the basis of (12), (13) and (14):

$$\frac{b}{b_s} = \frac{|u_1 - u_2|}{|u_1| + |u_2|}. \quad (15)$$

In the particular case of cocurrent motion of two boundless jets the velocities on the boundaries of the layer have identical signs, as a consequence of which the angle of the boundary layer growth decreases with an increase of the speed of cocurrent flow u_2 :

$$\frac{b}{b_s} = \pm \frac{u_1 - u_2}{u_1 + u_2}. \quad (16)$$

whereupon the minus sign is taken with $u_2 < u_1$.

During the spreading of a jet in a counterflow the speeds on the boundaries of the layer have different signs, i.e., the geometric difference in the speeds is equal to the sum of their absolute values, therefore

$$\frac{b}{b_s} = \frac{u_1 + u_2}{u_1 + u_2} = 1. \quad (17)$$

In other words, during the counter movement of the jets ($u_2 < 0$) the angle of the boundary layer growth does not depend on the relationship of velocities on the boundaries, i.e., the same as with the spreading of a jet in a motionless medium is obtained in all cases.

Figure 7.8 depicts the calculated curve which corresponds to formula (15) for the intervals of m from -1 to 0 and from 0 to $+1$:

$$\frac{\frac{1}{c} \frac{db}{dx}}{\frac{1}{c_0} \frac{db_0}{dx}} = 1 \quad \text{when } m \leq 0,$$

$$\frac{\frac{1}{c} \frac{db}{dx}}{\frac{1}{c_0} \frac{db_0}{dx}} = \frac{1-m}{1+m} \quad \text{when } m \geq 0.$$

In view of the complexity of determining from experiments the true value of b , the distance Δy_b between points with values of excess velocity $\Delta u_1 = 0.9\Delta u_0$ and $\Delta u_2 = 0.1\Delta u_0$ was used here as the boundary layer thickness. With a universal velocity profile the quantity Δy_b is in all cases just the very same fraction of the boundary layer thickness

$$\frac{\Delta y_b}{\Delta y_{b_0}} = \frac{b}{b_0}.$$

where b_0 - boundary layer thickness of submerged jet, Δy_{b_0} - value Δy_b for the submerged jet.

For comparison Fig. 7.8 gives the experimental points which at the same value of the experimental constant ($c = c_3$) lie close to the calculated curve in the range $-0.4 \leq m \leq 0.4$ but move away from it when $m > 0.5$. This result, observed also in shadow photographs of a jet, can be explained by the following.

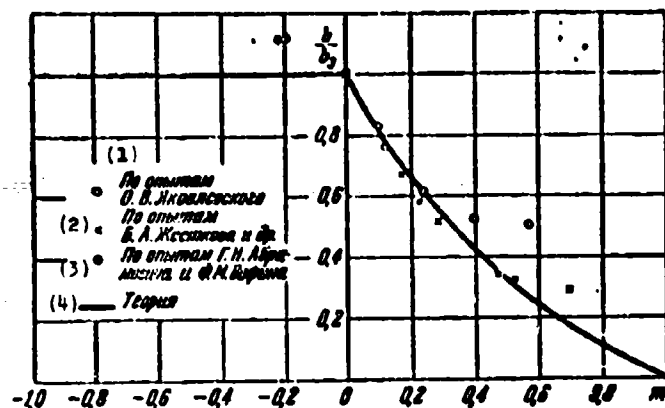


Fig. 7.8. Dependence of boundary layer thickness of a jet of noncompressible fluid on the speed of the external flow. KEY: (1) According to O. V. Yakovlevskiy's experiments; (2) According to the experiments of B. A. Zhestkov, et al.; (3) According to the experiments of G. N. Abramovich and F. M. Vafin; (4) Theory.

During the derivation of formula (12), we assumed that turbulence in the boundary layer gives rise to only a difference in the velocities on the boundaries, and outside the boundaries is completely absent, i.e., $v' \rightarrow 0$ when $m \rightarrow 1$. In actuality even in the "undisturbed" flow there is a certain initial turbulence, therefore when u_1 and u_2 are close to each other, i.e., the intensity of turbulence arising in the jet is less than the initial intensity of turbulence of undisturbed flow, the effect of the first ceases and the mixing is determined by the turbulence of undisturbed flow, which does not depend on the value of m . It is natural that in this area the angle of the boundary layer growth is barely connected with the relationship of velocities on the boundaries of the layer.

The results obtained for the zone of mixing of two boundless jets are valid also for the initial section of a jet of finite thickness spreading in cocurrent or counterflow, since in the initial section on both boundaries of the mixing zone the velocities remain constant.

The contours of the principal section of a jet of finite thickness during counter movement to the fluid encircling the jet, in view of the fact that the velocity of the counter movement does not affect the angle of thickening of mixing zone, remain approximately the same as in the submerged jet.

A more complex problem is determining the contours of the principal section of a jet in a cocurrent flow of fluid. In this case formula (12) acquires the following form

$$\frac{db}{dx} = \pm c \frac{u_m - u_n}{u_m + u_n} \quad (18)$$

where u_m - velocity on the axis of the principal section of the jet, u_n - speed of cocurrent flow (minus sign is taken when $u_n > u_m$). In connection with the fact that u_m changes on the axis of the jet, i.e., $u_m = u_m(x)$, the jet boundary in cocurrent flow should be curvilinear

$$\frac{db}{dx} = \text{var.}$$

To determine it, it is necessary to know the form of dependence $u_m(x)$, which can be obtained from the condition of conservation of momentum; the solution to this problem is given below.

In formulas (12)-(18) expression (11) is used for average speed, valid in the case of a noncompressible fluid. For values of $n = \rho_n/\rho_0$ differing significantly from unity it is necessary to consider the compressibility effect, for which in the denominators of formulas (12)-(18) the sum $(u_m + u_n)$ is replaced by $2|u|$, which can be determined from dependence (10). Then (18) takes the following form:

$$\pm c \frac{dx}{db} = \frac{2|u|}{u_m - u_n} = \frac{2 \int_0^b r^n dy}{\int_0^b r dy} \quad (19)$$

The excess speed ($\Delta u_m = u_m - u_H$) and the excess temperature ($\Delta T_m = T_m - T_H$) along the length of the principal section of a jet rapidly change, in connection with which the strong compressibility effect of gas on the form of the jet boundary is exhibited only in the transition section and the initial part of the principal section of the jet.

On almost the entire length of the principal section, as shown by experiments on supersonic and strongly heated subsonic jets, the jet boundary is weakly bent, and therefore instead of complex dependence (10) for average speed it is possible to utilize the simplified expression

$$u = \frac{\rho_m u_m + \rho_n u_n}{\rho_m + \rho_n}.$$

In this case instead of (19) we have

$$\pm c \frac{dx}{db} = \frac{2}{u_m - u_n} \frac{u_m + u_n}{1 + \frac{\rho_n}{\rho_m}}. \quad (20)$$

With the aid of the equation of state the density ratio in an isobaric jet is replaced by the temperature ratio

$$\frac{\rho_m}{\rho_n} = \frac{T_n}{T_m}. \quad (21)$$

Based on numerous experiments we take values of coefficient c in (19) for the initial section $c = 0.27$ and for the principal section $c = 0.22$.

§ 2. Change in the Parameters Along the Length of a Jet

In seeking laws governing a change in velocity, temperature and admixture concentration along the length of a turbulent gas

jet or a liquid jet, and also for determining the jet boundaries it is possible to use the conditions of conservation of momentum, enthalpy and mass of admixture, and also the law governing build-up of thickness of the jet (20), which we write in the following form:

$$\pm c \frac{dx}{db} = \frac{2m}{1-m} \frac{1}{\Delta u_m} + \frac{1}{1 + \frac{\theta-1}{2} \Delta \bar{T}_m}. \quad (22)$$

where

$$m = \frac{u_a}{u_{0m}}, \quad \theta = \frac{T_{0m}}{T_a}, \quad \Delta u_m = \frac{u_m - u_a}{u_{0m} - u_a}, \quad \Delta \bar{T}_m = \frac{T_m - T_a}{T_{0m} - T_a},$$

while u_{0m} , T_{0m} are the values of velocity and temperature on the axis of the initial jet cross-sectional area.

From comparison of the first and second terms in the right side of equation (22) it follows that when $m \neq 0$ the first term increasing without limit with a decrease in the axial velocity, usually exceeds in value the second term (which in this case approaches unity), and thus it is determining. Consequently, also for the case of a nonisothermal jet in cocurrent flow it is possible in the first approximation to use the same law governing increase of jet thickness, or as it is occasionally referred to as, the equation of propagation, which also holds for an isothermal jet, namely:

$$c \frac{dx}{db} = 1 + \frac{2m}{1-m} \frac{1}{\Delta u_m}. \quad (22a)$$

The most relieving effect of parameter θ on the characteristics of a jet is exhibited in the case of a submerged nonisothermal jet ($u_m = 0$), for which the equation of propagation will be written as (the second term of the right side of equality is retained (22)):

$$c \frac{dx}{db} = \frac{2}{1 + \frac{\theta}{2}} = \frac{1}{1 + \frac{\theta-1}{2} \frac{1}{k, s_m}}. \quad (22b)$$

This equation is correct both for a plane and for an axially symmetrical jet; in the latter case it is necessary only to replace half-thickness b by the radius of the jet r .

To establish from equation (22) the form of function $b(x)$ it is necessary to know the law of velocity change along the axis of the jet $\Delta u_m(x)$, which can be found with the equation of conservation of momentum. For an isobaric jet this equation takes the following form:

$$\int_0^M (u - u_m) dM = \int_0^{M_0} (u_0 - u_m) dM. \quad (23)$$

Here M - mass flow per second of gas (or liquid), flowing through an arbitrary transverse jet cross-sectional area; M_0 - same in the initial jet cross-sectional area, $dM = \rho u dF$ - mass flow per second of a stream filament in an arbitrary cross section. From equation (23) we obtain

$$\begin{aligned} \left(\frac{\Delta u_m}{\Delta u_{0m}} \right)^2 \int_0^1 \frac{\rho}{\rho_m} \frac{\Delta u}{\Delta u_m} \frac{u}{\Delta u_m} \frac{dF}{F} = \\ = \frac{F_0}{F} \left(\frac{u_{0m}}{\Delta u_{0m}} \right)^2 \left[\int_0^1 \frac{\rho_0 u_0}{\rho_m u_{0m}} \frac{dF_0}{F_0} - \frac{u_m}{u_{0m}} \int_0^1 \frac{\rho_0 u_0}{\rho_m u_{0m}} \frac{dF_0}{F_0} \right]. \end{aligned}$$

Utilizing the above designations

$$m = \frac{u_m}{u_{0m}}, \quad \frac{u_{0m}}{\Delta u_{0m}} = \frac{1}{1-m},$$

application of which is convenient with a uniform velocity field of external flow and nonuniform initial velocity field in the jet (here u_{0m} is the velocity on the axis of the jet in the initial cross section, $\Delta u_{0m} = u_{0m} - u_m$), and also the values

$$A_1 = \int_0^1 \frac{\rho}{\rho_{0m}} \frac{\Delta u}{\Delta u_m} \frac{dF}{F}, \quad A_2 = \int_0^1 \frac{\rho}{\rho_{0m}} \left(\frac{\Delta u}{\Delta u_m} \right)^2 \frac{dF}{F}, \quad (24)$$

$$n_{1u} = \int_0^1 \frac{\rho_0 u_0}{\rho_{0m} u_{0m}} \frac{dF_0}{F_0}, \quad n_{2u} = \int_0^1 \frac{\rho_0 u_0^2}{\rho_{0m} u_{0m}^2} \frac{dF_0}{F_0}, \quad (25)$$

$$\Delta n_m = \frac{\Delta u_m}{\Delta u_{0m}}, \quad (26)$$

we come to the following equation, which expresses the law of conservation of momentum in the jet:

$$\Delta u_m A_2 (1-m) + \Delta u_m A_1 m = \frac{F_0}{F} \frac{u_{0u}}{1-m}. \quad (27)$$

We will hence obtain the dependence of the velocity on the axis of the principal section of the jet on the relative cross-sectional area

$$\Delta n_m = \frac{\sqrt{m^2 A_1^2 + 4 \frac{F_0}{F} A_2 (n_{2u} - m n_{1u})} - m A_1}{2 A_2 (1-m)}.$$

or

$$\Delta n_m = \frac{m A_1}{2(1-m) A_2} \left(\sqrt{1 + p^2 \frac{F_0}{F}} - 1 \right), \quad (28)$$

where the parameter

$$p^2 = \frac{4(n_{2u} - m n_{1u})}{m^2 A_1^2}. \quad (29)$$

With uniform velocity and density fields in the initial jet cross-sectional area ($u_0 = u_{0m} = \text{const}$, $\rho_0 = \rho_{0m} = \text{const}$) $n_{1u} = 0$, $n_{2u} = 1$, in connection with which the right side of expression (27) is substantially simplified.

Let us compose now the equation of conservation of excess enthalpy for nonuniform velocity and temperature fields in the initial jet cross-sectional area

$$\int_0^M c_p (T - T_u) dM = \int_0^{M_0} c_{p0} (T_0 - T_u) dM \quad (30)$$

or in dimensionless form

$$(1-m) \frac{\Delta T_m}{\Delta T_{0m}} \frac{\Delta u_m}{\Delta u_{0m}} \int_0^1 \frac{c_p}{c_{p0m}} \frac{\rho}{\rho_{0m}} \frac{\Delta u}{\Delta u_m} \frac{\Delta T}{\Delta T_m} \frac{dP}{P} + \\ + m \frac{\Delta T_m}{\Delta T_{0m}} \int_0^1 \frac{c_p}{c_{p0m}} \frac{\rho}{\rho_{0m}} \frac{\Delta T}{\Delta T_m} \frac{dP}{P} = \frac{P_0}{P} \int_0^1 \frac{c_{p0}}{c_{p0m}} \frac{\rho_0}{\rho_{0m}} \frac{\Delta T_0}{\Delta T_{0m}} \frac{u_0}{u_{0m}} \frac{dP_0}{P_0}.$$

Introducing the designations

$$B_1 = \int_0^1 \frac{\rho}{\rho_{0m}} \frac{c_p}{c_{p0m}} \frac{\Delta T}{\Delta T_m} \frac{dP}{P}, \quad (31)$$

$$B_2 = \int_0^1 \frac{\rho}{\rho_{0m}} \frac{c_p}{c_{p0m}} \frac{\Delta u}{\Delta u_m} \frac{\Delta T}{\Delta T_m} \frac{dP}{P}, \quad (32)$$

$$n_r = \int_0^1 \frac{\rho_0}{\rho_{0m}} \frac{c_{p0}}{c_{p0m}} \frac{u_0}{u_{0m}} \frac{\Delta T_0}{\Delta T_{0m}} \frac{dP_0}{P_0}, \quad (33)$$

$$\Delta f_m = \frac{\Delta T_m}{\Delta T_{0m}}, \quad (34)$$

we bring the equation of conservation of excess enthalpy to the following form:

$$\Delta u_m \Delta T_m B_2 (1-m) - \Delta T_m B_1 m = \frac{P_0}{P} n_r. \quad (35)$$

If gas jets are mixed with uniform velocity, density and temperature fields in the initial cross section, then $n_r = 1$. After dividing the left and right sides of equation (27) by the corresponding parts of equation (35), it is possible to establish

the connection between dimensionless excess values of temperature and velocity on the axis of the principal section of the jet:

$$\Delta T_m = k_r \Delta u_m, \quad (36)$$

where

$$k_r = \frac{n_r(1-m) \Delta u_m \cdot \frac{1}{u_m} (1-m) + A_{1,m}}{n_{2u} - m n_{1u} \Delta u_m u_m (1-m) + u_{1,m}}. \quad (37)$$

In the case of a submerged jet ($\Delta u_m = u_m$, $m = 0$) with uniform initial velocity and temperature fields ($n_{1u} = n_{2u} = n_r = 1$)

$$k_{s,r} = \frac{\Delta T_m}{u_m} = \frac{A_1}{u_1} = \text{const}, \quad (38)$$

where

$$a_m = n_m / n_0 \quad (39)$$

In the case of mixing of jets of identical velocity ($m = 1$) with the uniform initial fields

$$k_{s,r} = \frac{A_1}{B_1} = \text{const}. \quad (40)$$

During the mixing of jets of different gases (or liquids) the density distribution depends also on the field of concentrations of each of the gases (or liquids) composing the mixture. The field of dimensionless excess concentration of any of the cases in the transverse jet cross-sectional area is subordinated to dependence (8a). The distribution of excess admixture concentration along the axis of the jet is established with the aid of the equation of conservation of excess admixture in the jet

$$\int_0^M (x - x_n) dM = \int_0^{M_0} (x_0 - x_n) dM_0 \quad (41)$$

which, after bringing to dimensionless form, can be presented thus:

$$\begin{aligned} (1-m) \frac{\Delta x_n}{\Delta x_{om}} \frac{\Delta u_m}{\Delta u_{om}} \int_0^1 \frac{\rho}{\rho_{om}} \frac{\Delta u}{\Delta u_m} \frac{\Delta x}{\Delta x_m} \frac{dP}{P} + \\ + m \frac{\Delta x_n}{\Delta x_{om}} \int_0^1 \frac{\rho}{\rho_{om}} \frac{\Delta x}{\Delta x_m} \frac{dP}{P} = F_0 \int_0^1 \frac{\rho}{\rho_{om}} \frac{u_0}{u_{om}} \frac{\Delta x_0}{\Delta x_{om}} \frac{dP_0}{P_0}. \end{aligned} \quad (42)$$

Let us designate

$$D_1 = \int_0^1 \frac{\rho}{\rho_{om}} \frac{\Delta u}{\Delta u_m} \frac{dP}{P}, \quad (43)$$

$$D_2 = \int_0^1 \frac{\rho}{\rho_{om}} \frac{\Delta u}{\Delta u_m} \frac{\Delta x}{\Delta x_m} \frac{dP}{P}, \quad (44)$$

$$n_0 = \int_0^1 \frac{\rho_0}{\rho_{om}} \frac{u_0}{u_{om}} \frac{\Delta x_0}{\Delta x_{om}} \frac{dP_0}{P_0}, \quad (45)$$

$$\Delta x_m = \frac{\Delta x_{om}}{\Delta x_{om}}. \quad (46)$$

Then the equation of conservation of excess impurity content will be written thus:

$$\Delta x_m \Delta u_m D_1 (1-m) + \Delta x_m D_2 m = \frac{F_0}{P} n_0. \quad (47)$$

After dividing the left and right sides of equation (27) by the corresponding parts of equation (47), we establish the connection between the admixture concentration and the velocity on the axis of the jet:

$$\Delta x_m = k \cdot \Delta u_m. \quad (48)$$

where

$$k_1 = \frac{n_1(1-m)}{n_{1u} - mn_{1u}} \frac{\Delta u_m A_1(1-m) + A_{1m}}{\Delta u_m D_1(1-m) + D_{1m}}. \quad (49)$$

In the case of a submerged jet ($m = 0$) with uniform initial velocity fields and admixture concentration ($n_{2u} = n_x = 1$)

$$k_{11} = \frac{\Delta \bar{u}_m}{n_m} = \frac{A_1}{D_1} = \text{const.} \quad (50)$$

In the case of the mixing of jets of identical velocity ($m = 1$) with uniform initial fields, we have

$$k_{11} = \frac{A_1}{D_1} = \text{const.} \quad (51)$$

Solving jointly equations (20), (27), (35) and (47), it is possible to find the dependences of change in thickness of jet, and also the velocity, temperature and admixture concentration along the axis of the principal section of the jet. To calculate the coefficients of initial nonuniformity n_{1u} , n_{2u} , n_T , n_x it is necessary to know the fields of velocity density, temperature and other parameters of liquid (or gas) in the initial jet cross-sectional area. Utilizing the fields of velocity (3), temperature (8) and admixture concentration (8a) in the cross sections of the principal section, it is possible to calculate the definite integrals A_1 , A_2 , B_1 , B_2 , D_1 and D_2 which are the coefficients of equations (27), (35) and (37).

For the uniform velocity, temperature and admixture concentration fields, in the initial jet cross-sectional area the family of curves which describe change in relative excess velocity Δu_m (and also temperature ΔT_m and concentration $\Delta \bar{x}_m$) in the dimensionless length of the jet¹ $\bar{x} = (x/b_0)$, has a parameter

¹ b_0 - half-width of the initial cross section of flat jet (or the initial radius of an axially symmetrical jet).

the quantity $m = u_w/u_0$ at $n = \rho_w/\rho_0 = \text{const}$ or n at $m = \text{const}$. With a decrease in m and increase of n the "attenuation" of the jet is accelerated.

The initial flow nonuniformity substantially distorts the effect of parameter m on the dependence $\Delta \bar{u}_m(\bar{x})$. With considerable initial nonuniformity (for example, during discharge from a long cylindrical pipe) the effect of m ceases to be detected. This can be judged from the experimental data for a subsonic jet (Fig. 7.9) and for a supersonic jet with $M_0 = 3$ (Fig. 7.10). The degree of preheating of jets θ in these experiments¹ was approximately identical (respectively $\theta = 1.85$ and $\theta = 2$).

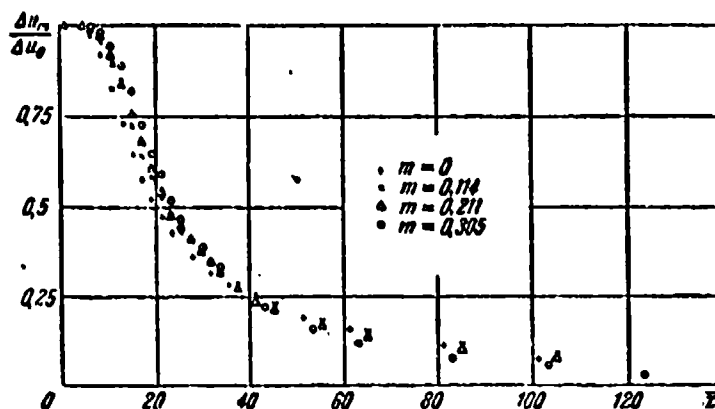


Fig. 7.9. Excess axial velocity in non-isothermal ($\theta = 1.85$) axisymmetric gas jet spreading in cocurrent flow ($m = \text{var}$); experimental data of O. V. Yakovlevskiy and V. K. Pechenkin.

¹For supersonic jets θ is understood as ratio of stagnation temperatures in the initial jet cross-sectional area and in the surrounding medium.

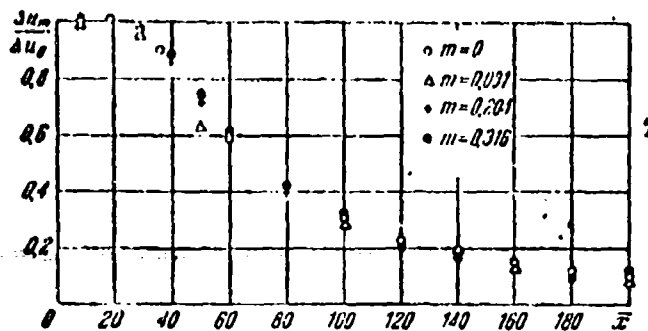


Fig. 7.10. Excess axial velocity in supersonic axisymmetric gas jet ($M_0 = 3$) spreading in cocurrent flow ($m = \text{var}$); experimental data of B. A. Zhestkov, et al.

Calculations and experiments show that conversion factors k_1 and k_2 , determined by equalities (37) and (49), barely change along the length of the jet and do not depend on the parameter of compressibility n .

Thus, if dependence $\Delta \bar{u}_m(\bar{x})$ is established, then it is easy to pass from it with the aid of (36), (37), (48) and (49) to dependences $\Delta \bar{T}_m(\bar{x})$ and $\Delta \bar{\kappa}_m(\bar{x})$; for this it is necessary to know, however, the variation factors in the initial jet cross-sectional area n_{1u} , n_{2u} , n_r and n_k .

If in (37) we disregard the effect of Δu_m in comparison with u , then for the case of uniform initial fields ($n_{1u} = n_{2u} = n_r = n_k = 1$) we will obtain the following approximate dependences:

for flat jet

$$k_1 = k_2 = 0.86 \frac{1 + 1.84m}{1 + 2.26m} \quad (52)$$

and for axially symmetrical jet

$$k_1 = k_2 = 0.745 \frac{1 + 2.86m}{1 + 3.76m} \quad (53)$$

More detailed presentation of the theory of a jet in a flow can be found in the author's monograph, references to which are given above.

§ 3. Subsonic Nonisothermal Jet of Simple Gas

Let us examine a subsonic jet of gas which is spreading in quiescent gas of the same composition. In this case ($r = 0$) the equation of momentum (27) is simplified and assumes the form

$$u_m^2 = \frac{F_0}{F} \frac{a_{2u}}{A_2}. \quad (54)$$

Here $\bar{u}_m = u_m/u_0$ - ratio of velocity on the axis in current jet cross-sectional area to velocity on the axis of the initial cross section, F - area of current cross section, F_0 area of the initial cross section.

The coefficients A_2 and n_{2u} are determined from (24) and (25) with the aid of dependences (3), (8), (21) and (36). To calculate A_2 it is possible also to make use of the following approximate dependences, which when $0.2 \leq \theta \leq 5$ and $Pr_\gamma = 0.5$ give an error of not more than 3%:

in the case of a flat jet:

$$A_2 = \frac{0.316\theta}{1 + 0.38\theta(\theta - 1)k_1 a_m}, \quad (55)$$

in the case of an axially symmetrical jet

$$A_2 = \frac{0.134\theta}{1 + 0.745(\theta - 1)k_1 a_m}. \quad (56)$$

From (54) on the basis of (55) and (56) we have for a flat submerged jet ($m = 0$)

$$\frac{0,316 n_m^2 \theta}{1 + 0,86 (\theta - 1) k_1 n_m} = \frac{n_{zg}}{\dot{b}}, \quad (57)$$

where according to (37)

$$k_1 = 0,86 \frac{n_1}{n_{zg}}, \quad (58)$$

and for the axially symmetrical jet

$$\frac{0,134 n_m^2 \theta}{1 + 0,745 (\theta - 1) k_1 n_m} = \frac{n_{zg}}{r^2}, \quad (59)$$

where

$$k_1 = 0,745 \frac{n_1}{n_{zg}}. \quad (60)$$

In these formulas for the ratios of the instantaneous value of half-thickness b or radius r of a jet to their values in the initial cross section (b_0, r_0) we introduce the designation

$$\dot{b} = \frac{b}{b_0}, \quad r = \frac{r}{r_0}.$$

Expressions similar to equalities (55)-(60) are obtained also for the case of very great preheating ($\theta \rightarrow \infty$), but we will not deal with this here.

Let us find now the velocity change along the length of the jet. Dividing variables in equation (22b) and integrating by parts (taking into account boundary condition $\bar{x} = \bar{x}_n^{-1}$, $\bar{b} = \bar{b}_n$, $\bar{u}_m = 1$), we have

\bar{x}_n - relative distance from the beginning of jet to the beginning of the principal section.

$$c(x - x_0) = \frac{b}{1 + \frac{\theta-1}{2} k_1 n_m} + \int_1^x \frac{\frac{\theta-1}{2} k_1 b d n_m}{(1 + \frac{\theta-1}{2} k_1 n_m)^2}.$$

Substituting here \bar{b} and k_1 from equation (57) and (58), after integration we will obtain for a flat nonisothermal jet

$$c(x - x_0) = \frac{n_m}{0.3115} \left[\frac{P(z)}{u_m} - P(z_0) \right], \quad (61)$$

where

$$z = \frac{\theta-1}{2} k_1 n_m, \quad z_0 = \frac{\theta-1}{2} k_1 n_{m0},$$

$$P(z) = 1 - 0.28z - 1.72z^2 + 0.28z^3 \ln \left| 1 + \frac{1}{z} \right|. \quad (62)$$

The graph of the $P(z)$ dependence is depicted on Fig. 7.11. As a result of the fact that $P(z) = 1$, formula (61) at $\theta = 1$ passes to the relationship for an isothermal submerged jet

$$c(x - x_0) = 3.16 n_m \left[\frac{1}{u_m} - 1 \right]. \quad (63)$$

After determining $u_m(x)$ from (61), it is not difficult to find from (36) the $\Delta T_m(x)$ dependence for change in axial temperature, and from (57) the thickness of the jet in an arbitrary cross section.

The results of calculations of the axial velocity and thickness of a jet according to formulas (61) and (57) with the different values of the parameter θ and uniform velocity and temperature profile in the initial jet cross-sectional area ($n_{2u} = n_r = 1$) are represented on Figs. 7.12 and 7.13. From examination of these figures it follows that the characteristics of propagation of nonisothermal and isothermal jets are substantially different. The heated jet washes out considerably

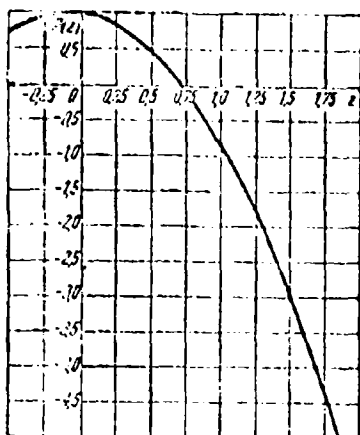


Fig. 7.11. Auxiliary function $P(z)$.

faster than the cooled: at a fixed distance from the nozzle it is thicker, but the velocity on its axis is less. It is interesting to note that bending of the jet boundaries at $\theta = 1$ is noticeable only at close distances from nozzle; in the examination of distant sections of a jet flow its boundaries can be considered virtually rectilinear, and the flare angle of the jet (or the coefficient of angular expansion) as weakly depending on the value of parameter θ . Figures 7.12 and 7.13 give the change of axial velocity and thickness of the jet depending on coordinate \bar{x} , calculated from the nozzle edge, from which the jet discharges, while in the above formulas the reference point coincides with the transition section of the jet ($\bar{x} = \bar{x}_n$). The quantity \bar{x}_n is determined by the configuration of the initial section of the jet, which is considered below.

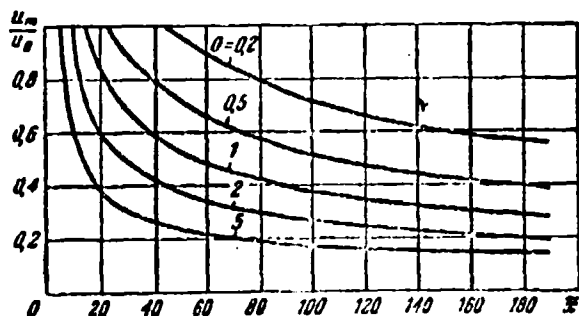


Fig. 7.12. Change of axial velocity in submerged nonisothermal plane-parallel gas jets (effect of parameter θ).

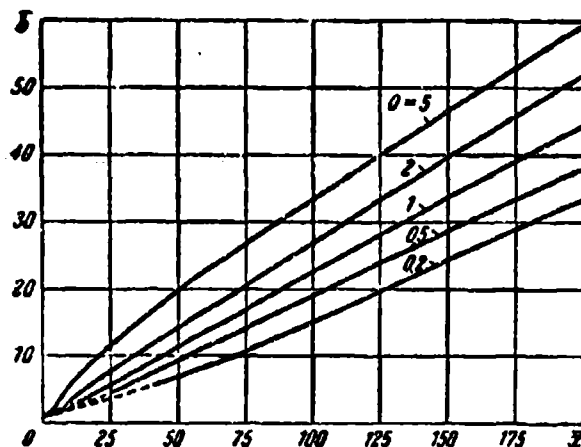


Fig. 7.13. Build-up of thickness in submerged nonisothermal plane-parallel gas jet (effect of parameter θ).

Integrating equations (22b) as applied to the case of an axially symmetrical jet, we obtain, taking into account boundary condition $\bar{x} = \bar{x}_n$, $\bar{r} = \bar{r}_n$, $\bar{u}_m = 1$:

$$c(x - x_n) = \frac{r}{1 + \frac{\theta-1}{2} k_r u_m} + \int_{\bar{r}_n}^{\bar{r}} \frac{\frac{\theta-1}{2} k_r r d\bar{r}}{\left(1 + \frac{\theta-1}{2} k_r u_m\right)^2}.$$

After substituting here for \bar{r} its expression in \bar{u}_m , according to formula (59) and after replacing k_r on the basis of (60), after integration let us find in implicit form the law of change in the axial velocity along the length of an axisymmetric non-isothermic jet

$$c(x - x_n) = \sqrt{\frac{n_{\infty}}{0.1346}} \left[\frac{R(x)}{n_m} - R(x_n) \right]. \quad (64)$$

Here

$$x = \frac{\theta-1}{2} k_r a_m, \quad x_n = \frac{\theta-1}{2} k_r a_n, \quad (65)$$

$$R(x) = \sqrt{1 + 1.40x} - 0.73x \operatorname{arctg}(1.47 \sqrt{1 + 1.40x}) - x \ln \left(\frac{1 + \sqrt{1 + 1.40x}}{1 - \sqrt{1 + 1.40x}} \right).$$

Auxiliary function $R(z)$ is depicted on Fig. 7.14. Let us note that formula (64) at $\theta = 1$ passes to the corresponding relationship for an isothermal axially symmetrical jet

$$\begin{aligned} c(x - x_n) &= \\ &= 2.73 \sqrt{n_{2u}} \left[\frac{1}{n_m} - 1 \right]. \end{aligned} \quad (66)$$

Knowing $u_m(x)$, it is possible to determine by formulas (36) and (59) the temperature on the axis of the jet and the radius of the jet in an arbitrary cross section.

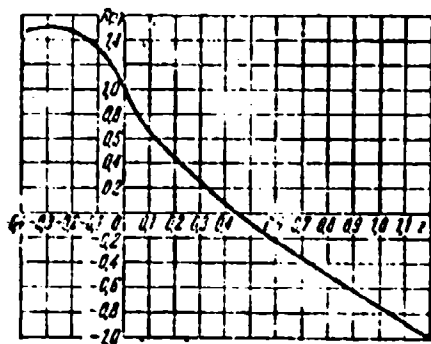


Fig. 7.14. Auxiliary function $R(z)$.

To illustrate the obtained results Figs. 7.15 and 7.16 depict the curve of axial velocity change, relative radius of an axially symmetrical jet with uniform initial velocity and temperature profile ($n_{2u} = n_r = 1$) at different values of parameter θ . As in the case of a flat jet, the velocity on the axis of a heated axially symmetrical jet ($\theta > 1$) attenuates faster than in an isothermal jet, but a cooled jet ($\theta < 1$) possesses considerably greater range¹ than an isothermal jet. Let us note

¹By the range of a jet is meant the distance from the nozzle on which the axial velocity of the jet drops to a determined given value, for example $\bar{u}_m = 0.5$.

that the bending of boundaries of a nonisothermal jet is noticeable only at close distances from the transition section, and appears more strongly the more θ differs from unity. With an increase in the distance from the nozzle of the jet the boundaries become virtually rectilinear, and the angle of inclination of the boundaries to the axis of the jet at $\theta = \text{var}$ approaches a constant value, equal to the slope angle for a jet of noncompressible fluid.

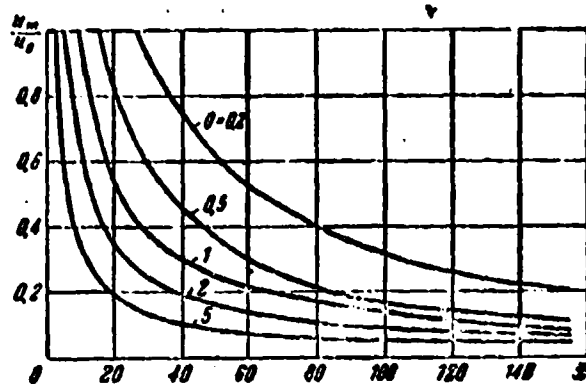


Fig. 7.15. Change of axial velocity in a nonisothermal axisymmetric submerged gas jet (effect of parameter θ).

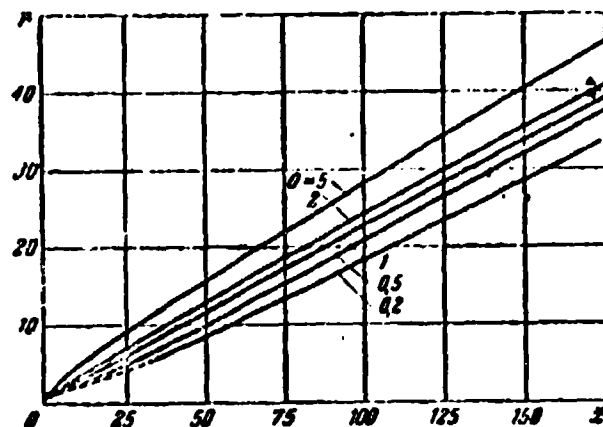


Fig. 7.16. Build-up of thickness of submerged nonisothermal axisymmetric gas jet (effect of parameter θ).

Build-up of thickness of both flat and axisymmetric non-isothermal jet when $\theta \approx 1$ and $m = 0$ occurs according to linear law:

$$\delta = \frac{n_{12}}{0.3163} + c(x - x_0) \quad (67)$$

$$\bar{r} = \sqrt{\frac{n_{12}}{0.1346}} + c(x - x_0) \quad (68)$$

It has already been mentioned that the abscissa of the transition cross section in which the principal section of the jet begins depends on the configuration of the initial section.

The change of the density ratio in the initial jet cross-sectional area and the surrounding medium (ρ_0/ρ_H) leads to a change in the length of the initial section in comparison with the isothermal case; during the propagation of a jet in a more solid medium the core of constant velocity (Fig. 7.1) is shortened, and in a less dense medium it is lengthened. This property of the initial section is explained by the following. Let, for example, a plane parallel air jet with density ρ_0 escape at a velocity of u_0 into a motionless air medium with density ρ_H (Fig. 7.17). Then in the zone of turbulent mixing a certain velocity, temperature and density distribution is established, which is described by dependences (5), (8) and (21).

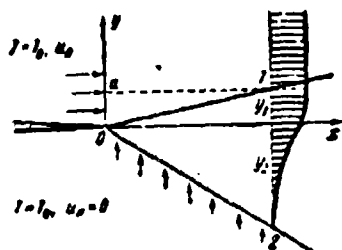


Fig. 7.17. Diagram of boundary layer of non-isothermal jet.

In view of the pressure constancy the per-second momenta at the entrance and exit from the contour, depicted on Fig. 7.17, are identical:

$$\rho u_0 y_1 = \int_{y_1}^{y_2} \rho u^2 dy. \quad (69)$$

Mass is not introduced through dotted line a-1, since the velocity vector u_0 is parallel to this line; through the outer edge of the submerged jet 0-2 air streams flow at right angles to the direction of propagation of the jet, therefore their momentum in projection onto the jet direction is equal to zero.

From (69), taking into account (5), (6), (7) and (21), we have

$$\frac{y_1}{y_1 - y_2} = \frac{y_1}{b} = \theta \int_0^1 \frac{2\tau_m^{1.5} - \tau_m^2}{1 + (\theta - 1)\tau_m^2} d\tau_m = \varphi(\theta). \quad (70)$$

After integration we have

$$\varphi(\theta) = \frac{1}{\theta - 1} - \frac{7}{2(\theta - 1)^2} - \frac{1}{(\theta - 1)^3} + \frac{\ln \theta}{(\theta - 1)^4} - \frac{4 \operatorname{arctg} \sqrt{\theta - 1}}{(\theta - 1)^{2.5}} \quad (71)$$

or, approximately,

$$\varphi(\theta) = \frac{\ln \theta}{\theta - 1} - \frac{0.45}{1 + 0.375(\theta - 1)}. \quad (72)$$

In view of the straightness of edges of the mixing zone in the initial section of the jet the quantity y_1/b is constant and depends only on θ . At the end of the initial section ($x = x_H$) the internal edges of the mixing zone meet ($y_1 = b_0$), therefore the relative length of the initial section ($\pi_H = x_H/b_0$) can be

obtained with the aid of (70) from the condition of similarity of triangles formed by rays 0-1 and 0-2 and by the cross sections parallel to line 1-2:

$$\frac{b}{x_n} = \gamma(\theta) \quad (73)$$

According to (20) the relative thickness of the mixing zone in the initial section of submerged jet

$$\frac{db}{dx} = \frac{b}{x} = 0.5c \left(1 + \frac{b_n}{b_0}\right) = 0.5c(1 + \theta) \quad (74)$$

The length of the initial section of the jet as a function of θ , calculated from formulas (71), (73) and (74), is graphed on Fig. 7.18.

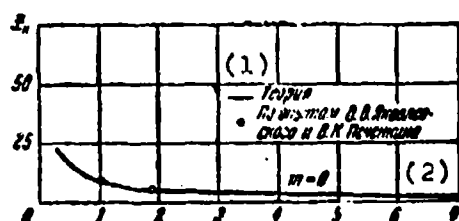


Fig. 7.18. Length of initial section of nonisothermal gas jet as a function of parameter θ . KEY: (1) Theory; (2) According to experiments of O. V. Yakovlevskiy and V. K. Pechenkin.

The abscissa of transition section can be found from (74), if we substitute for b the initial half-thickness of the principal section b_n , which is determined from (67) at $x = x_n$. Figure 7.19 depicts the results of calculations of \bar{x}_n for flat and axially symmetrical jets.

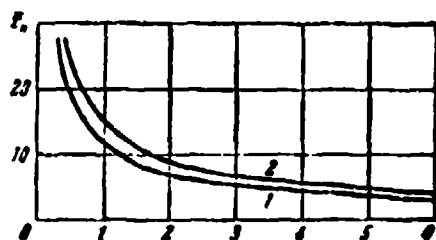


Fig. 7.19. Effect of degree of preheating θ on abscissa of transition section for axisymmetric (1) and flat (2) jets.

These values of \bar{x}_n were used in plotting the curves of $\bar{u}_m(\bar{x})$ and $\bar{b}(\bar{x})$ or $\bar{r}(\bar{x})$ on Figs. 7.12, 7.13, 7.15 and 7.16.

§ 4. Supersonic Isobaric Jet

Let us explain the basic properties of a supersonic jet escaping into a quiescent gas of the same composition, considering pressure in the jet and the surrounding medium to be identical. Let us use for this, as for a subsonic jet, the equation of momentum (54) and the equation of jet propagation (22b).

According to the experimental data of B. A. Zhestkov, et al., in a supersonic jet velocity profiles (3) and (5) are valid and also temperature profiles (7) and (8), if in them instead of stream temperature T we substitute the stagnation temperature T^* . Consequently, in the initial section of a submerged supersonic jet we have

$$\frac{\Delta T^*}{\Delta T_0^*} = \frac{T^* - T_0^*}{T_0^* - T_0^*} = \tau_{m0} \quad (75)$$

$$\frac{u}{u_0} = 1 - f(\eta_{m0}) \quad (76)$$

in the principal section correspondingly

$$\frac{\Delta T^*}{\Delta T_m^*} = \frac{T^* - T_m^*}{T_m^* - T_0^*} = \left(\frac{u}{u_m}\right)^{Pr}, \quad (77)$$

$$\frac{u}{u_m} = f(\eta) \quad (78)$$

where

$$f(\eta) = (1 - \eta^{1/2})^2. \quad (79)$$

In the initial section the ordinate $\eta_{m0} = y/b$ is read from the external boundary, and in the principal section $\eta = (y/b)$ is read from the axis of the jet.

Subsequently we take, as in a nonisothermal jet, $Pr_T = 0.5$. The density ratio is expressed through the stagnation temperatures:

$$\frac{\rho_n}{\rho_m} = \frac{T_m}{T_n} = \frac{T_m - A \frac{u_m^2}{2gc_g}}{T_n} \quad (80)$$

It is here taken into account that in the quiescent gas surrounding the jet the static temperature is equal to the stagnation temperature ($T_n = T_n^*$). Taking into account the equality $AR = c_p - c_v$ and introducing the designations

$$\lambda = \frac{u}{a_g}, \quad \theta^* = \frac{T_n^*}{T_n}, \quad \frac{c_p}{c_v} = \lambda, \quad \frac{\lambda - 1}{\lambda + 1} = a,$$

we present (80) in the following form:

$$\frac{\rho_n}{\rho_m} = \frac{AT_n^*}{3T_n} (\theta^* - 1) + 1 - a\lambda_0^2 \theta^* a_m^2 \quad (81)$$

In the particular case for the initial section ($\Delta T_m^* = \Delta T_0^*$, $\bar{u}_m = 1$)

$$\frac{\rho_n}{\rho_m} = \theta^* (1 - a\lambda_0^2) \quad (82)$$

For an axisymmetric supersonic jet when $\theta^* = 1$ we have

$$\frac{\rho_n}{\rho_m} = 1 - a\lambda_0^2 a_m^2 \quad (83)$$

$$\frac{\rho_n}{\rho_m} = 1 - a\lambda_0^2 \quad (83a)$$

Substituting equality (83) into (24), it is possible to find the value of the coefficient A_2 as a function of the velocity coefficient λ_0 . Since the obtained expression is unwieldy, it is more convenient to use the approximation formula

$$A_2 = 0.134(1 - a\lambda_0^2)[1 + 0.448a\lambda_0^2 a_m^2] \quad (84)$$

After substituting expression (83) into the equation of jet propagation (22b), we will obtain

$$c \frac{dx}{db} = \frac{2}{1 - a^2 \lambda_m^2} \quad (85)$$

or for the initial section ($\bar{u}_m = 1$)

$$c \frac{dx}{db} = \frac{2}{1 - a^2 \lambda^2} \quad (86)$$

From the joint solution of equations (85), (54) and (84) we establish the connection between axial velocity and distance for the principal section of a supersonic jet

$$c(x - x_0) = \sqrt{\frac{a_m}{0.134(1 - a^2 \lambda^2)}} \left[\frac{F(z)}{a_m} - F(z_0) \right] \quad (87)$$

The following designations are introduced

$$z = a_m \sqrt{\frac{a^2 \lambda^2}{2}}, \quad z_0 = \sqrt{\frac{a^2 \lambda^2}{2}}$$

and

$$F(z) = \frac{1}{(1 - z^2) \sqrt{1 + 0.9z^2}} - \frac{0.53z^2 \sqrt{1 + 0.9z^2}}{1 - z^2} - 1.07z \ln \frac{\sqrt{1 + 0.9z^2} + 1.39z}{\sqrt{1 - z^2}} \quad (88)$$

Function $F(z)$, calculated from equation (88), is depicted on Fig. 7.20.

As $\lambda_0 \rightarrow 0$ we have $z \rightarrow 0$ and $F(z) \rightarrow 1$, therefore formula (87) passes to relationship (66), obtained for a jet of non-compressible fluid. It should be noted that the compressibility effect of gas on velocity change along the axis of an axially symmetrical jet is determined mainly by the first factor in the right side of equation (87).

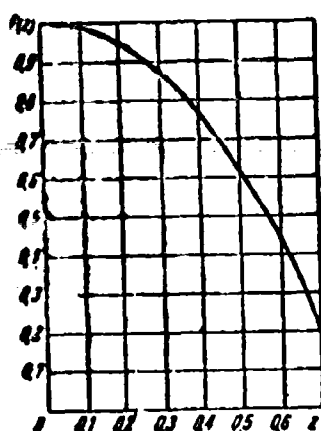


Fig. 7.20. Auxiliary function $F(z)$.

The curve of axial velocity change and build-up of depth of jet along its length, calculated respectively in equations (83) and (85) for $c = 0.22$ and $n_{2u} = 1$ at several values of the parameter λ_0^2 , are represented on Figs. 7.21 and 7.22. From analysis of these curves it follows that if the initial jet velocity exceeds the speed of sound, then the drop in velocity along the axis of the jet becomes less sharp than in the case of a low-speed jet; in this case with an increase in the velocity coefficient λ_0 this distinction is more and more noticeable.

As concerns the boundaries of a supersonic jet, generally speaking, they are curvilinear. In practice, however, this curvilinearity can be (Fig. 7.22) disregarded, and the jet boundaries can be approximated at a certain distance from the transition section by straight lines inclined toward the axis of the jet at the same angle as in a noncompressible fluid. The quantity \bar{x}_n (abscissa of transition section), is determined from the same procedure as in the case of a nonisothermal jet (use of equation (83a) for the density ratio). Dependence $\bar{x}_n(\lambda_0^2)$ is depicted on Fig. 7.23.

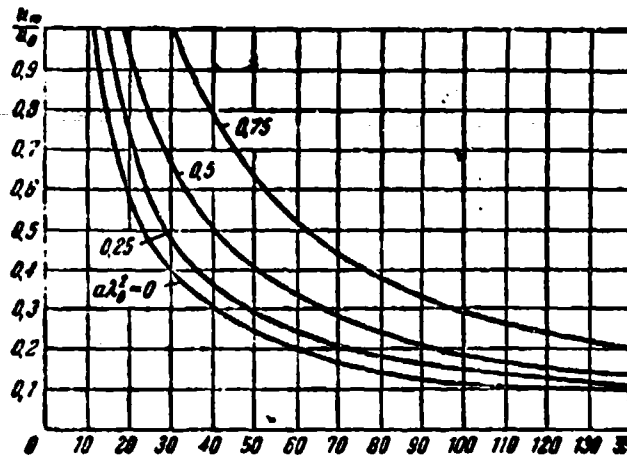


Fig. 7.21. Change of axial velocity in submerged axisymmetric supersonic gas jet (effect of parameter $a\lambda_0^2$).

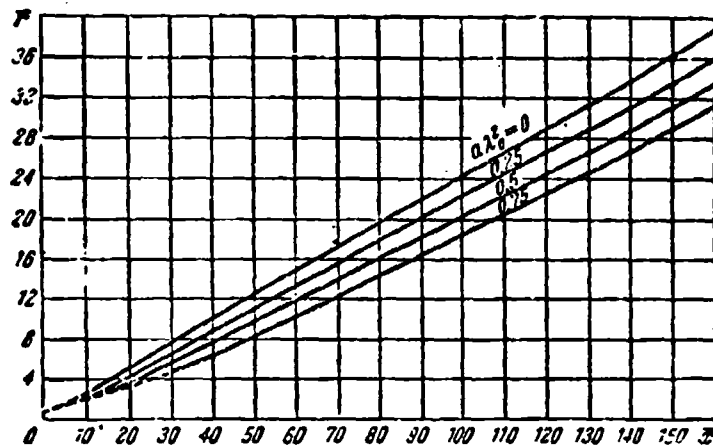


Fig. 7.22. Build-up of depth of submerged axisymmetric supersonic gas jet (effect of parameter $a\lambda_0^2$).

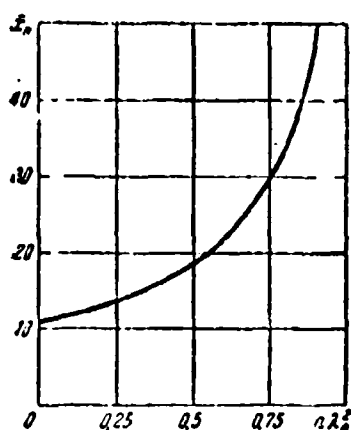


Fig. 7.23. Effect of discharge velocity ($a\lambda_0^2$) on abscissa of transition section in an axially symmetrical jet.

Concluding the examination of the properties of submerged supersonic jets, let us note that if their curvilinear boundaries are approximated by straight lines, then the slope angles toward the x-axis of these lines turn out to be independent of the parameter of compressibility $a\lambda_0^2$, and the point of intersection of these straight lines with the x-axis (pole of jet) changes its position relative to the nozzle edge depending on the value of $a\lambda_0^2$. The effect of parameter $a\lambda_0^2$ on polar distance \bar{x}_0 is shown on Fig. 7.24. The quantity $\bar{x}_0 = x_0/b$ characterizes the range of the jet; the results presented in Fig. 7.24 indicate a considerable increase in range with an increase of parameter $a\lambda_0^2$.

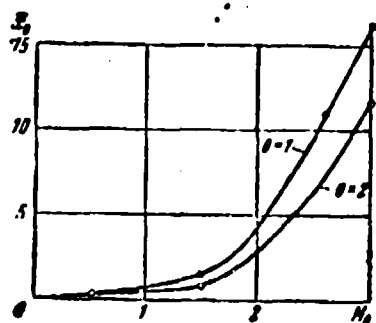


Fig. 7.24. Effect of discharge velocity (M_0) and degree of pre-heating θ on the position of the pole of an axially symmetrical jet according to experimental data of B. A. Zhestkov, M. M. Maximov, et al.

The simultaneous effect of preheating and initial velocity on the jet characteristics is connected with specific calculation difficulties. Let us say, however, that the heated supersonic jet washes out considerably faster than an isothermal jet at the same value of $a\lambda_0^2$, while the effect of preheating is amplified with an increase in $a\lambda_0^2$.

§ 5. Discharge of Supersonic Gas Jet From Nozzle in Off-Design Conditions

In the work of jet engines, different jet apparatuses, for example, ejectors, and in some other procedurally important cases, the discharge of the supersonic jet from a nozzle occurs in off-design conditions, when the pressure in the flow of gas at the nozzle exit differs from the pressure in the medium into which the jet is discharging. In this case both insufficient expansions of gas in nozzle ($p_a > p_H$), and overexpansion are possible ($p_a < p_H$). Because of this in the section of jet adjacent to the nozzle a system of expansion and compression waves appears, and also shock waves, because of which a gradual pressure equalization in the jet is achieved with the pressure predominating in the surrounding medium.

At a certain distance from the nozzle the pressure in the jet becomes equal to the pressure in the surrounding medium, and jet differs in no way from the ordinary calculated jet, which we examined above.

Conditions in the off-design discharge of a supersonic jet are characterized by the degree of off-design, which is the ratio of the real stagnation pressure in receiver p_0 to the calculated¹ pressure p_{00} , which can be approximately replaced

¹The pressure which corresponds to the calculated Mach number of the discharge, determined by the assigned area ratio of the critical and nozzle exit sections, is called the design pressure.

by the pressure ratio at the nozzle exit to the pressure in the surrounding medium:

$$n = \frac{P_e}{P_a} \sim \frac{P_e}{P_a}.$$

Let us pause at some experimental data relating to supersonic jets during off-design discharge from nozzles. In Fig. 7.25 below the solid lines show the change in total pressure p_{0x} referred to pressure in the receiver, along the axis of a supersonic ($M_a = 1.5$) off-design ($n = 5$) jet, and the dotted line shows maximum total pressure in the jet; the upper part of Fig. 7.25 shows the results of experimental research on the picture of flow in a supersonic jet during off-design conditions of discharge: the total-pressure profile in the transition jet cross-sections and the area of subsonic (shaded) and supersonic speed. As we see, in the initial section of the jet the maximum value of pressure does not occur on the axis of the jet. Experiments show that a certain distance from that cross section where the jet becomes isobaric ("isobaric cross section"), maximum speed is observed on the axis of the jet (beginning where the solid and dotted lines meet in the lower part of Fig. 7.25).

Utilizing conditions of momentum conservation between the nozzle-exit plane (subscript "a") and the "isobaric cross section" (subscript "c"), we have

$$\frac{G_a}{g} u_a + (p_a - p_a) F_a = \frac{G_c}{g} u_c \quad (89)$$

where G_a and G_c - weight discharges of air in the jet in cross sections a and c; u_a , u_c - mean values of velocity in these cross sections; F_a - area of nozzle in cross section a.

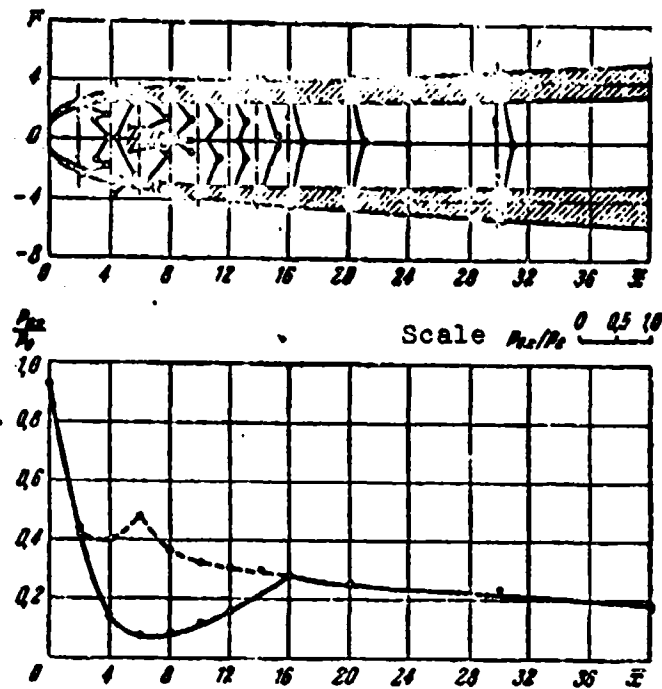


Fig. 7.25. Picture of flow and distribution of total pressure in supersonic off-design gas jet ($M_a = 1.5$; $n = 5$) according to the experiments of B. A. Zhestkov, M. M. Maximov, et al.

Passing to dimensionless quantities

$$\lambda = \frac{u}{a_{*}}, \quad \frac{G}{G_*} = \frac{u}{a_*} \frac{P_0}{P_{0*}} = \frac{P_0}{P_{0*}} \frac{u}{a_*} = \frac{2k}{k+1} \frac{\lambda^2}{1 - \frac{k-1}{k+1} \lambda^2},$$

from (89) we obtain (at constant value of critical speed)

$$\lambda_c = \frac{G_*}{G_c} \left[1 + \lambda_c^2 - \frac{1}{n} \left(1 - \frac{k-1}{k+1} \lambda_c^2 \right) \right]^{\frac{k+1}{2k}}. \quad (90)$$

The area of the isobaric jet cross-sectional area F_c is calculated with the aid of the equations of discharge and state¹:

¹More detailed analysis of change in the parameters of gas along the length of the initial section of off-design supersonic jet in one-dimensional formulation is given in § 6.

$$\frac{F_1}{F_2} = \frac{G_1 \lambda_1 u_1}{G_2 \lambda_2 u_2} = \frac{G_1 \lambda_1}{G_2 \lambda_2} \frac{1 - \frac{k-1}{k+1} \lambda_1^2}{1 - \frac{k-1}{k+1} \lambda_2^2} \quad (91)$$

Mixing leads to an increase in the flow mass and a sharp increase in the nonuniformity velocity profile, which in an isobaric cross section bears a typically jet nature. Because the jet draws substance from the surrounding medium, the quantity λ_c always should be somewhat lower than in the case of $G_a = G_c$. In this case with an increase of the parameter n the noted effect is exhibited more weakly.

Nonuniformity of the velocity profile in an isobaric jet cross sectional area leads to a considerable increase in the axial velocity (λ_{cm}) as compared with its mean value $\lambda_{cm} > \lambda_c$.

The above factors always act simultaneously, and, as we saw, have an effect on the value λ_{cm} . Figure 7.26 gives the curve calculated with the aid of (90) assuming the absence of mixing ($G_a = G_c$) for $\lambda_a = 1.37$ and $k = 1.4$. The experimental data taken from the experiments of B. A. Zhestkov, et al. (at $\lambda_a = 1.37$) show that with the large degrees of off-design ($n > 3$) neglect of the suction action of the jet leads to oversized calculated values of velocity in the isobaric cross section. When $n \approx 10$ the effect of suction and nonuniformity on λ_{cm} is mutually balanced, and the velocity on the axis of the jet in isobaric cross section becomes very close to λ_a .

Velocity on the flow axis after the jet becomes isobaric can be calculated on the basis of the momentum equation (taking into account inequality of nozzle pressure in surrounding medium) and the equation of jet propagation (85). In the case of an axially symmetrical jet we have

$$J = \int \rho u^2 2\pi r dr = \rho_a u_a^2 \pi r_a^2 + (p_a - p_a) \pi r_a^2. \quad (92)$$

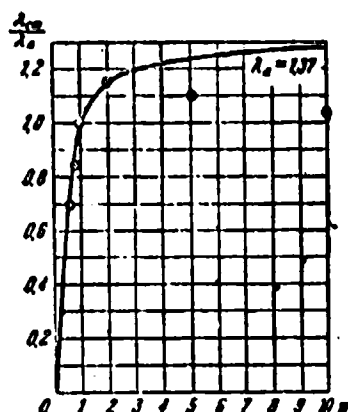


Fig. 7.26. Effect of degree of off-design n on relative axial velocity in an isobaric cross section according to experiments of B. A. Zhestkov, M. M. Maximov, et al. ($M_a = 1.5$).

The parameters of gas flow at the nozzle exit (designated in equation (92) by the subscript "a") can be defined by known gas parameters in the receiver and the geometric dimensions of the nozzle assuming that at any value $n > 1$ in the nozzle the same relative drop in pressures occurs as with design conditions of discharge.

Let us bring equation (92) to dimensionless form by dividing both sides by $\pi r_a^2 \rho_a \frac{2h}{h-1}$. After certain transformations we obtain

$$u_a^2 A_1 = \frac{1}{\rho_a} \left[n_{1,a} \cdot \frac{1-a)^2}{a^2} \left(\frac{a}{1+a} (n-1) \right) \right], \quad (93)$$

where $\bar{r} = r/r_a$, $a = (k-1)/k+1$, r - radius of jet. Comparing (93) with expression (54), we see that the momentum equation for an off-design jet differs from the corresponding expression in the case of calculated discharge by the factor

$$N = n + \frac{1-a)^2}{n_{1,a} a^2} \left(\frac{a}{1+a} (n-1) \right), \quad (94)$$

which depends only on the conditions in the initial jet cross-sectional area and does not change in terms of the x coordinate.

This fact makes it possible to utilize as a solution systems of equations (85) and (93), obtained above solution (87) for a supersonic gas jet in design conditions of discharge. The final formula for determining the axial velocity of an off-design jet takes the form

$$c(x - x_0) = \sqrt{\frac{N n_m}{0.134(1 - \alpha \lambda_a^2)}} \left[\frac{P(z)}{P_0} - F(x_0) \right], \quad (95)$$

whereupon function $F(z)$ is determined by formula (88). The build-up of jet thickness in this case is determined from equations (93) and (95).

From formula (95), and also equality (94) it follows that an off-design jet with $n > 1$ possesses considerably larger range than the corresponding (at the same values $\alpha \lambda_a^2$) isobaric supersonic jet; in this case the range of the jet, defined, for example, as the distance from the nozzle at which the axial velocity is half the initial, increases approximately as \sqrt{N} or, at large $\alpha \lambda_a^2$, as \sqrt{n} . From expression (94) it follows, furthermore, when the discharge velocity insignificantly differs from the sonic (parameter $\alpha \lambda_a^2$ is low), then even small off-design of a jet can lead to a noticeable increase in its range. For example, at $\alpha \lambda_a^2 = 0.2$ ($M_a = 1.11$) and $n = 1.2$ the value of N is 1.36, i.e., the range of the off-design jet proves to be 17% more than calculated.

In order to search for the value of the abscissa of the transition cross section \bar{x}_n , necessary for calculating the jet, it is necessary to know the characteristics of the turbulent expansion of the jet in its initial section. In view of the complexity of the theory of the initial section of an off-design jet, we usually utilize either the dependences obtained for the

corresponding calculated jet or experimental data. Dependence $\bar{x}_n(a\lambda_a^2, n)$, determined assuming the validity of relationships for the initial section of the calculated jet and in the case of off-design discharge, is depicted on Fig. 7.27.

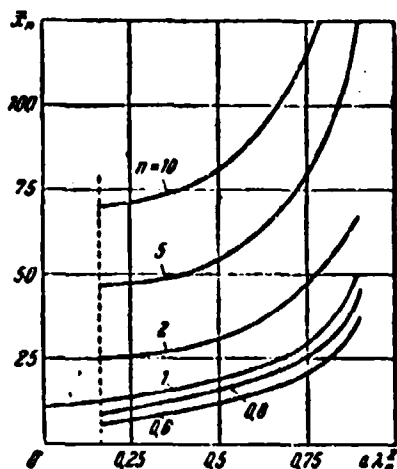


Fig. 7.27. Dependence of abscissa of transition section of supersonic off-design jets on parameters $a\lambda_0^2$ and n .

The comparison of values of axial velocity calculated according to formula (95) with the results of velocity measurements in supersonic off-design gas jets is presented on Figs. 7.28 and 7.29. The experimental data given on Fig. 7.28 are obtained for a nozzle design for $M_a = 1.5$ ($\lambda_a = 1.37$) at the following values of off-design parameter n : 0.8; 1; 2; 5; 10. Experimental values of velocity on Fig. 7.29 correspond to discharge from a nozzle designed for $M_a = 3$ with $n = 1$ and $n = 2$. From examination of these figures it follows that the theoretical results in the first approximation satisfactorily agree with the experimental data, although sometimes a noticeable quantitative disagreement between them is observed. The noted nonconformity can be the consequence of using in the initial section of the off-design jet dependence for a jet with the design discharge.

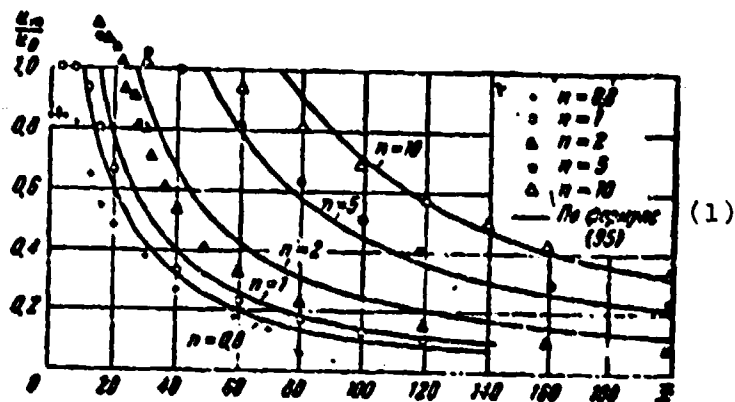


Fig. 7.28. Comparison of calculated and experimental values of axial velocity in a supersonic axisymmetric gas jet ($M_a = 1.5$) in calculated ($n = 1$) and off-design ($n = \text{var}$) systems of discharge according to the experiments of B. A. Zhestkov, M. M. Maximov, et al.
KEY: (1) According to formula.

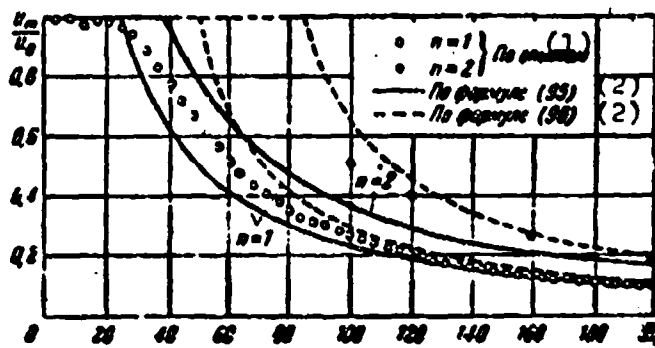


Fig. 7.29. Comparison of calculated and experimental values of axial velocity in a supersonic axisymmetric gas jet ($M_a = 3$) in calculated ($n = 1$) and off-design ($n = 2$) systems of discharge according to the experiments of B. A. Zhestkov, M. M. Maximov, et al.
KEY: (1) According to experiments; (2) According to formula.

Similar conclusions follow from analysis of Figs. 7.30 and 7.31, which represent experimental data on the arrangement of lines of half-velocity in supersonic jets at different values of the calculated Mach number M_a and off-design parameter n , and also results of the corresponding calculations according to formulas (93)-(95). As can be seen from examination of Figs. 7.30 and 7.31, the lines of half-velocity (and the corresponding boundaries) in supersonic off-design jets generally speaking are curvilinear, especially near the transition cross section, but the curvature of the boundaries is low, and therefore in the first approximation they can be replaced by straight lines. The angle of inclination of these lines does not depend on parameters $\alpha\lambda_a^2$ and n (the tangent of this angle, as in a jet of noncompressible fluid, is 0.22), and the position of the points of intersection with the x -axis relative to the nozzle edge (polar distance \bar{x}_0) changes depending on the values of $\alpha\lambda_a^2$ and n . The experimental dependence of value \bar{x}_0 on n for two values of M_a (or parameter $\alpha\lambda_a^2$) is given on Fig. 7.32.

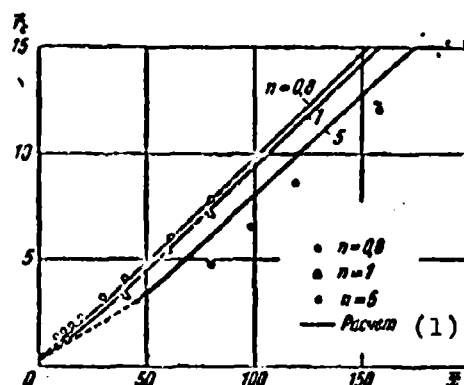


Fig. 7.30. Comparison of calculated and experimental values of "half radius" \bar{r}_c in supersonic ($M_a = 1.5$) gas jets during design and off-design conditions according to the experiments of B. A. Zhestkov, M. M. Maximov, et al.
KEY: (1) Calculation.

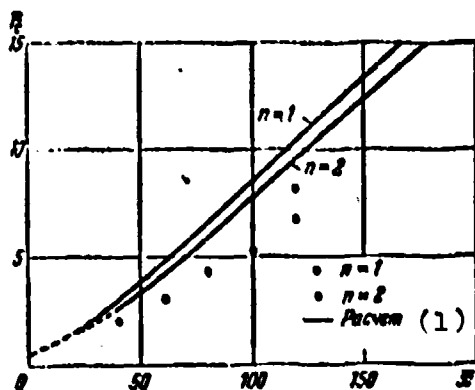


Fig. 7.31.

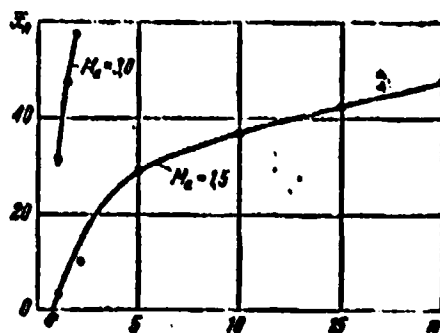


Fig. 7.32.

Fig. 7.31. Comparison of calculated and experimental values of "half radius" \bar{F}_c in supersonic ($M_a = 3$) gas jets during design and off-design conditions according to the experiments of B. A. Zhestkov, M. M. Maximov, et al.
KEY: (1) Calculation.

Fig. 7.32. Effect of the degree of off-design on position of the pole of a supersonic gas jet according to the experiments of B. A. Zhestkov, M. M. Maximov, et al.

As we see, with an increase both in the off-design parameter n and the value of λ_a^2 the pole of the jet shifts downstream. If we utilize the concept of the pole of a jet, assuming the boundaries of the principal section of the jet to be rectilinear, the formula for determining the axial velocity and thickness of an axially symmetrical jet assumes the form

$$c(x - x_0) = \frac{1}{n_m} \sqrt{\frac{n_m n + \frac{1 - \alpha \lambda_a^2}{\alpha} \frac{a}{1 + a} (n - 1)}{0.131 (1 - \alpha \lambda_a^2) (1 + 0.45 \alpha \lambda_a^2 n_m^2)}} \quad (96)$$

$$r = c(x - x_0) \quad (97)$$

The axial velocity attenuation curves, calculated from equation (96) for two values of parameter n (1.0 and 2.0 at $M_a = 3$) are

plotted by dotted lines on Fig. 7.25; in this case \bar{x}_0 is determined from the experimental data presented in Fig. 7.22. Analyzing the path of the calculated curves and comparing them with experimental points, it is possible to conclude that the curves which correspond to equation (96) in the area of transition and in the beginning principal section more strongly differ from the experimental values of axial velocity than the curves calculated from formula (95).

The method of calculating a supersonic jet with $n \neq 1$ given in this section should be considered as roughly approximate. It does not consider the concrete conditions of the development of a jet in the "gas-dynamic" section which adjoins the nozzle, on which the pressure (with $n \neq 1$) differs significantly from atmospheric. The weakest area of this method is the means of determining the abscissa of the transition cross section, and also the fact that it is suitable only for that part of the isobaric flow in which the velocity on the axis of the jet is maximum; in actuality, between the gas-dynamic section (where $p = p_0$) and this part of the isobaric flow is an isobaric zone with decreased velocity on the axis. The approximate theory of the gas-dynamic section of a jet is given below.

1.1. The One-Dimensional Theory of the Initial ("Gas-Dynamic") Section of an Off-Design Supersonic Jet

A characteristic feature of an off-design supersonic jet is the substantial nonuniformity of the flow: the parameters of the gas change considerably both for the length of the jet and for the radius of the transverse cross section. For calculating such a flow the method of characteristics is usually applied which makes it possible to find for the initial values of the parameters on the nozzle edge the parameters of the gas in the entire supersonic part of the flow which adjoins the nozzle. In a number of cases, however, it is necessary to know only some total flow characteristics, for example total pulse, the total pressure losses, the cross-sectional area, and the determination of the internal jet structure is not required. For the solution of such tasks, instead of the bulky and laborious method of characteristics it would be desirable to use simpler calculation methods.

Set forth below is one such method that is based on the averaging of the parameters of the jet in the transverse cross section and its approximate consideration as a one-dimensional gas flow.

Let us explain, first of all, how admissible it is to use the averaging of the parameters in the flow of such a large nonuniformity as an off-design supersonic jet where, for example, static pressure can decrease from the periphery to the axis 10-20 times and, in accordance with this, the rate of flow changes.

In the calculation of a jet the equations of energy, continuity, and momentum are utilized. Therefore, it is necessary that the

¹Cherkez, A. Ya., On the One-Dimensional Theory of the Off-Design Supersonic Gas Jet. News of AN USSR, Department of Technical Sciences, No. 5, 1962.

values of total energy, consumption and pulse of gas in the transverse cross section calculated according to the mean values of the parameters be equal to their real value in an initial nonuniform flow. Furthermore, for calculating it is important correctly to estimate the entropy of the flow: this makes it possible to utilize the condition of the retention of the value of total pressure in sections where there are no losses, and also to determine the real value of the total losses with respect to a change in the mean total pressure.

As is known (Chapter V), with the averaging of a nonuniform flow in general only three of its total characteristics can be maintained constant. However, for a supersonic flow with a constant stagnation temperature over the cross section, which is the initial section of an off-design jet of ideal gas in the absence of mixing, it is possible to find such mean values of parameters in the cross section upon transition to which the amounts of flow rate, total energy, pulse and entropy are retained simultaneously with the high degree of accuracy with an invariable cross-sectional area. We will also introduce these mean values of the parameters of a gas in the transverse cross sections of the initial section of the jet into the equations of continuity, energy, and pulses. The joint solutions of these equations therefore will also pertain to the mean values of the parameters, and the cross-sectional area hence determined will be equal to the real area of the corresponding cross sections of the jet. Almost all the basic properties of a flow in such a one-dimensional consideration do not change and are estimated correctly. Only one intrinsic property of the flow is lost, namely the equality of the static pressure on the jet boundaries and in the external environment; therefore, it is necessary to arbitrarily assume that in every transverse flow cross section there exists some constant mean static pressure p , in general distinct from the pressure of the external environment p_H .

Let us dwell on the case of a supersonic jet which escapes from an underexpanded nozzle, i.e., having overpressure $p_a > p_m$ at the nozzle edge (Fig. 7.33). The schematic picture of such a flow is described in § 2, Chapter IV.

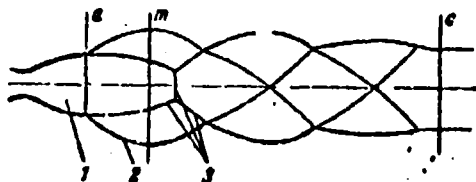


Fig. 7.33. Diagram of a jet which escapes from a nozzle with static overpressure in a stationary gas: 1 - nozzle; 2 - jet boundaries; 3 - shock waves.

We assume the gas ideal, we consider the parameters of the gas on the edge of the nozzle constant over the cross section, and the velocity vectors of gas on the nozzle edge - parallel to the nozzle axis. We disregard the mixing of the gas in the initial section with gas of the surrounding fixed environment.

Let us write the basic equations which connect the parameters of the gas in a free jet with the parameters in the outlet section of the nozzle. First, as a characteristic cross section of the initial section of the jet we select the maximum cross section of the first "barrel" (Fig. 7.33).

We record the equation of the equality of flow rates in the form

$$Q = Q_0 \quad (98)$$

or, utilizing the known expression of flow rate through the stagnation parameters p^* and T^* and the velocity coefficient λ :

$$\frac{\rho^* F_q(\lambda)}{\sqrt{T^*}} = \frac{\rho_0^* F_{q0}(\lambda_0)}{\sqrt{T_0^*}} \quad (99)$$

where subscript a pertains to the parameters in the nozzle outlet section. Values p^* and λ are the mean values of the total pressure and velocity coefficient in the cross section of a free jet in question.

According to the equation of the conservation of energy

$$G c_p T^* = G c_p T_a^* \quad (100)$$

with $G = G_a$ and $c_p = c_{p_a}$ the stagnation temperature in a jet remains constant. Therefore, the equation of continuity (99) assumes the form

$$q(\lambda) = \frac{1}{\sigma} \frac{1}{\lambda} q(\lambda_a) \quad (101)$$

Here $f = (F/F_a)$, and $\sigma = p^*/p_a^*$ is the coefficient of total pressure which estimates the total losses of total pressure on the section between the initial and considered cross-sections of the jet. In order to obtain the relation between the relative cross-sectional area f and the velocity coefficient λ in this cross section from equation (101), it is necessary to estimate the value of the coefficient of total pressure σ . For the first "barrel" of the underexpanded jet the total pressure losses can be disregarded since in a slot jet between the initial and maximum cross section shocks are absent, and in the axisymmetric underexpanded jet the intensity of curvilinear shock (envelope of lines of compression) near the nozzle is small. We will consider that also in an axially symmetrical jet for the first "barrel" $\sigma = 1$.

Let us write the equation of momentum for the section of the jet in question in the form

$$\frac{d}{dt} \int_V \rho u_n dV = p_n F_n - p F + \int_V \rho u_n (F - F_n) dV \quad (102)$$

where the last term of the right side is the axial component of the force of external pressure p_{μ} on the lateral surface of the jet.

Let us replace the expressions of the gas pulse in both cross sections in question according to formula (115) in Chapter V, taking into account in this case the fact that $G = G_a$ and $a_{\mu p} = a_{\mu p a}$. As a result we obtain

$$\frac{k+1}{2k} \frac{Q}{g} a_{\mu p} [z(\lambda) - z(\lambda_a)] = p_a F_a (f - 1) \quad (103)$$

We express in (103) the product $G a_{\mu p}$ according to formulas (108) and (110) in Chapter V

$$\frac{k+1}{2k} \frac{Q}{g} a_{\mu p} = \left(\frac{2}{k+1}\right)^{\frac{1}{k-1}} p^* F q(\lambda) = \left(\frac{2}{k+1}\right)^{\frac{1}{k-1}} p F y(\lambda)$$

through the parameters of gas in the nozzle outlet section. As a result we obtain

$$z(\lambda) = z(\lambda_a) + \left(\frac{k+1}{2}\right)^{\frac{1}{k-1}} \frac{f-1}{\Pi_{0q}(\lambda_a)} \quad (104)$$

or

$$z(\lambda) = z(\lambda_a) + \left(\frac{k+1}{2}\right)^{\frac{1}{k-1}} \frac{f-1}{\Pi_{0y}(\lambda_a)} \quad (105)$$

where the $\Pi_0 = p_a^*/p_{\mu}$ is the available pressure ratio in the jet, $n = p_a/p_{\mu}$ - the degree of the off-design of the jet $q(\lambda)$ and $y(\lambda)$ - the known gas-dynamic functions.

We note that according to equation (102) or to equations (104) and (105) the gas pulse in the jet does not remain constant but increases in proportion to the increase in the area of the jet because of the action of the force of external pressure.

Thus, we obtained two equations (101) and (104) containing two unknown values: the relative cross-sectional area f and the mean value of the velocity coefficient in this cross section λ . The joint solution of the equations and also the qualitative study of the laws governing the flow is most conveniently carried out graphically. The obtained graph is called the phase diagram of an off-design jet. Constructed on Fig. 7.34 for the initial parameters of the jet $M_a = 1.5$ ($\lambda_a = 1.365$) and $n = 6.8$ ($\Pi_0 = 25$) is the relation $\lambda = \lambda(f)$ according to the equation of flow rate (101) with $\sigma = 1$ (curve 1) and the same relation according to the equation of momentum (104) (curve 2). The intersection of obtained curves 1 and 2 gives two pairs of values of variables of f and λ that satisfy both equations. The first point of intersection $f = 1$ and $\lambda = \lambda_a$ corresponds to the initial parameters of the gas at the nozzle edge and is of no interest. The second point of intersection, as shown below, gives values f_m and λ_m in the maximum cross section of the first "barrel." Both points of intersection correspond to the supersonic flow velocity. From the value of functions $q(\lambda)$ and $z(\lambda)$, determined from equations (101) and (104), it is also possible to find the second, subsonic values of the velocity coefficient λ . However, these equations do not have joint solutions in the subsonic region.

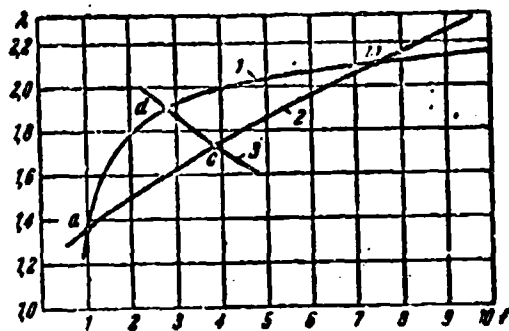


Fig. 7.34. The phase diagram of an underexpanded ($n > 1$) supersonic jet: 1 - equation of continuity (101); 2 - equation of momentum (104); 3 - equation of continuity (109); a - nozzle outlet cross section; m - maximum cross section of the first "barrel"; d - outlet cross section of an ideal calculated nozzle; c - isobaric cross section.

Let us examine in more detail the meaning of the obtained solution. At first sight it appears strange that the condition of constancy of the flow rate and the equation of momentum are simultaneously satisfied only in two cross sections of the initial section of the jet, whereas these conditions should be satisfied for any cross section of flow. However, one ought to consider that in equations (101) and (104) with the expression of the flow rate and momentum of the gas through the stagnation parameters and the velocity coefficient it was assumed that the velocity corresponding to the expansion from total pressure p^* to static pressure p in this cross section was directed along the axis of the jet so that the gas flow rate and its momentum in an axial direction are determined by the absolute gas velocity. The equations of the flow rate and momentum (101) and (104) are valid only for those cross sections of the flow in which the gas velocity can be assumed axial. Such a cross section, apart from the nozzle outlet section, in part of the jet in question is the maximum cross section of the first "barrel." Therefore, from the joint solution we obtain $f = f_m$ and $\lambda = \lambda_m$. In all the remaining intermediate cross sections of the divergent part of the first "barrel" there are radial component velocities, in consequence of which the equations of a one-dimensional flow (101) and (104), as can be seen from Fig. 7.34, are not satisfied simultaneously here.

This means that no flow exists with the axial direction of the velocity which, with given initial parameters at the nozzle edge and $p^* = \text{const}$ ($\sigma = 1$), could have a cross-sectional area equal to the area of any intermediate cross section of the first "barrel."

For determining the parameters of the gas in these intermediate cross sections, the expressions of flow rate and momentum should be written taking into account the radial velocity component. Using, as above, the mean values of the parameters of the gas in

each cross section, let us assume that the mean value of the radial velocity is such that the vector of the mean absolute velocity comprises some angle α with the axis of flow.

Above, in § 6 of Chapter V expressions for flow rate (123) and (125) and gas pulse (127) in a one-dimensional flow having the velocity component in a plane perpendicular to the axis were obtained.

With the aid of these expressions for the flow rate and momentum, it is possible to compose the equations of continuity and momentum for any cross sections of the initial section of the jet. These equations take the form

$$q(\lambda, z) = \frac{1}{z^k} q(\lambda_0) \lambda \quad (106)$$

$$z(\lambda, z) = z(\lambda_0) + \left(\frac{k+1}{2}\right)^{\frac{1}{k-1}} \frac{f-1}{n, q(\lambda_0)}. \quad (107)$$

For each selected cross-section of a jet with a relative area of $f = F/F_a$ with given initial flow parameters and value σ (specifically, for the first "barrel" with $\sigma = 1$) the obtained equations contain two unknown values λ and α . The joint solution of the equations is carried out graphically with the use of tables of gas-dynamic functions and a graph of the function $z(\lambda, \alpha)$ (see § 6, Chapter V), where λ is the coefficient of absolute velocity.

Figure 7.35 gives the results of such a calculation. As can be seen, in all intermediate cross sections some actual value of angle α is determined which seemingly compensates for the incompatibility of the equations of a one-dimensional parallel flow (101) and (104) for the intermediate cross sections of the barrels. It is natural that in cross sections $f = 1$ and $f = f_m$ for which equations (101) and (104) are satisfied simultaneously, we have $\alpha = 0$ and $\lambda_r = \lambda \sin \alpha = 0$.

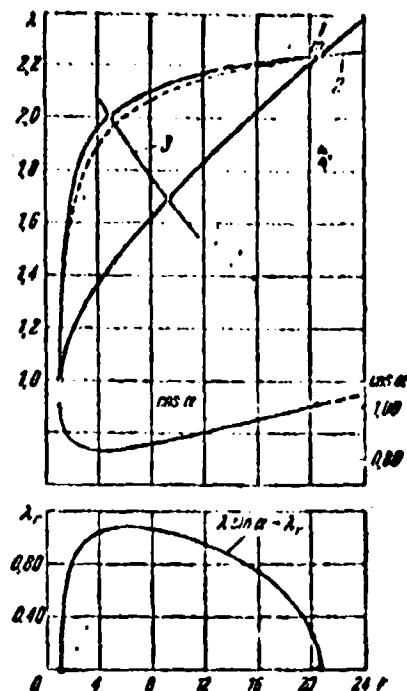


Fig. 7.35. The parameters of a gas in the intermediate cross sections of the first "barrels" of an off-design jet: 1 - the equation of momentum (104), 2, 3 - the equations of continuity (101) and (109), the dotted line is the coefficient of absolute velocity according to equations (106) and (107) ($M_a = 1.0$; $\Pi_0 = 46.5$; $n = 24.6$).

Let us note that the absolute velocity or the velocity coefficient λ in the intermediate cross sections (see dotted curve on the graph of Fig. 7.35) and, consequently, also the value of the static pressure $p = p^*\pi(\lambda)$, obtained during the calculation, taking into account the radial components of the velocity, are very close to the corresponding values obtained from the usual equation of flow rate (101) (unbroken curve) without correction for angle α .

If we attempt to determine the value of angle α , taking the area of cross sections more than F_m or less than F_a , then it will turn out that $\cos \alpha > 1$, and the radial component of the velocity

is an imaginary value. This indicates the physical impossibility of such a flow and, therefore, the fact that in the initial section of the underexpanded jet the cross-sectional area cannot become less than the nozzle outlet cross section F_a or larger than the area F_m found from the joint solution of equations (101) and (104); the value of f_m , therefore, is really the maximum relative area of the first "barrels" of the jet.

For determining the parameters of a jet in the cross sections following the maximum cross section of the first "barrel," it is possible to make use of the same equations which were derived above for the first "barrels" with the difference that value σ - the coefficient of total pressure - in equations (101) or (106) can no longer be assumed equal to unity. The losses in total pressure in the shock waves during the deceleration of a gas after over-expansion lead to the fact that at the end of the tapering portion of the first "barrels" and in all subsequent cross sections $p^* < p_a^*$ and $\sigma < 1$. Figure 7.36 presents the family of curves $\lambda = \lambda(f)$ obtained from the equation of continuity with $\sigma < 1$. The intersection of these curves with curve 2, calculated from the equation of momentum (104), gives the possible parameters of a gas in the maximum and minimum cross sections of the subsequent "barrels" of the initial section of the jet. From the phase diagram it is obvious that in each subsequent "barrel" maximum values of the area and velocity coefficient are less, but the minimum values are greater than in preceding one; a reduction in the total pressure leads to a decrease in the range of a change of the parameters of the gas in the "barrels." With a certain value of $\sigma = \sigma_{\min}$ $F_{\min} = F_{\max}$ is obtained; this shows that in a flow, if we do not consider mixing with the external environment, constant values of the parameters which correspond to point c of the phase diagram are established. This is also the limiting state of the gas attained in the initial section of an off-design jet, if we do not consider mixing with the external environment.

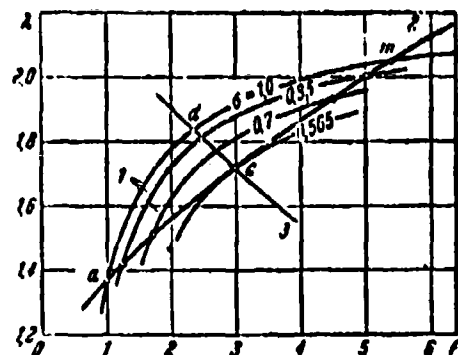


Fig. 7.36. The phase diagram of an off-design supersonic jet taking into account the total pressure losses: 1 - the equation of continuity (101); 2 - the equation of momentum; 3 - the equation of continuity (109).

It is possible to show that the static pressure in this cross section, called isobaric, is equal to the external pressure, in consequence of which a further change in the flow parameters also ceases. For determining the parameters of a gas in an isobaric cross section, let us write the condition of constancy of the flow rate, expressing the gas flow rate by the static pressure ($p_c = p_\infty$):

$$\frac{\rho_a F_a V(\lambda_c)}{\sqrt{T_c}} = \frac{\rho_\infty F_\infty q(\lambda_\infty)}{\sqrt{T_\infty}} \quad (108)$$

or

$$V(\lambda_c) = \Pi_\infty \frac{1}{\sqrt{T_c}} q(\lambda_\infty) \quad (109)$$

The joint solution of this equation with the equation of momentum in the form of (104) makes it possible to find values λ_c and $f_c = F_c/F_a$.

Let us note that in all cases $\lambda_c > 1$ is obtained from the calculation, i.e., with $G = \text{const}$. The jet at the end of the initial section always remains supersonic; the transition through the speed of sound becomes possible only as a result of mixing with the external environment which is not considered here.

According to the value λ_c , it is easy to determine total pressure $p_c^* = p_H / \pi(\lambda_c)$ and to calculate the value of the total losses of the total pressure of a gas in the initial section

$$\sigma_c = \frac{p_c^*}{p_a^*} = \frac{1}{\pi(\lambda_c)}. \quad (110)$$

Thus, the value of the total losses of total pressure in all "barrels" of the initial section can be determined without a detailed examination of the processes which proceed in the jet. The calculations show that these losses are very great and are determined mainly by the degree of off-design n (Fig. 7.37).

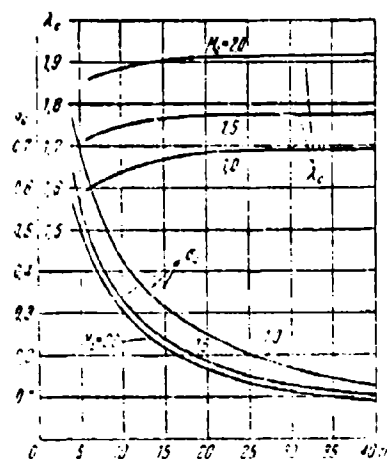


Fig. 7.37. The velocity coefficient of a gas in an isobaric cross section and the total losses of total pressure in the initial section of an off-design supersonic jet, $k = 1.4$.

On the phase diagram (Figs. 7.34, 7.36) curve 3, constructed according to equation (109), indicates possible states of gas flow (with given initial parameters) with which the mean static pressure is equal to p_H ; above this curve $p < p_H$, below $p > p_H$. It is easy to see that the point of intersection d of curve 3 with curve 1 ($p^* = p_a^*$) indicates the parameters of the gas with ideal expansion from p_a^* to p_H in a Laval nozzle; point c gives the parameters of a

free jet in an isobaric cross section. The phase diagram directly shows the qualitative relationships between the parameters of the gas at points c, m, d and a. Specifically, let us note that the area of the maximum and isobaric cross sections of a free jet with $n > 1$ is always obtained larger than the area of the outlet cross section of a design Laval nozzle. The smaller the section of free expansion of the gas, the closer to each other the parameters of the gas in states c, d, m and a.

The effect of the degree of off-design of a nozzle can be connected with a change in the external power effect on the jet. In fact, with an increase in the expansion ratio of the nozzle (decrease in n) part of the free flow is replaced by a supplementary part of the nozzle. Instead of external pressure p_μ variable pressure $p > p_\mu$ now acts on the jet boundaries, since $n > 1$. An increase in the force which acts on the jet in the direction of motion

$$P = \int_{(a)} (p - p_\mu) dF, \quad (111)$$

is equal to the force of excess pressure on the walls of the supplementary part of the nozzle. Value P will enter the right side of the equation of momentum (102) recorded for the section of flow from the initial output area of the nozzle to an arbitrary jet cross-section as a supplementary term; because of this, the pulse of the gas in a cross section with an area of F increases. Equation (104) for this case takes the form

$$z(\lambda) = z(\lambda_0) + \left(\frac{\lambda+1}{2} \right)^{\frac{1}{n-1}} \frac{1}{11.09(\lambda_0)} + KP, \quad (112)$$

where

$$K = \left(\frac{\lambda+1}{2} \right)^{\frac{1}{n-1}} \frac{1}{p_0^* F_{0*} q(\lambda_0)}.$$

The equation of continuity does not depend on the magnitude of force R . With the aid of the phase diagram (Fig. 7.38) it is easy to establish the qualitative influence of the force effect on the jet. The parameters of the gas in the maximum and isobaric cross sections are determined by the points of intersection of the invariable curves 1 and 3 with curve 2' constructed from equation (112). With $P > 0$, curve 2' always lies higher than the initial curve 2. Therefore, the areas of the maximum and isobaric cross sections are obtained smaller than in a free jet; the velocity coefficient λ_m in the maximum cross section decreases, while the velocity coefficient λ_c in the isobaric cross section increases. Thus, an increase in the force which acts on a flow in the direction of motion (or an increase in the reaction on the nozzle walls) leads to a decrease in the overexpansion of the jet in the "barrels" and to a decrease in the total losses of total pressure of the gas in the initial section of the jet. The result obtained with the aid of the phase diagram is not obvious. Actually, despite the fact that supplementary force P acts along the flow, the pulse of the gas in the maximum cross-section of the jet,

$$I_m = \frac{G}{g} u_m + p_m F_m = \text{const} \approx (p_m h)$$

as the joint solution of the equations of pulse and continuity shows, does not increase, but decreases, which is connected with a reduction in the area of this cross section.

The indicated method of the analysis of the force effect on a jet also turns out to be useful in the examination of more complex cases of gas flow. Being given the different initial parameters of the jet, according to the aforementioned relationships it is possible to determine the dependence of the parameters of the jet in characteristic jet cross sections on the degree of over-expansion and M number on the nozzle edge (Figs. 7.39, 7.40).

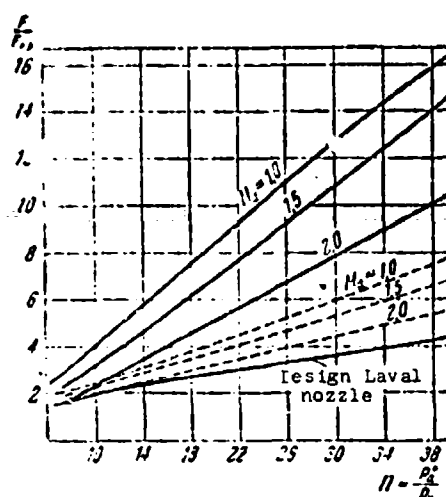


Fig. 7.40. The ratio of the areas of maximum and isobaric (dotted line) cross sections of an off-design supersonic jet to the area of critical cross section of a Laval nozzle, $k = 1.4$.

From the calculations carried out it follows that in all cases with $n > 1$ the mean value of the static pressure in the maximum jet cross-section

$$p_m = p_{0m}(\gamma_m)$$

is considerably lower than the external pressure p_H . The results of the calculation obtained over a wide range of initial parameters of the jet closely correspond to the approximate relation (for $n > 2.5$; $k = 1.4$)

$$\frac{p_m}{p_0} = \frac{1}{n} \div 0.07. \quad (113)$$

From Figs. 7.41, 7.42 it can be seen that the results of calculating the area (diameter) of the maximum and isobaric jet cross-sections according to the given method correspond well to the experimental data of different authors. Let us note that with the given initial parameters of the jet the conformity of the

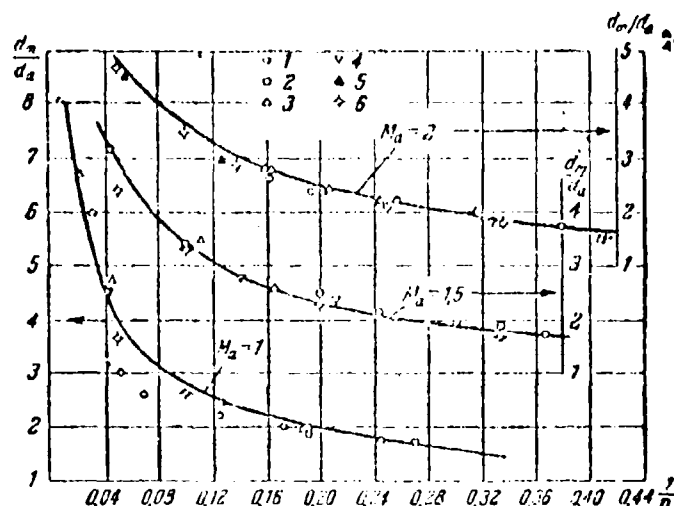


Fig. 7.41. The diameter of the maximum cross section of an underexpanded supersonic jet according to experimental and calculation data: 1 - I. P. Volkovaya's experiments; 2 - Tolomei-Melendier's experiments; 3 - G. A. Akimov's experiments; 4 - Ye. Lav's experiments; 5 - T. Adamson's experiments; 6 - calculation according to the method of characteristics. The solid lines are the calculation according to the one-dimensional theory, $k = 1.4$.

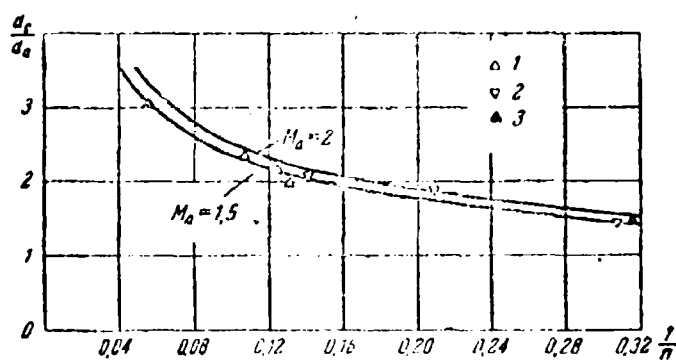


Fig. 7.42. The diameter of an isobaric jet cross-section according to experimental and calculation data: 1 - G. A. Akimov's experiments; 2 - Ye. Lav's experiments; 3 - T. Adamson's experiments. The solid lines are the calculation according to the one-dimensional theory, $k = 1.4$.

calculated and measured cross-sectional area simultaneously means that the mean values of the velocity in this cross section (see equation (104) and the value of the total pressure - coefficient σ (see equation (101)) also coincide.

From an examination of the phase diagram it is possible to obtain the qualitative results for a number of limiting conditions in the outflow. Specifically, during the outflow of gas into a void through a nozzle of finite dimensions ($p_H = 0$, $\Pi_0 = \infty$, $q(\lambda_a) \neq 0$) in the equation of momentum (104) the second term of the right side disappears, in consequence of which it assumes the form

$$z(\lambda) = z(\lambda_a) \text{ or } \lambda = \lambda_a$$

Curve 2 on the phase diagram (see Fig. 7.34) in this case is converted to a straight line parallel to the abscissa, and the point of its intersection with the invariable curve 1 which expresses the equation of continuity departs into infinity ($f_m \rightarrow \infty$, $\lambda_m \rightarrow \sqrt{k + 1/k - 1}$). This means that the jet which escapes into a void does not form "barrels," but it increases boundlessly in cross section, retaining the radial velocity component everywhere.

If the shaping of the nozzle does not assure obtaining a parallel uniform flow of gas in the outlet cross section as was accepted above, then in equations (101) and (104) one ought to consider the presence of a radial velocity component in cross section a . For this, as was done during the derivation of equations (106) and (107), one ought to replace functions $q(\lambda_a)$ and $z(\lambda_a)$, with the generalized functions $q(\lambda_a, \alpha_a)$ and $z(\lambda_a, \alpha_a)$, where α_a is the mean value of the angle between the vector of the absolute gas velocity at the nozzle outlet and the nozzle axis. For a conical nozzle, it is easy to obtain the following expression for the mean value of angle α :

$$\cos \alpha_a = \frac{2 \cos \beta}{1 + \cos \beta}, \quad (114a)$$

which with $\beta < 30^\circ$ is approximated with a sufficient degree of accuracy by the formula

$$\alpha_a \approx 0.7\beta. \quad (114b)$$

Here β is the angle between the generatrix of the cone and the axis.

The solution of the system of equations after substitution of the values $q(\lambda_a, \alpha_a)$ and $r(\lambda_a, \alpha_a)$ in the right side of (101) and (104) is also carried out for the case $\alpha_a = 0$. Calculations show that with an increase in the nozzle angle of taper the area of the maximum jet cross-sectional area increases, the overexpansion of the gas in the jet increases, and the total losses of total pressure with given values of Π_0 and λ_a grow.

In the solution of a number of problems, it is necessary to know the configuration of the initial part of the jet and the distance between the nozzle and the maximum cross section of the first "barrels." A one-dimensional examination of gas flows does not usually make it possible to obtain data of this type. Here, however, it is possible to indicate the method which makes it possible to approximately determine the outline of the expanding initial part of the jet on the basis of the results obtained from the one-dimensional calculation.

In the definition of the parameters of the gas in the intermediate cross sections of the first "barrels" for each cross section with an area of $\Pi < \Pi_m$ with the use of equations (106) and (107), as noted above, a certain value of the angle α can be found characterizing the value of the radial components of the gas velocity in this cross section. Angle α is comprised by the vector of the absolute mean-mean gas velocity and axis of the jet. In a real nonuniform flow, the angles of deflection of the velocity vectors from the axis are different at different points

of the cross section and increase from the axis to the periphery; therefore, the value of angle α found above will be some mean. However, taking into account that the major portion of the gas flow rate passes through the peripheral zone of the cross sections both due to its larger area and due to the low flow density in the central overexpanded part of the jet, it is possible to assume that this mean value of the angle will be close to the values of the divergence angle α_r at the jet boundary. Arbitrarily assuming that $\alpha_r = \alpha$, we obtain the possibility for the approximate construction of the jet boundaries.

The initial angle of deflection of the jet boundary at the nozzle edge where, due to the presence of a nucleus of undisturbed flow the indicated considerations are unacceptable, is determined analogous to the angle of the rotation of a supersonic flow which flows around an obtuse angle (see § 4 Chapter IV), from the formula

$$\alpha_0 = \beta + \delta \quad (115)$$

Here β is the angle between the tangent to the nozzle generatrix in the outlet section and the axis, and δ is the angle of rotation of the flow from the initial direction which is found from tables (see appendix) for given values of M number at the nozzle edge and ratio of pressures p_a^*/p_m or p_a/p_m . Instead of the tables, for determination of δ with $k = 1.40$ the approximate formula can be recommended (for $\lambda < 2.3$)

$$\delta = 7.6(\lambda_0^2 - \lambda^2) \quad (116)$$

where $\lambda_0 = \lambda(\Pi_0)$ is the velocity coefficient on the jet boundary (i.e., with the full expansion of the gas up to external pressure).

According to the size of the initial angle α_0 and values of angle α found from equations (106) and (107) for several (5-6) values of the relative cross-sectional area $f < f_m$, it is possible to

construct the approximate outlines of the expanding portion of the first "barrels." For this, added consecutively to the straight line drawn through the edge of nozzle at an angle of α_0 , at points corresponding to radii of selected intermediate cross sections r_1, r_2, r_3 , etc., are segments at angles $\alpha_1, \alpha_2, \alpha_3$, etc., up to the intersection with the straight line $r = r_m$; the obtained broken line is rounded off.

In spite of the arbitrariness of the given construction, the outline thus obtained closely corresponds to the form of jet visible in the photograph and also to the result of the calculation according to the method of characteristic if the degree of off-design of the jet does not exceed values $n = 100-150$ (Fig. 7.43).

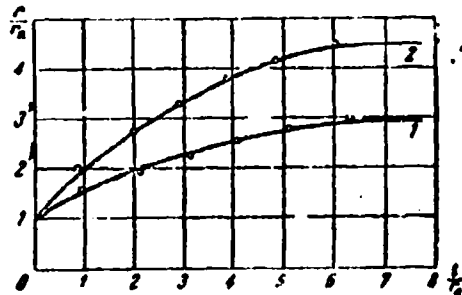


Fig. 7.43. Outline of the expanding portion of the first "barrels" of a supersonic jet. Curves - according to a shadow photograph of the jet, dots - the calculation for 6 cross sections: 1 - $M = 2.5$, $n = 6.43$, $\beta = 5^\circ$; 2 - $M = 1.0$, $n = 24.6$, $\beta = 0$, $k = 1.4$.

All the results presented above are obtained under the assumption that in the initial section of the jet there is no mixing with the environment. This is meaningful to the extent that it makes it possible to reveal the regular laws inherent in the jet itself and to determine the losses which appear in the process of the stabilization of the parameters of an off-design jet. With the large degree of off design, when the initial section is limited by one or two "barrels," the indicated assumption does not produce

considerable error. With a large length of section an increase in the flow mass can become noticeable, which will change the flow parameters in the isobaric cross section. The real mean values of the parameters can be obtained from a calculation similar to the one given above if, during the derivation of the fundamental equations, we consider the difference in the gas flow rate in the initial and final cross sections. In this, value ΔG or G/G_a should be given or determined from an examination of the turbulent mixing of the jet with the environment.

The presented design procedure according to mean values of the parameters in the basic sections of an off-design jet can also be extended to the case of outflow with overexpansion ($n < 1$).

In conclusion, let us recall that the presented one-dimensional theory does not permit obtaining data on the internal structure of a jet and distribution of parameters over its cross section; for this purpose it is necessary to use more complex methods, for example, the method of characteristics. At the same time, some of the results obtained above, for example the values of the parameters in an isobaric cross section, cannot be found by the method of characteristics without additional assumptions.

CHAPTER VIII

GAS FLOWS IN NOZZLES AND DIFFUSERS

§ 1. The Resistance of a Nozzle

The total pressure losses in a nozzle are usually reduced to friction losses. In the ideal case, in the absence of losses the rate of outflow from a nozzle is connected with the ratio of the static pressure in outlet cross section p_a to the total pressure in the nozzle p_{0c} by the known equality

$$\frac{p_a}{p_{0c}} = \left(1 - \frac{k-1}{k+1} \lambda_{a, \text{ideal}}^2\right)^{\frac{k}{k-1}}.$$

In the presence of losses the actual exhaust velocity is less than the ideal:

$$\lambda_a = \varphi \lambda_{a, \text{ideal}} \quad (1)$$

where φ is the velocity coefficient; its value usually equals $\varphi = 0.97-0.99$. Introducing the pressure coefficient which considers the total pressure losses in the nozzle $\sigma_c = p_{0a}/p_{0c}$ we obtain

$$\frac{p_a}{p_{0a}} = \frac{p_a}{\sigma_c p_{0c}} = \left(1 - \frac{k-1}{k+1} \lambda_a^2\right)^{\frac{k}{k-1}};$$

from which the dependence of the pressure coefficient on the velocity coefficient of the nozzle is established:

$$\sigma_c = \left[\frac{1 - \frac{k-1}{k+1} \lambda_{a \text{ и } d}^2}{1 - \frac{k-1}{k+1} \lambda_{a \text{ и } d}^2 \varphi^2} \right]^{\frac{k}{k-1}}. \quad (2)$$

For example with $\lambda_{a \text{ и } d} = 1$ and $\phi = 0.98$ we obtain $\sigma_c = 0.975$.

The relation $\sigma_c = f(\phi)$ with different values of M number in the outlet cross section is presented in Fig. 8.1; the curves are designed according to formula (2) with the use of expression (46) from Chapter I. Figure 8.1 shows that with discharge velocities which considerably exceed the speed of sound ($M > 1.5$), large total pressure losses correspond even to the moderate velocity losses ($\phi > 0.97$).

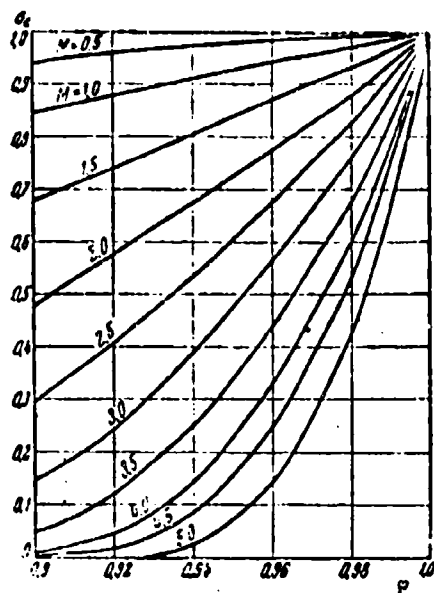


Fig. 8.1. The dependence of the coefficient of the total pressure on the velocity coefficient.

For the calculation of the gas flow rate through a nozzle taking losses into account, in formula (8) in Chapter IV one ought to substitute the value $p_0 = \sigma_c p_{0c}$.

In those cases when the field of total pressures in the nozzle entry cross section is uniform and the outlines of the nozzle are so smooth that there are no vertical regions and shock waves in it, the resistance of the nozzle is reduced to friction drag in the boundary layer. In view of the fact that the length of the nozzle usually is not greater than several nozzle diameters, the thickness of the boundary layer comprises a small fraction of the nozzle radius, i.e., the major part of the cross section of the nozzle is filled by the flow core which consists of jets of constant total pressure in which the parameters of the gas change according to the laws of an ideal adiabatic curve. In that case the total pressures in the flow core in the outlet and entrance cross sections of a nozzle are identical, but due to the existence of a boundary layer a precise value of the discharge velocity cannot be determined directly by formulas (2) and (3) or (4) of Chapter IV. However, it is possible to make use of these formulas if we introduce a correction into the value of the transverse cross-sectional area of the nozzle, applying the concept about the thickness of displacement of the boundary layer (see § 2, Chapter VI).

As is known, the displacement of a wall from its true position away from the nozzle axis by a distance equal to the displacement thickness (Fig. 8.2) leads to the fact that the distribution of static pressure and velocity over the deflected wall with its flow-around b , a viscous liquid turns out to be the same as over a true wall flowed around by an ideal fluid. In other words, by the appropriate increase in the transverse cross sections of the nozzle it is possible to compensate for the boundary layer effect on the distribution of velocity and pressure along the axis of the nozzle. Conversely, if we replace the given nozzle by a fictitious one whose outline in each cross section is shifted toward the nozzle axis by a distance equal to the displacement thickness δ^* , then the velocity distribution along the length of the fictitious nozzle can be determined according to isentropic formulas (2), (3) or (4) of Chapter IV, whereupon it turns out to be the same as in the given nozzle.

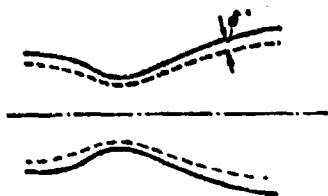


Fig. 8.2. Diagram of a change in the displacement thickness δ^* along the length of a nozzle.

In a plane-parallel nozzle the area of the fictitious cross section F_ϕ is found from the condition

$$\frac{F_\phi}{F} = 1 - \frac{2\delta^*}{b}, \quad (3)$$

where b is the width of the transverse cross section of the given nozzle.

In an axisymmetric nozzle

$$\frac{F_\phi}{F} = \left(1 - \frac{\delta^*}{R}\right)^2 \approx 1 - \frac{2\delta^*}{R}; \quad (4)$$

here R is the radius of the given nozzle.

Then the discharge velocity from the given nozzle is determined from the formula

$$\frac{F_{\phi \text{ up}}}{F_{\phi \text{ th}}} = \left(\frac{k+1}{2}\right)^{\frac{1}{k-1}} \lambda_a \left(1 - \frac{k-1}{k+1} \lambda_a^2\right)^{\frac{1}{k-1}} = q(\lambda_a) \quad (5)$$

In this formula $F_{\phi \text{ a}}$ - the discharge cross section of a fictitious nozzle, $F_{\phi \text{ up}}$ - the throat area of the fictitious nozzle.

In the core of the constant total pressure which fills the major part of the transverse cross section of a given nozzle, the gas velocity is determined by equation (5). In accordance with this value of velocity, using known formula (72) in Chapter I which corresponds to the ideal adiabatic process in a gas flow, it is

possible to find the static pressure in the corresponding transverse cross section of the given nozzle:

$$\frac{p}{p_0} = \left(1 - \frac{k-1}{k+1} \lambda^2\right)^{\frac{k}{k-1}}; \quad (6)$$

here p_0 is the total pressure on the axis of the nozzle whose value in all cross sections is identical.

The consideration of the boundary layer effect by means of the replacement of the true nozzle outline by a fictitious outline leads to the narrowing of the nozzle; therefore, in a subsonic flow the boundary layer causes an increase, and in a supersonic flow - a decrease in velocity (as compared with the case of the flow of a nonviscous gas in a nozzle of true outline).

Thus, in spite of the retention of the total pressure in the core of the flow, the velocity in the core in a subsonic nozzle proves to be more than in the ideal case: $\lambda_a > \lambda_{a \text{ ид}}$, and in a supersonic nozzle - less than in the ideal case: $\lambda_a < \lambda_{a \text{ ид}}$. In accordance with this, the static pressure in any cross section of a true nozzle with subsonic flow is reduced, and with supersonic flow is increased in comparison with the pressure in the same cross section of an ideal nozzle.

In view of the smallness of the corrections which consider the boundary layer effect on the velocity and the pressure, their value can be obtained by means of the expansion of formula (5) into a number. Omitting the indices in (5), we have

$$\frac{p}{p_0} = \frac{\left(\frac{2}{k+1}\right)^{\frac{1}{k-1}}}{\lambda \left(1 - \frac{k-1}{k+1} \lambda^2\right)^{\frac{1}{k-1}}}.$$

If a change in the transverse cross-sectional area by a small value of ΔF causes a change in the velocity also by a small value of $\Delta \lambda$, then with $k = \text{const}$

$$\frac{F + \Delta F}{F} = \frac{\lambda \left(1 - \frac{k-1}{k+1} \lambda^2\right)^{\frac{1}{k-1}}}{(1 + \Delta \lambda) \left[1 - \frac{k-1}{k+1} (\lambda + \Delta \lambda)^2\right]^{\frac{1}{k-1}}}.$$

After expansion into a binomial series and rejection of all terms with factors on the order of $\Delta \lambda^3$ and above as a result of the smallness we obtain

$$\frac{\Delta F}{F} = \frac{\Delta \lambda}{\lambda} \frac{\lambda^2 - 1}{1 - \frac{k-1}{k+1} \lambda^2} + \frac{\Delta \lambda^3 (3 - \lambda^2)}{(k+1) \left(1 - \frac{k-1}{k+1} \lambda^2\right)^2}. \quad (7)$$

In all cases except $\lambda = 1$, this formula can be simplified after also rejecting the term with factor $\Delta \lambda^2$. Then we have

$$\frac{\Delta F}{F} = \frac{\Delta \lambda}{\lambda} \frac{\lambda^2 - 1}{1 - \frac{k-1}{k+1} \lambda^2}. \quad (8)$$

In the case of $\lambda = 1$, i.e., in the vicinity of the supersonic nozzle throat, formula (7) acquires a very simple form:

$$\frac{\Delta F}{F} = \frac{k+1}{2} (\Delta \lambda). \quad (9)$$

Hence, it follows that an insignificant change in the cross-sectional area of the nozzle near the throat causes a noticeable velocity change. For example, a change in the area of the nozzle near the throat by 1% ($\Delta F/F = 0.01$) gives a velocity change of 0.009 ($\Delta \lambda = 0.09$).

Formula (8) establishes the connection between small deviation in the cross-sectional area and the corresponding small change in

the gas flow rate. Upon consideration of the boundary layer effect on the flow rate it is possible to introduce the displacement thickness instead of a change in the cross-sectional area; for an axisymmetric nozzle according to (4) we have

$$\frac{\Delta P}{P} \approx \frac{2\delta^*}{R} = 2\lambda^2.$$

Hence the connection between the displacement thickness and velocity change assumes the following form (with $\lambda \neq 1$):

$$\delta^* = \frac{1}{2} \lambda \frac{\lambda^2 - 1}{1 - \frac{k-1}{k+1} \lambda^2}. \quad (10)$$

For example, a change in the velocity coefficient by 3% with $k = 1.4$ and $\lambda = 1.5$ ($M = 1.73$) is achieved because of the displacement thickness δ^* , which comprises ~3% of the radius of the nozzle.

The small pressure changes caused by small velocity changes can also be calculated according to the formula obtained by means of the expansion of equality (72) of Chapter I into a binomial series and the rejection of all terms with the factors on the order of $\Delta\lambda^2$ and above. In fact,

$$\frac{P}{P_0} = \left(1 - \frac{k-1}{k+1} \lambda^2\right)^{\frac{k}{k-1}};$$

hence

$$\frac{P + \Delta P}{P} = \left[\frac{1 - \frac{k-1}{k+1} (\lambda + \Delta\lambda)^2}{1 - \frac{k-1}{k+1} \lambda^2} \right]^{\frac{k}{k-1}}$$

and, further,

$$\frac{\Delta P}{P} = - \frac{\Delta\lambda \cdot \frac{2k}{k+1} \lambda^2}{1 - \frac{k-1}{k+1} \lambda^2}. \quad (11)$$

For the example examined above ($\Delta\lambda/\lambda = 0.03$, $\lambda = 1.5$), from (11) we obtain $\Delta p/p \approx 0.12$. In the case of $\lambda = 1$, for the dependence of the pressure increase on the velocity increase we obtain the following simple formula:

$$\frac{\Delta p}{p} = -k\Delta\lambda \quad (12)$$

i.e., in the vicinity of the throat the pressure change is proportional to the velocity change.

In view of the presence of a boundary layer, the mean gas velocity in the transverse cross section is less than the velocity in the core of the flow: $\lambda_{cp} < \lambda_a$. For the calculation of the mean velocity for the mass of the gas

$$\lambda_{cp} = \frac{1}{Q} \int_0^Q \lambda_a dQ$$

it is possible to utilize the concept of the momentum thickness in the boundary layer δ^{**} (see Chapter VI). This value shows by what distance δ^{**} it is necessary to displace the nozzle outline (toward its axis) so that a uniform flow in the fictitious nozzle with the same velocity as in the flow core of a true nozzle would have the same per-second momentum as in a true nozzle. Then

$$\lambda Q_p = \lambda_a Q$$

Hence, the velocity coefficient which considers the boundary layer effect is equal to

$$\varphi = \frac{\lambda_{cp}}{\lambda_a} = \frac{Q_p}{Q} = \frac{F_p}{F} = 1 - 2\delta^{**}, \quad (13)$$

where

$$\delta^{**} = \frac{v^{**}}{K}.$$

Let us note that the value ϕ in formula (13) expresses the ratio of the mean velocity for the mass of the gas to the velocity in the flow core and not to the velocity in an ideal nozzle. The transition to the value

$$\psi = \frac{\lambda_{sp}}{\lambda_{no}}$$

can be realized in the following way:

$$\psi = \gamma \frac{\lambda_{no}}{\lambda_o} = (1 - 2\xi^{**}) \frac{\lambda_{no}}{\lambda_o},$$

where according to (10)

$$\xi^{**} = \frac{\lambda_{no} - \lambda_o}{2\lambda_{no}} \frac{\lambda_{no}^2 - 1}{1 - \frac{1}{\gamma} \lambda_{no}^2}.$$

The experiments of Keenan and Nauman¹ make it possible to estimate the ratio of the fictitious diameter of the nozzle outlet D_ϕ to the true diameter of the outlet (D_a) with different values of R and M numbers. The results of these experiments are reduced to a table.

Noz- zle	D_{sp}	D_a	M_a	R_a	$M_{a, no}$	$\frac{D_\phi}{D_o}$
1	0.562"	0.445"	2.06	$3.9 \cdot 10^4$	2.58	0.79
2	0.186"	0.498"	3.14	$3.9 \cdot 10^4$	3.56	0.82
3	0.175"	0.438"	—	$3.8 \cdot 10^4$	—	—
4	0.107"	0.498"	3.87	$1.2 \cdot 10^4$	4.80	0.87
5	0.184"	0.406"	2.84	$0.27 \cdot 10^4$	3.59	0.71

Diameters of the critical D_{sp} and outlet D_a cross sections are given in this table in inches and R_a numbers are calculated according to the outlet diameter of the nozzle. As we see, true

¹Keenan I., Nauman E. Journal of Applied Mechanics, No. 2, Vol. 13, June 1946.

values of the M_a number in the outlet cross section are lower than the calculated one ($M_a < M_{a_{ид}}$) and the fictitious diameter of the outlet aperture is less than the true by 18-33%, i.e., the dimensionless displacement thickness

$$\delta^* = 0.18 - 0.33,$$

whereupon the smaller values of the displacement thickness correspond to the higher values of R_a number.

The presence of large pressure gradients extremely complicates the boundary-layer calculation in nozzles, especially at supersonic speeds. The approximate design procedure of a turbulent boundary layer in a Laval nozzle developed by Bartz¹ is based on the following assumptions: the velocity profile and excess temperature in all cross sections of the nozzle are subordinated to "law 1/7," the local values of the friction coefficient on the wall and the boundary layer thicknesses are connected by the same relation as in the case of a plate, the Nusselt layer is calculated as one-dimensional (without consideration of the boundary layer effect). The results of such a calculation for the nozzle depicted on Fig. 8.3 are given on Fig. 8.4, where along the ordinate the thicknesses of the dynamic boundary layer δ are laid off (in inches), and along the abscissa the distance from the beginning of the nozzle to the current cross section is laid off, expressed in fractions of the reduced length of the nozzle x_n (in this example $x_n = 8.02''$). The calculation is performed for two cases when in the beginning of the nozzle the boundary layer thickness $\delta_0 = 0.188''$ and when $\delta_0 = 0$. The most important result of this calculation, confirmed by experimental data, consists in the fact that the boundary layer thickness in the throat is very small ($\delta_{np} = 0.028$; $\delta_{np}^* = 0.0035$) and virtually does not depend on the boundary layer thickness in

¹Bartz D. R., An Approximate Solution of Compressible Turbulent Boundary Layer Development, ASME Paper, N 54-A-153, 1954, Trans. ASME, v. 77, No. 2, 1955, p. 1235-1245.

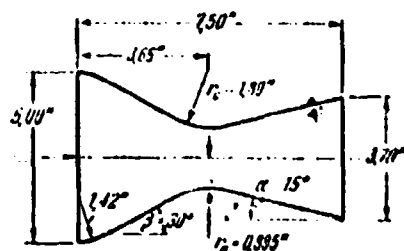


Fig. 8.3.

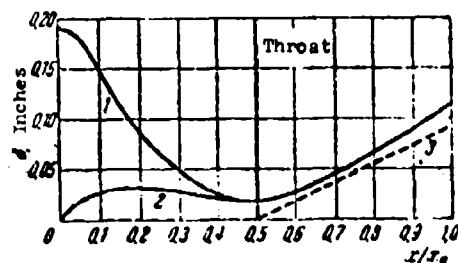


Fig. 8.4.

Fig. 8.3. Laval nozzle (from the work of Bartz).

Fig. 8.4. Change in the boundary layer thickness δ along the length of a conical Laval nozzle (see Fig. 8.3): 1 - thickness of layer in the initial cross section $\delta_0 = 0.188$ "; 2 - the same with $\delta_0 = 0$; 3 - thickness of layer in the throat $\delta_{np} = 0$.

the initial cross section of the nozzle. This means that the boundary layer thickness in the outlet cross section of a Laval nozzle can be approximately determined on the assumption that in the throat it is equal to zero ($\delta_{np} \approx 0$). This case is shown on Fig. 8.4 by the dotted curve.

The values of total pressure (taking into account the boundary layer) in the outlet section of a conical supersonic nozzle can be estimated approximately according to the following formula:¹

$$\left(\frac{p_0}{p_{0np}}\right)^{\frac{2\gamma}{\gamma-1}} = \left[\frac{1 + \frac{\gamma-1}{2} M^2}{\frac{\gamma+1}{2}} \right]^{\frac{\gamma+1}{\gamma-1}} \frac{M^{\frac{2\gamma}{\gamma-1}}}{e^{\frac{\gamma}{\gamma-1}}}, \quad (14)$$

here p_0 is the mean total pressure on the cross section at the outlet, p_{0np} - the same in the nozzle throat, M - the computed value of the Mach number, α - the half angle of aperture of the nozzle, c_f - the value of the coefficient of friction. The curves calculated from formula (14) with $k = 1.4$ are depicted on Fig. 8.5.

¹Evvard J., Diffusers and Nozzles - in the collection High Speed Aerodynamics and Jet Propulsion, v. VII, 1957, p. 638-654. Russkiy perevod Izd. inostr. lit., 1959.

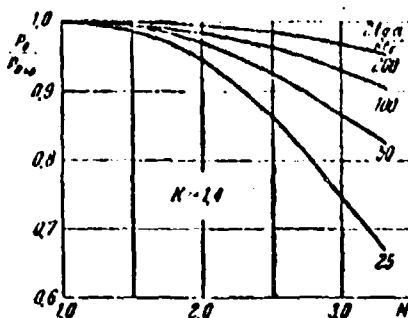


Fig. 8.5. Change in total pressure along the length of the nozzle, presented depending on the local value of the Mach number.

For calculating the value of the friction coefficient in a nozzle it is possible to use the approximate relation¹ which is in good agreement with the data of Chapter VI:

$$c_f = 0.003 \left[1 + 0.72 \frac{k-1}{2} M^2 \right]^{-0.378}. \quad (15)$$

Besides the friction drag, the losses connected with the nonuniformity of flow in the zone of the throat and the deviation of the flow from the axial direction at the nozzle exit are important.

The complete velocity coefficient of a nozzle ϕ can be presented in the form of the product of three coefficients which consider friction losses (ϕ_f), losses from the nonuniformity of flow in the throat of the nozzle (ϕ_p), and loss as a result of the deviation of the flow in the outlet section from the axial direction (ϕ_α):

$$\phi = \phi_f \phi_p \phi_\alpha. \quad (16)$$

Value ϕ_f is calculated with the aid of the methods of boundary-layer theory of a compressible gas (see Chapter VI).

¹Ahlberg J., Hamilton S., Migdal R., Nilson E. Truncated Perfect Nozzles in Optimum Nozzles Design, ARS J., 31, 1961, p. 614-620.

Value ϕ_p in conical nozzles depends mainly on the relative radius of curvature of the nozzle wall in the area of the throat; the corresponding experimental data of Rao¹ are approximated well by the exponential formula

$$\gamma_p = 1 - 0.032k \left(\frac{R_{kp}}{r} \right)^{1.4} \quad (17)$$

here k is the adiabatic index (in experiments $k = 1.23$ and 1.4), R_{kp} is the radius of the critical cross section (throat), and r is the radius of curvature of the nozzle wall in the area of the throat. In Rao's experiments relation R_{kp}/r changed from 0 to 1.

The coefficient ϕ_a for a uniform conical flow at the nozzle edge is determined from the mean value of the projection of the velocity vector to the nozzle axis

$$\gamma_a = \frac{1 + \cos \alpha}{2} \quad (18)$$

Here α is the half-angle of aperture of the nozzle.

If there are losses, then the maximum thrust is reached not with the design nozzle configuration, but with a certain under-expansion of the gas since a small contraction in the output pulse in this case is more than compensated for by a gain because of a decrease in losses.

The following analytical dependence of the optimum degree of expansion of the nozzle on the velocity coefficient is in good agreement with the experimental data:²

¹Rao G. V., Evaluation of Conical Nozzle Thrust Coefficient. ARS J., N 8, 1959, p. 606-607.

²Durham F. P., Thrust Characteristics of Underexpanded Nozzles, Jet Prop., N 12, 1955, p. 696-700.

$$\frac{F_a}{F_{kp}} = \sqrt{\frac{k-1}{k+1}} \frac{1 - \phi \left[1 - \left(\frac{p_a}{p_0} \right)^{\frac{k-1}{k}} \right]}{\frac{2}{k+1} \sqrt{\frac{p_a}{p_0}} \sqrt{1 - \left(\frac{p_a}{p_0} \right)^{\frac{k-1}{k}}}} \left[1 - \frac{1}{\phi^2} \frac{k-1}{k+1} \right]^{\frac{k}{k-1}}. \quad (19)$$

where F_a , F_{kp} are the areas of output and critical cross sections, p_a - pressure on the nozzle edge, p_0 - the total pressure at the outlet in the nozzle, ϕ - velocity coefficient of the nozzle, ϕ_{kp} - velocity coefficient taking into account losses only in the tapering portion of the nozzle. With $\phi = \phi_{kp} = 1$ formula (19) is identical with formula (4) in Chapter IV obtained for an ideal nozzle of which it is possible to be convinced after substituting relation (6) in (19).

Under conditions of outflow from a nozzle with large over-expansion, when a bridge-type shock is established on the nozzle edge (Fig. 8.6), the ratio of pressures on the edge p_H/p_a can prove to be higher than the critical one for the boundary layer of the nozzle with its interaction with the oblique shock wave ab. In this case the boundary-layer separation from the wall appears and the system of shocks displaces inside nozzle to cross section a', where the velocity is less ($\lambda'_a < \lambda_a$) and the pressure before the shocks is higher ($p'_a > p_a$) than in cross section a; with the proper decrease in the ratio of pressures in the oblique shock

$$\frac{p'_a}{p_a} = \bar{p}_{kp}(M) < \frac{p_a}{p_0}.$$

The system is stabilized and the outflow proceeds with separation from the wall at a supersonic speed less than in the design conditions. Beyond the locus of separation the pressure on the wall within the nozzle is equal to atmospheric pressure, in connection with which higher thrust is obtained than under the conditions of full overexpansion when in the outlet section of the nozzle rarefaction predominates (see § 2, Chapter IV). The calculation of the flow separation in the nozzles is a difficult

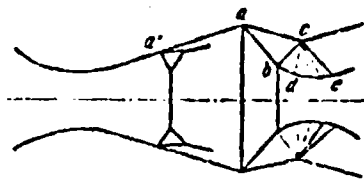


Fig. 8.6. Outflow from a Laval nozzle with strong overexpansion: abc - bridge-type shock on the edge, a' - shock within the nozzle caused by separation of flow.

task. Experimental study of this phenomenon made it possible to obtain the following generalized relation:¹

$$\frac{p_{0 \text{ отп}}}{p_{0 \text{ расч}}} = \frac{p_a}{p_{0 \text{ расч}}}^{0.336} \quad (20)$$

Here $p_{0 \text{ отп}}$ is the total pressure at which separation occurs, $p_{0 \text{ расч}}$ - the total pressure in the design mode. Another empirical relation is applied:²

$$\frac{p_a}{p_{0 \text{ отп}}} = 1 + 0.39 \left(\frac{p_a}{p_{0 \text{ расч}}} \right) \quad (21)$$

Only with the displacement of the system of shocks to the zone with Mach number $M \leq 1.3$ (see § 8, Chapter VI) does the boundary-layer separation cease and the system degenerates into a shock close to a straight line behind which a subsonic diffuser flow is established right up to the nozzle edge. The regions of the unstable gas flow in the nozzles are depicted on Fig. 8.7.

¹Ashwood P. F., Higgins D. G., The Influence of Design Pressure Ratio and Divergence Angle on the Thrust of Convergent-Divergent Propelling Nozzles. ARC CP N 325, 1957.

²Fraser R. P., Eisenklam P., Wilke D., Investigation of Supersonic Flow Separation in Nozzles, J. of Mech. Eng. Science, Vol. 1, N 3, 1959, pp. 267-279.

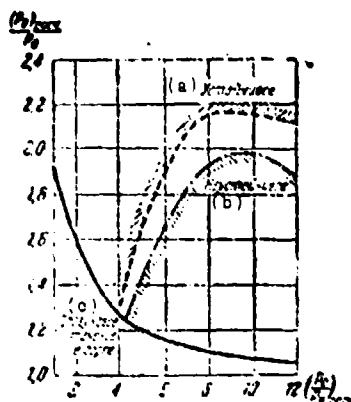


Fig. 8.7. Regions of unstable flow in Laval nozzles.

KEY: (a) Stable; (b) Unstable; (c) Subsonic flow in throat.

8.2. The Forms of Nozzles

Figure 8.3 shows a Laval nozzle composed of two cones connected by a neck which is described by a circular arc. Such nozzles are applied with not very large supersonic speeds of outflow ($M < 3$). It is recommended that the lateral angles of the tapering portion of the nozzle be taken within the limits of $15-30^\circ$, and of the expanding portion - within limits of $5-8^\circ$, and the radius of curvature of the wall of the neck should be not less than the throat diameter. Under these conditions such a conical nozzle provides (according to experimental data) a decrease in the pulse in comparison with the nozzles of special shape of not more than 1-2%.

For obtaining a uniform parallel flow (in connection with supersonic wind tunnels and the jet apparatuses with a very high velocity of outflows) nozzles are used with specially shaped walls for the construction of which methods of characteristics or functional series are employed.¹

¹Katskova O. N., Naumova I. N., Shmyglevskiy Yu. D., Shulishin N. P., The Experience of the calculation of plane and axisymmetric supersonic gas flows by the method of characteristics. The data processing center of the A. S. of the USSR, 1961.

Let us present a simple geometric method for the calculation of a nozzle¹ which provides outlines very close to optimum. The neck of such a nozzle is described by two circles: subsonic part - with a radius of $1.5 R_{np}$ and the supersonic part - with a radius of $0.4 R_{np}$, where R_{np} is the radius of the throat (Fig. 8.8). Drawn to the segment of the arc of a radius of $0.4 R_{np}$ at a given angle θ_N to the nozzle axis is tangent NQ up to the intersection with segment Qa which passes through the nozzle edge and is inclined toward the axis at a given angle θ_a (in the case of a wind tunnel $\theta_a = 0$). Segments NQ and Qa are divided into an equal number of sections, in which regard the dividing points of line Qa are connected with the like-named dividing points of line NQ; the envelope of the obtained grid of straight lines forms the sought nozzle contour.

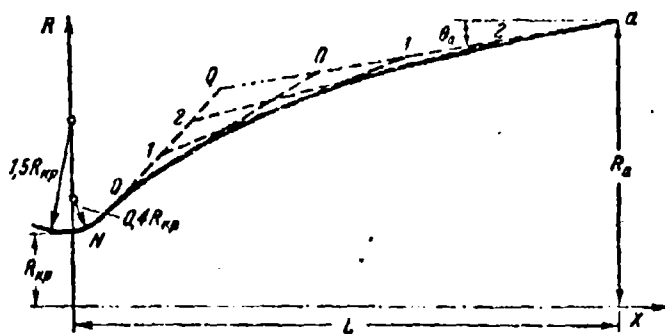


Fig. 8.8. Diagram of the construction of a nozzle outline.

Figure 8.9 presents graphs for determining the slope angles θ_N (solid lines) and θ_a (dotted line) for given values of relative length of a nozzle L/R_{np} and the relative radius of outlet cross section R_a/R_{np} . The quality of the described geometric method of the construction of nozzles can be judged from this example: the maximum linear deflection of the outline from the optimum,

¹Rac G., Approximation of Optimum Thrust Nozzle Contour. A. R. S. J., N 6, 1960, p. 561.

calculated with respect to a precise procedure, for nozzle

$$R_a = 5R_{kp}, \quad l = 12R_{kp} \text{ is } 0.03 R_{kp}.$$

The outline of the shortest possible nozzle is determined by the displacement of point N (Fig. 8.8) to the critical cross section ("angular nozzle"); angle θ_N is selected so that an increase in the Mach number in a Prandtl-Meyer flow (near point N) would occur up to the value of the Mach number on the nozzle edge.

There is great practical interest in a nozzle with an inner body, a schematic diagram of which is given on Fig. 8.10. In such a nozzle the gas flows along an annular channel (between the inner body and the cowl); the critical cross section can be regulated either by the longitudinal travel of the inner body or by the rotation of flaps on the cowl. Figure 8.11 depicts two types of nozzle with an inner body: a) with partial internal and b) with purely external expansion of the gas. In the first case, from the critical cross section to cross section A the supersonic jet is expanded in the channel, and beginning from point A the outer edge of the expanding jet is free. If point of inflection O of the supersonic part of the nozzle is placed in the critical cross section, then the characteristics exiting from it in the form of a beam (first family) are reflected from the cowl and the reflected characteristics (second family) fall on the walls of the inner body.

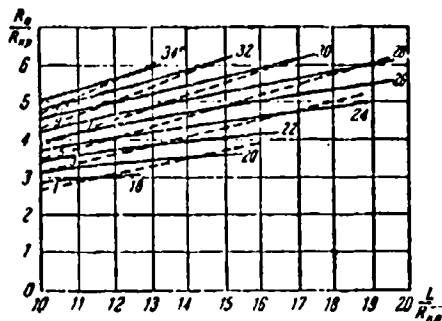


Fig. 8.9. The dependence of angles θ_N (solid lines) and θ_a (dotted line) on the relative values of length and radius on the nozzle edge.

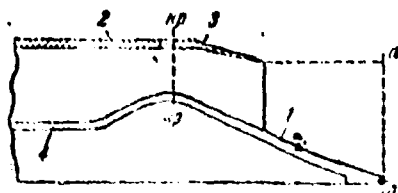


Fig. 8.10. Diagram of a nozzle with an inner body: 1 - inner body; 2 - cowl-ling; 3 - adjustable flaps; 4 - cooling air.

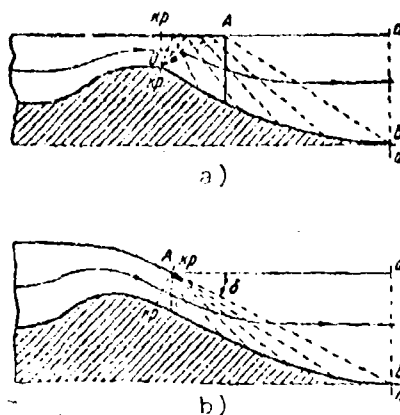


Fig. 8.11. Diagram of nozzles with an inner body: a) with point of inflection with mixed expansion; b) with purely external expansion.

Flow is turned toward the axis of symmetry, intersecting the characteristics of the first family, and then returns to the initial direction, intersecting the characteristics of the second family. The shape of the inner body is selected in such a way that at the point of fall of any characteristic the flow direction behind it would coincide with the direction of the wall; in this case the characteristics of the second family are not reflected from the inner body (they attenuate). Behind the extreme characteristic AB the gas flows evenly and rectilinearly.

In a nozzle with purely external expansion (Fig. 8.11b), the critical cross section and the point of inflection of flow are disposed on section A of the cowl-ling.

The expansion of a gas in this case is one-way, and the throat is inclined toward the axis by the angle δ equal to the angle of rotation of the gas flow near point A upon acceleration from critical velocity ($M = 1$) to the computed value of the Mach number (M_a) for this pressure ratio. The overall length of the part of the inner body protruding beyond the cowling (afterbody) is determined by the point of intersection of the last characteristic AB with the axis. Experiments show, however, that the afterbody of the inner body can be shortened by 30-50% without a noticeable reduction in the thrust.

In a nozzle throat made in accordance with the second scheme (Fig. 8.11b) the cowling should be parallel to the wall of the inner body; this leads to additional drag in connection with the losses to the external flow about the convergent section of the cowling.

With not very large design values of Mach number ($M_a \leq 2$) the inner body can be made conical.

Nozzles with an inner body are obtained considerably shorter than the usual Laval nozzles and unlike the latter give very small reductions in relative pulse at pressures considerably lower than designed (due to the absence of walls in the supersonic part the overexpansion of gas does not occur).

Figure 8.12 presents the experimental data of Pearson¹ on a change in the relative value of output pulse I with deviation from the design conditions ($p_{0a}/p_H = 8$) for the Laval nozzle and nozzle with an inner body (dotted line).

¹Krase W. H. Performance analysis of plug nozzles for turbojet and rocket exhausts, Paper A. S. M. E., N 58, A. 246, 1958.

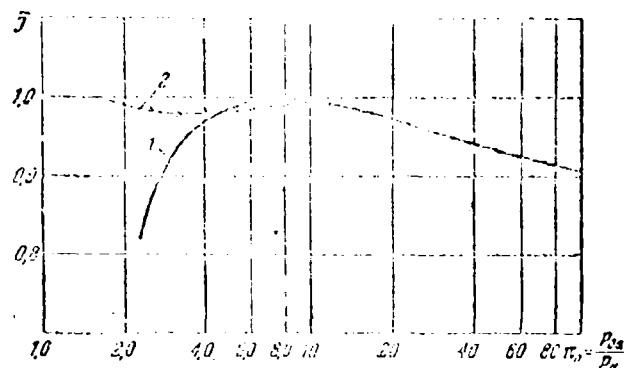


Fig. 8.13. Comparison of the characteristics of a liquid nozzle (1) and nozzle with an inner body (2).

The design expansion ratio of a nozzle with an inner body can be determined from the ratio of the cross-sectional area $a-a$ (Fig. 8.11) of a cylindrical surface which has the outlet cross section diameter of the nozzle to the throat area.

In the case of a plane nozzle the outline of the inner body is the flow line of a fluid element that leaves a convex angle.

In the case of an axisymmetric nozzle the outline of the inner body is found according to the method of characteristics. However, with a shortened afterbody the outline of an axisymmetric inner body is close to the flow line of a plane flow.

The scheme of a nozzle with a central insert is known (Fig. 8.13) whose throat is also circular, but the expansion of the supersonic flow in it occurs with rotation near the external wall and not the inner body. A central insert is formed a cavity with a free surface. The dimensions depend on the Mach number at the nozzle exit (with an increase in Mach number the cavity is reduced).

Great practical value, especially for JET (jet engines) is had by an ejector nozzle (Fig. 8.14) in which the combustion

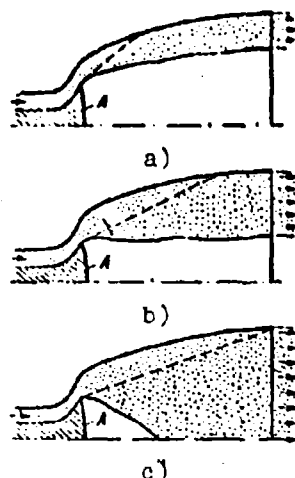


Fig. 8.13.

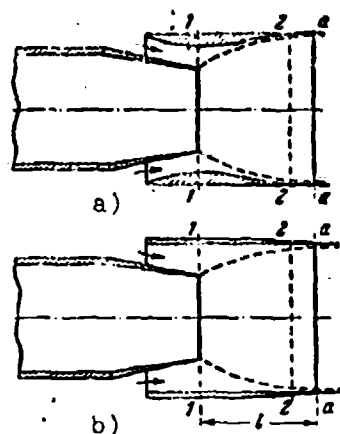


Fig. 8.14.

Fig. 8.13. Flow conditions in a nozzle with the central insert: a) at the ground; b) at the medium altitudes; c) at high altitudes.

Fig. 8.14. Diagrams of ejector nozzles: a) with the shaped cowling; b) with cylindrical cowling.

products of the engine escape through the simple narrowing nozzle placed inside an external cowling coaxial with it which has a special shape (Fig. 8.14a) or the form of a cylindrical ring (Fig. 8.14b). The critical velocity is established on the edge of the internal nozzle and if pressure here is higher than the surrounding pressure, then the central jet within the ejector is expanded, narrowing the flow cross sections of the airflow being ejected by it which enters an annular channel from the intermediate compressor stage or from the atmosphere.

The velocity of the ejected flow is usually less than the speed of sound; therefore, in the outlet section of the ejector it is accelerated. In some cross section 2-2 (Fig. 8.15) the pressures of two flows are equalized; the more the excess pressure in it, the further this cross section is located from the edge of the internal nozzle. The transverse dimension of the internal

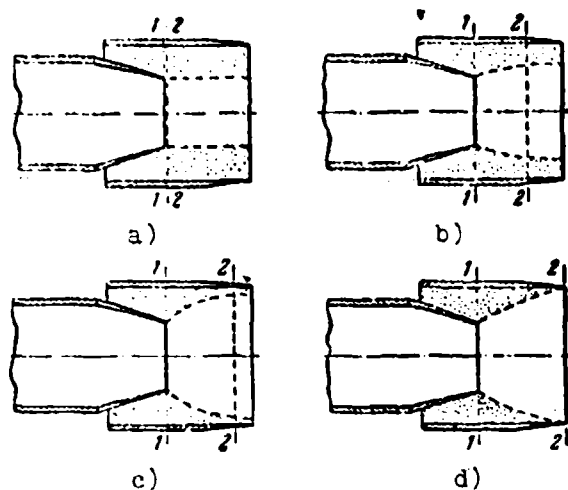


Fig. 8.15. Diagrams of flow in an ejector nozzle in off-design conditions: a) pressure on the edge of an internal nozzle equal to atmospheric; b) small pressure excess on the edge of an internal nozzle; c) critical mode of ejector; d) cutoff mode of the ejector.

jet increases, and of the ejected jet - decreases with an increase in the excess pressure in the internal nozzle. The configurations of two flows with different values of excess pressure are shown on Fig. 8.15. The operating mode of the ejector in which the secondary flow is accelerated (in cross section 2-2) to the speed of sound is called *critical* (Fig. 8.15c); if the central jet is expanded so much that it fills the entire outlet cross section of the ejector (Fig. 8.15d), then the *cutoff* condition begins where the flow rate of the ejected gas is equal to zero.

For the regulation of an ejector nozzle it is possible to install rotary flaps both on the internal nozzle and on the external cowling (Fig. 8.16).

If the parameters of the ejector nozzle are selected in such a way that in cross section 2-2 (Fig. 8.15) atmospheric pressure is obtained, then the expansion of the ejection gas will be complete; in this case, the thrust of the ejector nozzle is

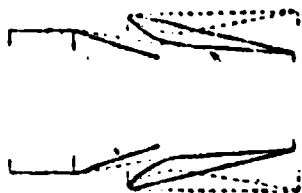


Fig. 8.16. Ejector nozzle with controllable cross sections of neck and edge.

greater than that of a simple tapered nozzle since the pressure on the part of the ejected gas on the wall of the internal nozzle is higher than atmospheric. The cross section of the cowling of an ejector nozzle should be such that in the design mode the flow rate of the ejected gas would decrease to the minimum necessary for the purposes of cooling the wall.

A reduction in the pressure excess in an ejector nozzle leads to a decrease in the velocity of the internal jet in cross section 2-2, which averts the possibility of the overexpansion of the gas and corresponding thrust loss (in comparison with a Laval nozzle).

A typical characteristic of an ejector nozzle of a TRD, i.e., the relation between the coefficient of ejection $k_{\text{эж}} = (G_{\text{эж}}/G_{\text{вн}})$ and the ratio of the total pressure of the internal jet to atmospheric pressure is depicted on Fig. 8.17. In order for the ejector nozzle to operate under the most advantageous conditions, it is necessary to regulate the flow rate of secondary air (with low flying speeds increasing the coefficient of ejection to values on the order of $k_{\text{эж}} = 0.1$ and reducing it with high speeds to a minimum on the order of $k_{\text{эж}} = 0.01-0.02$). The ratios of the total pressure of the ejected air in the nozzle to the total pressure in the inlet duct of the engine ($p_{0 \text{ эж}}/p_{0 \text{ д}}$) which can be recommended for obtaining the optimum modes for operation of the ejector nozzle at different flying speeds (or M_0) are given on Fig. 8.18.

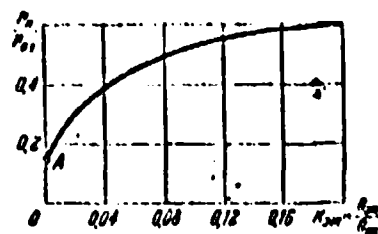


Fig. 8.17. The characteristic of an ejector nozzle.

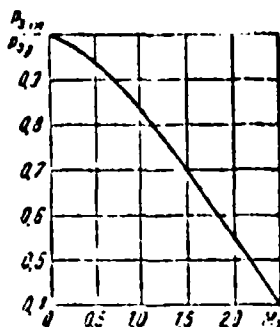


Fig. 8.18. The ratio of the total pressure of secondary air to the total pressure in the inlet duct of an engine for optimum conditions in the ejector nozzle.

The optimum relative length of an ejector nozzle which provides the smallest thrust losses in the design mode,¹

$$\bar{l} = \frac{l}{R_t} \approx 1 + 1.2,$$

where l is the distance from the edge of the internal nozzle to the edge of the cowling, R_t is the radius of the critical (outlet) cross section of the internal nozzle.

The thrust of an ejector nozzle is equal to the total pulse of two jets on the edge of the cowling. The parameters of jets with cylindrical cowling are determined from conditions for the maintenance of flow rate and pulse (not considering friction) between cross sections 1 and 2 of the edges of the internal nozzle

¹Person H., Holliday J., Smith S., A Theory of the Cylindrical Ejector Supersonic Propelling Nozzle, R. A. S. v. 62, NN 573, 574, 1958.

and the cowling (see the calculation of a gas ejector in Chapter IX) under the assumption of the absence of mixing of the jets. This task has two solutions from which they select the one in which the internal jet in cross section 2 is supersonic and the jet being ejected is subsonic or sonic. The extent to which data of such a calculation correspond to experimental data can be judged from Fig. 8.19 where along the ordinate the relation of the total pressures of two flows is laid off, and along the abscissa - the ratio of the total pressure of the internal jet to atmospheric pressure. The data presented pertain to the case where the ratio of the areas on the edge of the cowling F_a and the internal nozzle F_{np} is 1.73. Serving as the variable parameter for the curves is the product $k_{эм} \sqrt{(T_{01}/T_{0a})}$, where T_{01} and T_{0a} are the stagnation temperatures of external and internal jets. The horizontal sections of curves correspond to the critical modes of the nozzle.

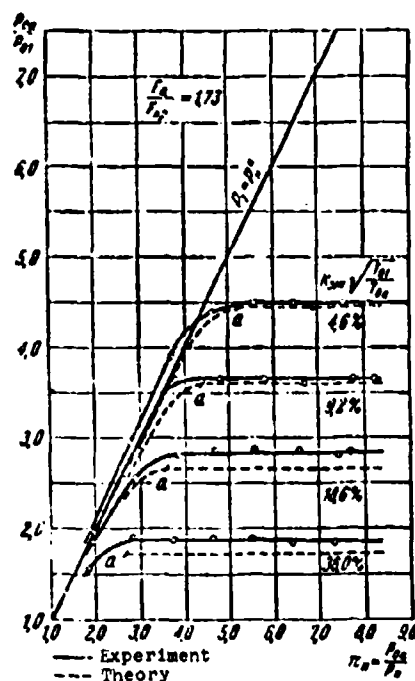


Fig. 8.19. Characteristics of an ejector nozzle ($F_a/F_{np} = 1.73$, $\bar{z} = 0.6$).

Losses in an ejector nozzle reach the minimum when the relation of the velocities of two jets on the edge of the internal nozzle is equal to the relation of their total enthalpies.¹

The typical nature of the dependences of the thrust of a TRD on the coefficient of ejection with different values of M_∞ number of flight is shown on Fig. 8.20. The dashed line connects the modes of the maximums of thrust. In view of the flatness of curves $P(k_{\text{эм}})$ it is possible to select the values of the coefficients of ejection considerably lower than optimum, which makes it possible to decrease the flow rate of secondary air.

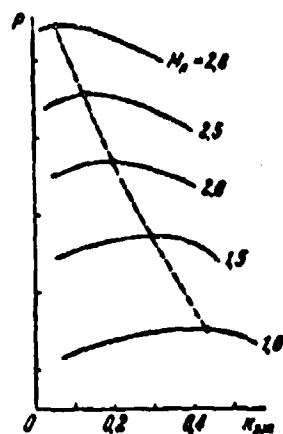


Fig. 8.20. For determining the optimum values of the coefficient of ejection.

§ 3. The Resistance of a Subsonic Diffuser

Let us examine the diffuser of an engine installed in a moving aircraft. Let the velocity of the aircraft be w_∞ , and the speed of sound which corresponds to the temperature of the

¹Knox R., The Optimized Ejector Nozzle Thrust Augmenter JASS, N 4, 1962, pp. 470-471.

atmosphere a_H . Let us introduce the designations: F_H is the transverse cross-sectional area of a jet at infinity in front of the engine, γ_H is the specific gravity of the air far in front of the engine, p_H - the pressure in the atmosphere. Let us designate the values of area, velocity, and pressure in the inlet of the diffuser F_e, w_e, p_e . The values of the same quantities at the end of the diffuser F_d, w_d, p_d .

The operation of a diffuser depends on the ratio of the flying speed to the velocity in its inlet. Let us first examine system $w_H < a_H$, i.e., subsonic flight. The rate of air flow through the engine, and therefore, through the diffuser G_e kgf/s.

It is possible to visualize the case where a jet enters a diffuser without a change in its configuration. The transverse cross-sectional area of a jet at infinity in front of the engine F_H in this case is equal to the area of the inlet of the diffuser F_e :

$$F_H = \frac{G_e}{\gamma_H w_H} = F_e$$

Generally, the form of the jet at the engine inlet is determined by the relation F_H/F_e . In the case given above $F_H = F_e$, consequently there is no transformation of the velocity and pressure in front of the diffuser (Fig. 8.21b):

$$w_e = w_H \text{ and } p_e = p_H$$

If the rate of air flow through the diffuser increases, then the jet will change its form as shown in Fig. 8.21c. A change in the form of the jet is accompanied by the transformation of the velocity and pressure:

$$w_e > w_H \quad p_e < p_H$$

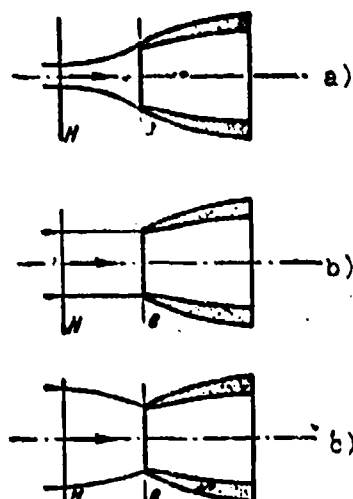


Fig. 8.21. Possible configurations of a jet in front of a diffuser.

With a decrease in the rate of air flow, the jet seemingly forms a diffuser even in the atmosphere (in front of the engine) in connection with a decrease in the velocity and a pressure increase (Fig. 8.21a).

With a constant air flow rate the form of the jet in front of the engine depends on the size of the inlet of the diffuser. Changing the dimensions of the diffuser, we can obtain any of three presented operating modes. Favorable for the operating conditions of the engine is the case where the flow decelerates somewhat even in front of the diffuser since the deceleration of the jet in front of the diffuser proceeds without any losses and the internal resistance of the diffuser decreases as a result of reduction of velocity at the entry. It is necessary, however, to note that besides internal losses one should also consider the external engine drag which increases with the shortening of the diffuser. This is explained by the fact that with the spreading of the flow in front of the nose of the engine the jets will approach its surface at large angles of attack and separation can be formed on the external surface of the nose (Fig. 8.22). For

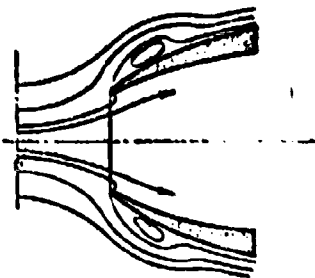


Fig. 8.22. Separation of jets with large diffuser inlet.

satisfaction of these contradictory requirements it is necessary to find optimum conditions for the operation of the inlet section of the engine.

Tests show that for a subsonic jet engine the optimum lies close to the mode

$$w_1 \approx 0.5 w_2.$$

If losses were absent in the diffuser, gas in any of its cross sections would have the very same total pressure equal (at the subsonic speeds of flight) to the total pressure in the incoming air jet. The presence of losses disturbs this equality, and the total pressure at the end of the diffuser is always lower than in the beginning:

$$p_{02} < p_{01}.$$

Static pressure along the diffuser, on the contrary, increases because of a decrease in velocity.

The value of hydraulic losses in the diffuser is conveniently expressed in fractions of velocity head in its broad cross section:

$$\Delta p_{02} = p_{01} - p_{02} = \frac{w_1^2}{2g_{01}} \zeta.$$

Here ζ_d is the coefficient of hydraulic resistance of the diffuser. Usually diffuser losses are relatively small: $\Delta p_{0d}/p_{0H} \ll 1$. Therefore, the density of the stagnated gas in a diffuser can be considered virtually constant $\rho_{0d} \approx \rho_{0H}$. Consequently, it is possible to accept

$$\Delta p_{0d} = \zeta_d \rho_{0H} \frac{w_d^2}{2}.$$

Let us reduce this formula to the dimensionless form:

$$1 - \frac{p_{0d}}{p_{0H}} = \zeta_d \frac{k}{k+1} \frac{w_d^2}{a_{0H}^2},$$

here

$$\frac{k p_{0H}}{\rho_{0H}} = a_{0H}^2 = \frac{k+1}{2} u_{kp}^2.$$

After the appropriate conversions we have

$$\sigma_d = \frac{p_{0d}}{p_{0H}} = 1 - \frac{k}{k+1} \zeta_d \lambda_d^2.$$

We note that $w_d/a_{0H} = \lambda_d$ is the velocity coefficient at the end of the diffuser. As a result, we obtain the following expression for the coefficient of the total pressure in the diffuser:

$$\sigma_d = 1 - \frac{k}{k+1} \zeta_d \lambda_d^2. \quad (22)$$

The resistance of the diffuser is composed of losses to friction and to vortex formations. Vortical losses are caused by the boundary-layer separation from the walls of the diffuser whose reasons are explained in Chapter VI: they depend on the diffuser cone angle and play the main role. With small diffuser cone angles hydraulic losses are small, but they increase in proportion to the increase in the angle. With an increase of cone angle the vortex zone moves from the end of the diffuser to its beginning and at wide angles the entire wall is covered with a vortical region.

Numerous experiments lead to the conclusion that vortex diffuser losses can be estimated as softened shock resistance (in comparison with the sudden expansion of the channel)

$$\Delta p_{\text{v}} = \psi \Delta p_{\text{sh}} \quad (23a)$$

where the shock loss is

$$\Delta p_{\text{sh}} = \rho \frac{(w_1 - w_2)^2}{2}.$$

Here ψ is the shock coefficient ($\psi < 1$). The experiments showed¹ that the shock coefficient ψ is a function of the diffuser cone angle α alone.

The corresponding relation for a rectilinear diffuser with circular cross section is given on Fig. 8.23. Corresponding to large cone angles ($\alpha > 40^\circ$) is $\psi \geq 1$, i.e., there is no softening of the shock. At angle $\alpha = 0$ we have $\psi = 0$, i.e., there is no shock. The maximum value of the shock coefficient ($\psi = 1.2$) is reached at angle $\alpha = 60^\circ$. In this case losses are even greater than with the sudden expansion of the channel, when $\psi = 1$. This is explained by the fact that the vortex zone in a right angle is stable, while with an inclined wall ($\alpha \approx 60^\circ$) the vortex zone is periodically carried away by the flow. Thus, added losses at such angles are caused by the expenditures of energy on the renewal of the vortex zone.

Usually diffusers are used with angles $\alpha = 6-10^\circ$. Corresponding to such values of cone angles are the values $\psi = 0.15-0.20$. In this region the visible separation of the jet from the wall of the diffuser is not observed.

¹Abramovich G. N. The Aerodynamics of the Local Resistances. Transactions of TsAGI, Issue 211, 1935.

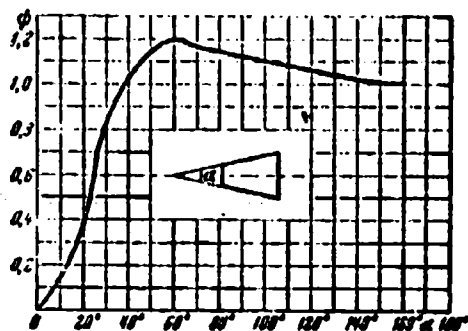


Fig. 8.23. The dependence of the shock coefficient on the diffuser cone angle of round cross-section.

If we disregard the change in air density within the limits of the diffuser, then we have

$$\bar{w}_2 = \frac{r_2}{r_1};$$

substituting this equality in (23a), we obtain

$$\zeta_d = \frac{\Delta p_{d, \text{fr}}}{p_{01} \frac{w_1^2}{2}} = \phi \left(\frac{r_2}{r_1} - 1 \right)^2. \quad (23b)$$

As an example let us compute the loss factor for a diffuser with the relationship of transverse cross sections $F_d/F_e = 3$ with cone angle $\alpha = 8^\circ$. It is possible to accept (taking into account friction) $\psi = 0.2$ for this case. Then $\zeta_d = 0.2 \cdot 4 = 0.8$, $\sigma_d = 1 - 0.44 \lambda_d^2$. The velocity coefficient at the end of the diffuser of a subsonic jet engine is usually on the order of $\lambda_d = 0.2-0.4$. Then

$$\sigma_d = 0.98 - 0.94.$$

We will not dwell on the calculation of friction drag since it is illuminated in sufficient detail in Chapter VI.

Experiments show that in diffusers with curvilinear side walls with large expansion angles the hydraulic losses can be substantially less¹ than in diffusers with rectilinear walls.

The results of the experimental determination of losses (including friction) in plane diffusers of one and the same length with a constant mean expansion angle $\alpha = 38^\circ 40'$ but with the different outlines of the lateral walls are given below. Figure 8.24 depicts the outlines of the tested diffusers. The first outline - a straight line, the second - a circular arc, the third corresponds to a constant pressure gradient along the length of the diffuser $dp/dx = \text{const}$, the fourth - to a constant velocity gradient $dw/dx = \text{const}$, and the fifth is constructed according to the formula

$$\frac{d}{dx} \left[\frac{d(1-\bar{p})}{dx} \frac{x}{1-\bar{p}} \right] = \text{const} > 0,$$

where \bar{p} is the dimensionless pressure determined from the relationship

$$\bar{p} = \frac{p - p_1}{\frac{\rho w_1^2}{2}}.$$

The smallest value of the drag coefficient $\zeta = 0.24$ is obtained for diffusers 3 and 4 with constant pressure gradient and constant velocity gradient. For diffuser 5 $\zeta = 0.26$, for diffuser 2 with the walls made along a circular arc the drag coefficient $\zeta = 0.27$ is obtained, and for diffuser 1 with straight walls $\zeta = 0.32$.

¹Idel'chik I. Ye., The Aerodynamics of Flow and Loss of Head in Diffusers. Collection of articles on industrial aerodynamics under the editorship of K. A. Ushakov, M., 1947.

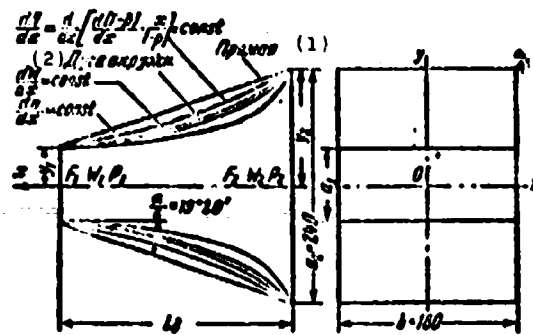


Fig. 8.24. The outlines of tested diffusers.
KEY: (1) Straight line; (2) Arc of circle.

Thus, in diffusers with constant pressure or velocity gradients a reduction in losses of approximately 25% is achieved in comparison with a straight diffuser.

Figure 8.25 depicts graphs of the dependence of the loss factor on length (i.e., on angle α) for diffusers of types 1 and 3. With sufficiently long (close to optimum) diffusers of these types the difference in losses becomes small.

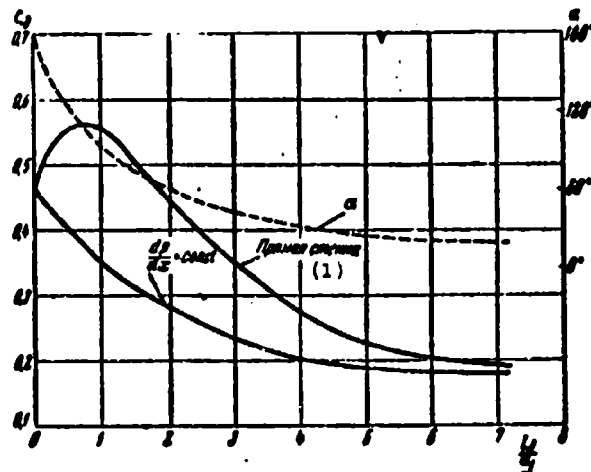


Fig. 8.25. The dependence of the loss factor on the length of the diffuser.
KEY: (1) Straight wall.

We examined the resistance of a diffuser under those conditions where it is possible to disregard the compressibility effect of the air which, as the experiments show, begins to show up in the value of the loss factor only in the case where the velocity in the diffuser inlet is close to the speed of sound ($\lambda_e > 0.7$).

Figure 8.26 presents graphs of the experimental dependences of the relation of the total pressures at the end and the beginning of a diffuser $\sigma_d = p_{0d}/p_{0e}$ on M_e number in a diffuser inlet¹ (with central expansion angles $\alpha = 4, 6, 8, 10^\circ$, diameter of entrance cross section 100 mm and the exit cross section diameter 222 mm). The sharp drop in the values of σ_d , which set in with values of M_e number of approximately 0.9 is explained by the fact that in these modes in the initial part of the diffuser a zone of supersonic velocity develops which is closed by the shock wave which introduced large wave drag. This can be judged from the curve on Fig. 8.27 which depicts the dependence of the M_e' number directly at the entry to the diffuser on the M_e number at a distance of one caliber in front of the entry to the diffuser.

A drawing of one of the diffusers (with $\alpha = 6^\circ$), tested by K. S. Stsillard, is presented on Fig. 8.28; the remaining diffusers of this series differed from that depicted on this figure only by the angle and accordingly by the length of the conical section.

To evaluate the effect of the R number on the resistance of the diffuser, K. S. Stsillard also tested geometrically similar diffusers of smaller size (with inlet diameter 18 mm). The results of tests of diffusers of increased and small sizes turned out to be close, which testifies to the weak effect of the R number on losses in a diffuser.

¹Stsillard K. S., The Investigation of Diffusers at High Velocities. Technical Notes of TsAGI, 1938.

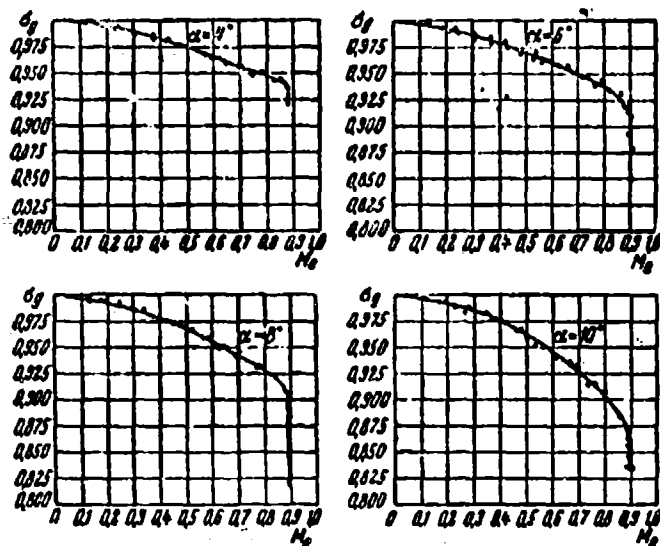


Fig. 8.26. The dependence of the total pressure coefficient in a diffuser on M_e number in front of a diffuser with expansion angles $\alpha = 4, 6, 8$ and 10° (according to K. S. Stsillard's experiments).

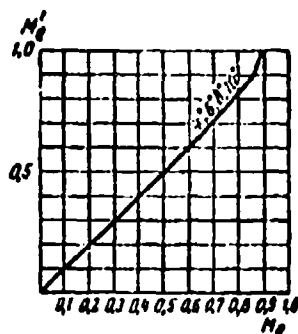


Fig. 8.27. The connection between the values of M number in the beginning (M_e) and the end (M_e') of the cylindrical entrance section of a diffuser (according to K. S. Stsillard's experiments).

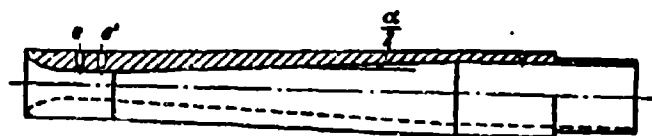


Fig. 8.28. Diagram of one of the diffusers tested by K. S. Stsillard.

Relation $\sigma_D = f(M_e)$ does not give a graphic representation of the effect of compressibility on drag since value σ_D changes with velocity even with a constant value of the loss factor. A convenient characteristic of losses during the flow of a compressible gas in a diffuser is the coefficient

$$\zeta_{cm} = \frac{L}{\frac{w_1^2}{2g}} = \frac{\frac{k}{k-1} RT_{0,1} \left[\left(\frac{p_{0,1}}{p_{0,2}} \right)^{\frac{k-1}{k}} - 1 \right]}{\frac{w_1^2}{2g}} \quad (24)$$

Here the numerator is the adiabatic work which must be expended in order to raise the total pressure in an ideal compressor at the end of the diffuser to the value of the total pressure in the beginning of the diffuser, and the denominator expresses the kinetic energy of a gas jet in the inlet of the diffuser.

Relations $\zeta_{cm} = f(M_e)$ for four of K. S. Stsillard's diffusers, recalculated for the curves on Fig. 8.26, are depicted on Fig. 8.29. As we see, the effect of compressibility of a gas on the value of the loss factor begins to be felt only at transonic velocities ($M_e > 0.7$). Some drop in the curves $\zeta_{cm} = f(M_e)$ in the region $M_e < 0.3$, where the compressibility effect is knowingly unthinkable, can be explained only by the effect of the R number which increases with an increase in M_e number.

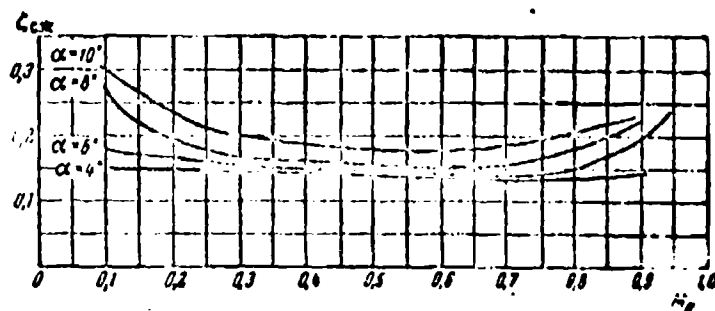


Fig. 8.29. The dependence of the drag coefficient of a diffuser on M_e number at the entry with expansion angles $\alpha = 4, 6, 8$ and 10° (according to K. S. Stsillard's experiments).

Let us now examine the operation of the diffuser of a VRD (jet engine) which has a usual ("subsonic") form with a supersonic flow velocity at the entry. A shock wave is formed in front of the entry to such a diffuser with a curvilinear front (Fig. 8.30). In the center section, i.e., in the one which intersects the working air jet which goes inside the engine, the shock should be a straight line. The latter ensues from the fact that the working jet retains its initial direction after the shock. Thus, the velocity in the working jet after the shock is subsonic.



Fig. 8.30. The shadow photograph of a supersonic flow in front of a simple diffuser.

Depending on the value of the inlet of the diffuser (F_e), one or other relationship occurs between the values of velocity after the shock (w_1) and at the entry to the diffuser (w_e). Two cases are fundamentally possible:

a) $w_1 > w_e$, i.e., the flow between the front of the shock and the inlet to the diffuser is decelerated;

b) $w_1 = w_e$, i.e., the velocity after the shock and the velocity at the inlet to the diffuser are identical.

Also possible is the case where the working jet enters the diffuser at supersonic velocity, then the shock wave is obtained not in front of the diffuser, but within it. Mode $w_1 < w_e$, i.e., the acceleration of the flow between the front of the shock and the entry to the diffuser, is not realized in practice.

Thus, in an engine with simple diffuser the deceleration of the entering jet at the supersonic initial velocity begins with a straight shock wave. The losses in shock and the flow parameters after the shock are determined from the formulas given in Chapter III.

Since the flow in a simple diffuser is subsonic even with supersonic flying speed ($\lambda_1 < 1$, $\lambda_e < 1$), hydraulic losses in the duct of such a diffuser can be calculated from formulas (22) and (23) of this chapter.

If for the case of subsonic speed of flight the total pressure losses with the deceleration of a working jet were determined only by the internal drag of the diffuser σ_d , then for the case of supersonic speed these losses also include external wave drag σ_n , i.e., are determined by the product of pressure coefficients in a straight shock and in the diffuser ($\sigma_n \sigma_d$).

§ 4. Supersonic Diffusers

By applying diffusers of special form it is possible to achieve a stepped slowing down of supersonic flow by means of different systems of oblique shock waves. Since in a usual step oblique shock the speed remains supersonic, then for the complete slowing down of flow it is necessary to place behind the last oblique shock a normal shock or a special ("strong") oblique shock which gives a transition to the subsonic speed of flow. In Fig. 3.12 the strong oblique shocks answer to the upper arms of curves $\alpha = f(\omega)$, lying higher than the maximums, whereupon the front of a strong oblique shock is located with respect to the incident flow at an angle of no less than 60° . Only under this condition ($\alpha > 60^\circ$) is it possible to obtain behind the front of an oblique shock a subsonic speed of flow ($M_1 < 1$).

The different combinations of shocks are investigated in the work of G. I. Petrov and Ye. F. Ukhov.¹ Let us examine the problem concerning a supersonic diffuser by utilizing the results of this work. We will turn first to the simplest layout of a supersonic diffuser in which the stagnation of flow is achieved by means of two shocks: an oblique and normal. In an oblique shock decrease in supersonic speed occurs, while in a normal shock - the lowered supersonic speed is transferred into subsonic.

Let us designate the velocity coefficient of the undisturbed flow by λ_∞ , the velocity coefficient behind the oblique shock by λ_1 , and the velocity coefficient behind the normal shock by $\lambda_k = (1/\lambda_1)$. As it was established above, an oblique shock wave is a normal shock in relation to the velocity components normal to its front. Thus the calculation of the first oblique shock of

¹G. I. Petrov and Ye. F. Ukhov, Calculation of the Restoration of Pressure upon Transition from Supersonic Flow to Subsonic in Different Systems of Step Shock Waves, M., 1947.

a system can be carried out according to the formulas for a normal shock. Formulas (38), (40), and (43) of Chapter III make it possible to calculate the change in the total pressure in an oblique shock wave.

Now, using expressions (21) and (24) of Chapter III, it is not difficult to determine the change in static and total pressures in a normal shock arranged behind an oblique shock. For this it is necessary only to consider that the velocity coefficient before the normal shock is λ_1 , then

$$\frac{p_n}{p_1} = \frac{\lambda_1 - \frac{k-1}{k+1}}{1 - \frac{k-1}{k+1} \lambda_1}, \quad \sigma_n = \frac{p_{0n}}{p_{01}} = \lambda_1^2 \left(\frac{1 - \frac{k-1}{k+1} \lambda_1}{1 - \frac{k-1}{k+1} \lambda_1^2} \right)^{\frac{1}{k-1}}. \quad (25)$$

The overall change in the total pressure in a supersonic diffuser, which contains oblique and normal shocks, is determined by the product of the pressure coefficients

$$\sigma_n \sigma_\alpha = \frac{p_{0n}}{p_{0\alpha}}. \quad (26)$$

With a change in the angle α between the front of an oblique shock and the direction of undisturbed flow the relations of the values of total and static pressures behind and before the system of shocks change.

Figure 8.31 depicts the charts of the dependence of the relations of the total pressures behind and before the system of shocks on the angle of the oblique shock at different values of velocity of undisturbed flow (i.e., at different values M_∞ or λ_∞), calculated for a diffuser with two shocks: oblique and following behind it a normal. For every value of M_∞ number (Fig. 8.31) there is a certain angle of oblique shock (α_{opt}), at which the restoration of the total pressure in the diffuser reaches a maximum; the less the flow velocity, the closer the optimum angle to a straight line. The dotted line A connects the points ($\alpha = \alpha_0$), in which the oblique shock degenerates into a weak wave; in this case the system consists of one normal shock. The dotted

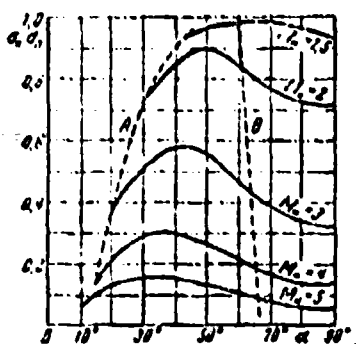


Fig. 8.31. The dependence of the relation of the total pressures behind and before a system of two shocks (oblique + normal) on the angle of the oblique shock.

line B connects the points, to the right of which the velocity behind the oblique shock is subsonic. In other words, the branch of each curve lying to the right of line B answers to a strong oblique shock, behind which there is no normal shock. With $\alpha = 90^\circ$ the strong oblique shock converts to a normal shock. By virtue of what was given on each of the curves the pressure coefficients $\sigma_n \sigma_n$ with $\alpha = 90^\circ$ and $\alpha = \alpha_0$ (angle of weak disturbance) obtained are identical.

Figure 8.31 shows that the superiority of the system - oblique shock with a subsequent normal shock over one normal shock - becomes significant only at $M \geq 1.5$. In the case $M_u = 2$ the optimum restoration of total pressure in a system of two shocks comprises $\sigma_n \sigma_n = 0.91$ (with $\alpha_{opt} = 50^\circ$), whereas one normal shock gives 0.72, i.e., 27% less. With $M_u = 3$ we have respectively for a system of two shocks $\sigma_n \sigma_n = 0.58$ ($\alpha_{opt} = 43^\circ$) and for one normal shock $\sigma_n = 0.33$ ($\alpha = 90^\circ$), i.e., two shocks give a gain in total pressure of approximately 70%. With a further increase in the velocity of incident flow the advantage of two shocks becomes even more considerable.

We examined in detail a system of two shocks. Applying the complex systems, which consist of three, four, and a greater number of shocks, it is possible to obtain better results than in a two-shock system. The calculation of any system of step shock waves is conducted with the help of formulas (38)-(52) of Chapter III and formulas (25), (26). It is possible to find the optimum modes for a complex system of shocks by means of consecutive

calculation. Let us indicate first how a system of three shocks (two oblique and a terminal normal) is calculated. In this case first the velocity coefficient (or Mach number) and the pressure behind the first oblique shock at different angles of slant of its front is determined, and on the basis of the already available data for every value of the velocity coefficient behind the first shock the optimum system from the remaining two shocks (oblique with a subsequent normal) is selected. As a result curves $\sigma_D = f(\alpha)$ are obtained which are similar to those given in Fig. 8.31; on them are established the optimum relationships for a system of three shocks. Further it is possible to find the optimum relationships for a system of four shocks (three oblique with a subsequent normal). For this it is necessary to conduct the calculation at different positions of the first oblique shock, selecting for every position of it (in terms of the value of velocity behind the first shock) the optimum system of three shocks. By the same consecutive calculation it is possible to determine the optimum modes for any assigned number of shocks.

Figure 8.32 gives the curves of the optimum values σ_D - the ratios of the total pressure behind a system of shocks to the total pressure before it depending on M_H number before the diffuser for the cases:

- 1) normal shock,
- 2) oblique shock with a subsequent normal shock,
- 3) two oblique shocks with a subsequent normal shock,
- 4) three oblique shocks with a subsequent normal shock.

The optimum modes are obtained in the described manner and correspond to the maximum restoration of total pressure. Figure 8.32 shows that the complex systems of shocks can give a large effect only at a very high velocity. So, with $M < 1.5$ good results are given by one normal shock, and more complex systems in this velocity range are not required. With $M \geq 1.5$ it is advantageous to apply a two-shock system (oblique with a subsequent normal). The advantages of a four-shock system (three oblique with a subsequent normal) become significant only at $M \geq 3$.

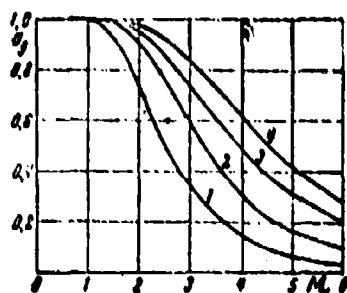


Fig. 8.32. The dependence of the optimum coefficient of total pressure in different systems of shock waves on Mach number in the incident flow.

Above we examined the different shock systems without depending on the configuration of the diffuser, which was necessary in order to realize the necessary system. The results obtained are applicable directly to plane diffusers and with insignificant changes to axisymmetric diffusers.

The schematic layout of a plane diffuser with two shock waves is depicted in Fig. 8.33. In order to obtain the first oblique shock with the necessary angle of slope α , one ought to install a wedge-shaped projection, deviating the flow by the angle ω , which for the assigned value of M_∞ is selected according to Fig. 3.12. The presence of a wedge does not disturb the external flow around the diffuser, if the distance OC is selected from the condition of encounter of the shock front OA with the edge of the inlet. The area of the inlet of the diffuser should be designed so that the flow velocity in it would be equal to the velocity behind the normal shock. In this case the normal shock is placed in plane CA and does not influence the external flow around the diffuser.

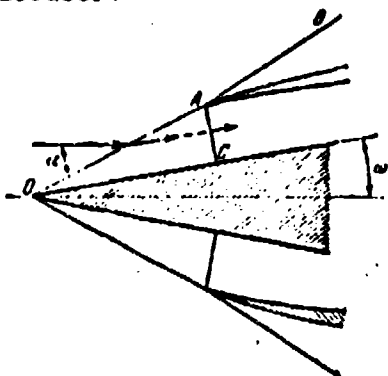


Fig. 8.33. Arrangement of a plane diffuser with two shocks: OA - first oblique shock, CA - normal shock, AB - oblique shock of external flow.

Figure 8.34 depicts the schematic diagram of the diffuser with three shock waves. In this case the surface of the wedge should have a fracture. The angle of deflection of undisturbed flow ω_1 and the angle of secondary deviation ω_2 are selected as before on the curves of Fig. 3.12 in accordance with the assigned slope angles of the first (α_1) and the second (α_2) oblique shocks also taking into account the velocities before the first (M_0) and before the second (M_1) shocks. The area of the inlet CA is selected based on the velocity behind the normal shock (M_2). Distances OD and DC are calculated from the condition of the intersection of shocks CA and DA on the edge of the inlet. Under these conditions through a system of three shocks passes only air which enters inside the diffuser: external flow is not agitated by this system of shocks.

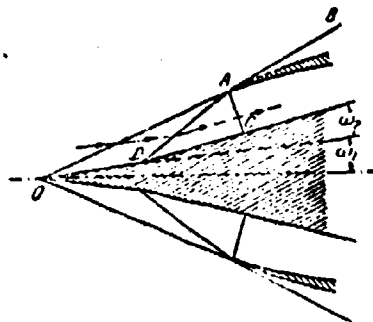


Fig. 8.34. Arrangement of a plane diffuser with three shocks: OA - the first oblique shock, DA - the second oblique shock, CA - normal shock, AB - oblique shock of external flow.

The schematic diagram of an axisymmetric supersonic diffuser does not differ from the diagram of a plane diffuser.

The states of the gas behind complex systems of axisymmetric and step shocks (with equal slope angles of shocks with identical ordinal numbers) should be close to each other. It is possible to be convinced of this as Fig. 8.35, in which are represented the relations of the values of the total pressures behind and before systems of two shocks (oblique with a subsequent normal) at the optimum slope angles of oblique shock depending on M_0 number of incident flow. One of the curves of Fig. 8.35

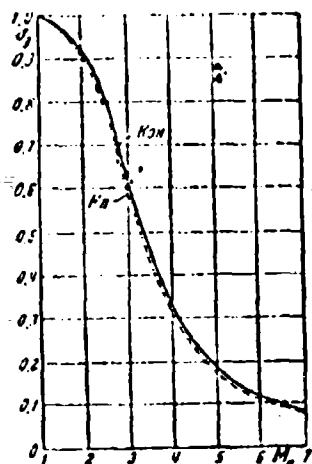


Fig. 8.35. The restoration of the total pressure behind a system of two shocks (oblique + normal) at optimum angles of oblique shock depending on the flow velocity for axisymmetric and plane (dotted line) flows.

corresponds to axisymmetric, the other (dotted line) - to a plane flow. During the calculation of a terminal normal shock in the axisymmetric case the velocity before it (λ_1) was determined from formula (53) in Chapter III. In a complex axisymmetric diffuser all shocks, except the first, can be considered virtually plane in view of the fact that they are situated in relatively narrow annular channels.

The analytical investigations carried out by G. I. Petrov and Ye. P. Ukhov,¹ and also by K. Oswatich,² showed that the maximum relation of total pressures (minimum of losses) in a system of several step oblique shock waves and a terminal normal shock equal to

$$(\pi_0)_{\max} = \pi_1 \pi_2 \dots \pi_n \quad (27)$$

is obtained when the oblique shocks have the identical intensity:

$$\pi_1 = \pi_2 = \pi_3 = \dots = \pi_n \quad (28)$$

With this condition from (27) we have

$$(\pi_0)_{\max} = \pi_n^{n-1} \pi_n \quad (29)$$

¹See footnote on page 580.

²Oswatich K., Der Druckrückgewinn bei Geschossen mit Ruckstossantrieb bei hohen Ueberschallgeschwindigkeiten. Forschungen und Entwicklungen des Heereswaffenamtes. Bericht N 2. 1005, Göttingen, January 1944.

Herman R. Supersonic inlet diffusers. Fizimatgiz, 1960.

Here m - the total number of shocks, $(m-1)$ - the number of oblique shocks, σ_n - the relation of the total pressures behind and before a single oblique shock, σ_n - the same for a normal shock.

From formula (40) in Chapter III it follows that with equal losses of total pressure ($\sigma_n = \text{idem}$) the coefficients of the normal components of velocity before the shock should be identical ($\lambda_{n1} = \lambda_{n2} = \dots = \text{idem}$, i.e., $M_{n1} = M_{n2} = \dots = \text{idem}$ or $M_{n1} \sin \alpha_1 = M_{n2} \sin \alpha_2 = \dots = \text{idem}$); because of this the relation of the static pressures, densities, and other parameters in all oblique shocks are the same ($\frac{p_2}{p_1} = \frac{p_3}{p_2} = \dots = \text{idem}$, $\frac{\rho_2}{\rho_1} = \frac{\rho_3}{\rho_2} = \dots = \text{idem}$, $\frac{T_2}{T_1} = \frac{T_3}{T_2} = \dots = \text{idem}$, $\frac{a_2}{a_1} = \frac{a_3}{a_2} = \dots = \text{idem}$) and the increases of entropy in them are equal ($s_2 - s_1 = s_3 - s_2 = \dots = \text{idem}$). Analytical investigation shows that all the parameters of a terminal normal shock in an optimum system differ only a little from the parameters of the single oblique shock of this system. So, in the range of values of Mach number of incident undisturbed flow $1.5 \leq M_{n1} \leq 5$ the relative value of the Mach number before the normal shock is virtually constant and equal to

$$M_{n-1} = 0.94 M_{n1} \sin \alpha_1 \quad (30)$$

Knowing value M_{n-1} , it is possible to calculate the velocity coefficient λ_{m-1} before the normal shock, the relation of the total and static pressures, and also all the other parameters behind and before the jump.

For the approximate precomputations it is possible to determine the Mach number before the normal shock based on the normal velocity component before the single oblique shock ($M_{n-1} \approx M_{n1} \sin \alpha_1$). Then the optimum relation of the total pressures in the system of shocks is equal to

$$(\sigma_1)_{opt} = \sigma_n^m \quad (31)$$

This expression gives a better approximation to the exact expression (29), the greater the number of shocks m in the system. When using the multishock system the intensity of every shock is relatively small, and this means that the velocity of subsonic flow behind the terminal normal shock is close to the speed of sound ($M_{n1} \approx 1$). But in this case a small jet contraction, which usually proceeds before the inlet of diffuser, is sufficient in order that in this opening the critical speed ($M_{n1} = 1$) would be established. Experiments show that this condition is realized in practice under basic conditions of operation of a multiple-shock diffuser in the system of an engine.

In that case the rate of air flow through the diffuser is determined from formula (8a) in Chapter IV:

$$G \approx 0.4 \frac{p_{0D}^* p_{0H}^*}{\sqrt{T_{0H}}} \text{ kgf/s.} \quad (32)$$

Here $p_{0D} = \sigma_D p_{0H}$ - the total pressure in the entrance section of the diffuser (behind the system of shocks); $T_{0D} = T_{0H}$ - the stagnation temperature in the entrance section of the diffuser, equal to the stagnation temperature in the incoming undisturbed flow; $F_{Bx} = F_{HP}$ - the entrance section area of the diffuser.

The rate of flow in the channels of an engine (specifically before the compressor and before the combustion chamber) usually should be considerably lower than the speed of sound, as a result of which the internal duct of the supersonic diffuser, where air arrives from the inlet, is made expanding. But if in the inlet the velocity is equal to critical, then such a channel can also work as the divergent section of the Laval nozzle with the formation of the supersonic flow being completed by an additional shock wave.

It is attempted to select the form of the internal duct and working conditions of the diffuser that the losses in supplementary shock, at least in the basic (calculated) system were as little as possible, and this is achieved by the maximally possible contraction in the supplementary supersonic zone of flow.

With a smooth form and small expansion angles of the initial part (neck) of the internal duct of the diffuser it is possible to avoid the boundary-layer separation in the shock (with $M_n < 3.5$), terminating the supplementary supersonic zone, and to reduce the losses of total pressure in the internal duct down to 3-5% ($\sigma_{\text{em}} = 0.97-0.95$).

The supersonic diffusers described above, in which the basic shock system is arranged before the inlet (before the cowl) are related to the category of diffusers with external compression (in spite of the presence of supplementary compression in the internal duct). If in such a diffuser all the shocks intersect at edge A of the cowl (Fig. 8.34), then, as already mentioned, the system of shocks does not disturb the external flow around the cowl. However, the internal wall of the cowl should be oriented on the direction of flow in a terminal normal shock, which the stronger it is deflected from the direction of the incoming undisturbed flow, the greater the oblique shocks on the central body of the diffuser.

In turn the external wall of the cowl makes up with the interior an angle of $\Delta\omega = 3-5^\circ$, therefore the angle of incidence of the face of the cowl with the incoming undisturbed flow is equal to

$$\omega_n = \sum_{k=1}^{n-1} \omega_k + \Delta\omega = \omega_n + \Delta\omega, \quad (33)$$

where ω_k - the deviation of the flow in a single oblique shock,

$\omega_n = \sum_{k=1}^{n-1} \omega_k$ - the total deviation of the flow in a system of oblique shocks.

In a multiple-shock diffuser with external compression the angle ω'_n is great and shock AB on the face of the cowl (Fig. 8.34) turns out to be intense. Such cases are possible where angle ω'_n is greater than the critical angle of rotation of flow

in a step oblique shock wave. In this case instead of step shock AB a detached curvilinear shock wave is formed which is united into one whole with the terminal normal shock of the system (Fig. 8.36) and leads to a great external drag of the cowl.

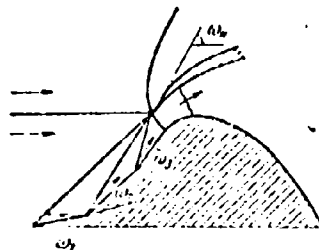


Fig. 8.36. The system of shocks at a cowl slope angle which exceeds the extreme value for an oblique shock.

In Fig. 8.37 the dotted line depicts the dependence of the critical angle of rotation of flow in a connected step shock on the Mach number w_{max} (M_{∞}) with $k = 1.4$. Here are plotted the curves of the values of total angle of rotation of flow ω_{Σ} in an optimum system of step shocks (for a diffuser with external compression), which consists of a various number of shocks ($m = 2, 3, 4$). As can be seen from Fig. 8.37, the total angle of rotation of flow in the optimum system of three shocks is approximately equal to the critical angle of rotation of undisturbed flow at the cowl, but in the case of four shocks - is greater than critical. In other words, with $m \geq 3$ (for $k = 1.4$) in an optimum diffuser with external compression the formation of a detached shock wave on the face of the cowl is unavoidable.

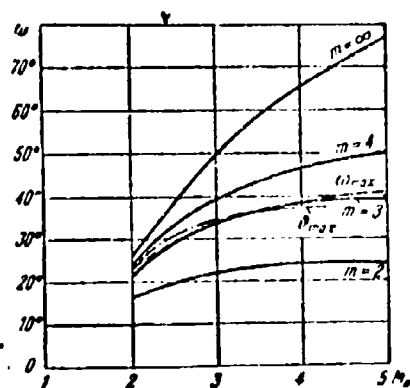


Fig. 8.37. The dependence of the total angle of rotation of flow in an optimum system of shocks on the Mach number with a different number m of shocks: ω_{max} - the maximum angle of rotation in an oblique shock, θ_{max} - the rotation of flow during isentropic compression about a central body.

As Fig. 8.32 shows, an increase in the number of shocks leads to a decrease in the total losses of total pressure in the system. With an increase in the number of shocks to infinity the losses in the system should drop to zero ($\sigma_d \rightarrow 1$), i.e., a transfer to isentropic stagnation is achieved. The form of the central body of a plane "isentropic" supersonic diffuser with external compression is depicted in Fig. 8.38.

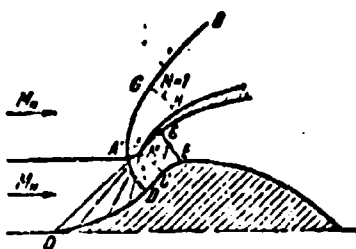


Fig. 8.38. Isentropic external compression in a supersonic diffuser.

The full angle of rotation of flow about such a central body is calculated from formulas and the tables of Prandtl-Mayer flow (see § 3 Chapter IV), since isentropic compression is reversed isentropic expansion.

In other words the angle of rotation of flow in a plane isentropic central body during stagnation from the value of M_∞ number to $M = 1$ is equal to the angle of rotation in a Prandtl-Mayer flow with expansion from $M = 1$ to $M = M_\infty$ ($\omega_\infty = \delta_\infty$). Curve $\delta_\infty(M_\infty)$ for $k = 1.4$ is given in Fig. 8.37 ($m = \infty$). If the beam of characteristics of the isentropic flow of compression converged on the edge of the diffuser cowl, then the jet entering into the diffuser would not disturb the external flow around the cowl.

In actuality the total isentropic stagnation of the flow of gas cannot be realized, since on the surface of the central body there is an increase in pressure which causes the deformation of the boundary layer velocity profile which leads to the breakaway of the latter. At the separation point of the boundary layer a strong disturbance of supersonic flow appears, as a result of which a shock wave is formed (Fig. 8.38) which converts to a shock wave of external flow around the cowl.

All the same the selection of the corresponding form of central body, especially with the realization of the boundary-layer bleed, makes it possible to partially utilize isentropic stagnation of flow in a diffuser of external compression and to obtain the recovery of pressure somewhat higher than in a three- or four-shock diffuser.

If the point of intersection of shocks (or the Mach waves in an isentropic diffuser) does not coincide with the edge of the cowling, then from this point to the side of external flow the shock wave, the intensity of which is determined by two conditions will move away. These conditions are:

- 1) the agreement of the direction of external flow and internal jet;
- 2) the equality of pressure on both sides of the surface which separates the external flow from the internal jet.

The curve of the values of angle of rotation of flow θ_{max} , determined by these conditions, is given in Fig. 8.37 (for isentropic compression). If the angle of rotation of streams in a shock proves to be more than the maximum possible at this velocity of incoming flow, then the shock is converted into a curvilinear shock wave which penetrates the internal flow and pulls itself to the wall of the central body (Fig. 8.36). Behind the curvilinear wave the supersonic flow is broken down both near the external and internal walls of the cowling.

For a decrease in the external drag diffusers with incomplete (partial) external compression are used (Fig. 8.39). In such a diffuser the cowling comprises with the direction of undisturbed flow a smaller angle than the last face of the central body. Thus flow encounters the internal surface of the cowling at a certain angle and is forced to be deflected with the formation of an oblique shock AC, which goes from the edge of the cowling to that part of the central body which is arranged in the internal duct of the diffuser; the terminal normal shock EF is disposed

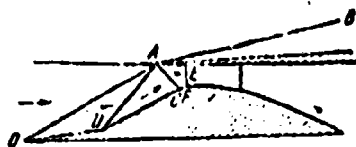


Fig. 8.39. Supersonic diffuser with partial external compression.

near the narrow cross section of the internal duct. The diffuser cowl with partial external compression can have a low external drag. If the cowl is directed parallel to the velocity vector of undisturbed flow, then its external wave resistance is close to zero.

A supersonic diffuser with total internal compression can be realized without a central body (Fig. 8.40). In such a diffuser the oblique shock will move away from the edge of cowl A and intersects at point O on the axis of the diffuser with the shock which goes from the opposite edge. The flow of gas in shock AO deviates from the initial direction and becomes parallel to wall AC. At point O the lines of flow are forced to return to the initial direction, in connection with which the reflected shock OD appears. At point D the flow again deviates from the axial direction and becomes parallel to the wall of the diffuser; this causes a new shock which is reflected from the axis of the diffuser, forming the following shock, etc. Since in the shock waves the flow is decelerated, then the maximum angle of rotation in every subsequent jump is less than in the preceding. The described process is continued until the required deviation of flow angle turns out to be greater than maximum ($\omega > \omega_{\max}$); with the advent of this mode instead of the next step shock a curvilinear shock wave EF is formed, behind which the flow becomes subsonic. Further flow in the converging channel occurs with an increase in velocity, whereupon in the narrow cross section the velocity should be below or equal to critical; in the latter case behind the narrow cross section a supplementary supersonic zone terminated by the shock wave GH can arise.

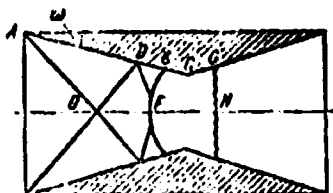


Fig. 8.40. Supersonic diffuser with internal compression.

At a very low slope angle of the side wall of the diffuser with total internal compression ($\omega < 1^\circ$) partial isentropic stagnation is possible; it is attained up to the place of the boundary-layer separation which causes the shock wave.

A supersonic diffuser with total internal compression is utilized in wind tunnels. As a result of partial isentropic compression in a diffuser of narrow angle it is possible to cut the losses in half in comparison with the same in a normal shock (calculated according to the Mach number before the diffuser).

The boundary layer influences the work of the diffuser not only in the case of isentropic compression. In diffusers of other layouts the boundary layer effect is also very perceptible; it does not influence only the first shock, which is established in the case of encounter of undisturbed flow with the leading edge of the central body or cowling.

All the subsequent shocks appear or are reflected in places of interaction of the boundary layer with the shock (in the case of a drop in pressures on the shock above "critical," see § 6, Chapter VI). As a result of this interaction the losses of pressure increase, and the shock waves are transformed and displaced. If the latter fact is not taken into account when selecting the form of the central body of a diffuser with external compression, then the intersection of all shocks on the edge of the cowling will not be ensured, (Fig. 8.41), due to which the external flow around the diffuser will be disturbed. One ought to keep in mind also the viscosity effect when selecting the transverse dimensions of the

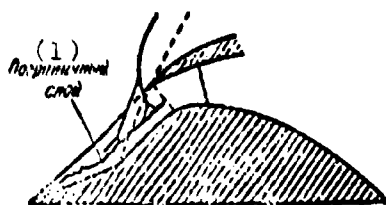


Fig. 8.41. The distortion of the system of shocks during their interaction with the boundary layer. Dotted line - shocks in an ideal gas, solid lines - shocks in a viscous gas.

KEY: (1) Boundary layer.

channel of the diffuser (by means of an increase in the flow areas in accordance with the build-up, along the length of the channel, of the displacement thickness of the boundary layer as this was shown in the example of a nozzle in § 1 of this Chapter).

Up to now we examined supersonic diffusers working on the basic, calculated value of the incoming flow velocity. During a deviation from the design conditions the form of the system of shocks changes, in connection with which some of the assigned conditions are disrupted. Specifically in an uncontrolled diffuser with external compression with a decrease in the Mach number of incident flow the shock waves become steeper (Fig. 8.42); due to this the extreme flow line of the internal jet (getting into the diffuser) passes through points abA, being diverted in every shock of the system. But then the jet cross-section F_{OH} , which is enclosed by the diffuser, proves to be less than under calculated conditions, for which it is equal to total cross section F_{OA} (from edge A of the cowling to the axis of the diffuser, see for example Fig. 8.39).

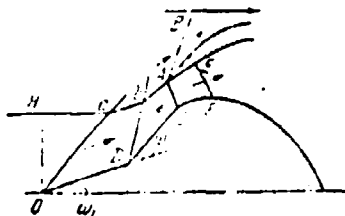


Fig. 8.42. The form of the jet which enters the diffuser at a flight velocity lower than calculated.

The relation

$$\tau = \frac{P_{0H}}{P_{0A}}$$

is called the flow coefficient. Losses in the internal jet, as can be seen from Fig. 8.42,¹ should not depend on whether or not the shocks on edge A of the cowl intersect; the external resistance of the diffuser under the action of the shifted shocks increases, since part of the flow which flows around the diffuser is forced to cross these shocks up to encounter with the cowl.

The nature of the dependence of the coefficient of total pressure σ_D and the flow coefficient on the Mach number in a three-shock diffuser of permanent form (with external compression) is shown in Fig. 8.43 (calculated value $M_H = 3$). Here are plotted the curves $\sigma_{opt}(M_H)$ and $\phi_{opt}(M_H)$ for an optimum diffuser (dotted line), the geometric form of which with a change in value M_H should change (ideally regulated diffuser). Under all conditions, except calculated, a non-variable diffuser has a value σ_D lower than optimum; values $\phi < 1$ are obtained only in the range of values M_H lower than calculated.

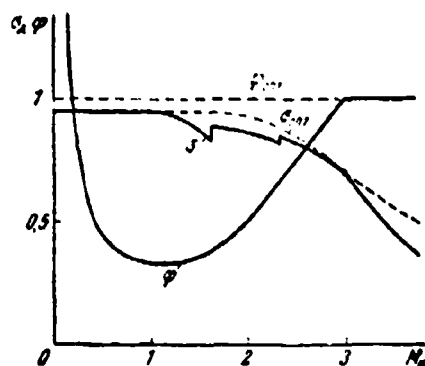


Fig. 8.43. Dependence on flight velocity of the coefficients of total pressure and flow for a three-shock supersonic diffuser with external compression which has the optimum characteristics with $M_{HP} = 3$.

The calculation of curves in Fig. 8.43 is done in the following manner. According to Fig. 8.32 the value $(\sigma_D)_{max} = 0.73$ is taken for the optimum system of three shocks with $M_H = 3$ and multiplied by the total pressure recovery coefficient of the internal part of

¹Shocks in Fig. 8.42 are constructed without allowing for the boundary layer effects.

the diffuser (we accept $\sigma_{BH} = 0.95$); the product of these coefficients characterizes total losses within the diffuser under design conditions ($\sigma_n = 0.7$) for which the flow coefficient is close to unity $\phi = 0.98-1$. The approximate value σ_n for a single oblique shock of an optimum three-shock system according to (31) $\sigma_n = \sqrt{3} = 0.89$. Answering to this value σ_n on the basis of (25) is the coefficient of normal velocity component (with $k = 1.4$) $\lambda_{nn} = 1.43$ and Mach number calculated on the normal velocity component of incoming flow:

$$M_{nn} = \sqrt{\frac{\frac{2}{k+1} \lambda_{nn}^2}{1 - \frac{k-1}{k+1} \lambda_{nn}^2}} = M_n \sin \alpha_1 = 1.6.$$

Hence the angle of inclination of the first shock $\alpha_1 = \arcsin 1.6/3 = 32^\circ$. On the curves in Fig. 3.12 of Chapter III we find the angle of the first wedge of the central body (with $M_n = 3$ and $\alpha_1 = 32^\circ$) $\omega_1 = 15^\circ$ and in Fig. 3.19 of Chapter III - the Mach number behind the first shock $M_1 = 2.3$.

The value of the Mach number for a normal velocity component before the second shock in an optimum system should be the same as before the first shock $M_{nn} = M_{1n} = M_1 \sin \alpha_2 = 1.6$. Hence the angle of inclination of the second shock to the flow direction behind the first shock

$$\alpha_2 = \arcsin \frac{1.6}{2.3} = 44^\circ,$$

to which corresponds the flow angle of deviation on the second step of the wedge $\omega_2 = 18^\circ$. The total angle of rotation of flow in the optimum system of shocks in question $(\omega_1 + \omega_2) = 33^\circ$, and the Mach number behind the second shock $M_2 = 1.6$. The refined value of the Mach number before the terminal normal shock according to (30) $M_{m-1} = 0.94 M_{nn} = 1.5$.

Now it is possible to refine the calculation of the system of shocks, for which one ought to determine the value σ_n in a normal shock with $M_{m-1} = 1.5$, value σ'_n in each of two identical oblique shocks

$$v_i = \sqrt{\frac{v_{i, \max}}{M_n}},$$

the velocity coefficient and Mach number for normal component velocity in oblique shocks λ_{Hn}' and M_{Hn}' , the slope angles of oblique shocks α_1' and α_2' , and the angles of steps on the central body of the diffuser ω_{Hn}' , ω_1' . After this it is possible to refine the values of the Mach number M_{m-1} before the terminal normal shock. In view of the fact that the refined values differ little from those obtained in the first approximation, we will not give them.

For the facilitation of the calculations it is possible to make use of Fig. 8.44, in which are given the curves $M_{Hn}' \sin \alpha_1' = f(M_{Hn})$, which correspond to the data of an optimum diffuser with systems of two, three, and four shocks. Figure 8.45a, b, and c depict the charts of the angles of deflection of flow in oblique shocks $\omega(M_{Hn})$ for the same three systems, in Fig. 8.46a, b - the values of the Mach numbers behind oblique shocks, while in Fig. 8.47a, b, c - the value of the slope angles of shocks in these systems.

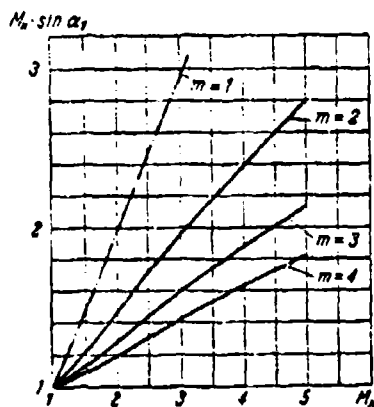


Fig. 8.44. Normal component $M_{Hn}' \sin \alpha_1'$ depending on M_{Hn} for an optimum system of m jumps.

The described procedure is related to the calculation of a plane supersonic diffuser with external compression and an optimum shock system under design conditions, during which all the shocks intersect at the edge of the cowl.

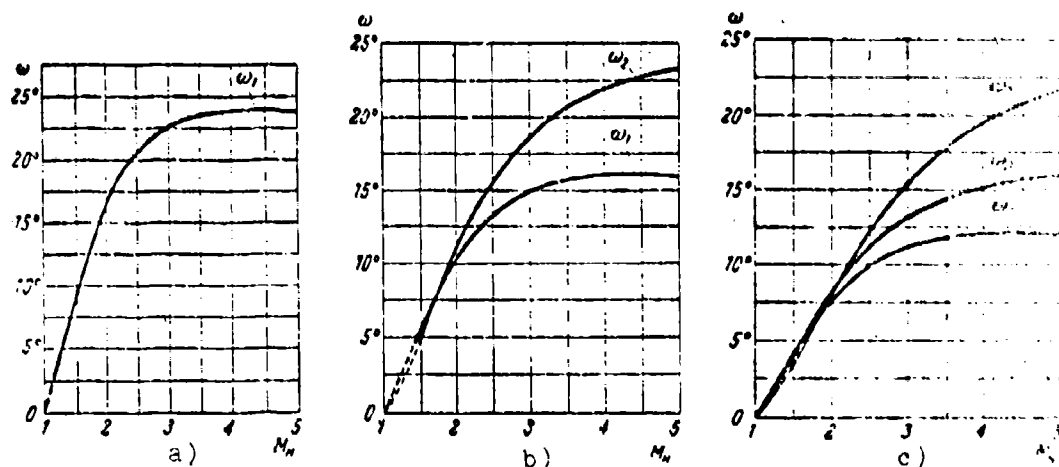


Fig. 8.45. The dependence of the angles of deflection of flow in the shock of an optimum system on M_∞ : a) with $m = 2$, b) with $m = 3$, c) with $m = 4$.

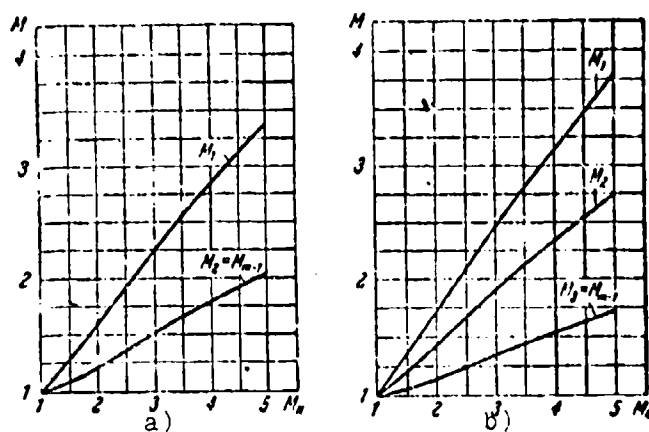


Fig. 8.46. The dependence of the Mach number behind oblique jumps of an optimum system on M_∞ : a) with $m = 3$, b) with $m = 4$.

At a flying speed lower than calculated and a fixed shape of diffuser, as has already been said, the shock-wave angles will become greater. For example, if $M_\infty = 2.5$, then for the described diffuser we will obtain the angle of slope of the first shock $\alpha_1 = 36^\circ$ (with $\omega_1 = 15^\circ$), the Mach number for the normal

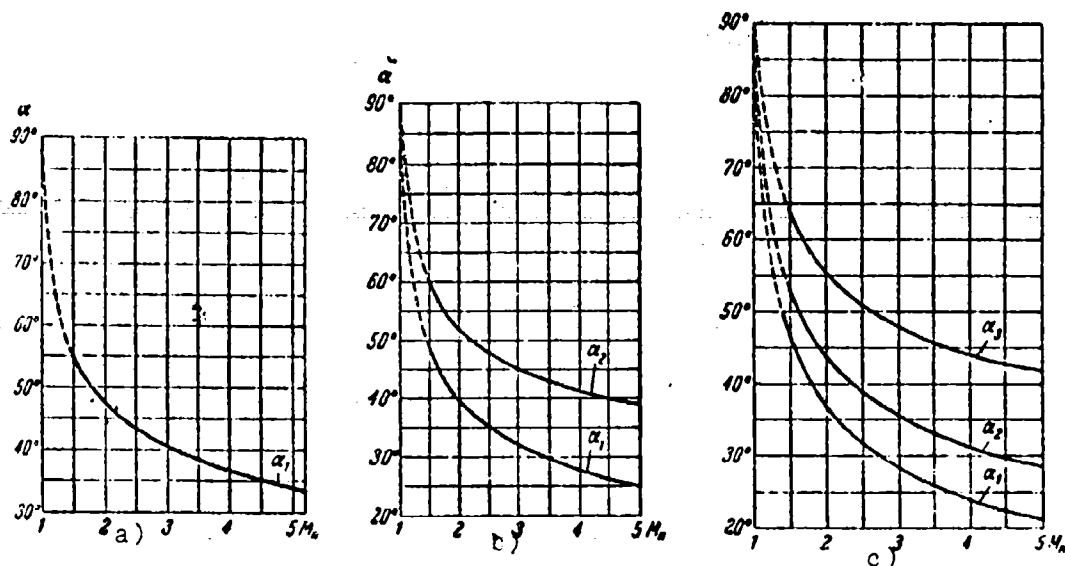


Fig. 8.47. The slope angles of shocks: a) with $m = 2$, b) with $m = 3$, c) with $m = 4$.

velocity component before the first shock $M_{Hn} = M_H \sin \alpha_1 = 1.48$, and the corresponding values of the velocity coefficient $\lambda_{Hn} = 1.35$. The coefficient of total pressure in the first shock comprises in this case $\sigma_{H1} = 0.936$, the Mach number behind the first shock $M_1 = 1.9$, the angle of slope toward the flow of the second shock $\alpha_1 = \arcsin 1.48/1.9 = 53^\circ$ (with $\omega_2 = 18^\circ$), the coefficient of total pressure in the second shock $\sigma_{H2} = 0.929$, the Mach number before the terminal normal shock $M_{m-1} = 1.2$, the coefficient of total pressure in the normal shock $\sigma_n = 0.993$, and the total values of this coefficient

$$\sigma_A = \sigma_{H1} \sigma_{H2} \sigma_n = 0.825.$$

If the angle of rotation of flow in the second oblique shock proves to be more than maximally possible ($\omega_2 > \omega_{\max}$) with M_1 value obtained, then instead of a three-shock system a two-shock is realized ($\sigma_{H2} \approx 1$); the approximate value of the pressure coefficient in this case is equal to

$$\sigma_A = \sigma_{H1} \sigma_n.$$

whereupon σ_m is calculated from the value of the Mach number behind the first shock.

The flow coefficient $\phi = F_m/F_{0A}$ at a velocity equal to or greater than calculated, is close to a unit. At low values of M_m the dependence $\phi(M_m)$ for a diffuser with external compression is determined from the condition of equality of rate of flow in the intake (critical) cross section and before the system of shocks

$$\sigma'_A \rho_{HP} a_{HP} F_{HP} = \rho_m \omega_m F_m.$$

Here $(\sigma'_A \rho_{HP})$ - the air density in the critical cross section, calculated taking into account the losses of total pressure in the system of shocks (not allowing for losses in the internal part of the diffuser: $\sigma'_A = \sigma_A/\sigma_{BH}$). Hence, utilizing expression (109) of Chapter V, we have

$$\frac{F_m}{F_{HP}} = \frac{\sigma'_A \lambda_{HP} a_{HP}}{\rho_m \omega_m} = \frac{\sigma'_A}{q(\lambda_m)}. \quad (34)$$

Under design conditions the jet cross-sectional area covered by the diffuser is equal to the total cross section of the latter in the intake plane ($F_m = F_A$), therefore

$$\frac{F_A}{F_{HP}} = \frac{\sigma'_A}{q(\lambda_{HP})}. \quad (35)$$

where λ_{HP} is the calculated velocity coefficient of incident flow. After dividing (34) and (35) termwise we obtain the expression for the flow coefficient of the diffuser

$$\phi = \frac{F_m}{F_A} = \frac{\sigma'_A}{\sigma'_{HP}} \frac{q(\lambda_{HP})}{q(\lambda_m)}. \quad (36)$$

For any diffuser we have

$$\begin{aligned} \sigma'_A &= \sigma'_{HP} & \text{and } \tau &\approx 1 & \text{when } \lambda_m &= \lambda_{HP}, \\ \sigma'_A &= 1, q(\lambda_m) = 1 & \text{and } \tau &= \frac{q(\lambda_{HP})}{\sigma'_{HP}} & \text{when } \lambda_m &= 1, \\ \sigma'_A &= 1, q(\lambda_m) \rightarrow 0 & \text{and } \tau &\rightarrow \infty & \text{when } \lambda_m &\rightarrow 0. \end{aligned}$$

For $1 < \lambda_H < \lambda_{HP}$ in terms of the rated value λ_H we find with the help of the table of gas-dynamic functions the value $q(\lambda_H)$ and calculate the coefficient of total pressure in the system of shocks σ_d , which is obtained on the central body of a diffuser of assigned form. For example, for an optimum diffuser with external compression under design conditions $\lambda_{HP} = 1.97$ ($M_{HP} = 3$), $\sigma_d = 0.73$ was obtained above; for the same diffuser with $M_H = 2.5$ ($\lambda_H = 1.825$, $q(\lambda_H) = 0.38$, $\sigma'_d = 0.825$ was found to which according to (36) corresponds $\phi = 0.76$. Curves $\phi(M_H)$ and $\sigma_d(M_H)$ calculated from such a method are given in Fig. 8.43. Steps on the curve $\sigma_d(M_H)$ correspond to transfers from a three-shock system to two-shock and from the latter to one normal shock.

By the dotted line, as noted earlier, the curves were plotted which corresponded to the ideally adjustable three-shock diffuser, in which the forms of the central body and cowling, and also the flow area of the throat change according to such a law, that for every value of velocity an optimum system of three shocks which intersect on the edge of cowling is established.

At values of velocity higher than calculated ($M_H > M_{HP}$) it is possible to assume $\phi = 1$ and $\sigma'_d < \sigma'_{d \text{ опт}}$. The first of these conditions is connected with the fact that the shocks in this system are not focused on the edge of the cowling, but are enveloped inside the diffuser (Fig. 8.48), as a result of which in the inlet of the diffuser the jet of undisturbed flow arrives, the cross section of which is equal to the cross section of the diffuser.

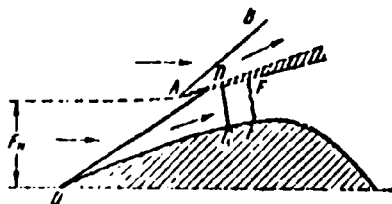


Fig. 8.48. Flow at the entry to the diffuser at a flying speed greater than calculated.

The second condition ($\sigma'_D < \sigma'_D \text{ on } \tau$) is predetermined by the fact that with $M_H > M_{HP}$ the gas density in the critical cross section is higher than under design conditions (in spite of the increase of losses, the total pressure behind the system of shocks with an increase in velocity increases). Due to this the throat (D) of an uncontrolled diffuser with $M_H > M_{HP}$ turns out to be overexpanded and the velocity obtained in it is higher than critical. But then after the throat occurs a further acceleration of supersonic flow, which leads to the enhanced intensity of normal shock EF, terminating the supersonic zone (value σ_n decreases as a result of the increase of the value of Mach number M_{m-1} before the normal shock).

When the inlet diffuser is operating at a velocity lower than calculated, when into the diffuser a jet of incomplete cross section ($\phi < 1$) is trapped, there appears (as has already been indicated during the discussion of the diagram of flow depicted in Fig. 8.42) a force of supplementary external drag, equal to projection on the direction of flow of the force of the excess pressure acting on surface abA:

$$X_{don} = (p_1 - p_n) l_1 \sin \omega_1 + (p_2 - p_n) l_2 \sin \omega_2. \quad (37)$$

Here l_1, l_2 - the lengths of segments ab, bA; ω_1, ω_2 - the slope angles of these segments which are parallel to the corresponding sections of the central body; p_1, p_2 - pressures behind the first and second oblique jumps. After dividing force X_{don} by the dynamic head of incident flow and the area of the frontal cross section of the cowl F_A , we will obtain the coefficient of supplementary resistance of a "liquid outline" abA:

$$c_{x\pi} = \frac{X_{don}}{\rho_n \frac{w_n^2}{2} F_A}. \quad (38)$$

The greatest value of coefficient $c_{x\pi}$ takes place in the case of formation before the diffuser of a curvilinear shock wave (Fig. 8.49), when on the boundary of the internal jet aA the pressure is approximately the same as behind the normal shock wave:

$$(c_{x,a})_{\max} = \frac{X_{\text{son}}}{\rho_n \frac{\omega_n^2}{2} F_A} = \frac{1}{\frac{\rho_n \omega_n^2}{2} F_A} (p_n - p_a) (F_A - F_a) = \frac{p_n - p_a}{\frac{1}{2} \rho_n \omega_n^2} (1 - \varphi) \quad (39)$$

Here p_n - pressure behind the normal shock at a velocity which corresponds to the Mach number M_n ; F_a - the cross-sectional area of the jet in point a, F_A - the cross-sectional area of the diffuser in the plane of the inlet opening.

Substituting in (39) expression (45) from Chapter III for pressure behind a normal shock, we will obtain

$$(c_{x,a})_{\max} = \frac{4}{k+1} \frac{M_n^2 - 1}{M_n^2} (1 - \varphi) \quad (40)$$

With $M_n \leq 1$ supplementary resistance disappears in connection with the absence of shock waves.



Fig. 8.49. Flow around a diffuser with a curvilinear wave before it.

Figure 8.50 depicts the results of calculating dependences $\phi(M_n)$ and $c_{x,n}(M_n)$ for supersonic diffusers with a single-stage and two-stage central body, which has the different total angles of rotation of flow $\omega_n = \omega_1 + \omega_2$. As we see, at just one value of total angle of rotation of

flow the curves $\phi(M_n)$ and $c_{x,n}(M_n)$ for two-stage and single-stage wedges differ little.

The operation of the diffuser is influenced by the angle of attack γ (angle between the axis of the diffuser and the direction of incident flow), with an increase in which the coefficients of total pressure σ and the rate of flow ϕ decrease and additional drag $c_{x,n}$ increases. The nature of dependences $\sigma(\gamma)$, $\phi(\gamma)$ and $c_{x,n}(\gamma)$ for the different types of air intakes is dissimilar.

Up to now we cited data on the operation of plane supersonic diffusers. The basic dependences for axisymmetric, and also

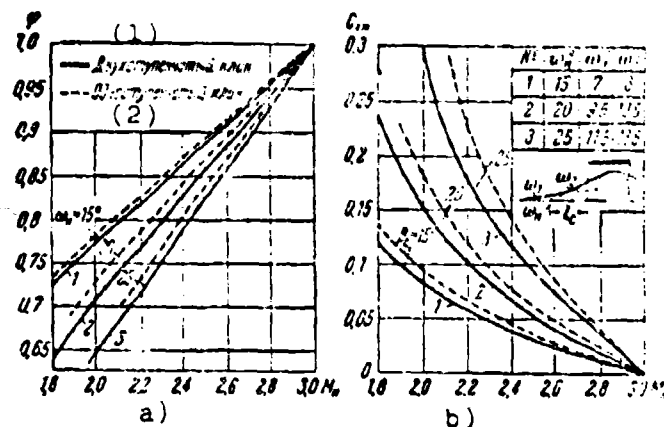


Fig. 8.50. Comparison of values ϕ and $c_{x m}$ for one- and two-stage wedges.
KEY: (1) Two-stage wedge; (2) Single-stage wedge.

lateral¹ and other types of diffusers have the same nature, but their calculation presents great difficulties.

In the examination of diffusers it was assumed that in the throat of a diffuser the velocity was equal to critical, and behind the throat there is a small supersonic zone terminated by a supplementary shock wave. In that case the system of shocks and the rate of air flow at the entry to the diffuser do not depend on the engine power rating.

However, with deep throttling of the engine (considerable change in the number of revolutions or nozzle area, etc.) the indicated operating mode of the diffuser - air intake is disturbed. So, with a decrease in the volume flow rate through the engine the counterpressure behind the diffuser increases, in connection with which the supplementary supersonic zone is reduced and losses

¹Lateral diffusers are those attached to the fuselage or the wing surface of a flight vehicle, i.e., having a common wall with any part of the latter.

in the supplementary shock drop (σ_A increases). Under certain throttling conditions the supplementary supersonic zone in the diffuser disappears. A further decrease in the rate of flow leads to the fact that in the throat of the diffuser a subsonic velocity is established whereupon the throttling begins to affect the intensity of the terminal shock wave of the intake system: due to a decrease in the rate of flow the velocity behind the shock decreases, which makes it necessary to displace it into the area of larger values of the velocity before it, but in this case the system of shocks will not be focused on the edge of the cowl.

Beginning from this system an increase is observed in the losses of total pressure and the external drag and a reduction of the flow coefficient in the diffuser. An increase in the intensity of the terminal shock wave can lead to the fact that a drop in the pressures on it will become higher than critical for the boundary layer and a breakaway of the latter will arise, whereupon vortex formations will cause the fluctuations of the rate of air flow and the location of the system of shocks.

At the moment of the greatest decrease in the rate of flow the system of shocks is converted into a curvilinear shock wave, ejected forward beyond the limits of the central body. This leads to the elimination of the boundary-layer separation and an increase in the rate of air flow, as a result of which the system of shocks is restored, and its terminating shock will approach that place, where again the boundary-layer separation occurs, etc. Under these conditions a strong vibration ("surging") of the engine is observed - low-frequency pulsations of pressure connected with the fluctuation in the rate of air flow. In view of the possible failure of the engine it cannot operate under the conditions of surging.

With an increase in the volumetric rate of air flow in the engine (higher than calculated) the supplementary supersonic zone

(behind the throat of the diffuser) is expanded and the supplementary shock is displaced into the area of greater velocities, due to which the losses of total pressure in it increase and the air density before the engine drops (this provides the increase of volume flow rate with a constant rate of flow through the diffuser).

With a certain increase in the volume flow rate the supplementary shock becomes so intense that it causes the boundary-layer separation (in the internal duct behind the throat of the diffuser). Characteristic for this system are the high-frequency pulsations of pressure accompanied by a high unpleasant sound - "buzzing." Surging and "buzzing" limit the throttle operating mode of an engine equipped with a diffuser.

The source of strong pulsations can also be the surface of the tangential rupture of velocity (from the point of intersection of shocks), if it enters inside the diffuser. The typical curves of dependence of values σ_d and $c_{x\infty}$ on the relative volumetric rate of air flow V/V_p (ratio of real flow rate V to calculated V_p) at different values of Mach number M_H are given in Fig. 8.51. They apply also for the throttle characteristics of diffusers in the form of dependence $\sigma_d(\phi)$ and $c_{x\infty}(\phi)$ with $M_H = \text{const}$ (Fig. 8.52).

For the expansion of the operating range of throttle systems and improvement of the diffuser characteristics at off-design flying speeds different methods for the control of diffusers are resorted to (change in the flow area of the throat and relative position of the central body and cowl, the discharge of air through openings in the wall of the diffuser, the control by suction or bleeding of the boundary-layer on the central body or on the cowl, etc.). These are described in specialized literature.¹ The regulation of rate of flow of air through the throat

¹See the books by R. Herman and Yu. N. Nechaev which are given in the bibliography.

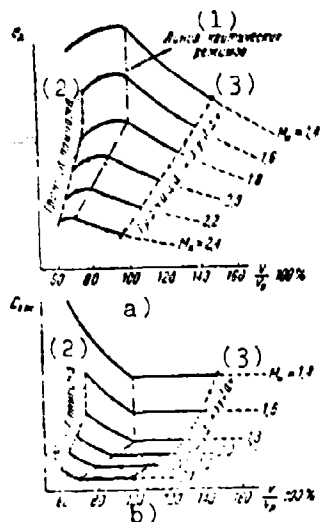


Fig. 8.51.

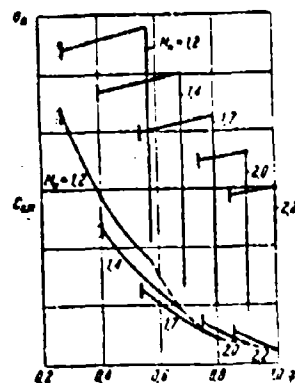


Fig. 8.52.

Fig. 8.51. The characteristics of an uncontrolled intake supersonic diffuser with $M_{HP} = 2.2$.

KEY: (1) Line of critical conditions; (2) Surge line; (3) Boundary of "buzzing."

Fig. 8.52. The throttle characteristic of an uncontrolled supersonic diffuser.

of a supersonic diffuser is also necessary for placing the latter in operational conditions ("starting"). The fact is that the calculated flow velocity is established not suddenly, but by means of transfer from the rest position to motion at a gradually increasing velocity. Let us examine this process in an example of the operation of a wind tunnel diffuser (Fig. 8.53). The acceleration of the air flow in a wind tunnel takes place in the following manner. First - with the starting of the tunnel - the velocity in its channel everywhere is lower than sonic and has the greatest value in the narrowest place - the throat of the nozzle (g.s). Gradually increasing the flow rate of air leads to conditions in which the velocity in the throat of the nozzle becomes critical, but in all remaining cross sections remains subsonic.

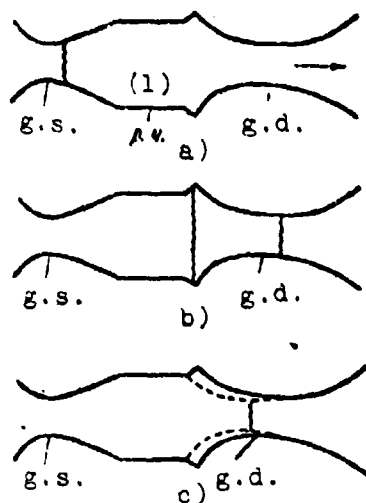


Fig. 8.53. The different flow conditions of gas in a wind tunnel: a) shock is located in the Laval nozzle (insufficient evacuation before the exhaustor), b) flow in the test section of the tube supersonic (system after "starting"), c) operational conditions (with a narrowed diffuser throat). KEY: (1) p.v. = r.ch. - test section.

A further increase in the volume flow rate at the exit from the tube (in the exhaustor) is not accompanied by an increase of weight rate in the throat of the nozzle, however, it leads to the appearance of a supersonic zone behind the throat of the nozzle which is terminated by a shock wave (Fig. 8.53a); in the latter the total pressure and density of the stagnation gas decrease, producing a relative increase in the volume flow rate in the diffuser of the tube, the throat (g.d.) of which therefore must have an area greater than the throat of the nozzle:

$F_{r,d} > F_{r,c}$. Under certain operating conditions of the exhaustor the density of the decelerated air because of losses in shock can decrease so much that the velocity in the throat of the diffuser will become critical. At the identical values of stagnation temperature ($T_0 = \text{const}$) an identical critical velocity is established both in the throat of the nozzle and the diffuser ($a_{kp} = \text{idem}$). Then from the equation of continuity we have

$$\rho_{c,d} V_{c,d} = \rho_{c,n} V_{c,n}$$

Gas density in the critical cross section with $T_0 = \text{const}$ is proportional to the total pressure

$$\frac{p_{r,A}}{p_{r,c}} = \frac{p_{r,A}}{p_{r,c}} = \sigma(M) \quad (41)$$

which changes because of losses in shock. Thus the areas of two throats during critical conditions in them are connected by the relationship

$$f = \frac{p_{r,A}}{p_{r,c}} = \frac{p_{r,s}}{p_{r,A}} = \frac{1}{\sigma} \quad (42)$$

In order that in the wind-tunnel test section the necessary supersonic speed (M_H) would be obtained, the shock wave should be located at the end of the test section. After the shock (in the tapering channel of the diffuser) the subsonic flow is accelerated and only in the throat of diffuser the velocity again becomes critical. Behind the throat of the diffuser a supplementary supersonic zone is formed which is terminated by a shock whose intensity is greater, the stronger the evacuation which is created by the exhaustor of the tube.

Thus the value $\sigma(M)$, on which according to (42) depends the relative size of the "critical" throat of diffuser, in turn is determined by the intensity of the shock, which corresponds to the Mach number in the test section. If we consider that a normal shock appears, then according to formula (24) in Chapter III

$$\sigma = \lambda_H^2 \left[\frac{1 - \frac{k-1}{k+1} \lambda_H^2}{1 - \frac{k-1}{k+1} \frac{1}{\lambda_H^2}} \right]^{\frac{1}{k-1}}.$$

where λ_H - the velocity coefficient in the test section of the tube. Converting to gas-dynamic functions from Chapter V we find

$$\sigma = \frac{q(\lambda_H)}{\sqrt{\left(\frac{1}{\lambda_H}\right)}} \quad (43)$$

From (42) and (43) it follows that for the output of a wind tunnel on the rated value of supersonic speed the relative cross section of the throat of the diffuser should be no less than the following value:

$$f = \frac{p_{r,a}}{p_{r,e}} = \frac{q\left(\frac{1}{\lambda_n}\right)}{q(\lambda_n)}. \quad (44)$$

If we make the relative cross section of the throat of the diffuser somewhat larger than according to formula (44), then it is possible to "extend" the shock wave from the test section into the divergent section of the diffuser (Fig. 8.53c), then in the narrowing section of the diffuser will be established a decelerating (after the test section) supersonic gas flow, whereupon in the throat of the diffuser the velocity coefficient $\lambda_{r,a} > 1$; according to formula (4) in Chapter IV we have

$$f = \frac{1}{\lambda_{r,a}} \left[\frac{\frac{2}{k+1}}{1 - \frac{2}{k+1} \lambda_{r,a}^2} \right]^{\frac{1}{k-1}}$$

or

$$f = \frac{1}{q(\lambda_{r,a})} = \frac{q\left(\frac{1}{\lambda_n}\right)}{q(\lambda_n)}. \quad (45)$$

After the shock passed into the expanding part of the diffuser it is possible, by smoothly narrowing (regulating) the throat of the diffuser, to gradually decrease the velocity in it down to the critical value, and then, weakening the evacuation of the exhaustor, to bring the shock wave in the divergent section of the diffuser almost to its throat (dotted line in Fig. 8.53c). Under such operational conditions the throat of the diffuser should be only somewhat larger than the throat of the nozzle (because of the displacement thickness of the boundary layer, i.e., only in connection with friction losses), and the loss of total pressure in the diffuser (in the shock) becomes considerably less than under the conditions of starting.

The ratio of the cross section area of the throat of the diffuser to the cross-sectional area of the jet of undisturbed flow F_w (the test section of the tube) according to (42), (44), and (45)

$$\bar{F}_{r,d} = \frac{F_{r,d}}{F_H} = \frac{F_{r,d}}{F_{r,c}} \frac{F_{r,c}}{F_H} = \frac{q(\bar{F}_H)}{q(\bar{F}_H)} = q\left(\frac{1}{\lambda_H}\right). \quad (46)$$

The values of the relative throat area of the diffuser $\bar{F}_{r,d}(M_H)$, necessary for the starting of the latter, and relative throat area $\bar{F}_{r,c}(M_H) = \frac{F_{r,c}}{F_H}$ at $k = 1.4$ are given in Fig. 8.54. It is

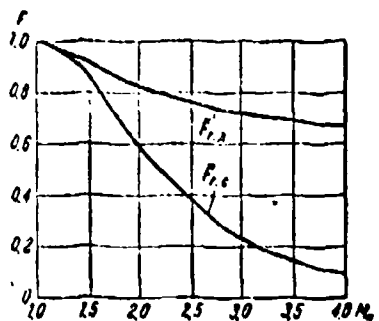


Fig. 8.54. The relative values of the areas of the throat of the diffuser (during "starting") and the wind-tunnel nozzle.

diffuser $M_{r,d}$, necessary for the "overshoot" through it of a normal shock wave (before the contraction of the throat of the diffuser), is approximately 0.875 from the value of the Mach number in incident flow M_H (for $M_H = 1.5-5$ with $k = 1.4$). The described features of the starting of a wind tunnel diffuser are related also to the starting of the inlet diffuser of an engine. In order to realize the calculated system of shocks by converting from low flying speeds to rated speed, one ought at low speeds to expand the throat of the diffuser (or to let the excess part of the air

before the throat pass outside), and based on the output on the rated speed to narrow the throat (to the calculated dimension) or to discontinue air bleeding (to cover the opening for bypass). Without this the starting of a supersonic diffuser under design conditions is impossible.

¹As was noted, after the outlet of the diffuser under design conditions the cross section of the throat of the diffuser is only a little (by the displacement thickness of the boundary layer) larger than the cross section of the throat of an ideal nozzle.

CHAPTER X

THE ELEMENTS OF GAS DYNAMICS OF THE AIRFOIL AND RECTILINEAR AIRFOIL CASCADE

§ 1. The Basic Geometric Parameters of the Airfoil and Rectilinear Airfoil Cascade

The rounded forward section (leading edge) and the pointed trailing edge (Fig. 10.1) are characteristic for the usual subsonic airfoil. The supersonic profile, unlike the subsonic, has a sharp (tapered) leading edge. In a number of cases the contour of such a profile is composed of rectilinear sections (Fig. 10.2)

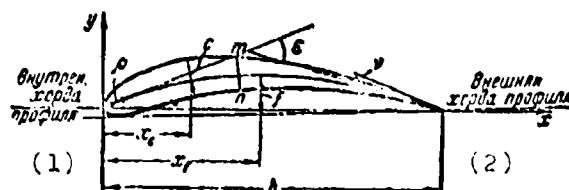


Fig. 10.1. Geometric parameters of subsonic airfoil.
KEY: (1) Internal airfoil chord. (2) External airfoil chord.

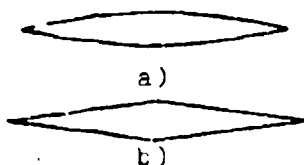


Fig. 10.2. Supersonic profiles: a) lenticular, b) double-wedge.

By the average line or the arc (small arc) of the profile we mean the locus at the centers inscribed in the outline of circumferences. After determining this line of the given profile, it is possible to construct a symmetrical section (with a straight center line) which has ordinates equal to the corresponding distances of the profile's points from the axial arc. If we now bend the symmetrical section so that its axis of symmetry would pass to the center line and the ordinates of symmetrical points would lie on the same normal to it, then we obtain this profile. Thus, any shape can be obtained by bending a certain symmetrical shape.

For determining the position of the profile with respect to the flow, and also as a characteristic dimension, we introduce the concept of airfoil chord. The internal airfoil chord is the line segment connecting the two most distant points of the axial profile arc. For the slightly bent profiles the chord determined in this way is virtually coincidental with the straight line section connecting the two most distant points of the profile. The coordinates of the profile points are usually given in fractions of the chord length, which is assumed to be the horizontal axis.

The profile configuration is determined by a series of geometric parameters. Let us give the principal one. The relative profile thickness c is the quotient of the division of the maximum profile thickness c (Fig. 10.1) by the chord length b : $\bar{c} = c/b$. The center-line camber \bar{f} or the relative camber, is the ratio of the maximum bending deflection of axial arc f to the chord length: $\bar{f} = f/b$. The positions of the maximum profile thickness and maximum bending deflection of the axial arc are important parameters and are determined respectively by the values of relative abscissae

$$x_c = x_c/b \quad \text{and} \quad x_f = x_f/b.$$

The profile camber can also be characterized by the angle of bending of center line ϵ , i.e., by the angle between the tangents to the axial arc at the nose and the rear point, called the leading and rear tangents of the profile respectively (Fig. 10.1). For a circular small arc, angle ϵ is equal to its central angle. In this case

$$\gamma = \frac{1}{8} \lg \frac{\epsilon}{4}.$$

After selecting a certain form for the axial small arc and the shape of the initial symmetrical profile, it is possible to obtain a family (series) of profiles with a continuous change in the center-line cambers and thicknesses.

A rectilinear airfoil cascade is the name applied to a combination of an infinite number of equally arranged identical airfoils which are equidistant from one another. The line which connects the corresponding profile points in the cascade is called the *cascade front* and the normal to it - the *axis of the cascade* (Fig. 10.3).

The problem of the flow around a rectilinear cascade is encountered in axial-flow compressors and turbines in the study of flow through the fixed and rotating vane rings with cylindrical stream surfaces. In this case the elementary rim, i.e., the vane ring limited by two close stream surfaces can be converted to a rectilinear cascade by developing it into planes; in order for the flow around all airfoils to be identical (as in the vane ring), the cascade should consist of infinite number of airfoils.

The relative position of airfoils in a rectilinear cascade is unambiguously determined by two parameters: distance between the adjacent airfoils called cascade pitch t , and the angle between the airfoil chord and the front, which is called setting angle β . Instead of setting angle β , sometimes the concept of stagger is used, which implies the distance a between the normals to the chords of two adjacent profiles, drawn at similar points.

As seen from the drawing, $a/t = \bar{a} = -\cos \theta$, and, consequently, the forward stagger corresponds to values $\theta > \pi/2$, while the backward stagger - to values $\theta < \pi/2$. The position of this airfoil in the cascade can also be characterized by one of the angles ϕ_1 or ϕ_2 (Fig. 10.3) formed by the front and rear tangents of the profile with the front of the cascade, respectively. The difference of these angles determines the bending of the profile $\epsilon = \phi_2 - \phi_1$.

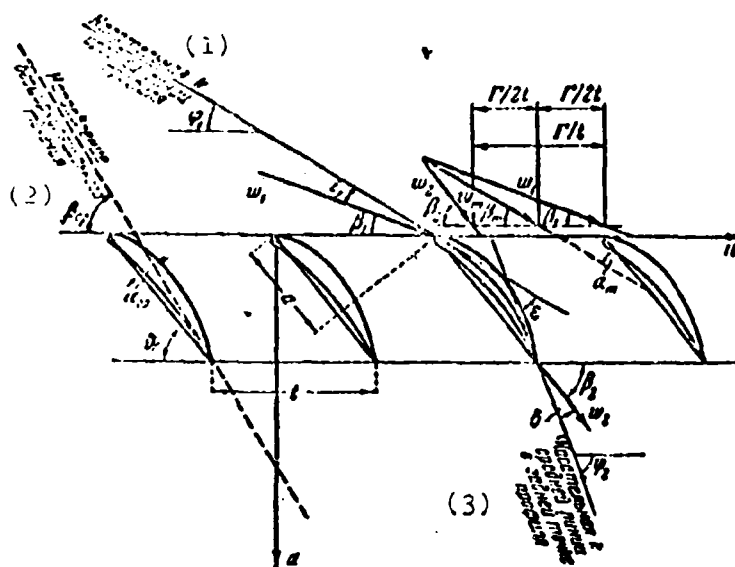


Fig. 10.3. Rectilinear cascade.
 KEY: (1) Tangent to the center profile line.
 (2) Direction of noncirculatory flow. (3)
 Tangent to the center line at the rear point
 of a profile.

The cascade pitch value referred to the chord length of the profile is called *relative cascade pitch* $\bar{t} = t/b$; the reciprocal value is called the *cascade solidity* $\tau = b/t$. Thus, a rectilinear cascade can be unambiguously determined by the form of a profile, by solidity and value of the setting angle.

The position of the profile and airfoil cascade with respect to the incident flow is characterized by the angle of attack; in the case of a unitary profile - it is angle α between the direction of the speed at infinity and the chord (Fig. 10.1); in the case of the airfoil cascade - it is angle i between velocity w_1 and the forward tangent to the profile arc. The angle between w_2 and the rear tangent is called the *flow angle of lag* δ (Fig. 10.3). Angle β_1 between the direction of inlet velocity w_1 and the cascade front is called the angle of entry; accordingly, angle β_2 between the outlet velocity w_2 and the cascade front is called the *angle of departure*. The difference in these angles $\Delta\beta = \beta_2 - \beta_1 = \epsilon - \delta + i$ determines the rotation of flow in the cascade.

In aerodynamics a distinction is made between the direct and inverse problems of flow around a unitary profile or the airfoil cascade.

By direct problem for a unitary profile we usually mean the determination of pressure distribution along the surface of this profile at a given velocity field far ahead of the profile. The determination of the geometry of a profile, which provides certain pressure distribution along its surface, is called the *inverse problem*.

In aerodynamics of the airfoil cascade both these problems are usually examined as applied to the total parameters of the cascade. Here, by direct problem we mean the determination of aerodynamic forces and the angle of departure of the flow at a given velocity field ahead of the cascade of certain configuration. In the case of flow of a viscous fluid or gas, there is also a need for determining the total pressure losses.

Accordingly, by the inverse problem we mean the determination of configuration of the cascade which turns a given flow to angle $\Delta\beta$, forming angle β_1 with the front of the cascade. In such a

setting there usually is no unique solution for the inverse problem. There is an infinite number of cascades which differ from one another in their geometric parameters and profile shapes, which satisfy the posed conditions. The problem becomes unique with the imposition of additional conditions. In the case of a potential flow these conditions are usually imposed on the geometry of the cascade or on the pressure distribution along the profile or, finally, on the combination of the indicated factors. In the case of a viscous flow, the optimum cascade (with minimal losses) is found from the whole multitude of cascades which achieve the given angle of rotation.

§ 2. Zhukovskiy's (Joukowski's) Theorem on the Power Effect of a Potential Flow on the Airfoil in the Cascade

Let us examine the flow around a rectilinear infinite cascade of airfoils by the steady flow of gas. We will assume that the airfoils which form the cascade have an infinite span and the flow is plane-parallel.

Let us determine the force with which the flow affects the airfoil surface of unit length. Let us draw sections 1-1 and 2-2 which are parallel to the cascade front (Fig. 10.4) and are so distant from it that it is possible to assume that the speed and pressure in each of these sections are constant. Let us select any flow line $A_1 A_2$ and draw another flow line $B_1 B_2$ at a distance of one pitch from the first flow line. It is obvious that these flow lines are congruent, i.e., they coincide when superimposed. Applying the equation of momentum to the volume of fluid limited by sections of straight lines $a_1 b_1$ and $a_2 b_2$ and by sections of flow lines $a_1 a_2$ and $b_1 b_2$, we will obtain (see § 5 Chapter I) the following expressions for the projections, on the front and the axis of the cascade, of the resultant of all forces applied to the fluid volume:

$$P_u = M(\omega_{1u} - \omega_{2u}) \quad (1)$$

$$P_a = M(\omega_{1a} - \omega_{2a}) \quad (2)$$

where M - fluid mass passing through the section, which is equal to one cascade pitch,¹ in unit time and which is determined by the equation of continuity

$$M = \rho_1 \omega_{1a} t = \rho_2 \omega_{2a} t. \quad (3)$$

On the other hand, the forces can be determined by adding the projections of all forces which act on volume $a_1 b_1 b_2 a_2$, i.e., the forces of pressure along contour $a_1 b_1 b_2 a_2$ and the reactions from the force applied to the airfoil surface (we disregard the gravitational forces). Designating the components of forces applied to the airfoil in terms of R_u and R_a and noting that the resultant forces of pressure applied to the sections of flow lines $a_1 a_2$ and $b_1 b_2$ are equal and are directed to opposite sides, we have

$$P_u = -R_u \quad \text{and} \quad P_a = -R_a + (\rho_1 - \rho_2)t.$$

Substituting the last equalities into expressions (1) and (2), we obtain

$$R_u = M(\omega_{1u} - \omega_{2u}) \quad (4)$$

$$R_a = M(\omega_{1a} - \omega_{2a}) + t(\rho_1 - \rho_2) \quad (5)$$

Let us determine the value of circulation Γ_{OH} along contour $a_1 b_1 b_2 a_2$. By bypassing the contour in forward direction, i.e., clockwise, we have the following values of circulation for the frontal sections of the contour:

$$\Gamma_{a_1 b_1} = t\omega_1 \cos \beta_1 = t\omega_{1u} \quad \Gamma_{b_2 a_2} = t\omega_2 \cos \beta_2 = -t\omega_{2u}$$

¹Here and subsequently the thickness of the jet in the direction of the perpendicular to the plane of the drawing is equal to unity.

Subsequently, we will limit ourselves to the examination of a potential flow. As was proven in § 11 Chapter II, in the case a potential (Vortex-free) flow circulation Γ_{OH} along certain contour $a_1 b_1 b_2 a_2$ is equal to circulation Γ in any contour enveloping the airfoil including also the surface of the airfoil itself, i.e., $\Gamma_{OH} = \Gamma$, and, consequently, in the potential flow

$$R_s = M \frac{\Gamma}{l}. \quad (8)$$

In the incompressible flow we have

$$w_{1s} = w_{2s} = w_s, \quad M = \rho w_s$$

In the absence of losses we also have

$$p_1 - p_2 = \frac{\rho}{2} [w_1^2 - w_2^2].$$

According to (4) and (8), for the potential flow of the incompressible fluid we obtain

$$\begin{aligned} R_s &= \frac{\rho}{2} [w_{1s}^2 - w_{2s}^2] = \frac{\rho}{2} (w_{1s}^2 - w_{2s}^2) \\ R_s &= \rho w_s^2 l. \end{aligned}$$

Based on the velocity triangle on Fig. 10.3, it follows that

$$\frac{w_{1s}}{2} + \frac{w_{2s}}{2} = w_m, \quad (9)$$

$$w_{1s} = w_{2s} = w_m. \quad (10)$$

Here, w_m is understood to be the geometric mean velocity

$$w_m = \frac{w_1 + w_2}{2}.$$

The direction of the geometric mean velocity is determined from the obvious expression

$$\operatorname{ctg} \beta_m = \frac{1}{2} (\operatorname{ctg} \beta_1 + \operatorname{ctg} \beta_2). \quad (11)$$

In accordance with (6), (9) and (10), we have

$$R_x = -\rho l' \alpha_{m\alpha} \quad (12)$$

$$R_z = \rho l' \alpha_{m\alpha} \quad (13)$$

From these expressions for the force components of pressure it follows that in a potential flow of an incompressible fluid the value of all resultant aerodynamic forces applied to the cascade airfoil is equal to the product of the fluid density times the value of the geometric half-sum of velocities and the value of circulation around the airfoil

$$R = \rho \alpha_m l' \quad (14)$$

Force R is directed at right angles to the geometric half-sum of velocities. In order to obtain the direction of this force, it is necessary to turn the geometric half-sum to an angle of $\pi/2$ to the direction opposite to that of circulation. This theorem for the airfoil cascade was first obtained by N. Ye. Joukowski in 1912.

At subsonic speeds of an isentropic gas flow it is possible to use the equation of the resultant in form (14), determining only density value $\rho = \rho_m'$ according to the formula

$$\frac{1}{\rho_m} = \frac{1}{2} \left(\frac{1}{\rho_1} + \frac{1}{\rho_2} \right).$$

In this case the Joukowski theorem for the cascade in an isentropic flow of compressible gas is fulfilled precisely if we replace the true curve of the isentropic process by the straight line tangent to it at point $(p_0, 1/\rho_0)$.¹ In this case the direction

¹E. M. Berzon, on the Force Acting on Airfoil in a Cascade. The transactions of the Leningrad Military Engineering Air Academy, iss. 27, 1949; Loytsyanskiy L. G., the generalization of Joukowski's formula in the case when the cascade airfoil is streamlined by compressible gas at subsonic speeds. Appl. math. and mech., No. 2, tn. XIII, 1949; Loytsyanskiy L. G., Fluid and gas mechanics. Tekhteorizdat, 1950; Bloch E. L., Balter A. Ye. and Dovzhik S. A., N. Ye. Joukowski's Theorem on the airfoil's lift force in a cascade, streamlined by compressible gas. In coll. "Industrial Aerodynamics," iss. 4. 1953.

of the resultant at not very high subsonic speeds turns out to be very close to the normal to the geometric half-sum of current densities

$$J_m = (\rho w)_m = \frac{\rho_1 w_1 + \rho_2 w_2}{2}$$

In the general case of gas flow the resultant can be presented as the sum of two components, i.e., of the Joukowski force, equal in magnitude $(\rho w)_m \Gamma$ and directed along the normal to the geometric half-sum of current densities and certain additional force directed along the axis.¹

Let us determine the power effect of a potential flow of the incompressible fluid on a unitary airfoil. For this we will direct cascade pitch t toward infinity. We will obtain the unitary airfoil within the limit. It is obvious that if we consider the flow parameters ahead of the cascade to be fixed, then when $t \rightarrow \infty$ we have

$$w_{2\infty} = w_{1\infty}, \quad \beta_2 = \beta_1, \quad w_{2\infty} = w_1$$

and, therefore, according to (14)

$$R = \rho w_1 \Gamma. \quad (15)$$

Here Γ - still the circulation of velocity, taken for any contour enveloping this unitary airfoil. Thus, we can formulate the following theorem: during the potential flow around a unitary airfoil, the resultant of force applied to the airfoil is equal to the product of the density and velocity of the incident flow times circulation the value Γ around the airfoil. To find the direction of the resultant which, in this case, is the lift force

¹Sedov L. I., Hydroaerodynamic forces during the flow of a compressible fluid around airfoils. Proceedings of the Academy of Sciences USSR, No. 6 tn. 1 XIII, 1948 (see also G. Yu. Stepanov's article in the survey bulletin "Aircraft Engine Production" No. 4, (1949)).

we have to swing the velocity vector through an angle of $\pi/2$ in the direction opposite to that of circulation.

This important theorem was first obtained by N. Ye. Joukowski in 1906. Subsequently, in 1934 M. V. Keldysh and F. I. Frankl' verified this theorem for the gas flow, limiting themselves to relatively low Mach numbers. The derivation of the Joukowski theorem for a gas was made by L. I. Sedov in 1948 by passing to the limit.

§ 3. Effect of Viscosity on the Power Influence of Flow

The flow of viscous fluid around the cascade produces a wake, an area of reduced total pressure, where in fact all losses which appear in the boundary layer are concentrated.

Let us examine a volume of fluid limited by two adjacent congruent stream surfaces, by section 1-1, located far ahead of the cascade and by certain section z-z behind it (Fig. 10.5). As shown by the experiments, the equalization of the flow velocities with respect to direction, connected with the equalization of static pressure is achieved in the immediate proximity behind the cascade (at a distance of fractions of the airfoil chord from the edge of the cascade).

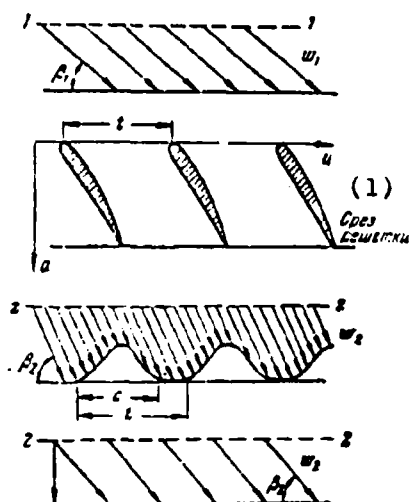


Fig. 10.5. Streamlining of the airfoil cascade by the viscous fluid.
KEY: (1) Edge of the cascade.

Applying the theorem of momentum to the selected volume of fluids, we have

$$R_a = t(p_1 - p_2) + \rho_1 w_{1a} t - \int_0^t \rho w_a^2 dz, \quad (16)$$

$$\begin{aligned} R_u &= \rho_1 t w_{1u} w_{1a} - \int_0^t \rho w_a w_u dz = \\ &= \rho_1 t w_{1a} \operatorname{ctg} \beta_1 - \operatorname{ctg} \beta_2 \int_0^t \rho w_a^2 dz. \end{aligned} \quad (17)$$

Let us assume approximately that with a continuous flow around the cascade the direction of velocities in section z - z is identical for the viscous and potential flows, i.e., let us assume that

$$\beta_z = \beta_{z \text{ pot}} = \beta_{z \text{ vis}}$$

In this case the effect of viscosity will be apparent only in the uneven distribution of velocities at the exit from the cascade.

Assuming that in expressions (16) and (17) the velocities behind the cascade are constant, we obtain the following formulas for the axial and tangential components of forces which act on the cascade streamlined by the potential flow of incompressible fluid:

$$R_{a \text{ pot}} = t(p_1 - p_{2 \text{ pot}}), \quad (18)$$

$$R_{u \text{ pot}} = \rho t w_a^2 (\operatorname{ctg} \beta_1 - \operatorname{ctg} \beta_2). \quad (19)$$

By deducting expressions (16) and (17) term by term from (18) and (19), we obtain

$$\Delta R_a = R_{a \text{ pot}} - R_a = t(p_1 - p_{2 \text{ pot}}) - t \rho \left[\int_0^1 w_a^2 dz - w_{1a}^2 \right], \quad (20)$$

$$\Delta R_u = R_{u \text{ pot}} - R_u = \rho t \left[\int_0^1 w_a^2 dz - w_{1a}^2 \right] \operatorname{ctg} \beta_2, \quad (21)$$

where $\bar{z} = z/t$.

There are no losses in the core of the flow

$$p_{z \text{ not}} + \frac{\rho w_{z \text{ not}}^2}{2} = p_z + \frac{\rho w_{z \text{ max}}^2}{2}. \quad (22)$$

Hence it follows that

$$p_z - p_{z \text{ not}} = \frac{\rho}{2} (w_{z \text{ not}}^2 - w_{z \text{ max}}^2).$$

According to the equation of continuity

$$w_{1u} = \frac{1}{l} \int_0^l w_n dz = \int_0^1 w_n dz. \quad (23)$$

Taking into account the two last expressions, formulas (21) and (20) assume the form

$$\Delta R_a = \frac{1}{2} \rho (w_{z \text{ not}}^2 - w_{z \text{ max}}^2) + \rho \left[\int_0^1 w_n^2 dz - \left(\int_0^1 w_n dz \right)^2 \right], \quad (24)$$

$$\Delta R_a = \rho \left[\int_0^1 w_n^2 dz - \left(\int_0^1 w_n dz \right)^2 \right] \operatorname{ctg} \beta_z. \quad (25)$$

Since $w_{z \text{ not}} \leq w_{z \text{ max}}$ and for any function $w(z)$ the following inequality is valid:

$$\int w^2(z) dz > \left(\int w(z) dz \right)^2, \quad (26)$$

then value ΔR_a is the sum of two components of opposite signs. In the general case this does not make it possible for us to make a conclusion concerning the sign of the viscosity effect on the axial component value of the resultant force.

The sign of addition to another component, ΔR_u , according to (25), is determined by the angle of departure of flow β_z . With $\beta_z = \pi/2$, i.e., with the axial departure of flow from the cascade, $\Delta R_u = 0$, and, consequently, in this case, the viscosity effect is generally absent: the circumferential component of the resultant force is determined only by spiral, by the relative value of the circumferential velocity component.

For the cascades in which $\beta_2 > \beta_1$, value R_u in the potential flow is always positive according to (19).¹ Therefore in such cascades, when $\beta_2 < \pi/2$, the presence of viscosity leads to a decrease, and with $\beta_2 > \pi/2$ it leads to an increase in the circumferential component of the resultant force.

In cascades with angles $\beta_2 < \beta_1$, value R_u in the potential flow is negative and therefore, here, in accordance with (25), the presence of viscosity always leads to an increase in the absolute value circumferential force.

Usually, cascades are differentiated depending on the calculated ratio of velocities at the entrance and the exit.

A *convergent cascade* is one which has $p_2 < p_1$. The flow passing through such a cascade increases its speed; during this, the static pressure in it drops. At of the same angles β_1 the convergent cascades can be of two types: with angle $\beta_2 > \beta_1$ and with angle $\beta_2 > \pi - \beta_1$.

The cascade in which a stagnation of flow occurs ($p_2 > p_1$) is called the *diffuser cascade*. The stagnation of flow is naturally accompanied by an increase in static pressure. The diffuser cascades encompass the area of angles

$$\pi - \beta_1 > \beta_2 > \beta_1.$$

The cascade in which the change is only in the direction of velocity, while its value remains constant ($p_2 = p_1$), is called an *active cascade*. In this cascade $\beta_2 = \pi - \beta_1$.

¹Without disturbing generality, we will always assume $\beta_1 \leq \pi/2$.

The results obtained above can now be formulated in the following manner. In the convergent and active cascades the presence of viscosity always leads to an increase in the circumferential force as compared with its value in the potential flow. The viscosity also has the same effect in the diffuser cascades which turn the flow to angle $\beta_z > \pi/2$. In the diffuser cascades with $\beta_z < \pi/2$ the viscosity effect is inverse - it leads to a decrease in the circumferential component of the resultant force.

During the viscous fluid flow in the space behind the cascade, as a result of mixing, there is a gradual equalization of the velocity fields. As a result, beginning with a certain section 2-2 sufficiently removed from the cascade, there is already a uniform flow whose parameters can be determined with the aid of the equations of continuity and momentum. Thus, for instance, in the case of the incompressible fluid the axial velocity of the equalized flow is equal to the axial velocity of the incoming flow, and the static pressure and circumferential velocity are determined from the following equations which represent projections of the momentum on axes a and u , respectively.

$$\left. \begin{aligned} \rho w_{1a} t - \rho \int_0^l w_a^2 dz &= (p_s - p_a) t, \\ \rho t w_{1u} w_{1a} &= \rho \int_0^l w_a w_u dz. \end{aligned} \right\} \quad (27)$$

Replacing in the last expression

$$w_u = w_a \operatorname{ctg} \beta$$

and taking into account that according to the equation of continuity

$$\rho w_{1a} t = \rho \int_0^l w_a dz,$$

we obtain

$$\operatorname{ctg} \beta_2 = \frac{\int_0^1 w_2^2 dz}{\int_0^1 w_2 dz} \operatorname{ctg} \beta_1 \quad (28)$$

where $\bar{z} = z/t$.

The condition of compressibility somewhat complicates the determination of the equilized gas flow parameters.¹ Replacing in the expression for the projection of momenta on axis u

$$\int_0^M w_1 \cos \beta_1 dM = M w_2 \cos \beta_2$$

the value of elementary mass according to formula (111) in Chapter V

$$dM = V \sqrt{\frac{k \left(\frac{2}{k+1} \right)^{\frac{k+1}{k-1}}}{gR}} \frac{p_2}{\sqrt{T_2}} y(\lambda_2) \sin \beta_2 dz,$$

we will obtain the following expression for the coefficient of the circumferential velocity component of the equilized flow:

$$\lambda_{2u} = \lambda_2 \cos \beta_2 = \frac{\int_0^1 \lambda_2 y(\lambda_2) dz}{\int_0^1 y(\lambda_2) dz} \cos \beta_2$$

To determine angle β_2 , we write the theorem of momentum in the projection in the direction of the equilized flow

$$M w_1 - \int_0^M w_1 \cos (\beta_1 - \beta_2) dM = (p_1 - p_2) t \sin \beta_2$$

¹Ginsburg S. I., Total Power Effect of the Stationary Plane Flow on the Rectilinear Airfoil Cascade. In coll. "Bladed machines and Jet Apparatuses," iss. 3, "Mechanical Engineering," 1968.

which, taking into account (126) and (127) in Chapter V, we rewrite in the following dimensionless form:

$$z(\beta_2) = \frac{2k}{k+1} \lambda_{2n} \cos(\beta_2 - \beta_1) + \left(\frac{2}{k+1}\right)^{\frac{1}{k-1}} \frac{\sin \beta_2}{\sin \beta_2 \int_0^1 y(\lambda_2) dz}.$$

Hence, after elementary transformation we obtain

$$a - b \sin^2 \beta_2 + c \sin 2\beta_2 = 0, \quad (29)$$

where

$$a = \frac{k-1}{k+1} \lambda_{2n} - \frac{1}{\lambda_{2n}}, \quad b = \frac{2k}{k+1} \lambda_{2n} - \frac{1}{\lambda_{2n}}, \\ c = \frac{2k}{k+1} \lambda_{2n} \lg \beta_2 + \frac{1}{2 \left(\frac{2}{k+1}\right)^{\frac{1}{k-1}} \sin \beta_2 \int_0^1 y(\lambda_2) dz}.$$

Equation (29) can be transformed into the form

$$A \sin^4 \beta_2 - B \sin^2 \beta_2 + 1 = 0. \quad (29a)$$

here

$$A = \frac{b^2}{a^2} + 4 \frac{c^2}{a^2}, \quad B = 2 \frac{b}{a} + 4 \frac{c}{a}.$$

After determining flow direction (β_2), from (29a), we compute the velocity

$$\lambda_2 = \frac{\lambda_{2n}}{\cos \beta_2},$$

and from the equation of continuity written for sections z-z and z'-z',

$$p_2 \sin \beta_2 \int_0^1 y(\lambda_2) dz = p_{02} q(\lambda_2) \sin \beta_2$$

depending on static pressure p_2 directly behind the cascade, we find the total pressure p_{02} of the equilized flow, total losses in total pressure

$$\Delta p_0 = p_{01} - p_{02}$$

and the coefficient of total hydraulic losses

$$\zeta = \frac{\Delta p_{\text{tot}}}{\rho_1 \frac{w_1^2}{2}}.$$

This coefficient takes into account the losses both strictly in the cascade (in its vane channels) and those due to the equalization of the flow in the space behind the cascade.

Let us now find the losses strictly in the cascade. For this we carry out on isentropic averaging of the flow in section z-z, i.e., we find a steady flow with the same entropy as that in a nonuniform flow.¹ At a constant static pressure we have²

$$\ln \frac{p_{0z}}{p_{0z \text{ из}}} = \frac{\int_0^1 \frac{\lambda}{\tau(k)} \ln \tau(k) dk}{\int_0^1 \frac{1}{\tau(k)} dk}.$$

After obtaining the mean isentropic total pressure $p_{0z \text{ из}}$ in cross section z-z from the last expression using the known static pressure and the specified distribution of velocities, we find the loss in the cascade itself

$$\Delta p_{\text{сеч}} = p_{01} - p_{0z \text{ из}}$$

and the losses caused by the equalization of the flow velocities behind it:

$$\Delta p_{\text{равн}} = p_{0z \text{ из}} - p_{02}.$$

¹Sedov L. I., Chernyy G. G., The Averaging of Nonuniform Gas in the Channels. Collection of articles under the editorship of L. I. Sedov, No. 12, iss. 4. Oborongiz, 1954.

²Korostelev Yu. A., Klimovskiy K. K., The Averaging of Parameters of the Nonuniform Airflow as applied to the axial-flow compressor. Collection of articles under the editorship of L. I. Sedov, No. 13, iss. 5. Oborongiz, 1954.

The losses in the cascade during its continuous streamlining by a subsonic flow can also be expressed directly in term of the boundary layer parameters on the trailing edges of its airfoils.

Having determined the power losses in the wake behind the cascade, which consists of boundary layers having converged from the upper (convex) and lower (concave) profile surfaces, and bearing in mind that in the remaining section the flow is isentropic, we obtain the following expression for the loss factor in the cascade:¹

$$\zeta_p = \frac{\Delta p_{ep}}{\rho_1 \frac{w^2}{2}} = \left(\frac{\delta_1 \sin \beta_1}{\rho_{H1} \sin \beta_1} \right)^2 \frac{\Delta^{***}}{(1-\Delta^*)^2}.$$

Here ρ_{H1} - value of density on the boundary layer border

$$\Delta^* = \frac{\delta_{HB}^* + \delta_{HH}^*}{l \sin \beta_2} = \frac{\delta/l}{\sin \beta_2} (\delta_{HB}^* + \delta_{HH}^*),$$

$$\Delta^{***} = \frac{\delta_{HB}^{***} + \delta_{HH}^{***}}{l \sin \beta_2} = \frac{\delta/l}{\sin \beta_2} (\delta_{HB}^{***} + \delta_{HH}^{***}),$$

where δ_{HB}^* , δ_{HH}^* - displacement thicknesses on the trailing edge for the boundary layer on the upper and lower profile surface respectively, δ_{HB}^{***} , δ_{HH}^{***} - energy loss thicknesses in the boundary layer on the trailing edge (see Chapter VI). For the incompressible fluid $\rho_1 = \rho_{H1}$ and the loss factor

$$\zeta_p = \left(\frac{\sin \beta_1}{\sin \beta_2} \right)^2 \frac{\Delta^{***}}{(1-\Delta^*)^2}.$$

Further, we will limit ourselves to an examination of incompressible fluid flow. In this case the following inequality² follows from expression (28) and condition (26)

$$\operatorname{ctg} \beta_1 > \operatorname{ctg} \beta_2. \quad (30)$$

¹Ginevskiy A. S., Dovzhik S. A., Gas viscosity effect on the cascade characteristics. In coll. "Industrial Aerodynamics," iss. 11. Oborongiz, 1958.

²This relationship was obtained by Yu. A. Korostelev in 1953.

Thus, the direction of the equalized flow is always closer to the direction of the cascade front than the direction of the initial nonuniform flow. This means that in the convergent and active cascades, it appears that the viscosity effect leads to an increase in the deflection of the flow by the cascade, i.e., to a decrease in the initial angle of lag and, sometimes, even to the development of the advance angle of the flow.

The influence of viscosity has the same effect in the diffuser cascades which have $\beta_z > \pi/2$. In the diffuser cascades which have $\beta_z < \pi/2$, the viscosity effect is inverse, i.e., it leads to a decrease in the effective deflection of the flow by the cascade, i.e., to the appearance of seemingly complementary angle of lag. These conclusions are in complete agreement with the results obtained above on the viscosity effect on the circumferential component value of the resultant.

Using the known parameters of the equalized flow the power effect on the cascade can be determined directly by formulas (4), (5) obtained for a uniform flow.

For the viscous incompressible fluid flow we have

$$p_1 - p_2 = \frac{\rho}{2} (\omega_1^2 - \omega_2^2) + h_w = -\rho \frac{\Gamma_{cs}}{r} \omega_{m2} + h_w,$$

and according to (5)

$$R_a = -\rho \Gamma_{cs} \omega_{m2} + h_w f. \quad (31)$$

Here h_w are the total losses of total pressure, referred to 1 m² of fluid flowing from cross section 1-1 to cross section 2-2. The total losses include both the losses which arise during a direct flow around the cascade and losses connected with a complete equalization of the flow in the space behind the cascade.

The circumferential component force is found from formula (7)

$$R_u = \rho \omega_{m2} \Gamma_{or} \quad (32)$$

The last two expressions make it possible for one to generalize the Joukowski theorem as follows: the resultant of all forces applied to the cascade profile as it is being streamlined by a flow of viscous incompressible fluid is equal to the vector sum of the Joukowski circulation force $G = \rho w_m \Gamma_{OH}$ directed along the normal to the geometric half-sum of velocities and certain additional force $F_a = h_w t$, always directed along the axis of the cascade.

The projection of the resultant on the direction of the normal to the geometric mean velocity w_m is called airfoil lift force R_y in the cascade. During a potential flow around the cascade the lift is equal to the Joukowski circulation force $R_y = G$.

The other resultant projection on the direction of mean geometric velocity R_x we will call the viscous force, thereby characterizing the reason for its development, because in a potential flow of incompressible fluid it is equal to zero.

Comparing the streamlining of this cascade by the viscous and potential flows of incompressible fluid at the same (with respect to magnitude and direction) geometric mean velocity w_m , we note that the viscosity effect is twofold: it leads both to the change in the Joukowski circulation force G and to the appearance of additional axial force F_a . As a result viscous force (resistance) R_x is developed which is equal to the projection of force F_a on the direction of the geometric mean velocity, and also there is a change in the value of lift R_y . This change is determined by the relationship between the corresponding projection of the additional axial force and the change in the Joukowski circulation force

$$\Delta R_y = \Delta G - F \cos \beta_m$$

If in the vane channels of a dense cascade a complete equilization of the velocity fields is achieved as a result of turbulent mixing the flow on the edge of the cascade is uniform,¹ then the viscosity effect is limited only by the development of axial force F_a , Joukowski force remains the same, since the value of circulation Γ_{0H} does not change. In this particular case

$$\Delta R_y = -F_a \cos \beta_m = -h_a t \cos \beta_m,$$

and, therefore, in the viscous flow the airfoil lift in the convergent cascade is greater, while in the diffuser cascade it is less, than the Joukowski circulation force (Fig. 10.6). In an active cascade, just as in the potential flow, the lift is equal to that of circulation.

The resultant projection on the direction normal to the incident flow is called lift R_y of the unitary profile. Another projection of the resultant force normal to it is called the profile resisting force R_x .

In the potential flow the profile is affected only by the forces of pressure, whose resultant, according to the Joukowski theorem, is equal to airfoil lift $R = R_y$. The resistance is absent when $R_x = 0$. The effect of viscosity is evident in both the appearance of the tangential forces, forces of friction, on the profile surface and the redistribution of pressure forces. As a result, in a viscous flow there is a change in the lift and the appearance of the profile drag force which consists of pressure resistance R_{xp} and friction drag R_{xf} . These total force components of the profile drag

$$R_x = R_{xp} + R_{xf} \quad (53)$$

¹Strictly speaking, such a case is hypothetical. Actually, with a sufficient length of the channel a certain distribution of velocities is established, which does not change any further (see Chapter VI).

are equal to the projection on the direction of motion of the resultant normal and tangential forces respectively, which act on the profile surface.

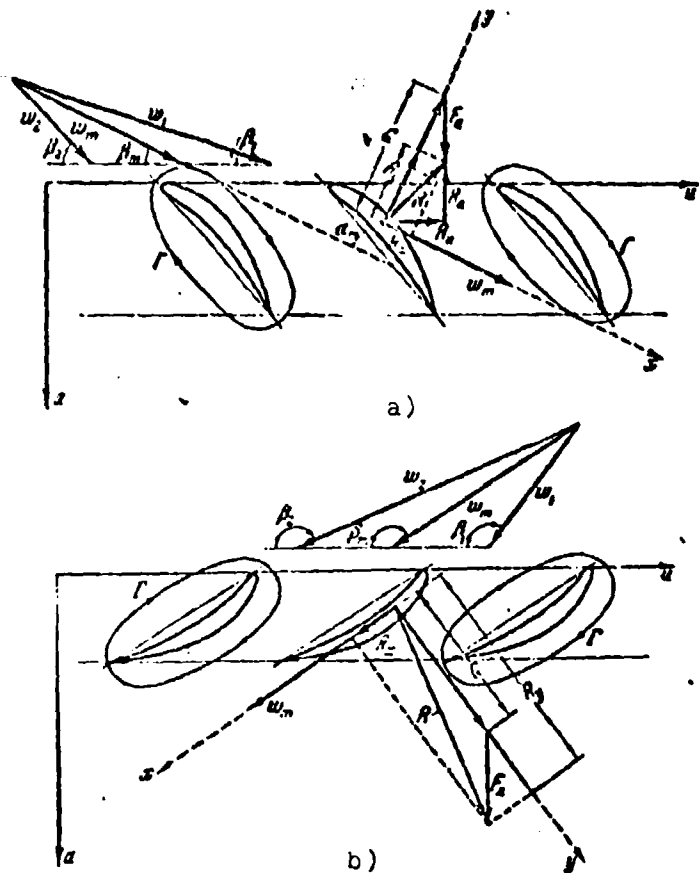


Fig. 10.6. The effect of viscosity on the power effect of the incompressible flow on the dense cascade (complete equalization in the vane channels): a) Diffuser cascade; b) Convergent cascade.

The ratio of airfoil lift to its resistance is called the quality of the profile

$$K' = \frac{R_y}{R_x}.$$

The reciprocal value is the inverse quality of the profile

$$\mu = \frac{1}{K} = \frac{R_x}{R_y} = \tan \epsilon.$$

Here ϵ is the angle between the direction of lift and the resultant force. In the potential flow $\epsilon = 0$.

5.4. Aerodynamic Coefficients

For the convenience of the analysis and the use of experimental data, we introduce the dimensionless coefficients of the characteristic forces, dividing their value necessary per unit length of the span by the product of airfoil chord times the dynamic head of incident flow.

The dimensionless force coefficients of the profile or airfoil cascade of given geometry depend on the angle of attack and on the similarity criteria, Mach number, Reynolds, numbers, etc.

For the unitary profile, characteristic forces are lift R_y and frontal or profile drag R_x . The dimensionless coefficients of these forces,

$$c_y = \frac{R_y}{\frac{\rho_1 \omega^2}{2} b} \quad (34)$$

$$c_x = \frac{R_x}{\frac{\rho_1 \omega^2}{2} b} \quad (35)$$

are called the lift coefficient and the coefficient of profile drag, respectively. According to (33) the coefficient of profile drag can be presented as the sum of the pressure drag coefficient c_{xp} and the coefficient of friction drag c_{xf} :

$$c_x = \frac{R_{xp}}{\frac{\rho_1 \omega^2}{2} b} + \frac{R_{xf}}{\frac{\rho_1 \omega^2}{2} b} = c_{xp} + c_{xf}$$

Here, unlike the friction coefficient of plate c_f , the friction drag coefficient of the profile is designated in terms of c_{xf} . Sometimes the concept of the shape's resistance is introduced. The drag coefficient of shape is understood to be the difference between the coefficient of profile drag and the friction coefficient of a flat plate which has the same surface as this airfoil:¹

$$c_{x\text{shape}} = c_{xnp} - 2c_f = c_{xa} - (c_{xf} - 2c_f)$$

For the airfoil cascade the frontal and axial forces are characteristic. The frontal component R_u of the resultant force determines the energy effect of the compressor impeller or turbine. Rotor and axial component R_a characterizes that force which should be absorbed by the bearings or special devices.

The dimensionless coefficients of these components are determined by the known parameters the flow at infinity ahead of the cascade

$$c_x = \frac{R_x}{\rho_1 \frac{w_1^2}{2}}, \quad c_a = \frac{R_a}{\rho_1 \frac{w_1^2}{2}}.$$

According to (3), (4) and (5), for a profile of unit length ($l = 1$) in the cascade we have

$$c_x = \frac{R_x}{\rho_1 \frac{w_1^2}{2} b} = -\frac{2}{b} \frac{\Delta w_x}{w_1} \sin \beta_1. \quad (36)$$

$$c_a = \frac{R_a}{\rho_1 \frac{w_1^2}{2} b} = -\frac{1}{b} \left(\frac{\Delta p}{\rho_1 \frac{w_1^2}{2}} + 2 \frac{\Delta w_a}{w_1} \sin \beta_1 \right). \quad (37)$$

The dimensionless pressure differential

$$\frac{\Delta p}{\rho_1 \frac{w_1^2}{2}} = \frac{2\rho_2}{\rho_1 w_1^2} \left(\frac{p_2}{\rho_2} - 1 \right) = \frac{2gRT_1}{w_1^2} \left(\frac{p_2}{p_1} - 1 \right)$$

¹Factor 2 with c_f takes into account the friction on both sides of the plate.

can be presented using the gas-dynamic functions (§ 6 Chapter V, in the following form:

$$\frac{\lambda p}{\rho_1 w_1^2} = \frac{k+1}{k} \frac{\varepsilon(\lambda_1)}{\lambda_1^2} \left[\frac{\pi(\lambda_1)}{\pi(\lambda_1)} a - 1 \right]. \quad (38)$$

In this case it is assumed that all losses are concentrated in the space between cross sections 1-1 and 2-2 and can be taken into account by the value of the conservation coefficient of total pressure $c = p_{20}/p_{10}$. In the absence of heat exchange with the external medium

$$T_{10} = T_{20} \quad a_{*p1} = a_{*p2} = a_{*p} \quad (39)$$

and, consequently,

$$\frac{\Delta w_\theta}{w_1} = \frac{w_{2\theta} - w_{1\theta}}{w_1} = \frac{w_2}{w_1} \sin \beta_2 - \sin \beta_1 = \frac{\lambda_2}{\lambda_1} \sin \beta_2 - \sin \beta_1. \quad (40)$$

$$\frac{\Delta w_R}{w_1} = \frac{w_{2R} - w_{1R}}{w_1} = \frac{w_2}{w_1} \cos \beta_2 - \cos \beta_1 = \frac{\lambda_2}{\lambda_1} \cos \beta_2 - \cos \beta_1. \quad (41)$$

After substituting (38), (40) and (41) into formulas (36) and (37), we obtain

$$c_u = -\frac{2}{b_2} \left(\frac{\lambda_2}{\lambda_1} \cos \beta_2 - \cos \beta_1 \right) \sin \beta_1, \quad \text{and} \quad (42)$$

$$c_a = -\frac{1}{b_2} \left[\frac{k+1}{k} \frac{\varepsilon(\lambda_1)}{\lambda_1^2} \left(\frac{\pi(\lambda_2)}{\pi(\lambda_1)} a - 1 \right) + 2 \left(\frac{\lambda_2}{\lambda_1} \sin \beta_2 - \sin \beta_1 \right) \sin \beta_1 \right], \quad (43)$$

respectively.

From the equation of state with $T_0 = \text{const}$, we have

$$\frac{p_{21}}{\rho_{21}} = \frac{p_{20}}{\rho_{20}} = \frac{p_{*p2}}{\rho_{*p2}}.$$

Thus, the equation of continuity

$$\frac{\rho_1 w_1}{\rho_{*p1} a_{*p1}} \sin \beta_1 = \frac{\rho_2 w_2}{\rho_{*p2} a_{*p2}} \frac{p_{*p2}}{p_{*p1}} \frac{a_{*p2}}{a_{*p1}} \sin \beta_2$$

taking into account condition (39), can be written in the following dimensionless form:

$$q(\lambda_1) \sin \beta_1 = a q(\lambda_2) \sin \beta_2 \quad (44)$$

or

$$q_{1a} = a q_{2a}.$$

Here q_{2a} is the relative flow rate by which it is understood to be the ratio

$$q_a = q(\lambda) \sin \beta = \frac{p w \sin \beta}{p_{xp} a_{xp}}. \quad (45)$$

In accordance with (44), expression (38) for the dimensionless pressure differential we write in the following form:

$$\frac{\Delta p}{p_1 \frac{w_1}{2}} = \frac{k+1}{k} \frac{1}{\pi(\lambda_1)} \frac{1}{\lambda_1} \left[\frac{\pi(\lambda_2) q(\lambda_2) \sin \beta_2}{q(\lambda_1) \sin \beta_1} - \pi(\lambda_1) \right], \quad (46)$$

or according to the determination of gas-dynamic functions (see Chapter V).

$$\frac{\Delta p}{p_1 \frac{w_1}{2}} = \frac{k+1}{k} \left(\frac{k+1}{2} \right)^{\frac{1}{k-1}} \frac{1}{\lambda_1} \left[\frac{\sin \beta_2}{y(\lambda_2) \sin \beta_1} - \frac{1}{y(\lambda_1)} \right]. \quad (47)$$

Thus, from (43) we have

$$c_a = -\frac{1}{b_1} \left[\frac{m}{\lambda_1} \left(\frac{\sin \beta_2}{y(\lambda_2) \sin \beta_1} - \frac{1}{y(\lambda_1)} \right) - 2 \left(\frac{\lambda_2}{\lambda_1} \sin \beta_2 - \sin \beta_1 \right) \sin \beta_1 \right], \quad (48)$$

where

$$m = \frac{k+1}{k} \left(\frac{k+1}{2} \right)^{\frac{1}{k-1}}. \quad (49)$$

In the case of an incompressible fluid the expression for coefficients (36) and (37) assume the following form

$$c_a = \frac{2}{b_1} \frac{\sin \beta_1 \sin (\beta_2 - \beta_1)}{\sin \beta_2} = \frac{2}{b_1} \sin^2 \beta_1 (\operatorname{ctg} \beta_2 - \operatorname{ctg} \beta_1). \quad (50)$$

$$c_a = \frac{1}{b/t} \left(\frac{\sin^2 \beta_1}{\sin^2 \beta_0} + k - 1 \right), \quad (51)$$

where

$$k = \frac{p_{02} - p_{01}}{p_1 w_1^2 / 2}. \quad (52)$$

In a number of cases during the streamlining of airfoil cascades by an incompressible fluid flow the lift - the force directed along the normal to the geometric mean velocity w_m - and the force caused by the presence of viscosity and directed along w_m are assumed to be the quality characteristic. In this case, for the formation of dimensionless coefficients we divide the corresponding components of the resultant by the dynamic head calculated by the geometric mean velocity. Thus, we have

$$c_y = \frac{R_y}{\frac{w_m^2}{2} b}, \quad c_x = \frac{R_x}{\frac{w_m^2}{2} b}. \quad (53)$$

The aerodynamic forces which act on the profile in the cascade cannot be as large as desired. With the aid of the expressions obtained above it is possible to show that in air isentropic flow the circumferential force necessary per unit area of the cascade achieves the maximum value

$$\left(\frac{R_\theta}{t} \right)_{\max} = \frac{2p_0}{k-1} \quad (54)$$

when $\beta_1 = \frac{\pi}{4}$ and $\lambda_1 = \lambda_0 = \sqrt{\frac{k+1}{k}} > 1$. In incompressible fluid $(R_u/t)_{\max} = 2p_0$ (see the reference on page 527).

§ 5. Profile in a Plane Flow of Incompressible Fluid

Let us first examine the potential flow of incompressible fluid. In this case the problem of the flow around a body of

a given form is reduced to finding a function of velocity potential $\phi(x, y)$.

Knowing the velocity potential, it is possible to find its corresponding flow. This problem consists of determining stream function $\psi(x, y)$ by the known function of potential $\phi(x, y)$.

According to (95a) and (97) Chapter II, between these two functions there are the following differential relationships:

$$\frac{\partial \eta}{\partial x} = \frac{\partial \psi}{\partial y}, \quad (55)$$

$$\frac{\partial \eta}{\partial y} = -\frac{\partial \psi}{\partial x}. \quad (56)$$

Integrating both sides of (55) with respect to y , we have

$$\psi = \int \frac{\partial \eta}{\partial x} dy + C(x). \quad (57)$$

Now, differentiating both sides of the last expression with respect to x , we obtain the following equation for determining the arbitrary function of $C(x)$, taking into account (56):

$$\frac{\partial \eta}{\partial y} + \frac{\partial}{\partial x} \int \frac{\partial \eta}{\partial x} dy + \frac{dC(x)}{dx} = 0. \quad (58)$$

If, for example,

$$\varphi = \left(x + \frac{x}{x^2 + y^2} \right) \omega_1, \quad (59)$$

then the calculations carried out in accordance with (57) and (56) yield

$$\psi = \left(y - \frac{y}{x^2 + y^2} \right) \omega_1.$$

In order to find the equation of the flow line, let us equate the stream function to the constant

$$y - \frac{y}{x^2 + y^2} = \text{const} = C_2.$$

Assuming $C = 0$, we obtain the zero flow line which is composed of axis x and the circumference of a unit radius with the center at the origin of the coordinates (Fig. 10.7a).

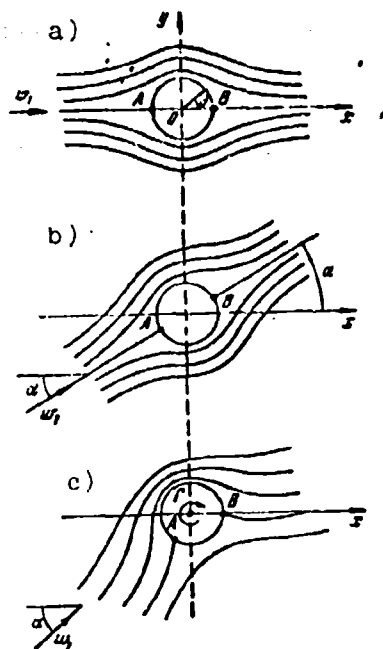


Fig. 10.7. Streamlining of a circle by the potential flow of an incompressible fluid: a) without circulation at the zero angle of attack ($\alpha = 0$), b) without circulation with $\alpha \neq 0$, c) streamlining with circulation.

For the velocity components we have the following expressions:

$$u = \frac{\partial \varphi}{\partial x} = w_1 - \frac{x^2 - y^2}{(x^2 + y^2)^{3/2}} w_1, \quad v = \frac{\partial \varphi}{\partial y} = -\frac{2xy}{(x^2 + y^2)^{3/2}} w_1.$$

Proceeding to the polar coordinates with the origin at the center of the circle, we obtain

$$u = \left(1 - \frac{\cos^2 \theta - \sin^2 \theta}{r^3}\right) w_1, \quad v = -\frac{2 \cos \theta \sin \theta}{r^3} w_1. \quad (60)$$

From this it is apparent that at an infinite distance from the circle the flow is uniform and proceeds at velocity w_1 , directed along axis x .

According to (60) the velocity projections on the radial and normal directions to the flow line are equal to

$$\begin{aligned} w_r &= u \cos \theta - v \sin \theta = w_1 \left(1 - \frac{1}{r^2}\right) \cos \theta, \\ w_n &= u \sin \theta + v \cos \theta = w_1 \left(1 + \frac{1}{r^2}\right) \sin \theta, \end{aligned}$$

respectively.

In this case the value of circulation relative to the circumference is

$$\Gamma = \int w_n dS = \int_0^{2\pi} w_n r d\theta = -w_1 \left(1 - \frac{1}{r^2}\right) r \int_0^{2\pi} \sin \theta d\theta = 0.$$

Thus, expression (59) is the velocity potential of noncirculatory flow around the circle of a unit radius by a uniform flow which has velocity w_1 , directed along axis x .

Since on the circumference itself ($r = 1$) the radial velocity component is equal to zero, then $w = w_s = 2w_1 \sin \theta$. Hence, it follows that the maximum streamline velocity which is observed when $\theta = \pi/2$ and $\theta = 3\pi/2$ is equal to the doubled velocity of the incident flow. At $\theta = 0$ and $\theta = \pi$ the velocities are equal to zero and the corresponding points are critical. The latter, evidently is because it is the result of the symmetry of the flow. During the flow around the circle at a certain angle α to axis x the critical points will shift along the circumference by the same angle value (Fig. 10.7b).

For obtaining a circulation flow around the circle let us impose on the flow examined above a purely circulatory flow from a single vortex, after placing it at the origin of the coordinates, i.e., in the center of the circle. The velocity induced by point vortex with circulation Γ is equal to $\Gamma/2\pi r$ in magnitude and is always directed along the normal to the radius-vector.

Adding these velocities with those of the noncirculatory flow around the circle, we obtain the unknown expression for the velocity distribution along the circumference during its circulatory streamlining.

$$\vec{v} = 2w_1 \sin \theta + \frac{\Gamma}{2\pi} \quad (61)$$

The last expression allows for an easy determination of the necessary circulation at which one of the critical points, for example B, retains an invariable position during a change in the direction of an incoming flow on the circumference. For example, let us assume that the circle is streamlined by a non-circulatory flow at a zero angle of attack (which we will conditionally reckon from diameter AB). In this case, one of the critical points will be point B. In order for this point to remain critical and at a certain angle of attack $\alpha = -\theta$ when the circle is streamlined, it is necessary, as this follows from (61), to apply circulation $\Gamma = 2\pi w_1 \sin \alpha$.

Knowing the flow around a circle with a unitary radius, also it is possible, with the aid of the conformal mapping of the area external to this profile onto the area external to the circle, to construct a flow around an arbitrary profile. In this case, the property of the invariability of circulation is used during the conformal transformation.¹ However, in this case, the problem of streamlining a profile by a flow with known velocity and its direction at infinity has a countless number of solutions which depend on the selection of circulation Γ . An additional condition is necessary which determines the value of circulation. Such a condition was indicated by S. A. Chaplygin in 1909; prior to this work there was no effective mathematical method for solving the

¹L. G. Loitsyanskiy, Fluid and Gas Mechanics, Tekhteorizdat, M. - L., 1950.

problem of flow around a profile, i.e., there was virtually no theoretical airfoil aerodynamics.

For the purpose of clarification of this condition, let us examine the flow of an incompressible fluid around the profile which has a sharp trailing edge whose presence is characteristic of the contemporary aerodynamic airfoils. First, let us assume that the velocity circulation is absent ($\Gamma = 0$), i.e., there is no lift. In this hypothetical case, the obtained picture of the so-called noncirculatory streamlining of a profile can be constructed by well-known methods of theoretical hydrodynamics.

The picture of noncirculatory flow around a profile has the following basic features. Incident flow is divided at the profile into two parts which flow around its upper and lower surfaces, respectively (Fig. 10.8a). Point A in which the jets separate and the flow has zero velocity is called the *leading critical point* or the point of stream separation. Point C where the jets converge again is called the *convergence point* of the stream or the rear critical point.

A change in the angle of attack leads to a change in the positions of leading and rear critical points. For example, in the case depicted on Fig. 10.8, with an increase in the angle of attack the leading critical point moves along the lower surface, approaching the trailing edge of the profile, and the rear critical point moving over the upper surface approaches the frontal part of the profile; a decrease in the angle of attack leads to the displacement of the point, at which the jets branch out, to the side of the snout, and the point at which the jets converge - toward the tail section of the profile.

In the general case due to the fact that the sharp trailing edge cannot be streamlined, such a flow is accompanied by the

separation of the flow from the profile surface. Only at a certain particular angle of attack (usually negative) the point of convergence of jets coincides with the trailing edge of the profile, i.e., a continuous noncirculatory flow is obtained; the corresponding angle of attack α_0 is called the angle of zero lift.

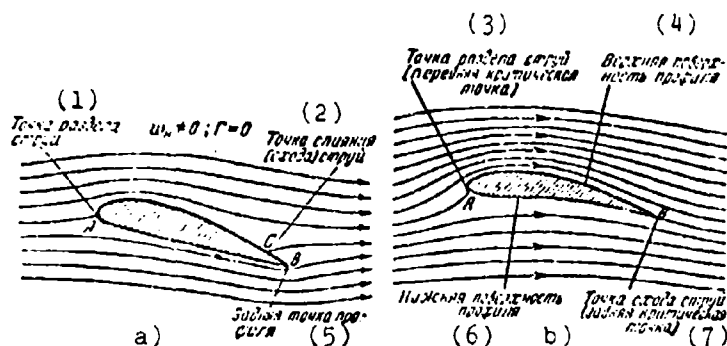


Fig. 10.8. Streamlining of the profile by a potential flow of incompressible fluid: a) without circulation, b) with circulation.
KEY: (1) Point of jet separation. (2) Convergence point of jets. (3) Point of jet separation (leading critical point). (4) Upper profile surface. (5) Rear point of the profile. (6) Lower profile surface. (7) Point of jet convergence (rear critical point).

Now, let us examine another limiting case of the flow around a profiles purely circulatory streamlining. By the purely circulatory flow we will understand it to be the flow caused only by the presence of circulation around the airfoil in the absence of incident flow, when $w_\infty = 0$, $\Gamma \neq 0$. An example of the purely circulatory flow is the circulatory flow examined in Chapter II, whose velocity field is caused by a single vortex. In the case of a purely circulatory flow, the leading and rear critical points are absent and the flow lines represent closed curves enveloping the profile. Such a flow independently of the circulation requires the presence of an infinite velocity at the point lying on the trailing edge of the profile and, therefore, just as the noncirculatory flow cannot be realized without the discontinuity of the flow.

The general case of a plane-parallel flow around a profile can be obtained by the superposition of these two limiting cases of flow, noncirculatory and purely circulatory. One can be convinced from the construction of a picture of streamlining that, as a result of the superposition of the purely circulatory flow on the noncirculatory flow the rear critical point, during a forward circulation ($\Gamma > 0$), is displaced toward the tail section, and during a backward circulation ($\Gamma < 0$) - toward the frontal profile section.¹

By specifying value Γ , we unambiguously determine the position of the rear critical point at a given direction of the noncirculatory flow, i.e., at a specified direction of the velocity far from the profile.

It is obvious that at a certain well-defined value of circulation Γ around the profile, the rear critical point will coincide with the rear sharp edge of the profile (Fig. 10.8). In this solitary case the circulation flow can be physically realized by a continuous flow. For all other values of circulation, the streamlining of the trailing edge is required which, as was indicated, is impossible without the discontinuation of the flow.

This condition was first expressed by S. A. Chaplygin, called the Chaplygina-Joukowski postulate, and it can be formulated as follows: during a continuous flow around a profile, circulation Γ is developed around it of such magnitude at which the rear sharp edge is the point of stream convergence. The Chaplygin-Joukowski postulate makes it possible for one to calculate the circulation around the airfoil and, consequently, with the aid of the Joukowski theorem, also the airfoil lift.

¹We remind you that by forward we mean a clockwise direction.

Let us examine a physical system of the flow around a profile in which a lift is developed, i.e., the force of fluid pressure on the profile, directed at a right angle to the velocity of an undisturbed flow. As we have observed, in the flow around the profile there arises a circulation as a result of the superposition of which on the incident flow the velocities over the profile become greater, while under the profile they become less than that of the undisturbed flow. Because of this the pressure over the profile is reduced, while under the profile it is increased, which leads to the appearance of a lift. The development of fluid circulation around the profile, in turn, is explained by the following. At the initial moment, the flow around the profile is noncirculatory but, in this case, in the area between the point of stream convergence (on the upper profile surface) and the rear sharp edge of the profile there develops a stagnation zone of the flow. The fluid interface surface (boundary between the stagnation zone and the stream which flows from the trailing edge), as shown by observations, is twisted into a vortex which is entailed by the flow. However, the vorticity did not occur in the incident flow; consequently, the circulation along the contour enveloping the profile and the vortex was equal to zero. However, if this contour were divided by a line which separates the profile from the vortex, then in each of the two new contours the circulation does not equal to zero. It is obvious that these circulations should be equal in magnitude, but opposite in direction.

Thus, the starting vortex which breaks away from the trailing profile edge causes the development of the circulation around the profile which in fact creates lift. In the photograph of airfoil in planing (Fig. 10.9) both the starting vortex and the circulatory flow around the profile are visible.

Let us note that the the particular case of a continuous circulatory flow examined above is an example of fulfillment of the Kutta-Joukowski condition for mode I.

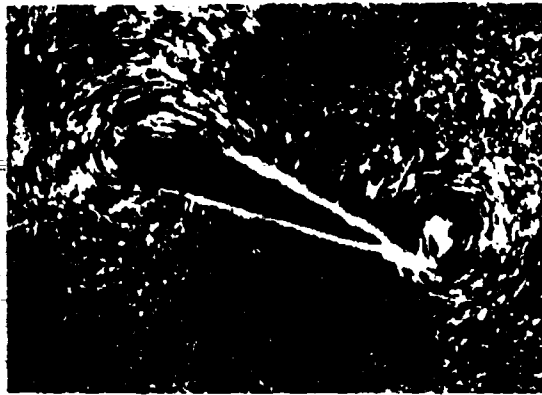


Fig. 10.9. A photograph of the starting vortex.

Such a continuous noncirculatory flow (with $\Gamma = 0$) is the only possible case when the noncirculatory flow is actually realized; otherwise it is only a conceptual component of the true flow which also includes the circulatory flow.

Now, let us assume that during the conformal transformation of certain arbitrary profile on the circle of a unit radius the trailing edge of airfoil B_1 passes to point B of the circle (Fig. 10.10). This means that the noncirculatory direction of the flow around the circle, which corresponds to the noncirculatory flow around the profile, is parallel to the diameter of the circle, passing through point B. Now, if the profile and the circle, respectively, are streamlined at an angle of $(\alpha - \alpha_0)$ to this noncirculatory direction, then in order for points B_1 and B to remain coincidental with the point of stream convergence, it is necessary, in accordance with what has been said above, to apply the circulation

$$\Gamma = m_\alpha b u_1 \sin(\alpha - \alpha_0), \quad (62)$$

where m_α is the proportionality factor which depends only on the airfoil shape, α_0 - zero-lift angle, i.e., of a continuous noncirculatory flow.

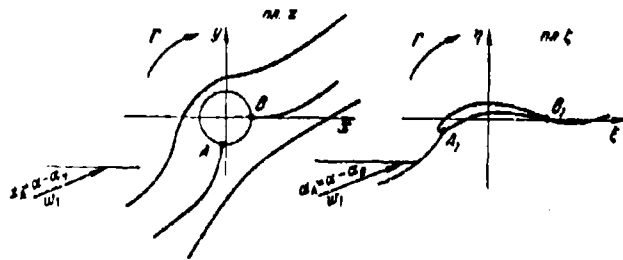


Fig. 10.10. The conformal mapping of the profile exterior on the exterior of the circle of a unit radius.

The lift coefficient, according to (15), (34) and (62), comprises

$$c_y = \frac{2\Gamma}{b w_1} = 2m_\infty \sin(\alpha - \alpha_0).$$

Hence we have

$$\left(\frac{dc_y}{dz} \right)_{z=z_0} = 2m_\infty.$$

Since the angles of attack generally used are small, then it is possible to assume that $\sin(\alpha - \alpha_0) \approx \alpha - \alpha_0$. Using this approximation, we have

$$c_y = 2m_\infty(\alpha - \alpha_0).$$

Introducing the so-called aerodynamic angle of attack

$$\alpha_A = \alpha - \alpha_0,$$

i.e., the angle between the direction of velocity at infinity and the zero-lift direction, we obtain

$$c_y = 2m_\infty \alpha_A.$$

In symmetrical profiles the chord coincides with the axis of symmetry, as a result of which, zero-lift angle $\alpha_0 = 0$. For the small arc of the circle the direction of the noncirculatory streamlining corresponds to the straight line passing through the trailing edge and the center of the profile.

Using data of the Joukowski profile, it is possible to obtain the following approximation formula for determining value dc_y/da of an arbitrary profile:¹

$$\frac{dc_y}{da} = 2\pi(1 + 0.77c) \sqrt{1 + \left(\frac{f}{c}\right)^2}.$$

In this formula, one of the factors takes into account the camber and another - its thickness.

In the conventional airfoils the value of $(f/2)^2$ is negligible and, therefore, for them it is assumed that

$$\frac{dc_y}{da} = 2\pi(1 + 0.77c).$$

Assuming that in the last expression $c = 0$, for a flat plate we obtain

$$\frac{dc_y}{da} = 2\pi.$$

and, therefore,

$$c_y = 2\pi a.$$

In the potential flow the tangential forces are absent and, therefore, it would seem that the resultant of all pressure forces applied to the plate should be directed along the normal to it and not at a right angle to the incident flow velocity, as this follows from the Joukowski theorem. This apparent paradox is explained by the fact that, besides the normal forces which act on the upper and lower plate surfaces, at the plates leading edge a pull directed along the plate is developed of such magnitude at which the resultant turns out to be directed along the normal

¹See "Aerodynamics," V. II, under the editorship of V. F. Dyurend. Oborongiz, M.-L., 1939.

to the incident flow velocity. The development of this pull is connected with the appearance of the infinitely high negative pressure, at the leading edge theoretically permissible in the mathematical model of ideal fluid.

Let us note that, as has already been indicated (Chapter II), due to the unreality of such a pressure the continuous streamlining becomes impossible, and the separation of stream from the leading sharp edge of the plate occurs.

Thus, the use of the mathematical methods described above for determining the flow around the plate or other profiles with sharp leading and trailing edges by an inviscid flow, strictly speaking, bears a somewhat conditional nature.

The only exception is the case of airfoil streamlining under such an angle of attack at which the branch point of streams coincides with the sharp leading edge.¹ At this case, both sharp edges, leading and trailing, lie on the interface of streams which flow around the upper and lower side of the profile, and jets of fluid smoothly enter and depart from it.

Up to this point we examined the flow around a profile by an ideal fluid. Let us present some concepts concerning the effect of viscosity. Fluid viscosity brings about changes into the picture of flow and results in a difference between the derivations of the theory of the potential flow around a profile and the experimental data. The effect of viscosity in the case of well-streamlined bodies is evident only in the fine boundary layer outside of which the motion can be considered to be potential, i.e., vortex-free.

¹Sometimes, this angle is called the angle of attack of the shock-free streamline flow.

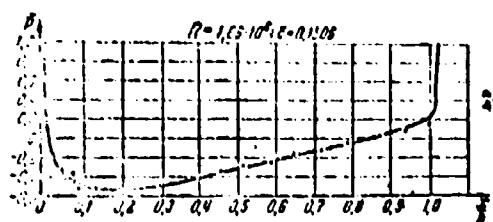


Fig. 10.11. Comparison of the experimental and theoretical pressure curves for a symmetrical Joukowski profile with a relative thickness $\bar{c} = 0.1506$ at a zero angle of incidence: curve - calculation, exes - experiment.

In Chapter VI a detailed examination is made of the streamline flow with friction of a flat plate placed in parallel to the direction of the flow; in this case, the pressure in the flow is virtually unchanged. However, during the flow of a viscous fluid around the profile the pressure near its surface is changed substantially. Based on this the entire flow near the profile should be divided into two principal sections: convergent section in which the velocity increases and the pressure drops accordingly, i.e., the pressure gradient is negative ($dp/dx < 0$), and the diffuser section in which the velocity decreases while the pressure increases, i.e., the pressure gradient is positive ($dp/dx > 0$).

The lower surface and the forward section of the upper surface of the profile (up to the point of minimum pressures p_{\min}) pertain to the convergent section. The rear section of the upper surface (from the point of minimum pressure to the trailing edge) pertains to the diffuser section. In the convergent section the flow proceeds toward the side of pressure drop and, therefore, there is no danger of the boundary-layer separation from the profile surface. In the diffuser section the motion is directed toward the side of pressure increase, which, as noted in Chapter VI, with high gradients of pressure leads to the possibility of the boundary-layer separation.

These suppositions are confirmed by numerous experiments done on diffusers, convergent channels and airfoils.

Figure 10.11 shows a comparison of curves of the dimensionless quantities of pressure $\bar{p} = (p - p_1)/0.5\rho w_1^2$ along the surface, obtained from an experiment with the data of the theory of the potential flow with the zero angle of attack for a symmetrical Joukowski profile.

As we see, the difference between the theoretical and experimental data on pressure distribution is only in the profile's afterbody. This result is valid not only with a zero angle, but also with small angles of attack.

To illustrate the relationship between the pressure drag and the friction drag, Fig. 10.12 shows the results of experimental studies during the zero angle of attack of a series of seven symmetrical Joukowski profiles with a relative thickness $\bar{c} = 0.05; 0.10; 0.15; 0.21; 0.27; 0.33; 0.40$.

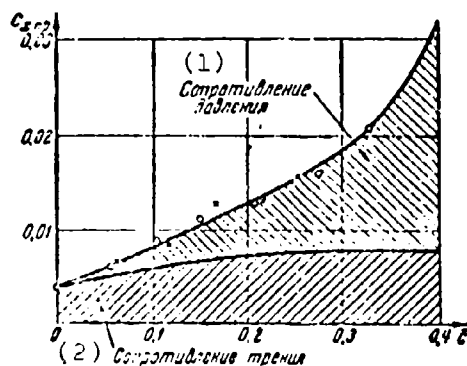


Fig. 10.12. The relationship between the friction drag and the pressure drag depending on the relative airfoil thickness \bar{c} for a symmetrical Joukowski profile, according to the data of purging at a zero angle of attack.

KEY: (1) Pressure drag. (2) Friction drag.

As we see, in the thin airfoils the overwhelming portion of the profile drag is composed of the friction drag; for example, in the case $\bar{c} = 0.1$ the fraction constitutes up to 75% of the

profile drag. With an increase in the relative thickness due to the pressure gradient increase in the diffuser section of the profile, there is an increase in the total profile drag and a decrease in the friction drag portion. With $\bar{c} > 0.25$ the pressure drag predominates over the friction drag; with $\bar{c} = 0.4$ the former constitutes ~70% of the total profile drag.

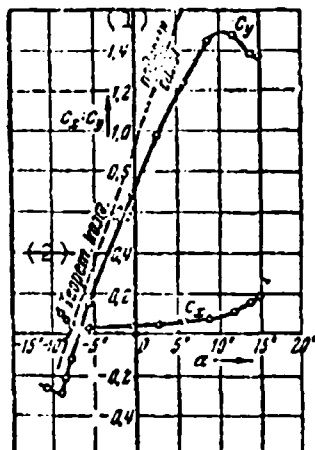


Fig. 10.13. Experimental curved $c_y(\alpha)$ and $c_x(\alpha)$ for a unitary profile.
KEY: (1) Lift. (2) Theoretical coefficient.

Let us proceed to the problem concerning the effect of viscosity on the lift. A typical experimental curve $c_y(\alpha)$ for an aerodynamic profile is depicted on Fig. 10.13. First, the experimental curve of $c_y(\alpha)$ has a significant rectilinear segment, as this follows from the theory of a potential flow; however, experimental values $(dc_y/d\alpha)$, ... prove to be less than the theoretical.

Increasing the angle of attack intensifies the diffusivity of a flow on the upper surface, which increases the divergence between the experiment and the theory. With a critical value of the angle of attack α_{kp} the lift coefficient reaches a maximum ($c_y = c_{y \max}$), whereupon there is a drop in value c_y with an increase in the angle of attack. The sharp deviation of dependence $c_y(\alpha)$ from the linear with large angles of attack is caused by the boundary-layer separation, which propagates to an ever larger

portion of the upper profile surface with an increased angle of attack and leads to rapid increase in the frontal drag coefficient c_x simultaneously.

§ 6. Streamlining of a Profile by a Subsonic Gas Flow

At low Mach number values of gas flow ($M < 0.3-0.5$) the velocity value does not affect the nature of pressure distribution along the contour of the streamlined profile. At higher Mach number values ($M \leq M_{kp}$) an increase in the velocity of the incident flow leads to a change the pressure curve; however, the general nature of the pressure curve remains the same.

An increase in the rarefaction corresponds to an increase in the local velocities on the profile; at the point of minimum pressure p_{min} the velocity reaches a maximum value. At a certain Mach number value of the incident flow the minimum pressure becomes critical:¹

$$p_{min} = p_{sp} = \left(\frac{2}{k+1} \right)^{\frac{k}{k-1}} p_0$$

where p_0 is the total pressure of the incident flow; at point p_{kp} the flow velocity is equal to the local speed of sound $M = 1$. Mach number $M = M_{kp}$ of the incident flow at which a sonic speed is developed any place on the profile is called *critical*. With a further increase in the Mach number of the incident flow, i.e., when $M_1 > M_{kp}$, we have an area of the flow, developed near the profile surface, with supersonic speeds, as a result of which the flow acquires new qualities. Value M_{kp} is the boundary of the

¹Value p_{min} can be obtained from formula (68), Chapter I, assuming that $M = 1$.

two principal streamlining conditions of profile at a subsonic speed of the incident flow, subcritical ($M_1 < M_{kp}$) and supercritical ($M_1 > M_{kp}$).

Let us consider in more detail the streamlining of a certain profile by a subsonic, isentropic, uniform gas flow at velocity w_1 directed along axis x , pressure p_1 the (speed of sound a_1).

In the general case the gas-dynamic parameters of any point of the flow can be expressed thus:

$$u = w_1 + u', \quad v = v', \quad p = p_1 + p', \quad \rho = \rho_1 + \rho', \quad a = a_1 + a'. \quad (63)$$

Here u' , v' , p' , ρ' and a' are values which characterize the perturbation of a uniform flow by this profile.

Further, we will limit ourselves to the examination of only the thin and slightly bent profiles streamlined at such small angles of attack at which the perturbations are so low that the squares and products u' , v' , p' , ρ' , a' and of their derivatives with respect to the coordinates can be disregarded. Under this assumption equation (100), Chapter II, which we rewrite beforehand as:

$$(a^2 - u^2) \frac{\partial u}{\partial x} - uv \left(\frac{\partial v}{\partial x} + \frac{\partial u}{\partial y} \right) + (a^2 - v^2) \frac{\partial v}{\partial y} = 0,$$

assumes the following form:

$$(a_1^2 - w_1^2) \frac{\partial u'}{\partial x} + a_1^2 \frac{\partial v'}{\partial y} = 0$$

or

$$(1 - M_1^2) \frac{\partial u'}{\partial x} + \frac{\partial v'}{\partial y} = 0. \quad (64)$$

Introducing potential ϕ' of the perturbations

$$\frac{\partial \phi'}{\partial x} = u', \quad \frac{\partial \phi'}{\partial y} = v'.$$

we represent velocity potential ϕ as the sum of the potential of the uniform flow $\phi_{\text{одн}} = w_1 x$ and the potential of the perturbations

$$\varphi = w_1 x + \varphi'. \quad (65)$$

Differentiating both sides of this expression

$$\frac{\partial \varphi}{\partial x} = \frac{\partial \varphi'}{\partial x} = \frac{\partial u}{\partial x}, \quad \frac{\partial \varphi}{\partial y} = \frac{\partial \varphi'}{\partial y} = \frac{\partial v}{\partial y},$$

after the substitution in (64), we obtain

$$\frac{\partial^2 \varphi}{\partial x^2} (1 - M^2) + \frac{\partial^2 \varphi}{\partial y^2} = 0. \quad (66)$$

From the equation of continuity

$$\frac{\partial(\rho u)}{\partial x} + \frac{\partial(\rho v)}{\partial y} = 0$$

it follows that by analogy with an incompressible fluid flow (see Chapter II) there is stream function ϕ which corresponds to the condition

$$\frac{\partial \phi}{\partial x} = u, \quad \frac{\partial \phi}{\partial y} = -v. \quad (67)$$

This stream function ϕ we will divide into the stream function of a uniform flow $\phi_{\text{одн}} = w_1 y$ and the stream function of perturbations ϕ' which corresponds to the deviation of the real flow from the uniform flow

$$\phi = w_1 y + \phi'. \quad (68)$$

Substituting values (63) into (67) and taking into account the last relationship, we obtain

$$\left(\frac{\partial \phi}{\partial x} \right) (w_1 + u') = w_1 + \frac{\partial \phi'}{\partial x}, \quad \frac{\partial \phi}{\partial y} = -v = -\frac{\partial \phi'}{\partial y}.$$

With an accuracy to the small second order terms, from this we have

$$u' + \frac{\partial \phi'}{\partial x} w_1 = \frac{\partial \phi'}{\partial x}, \quad v = -\frac{\partial \phi'}{\partial y}.$$

From the equation of enthalpy for an isentropic flow (see § 3 Chapter I)

$$\frac{w^2}{2} + \frac{a^2}{\gamma-1} \left(\frac{\rho}{\rho_0} \right)^{\gamma-1} = \frac{w_0^2}{2} + \frac{a_0^2}{\gamma-1}$$

under the same assumptions, we have

$$\frac{p'}{\rho_0} = - \frac{w_0 a_0'}{a_0^2},$$

and correspondingly

$$u' = \frac{1}{1-M_0^2} \frac{\partial \psi'}{\partial y}.$$

Thus

$$\left. \begin{aligned} \frac{\partial \sigma}{\partial x} &= \frac{\partial \sigma'}{\partial x} = - \frac{\partial^2 \psi'}{\partial x^2} = - \frac{\partial^2 \psi}{\partial x^2} \\ \frac{\partial u}{\partial y} &= \frac{\partial u'}{\partial y} = \frac{1}{1-M_0^2} \frac{\partial^2 \psi'}{\partial y^2} = \frac{1}{1-M_0^2} \frac{\partial^2 \psi}{\partial y^2} \end{aligned} \right\} \quad (69)$$

Substituting these expressions into the condition of non-vorticity of the flow

$$\frac{\partial u}{\partial y} - \frac{\partial \sigma}{\partial x} = 0,$$

we obtain

$$\left. \begin{aligned} \frac{\partial^2 \psi}{\partial x^2} + \frac{1}{1-M_0^2} \frac{\partial^2 \psi}{\partial y^2} &= 0, \\ \frac{\partial^2 \psi}{\partial x^2} + \frac{1}{1-M_0^2} \frac{\partial^2 \psi}{\partial y^2} &= 0. \end{aligned} \right\} \quad (70)$$

Thus, the gas streamlining of the thin slightly bent profiles at small angles of attack is described approximately by linear equations in partial derivatives (66) and (70). These equations are the linearized equations of a plane vortex-free motion of compressible gas.

When $M < 1$ these equations pertain to an elliptical type of equations in the partial derivatives, when $M_1 > 1$ - to a hyperbolic.

Here, limiting ourselves only to subsonic speeds ($M_1 < 1$), we introduce the following new independent variables in place of x and y :

$$x_1 = x, \quad y_1 = y \sqrt{1 - M_1^2}.$$

Substituting into (66) the derivative values of the velocity potential

$$\begin{aligned} \frac{\partial \varphi}{\partial x_1} &= \frac{\partial \varphi}{\partial x}, \quad \frac{\partial \varphi}{\partial y_1} = \frac{\partial \varphi}{\partial y} \frac{dy}{dy_1} = \frac{\partial \varphi}{\partial y} \sqrt{1 - M_1^2}, \\ \frac{\partial^2 \varphi}{\partial y_1^2} &= \frac{\partial}{\partial y_1} \left(\frac{\partial \varphi}{\partial y_1} \sqrt{1 - M_1^2} \right) \frac{dy_1}{dy} = \frac{\partial^2 \varphi}{\partial y^2} (1 - M_1^2), \end{aligned}$$

after reducing by $(1 - M_1^2)$, we obtain the Laplace equation for an incompressible fluid

$$\frac{\partial^2 \varphi}{\partial x_1^2} + \frac{\partial^2 \varphi}{\partial y_1^2} = 0.$$

This equation defines a certain potential motion of incompressible fluid in plane x_1, y_1 , which corresponds to a given motion of compressible gas in initial plane x, y . In this motion of the velocity of incompressible fluid is

$$\begin{aligned} u_1 &= \frac{\partial \varphi}{\partial x_1} = \frac{\partial \varphi}{\partial x} = u, \\ v_1 &= \frac{\partial \varphi}{\partial y_1} = \frac{v}{\sqrt{1 - M_1^2}}. \end{aligned}$$

Hence it follows that the tangents of the slope angles to axis x , which are tangential to the flow lines, equal to v/u , in an incompressible flow they will be $(1 - M_1^2)^{-1/2}$ times greater than in the initial flow of compressible gas. Thus, any thin profile

streamlined by subsonic gas flow corresponds to the following thickened profile in an compressible fluid (Fig. 10.14):

$$c_i = \frac{\bar{c}}{\sqrt{1-M_1^2}},$$

which is streamlined by a flow which is at a greater angle of attack than the initial

$$\alpha' = \frac{\alpha}{\sqrt{1-M_1^2}}.$$

The deformation of the profile turns out to be so insignificant that for determining the lift coefficient c_y it suffices to consider only the change in the angle of attack. In this case it is assumed that both angles of attack α and α' are sufficiently small; the reckoning of these angles is accomplished from the zero-lift direction. It is obvious that the zero-lift angle in the symmetrical airfoil is always equal to zero, i.e., it does not depend on the M_1 number of the incident flow; with sufficient practical accuracy it is possible to assume that the value of the zero-lift angle in the slightly bent aviation profiles is also independent of the M_1 number value. In the gas and equivalent flows of incompressible fluid (under the condition that $M_1 < M_{kp}$) the lift coefficient values must be identical $c_y = c'_y$. Since when reckoning the angle of attack from the zero-lift direction we have

$$c_y = \left(\frac{dc_y}{d\alpha} \right) \alpha, \quad c'_y = \left(\frac{dc'_y}{d\alpha'} \right) \alpha',$$

then

$$\left(\frac{dc_y}{d\alpha} \right) = \frac{\left(\frac{dc'_y}{d\alpha'} \right)}{\sqrt{1-M_1^2}}.$$

Hence, it follows that with the same angles of attack the following relationship should be valid in the gas and incompressible fluid:

$$c_y = c'_y \frac{1}{\sqrt{1-M_1^2}}.$$

Consequently, for obtaining value c_y with the given values M_1 number of the incident flow and the angle of attack α , it is sufficient that the lift coefficient taken from the purging of the profile at low speeds and the same angle of attack be multiplied by value $\frac{1}{\sqrt{1-M_1^2}}$. Values c_y thus obtained coincide well with the

experimental data right up to the critical Mach number value, the thinner the profile the greater the value. With a further increase in the Mach number the streamline flow becomes supercritical and a sharp decrease in value c_y is observed. Thus, to calculate the total effect of compressibility on the airfoil lift in the sub-critical area it is possible, with a sufficient practical accuracy, to use the formulas of the Prandtl-Glauert approximation theory presented here. According to this theory the effect of compressibility leads to the proportional change in pressure at all points of this profile

$$p = \frac{p - p_1}{\rho_1 \frac{a_1^2}{2}} = \frac{p_{\text{нез}}}{\sqrt{1-M_1^2}}. \quad (71)$$

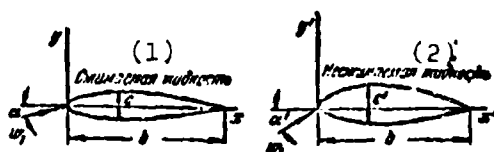


Fig. 10.14. Diagram of the transition from the profile in a compressible gas flow to the equivalent profile in an incompressible fluid.

KEY: (1) Compressible fluid. (2) Incompressible fluid.

The comparison of this formula with the experiment results¹ (Fig. 10.15) shows that its accuracy decreases with an increase in the

¹Stack G, Lindsey W. F. and Littel R. E., Report NACA, No 646, 1938.

Mach number. There is less disagreement between the experimental data when the calculations are carried out according to Sedov¹ and Karman-Tsien.² It should be noted that the Karman-Tsien formula

$$\rho = \frac{\rho_{\text{векс}}}{\sqrt{1-M^2} + \frac{M^2 \rho_{\text{векс}}}{2(1+\sqrt{1+M^2})}}$$

at low Mach numbers converts to the Prandtl-Glauert formula (71).

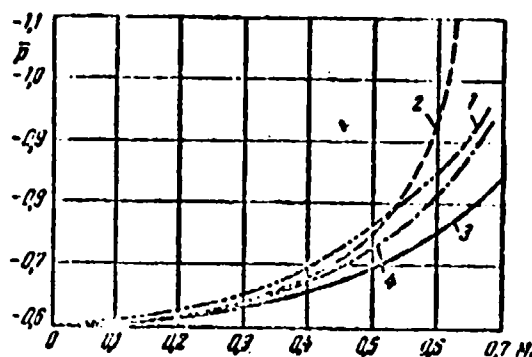


Fig. 10.15. A comparison of different methods for an approximate determination of pressure coefficients for compressible fluid: 1 - experiment, 2 - according to Karman-Tsien, 3 - according to Prandtl-Glauert, 4 - according to Sedov.

For determining the compressibility effect on the velocity and pressure distribution at subcritical velocities along the profile, it is possible to use also another approximation theory based on the hypothesis of "solidification" of the flow lines

¹Sedov L. I., Two-dimensional problems of hydrodynamics and aerodynamics. Gostekhteorizdat, M.-L., 1950.

²Karman T and Tsien, J. of Aeronautical Sciences, #12, 1939. In this work the approximate method indicated by Chaplygin for replacing the real isentrope by the straight line tangent to it.

during the streamlining of a given body by potential flows of incompressible fluid and compressible gas.¹

According to the equation of continuity, for an elementary flow stream adjacent to the profile in an isentropic flow of gas the following relationship is valid:

$$\frac{\Delta P_1}{\Delta P} = \frac{\rho w}{\rho_1 w_1} = \frac{q(\lambda)}{q(\lambda_1)}.$$

Here index "1" designates the parameters of an elementary stream far ahead of the profile.

Since in the incompressible fluid

$$\frac{\Delta P_1}{\Delta P} = \left(\frac{w}{w_1} \right)_{\text{const}},$$

then from the foregoing expression it follows that under the condition of invariability of the flow lines the following equality is valid in the flows of the incompressible and compressible fluids:

$$\left(\frac{w}{w_1} \right)_{\text{const}} = \frac{q(\lambda)}{q(\lambda_1)}. \quad (72)$$

If in an incompressible flow the velocity at a certain point on the profile reaches a maximum value, then the critical value of the velocity coefficient of incident flow λ_{kp} is determined from (72) under the condition that at this point $\lambda = 1$. Then we have

¹S. R. Nuzhnin showed ("The theory of gas flow around bodies at high subsonic speeds.") Applied Math. and Mech., Vol. 10, Iss. 5-6, 1945), that the problem of continuous streamlining of a given body by an irrotational flow of compressible fluid can be reduced to the problem of vortex flow around a given body by an incompressible fluid. In this case it turns out that the flow lines in both flows will remain constant. Disregarding the vorticity we arrive at the confirmation of the hypothesis of solidification of the flow lines.

$$q(\lambda_{kp}) = \frac{1}{\left(\frac{w}{w_1}\right)_{\max \text{ Hess}}} = \frac{1}{\sqrt{1 - \bar{p}_{\min \text{ Hess}}}}.$$

The dependence of critical Mach number calculated according to this formula on the minimum pressure on a profile in the incompressible flow is given in Fig. 10.16 (dashed line). The same figure shows the dependence calculated by the S. A. Khristianovich method.¹ The hypothesis of solidification gives lower M_{kp} values, moreover, the difference is somewhat increased with an increase in the rarefaction on the profile, i.e., with an increase in the profile thickness at a fixed angle of attack.

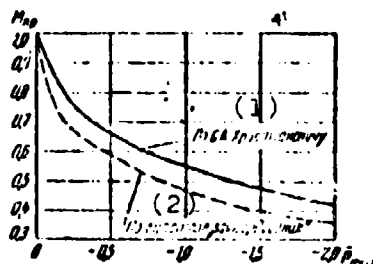


Fig. 10.16. The dependence of critical Mach number M_{kp}

on minimum pressure \bar{p}_{min} on the profile.

KEY: (1) According to S. A. Khristianovich. (2) According to the hypothesis of "solidification."

Value λ_{kp} and, consequently, also M_{kp} depend on the same factors as value \bar{p}_{min} , i.e., on the configuration of the profile and angle of attack.

The thin and slightly bent profiles correspond to the greater M_{kp} values. As established on the basis of experimentation with the ordinary aviation airfoils, a decrease in the profile thickness of 5% leads to an increase in M_{kp} by a value from 0.03 to 0.05, while a decrease in camber $f = f/b$ from 5% down to 0 leads to an increase in M_{kp} approximately by value from 0.1 to 0.12. To

¹Khristianovich S. A., Streamlining of bodies by gas at high subsonic speeds. Works of TsAGI, Iss. 481, 1940.

increase the M_{kp} it is advantageous to situate the points of greatest camber and profile thickness at a distance equal to 0.4-0.5 of the chord from the leading edge of the profile. The nose shape of the profile also has a significant effect on the M_{kp} value.

An increase in the angle of attack leads to an increase in the rarefaction on the upper profile surface, and therefore, to a decrease in value M_{kp} .

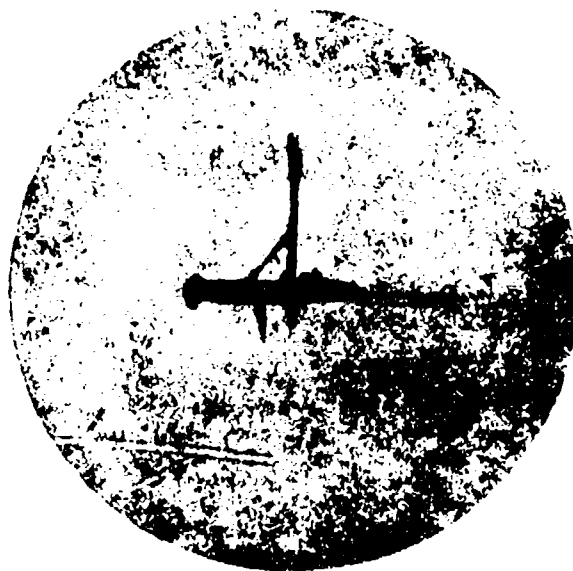


Fig. 10.17. A shadow photograph of transonic streamlining of a unitary profile.

With $M_1 > M_{kp}$, as has already been indicated, the zone of supersonic speed is formed which ends in shock waves. This is quite evident on Fig. 10.17 which shows a photograph of the corresponding pattern of streamlining of the aviation profile obtained by V. S. Tatarenchikov.¹ Behind the system of shocks

¹Levinson Ya. I. Aerodynamics of high-speeds. Oborongiz, 1950.

the breakaway of flow from the profile is visible. The presence of shocks and separation leads to an increase in the frontal airfoil drag, a decrease in lift convergence and a sharp change in the nature of pressure distribution on the profile.

Let us note that the Mach number at which a sharp increase in c_x begins and the Mach number which corresponds to the beginning of a decrease in c_y are dissimilar; this is explained by the different nature of effect the shock waves have on drag and lift. It is obvious that both these numbers are greater than the critical. With an increase in number M_1 the supersonic zone is expanded in the incident flow (in the area where $M_1 > M_{KP}$) and the system of shock waves moves toward the trailing edge of the profile. In this case there is a sharp increase in the profile drag. With $M_1 > 1$ a supersonic streamlining of profile is formed, which we shall consider below.

§ 7. Supersonic Streamlining of Airfoil

Usually, when $M_1 > 1$, special supersonic airfoils with a sharp leading edge are used. This edge significantly decreases the drag at supersonic speed as compared with an ordinary subsonic airfoil with a rounded leading edge. As an example of the simplest supersonic profile we will examine a flat fixed plate onto which plane steady gas flow advances.

Let the plate be tilted at angle i toward the direction of the incident flow (Fig. 10.18). The flow around such a plate can be fully calculated using the theory of oblique shock waves and the theory of streamlining of the external obtuse angle. In this case one assumes that the flow behind the plate again assumes the direction of an incident flow. Let us designate the velocity coefficient of the flow advancing toward the plate in

terms of λ_1 and the pressure in this flow - by p_1 . The velocity coefficient of the flow along the upper side of the plate we designate by λ_B and the pressure in this flow - by p_B . For the flow which runs off from the upper side of the plate, these parameters we designate by λ_2 and p_2 . For the stream which flows along the lower side of the plate, the corresponding parameters we designate by λ_H , p_H , and λ_3 , p_3 .

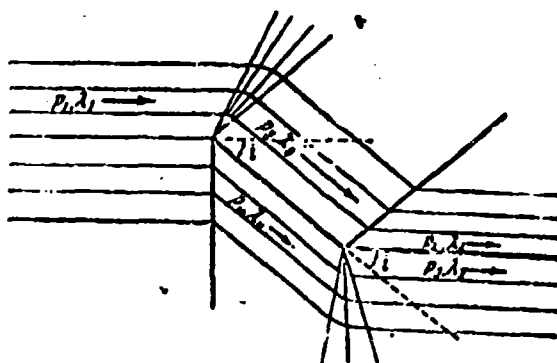


Fig. 10.18. A diagram of supersonic flow around a plate.

During the flow around the upper side of the plate, at the leading edge the flow is deflected at angle 1 and becomes parallel to the direction of the plate, i.e., a pattern is developed which is similar to the flow around the external obtuse angle. Values λ_B and p_B can be determined by the formulas given § 3 Chapter IV. For the calculation it is convenient to use the table of appendix I at the end of the book. At the trailing edge of the plate the flow should again be deflected at angle 1 in opposite direction, i.e., an oblique shock wave is developed because we have a picture similar to the flow around a wedge with angle 1 at the top. Values λ_2 and p_2 are determined by the formulas for an oblique shock wave, given in Chapter III. The following inequalities are obvious:

$$\lambda_2 < \lambda_B, \quad p_2 > p_B, \quad \text{and} \quad \lambda_3 > \lambda_1, \quad p_3 < p_1$$

During the flow around the lower side of the plate an oblique shock wave is formed at the leading edge in passing through which the flow is deflected at angle i . Values λ_H and p_H can be found by the formulas for the oblique shock wave. At the trailing edge the flow will be deflected at angle i in opposite direction. Values λ_3 and p_3 are determined by the formulas for the streamlining of the external obtuse angle. Here $\lambda_H < \lambda_1$, $p_H > p_1$ and $\lambda_3 > \lambda_H$, $p_3 < p_H$.

The pressure in the flow which runs off from the upper side of the plate should be equal to the pressure in the flow which runs off from the lower side $p_2 = p_3$. The velocities of these two flows can be different in value, but their direction is the same. Thus, λ_2 may not equal to λ_3 .¹

Force R , which acts on plate is equal to $(p_H - p_B)F$ where $F = bl$ - the plate area. Thus, the lift of a flat plate per unit length of the span is determined by the formula

$$R_y = (p_H - p_B) b \cos i,$$

and the frontal drag - by formula

$$R_x = (p_H - p_B) b \sin i.$$

Consequently,

$$c_y = \frac{R_y}{\rho_1 \frac{w_1^2}{2} b} = \frac{p_H - p_B}{\rho_1 \frac{w_1^2}{2}} \cos i,$$

$$c_x = \frac{R_x}{\rho_1 \frac{w_1^2}{2} b} = \frac{p_H - p_B}{\rho_1 \frac{w_1^2}{2}} \sin i.$$

¹A more thorough investigation shows that the direction of the flow which runs off from the plate does not coincide with the direction of the incident flow. This direction is determined from the condition of equality of pressures and the sameness of the velocity direction in the flows which run off from the upper and lower sides of the plate. However the deflection of the flow by the plate is very small and with $M_1 < 3$ does not exceed 1° , thus, the scheme presented here can be used for practical calculations.

Using the equation of state

$$\rho_1 = \frac{p_1}{R T_1}$$

and expressing the flow velocity in terms of the Mach number

$$w_1 = M_1 a_1 = M_1 \sqrt{\gamma R T_1}$$

we reduce the formulas for c_y and c_x to the form

$$c_y = \frac{2}{\gamma M_1^2} \left(\frac{p_2}{p_1} - \frac{p_3}{p_1} \right) \cos i,$$

$$c_x = \frac{2}{\gamma M_1^2} \left(\frac{p_2}{p_1} - \frac{p_3}{p_1} \right) \sin i.$$

The composed scheme for calculating the streamlining of a flat plate becomes unsuitable for the following two cases.

First, if angle of attack $i > i_{np}$ for the given number M_1 of the incident flow; in this case, during the flow around the upper side of the plate there is flow separation. This case is of low practical significance, because when $M \leq 10$ the maximum angles of attack $i_{np} \geq 25^\circ$.

Second, if angle of attack i exceeds the maximum angle of deflection of the flow in the oblique shock wave ω_{max} for the given number M_1 of the incident flow (see Fig. 3.12); when $i > \omega_{max}$ a separated shock wave with curvilinear front is formed ahead of the lower side of the plate. The calculation of such a flow is a very complex problem. The case when $i > \omega_{max}$ can occur with very small M_1 numbers (for example for $M_1 = 1.5$, angle $i = 12^\circ$).

It is important to note that when $M_1 < 6.4$, ω_{max} is always less than i_{np} and, consequently, the reason for the inapplicability of this calculation scheme is the formation of the separated curvilinear shock wave ahead of the plate. With very large M_1 numbers it is the opposite, $i_{np} < \omega_{max}$ and the reason for the

inapplicability of the calculation scheme is the flow separation during the flow around the upper side of the plate.

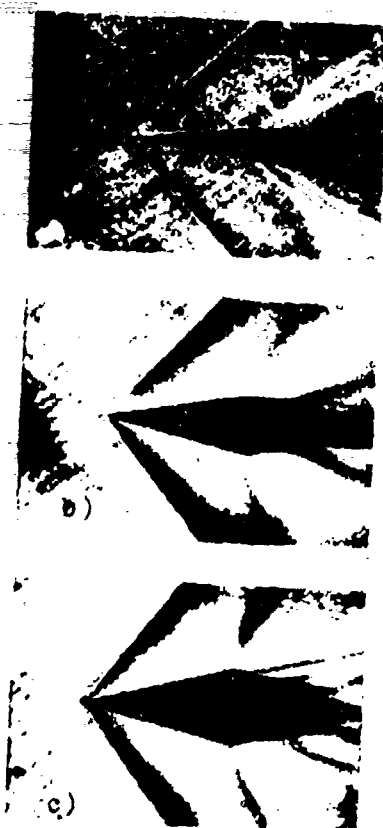


Fig. 10.19. Shadow photographs of supersonic flow around a double-wedge airfoil at the zero angle of attack with $M_1 = 1.7$. Semiapex angle of the rhomb: a) $\omega = 7^\circ$, b) $\omega = 12^\circ$, c) $\omega = 14^\circ$.

Figure 10.19 shows the photographs of supersonic streamlining of the double-wedge airfoils of varied thickness in a wind tunnel at zero-angle of attack. Each of these photographs shows distinctly the shock waves at the leading edge of the profile, clusters of characteristics at the upper and lower convex angles of profiles and characteristics resulting from the unevennesses on the walls of the wind tunnel by whose slope the flow velocity in the tunnel can be judged.

The theory of oblique shock waves and the theory of the flow around the external obtuse angle make it possible for one to calculate the flow around any profile whose contour is composed of rectilinear sections.¹

¹See, for example, Chapter VIII of the proceeding publication of this book. Gostekhteorizdat, M., 1953.

To construct a flow with small angles of attack around the thin and slightly bent profiles of any configuration, we can use equations (66) and (70) obtained for the case.

Introducing the designation

$$\omega^2 = M_1^2 - 1,$$

we rewrite (70) with $M_1 > 1$ thus:

$$\frac{\partial^2 \psi}{\partial x^2} - \frac{1}{\omega^2} \frac{\partial^2 \psi}{\partial y^2} = 0. \quad (73)$$

As anyone can easily check by substitution, this equation, called the wave equation, has the following general solution:

$$\psi = f_1(x - \omega y) + f_2(x + \omega y).$$

Here f_1 and f_2 are the symbols of arbitrary functions. Let us examine the two partial solutions of equation (73)

$$x - \omega y = \text{const}, \quad x + \omega y = \text{const},$$

representing two families of straight lines

$$y = \frac{1}{\omega} x + c_1, \quad y = -\frac{1}{\omega} x + c_2,$$

forming the following angles with axis x and, consequently, also with the direction of the incident flow respectively:

$$\gamma_1 = \arctg \frac{1}{\sqrt{M_1^2 - 1}} = \arcsin \frac{1}{M_1}, \quad \gamma_2 = \arctg \frac{-1}{\sqrt{M_1^2 - 1}} = -\arcsin \frac{1}{M_1},$$

which are equal to the Mach angles of uniform flow α , i.e., to the angles between the velocity direction of the incident flow and the Mach waves. Along these straight lines which are the characteristics of the examined wave equation (73), values ψ , u' , v' assume constant values $\psi(c)$, $u'(c)$ etc., specifically equal to the values of these quantities on the very surface of the profile. The streamlining pattern of such a profile, formed of two curves

$$y_1 = h_1(x) \quad \text{and} \quad y_2 = h_2(x)$$

is given in Fig. 10.20.

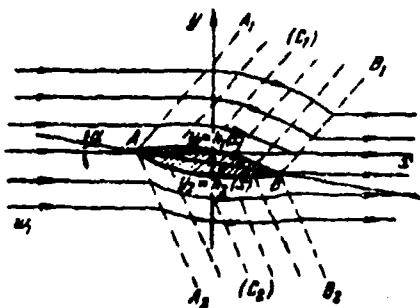


Fig. 10.20. Streamlining the profile by a supersonic flow.

The Mach waves AA_1 and AA_2 , drawn through leading edge A respectively and waves BB_1 and BB_2 drawn through trailing edge B respectively separate the area of disturbed plane-parallel flow from that of undisturbed.

Between these boundary lines of perturbation we find the flow disturbed by the profile surface. Along each of the lines between the two infinitely close characteristics, i.e., Mach waves, the flow is identical to flow in the immediate proximity of the corresponding surface element of the profile. In accordance with this, all flow lines above the upper surface are equidistant to curve $h_1(x)$, while the flow lines above the lower surface are equidistant to another curve $h_2(x)$.

The solution of the problem is reduced to determining function ψ constant on every flow line. Let us assume that on the profile surface the stream function is equal to zero, i.e., $\psi = 0$ when $y = h(x)$. According to (68) this is equivalent to condition $\psi' = -w_1 h(x)$ when $y = h(x)$.

Taking into consideration that the profile is thin, we will require a precise fulfillment of the boundary condition not on

the profile surface itself but approximately on axis OX. In this case the boundary conditions will be written as:

$$y=0, \psi=0 \quad \text{then} \quad y=0, \psi'=-w_1 h(x). \quad (74)$$

For the upper surface, where there are characteristics of the first family, we will seek the solution in the form

$$\psi'_{0,n} = Ah(x - wy),$$

where A - arbitrary value determined from boundary condition (74). Since $\psi'_{0,n} = Ah(x) = -w_1 h(x)$ when $y = 0$, then $A = -w_1$.

Consequently, we finally have

$$\psi'_{0,n} = -w_1 h(x - wy)$$

According to (69), for the upper surface we obtain

$$\left. \begin{aligned} u' &= -\frac{1}{1-M_1^2} \frac{\partial \psi'}{\partial y} = -\frac{w_1}{1-M_1^2} \frac{dh}{dx} \\ v' &= -\frac{\partial \psi'}{\partial x} = w_1 \frac{dh}{dx} \end{aligned} \right\} \quad (75)$$

Similarly, for the lower surface where there are characteristics of the second family

$$\psi'_{n,n} = -w_1 h(x + yw)$$

and accordingly

$$\left. \begin{aligned} u' &= \frac{w_1}{1-M_1^2} \frac{dh}{dx} \\ v' &= -w_1 \frac{dh}{dx} \end{aligned} \right\} \quad (76)$$

Presenting to the Bernoulli equation for the isentropic flow (§ 4, Chapter I)

$$\frac{w^2}{2} + \frac{k}{k-1} \left(\frac{p}{\rho_1} \right)^{\frac{k-1}{k}} = \frac{w_1^2}{2} + \frac{k}{k-1} \frac{p_1}{\rho_1}$$

the expression for the flow parameters in form (63) and disregarding the squares of small values, we have

$$p = \frac{p_1 - p_2}{\rho_1 \frac{w_1}{2}} = \frac{p_1 - p_2}{\rho_1 \frac{w_1}{2}} = -\frac{2H}{w_1}.$$

Now, according to (75) and (76) we obtain the following expressions for a dimensionless pressure on the upper and lower profile surfaces:

$$p_{u.s.} = \frac{2h'_1(x)}{\sqrt{M_1^2 - 1}}, \quad p_{l.s.} = -\frac{2h'_2(x)}{\sqrt{M_1^2 - 1}}. \quad (77)$$

Let us find the drag and lift coefficients. For the surface element

$$\begin{aligned} dR_x &= p dS \sin \theta = p dy = p \frac{dy}{dx} = p h'_1(x) dx, \\ dR_y &= -p dS \cos \theta = -p dx, \end{aligned}$$

and according to (77), after summation we obtain for both surfaces

$$\left. \begin{aligned} c_x &= \frac{R_x}{\frac{1}{2} \rho_1 w_1^2} = \frac{2}{b \sqrt{M_1^2 - 1}} \int_{x_A}^{x_B} \{ |h'_1(x)|^2 + |h'_2(x)|^2 \} dx, \\ c_y &= \frac{R_y}{\frac{1}{2} \rho_1 w_1^2} = \frac{4}{\sqrt{M_1^2 - 1}} \frac{y_B - y_A}{b}. \end{aligned} \right\} \quad (78)$$

Here y_A and y_B are the coordinates of points B and A. For a thin profile the following approximate equality is valid

$$\frac{y_B - y_A}{b} = \frac{y_B - y_A}{x_B - x_A} \approx L$$

Then from (78), we have

$$c_y = \frac{4L}{\sqrt{M_1^2 - 1}}. \quad (79)$$

Thus, the lift coefficient of a thin profile does not depend on its shape, but is determined only by the angle of attack and the Mach number of the incident flow.

The coefficient of wave drag c_x , as compared with lift coefficient c_y , represents a small value of the second order. Thus, for instance, for the plate

$$h'_1(x) = h'_2(x) = -1,$$

and according to (78)

$$c_x = \frac{4\alpha^2}{\sqrt{M_1^2 - 1}}. \quad (80)$$

This formula for the drag coefficient can also be obtained directly from the lift coefficient (79), taking into account that the resultant of the forces applied to a flat plate in supersonic inviscid flow is always directed along the normal to it and, therefore,

$$c_x = c_y \tan \alpha \approx c_y \alpha. \quad (81)$$

With the angles of attack $\alpha < 15^\circ$ the calculation of coefficients c_y and c_x for a flat plate, using approximation formulas (79) and (80), yields a satisfactory agreement with the precise calculation presented above in this paragraph.

The plate, as compared with other thin profiles with the same angle of attack, has the smallest wave-drag coefficient. Thus, for instance, in accordance with (78), for the profile formed from two arcs of the circle with an identical radius (lens)

$$c_x = \frac{4\alpha^2}{\sqrt{M_1^2 - 1}} + \frac{16}{3\sqrt{M_1^2 - 1}} \left(\frac{c}{b} \right)^2 = c_{x0} + \frac{16c^2}{3\sqrt{M_1^2 - 1}}.$$

The additional component to the wave-drag coefficient of the plate depends on the relative thickness ratio of the profile $\bar{c} = c/b$.

§ 8. Streamlining of Airfoil Cascade by the Flow of an Incompressible Fluid

Let us examine the streamlining by a potential flow of incompressible fluid of a rectilinear cascade composed of profiles which have a sharp trailing edge. Just as for the case of a unitary profile, it is possible to find the direction of a non-circulatory flow at which the sharp edge is the point of stream convergence; the corresponding angle between the direction of a noncirculatory flow and the front of the cascade we designate as β_0 .

The circulation value for the profile located in the cascade and streamlined by an ideal incompressible fluid is determined from the same expression, as for the unitary profile except instead of the incident flow velocity, as this was done in the case of the isolated airfoil, one should, in accordance with N. Ye. Joukowski's theorem, substitute the value of the geometric half-sum of velocities w_m ahead of and behind the cascade. Angle of attack α_m is defined as the angle between the airfoil chord and the direction of velocity w_m .

Thus, we can write

$$\Gamma_p = m_p b w_m \sin(\alpha_m - \alpha_{0p}),$$

where m_p - proportionality factor depending on the profile shape and the cascade parameters, α_{0p} is the angle between the zero-lift direction and the airfoil chord.

Substituting this value of circulation into (14), we obtain the following in accordance with (53):

$$c_{yp} = 2m_p \sin(\alpha_m - \alpha_{0p})$$

or

$$c_{yp} = \left(\frac{dc_y}{d\alpha} \right)_{\alpha=\alpha_{0p}} \sin(\alpha_m - \alpha_{0p}) = \left(\frac{dc_y}{d\alpha} \right)_{\alpha=\alpha_{0p}} \sin(\beta_0' - \beta_m) \quad (82)$$

where β_0 is the angle between the zero-lift direction and the front of the cascade.

For the angles generally used in practice it is possible to assume that

$$\sin(\alpha_m - \alpha_{op}) \approx \alpha_m - \alpha_{op}$$

Then from (82) we have

$$c_{yp} = \frac{dc_p}{d\alpha} (\alpha_m - \alpha_{op}) = \frac{dc_p}{d\alpha} \alpha_{Ap}$$

where

$$\alpha_{Ap} = \alpha_m - \alpha_{op}$$

Let us note that if for the isolated profile value $dc_p/d\alpha$ and zero-lift angle α_0 depend only on the profile shape, then in the case of a cascade, in addition, these values depend also on the cascade parameters: denseness $\tau = b/t$ and setting angle φ .

Evidently when the cascade pitch approaches infinity ($\tau \rightarrow 0$) value of $dc_p/d\alpha$ and α_{0p} tend toward their values respectively for the isolated profile.

Based on (11) and (82), after elementary transformations, we come to the following relationship between the angles of entry and departure:¹

$$\operatorname{ctg} \beta_2 = A \operatorname{ctg} \beta_1 + B, \quad (83)$$

where A and B - constants for a given airfoil cascade with the value

¹For a detailed derivation, see Chapter VIII of the previous publication of this book.

$$A = \frac{1 - \frac{\tau}{4} \frac{dc_y}{da} \sin \beta_0}{1 + \frac{\tau}{4} \frac{dc_y}{da} \sin \beta_0}, \quad B = \frac{\frac{\tau}{2} \frac{dc_y}{da} \cos \beta_0}{1 + \frac{\tau}{4} \frac{dc_y}{da} \sin \beta_0}.$$

With an increase in denseness coefficient A decreases, therefore, beginning with certain denseness τ the first term in the right side of expression (83) can be disregarded. Consequently, with large values τ the angle of departure ceases to depend on the angle of entry, becoming the following constant value for these cascade parameters:

$$\operatorname{ctg} \beta_2 \approx B = \text{const.}$$

In this case the flow at the outlet is determined only by the output part of the vane channel, i.e., it does not depend on the conditions of entry. If the condition of constancy of the angle of departure $\beta_2 = \text{const}$ is observed, then the flow direction at the output coincides with the zero-lift direction $\beta_2 = \beta_0$, because in this case $\beta_1 = \beta_2$, i.e., the flow in the cascade is not deflected. In the general case, the expression for angle β_0 is found from formula (83), written for the noncirculatory mode of cascade streamlining in the form

$$\operatorname{ctg} \beta_0 = \frac{B}{1-A}.$$

Figures 10.21 and 10.22 show the charts of functions A and B for the cascade of flat plates¹ depending on denseness τ , at the various setting angles α . Based on the examination of these graphs, when $\tau > 1$ value A becomes on the order of $A < 0.1$; however, value B asymptotically approaches $\operatorname{ctg} \alpha$ and when $\tau \geq 1.2$ it can be assumed to be constant.

¹The problem of flow around a cascade of flat plates was solved for the first time by S. A. Chaplygin in 1912; then a simpler solution was obtained by N. Ye. Joukowski in 1915.

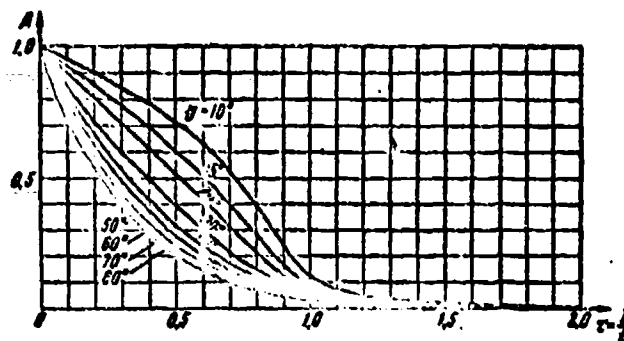


Fig. 10.21. Coefficient A for the cascade of plates.

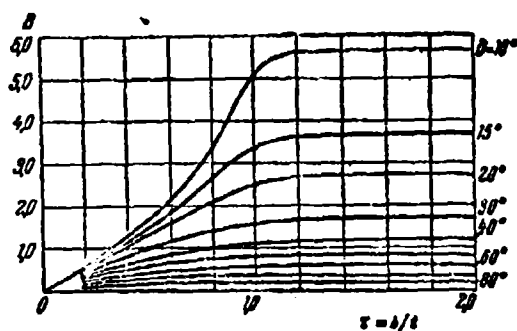


Fig. 10.22. Coefficient B for the cascade of plates.

Using values A and B the values so-called "angle of lag" δ are calculated and plotted in Fig. 10.23 as an example, i.e., the angle between the flow direction at the output and the direction of plates: $\delta = \beta_1 - \beta_2$. As we see, with an increase in denseness the angle of lag rapidly decreases; for example, in the case $\beta_1 = 30^\circ$ the angle of lag for denseness $\tau = 0.5$ comprises $\delta = 11^\circ$, whereas with $\tau = 1$ we have $\delta = 2^\circ$.

In the general case the problem of streamlining of the airfoil cascade by a potential flow of incompressible fluid is usually solved either by the method of conformal mapping or by the vortex method.

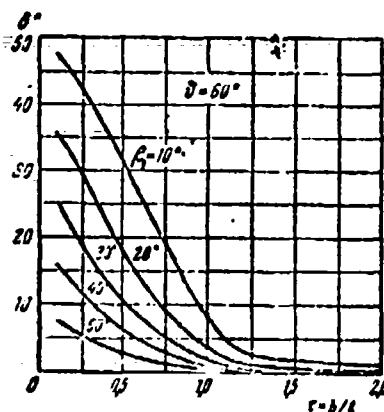


Fig. 10.23. The dependence of the angle of lag δ on denseness τ for the cascade of plates.

In the first method it is assumed that the flow around any cascade of the simplest bodies is known. As an example of such a cascade we use a cascade of circles or a cascade of ovals close to them. Further, with the aid of some simple mapping function, the area external with respect to this cascade is conformally converted into an exterior of a certain airfoil cascade whose configuration depends on the form of the mapping function. The cascade thus obtained in which the flow is already determined is usually called the cascade of theoretical or analytical profiles.¹

A considerably more complex for this method is the solution of a direct problem - a construction of flow around certain airfoil cascade. In this case, a more effective method of solution, especially, bearing in mind the use of contemporary electronic computers, is the second method, the vortex method. This method as applied to the cascade composed of thin airfoils - small arcs of given shape - consists of the following. Each

¹See, for example, Bloch E. L., A Study of a Two-Dimensional Cascade Composed of Theoretical Profiles of Finite Thickness. The works of TsAGI Issue 611, 1947.

profile is replaced by a vortical layer with intensity $\gamma(S)$, where S is the arc length reckoned from the leading edge of the profile (Fig. 10.24). The intensity of vortical layer $\gamma(S)$ is selected from the condition of the normal vector component of velocity vanishing at any point of the profile, which is equal to the vector sum of the velocity of a uniform incident flow and the velocities induced at this point from the entire infinite system of vortices.

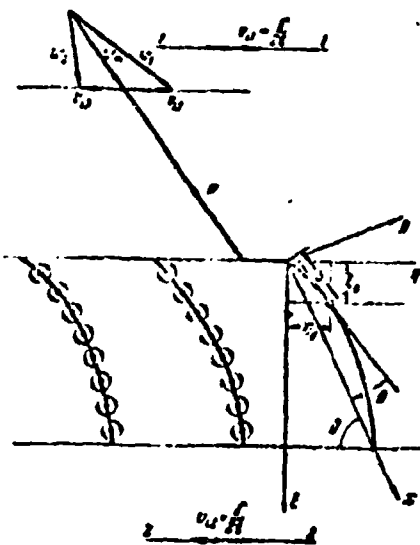


Fig. 10.24. A scheme for replacing the small arcs by vortical layers.

In this case it is necessary to bear in mind that the velocity induced far ahead of the cascade as an infinite chain of vortices with intensity Γ , unlike the unitary vortex, does not vanish but is equal to $\Gamma/2t$ and is directed at a right angle to the front of the cascade.¹ Thus, even though the direct replacement of the small arcs by the corresponding vortical

¹See, for example, Chapter II of the book by G. M. Abramovich "Applied Gas Dynamics," Publication 2, Tekhteorizdat, 1953.

layers in the cascade, satisfies the boundary conditions on the profile surfaces (conditions of impenetrability, $w_n = 0$), it results, however, in the disturbance of the boundary conditions far ahead and behind the cascade.

To account for this fact, instead of the flow around this cascade of physical profiles by a given flow at infinity, we need to examine the flow around the cascade with corresponding vortical layers by the flow having the velocity equal to the geometric mean velocity $w_m = 1/2(w_1 + w_2)$. However, to determine the magnitude and direction of this velocity according to the given velocity w_1 , it is necessary to know circulation Γ around the profile, the value of which is to be determined.

Usually, this is done in the following manner. The cascade of physical profiles is replaced by the cascade of vortical layers and its forward motion is examined at a given velocity v in a static fluid. In the reverse motion the cascade is static and is streamlined by a flow with velocity w_1 so that half of the geometric sum of this velocity and the velocity w_2 behind the cascade is equal to $-v$.

According to the N. Ye. Joukowski theorem (see § 2), the resultant of the aerodynamic forces which act on the static cascade is directed along the normal to the geometric mean velocity, i.e., in our case it is along the normal to velocity v . Thus, during the motion of a cascade of vortical layers in a static fluid the resultant is directed along the normal to the direction of motion, i.e., there is no resistance. Another case; the same forward motion of a cascade of physical profiles in a static fluid. Here there is no disturbance of flow at an infinity ahead of the cascade. Thus, with the reversal of motion we arrive at a static cascade streamlined by a flow with velocity $w_1 = -v$. Since the projection of the resultant of forces on the direction of the flow advancing onto the cascade, according

to the Joukowski theorem, is always different from zero, then, depending on the sign of this component, the motion of a cascade of physical profiles in a static fluid always occurs either in the presence of the resisting forces or under the action of the pull directed along the motion.¹

Turning again to the forward motion of the cascade of vortical layers and designating the disturbed velocity of the previously static fluid in terms of v_1 , we write the condition of the absence of flow separation during the flow around the profiles in the form

$$v_n + v_{1n} = 0. \quad (84)$$

Adding all the velocities induced by an infinite system of vortices at the fixed point of a profile, we obtain²

$$v_{1n} = \frac{1}{2\pi} \int \Gamma(S) \gamma_n(\xi, \eta, \xi_0, \eta_0) dS. \quad (85)$$

Here

$$\gamma_n(\xi, \eta, \xi_0, \eta_0) = \frac{\frac{1}{2} \sin 2\bar{\eta}}{\sin^2 \bar{\eta} + \sin^2 \bar{\xi}} \cos(\bar{\theta} + \bar{\psi}) + \frac{\frac{1}{2} \sin 2\bar{\xi}}{\sin^2 \bar{\eta} + \sin^2 \bar{\xi}} \sin(\bar{\theta} + \bar{\psi}),$$

$$\bar{\xi} = \pi \frac{\xi - \xi_0}{l}, \quad \bar{\eta} = \pi \frac{\eta - \eta_0}{l};$$

where $\bar{\theta}$ is the angle between the tangent to the profile contour at a particular point and the profile chord; ξ, η, ξ_0 , and η_0 are the coordinates of the flowing and fixed points of the

¹It is not difficult to show that during the motion of a diffuser cascade, we have the resisting force and, correspondingly during the motion of a convergent cascade - pulling force. In an active cascade the resultant is directed along the normal to the motion.

²Belotserkovskiy S. M., Ginevskiy A. S., Polonskiy Ya. Ye., The Power and Moment Aerodynamic Characteristics of the Thin Airfoil Cascades. In the Coll. of "Industrial Aerodynamics," No. 22, Oborongiz, M., 1962.

examined cascade profile, respectively. The normal velocity component at a particular profile point during the forward cascade motion at velocity v will be

$$v_n = v [\sin(\theta - \beta_m) \cos \theta + \cos(\theta - \beta_m) \sin \theta] \quad (86)$$

The substitution of (85) and (86) into (84) leads to the following integral equation for determining $\gamma(S)$:

$$\frac{1}{2\pi i} \int \gamma(S) \gamma_n(t, \eta, \xi, \eta_n) dS = \sin(\theta - \beta_m) \cos \theta + \cos(\theta - \beta_m) \sin \theta.$$

Replacing the continuous vortical layer by discrete vortices, we reduce the solution of integral equation to the solution of a system of linear algebraic equations.

Thus, with the aid of an electronic computer, we made a thorough calculation of coefficients A and B for the thin airfoil cascades over a wide range of a change in the geometric parameters of the cascade and profile.¹ Using these materials, one can easily solve the direct and inverse problems of the airfoil cascade aerodynamics in a potential flow of incompressible fluid.

As the denseness of the cascade is decreased, the velocity induced on this small arc by the vortices located on the other small arcs decreases and disappears in the extreme case of a unitary small arc, when the induced velocity is determined only by the vortices located on the small arc itself. Now, assuming that the vortices are not on the unitary small arc but on its chord, we obtain the following expression for the velocity

¹See footnote 2 on preceding page.

induced by the entire system of vortices at point x_1 of the chord:

$$v_1(x_1) = \int \frac{\gamma(x) dx}{2\pi(x-x_1)}.$$

Limiting ourselves only to the slightly bent small arcs, we assume this velocity calculated on the airfoil chord to be equal to the induced velocity at the corresponding point x_1 on the small arc surface. If, furthermore, we limit ourselves also to the small angles of attack, then the condition when the normal velocity component on the profile is equal to zero, which expresses the condition of its continuous streamlining is written as:

$$\alpha + \frac{1}{2\pi w_1} \int \frac{\gamma(x)}{x-x_1} dx = \frac{dy}{dx}.$$

Here, on the right side, is the derivative of the small arc coordinate along axis x , which coincides with the airfoil chord. As a result of the solution of an integral equation with respect to $\gamma(x)$ with the aid of trigonometric series, we obtain the following expression for the lift coefficient of the slightly bent thin profile:¹

$$c_y = 2\pi \left(A_0 + \frac{A_1}{2} \right).$$

where A_0 and A_1 are coefficients of the Fourier series

$$A_0 = \alpha - \frac{1}{\pi} \int \frac{dy}{dx} d\varphi, \quad A_1 = \frac{2}{\pi} \int \frac{dy}{dx} \cos \varphi d\varphi.$$

¹See Glauert N., The Airfoil and Prop Theory. Gostekhizdat, 1931.

and φ is a new independent variable determined by the equality

$$x = \frac{b}{2}(1 - \cos \varphi).$$

For a flat plate we have

$$\frac{dy}{dx} = 0 \quad \text{and} \quad c_y = 2\pi\alpha.$$

This expression coincides with the formula given in the preceding paragraph.

Knowing the values of coefficients A and B for this cascade, according to (50), (51) and (83), we find¹

$$\begin{aligned} c_x &= 2[(1-A)\operatorname{ctg} \beta_1 - B] \sin^2 \beta_1, \\ c_y &= -[(1-A)\operatorname{ctg}^2 \beta_1 + 2AB \operatorname{ctg} \beta_1 - B^2] \sin^2 \beta_1, \end{aligned}$$

and consequently

$$c_R = \sqrt{c_x^2 + c_y^2}.$$

For the dense diffuser cascade of thin strongly bent profiles Fig. 10.25 shows the dependences of the coefficients of the resultant of forces on the angle of attack

$$c_R = \frac{R}{\frac{w_1}{2} b} \quad \text{and} \quad c_y = \frac{R}{\frac{w_2}{2} b}.$$

With a fixed velocity value w_1 of the incident flow the value of coefficient c_R and, consequently, also the resultant of the aerodynamic forces applied to the cascade profile at a certain relatively small angle of attack reaches a maximum value.

¹Since the flow is potential, we assume that $\xi = 0$.

It has been indicated earlier that for a unitary profile the presence of a maximum of the resultant always presupposes the development of intense flow separation from the upper profile surface. This is why such critical angle of attack of the isolated profile is frequently called the separation angle of attack. A different case is in the cascade. Here, as we see, achieving a maximum by the resultant is not necessarily connected with the flow separation, but occurs also during a continuous potential flow around the airfoil cascade.

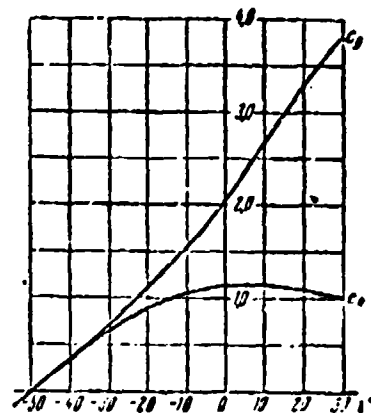
This is explained by the fact that the cascades composed of airfoils with large camber operate at very large aerodynamic angles of attack reckoned from the direction of a noncirculatory flow.

Thus, for instance, in the case given in Fig. 10.25 the direction of a noncirculatory flow (Fig. 10.3) forms the angle

$$\beta_0 = \beta_1 = \gamma_1 = 0 + \frac{\epsilon}{2} = 67.5^\circ,$$

and with zero angle of attack ($i = 0$) the aerodynamic angle of attack is equal to 45° . The resultant force reaches a maximum value when $i = 7^\circ$, which corresponds to the aerodynamic angle of attack $\alpha_A = 52^\circ$. The possibility of a continuous flow around the profiles at such angles of attack is connected with a specific nature of the flow in a very dense cascade.

Fig. 10.25. The dependence of dimensionless coefficients c_R and c_y on the angle of attack for a dense cascade of thin small arcs; $\epsilon = 65^\circ$, $\epsilon = 50^\circ$.



It should be noted that the use of lift coefficient c_y impedes the determination of the critical angle of attack; in this case the value of the resultant is referred to the dynamic head calculated by the geometric mean velocity $\sqrt{\frac{w_1^2 + w_2^2}{2}}$, which does not remain constant with a change in the angle of attack and fixed value w_1 .

Let us now examine certain problems which pertain to the streamlining of airfoil cascades by a flow of viscous incompressible fluid, in the case of the diffuser cascades. The latter is connected with the fact that in the decelerating flow characteristic for a diffuser cascade, conditions are created which contribute to earlier boundary-layer separation. In fact, these situations lead to larger total pressure losses in the diffuser cascades in comparison with the convergent in which the accelerating flow prevents the boundary-layer separation.

The first experimental study of the flow around cascades by an air stream at low velocities was done by N. Ye. Joukowski in 1902 at the laboratory of Moscow University. The tested cascade of plates was connected to the aerodynamic balances which were instrumental in determining the lift coefficient of a plate in the cascade.

At the present there are many experimental data obtained as a result of a systematic study of the diffuser cascades,^{1,2,3} which make it possible for us to solve successfully both the direct and inverse problems of cascade aerodynamics. In these

¹Howell A. R., The Hydrodynamics of the Axial-Flow Compressor. In Coll. of "Development of Gas Turbines," under the editorship of V. L. Aleksandrov. B. N. Vol., MAP, 1947.

²Bunimovich A. I., Svyatogorov A. A., Generalization of Results of the Study of Two-Dimensional Compressor Cascades at a Subsonic Speed. In Coll. of "Bladed Machines and Jet Apparatuses," Iss. 2, "Mechanical Engineering," M. 1967.

³Komarov A. P., Study of Two-Dimensional Compressor Cascades. In Coll. of "Bladed Machines and Jet Apparatuses," Iss. 2, "Mechanical Engineering," M., 1967.

experiments, one usually measured the velocities and angles ahead of and behind the cascade respectively and a direct measurement was made of the difference in total pressures. In a number of cases, pressure distribution along the profile surface was also determined.

We should bear in mind that in these experiments, just as in the majority of others, the flow direction behind the cascade was determined in the immediate vicinity of its edge, where it is still nonuniform. Therefore, for determining the effective deflection of flow by the cascade, using the measured velocity distribution one should find the direction of the equalized flow according to (28). In the case of the continuous angles of attack this direction can be determined by the parameters of the boundary layer on the trailing edges of profiles.¹

Figure 10.26 shows the experimental dependences obtained by A. P. Komarov for losses ζ and angle of turn $\Delta\beta$ of the flow in the cascade on the angle of attack. It is evident that at first the dependence of the angle of turn of the flow on the angle of attack is linear. Then, at a certain value of the angle of attack, usually called the angle of separation, the value of the angle of flow deflection by the cascade reaches a maximum value. An intense flow separation from the upper profile surface starts at this angle of attack and the losses increase considerably. A further increase in the angle of attack leads to a decrease in the angle of deflection, accompanied by an intense increase in losses.

Another characteristic angle of attack is that at which the total pressure losses in the cascade become minimal. In

¹Ginevskiy A. S., Study of the Aerodynamic Characteristics of Airfoil Cascades of the Axial-Flow Compressor. Author's dissertation abstract, 1956.

this case the flow direction far ahead of the cascade is close to that shock-free, i.e., to a direction at which the branch point of streams during the flow around a profile coincides with the point of its maximum camber.

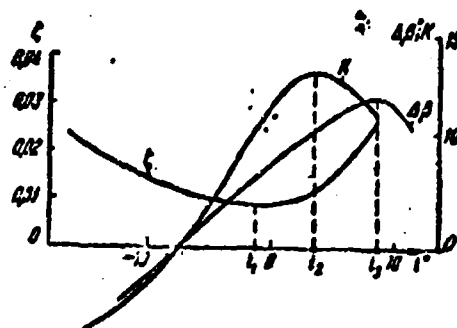


Fig. 10.26. Dependence of the loss factor, angle of flow deflection and quality on the angle of attack for the airfoil cascade with $\epsilon = 10$; $b/t = 1.0$ and $\delta = 50^\circ$, α_1 - angle of attack with minimum losses, α_2 - angle of attack with a maximum cascade quality, α_3 - angle of attack during a maximum flow deflection by the cascade (separation angle of attack).

To evaluate the aerodynamic perfection of the airfoil cascade one can use¹ the concept of quality K of the cascade (not to confuse with the quality of profile in the cascade)

$$K = \frac{R_u}{P_a}$$

Here R_u is that useful frontal force in order to obtain which one uses this cascade, and F_a is the axial force whose appearance is connected only with the irreversible total pressure losses

¹S. I. Ginsburg, Elements of Gas Dynamics of the Axial-Flow Compressors and Turbines. Chapter IX in the first publication of this book. The Gostekhteorizdat, M. - L., 1951.

in the cascade. The greater the value of K , the more perfect is the cascade. In an inviscid flow the losses are absent, axial additional force disappears and $K = \infty$.

In certain instances it is convenient to use the value called the inverse quality of a cascade:

$$\nu = \frac{1}{K} = \frac{P_d}{P_a}$$

The quality of the cascade predetermines the efficiency of the elementary cross section of the rotor of the axial stage in which this cascade is being used. The cascade quality maximum corresponds to the maximum of the efficiency.

According to (4) and (32), the quality of the cascade

$$K = \frac{\rho w_a \Delta w_a}{h_w}$$

and, correspondingly, inverse quality of the cascade is expressed in terms of the drag coefficient value and the angles of entrance and departure values

$$\nu = \frac{2 \sin^2 \beta_1 (\operatorname{ctg} \beta_1 - \operatorname{ctg} \beta_2)}{c}$$

At a certain value of the angle of attack $i = i_2$ the quality value of a given cascade reaches a maximum. Such a system of flow around the cascade is called optimal. In the general case, the system of minimum losses and the optimal system do not coincide with one another.

An increase in the optimum angle of attack i_2 observed in Fig. 10.26 as compared with the angle of attack i_1 of the minimum

losses, is due to the relatively flat nature of dependence $\zeta(i)$. Because of this, the increase in the angle of attack, which leads to an increase in Δw_u and, consequently, also an increase in circumferential force R_u , will have a slight effect on the increase in losses, hence, also on the additional axial force F_a . As a result, the numerator of the expression for v will, up to a certain angle of attack, increase faster than the denominator, and, correspondingly, the point of the maximum quality value of the cascade will shift to the side of large angle of attack values.

With an increase in profile camber the dependence of the loss factor on the angle of attack becomes steeper and, as a result, there is a convergence of both extreme points. Beginning with the angle of profile camber $\epsilon = 60^\circ$, the angle of attack which corresponds to the minimum of losses is virtually coincidental with the optimum angle of attack.

The degree of deceleration of the flow in a two-dimensional diffuser cascade and the corresponding pressure gradient value or, in other words, the aerodynamic load factor of the cascade can be compared with those in equivalent two-dimensional diffuser (Fig. 10.27) whose lateral sides are equal to the length of the axial profile arc and the areas of inlet and outlet cross sections are equal to the corresponding areas of the examined cascade at a given direction, the flow advancing onto it. The central angle α_g of such equivalent diffuser of a two-dimensional cascade is determined from the relationship

$$\sin \frac{\alpha_g}{2} = \frac{n_2 - n_1}{2S} = \frac{l (\sin \beta_2 - \sin \beta_1)}{2S},$$

where S is the length of the axial profile arc.

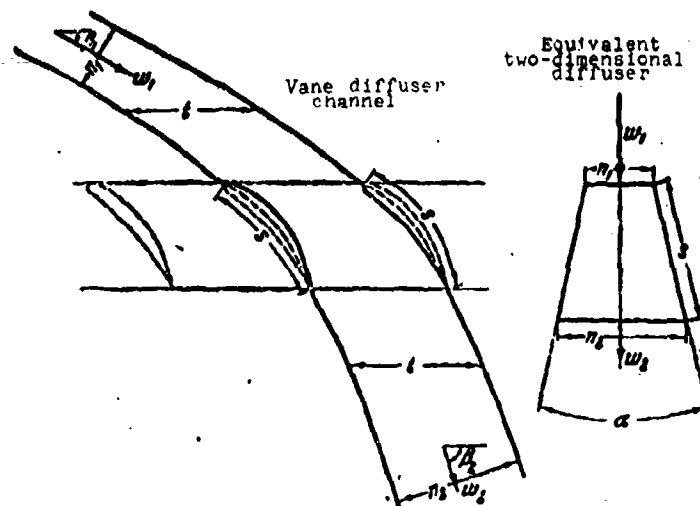


Fig. 10.27. A diagram of transition from the vane diffuser channel to the equivalent two-dimensional diffuser.

For the slightly bent profiles it is possible to assume that $S = b$. Under this condition we have

$$\sin \frac{\alpha_0}{2} = \frac{\sin \beta_2 - \sin \beta_1}{2\epsilon}.$$

The diffuser angles used in practice are small, therefore, it is possible to assume that

$$\alpha_0 = 2\varphi_0 = \frac{\sin \beta_2 - \sin \beta_1}{\epsilon}. \quad (87)$$

It is important to note that an equivalent two-dimensional diffuser is determined not only by the angle of expansion but also by the length or value of ratio n_2/n_1 . This fact is confirmed¹ by the data of experimental determination of the expansion

¹Polsin I., Stromungsunters an einem ebenen Diffusor, Ingenier - Archiv, Heft 5, 1940.

angles of a two-dimensional diffuser, at which a flow separation occurs, depending on ratio n_2/n_1 .

The relative length of channels with constant cross section is usually characterized by the ratio of channel length l to its width n . For the channels with variable cross section, the characteristic value is the average value of its width

$$n_{cp} = \frac{1}{2}(n_1 + n_2).$$

Accordingly, for the vane channel we obtain

$$n_{cp} = \frac{l(\sin \beta_1 + \sin \beta_2)}{2},$$

and, therefore, its relative length can be found from the following expression:

$$\bar{l} = \frac{l}{n_{cp}} = \frac{1}{2} \frac{b}{l} (\sin \beta_1 + \sin \beta_2)$$

The angle of an equivalent two-dimensional diffuser and its relative length determine the maximum aerodynamic load factor of a two-dimensional diffuser cascade, which is achieved at the so-called "separation or critical" angle of attack when the angle of turn of the flow in the cascade reaches a maximum value. This is evident from the examination of Fig. 10.28, where the results of the calculation carried out by Ye. A. Lokshtanov are plotted for dependence $\alpha_{np}(\bar{l})$ on the boundary of a continuous flow around the cascades according to the experimental data of Howell¹ and also shown are the experimental results of blowing of the two-dimensional straight diffusers, reconstructed in the same manner.

¹Howell A. R., Hydrodynamics of Axial-Flow Compressor. Coll. of "Development of Gas Turbines," under the editorship of V. L. Aleksandrov. B. N. Vol., MAP, 1947.

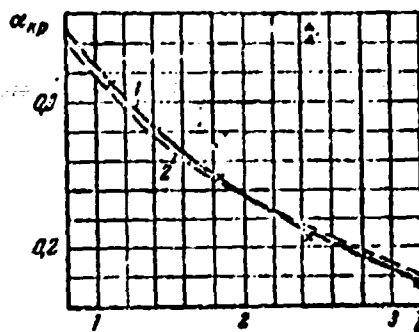


Fig. 10.28. A comparison of dependences $\alpha_{kp} = f(\bar{l})$ for two-dimensional diffusers (1) and for diffuser cascades (2).

The comparison of curves on Fig. 10.28 shows that the dependence $\alpha_{kp}(\bar{l})$ obtained for critical deviation of the flow in diffuser cascades is virtually completely coincidental with the curve corresponding to the onset of stable flow separating in a two-dimensional diffuser.

It is known that with a known value of the area ratio there is an optimum expansion angle in a straight diffuser at which the total losses composed of the losses due to friction and vortex formation achieve a minimum value. Hence, it is possible to assume that according to expression for α_0 the optimum cascade density value should depend only on angles β_2 and β_1 . Actually, the results of the experimental study of cascades indicate the existence of such a dependence. As the denseness increases in comparison with its optimum value, the increase in losses due to friction exceeds the decrease in losses caused by the flow separation. With a decreased denseness the opposite is observed. Qualitatively, the same phenomena occur also in a two-dimensional diffuser when its length changes in the inlet and outlet cross sections of the given areas or, the same occurs when there is a change in the expansion angle. Although, qualitatively, the

dependence of optimum denseness on angles β_2 and β_1 is found in accordance with the existence of an optimum expansion angle in a two-dimensional diffuser; however, the corresponding value does not prove to be constant for different cascades. This indicates that the losses in an equivalent two-dimensional diffuser differ from losses in the cascade. The latter is connected with the fact that the examined equivalent dimensional diffuser determined by the flow parameters ahead of and behind the cascade does not permit one to make a sufficiently complete consideration of the peculiarities of fluid flow in the vane channel. With small angles, especially in cascades with thick profiles, the flow is first accelerated, reaches maximum velocity w_{\max} in the narrowest cross section of the vane channel (in the throat) and only then the deceleration of the flow begins. In this case the diffuser effect of a cascade should be characterized by the angle of expansion and the length of an equivalent rectilinear two-dimensional channel which corresponds to the second diffuser vane channel section. The expansion angle of this part of the channel is

$$\alpha_2 = \frac{(\sin \beta_2)_2 - F_2}{S_2}.$$

Here F_2 - width of the narrowest section in the vane channel, while S_2 - arc length of the center line of its diffuser section. Assuming approximately for cascades with large setting angle

$$S_2 \approx b, \quad F_2 \approx t \sin \beta_2 - c,$$

where β_2 - angle of slope in the center line in the throat of the vane channel, and c - maximum profile thickness, we obtain

$$\alpha_2' = \frac{\sin \beta_2 - \sin \beta_1 + \frac{c}{t}}{b/t}.$$

With small separation-free angles of attack the losses in the cascade arise primarily on a convex, profile surface having

the highest diffuser factor, which has a relatively thicker boundary layer. In accordance with this, one of the most effective parameters which characterize the losses in the indicated flow conditions is the coefficient of diffusivity

$$D_s = \frac{w_{\max} - w_2}{w_1},$$

which estimates the degree of deceleration of the flow from a maximum velocity w_{\max} on a convex profile wall to flow velocity w_2 at the exit from the cascade.

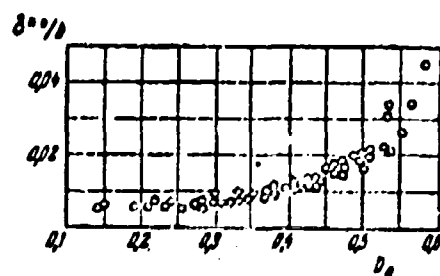


Fig. 10.29. Dependence of the relative value of the momentum loss in the wake behind the profile in the cascade with an optimum angle of attack on diffuser coefficient D_s (calculated according to the distribution of pressure along the profile).

In a number of cases the diffusivity of cascades is also characterized by coefficient D called the total diffusivity coefficient:¹

$$D = \left(1 - \frac{\sin \beta_2}{\sin \beta_1}\right) + \frac{\sin \beta_1}{2b_1} (\log \beta_1 - \log \beta_2)$$

Figure 10.29 shows the experimental dependence of the relative thickness of the momentum loss in the wake behind the cascade (the value is proportional to the losses in total pressure) on the diffusivity coefficient determined by the pressure

¹Lieblein G., Schrenk E. I. and Frederick, R. L., Diffusion Factor for Estimating Losses and Limiting Blade Loadings in Axial - Flow-compressor Blade Elements. NACA RM 53D01, 1953.

distribution on the upper profile surface. These data are obtained on the basis of the results of the experimental study of cascades composed of the NACA profiles over a wide range of change in the denseness, angle of curvature and angle of entry.¹ It is evident that there is a universal relationship between the relative thickness of the momentum loss and the coefficient of diffusivity. With an increase in the diffusivity coefficient we observed an increase in losses - at first a very gradual, and then more intense. With high diffusivity coefficient values (more than 0.5) the boundary-layer separation on the convex surface causes a rapid increase in the relative momentum loss thickness. With zero value of the diffusivity coefficient the momentum loss thickness does not equal to zero. This is due to presence of losses due to friction and, to a lesser degree, also to the effect of the finite thickness of the trailing edge.

The results of the experiments carried out on cascades composed of a different kind of profiles, also indicate the presence of a universal relationship between the losses at the optimum angle of attack and the value of the total diffusivity coefficient D .

§ 9. Streamlining of Airfoil Cascade by a Subsonic Flow of Gas

A subsonic streamlining of a cascade composed of subsonic profiles, just as the subsonic streamlining of a unitary profile examined above, is subdivided into two types - subcritical and supercritical. It is obvious that value M_{1*cr} which corresponds to the critical incident flow velocity at which, somewhere on the

¹Herrig L. Y., Emery, J. C. and Erwin J. R. Systematic Two - Dimensional Cascade Tests of NACA 65 - Series Compressor Blades at Low Speeds, NACA RML 51031, 1951.

profile, a velocity equal to the speed of sound arises, which ultimately depends on the value of highest rarefaction on the profile (usually, M_{1kp} is found from condition $d\zeta/dM_1 \approx 0.1$). The experimental dependence curve of M_{1kp} on angle of attack α is represented in Fig. 10.30 for a typical diffuser cascade.

It should be noted that for a profile in the cascade the effect of boundary layer on value M_{1kp} is exhibited to a considerably larger degree than for a unitary profile. This is due to the limitedness of the flow during a flow around a profile in the cascade.

The special features of the flow are exhibited most prominently at supercritical velocities. When $M_1 > M_{1kp}$ a supersonic zone is formed in the cascade vane channels which increases in proportion to the increase in number M_1 and which is consummated by a much more complex system of shocks than that of a unitary profile as a result of their reflection from the adjacent surfaces.

Unlike the unitary profile for which the incident flow velocity can be as high as desired, the flow around a cascade is limited by a certain maximum Mach number

$$M_{1kp} \leq M_{1max} \leq 1.$$

The onset of critical condition, earlier than that of maximum flow rate (M_{1max}), is due to the uneven distribution of flow parameters along the cross sections of the vane channel. With constant velocity and total pressure in the narrow cross section of the channel both these conditions should begin simultaneously, with the same number M_1 . Let us determine value M_{1max} under this supposition. In this case, we will assume that in the narrow cross section, "throat," the flow is uniform and its direction does not depend on the angle of attack. According to the equation of continuity, we have

$$\lambda q(\lambda_1) \sin \beta_1 = \sigma_{ex} q(\lambda_1) f_r$$

Here $\sigma_{ex} = P_{0r}/P_{01}$ - pressure coefficient defining losses in total pressure in the inlet cross section up to the critical cross section whose width is f_r , and λ_r is the flow velocity coefficient. Assuming that $\lambda_r = 1$, from the equation of continuity we obtain the following expression for determining the maximum flow velocity ahead of the cascade:

$$q(\lambda_{1max}) = \sigma_{ex} \frac{f_r}{l \sin \beta_1}$$

For an isentropic flow ($\sigma_{ex} = 1$), we have

$$q(\lambda_{1max}) = \frac{f_r}{l \sin \beta_1}$$

From the last expression it is evident that when

$$\beta_1 \leq \arcsin \frac{f_r}{l} \text{ or } F_1 = l \sin \beta_1 \leq f_r$$

the velocity of a subsonic incident flow is unlimited, and for the examined case of subsonic flows $M_{1max} = 1$. The limitation on number M_1 in the absence of losses develops at large angles β_1 when the stream area F_1 which enters the vane channel exceeds the area of its critical cross section f_r . In this case an increase in angle β_1 , i.e., a decrease in the angle of attack, should lead to a decrease in number M_{1max} . The results of the experiment, given in Fig. 10.30, confirm this fact. The considerable limitation on number M_{1max} observed in the experiments, with large angles of attack when the area of the entering stream is less than that of the critical cross section of the vane channel is due, first of all, to the effect of losses.

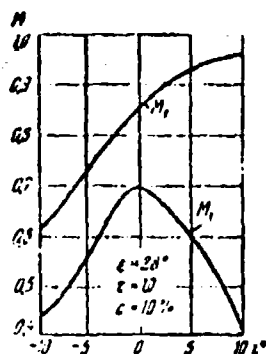


Fig. 10.30. Experimental dependence of $M_{1\text{ep}}$ and $M_{1\text{max}}$ on angle of attack α_1 for a typical diffuser cascade.

The simplest of the approximate methods for estimating the effect of compressibility during a subcritical flow is based on the hypothesis of "solidification" of the flow lines mentioned earlier, i.e., under the assumption that the flow lines in a compressible gas flow coincide with the flow lines of incompressible fluid.

For the airfoil cascade this, in particular, means that at fixed angle β_1 the flow direction behind the cascade should not depend on number $M_1 < M_{1\text{ep}}$. In other words, dependence $\beta_2(\beta_1)$ remains the same as with a flow of incompressible fluid around this cascade.

Under such assumption the effect of compressibility on the value, for example, of the circumferential force is connected only with a change in the axial gas velocity component behind the cascade. Depending on the nature of flow through the cascade, the axial velocity behind it either increases (convergent cascade) or decreases (diffuser cascade). In accordance with this, there is also a change in the flow twist value behind the cascade and, consequently, with a fixed flow twist value ahead of the cascade there is a change in value Δw_u , which is proportional to circumferential force R_u .

At subcritical velocities it is possible, just as in the case of a unitary profile, to replace the gas flow around the cascade with the flow of incompressible fluid around a certain equivalent cascade. Two methods of construction of an equivalent cascade are possible which are based on the analysis of the equations of gas dynamics.¹ In view of the simplicity of physical substantiation of these methods, let us describe them without resorting to the analysis of the equations. Let us first consider the simplest case - a cascade of symmetrical profiles with zero stagger and zero angle of attack. Treating each profile in the cascade as an isolated profile, i.e., increasing its transverse dimensions by $1/\sqrt{1-M_1^2}$ times we obtain an equivalent cascade of the same pitch t , but composed of profiles having a larger relative thickness:

$$c' = \frac{c}{\sqrt{1-M_1^2}}.$$

The same effect can be obtained by proceeding to a more close-spaced cascade without deforming the profiles, for which it is necessary to change the distance between the profiles, calculated in the direction of the normal to the incident flow, by $\sqrt{1-M_1^2}$.

In the case of symmetrical profiles with zero stagger and zero angle of attack, the same result is obtained by a corresponding change in the cascade pitch:

$$t' = t \sqrt{1-M_1^2}.$$

Both indicated methods for constructing an equivalent cascade are entirely equal in this case when the profile thickness is small in comparison with the cascade pitch. Let us note that the

¹Sedov L. I., Two-Dimensional Problems of Hydrodynamics and Aerodynamics. Gostekhizdat, 1950.

second method is more suitable for the analysis and calculations, because in it the profile itself remains unchanged. Let us now consider the streamlining of the cascade with asymmetric profiles and values of stagger and angle of attack which are different from zero, however, limiting ourselves to the case of thin profiles and small angles of attack. Let us introduce a new concept - *aerodynamic cascade pitch* h which is equal to the distance between two straight lines drawn through the corresponding points of the adjacent profiles parallel to the geometric half-sum (w_m) of the entrance and exit velocities. Applying the second method of construction, we obtain an equivalent cascade (Fig. 10.31) consisting of the same profiles but with a smaller aerodynamic pitch:

$$h' = h \sqrt{1 - M_m^2};$$

here value M_m is most simply calculated from the known transfer formula

$$M_m^2 = \frac{\frac{2}{k+1} \lambda_m^2}{1 - \frac{k-1}{k+1} \lambda_m^2},$$

where

$$\lambda_m = \frac{w_m}{a_{\infty}}, \quad a_{\infty} = \sqrt{\frac{2k}{k+1} gRT_{\infty}}.$$

A change in the aerodynamic pitch leads to a change in the geometric parameters of the cascade. Designating all parameters which pertain to the equivalent cascade in the flow of incompressible fluid by dashed lines, we find the following from triangles B_0B_1D and $B_0B_1'D$ (Fig. 10.31)

$$\lg(\psi' - \alpha_p) = \frac{B_1'D}{B_0'D} = \frac{h'}{B_0'D}, \quad \lg(\psi - \alpha_p) = \frac{B_1D}{B_0'D} = \frac{h}{B_0'D},$$

from which

$$\tan(\theta' - \alpha_p) = \frac{h}{h'} \tan(\theta - \alpha_p)$$

and, consequently

$$\tan(\theta' - \alpha_p) = \sqrt{1 - M_m^2} \tan(\theta - \alpha_p)$$

or

$$\tan(\theta' - \alpha_p) = \sqrt{1 - M_m^2} \tan \beta_m$$

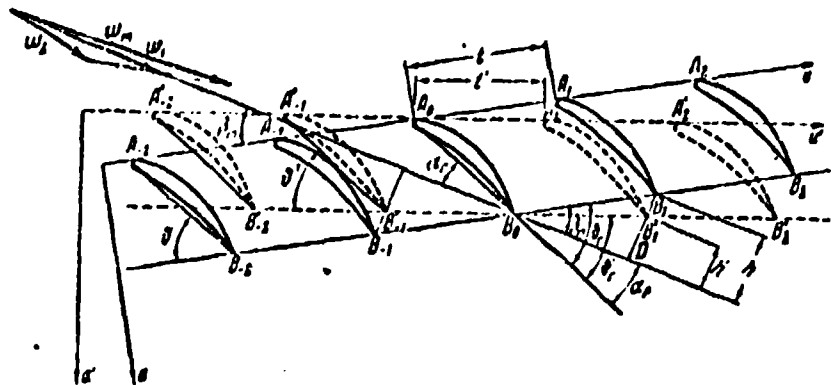


Fig. 10.31. The original airfoil cascade in gas and its equivalent cascade in an incompressible fluid.

Here β_m is the angle between the direction of velocity w_m and the front of the cascade. After determining from the last expression setting angle β' of the equivalent cascade, we find its pitch t' from the following obvious formula:

$$t' = \frac{h'}{h} t \frac{\sin(\theta - \alpha_p)}{\sin(\theta' - \alpha_p)}$$

after dividing both sides of this expression by the airfoil chord, which according to the condition of construction is unchanged, we obtain the denseness of the equivalent cascade:

$$\tau' = \tau \sqrt{1 - \sin^2 \beta_m M_m^2}$$

Knowing the geometric parameters of the equivalent cascade, we determine the angle of attack when it is streamlined by an incompressible fluid, at which the lift coefficient has the same value as in the original cascade, for which we use the relationship given above for the isolated profile:

$$\alpha' = \frac{\alpha}{\sqrt{1-M_\infty^2}}.$$

Based on linear dependence between the angle of attack and the lift coefficient, it is possible, just as in the case of a unitary profile, instead of calculating the change in the angle of attack when $c_y = \text{const}$ to determine the change in c_y when $\alpha = \text{const}$.

Let us now examine some results of the systematic experimental studies carried out by A. I. Bunimovich and A. A. Svyatogorov¹ on subsonic cascades over a wide range of change in numbers M_1 and the angles of attack.

With an increase in number M_1 the losses increase and the nonuniformity of flow behind the cascade increases accordingly. Therefore, when using the results of the experimental studies of cascades at large subsonic speeds one should consider even to a greater extent than with low speeds, the supplementary rotation of flow during its equalization, which leads to an increase in the angle of lag in the diffuser cascade when $\beta_2 < \pi/2$, i.e., to a decrease in the effective angle of deflection of flow by the cascade.

¹Bunimovich and Svyatogorov A. A., The Aerodynamic Characteristics of Two-Dimensional Compressor Cascades at High Subsonic Speed. In Coll. of "Bladed Machines and Jet Apparatuses," Iss. 2 "Mechanical Engineering," 1967.

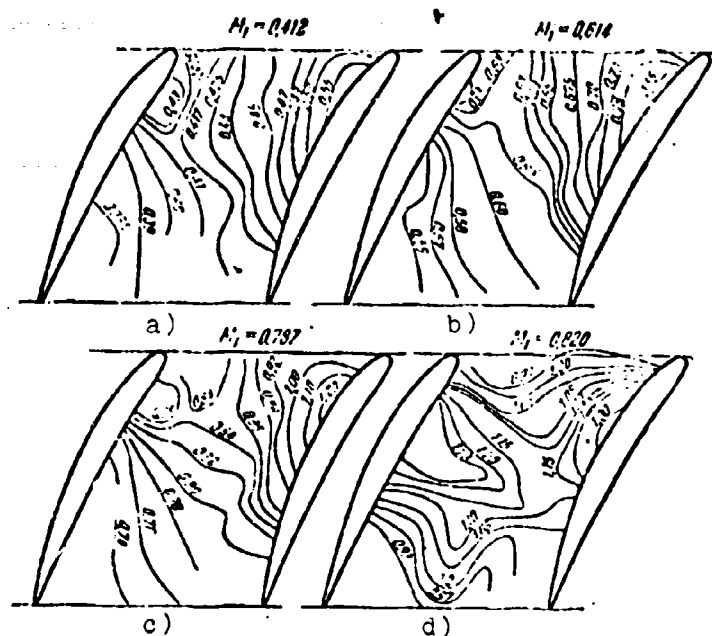


Fig. 10.32. Velocity distribution in the vane channels of the cascade with $b/t = 1.3$, $\delta = 62.6^\circ$ and $\epsilon = 27.6^\circ$ with the angle of attack $\alpha = 0$ and different numbers M_1 of the incident flow.

In the general case this supplementary rotation of flow can be found from equation (29), using the measured velocity distribution on the edge of the cascade; for the separation-free angles of attack it suffices to know the parameters of the boundary layer on the trailing edges of profiles.¹

Figure 10.32 shows the results of measured velocities in the cascade vane channel with a zero angle of attack. These data are presented in the form of curves of constant M numbers.

¹Refer to references on pages 690 and 691.

When $M_1 = 0.412$ the flow is essentially subsonic. Maximum value $M = 0.55$ occurs in a small zone on the upper profile surface near its leading edge. With an increase in the velocity up to $M_1 = 0.614$ the flow everywhere still remains subsonic; maximum Mach number in the zone of increased velocities does not exceed 0.9. A further increase in the velocity ($M_1 = 0.787$) leads to the appearance of a relatively noticeable area of supersonic speeds. Thus, for the examined cascade critical number M_{1kp} at this angle of attack is between the values of numbers $M_1 = 0.614$ and $M_1 = 0.787$. It is interesting to note that in the whole speed range examined the location of the lines of constant velocity values and, in particular, the location of the area of increased M numbers changes slightly despite the appearance of supersonic speeds with $M_1 = 0.787$.

The picture changes sharply when number M_1 of the incident flow becomes equal to 0.82. In this case the sonic line ($M = 1.0$) intersects the entire vane channel, settling in the inlet section. This means that the choking of cascade has occurred and number $M_1 = 0.82$ is the maximum Mach number of this cascade at the zero angle of attack; behind line $M = 1$ the flow is accelerated to values $M = 1.2-1.25$, then decelerates and, before it leaves the channel becomes subsonic. As a result, there is a subsonic flow with essentially uneven distribution of velocities behind the cascade, which, as this was already indicated above, leads to an increase in the angle of lag, i.e., to a decrease in the effective angle of deflection of the flow by the cascade.

With the choking of the cascade the Mach number reaches a maximum value and no longer determines unambiguously the magnitude of losses - the cascade characteristic becomes vertical ($d\zeta/dM_1 \rightarrow \infty$); also, the angle of deflection of the flow by the cascade is decreased (Fig. 10.33).

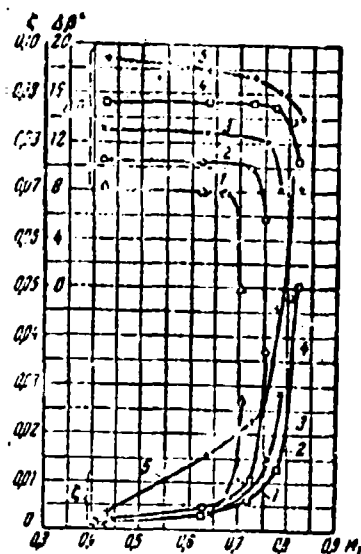


Fig. 10.34. The dependence of loss factor ξ and the angle of deflection $\Delta\beta$ of the flow on number M_1 at different angles of attack for a diffuser cascade ($\epsilon = 15^\circ$, $b/t = 1.3$, $\beta = 62.6^\circ$):
 1 - $i = -2.5^\circ$; 2 - $i = 0^\circ$;
 3 - $i = +2.5^\circ$; 4 - $i = +5^\circ$;
 5 - $i = +10^\circ$.

For this flow the pressure ratio behind the cascade to its value ahead of it p_2/p_1 becomes the determining parameter.

As the counterpressure decreases the acceleration of supersonic flow increases and, consequently, also the intensity of its deceleration, as a result of which, there is an increase in losses. The opposite phenomenon is observed with increased counterpressure.

The dependence of the loss factor in the cascade on the angle of attack at different M_1 numbers is constructed in Fig. 10.34. The angle-of-attack range in which the loss factor changes slightly depends on the M_1 number and decreases with an increase in the latter. With large M_1 numbers the curves of the loss factor dependence on the angle of attack are characterized by the presence of a clear minimum which corresponds to the maximum value of critical number M_{kp} . As shown by the analysis of the experimental data, at this angle of attack the stream area ahead of the cascade, necessary for one vane channel, is equal to that of the narrowest cross section of the vane channel.

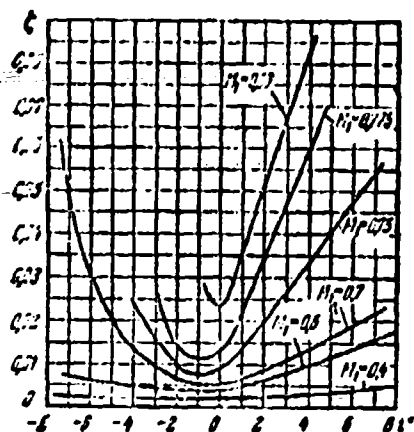


Fig. 10.34. The dependence of loss factor ξ on the angle of attack at various M_1 numbers for a diffuser cascade ($\epsilon = 27.6^\circ$, $b/t = 1.3$; $\delta = 62.6^\circ$).

We examined the results of the experimental study of the diffuser cascades used mainly in the axial-flow compressors.

As shown by the experiments, the convergent flow pattern in the cascades of axial-flow turbines permits one with a proper selection of the profile and cascade parameters to insure a continuous flow in a certain angle-of-attack range and, as a result, to obtain a smooth acceleration of the flow up to the speed of sound at the exit from the cascade.¹

§ 10. Streamlining of a Supersonic Airfoil Cascade by a Gas Flow with Supersonic Axial Velocity Component

During a supersonic streamlining of cascades composed of ordinary subsonic profile with rounded leading edges, a curvilinear shock wave is formed ahead of every profile (Fig. 10.35), behind which is a zone of subsonic speeds. However, further, the speed again increases so that supersonic speeds are obtained

¹See for example, Chapter VI.I in the preceding publication of this book. Gostekhteorizdat, M. 1953.

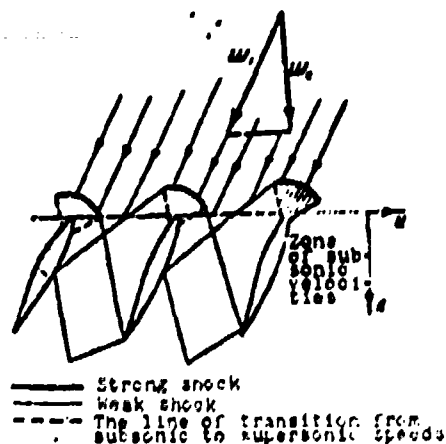


Fig. 10.35. Diagram of a supersonic flow around the airfoil cascade with a blunt leading edge.

almost everywhere on the profile surface. In a dense cascade the individual shock waves formed before every profile can merge into one shock wave of periodic nature. Shock waves lead to considerable losses. To avoid this, the cascades for supersonic flows are composed of supersonic profiles with a sharp leading edge which does not cause a curvilinear wave in the designed conditions of flow (Fig. 10.36).

In analyzing a supersonic streamlining of cascades, a distinction is made between the cases when the axial velocity component of incident flow w_{1a} is greater and less than the speed of sound.

When $w_{1a} > a_1$ the characteristics are directed inside the cascade, i.e., there is no interference between the cascade and incident flow (Fig. 10.38) and, therefore, it is sufficient to examine only the flow in the vane channels and in the immediate vicinity behind the cascade's edge.

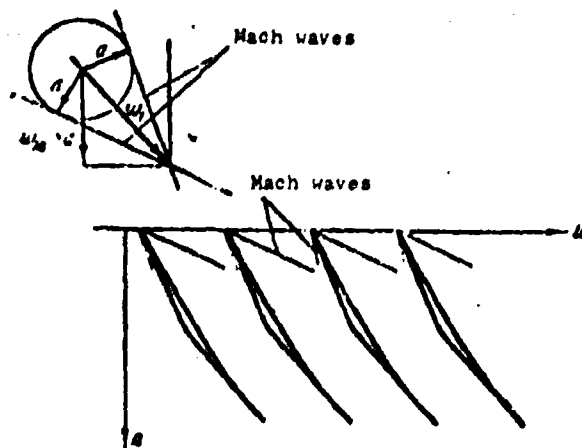


Fig. 10.36. Flow about a profile cascade with acute leading edge with supersonic axial velocity component.

These flows are defined not only by the parameters of the incident flow - by the M_1 number and by angle of attack α as this occurs, for example, during a subsonic streamlining of the cascades,¹ but also by the counterpressure, i.e., by pressure value p_2 in a cross section far beyond the cascade. The dimensionless value of pressure ratio $\epsilon = p_2/p_1$ ahead of and behind the cascade has a certain range of possible values, which depends for this cascade, on the parameters of the flow advancing onto it.

Minimum value ϵ_{\min} is determined by that minimum value of counterpressure $p_{2\min}$ at which the disturbances begin to affect the flow in the outlet section of the cascade's vane channels if this value is exceeded.

¹Excluding their choking conditions.

The maximum counterpressure (ϵ_{\max}) is determined by the achievement of that $p_{2\max}$ at which a further pressure increase leads to the disruption of the flow at an infinity ahead of the cascade.

Let us first examine the streamlining of cascades at small angles of attack, which are composed of slightly bent supersonic profiles.¹ In this case, as this has already been indicated in a similar statement of the problem in § 7, the disturbances introduced into the supersonic flow by the profile are weak, and therefore propagate only in the area limited by the characteristics - Mach waves from sharp leading edge (Fig. 10.20). In accordance with this the interference between the cascade profiles will be determined by its density. When the cascade density is less than or equal to critical density

$$\left(\frac{\rho}{\rho^*}\right)_{\text{c.p.}} = \frac{\sin [\theta - (\alpha + \beta)]}{\sin (\alpha + \beta)},$$

defined from the condition that the Mach wave leaving the leading edge of a given profile passes through the trailing edge of the adjacent profile (Fig. 10.37a), interference between profiles is absent - they are streamlined as though one. In this case interference between Mach waves from every profile begins only after the edge of the cascade (Fig. 10.37b). As a result of this interference the velocity field after the cascade up to infinity turns out to be periodic, not only along the front of the cascade, but also along the flow.

¹Keldysh V. V., Airfoil Cascades in Supersonic Flow. In the Collection of Theoretical Works on Aerodynamics. Oborongiz, 1957.

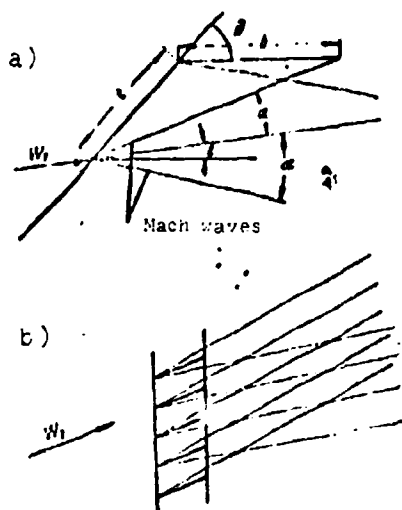


Fig. 10.37. Flow about cascades of thin weakly bent profiles with small angles of attack: a) in determining critical density; b) flow when $b/t < (b/t)_{cp}$.

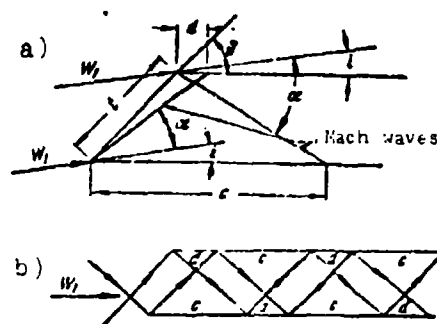


Fig. 10.38. Flow about cascades of thin weakly bent profiles at small angles of attack with density greater than critical: a) sections of profile in cascade outside zone of perturbation of adjacent profiles; b) reflection of Mach wave within profile cascade.

Thus, the velocity field after the cascade will be periodic in two ways.

When density exceeds critical density, only the sections of the profile (Fig. 10.38a)

$$\left. \begin{aligned} c &= l \sin \theta [\operatorname{ctg}(\alpha - \theta) + \operatorname{ctg} \theta] \\ d &= l \sin \theta [\operatorname{ctg}(\alpha + \theta) - \operatorname{ctg} \theta] \end{aligned} \right\} \quad (88)$$

adjacent to its leading edge are outside the zone of perturbation of adjacent profiles. In these sections the pressure will be the same as on an isolated profile, and therefore can be found from the formulas given in § 6. Pressure distribution in the remaining part of the profile will depend on the nature of the

consecutive reflections of Mach waves on the surfaces of two adjacent profiles (Fig. 10.38b). If one assumes that the reflection of Mach waves within the cascade proceeds not from the contour of the profile, but from its chord, then the number of reflections will be a certain equal to integer n , related to chord length and the quantities c and d by the condition.

$$b = (c + d)n + \Delta, \quad 0 \leq \Delta \leq c + d \quad (89)$$

or in dimensionless form

$$1 = (\bar{c} + \bar{d})n + \bar{\Delta}, \quad 0 \leq \bar{\Delta} \leq \bar{c} + \bar{d}. \quad (90)$$

If $\Delta = 0$, all Mach waves incident on a profile from undisturbed flow will reflect within the cascade $2n$ times (Fig. 10.38b); if $0 \leq \Delta \leq c + d$, the number of reflections of the different Mach waves within the cascade will change from $2n$ to $2(n + 1)$. The quantity Δ can be expressed also in the form (Fig. 10.39)

$$\Delta = d + \delta c = c + \delta d.$$

Utilizing relationships for linearized flow given in §§ 6 and 7, and after determining with the aid of the Mach waves pressure distribution over the profile, V. V. Keldysh used a series of simplifying transformations to obtain the following expression for the profile lift coefficient:

$$C_L = \frac{4\pi}{1 - M_\infty^2} A, \quad (91)$$

where the coefficient A , depending on Δ , has the following values:

$$\Delta \leq d; \quad A = A_1 = i\bar{\Delta} + \sum_{n=1}^{\infty} \left(\int_{a_n} y_{1n} dx + \int_{c_n} y_{2n} dx \right), \quad (92)$$

$$d \leq \Delta \leq c, \quad A = A_1 = ld - \int_{d_{n+1}} y_{11} dx + \sum_{i=1}^n \left(\int_{d_{2i}} y_{11} dx - \int_{d_{2i-1}} y_{11} dx \right) \quad (93)$$

$$c \leq \Delta \leq c + d, \quad A = A_2 = \\ = l(c + d - \Delta) + \int_0^d y_{11} dx + \int_0^c y_{11} dx + \sum_{i=1}^n \left(\int_{d_{2i}} y_{11} dx + \int_{d_{2i}} y_{11} dx \right) \quad (94)$$

The integrals \int_{c_i} and \int_{d_i} are taken respectively over intervals c and d . The index "i" indicates the order of the interval, assuming that the profile chord is broken (beginning from the trailing edge) into intervals whose lengths are in turn c and d , while for the upper contour the length of the first interval is equal to d , and for the lower c (Fig. 10.39).

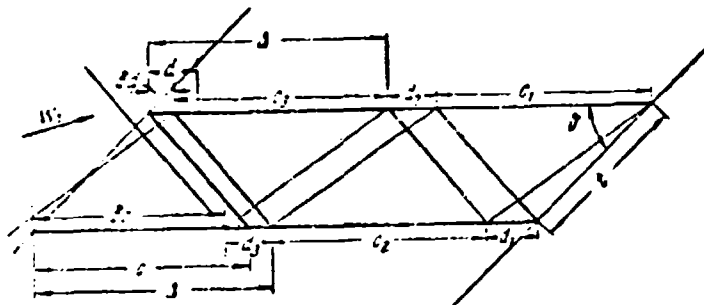


Fig. 10.39. Used in constructing the reflections of Mach waves.

From the above formulas it may be concluded that, unlike an isolated profile, the profile lift coefficient in the cascade depends on its form. The effect of the cascade weakens in proportion to the decrease in density, i.e., in proportion to the decrease in the number of reflections.

When $n = 0$, according to (92) we have $A = 1_2$, and therefore, the expression for c_y no longer depends on the form of the

profile and completely coincides with formula (79), obtained in § 7 for an isolated profile. This agrees also with the fact that when $n = 0$ profile chord $b \leq d$, i.e., the cascade density proves to be less than critical, and therefore there is no interaction of profiles in the cascade - they are streamlined as isolated (Fig. 10.37b).

For a plate $y' = 0$ and according to (92), (93) and (94) for cascades of plates

$$A_1 = \Delta t \quad A_2 = dt \quad A_3 = (c + d - \Delta)t. \quad (95)$$

Thus, at a given number M_1 and angle of attack i the interference of plates in the cascade always leads to a decrease in the lift coefficient in comparison with its value for an isolated plate (79). A similar conclusion can be made also for the drag coefficient, since for a plate (see page 677)

$$c_x = c_y \lg l.$$

The power effect of the profile cascade on the flow is determined by the size of the product $c_y b/t$. For a cascade of plates in accordance with (95) we have

$$\left. \begin{array}{ll} \text{with } \Delta \leq d & c_y b/t = \frac{\Delta}{t} l, \\ \text{with } d \leq \Delta \leq c & c_y b/t = \frac{d}{t} l, \\ \text{with } c \leq \Delta \leq c + d & c_y b/t = (c + d - \Delta) \frac{l}{t}. \end{array} \right\} \quad (96)$$

Here, unlike the usual dense subsonic cascades, the value of the product $c_y b/t$ already remains constant, and is strictly a periodic function of density with period $T = c + d$. In this case in accordance with (88) the maximum value of the product $c_y b/t$ composes

$$(c_y b/t)_{\max} = \frac{4l}{\sqrt{M_1^2 - 1}} (1 - M_1^2 \sin^2 \theta - \cos \theta).$$

Similar values for cascades composed of rhombs and isosceles triangles are respectively equal to

$$c_y \left(\frac{b}{t} \right)_{\max} = \frac{4(1+\varepsilon)}{1-M_1^2-1} (1-M_1^2-1 \sin \theta - \cos \theta),$$

$$c_x \left(\frac{b}{t} \right)_{\max} = \frac{4(1+\varepsilon)}{1-M_1^2-1} (1-M_1^2-1 \sin \theta - \cos \theta).$$

In these formulas the quantity c , as before, is the relative thickness of the profile. According to (96) the minimum value of $c_y b/t$ for a cascade of plates is zero when $\Delta = 0$, i.e., when $b = n(c + d)$. In this case (see Fig. 10.39) as a result of the mutual interference of plates there is no overall power effect of flow on the cascade.

Let us recall that all the above conclusions are obtained by means of linearization of the equations of flow, and therefore are valid only with slight disturbances.

The application of a known graphoanalytical method¹ makes it possible to forego the aforementioned assumptions of smallness of the perturbations, and to solve the problem of flow about an arbitrary cascade of supersonic profiles (with $M_{1a} > 1$) for any angles by means of consecutive construction of flow in vane channels and in the space after the edge of the cascade. In this case the flow in vane channels and, consequently, also the profile pressure distribution are determined not only by the parameters of the incident flow, but also by the assigned level of counter pressure. Thus, for this cascade we can obtain the dependence of resultant on p_2/p_1 at different fixed values of M_1 and angle of attack i . However, such a method is generally very bulky, and impedes obtaining general conclusions.

¹Kochin N. Ye., Kibel' I. A. and Rose N. V., Theoretical Hydromechanics, Pt. II. OGIZ, M., 1948.

Let us show possible systems of flow about cascades in the presence of strong perturbations in the example of cascades composed of the simplest supersonic profiles - flat plates. Let us pause first at flow about such a cascade at zero angle of attack.

If the axial component of the velocity of flow incident on a cascade of plates at zero angle of attack is more than or equal to the speed of sound, then with a decrease in the pressure after the cascade, in comparison with its value before it, there is no power effect of flow on the plate. This is connected with the fact that when $M_{1a} = M_1 \sin \alpha \geq 1.0$, the characteristic at the exit either coincides with the front (when $M_{1a} = 1.0$) or goes beyond the limits of the cascade (when $M_{1a} > 1.0$), and therefore any decrease in pressure p_2 in comparison with p_1 has no effect on pressure distribution over the plate.

With a pressure increase after the cascade to a certain value of p_{2min} , the power effect is also absent. The corresponding values of p_{2min} and ϵ_{min} are determined from the condition of formation of an oblique shock wave on the edge of the cascade (Fig. 10.40a). In this case the angle of lag is positive and equal to the angle of rotation of flow in the oblique shock.

With a further increase in the pressure, i.e., $p_2 > p_{2min}$ or $\epsilon > \epsilon_{min}$, the front of the oblique shock passes above the front of the cascade, and this leads to redistribution of pressure in section CB of the lower surface, which adjoins the trailing edge of the plate (Fig. 10.40b). Consequently, in this case there is a power effect of flow on the plate. The resultant of pressure forces is directed toward the positive direction of the n -axis. In proportion to the throttling, i.e., in proportion to the increase in pressure p_2 , point C moves upstream and the power effect increases; angle of lag δ and angle of rotation of

flow in the oblique shock decrease and the oblique shock becomes close to a forward shock.

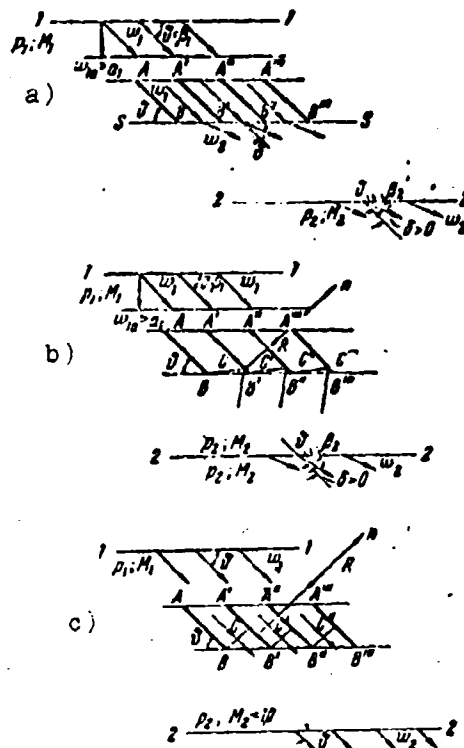


Fig. 10.40. Flow around cascade of plates by a flow with supersonic axial velocity component at zero angle of attack and different values of pressure p_2 after the cascade: a) at pressure p_2 equal to pressure after oblique shock; b) at large pressure; c) at maximum pressure p_2 equal to pressure after normal shock.

At a certain value $p_2 = p_{2\max}$ the shock becomes a forward shock, and directly after the cascade there is a uniform subsonic flow¹ (Fig. 10.40c), directed over the plate, i.e., with zero angle of lag; a further increase in the counterpressure (in comparison with the normal shock) turns out to be impossible, i.e., the flow becomes unstable and the normal shock, moving upstream, makes the given flow impossible at infinity before the cascade. Thus, the value of ϵ which corresponds to a normal shock is maximally possible, corresponding to a system of maximum throttling of a cascade with the preassigned M_1 number.

At positive angles of attack at the upper surface near the leading point of profile A appears a Prandtl-Meyer flow, in which part of the flow which encounters this vane channel is turned through an angle equal to the angle of attack α (Fig. 10.41a). The direction of the remaining part of the flow changes through the same angle in the oblique shock, going from the leading edge in the lower surface of the blade.

The corresponding picture is observed with negative angles of attack (Fig. 10.41b). In both cases the flow above broken line A'C'A", composed of a section of the front of the oblique shock and a section of the characteristic of incident flow, remains undisturbed and uniform. This position is not retained, however, at all angles of attack.

If the positive angle of attack becomes so large that it exceeds the maximum angle of flow rotation in the oblique shock wave for a given M_1 , then before the cascade appears a curvilinear shock wave.

¹Remember that this examination is being carried out with the simplifying assumption of no viscosity forces. In real flow as a result of interaction between shock and wall boundary layer of the vane channel (with sufficient pressure increase in shock) separation develops and flow after the cascade becomes nonuniform.

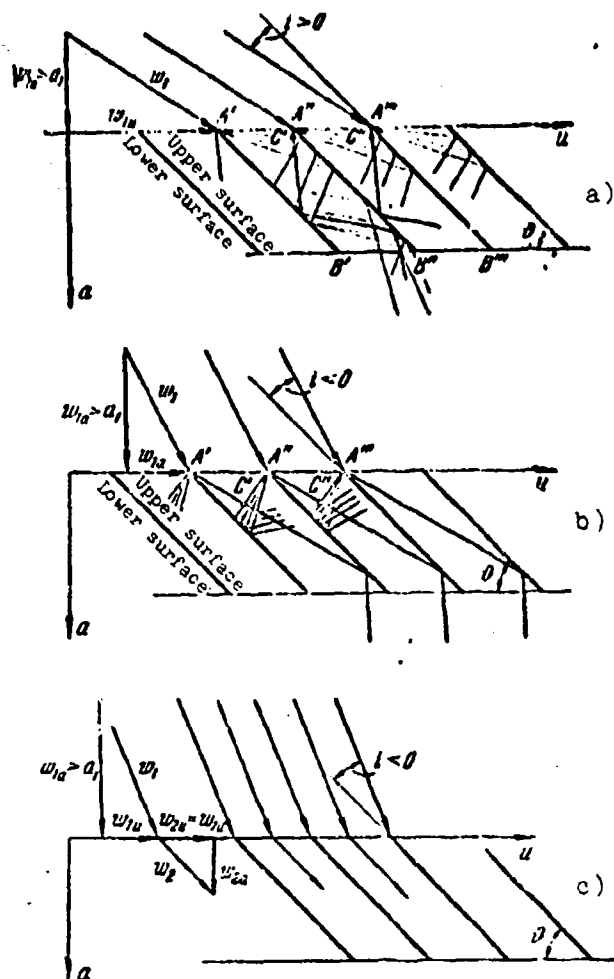


Fig. 10.41. Flow around a cascade of plates by a flow with supersonic axial velocity component at different angles of attack: a) positive angles of attack; b) negative angles of attack; c) negative angles of attack; front of oblique shock coincides with the front of a cascade.

With an increase in negative angle of attack characteristics A''C' recede from the front of the cascade, the plane of the oblique shock approaches it, and at a certain angle of attack

the front of the oblique shock coincides with the front of the cascade (Fig. 10.41c). In this case at the entry to vane channel flow is steady. The absolute value of angle of attack $|i_{\alpha}|$ at which for the assigned values of M_1 and set cascade angle θ an oblique shock develops, which coincides with the front of the cascade, is determined from the following obvious relationship:

$$\gamma - i_{\alpha} = 0.$$

Here γ is the angle between the plane of the oblique shock and the direction of flow onto a plane wedge with vertex angle $\theta = |i_{\alpha}|$.

It is known that when $M_1 = \text{const}$, the dependence $v(\gamma)$ is ambiguous; however, only the first value is usually realized which corresponds to a smaller increase in the static pressure in the shock. In this case in almost all the range of possible values, the velocity after the shock turns out to be supersonic (Fig. 10.42). Only in the area of large angles of setting is velocity after an oblique shock subsonic. This is an example of realization of the second branch of the $v(\gamma)$ dependence, which corresponds to a larger increase in the static pressure. It is interesting to note that when $M \geq 2$ in the small area of the angles of setting close to $|i_{\alpha}|_{\min}$, and with given M_1 and θ there are two values of the angle of attack and pressure drop at which the plane of the oblique shock coincides with the front of the cascade.

The above cases of flow about a cascade of plates at non zero angles of attack occur at minimum counterpressure, when within the vane channels and in the space after the cascade flow is supersonic.

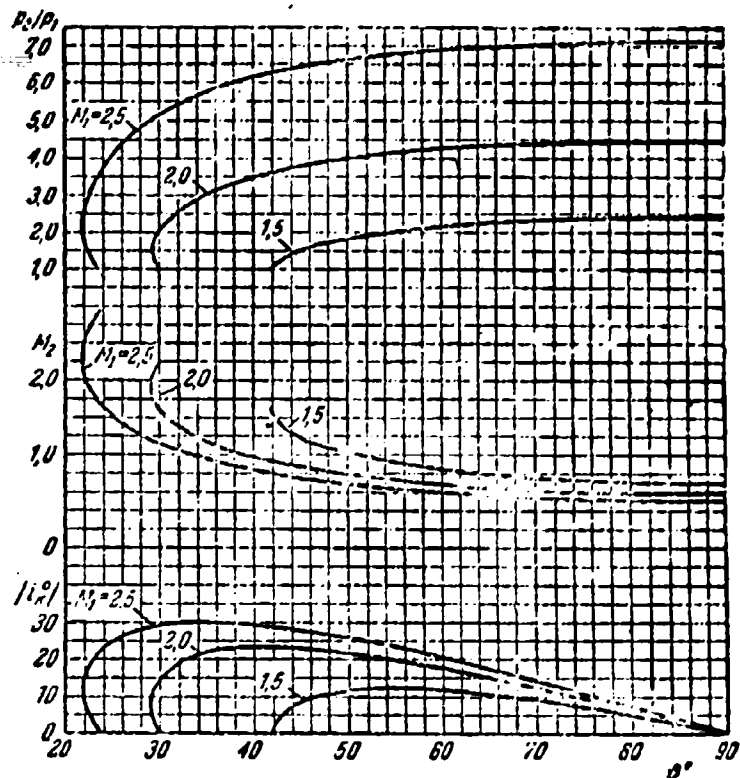


Fig. 10.42. Flow parameters before and after cascade of flat plates as a function of the angle of setting when an oblique shock arises along the front of the cascade.

With a pressure increase after the cascade the calculated flow picture in the exit part of the vane channel begins to be destroyed - an area of subsonic flows appears, and pressure distribution over the surface of the plate changes, which changes the value of the resultant force on the plate. With an increase in throttling, the area of subsonic flows increases, moving upstream. At a certain value of p_2 disturbances begin to go beyond the front of the cascade. With a further pressure increase, although there is subsequent rearrangement of the flow directly before the cascade, the flow at infinity before it still remains

undisturbed. Finally, at certain pressure p_2' disturbances begin to propagate throughout the entire flow area. This is the maximum pressure at which the assigned supersonic flow at infinity before the cascade is still possible.

Let us now move on directly to determining the power effect of supersonic flow on a cascade.

If we are limited only to searching for the magnitude of the resultant, then such a problem for cascades of plates when $M_{\infty} \geq 1$ has a simple solution in any parameters of incident flow and assigned counterpressure. To solve this problem it is sufficient to determine¹ the parameters of steady flow far beyond the cascade in terms of known values of M_1 , i and $\epsilon = p_2/p_1$.

In this case it is assumed that the viscosity effect during flow about the cascade proper is negligibly small, and accordingly friction on the plates can be taken as zero. The viscosity effect begins to be pronounced only after the cascade, where turbulent mixing makes the flow completely balanced. The balancing of the flow leads to added losses (in comparison with the losses appearing during flow about cascade by an inviscid flow of gas); however, it does not affect the flow about the cascade itself and, consequently also the power effect of the flow. The presence of added losses affects only the value of the static pressure of the balanced flow p_2 in the cross section far beyond the cascade. The value of the resultant force applied to the profile in this case will not change.

¹See reference on page 726.

The zero friction on plate is identical to zero tangential component of the resultant force

$$R_t = R_n \sin \theta - R_o \cos \theta = 0,$$

which, taking into account expressions (42) and (48) can be written in the form

$$\frac{b}{l} \epsilon_1 = -\frac{R_t}{\rho_1 \frac{\omega}{2} l} = 2 \left[\cos i - \frac{\lambda_2}{\lambda_1} \cos i \right] \sin (\theta - \eta) - \frac{m}{\lambda_1} \left[\frac{\sin (\theta - \eta)}{y(\lambda_2)} - \frac{\sin \theta}{y(\lambda_1)} \right] = 0. \quad (97)$$

This expression is a supplementary equation, which makes it possible as will be shown later, to close the system of equations for a cascade of plates, to determine the parameters of the balanced flow far beyond it and, in the last analysis, to find the value of the resultant force on the profile.

Using the gas-dynamic functions (see Chapter V), we have

$$\epsilon = \frac{p_1}{p_2} = \frac{p_{12}}{p_{21}} \frac{p_1}{p_2} = \epsilon \frac{\pi(\lambda_2)}{\pi(\lambda_1)}.$$

The continuity condition (44) gives

$$\frac{q(\lambda_1)}{\pi(\lambda_1)} \sin \beta_1 = \epsilon \frac{q(\lambda_2)}{\pi(\lambda_2)} \sin \beta_2 \quad (98)$$

or

$$y(\lambda_1) \sin (\theta - \delta) = \frac{y(\lambda_2) \sin (\theta - \eta)}{\epsilon}. \quad (99)$$

After substituting in (99) the expressions for $y(\lambda_2)$, we will obtain

$$\frac{k-1}{k+1} \lambda_2^2 d + \lambda_2 \sin (\theta - \delta) - d = 0, \quad (100)$$

$$d = \frac{y(\lambda_1) \sin(\theta - \delta)}{\left(\frac{k+1}{2}\right)^{\frac{1}{k-1}}}. \quad (101)$$

In accordance with this the condition of zero tangential force component is written as follows:

$$\lambda_2 \cos \delta = \lambda_1 \cos \delta - \frac{\sin \theta}{2 \sin(\delta - \theta)} \frac{m}{y(\lambda_1)} [e - 1] \quad (102)$$

or

$$\lambda_2 \cos \delta = e, \quad (103)$$

where the e designates the right side of expression (102), which can be determined by assigned quantities λ , i , a and θ .

Eliminating λ_2 from (102) and (103), we obtain a quadratic equation relative to the tangent of the angle of lag δ

$$\text{tg}^2 \delta - 2b \text{tg} \delta + c = 0. \quad (104)$$

Here

$$b = \frac{k+1}{2(k-1)} \frac{\cos \theta}{ed}, \quad c = 1 + \frac{k+1}{k-1} \frac{\sin \theta}{ed} - \frac{k+1}{k-1} \frac{1}{e^2}.$$

In the case of zero angle of attack

$$b = \frac{k+1}{k-1} \left(\frac{k+1}{2}\right)^{\frac{1}{k-1}} \frac{1}{2[y(\lambda_1) - m(e-1)]}$$

and

$$c = 1 + \frac{2b}{\text{tg} \theta} - \frac{k+1}{k-1} \frac{4[y(\lambda_1)]^2}{[2y(\lambda_1) - m(e-1)]}.$$

If, furthermore, we assume $\lambda_1 = 1$, then

$$b = \frac{2k}{k-1} \frac{\epsilon \cot \theta}{1-\epsilon},$$

$$c = 1 + \frac{2k}{k-1} \frac{\epsilon}{1+\frac{\epsilon}{k-1}} - \frac{k+1}{k-1} \frac{k^2}{(1+\frac{\epsilon}{k-1})^2},$$

and equation (104) matches the equation obtained previously by G. Yu. Stepanov.

This, the dependence of the power effect of a flow with supersonic axial velocity component on the pressure drop can be determined, if for each series of arbitrarily assigned values of ϵ we use (104) and (100) to find the appropriate values of the angle of lag θ and the velocity coefficient of the flow λ_2 far beyond the cascade. Since the resultant of forces on the plate is directed along the normal to it

$$R = R_n = \frac{R_a}{\sin \theta}, \quad (105)$$

and, according to (42), the coefficient of the resultant force is written thus:

$$\frac{b}{\epsilon} c_n = \frac{Rb/\epsilon}{\rho_1 \frac{u_1}{2} b} = 2 \frac{\sin(\theta - \theta_1)}{\sin \theta} \left[\cos(\theta - \theta_1) - \frac{\lambda_1}{\lambda_2} \cos(\theta - \theta_2) \right]. \quad (106)$$

The problem of determining the range of the possible values of pressure drop at which the flow in question can be realized is very important. The minimum value of ϵ is determined from the condition that the axial flow velocity after the cascade reaches the speed of sound, i.e., $M_{2a} = 1$. With a further decrease of ϵ flow is impossible, since it requires the formation of expansion shocks.¹ In accordance with this ϵ_{\min} is characterized by minimum value of losses (i.e., $d\sigma/d\epsilon = 0$).

One feature is the case of zero angle of attack. In this case the value ϵ_{\min} is determined from the condition that the

¹Stepanov G. Yu., The Hydrodynamics of Turbomachines. Fizmatgiz, 1962.

counterpressure reaches a level at which in a section of the cascade an oblique shock develops, directed along the front of the cascade.

The greatest difficulties appear during the determining of maximally possible counterpressure. As has already been indicated, in the case of zero angle of attack the maximum value of ϵ corresponds to such pressure after the cascade at which a normal shock appears in its vane channels. In this case the losses become greatest, which means that in this limit case $d\sigma/d\epsilon = 0$.

A further pressure increase is impossible: the shock moves upstream and disrupts flow at infinity.

The value ϵ_{\max} in the general case of flow is determined by analogy with zero angle of attack from the condition of minimum value of the coefficient σ ($d\sigma/d\epsilon = 0$). As calculations show, such limit conditions of counterpressure when $i \neq 0$ correspond to zero angle of lag and to the presence of a normal shock in the exit section of the cascade vane channel.

Thus, the range of possible values of ϵ for this cascade of plates at fixed values of M_1 and angle of attack i , can be defined as the interval between the two extrema of the $\sigma(\epsilon)$ dependence.

As an example Fig. 10.43 gives the dependence of the coefficients of the resultant force and flow parameters after a cascade of plates on ϵ with supersonic streamlining under positive angle of attack. Here the limit values of the resultant were determined at the points of the extreme value of the total pressure loss. Minimum losses correspond to axial velocity after cascade being equal to the speed of sound, and the maximum losses correspond to the presence of a normal shock within the vane channel.

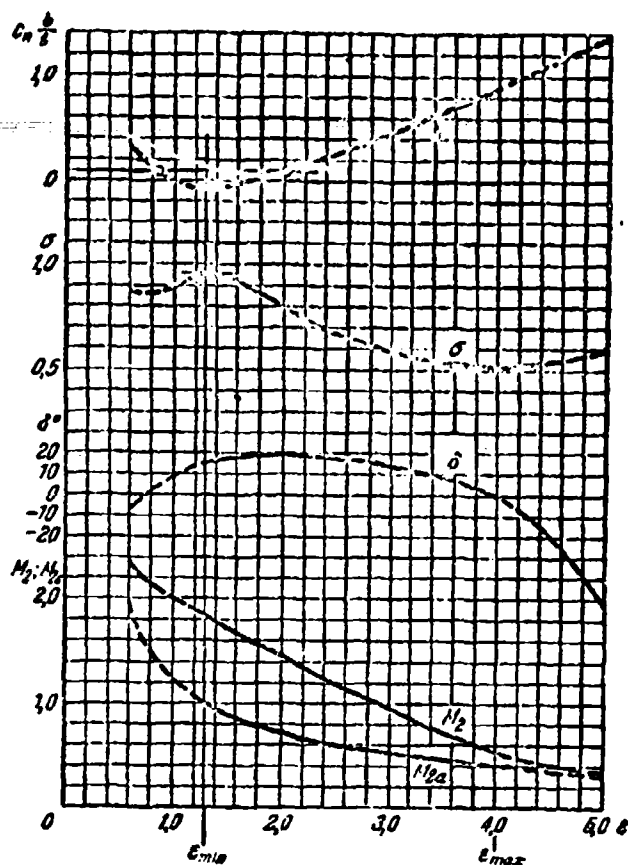


Fig. 10.43. Coefficient of resultant force and flow parameters after a cascade of plates as a function of $\epsilon = p_2/p_1$ when $\beta = 45^\circ$, $\alpha = 9^\circ$ and $M_1 = 2.0$.

All the above cases of a flow around a cascade of plates with supersonic axial velocity component are possible only beginning with a specific critical density. For example, flow at zero angle of attack with a normal shock (Fig. 10.40c) is possible only when $b/t \geq \cos \beta$. In this case the critical density does not depend on M_1 , and is numerically equal to $\cos \beta$.

At positive angle of attack the critical density, as has already been indicated above, is determined by the intersection of the Mach wave from the leading edge with the adjacent profile (Fig. 10.37a). Analogously, at negative angles of attack the critical density is determined by the point of intersection with the adjacent profile front of an oblique shock.

When density is less than critical (widely-spaced cascade), the interference of the flow between profiles disappears, and they are streamlined as a unit. In accordance with this the coefficient of the resultant force on a plate in widely-spaced cascade with angles of attack $i \leq 15^\circ$ according to (79) and (80) is determined by the expression

$$c_n = 4i \sqrt{\frac{1+i^2}{M_1^2 - 1}}.$$

Interference between the Mach waves and shock waves appears in this case only after the cascade (Fig. 10.44). The velocity coefficient λ_2 and the angle of lag δ can be found from the joint solution of equations (97) and (106). The total pressure after the cascade will be determined from the equation of continuity, and the static pressure will be determined from the Bernoulli equation.¹

§ 11. Flow Around a Cascade of Supersonic Profiles by an Inviscid Flow of Gas with Subsonic Axial Velocity Component

Let us first deal with a supersonic flow about cascades with subsonic axial velocity component. If at fixed M_1 we decrease the axial component of the approach stream velocity, the

¹In certain cases it can seem that no solution exists. This means that such conditions of flow about cascades of plates of subcritical density are unrealizable under the condition of total balancing of the flow after them.

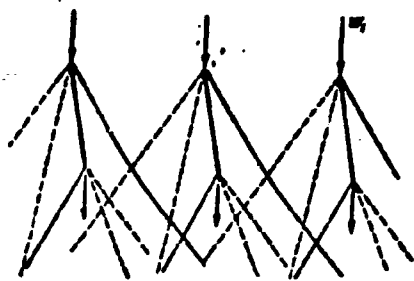


Fig. 10.44. The case of supersonic flow about a cascade of plates ($M_1 = 2.6$; $i = 10^\circ$), when interference between the waves from each profile begins after the cascade edge. The dotted lines are the Mach waves and the solid lines are shocks.

characteristic direction will approach the direction of the front of the cascade and when $M_{1a} = 1$ both directions will coincide. When $w_{1a} < a_1$, the characteristics are directed above the front of the cascade, and in this case, just as during subsonic flow around a cascade, there is interference between the incoming supersonic flow and the cascade. The disturbances from the leading edges of plates and the disturbances created after cascade propagate upstream. Pressure after the cascade no longer can be an assigned parameter: it unambiguously depends on the number M_1 and the incidence of the flow incoming to the cascade. Thus, in spite of the supersonic speed at infinity, such flow about a cascade in a sense is analogously subsonic.

An exception is the case of flow about the cascades of plates at zero angle of attack, in which the flow direction coincides with the direction of the plates. In this case disturbances before a cascade of infinitely thin plates are absent, and in the intake part of the vane channels is a uniform supersonic flow, which prevents (independently of the amount of axial velocity), the spread of disturbances after a cascade to the flow region before it.

Note that the examined property of flow about cascades of thin plates at zero angle of attack extends also to the case of cascades of infinitely thin bent profiles composed of a rectilinear section of sufficient length l and coupled small arc

(Fig. 10.45). The minimum length of rectilinear section is determined by the requirement that the Mach wave which propagates from the coupling point does not go beyond the front of the cascade. With nonobservance of this condition the weak disturbances caused by flow around the coupled arc will disturb the uniformity of the flow before the cascade.

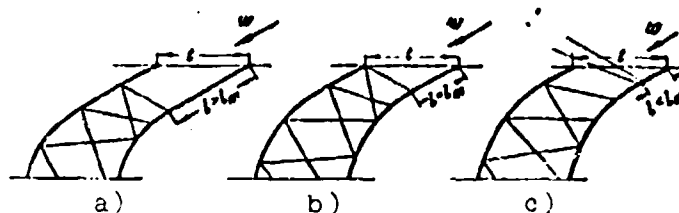


Fig. 10.45. In determining minimum length of a rectilinear section of an infinitely thin cascade profile in which there are no disturbances before it ($i = 0$).

In further examination we are restricted only to a cascade of plates.¹ In accordance with what has been said above, the flow about such a cascade at zero angle of attack becomes ambiguous, and is also determined by (besides the number M_1 of the incident flow) the quantity $\epsilon = p_2/p_1$, i.e., by the pressure ratio at infinity before the cascade and after it. In the case of equal pressures ($\epsilon = 1.0$) the flow passes through a cascade of plates undisturbed, and the power effect on the cascade naturally is absent.

When the axial component of the approach stream velocity is less than the speed of sound ($M_{1a} < 1$), any breakdown of the condition $\epsilon = 1$ leads to a power effect of flow on the cascade

¹See Ginsburg S. I., Total Power Effect of a Flow of Gas on a Cascade of Plates. In Coll. "Strength and Dynamics of Aircraft Engines," No. 3, "Mechanical Engineering," 1, 1966.

of plates. If $\epsilon < 1$, i.e., if pressure after the cascade is less than before it, then at the exit from the vane channel flow is formed with expansion near the trailing edge B of the plate (Fig. 10.46), i.e., flow accelerates with simultaneous rotation toward greater angles. As a result, the angle of lag of flow far beyond the cascade becomes negative.

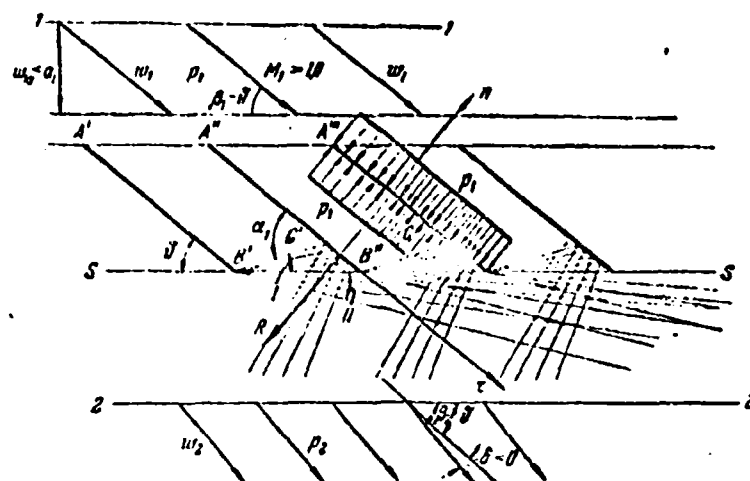


Fig. 10.46. Flow about a cascade of plates by supersonic flow with subsonic axial component velocity component at zero angle of attack and $p_2 < p_1$.

In the entire area of flow above the characteristic B'C' inclined toward the plate at an angle $\alpha_1 = \arcsin 1/M_1$ the flow remains undisturbed. This means that over the entire upper surface of the plate and over part of its lower surface A"C', the pressure is the same as in incident flow p_1 . A change in pressure distribution will be observed only in the section of plate C'B", where there is reflection of characteristics. On this section rarefaction dominates and therefore the resultant is always directed opposite to the positive direction of axis n. The value of the resultant depends on M_1 , the length of section C'B" and the degree of rarefaction ϵ . It is obvious

that with fixed values of the first two quantities the resultant increases with a decrease of ϵ . At a certain value of ϵ the axial velocity far beyond the cascade reaches the speed of sound, and characteristic becomes parallel to the front of the cascade. In this case the disturbances at infinity after the cascade do not spread upstream. With an increase of pressure after the cascade ($\epsilon > 1$) in the outlet part of the vane channel a system of shocks is formed, which leads to a pressure increase on the lower surface and the development of a force which acts in the positive direction of the n -axis. With an increase of p_2 this force increases, and the angle of lag decreases. At a certain value of $p_2 = p_{2\max}$ and respectively $\epsilon = \epsilon_{\max}$ in the vane channel a normal shock is formed, and at the exit from the cascade a subsonic flow with zero angle of lag is established (Fig. 10.40).

As an example Fig. 10.47 gives the dependence of $c_n b/t$ on ϵ with different Mach numbers of the supersonic flow on a cascade of plates ($\beta = 30^\circ$) at zero angle of attack.

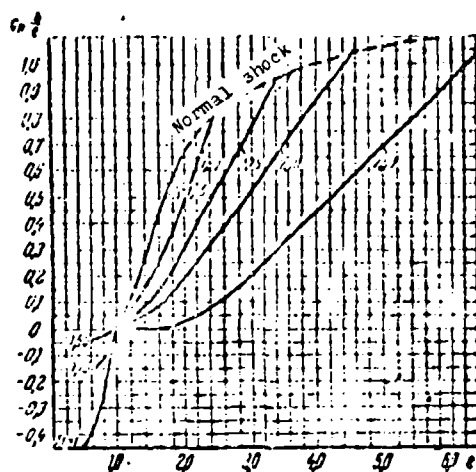


Fig. 10.47. Dependence of the coefficient of resultant force for a cascade of plates on $\epsilon = p_2/p_1$ ($\beta = 30^\circ$, $i = 0$).

At $M_1 < 2.0$ the quantity $M_{1a} < 1$ and respectively the power effect of the flow exists both with an increase and a decrease after the cascade. When $M_1 = 2.0$, the axial components of the

approach stream velocity becomes equal to the speed of sound, and in accordance with this the power effect of the flow when $M_1 \geq 2.0$ appears only with a pressure increase after the cascade. The limit values of the resultant force with this M_1 number were determined respectively either from the condition of formation of a normal shock, or from the condition of axial velocity after the cascade being equal to the speed of sound.

At positive angles of attack before a cascade, as indicated by G. I. Taganov and experimentally confirmed by L. A. Suslennikov (see § 14), a system of disconnected shock waves is formed (Fig. 10.48). Near the leading edge of every plate appears Prandtl-Meyer flow, in which the flow is accelerated from the speed of sound to a certain supersonic speed which exceeds the velocity at infinity before the cascade. Rarefaction waves from the leading edge are incident on adjacent shock waves, and weaken them; however, near a plate shock waves retain considerable intensity.

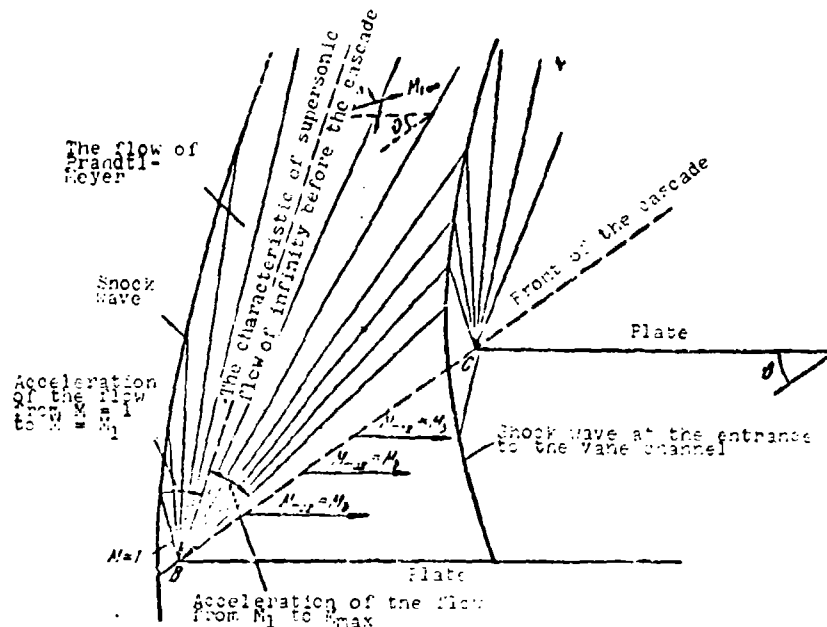


Fig. 10.48. Diagram of flow around a dense cascade of flat plates by a supersonic flow with subsonic axial velocity component ($i < 0$).

From tables for Prandtl-Meyer flow it is possible to find the necessary value of the angle of rotation of the flow to accelerate it from $M = 1.0$ to the value of M at infinity before the cascade. This angle determines the direction of flow at sonic speed around the leading edges of the plates. The maximum speed to which flow is accelerated is determined in this case by the angle of its rotation with assigned direction at infinity before the direction of the plates. This angle is equal to the angle of attack.

Thus, supersonic flow before hitting the vane channel passes through an infinite system of shock waves with gradually increasing intensity; in the area between adjacent shock waves the flow accelerates to ever higher speeds (with approach to the front of the cascade). Before the section of shock wave at the entry to the vane channel flow moves forward with Mach number, equal to M_{max} . In this section there is the most intense deceleration of the flow as a result of which at the vane channel exit subsonic flow develops. In this case the amount of total pressure losses in the different elementary streams which passed through the system of shock waves will be different, since the intensity of waves drops off from left to right. Consequently, in the examined streamlining of a cascade by an ideal inviscid gas flow in the vane channel section sufficiently removed from the inlet, where static pressure, and, therefore, also the direction of the velocity are already constant along its width, the velocity will remain variable. For the purpose of simplification of the problem we will assume that, as a result of a turbulent exchange between streams, the flow within the vane channels is completely equalized and in accordance with this a uniform, with respect to pitch, flow with constant static and total pressures is stabilized behind the cascade; moreover, the direction of this flow coincides with the direction of the plates (angle of lag α is equal to zero). It is important to note that the

assumption about the equalization of the flow in the vane channels made here differs significantly from that made in the preceding paragraph concerning the equalization of the flow in the cross section far beyond the cascade. In this last case we only somewhat overstate the losses in comparison with those which occur in an inviscid gas flow, leaving the flow as invariable in the cascade itself, and, consequently, the power effect of flow on it also as invariable. We have another matter when equalizing the flow in the blade channels, where as a result of the flow change in the cascade itself, there is not only an increase in losses but also a change in the value of the resultant as compared with its value in an ideal, inviscid gas flow. Of course, it is possible to assume that the flow equalization occurs also beyond the cascade. However, nevertheless, this would not make it possible for one to solve the problem completely since the angle of lag value arising during such equalization itself is determined by the velocity distribution in the outlet cross section of the vane channel.

Taking into account the aforesaid, from the condition of the tangential force coefficient equaling zero (97), we obtain the following expression for the velocity coefficient of flow beyond the cascade.

$$z(l_2) = \frac{2k}{k+1} \lambda_1 \cos l + \frac{\sin \theta}{\sin(\theta + l)} \cdot \frac{z(l_1)}{\lambda_1}. \quad (107)$$

Replacing in (107)

$$\frac{z(l_1)}{\lambda_1} = \frac{1 - \frac{k-1}{k+1} \lambda_1^2}{\lambda_1^2} \Rightarrow z(l_1) = \frac{2k}{k+1} \lambda_1, \\ 0 = \beta_0, \quad l = \theta - \beta_1 \Rightarrow \beta_1 = \theta.$$

we obtain the following expression derived by G. I. Taganov in 1952:¹

$$z(\lambda_2) = \left[z(\lambda_1) - \frac{2k}{k+1} \lambda_1 \right] \frac{\sin \beta_1}{\sin \beta_2} + 2 \frac{k}{k+1} \lambda_1 \cos(\beta_1 - \beta_2) \quad (108)$$

The total pressure beyond the cascade and the loss factor are found from the equation of continuity

$$\frac{p_{02}}{p_{01}} = 1 = \frac{q(\lambda_1) \sin \beta_1}{q(\lambda_2) \sin \beta_2}$$

The calculations show that the relative percentage of losses due to the equalization of the flow in vane channels is very low, therefore, with a sufficient practical accuracy it is possible to ascribe the total losses determined according to (107) only to the losses in a system of shock waves. The static pressure is determined with the aid of the corresponding gas-dynamic function

$$p_1 = p_{01} \Pi(\lambda_1)$$

When determining λ_2 from (107) it is necessary to bear in mind that gas-dynamic function $z(\lambda)$ whose value

$$z < \sqrt{\frac{k-1}{k+1}} + \sqrt{\frac{k-1}{k+1}}$$

is ambiguous: one root of the equation

$$z(\lambda_2) = \lambda_2 + \frac{1}{\lambda_2} = \text{const}$$

corresponds to subsonic ($\lambda_2^I < 1$), while another corresponds to supersonic speed ($\lambda_2^{II} > 1$). These speeds are connected to one

¹Taganov, G. I., Total Pressure Losses in a System of Curvilinear Shock Waves Ahead of the Cascade Composed of Flat Plates. Collection of Theoretical Works on Aerodynamics. Oborongiz, 1957.

another by the relationship

$$M_1 M_2 = 1.$$

For a cascade with $\beta = 48^\circ$ when $i = 9^\circ$ the dependence $\sigma(M_1)$, obtained for both root values of equation (107) is given in Fig. 10.49. It is evident that with axial incident flow velocity component being less than the speed of sound, condition $\sigma < 1$ is observed only at subsonic speed beyond the cascade. This means that only such a flow is possible. The generality of this conclusion is confirmed by the fact that only at subsonic speed and in the absence of critical cross section in the vane channel do the disturbances beyond the cascade propagate into the zone of flow ahead of it.

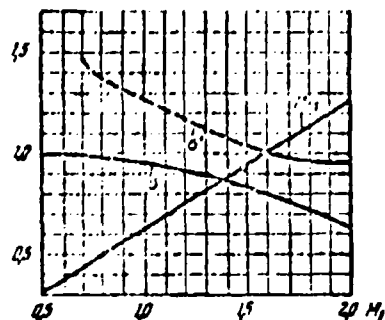


Fig. 10.49. Dependence of the total pressure coefficient in a dense cascade of flat plates with $\beta = 48^\circ$ and $i = 9^\circ$ on the M_1 number of incident flow for subsonic (σ') and supersonic (σ'') roots of equation (107).

Figure 10.50 shows the dependence of relative total pressure losses on the angle of attack for a dense cascade of plates with the different values of the setting angles but with the same incident flow velocity. With zero angle of attack the losses do not depend on angle β and are equal in magnitude to the losses in a normal shock. An increase in the angle of attack leads to the difference in losses. The larger the setting angle, the smaller the losses in a system of shock waves. With $i = 10^\circ$ the losses in the cascade with $\beta = 30^\circ$ are two times greater than with $\beta = 70^\circ$. On this figure the losses in a normal shock with Mach number $M = M_{\max}$ are plotted by the dashed line. The losses determined in this manner do not depend

on the setting angle of the plates, but depend only on the angle of attack. With large angles of setting these losses are greater than the true losses in a system of shock waves.

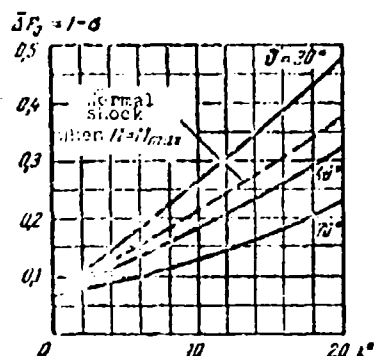


Fig. 10.50. The dependence of relative total pressure losses on the angle of attack in dense cascades of flat plates with different setting angles when $M_1 = 1.5$.

Using the known value λ_2 the coefficient of the resultant force can be found from equation (106), which in the case $\delta = 0$ will be written thus:

$$c_n \frac{b}{l} = 2 \sin(\theta - \alpha) \left[\left(\cos \alpha - \frac{\lambda_2}{\lambda_1} \right) \operatorname{ctg} \theta - \sin \alpha \right]. \quad (109)$$

Let us now consider the streamlining of a cascade of plates by a subsonic, inviscid, therefore, isentropic gas flow.

The streamlining of any cascade of supersonic profiles by a subsonic flow is always accompanied by a separation of the streams from sharp leading edges. Separation flow around a cascade of plates by the potential subsonic flow is schematically shown in Fig. 10.51. The separation of streams occurs from the leading and trailing edges. The speeds and pressures on the stream boundaries are constant. The flow line which passes along the plate, at a point of zero velocity, is divided into lines going upstream (bc_1) and downstream (bc_2). At an infinity beyond the cascade there is a periodic series of parallel streams of width h at constant velocity w_2 . With high cascade density the direction of these streams can be considered as coincidental

with the direction of plates, i.e., $\beta_2 = \beta$. Then from the theorem of momentum for volume $a_1 b_1 b_2 a_2$ we have in projections onto axes n and τ

$$\Delta l (w_1 - w_1 \cos l) = (p_1 - p_2) l \sin \theta, \quad (110)$$

$$- \Delta l w_1 \sin l = - (p_1 - p_2) l \cos \theta - R_x \quad (111)$$

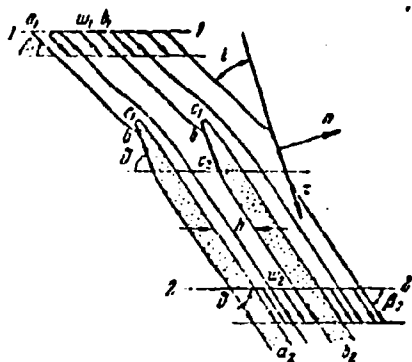


Fig. 10.51. Diagram of separation flow around a cascade of plates by an isentropic flow at sub-critical speeds.

Transforming equality (110) with the aid of the equations of continuity and Bernoulli, we obtain when $\rho = \text{const}$ (see reference on page 629):

$$\left(\frac{w_2}{w_1}\right)^2 - 2 \frac{\sin(\theta - l)}{\sin \theta} \frac{w_2}{w_1} + 2 \frac{\cos l \sin(\theta - l)}{\sin \theta} - 1 = 0. \quad (112)$$

One of the roots of this quadratic equation can be disregarded, since according to the condition $\bar{h} = h/t \leq 1$. Then from equation (112), when $l > 0$, we have

$$\frac{w_2}{w_1} = \frac{\sin(\theta - l)}{\sin \theta} + \frac{\sin l}{\sin \theta}, \quad (113)$$

and from the equation of flow rate

$$h = \frac{\sin(\theta - l)}{\sin(\theta - l) + \sin l}. \quad (114)$$

From equality (113) it follows that with an increase in the angle of attack the flow velocity beyond the cascade, when

$w_1 = \text{const}$, first increases, reaches a maximum when $i = \theta/2$, and then decreases. This is due to the two opposite tendencies which arise with an increase in the angle of attack and the fixed velocity of the flow advancing onto the cascade. On one hand, according to (114), relative width \bar{h} of the stream in the vane channel decreases monotonically, and this should lead to an increase in velocity w_2 ; on the other hand, with an increase in the angle of attack there is a monotonic decrease in the mass gas flow rate through the cascade which in turn leads to a decrease in the velocity at the exit from it. After the transformation of equality (111), we obtain the following expression for the coefficient of the resultant force in the flow of incompressible fluid:

$$c_n \frac{b}{l} = \frac{\sin(\theta - i) \sin i}{\cos^2 \frac{\theta}{2}}. \quad (115)$$

From (115) it follows that with the angle of attack $i_{\text{np}} = \theta/2$ value of the resultant force reaches a maximum. For the flow of compressible gas, by virtue of the isentropicity of the flow ($\sigma = 1.0$) according to (39), we have

$$\frac{p_1 - p_2}{\rho_1 \frac{w_1^2}{2}} = \frac{k+1}{k} \frac{\lambda_1}{\lambda_2} \left[1 - \frac{\pi(\lambda_2)}{\pi(\lambda_1)} \right].$$

Using this relationship, we transform equations (110) and (111) to the form

$$\lambda_2 = \frac{k+1}{k} \frac{\lambda_1}{\lambda_2} \left[1 - \frac{\pi(\lambda_2)}{\pi(\lambda_1)} \right] \frac{\sin \theta}{2 \sin(\theta - i)} + \lambda_1 \cos i, \quad (116)$$

$$c_n b/l = 2 \sin(\theta - i) \left[\left(\frac{\lambda_1}{\lambda_2} \cos i - \frac{\lambda_1}{\lambda_2} \right) \operatorname{ctg} \theta + \sin i \right]. \quad (117)$$

Considering values λ_2 , i and θ as known, it is possible to graphically solve equation (116) with respect to λ_1 and then, with the aid of the equation of continuity, to find the relative width of the stream:

$$h = \frac{h}{t} = \frac{q(\lambda_1) \sin(\theta - \theta_1)}{q(\lambda_1) \sin \theta}.$$

The dependences of λ_2 and \bar{h} on the angle of attack with values $M_1 = 0.75$ and $\beta = 70^\circ$ are given in Fig. 10.52. They are similar to the analogous dependences for an incompressible fluid flow (see the reference on page 734).

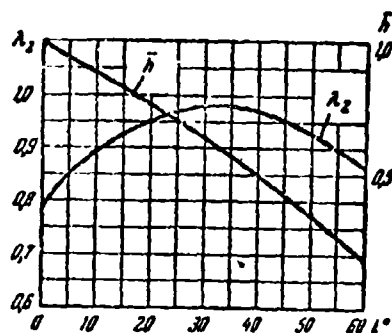


Fig. 10.52. Dependence of λ_2 and \bar{h} on the angle of attack when $M_1 = 0.75$ and $\beta = 70^\circ$.

As an example, dependence $c_n b/t = f(\alpha)$, calculated from equation (117) is given on Fig. 10.53. The same figure shows the calculation results of a similar dependence for the case of a continuous flow around the same cascade. The comparison of these dependences shows that the flow separation from the leading edge leads to a very sharp decrease in the value of the resultant. Simultaneously, there is also a substantial decrease in the critical angle of attack characterized by the maximum value of the resultant. Bearing in mind that λ_2 is the maximum value of the velocity coefficient in the entire area of flow, with the aid of equation (116) it is possible to determine the maximum value $\lambda_1 = \lambda_{1\text{кр}}$ at which the flow is still subcritical.

For this, in expression (116) one should assume that $\lambda_2 = 1$ and solve the obtained equation with respect to λ_{1kp} at the given angles of attack and setting angles.

The calculation results given in Fig. 10.54 agree with the nature of the dependence of λ_2 on i in Fig. 10.52.

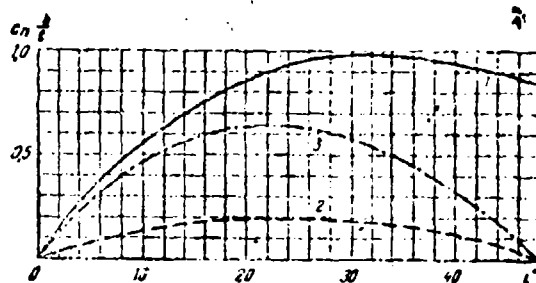


Fig. 10.53. Dependence of $c_n b/t$ on the angle of attack for the cascade of plates when $\beta = 48^\circ$ with $M_1 = 0.75$:

1 - a continuous isentropic flow; 2 - flow with stream separation without mixing in the vane channels; 3 - with a complete equalization of the flows in the vane channels.

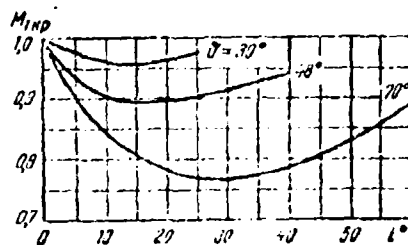


Fig. 10.54. Dependence of M_{1kp} on the angle of attack for a dense cascade of plates streamlined by an isentropic gas flow with stream separation from the leading edges.

§ 12. The Effect of Viscosity on Flow
Around Supersonic Airfoil Cascades. A
Solid Cascade of Plates¹

Let us first examine the effect of viscosity on an example of cascades of plates with zero incidence.

In the case of inviscid flow of a liquid and subsonic gas flow the power effect of the flow on a cascade of plates with $l = 0$ is absent. In accordance with this, the cascade does not divert the flow from its initial direction, and the angle of deviation will be equal to zero independently of denseness and setting angle. The presence of forces of friction during the flow of a viscous flow about the cascade leads to the formation of tangential force R_t and correspondingly to a deviation of flow by the cascade which is the greater, the greater this force is. At the same time, the formation of a boundary layer causes acceleration of external flow and, consequently, also to the appearance of a pressure gradient along the plate. The resultant force of the pressure in general ceases to be equal to zero - there appears normal force R_n . Limiting ourselves to an examination only of cascades of low solidity for which it is possible to disregard the mentioned effect of the acceleration of external flow, i.e., assuming that $R_n = 0$, we have

$$R_x = R_t \cos \theta$$

or

$$c_x = c_t \cos \theta.$$

In the case of an incompressible fluid according to (50) we obtain the following dependence between the angle of flow exit β_2 and the coefficient of tangential force:

$$\operatorname{ctg} \beta_2 = \operatorname{ctg} \theta \left(1 - \frac{c_t l}{2 \sin \theta} \right).$$

¹See references on pages 629 and 734.

If the fluid is inviscid, $c_f = 0$, and therefore, $\beta_1 = \delta = \beta_2$, i.e., the flow which flows through a cascade of plates at zero incidence does not change the initial direction. In the case of a viscous fluid $\beta_1 > \delta$, i.e., the angle of deviation is negative

$$\delta = \delta - \beta_1 < 0.$$

The greater the drag coefficient and the greater the cascade solidity, the more considerable is the deviation of the flow. With an increase in the setting angle a decrease in δ is observed. With $\theta = \pi/2$ independently of the value of $c_f b/t$ we have $\delta = 0$. This is also easy to conclude from the condition of symmetry of flow.

Correct to the assumptions, made above, the value of c_f can be taken as equal to the doubled drag coefficient of the plate c_p . Utilizing the data regarding the value of this coefficient with various Reynolds numbers given in Chapter VI, it is possible to obtain the dependence of the angle of deviation on the Reynolds number. Thus, for instance, with $R = 10^6$ in the case of laminar conditions over entire length of the blade $c_p = 0.0015$, while in the case of a turbulent condition, $c_p = 0.005$. The lead angles of flow in a cascade with $\theta = 30^\circ$ and $b/t = 1.0$ will comprise respectively $0^\circ 4'$ and $0^\circ 14'$.

The relatively low values of the coefficient of friction and the respectively insignificant angles of deviation make it possible to disregard the forces of friction on the plates in determining pitot losses and total power effect of a viscous flow of liquid and gas on a cascade of such airfoils. This is all the more correct since with an increase in the Mach number of the flow incident to the plate the coefficient of friction drag decreases (see Chapter VI).

At angles of incidence different from zero, the nature of the viscosity effect depends on whether the flow that encounters the cascade is subsonic or supersonic.

In a subsonic flow the specific effect of viscosity is expressed, in the first place, in the fact that during the separation of jets from the sharp leading edges of supersonic airfoils an eddy is formed which seemingly rounds off the knife edges. As a result, the viscous flow no longer flows around the sharp leading edge of the airfoil, but about this eddy; however, with small angles of incidence the flow on departure differs little from nonseparable (Fig. 10.55). In the second place, the effect of viscosity is expressed in the fact that, when at sufficiently great angles of incidence stalled flow appears, as a result of turbulent mixing it will gradually be eroded, and with a sufficiently large extent of the vane channel, i.e., with a sufficiently solid cascade, the area of separation closes and on departure from the cascade the flow will evenly fill the whole cross section of the channel (Fig. 10.56).

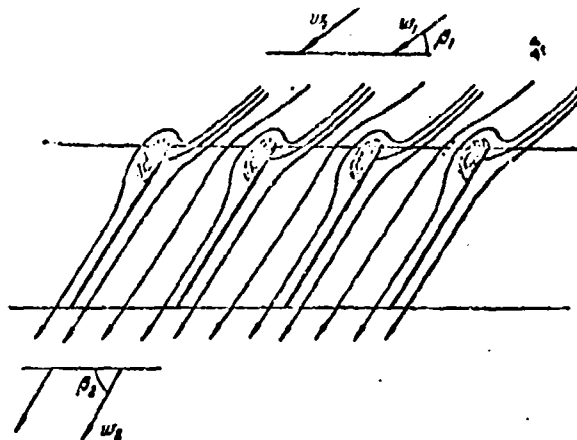


Fig. 10.55. Diagram of flow around a cascade of plates by a viscous subsonic flow with the formation of an eddy at sharp leading edges.

Both aforementioned factors give rise to the formation of pitot losses and to the equalizing of velocities in the exit sections of the vane channels. As a result of equalizing, the resultant is increased in comparison with its value during the

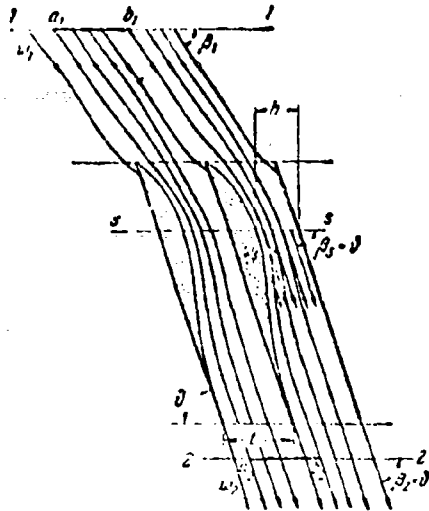


Fig. 10.56. Diagram of stalled flow with full mixing of the flow in the vane channels of a solid grid of plates.

Flow of an isentropic flow about this cascade with separation of jets from the leading edges.

Thus, during subsonic flow around the cascade, the viscosity independently of the mechanism of its effect, gives rise to the formation of losses and an increase in the resultant. It is a different matter with the effect of viscosity during the flow of a supersonic flow about the cascades. In this case, in an inviscid flow of gas there is achieved a nonseparated flow around airfoils with a sharp leading edge. In the presence of viscosity there appears a boundary layer whose interaction with a shock wave of sufficient intensity falling on it gives rise to the formation at the surface of the airfoil of λ -shaped shock, after which boundary-layer separation occurs (see Chapter VI). As a result, the nonuniformity in the velocity distribution over the cascade pitch increases, and consequently, the angle of deviation of flow increases and the resultant force applied to the airfoil in the cascade decreases correspondingly. In so doing, the pitot losses may even decrease.

Let us illustrate the considerations expressed here in an example of a cascade of plates. Let us examine first the flow of a subsonic flow about such a cascade. We will consider that the cascade solidity is so great that as a result of intense turbulent mixing on departure from the cascade there is a flow uniform in pitch, parallel to the plates.

Determining with the aid of expressions (50) and (51) the coefficient of tangential component resultant c_t and equating it to zero, we obtain the following expression for the loss coefficient of the flow of a viscous incompressible fluid:

$$\zeta = \frac{\sin^2 \theta}{\sin^2 \theta_0}.$$

The same expression for the loss coefficient can be obtained according to Borda's formula if one assumes that a sudden expansion of uniform jet occurs with an area of $F_1 = h \sin \theta$ to area $F_2 = t \sin \theta$ (Fig. 10.56).

From equation (50) we have ($\beta_1 = 0 - L$, $\beta_2 = 0$)

$$c_n \frac{b}{t} = \frac{c_n \frac{b}{t}}{\sin \theta} = 2 \frac{\sin (\theta - L) \sin \theta}{\sin^2 \theta}.$$

Comparing this expression with (115) we conclude that in a solid cascade the viscosity effect leads to an increase in the coefficient of resultant of $\left(1, 2 \sin^2 \frac{\theta}{2}\right)^{-1}$ once. With an increase in the angle of incidence, the viscosity effect on the power effect of the flow decreases and becomes zero with $\theta = \frac{\pi}{2}$. The latter is connected with the fact that according to (50) when $\beta_2 = \frac{\pi}{2}$ the whirl constituent of the resultant, and consequently, in the case in question, the resultant itself no longer depend on the velocities on departure from the cascade and are determined only by the value of the velocity at inlet to it.

For determining the resultant during flow around a solid cascade of plates of a viscous flow of a compressible gas at subsonic velocities equations (107) and (109) should be used.

It is natural that in so doing in (107) only the subsonic value of λ_2 is selected. Although the indicated equation was utilized earlier for determining losses during flow around cascades of plates of a supersonic flow, however, the generality of the assumptions made during the derivation of this equation makes it possible to employ it (if we disregard the forces of friction on the plates) also in the case in question. Moreover, if as has already been indicated above, equation (107) makes it possible to only approximately determine losses in an infinite system of shock waves, then this equation accurately determines losses to the equalizing of flow in the vane channels of a solid cascade of plates flowed around with a subsonic flow. This is also confirmed by the fact that the losses to equalizing thus determined, just as in an incompressible fluid, completely coincide with losses according to Borda calculated for a compressible gas according to the previously found values of h and λ_2 in a potential flow.

The dependence of $c_n b/t(1)$ with $M_1 = 0.75$ is given in Fig. 10.53. There, similar dependences are also plotted during the flow of an isentropic flow about a solid cascade without separation and with separation of jets. As already indicated earlier, the separation of jets from the leading edge while maintaining the potential flow pattern leads to a sharp decrease in the resultant force. At small angles of incidence, the equalizing of flow in the vane channels as a result of turbulent mixing, to a considerable degree, compensates for this sharp drop in the force. In proportion to the increase in the angles of incidence, this compensation as a result of the intense increase of losses decreases substantially.

During flow around a cascade of plates of a supersonic flow with a subsonic axial component of velocity, the viscosity effect is basically exhibited in the interaction between the boundary layer on the plate and the shock wave falling on it.

In Chapter VI it was indicated that in this case, with a "critical" ratio of static pressures in the shock, near the wall there appears a λ -shaped shock after which boundary-layer separation occurs. The presence of separation leads to an essential redistribution of pressure. The change in the total losses and value of the resultant depends, to a considerable degree, on the solidity of the cascade. If the solidity of the cascade is so great that the separated flow within the vane channel is completely equalized (Fig. 10.57a), then according to the theorem of flow impulses (disregarding, as before, the forces of friction applied to the plate) the total quantity of losses remains the same as for the case examined above where the viscosity effect was not considered, there will occur only a redistribution of the losses between the zone of shock waves and the area of equalizing the flow. An increase in the losses to equalization is completely compensated for by a decrease in the losses in the shock waves connected with the formation of a system of oblique shocks. In the case of complete equalization of flow in the vane channels of a solid cascade there are no reasons for the emergence of an angle of deviation. With zero angle of deviation and the retention of the same value of σ the resultant of all forces of pressure remains constant in spite of their essential redistribution along the chord.

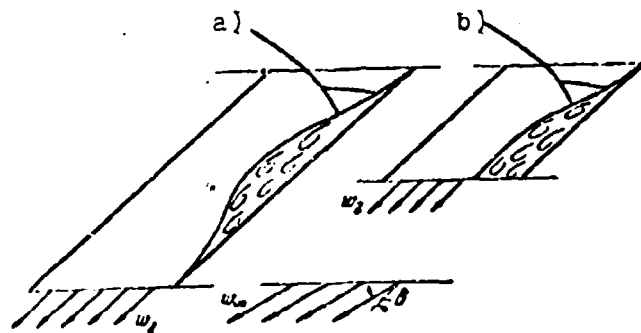


Fig. 10.57. Diagram of flow around a cascade of plates of a supersonic flow of a viscous gas with subsonic axial component of a velocity ($M_{1a} < 1.0$) and with a supercritical drop in the pressure in the shock wave: a) solid cascade, b) widely spaced cascade.

In a widely spaced cascade the equalizing of flow occurs mainly after the cascade (Fig. 10.57b), and therefore is connected as was shown earlier, with the appearance of the angle of deviation, which can be very considerable; the flow separation after the λ -shaped shock in this case can lead to a decrease in the resultant force applied to the plate. With a given number M_1 at an infinity M_k number before the latter, the shock wave is the greater, the greater the angle of incidence. Consequently, with an increase in the angle of incidence there is an increase in the intensity of flow breakaway in a λ -shaped shock. Hence, it may be concluded that the effect of viscosity on the value of the resultant force should increase with an increase in the angle of incidence. Determination of the viscosity effect actually is reduced to determining the effect of the angle of deviation of flow after the cascade on the magnitude of losses and the value of the resultant. Similar results of calculations (Fig. 10.58) show that

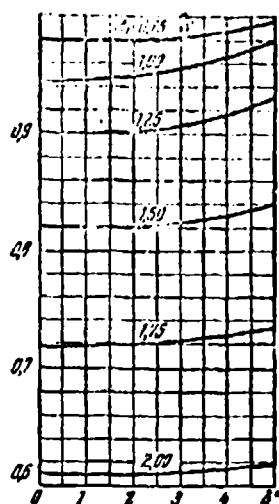


Fig. 10.58. Dependence of σ on the angle of deviation δ for various values of M_1 during flow around a cascade of plates ($\delta = 30^\circ$, $1 = 6^\circ$).

the total losses decrease with an increase in the angle of deviation. Such a decrease in losses at subsonic speeds is explained by the fact that the equalizing of the flow in space after the cascade occurs with less losses than in the vane channels. This circumstance explains the fact that the decrease in wave losses in a system of oblique shocks (with λ -shaped shock) which remains the same as in a solid cascade, overlaps the increase in the losses connected with the turbulent mixing of the flow detached from the plate in a widely spaced cascade. The resultant force with an increase of the angle of deviation also decreases (Fig. 10.59) whereby the relative drop in the coefficient of resultant force c_n is weakened with an increase of the

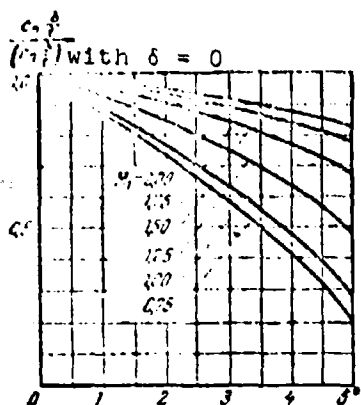


Fig. 10.59. Dependence of the value of $c_n b/t$ referred to its value with $\delta = 0$, on the angle of deviation ($\delta = 30^\circ$, $1 = 6^\circ$).

number M_1 . Such nature of the effect of the angle of deviation is explained by the fact that with an increase in number M_1 an ever greater portion of the composite force which acts on the plate is connected with a change in the momentum in the system of shock waves in the intake part of the vane channel and, to a lesser degree, depends on the angle of deviation. Thus its value basically is determined only by angle of incidence and by the number M_1 .

The analysis carried out above on the different cases of flow around a cascade of plates of a viscous gas shows that if we restrict ourselves to the examination only of such solid cascades of plates for which on outlet from the vane channels the flow is always uniform, then in the entire possible range of change in M_1 numbers and angles of incidence the value of the velocity coefficient after the cascade λ_2 is determined by one universal equation (107).

If in this case, the axial velocity of the flow incoming to the cascade is less than the speed of sound ($M_{1a} < 1$), then of the two roots of equation (107) only the subsonic values of λ_2 have a physical sense. But if $M_{1a} \geq 1$, then both roots of the equation have a physical sense whereby realization of one of the two systems connected with condition $\lambda_2'' \lambda_2' = 1.0$, is determined by the value of static pressure p_2 after the cascade. At less pressure $p_2 = p_{2min}$, the flow after the cascade will be supersonic ($\lambda_2 = \lambda_2'' > 1$), while at greater pressure $p_2 = p_{2max}$ - subsonic ($\lambda_2 = \lambda_2' < 1$).

These values of p_2 differ from one another by the value of the increase in static pressure in the normal shock.

Knowledge of value of λ_2 makes it possible according to (109) to determine the power characteristic of this cascade, i.e., the dependence of $c_n(i)$ with different M_1 numbers.

Figure 10.60 gives the power characteristic of a solid cascade of plates in a viscous flow of gas over a wide range of M_1 numbers at positive angles of incidence. In those cases when the power effect is ambiguous ($i = 0$ or $M_{1a} > 1$), the value of the coefficient of the resultant of c_n was taken which corresponded to the maximum possible pressure after the cascade. At zero angle of incidence and at supersonic velocity this system is realized with the emergence of a normal shock in the vane channels of the cascade.

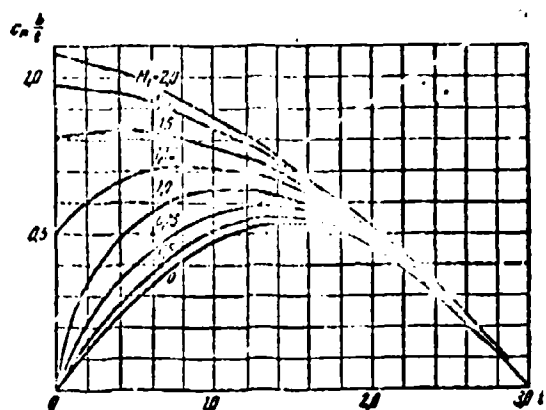


Fig. 10.60. Dependence of $c_n b/t$ on the angle of incidence for a solid cascade of plates during flow of turbulent flow around it of a gas ($\delta = 30^\circ$).

With an increase in the angle of incidence to i_{np} the resultant force first increases from zero value to the maximum, and then monotonically decreases. With an increase in the M_1 number the point of maximum of force is shifted in the direction of the lesser angles of incidence with simultaneous increase in the value of the force coefficient; at a certain value of the number $M_1 > 1$ the value of i_{np} reaches zero value.

In an example of a solid cascade of plates let us examine the question concerning the range of possible values of the parameters of incident flow: the M_1 number and the angle of incidence i .

If the flow velocity in the exit section of the vane channels of the cascade of plates reaches the speed of sound ($\lambda_{2k} = 1$), then the so-called cutoff condition begins which limits the area of possible values of the angles of incidence i and M_1 numbers during flow about the cascade.

Independently of the value of the Mach number and the angle of incidence, if choking of the cascade begins, then the flow after it becomes ambiguous and is determined by the relation of the static pressures $\epsilon = p_2/p_1$.

Dependence of the parameters of equalized flow in cross section 2-2 far beyond the cascade on ϵ can be obtained with the aid of expressions (100) and (104).

The maximum possible pressure p_2 is equal to the pressure in the exit section of the vane channel. In this case, directly at the edge of the cascade there is a steady flow and correspondingly the angle of deviation is equal to zero, and the velocity far beyond the cascade is equal to the flow velocity in the exit section of the vane channel $\lambda_2 = \lambda_{2k}$.

The minimum value of p_2 is determined by the condition of achievement of axial velocity after the cascade of the speed of sound ($M_{2a} = 1.0$). With non-stalling isentropic flow ($\sigma = 1.0$) choking of a solid cascade of plates is possible only at negative angles of incidence. The value of the velocity coefficient at which the choking condition of a cascade of plates begins (with the given angle of incidence), in this case is found directly from the equation of continuity

$$q(\lambda_1) = \frac{\sin \theta}{\sin(\theta - i)}.$$

Here the choking condition of the cascade is noted by the subscript "a." As can be seen from the last expression, for each fixed value of negative angle of incidence ($i < 0$) there are two values of velocities, one subsonic ($\lambda_{1a,a} < 1$), and another supersonic ($\lambda_{1a,c} > 1$), at which choking of the cascade occurs.

Curves $\lambda_{1a}(i)$ limit the area of velocities and angles of incidence in which even isentropic flows are impossible. As an example, Fig. 10.61 gives the dependences of $\lambda_{1a}(i)$ for $\beta = 30^\circ$ at negative angles of incidence.

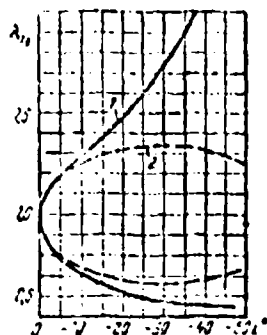


Fig. 10.61. Dependence of the velocity coefficient of incident flow on the angle of incidence $i < 0$ with choking of a solid cascade of plates ($\beta = 30^\circ$): 1 - in isentropic flow, 2 - taking losses into account.

For determining the velocity coefficient with which choking of a cascade of plates begins, taking into account the actual losses in the turbulent flow of a gas, let us make use of relationship (107). Assuming that in this expression $\lambda_2 = 1.0$, we obtain the following equation of relatively unknown value λ_{1a} :

$$\lambda_{1a} - 2b\lambda_{1a} + b \frac{\sin \theta}{\sin(\theta - i)} = 0, \quad (118)$$

where

$$b = \frac{(k+1) \sin(\theta - i)}{2k \cos \theta \sin(\theta - i) - (k-1) \sin \theta}. \quad (119)$$

The presence of losses (Fig. 10.61) leads to a marked decrease in the range of values (λ_1, i), in which flow is possible. The effect of losses increases with an increase in the absolute values

of the angles of incidence and with an increase in the setting angle of the cascade. At supersonic velocities the effect of losses on contraction of the area of possible parameters of incident flow is expressed more strongly than with subsonic, which, probably, is caused by large losses at supersonic velocities.

Choking of the cascade at positive angles of incidence is connected only with the appearance of losses. With a fixed number λ_1 the losses grow with an increase in the angle of incidence, but simultaneously the gas flow rate through the cascade decreases as a result of reduction of the cross section of jets before it. As a result, it turns out that choking of a solid cascade of plates appears only at sufficiently high angles of incidences.¹ At less positive angles of incidence the cascade is not choked. Complex values of the roots of equation (118) correspond to this case.

§ 13. Construction of Purely Supersonic Cascades

Let us examine the reverse problem - the construction of a supersonic cascade which turns flow at a given angle.

Depending on the calculated values of M numbers on entry and exit we distinguish cascades which are purely supersonic ($M_1 > 1, M_2 > 1$) and cascades with the mixed flow: convergent ($M_1 < 1, M_2 > 1$) and divergent ($M_1 > 1, M_2 < 1$). Each of these types of cascade differs in the method of profiling.

¹Detailed analysis of possible systems of flow about a solid cascade of plates is given in the work: Ludwig M., Über das Verhalten kompressibler Medium bei der Strömung durch gerade Schaufelgitter, Forsch. Ing., Wes. 22, N 6, 1956. See also reference on page 740.

We will first acquaint ourselves with the methods of constructing purely supersonic isentropic cascades. The four parameters β_1 , β_1 , λ_2 , and β_2 , which determine the flow before and after the cascade are not independent but are connected by the equation of continuity. Thus, in the construction of a cascade it is possible to assign only three arbitrary parameters, i.e., isentropic cascades in general are three-parameter cascades. But if in the construction of a cascade we make use, for example, of the laws governing supersonic flow around an obtuse angle (Chapter IV) giving an additional dependence between the deflection of the flow and the values of numbers M_1 and M_2 , then the number of independent parameters will be reduced to two.

As an example let us examine a supersonic two-parameter convergent cascade.¹ By assigning two parameters - the deflection and the number M_1 in the incident flow it is possible to find number M_2 after deflection and change of pressure p_2/p_1 . According to the numbers M_1 and M_2 we construct (Fig. 10.62a) the appropriate characteristics and conduct at a distance r_0 two flow lines, each of which consists of two segments of straight lines and a curvilinear section determined from equation (29) in Chapter IV. Let us continue the rectilinear segments 1-1 and 2-2 which are tangents to the curvilinear section of the flow line before their intersection at point O'. As a result of construction we obtain a certain airfoil (with infinitely thin leading and trailing edges) which causes no disturbances in the flow.

Repeating a similar procedure of construction in connection with point O', we obtain a second airfoil section of the cascade identical to the first, and then all remaining airfoils. Such a cascade does not have wave drag, and therefore the flow in it, if we disregard friction, is isentropic.

¹E. Straus, Schaufelgitter für Überschallgeschwindigkeit ohne Wellenwiderstand. Technische Berichte ZWB, Berlin - Adlershof, 1944, Bd. 11, Heft 10.

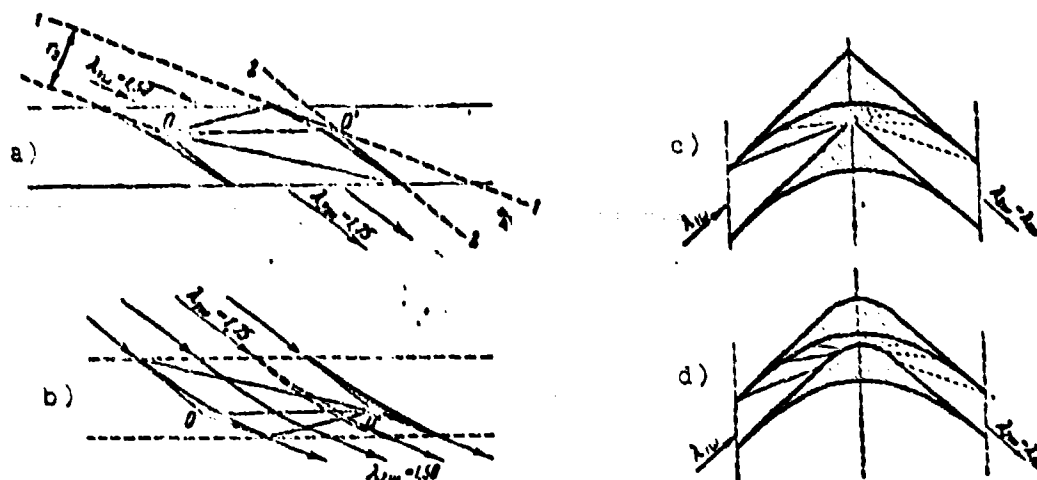


Fig. 10.62. Two-parameter supersonic cascades without wave drag, constructed with the use of laws governing flow around an obtuse angle: a) convergent cascade; b) divergent cascade (obtained by reversal of flow in a convergent cascade); c) an active cascade of broken airfoils; d) an active cascade of curvilinear airfoils.

Turning flow, it is not difficult to convert the constructed convergent cascade into a divergent (Fig. 10.62b); however, in the latter case the area of flow where compression of gas occurs, can prove to be the site of formation of shock waves and wave losses.

Utilizing a flow with compression about an obtuse angle (turned flow with expansion), let us construct a certain section of curvilinear channel with a smooth decrease in the pressure down to certain value of p . If we now add a symmetrical second section in which the flow of expansion from pressure p to initial pressure p_1 is achieved, then we will obtain a curvilinear active channel, and therefore we will be able to construct an active airfoil cascade (Fig. 10.62c).¹ In this case it is assumed that the flow

¹Stodola A., Dampf- und Gasturbinen. Ver. Springer, 1924.

of compression occurs without losses, although in actuality this is highly improbable. Analogously, it is possible to construct a cascade, each airfoil of which is formed by any two flow lines for the flow about a right angle; in this case the surface of the airfoil has a curvilinear, but not a broken form (Fig. 10.62d).

Let us proceed to the construction of an arbitrary supersonic three-parameter cascade. The simple method of constructing such cascades indicated by S. I. Ginsburg in 1950 is based on the use of two Prandtl-Meyer flows with different angles of turn on the flows.

Let us assume that the parameters of the unknown grid λ_1 , β_1 , and β_2 are given. From the equations of continuity we find the fourth parameter λ_2 . Let us examine now two cases of flow (Fig. 10.63) about the angle: flow with compression and a decrease in velocity from λ_1 to a certain value λ_0 less than λ_1 and λ_2 , and a turn of flow through angle β_{01} (Fig. 10.63a); and flow with expansion and an increase in velocity from λ_0 to λ_2 and a turn of flow through angle β_{02} (Fig. 10.63b).

Connecting both flows consecutively, we will obtain the channel depicted in Fig. 10.63c. In this channel at first there is a divergent section B_1A_1O , further in the area of the isosceles triangle OA_1A_2 we have a uniform progressive flow with velocity coefficient λ_0 , then follows the convergent section OA_2B_2 . At points B_1 and B_2 let us conduct tangents to curves B_1A_1 and B_2A_2 to their intersection at point O_1 (Fig. 10.63d).

Thus, we will obtain a certain airfoil section $B_1O_1B_2$. By consecutively shifting this airfoil along straight line O_1O_1' a distance B_1B_1' it is possible to construct a cascade from these airfoils with pitch $t = B_1B_1'$. The flow which encounters this grid at angle β_1 with velocity coefficient λ_1 will be turned through an angle

$$\Delta\beta = \beta_2 - \beta_1 = \beta_{01} + \beta_{02}$$

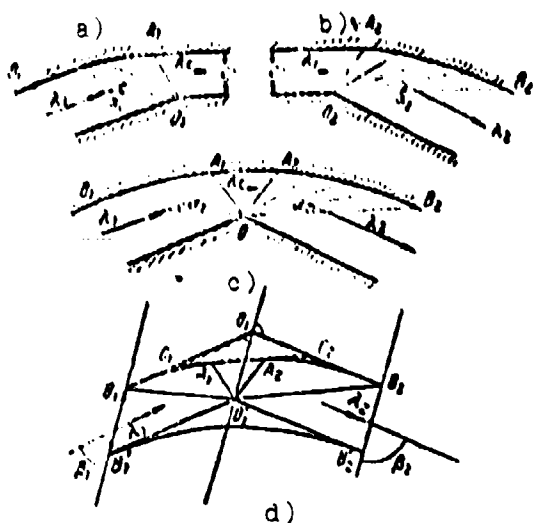


Fig. 10.63. To construct a three-parameter purely supersonic cascade without wave drag.

If we continue the straight line segment A_1A_2 before intersection with straight lines B_1O_1 and B_2O_1 , then it will turn out that the airfoil which forms the cascade consists of three parts: 1) triangle $O_1C_1C_2$; 2) the airfoil of the two-parameter divergent cascade $B_1C_1A_1B_1$; 3) the airfoil of the two-parameter convergent cascade $A_2C_2B_2A_2$. As already indicated above, the divergent section of the vane channel of the cascade should be constructed in such a way that the characteristic curves do not intersect. This can easily be done by rounding off the angle.

Thus, if three arbitrary flow parameters λ_1 , β_1 and β_2 are given, then for the construction of a cascade which satisfies these conditions, it is only necessary to determine the value of λ_c .

Figure 10.64 gives the graphs to permit finding λ_c for the given values of β_1 and β_2 at the fixed value of $\lambda_1 = 1.5$. The area of possible values of angles β_1 and β_2 , obtained from a condition of isentropicity of flow is delimited by the shaded curves. The values of the angles of the cascade being designed naturally should lie in this area. However, since in the method of construction of the cascade in question we should satisfy the

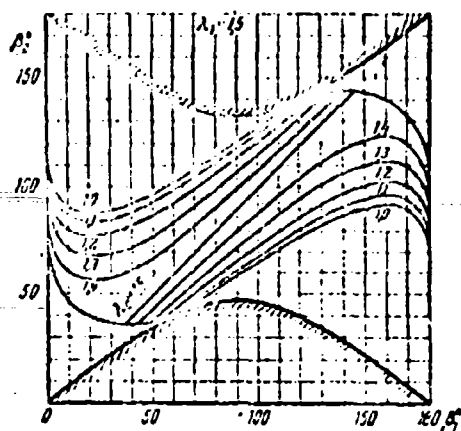


Fig. 10.64. Graphs of λ_c (β_1 , β_2) for a three-parameter isentropic cascade with $\lambda_1 = 1.5$.

additional condition $\lambda_c \geq 1$, the area of possible values of angles β_1 and β_2 is additionally limited by curves $\lambda_c = 1$.

Limitations on the possible values of the parameters of supersonic cascades appearing in their construction with the aid of Prandtl-Meyer flows can be completely removed with the use of a more general method of construction proposed by A. M. Domashenko in 1951 and based on "gluing" any supersonic flow for which there is an exact solution to the Prandtl-Meyer flows. This method makes it possible, by utilizing an exact solution for a potential vortex to construct a supersonic isentropic cascade for almost any parameters.¹

The methods given above for the construction of supersonic isentropic cascades possess that common disadvantage, that, in the first place, the leading and trailing edges of the vanes are made infinitely thin (they have a zero angle of taper) and, in the

¹The method of constructing an almost arbitrary supersonic cascade with the use of a flow from a potential vortex is also examined in a later work: Oswatitsch K., Potential-Gitter für Überschallgeschwindigkeiten, Zeitschrift für Flugwiss. 4, N 1-2, 1956.

second place, there is assumed to be isentropic deceleration of flow in the diffuser part of the vane channel.

The presence of thin intake and outlet edges hinders the manufacture of such vanes, creates the danger of the emergence of vibrations, and hinders their use at high temperatures. The realization of isentropic deceleration over a wide range of values of velocity coefficients λ is impossible without boundary layer control. In actuality, instead of the smooth process of isentropic deceleration a certain system of shock waves appears, losses of pressure increase sharply and the design diagram of flow is disturbed.

The indicated deficiencies can be eliminated if we organize the deceleration of flow in a system of oblique shocks. Such deceleration, as shown by experiments with flat and axisymmetric models, can be realized whereby the airfoil in this case has a leading edge with a finite angle of taper.

Given the velocity coefficient of incident flow λ_1 , the number of oblique shocks m , and the value of the velocity coefficient λ_m to which the flow should be decelerated ($1 \leq \lambda_m < \lambda_1$), it is possible to find the total value of the angle of turn and the total value of the total pressure drop in the diffuser part of vane channel. Losses can be reduced to a minimum if we utilize the optimum system of shocks for the assigned values of λ_1 , λ_m and number of shocks m .

Let us examine the method of constructing "shock" cascades in a concrete example. Let us assume that it is required to construct a cascade, the vane channel of which has a divergent part where the velocity decreases from a value of $\lambda_1 = 2$ to a value of $\lambda_c = 1.2$, and a convergent part in which the flow is accelerated from the value of velocity coefficient $\lambda_c = 1.2$ to a value of $\lambda_2 = 1.8$. Let us assume that this requires the number of shocks $m = 3$. With the aid of the graphs given in Chapter III, we find

that during the deceleration of flow in an optimum system of shocks from $\lambda_1 = 2$ to $\lambda_0 = 1.2$ the values of the velocity coefficients after each of the shocks comprise

$$\lambda_1' = 1.84, \quad \lambda_1'' = 1.60, \quad \lambda_1''' = 1.20,$$

and the corresponding values of the angles of turn

$$\alpha_1 = 11^\circ 30', \quad \alpha_2 = 14^\circ 30', \quad \alpha_3 = 17^\circ 30'.$$

In this case, the values of the angles between direction of the free stream and the front of the corresponding shock comprise

$$\gamma_1 = 27^\circ 40', \quad \gamma_2 = 36^\circ, \quad \gamma_3 = 51^\circ 30'.$$

Using the indicated values, we construct (Fig. 10.65) line ABCD consisting of straight segments AB, BC, CD, parallel with respect to the flow directions after each of the shocks. Let us select the lengths of segments AB, BC in such a way that all shocks intersect at point O through which let us conduct straight line ON at an angle β_{02} equal to the value of the necessary angle of turn of the flow for isentropic expansion from λ_0 to λ_2 . In our case, we have $\lambda_0 = 1.20$, $\lambda_2 = 1.8$. Then, from tables for Prandtl-Meyer flow (see Appendix I) we find $\beta_{02} = 32^\circ 24'$.

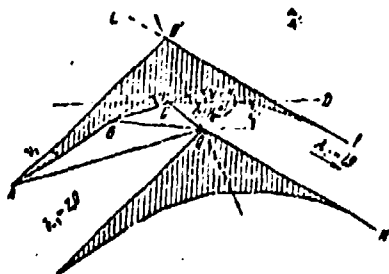


Fig. 10.65. To construct a three-shock purely supersonic cascade.

If now for the given value of n_0 (Fig. 10.65) we outline the flow line of the flow about the angle, then straight line CD will be tangent to it at point K of the intersection of the flow quantity after the last shock with direction CD. Tangent FL to the flow line at point F will be parallel to line ON.

Conducting through point A a straight line parallel to the direction of the flow incoming to the cascade before intersection with tangent FL at point O', we obtain a certain closed outline-shape of the cascade.

The axis of this cascade will be straight line OO'; its pitch is equal to the length of segment OO'.

Let us note that the process of deceleration in oblique shocks can be applied not to the entire length of the divergent section, but only to part of it. As an example, Fig. 10.66a depicts a cascade in which the process of deceleration in oblique shocks is achieved only in parts of the divergent section from $\lambda_1 = 2$ to $\lambda = 1.6$. In the remaining section, provision is made for isentropic deceleration from $\lambda = 1.6$ to $\lambda_{cp} = 1.2$.

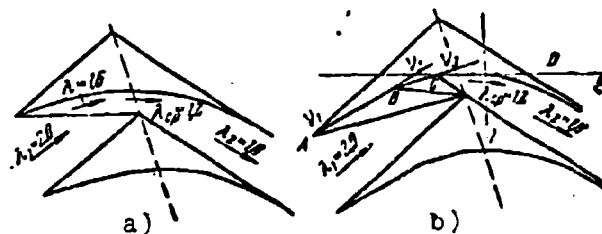


Fig. 10.66. Examples of combined shock supersonic cascades: a) a single-shock cascade with partial deceleration of flow by an oblique shock; b) a three-shock cascade with finite thickness of the trailing edge.

It is also possible to construct vanes with finite thickness of the trailing edge (see Fig. 10.66b). In this case, added losses appear connected with the formation of pressure jumps at the exit edges and further equalizing of the flow. By analogy with the subsonic flow, here it is possible to speak about a Borda-Carnot "oblique" shock.

It is also possible to visualize a supersonic cascade in the vane channels of which is a convergent section absent, and the compression of gas occurs only in shock waves. For the construction of such a divergent cascade we utilize airfoils in the form of triangles, directing flow with a given M_1 number parallel to the side of triangle $A'O'$ (Fig. 10.67a); the angle of triangle at point A' is selected as less than the critical angle for an oblique shock with this value of M_1 .

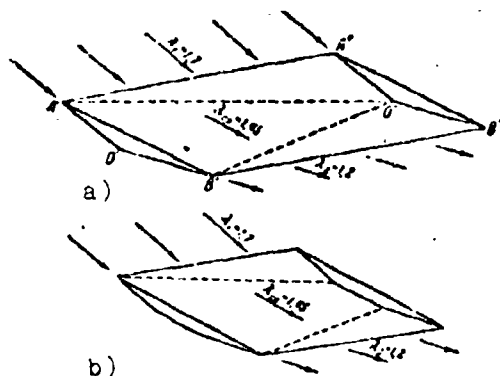


Fig. 10.67. Purely shock supersonic cascade possessing wave drag: a) a cascade of triangles; b) a cascade of trapezoids.

In the area $A'O''B'$ lower than the shock wave $A'O''$ there is achieved a uniform flow of gas parallel to wall $A'B'$, with velocity $\lambda_{cp} < \lambda_1$ and pressure $p_{cp} > p_1$. After point B' the particles of gas enter the high-pressure area ($p_2 > p_{cp}$), in connection with which a second shock wave appears in which the flow again changes its direction. The apex of the following airfoil of the cascade is placed at the point of intersection of shocks O'' , and the boundaries $O''B''$ and $O'B'$ are conducted parallel to the direction of flow after the second shock. Thus, the triangular airfoils $A'B'O'$ and $A''B''O''$ are arranged in parallel.

Continuing the process of construction of these airfoils, we obtain an infinite rectilinear cascade of triangles.¹

¹E. Straus, Schaufelgitter für Überschallgeschwindigkeit ohne Wellenwiderstand. Technische Berichte ZWB, Berlin - Adlershof, 1944, Bd. 11, Heft 10.

This cascade possesses wave drag determined according to known formulas for pitot losses in a system of two oblique shocks. Let us note that in a similar manner it is possible to obtain a cascade which consists of trapezoids (Fig. 10.67b) which has a higher solidity than the corresponding cascade of triangles.

§ 14. Construction of Supersonic Cascades with Mixed Flow

Let us move on now to the construction of supersonic cascades in which transition through the speed of sound occurs.

Let us first examine a convergent cascade of such type ($\lambda_1 < 1$, $\lambda_2 > 1$) which is employed in the nozzle (directing) cascades of turbines. Flow enters such a cascade at low subsonic velocity at an angle $\beta_1 = \pi/2$, and at exit from it becomes supersonic, directed under a given angle β_2 to the front of the cascade.

Let us examine one of the methods of the construction of such supersonic cascades lacking wave drag.¹ Flow in the vane channel is divided into two consecutive parts. First in the straight part, which is the usual Laval nozzle, flow is accelerated from the assigned subsonic velocity ($\lambda_1 < 1$) to a certain supersonic speed $\lambda_c < \lambda_2$. The turning of the flow through angle $\Delta\beta$ is achieved in the flow with expansion about the obtuse angle at which further acceleration of flow to λ_2 occurs. For this purpose, the lower wall of the nozzle (Fig. 10.68) is continued straight at angle $\Delta\beta$ to the nozzle axis, the upper wall is first continued parallel to the axis to point A of intersection with the characteristic in the nozzle exit section OK, and then along the flow line of the flow about apex O of an obtuse angle.

¹This method was proposed by author of the present Chapter in 1950.

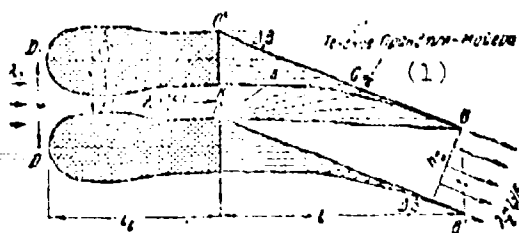


Fig. 10.58. Diagram of construction of intake guide cascade with transition through the speed of sound without wave drag and with turning only of the supersonic flow.

KEY: (1) Prandtl-Glauert flow.

If now at point E we conduct a tangent parallel line OB' to the intersection with the normal to the nozzle axis carried out through point O and again construct the outline of the straight nozzle so that its end point coincides with point O' , we then obtain a certain airfoil. Continuing this process of construction without limit, we form a guide cascade deflecting the flow to the given angle and imparting the necessary velocity.

The shape of this cascade will consist of three parts:

1) symmetrical airfoil $D_1C'KD_1$ whose outlines form a straight nozzle; 2) rectilinear triangle $C'KC$; 3) airfoil ABC of a two-parameter convergent cascade.

Cascades thus constructed ensure obtaining good uniformity of flow with pitch; their main disadvantage is the limitation on the size of the possible angle of turn of the flow.

For an increase in the total angle of turn of the flow, it should be achieved not only in the supersonic, but in the subsonic part of the vane channel (Fig. 10.69). With such grids, however, great nonuniformity of flow is created as a result of the difficulty of obtaining uniform velocity distribution in the throat to a Laval nozzle with a curvilinear axis. Nonuniformity increases, when, as so often is the case in practice, the entire assigned

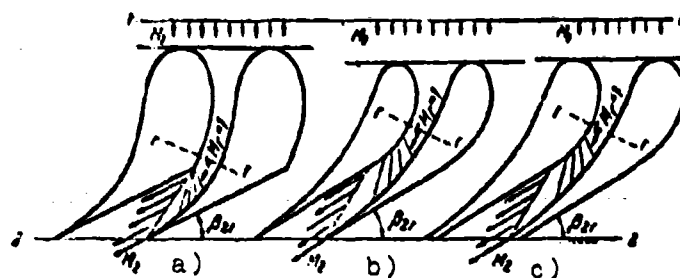


Fig. 10.69. Diagram of construction of intake guide cascades with transition through the speed of sound and with turning of flow in the subsonic and supersonic parts of the vane channel: a) with angular point; b) with smooth profiling; c) with finite thickness of trailing edge.

turn of the flow of the nozzle cascade is accomplished in the subsonic part of the vane channels. In this case, in the supersonic part of the vane channel consisting of half the usual flat symmetrical Laval nozzle, there occurs only acceleration of flow from the speed of sound to the assigned value of velocity on outlet from the grid (Fig. 10.70).

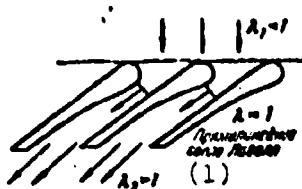


Fig. 10.70. Intake guide cascade with transition through the speed of sound and with turn of flow only in the subsonic part of the vane channel.

KEY: (1) Rectilinear Laval nozzle.

Flow in the oblique section of a supersonic nozzle cascade (Fig. 10.68) under off-design conditions is the same as in a cascade of plates with setting angle $\beta = \beta_{2r}$, being streamlined by a flow at zero angle of incidence with velocity coefficient $\lambda_1 = \lambda_{2p}$. This makes it possible with the aid of expressions (79) and (81) to determine the value and direction of the velocity in cross section 3-3 after the cascade (where the flow after mixing can already be considered uniform). The pitot losses in the

oblique section and with the subsequent equalizing of the flow are found from the equation of flow

$$q(\rho_p) \sin \beta_r = \gamma q(\rho_2) \sin \beta_r$$

As an example, Fig. 10.11 gives the parameters of the equalized flow after expansion in the oblique exit of such a cascade at different computed values of $\beta_2 = \beta_{2p}$ and M_{3pa} . These parameters are constructed depending on $\varepsilon = p_1/p_2$ - the pressure ratio far beyond the cascade p_2 to the calculated value of p_{3a} . It must be kept in mind that under design conditions $p_3 = p_{3p} = p_{2p}$.

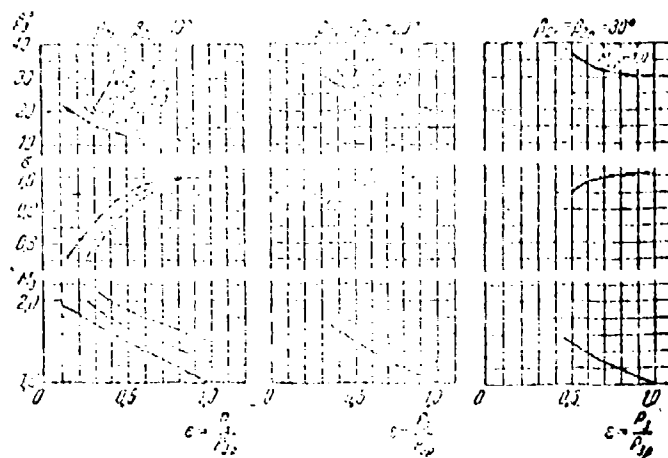


Fig. 10.11. Parameters of equalized flow after flow with expansion in the oblique exit of a cascade depending on the value of the pressure in section 3-3 located far beyond the cascade.

The dependence in Fig. 10.11 is constructed in the range of values $\varepsilon_{\min} \leq \varepsilon \leq 1$, where the value of ε_{\min} is determined from the condition $M_{3a} = 1.0$. At pressures p_2 , greater than calculated, there appears a system of oblique shocks which converts with a further pressure increase to a normal-type shock in the same way as it occurs during outflow from the nozzle (§ 1 Chapter VIII).

(With pressure after the cascade p_2 less than calculated, there is established flow with expansion in the oblique exit with which the beam of characteristics converges on the trailing edge of the airfoil. Unlike the isentropic outflow from a separate nozzle with oblique exit examined in Chapter IV, in the case of a nozzle cascade in the oblique exit the pitot losses appear in a certain shock wave system. These shocks are obtained as a result of interference between the nozzles which leads to overexpansion and subsequent compression of flow on exit from the cascade.

With sufficiently great counterpressure, the flow everywhere becomes subsonic; the presence in this case of an angular point on the airfoil causes local turbulence of flow, and connected with this, added losses and distortion of the velocity field at the edge of the cascade. To eliminate this deficiency, it is possible as with the profiling of purely supersonic cascades, to replace the broken line with a smooth line, for example, by the circular arc, or one of the flow lines of the flow about the angle (Fig. 10.69b).

(Another, structural deficiency in the airfoils in question is connected with the presence of a thin trailing edge. It can be easily overcome by construction of an airfoil with finite thickness of trailing edge Δ with a corresponding increase in pitch t and a decrease in velocity on entry (Fig. 10.69c). In this case one ought, however, to consider that as a result of equalizing of the velocity field after the cascade there will arise losses and turning of flow which can no longer be unambiguously defined from a Bernoulli equation, equations of momentum and flow in the same way as was done above for cascades with infinitely thin trailing edges. This is connected with the fact that in the momentum equation a new value will enter - static pressure on the airfoil edges p_n , which at supersonic flow velocity at the edge of the cascade requires special determining.

In practice, frequently for obtaining supersonic velocity after the nozzle cascade they are equipped with contracted channels, and for calculation the necessary calculated value of $M_2 > 1$, use is made of flow in the oblique exit which always occurs with cascade no. 1 in a flow from the front of the cascade. Therefore, to spin off flow in the vane channels of such cascades should be correspondingly increased (in comparison with the rated value of M_2). The value of the angle of deflection of flow can be approximately calculated with the aid of the expressions obtained¹ for cascade of plates on the assumption that $\beta = 0$ and $M_1 = 1$. The error of approximation of these formulas in connection with this, with a reservation is determined by the fact that 1) the plates in cascade have a finite thickness of the trailing edge; 2) the leading part of the vanes which find an oblique exit, is not always straight; 3) in the throat section the flow is not strictly uniform.

Let us consider now a cascade of plates cascades with transition through the speed of sound ($M_1 < 1$, $M_2 > 1$). The method of constructing such cascades is based on the fact that first in the supersonic part of the vane channel, in a shock or in a system of shocks the deceleration of flow of subsonic velocity is achieved. In the remaining subsonic part of the channel further deceleration of the subsonic flow occurs and the necessary turning is achieved.

Let us dwell on cascades with transition through the speed of sound in a normal shock. Figure 1.40 depicts a cascade of plates calculated for such a shock at the angle of incidence. In this case, on the vane there appears a normal shock also without change in the initial flow direction. In general, the necessary turn of flow through angle $\Delta\beta$ is achieved by means of bending the subsonic part of the vane channel. Thus, the design of the vane

¹See reference on page 139.

Reproduced from
best available copy.

consists of a rectilinear segment of length $l = l_p = t \cos \beta_1$ and combined with it a curvilinear small arc (Fig. 10.72). Given the angle of an equivalent plane diffuser α_g , it is possible to determine the necessary extent of the subsonic part of the channel. Approximately replacing the curvilinear axis of channel by the circular arc R_d and disregarding the angle of deviation, we obtain

$$\operatorname{tg} \frac{\alpha_g}{2} = \frac{t \sin \beta_2 - t \sin \beta_1}{2R_d \lambda_{d1}}$$

or

$$\frac{R_d}{t} \approx \frac{\sin \beta_2 - \sin \beta_1}{\alpha_g \lambda_{d1}}.$$

The value of α_g can be approximately selected from the data of blowing through plane diffusers with a velocity coefficient equal to its value λ_{d1} on entry to the subsonic part of the channel (Chapter VIII).

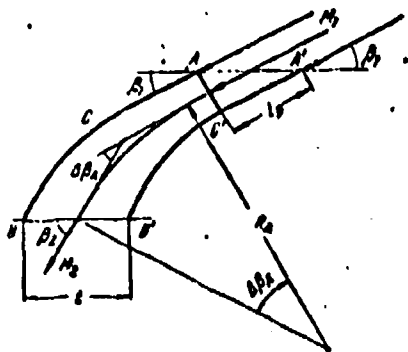


Fig. 10.72. Supersonic divergent cascade of infinitely thin airfoils with transition through the speed of sound in a normal shock.

The cascades of plates described above with normal shock on entry require, strictly speaking, infinitely thin leading edges. This condition in actuality can never be fulfilled, in consequence of which the design diagram of flow cannot be realized, since the basic property of a normal shock is disturbed - the equality of the transverse cross-section of the jet.

As a result, before the cascade a system of disconnected shock waves appears, similar to that which appears during flow at a positive angle of incidence ($\lambda_1 > 1$, $\lambda_{1a} < 1$) of cascades of

infinitely thin plates (Fig. 10.48), but with a specific picture of flow in the zone of flow around the leading edge.

With large values of number M_1 the losses in a normal shock increase substantially, and for the purpose of reducing them, just as in a supersonic diffuser, it is advantageous to achieve transition through the speed of sound in a system of oblique shocks with a terminal normal shock. Figure 10.73 depicts such a cascade with the simplest system of shocks (one oblique + a normal) calculated for number $M_1 = 2.0$. The intensity of the first oblique shock determined by the angle of turn at the leading edge of the airfoil is selected from the condition of minimum total loss in the system of shocks. Thus, the turn of the flow in the cascade is here achieved only in an oblique shock. Deceleration of subsonic flow in the vane channel is absent. It occurs in the process of turbulent mixing after the cascade and is accompanied by a change in the direction of flow, which reduces the total turn of flow in the cascade. The intensity of the losses and the additional turn which depend on the thickness of the trailing edges and Mach number after the normal shock can be determined on the basis of the condition of conservation of momentum in the space beyond the edge and with the aid of continuity and Bernoulli equations. For this, it is sufficient to use the expressions given in § 3, having first determined the values of the integrals entering there. In the case of the velocity distribution in question we have

$$\int \lambda_1 y(\lambda_1) d\bar{x} = h \lambda_1 y(\lambda_1), \quad \int y(\lambda_1) d\bar{x} = h y(\lambda_1)$$

and also

$$\lambda_{\infty} = \frac{\int \lambda_1 y(\lambda_1) d\bar{x}}{\int y(\lambda_1) d\bar{x}} \cos \beta_1 = \lambda_1 \cos \theta = \lambda_{1r}$$

Correspondingly, the coefficients of quadratic equation (29a) relative to $\sin^2 \beta_{\infty}$ can be presented in the form

$$h = \frac{\left(1 - \frac{2\gamma}{\gamma+1} M_\infty^2\right)^2 + \left(\frac{2}{\gamma+1} M_\infty^2 \sin^2 \theta + \frac{\gamma(\gamma-1)}{2} \cot^2 \theta\right)^2}{\left(1 - \frac{2\gamma}{\gamma+1} M_\infty^2\right)^2}$$

$$h = \frac{2\left(1 - \frac{2\gamma}{\gamma+1} M_\infty^2\right) + \left(\frac{2}{\gamma+1} M_\infty^2 \sin^2 \theta + \frac{\gamma(\gamma-1)}{2} \cot^2 \theta\right)^2}{\left(1 - \frac{2\gamma}{\gamma+1} M_\infty^2\right)^2}$$

The pitot losses are found from the equation of continuity

$$\frac{p_{02} - p_{01}}{p_{01}} = 1 - \frac{q(p_2) L_{02} A_2}{q(p_1) L_{01} A_1}$$

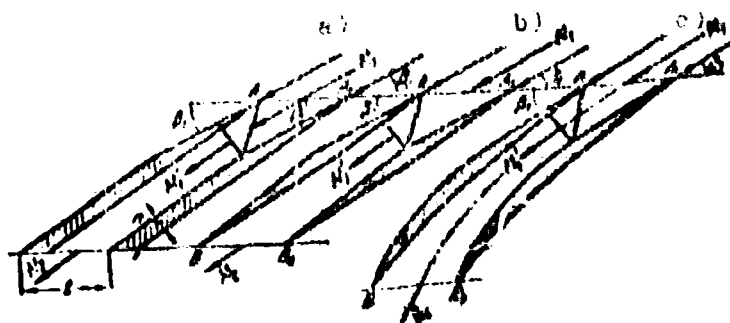


Fig. 10.73. Supersonic divergent cascade with transition through the speed of sound in a system of shocks: one oblique + a normal terminal; a) with flow velocity constant in value and direction in the subsonic part of the vane channel; b) with deceleration of flow in the subsonic part of the vane channel without turning it; c) with deceleration and turning of flow in the subsonic part of the vane channel.

If equalization of velocities in the space beyond the cascade occurred without simultaneous turning of the flow (for example with the aid of a second cascade of infinitely thin plates), then the losses would be equal to losses in a border shock. The calculations show that in magnitude these losses considerably exceed the losses which appear with equalizing of flow in free space beyond the cascade. This is especially easy to trace in an example of low values γ , when the compressibility of air can be

disregarded. In the case of an incompressible fluid we have
 $w_{\infty 1} = w_{2a}$, $w_{\infty 2} = w_{2a}(1 - \bar{\Delta})$, where $\bar{\Delta} = n/t \sin \phi$, and

$$\operatorname{tg} \beta_{\infty} = (1 - \bar{\Delta}) \operatorname{tg} \theta.$$

i.e., the greater the thickness of trailing edges, the greater the angle of deviation. Thus, for instance, with $\phi = 45^\circ$, value of the angle of deviation δ with $\bar{\Delta} = 0.1$ is 3° and increases to 10° with $\bar{\Delta} = 0.2$.

From the equation of the momentum in projection in an axial direction

$$M(w_{\infty 2} - w_{\infty 1}) = (p_1 - p_{\infty})t$$

it follows that

$$p_1 - p_{\infty} = \rho w_{\infty 1}(w_{\infty 1} - w_{\infty 2})$$

Thus, in the free space beyond the cascade

$$\Delta p_s = p_1 + \frac{\rho w_1^2}{2} - p_{\infty} - \frac{\rho w_{\infty}^2}{2} = \frac{\rho}{2} (w_{1s} - w_{\infty s})^2 = \frac{\rho}{2} w_{\infty s}^2 \bar{\Delta}^2.$$

The pitot losses during sudden expansion of the area of a rectilinear channel with $(t - h) \sin \phi$ to $t \sin \phi$ comprise (see Chapter I)

$$\Delta p_{es} = \frac{\rho}{2} (w_1 - w_{\infty})^2.$$

Since

$$w_{\infty} = w_1(1 - \bar{\Delta}),$$

then

$$\Delta p_{es} = \frac{\rho}{2} w_1^2 \bar{\Delta}^2.$$

From a comparison with the foregoing formula for pitot losses we have

$$\frac{\Delta p_s}{\Delta p_{es}} = \sin^2 \theta.$$

As we see, losses with the equalizing of flow in the free space beyond the cascade decrease in comparison with the losses by Borda shock in a corresponding rectilinear channel with a decrease in

angle δ . With large values of angle δ , the difference between these losses drops and becomes zero with $\delta = 90^\circ$. The latter result is the obvious consequence of the symmetry of flow in the free space beyond the cascade at such an angle of setting.

To reduce the angle of deviation, and therefore, to increase the effective angle of turn of the flow by the cascade, it is necessary to reduce the thickness of the trailing edges of the airfoils, additionally retarding the flow (after passage through the system of shocks) in a rectilinear subsonic diffuser (Fig. 10.73b). In so doing there will be a simultaneous decrease also in the losses by equalizing the flow in the space beyond the cascade.

At first, this reduction in losses will exceed the increase in the losses in the subsonic part of the vane channel and thus the total losses in the cascade will decrease. Subsequently, in proportion to the refining of the trailing edge of the airfoil and a corresponding increase in the expansion angle of diffuser it may prove that the increase in losses in the subsonic part of the vane channel will no longer be compensated for by a decrease in the losses by the equalizing of the flow after the cascade. In other words, with a certain optimum thickness of the trailing edges, the total losses in the cascade can become minimum. This is confirmed by experiments on rectilinear diffusers which show that in a number of cases the optimum is a staged diffuser in which deceleration of air is achieved first in the diffuser with less than initial, by the expansion angle, and then during sudden expansion.

The aforementioned considerations become even more essential in connection with subsonic divergent cascades where the relative percentage of intake losses is many times less. On the strength of these considerations, K. A. Ushakov proposed a subsonic divergent cascade composed of winged airfoils with blunt trailing edge. A decrease in the angle of turn of flow in such a cascade in comparison with a cascade of the usual shapes with sharp

trailing edge is compensated for by the large angle of bending of the center line of its airfoils. In general, the necessary turn of flow $\Delta\beta$ by a supersonic cascade is achieved as a result of deflection of the supersonic flow in an oblique shock $\Delta\beta_c = \nu$ and the deflection of the subsonic flow $\Delta\beta_d$ in the curvilinear subsonic part of the vane channel (Fig. 10.73c)

$$\Delta\beta = \Delta\beta_c + \Delta\beta_d = \nu + \Delta\beta_d$$

It is important to note that in a supersonic divergent cascade the presence of the angle of deviation has substantially less effect on the relative change in the value of Δw_u , and, consequently also circumferential force R_u proportional to it than in an incompressible flow. This is illustrated by the velocity triangles given in Fig. 10.74 constructed for a supersonic flow and an incompressible flow at one and the same entrance angles and equal angles of deviation.

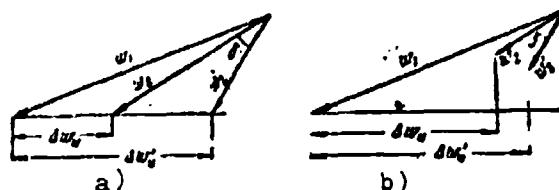


Fig. 10.74. Effect of angle of deviation on value of Δw_u : a) incompressible flow; b) supersonic flow before the cascade and deceleration in it to subsonic velocity.

The advantage in the type of cascades in question with oblique shock in comparison with cascades calculated for one normal shock consists not only of the fact that the flow through these cascades, especially with high M_1 numbers, occurs with less

losses,¹ but also in the fact that their airfoils have a finite thickness unlike the infinitely thin airfoils of which, strictly speaking, a cascade with normal shock on entry should consist. Among the deficiencies in the cascades in question one should include the difficulty of bringing them to a condition of flow corresponding to the design Mach number.

Figure 10.75 gives diagrams of flow both with design and with off-design M_1 numbers; the angle of incidence in all these cases is taken as design: $i = 0$. With an increase in the flow velocity in comparison with its design value the front of an oblique shock passes more sloping, and as a result, there appears interaction between this shock and flow with rarefaction which becomes complicated in proportion to the reflection of the shocks and characteristics from the walls of the vane channel (Fig. 10.75b). With a decrease in M_1 number, the front of the oblique jump passes more steeply, in consequence of which, flow with rarefaction interacts only with reflected shocks (Fig. 10.75c). Such a picture of flow is possible, however, only up to a specific M_1 number equal to the maximum M_1 number for flow around a wedge.

It is known that with Mach numbers less than maximum, the flow about a wedge with formation of an oblique shock becomes impossible, and at a certain distance from the apex of the wedge a disconnected shock wave is established. However if the flow about a unit wedge with a boundless decrease in M_1 number is nevertheless possible (only the picture of flow changes), then the possibility of flow about cascades composed of wedge-shaped airfoils is limited to a condition of flow choking in the narrow cross section of the vane channels.

¹In this case, they have in view only losses which appear in shocks (without allowing for the effect of viscosity). In an actual flow, the interaction of the falling shock with the boundary layer on the airfoil complicates the flow and does not make such an obvious gain in losses. A normal shock, although of greater intensity interacts with a thinner boundary layer than an oblique shock which passes within the channel.

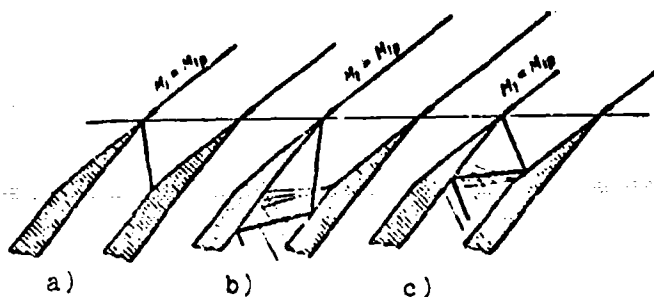


Fig. 10.75. Flow around a supersonic cascade of wedge-shaped airfoils: a) $M_1 = M_{1p}$; b) $M_1 > M_{1p}$; c) $M_1 < M_{1p}$.

On going to design conditions, i.e., during "starting" of the cascade there occurs a monotonic increase in M_1 number of incident flow from $M_1 = 1$ up to the design M_1 number. The limitation in minimum M_1 number makes it impossible to start the cascade without special adjustment similar to that which is employed in starting a wind tunnel with a supersonic diffuser.

Such adjustment in the cascade is simpler than in the wind tunnel, since it is possible to carry it out not only by reducing the area of the throat section of vane channels, but also by a corresponding reduction of area of the entering jet by means of an increase in the angle of incidence. Figure 10.76 for the cascade of wedges designed for number $M_{1p} = 1.5$ gives the dependences of the minimum angle of incidence i_{\min} , necessary for "starting" this cascade. One of the curves is constructed under assumption of isentropicity of flow, the other - taking into account losses in the shock waves computed according to (107). These dependences show that the presence of losses shows up noticeably in an increase in the minimum value of the angle of incidence. So, with $M_1 = 1.0$, the value of the minimum angle of incidence is equal to $\sim 4^\circ$ for an isentropic flow, and increases to 10° in the presence of losses.

Let us examine now some results of the experimental research on supersonic divergent cascades calculated for deceleration of

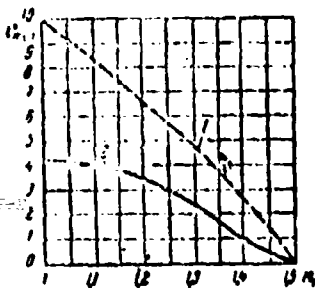


Fig. 10.76. Dependence of minimum angle of incidence on M_1 number for a two-shock divergent cascade with angle of wedge $\omega = 10^\circ$ ($\theta_{lp} = 30^\circ$, $M_{lp} = 1.5$): 1 - under the assumption of isentropicity of flow; 2 - taking into account the losses determined approximately according to formula (107) for a solid cascade of plates.

a supersonic flow with a subsonic axial component of velocity. Let us dwell on the experiments with an isolated vane channel carried out by S. I. Ginsburg and by L. A. Suslennikov. With a subsonic axial component of velocity such a replacement of an infinite cascade by a single channel having the same leading edges as for the cascade airfoil is valid only at zero angle of incidence and when length l_1 of the straight portion of convex surface is such that the characteristic which goes from the end of this segment does not emerge beyond the front of the cascade (Fig. 10.45).

Figure 10.77 depicts a cascade, the vane channel of which was tested at zero angle of incidence, with several values of M_1 numbers and various counterpressures. The cascade is designed for $M = 1.5$ and has an angle of taper of leading edge $\omega = 6^\circ$. The convex surface of the airfoil consists of a straight segment and combined with it a circular arc. The results of experiment are given in Fig. 10.78 which shows the distribution by section after the channel of the coefficient $\sigma = p_{02}/p_{01}$ of the values of number $M_1 = 1.36; 1.5; 1.65$. These data pertain to the design position of the terminal shock located directly after the first shock. Figure 10.78 shows that at all velocities of the incident flow the pitot losses in the flow core are comparatively small and close to the losses in the calculated system of shocks. With approach to the convex wall, the losses increase sharply, which is explained by the boundary-layer separation after the λ -shaped part of the terminal shock and the further development of separation

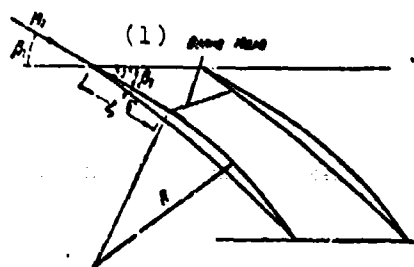


Fig. 10.77.

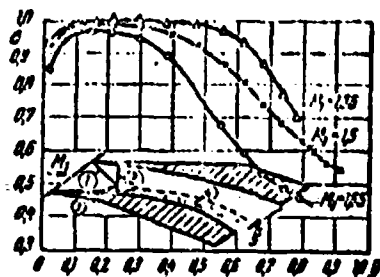


Fig. 10.78.

Fig. 10.77. Supersonic cascade of wedge-shaped airfoils, the vane channel of which was tested under isolated conditions.

KEY: (1) Mach wave.

Fig. 10.78. Distribution of the relative total pressure $\sigma = p_{02}/p_{01}$ according to pitch after the vane channel during design position of the terminal shock and various Mach numbers of incident flow: 1 - oblique shock; 2 - terminal normal shock; 3 - λ -shaped shock; 4 - zone of flow separation.

in the subsonic diffuser part of the channel. The latter circumstance is confirmed by the fact that during testing of another channel with the same supersonic part but with substantially less diffusivity of the subsonic section ($\alpha_3 = 1.5^\circ$ instead of $\alpha_3 = 7^\circ$) the drop in the total pressure begins considerably nearer to the convex wall and occurs considerably weaker than for the initial channel (Fig. 10.79). Averaging of the experimental data given in Fig. 10.78 gives the following mean values of the loss coefficient:

$$\Delta p_{0,sp} = \frac{p_{01} - p_{01sp}}{p_{01}} = 1 - \sigma_{sp}$$

M_1	1.36	1.50	1.65
$\Delta p_{0,sp}$	0.12	0.165	0.280

The increase in the pitot losses with an increase in the velocity of the incident flow is caused by the increase in the losses in the center section of the flow (connected directly with losses in the system of shocks) and by the increase of the intensity of the boundary-layer separation as a result of an increase in

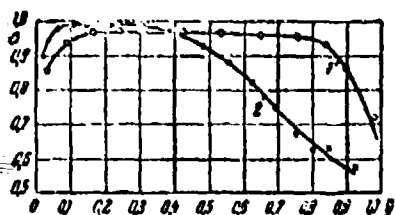


Fig. 10.79. Distribution of total pressure according to pitch after the vane channels of two supersonic cascades which differ only by the angle of the equivalent plane diffuser for the subsonic part of the vane channels with $M_1 = 1.5$, $i = 0$ and maximum counter-pressure: 1 - initial channel; 2 - channel with the reduced diffusivity of the subsonic part.

velocity before the terminal jump and its displacement downstream together with the point of fall in the oblique shock. The latter is characterized by displacement to the convex side of the channel of the point of steep drop in the distribution curve of total pressure for pitch after the channel (Fig. 10.78).

The results of investigation of another channel close in configuration with the same design number $M_1 = 1.5$, but with different positions of the terminal shock are given in Fig. 10.80. The smallest losses, as the graphs show, are observed in the design position of the shocks, when on entry to the vane channel one oblique shock and directly following it a normal terminal shock are used (curve 1). With a decrease in pressure in comparison with the designed, the shock moves downstream and losses begin to increase (curve 2) at first unessentially, and then very sharply and reach a value of $\Delta \bar{p}_{0\text{ cp}} = 0.24$ in the extreme position of the terminal shock (curve 3) instead of $\Delta \bar{p}_{0\text{ cp}} = 0.10$ at its calculated position. Such an increase of losses is connected with the increasing intensity of separation during movement of the shock in the diffuser channel. In this case, the separation appearing and developing at the convex wall of the channel leads to acceleration of flow at the opposite - the concave wall, and as a consequence of this, to a decrease in the losses in this zone of flow (curve 3). At the certain increased counterpressure on inlet to the channel there appears one normal shock instead of calculated system of two shocks. The replacement of two shocks by one shock of greater intensity produces an increase in the losses also in

the central and in the near-wall parts of the flow (curve 4, Fig. 10.80). The latter circumstance is the result of the interaction of the shock of greater intensity with the boundary layer.

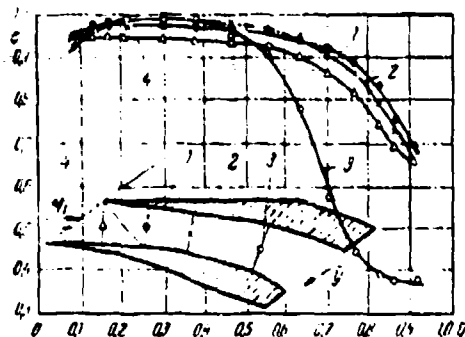


Fig. 10.80. Distribution of relative total pressure $\sigma = p_{02}/p_{01}$ according to pitch after the channel with $M_1 = 1.5$ and various positions of the terminal shock (symbols and numerals on the curves show the approximate location of the terminal shock).

Experimental research on the initial supersonic cascade (Fig. 10.77) with angles of incidence $\alpha \neq 0$ was carried out by L. A. Suslennikov¹ on a rotor with cylindrical form of blading and with the height of the blades composing a total of 0.1 part of the diameter. For such vanes a change in the flow parameters on a radius is so insignificant that it can be disregarded and to consider the rotor as revolving cascade with the constant flow parameters on a radius.

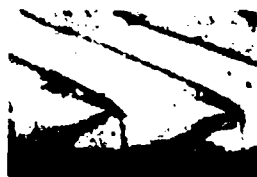
Instantaneous photographs of cascade flow obtained on a Toepler-Foucault instrument with the aid of cylindrical optics are given in Fig. 10.81.

From these photographs it is distinctly evident that before the cascade there is a periodic system of shock waves. Before the leading edge of each vane a curvilinear shock wave is established,

¹L. A. Suslennikov, The use of optical methods for studying flow in the blading rings of an axial-flow compressor. In a collection "Rotodynamic machines and jet apparatuses," issue I. "Mechanical Engineering," M., 1966.



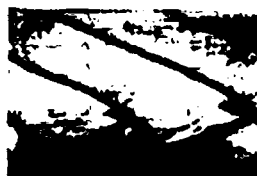
(1) *rotating wheel* (2) *No flow*



$M = 1.27$ $i = 2.7^\circ$



$M = 1.27$ $i = 3.3^\circ$



$M = 1.23$ $i = 3.9^\circ$



$M = 1.23$ $i = 4.5^\circ$

Fig. 10.81. Instantaneous Schlieren photographs of flow about a rotating wheel with wedge-shaped blades (rotating superersonic cascade) by a supersonic flow.
KEY: (1) Wheel is stationary; (2) No flow.

one of the branches of which departs forward, agitating the flow before the cascade, and the other branch drops on the airfoil of the adjacent vane. The form and the position of the shock waves depend on the angle of incidence.

With small angles of incidence the shock wave consists of two branches - one is located before the cascade and the second enters into the vane channel and represents essentially an oblique shock. As the angle of incidence, increases the shock wave is straightened, simultaneously moving upstream. At the greatest angle of incidence, the shock wave is close to the normal shock located at a noticeable distance from the leading edge of the airfoil.

§ 15. Certain Findings Regarding Spatial Flow Around a Single Airfoil and a Cascade of Airfoils

In the foregoing paragraphs we examined the flow of a plane-parallel fluid flow around an airfoil. Such a flow can be realized only on an infinite-span airfoil.

Let us now dwell on the basic questions of the theory of an airfoil of finite span. An infinite airfoil affects its circumfluent fluid flow as an infinite vortex filament. In other words, it may be considered that into the airfoil, as it were, a so-called bound vortex is placed. As is known from hydrodynamics, the vortex can terminate only on the boundaries of the flow or be closed. Therefore, a bound vortex cannot suddenly terminate on the tips of a finite-span airfoil (Fig. 10.82); its free ends, called vortex curls go beyond the limits of span l and being caught up by the general flow of the liquid, are extended over the flow lines into infinity.

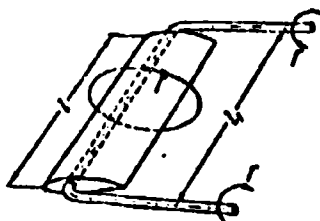


Fig. 10.82. Aerodynamic configuration of a finite-span airfoil with a horseshoe vortex of constant circulation.

If circulation around the airfoil is constant, then such a finite-span airfoil can be replaced by a horseshoe vortex. In actuality, the circulation over a finite-span airfoil usually changes, and in general, the airfoil can be replaced by a system of an infinite number of horseshoe vortices forming a continuous vortex sheet (Fig. 10.83) which, as studies show, is unstable and after the airfoil is turned into two vortex curls (Fig. 10.84). With an airfoil of rectangular form, the vortex curls run off mainly from the tips, therefore such an airfoil can be replaced approximately by one horseshoe vortex with constant circulation.

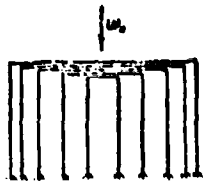


Fig. 10.83.



Fig. 10.84.

Fig. 10.83. Diagram of horseshoe vortices for an airfoil with variable circulation spanwise.

Fig. 10.84. Diagram of turning of a vortex sheet after an airfoil into two vortex curls.

Experiments confirm well the described hydrodynamic diagram of an airfoil of finite span. Taking into account the action of those vortices disappearing from the tips of the airfoil, it is possible to establish the effect of the span of the airfoil on its aerodynamic properties.

For this, the average induced velocity over the span of the airfoil being caused by vortex curls and usually called the downwash velocity w_{y0} is determined. It can be shown that

$$w_{y0} = -\frac{2}{\pi} \frac{b}{l} \alpha = -\frac{2}{\pi \lambda} \alpha$$

here the value $\lambda = l/b$ designates relative span, or aspect ratio.

Correspondingly, for the angle of downwash of flow $\Delta\alpha$ we have the following important formula of the theory of an airfoil of finite span¹:

$$\Delta\alpha = \frac{2}{\pi \lambda} \alpha$$

If the airfoil stands in a flow at an angle of attack α , then the true (aerodynamic) angle of attack comprises (Fig. 10.85)

$$\alpha_1 = \alpha - \Delta\alpha$$

¹See the more detailed presentation of the theory of an airfoil of finite span in B. N. Yur'yev's book "Experimental Aerodynamics," part II. Oborongiz, 1938.

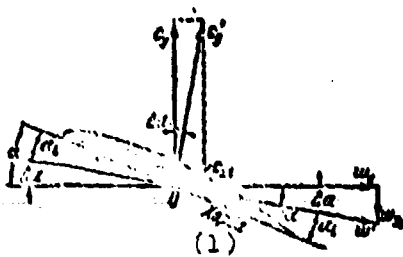


Fig. 10.85. Downwash after an airfoil of finite span.
KEY: (1) Chord.

For an infinite-span airfoil ($\lambda = \infty$) the angle of downwash is equal to zero ($\Delta\alpha = 0$), i.e., the true angle of attack is equal to apparent (α). The smaller the relative span of the airfoil λ , the greater the downwash angle, and therefore, the smaller the true angle of attack.

In connection with the downwash the lift vector of the airfoil is turned to the same angle $\Delta\alpha$, since its direction is always at right angles to the true direction of flow (Fig. 10.85). The projection of the lift of an airfoil of finite span¹ on the free-stream direction constitutes the force of so-called "induced drag":

$$R_{xi} = R_l \sin \Delta\alpha.$$

Converting to dimensionless quantities and taking into account the smallness of the downwash angle ($\sin \Delta\alpha \approx \Delta\alpha$), we obtain the formula for determining the so-called "coefficient of induced drag" of an airfoil of finite span

$$c_{xi} = c_l \Delta\alpha = \frac{c_l^2}{\pi\lambda}.$$

Thus, the effect of the finite span of the airfoil is expressed in the appearance of a special kind of (induced) drag even in the case of flow of an ideal fluid around an airfoil.

In view of the fact that the lift coefficient is proportional to the aerodynamic angle of attack, the expression for the

¹In view of the fact that the angles of downwash are small, lift with downwash barely changes ($c_l' \approx c_l$).

coefficient of induced drag in a subsonic flow of a compressible gas remains the same as in an incompressible fluid (at subsonic velocity the vortices running off from the tips of the airfoil, as before, affect the flow along the entire span of the airfoil).

During supersonic flow, the disturbing action of the end section of the airfoil is propagated only within a cone of weak disturbances with the apex in the leading edge of the end section. This leads to an essential decrease in the induced drag which, generally speaking, can be reduced to zero if the airfoil tips are cut so that the disturbance cones going out from the leading edges of the tip sections do not include within themselves elements of the airfoil. In this case, at supersonic flight speed all wing sections will be flowed around just as an infinite-span airfoil.

Earlier in the examination of an infinite-span airfoil it was assumed that the flow remains two-dimensional and that the direction of the approach stream velocity is at right angles to the leading edge of the airfoil. Let us examine now an infinite-span airfoil being blown at an angle to leading edge, or an airfoil equivalent to it which is moving in air with certain side slip characterized by angle β (Fig. 10.86). In this case, as before, we will consider that the airfoil chord and profile are constant along the span.

We shall break the total flow velocity w_1 down into two components: parallel to the leading edge and at right angles to it.

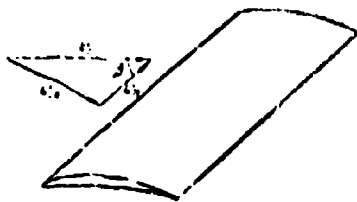


Fig. 10.86. Oblique flow about a wing.

Parallel to the span of the airfoil the velocity component $w_1 \cos \beta$ during flow about the airfoil does not change and therefore it has no effect on the pressure distribution over the airfoil which is determined only as the normal velocity component $w_1 \sin \beta$.

Thus, the side slip of an infinite-span airfoil does not affect pressure distribution over its surface. Consequently, the Mach number which determines the nature of flow about the airfoil is no longer the number $M_1 = w_1/a_1$ but the effective Mach number

$$M_{1\beta} = \frac{w_1 \sin \beta}{a_1} = M_1 \sin \beta$$

Thus, by giving the wing a swept-back form, it is possible, for example, to delay the moment of emergence of shock stall for a wing with this shape to high M_1 numbers. This method of reducing drag has found wide application in the practice of modern aircraft construction.

The presence of a velocity component along the span of a swept-back wing causes displacement of the boundary layer in this direction. This leads to a deterioration in the flow and to a decrease in the angle of stall at the tip profiles. In practice, for the elimination of this harmful effect of viscosity use is made of "combs" - projections along chord and preventing overflowing of the boundary layer.

Let us now examine certain questions of three-dimensional flow of a liquid in rotodynamic machines.

In those rotodynamic machines whose rims operate in virtually unrestricted flow (air and water propellers, windmills), from the tips of their blades, just as in a single airfoil of finite elongation, bound vortices run off. As a result, an additional induced drag appears the calculation of which, by comparison with a single airfoil, is complicated by the presence of mutual interference between the vortex curls running from the tip of each blade.¹

¹N. E. Joukowski, Vortex theory of a screw propeller. Tekhteorizdat, 1950.

Vortex curls of this type cannot arise in the turbomachines of other types (axial-flow compressors and fans, axial-flow turbines) which differ by the fact that their blades are limited at the ends by the surface of an annular channel.¹ As a result of this, the induced drag either does not appear at all or it has a secondary value.

The three-dimensional character of flow in the rotodynamic machines of the type in question is basically expressed in those limitations on possible distribution of flow parameters over the span of the blades which are imposed, for example, by one or another form of surface current adopted.² Friction on the walls of an annular channel, especially in the area of the vane channels, leads to amplifying the effect of viscosity on the character of three-dimensional flow.

As the simplest example having a direct relation to the phenomena which occur during flow by a flow of a viscous liquid about fixed vane channels, let us examine the flow about a cascade of straight airfoils of constant profile limited by two parallel planes normal to the generating lines of the airfoils (Fig. 10.87).

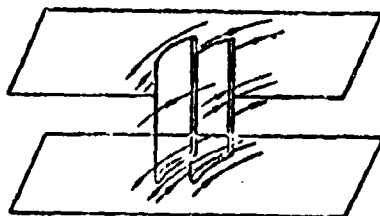


Fig. 10.87. Flow of a potential flow about a cascade of airfoils of finite aspect ratio located between two parallel planes.

In the case of an ideal inviscid fluid the flow in question is two-dimensional. This means that over the entire span of the

¹The very small radial clearances between the surface of the annular channel and the ends of the rotor wheel blades - rotating vane rings - can be disregarded.

²For greater detail see, for example, S. I. Ginsburg, Elements of gas dynamics of compressors and turbines, Chapter IX in the earlier edition of this book.

blade, including on the planes which limit the cascade, there is the same two-dimensional flow regardless of the amount of aspect ratio $\lambda = l/b$ constituting this cascade.

With the usual angles of incidence the pressure on the convex wall of the airfoil is always less than on the concave. As a result, in the vane channel the forces of pressure increase in direction from the convex to the concave surfaces of the airfoils. In a flow of inviscid liquid and gas this pressure gradient is completely balanced by the centrifugal force which appears during the motion of particles along curved paths (Fig. 10.38)

$$\frac{\partial p}{\partial n} \Delta n \Delta F = \Delta m \frac{w^2}{R}.$$

Here R - the radius of curvature of the flow line at the given point. Taking into account the fact that $\Delta m = \rho \Delta n \Delta F$, we have

$$\frac{1}{\rho} \frac{\partial p}{\partial n} = \frac{w^2}{R}.$$

As has already been indicated, during non-separating flow the viscosity effect is limited to a thin surface layer. Outside this layer the flow differs little from the flow of an ideal fluid. Hence it follows that the viscosity effect barely shows up in the flow in the middle sections - it remains virtually undisturbed.

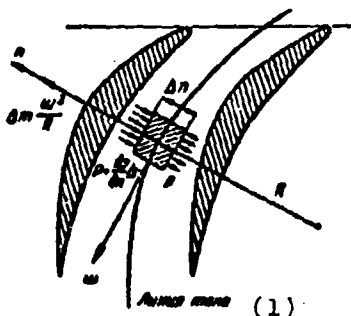


Fig. 10.88. Flow in a plane curvilinear vane channel.
KEY: (1) Flow line.

The greatest disturbances of flow will occur in the boundary layer of flat walls which limit flow. A decrease in the velocity in this layer leads to the fact that the pressure gradient, which in the boundary layer remains the same as in the core of the flow, will no longer be balanced by centrifugal force. Because of this,

in the boundary layer overflowing of fluid will begin in the direction of the pressure gradient - from concave wall to convex. The intensity of this overflowing will increase in proportion to proximity to the wall. Falling on the convex surface of the airfoil, part of this fluid will be taken away by the main flow. As a result, at the upper and lower surface there will arise two vortices of identical intensity, but with counterrotation (Fig. 10.89). Such a vortex system is called a *paired vortex*. The expenditure of energy on vortex formation leads to pitot losses, i.e., to the emergence of additional, so-called "secondary losses."

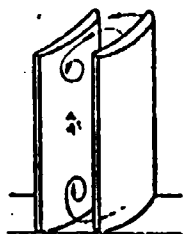


Fig. 10.89. Formation of a paired vortex during flow of a viscous flow about a cascade of airfoils located between two parallel planes.

Figure 10.90 shows the distribution of the loss coefficient over the span of the vane for impulse and convergent cascades.¹ In the middle part of the vane the losses are connected only with the flow about the airfoil and therefore are constant over the span. They are called profile losses. The losses connected with vortex formation and flow at the walls have a local character and down to a certain minimum value of aspect ratio do not depend on it. In other words, the relative percentage

of tip losses decreases linearly with an increase in aspect ratio. In proportion to the decrease in the aspect ratio, the vortex regions come together and with a certain λ_{\min} only one area of increased losses is detected, located in the middle sections of the vane. Figure 10.91 gives the dependence¹ of λ_{\min} on the value

$$\bar{\Delta p_t} = \frac{p_1 - p_2}{\rho \frac{u_1^2}{2}}.$$

¹M. Ye. Deutsch, T. S. Samoylovich, Fundamentals of aerodynamics of axial turbomachines. M., Mashgiz, 1959.

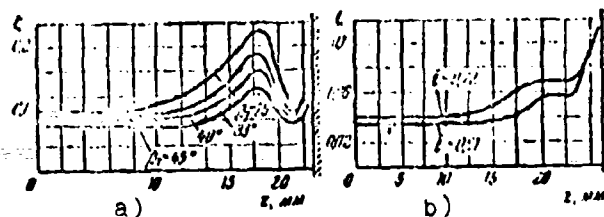


Fig. 10.90. Distribution of losses over the span of an airfoil in a cascade: a) impulse cascade with $\lambda = 2.25$; b) convergent cascade with $\lambda = 1.2$; z - distance from the mid-span section.

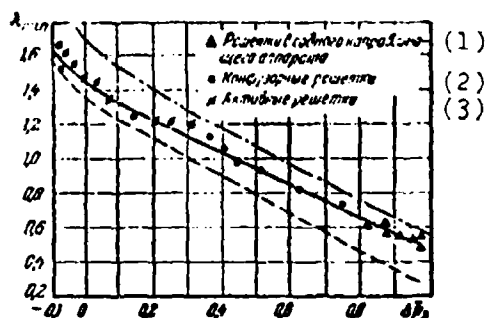


Fig. 10.91. Dependence of minimum aspect ratio of the airfoils of a cascade λ_{\min} with which joining of secondary flows occurs from Δp_2 .

KEY: (1) Cascades of intake guide device; (2) Convergent cascades; (3) Impulse cascades.

The graph in Fig. 10.91 shows that with an increase in $\overline{\Delta p}_2$ a drop in λ_{\min} occurs which indirectly testifies to a decrease in the intensity of vortex formation. This is connected with the increase in the convergent effect, i.e., with a general acceleration of flow which leads to a decrease in the boundary layer thickness and thus to weakening of the viscosity effect. With a decrease in $\overline{\Delta p}_2$, especially when this value becomes negative and flow becomes divergent, the reverse effect is observed.

In a direct diffuser cascade, as during any flow with deceleration, a considerable portion of the losses is usually caused by the emergence of flow separations. In the same way as for evaluating the degree of total diffusivity of a two-dimensional cascade in § 3 the concept of an equivalent two-dimensional rectilinear diffuser was introduced here, in the presence of a

three-dimensional character of flow, as one of the estimates, in a number of cases the representation of an equivalent circular diffuser is employed which was first introduced in connection with rotodynamic machines by K. A. Ushakov. The equivalent circular diffuser (Fig. 10.92) has an extent equal to the length of the center line of the vane channel and its sections F_1 and F_2 are equivalent to the corresponding flow areas before the cascade and after it

$$\left. \begin{aligned} F_1 &= \pi R^2 \sin^2 \beta_1 = \frac{\pi l^2}{4}, \\ F_2 &= \pi R^2 \sin^2 \beta_2 = \frac{\pi l^2}{4}. \end{aligned} \right\} \quad (120)$$

The expansion angle of the equivalent circular diffuser is determined from the obvious relationship

$$\tan^2 \frac{\alpha}{2} = \frac{F_2 - F_1}{S^2}.$$

Taking into account that α is small for not very curved channels $S \approx b$, according to (120) we have

$$\alpha = \frac{V_2}{V_1} \sqrt{\frac{F_2 - F_1}{b^2}} = \frac{V_2}{V_1} \sqrt{\sin^2 \beta_2 - \sin^2 \beta_1} \quad (121)$$

Thus, the angle of the equivalent diffuser is proportional to the root from the aspect ratio of the airfoils and inversely proportional to the root from the solidity of the cascade.

In a limited range of change in the cascade parameters, the application of the concept about an equivalent circular diffuser turned out to be sufficiently effective. Specifically, with the aid of this concept it was possible to explain the fact observed in practice of the increase of losses in a diffuser circular grid with an increase in the aspect ratio of the vanes. However, the use of angle α_k as the parameter of diffusivity over a wide range of change in the geometry of the cascade and airfoil encounters serious difficulties. Thus, for instance, from expression (121) it follows that with an increase in aspect ratio, the angle α_k monotonically increases. Meanwhile, from general considerations it is clear that with an increase in aspect ratio the effect of

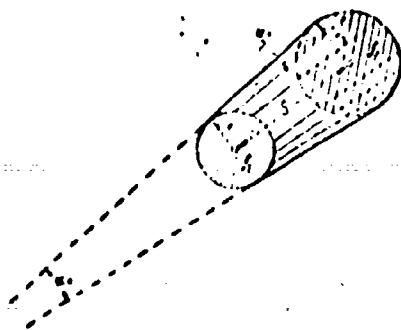


Fig. 10.92. Circular diffuser equivalent to the vane channel of a divergent cascade of airfoils of finite aspect ratio.

end effects decreases and with the tendency of elongation of vanes to infinity, the flow becomes two-dimensional, and therefore, the expression for the parameter of diffusivity should convert to expression (87) for the equivalent plane diffuser of a cascade of airfoils. Such nonconformity is the result of the replacement of this channel by an equivalent channel of different configuration. If, in the same way as was done for a foil cascade, the equivalent channel is constructed by means of straightening this vane channel (Fig. 10.93) and its diffusivity, following Ye. A. Lokshtanov, we characterize by a certain average in swept area F the value of the angle

$$\varphi_{cp} = \frac{1}{F} \int_F \varphi dF \quad (122)$$

(φ - the angle between the element of area and axis of the channel), then with a monotonic increase in aspect ratio φ_{cp} will approach a certain finite quantity equal to value of φ_{cp} for a foil cascade of airfoils.

If angles φ are small then (Fig. 10.93)

$$\varphi_{cp} = \frac{1}{F} \int \sin \varphi dF = \frac{f_2 - f_1}{SU_{cp}} \quad (123)$$

Here S is the length of the channel, U_{cp} - its average perimeter.

Substituting in (123) the values

$$f_1 = l \sin \beta_1, \quad f_2 = l \sin \beta_2$$

$$U_{cp} = \frac{U_1 + U_2}{2} = 2l + l(\sin \beta_1 + \sin \beta_2)$$

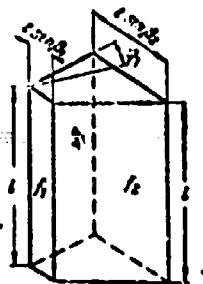


Fig. 10.93. Tetrahedral rectilinear symmetrical channel equivalent to the vane channel of a diffuser cascade of airfoils of finite aspect ratio.

and assuming that $S \approx b$, we obtain

$$\varphi_{cp} = \frac{l (\sin \beta_1 - \sin \beta_2)}{b \left[2 + \frac{h}{l} (\sin \beta_1 + \sin \beta_2) \right]}.$$

This expression, taking into account (87), can be written thus:

$$\varphi_{cp} = \frac{2}{2 + \frac{1}{\lambda b/l} (\sin \beta_1 + \sin \beta_2)} \varphi_v.$$

With an increase in aspect ratio ϕ_{cp} monotonically increases with λ , approaching infinity, it approaches its maximum value - the lateral angle of the equivalent plane diffuser ϕ_g for this airfoil cascade. For an incompressible fluid we have

$$\frac{f_2}{f_1} = \frac{w_1}{w_2} = \frac{w_1 - w_2}{w_2} + 1 = \frac{\Delta w}{w_2} + 1$$

and correspondingly

$$\varphi_{cp} = \frac{f_1}{F} \left(\frac{f_2}{f_1} - 1 \right) = \frac{\Delta w w_2}{F f_1}.$$

The numerator here characterizes the degree of deceleration of flow, and the denominator determines by itself the relative extent of the channel. Thus, the value ϕ_{cp} determines the average velocity gradient, and therefore, the static pressure. Therefore ϕ_{cp} can be considered the measure of the aerodynamic load state of a divergent cascade of airfoils. With an increase in aspect ratio the aerodynamic load state grows, and consequently, separation losses increase. In this case it is necessary to bear in mind, as has already been indicated above, an increase in aspect ratio leads to a relative decrease in the secondary losses connected with the formation of a paired vortex. Hence, it follows that with a certain optimum aspect ratio λ_{opt} the value of the total losses becomes minimum.¹ With $\lambda < \lambda_{opt}$ an increase in

¹As experimental studies show, in a number of cases the optimum aspect ratio of divergent cascades is close to one.

elongation leads to a decrease in total losses, since here the losses to vortex formation will be determining. With $\lambda > \lambda_{crit}$ the profile losses become determining and, correspondingly, an increase in the total pitot losses.

It is another matter in a convergent grid. Here, as a rule, flow is nonseparable and the total losses are determined only by friction losses and by losses to the formation of the paired vortex. Therefore, an increase in the aspect ratio wings constituting a convergent cascade leads to a monotonic decrease in total losses.

Such a distinction in the nature of the effect of aspect ratio on the total losses in divergent and convergent grids is confirmed both by results of experimental research on them and also by the practice of compressor and turbine construction.

CHAPTER XI

HYPERSONIC GAS FLOWS

§ 1. Change in the Parameters of a Gas in an Isentropic Hypersonic Flow

Gas flows at a velocity which considerably exceeds the speed of sound, sometimes called hypersonic flows, possess a series of distinctive features.

Let us express in an explicit form the influence of a change in the rate of flow on the basic parameters of a gas.

In a unit stream of gas in the absence of losses and external work according to the equation of Bernoulli (52) of Chapter I we have

$$dp = -\rho w dw.$$

Hence with the help of the known expression for the speed of sound (34) of Chapter I we obtain the relationship which connects pressure change with the velocity change

$$\frac{dp}{p} = -\lambda M^2 \frac{dw}{w}. \quad (1)$$

The equation of conservation of enthalpy of a stream during adiabatic flow can be presented in the form

$$dT = -\frac{k-1}{kR} \omega d\omega.$$

After simple conversions from here follows

$$\frac{dT}{T} = 2 \frac{d\omega}{\omega} = -(k-1) M^2 \frac{d\omega}{\omega}. \quad (2)$$

Differentiating the equation of state of an ideal gas and utilizing relationships (1) and (2), we obtain a similar dependence for the density change

$$\frac{dp}{p} = \frac{dp}{\rho} - \frac{dT}{T} = -M^2 \frac{d\omega}{\omega}. \quad (3)$$

Differentiating the equality $w = Ma$ and expressing the speed of sound through the gas temperature, we find with the help of (2) the relationship

$$\frac{dM}{M} = \left(1 + \frac{k-1}{2} M^2\right) \frac{d\omega}{\omega}. \quad (4)$$

Relationships (1)-(4) show that at subsonic speeds ($M < 1$) an insignificant change of pressure, density, and temperature of the gas occurs with a change in velocity, but the Mach number depends on velocity linearly. On the contrary, at hypersonic speeds ($M \gg 1$) even a small change in the rate of flow leads to a noticeable change in the state of the gas and Mach number.

With $M \gg 1$ in the right side of expression (4) it is possible to disregard unity, then we have

$$\frac{dM}{M} \approx \frac{k-1}{2} M^2 \frac{d\omega}{\omega}. \quad (5)$$

Eliminating from (1) and (5) the factor $d\omega/\omega$ and carrying out integration, we obtain the characteristic, for hypersonic flows, dependence of pressure on Mach number

$$\frac{p}{p_\infty} = \left(\frac{M_\infty}{M}\right)^{\frac{2k}{k-1}}. \quad (6)$$

From (2) and (5) in a similar manner the dependence of temperature on the Mach number is derived

$$\frac{T}{T_0} = \left(\frac{M_0}{M}\right)^2. \quad (7)$$

From which follow the corresponding expressions for the speed of sound

$$\frac{a}{a_0} = \frac{M_0}{M} \quad (8)$$

and the gas density

$$\frac{\rho}{\rho_0} = \left(\frac{M_0}{M}\right)^{\frac{2}{\gamma-1}}. \quad (9)$$

Integrating expression (5), we establish the connection between the flow velocity and the Mach number

$$\frac{w}{w_0} \sim 1 + \left(\frac{1}{M_0^2} - \frac{1}{M^2}\right) \frac{1}{\gamma-1}. \quad (10)$$

During the derivation of equation (10) the function $\ln w/w_0$ was expanded in a series by degrees $(w/w_0 - 1)$, whereupon in view of the proximity of relation w/w_0 to unity all the nonlinear terms of this series were rejected.

In expressions (6)-(10) the values without indices correspond to the current values of the parameters of the gas, and the values with the index "0" - to their initial values.

§ 2. Hypersonic Flow Around a Convex Obtuse Angle

Let us examine the features of flow at a very high speed around a convex obtuse angle - the hypersonic Prandtl-Mayer flow (Fig. 11.1). The mass flow per second of the gas between the arbitrary flow line and the pole of flow 0 is constant and can be

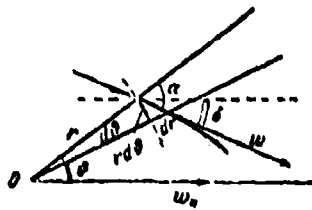


Fig. 11.1. Diagram of a flow around a convex angle.

calculated by the velocity component normal to the characteristic, which is equal to the speed of sound

$$\rho a r = \text{const.}$$

Hence after differentiation we have

$$\frac{dp}{p} + \frac{da}{a} + \frac{dr}{r} = 0. \quad (11)$$

The Mach angle (between the flow line and the characteristic) in the case of hypersonic speed ($M \gg 1$) is determined by the following approximate dependence:

$$\alpha = \arcsin \frac{1}{M} \approx \frac{1}{M}. \quad (12)$$

If δ is the angle of deflection of flow from the initial direction, and θ is the angle between the assigned characteristic and the initial flow direction, then obviously

$$\theta = \alpha + \delta = \frac{1}{M} + \delta. \quad (13)$$

Here it is taken into consideration that the reference directions of angles α and δ are opposite ($\alpha > 0$, $\delta < 0$, since reading is counterclockwise).

Figure 11.1 shows that

$$\frac{1}{r} \frac{dr}{d\theta} = \frac{dr}{r d\theta} = -\cot \alpha = -M, \quad (14)$$

since with $M \gg 1$ according to (12)

$$\alpha \approx \frac{1}{M^2} \approx M$$

Substituting (14) in (11) we have

$$\frac{d}{dx} + \frac{d}{dx} - M \frac{d}{dx} = 0$$

from which on the basis of (2), (3), and (5) we obtain

$$\frac{d}{dx} = \frac{1}{M^2} \frac{dM}{dx}$$

Integrating this equation and taking into account relationships (12) and (13) when to the initial value $\alpha = \alpha_0$ answers $\delta_0 = 0$, we obtain for hypersonic flow the following connection between Mach number and the angle of a deviation of the flow:

$$\delta = \frac{1}{2} \left(\frac{1}{M} - \frac{1}{M_0} \right); \quad (15)$$

here M and M_0 are the current and initial values of Mach number. Solving equation (15) relative to the current value of the Mach number

$$\frac{1}{M} = \left(1 + \frac{2}{M_0} \right) \delta, \quad (16)$$

and substituting this value into expressions (6)-(10), we will obtain formulas for determining the current values of pressure, density, temperature, speed of sound, and flow velocity during hypersonic flow around a convex obtuse angle.

Specifically for pressure we have

$$\frac{p}{p_0} = \left(1 + \frac{2}{M_0} \delta \right)^{-\frac{2}{\gamma-1}}. \quad (17)$$

The calculations show that all the formulas obtained thusly are accurate with $M_1 > 5$

The maximum angle of deviation of flow δ_{np} corresponds to the expansion of gas to total pressure (p = 0). Then from (16) we have

$$\delta_{np} = -\frac{2}{(k-1)M_1^2} \quad (17)$$

let us recall that during a clockwise deviation in the flow the angle is considered negative ($\delta < 0$).

As we see, the product of the angle of deviation of flow by the initial value of the Mach number $M_1 \delta$, which enters into all the design equations as the combined value, is the basic parameter which determines this flow.

If we are restricted to the case of a low deviation in the flow around a convex obtuse angle and present a change in the full speed as a disturbance which is characterized by the appearance of two supplementary velocity components u and v , then as it follows from Fig. 11.2,

$$w_1 + u = w \cos \delta, \quad v = w \sin \delta \quad (18)$$

At small angles of deflection of flow

$$\cos \delta \approx 1 - \frac{\delta^2}{2}, \quad \sin \delta \approx \delta,$$

therefore

$$u = w \left(1 - \frac{\delta^2}{2}\right) - w_1, \quad v = w \delta \quad (19)$$

Hence with the help of (10) and (15a) we obtain

$$\frac{u}{w_1} = -\left(\frac{1}{M_1^2} - \frac{k+1}{4}\right)\delta^2, \quad \frac{v}{w_1} = \delta \quad (20)$$

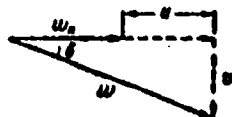


Fig. 11.2. Diagram of the vectors of velocity and disturbances during a deviation of flow around a convex angle.

In the first of these expressions as a result of smallness the terms with factors δ^3 and δ^4 are rejected, in the second - with factors δ^2 and δ^3 .

As we see, in hypersonic flow near a convex angle the transverse disturbance of flow velocity exceeds by at least an order the longitudinal disturbance ($v \gg u$). This means that during the flow there was a seemingly particle displacement along the normal to the direction of undisturbed flow and the value of the longitudinal velocity virtually does not change.

§ 3. Plane Shock Wave in a Hypersonic Flow

Let us pause now on the relationships which characterize a plane shock wave which appears during flow around a concave obtuse angle at hypersonic speed. In a plane oblique shock wave a density the change according to (47) of Chapter III will be

$$\frac{\rho}{\rho_n} = \frac{\frac{k+1}{k-1}}{1 + \frac{2}{k-1} M_n^2 \sin^2 \alpha}. \quad (21)$$

Here α is the angle of inclination of the shock front to the velocity vector w_n .

Pressure change in such a wave according to (45) of Chapter III

$$\left. \begin{aligned} \frac{p}{p_n} &= \frac{2k}{k+1} M_n^2 \sin^2 \alpha - \frac{k-1}{k+1} \\ \text{or} \quad \frac{p-p_n}{\rho_n w_n^2} &= \frac{2}{k+1} \left(\sin^2 \alpha - \frac{1}{M_n^2} \right). \end{aligned} \right\} \quad (22)$$

The dependence of the angle of deflection of flow in a shock wave on the slope of front α is determined from (50) of Chapter III

$$\omega = \alpha - \beta, \quad \operatorname{tg} \beta = \frac{k-1}{k+1} \left(1 + \frac{2}{k-1} \frac{1}{M_1^2 \sin^2 \alpha} \right) \operatorname{tg} \alpha, \quad (23)$$

where β is the angle between vectors of velocity behind the shock wave and the front of the latter.

From here we obtain after the elementary conversions

$$\operatorname{tg} \omega = \operatorname{ctg} \alpha \frac{\sin^2 \alpha - \frac{1}{M_1^2}}{\frac{k+1}{2} - \left(\sin^2 \alpha - \frac{1}{M_1^2} \right)}. \quad (24)$$

From (21) and (22) with the help of the equation of state it is possible to derive the appropriate dependences for the relation of temperatures and values of the speed of sound in a shock wave.

The velocity disturbances in a shock wave (u, v) we find from the obvious relationships

$$u = w \cos \omega - w_n, \quad v = w \sin \omega, \quad (25)$$

whereupon in accordance with the deflection circuit of velocities in a shock wave (Fig. 11.3) we have

$$u = w_n \left(\frac{\cos \alpha \cos \omega}{\cos \beta} - 1 \right), \quad v = w_n \frac{\cos \alpha}{\cos \beta} \sin \omega. \quad (26)$$

Replacing $\cos \beta = \cos (\alpha - \omega)$, after elementary conversions we obtain

$$\begin{aligned} v &= w_n \frac{2}{k+1} \operatorname{ctg} \alpha \left(\sin^2 \alpha - \frac{1}{M_1^2} \right), \\ u &= -w_n \frac{2}{k+1} \left(\sin^2 \alpha - \frac{1}{M_1^2} \right). \end{aligned} \quad (27)$$

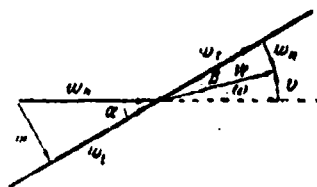


Fig. 11.3. The deflection diagram of flow in a shock wave.

From relationship (24) it follows that at hypersonic speeds ($M_H > 5$) the angle of inclination of the shock front α is close to the angle of deviation of the flow in the shock ω , in connection with which the layer of the condensed gas found between the shock front and the body surface turns out to be very fine.

In sufficiently intensive shock waves ($p/p_H \gg 10$) there is always the inequality

$$\sin \alpha > \frac{1}{M_H}. \quad (28)$$

At any arbitrary small fixed value of the angle of deflection of flow ω it is possible to achieve such a value of the Mach number at which condition (28) will be executed. Consequently in relationships (21)-(27) it is possible to disregard terms $1/M_H^2$, and then it will turn out that the dimensionless values of the velocity disturbances u/w_H , v/w_H , dimensionless density ρ/ρ_H , and the angle of inclination of the shock front α do not depend on M_H , but the dimensionless values of pressure p/p_H (and temperature T/T_H) are proportional to value M_H^2 :

$$\left. \begin{aligned} \frac{u}{w_H} &= -\frac{2}{k+1} \sin^2 \alpha, & \frac{v}{w_H} &= \frac{2}{k+1} \sin \alpha \cos \alpha, \\ \frac{p-p_H}{\rho_H w_H^2} &= \frac{2}{k+1} \sin^2 \alpha \quad \text{or} \quad \frac{p}{\rho_H} = \frac{2k}{k+1} M_H^2 \sin^2 \alpha, \\ \frac{\rho}{\rho_H} &= \frac{k+1}{k-1}, & \tan \omega &= \frac{\frac{2}{k+1} \sin \alpha \cos \alpha}{1 - \frac{2}{k+1} \sin^2 \alpha}. \end{aligned} \right\} \quad (29)$$

Thus at high hypersonic speeds in the area behind intensive shock waves a certain limiting condition of the gas flow is observed. During this its characteristic dimensionless parameters

and the aerodynamic coefficients do not depend on the value of the M_H number. We observed similar features of gas flow at very low - subsonic - speeds ($M_H \rightarrow 0$), when the properties of flow also do not depend on value M_H (incompressible liquid).

Experiments show that the indicated limiting condition of gas flow (with $M_H \rightarrow \infty$) is reached virtually at comparatively moderate values of M_H number.

Testifying to this, for example, are the experimental dependences of the resistance coefficients $c_x(M_H)$ of a sphere and cylinder with a conical nose section as depicted in Fig. 11.4; as we see, already with $M = 3-4$ the values c_x are very close to asymptotic, corresponding to $M_H \rightarrow \infty$; the stability of the values of aerodynamic coefficients testifies to the invariability of the entire picture of gas flow near a body.

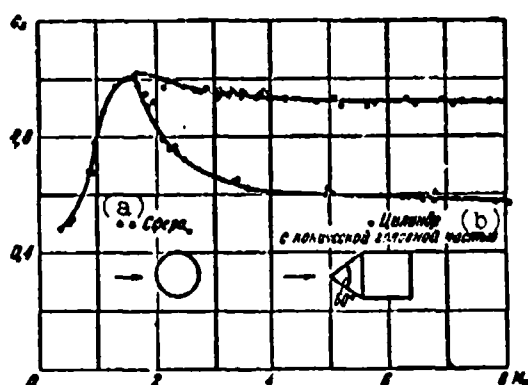


Fig. 11.4. The dependence of the drag coefficients of a sphere and cylinder with a conical forward section on the Mach number.
KEY: (a) Sphere; (b) Cylinder with conical nose section.

A general strict proof of the indicated self-similarity of flows at high supersonic speed was given for the first time by S. V. Valander in 1949.¹

¹See Chernyy, G. G. Gas flows at high supersonic speed. Fizmatgiz, 1960.

If the shock wave is insufficiently intensive, i.e., the angle of deviation of flow ω in it is small, then at hypersonic speed angle α is also small; carrying out the substitutions

$$\sin \alpha \approx \alpha, \quad \sin \omega \approx \omega, \quad \cos \alpha \approx 1, \quad \cos \omega \approx 1,$$

and designating $\alpha M_H = K_\alpha$, $\omega M_H = K_\omega$, we will obtain from (24)

$$\omega = \frac{1 - K_\alpha^2}{\frac{k+1}{2} - \frac{1}{K_\alpha^2}} \quad (30)$$

from which with $\alpha \ll 1$

$$K_\omega = \frac{k+1}{2} K_\alpha + \sqrt{\left(\frac{k+1}{2} K_\alpha\right)^2 + 1}. \quad (31)$$

Correspondingly from equality (21) we obtain

$$\frac{p}{p_0} = \frac{\frac{k+1}{2}}{1 + \frac{k-1}{2} K_\omega^2}. \quad (32)$$

from equality (22)

$$\frac{p}{p_0} = 1 + \frac{2k}{k+1} (K_\omega^2 - 1) \quad (33)$$

from equalities (27)

$$\frac{u}{u_0} = -\frac{2}{k+1} \frac{K_\omega^2 - 1}{K_\omega^2}, \quad \text{and} \quad \frac{v}{u_0} = 1. \quad (34)$$

Now we find the Mach number behind the shock wave

$$M' = M_1 \frac{u'}{u_1} \frac{p_1}{p_0}. \quad (35)$$

As it follows from (34), in the case of hypersonic flow the relative gas velocity on a shock at a narrow angle of the latter barely changes ($w \approx w_H$). Then from (35) with the help of (32) and (33) we obtain

$$\frac{M_2^2}{M_1^2} \approx \left[\frac{2k}{k+1} M_{1\alpha}^2 - \frac{k-1}{k+1} \right] \left[\frac{k-1}{k+1} + \frac{2}{k+1} M_{1\alpha}^2 \right]. \quad (36)$$

In the extreme case, when $M_H \rightarrow \infty$, we have

$$M = \frac{k+1}{2} \frac{1}{\sqrt{2k(k-1)}}.$$

With $M_H \rightarrow \infty$ according to (31) $\alpha = \omega(k+1)/2$, therefore

$$M = \frac{1}{2} \sqrt{\frac{2}{k(k-1)}}. \quad (37)$$

In other words, in the case $M_H \rightarrow \infty$ at low slope angles of shock α the Mach number behind the shock will be large. If the shock is of low intensity, then the Mach numbers before and behind the shock at hypersonic speed have a value of the same order.

In the examination of Prandtl-Mayer flow (§ 2) we represented all the parameters in the function of the angle of deflection of flow, whereas for flow behind a shock wave we found the dependences containing the angle of the shock wave itself.

Using expression (31), we obtain

$$\begin{aligned} M_{1\alpha}^2 - 1 &= \frac{k+1}{2} (M_{1\alpha}) (M_{1\omega}) = \\ &= \frac{k+1}{2} (M_{1\omega}) \left[\frac{k+1}{4} M_{1\omega}^2 + \sqrt{\left(\frac{k+1}{4} M_{1\omega}^2 - 1 \right)} \right] \end{aligned} \quad (38)$$

or for strong disturbances ($M_{1\omega} \gg 1$)

$$\begin{aligned} M_{1\alpha}^2 - 1 &= 2 \left(\frac{k+1}{4} M_{1\omega} \right)^2 \left[1 + \sqrt{1 + \frac{1}{\left(\frac{k+1}{4} M_{1\omega} \right)^2}} \right] \sim \\ &\sim \left(\frac{k+1}{2} M_{1\omega} \right)^2. \end{aligned} \quad (39)$$

Substituting (39) into formulas (31)-(34), it is possible to present the changes in pressure and density in a shock wave, and also the values of the velocity disturbances in the function of the angle of deflection of flow (angle of incidence of flow with the body surface).

From these dependences it follows that at hypersonic speeds in a step oblique shock wave the change of the parameters is determined (as during Prandtl-Mayer flow) by one criterion $K_w = M_w \omega$ - by the product of the Mach number by the angle of deviation of flow.

§ 4. Hypersonic Flow Around a Flat Plate at a Small Angle of Incidence

The expressions obtained in §§ 2 and 3 make it possible to derive simple formulas for the coefficients of lift and resistance of a plate flown around by a gas flow at a high supersonic speed with a small angle of incidence.

The coefficient of the total aerodynamic force directed at right angles to the plate is equal to

$$c = \frac{p' - p''}{\rho_a \frac{w_a^2}{2}} = \left(\frac{p'}{\rho_a} - \frac{p''}{\rho_a} \right) \frac{2}{k M_a^2}. \quad (40)$$

Here the minuend is the dimensionless pressure on the lower side of the plate (behind the shock), according to (33) equal to

$$\frac{p'}{\rho_a} = 1 + \frac{2k}{k+1} (M_a^2 \sin^2 \omega - 1)$$

The subtrahend in the right side of equality (40) represents the dimensionless pressure from the upper side of the plate (as during the flow around a convex obtuse angle), which on the basis of (16) with $\delta = -\omega$ takes the form

$$\frac{p'}{p_\infty} = \left(1 - \frac{k-1}{2} M_\infty^2 \omega^2\right)^{\frac{2k}{k-1}}.$$

Converting equality (40) with the help of the expressions obtained and utilizing (38) we obtain

$$c = \left\{ \frac{k+1}{2} + \sqrt{\frac{(k-1)^2}{2} + \frac{1}{M_\infty^2 \omega^2}} + \frac{2}{k M_\infty^2 \omega^2} \left[1 - \left(1 - \frac{k-1}{2} M_\infty^2 \omega^2\right)^{\frac{2k}{k-1}} \right] \right\} \omega^2. \quad (41)$$

If the angle of incidence of the plate ω is equal to or greater than the critical angle of rotation of flow during Prandtl-Mayer flow, which is determined by (17), then on the upper side of the plate a total vacuum is established. In this case the value which stands in the brackets of expression (41) is equal to zero.

At small angles of incidence the coefficients of lift c_y and resistance c_x are connected with the coefficient of total aerodynamic force in the following manner:

$$c_y = c \cos \omega \approx c, \quad c_x = c \sin \omega \approx c\omega \approx c_y \omega. \quad (42)$$

With $M_\infty \rightarrow \infty$ we have

$$c_y = (k+1)\omega^2, \quad c_x = (k+1)\omega^3.$$

As we see, the aerodynamic coefficients at very large values of M_∞ and at small angles of incidence are very low and, furthermore, they depend on value M_∞ ; in general these coefficients depend on the criterion K_ω .

§ 5. Concerning the Hypersonic Flow Around Narrow Ogival Bodies

The results obtained in §§ 2-4 can be applied directly to the calculation of hypersonic flow around a narrow ogival body, since the flow at the surface of such a body is either a flow behind an

oblique shock wave (at a positive angle of deflection of flow) or Prandtl-Mayer flow (at a negative angle of deflection of flow).

As it was already shown above, in such cases at small angles of tapering of a body and small angles of incidence the basic similarity criterion are the products of the Mach number of incident flow M_∞ by a certain characteristic angle τ . By τ can be implied the angle of deflection of flow $\tau = \omega$ (angle of inclination of the body surface to incident flow) or the relative thickness of the body $\tau = d/l$ (ratio of the maximum transverse dimension to the length of the body), since in the case of a narrow body these values are proportional. The fine pointed bodies in which the criterion $K_\tau = M_\infty \tau = \text{idem}$ we will subsequently call affine-similar. It is clear that the retention of affine-similar flow around a body during a change in the angle of incidence δ is achieved in such a case when the latter is proportional to the characteristic angle of the body, i.e., under the condition $\delta/\tau = \text{idem}$. Thus the relative values of velocities, the coefficients of aerodynamic forces, and other factors which characterize the hypersonic flow around a narrow body retain their values if the values $M\tau$ and δ/τ do not change.

This is confirmed by the experimental data given in Fig. 11.5, in which are depicted the curves of dimensionless values of excess pressure on the surface of a cylinder with an ogival nose section, obtained at different values of Mach number and for different values of relative thickness of the ogive section (at zero angle of incidence). As we see, the curves of pressure distribution are universal with $M = \text{var}$ and $\tau = \text{var}$, if the condition affine similarity - $M\tau = \text{idem}$ - is maintained.

In G. G. Chernyy's monograph it is shown that the area of action of the law of similarity for a hypersonic flow around a narrow ogival body is determined approximately by the following boundaries:

$$M > 2, \quad \tau = \frac{d}{l} < 0.5.$$

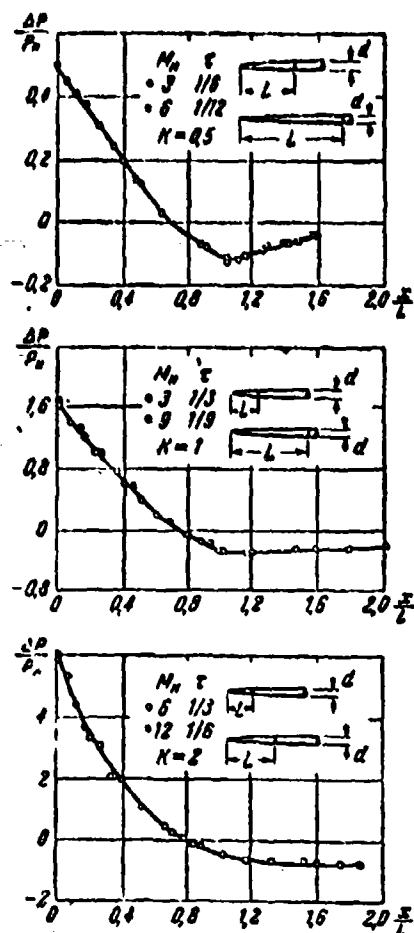


Fig. 11.5. Pressure distribution during flow around affine-similar bodies at high supersonic speed.

Let us note that the area of applicability of the law of similarity is considerably expanded, if instead of value $M_\infty \tau$ we take the value $\tau \sqrt{M_\infty^2 - 1}$ as the similarity criterion. It was shown above that during hypersonic flow around a narrow body the longitudinal disturbance of velocity is negligible $|u| \ll |w|$, and the transverse speed is proportional to the angle of the surface slope of the body

$$v = \tau w.$$

In other words, a narrow body separates the layers of a circumfluent gas as if in every layer (independent of adjacent layers) the displacement of gas by an impenetrable mobile piston occurs in a direction perpendicular to the direction of motion of the body. If the entire area of flow is broken down by planes perpendicular to the velocity of incoming stream into many layers, then in each of them an unsteady motion directed only parallel to these planes will be observed.

This feature of hypersonic flows was called the law of plane cross sections, with the help of which it is not difficult to determine the resistance of a body, equal to the work of expansion of the corresponding form of an equivalent piston, being accomplished on a gas in a layer during the time of passage of the body through this layer. The outline of the piston at every point in time and the normal velocity of its points are determined by the form of the body, and the pressure on its surface is found from the solution of the corresponding problem of the unsteady flow of gas.¹

§ 6. The Newton Law of Resistance

Considerable accumulated experience shows that for calculating the resistance of a body during hypersonic flow it is possible to utilize the law of resistance of Newton, who assumed that the driving fluid consists of identical particles which fill the space evenly and which do not interact with each other; during collision with a body the particles lose the momentum component normal to the body surface (inelastic impact), as a result of which the force of pressure of flow on the body appears. The excess pressure of the fluid on the sections of body located behind its greatest cross section, i.e., in the aerodynamic shadow (Fig. 11.6), Newton considered equal to zero.

¹For more detail about the application of the law of plane cross sections see G. G. Chernyy's monograph.



Fig. 11.6. Flow around a body which corresponds to Newton's model.

If the surface element of a body with area dF is tilted toward the incident flow at an angle ω , then the mass of gas in which the loss of momentum occurs is equal to $\rho w \sin \omega dF$, and the normal ("lost") velocity component is $w \sin \omega$, therefore the normal component of the force of pressure according to the law of Newton

$$dP = \rho w^2 \sin^2 \omega dF, \quad (43)$$

and the value of the local increase in gas pressure

$$p - p_\infty = \frac{dP}{dF} = \rho w^2 \sin^2 \omega. \quad (44)$$

In a general case of flow around a body Newton's supposition, it goes without saying, is not justified in connection with the fact that the disturbance caused by the body in the flow is propagated to a great distance from the body and with distance from the body is gradually attenuated, i.e., the adjacent streams of gas have different directions and velocities. However, during the flow around a body at high supersonic speed Newton's law becomes valid, since in this case the shock wave is located close to the body surface and all the streams up to the shock wave have identical direction and velocity (undisturbed flow), but behind the shock wave they move in a thin layer between it and the body and acquire almost identical velocities parallel to the body surface. The higher the Mach number and narrower the body, the nearer to reality is Newton's theory. At the same time it should

be noted that even in the extreme case $M \rightarrow \infty$ Newton's law answers to a precise solution of the problem only at $k = 1$.

If $k \neq 1$, then Newton's law is inaccurate even with $M \rightarrow \infty$, since in this case from the exact solution (29) we have

$$p - p_0 = \frac{2}{k+1} \rho_0 c^2 \sin^2 \alpha, \quad \text{tg } \alpha = \frac{1}{k} \sqrt{\frac{1}{k+1} + 1}. \quad (45)$$

However, practical calculation of pressure distribution over a body surface which is flown over by a hypersonic flow with the help of Newton's law gives in many instances satisfactory results, in spite of the fact that the viscosity effect is not considered in Newton's theory.

Figure 11.7 shows dimensionless pressure ($p = p - p_0 / \rho_0 u_\infty^2$) at different points of the surface of a cone with a central angle of 10° ($\alpha = 5^\circ$), covered by a flow of air with $M_\infty = 6.9$ at an angle of incidence $\delta = 1.7^\circ$. The curve in Fig. 11.7 is calculated according to Newton's formula (45). As we see, the experimental points lie sufficiently close to the theoretical curve.

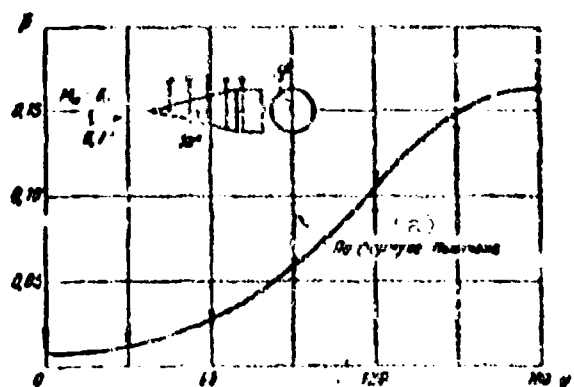


Fig. 11.7. Pressure distribution over the surface of a cone which is flown over by a flow at the angle of incidence. Comparison of Newton's formula and experimental data.

KEY: (a) According to Newton's formula.

The suitability of Newton's formula for calculating pressure on a body, which attests to the fact that the local flow pattern is determined by the local "angle of impact" of the body surface with an undisturbed flow, led to the thought about the possibility of calculating hypersonic flow around a pointed body by the method of tangential wedges (for an axisymmetrical body - tangential cones). In this method, proposed by S. V. Valander in 1949, it is assumed that the local pressure at any point on the surface of an arbitrary body is the same as on a wedge (cone), tangent to the surface at this point.

The method of tangential wedges (cones) is less convenient than Newton's formula, since in general the dependence of pressure on the wedge on its angle is represented in an implicit form, and on a cone it is determined only by numerical methods.

However, in hypersonic approximation these dependences, as it was shown in § 3, can be obtained in an explicit analytical form.

It was noticed that it is possible to attain considerably better agreement of calculated and experimental data, if in the following manner we modify Newton's formula:

$$p = p^* \frac{\sin^2 \omega}{\sin^2 \omega^*}; \quad (46)$$

here p^* - dimensionless pressure at the tip of the body, which it is easy to calculate according to the theory of supersonic flows of an ideal gas with assigned ω^* - the angle between the tangent to the outline of body at this point and the direction of the incoming flow; ω - similar angle in an arbitrary point of the outline.

Figure 11.8 gives the pressure distribution over the surface of symmetrical longitudinal-streamlined cylinders of different length with an ellipsoid nose section at $M = 4$; the solid line,

calculated from a refined Newton's formula (46), passes close to the experimental points.

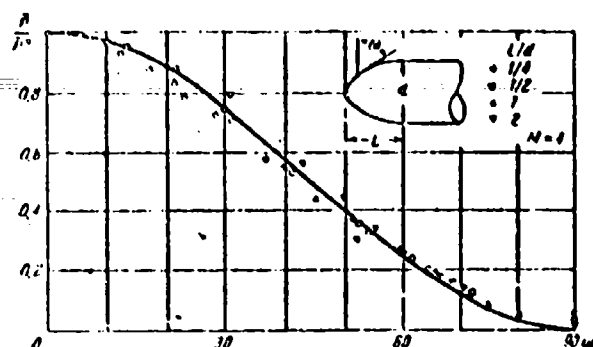


Fig. 11.8. Pressure distribution over the surface of cylinders, streamlined in a longitudinal direction, with a nose section in the form of ellipsoids of rotation.

Figure 11.9 depicts the picture of pressure distribution along the length of a cone with a spherical nose section of radius R (central expansion angle of cone $2\omega = 80^\circ$) at values of Mach number $M = 5.6-5.8$; the curve calculated by formula (46) passes close to the experimental points.

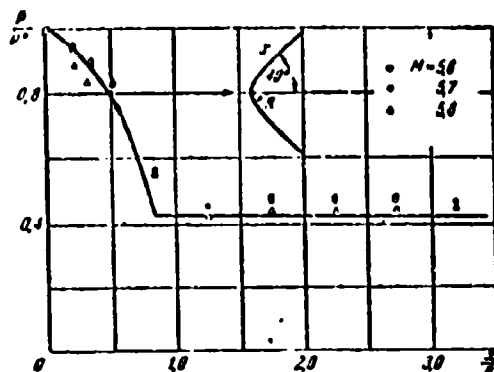


Fig. 11.9. Pressure distribution on the surface of a cone with a spherical nose section.

Let us note that calculations according to Newton's formula give good results for bodies of a convex form; in the case of bodies with a concave form the computed values obtained for the forces of pressure are understated. This is explained by the fact that in actuality the layer of gas included between the shock wave and the body surface is not infinitely fine, therefore with a curvilinear form of this layer a pressure gradient according to its thickness appears; the difference of pressure on the body surfaces and the shock wave is induced by centrifugal force. When this is considered it is possible to obtain a correction to Newton's formula, which was introduced for the first time by Busemann.

With the help of Newton's formula it is possible to solve the problem concerning the form of the body of the least resistance at certain assigned conditions (with assigned volume and length of body or with assigned areas of the greatest cross section and length, etc.).

For the solution of such a problem it is necessary first of all to compose expressions for the forces which act on the body.

The projection of the elementary force of pressure on the direction of motion - frontal resistance - according to (43)

$$dP_x = dP \sin \alpha = \rho_n w_n^2 \sin^3 \alpha dF,$$

from which the total resisting force

$$P_x = \rho_n w_n^2 \int \sin^3 \alpha dF = \rho_n w_n^2 \int \sin^3 \alpha dF_y, \quad (47)$$

where F - the body surface, F_y - its projection on a plane normal to the direction of motion.

The transverse component of elementary force of pressure - lift

$$dP_y = -\rho_\infty \omega_\infty^2 \sin^2 \omega \cos \omega dF.$$

From here the total value of lift

$$P_y = -\rho_\infty \omega_\infty^2 \int_0^F \sin^2 \omega \cos \omega dF = -\rho_\infty \omega_\infty^2 \int_0^F \sin \omega \cos \omega dF_y. \quad (48)$$

Being given one form or another of the dependence of the slope angle of the surface on length, it is possible to integrate (47) and (48) and obtain analytical dependences, which then are used, in particular, for finding the optimum values of the geometric parameters of the body under any assigned conditions by means of the solution of a problem on the minimum of value P_x .

With the help of Newton's formula it is not difficult, for example, to show that during hypersonic flow a blunt-nosed cone with a smaller lateral angle can have less resistance than a pointed cone with a larger angle (Fig. 11.10).

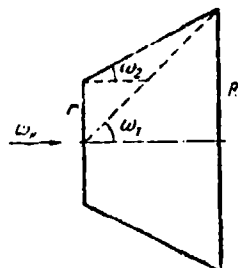


Fig. 11.10. Truncated and full cones of equal length with identical midsection cross sections.

If the "area" in the nose of a blunt-nosed cone has a radius r and its lateral angle ω_2 , but at the "pointed" cone of same length and same maximum radius R the lateral angle ω_1 , then according to (47) the relation of the forces of resistance of these bodies comprises

$$f = \frac{P_{x2}}{P_{x1}} = \frac{r^2 + (R^2 - r^2) \sin^2 \omega_2}{R^2 \sin^2 \omega_1}.$$

where

$$\sin^2 \omega_2 = \frac{(R-r)^2}{(R-r)^2 + x^2}, \quad \sin^2 \omega_1 = \frac{K^2}{R^2 + x^2}.$$

Substituting these expressions and introducing the dimensionless designations $\bar{x} = x/R$, $\bar{r} = r/R$, we finally obtain

$$f = (1 + \bar{x}^2) \frac{(1 - \bar{r})^2 + \bar{r}^2 \bar{x}^2}{(1 - \bar{r})^2 + \bar{x}^2}.$$

Equating to zero the first-order derivative of function f , we find the optimum value of radius \bar{r}_{opt} to which corresponds the minimum of the value of this function, i.e., the minimum of resistance

$$\bar{r}_{\text{opt}} = 1 + 0.5\bar{x}^2 - \sqrt{\bar{x}^2 + 0.25\bar{x}^4}.$$

For example, with $\bar{x} = 1$ we have $\bar{r}_{\text{opt}} = 0.38$ and $f_{\text{min}} = 0.76$, i.e., the resistance of the optimum truncated cone proves to be 24% less than for a standard cone of the same length.

Solving this problem for a wedge by the same method, it is possible to be convinced of the fact that according to the calculation an "optimum" truncated wedge is obtained only with $\bar{x} < 1$ ($\omega > 45^\circ$), i.e., at such a large central expansion angle that apparently the practical significance of the solution is lost.

Let us pause now on the correction of Busemann to Newton's formula mentioned above for the case of flow around a curvilinear surface. In view of the fact that the layer of gas, which consists of particles included between the body surface and the shock wave, is not infinitely fine, the pressure directly behind the wave in the case of a curvilinear trajectory of particles is not equal to the pressure on the surface; the difference in these pressures is caused by the action of centrifugal force.

In an elementary layer with a thickness $d\delta$ this pressure difference evidently is equal to

$$dp = \rho w^2 \frac{d\delta}{R}.$$

where R - the radius of curvature of the layer, ρ , w - the values of the density of the gas and velocity of motion in the layer (along the flow line).

From the continuity condition we have

$$\rho w l d\delta = \rho_n w_n dF_n$$

Here l - the width of a layer on a normal to the plane of drawing, F_n - the cross-sectional area of a body with a plane normal to the direction of incident flow. Substituting the value $d\delta$ from this equality into the preceding one, we have

$$dp = \frac{\rho_n w_n^2}{R} w dF_n$$

After integration we obtain the pressure change across the layer due to centrifugal force

$$p - p_\infty = \frac{\rho_n w_n^2}{R} \int_{F_\infty}^{F_2} w dF_n$$

The velocity component, tangent to the surface of the body, in the case of encounter of particles with the body does not change, therefore, $w = w_\infty \cos \omega$. Since the radius of curvature of the surface

$$R = -\frac{ds}{d\omega} = -\frac{dF}{\sin \omega ds},$$

where s is the length measured on the contour of the body, then the pressure difference on the wall and on the boundary of the layer

$$p_w - p = \rho_a \omega_a^2 \sin^2 \alpha \int_{F_0}^F \cos \alpha dF,$$

The pressure on the boundary of the layer is determined from Newton's formula (46), therefore excess pressure on the wall taking into account centrifugal force is equal to

$$p_w - p_a = \rho_a \omega_a^2 \left(\sin^2 \alpha + \sin \alpha \int_{F_0}^F \cos \alpha dF \right). \quad (49)$$

This dependence was obtained for the first time by Busemann and called the Newton-Busemann formula. For bodies of convex form calculation to the initial Newton law (44) gives results which are closer to experimental data than the calculation according to refined formula (49). This is explained by the fact that according to Newton's formula the pressure obtained is lower than true (since the angle of encounter of flow with the shock wave α is greater than the angle of encounter with the body ω , which figures in Newton's formula), and for a convex body the correction for centrifugal force additionally decreases the pressure. On the contrary, in the case of a concave body the correction for centrifugal force is positive, i.e., it compensates for the understated pressure which is given by Newton's law. The comparison of the calculations with experimental data shows that for a concave body formula (49) gives better results than formula (44).

§ 7. The Influence of Minor Blunting of the Front End of a Narrow Body on Flow Around It at Hypersonic Speeds

During hypersonic flow around a narrow body with a blunted nose section a detached shock wave is formed. In its forward section the pressure increases so strongly that even with small dimensions of blunting the aerodynamic drag can increase substantially. This fact cannot be bypassed in connection with the fact that real bodies (wings, fuselages, missile bodies) are always

blunted. To carry out flight with an ideally pointed body is impossible if only because at high velocities of flight the heating of air about the nose of the body is so considerable that the pointed end would unavoidably be fused.

Let us assume in the first approximation that the resistance of a blunted narrow body is equal to the sum of the resistance of blunting P_{x1} and the resistance of the remaining part of the body P_{x2} , the pressure on which is determined from the theory of hypersonic flow around a pointed body (§ 5). The relation of these resistances according to (29), (33), and (39):

$$\frac{P_{x1}}{P_n} \sim \frac{F_{y1}}{F_n}. \quad (50)$$

Here ω - the angle between the lateral surface of the body and the direction of incident flow, F_{y1} , F_{y2} - projections on the plane perpendicular to the direction of incident flow, surfaces with respect to the blunted part, and the entire remaining body.

Hence it is apparent that the additional resistance caused by the blunting of a narrow body is comparable with the resistance of the initial pointed body with a very low relative area of blunting

$$\frac{F_{y1}}{F_n} \sim \omega^2. \quad (51)$$

For example at an angle of deflection of flow $\omega = 5^\circ = 0.087$ rad the resistance of a blunted body with a relative area of blunting $F_{y1}/F_{y2} \approx 0.0075$ is approximately doubled. Let us replace the area ratio by the ratio of linear dimensions

$$\frac{r_{y1}}{r_n} = \left(\frac{d}{D}\right)^2. \quad (52)$$

Here d - the transverse dimension of the blunted part, $D = \omega L$ - the linear dimensions of the maximum cross section of the body, L - the length of the body, v - the exponent, equal to a unit for plane bodies and to two for axially symmetrical bodies.

Thus, we have for a wedge

$$\frac{F_p}{F_n} = \frac{d}{D},$$

and for a cone

$$\frac{F_p}{F_n} = \left(\frac{d}{D}\right)^2.$$

The relative linear dimensions of the blunted part of a narrow body, in which the resistance during hypersonic flow is two times greater than for the same pointed body is connected with the angle of deviation in the flow by the relationship

$$\frac{d}{D} \sim \omega^{\frac{2}{v}} \text{ or } \frac{d}{L} \sim \omega^{\frac{2}{v}}.$$

In the example examined above ($\omega = 0.087$ radians) the relative dimensions of blunting in a wedge $(d/D) \sim \omega^2 \approx 0.0075$, in a cone $(d/D) \approx 0.087$.

A detailed examination of the problem of hypersonic flow around a narrow body shows that blunting of the nose section of the body causes a significant distortion in the picture of pressure distribution on a considerable part of the lateral surface of the body. Figure 11.11 shows the dimensionless distribution of excess pressure along the length of a plate with wedge-shaped and semi-circular leading edges. The expansion angle of the leading wedge was selected for each value of Mach number in incident flow ($M_\infty = 5.00; 6.86; 9.50$) so that the velocity behind a front-connected shock was equal to the speed of sound ($M_1 = 1$), and the plate with a semicircular edge was tested with $M = 14$.

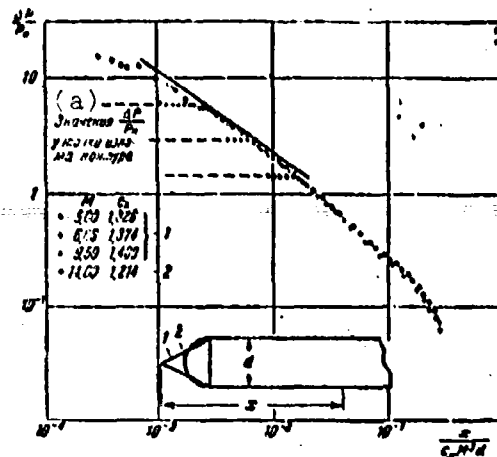


Fig. 11.11. Pressure distribution on a plate with wedge-shaped (1) and rounded (2) edges.
KEY: (a) Values $\Delta P/P_\infty$ at the point of break in contour.

The dimensionless curves

$$\frac{\Delta P}{P_\infty} = \frac{P - P_\infty}{P_\infty} = f\left(\frac{x}{c_x M^2 d}\right)$$

will move away from a certain universal dependence only near the breaking point of the outline; value c_x for the nose of a wedge-shaped body was determined according to the theory of an oblique shock wave, and for a semicircular form - according to the refined Newton formula ($c_x = 2/3\pi$). The calculated dependence (solid line)

$$\frac{\Delta P}{P_\infty} = 0.12 \left(c_x M^2 \frac{d}{x} \right)^{2.3}$$

agrees satisfactorily with experimental data.

This approximate dependence is obtained with the help of the theory of point burst and the hypothesis of plane cross sections, whereupon the force which acts on the blunted nose of a body is

considered as an additional concentrated force. Without dwelling in more detail on the theory of hypersonic flow around blunted narrow bodies, let us refer those who are interested in this equation to special monographs.¹

Let us note in conclusion only one interesting feature of the flow around a narrow blunt-nosed cone, discovered by both theoretical and experimental means, which consists of the fact that the excess pressure (Fig. 11.12) on part of the surface of a blunt-nosed cone turns out to be lower than for a pointed cone. In other words, the effect of the flow around a blunted nose on the adjacent areas of flow can lead to the fact that with a certain "degree of bluntness" of a cone its resistance will prove to be lower than for a sharp-nosed cone (in Fig. 11.12 the unbroken curve is calculated; here for a comparison is given the curve of pressure distribution according to the generatrix of a sharp-nosed cone (dotted line)).

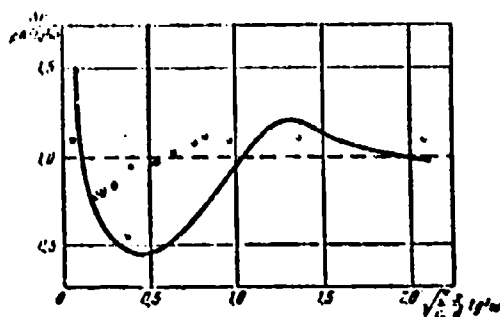


Fig. 11.12. Pressure on the surface of a blunt-nosed cone.

§ 8. The Viscosity Effect in Hypersonic Flows

The viscosity effect in hypersonic flows, on which we did not dwell in the foregoing paragraphs of the chapter, is a complex problem.

¹Chernyy, G. G. Gas flow at high supersonic speed. Fizmatgiz, 1969; Kheyz U. D. and Probstin R. F. The theory of hypersonic flows. Publishing house of foreign literature, 1962.

When the boundary layer is considerably narrower than the shock layer (zone between the shock wave and the body surface), the calculation of the stresses of friction and heat exchange is done by the usual methods developed in the boundary-layer theory (Chapter VI).

True, at hypersonic speeds the gas temperature as a result of the stagnation of flow in the shock waves and the boundary layer can turn out to be very high, and then it is necessary to consider not only the compressibility of the gas, but also dissociation, and at temperatures above 5000 the ionization of gas. Furthermore, in a hypersonic boundary layer during flow around a sharp-nosed narrow body (or even a flat plate placed along the flow) a longitudinal pressure gradient appears, since, as is known, the boundary layer affects the external flow the same as the thickening of the body (by the magnitude of the displacement thickness of the boundary layer), causing the formation of shock waves (Fig. 11.13). In other words, the boundary layer can create in the external flow on a sharp-nosed body "its own" shock layer, which begins from the leading edge of the body; during flow around a body with a blunted nose usually this is not observed, in connection with the fact that in the boundary layer behind the detached shock wave the velocities are subsonic or temporarily exceed the speed of sound.

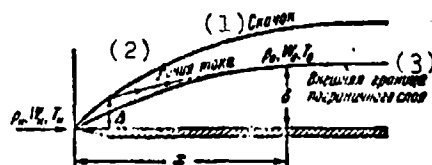


Fig. 11.13. Diagram of the boundary layer and the shock layer induced by it.
KEY: (1) Shock; (2) Flow line; (3) Boundary layer outer edge.

The theoretical and experimental investigations of the hypersonic boundary layer, which causes on a plate and on a narrow body (wedge, cone) the appearance of a shock layer with a longitudinal

pressure gradient, were carried out in the works of Becker, Lees and Frobstein, Bertram, Kendall, etc. (see the monograph of Kheyz and Frobstein).

The essence of the theoretical approach to the solution of this problem consists of the following. The pressure in each cross section of the boundary layer is considered constant and dependent on the total angle of rotation of flow

$$\omega = \omega_0 + \frac{d\delta^*}{dx};$$

here ω_0 - the local angle of deflection of the body surface from the direction of undisturbed flow, $\Delta\omega = d\delta^*/dx$ - the additional deviation of flow which corresponds to the displacement thickness δ^* of the boundary layer (in view of the smallness of angles we consider the tangent of the angle equal to the angle itself measured in radians). Value δ^* can be determined approximately, utilizing the known methods of calculation of the boundary layer without the pressure gradient; during calculation of δ^* the pressure is accepted in the first approximation as the same as in a flow without a boundary layer; the viscosity-temperature dependence is approximated by the linear function

$$\frac{\mu_w}{\mu_0} = c_\infty \frac{T_0}{T_w},$$

where the index "w" is related to values on the wall, and index "0" is related to the boundary of the layer.

In turn the change of pressure caused by a deviation in the external flow under the effect of a body of increased thickness, as a result of the build-up of the boundary layer, can be calculated with the help of a refined Newton formula (44) or according to the method of tangential wedges or cones.

In summation, for example, for a flat plate the following approximation formula is obtained for dimensionless pressure in a laminar boundary layer (with $k = 1.4$ and $Pr = 0.725$):

$$\frac{p}{p_\infty} = 1 + 0.312 \chi + 0.052 \chi^2, \quad (53)$$

where the interaction factor of the layer with the flow

$$\chi = \frac{M_\infty^2 \sqrt{r_\infty}}{\sqrt{R_{x_\infty}}},$$

Here the index ∞ corresponds to the parameters of undisturbed flow, $R_{x_\infty} = \rho_\infty x / \mu_\infty$ - Reynolds number.

A comparison of calculation data with the experimental data of Bertram and Kendall, given in Fig. 11.14, gives satisfactory results with $\chi \leq 4$; Reynolds numbers, calculated according to the thickness of the leading edge of the plate, were equal respectively in Bertram's experiments to approximately 40, in Kendall's experiments to approximately 100.

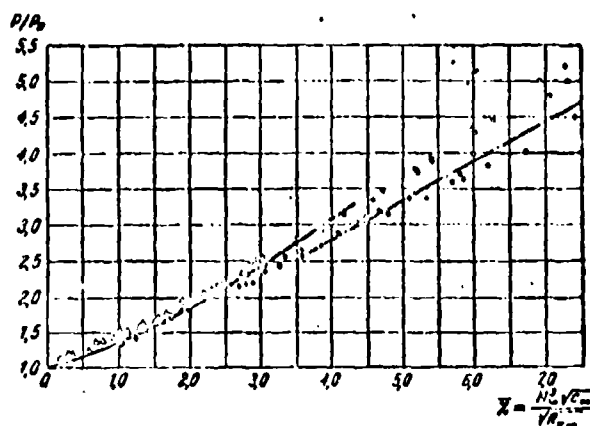


Fig. 11.14. Pressure on a heat-insulated plate during weak and strong (dotted line) interactions.

Figure 11.15 depicts the picture of flow in a heat-insulated plate, calculated and determined experimentally in Kendall's work; the figure gives the boundary layer outer edge and the shock wave caused by it, and also the flow lines and Mach waves. The experimental and calculation data of Kendall virtually coincide in the entire zone of flow.

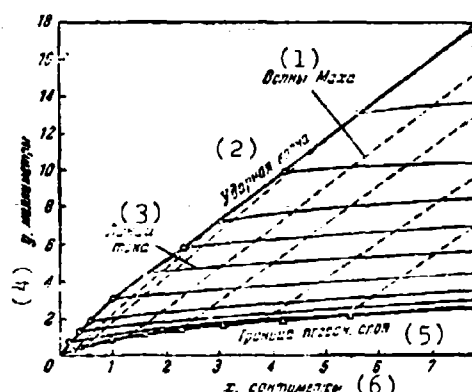


Fig. 11.15. The field of flow near a heat-insulated plate (according to Kendall).
KEY: (1) Mach waves; (2) Shock wave; (3) Flow lines; (4) y, millimeters; (5) Limit of boundary layer; (6) x, centimeters.

Let us note that the longitudinal pressure gradient shows up in the stress level of friction on the wall, but it affects heat exchange weakly, of which it is possible to be convinced by calculating the boundary-layer in the second approximation taking into account the previously determined pressure gradient.

It is accepted to call the examined type of interaction of boundary layer with an external hypersonic flow a weak interaction, since in this case the disturbance of only part of the shock layer by the hypersonic boundary layer is observed.

We are dealing with a weak interaction when the intensity of the build-up of the displacement thickness of the boundary layer is low in comparison with the angle of encounter of flow with the body surface

$$\frac{d\delta^*}{dx} < 1$$

or under the condition

$$K = M_\infty \left(w_\infty + \frac{d\delta^*}{dx} \right) < 1.$$

But if

$$\frac{d\delta^*}{dx} > 1 \text{ or } K > 1,$$

then we are speaking about a strong interaction, during which the entire area of the shock layer, including the viscous boundary layer, should be considered in the theoretical solution as a unit.

The approximate computation, based on the use of the method of tangential wedges, gives for pressure in a shock layer during a strong interaction the linear dependence

$$\frac{p}{p_\infty} = 0.514x - 0.739. \quad (54)$$

depicted in Fig. 11.14 by the dot-dash line, which passes comparatively close to the experimental points at values $\bar{x} \geq 4$. The details of the theoretical calculation of a strong interaction can be found in the cited book by Kheyz and Probstin.

One ought to emphasize that the picture of the interaction of a boundary layer with an incoming steady flow examined by us was restricted to the case of a body with a pointed leading section. The blunting of the nose of the body, and also the non-uniformity of external flow (for example, with a strongly bent head shock wave) introduce additional changes into pressure distribution. These forms of interaction are examined in the monograph of Kheyz and Probstin.

CHAPTER XII

FLOWS OF RAREFIED GAS

§ 1. Different Types of the Flows of Rarefield Gases

Up till now we examined gas flows in which the gas was a continuum; this is correct when the length of the mean free path of molecules of the gas l is very low in comparison with the characteristic dimension of the gas flow of L .

In some problems of gas dynamics the characteristic dimension is the boundary-layer thickness and in another - the thickness or the length of the streamlined body. The dimensionless relation

$$K = \frac{l}{L}, \quad (1)$$

which determines the nature of the medium, is called the *Knudsen number*.

At normal pressure the value of the mean free path of the molecules consists of millions of a centimeter. With the lowering of the gas density the mean free path of the molecules increases inversely proportional to the density, and if it becomes commensurable with the characteristic dimensions of the flow, then the discrete structure of the gas begins to affect the laws of gas dynamics and heat exchange.

Knudsen's number can be expressed by the known similarity criteria - the Mach M and Reynolds R numbers, for this one should use Chapman's formula from the kinetic theory of gases, which connects the kinematic viscosity with the mean free path and the average velocity of the motion of the molecules \bar{c} :

$$\nu = 0.499 l \bar{c} \approx \frac{1}{2} l \bar{c}. \quad (2)$$

The average velocity of the molecules is expressed as the speed of sound a

$$\bar{c} = a \sqrt{\frac{5}{3}}, \text{ where } k = \frac{c_p}{c_v}. \quad (3)$$

Then from (2) and (3) we have

$$l = 1.26 \frac{\nu}{a} \sqrt{k}. \quad (4)$$

Substituting (4) into (1), we obtain the dependence of the Knudsen's number on the ratio of the Mach number to the Reynolds number

$$K = \frac{l}{L} = 1.26 \frac{\nu}{a L} \sqrt{k} = 1.26 \frac{M}{R_L} \sqrt{k}. \quad (5)$$

From the boundary-layer theory, it follows that at large values of the Reynolds number ($R_L \gg 1$) the boundary-layer thickness δ is inversely proportional to the square root of the Reynolds number

$$\frac{\delta}{x} \sim \frac{1}{\sqrt{R_L}},$$

where x is the length of the body. Therefore, if the discussion is about the fluid friction or heat exchange, when the characteristic dimension is the boundary-layer thickness ($L = \delta$), then when $R_x \gg 1$, according to (5), the Knudsen number becomes proportional

to the ratio of the Mach number to the square root of the Reynolds number

$$H \sim \frac{M}{\sqrt{R_x}} \quad (6)$$

At small values of the Reynolds number ($R_x \leq 1$) the boundary-layer thickness is comparable with the length of the body ($\delta \sim x$), and therefore

$$H \sim \frac{M}{R_x} \quad (7)$$

The available theoretical and experimental data indicate the fact that at the very low values of the Knudsen's number ($H < 0.01$) the gas behaves as a continuum. In the interval of values of the Knudsen number of $0.01 < H < 0.1$ it also is possible to use equations of gas dynamics of the continuum; however, in this case, as it will be shown below, in the boundary conditions on the rigid surface one should correct for the so-called "slip" and "temperature jump."

At very large values of the Knudsen number ($H > 1$) the boundary layer at the body surface is not formed, since the molecules re-emitted (reflected) by the surface of the body collide with molecules of the external flow at a distance remote from it, i.e., body does not introduce distortions into the velocity field of external flow. For this mode of the "free-molecular flow of gas," which according to the available data is observed when $M/R_x > 3$, the friction and heat exchange on the surface of the streamlined body are calculated from the condition of a single collision of the molecules of gas with the surface.

The transition region between the mode with slip and free-molecular mode remains up to now little studied, since in it one must consider both the collisions of the molecules between themselves and their repeated collisions with the body, and this creates great theoretical difficulties.

Plotted on Fig. 12.1 are the boundaries of different flow conditions of the gas in coordinates $M = f(R_x)$, which include 1) the lower boundary of the free molecular flow, which corresponds to value $M/R_x = 3$; 2) the upper limit of the flow with slip which corresponds to the value $M/\sqrt{R_x} = 0.1$; 3) the upper limit of flows for a continuum, where $M/\sqrt{R_x} = 0.01$. Table 1 depicts the approximate dependence of the mean free path of molecules on height calculated from formula (4) for a standard atmosphere.

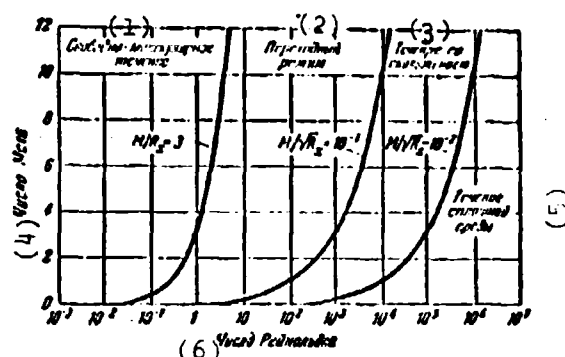


Fig. 12. 1. Boundaries of different flow conditions of rarefied gas.

KEY: (1) Free-molecular flow; (2) Transient condition; (3) Flow with slip; (4) Mach number; (5) Flow of continuum; (6) Reynolds number.

Table 1.

(1)		0	25	50	75	100	125	150	175	200
(2)	Высота H [км]									
	Длина свободного пробега l [м]	$6.9 \cdot 10^{-5}$	$2.2 \cdot 10^{-4}$	$7.8 \cdot 10^{-4}$	$2.0 \cdot 10^{-3}$	$5.5 \cdot 10^{-3}$	2.3	18	60	300

KEY: (1) Height H [km]; (2) Mean free path l [m].

Comparing data of Fig. 12.1 and Table 1, it is possible to obtain the concept of the connection between the flight altitude and the boundaries of different modes.

For a rocket 3 m long the effect of slip begins to be exhibited at the height of 50 km at $M = 1$ and 30 km at $M = 4$. Free - molecular flow is established at any flight speed, beginning at the height of 140 km.

§ 2. Jumps of Velocity and Temperature at the Wall During Gas Flow with Slip

If the mean free path of the molecules l is not negligible in comparison with the thickness of the boundary layer δ but is considerably less than the latter, $l < \delta$, then the velocity profile of the directed flow of gas at the wall has the form depicted on Fig. 12.2. The difference in the velocity in layers remote from each other at a distance of the mean free path, obviously, is equal to

$$\Delta w \sim l \frac{\partial w}{\partial y}$$

Consequently, the molecules which are located at distance l from the wall have a directed velocity relative to it

$$w_l = l \left(\frac{\partial w}{\partial y} \right)_R + w_R = \frac{l}{\delta} w_0 \frac{\partial \left(\frac{w}{w_0} \right)}{\partial \left(\frac{y}{\delta} \right)} + w_0 \frac{w_R}{w_0}, \quad (8)$$

where w_R is the velocity jump at the wall, i.e., the velocity value in the layer of gas which directly adjoins the wall, w_0 is the velocity of the undisturbed flow of gas. In accomplishing the mean free path l , the molecules retain their velocity, i.e., hit the wall at a final velocity w_l . As the experiments of Milliken¹ and other researchers showed, a considerable part of the

¹Milliken P. A., The isolation of an ion, a precision measurement of its charge, and the correction of Stoney's law. Phys. Rev. XXXII, No. 4, p. 345-355 (1928).

molecules with impact against the wall is absorbed by it and then reemitted (emitted), having lost completely the velocity of the ordered motion w_x . Let us designate a portion of these "diffusely" reflected molecules by the letter σ ; the remaining molecules, the algebraic number of which is equal to $1 - \sigma$, are "mirror" reflected i.e., after reflection they retain the velocity w_x which they had prior to the impact against the wall.

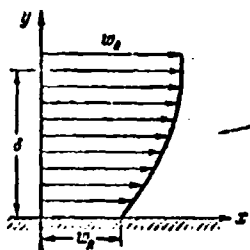


Fig. 12.2. Velocity profile at the wall during flow with slip.

Taking that given into account, it is possible to determine the average directed velocity of the layer of gas directly at the wall, on the basis of the fact that this layer consists of half of the molecules arriving at the wall and half of those reflected from it.

$$w_R = \frac{1}{2} \left[w_R + l \left(\frac{\partial w}{\partial y} \right)_R \right] + \frac{1}{2} (1 - \sigma) \left[w_R + l \left(\frac{\partial w}{\partial y} \right)_R \right] + \frac{1}{2} \sigma \cdot 0.$$

Thus, the velocity of "slip" of the gas at the wall is equal to

$$w_R = \frac{2 - \sigma}{\sigma} l \left(\frac{\partial w}{\partial y} \right)_R. \quad (9)$$

The table given below contains values of the coefficient σ found by different experimenters for cases of the interaction of different gases with surfaces of a different nature.

Surface \ Gas	Air	Carbon dioxide	Hydrogen	Helium
Brass	1	—	—	—
Old varnish	1	—	—	—
Varnish, fresh	0.79	—	—	—
Oil paint	0.925	0.92	0.93	0.87
Glass	0.89	—	—	—

In view of the fact that the portion of diffusely reflected molecules is close to unity ($\sigma \approx 1$), we have approximately

$$w_R \approx l \left(\frac{\partial w}{\partial y} \right)_R = \frac{l}{\delta} w_0 \left[\frac{\partial \left(\frac{w}{w_0} \right)}{\partial \left(\frac{y}{\delta} \right)} \right]_R. \quad (10)$$

Hence it follows that in the dense gas ($l \ll \delta$) the slip is virtually absent ($w_R = 0$), i.e., the molecules "adhere" to the wall, as is accepted in the standard gas dynamics; in the greatly rarefied gas ($l > \delta$) the slip velocity is close to the velocity of the undisturbed flow of gas outside the boundary layer ($w_R \approx w_0$). In flow with slip velocity the velocity at the wall is subordinated to the condition (9), which is usually replaced by approximate condition (10).

It should be noted that the condition of slip (9) is not completely precise when at the low absolute pressure of the gas there is a substantial change in temperature along the length of the wall, since the longitudinal gradient of temperature causes the "thermal diffusion" directed flow of molecules to the side of the increasing temperature (see, for example, § 8). Such flow induced by a difference in temperatures was called "temperature creep."

Kennard¹ showed that the rate of the temperature creep at the wall is equal to

$$w_{RT} = \frac{3}{4} \frac{\mu}{p} \left(\frac{\partial T}{\partial x} \right)_R; \quad (11)$$

Here p and T are gas density and temperature at the wall, μ - the coefficient of viscosity, x - the distance calculated along the wall. Thus, the refined boundary condition, which characterizes the velocity jump at the wall, should take the following form:

¹Kennard J. C., Kinetic Theory of Gases, McGraw-Hill, 1938.

$$u_R = \frac{2-\epsilon}{\epsilon} \left(\frac{\partial u}{\partial y} \right)_R + \frac{3}{4} \frac{\mu}{RT} \left(\frac{\partial T}{\partial x} \right)_R. \quad (12)$$

The second term of the relation (12), which considers the temperature creep, can most frequently be disregarded, since with high longitudinal temperature gradients and very large rarefactions, when this term is especially important, the free molecular gas flow without a hydrodynamic boundary layer is usually realized. However, in some special cases (for example, the flow around the nose section of a rocket during its entry into comparatively dense layers of the atmosphere) condition (12) is used completely.

Let us discuss now the question concerning the temperature jump at the wall during flow conditions with slip.

The capture of the molecules by the wall and the subsequent reemission lead to the fact that the reflected molecules have a temperature close to the wall temperature. Let us introduce the so-called accommodation coefficient

$$\alpha = \frac{dE_I - dE_R}{dE_I - dE_w}; \quad (13)$$

here dE_I and dE_R are energy flows, respectively, brought by the molecules which fall on the infinitesimal surface element and taken away by the re-emitted molecules, dE_w is the energy flow by which the re-emitted molecules would take away if they possessed Maxwellian velocity distribution at the wall temperature. With total accommodation ($\alpha = 1$) $dE_R = dE_w$, in the absence of accommodation ($\alpha = 0$) $dE_I = dE_R$. Experiments show that frequently the value of coefficient α is close to unity, which can be judged from the accompanying table of experimental values of α for air found by Wiedmann.¹

¹Wiedmann M. L., Trans. Am. Soc. Mech. Eng. v. 68, p. 57, 1946 (Russian translation: Collection "Mekhanika, No. 4, 1951).

Table 3.

Surface	α	Surface	α
Uniform varnish on bronze	0.88-0.89	Cast steel of machine treatment	0.87-0.88
Polish bronze	0.91-0.94	Etched cast steel	0.89-0.96
Bronze of machine treatment	0.89-0.93	Polished aluminum	0.87-0.95
Etched bronze	0.93-0.95	Aluminum of machine treatment	0.95-0.97
Polished cast steel	0.87-0.93	Etched aluminum	0.89-0.97

From the table it follows that the finish of the metal does not virtually affect the value of the accommodation coefficient.

Dickins¹ determined the following values of the accommodation coefficients for different gases during their interaction with the surface of platinum:

Table 4.

Type of gas	α	Type of gas	α
Hydrogen	0.35	Nitrous oxide	0.90
Helium	0.51	Air	0.91
Argon	0.88	Carbon monoxide	0.91
Ammonia	0.88	Carbon dioxide	0.92
Nitrogen	0.90	Sulfur gas	0.95
Oxygen	0.90		

As we see, gases of very low molecular weight (hydrogen and helium) are weakly accommodated by the wall; all the remaining gases have an accommodation coefficient of approximately 0.9 and above.

¹Dickins B. G., Proc. Roy. Soc. A 143, p. 517, 1933.

If the dissociation effect is unessential, then at subsonic velocity of the flow of gas, when the kinetic flow energy is relatively low, the accommodation coefficient can be expressed in terms of the appropriate values of temperature

$$\alpha = \frac{T_i - T_g}{T_i - T_w}. \quad (14)$$

Let us determine the value of the temperature jump near the wall ($\Delta T_R = T_R - T_w$) in the flow with slip. This problem is somewhat more complex than the definition of the velocity jump, since for the temperature change in the direction of the normal to wall affects not only the molecular thermal conductivity but also the heat which is released in the process of molecular friction. The per-second flow through a unit area of side surface of the gas layer in the direction of the normal to it (Fig. 12.2), according to the Fourier law, is equal to

$$q = \lambda \frac{\partial T}{\partial y}.$$

The per-second mass flow rate of molecules through a unit area in the same direction, according to (71)¹ is

$$O_x = g \cdot M_x = \frac{1}{4} \rho g c.$$

A change in the temperature of the molecules for the extent of the thickness of the layer is equal to the ratio of the inflow of heat to the inflow of the substance multiplied by the heat capacity

$$\Delta T_i = \frac{q}{c_p O_x} = \frac{4\lambda}{\rho g c_p} \frac{\partial T}{\partial y}.$$

¹See below, § 6.

After substituting into this equality the expression for the Prandtl number, which characterizes the ratio of the heat of friction to the heat removed by thermal conductivity $Pr = \mu c_p / \lambda$, we obtain

$$\Delta T_i = \frac{\eta}{\rho Pr} \frac{\partial T}{\partial y}. \quad (15)$$

Finally, in using expression (2) for the molecular viscosity of gas, we have

$$\Delta T_i = \frac{2}{Pr} l \frac{\partial T}{\partial y}. \quad (16)$$

Thus, calculation of the thermal conductivity and heat of friction shows that the effective temperature change in the layer, the thickness of which is equal to one mean free path of the molecules, is $(2/Pr)$ times more than that in the absence of the interaction between the molecules. By producing now the calculations similar to those made in determining the velocity jump, let us find the temperature jump at the wall in the flow with slip, whereupon the excess temperature in the layer of gas at the wall will be considered equal to the arithmetic mean between the excess temperatures of the molecules falling on the wall and re-emitted taking into account the accommodation coefficient α (14), which for the temperature plays the same role as that of the diffuse reflection factor for the velocity¹

$$\Delta T_K = \frac{1}{2} \left[\Delta T_K + \frac{2l}{Pr} \left(\frac{\partial T}{\partial y} \right)_K \right] + \frac{1}{2} (1 - \alpha) \left[\Delta T_K + \frac{2l}{Pr} \left(\frac{\partial T}{\partial y} \right)_K \right] + \frac{1}{2} \alpha \cdot 0.$$

Hence we obtain for the temperature jump at the wall

¹The portion α of the total number of molecules is reflected with the temperature equal to the wall temperature, and the remaining part of the molecules $(1 - \alpha)$ retains that temperature which it had prior to collision.

$$\Delta T_R = T_R - T_\infty = \frac{2-\alpha}{\alpha} \frac{2\eta}{\rho r} \left(\frac{\partial T}{\partial y} \right)_R. \quad (17)$$

For gases whose Prandtl number is close to unity with an accuracy sufficient for practical purposes, it is possible to use the simplified relation

$$\Delta T_R = \frac{2-\alpha}{\alpha} 2\eta \left(\frac{\partial T}{\partial y} \right)_R. \quad (18)$$

When $\alpha = 1$ we have

$$\Delta T_R = 2\eta \left(\frac{\partial T}{\partial y} \right)_R. \quad (19)$$

Formulas (17)-(19) for the temperature jump at wall are valid only at moderate flow velocities ($M = 0$, $T = T^*$). In the case of supersonic velocities, it follows to refine them. Formula (12) for the velocity jump is valid at high speeds.

As follows from Fig. 12.1, the conditions of flow with slip are observed at such moderate values of the Reynolds numbers for which the real one is the existence of only the laminar boundary layer, and therefore below laminar flows with slip are examined.

§ 3. Gas Flow with Slip in the Tube

To establish the laws governing the laminar gas flow with slip, in a tube of round cross section one should, first of all, compile the balance of forces applied to the cylindrical fluid element with a moving radius r and length dx (Fig. 12.3)

$$- \pi r^2 dp = - \tau 2\pi r dx, \quad (20)$$

where τ is the stress of friction on the side surface of the element and dp is the pressure difference on its ends.

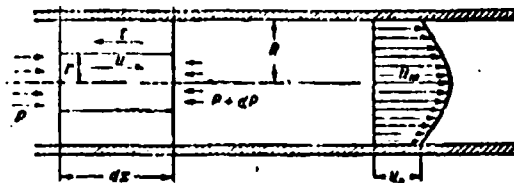


Fig. 12.3. Laminar gas flow with slip in a tube.

Here we disregarded the small value of the change in momentum in the direction of the axis of the tube, which is caused by the density change of the gas, which in turn is caused by the pressure change. Expressing the stresses of friction according to Newton's formula, from (20) we have

$$\frac{dp}{dx} = -\frac{2}{r} \mu \frac{du}{dr}. \quad (21)$$

Hence after integration in the boundary conditions, which consider the slip velocity on the wall ($u = u_R$ when $r = R$), we obtain

$$u - u_R = \frac{1}{\mu} \frac{dp}{dx} \frac{R^2 - r^2}{4}.$$

On the axis of the tube (when $r = 0$) we have

$$u_m - u_R = \frac{1}{\mu} \frac{dp}{dx} \frac{R^2}{4}.$$

This gives the following final dependence for the dimensionless velocity profile in a tube with slip:

$$\frac{u - u_R}{u_m - u_R} = 1 - \frac{r^2}{R^2}. \quad (22)$$

The velocity gradient at the wall in such a flow is

$$\left(\frac{du}{dr}\right)_R = -\frac{2(u_m - u_R)}{R}, \quad (23)$$

and the stress of friction on the wall is

$$\tau_R = - \frac{2\mu (u_m - u_R)}{R}. \quad (24)$$

The average rate of flow in the tube proves to be equal to the arithmetic mean between the velocities on the axis and at the wall

$$U = \frac{\int_0^R u 2\pi r dr}{\pi R^2} = (u_m - u_R) \int_0^R \frac{2}{R^2} \left(1 - \frac{r^2}{R^2}\right) r dr + u_R = \frac{1}{2} (u_m + u_R) \quad (25)$$

Equation (21) leads to the following formula for determining the pressure drop along the length of the tube:

$$dp = \frac{2\tau_R}{R} dx = - \frac{4(u_m - u_R)\mu}{R^2} dx$$

or in a dimensionless form, after replacement, $D = 2R$

$$\frac{dp}{\frac{1}{2}\rho U^2} = - \frac{64\mu}{\rho U D} \frac{dx}{D} \frac{u_m - u_R}{u_m + u_R}. \quad (26)$$

Let us exclude the slip velocity from the obtained expressions for which we will use the boundary condition (9) established in § 2

$$u_R = - c l \left(\frac{du}{dr} \right)_R, \text{ where } c = \frac{2-\sigma}{\sigma}. \quad (9a)$$

Here taken in front of the derivative a minus sign in order that the value of velocity on the wall would be positive ($u_R > 0$) at a negative value (23) of the velocity gradient. Substituting into (9a) the value of the derivative from (23), we find

$$u_R = \frac{u_m}{1 + \frac{R}{2\alpha}} = \frac{u_m}{1 + \frac{D}{4\alpha}} \quad (27)$$

Using formulas (21), (27), (22) and (26), we arrive at the following expressions for the maximum velocity:

$$u_m = U \frac{1 + 4\epsilon \frac{l}{D}}{0.5 + 4\epsilon \frac{l}{D}} \quad (28)$$

for the velocity at the wall

$$u_R = U \frac{4\epsilon \frac{l}{D}}{0.5 + 4\epsilon \frac{l}{D}} \quad (29)$$

for the current value of the velocity

$$u = U \frac{1 + 4\epsilon \frac{l}{D} - 4\epsilon^2 \frac{l^2}{D^2}}{0.5 + 4\epsilon \frac{l}{D}} \quad (30)$$

for the pressure drop along the length of the tube

$$\frac{dp}{\frac{1}{2} \rho U^2} = - \frac{64\mu}{\rho U D} \frac{1}{1 + 8\epsilon \frac{l}{D}} \frac{dx}{D} \quad (31)$$

or, in accordance with the Darcy formula

$$\frac{dp}{\frac{1}{2} \rho U^2} = - \zeta \frac{dx}{D}, \quad \text{and} \quad \zeta = \frac{64}{Re \left(1 + 8\epsilon \frac{l}{D}\right)} \quad (32)$$

In (32) the Reynolds number is determined by the diameter of the tube and mean flow rate

$$R_D = \frac{\rho U D}{\mu}$$

From the continuity condition it follows that along the tube of constant cross section the current density is not changed ($\rho U = \rho_0 U_0 = \text{const}$) if gas temperature is constant, and therefore the Reynolds number for all the cross sections has the same value. In this case the coefficient of friction ζ along the length of the tube changes only as a result of the change in value in the mean free path of the molecule, which depends on the local value of density $l = l_0 \rho_0 / \rho$ (subscript "0" corresponds to the initial cross section of the tube). By substituting this value into (31), we obtain when $T = \text{const}$

$$dp = -\frac{\zeta_0}{2D} \frac{\left(1 + 8\epsilon \frac{l_0}{D}\right) dx}{\frac{l_0}{\rho_0} \left(1 + 8\epsilon \frac{l_0}{D} \frac{\rho_0}{\rho}\right)} \rho_0 U_0 \quad (33)$$

where

$$\zeta_0 = \frac{64}{R_D \left(1 + 8\epsilon \frac{l_0}{D}\right)}$$

is the value of the coefficient of friction at the beginning of the tube. Using the equation of state for an ideal gas, from (33) we obtain the differential equation

$$\frac{\rho dp}{\rho_0} + 8\epsilon \frac{l_0}{D} dp = -\frac{\zeta_0}{2D} \rho_0 U_0 \left(1 + 8\epsilon \frac{l_0}{D}\right) dx,$$

which after integration, taking into account the boundary condition

$$p = p_0 \quad \text{when } x = 0$$

and some elementary conversions, gives (when $\Delta p = p - p_0$)

$$\left(\frac{\Delta p}{p_0}\right)^2 + 2 \frac{\Delta p}{p_0} \left(1 + 8c \frac{l}{D}\right) + \frac{c}{D} \frac{p_0 U^2}{p_0} \left(1 + 8c \frac{l}{D}\right) x = 0.$$

Hence it follows that

$$\frac{\Delta p}{p_0} = \left| \sqrt{1 - \frac{c p_0 U^2 x}{D p_0 \left(1 + 8c \frac{l}{D}\right)}} - 1 \right| \left(1 + 8c \frac{l}{D}\right). \quad (34)$$

where x is the overall length of the tube. In this solution one root is rejected (with a negative sign) as not corresponding to the physical conditions of the problem ($\Delta p = -2p_0$ when $x = 0$). If that being subtracted under the radical is considerably less than one, then the approximate solution is correct, which makes it possible to determine the pressure drop in the tube not allowing for the compressibility of the gas

$$\frac{\Delta p}{\frac{1}{2} \rho U^2} = -\frac{c}{D} x. \quad (35)$$

Let us substitute in (34) $c = (2 - \sigma)/\sigma$, and also on the basis of (5) the value

$$\frac{l}{D} = 1.26 \sqrt{k} \frac{\mu}{\rho D_0} = 1.26 \sqrt{k} \frac{M_0}{R_D}.$$

Having in mind that

$$\frac{p_0 U^2}{p_0} = k M_0^2$$

we obtain when $\sigma = 1$

$$\frac{p}{p_0} = \left[\sqrt{1 - \frac{\zeta k M_0^2 x}{D(1 + 10\sqrt{k} \frac{M_0}{R_D})}} - 1 \right] (1 + 10\sqrt{k} \frac{M_0}{R_D}). \quad (36)$$

where

$$\zeta = \frac{64}{R_D(1 + 10\sqrt{k} \frac{M_0}{R_D})}.$$

Let us recall that solution (36) is correct only when $M_0 \ll 1$. The dependence of the coefficient of friction ζ on the Reynolds number at different values of the Mach number is represented on Fig. 12.4. It agrees well with the experimental data of Knudsen and other researchers.

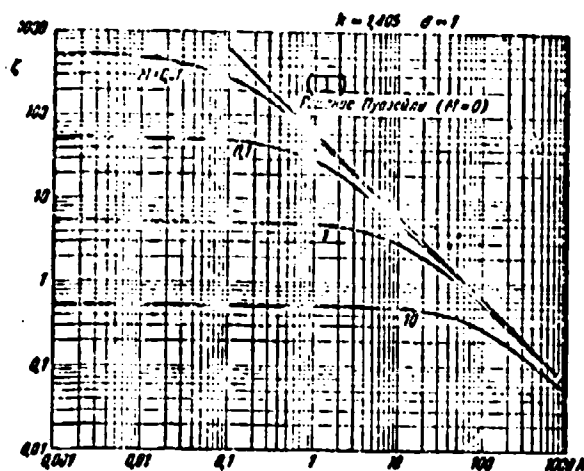


Fig. 12.4. Dependence of the coefficient of friction during flow with slip in a tube on the R number at different values of the Mach number. KEY: (1) Poiseuille solution ($M = 0$).

§ 4. External Drag of Bodies in the Flow of Rarefied Gas in the Presence of Slip

For the first time the effect of slip on the drag of the body was detected by Milliken¹ in 1911 during the study of the velocity of the drop of small oil drops in air under the action of gravity and also the lift velocity against the gravity of charged drops found in a vertically directed electrical field.

These studies of Milliken made it possible to determine the hydrodynamic effect of slip and also to measure with high precision the magnitude of the charge of the electron.

The small drops, which move at low speed in the continuum, have the form of a sphere, the drag force of which at the low values of the Reynolds number $R_e = \frac{\rho u_0 a}{\mu} \ll 1$ is determined from the Stokes formula

$$X = 6\pi\mu a u_0 \quad (37)$$

where a is the radius of the sphere, μ is the viscosity of the air, and u_0 is the velocity of the undisturbed incident flow.

Formula (37) is obtained from the accurate solution of the Navier-Stokes equation for the slow flow of incompressible fluid, when the inertia terms which are on the left side of the equation can be disregarded; the boundary condition is the equality of the rate of flow on the surface of the sphere to zero.

If we consider the slip, i.e., assume according to (9) that the slip velocity on the wall is proportional to the Knudsen

¹Collection "Gas dynamics," page 260. Publishing House of Foreign Literature, 1950.

number, then as Basset¹ showed as long ago as 1888, the modified law of the drag of the sphere is valid:

$$X = 6\pi\eta u_0 \frac{1 + 2A \frac{l}{a}}{1 + 3A \frac{l}{a}}, \quad (38)$$

where A is the proportionality factor (according to the Milliken experiments² A = 1.22, which according to (9) answers to value $\sigma = 0.9$). Expansion power of the series of the last additional factor of the parameter $A \frac{l}{a}$ leads to the following approximation formula of the drag of the sphere with slip:

$$X = 6\pi\eta u_0 \left(1 + A \frac{l}{a}\right)^{-1}, \quad (39)$$

valid at $\frac{l}{a} \leq 0.5$, subsonic velocity and low values of the Reynolds number.

The dimensionless coefficient of drag of the sphere, according to Milliken when $M < 1$

$$c_x = \frac{\lambda}{\frac{1}{2} \rho u_0^2 a^2} = \frac{12}{R_a \left(1 + 1.2 \frac{l}{a}\right)}. \quad (40)$$

The experiments of Kane³, carried out in the interval $2.05 \leq M \leq 2.81$ and $15 \leq R_a \leq 786$, did not detect the effect of the Mach number and led to the following empirical formula:

¹Basset A. B., A Treatise on Hydrodynamics, V. II, P. 271, 1888.

²Milliken gives the value A = 0.864; however, in the calculation of mean free path in terms of the value of the coefficient of viscosity, he used the obsolete dependence of Maxwell $\mu = 0.35 \rho \bar{c} l$, whereas at present the most accurate is considered to be Chapman's formula $\mu = 0.499 \rho \bar{c} l$, which also gives A = 1.22.

³Kane, E. D., J. Aeron, Sci. 18, p. 259, 1951. Russian translation in the collection: Problems of Rocket Technology, No. 2, pages 54-69, Publishing House Foreign Literature, 1953.

$$c_x = \left(0.97 + \frac{1.92}{R_a}\right) \left(1 + \frac{1}{R_a}\right)^0. \quad (41)$$

Kane determined the values of R_a according to the velocity and density of the air after the normal shock. When $R_a < 80$ the drag of the sphere, according to Milliken, is higher than that according to Kane (at low R_a the role of friction is relatively great, but it is decreased because of the intensification of the slip with an increase in M); at $R_a > 80$ the drag according to Milliken is less than that according to Kane (at large R_a there prevails the wave drag, which appears more greatly at large values of the Mach number).

The drag of the cylinder with its transverse flow with slip is examined by Chiang,¹ who obtained the following theoretical formula for the drag coefficient of the cylinder referred to the cross section $2aL$ (length of the cylinder L , radius a):

$$c_x = \frac{X}{\frac{1}{2} \rho u^2 2aL} = \frac{4a}{R_a \left[\ln \frac{4}{R_a} - 1.2M + 1.25 \sqrt{\frac{2-M}{1+M}} \frac{1}{R_a} \right]}. \quad (42)$$

where

$$R_a = \frac{\rho u^2}{\mu}.$$

There are no experimental data on the drag of the cylinder with slip at the present.

¹Collection: "Gas dynamics," page 341, Publishing of Foreign Literature, 1950.

§ 5. Free Molecular Gas Flows and Elements of the Kinetic Theory of Gases

The free molecular flow conditions are observed in the greatly rarefied gas, when the Knudsen number is considerably greater than one ($\frac{M}{R_x} \geq 3$).

Despite the fact that the collision rate of the molecules in the volume element during this condition is negligible, the number of molecules per unit volume is great enough in order that it would be possible to determine the mean macroscopic properties of the gas. For example, at a height of 150 km, when the mean free path is $\lambda = 18$ m, the number of molecules in 1 cm^3 is $2.5 \cdot 10^{11}$.

Let us establish the properties of the gas which are determined by features of the motion of its molecules. Let us examine for this the volume element $d\tau = dx dy dz$ filled by a large number of moving and rarely colliding molecules $nd\tau$, where n is the local molecule concentration in the physical volume, i.e., the quantity of molecules per unit volume.

The instantaneous values of the projections of velocity u , v , and w of separate molecules in volume $d\tau$ are distinguished very greatly. It is possible to sort out the molecules according to the velocity of motion, having in mind that the velocities depend on the coordinates x , y , and z and time t . The concept of the distribution of molecules in volume $d\tau$ according to velocity of motion gives the velocity distribution function introduced by Maxwell

$$f(u, v, w)$$

which estimates the portion of the total number of molecules (in volume $d\tau$), which possess velocity u , v , and w .

In other words, if all the molecules of the physical volume dt are arranged in the space of velocities u , v , and w , then in the elementary region of the velocity space

$$du dv dw$$

there will be concentrated $(n f dt) du dv dw$ molecules whose velocity are included in the indicated intervals; the value which is in the parenthesis is the concentration of molecules in the velocity space.

The total number of molecules in the physical volume can be obtained by means of integration over the velocity space

$$ndt = \int (n f dt) du$$

Since the total number of molecules depends only on the coordinates and time, it is possible to bring it out from under the sign of the integral and reduce it

Thus, the velocity distribution function should satisfy the following condition

$$\int f dt = 1. \quad (43)$$

An important role of the velocity distribution function is revealed, for example, in the determining of the mean value of any value Q , which depends only on components of velocities of the molecules.

The quantity Q which possess all molecules of the element dt is equal¹ to $\sum Q$, but the number of molecules in this element is ndt , and therefore the mean value \bar{Q} is

¹Patterson G. N., Molecular flow of gases. Fizmatgiz, M., 1960.

$$\bar{Q} = \frac{\int Q(n f dv) dv}{n \int f dv} = \int Q f dv \quad (44)$$

Specifically, the mean value of the component of the velocity u

$$\bar{u} = \int u f dv. \quad (45)$$

Maxwell found the following expression for the velocity distribution function of the quiescent gas:

$$f = a \exp\left(-\frac{E}{\theta}\right). \quad (46)$$

where a and θ are constants determined below, and value

$$E = \frac{1}{2} m c^2 = \frac{m}{2} (u^2 + v^2 + w^2)$$

is the kinetic energy of the molecule which corresponds to the instantaneous value of the total velocity of its random motion c . We will define constant a on the basis of condition (43)

$$\int f dv = a \int_{-\infty}^{\infty} \exp\left(-\frac{E}{\theta}\right) dv = 1.$$

This integral can be represented as the product of three identical integrals

$$\int_{-\infty}^{\infty} \exp\left(-\frac{mu^2}{2\theta}\right) du \int_{-\infty}^{\infty} \exp\left(-\frac{mv^2}{2\theta}\right) dv \int_{-\infty}^{\infty} \exp\left(-\frac{mw^2}{2\theta}\right) dw = V \left(\frac{2\pi\theta}{m}\right)^{3/2}.$$

thus, we have

$$a = \left(\frac{m}{2\pi\theta}\right)^{3/2}. \quad (47)$$

In order to determine the parameter θ , let us compute the mean value of the square of each component of velocity of the motion of the molecule according to method (45)

$$u^2 = v^2 = w^2 = \frac{1}{3} c^2 = \frac{1}{3} \int c^2 \exp \left[-\frac{\pi (u^2 + v^2 + w^2)}{2\theta^2} \right] du = \frac{\theta^2}{\pi}.$$

Hence we have

$$\frac{1}{2} m \overline{c^2} = \frac{3}{2} \theta^2. \quad (48)$$

where $m \overline{c^2} / 2$ is the internal energy of the molecule determined in terms of the mean value of the square of its total velocity. By substituting (47) and (48) into (46), we will obtain the velocity distribution function of Maxwell's molecules in the final form

$$f = \left(\frac{3}{2\pi\theta^2} \right)^{3/2} \exp \left(-\frac{3c^2}{2\theta^2} \right). \quad (49)$$

It is sometimes convenient with the calculations to turn from the velocity components u , v , and w to the total velocity c ; for this the polar (spherical) coordinates are introduced, c , ϕ , θ , where ϕ is the angle between the vectors of velocity and the polar axis Oz , and θ is the angle between planes zOc and zOx (Fig. 12.5).

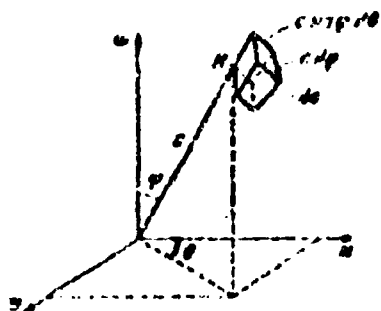


Fig. 12.5. Volume element in the velocity space (transfer from the rectangular to spherical coordinates).

In the spherical coordinates the element of the velocity space is equal to

$$dV = c^2 \sin \phi \, d\phi \, d\theta \, dc. \quad (50)$$

Therefore, the number of the molecules in the element of volume dV , the velocities of which lie in the interval c and $c + dc$, and the directions of motion - in the

Intervals $\phi, \phi + d\phi$ and $\theta, \theta + d\theta$ consists of

$$nc^3 f \sin \gamma d\gamma d\theta dc d\tau. \quad (51)$$

Integrating this expression by ϕ and θ for all possible directions ($0 \leq \phi \leq \pi, 0 \leq \theta \leq 2\pi$), we will obtain the total number of molecules which have velocities in the interval c and $c + dc$:

$$nc^3 f \left[\int_0^\pi \left(\int_0^{2\pi} \sin \gamma d\gamma \right) d\theta \right] dc d\tau = 4\pi nc^3 f dc d\tau. \quad (52)$$

The total number of molecules in the volume element $d\tau$ for the entire velocity range ($0 \leq c \leq \infty$) is determined, obviously, by the following:

$$nd\tau = \left[\int_0^\infty 4\pi nc^3 f dc \right] d\tau. \quad (53)$$

Because of this condition (43) in polar coordinates takes the form

$$4\pi \int_0^\infty c^3 f dc = 1 \quad (54)$$

and, therefore, the mean value of any Q , which depends only on the components of velocity, is found from the expression

$$\bar{Q} = 4\pi \int_0^\infty Q c^3 f dc. \quad (55)$$

Let us write the mean value of the square of the velocity in polar coordinates

$$\bar{c}^2 = 4\pi \int_0^\infty c^5 f dc. \quad (56)$$

It is easy to be convinced of the fact that, by substituting into equations (54) and (56) expression (49) for f , we turn them into identities; this means that parameters a and θ in the Cartesian and spherical coordinates are identical.

Figure 12.6 depicts the change of function $F = fc^2$ depending on c for two values of parameter \bar{c}^2 . As is evident, at a certain value of velocity $c = c_m$ function F has a maximum.

Solving the elementary problem for the search of the maximum of function (fc^2) , we find the value of the most probable velocity of the molecules

$$c_m = \sqrt{\frac{2a^2}{3}} = 0.816 \sqrt{a^2} \quad (57)$$

Let us express with the aid of (49) and (56) the arithmetic mean velocity of the molecules by the mean square velocity

$$\bar{c} = 4\pi \int_0^\infty c^3 f dc = 2 \sqrt{\frac{2a^2}{3\pi}} = 0.922 \sqrt{a^2}. \quad (57a)$$

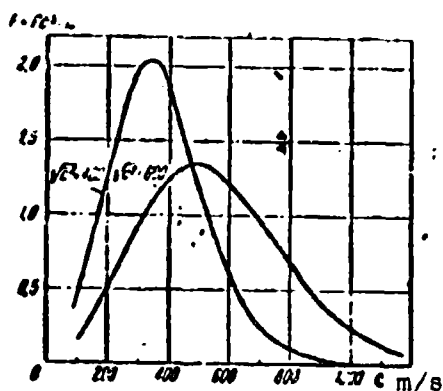


Fig. 12.6. Distribution functions for two values of the mean square velocity of molecules.

By substituting (57) into (49), we obtain a more convenient expression for the distribution function of Maxwell

$$f = \left(\frac{1}{\pi c_m^2} \right)^{3/2} \exp \left(-\frac{c^2}{c_m^2} \right). \quad (58)$$

As can be seen from Fig. 12.6, with an increase in value of the most probable velocity c_m (or the mean quadratic \bar{c}^2), the algebraic number of molecules which have high velocities increases.

The motion of the molecules affects the macroscopic properties of the gas. The gas pressure on the wall can be defined as the force which appears as a result of the change in the component normal to wall of the total momentum of molecules during their collision with the wall; in this case the molecule and wall are considered as being absolutely elastic solids.

Let us position the wall along the normal to the horizontal axis (Fig. 12.7), and let us determine the quantity of molecules which will be encountered with the elementary area with dimension dF per unit time. Let us examine first the molecules with the velocity of motion c ; hitting in one second against this area will be half of the entire quantity of molecules of the given velocity, which fill the cylinder with the generatrix c and the area of the base dF (the second half of the molecules of this velocity in view of the randomness of their motion at this same time interval moves in the opposite direction, i.e., it is driven away from the wall). This quantity is

$$\frac{1}{2} n f u dF d\omega, \quad (59)$$

where n is the total number of molecules per unit volume, f - value of the function which corresponds to the velocity c , $u dF$ - volume of the elementary cylinder, and $d\omega = du dv dw$ - element of the velocity space.

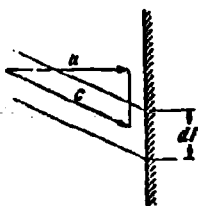


Fig. 12.7. Determining the number of molecules encountered with the wall per unit time.

The total mass of the molecules which collide with the area dF for one second is equal to

$$\frac{1}{2} nm f u dF d\omega = \frac{1}{2} \rho f u dF d\omega,$$

where $\rho = nm$ is the gas density, and m is the mass of one molecule. With elastic impact against the wall the normal component of velocity of the molecule changes to the opposite value, which corresponds to a change in the corresponding projection of the momentum for one second by the value

$$\frac{1}{2} \rho f \cdot 2u^2 dF d\omega = \rho u^2 f dF d\omega. \quad (60)$$

In summing up the changes in the momentum of the molecules in the whole velocity range ($0 \leq c \leq \infty$), we will obtain the total change in the normal projection of the momentum for one second equal to the averaged force of pressure of the molecules on area dF :

$$dP = \left[\int_0^\infty u^2 f d\omega \right] \rho dF,$$

here values ρ and dF , as being independent of the distribution of molecules according to the velocities, are removed from under the integral sign.

In converting, as in formulas (50)-(55), to the polar coordinates and referring to the force of pressure to the area, we obtain the following formula for determining the value of pressure:

$$p = \frac{dP}{dF} = \frac{1}{2} \rho \int_0^\infty u^2 c^4 f dc$$

or

$$p = \rho \bar{u}^2,$$

where \bar{u}^2 is the mean square velocity of the motion of molecules in the direction of the normal to the wall equal according to (44) and (55) to

$$\bar{u}^2 = 4\pi \int_0^\infty u^2 c^2 / dc = \int_0^\infty u^2 / d\omega.$$

Since during random motion all directions are equivalent to

$$\bar{u}^2 = \bar{v}^2 = \bar{w}^2 = \frac{c^2}{3},$$

then the gas pressure on the wall is equal to

$$p = \frac{1}{3} \rho c^2 \quad (61)$$

or, in accordance with (57),

$$p = \frac{1}{3} \rho c^2.$$

Since it was accepted that the momentum of the molecules hitting against the wall is equal to the momentum of the reflected molecules, then the obtained value of pressure is added from two equal parts: the pressure of the hitting molecules and pressure of the reflected molecules

$$p = p_1 + p_2$$

where

$$p_1 = p_2 = \frac{1}{3} \rho \bar{c}^2.$$

From (61) we obtain the expression for the mean square velocity of the motion of the molecules

$$\sqrt{\bar{c}^2} = \sqrt{\frac{3p}{\rho}}. \quad (62)$$

In comparing (62) with the known expression for the speed of sound in the gas

$$a = \sqrt{\frac{\gamma p}{\rho}},$$

we can connect the mean square velocity of the molecules with the speed of sound

$$\sqrt{\bar{c}^2} = a \sqrt{\frac{3}{\gamma}}. \quad (63)$$

§ 6. Pressure and Stress of Friction During the Free Molecular Flow Around a Solid

During the study of the free molecular flow of gas, one should consider the fact that together with the random motion of the molecules there is ordered motion of the finite masses of the gas.

In the first works of Epstein¹ and Smoluchowski² which are devoted to the free molecular gas flow around a solid, it was

¹Epstein, P. S., on the drag of spheres with motion in gases In Collection: "Gas dynamics." Publishing House of Foreign Literature, 1950.

²Smoluchowski M., Zur kinetische Theorie der Transpiration und Diffusion verdünnter Gase, Annal. der Physik, V. 33, 1559-70, 1910.

assumed that the velocity of the ordered motion of gas was low as compared with the average velocity of the random motion of the molecules. We will not begin to use this limitation, and let us give the solution to the problem for the arbitrary value of the Mach number in the gas flow incident on the body. As Chiang¹ showed such a general solution has a sufficiently simple form.

It is advantageous to examine the streamline flow of a body by rarefied gases in a rectangular system of coordinates, since in this case the similar velocity components of the random and ordered motions are conveniently grouped.

If the gas is greatly rarefied, then the collisions of the molecules between themselves and with the body surface are so rare that the molecules reemitted by the surface do not virtually disturb the undisturbed flow of gas incoming to the body and do not disturb the Maxwellian distribution of the random velocities (u, v, w) of molecules in this gas. The distribution function of Maxwell according to (58) can be represented in the form

$$f = \left(\frac{1}{\pi c_m^2} \right)^{3/2} \exp \left[- \frac{u^2 + v^2 + w^2}{c_m^2} \right]. \quad (64)$$

If the ordered motion of the gas occurs with the velocity

$$C = \sqrt{U^2 + V^2 + W^2}, \quad (65)$$

then the total velocity of the molecules are respectively equal to

$$u_1 = U + u, \quad v_1 = V + v, \quad w_1 = W + w. \quad (66)$$

¹Chiang, Kh. Sh., Aerodynamics of Rarefied Gases. In the Collection: "Gas Dynamics." Publishing House of Foreign Literature, 1950.

Let us arrange the rectangular coordinate system in such a way that the x-axis is perpendicular to the surface element of the body dF (Fig. 12.8), and let us determine the force of pressure of the moving gas on the area dF following the same considerations as in the previous paragraph (in the determining of the pressure on the wall of stationary gas).

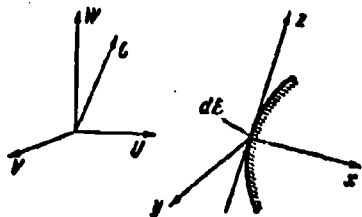


Fig. 12.8. Determination of the pressure force of gas on the wall with molecular flow.

In the stationary coordinate system the number of molecules in a unit volume, which have velocities of random motion in the interval u and $u + du$, v and $v + dv$, w and $w + dw$ is equal to $nfdw$; in one second dF those molecules which fill cylinder with the base dF and generatrix manage to hit against the area.

$$c_1 = \sqrt{u_1^2 + v_1^2 + w_1^2}$$

The volume of this cylinder is equal to $u_1 dF$. Therefore, the total number of molecules at a rate of u_1 , which transmit momentum to area dF , is

$$n f u_1 dF du dv dw = n f u_1 dF du_1 dv_1 dw_1$$

Here assumption about the constancy of the velocity of the directed motion of the gas is used.

The total number of molecules N which hit against the unit element of the area will be obtained by means of the integration of the last expression over the entire range of the change in velocities of the molecules. Taking (64) into account, we have

$$N = n \left(\frac{1}{\pi^{3/2}} \right)^{1/2} \int_{-\infty}^{\infty} dv_1 \int_{-\infty}^{\infty} dw_1 \int_{-\infty}^{\infty} u_1 \times \exp \left[- \frac{(u_1 - U)^2 + (v_1 - V)^2 + (w_1 - W)^2}{c_m^2} \right] du_1. \quad (67)$$

The lower limit in the last integral is equal to zero and not $-\infty$, since the molecules with the negative values of the normal component of velocity ($u < 0$) with the surface of the body will not be encountered.

It is not difficult to show that the triple integral in (67) is reduced to the product of the following three integrals:

$$\int_{-\infty}^{\infty} \exp\left[-\frac{(v_1 - U)^2}{c_m^2}\right] dv_1 = c_m \sqrt{\pi}, \quad (68a)$$

$$\int_{-\infty}^{\infty} \exp\left[-\frac{(w_1 - W)^2}{c_m^2}\right] dw_1 = c_m \sqrt{\pi}, \quad (68b)$$

$$\begin{aligned} \int_0^{\infty} u_1 \exp\left[-\frac{(u_1 - U)^2}{c_m^2}\right] du_1 = \\ = \frac{c_m}{2} \left\{ \exp\left[-\frac{U^2}{c_m^2}\right] + \frac{U \sqrt{\pi}}{c_m} \left[1 + \operatorname{erf}\left(\frac{U}{c_m}\right) \right] \right\}. \end{aligned} \quad (68c)$$

Used in this recording is a conventional designation for the probability integral:

$$\operatorname{erf}(t) = \frac{2}{\sqrt{\pi}} \int_0^t e^{-x^2} dx,$$

the values of which are taken from the tables [let us note that when $t = \infty$ $\operatorname{erf}(\infty) = 1$]. Substituting the expressions (68) into (67), we obtain the following formula for determining the number of molecules hitting per unit time against the unit area of the body's surface:

$$N = \frac{n c_m}{2} \left\{ \frac{1}{\sqrt{\pi}} \exp\left(-\frac{U^2}{c_m^2}\right) + \frac{U}{c_m} \left[1 + \operatorname{erf}\left(\frac{U}{c_m}\right) \right] \right\}. \quad (69)$$

In the particular case of stationary gas ($U = 0$) we obtain

$$N_0 = \frac{n c_m}{2 \sqrt{\pi}}. \quad (69a)$$

The per-second mass flow of molecules which fall on the unit area of the body's surface:

$$\Delta I_x = mN = \frac{1}{2} \rho c_m \left\{ \frac{1}{c_m^2} \exp \left[-\frac{U^2}{c_m^2} \right] + \frac{U}{c_m} \left[1 + \operatorname{erf} \left(\frac{U}{c_m} \right) \right] \right\}. \quad (70)$$

For stationary gas ($U = 0$), according to (57) and (57a), we have

$$\Delta I_x = \rho \frac{c_m^2}{2\sqrt{\pi}} = \frac{1}{2} \rho c_m^2. \quad (71)$$

In determining the aerodynamic forces which appear on a unit area of the body during free molecular flow, it is necessary to keep in mind that the projection of the aerodynamic force is equal to the difference in the projections on the same axis of the momenta of the per-second mass of molecules falling on the area and reflected from it.

The projection on the x-axis of the per-second momentum of molecules with velocity in the interval $u, u + du; v, v + dv; w, w + dw$, which fall on the surface of the unit area, obviously, is equal to

$$\rho f u_x^2 du dv dw.$$

The projection on the normal of the per-second momentum of all the molecules comprises, taking into account (64),

$$I_{x1} = \rho \left(\frac{1}{\pi c_m^2} \right)^{\frac{3}{2}} \int_{-\infty}^{\infty} du_1 \int_{-\infty}^{\infty} dv_1 \int_{-\infty}^{\infty} dw_1 u_1^2 \times \\ \times \exp \left[-\frac{(u_1 + U)^2 + (v_1 - V)^2 + (w_1 - W)^2}{c_m^2} \right] du_1. \quad (72)$$

As in the determining of the number of molecules hitting the surface (see formulas (67) and (68)), let us replace the triple

integral in (72) by the product of the three integrals. Two of them were found earlier than (68a) and (68b)

$$\int_{-\infty}^{\infty} \exp\left[-\frac{(v_1 - V)^2}{c_m^2}\right] dv_1 = \int_{-\infty}^{\infty} \exp\left[-\frac{(\omega_1 - V)^2}{c_m^2}\right] d\omega_1 = c_m \sqrt{\pi},$$

and the third in this case takes the form

$$\begin{aligned} \int_{-\infty}^{\infty} u_1^2 \exp\left[-\frac{(u_1 - U)^2}{c_m^2}\right] du_1 = \\ = \left(\frac{c_m^2}{2} + c_m U\right) \left[1 + \operatorname{erf}\left(\frac{U}{c_m}\right)\right] + \frac{1}{2} c_m U \exp\left[-\frac{U^2}{c_m^2}\right]. \end{aligned} \quad (73)$$

Let us note that with integration (73) the following known relationships were taken into consideration:

$$\begin{aligned} \int x^2 e^{-x^2} dx &= \frac{1}{2} \left(\int e^{-x^2} dx - x e^{-x^2} \right), \\ \int x e^{-x^2} dx &= -\frac{1}{2} \int e^{-x^2} dx = -\frac{1}{2} e^{-x^2}. \end{aligned} \quad (74)$$

By substituting the found values of the integrals into (72), we determine projection on the normal (x-axis) of the per-second momentum of the molecules which fall on the unit surface area of the body:

$$I_{x1} = \frac{1}{2\sqrt{\pi}} \rho c_m U \exp\left(-\frac{U^2}{c_m^2}\right) + \rho \left(\frac{c_m^2}{4} + \frac{U^2}{2}\right) \left[1 + \operatorname{erf}\left(\frac{U}{c_m}\right)\right]. \quad (75)$$

In two limiting cases, $U = 0$ and $U \gg c_m$, expression (75) is greatly simplified. When $U = 0$ (ordered gas flow is absent)

$$I_{x1} = \frac{1}{4} \rho c_m^2. \quad (76)$$

At $U \gg c_m$ (the flow velocity is considerably greater than the probable velocity of the random motion of the molecules)

$$I_{x1} = p \left(\frac{1}{\gamma} c_m + U^2 \right), \quad (77)$$

since in this case

$$\exp \left[-\frac{U^2}{c_m^2} \right] \sim 0, \quad \operatorname{erf} \left(\frac{U}{c_m} \right) \sim 1.$$

Let us now find the component tangential to the body surface of the per-second momentum of molecules which fall on the unit area (projection on the z-axis).

For the molecules whose velocities lie in the narrow interval of the value

$$u, u+du; v, v+dv; w, w+dw,$$

the tangential projection of the per-second momentum is equal to

$$-p u_1 w_1 du_1 dv_1 dw_1. \quad (78)$$

For all molecules we have, by analogy with (67) or (72),

$$I_{x1} = p \left(\frac{1}{\gamma c_m^2} \right)^{\frac{3}{2}} \int_{-\infty}^{\infty} dv_1 \int_{-\infty}^{\infty} w_1 dw_1 \int_{-\infty}^{\infty} u_1 \times \\ \times \exp \left[-\frac{(u_1 - U)^2 + (v_1 - V)^2 + (w_1 - W)^2}{c_m^2} \right] du_1. \quad (79)$$

Let us replace, as before, the triple integral in (79) by the product of the three integrals. Values of two of them are already known (see (68a) and (68c)), and the third is easily determined by analogy with (68b)

$$\int_{-\infty}^{\infty} w_1 \exp \left[-\frac{(w_1 - W)^2}{c_m^2} \right] dw_1 = W c_m \sqrt{\pi}. \quad (80)$$

Substituting (68a), (68c) and (80) into expression (79), we find the component tangential to the body's surface of the per-second momentum of the molecules which hit against the surface of the unit area:

$$I_{11} = \frac{1}{2} \rho_m W \left\{ \frac{1}{2} \exp\left(-\frac{U^2}{c_m^2}\right) + \frac{U}{c_m} \left[1 + \operatorname{erf}\left(\frac{U}{c_m}\right) \right] \right\}. \quad (81)$$

In the case of the quiescent gas ($U = W = 0$), as one would expect, the tangential component of the momentum of the molecules is equal to zero, since the momenta of the molecules of the opposite direction cancel out.

If the flow velocity of the gas considerably exceeds the probable velocity of motion of the molecules ($U \gg c_m$), then, as has already been indicated, in the derivation of expression (77),

$$\exp\left(-\frac{U^2}{c_m^2}\right) = 0, \quad \operatorname{erf}\left(\frac{U}{c_m}\right) = 1;$$

and therefore, according to (81), the tangential component of the per-second momentum of the molecules hitting against the plate

$$I_{11} = \rho U W. \quad (82)$$

Let us now find the per-second momentum for the molecules re-emitted (reflected) by the body's surface.

If the molecules are mirror reflected, then we deal with the inverted re-emission, when for the incident and reflected molecules the normal components of the momenta are equal in magnitude but opposite in sign (normal velocity with reflection reverses the sign)

$$I_{11} = -I_{12}. \quad (83)$$

and the tangential components of the momenta before and after the reflection are identical both in value and direction (the tangential velocity with reflection is retained)

$$I_{n1} = I_{n2} = I_{nt} \quad (84)$$

If the molecules are emitted by the surface in a diffuse manner (with the normal Maxwellian velocity distribution of random motion), then in view of the absence of the preferred direction of the molecule the tangential component of the momentum after reflection is equal to zero.

$$I_{n1} = I_{n2} = 0. \quad (85)$$

The normal component of the per-second momentum with diffuse reflection can be found with the aid of the following considerations. Since after the diffuse reflection the molecules of the gas lose the average forward gas velocity ($c_x = 0$), then the per-second mass of the molecules being reflected by the unit area of the body's surface is determined by expression (71)

$$M_{n1} = \frac{1}{2} \rho c_{m1}^2 \quad (86)$$

Here c_{m1} is the probable velocity of the molecules at the temperature of re-emission not equal to the temperature of the incident flow.

The normal component of the per-second momentum of the molecules diffusely reflected by the wall (when $c_x = 0$) is defined from (76)

$$I_{n1} = \frac{1}{4} \rho c_{m1}^3 \quad (87)$$

If comparing (86) and (87), we have

$$I_{xA} = \frac{V_{\infty}}{2} M_{xA} c_{mAx} \quad (88)$$

It is not difficult to find the value I_{xA} on the basis of the fact that the mass of the molecules reflected from the wall is equal to mass of the molecules hitting against it ($M_{xA} = M_x$), but then, after substituting (70) into (88), we have

$$I_{xA} = \frac{1}{4} \rho c_m c_{mAx} \left\{ \exp\left[-\frac{U^2}{c_m^2}\right] + \frac{UV_{\infty}}{c_m^2} \left[1 + \operatorname{erf}\left(\frac{U}{c_m}\right)\right] \right\}. \quad (89)$$

Since the velocity of the random motion of the molecules is proportional to the square root of the temperature, then the probable velocity of the reflected molecules can be expressed in terms of the probable velocity of the molecules and incident flow, and the ratio of temperatures

$$c_{mA} = c_m \sqrt{\frac{T_A}{T_{\infty}}}. \quad (90)$$

Here T_{∞} is the temperature in the undisturbed incident flow, and T_A is the temperature of the molecules after reflection from the wall, which depends on the wall temperature T_w and the accommodation coefficient α .

Let us assume that the portion of the diffusely reflected molecules consist of σ , then the energy of these molecules is proportional to the value σT_A , and the energy of the mirror reflected molecules is proportional to $(1 - \sigma) T_{\infty}^*$. The total energy of the molecules reflected by the surface is proportional to the value

$$\sigma T_A + (1 - \sigma) T_{\infty}^*$$

As was shown in § 2, the accommodation coefficient is called the ratio of the actual change in the energy of the molecules with

reflection from the wall to its maximally possible change, which takes with the full accommodation of the molecules when the temperature of the reflected molecules is equal to the wall temperature T_w . Therefore, we have

$$\alpha = \frac{T_A^2 - [\sigma T_A + (1 - \sigma) T_w^2]}{T_A^2 - T_w^2} = \frac{\sigma(T_A^2 - T_w^2)}{T_A^2 - T_w^2}. \quad (91)$$

Using this formula, it is possible from the known values of coefficients α and σ to find the temperature of the diffusely reflected molecules T_d and then according to formula (90) - the probable velocity of the molecules $c_{m d}$. The obtained information is sufficient for determining the aerodynamic forces which appear on the body under varied conditions of the free molecular flow.

The projection of the force is equal to the change in the corresponding projection of the per-second momentum of molecules (with impact and reflection)

$$P_x = I_{x1} - I_{x2} \quad P_z = I_{z1} - I_{z2} \quad (92)$$

If the portion of the diffusely reflected molecules is σ , and the mirror reflected molecules $(1 - \sigma)$, then

$$\left. \begin{aligned} P_x &= I_{x1} - [-\sigma I_{x2} + (1 - \sigma) I_{x2}] \\ P_z &= I_{z1} - [-\sigma I_{z2} + (1 - \sigma) I_{z2}] \end{aligned} \right\} \quad (93)$$

or on the basis of (83) and (84)

$$P_x = (2 - \sigma) I_{x1} + \sigma I_{x2} \quad P_z = \sigma I_{z1} \quad (94)$$

By using expressions (94), (75) and (90), we obtain the final expression for the pressure, which exerts the free molecular gas

flow on the surface element oriented along the normal to the velocity component of the undisturbed flow of gas:

$$p = P_x = \frac{1}{2} \rho c_m^2 \left\{ \left[\frac{2-\sigma}{\sqrt{\pi}} \frac{U}{c_m} + \frac{\sigma}{2} \sqrt{\frac{T_A}{T_m}} \right] \exp\left(-\frac{U^2}{c_m^2}\right) + \left[\left(\frac{1}{2} + \frac{U^2}{c_m^2}\right)(2-\sigma) + \frac{\sigma}{2} \sqrt{\frac{T_A}{T_m}} \frac{U}{c_m} \sqrt{\frac{T_A}{T_m}} \right] \left[1 + \operatorname{erf}\left(\frac{U}{c_m}\right) \right] \right\}. \quad (95)$$

Similarly, from (94), (80), (85) and (90), we derive the general formula for the stress of friction on the surface element during the free molecular flow

$$\tau = P_z = \frac{1}{2} \sigma \rho c_m W \left\{ \frac{1}{\sqrt{\pi}} \exp\left(-\frac{U^2}{c_m^2}\right) + \frac{U}{c_m} \left[1 + \operatorname{erf}\left(\frac{U}{c_m}\right) \right] \right\}. \quad (96)$$

In the particular case of the undisturbed flow perpendicular to the body surface ($C = U$, $V = 0$, $W = 0$), the tangential stress (friction) is equal to zero

$$\tau_m = 0. \quad (97)$$

In the particular case of the flow parallel to the body's surface ($C = W$, $U = 0$, $V = 0$), the pressure

$$p = \frac{1}{4} \rho c_m^2 \left[2 + \sigma \left(\sqrt{\frac{T_A}{T_m}} - 1 \right) \right] \quad (98)$$

and the stress of friction

$$\tau = \frac{\sigma}{2\sqrt{\pi}} \rho c_m C \quad (99)$$

With the completely diffuse reflection of the molecules from the wall ($\sigma = 1$) we have

$$\rho = \frac{1}{4} \rho c_m^2 \left(1 + \sqrt{\frac{T_A}{T_n}}\right),$$

$$\tau = \frac{1}{2 \sqrt{\pi}} \rho c_m C \quad (100)$$

In formulas (95) and (96) the approach stream velocity is considered to be positive if vector U is directed toward the streamlined surface and negative if this vector is directed from the surface. In other words, in the calculation of forces which appear on the front side of the body (turned toward the incident flow), it is necessary to consider the velocity positive ($U > 0$), and on the rear side of the body - negative ($U < 0$).

Since here understood by U is the absolute value of the velocity, then for the front part of the body ($U > 0$) formulas (95) and (96) are suitable without changes ($p_n = p$, $\tau_n = \tau$); for the rear side of the body ($U < 0$) formulas (95) and (96) must be written in the following form:

$$\rho_s = \frac{1}{2} \rho c_m^2 \left\{ \left[-\frac{2-s}{\sqrt{\pi}} \frac{U}{c_m} + \frac{s}{2} \sqrt{\frac{T_A}{T_n}} \right] \exp\left(-\frac{U^2}{c_m^2}\right) + \right.$$

$$\left. + \left[(2-s) \left(\frac{1}{2} + \frac{U^2}{c_m^2} \right) - \frac{s \sqrt{\pi}}{2} \frac{U}{c_m} \sqrt{\frac{T_A}{T_n}} \right] \left[1 - \operatorname{erf}\left(\frac{U}{c_m}\right) \right] \right\}. \quad (101)$$

$$\tau_s = \frac{1}{2} \rho c_m W \left\{ \frac{1}{\sqrt{\pi}} \exp\left(-\frac{U^2}{c_m^2}\right) - \frac{U}{c_m} \left[1 - \operatorname{erf}\left(\frac{U}{c_m}\right) \right] \right\}. \quad (102)$$

For the facilitation of the calculations according to formulas (95), (96), (101) and (102), Table 5 gives values of functions $\exp\left(-\frac{U^2}{c_m^2}\right)$ and $\operatorname{erf}\left(\frac{U}{c_m}\right)$ for different $s = \frac{U}{c_m}$. According to these data, curves on Fig. 12.9 are also plotted.

Table 5.

$\frac{U}{c_m}$	$\frac{U^2}{c_m^2}$	$\exp\left(-\frac{U^2}{c_m^2}\right)$	$\operatorname{erf}\left(\frac{U}{c_m}\right)$
0	0	1	0
0.1	0.01	0.9900	0.1123
0.2	0.04	0.9806	0.2227
0.3	0.09	0.9139	0.3286
0.4	0.16	0.8521	0.4284
0.5	0.25	0.7788	0.5205
0.6	0.36	0.6977	0.6039
0.7	0.49	0.6026	0.6778
0.8	0.64	0.5274	0.7421
0.9	0.81	0.4449	0.7981
1	1	0.3679	0.8127
1.1	1.21	0.2982	0.8802
1.2	1.44	0.2369	0.9103
1.3	1.69	0.1843	0.9310
1.4	1.96	0.1409	0.9523
1.5	2.25	0.1054	0.9661
1.6	2.56	0.0773	0.9763
1.7	2.89	0.0556	0.9838
1.8	3.24	0.0392	0.9891
1.9	3.61	0.0271	0.9928
2	4	0.0183	0.9953
3	9	0	1

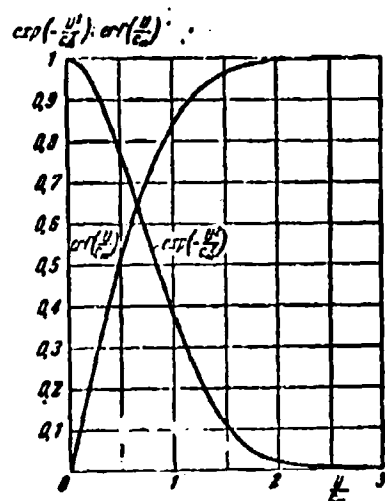


Fig. 12.9. Auxiliary functions:

$\exp\left(-\frac{U^2}{c_m^2}\right)$ and $\operatorname{erf}\left(\frac{U}{c_m}\right)$.

§ 7. Calculation of Aerodynamic Forces with Free Molecular Flow Around Solids

Shown in the preceding paragraph are methods of the determining of the normal and tangential stresses which appear on the surface element of the body's surface with free molecular flow.

Let us find the aerodynamic forces which act on body as a whole.

Let us assume that the velocity vector of the undisturbed flow C consists of angle β with the surface element of the body (local angle of attack), then the angle φ between vector C and normal to the surface (Fig. 12.10)

$$\varphi = \frac{\pi}{2} - \beta$$

Consequently, the projections of the velocity on the normal and tangent to the surface are, respectively,

$$\begin{aligned} U &= C \cos \varphi = C \sin \beta, \\ W &= C \sin \varphi = C \cos \beta. \end{aligned} \quad (103)$$

Let us determine the forces which act on the plate. The aerodynamic force component normal to plate is equal to the product of the area of the plate by the difference in pressure applied to its front and rear sides

$$P_n = (p_n - p_d) F. \quad (104)$$

The tangential force is equal to the product of the area of the plate by the sum of the stresses of friction which appear on its both sides:

$$P_t = (\tau_n + \tau_d) F. \quad (105)$$

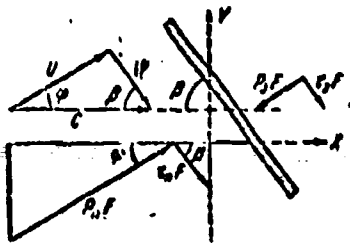


Fig. 12.10. On the determining of aerodynamic forces on the plate with a free-molecule flow of gas.

Substituting (103), (95) and (101) into (104) and taking for simplicity $\sigma = 1$, $T_{\Delta n} = T_{\Delta z} = T_n$, let us find the value of the normal force

$$P_n = \frac{1}{2} \rho c_m^2 F \left\{ \left[\frac{2}{\sqrt{\pi}} \frac{C \sin \beta}{c_m} \exp \left(-\frac{C^2 \sin^2 \beta}{c_m^2} \right) + \sqrt{\pi} \frac{C \sin \beta}{c_m} + \left[1 + 2 \frac{C^2 \sin^2 \beta}{c_m^2} \right] \operatorname{erf} \left(\frac{C \sin \beta}{c_m} \right) \right] \right\}. \quad (106)$$

On the basis of (103), (96) and (102), we will obtain from (105) the value of the tangential force

$$P_t = \rho c_m C \cos \beta F \left\{ \frac{1}{\sqrt{\pi}} \exp \left(-\frac{C^2 \sin^2 \beta}{c_m^2} \right) + \frac{C \sin \beta}{c_m} \operatorname{erf} \left(\frac{C \sin \beta}{c_m} \right) \right\}. \quad (107)$$

Now it is not difficult to determine the total aerodynamic force directed perpendicular to the approach stream velocity, i.e., the lift on the plate

$$P_y = P_n \cos \beta - P_t \sin \beta = \frac{1}{2} \rho c_m^2 \cos \beta \left[\frac{C \sin \beta}{c_m} \sqrt{\pi} + \operatorname{erf} \left(\frac{C \sin \beta}{c_m} \right) \right] \quad (108)$$

and the total aerodynamic force directed along the approach stream velocity, i.e., the drag force of the plate

$$P_x = P_n \sin \beta + P_t \cos \beta = \frac{1}{2} \rho c_m^2 \left\{ \frac{2}{\sqrt{\pi}} \frac{C}{c_m} \exp\left(-\frac{C^2 \sin^2 \beta}{c_m^2}\right) + \sqrt{\pi} \frac{C \sin^2 \beta}{c_m} + \left[1 + 2 \frac{C^2}{c_m^2}\right] \sin \beta \operatorname{erf}\left(\frac{C \sin \beta}{c_m}\right) \right\}. \quad (109)$$

Let us find from (108) and (109) the aerodynamic coefficients of the plate with free molecular streamline flow

$$c_y = \frac{P_y}{\frac{1}{2} \rho C^2 F} = \cos \beta \sin^2 \beta \left[\sqrt{\pi} \frac{C}{c_m \sin \beta} + \frac{c_m^2}{C^2 \sin^2 \beta} \operatorname{erf}\left(\frac{C \sin \beta}{c_m}\right) \right], \quad (110)$$

$$c_x = \frac{P_x}{\frac{1}{2} \rho C^2 F} = \sin \beta \left[\frac{2}{\sqrt{\pi}} \frac{C}{c_m \sin \beta} \exp\left(-\frac{C^2 \sin^2 \beta}{c_m^2}\right) + \sqrt{\pi} \frac{C}{c_m} \sin \beta + \left(\frac{c_m^2}{C^2} + 2\right) \operatorname{erf}\left(\frac{C \sin \beta}{c_m}\right) \right]. \quad (111)$$

Coefficients c_y and c_x can be expressed as a function of the Mach number, if with the aid of (57) and (63) the probable velocity of the random motion of molecules c_m is replaced by the speed of sound. In accordance with this we have

$$s = \frac{C}{c_m} = M \sqrt{\frac{\gamma}{2}}. \quad (112)$$

Dependences $c_y(M)$, and $c_x(M)$ for several values of the angle of attack of the plate are presented on Fig. 12.11 and Fig. 12.12.

Aerodynamic forces with free molecular streamline flow can be calculated for bodies of a more complex shape than can flat plates, but in this case it is advantageous to make the calculation for the front and rear sides of the body separately, using the corresponding expressions (95) and (96) or (101) and (102) for the normal and tangential stresses.

The calculation of aerodynamic forces with free molecular transverse streamline flow around a circular cylinder of infinite length is feasible.

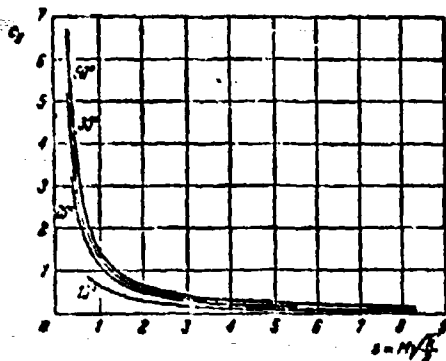


Fig. 12.11.

Fig. 12.11. Dependence of the lift coefficient of the plate on the Mach number with free-molecule flow of the gas.

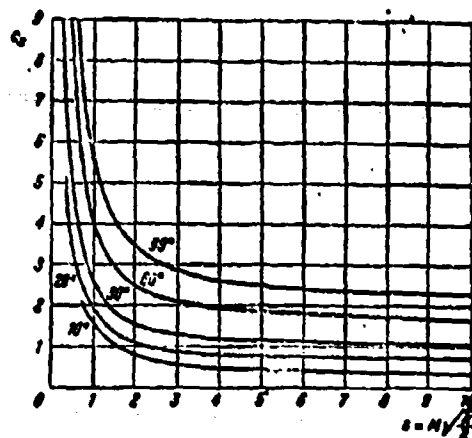


Fig. 12.12.

Fig. 12.12. Dependence of the drag coefficient of the plate on the Mach number with the molecular flow of the gas.

The projection of the aerodynamic force applied to the surface element dF onto the free-stream direction (drag), in accordance with Fig. 12.13, is equal to

$$dP_{xx} = (\rho \sin \beta + \tau \cos \beta) dF, \quad dP_{xx} = (-\rho \sin \beta + \tau \cos \beta) dF. \quad (113)$$

The projection of the same force onto the perpendicular to the free-stream direction

$$dP_{yy} = (\rho \cos \beta - \tau \sin \beta) dF, \quad dP_{yy} = (\rho \cos \beta + \tau \sin \beta) dF. \quad (114)$$

After integrating these expressions within limits of β_1 (the lower edge of the body's surface) to β_2 (upper edge), we obtain the values of the drag P_x and lift P_y , which act on the assigned section of the body's surface. In the particular case of the cylinder (Fig. 12.13) there is no lift ($P_y = 0$), and drag can be obtained from (113) by means of (95) and (96) for the front side of the cylinder (unit length)

$$P_{x0} = \frac{1}{2} \rho C^2 2R \int_0^{\frac{\pi}{2}} \left\{ \left(\frac{1}{2} \frac{C}{c_m} + \frac{1}{2} \sin \beta \right) \exp \left(-\frac{C^2 \sin^2 \beta}{c_m^2} \right) + \right. \\ \left. + \left(\frac{1}{2} + \frac{C^2}{c_m^2} + \frac{1}{2} \frac{C \sin \beta}{c_m} \right) \sin \beta \left[1 + \operatorname{erf} \left(\frac{C \sin \beta}{c_m} \right) \right] \right\} d\beta \quad (115)$$

where $dF = -Rd\phi = R d\beta$. In a similar manner, with the aid of (101) and (102) for the rear side of the cylinder, we obtain

$$P_{x2} = \frac{1}{2} \rho C^2 2R \int_0^{\frac{\pi}{2}} \left\{ \left(\frac{1}{2} \frac{C}{c_m} - \frac{1}{2} \sin \beta \right) \exp \left(-\frac{C^2 \sin^2 \beta}{c_m^2} \right) + \right. \\ \left. + \left(-\frac{1}{2} - \frac{C^2}{c_m^2} + \frac{1}{2} \frac{C \sin \beta}{c_m} \right) \sin \beta \left[1 - \operatorname{erf} \left(\frac{C \sin \beta}{c_m} \right) \right] \right\} d\beta \quad (116)$$

The drag coefficient of the cylinder

$$c_x = \frac{P_{x0} + P_{x2}}{\frac{1}{2} \rho C^2 2R}$$

By using relations (115) and (116) and introducing notation $\epsilon = \frac{C}{c_m}$, we have¹⁾

$$c_x = \frac{2}{\pi} \int_0^{\frac{\pi}{2}} e^{-\epsilon^2 \sin^2 \beta} d\beta + \left(\frac{1}{2} + 2 \right) \int_0^{\frac{\pi}{2}} \sin \beta \operatorname{erf}(\epsilon \sin \beta) d\beta - \frac{1}{2} + \\ + \frac{1}{2} \int_0^{\frac{\pi}{2}} \sin^2 \beta d\beta \quad (117)$$

¹⁾ It is obvious (see Fig. 12.13) that the expression for c_x can be obtained (as for the plate) from formula

$$c_x = \frac{1}{\frac{1}{2} \rho C^2 2R} \int_0^{\frac{\pi}{2}} [(P_{x0} - P_{x2}) \sin \beta + (q_0 + q_2 \cos \beta)] d\beta$$

Values of the integrals which enter into expressions (117) will be

$$F_1 = \int_0^{\pi} e^{-s \sin \beta} d\beta = \frac{\pi}{2} e^{-\frac{s}{2}} I_0$$

$$F_2 = \int_0^{\pi} \sin \beta \operatorname{erf}(s \sin \beta) d\beta = \frac{\sqrt{\pi}}{2} e^{-\frac{s^2}{4}} (I_0 + I_1)$$

$$F_3 = \int_0^{\pi} \sin^2 \beta d\beta = \frac{\pi}{4}$$

Here the values

$$J_0 = \frac{1}{\pi} \int_0^{\pi} \frac{e^{\frac{s^2}{2} x} dx}{\sqrt{1-x^2}}, \quad J_1 = \frac{1}{2\pi} s^2 \int_0^{\pi} e^{\frac{s^2}{2} x} \sqrt{1-x^2} dx$$

are the so-called modified Bessel functions of the order of 0 and 1, respectively. Values $J_0(s)$ and $J_1(s)$ are given on Fig. 12.14.

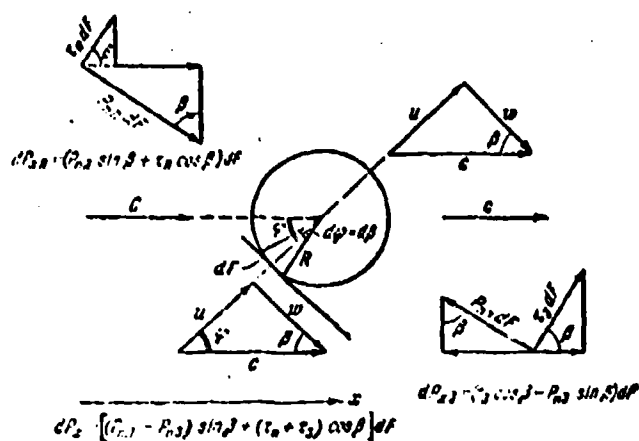


Fig. 12.13. The determining of projections of forces of pressure and friction on the flow direction with transverse streamline flow around the cylinder.

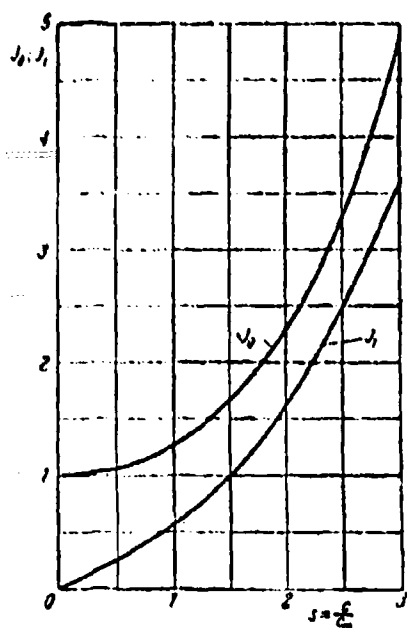


Fig. 12.14. The modified Bessel functions of the zeroth and first order.

By substituting values F_1 , F_2 , and F_3 into equation (117), we obtain finally

$$c_x = \frac{\sqrt{\pi}}{s} \left\{ s^{-\frac{1}{2}} s^{\frac{1}{2}} \left[I_0 + \left(\frac{1}{2} + s^2 \right) (I_0 + I_1) \right] + \frac{\pi}{4} \right\}.$$

Figure 12.15 depicts the dependence calculated in formula (117) of the drag coefficient of the cylinder on the number $s = c/c_m$ with its free-molecular streamline flow of helium. For a comparison on this graph the experimental points obtained by Stalder, Goodwin and Creager¹ in a wind tunnel.

In the search of aerodynamic forces which appear with the free-molecular flow about the plate and cylinder, it was assumed that the surface temperature of the body was equal to the temperature of the undisturbed incident flow. The determining of the actual temperature of the body in free-molecular flow is an independent problem,² which we will not discuss here.

¹Stalder J. R., Goodwin G., Creager M. O., NACA Reprt 1037, 1951.

²Patterson, G. N., Molecular Flow of Gases. Fizmatgiz, M., 1960.

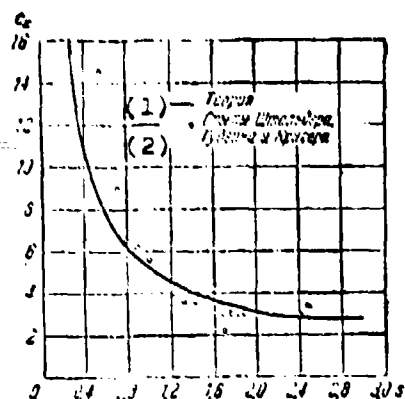


Fig. 12.15. Dependence of the drag coefficient on the s number with transverse streamline flow around the cylinder.

KEY: (1) Theory; (2) Experiments of Stalder, Goodwin and Greager.

12.6. The Free-Molecular Gas Flow in a Long Tube

The free-molecular flow in a long tube is understood to be a flow in which the mean free path of the molecules λ is much greater than the diameter of the tube d . In this case it is necessary to consider the collisions of the molecules with the walls, but it is possible to disregard collisions of the molecules between themselves, and therefore, the Maxwellian velocity distribution of the random motion of the molecules, which is established with reflection from the walls within the tube, is not disturbed.

Let us find the molecular mass which passes per unit time through the cross section of the tube (Fig. 12.16). For this purpose let us cut out the surface element dF in cross section 2 of the tube, and let us determine the number of molecules reflected by walls of the tube which will cross this area.

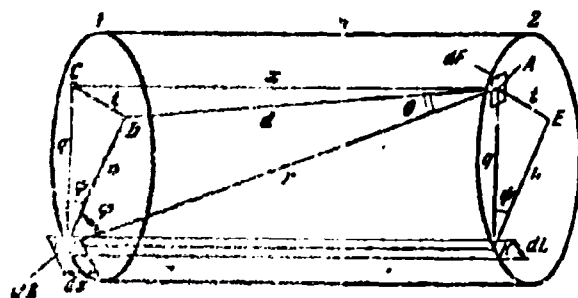


Fig. 12.16. The determining of the gas flow rate in the tube with molecular flow.

Let us assume that the surface element of the tube reflecting the molecules, with an area of $d\delta$ and length of dx , is located in cross section 1, standing at a distance of x , from cross section 2, and the radius vector rk , which connects areas dF and $d\delta$, has the length r and forms the angle θ with the axis of the tube.

The per-second molecular mass, reflected by area $d\delta$ in the direction of the normal to the wall, according to (71) is equal to

$$dM_n = \frac{1}{4} \rho_1 \bar{c} d\delta,$$

where ρ_1 is the gas density in cross section 1 (in the vicinity of area $d\delta$), and \bar{c} - the average speed of the molecules. The projection of the area $d\delta$ onto the plane normal to the radius vector r is $\cos \varphi d\delta$, where φ is the angle between the radius vector r and the normal to the area $d\delta$ (i.e., the direction of the radius of the tube). The flow rate per second of the molecules which fall from area $d\delta$ onto area dF is thus determined by expression

$$dM_n = \frac{1}{4} \rho_1 \bar{c} \cos \varphi d\delta \frac{d\Omega}{\pi}. \quad (118)$$

Here $d\Omega$ is the solid angle at which the area dF is visible from the center of area $d\delta$, and the ratio $d\Omega/\pi$ is equal to the portion of the total number of molecules, which are reflected by the area $d\delta$ into the whole internal hemisphere covering it, which falls onto the area dF .

By definition, the solid angle $d\Omega$, which covers the area dF , is equal to the ratio of the projection of this area onto the plane normal to the radius vector r to the square of the value of the radius vector

$$d\Omega = \frac{\cos \theta dF}{r^2}. \quad (119)$$

Let us designate by ϕ the angle between the segment of the straight line connecting the center of the area dF with the point of intersection of the generatrix of the tube drawn from the center of the area $d\delta$ with the plane of cross section 2, and let us drop a perpendicular t from the center of area dF onto the normal to the

wall of the tube n. From a comparison (Fig. 12.16) of the two right triangles BCD and ACD with triangle ABD, which has common sides with them, it follows that $\triangle ABD$ is a right triangle, therefore we have the equalities

$$r \cos \varphi = q \cos \psi, \quad r \cos \theta = x. \quad (120)$$

Substituting (119) and (120) into (118), we arrive at the following expression for the elementary molecular mass being reflected by the surface element of the tube $d\delta$ (in cross section 1) onto element dF of cross section 2:

$$dM_{11} = \frac{1}{4\pi r^2} \rho_1 c \cos \varphi \cos \theta d\delta dF = \frac{1}{4\pi r^2} \rho_1 c dF q \cos \psi x dL dx. \quad (121)$$

Here the elementary arc of the perimeter of the tube

$$dL = r_0 d\phi = \frac{r_0}{dx} dx,$$

whereupon $d\phi$ is the angle being subtended by the elementary arc dL , and r_0 is the radius of the tube. Since $r^2 = x^2 + q^2$, from (121) we have

$$dM_{11} = \frac{c dF}{4\pi} \frac{\rho_1 x dx}{(q^2 + x^2)^{3/2}} q \cos \psi dL.$$

It is natural that from the element dF of cross section 2 there proceeds the flow of molecules to the surface element of the tube $d\delta$ located in cross section 1; this "reverse" flow differs from the flow examined above by sign, and also by the fact that the gas density in cross section 2 has another value; thus, the mass flow per second of the "reverse" flow consists of

$$dM_{12} = -\frac{c dF}{4\pi} \frac{\rho_2 x dx}{(q^2 + x^2)^{3/2}} q \cos \psi dL.$$

Here the average velocity \bar{c} is taken as the same as that for dM_{r1} in view of the temperature constancy.

The resultant flow of molecules in the direction of the drop in density has the mass flow per second

$$\begin{aligned} dM &= dM_{r1} + dM_{r2} = \\ &= \frac{2 dF (p_1 - p_2) x dx}{(q^2 + x^2)^{3/2}} q \cos \psi dL. \end{aligned} \quad (122)$$

Let us examine the case of the flow in which the density gradient along the length of the tube is small, and therefore it is possible to take

$$p_1 - p_2 = x \frac{dp}{dx}. \quad (123)$$

By substituting (123) into (122), we arrive at the final form of the expression for the resultant per-second molecular mass which arrives from the surface element of the tube $d\delta$ to the element of the cross section dF :

$$dM = - \frac{2 dF}{4\pi} \frac{x^2 dx}{(q^2 + x^2)^{3/2}} \frac{dp}{dx} q \cos \psi dL. \quad (124)$$

Let us draw in cross section 2 through point A - the center of the area dF - an arbitrary reference line MN (Fig. 12.17), which forms with segment $\overline{AK} = q$ angle γ . Since the element of the perimeter of the tube dL in the vicinity of point K is evident from dF at angle $d\gamma$, then the projection of arc dL on the normal to segment \overline{AK}

$$q d\gamma = \cos \psi dL. \quad (125)$$

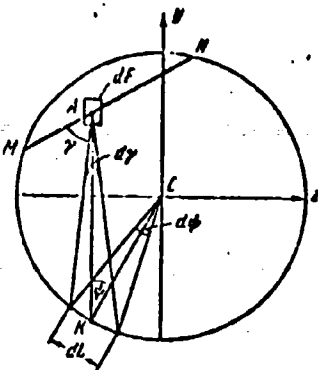


Fig. 12.17. The determining of the gas flow through the surface element of the cross section of the tube with molecular flow.

If we substitute the relation (125) into (124) and integrate the obtained expression within limits of $-\infty \leq x \leq \infty$, $0 \leq y \leq 2\pi$, i.e., solve the problem for an infinitely long circular tube, then the following expression for the per-second mass gas flow rate through the unit area of the cross section will be obtained:

$$\frac{dM}{dF} = -\frac{c}{4\pi} \frac{d\rho}{dx} \int_0^{2\pi} \int_{-\infty}^{\infty} \frac{q^2 x^2 dx}{(q^2 + x^2)^2} dy. \quad (126)$$

The density gradient of the gas along the length of the tube is taken in (126)

as being constant in connection with the fact that the mass gas flow rate from the condition of the stationarity of the flow should be constant.

By calculating preliminarily the integral

$$\int_{-\infty}^{\infty} \frac{x^2 dx}{(q^2 + x^2)^2} = \frac{1}{2} \int_{-\infty}^{\infty} \frac{dx}{q^2 + x^2} = \frac{1}{2q} \operatorname{arctg} \left(\frac{x}{q} \right) \Big|_{-\infty}^{+\infty} = \frac{\pi}{2q} \quad (127)$$

and substituting the value (127) into (126), we have

$$\frac{dM}{dF} = -\frac{c}{8} \frac{d\rho}{dx} \int_0^{2\pi} q dy \quad (128)$$

and, further,

$$M = -\frac{c}{8} \frac{d\rho}{dx} \int dF \int_0^{2\pi} q dy. \quad (129)$$

For a tube of round cross section this double integral can be converted in the following way (since the integral value $\int q d\gamma$ for a circle does not depend on the initial position of the ray q):

$$\int_F dF \int_0^{2\pi} q d\gamma = \int_0^{2\pi} d\gamma \int_F q dF = 2\pi \int q dP. \quad (130)$$

In the rectangular coordinate system, if we select for q the direction of y -axis (Fig. 12.17), we will obtain

$$\int q dF = \int_0^{r_0} dz \int_{-\sqrt{r_0^2 - z^2}}^{\sqrt{r_0^2 - z^2}} (y) dy = \frac{\pi}{3} r_0^3. \quad (131)$$

By substituting (131) into (130) and then into (125), we obtain the following expression for the per-second mass gas flow rate along the long circular tube:

$$M = -\frac{2\pi}{3} r_0^3 \frac{dp}{dx}. \quad (132)$$

At a constant density gradient and constant temperature from the equation of state, we have

$$\frac{dp}{dx} = \frac{\rho}{RT} \frac{dP}{dx} = \frac{\rho_1 - \rho_2}{RTl} = -\frac{\rho_1}{l} \left(1 - \frac{\rho_2}{\rho_1}\right),$$

where l is the length of the tube along which the pressure changes from p_1 to p_2 .

The final formula for the gas flow rate per second with free molecular flow along the long circular tube takes the following form:

$$M = \frac{2}{3} \frac{r_0^3}{l} \rho_1 \epsilon \pi r_0^2 \left(1 - \frac{\rho_2}{\rho_1}\right). \quad (133)$$

Hence the average velocity in the arbitrary cross section of the tube

$$U = \frac{M}{\pi r^2 l} = \frac{2}{3} \frac{r_2}{l} \frac{p_1}{p} \left(1 - \frac{p_2}{p_1}\right) c, \quad (134)$$

the average velocity in the initial cross section of the tube

$$U_1 = \frac{2}{3} \frac{r_2}{l} \left(1 - \frac{p_2}{p_1}\right) c \quad (135)$$

and in the final cross section of the tube

$$U_2 = \frac{2}{3} \frac{r_2}{l} \left(\frac{p_1}{p_2} - 1\right) c. \quad (136)$$

The value \bar{c} is the average velocity of the random motion of the molecules according to (57a)

$$c = \sqrt{\frac{8kT}{\pi m}}.$$

With a very large pressure drop in the tube ($p_2 \ll p_1$), we have, respectively

$$U = \frac{2}{3} \frac{r_2}{l} \frac{p_1}{p} c, \quad U_1 = \frac{2}{3} \frac{r_2}{l} c, \quad U_2 = \frac{2}{3} \frac{r_2}{l} \frac{p_1}{p_2} c. \quad (137)$$

From expressions (134)-(137) it is evident that the value of the average flow rate of the gas during free-molecular conditions does not depend on the density (or pressure) of the gas.

Relation (133) makes it possible to find the time necessary for the assigned lowering of pressure in the vessel, which is found under much rarefaction. For example, Kennard¹ calculated that in a

¹Kennard E. H., Kinetic theory of gases, McGraw-Hill B. C., New York-London, 1938.

flask 1 l in volume with the initial pressure of 0.01 mm Hg, with its connection with high vacuum ($p_2/p_1 = 0$) by means of a tube whose length is 30 cm and whose diameter is 2 mm, the pressure is lowered twice after 3 min.

As we see, the evacuation of gas from the vessel at great rarefaction is a very slow process.

However, if the flow in the tube in the indicated example of Kennard occurred according to the law of Poiseuille (as for the continuous medium), then for a reduction of pressure in the flask of two times, not 3 minutes but two hours would be required.

Above we determined the gas flow rate in the long tube with the completely diffuse reflection of molecules by the walls; if part of the molecules σ is reflected diffusely, and the remaining molecules are mirror reflected, then the flow rate of the gas along the tube increases (the velocity of motion along the tube of the mirror reflected molecules after impacts against the wall does not change). Smoluchowski¹ showed that an increase in the gas flow rate in this case occurs in the ratio

$$\frac{M}{M_0} = \frac{2-\sigma}{\sigma}, \quad (138)$$

where M_0 is the flow rate per second with the completely diffuse reflection, which is determined from formula (133).

Knudsen's experiments,² in which different gases (hydrogen, oxygen and carbon dioxide) were drawn through a glass capillary

¹Smoluchowski M., Zur kinetischen Theorie der Transpiration und Diffusion verdünnter Gase, Annalen der Physik, V. 33, P. 1559, 1910.

²Knudsen M., a) Die Gesetze der Molekularströmung und der innere Reibungsströmung der Gase durch Röhren, Annalen der Physik, Bd. 28, s. 75, 1908; b) Molekularströmung des Wasserstoffs durch Röhren. Annalen der Physik, Bd. 35, S. 359, 1911.

tube with a length of 12 cm and with an inside diameter of approximately 0.3 mm, confirm the formulas given above (for $\sigma = 1$). Gaede¹, who later, and more thoroughly made similar experiments with hydrogen and nitrogen (suction was conducted with the aid of a glass tube approximately 0.2 mm in diameter), also confirmed design equation but revealed that at a pressure above 0.01 mm Hg the experimental value of the gas flow rate becomes several percent lower than that of the theoretical (when $\sigma = 1$).

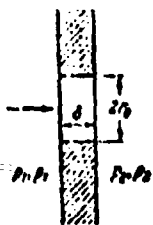
Leviyen and others studied the molecular flow of dry air along a metallic tube whose length is 80 cm and diameter is 4 cm; in the experiments the gas flow rate and values of pressure at distances of 10, 30, 50 and 70 cm from the end of the tube were measured; as a result the following facts were confirmed: the constancy of the pressure gradient along the length of the tube and the linear connection between the pressure difference on ends and the gas flow rate per second; it was found that at the low rates of flow $\sigma \approx 1$, upon transition to high velocity the value σ was decreased.

§ 9. The Molecular Outflow of Gas Through the Opening in the Wall and Through the Short Tube

Let us examine the free molecular overflow of gas through the opening of radius r_0 in the wall (Fig. 12.18), on both sides of which the pressures, temperatures and gas densities are dissimilar.

Let us assume that the wall thickness δ is comparable with the length of the mean free path of the molecules, in consequence of which only a single collision of the molecule with the internal surface bounding the opening is possible.

¹Gaede W., Die aussere Reibung der Gase, Annalen der Physik Bd. 41, S. 289, 1913.



The per-second molecular mass which enters into the opening from zone 1 into zone 2, according to (71), is

$$M_{12} = \frac{1}{4} p_1 c_1 \pi r_0^2$$

Fig. 12.18. The calculation of molecular outflow through the opening in the wall.

The per-second molecular mass hitting against the internal surface of the opening is approximately equal to

$$M_0 = \frac{1}{4} p_1 c_1 2\pi r_0 \delta.$$

The latter expression is not accurate, since states of the gas within the opening and in zone 1 differ. About half of mass M_0 comes from zone 1 and after reflection from the wall is divided into two equal parts, one of which is reflected into zone 1; in summation, flowing from zone 1 into the opening is the mass flow per second

$$M_1 = M_{12} - \frac{1}{4} M_0 = \frac{1}{4} p_1 c_1 \pi r_0^2 \left(1 - \frac{\delta}{2r_0}\right).$$

Determined similarly is the mass which escapes into the opening of zone 2:

$$M_2 = \frac{1}{4} p_2 c_2 \pi r_0^2 \left(1 - \frac{\delta}{2r_0}\right).$$

The total gas flow rate, which is established in direction to zone 2 in which the value $p\bar{c}$ has a smaller value, obviously, is equal to

$$M = M_1 - M_2 = \frac{1}{4} (p_1 c_1 - p_2 c_2) \left(1 - \frac{\delta}{2r_0}\right) \pi r_0^2 \quad (139)$$

or on the basis of the equation of state and relations (3)

$$M = r_0 \left(1 - \frac{\delta}{2r_0}\right) \left(\frac{p_1}{V T_1} - \frac{p_2}{V T_2}\right) \sqrt{\frac{\pi}{2gR}}. \quad (140)$$

We obtained for the free molecular outflow through the opening in the wall expression (140) of a more general form than that in § 8 for a long tube, since (140) considers not only the pressure difference, but also the difference in temperatures on both sides of the wall.

In the case of a very thin wall ($\delta = 0$) the flow rate per second through the opening is determined by the following formula:

$$M = r_0 \left(\frac{p_1}{V T_1} - \frac{p_2}{V T_2}\right) \sqrt{\frac{\pi}{2gR}}. \quad (141)$$

From formulas (140) and (141) it follows that the molecular outflow is possible even in the direction of higher pressure (if the square root of the temperature increases more greatly than that of the pressure); at equal pressures the outflow occurs in the direction of the higher temperature (thermal diffusion); equilibrium (zero flow rate) is established under the condition

$$\frac{p_1}{V T_1} = \frac{p_2}{V T_2}.$$

Formulas, (133) and (140) are not suitable for a short tube if its length l is considerably greater than the mean free path of the molecule. For this case the Clausius¹ obtained the numerical solution which, with an accuracy of up to 1.5%, is approximated (when $T = \text{const}$) by formula

$$M = \frac{20 + \frac{8l}{r_0}}{20 + \frac{19l}{r_0} + 3\left(\frac{l}{r_0}\right)^2} r_0 (p_1 - p_2) \sqrt{\frac{\pi}{2gRT}}. \quad (142)$$

¹Clausius P., Über die Stromung sehr verdünnter gases durch Rohren. Ann. der Physik, Bd. 2, S. 961, 1932.

CHAPTER XIII

ELEMENTS OF MAGNETIC GAS DYNAMICS

§ 1. Introduction

With the motion of an electroconductive fluid in electrical and magnetic fields there appears an electromagnetic body force (e. b. f.), occasionally referred to as the *ponderomotive force*, which acts on all particles of the fluid. Furthermore, in the passage of electrical current through the fluid, Joule heat is liberated.

In the study of the motion of electroconductive fluid in electrical and magnetic fields, it is necessary to consider these two new effects, introducing into the equations of motion and energy the appropriate additional terms. This circumstance leads to an increase in the number of variables and to the need for a corresponding increase in the number of equations; such additional equations are Maxwell's equations of electrodynamics. The combination of the equations of Maxwell, equations of Navier-Stokes, into which electromagnetic volume forces are introduced, equation of energy, which includes Joule heat, and the equations of state is the system of the differential equations of magnetic hydrogas dynamics.

At high temperatures on the order of several thousands of degrees, and also at very low pressures, the gasses are found in an ionized state and therefore are electroconductive, similar to liquid metals and some other drop liquid-electrolytes; that which was said above about the effect of electrical and magnetic fields on an electroconductive fluid and the account of this effect is referred also to ionized gas.

The development of magnetic hydrogas dynamics require astrophysics, aviation and rocket engineering, and also power engineering.

Astrophysics is the study of the internal structure of the sun and other stars in which the gas is found in a highly ionized state under the action of very high temperatures, and also the study of "cold" interstellar gas ionized and its very low density.

Contemporary aviation and rocket engineering developes vehicles which fly in the atmosphere at a velocity of the order of several kilometers per second. The temperature of the air near the surface of the body which has such a velocity approaches the temperature of an electrical arc, in consequence of which the air is noticeably ionized. If we apply electrical and magnetic fields to such an air flow, then there will arise an electromagnetic body force, which under specific conditions will prove to be comparable in value with the aerodynamic forces.

The feature of electromagnetic body forces is the fact that unlike other body forces (gravity, inertial forces) it cannot be controlled, affecting the electrical and magnetic fields causing it. By changing the value of electromagnetic force, it is possible to affect the intensity and shape of the shock waves, increase the critical value of the Reynolds number upon the transition of laminar flow conditions into turbulent, retard or accelerate the flow of the electroconductive fluid (or gas), and cause the deformation velocity profile and the boundary-layer separation.

By using the electroconductive fluid or gas, it is possible to create a generator of electrical current in which the direct transition of thermal energy into electrical is achieved; magnetic dosing devices, flow meters and pumps for the pumping of mercury and liquid metals find use; other fields of the use of magnetic hydrogas dynamics in technology are known, for example, in instrument manufacture.

At present two regions of hydromagnetics clearly appear: in the first it is considered that the medium possesses infinite conductivity (astrophysics), and in the second the medium of finite conductivity (magnetic gas dynamics of different technical apparatuses) is dealt with.

In one of the paragraphs of this chapter some properties of magnetic gas-dynamic waves which are possible only in an infinite conducting medium are examined; in the remaining paragraphs we are speaking only about the media of the finite conductivity.

§ 2. Elements of Electrostatics and Electrodynamics

The interaction between two point electrical charges q_1 and q_2 , which are located at a distance r from each other, is described by Coulomb's law

$$f = \pm \frac{q_1 q_2}{r^2}. \quad (1)$$

Here f is measured in dynes, r - in centimeters, q - in units of the charge of the CGSE. In technology another unit - 1 coulomb = $3 \cdot 10^9$ CGSE units of a charge - is accepted.

From Coulomb's law (1) it follows that around the given electrical charge a force field called electrostatic field is formed. Placing the positive charge q_2 into the electrostatic field of charge q_1 and measuring the force f applied to it,

all the values of the electric field intensity at its point

$$\vec{E} = \frac{1}{\epsilon_0} \vec{p} \quad (2)$$

If the field is created by several point charges, then its intensity is equal to the vector sum of the intensities of the fields of separate charges.

If we draw in the given field a line, in all points of which the vector of intensity is tangent to it, then we will obtain the line of intensity, which is similar to the flow line in the stationary velocity field.

The lines of intensity are drawn usually so that through a unit of area of any area ΔS normal to it there would pass a number of lines N equal to the value of the local intensity of the field:

$$\frac{\Delta N}{\Delta S} = E.$$

Then the number of lines passing through the arbitrarily located area ΔS , obviously, will be

$$\Delta N = E \Delta S \text{ or } N = \int E_n dS. \quad (3)$$

where E_n is the projection of intensity onto the normal to the area.

According to the Gauss theorem, the flow of intensity through any closed surface is equal to product of 4π by the algebraic sum of the charges contained by it

$$N = 4\pi \sum q. \quad (4)$$

Let us introduce function V , which is called the potential of the point charge q :

$$V = \frac{q}{r} \quad (5)$$

The potential difference at two points of the field measures the work of the movement of a single positive charge of one point into another

$$V_1 - V_2 = \frac{q_1}{r_1} - \frac{q_1}{r_2} = \frac{A}{q_1}. \quad (6)$$

The potential of the point of the field is equal to the work of the movement of a single positive charge from this point to infinity ($V = \frac{q_1}{\infty} = 0$).

From (2) and (6) it follows that between the work of the movement of charge A and the intensity of the field E_r there is the following connection:

$$A = q_1 \int E_r dr \quad \text{or} \quad \int E_r dr = V_1 - V_2. \quad (7)$$

With movement of a charge over a closed circuit ($V_1 = V_2$), the work is equal to zero

$$\oint E_r dr = 0. \quad (8)$$

As is known from the field theory, the left side of expression (8) is the circulation of vector E_r on the closed circuit. The equality of the circulation to zero indicates that the electrostatic field is the potential.

The family of equipotential surfaces is orthogonal to the family of the lines of intensity.

By differentiating the second of expressions (7) along the line of intensity, we have

$$E_r = -\frac{dV}{dr}. \quad (9)$$

Thus, the electrical intensity is numerically equal to the potential gradient along the normal to the equipotential surface.

In the three-dimensional electrostatic field

$$E_x = -\frac{\partial V}{\partial x}, \quad E_y = -\frac{\partial V}{\partial y}, \quad E_z = -\frac{\partial V}{\partial z} \quad (10)$$

or in vector form

$$\mathbf{E} = -\text{grad } V. \quad (10a)$$

In the CGSE system the unit of potential difference is the erg (dyne \times centimeter); in technology a value 300 times less is used: volt = (1/300) of a CGSE unit of potential difference.

If charge q is not concentrated at the point but is distributed evenly over surface S or volume v , then usually used are concepts about the surface or bulk density of the charge

$$\sigma_s = \frac{q}{S}, \quad \rho_v = \frac{q}{v}. \quad (11)$$

From expression (3) and the Ostrogradskiy-Gauss theorem (4) there follows the relation which connects the total flow of the electrical intensity on the surface with the density of charges in the volume v covered by this surface

$$\oint \mathbf{E}_n dS = 4\pi \int \rho_v dv \quad (12)$$

(here n is the external normal to surface S). Let us establish the connection between the intensity, potential and bulk density of the charges. For this let us isolate in the rectangular coordinate system the parallelepiped element with volume $dv = dx dy dz$ with charge $dq = \rho_v dx dy dz$. A voltage difference on the opposite sides parallel to the plane yz is equal to

$\frac{\partial E_x}{\partial x} dx$, on the remaining two pairs of sides respectively $\frac{\partial E_y}{\partial y} dy$ and $\frac{\partial E_z}{\partial z} dz$.

By means of (3) let us determine the difference in the total flows of intensity on opposite sides of the parallelepiped

$$dN_x = \left[\left(E_x + \frac{\partial E_x}{\partial x} dx \right) - E_x \right] dy dz = \frac{\partial E_x}{\partial x} dx dy dz,$$

$$dN_y = \frac{\partial E_y}{\partial y} dx dy dz, \quad dN_z = \frac{\partial E_z}{\partial z} dx dy dz.$$

Consequently, a change in the flow of intensity on the entire surface of the parallelepiped

$$dN = dN_x + dN_y + dN_z = \left(\frac{\partial E_x}{\partial x} + \frac{\partial E_y}{\partial y} + \frac{\partial E_z}{\partial z} \right) dx dy dz.$$

From the Ostrogradskiy-Gauss theorem (4), we have

$$dN = 4\pi dq = 4\pi \rho_0 dx dy dz$$

or, by replacing dN ,

$$\frac{\partial E_x}{\partial x} + \frac{\partial E_y}{\partial y} + \frac{\partial E_z}{\partial z} = 4\pi \rho_0 \quad (13)$$

In vector form equation (13) can be written in the form

$$\operatorname{div} \mathbf{E} = 4\pi \rho_0 \quad (13a)$$

According to the field theory, this equation results directly from (12). Components, of the vector of electrical field intensity E_x , E_y and E_z , on the basis of (10), can be replaced by derivatives of the potential, and then (13) takes the following form:

$$\frac{\partial^2 V}{\partial x^2} + \frac{\partial^2 V}{\partial y^2} + \frac{\partial^2 V}{\partial z^2} = -4\pi \rho_0 \quad \text{or} \quad \Delta V = -4\pi \rho_0 \quad (14)$$

Dependences (13) and (14) play in electrostatics the same role as the equation of continuity in hydrodynamics. The majority of the bodies is divided into two classes: into conductors, which transmit charges (electrification), and dielectrics, which do not transmit the charges.

In the dielectric, unlike the void where the lines of intensity are extended from some free charges to others, or depart to infinity, part of the lines of intensity should be broken into bound charges which appears as a result of polarization.

In order to avoid the discontinuity of the lines of force, one introduces an additional concept - *the vector of the electrostatic induction*

$$\mathbf{D} = \epsilon \mathbf{E}, \quad (15)$$

which is parallel to the vector of intensity (ϵ - permittivity of the medium). It is not difficult to show that lines of the vector of induction (unlike the line of intensity) in the direction of the normal to the uncharged boundary surface of the two media¹ are retained, being broken only on free charges, and the tangential components undergo discontinuity

$$D_{1n} = D_{2n}, \quad \frac{D_{1t}}{\epsilon_1} = \frac{D_{2t}}{\epsilon_2}. \quad (15a)$$

Components, of the vector of electrostatic intensity behave in the opposite manner, and therefore valid for them are the relations

$$\epsilon_1 E_{1n} = \epsilon_2 E_{2n}, \quad E_{1t} = E_{2t}.$$

Let us take the number of flow lines of the vector of induction which intersect the unit of area of the surface element ΔS_n , perpendicular to the vector of induction, equal to the magnitude of vector induction

$$\frac{\Delta N}{\Delta S_n} = D.$$

For the arbitrarily oriented area ΔS , we will obtain

$$\Delta N = D \Delta S \cos \alpha = D_n \Delta S,$$

where D_n is the projection of the vector of induction onto the normal to the area ΔS , and α is the angle between the normals to

¹We have in mind the surface on which there are no free charges.

areas ΔS and ΔS_n . The flow vector of induction through the finite surface is equal to

$$N = \int D_n dS. \quad (16)$$

Relation (13) can be extended to the vector of induction if into the right side we substitute the density of the free charges: ρ_0

$$\frac{\partial D_x}{\partial x} + \frac{\partial D_y}{\partial y} + \frac{\partial D_z}{\partial z} = 4\pi\rho_0 \quad (17)$$

or in vector form

$$\text{div } D = 4\pi\rho_0. \quad (17a)$$

From the foregoing it follows that the integral relation (8) can also be extended to the induction flow of the electrostatic field (16), after substituting into the right side the density of the free charges:

$$\int D_n dS = 4\pi \int \rho_0 d\sigma. \quad (18)$$

The force of electrical current is measured by the quantity of electricity transferred through this area per unit time:

$$I = \left| \frac{dq}{dt} \right|. \quad (19)$$

In the CGSE system unit of the force of current corresponds to the transfer in one second of one CGSE unit of a quantity of electricity. In practice as the unit of the force of current we take

$$1 \text{ ampere} = \frac{1 \text{ coulomb}}{1 \text{ second}} = 3 \cdot 10^9 \text{ CGSE units of the force of current.}$$

According to the Ohm's law established experimentally, we have

$$I = \frac{V_1 - V_2}{R}. \quad (20)$$

where $V_1 - V_2$ is the potential difference on ends of the conductor,
 R - the resistance of the conductor.

For a conductor of constant section S and length l the resistance is equal to

$$R = \nu_R \frac{l}{S}, \quad (21)$$

where ν_R is the resistivity of the material. In a practical system the resistance is measured in ohms, whereupon

$$1 \Omega = \frac{1V}{1A} = \frac{1}{9 \cdot 10^{11}} \text{ CGSE units of resistance.}$$

The unit of resistivity in a practical system is usually taken from the resistance of a conductor 1 m long having a cross section of 1 mm²

$$1 \text{ tech. unit of resistance} = 1 \Omega \frac{0.01 \text{ cm}^2}{100 \text{ cm}} = 10^{-4} \Omega \cdot \text{cm}.$$

Used also is specific conductivity (or electrical conductivity)

$$\sigma_R = \frac{1}{\nu_R} \frac{\text{cm}^1}{\text{cm}^1}.$$

Values of resistivity and electrical conductivity of some substances when $t = 0^\circ\text{C}$ are given in the table.

Conductor	$\nu_R \Omega \cdot \text{cm}$	$\sigma_R, \frac{\text{mho}}{\text{cm}}$
Aluminum	$2.53 \cdot 10^{-6}$	$39.50 \cdot 10^4$
Graphite	$39.20 \cdot 10^{-6}$	$2.55 \cdot 10^4$
Pure iron	$8.69 \cdot 10^{-6}$	$11.48 \cdot 10^4$
Pure copper	$1.55 \cdot 10^{-6}$	$64.50 \cdot 10^4$
Mercury	$94.30 \cdot 10^{-6}$	$1.06 \cdot 10^4$
Pure water	$0.50 \cdot 10^7$	$2 \cdot 10^{-7}$
Saline water (saturated at 25°C)	4	$2.5 \cdot 10^{-1}$

¹Unit of conductivity [mho] = [cm⁻¹].

Data on the conductivity of thermally ionized pure air can be borrowed from works of Lin, Sears, and also Chinitz, Eisen and Grass¹, who measured it behind a shock wave in a shock wind tunnel; the initial pressure before the shock wave was 1 mm Hg, the initial temperature of the air was close to 300°K, the temperature after shock wave was determined according to values of the Mach number. Figure 13.1 gives curves of the conductivity of pure air and air which contains as an impurity 0.1% by weight of potassium vapors and 0.01 and 0.001% of cesium vapors. The calculated curves of the dependence of the conductivity of air on temperature at different pressures are given on Fig. 13.2.

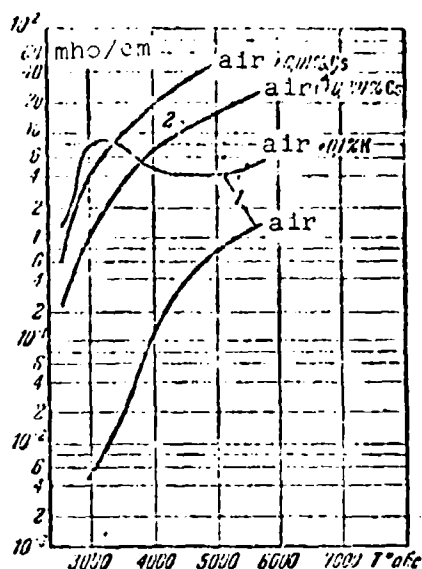


Fig. 13.1. Electrical conductivity of pure air and air with additives of potassium and cesium at

$p = 10^3$ atm (abs).

The current strength is a scalar value. For determining not only the quantity of the electricity being transferred but also the directions of the transfer, we use the vector of the current density whose value is

$$j = \frac{\Delta I}{\Delta S_n} = \frac{\Delta I}{\Delta S \cos \alpha}. \quad (22)$$

Here ΔS_n is the surface of the area oriented along the normal to the direction of flow ΔI , whereupon the current of positive charges is considered positive; in expression (22) value α is the angle between the normal to the area ΔS and the vector of the current density.

The current flows in the direction of the drop in potential,

¹Lin, S. C., Electrical conductivity of thermally ionized air produced in a shock tube, AVCO Res. Note 26, 1957. Sears, W. R., ARS J. No. 6, V. 29, 1959. Chinitz, L., Eisen C., Grass R., ARS, J., No. 8, V. 29, 1959.

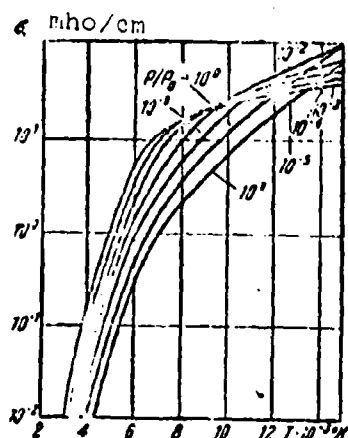


Fig. 13.2. Electrical conductivity of air at different pressures.

i.e., the vector of the current density is parallel to the vector of intensity E . In connection with this, the formula of Ohm's law can be modified, having presented it in vector form.

In fact,

$$\Delta I = -\frac{\Delta V}{R} = -r_R \frac{\Delta S_a}{\Delta I} \Delta V,$$

whence

$$\frac{\Delta I}{\Delta S_a} = -r_R \frac{\Delta V}{\Delta I}.$$

Since $\mathbf{j} \parallel \mathbf{E}$, then according to (9) and (22)

$$\mathbf{j} = r_R \mathbf{E} \quad (23)$$

If the current flows through the closed surface ΔS , then the positive direction of the current corresponds to the external normals to this surface. The losses of charges within the closed surface ΔS , designated by Δq , is equal to the sum of the elementary currents which flow through this surface:

$$\Delta I = \sum \mathbf{j}_n \Delta S \Delta t = -\Delta q$$

or

$$I = \int \mathbf{j}_n dS = -\frac{dq}{dt}. \quad (24)$$

The distribution of electric current can be represented with the aid of flow lines; at each point of the field the direction of the vector of current density is tangential to the flow line.

If the charge within the closed surface does not change, then all the flow lines intersect this surface or are closed within it. The flow lines are broken only at those places where there is a loss (or an accumulation) of the charges.

Let us formulate the equation of the conservation of the charge in differential form. In a parallelepiped element with sides dx , dy and dz at the bulk density of the charges ρ_v during time dt there occurs a change in the charge by the value

$$dq = \left(\frac{\partial \rho_v}{\partial t} dt \right) dx dy dz.$$

This change is caused by the difference in current strengths on opposite faces

$$\begin{aligned} \left[\left(j_x + \frac{\partial j_x}{\partial x} dx \right) - j_x \right] dy dz dt &= \frac{\partial j_x}{\partial x} dx dy dz dt, \\ \left[\left(j_y + \frac{\partial j_y}{\partial y} dy \right) - j_y \right] dx dz dt &= \frac{\partial j_y}{\partial y} dx dy dz dt, \\ \left[\left(j_z + \frac{\partial j_z}{\partial z} dz \right) - j_z \right] dx dy dt &= \frac{\partial j_z}{\partial z} dx dy dz dt. \end{aligned}$$

Thus, we have

$$\frac{\partial j_x}{\partial x} + \frac{\partial j_y}{\partial y} + \frac{\partial j_z}{\partial z} = - \frac{\partial \rho_v}{\partial t} \quad (25)$$

or in the vector form

$$\operatorname{div} \mathbf{j} = - \frac{\partial \rho_v}{\partial t}. \quad (25a)$$

If in the circuit $V_1 > V_2$, then current always flows from one V_1 to V_2 ; in order that the circuit would be closed, the current within the electrical battery - current source - should flow in the opposite direction, i.e., from a negative electrode to a positive one. This is achieved because so-called electromotive force \mathcal{E} (emf), which balances the potential difference in external circuit and the drop in potential on internal resistance R_0 of the battery:

$$\mathcal{E} = V_1 - V_2 + IR_0 \quad (26)$$

The sources of emf can be chemical reactions (in a battery), electromagnetic induction (in a generator), and so on.

Let us discuss the heating effect of the electrical current. The quantity of electricity transferred from one end of the conductor to the other during time t equal to It produces work proportional to the potential difference

$$A = R(V_1 - V_2) \quad (27)$$

Hence, on the basis of the Ohm's law, we have

$$A = I^2 R t \quad (27a)$$

Work proceeds for the heating of the conductor. At the current strength $I = 1$ A during time $t = 1$ s, the quantity of electricity $q = 1$ coulomb $= 3 \cdot 10^9$ CGSE units is transferred. With a potential difference of 1 volt, in this case the work accomplished is

$$1 \text{ C} \times 1 \text{ V} = \frac{3 \cdot 10^9}{300} \text{ erg} = 10^7 \text{ erg} = 1 \text{ J}$$

The ratio of heat power A/t to the volume of the conductor Sl is called the *density of the heat power*

$$w = \frac{A}{Sl}.$$

Hence, on the basis (22), (27a) and (21), we have

$$w = \frac{I^2}{\sigma_R} \frac{J}{\text{cm}^3 \cdot \text{s}} \quad (28)$$

or, taking into account (23),

$$w = \sigma_R E^2 = jE. \quad (28a)$$

With superconductivity ($\sigma_R \rightarrow \infty$), according to (28), the density of the heat release tends to zero.

The total power released in the circuit consists of powers of external and internal parts of the circuit: $w = I^2 R$, i.e., total

power is equal to the product of the current strength by the electromotive force.

Around the conductor, along which the electric current flows, there appears a magnetic field being characterized by lines of the magnetic field strength; tangent at any point of such a line coincides with the direction of the vector of intensity H of the magnetic field.

Around the long straight conductor lines of the magnetic field strength have the form of concentric circles: their direction is determined by the so-called right-hand rule: if the forward motion of the gimlet coincides with the direction of the flow, then the direction of rotation of its grip coincides with the direction of the magnetic lines of intensity.

The magnetic field of a solenoid, i.e., a system of identical circular currents (turns) with a common rectilinear axis, is presented on Fig. 13.3. In the middle part of the internal cavity of the solenoid, the magnetic lines are parallel to the axis of solenoid; at the ends of the solenoid the magnetic lines are bent and emerge outside, being closed outside the solenoid, where the field becomes very weak.

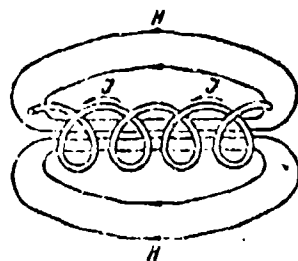


Fig. 13.3. Magnetic field of a solenoid.

Conducted through a unit of surface ΔS_n , normal to lines of the magnetic field strength, as is accepted in the field theory, is the number of lines equal to the intensity value. If the normal to the area ΔS is located at angle α to the lines of intensity, then we have $\Delta S_n = \Delta S \cos \alpha$, whence the total number of lines

$$\Delta V = I \Delta S \cos \alpha.$$

Since $H \cos \alpha = H_n$ is a projection of the vector of intensity on the normal to the area, then

$$\Delta N = H_n \Delta S. \quad (29)$$

The direction of the external normal is usually considered positive.

Unlike the lines of the electrostatic intensity, which are broken on the charges, the lines of the magnetic field strength are always closed, since magnetic charges in nature there do not exist. Therefore, the total flux of the magnetic field strength through the closed surface S is always equal to zero

$$\oint_S H_n dS = 0. \quad (30)$$

The continuity condition of the magnetic field can, by analogy with the hydrodynamic condition, be written thus:

$$\frac{\partial H_x}{\partial x} + \frac{\partial H_y}{\partial y} + \frac{\partial H_z}{\partial z} = 0$$

or

$$\operatorname{div} H = 0. \quad (31)$$

The magnetic field strength H at the given point is determined by the action of all the individual sections of the wire. According to the law of Laplace and Bio-Savart based on the experiment, the circuit element Δl , along which the current flows by force I , creates at point A of the space (Fig. 13.4), which is found at distance r from the element Δl , the magnetic field with intensity

$$\Delta H = \frac{I \Delta l \sin \alpha}{r^2}, \quad (32)$$

where α is the angle between Δl and r (the direction of flow I is considered positive).

In vector form the magnetic field strength at point A

$$\Delta H = \frac{I \Delta l \times r}{r^3}. \quad (32a)$$

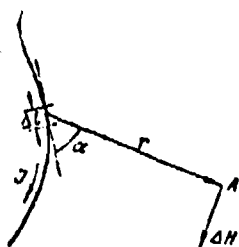


Fig. 13.4. Determination of the field of magnetic field strength around a conductor with current.

here $[dl \times r]$ is the vector product, whereupon $dl \times r$ is the element of length dl in the direction of the flow and its radius vector r - the direction from element dl to point A.

The total intensity H at point A is the vector sum

$$H = \sum dH, \quad (13.1)$$

which is formed by the intensities which are created by all the elements of the circuit (conductor).

In the case of a rectilinear conductor (Fig. 13.5), the intensities from all of its sections are directed equally, in consequence of which

$$H = \frac{r_0}{\sin \alpha} \quad \text{or} \quad \frac{H}{r_0} = \frac{dl}{r^2 \sin \alpha} = \frac{1}{r_0^2},$$

where r_0 is shortest distance from dl to point A. From the basis of (32) and (33) for an infinitely long straight conductor, we have

$$H = \int \frac{I \sin \alpha \, dl}{r^2} = \frac{2I}{r_0}.$$

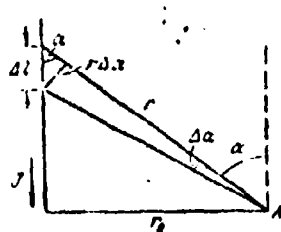


Fig. 13.5. Determination of the magnetic field of a rectilinear conductor with current.

From this formula it follows that at a distance of $r_0 = 1$ cm. from the infinitely long conductor, along which flows a current of $I = 10$ GSE units of current force, the magnetic field $H = 10$ GSE units of intensity appears. The

projections of the vector of intensity (32a) on the axis of the angular coordinate system xyz are

$$\left. \begin{aligned} \Delta H_x &= \frac{I(\Delta l_y r_z - \Delta l_z r_y)}{r^3}, \\ \Delta H_y &= \frac{I(\Delta l_z r_x - \Delta l_x r_z)}{r^3}, \\ \Delta H_z &= \frac{I(\Delta l_x r_y - \Delta l_y r_x)}{r^3}, \end{aligned} \right\} \quad (34)$$

and here the subscripts denote the projections of vectors Δl and r on the appropriate coordinate axes. Similar relations determine in hydrodynamics the velocity field induced by the vortex filament.

The experiments of Faraday and Ampere showed that acting on any conductor with current put into the magnetic field is an electromagnetic force. Ampere established that this force

$$\Delta f = \frac{1}{c^2} I H_n \Delta l = \frac{1}{c^2} I H \Delta l \sin \alpha, \quad (35)$$

The direction Δf is perpendicular to the plane of vectors Δl and H and is determined by the left-hand rule: if the palm of left hand is arranged so that the component of intensity H_n perpendicular to Δl is directed to the palm, and the four elongated fingers are directed along the current I , then the thumb set aside will indicate the direction of force.

In vector form the Ampere law takes the form

$$\Delta f = \frac{1}{c^2} I [\Delta l \times H], \quad (36)$$

where the direction Δl coincides with the direction of flow.

After placing into formula (35) the proportionality factor, equal to unity, it is possible to construct the electromagnetic system of CGSM units. In this system of units the Ampere law will be written in the form

$$\Delta f = I H \Delta l \sin \alpha \quad (37)$$

It is not difficult to notice that in the new system (CGSM) the unit of the force of current is c times more than that in the CGSE system. Since $c = 3 \cdot 10^{10}$ cm/s, then

$$1\text{CGSM unit of current force} = 3 \cdot 10^{10} \text{ CGSE units} = 10 \text{ A.}$$

A unit of a quantity of electricity $Q = It$ and a unit of magnetic field strength in the CGSM system are also c times more than those in the CGSE system, $1\text{CGSM unit of a quantity of electricity} = 3 \cdot 10^{10} \text{ CGSE units of a quantity of electricity} = 10 \text{ coulombs}$; $1\text{CGSM unit of intensity} = 3 \cdot 10^{10} \text{ CGSE units of intensity} = 1 \text{ oersted}$.

The force Δf in both systems of units is measured in dynes.

Subsequently, we will use the combined system of units of Gauss, in which the electric intensity is measured in CGSE units, and the magnetic field strength is measured in CGSM units.

Let us formulate the expression for circulation of a vector of magnetic field strength along a closed loop L . If the conductor is arranged from the circuit element at a distance r (Fig. 13.6), then the length of the circuit element can be expressed by the angle at which it is visible from the line of the electrical current: $dL = r d\varphi$. The product of the length of the circuit element by the component of vector of intensity tangential to it in mixed units is

$$H_t dL = \frac{1}{c} \frac{2I}{r} r d\varphi = \frac{1}{c} 2I d\varphi.$$

The value of the circulation of the vector H along the closed loop L is equal therefore to

$$\oint H_t dL = \frac{1}{c} 2I \int_0^{2\pi} d\varphi = \frac{4\pi}{c} I. \quad (38)$$

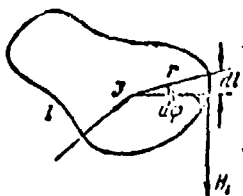


Fig. 13.6. Determination of the circulation of the vector of magnetic field strength along the closed circuit L.

Thus, unlike the electrostatic field, which according to (8) is the potential field, the magnetic field proves to be the vortex field (circulation of the vector H along the closed loop is not equal to zero).

The given information, strictly speaking, is valid only in the case of the formation of the magnetic field in a void. The experiment shows that properties of the medium, in which the conductors with current are placed, affect the intensity of the fields.

If we place the conductor with the current into a medium which is magnetized (magnetics), then there appears the additional magnetic field strength H' which is totaled with the intensity of the external field H_0 : the resulting intensity B is called the vector of magnetic induction

$$B = \mu_B H_0 = H_0 + H', \quad (39)$$

where μ_B is the magnetic permeability of the medium. The value B in the CGSM system of units is measured in gauss (numerically the gauss is equal to the oersted). If in a void the Ampere force, according to (35), is determined by the intensity of the external field H_0 (in the Gaussian system of units)

$$\Delta f = \frac{1}{c} H_0 \Delta l \sin \alpha,$$

then in magnetics it depends on the total intensity, i.e., on the vector of magnetic induction $B = H_0 + H'$:

$$\Delta f = \frac{1}{c} B \Delta l \sin \alpha = \frac{1}{c} \int B \Delta v \sin \alpha, \quad (40)$$

where $\Delta v = \Delta S$ is the volume of the section Δl of the conductor which has cross section S . In vector form the Ampere force in mixed units

$$\Delta f = \frac{1}{c} [J \times B] \Delta v. \quad (40a)$$

The projections of the Ampere force on the axis of the rectangular coordinate system are

$$\left. \begin{aligned} \Delta f_x &= \frac{1}{c} \Delta v (J_y B_z - J_z B_y), \\ \Delta f_y &= \frac{1}{c} \Delta v (J_z B_x - J_x B_z), \\ \Delta f_z &= \frac{1}{c} \Delta v (J_x B_y - J_y B_x). \end{aligned} \right\} \quad (41)$$

For gases and plasma (ionized gas) the electrical and magnetic permeability has virtually the same value as that in a void ($\epsilon \approx 1$, $\mu_B \approx 1$), and therefore in equations of magnetic gas dynamics it is possible to manage without the vectors of electrostatic and magnetic induction, i.e., it is possible not to consider the phenomena of the polarization and magnetization of the medium.

In a way similar to the lines of intensity which characterize the magnetic field in a void it is possible to construct lines of magnetic induction. Drawn through a unit of surface normal to the induction lines is a number of lines equal to the local value of the vector of induction; the total number of induction lines which intersect the surface element ΔS_n normal to them comprises the elementary flow of the magnetic induction.

$$\Delta \Phi = B \Delta S_n = B_n \Delta S. \quad (42)$$

The induction lines coming out from the volume limited by this surface give a positive flow and those entering into this volume - a negative flow; the lines of magnetic induction are always closed, and therefore, for them there should be fulfilled the continuity condition

$$\operatorname{div} B = \frac{\partial B_x}{\partial x} + \frac{\partial B_y}{\partial y} + \frac{\partial B_z}{\partial z} = 0. \quad (43)$$

The total flow of induction through surface S

$$\Phi = \int B_n dS. \quad (44)$$

For the closed surface we always have $\Phi = 0$. In the CGSM system the flow of induction is measured in the Maxwells: 1 Maxwell = 1 gauss \times 1 cm².

It is possible to show that with the intersection of the boundary of two media with different values of permeability μ_1 and μ_2 , the normal component of magnetic induction is retained (if on the boundary there are no surface currents), and tangential component undergoes discontinuity

$$B_{1n} = B_{2n}, \quad \frac{B_{1t}}{\mu_1} = \frac{B_{2t}}{\mu_2}. \quad (45)$$

The components of the magnetic field strength behave in an opposite manner:

$$H_{1t} = H_{2t}, \quad \mu_1 H_{1n} = \mu_2 H_{2n}. \quad (46)$$

In other words, in the flow of induction directed along the normal to the boundary surface of the magnetics and in the absence of surface currents, the vector of induction is not changed, and the vector of intensity undergoes a jump. The magnetic flow, in certain cases, passes over wholly from one medium to another (series connection), and other cases it branches out into separate parts, which then merge (connection in parallel).

Electric current is a flow of charged particles: electrons and ions. Therefore the ampere force which acts on the conductor is composed of forces applied to the moving charges.

If the charged particles move within the solid or liquid body, then because of their collisions with the molecules or atoms of the body the Ampere force is transferred to the body. For example, if side walls of a circular vessel filled with a conducting fluid are electrodes to which the current is conducted, and the bottom is an insulator installed on the pole of a forward magnet, then the current flows along radii, and the vector of the magnetic field strength is parallel to the walls. In this case the fluid in the vessel arrives into circular motion (the Ampere force acts in the same direction on positive and negative charges, since they move in opposite directions).

The current strength I is equal to the total charge transferred per unit time in the cross section of the conductor:

$$I = en_0 WS = \rho_0 WS. \quad (47)$$

Here e is the value of the separate charge, n_0 - the number of the moving charges per unit volume, W - the velocity of their motion, S - the cross-sectional area of the conductor.

Substituting this expression into (37), we obtain the ampere force applied to the total charge on the section with length Δl :

$$\Delta f = \frac{1}{c} en_0 W \Delta l H \sin \alpha$$

The number of charges which move along the section of conductor Δl :

$$n' = n_0 S \Delta l,$$

and therefore the force which acts on one moving charge:

$$\Delta f' = \frac{\Delta f}{n'} = \frac{1}{c} e W H \sin \alpha. \quad (48)$$

Here the charge is measured in CGSE units and the intensity in oersteds. The force $\Delta f'$, called the Lorentz force, is perpendicular to the plane at which vectors W and H lie: for a

positive charge it is determined by the left-hand rule. If $W \perp H$, then the force has a greatest value ($\sin \alpha = 1$), if $W \parallel H$, then the force is equal to zero ($\sin \alpha = 0$).

In vector form the Lorentz law takes the form

$$\Delta f = \frac{e}{c} [W \times H], \quad (49)$$

and in projections on rectangular coordinate of the axis (in the mixed units)

$$\left. \begin{aligned} \Delta f_x &= \frac{e}{c} (vH_z - wH_y), \\ \Delta f_y &= \frac{e}{c} (wH_x - uH_z), \\ \Delta f_z &= \frac{e}{c} (uH_y - vH_x). \end{aligned} \right\} \quad (50)$$

Here u , v and w are components of the velocity vector W . If acting on the charges is also the electrical field, then added to the Lorentz force will be the Coulomb force, which according to (2) is equal to eE . The total electromagnetic force which acts on the charge will in this case be

$$\Delta f = e \left\{ E + \frac{1}{c} [W \times H] \right\}. \quad (51)$$

The electromagnetic force applied to a single charge is very low, but it is necessary to keep in mind that with usual currents a very large number of charges is transferred, in consequence of which the force applied to conductive body can prove to be considerable.

If the electrical and magnetic fields are mutually perpendicular ($E \perp H$), then under the condition

$$E = -\frac{1}{c} [W \times H]$$

the Coulomb and Lorentz forces are balanced, i.e., the resulting electromagnetic force is equal to zero ($\Delta f = 0$). In this case the charge moves along the inertia at a constant velocity, which

is called the *drift velocity* and is equal in magnitude to

$$w_d = \frac{cE}{H}. \quad (52)$$

When $E = E_x$, $H = H_y$ and $\Delta f_x = 0$, we have $w = w_d$. A comparison of (51) with (2) leads to the conclusion that the presence of the electromagnetic force Δf , which acts on the moving charge, is equivalent to existence in the fixed coordinate system of an electrical field with the intensity

$$E_1 = E + \frac{1}{c}(W \times H). \quad (53)$$

This expression is correct for the moving conducting fluid. By substituting (53) into the right side (23), we obtain the expression which is called the *generalized Ohm's law* for the flow of the isotropic conducting fluid (in mixed units)

$$J = \sigma_R \left\{ E + \frac{1}{c}(W \times H) \right\}. \quad (54)$$

Here W is the velocity vector of the fluid flow (and not the speed of motion of the charges in it).

In (54) component E corresponds to the conduction current in the fixed coordinate system and term $E' = \frac{1}{c}[W \times H]$ - to the additional current induced by magnetic field in the moving fluid. If the charges move not in a void but in magnetics ($B \neq H$), then the generalized Ohm's law in mixed units takes the following form

$$J = \sigma_R \left\{ E + \frac{1}{c}(W \times B) \right\}. \quad (55)$$

The projections of the vector of the current density (55) on the axis of the rectangular coordinate system comprise (in mixed units)

$$\left. \begin{aligned} J_x &= \sigma_R \left[E_x + \frac{1}{c}(vB_z - wB_y) \right], \\ J_y &= \sigma_R \left[E_y + \frac{1}{c}(wB_x - vB_z) \right], \\ J_z &= \sigma_R \left[E_z + \frac{1}{c}(uB_y - vB_x) \right]. \end{aligned} \right\} \quad (56)$$

In 1831 Faraday discovered the phenomenon of *electromagnetic induction* which consists in the fact that with a change in the flow of induction through any closed circuit in it there appears an electrical current caused by the electromotive force of induction: this inductive current appears with the approach of the magnet or conductor with current toward the closed conductor, with the rotation of the closed conductor in a magnetostatic field, and so on.

The direction and force of the inductive current are such that the intrinsic flow of magnetic induction being created by it compensates for that change in the external flow of induction which causes it; as a result there appear forces which counteract the relative movement of these two flows of magnetic induction.

On the basis of the law of the conservation of energy, Faraday established the relationship between the electromotive force of induction \mathcal{E}_i and the rate of the change in the induction flow through the circuit $\partial\Phi/\partial t$

$$\mathcal{E}_i = -\frac{\partial\Phi}{\partial t}. \quad (57)$$

The relation (57), called the *law of electromagnetic induction of Faraday*, establishes the value and direction of the emf of induction.

In the CGSM system emf of induction is measured in *maxwells/s*

$$1 \text{ maxwell} = \frac{1}{3 \cdot 10^{10}} \text{ CGSE units of emf} = 10^{-8} \text{ V.}$$

In technology the emf of induction is measured in the webers

$$1 \text{ weber} = 10^8 \text{ maxwells.}$$

In this case relation (57) gives

$$\mathcal{E}_1 \text{ (volt)} = - \frac{\partial \Phi}{\partial t} \frac{\text{weber}}{\text{s}}.$$

In the mixed system of units, when Φ is measured in CGSM units, and \mathcal{E}_1 - in CGSE units, we have

$$\mathcal{E}_1 = - \frac{1}{c} \frac{\partial \Phi}{\partial t}. \quad (57a)$$

If conductor is stationary, and the value of magnetic induction changes, then for the explanation of electromagnetic induction it is necessary to assume that in this case at each point of space an electrical force appears. This hypothesis, confirmed by experiments, was assumed by Maxwell as a basis of the theory of the electrical field.

The electrical field changing with time gives rise to a magnetic field; for with an evenly changing electrical field ($\frac{\partial D}{\partial t} = \text{const}$) a magnetostatic field is obtained.

If placed into an alternating magnetic field is a fixed conductor, then the flow of magnetic induction through the cross section of the circuit included by the conductor changes, in connection with which in the conductor according to the Faraday law there appears an emf of induction

$$|\mathcal{E}_1| = \frac{d\Phi}{dt}$$

and along it current flows. Thus, the alternating magnetic field gives rise to an electrical field.

Both alternating fields - electrical and magnetic - connected with each other, form an *electromagnetic field*.

The electrical field, generated by the alternating magnetic field, has a vortex nature, i.e., differs significantly from the potential electrostatic field of fixed charges.

The vortex nature of the magnetic field results from relation (38).

Taking (22) into account, from (38) we obtain for direct current¹

$$\oint H_1 dl = \frac{4\pi}{c} \int j_n dS. \quad (58)$$

A similar relation can also be obtained for an electrical vorticity field. According to (57a) the emf of induction

$$\mathcal{E}_1 = -\frac{1}{c} \frac{\partial \Phi}{\partial t},$$

where the flow of magnetic induction

$$\Phi = \int B_n dS.$$

Thus, we have

$$\mathcal{E}_1 = -\frac{1}{c} \frac{\partial}{\partial t} \int B_n dS = -\frac{1}{c} \int \frac{\partial B_n}{\partial t} dS.$$

On the basis of (7) and (26) the emf is expressed in terms of the intensity of the electric field (when $R_0 = 0$)

$$\mathcal{E}_1 = \oint E_1 dl,$$

and, therefore,

$$\oint E_1 dl = -\frac{1}{c} \int \frac{\partial B_n}{\partial t} dS. \quad (59)$$

The electrical field is vortex (electromagnetic) if the right side of expression (59) is different from zero, and it becomes potential if the right side is equal to zero ($\frac{\partial B_n}{\partial t} = 0$), i.e., if the magnetic field is constant or absent.

¹Below we will be limited to an examination of direct current.

§ 3. Electromagnetic Fields

In the preceding paragraph it is shown that the electromagnetic fields are described in general by the following system of Maxwell's integral relations:

1. Relation (58) which connects the circulation of the vector of the magnetic field strength H over a closed circuit L with the total force of the direct current which flows through the area S included by this circuit:

$$\oint_L H_i dl = \frac{1}{c} \int_S 4\pi j_n dS.$$

2. Relation (18), which connects the total flow of the electrostatic induction through the closed surface of area S with the total free charge in the volume v included by this area:

$$\int_S D_n dS = 4\pi \int_v \rho_{\text{free}} dv.$$

3. Relation (59) which connects the circulation of the vector of electrical intensity E over the closed circuit L with the rate of change in time of the vector of magnetic induction through the area included by this circuit:

$$\oint_L E_i dl = -\frac{1}{c} \int_S \frac{\partial B_n}{\partial t} dS.$$

4. Relation (44), which is indicative of the flow continuity of magnetic induction B through the closed surface:

$$\int_S B_n dS = 0.$$

It is necessary to add expressions (15) and (39) to these integral relations, by means of which it is possible to pass from the vectors of intensity of the electromagnetic fields to the vectors of induction

$$D = \epsilon E, \quad B = \mu H,$$

and the generalized Ohm's law (55)

$$J = j_R \left\{ E + \frac{1}{c} [W \times B] \right\}.$$

In these formulas the electrical values are measured in CGSE units (j , E , D , ρ_{v0}), magnetic values - in CGSM units (H , B), forces - in dynes, velocity - in cm/s. Of course, it is possible with the aid of the corresponding coefficients to turn to any other system of units.

Let us now derive the Maxwell equations in differential form, and let us divide them into two systems. We will obtain the first system for the magnetic field of direct current.

Since the lines of magnetic field strength lie in a plane perpendicular to the direction of the flow, the projection of the current density j_z (Fig. 13.7) is connected only with projections H_x and H_y of the magnetic field strengths at the same point of space. The circulation of the vector of intensity along an infinitesimal circuit $abcd$ consists of the following terms (the circuit is counterclockwise):

$$\begin{aligned} \Gamma_{abcd} = & -H_y dy + H_x dx + \left(H_y + \frac{\partial H_y}{\partial x} dx \right) dy - \\ & - \left(H_x + \frac{\partial H_x}{\partial y} dy \right) dx = \left(\frac{\partial H_y}{\partial x} - \frac{\partial H_x}{\partial y} \right) dx dy. \end{aligned}$$



Fig. 13.7. The coordinate system (on the derivation of the Maxwell equations).

On the other hand, according to (58), the circulation of the vector H should be equal to the force of current flowing through this area multiplied by 4π :

$$\Gamma_{abcd} = \frac{1}{c} 4\pi I_z = \frac{1}{c} \pi j_z dx dy.$$

Thus, we have

$$\frac{\partial H_y}{\partial x} - \frac{\partial H_x}{\partial y} = \frac{1}{c} 4\pi j_z \quad (60)$$

Similarly, for components of the current density along the other axes, we find

$$\frac{\partial H_x}{\partial y} - \frac{\partial H_y}{\partial x} = \frac{1}{c} 4\pi j_z, \quad \frac{\partial H_z}{\partial x} - \frac{\partial H_x}{\partial z} = \frac{1}{c} 4\pi j_y \quad (60a)$$

Equations (60), recorded in the mixed system of Gauss units, connect the current density of conductivity j with the spatial derivatives of the magnetic field strength H . If to equations (60) we add equation (17), which connects the vector of the electrostatic induction D with the density distribution of free charges in the volume ρ_{v0}

$$\frac{\partial D_x}{\partial x} + \frac{\partial D_y}{\partial y} + \frac{\partial D_z}{\partial z} = 4\pi \rho_{v0}$$

then we will obtain the first system of Maxwell equations, which in vector form can then be represented as:

$$\text{rot } H = \frac{4\pi}{c} j, \quad \text{div } D = 4\pi \rho_{v0} \quad (61)$$

This system is valid for the uniform magnetics which entirely fill the whole field, since in this case the magnetic field strength of the currents does not depend on the permeability of the medium.

We will obtain the second system of equations of Maxwell, utilizing the generalization given by it of the law of induction of Faraday.

Let us formulate the expression for the circulation of the intensity of the electrical field E along an infinitesimal circuit $abcd$ (Fig. 13.7), caused by a change in time of the vector of magnetic induction $\frac{\partial B}{\partial t}$ perpendicular to vector E :

$$\begin{aligned} \Gamma_{\text{induced}} = -E_y dy + E_x dx + \left(E_z + \frac{\partial F_z}{\partial y} dx \right) dy - \\ - \left(E_z + \frac{\partial F_z}{\partial x} dy \right) dx = \left(\frac{\partial F_x}{\partial y} - \frac{\partial F_y}{\partial x} \right) dy dx. \end{aligned}$$

The circulation of the vector E along the closed circuit is equal to the derived flow of magnetic induction through the area included by this circuit, taken with a minus sign

$$\Gamma = -\frac{1}{c} \frac{\partial \Phi}{\partial t} = -\frac{1}{c} \frac{\partial B_z}{\partial t} dx dy.$$

Hence we have

$$\frac{\partial E_y}{\partial x} - \frac{\partial E_x}{\partial y} = -\frac{1}{c} \frac{\partial B_z}{\partial t}. \quad (62)$$

By analogy we also have

$$\frac{\partial E_z}{\partial y} - \frac{\partial E_y}{\partial z} = -\frac{1}{c} \frac{\partial B_x}{\partial t}, \quad \frac{\partial E_x}{\partial z} - \frac{\partial E_z}{\partial x} = -\frac{1}{c} \frac{\partial B_y}{\partial t}. \quad (62a)$$

Adding to equations (62) the equation of the continuity of the lines of magnetic induction (43)

$$\frac{\partial B_x}{\partial x} + \frac{\partial B_y}{\partial y} + \frac{\partial B_z}{\partial z} = 0,$$

we obtain the second system of Maxwell equations, which in vector form takes the form

$$\text{rot } E = -\frac{1}{c} \frac{\partial B}{\partial t}, \quad \text{div } B = 0. \quad (63)$$

In the case of an inhomogeneous medium on the boundaries of its separate sections, in the absence of surface charges and currents conditions (15a) and (45) should be fulfilled:

$$\begin{aligned} D_{1n} &= D_{2n}, & \frac{D_{1t}}{\epsilon_1} &= \frac{D_{2t}}{\epsilon_2}, \\ B_{1n} &= B_{2n}, & \frac{B_{1t}}{\mu_1} &= \frac{B_{2t}}{\mu_2}. \end{aligned}$$

Let us exclude from the differential Maxwell equations the vectors of current density j and the electrical field strength of current E . For this let us use Ohm's law (55), having converted it into the equation of vorticity of the field of current density (in mixed units):

$$\text{rot } J = \frac{1}{c} \left\{ \text{rot } E + \frac{1}{c} \text{rot} [W \times B] \right\}. \quad (64)$$

Let us replace the equation for the vorticity of the vector of the magnetic field strength (61) with the aid of (39) with the equation of vorticity of the vector of magnetic induction

$$\text{rot } B = \frac{1}{c} 4\pi \mu_R J. \quad (65)$$

As is known from the field theory,

$$\text{rot rot } B = -\Delta B = -\left(\frac{\partial^2 B}{\partial x^2} + \frac{\partial^2 B}{\partial y^2} + \frac{\partial^2 B}{\partial z^2} \right). \quad (66)$$

From (64), (65) and (66) we find when $\sigma_R = \text{const}$

$$-\Delta B = \frac{4\pi}{c} \mu_R \text{rot } J = \frac{4\pi \mu_R}{c} \left\{ \text{rot } E + \frac{1}{c} \text{rot} [W \times B] \right\}. \quad (67)$$

From equation (63) we have

$$\text{rot } E = -\frac{1}{c} \frac{\partial B}{\partial t}.$$

Substituting this result into (67), we obtain

$$\frac{\partial B}{\partial t} = \text{rot} [W \times B] + \frac{c^2}{4\pi \mu_R^2 R} \Delta B. \quad (68)$$

This equation, which connects the magnetic field with the velocity field in the electro conductive fluid, is called the *equation of magnetic induction*.

In the case of very great electrical conductivity of the medium ($\sigma_R \rightarrow \infty$), the second term of the right side of equation (68) can be disregarded, in connection with which it acquires the following form:

$$\frac{\partial B}{\partial t} = \text{rot} [W \times B]. \quad (68a)$$

This equation is identical to the equation of vorticity in the hydrodynamics of an ideal fluid, which means that the lines of the vortex move together with the fluid. But in this case the question is of lines of the magnetic field, which prove to be rigidly connected with the substance - "frozen in," and if the particles of fluid move, then the lines of magnetic induction move together with them (the particles cannot cross the induction lines).

The "freezing in" of the magnetic lines is connected with the fact that with a change in the vector flux of magnetic induction through the circuit, in it there appear electrical currents which prevent a change in this flow, and the larger they are, the higher σ_R ; when $\sigma_R \rightarrow \infty$ a change in the flow of induction becomes impossible. Motion along the lines of force does not affect the field; with motion in a transverse direction the lines of force are completely carried away together with the substance (if $\sigma_R \rightarrow \infty$).

In the case of a stationary medium ($W = 0$) the equation of induction takes the form of the equation of diffusion or non-stationary thermal conductivity (Fourier equation)

$$\frac{\partial B}{\partial t} = \frac{c^2}{4\pi\sigma_R} \Delta B. \quad (68b)$$

It shows that in a body which is located in a magnetic field of external sources, the magnetic field disappears not immediately after their disconnection; the magnetic lines of force gradually "filter" through the body and are attenuated.

For example, in a copper sphere 1 m in radius the magnetic field attenuates in approximately 10 seconds: the higher the conductivity, the weaker the attenuation of the field.

The value

$$\frac{c^2}{4\pi\mu H^2 R} = \eta_m \quad (69)$$

which is similar to the transfer coefficient in equations of diffusion and thermal conductivity and having a dimensionality of kinematic viscosity, was called *magnetic viscosity*. The numerical values of magnetic viscosity are usually considerably more than the values of kinematic viscosity. In general, when not one of the terms on the right side of the equation of magnetic induction can be disregarded, the lines of force attempt to move together with the substance and are simultaneously filtered through the substance.

Given in Appendix V is a table of fundamental units used into electrodynamics and in different measuring systems, whereupon each value is compared with the number of units of the CGSE system corresponding to it. From this table it is evident that a shortcoming in the SI system is the fact that in it the magnetic permeability and electrical induction of the vacuum are dimensional values different from unity.

§ 4. Equations of Magnetic Gas Dynamics

The equations of hydrodynamics (and gas dynamics) of an electroconductive fluid in the presence of electrical and magnetic fields should, unlike the equations of hydrodynamics of a nonconductive fluid, contain an additional term which considers the electromagnetic body force.

Acting on the element of the volume of the conductor (or the conducting fluid) dv , if along it there flows a current with density j , on the side of magnetic field is the Ampere force (40a)

$$df_H = j \times B dv,$$

and on the side of the electrical field - the Coulomb force (3)

$$df_c = E \rho_{v0} dv,$$

where ρ_{v0} is the density of the charges in the volume dv ($\rho_{v0} dv = dq$).

Thus, the total body electromagnetic force applied to volume dv (in mixed units):

$$df = df_c + df_H = \left\{ \rho_{v0} E + \frac{1}{c} [J \times B] \right\} dv, \quad (70)$$

the force which acts per unit volume

$$F = \frac{df}{dv} = F_c + F_H = \rho_{v0} E + \frac{1}{c} [J \times B]. \quad (71)$$

An evaluation of the order of terms in the relation (70) shows that the Coulomb force can frequently be disregarded¹. Then,

¹The relative value of the Coulomb force is estimated in the following manner:

$$\frac{|\rho_{v0} E|}{\left| \frac{1}{c} [J \times B] \right|} \sim \frac{\rho_{v0} L^2 c^2}{\sigma_R W B^2},$$

where

$$\rho_{v0} = \frac{1}{4\pi} \operatorname{div} D \sim \frac{1}{4\pi L} \epsilon E.$$

Hence

$$\frac{|\rho_{v0} E|}{\left| \frac{1}{c} [J \times B] \right|} \sim \frac{\epsilon^2 E^2}{W^2 B^2} \frac{\epsilon W}{4\pi L \sigma_R}.$$

According to (52), $\epsilon E/B = W_d$ is the drift velocity which, as is known, is the value of the order of the flow velocity, ϵ - the order of unity, linear dimension L - the order of 10^2 cm, σ_R - the order of mho/cm or in the gauss system - the order of $9 \cdot 10^{11}$.

Thus, even at flow velocities W of order of 10^2 km/s, the relative value of the Coulomb force is of the order of 10^{-8} .

taking into account (65), we obtain for the electromagnetic force applied to the unit of volume the expression

$$\mathbf{F} = \frac{1}{c} [\mathbf{J} \times \mathbf{B}] = \frac{1}{4\pi\mu_B} [\text{rot } \mathbf{B} \times \mathbf{B}]. \quad (72)$$

Projections of the vector of the electromagnetic force on the axis of the rectangular coordinate system are

$$\left. \begin{aligned} F_x &= \frac{1}{c} (J_y B_z - J_z B_y) \\ F_y &= \frac{1}{c} (J_z B_x - J_x B_z) \\ F_z &= \frac{1}{c} (J_x B_y - J_y B_x) \end{aligned} \right\} \quad (72a)$$

or in another form (with replacement according to (65) of the vector of the current density by the rotor of the vector of magnetic induction)

$$\left. \begin{aligned} 4\pi\mu_B F_x &= a_y B_z - a_z B_y = B_x \frac{\partial B_x}{\partial x} + B_y \frac{\partial B_x}{\partial y} + B_z \frac{\partial B_x}{\partial z} - \frac{1}{2} \frac{\partial B^2}{\partial x} \\ 4\pi\mu_B F_y &= a_z B_x - a_x B_z = B_x \frac{\partial B_y}{\partial x} + B_y \frac{\partial B_y}{\partial y} + B_z \frac{\partial B_y}{\partial z} - \frac{1}{2} \frac{\partial B^2}{\partial y} \\ 4\pi\mu_B F_z &= a_x B_y - a_y B_x = B_x \frac{\partial B_z}{\partial x} + B_y \frac{\partial B_z}{\partial y} + B_z \frac{\partial B_z}{\partial z} - \frac{1}{2} \frac{\partial B^2}{\partial z} \end{aligned} \right\} \quad (72b)$$

Here $B^2 = B_x^2 + B_y^2 + B_z^2$ - magnitude of magnetic induction vector, $\mathbf{a} = \text{rot } \mathbf{B}$. In the derivation of expressions (72b) the continuity condition of magnetic lines of force was used also (43).

Adding force \mathbf{F} (70) to the right side of equation (28) from Chapter II, we obtain the equation of motion of the electrical conductivity of the fluid in electrical and magnetic fields in vector form (at $\mu = \text{const.}$)

$$\rho \frac{d\mathbf{W}}{dt} = \mathbf{R} - \text{grad } p + \mu \Delta \mathbf{W} + \frac{1}{3} \mu \text{grad } (\text{div } \mathbf{W}) + \frac{1}{c} [\mathbf{J} \times \mathbf{B}] \quad (73)$$

or

$$\begin{aligned} \rho \frac{d\mathbf{W}}{dt} &= \mathbf{R} - \text{grad } p + \mu \Delta \mathbf{W} + \\ &+ \frac{1}{3} \mu \text{grad } (\text{div } \mathbf{W}) + \frac{1}{4\pi\mu_B} [\text{rot } \mathbf{B} \times \mathbf{B}]. \end{aligned} \quad (73a)$$

For gas the system of differential equations should include the equation of energy. In the case of an electroconductive fluid which is in magnetic and electric fields, the right side of equation of energy (42) from Chapter II should contain an additive term (26) expressing the density of Joule heat release (heat release per unit volume). Then the equation of energy for the electroconductive fluid takes on the following form (with $\lambda = \text{const.}$, $\mu = \text{const.}$):

$$\rho S \frac{di}{dt} = A \frac{dp}{dt} + \lambda \Delta T + A \mu \Phi + A \frac{I^2}{\sigma_R} \quad (74)$$

or, taking into account (65),

$$\rho S \frac{di}{dt} = A \frac{dp}{dt} + \lambda \Delta T + A \mu \Phi + \frac{Ac^2}{4\pi\mu_B^2} [\text{rot } B]^2. \quad (74a)$$

To equations (73) and (74) we must add the equation of magnetic induction (68)

$$\frac{\partial B}{\partial t} = \text{rot} [W \times B] + \frac{c^2}{4\pi\mu_B^2} \Delta B, \quad (75)$$

the hydrodynamic equation of continuity

$$\frac{\partial \rho}{\partial t} + \text{div}_F W = 0 \quad (76)$$

and then the equation of state

$$p = f(\rho, T), \quad (77)$$

which in the case of an ideal gas is replaced by the Clapeyron equation. The system of equations (73a)-(77) is the total system of differential equations of magnetic gas dynamics.

If the equation of motion is utilized in the form of (73), the system of equations must be augmented by the equation of Ohm's law (55), the Maxwell equation (63), and also equations (65) and (68).

In these equations we disregard the electrostatic Coulomb force; if one takes into account the Coulomb force, then the system of equations of electromagnetic gas dynamics will be obtained.

For an incompressible fluid the system of equations (73)-(77) is simplified, since the equations of motion are solved independently of the equation of energy, the equation of state (77) is no longer necessary, and the equations of continuity (76) and motion (73) take on a simpler form.

Thus, the total system of equations of the hydromagnetics of an incompressible fluid in vector form consists of the equation of motion

$$\rho \frac{dW}{dt} = R - \text{grad} p + \mu \Delta W + \frac{1}{c} [J \times B] \quad (78)$$

or

$$\rho \frac{dW}{dt} = R - \text{grad} p + \mu \Delta W + \frac{1}{4\pi c} [\text{rot} B \times B], \quad (78a)$$

the equation of energy, solved independently of the remaining equations

$$\rho c_p \frac{dT}{dt} = A \frac{dp}{dt} + \Delta T + \Delta \Phi + A \frac{J^2}{\sigma}, \quad (79)$$

the equation of magnetic induction

$$\frac{\partial B}{\partial t} = \text{rot} [W \times B] + \frac{c^2}{4\pi \sigma R} \Delta B, \quad (80)$$

the equation of continuity

$$\text{div} W = 0.$$

If the equations of motion and energy are written in the form of (78) and (79), then to obtain a closed system it is necessary to add the equation of Ohm's law (55), the Maxwell equation (63) and equation (64).

If we pass to projections onto the axis of the orthogonal coordinate system xyz , then the vector equation of motion (78) is broken down into three equations of motion:

$$\left. \begin{aligned} \rho \left(\frac{du}{dt} + u \frac{\partial u}{\partial x} + v \frac{\partial u}{\partial y} + w \frac{\partial u}{\partial z} \right) &= \\ &= - \frac{\partial p}{\partial x} + \mu \left(\frac{\partial^2 u}{\partial x^2} + \frac{\partial^2 u}{\partial y^2} + \frac{\partial^2 u}{\partial z^2} \right) + \frac{1}{c} (J_x B_z - J_z B_x), \\ \rho \left(\frac{dv}{dt} + u \frac{\partial v}{\partial x} + v \frac{\partial v}{\partial y} + w \frac{\partial v}{\partial z} \right) &= \\ &= - \frac{\partial p}{\partial y} + \mu \left(\frac{\partial^2 v}{\partial x^2} + \frac{\partial^2 v}{\partial y^2} + \frac{\partial^2 v}{\partial z^2} \right) + \frac{1}{c} (J_z B_x - J_x B_z), \\ \rho \left(\frac{dw}{dt} + u \frac{\partial w}{\partial x} + v \frac{\partial w}{\partial y} + w \frac{\partial w}{\partial z} \right) &= \\ &= - \frac{\partial p}{\partial z} + \mu \left(\frac{\partial^2 w}{\partial x^2} + \frac{\partial^2 w}{\partial y^2} + \frac{\partial^2 w}{\partial z^2} \right) + \frac{1}{c} (J_y B_z - J_z B_y), \end{aligned} \right\} \quad (82)$$

Utilizing (72a) and (7.1), the three equations of motion can be brought to the following form:

$$\left. \begin{aligned} \rho \left(\frac{du}{dt} + u \frac{\partial u}{\partial x} + v \frac{\partial u}{\partial y} + w \frac{\partial u}{\partial z} \right) &= - \frac{\partial p}{\partial x} + \\ &+ \mu \left(\frac{\partial^2 u}{\partial x^2} + \frac{\partial^2 u}{\partial y^2} + \frac{\partial^2 u}{\partial z^2} \right) + \frac{1}{c} \left(B_z \frac{\partial H}{\partial x} + B_x \frac{\partial H}{\partial z} + B_x \frac{\partial B_z}{\partial x} \right), \\ \rho \left(\frac{dv}{dt} + u \frac{\partial v}{\partial x} + v \frac{\partial v}{\partial y} + w \frac{\partial v}{\partial z} \right) &= - \frac{\partial p}{\partial y} + \\ &+ \mu \left(\frac{\partial^2 v}{\partial x^2} + \frac{\partial^2 v}{\partial y^2} + \frac{\partial^2 v}{\partial z^2} \right) + \frac{1}{c} \left(B_x \frac{\partial H}{\partial y} + B_y \frac{\partial H}{\partial x} + B_z \frac{\partial B_x}{\partial y} \right), \\ \rho \left(\frac{dw}{dt} + u \frac{\partial w}{\partial x} + v \frac{\partial w}{\partial y} + w \frac{\partial w}{\partial z} \right) &= - \frac{\partial p}{\partial z} + \\ &+ \mu \left(\frac{\partial^2 w}{\partial x^2} + \frac{\partial^2 w}{\partial y^2} + \frac{\partial^2 w}{\partial z^2} \right) + \frac{1}{c} \left(B_y \frac{\partial H}{\partial z} + B_z \frac{\partial H}{\partial y} + B_z \frac{\partial B_y}{\partial z} \right). \end{aligned} \right\} \quad (82a)$$

These equations are written in the form

$$F_i = \rho \left(\frac{dw_i}{dt} + \dots \right) \quad (83)$$

where the effective mass m_i is the sum of hydrodynamic (p) and magnetic $\left(\frac{1}{c} \frac{\partial H}{\partial x_i} \right)$ forces.

Let us note that in equations (82) the nonelectromagnetic forces (gravity, centrifugal force, etc.) are omitted for brevity.

The vector equation of induction (80) in the orthogonal coordinate system also breaks down into three equations:

$$\left. \begin{aligned} \frac{dB_x}{dt} &= \frac{c^2}{4\pi\epsilon_0 B^2 R} \left[\frac{\partial^2 B_x}{\partial x^2} + \frac{\partial^2 B_x}{\partial y^2} + \frac{\partial^2 B_x}{\partial z^2} \right] + \frac{\partial u B_x}{\partial x} + \\ &\quad + \frac{\partial u B_x}{\partial y} + \frac{\partial u B_x}{\partial z} - B_x \left(\frac{\partial u}{\partial x} + \frac{\partial v}{\partial y} + \frac{\partial w}{\partial z} \right), \\ \frac{dB_y}{dt} &= \frac{c^2}{4\pi\epsilon_0 B^2 R} \left[\frac{\partial^2 B_y}{\partial x^2} + \frac{\partial^2 B_y}{\partial y^2} + \frac{\partial^2 B_y}{\partial z^2} \right] + \frac{\partial v B_y}{\partial x} + \\ &\quad + \frac{\partial v B_y}{\partial y} + \frac{\partial v B_y}{\partial z} - B_y \left(\frac{\partial u}{\partial x} + \frac{\partial v}{\partial y} + \frac{\partial w}{\partial z} \right), \\ \frac{dB_z}{dt} &= \frac{c^2}{4\pi\epsilon_0 B^2 R} \left[\frac{\partial^2 B_z}{\partial x^2} + \frac{\partial^2 B_z}{\partial y^2} + \frac{\partial^2 B_z}{\partial z^2} \right] + \frac{\partial w B_z}{\partial x} + \\ &\quad + \frac{\partial w B_z}{\partial y} + \frac{\partial w B_z}{\partial z} - B_z \left(\frac{\partial u}{\partial x} + \frac{\partial v}{\partial y} + \frac{\partial w}{\partial z} \right). \end{aligned} \right\} \quad (84)$$

In the equation of energy (74) the term which considers Joule heat can be expressed by magnetic induction. For this we must use the Maxwell equation (67). As a result, we will obtain

$$\rho g \frac{dl}{dt} = A \frac{dp}{dt} + \lambda \Delta T + A_1 \Phi + \frac{Ac^2}{(4\pi\epsilon_0)^2 R} (\text{rot } B)^2, \quad (85)$$

where, in accordance with field theory, the quantity

$$(\text{rot } B)^2 = \left(\frac{\partial B}{\partial x} \right)^2 + \left(\frac{\partial B}{\partial y} \right)^2 + \left(\frac{\partial B}{\partial z} \right)^2. \quad (86)$$

The equation of Ohm's law (55) in projections onto the axis of the coordinates takes the form

$$\left. \begin{aligned} J_x &= z_R \left[E_x + \frac{1}{c} (v B_z - w B_y) \right], \\ J_y &= z_R \left[E_y + \frac{1}{c} (w B_x - u B_z) \right], \\ J_z &= z_R \left[E_z + \frac{1}{c} (u B_y - v B_x) \right]. \end{aligned} \right\} \quad (87)$$

When $\rho = \text{const.}$ the hydrodynamic equation of continuity takes the form

$$\frac{\partial u}{\partial x} + \frac{\partial v}{\partial y} + \frac{\partial w}{\partial z} = 0,$$

and therefore the equations of magnetic induction (64) are simplified, since the last terms on their right sides are zero.

In many concrete cases the equations of motion and induction can be substantially simplified by neglecting these or other relatively small terms.

Chapter II presents several versions of the equation of energy for gas flow. Frequently the equation of energy is used in a form in which enthalpy and kinetic energy are combined into total enthalpy; such is equation (49) from § 6 of Chapter II. In order to arrive at the appropriate form of the equation of the energy of hydromagnetics, we must project the additive term of the equation of motion (electromagnetic force)

$$\mathbf{f} = \frac{1}{c} [\mathbf{j} \times \mathbf{B}]$$

onto the axis of the orthogonal coordinate system and then multiply every projection of this vector by the appropriate projection of velocity; after adding the three obtained products, we find an additional electromagnetic term to equation (45) of Chapter II

$$\begin{aligned} j_x u + j_y v + j_z w = & \frac{1}{c} [u(j_y B_z - j_z B_y) + v(j_z B_x - j_x B_z) + \\ & + w(j_x B_y - j_y B_x)] = \frac{1}{c} [j_x (w B_y - v B_z) + j_y (u B_z - w B_x) + \\ & + j_z (v B_x - u B_y)]. \end{aligned}$$

This expression employs expressions (72a) for the components of electromagnetic force. In other words, the scalar product of velocity by the electromagnetic force vector was presented in the form

$$\mathbf{w} \cdot \mathbf{f} = -\frac{1}{c} \mathbf{j} \cdot [\mathbf{w} \times \mathbf{B}].$$

From the Ohm's law (55) follows

$$\frac{j}{\sigma_R} - E = \frac{1}{c} [W \times B].$$

Substituting this result into the foregoing equality, we find

$$W \cdot j = - \frac{j^2}{\sigma_R} + j \cdot E.$$

If this additive term, expressing the work of electromagnetic force, is added to Joule heat

$$Q_e = \frac{j^2}{\sigma_R}, \quad (88)$$

we will obtain resultant expressions for the additive "electromagnetic" term of the equation of energy

$$Q_H = j \cdot E. \quad (89)$$

This quantity must be added to the right side of equation (49) of Chapter II; then the equation of energy of gas in the presence of an electromagnetic field is written in the following form:

$$\rho \frac{dU}{dt} = A \frac{\partial p}{\partial t} + \lambda \Delta T + \mu \Delta \left(\frac{W^2}{2} \right) + \frac{A}{4\pi} [W \times \nabla] \operatorname{div} W + A j \cdot E. \quad (90)$$

Here the coefficient A (heat equivalent of mechanical work) is added to the last term, because in (89) this term is expressed in mechanical units.

In a number of cases the work of electromagnetic forces is represented in another form, which can be obtained if we use (65) to replace current density in scalar product (89) by magnetic induction

$$Q_H = \frac{cE}{4\pi\mu_B} \operatorname{rot} B \quad (91)$$

and use the known formula from field theory

$$\operatorname{div} [E \times B] = B \operatorname{rot} E - E \operatorname{rot} B.$$

In the case of a stationary magnetic field ($\frac{\partial B}{\partial t} = 0$) from (83) we have not $E = 0$, and therefore

$$E \text{ rot } B = -\text{div} [E \times B].$$

Substituting this result into (91), we come to the following expression for the additive electromagnetic term to the equation of energy:

$$Q_H = -\frac{c}{4\pi\mu_0} \text{div} [E \times B]. \quad (92)$$

After replacing in (90) the last term by expression (92), we obtain one additional form of the equation of energy of magnetic gas dynamics:

$$\rho g \frac{dl_0}{dt} = A \frac{\partial p}{\partial t} + \lambda \Delta T + A \mu \Delta \left(\frac{W^2}{2} \right) + \\ + \frac{A}{3} \mu [W \times \nabla] \text{div } W - \frac{Ac}{4\pi\mu_0} \text{div} [E \times B]. \quad (93)$$

In the stationary case and in the absence of viscosity and thermal conductivity the equation of energy (93) assumes the form

$$\rho g \frac{dl_0}{dt} = -\frac{Ac}{4\pi\mu_0} \text{div} [E \times B]. \quad (94)$$

§ 5. The Similarity Criteria in Hydromagnetics¹

With the additive term in the equation of motion of an electroconductive fluid in a magnetic field (82) we must introduce a new similarity criterion considering the ratio of magnetic force to the force of inertia. Following the method given in § 7 of Chapter II, let us bring the last term of the right side of

¹Bai Shi-yi and, Magnetic gas dynamics and dynamics of plasma. "MIR," M., 1964.

equation (82) to a dimensionless form by dividing by $\frac{\rho_0 U_0^2}{l}$. As a result we will obtain

$$\frac{j_0 B_0 l}{\rho_0 U_0^2 c} \left(\frac{j_0 B_0}{j_0 B_0} - \frac{j_0 B_0}{j_0 B_0} \right).$$

Here l - characteristic dimension, ρ_0 , U_0 , j_0 , B_0 - values of fluid density, velocity, current density and magnetic induction at a certain characteristic point of flow. If the electromagnetic force is written as in equation of motion (82a), then in dimensionless form the corresponding term of this equation can be presented in the form

$$\frac{j_0 B_0 l}{4\pi \rho_0 U_0^2 c} \left[\frac{n_x}{B_0} \frac{\partial \frac{n_x}{B_0}}{\partial \frac{x}{l}} + \frac{B_y}{B_0} \frac{\partial \frac{n_x}{B_0}}{\partial \frac{y}{l}} + \frac{n_z}{B_0} \frac{\partial \frac{n_x}{B_0}}{\partial \frac{z}{l}} - \frac{1}{2} \frac{\partial \left(\frac{n_x}{B_0} \right)^2}{\partial \frac{x}{l}} \right].$$

The dynamic similarity of flow about model and full-scale object (see § 7 Chapter II) in an electroconductive fluid in the presence of an external magnetic field obviously requires that model and nature have identical values of the term

$$\dots \sim \frac{j_0 B_0 l}{\rho_0 U_0^2 c} = S_j = \text{idem} \quad (95)$$

or, taking into account the fact that according to (65) $j_0 \approx \frac{c}{4\pi \mu_0} \frac{B_0}{l}$, we have

$$\frac{B_0^2}{4\pi \mu_0^2 U_0^2 c} = S_n = \text{const.} \quad (96)$$

This term characterizes the relation of magnetic and kinetic energies of a unit volume. The quantity $A = \sqrt{S_n}$ is called *Alfven's number*. It goes without saying that it is necessary that the remaining hydrodynamic similarity criteria (Strouhal, Froude, Mach and Reynolds numbers) also be respectively identical.

Taking into account that with the final conductivity, according to Ohm's law (55) the current density induced by magnetic field is proportional to the relation

$$\frac{j_0 U_0 B_0}{c} \sim j_0$$

it is possible to obtain from (95) the criterion of magneto-hydrodynamic interaction, which expresses the ratio of magnetic force from the induced currents to the force of inertia

$$S_0 = \frac{j_0 D^2}{\rho_0 U_0 c^2} = \text{idem.} \quad (97)$$

The criterion S_0 is called the *parameter of magnetohydrodynamic interaction*.

Let us bring to dimensionless form the terms of the equation of Ohm's law (87)

$$\frac{j_x}{j_0} = \frac{\sigma_R E_0}{j_0} \left[\frac{E_x}{E_0} + \frac{1}{c} \frac{U_0 B_0}{E_0} \left(\frac{v B_x}{U_0 B_0} - \frac{w B_y}{U_0 B_0} \right) \right].$$

If j_0 is the conduction current at a characteristic point, then according to (23) $j_0 = \sigma_{R0} E_0$. Hence follows

$$\frac{j_x}{j_0} = \frac{\sigma_R}{\sigma_{R0}} \left[\frac{E_x}{E_0} + \frac{1}{c} \frac{U_0 B_0}{E_0} \left(\frac{v B_x}{U_0 B_0} - \frac{w B_y}{U_0 B_0} \right) \right].$$

Here the ratio of current induced by the magnetic field to external electric field current is determined at $\sigma_R = \sigma_{R0}$ by the dimensionless criterion

$$\Pi = \frac{U_0 B_0}{c E_0} = \frac{U_0}{c E_0 B_0} = \frac{U_0}{W_A}. \quad (98)$$

Here W_A is the drift velocity (52), determined earlier in § 2. The quantity

$$\Theta = \frac{S_0}{\Pi}, \quad (99)$$

characterizing the ratio of electromagnetic force from current imposed from without to the force of inertia is the criterion of electrohydrodynamic interaction.

Let us bring to dimensionless form the equation of magnetic induction (84)

$$i, U_0 \frac{d \frac{B_x}{B_0}}{d t} = \frac{c^2}{4\pi\mu_0^2 R^2 U_0} \left[\frac{\partial^2 \frac{B_x}{B_0}}{\partial \left(\frac{x}{l}\right)^2} + \frac{\partial^2 \frac{B_x}{B_0}}{\partial \left(\frac{y}{l}\right)^2} + \frac{\partial^2 \frac{B_x}{B_0}}{\partial \left(\frac{z}{l}\right)^2} \right] + \\ + \frac{\partial \frac{UB_x}{U_0 B_0}}{\partial \frac{x}{l}} + \frac{\partial \frac{UB_y}{U_0 B_0}}{\partial \frac{y}{l}} + \frac{\partial \frac{UB_z}{U_0 B_0}}{\partial \frac{z}{l}} - \frac{B_x}{B_0} \left[\frac{\partial \frac{u}{U_0}}{\partial \frac{x}{l}} + \frac{\partial \frac{v}{U_0}}{\partial \frac{y}{l}} + \frac{\partial \frac{w}{U_0}}{\partial \frac{z}{l}} \right]. \quad (100)$$

On the left side of (100) is an already known dimensionless factor - the Strouhal number ($SH = l/U_0 t_0$). In the right side appears a new dimensionless factor, the reciprocal of which is called the *magnetic Reynolds number*

$$R_H = \frac{4\pi\mu_0^2 R^2 U_0}{c^2} = \frac{l U_0}{\nu_H}. \quad (101)$$

This criterion characterizes the ratio of the magnetic field from induced currents to a superimposed external magnetic field¹. Sometimes the ratio of magnetic Reynolds number to the usual Reynolds number is used, i.e., Prandtl's magnetic number

$$Pr_m = \frac{R_H}{R} = \frac{4\pi\mu_0^2 R^2 \nu}{c^2} = \frac{\nu}{\nu_H}, \quad (102)$$

which is the ratio of ordinary viscosity to magnetic viscosity. If we multiply the criterion of magnetohydrodynamic interaction (97) by the Reynolds number, we will obtain the ratio of magnetic

¹The magnetic field from the induced currents is determined from the known relation

$$|\text{rot } B_i| = \frac{4\pi\mu_0}{c} |j| \sim \frac{4\pi\mu_0}{c^2} \sigma_R U_0 B_0$$

where $|\text{rot } B_i| \sim \frac{B_i}{l}$, B_0 is external field intensity. We hence have

$$\frac{B_i}{B_0} \sim \frac{4\pi\mu_0^2 R^2 U_0}{c^2} = R_H.$$

force from a field induced by magnetic current to viscosity force

$$S.R = \frac{\sigma_R l^2}{\rho_0 \nu} \frac{U_0}{\nu} = \frac{\sigma_R l^2 U_0}{\rho_0 \nu^2}.$$

The square root of this quantity is called *Hartman's number*

$$Ha = \frac{R_H l}{\nu} \sqrt{\frac{\sigma_R}{\mu}}. \quad (103)$$

Here $\nu = \rho_0^{-1}$ is the coefficient of dynamic viscosity. In the determination of Hartman's number, the characteristic l is the transverse dimension of the channel. Hartman's number is the basic similarity criterion in such magnetohydrodynamic problems in which a significant role belongs to viscosity forces.

Of the enumerated supplementary criteria of hydromagnetics only three are mutually independent (for example, the R , Ha and R_H numbers). The remaining parameters S , \mathfrak{E} , Pr_m) can be obtained from the given relationships as derivatives.

For some values of the separate similarity criteria the system of equations of hydromagnetics permits simplifications. So, when $R_H \ll 1$ it is possible to disregard magnetic fields from the induced currents and to consider that flow occurs only under the action of an external magnetic field. We deal with this type of flows in magnetic hydrodynamic channels (motion in the presence of electromagnetic fields of technical plasma or liquid metal in pipes, channels of magnetic pumps and magnetic gas-dynamic generators of electric current) and in the case of flows about a body, when the electrical conductivity of the medium is not very great.

When $R_H \gg 1$ the magnetic field turns out to be "frozen" into the substance and moves together with it; this area of magnetic gas dynamics is used in astrophysics, where very extended areas of greatly rarefied interstellar gas of sufficient conductivity or highly conducting stellar substance heated to millions of degrees (for example solar prominences) are dealt with.

During laboratory tests on liquid metals usually $R_H = 0.01-0.1$, and Hartman's number can reach the order of several hundred; in experiments on technical plasma (temperature on the order of 10^4 °K) a value of $R_H = 1$ is possible, whereas the number Π can be both less than and more than unity.

§ 6. Flow of Viscous Electroconductive Fluid Along a Plane Channel in a Transverse Magnetic Field

Let us examine the so-called "Hartman" flow - a laminar flow of incompressible electroconductive fluid along a plane channel of constant cross section (Fig. 13.8) in the presence of a permanent external transverse magnetic field with magnetic induction

$$B_y = B_0$$

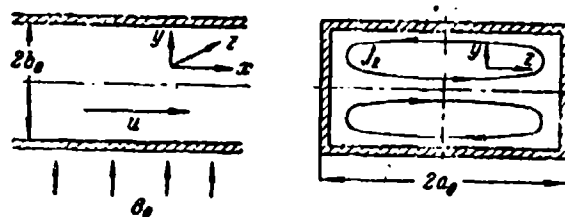


Fig. 13.8. Plane viscous fluid flow in a transverse magnetic field.

Along the length of the channel (section of stabilized flow) only pressure changes ($\partial p / \partial x \neq 0$); the remaining parameters remain constant ($\frac{\partial W}{\partial x} = \frac{\partial B}{\partial x} = 0$). With sufficiently large relative channel width ($a \gg b$) the flow can be considered plane-parallel, during which the velocity and the induction do not change in the direction of the z -axis ($\frac{\partial W}{\partial z} = \frac{\partial B}{\partial z} = 0$), and the transverse velocities of components are absent ($v = 0, w = 0$).

¹Hartmann, Theory of the laminar flow in a homogeneous magnetic field, Kgl. Danske Videnskab, Math. -fys., Medd., 15, No. 6, 1937.

From the equation of continuity of the lines of magnetic induction (43) we have

$$\operatorname{div} B = 0 \text{ or } \frac{\partial B_x}{\partial x} + \frac{\partial B_y}{\partial y} + \frac{\partial B_z}{\partial z} = 0.$$

As a result of condition $\frac{\partial B_x}{\partial x} = \frac{\partial B_z}{\partial z} = 0$ we also have $\frac{\partial B_y}{\partial y} = 0$ or $B_y = \text{const} = B_0$, i.e., magnetic induction within the channel in the direction of the y-axis does not change

From equation (63) for a magnetostatic field, there follows $\operatorname{rot} E = 0$. Hence, under the assumption that $\frac{\partial}{\partial x} = \frac{\partial}{\partial y} = 0$, we obtain $E_z = \text{const}$, $E_x = \text{const}$. From the condition of the absence of current in direction x, it is necessary to take $E_x = 0$. From the equation $\operatorname{div} j = 0$ we have $j_y = \text{const}$. Assuming the walls $y = \pm b$ to be nonconductive, we have $j_y = 0$. Then from Ohm's law it follows that $E_z = \frac{1}{\sigma_R} j_z = 0$.

According to the Ohm's law the current density in projection onto the z-axis is equal to

$$j_z = \sigma_R \left[E_z + \frac{1}{c} u B_0 \right]. \quad (104)$$

If the side walls $z = \pm a$ are also insulators, then the total current in the direction of the z-axis

$$I_z = \int_{-b}^b j_z dy = \sigma_R \left[E_z 2b + \frac{B_0}{c} \int_{-b}^b u dy \right] = 0.$$

Since the value

$$\frac{1}{2b} \int_{-b}^b u dy = u_{cp}$$

is the average flow velocity, the electric field intensity

$$E_z = - \frac{B_0 u_{cp}}{c}. \quad (105)$$

Substituting (105) into (104), we arrive at the final expression for the current density

$$j_z = \frac{e \kappa B_0}{c} (u - u_{cp}) \quad (106)$$

As we see, despite the fact that the total current strength is equal to zero, current in the direction of the z-axis flows, whereupon in layers at low velocity ($u < u_{cp}$) the current density is negative, and in layers of high speed ($u > u_{cp}$) it is positive

The electromagnetic force - the last term on the right side of equation (82) - in this case is

$$F_x = -\frac{1}{c} j_z B_0 = -\frac{e \kappa B_0^2}{c^2} (u - u_{cp}) \quad (107)$$

From (107) it follows that in the middle part of the cross section of the channel the electromagnetic force is negative (brakes the flow) and near the walls is positive (accelerates the flow). Since $I_z = 0$, the total electromagnetic force applied to the entire flow is also equal to zero. In connection with the account given, the equation of motion (82) along the x-axis is written thus:

$$0 = -\frac{\partial p}{\partial x} + \mu \frac{\partial^2 u}{\partial y^2} - \frac{1}{c} j_z B_0 \quad (108)$$

Hence, on the basis of (106) we have

$$A = \frac{\partial p}{\partial x} - u_{cp} \frac{e \kappa B_0^2}{c^2} = \mu \frac{\partial^2 u}{\partial y^2} - \frac{1}{c^2} e \kappa B_0^2 u \quad (108a)$$

From the equation of motion (82a) for the y-axis we have

$$\frac{\partial \rho}{\partial y} = \frac{\partial}{\partial y} \left(\rho + \frac{B_0^2}{8\pi\mu_B} \right) = 0,$$

whence it follows that the quantity $\partial p / \partial x$ does not depend on y.

The left side of equation (108a) depends only on x and right only on y, and therefore A should be a constant value ($A = \text{const}$).

After reduction to a dimensionless form we have

$$n = \frac{\Delta b^2}{\mu u_{cp}} = \frac{\partial^2 n}{\partial y^2} - \text{Ha}^2 n. \quad (109)$$

Here $\text{Ha} = \frac{\Delta b}{c} \sqrt{\frac{\rho R}{\mu}}$ - the Hartman number, n - dimensionless coefficient, $a = \frac{u}{u_{cp}}$, $y = \frac{y}{b}$ - dimensionless values of velocity and distance from the axis of the channel.

The integral of this heterogeneous linear equation with constant coefficients is

$$n = C_1 \text{ch}(\text{Ha} y) + C_2 \text{sh}(\text{Ha} y) + \frac{n}{\text{Ha}^2}.$$

From the boundary conditions $\bar{u} = 0$ when $\bar{y} = \pm 1$ we determine the integration constants

$$C_1 = -\frac{n}{\text{Ha}^2 \text{ch Ha}}, \quad C_2 = 0.$$

Thus, the rate of flow of fluid in the channel

$$a = \frac{n}{\text{Ha}^2} \left[1 - \frac{\text{ch}(\text{Ha} y)}{\text{ch Ha}} \right]. \quad (110)$$

From a determination of the average velocity (for half of a channel)

$$u_{cp} = \frac{1}{b} \int_0^b u dy = u_{cp} \int_0^1 a dy$$

there follows

$$\int_0^1 a dy = 1.$$

Substituting value \bar{u} from (110) into this integral, we have

$$1 = \frac{n}{\text{Ha}^2} \left[1 - \frac{\text{th Ha}}{\text{Ha}} \right] \text{ or } \frac{n}{\text{Ha}^2} = \frac{\text{Ha}}{\text{Ha} - \text{th Ha}}.$$

Substituting this result into (110), we arrive at the final expression for the flow velocity

$$u = Ha \frac{\operatorname{ch} Ha - \operatorname{ch}(y Ha)}{Ha \operatorname{ch} Ha - \operatorname{sh} Ha} \quad (111)$$

When $Ha \rightarrow 0$ we have

$$u = \frac{3}{2} (1 - y^2)$$

i.e., the maximum velocity profile in the channel for a not electrically conductive liquid, as one would expect, is Poiseuille's profile (see Chapter II). The maximum value of velocity on the axis of the channel (when $\bar{y} = 0$), according to (111), is equal to

$$u_m = \frac{Ha (\operatorname{ch} Ha - 1)}{Ha \operatorname{ch} Ha - \operatorname{sh} Ha} \quad (111a)$$

The velocity profile in the cross section of the channel at different values of Ha numbers, calculated by means of (111), are shown on Fig. 13.9. The intensification of the magnetic field leads to the smoothing (flattening) of the velocity profile. When $Ha = \infty$ we have $\bar{u} = \bar{u}_m = 1$. As is evident on Fig. 13.9, at large values of the Hartman number, the flow consists of a nucleus of constant velocity and comparatively thin boundary layer.

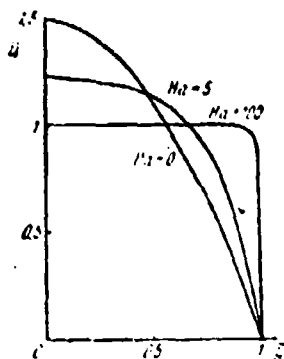


Fig. 13.9. Velocity profile at different values of the Hartman number.

The smoothing velocity profile with an increase in the Hartman number leads to an increase in the velocity gradient at the wall, which produces an increase in the force of friction.

The velocity gradient according to (111)

$$\frac{\partial u}{\partial y} = \frac{u_{cp}}{b} \frac{dh}{dy} = -\frac{u_{cp}}{b} \frac{Ha^2 \operatorname{sh}(y Ha)}{Ha \operatorname{ch} Ha - \operatorname{sh} Ha}.$$

Hence, according to Newton's formula we find the frictional stress at the wall (when $y = b$, i.e., $\bar{y} = 1$)

$$\tau_w = -\mu \left(\frac{\partial u}{\partial y} \right)_w = \frac{\mu_c \mu}{b} \frac{Ha^2 \operatorname{ch} Ha}{Ha \operatorname{ch} Ha - \operatorname{sh} Ha}$$

or in a dimensionless form

$$c_f = \frac{\tau_w}{\frac{\rho u_c^2}{2}} = \frac{2}{R} \frac{Ha^2 \operatorname{ch} Ha}{Ha \operatorname{ch} Ha - \operatorname{sh} Ha}. \quad (112)$$

Here $R = \mu_c b / \mu$ is the Reynolds number. When $Ha \rightarrow \infty$ we have $c_f \rightarrow \infty$ when $Ha \rightarrow 0$, from (112) we obtain the well-known Poiseuille equation

$$c_{f0} = \frac{6}{R}. \quad (112a)$$

Having divided term by term (112) into (112a), let us find the ratio of the coefficients of friction in the presence and absence of the magnetic field

$$\bar{c}_f = \frac{c_f}{c_{f0}} = \frac{Ha^2}{3} \frac{\operatorname{ch} Ha}{Ha - \operatorname{sh} Ha}. \quad (113)$$

At large values of the Hartman number ($Ha \geq 3$) $\operatorname{th} Ha \sim 1$, and therefore in the case of a strong magnetic field, formula (113) takes the following form:

$$\bar{c}_f = \frac{1}{3} Ha. \quad (113a)$$

Functions (111a) and (113) are shown graphically on Fig. 13.10. The experiments of Hartman, Lazarus and Margetroyt¹ confirm the validity of the laws found above governing the Hartman flow.

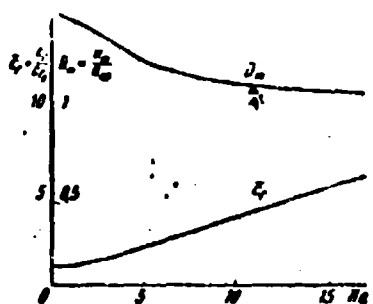


Fig. 13.10. Dependence of the maximum speed and coefficient of friction on the Hartman number.

¹Harris, L. S., Magnetohydrodynamic channel flows. Publishing House of Foreign Literature, M., 1963.

The pressure change along the length of the channel can be found from equality (108), under condition that on the wall $u = u_w = 0$:

$$A = \frac{\partial p}{\partial x} - \frac{u_{cp}^2 R B_0^2}{c^2} = \mu \left(\frac{\partial^2 u}{\partial y^2} \right)_w.$$

According to (111)

$$\frac{\partial^2 u}{\partial y^2} = \frac{u_{cp}}{b} \frac{\partial^2 \bar{u}}{\partial \bar{y}^2} = - \frac{u_{cp}}{b^2} \frac{Ha^2 \operatorname{ch}(\bar{y} Ha)}{Ha \operatorname{ch} Ha - \operatorname{th} Ha}.$$

At the wall when $\bar{y} = 1$ we have

$$\left(\frac{\partial^2 u}{\partial y^2} \right)_w = - \frac{u_{cp}}{b^2} \frac{Ha^2}{Ha - \operatorname{th} Ha}.$$

Consequently,

$$A = \frac{\partial p}{\partial x} - \frac{u_{cp}^2 R B_0^2}{c^2} = - \frac{\mu u_{cp}}{b^2} \frac{Ha^2}{Ha - \operatorname{th} Ha}$$

or in a dimensionless form when $\bar{x} = x/b$

$$\frac{\partial p}{\partial \bar{x}} = \frac{2b}{\mu u_{cp}} \frac{\partial p}{\partial x} = - \frac{2}{R} \frac{Ha^2 \operatorname{th} Ha}{Ha - \operatorname{th} Ha}. \quad (114)$$

From a comparison of (114) with expression (112) we have

$$\frac{\partial p}{\partial \bar{x}} = -c_f. \quad (114a)$$

This result can also be obtained on the basis of the fact noted above that in the Hartman flow the total electromagnetic force is equal to zero, in consequence of which the pressure change is balanced by the force of friction on the wall

$$2\tau_w dx = -2b \frac{\partial p}{\partial \bar{x}} dx, \quad \text{i.e.} \quad \frac{\partial p}{\partial \bar{x}} = -c_f.$$

In the presence of the total electromagnetic force condition $I_z = 0$ is not fulfilled, and equality (114a) is incorrect.

Let us discuss now the electromagnetic features of the Hartman flow. From the Maxwell law (60a) and formula (106) we obtain in the projection onto the z-axis

$$\frac{\partial U_y}{\partial x} - \frac{\partial B_x}{\partial y} = -\frac{4\pi\mu_0^2 R B_0}{c^2} (u - u_{cp})$$

Since according to condition $\frac{\partial B_y}{\partial x} = 0$,

$$\frac{\partial B_x}{\partial y} = -\frac{4\pi\mu_0^2 R}{c^2} (u_{cp} - u)$$

or in accordance with (101)

$$\frac{\partial B_x}{\partial y} = R_H (1 - \eta)$$

Hence, taking into account (111), we have

$$\frac{B_x}{B_0} = R_H \left[y - \frac{Ha}{ch Ha} \frac{y ch Ha}{sh Ha} + \frac{sh(y Ha)}{Ha ch Ha - sh Ha} \right] + C$$

Considering the boundary conditions $B_x = 0$ when $\bar{y} = 1$ and $\bar{y} = 0$ (in the absence of the total current the induced magnetic field outside the channel is absent), we find that $C = 0$ is constant. As a result we obtain

$$\frac{B_x}{B_0} = R_H \frac{sh(y Ha) - y sh Ha}{Ha ch Ha - sh Ha}. \quad (115)$$

Thus, in the Hartman flow there appears the magnetic induction in the direction of the x-axis, the relative value of which is proportional to the value of the magnetic Reynolds number.

In connection with the presence of magnetic induction B_x , the pressure on the cross section of the channel is variable. The pressure change in a transverse direction can be determined from the equation of motion (82) in the direction of the y-axis.

Under conditions of this problem ($v = 0$, $w = 0$, and also $\frac{\partial}{\partial x} = \frac{\partial}{\partial z} = 0$ for all values except pressure) the equation of motion in the projection onto the y-axis takes the following form

$$0 = -\frac{\partial p}{\partial y} + \frac{1}{c} j_z B_x$$

or

$$0 = -\frac{\partial p}{\partial y} + \frac{\epsilon_R n_0^2 u_{cp}}{c^2} \frac{B_x}{B_0} (a-1)$$

Hence we obtain

$$\frac{\partial p}{\partial y} = -\frac{\epsilon_R B_0^2 u_{cp}}{c^2} \frac{B_x}{B_0} (1-a)$$

or in a dimensionless form for $\bar{p} = 2p/\rho u_{cp}^2$, $\bar{y} = y/b$ and S_0 , determined from

$$\frac{\partial \bar{p}}{\partial \bar{y}} = -2S_0 \frac{B_x}{B_0} (1-a) \quad (116)$$

Thus, the pressure gradient in a transverse direction is proportional to the value of the criterion of magnetic gas-dynamic interaction S_0 .

The calculations carried out according to formulas (116), (115) and (111) show that the transverse pressure gradient is considerably less than the longitudinal $\frac{\partial p}{\partial y} < \frac{\partial p}{\partial x}$.

Figure 13.11 shows curves of the distribution of dimensionless quantities of the electric current density j_z^* , magnetic induction (B_x^*) and pressure gradient p^* with respect to the height of the channel, calculated, respectively, according to formulas (106), (111), (115) and (116), when $Ha = 5$

$$j_z^* = \frac{c}{\epsilon_R B_0^2 u_{cp}} j_z = a - 1, \quad B_x^* = \frac{1}{R_H} \frac{B_x}{B_0} = \frac{\text{sh } y Ha - y \text{sh } Ha}{Ha \text{ch } Ha - \text{sh } Ha},$$

$$p^* = \frac{1}{2S_0 R_H} \frac{\partial p}{\partial y} = -B_x^*/a.$$

Here

$$R_H = \frac{4\pi u_{cp}^2 \epsilon_R b u_{cp}}{c^2}, \quad S_0 = \frac{\epsilon_R b B_0^2}{4\pi u_{cp}^2}.$$

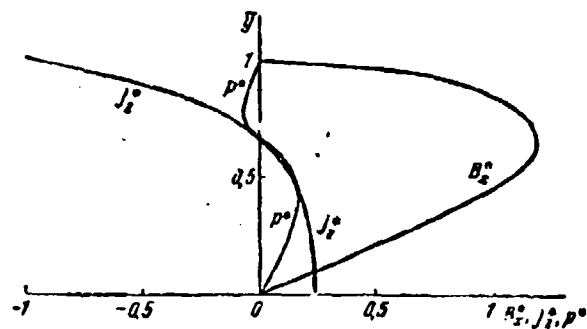


Fig. 13.11. Curves of the density distributions of current, magnetic induction and pressure gradient in the cross section of the channel when $Ha = 5$.

§ 7. Magnetohydrodynamic Pumps, Accelerators, Chokes and Generators

The electromagnetic force which is caused by electric and magnetic fields applied to a flow of a conducting liquid can be directed along the flow or against the flow. In the first case the electromagnetic force can be utilized as a means for a pressure increase (electromagnetic pump) or as means for an increase in the rate of flow (jet engine). In the second case the electromagnetic force slows down the flow (electromagnetic choke).¹

If the electric current being induced by a magnetic field in a fluid flow is directed into an external circuit, then a magnetohydrodynamic current generator (MHD generator) will be obtained.

The dependence of the induced potential differences on the average flow velocity is utilized for the measurement of the fluid flow rate (magnetohydrodynamic flow meter).

All these methods of using electro-MHD effects can be examined in the example of a flow of an electro-conductive fluid in a flat channel which is placed into an electromagnetic field; one case of such a flow is analyzed in the foregoing paragraph (Hartman's problem).

In a Hartman flow it was assumed that the walls of the channel are insulators and the total electric current which appears in the direction perpendicular both to the velocity vector and to the vector of induction of the superimposed magnetic field is equal to zero, as a result of which total electromagnetic force is also equal to zero.

¹Sherkliff D. A. The theory of electromagnetic measurement of flow rate. "MIR," M., 1965.

If the lateral walls of the channel ($z = \pm a$) are electrodes connected with an external electric circuit, then the electromotive force maintains the potential difference on these electrodes.

Within the channel (Fig. 13.12) the current flows from electrode 1 to electrode 2, in the external circuit - in the opposite direction. The average current density in the channel according to (104)

$$j_{zcp} = \frac{1}{2b} \int_0^b j_z dy = \sigma_R \left(-E_0 + \frac{u_R B_0}{c} \right), \quad (117)$$

and the local current density

$$j_z = \sigma_R \left(-E_0 + \frac{u_R B_0}{c} \right). \quad (117a)$$

For Hartman flow ($j_{zcp} = 0$) from a comparison of (104) and (117) we obtain the already known equality (105)

$$-E_0 = E_1 = \frac{u_{cp} B_0}{c}.$$

If the electrodes are short-circuited (external resistance $R = 0$) then the electric current strength is equal to zero ($E_0 = 0$) and the current density

$$j_{zcp} = \frac{\sigma_R B_0 u_{cp}}{c}.$$

In this case according to (107) an inhibiting electromagnetic force is applied to the flow

$$F_x = -\frac{1}{c} j_{zcp} B_0 = -\frac{\sigma_R B_0^2 u_{cp}}{c}.$$

In general the expression (117) is convenient to present in the following form:

$$j_{zcp} = \frac{\sigma_R B_0}{c} (u_{cp} - W_A). \quad (118)$$

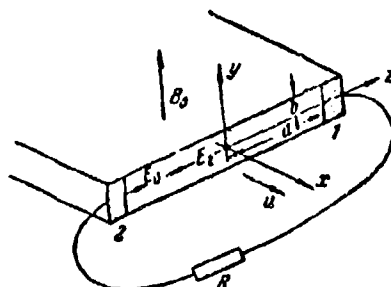


Fig. 13.12. Diagram of a channel with lateral wall-electrodes.

where the subtrahend $W_d = cE_0/B_0$ is the drift velocity.

In order that the channel would work under the conditions of an MHD generator ($j_z > 0$), it is necessary that the average flow velocity would be greater than the drift velocity; in the case of operation of the channel under the conditions of a pump or accelerator ($j_z < 0$) the average velocity in the channel is less than the drift velocity. The sign of current density determines the direction of electromagnetic force. On the basis of (107) we conclude that in an MHD generator the electromagnetic force is directed against the flow ($F_x < 0$), and in a pump and accelerator - along the flow ($F_x > 0$); the pressure gradient along the length of the channel (not allowing for friction) in an MHD generator should be negative ($\partial p / \partial x < 0$), and in a pump or accelerator - positive ($\partial p / \partial x > 0$).¹

In all apparatuses examined in this paragraph which use the motion of a noncompressible fluid along a flat channel of constant section the equation of motion (108) is useful; with the help of (105) it can be given the following form:

$$\Lambda = \frac{\partial p}{\partial x} - \frac{c_R^2 B_0}{c} = \mu \frac{\partial^2 u}{\partial y^2} - \frac{c_R^2 j_z^2}{c^2}. \quad (119)$$

¹The indicated inequalities for $\partial p / \partial x$ are valid in the case of a liquid metal; in a gas they cannot be fulfilled.

Equation (119) is identical to equation (108a), the solution of which was obtained in the previous paragraph. In connection with this the profile of relative velocity in the cross section of channel $\bar{u}(\bar{y})$ and the relative value of the coefficient of friction \bar{c}_f do not depend on value E_0 and are described in all cases by equations (111) and (113) respectively.

Substituting in (119) the value A , found in § 6 for Hartman flow, we come to the expression for the pressure gradient in the direction of flow

$$\frac{\partial p}{\partial x} = A + \frac{e_R E_0 B_0}{c} = -\frac{\mu u_{cp}}{b^2} \frac{Ha^2}{Ha - \ln Ha} + \frac{e_R E_0 B_0}{c}. \quad (120)$$

As we see, in the case of an electromagnetic pump ($\partial p / \partial x > 0$) the intensity of the electric field should be sufficiently great in order that the right side (120) would turn out to be positive.

In an MHD generator ($\partial p / \partial x < 0$) the electric field intensity should be such that the sign of the right side (120) would be negative.

For constant electric and magnetic fields in all electro-MHD apparatuses in which the fluid flows along a channel of constant section the pressure gradient along the length of the channel does not change, therefore, a drop in pressure in a channel with length x

$$\Delta p = x \frac{\partial p}{\partial x} = x \left(\frac{e_R E_0 B_0}{c} - \frac{\mu u_{cp}}{b^2} \frac{Ha^2}{Ha - \ln Ha} \right). \quad (121)$$

Utilizing expressions (97) and (98), we obtain from (121) the dimensionless magnitude of drop in pressure

$$\frac{\Delta p}{\rho u_{cp}^2} = 2 \frac{x}{b} S_0 \left(\frac{1}{\Pi} - \frac{Ha}{Ha - \ln Ha} \right). \quad (122)$$

Here

$$\Pi = \frac{u_{cp}}{W_A}, \quad S_0 = \frac{u_R u_{cp}}{R} = \frac{Ha^2}{R}.$$

In a pump or accelerator ($\Pi < 1$) the subtrahend in parenthesis is less than the minuend, while in an MHD generator ($\Pi > 1$) - vice versa.

For Hartman flow ($\Pi = 1$) taking into account (112) we have

$$\frac{2\Delta p}{\mu u_{cp}} = \frac{\pi}{b} c_f.$$

§ 6. The Entry of the Flow of an Electro-Conductive Fluid into a Magnetic Field and Discharge from It

Near the electrode tips the electric field is non-uniform, in connection with which the electric current density in these places is changed in value and direction.

Let us examine the flow of an electro-conductive fluid in the zone of entry into a section of channel with a magnetic field (Fig. 13.13). Let us designate the height of the channel (electrode separation) $2a$, and the width of the channel $2b$. We will consider the channel flow two-dimensional, which is admissible under the condition $b \gg a$. The beginning of the electrodes is located in plane $x = 0$; with $x < 0$ the walls of the channel are not electrically conductive.

The magnetic field in the area $x < 0$ is absent ($B = 0$), and in area $x > 0$ it is constant and is oriented along axis y in a negative direction ($B_x = 0, B_y = B < 0, B_z = 0$), i.e., at right angles to the plane of the drawing in Fig. 13.13.

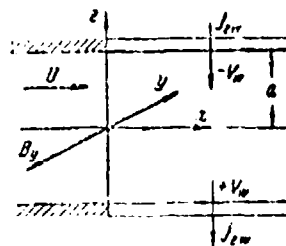


Fig. 14.13. The diagram of flow upon entry into a section of channel with a magnetic field.

The viscosity of the fluid is not taken into consideration, so that the flow with $x = -\infty$ is uniform (speed W is constant and directed along the x -axis). The magnetic Reynolds number we assume small ($R_H \ll 1$).¹

For simplicity we consider the fluid incompressible ($\rho = \text{const}$), and flow is steady.

Near the electrode tips the lines of electric current are deformed and cause the distortion of the velocity field

$$u = U + u', \quad w = w'. \quad (123)$$

Additional velocities (disturbances) u' , w' along the axes x and z we consider low relative to the initial velocity W , i.e., $u' \ll W$, $w' \ll W$.

This problem can be solved by the method of successive approximations. In the first approximation the equations of motion (92) along axes x and z take the following form:

$$\left. \begin{aligned} \rho W \frac{\partial u'}{\partial x} + \frac{\partial p}{\partial x} &= -\frac{1}{c} J_y B_y \\ \rho W \frac{\partial w'}{\partial x} + \frac{\partial p}{\partial z} &= \frac{1}{c} J_y B_y \end{aligned} \right\} \quad (124)$$

¹Sutton G. W., Carlson A. W. EHD effects in inviscid flow in a magnetohydrodynamics channel. Journal of Fluid Mech., v. 11, p. 1, 123-131, 1961.

The components of electric current density in the first approximation (with $W = \text{const}$) according to (87) are determined as

$$I_x = \sigma_R E_x, \quad I_z = \sigma_R \left(E_z + \frac{1}{c} WB \right). \quad (125)$$

Here $B = 0$ with $x < 0$, $B = \text{const} < 0$ with $x > 0$.

If on section $x > 0$ at a sufficient distance from cross section $x = 0$ the walls ($z = \pm a$) are electrically insulated, then the transverse component of current at the walls will be equal to zero

$$I_{z0} = \sigma_R \left(E_{z0} + \frac{1}{c} WB \right) = 0.$$

From here we have

$$E_{z0} = -\frac{\partial V}{\partial z} = -\frac{1}{c} WB > 0$$

or in the case $B < 0$

$$\frac{\partial V}{\partial z} < 0.$$

Consequently positive charges are accumulated at the lower wall of the channel, and negative are accumulated on the upper wall. If the isolated walls are replaced by electrodes, then the lower electrode will be positive, and the upper - negative. After connecting the electrodes by an external circuit, we will obtain in it an electric current which goes from the positive electrode to the negative.

In the case of a stationary two-dimensional electric field according to (25) we have

$$\frac{\partial I_x}{\partial x} + \frac{\partial I_z}{\partial z} = 0. \quad (126)$$

From the zero approximation we obtain with the help of (125) the equation for the field of electrical strength

$$\frac{\partial E_y}{\partial y} + \frac{\partial E_z}{\partial z} = 0, \quad (127)$$

valid with $\lambda = \text{const}$ and $r = 1/2$ in the entire zone of flow ($-a \leq y \leq a$).

Introducing in (127) according to (20) the electric potential V

$$E_x = -\frac{\partial V}{\partial x}, \quad E_z = -\frac{\partial V}{\partial z},$$

we obtain the Laplace equation

$$\frac{\partial^2 V}{\partial x^2} + \frac{\partial^2 V}{\partial z^2} = 0. \quad (128)$$

The boundary conditions in the zone of arrangement of electrodes ($x > 0$)

$$z = \pm a, \quad V_0 = \pm V_0, \quad (129)$$

The value of potential on an electrode (V_0) with high conductivity of the latter is virtually constant.

In the zone of insulated walls ($x < 0$) the boundary conditions are written in the form

$$z = \pm a, \quad E_{z0} = j_{z0} = 0, \quad \text{i.e.,} \quad \left(\frac{\partial V}{\partial z}\right)_0 = 0. \quad (130)$$

The solution of the Laplace equation (128), which satisfies boundary conditions (129) and (130), can be presented in the form

$$V = V_0 \frac{x^2}{a^2}. \quad (131)$$

where

$$\xi = \arcsin \left[\pm \sqrt{\frac{e^{i\xi} + 1}{2}} - \sqrt{\frac{(e^{i\xi} + 1)^2}{4} - e^{i\xi} \cos^2 \eta} \right], \quad (132)$$

$$\bar{x} = \frac{\pi}{2a} \pi, \quad \eta = \frac{\pi + a}{2a} \pi. \quad (133)$$

The plus sign in (132) corresponds to values $\pi > \eta > \pi/2$, minus - to values $\pi/2 > \eta > 0$.

It is possible to be convinced of the validity of solution (132) by substituting it into the Laplace equation (128) which in variables (133) is reduced to the form

$$\frac{\partial^2 \xi}{\partial \bar{x}^2} + \frac{\partial^2 \xi}{\partial \eta^2} = 0. \quad (134)$$

Let us replace in expressions (126) for the components of current density the components of electric field strength (E_x, E_z) with the derivatives of electric potential ($\partial V/\partial x, \partial V/\partial z$), making use of expressions (131) and (133):

$$\left. \begin{aligned} j_x &= -\epsilon_R \frac{\partial V}{\partial x} = \pm \frac{\epsilon_R V_0}{a} \frac{\partial \xi}{\partial \bar{x}}, \\ j_z &= \epsilon_R \left[-\frac{\partial V}{\partial z} + \frac{WB}{c} \right] = \epsilon_R \left[\frac{V_0}{a} \left(\mp \frac{\partial \xi}{\partial \eta} \right) + \frac{WB}{c} \right]. \end{aligned} \right\} \quad (135)$$

With the selected signs the transverse component of current density j_z caused by the electrical field, as it was shown, is directed from the bottom to the top ($\partial V/\partial z < 0$). The longitudinal component of current density j_x in the upper part of the channel is positive, and in the lower part negative; on the axis of the channel $j_x = 0$.

The transverse component of current density j_z within the channel on the section with electrodes in zone $x \rightarrow \infty$ (where $\xi < 0$) is directed from the negative electrode to the positive (downward), since here the current which is induced by the magnetic field

prevailing in the region of the laminated walls ($R = 0$) there is a current induced by the magnetic field, and therefore here vector J_z is an odd function of y (from bottom to top). Thus with the entry of a fluid into a magnetic field a zone of closed circulation of vector J_z appears in which the latter changes its direction to the opposite.

The density of the total current ($j = \sqrt{j_x^2 + j_z^2}$), calculated with the help of formula (136) for the case $aWB/cV_w = 2$, is plotted in Fig. 12.14.

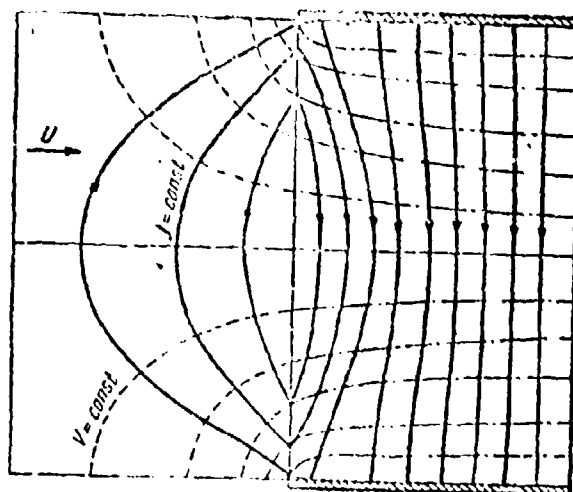


Fig. 12.14. Lines of equal values of potential and current density upon entry of a flow into a magnetic field.

Utilizing equations of motion (124), it is possible to find the change in the average static pressure by area along the length of the channel. Integrating the first of equations (124) within the limits from $-a$ to $+a$ and dividing all its terms by $2a$, we obtain

$$\frac{1}{2a} \int_{-a}^{+a} \rho W \frac{\partial u'}{\partial x} dz = -\frac{1}{2a} \int_{-a}^{+a} \frac{\partial p}{\partial x} dz - \frac{n}{2ac} \int_{-a}^{+a} J_z dz. \quad (136)$$

Let us rewrite equation (136) in the form

$$\frac{1}{2a} \frac{\partial}{\partial x} \int_{-\infty}^{\infty} n' dz = -\frac{1}{2a} \frac{\partial}{\partial x} \int_{-\infty}^{\infty} p dz - \frac{B}{2ac} \int_{-\infty}^{\infty} j_z dz, \quad (136a)$$

Let us introduce the designations

$$\frac{1}{2a} \int_{-\infty}^{\infty} p dz = p_{cp}, \quad \frac{1}{2a} \int_{-\infty}^{\infty} j_z dz = j_{zcp} \quad (137)$$

Taking into account that from the continuity condition follows

$$\int_{-\infty}^{\infty} n' dz = 0,$$

from equation (136a) we have

$$\frac{\partial p_{cp}}{\partial x} = -\frac{B}{C} j_{zcp} \quad (138)$$

With $x < 0$ $B = 0$, therefore p_{cp} on section $-\infty < x < 0$ along the length does not change. Let us calculate $\partial p_{cp}/\partial x$ on the section of distribution of the electrodes ($x > 0$).

Utilizing relationships (135) and (132), we find the average cross sectional value of the component of current density j_z cp

$$j_{zcp} = \sigma_R \left[\mp \frac{V_R}{a} \int_{-\infty}^{\infty} \frac{\partial x'}{\partial \eta} d\eta \frac{\partial z}{\partial \eta} \frac{1}{2a} + \frac{VB}{c} \right].$$

It is obvious that integral $\int_{-\infty}^{\infty} \frac{\partial x'}{\partial \eta} d\eta$ is equal to the difference in the values of function \bar{x}' in points π and 0, i.e.,

$$\mp \int_{-\infty}^{\infty} \frac{\partial x'}{\partial \eta} d\eta = \pi.$$

Consequently,

$$J_{z,p} = \sigma R \left[\frac{V_w}{a} + \frac{WB}{c} \right], \quad (139)$$

i.e., the average cross sectional value of the component of current $J_{z,p}$ on the section of distribution of electrodes does not change. Utilizing relationship (139), from equation (138) we find

$$\frac{dp_p}{dx} = -\frac{\sigma R D}{c} \left[\frac{V_w}{a} + \frac{WB}{c} \right].$$

Thus, it turns out that the gradient of mean pressure dp_p/dx along the length of the channel (with $x > 0$) is a constant value. After designating the mean value of static pressure in section $x = 0$ through p_0 , we finally have with $x > 0$

$$p_p - p_0 = -\frac{\sigma R D}{c} \left[\frac{V_w}{a} + \frac{WB}{c} \right] x. \quad (140)$$

Utilizing an electric field of first approximation, it is possible to determine the velocity field of first approximation, for which one ought to turn to the equations of motion (124).¹

We examined the problem concerning the flow of a fluid in a section located directly before the inlet to a channel with a magnetic field.

The problem of the flow discharge of fluid from a magnetic field is solved analogously; however, in this case when using the same equations one should change to the opposite sign of variable \bar{x} .

¹See footnote on page 962.

The solution of the Laplace equation (134) for the stream or discharge from a field we present in the form

$$V_{\text{out}} = V_{\text{in}} \frac{x'}{x}, \quad (135)$$

where $\bar{x}' = x'/a$ is determined from (132) by taking into account the sign before \bar{x}

$$x' = ax \sin \left(\frac{\pi}{2} \sqrt{\frac{e^{-u} + 1}{2}} - \sqrt{\frac{(e^{-u} + 1)^2}{4} - e^{-u} \cos^2 \eta} \right). \quad (136)$$

In this case at the boundary we accept the conditions

$$\begin{aligned} x < 0, \quad V_{\text{out}} &= V_{\text{in}} \quad \text{for } y = 0, \pi \\ x > 0, \quad \frac{\partial V}{\partial y} &= 0 \quad \text{for } y = 0, \pi. \end{aligned}$$

Taking into account the connection between the stream and velocity functions \bar{x}' and \bar{y}'

$$\frac{\partial x'}{\partial t} = -\frac{\partial t}{\partial x}, \quad \frac{\partial x'}{\partial y} = \frac{\partial t}{\partial y},$$

we find that the direction of the transverse component of current density remains the same as in the section of entry into a field, but the direction of the longitudinal component of current density changes to inverse

$$J_x < 0 \text{ with } x > \frac{a}{2}, \quad J_x > 0 \text{ with } x < \frac{a}{2}.$$

The sign of the longitudinal pressure gradient remains before (negative), in other words into the field the current and magnetic field and entry into it are always directed against (resistance) drag. The directions of the transverse velocity of pressure during exit and entry of a fluid flow from a magnetic field are opposite.

§ 9. The Equations of Magnetic Gas Dynamics for a Unit Stream

The concept "unit stream" in magnetic hydrogasdynamics does not have such a universal application as in usual gas dynamics, since only in a few cases is it possible to consider as constant in the cross section of the stream the values and directions of the vectors of electrical strength and magnetic induction, and together with them the vectors of current density and electromagnetic force.

Let us give two examples of the magnetogasdynamic flows in which the idea of a unit stream is strictly valid:

1. A channel of constant section $z = \pm a$, formed by two parallel walls along which in direction x a conducting gas moves; the walls of the channel are opposite electrodes of infinite conductivity, and viscosity and thermal conductivity are not considered.

If on the walls a potential difference is supported, then an electric current j_z appears which induces "its own" magnetic field, the lines of intensity of which according to the thumb rule are directed at right angles to the flow plane (along axis y).

Flow in such a channel is equivalent to the flow of a unit stream which is found in constant lattice-type electromagnetic fields $W(u, 0, 0)$, $E(0, 0, E_z)$, $B(0, B_y, 0)$, $f(f_x, 0, 0)$.

2. The uniform flow of the gas before and behind a direct magnetogasdynamic wave (with lines of magnetic induction perpendicular to the direction of flow). This case is examined in detail in § 10.

Let us write the equations of magnetic gas dynamics for a unit stream of gas, disregarding the viscosity and the thermal

conductivity of the fluid. We will consider the motion of the fluid steady-state, magnetic field - stationary, and the vector $[E \times B]$, which determines the work of electromagnetic force (see (24)), - directed parallel to the velocity vector W . In this case the vector flux $[E \times B]$ is directed along the normal to the cross section of the stream.

As is known from the field theory,

$$\operatorname{div}[E \times B] = \lim_{\Delta v \rightarrow 0} \frac{1}{\Delta v} \int_S [E \times B]_n dS,$$

where Δv - the volume being included by the closed surface S , through which passes the vector flux $[E \times B]_n$, n - external standard to surface S . In our case, with a low extent of volume Δv , we have

$$\int_S [E \times B]_n dS = \Delta([E \times B]_n F).$$

Here F - the cross-sectional area of the stream tube, index l indicates that the projection of vector $[E \times B]$ is taken on the flow line. The volume of the section of the stream tube with length dl is equal to $dv = Fdl$, therefore

$$\operatorname{div}[E \times B] = \frac{1}{F} \frac{d}{dl}([E \times B]_n F).$$

Substituting this expression into the equation of energy (24) and taking into account that $W = dl/dt$, we obtain

$$\rho_0 W F \frac{dl}{dt} = - \frac{Ac}{4\pi\mu_0} \frac{d}{dl}([E \times B]_n F).$$

Since the per-second weight rate of the fluid

$$\rho_0 W F = Q_{cr} = \text{const}$$

along the stream tube does not change, then after integration we have

$$\rho g W l_0 + \frac{Ac}{4\pi\mu_0} [E \times B]_l = \text{const.}$$

From here we obtain the effective value of total enthalpy

$$l_e = l_0 + \frac{Ac [E \times B]_l}{4\pi\mu_0 \rho W} = \text{const}$$

or

$$l_e = l + A \frac{W^2}{2g} + \frac{Ac [E \times B]_l}{4\pi\mu_0 \rho W}. \quad (143)$$

Thus the effective value of total enthalpy l_{0e} , which includes electromagnetic energy, remains constant along the stream tube if the flow of electromagnetic energy is directed along the velocity vector.

In the case $E = 0$ or with parallelism of the vectors of strengths of electric and magnetic fields ($E \parallel H$) equation (143) expresses the condition of constancy of total enthalpy for an energy isolated stream $l_0 = \text{const.}$ With the help of equations (55) and (65) it is possible to eliminate vector E from the equation of energy. In fact,

$$E = \frac{1}{c} (v_H \text{rot } B - [W \times B]),$$

from which

$$[E \times B] = \frac{1}{c} (v_H [\text{rot } B \times B] - [[W \times B] \times B]).$$

In a projection on the direction of the flow line we obtain

$$[E \times B]_l = \frac{1}{c} [v_H [\text{rot } B \times B]_l + u(B_l^2 - B_n^2)].$$

Here it is assumed that the x-axis is directed along the stream ($v = w = 0$). Substituting the latter expression in (143),

we obtain the equation of energy for a stream under the condition $E \perp W, B \perp W$

$$I_{\kappa} = I_0 + \frac{AB^2}{4\pi^2 \mu_0 g p} + \frac{A v_H}{4\pi^2 \mu_0 g p W} [\text{rot } B \times B]_x = \text{const.} \quad (144)$$

In view of the fact that in the cross section of the unit stream all the parameters are accepted as constant ($\frac{\partial}{\partial y} = \frac{\partial}{\partial z} = 0$), expression (144) can be simplified.

In fact, in this case ($v = w = B_x = B_z = E_x = E_y = 0$, i.e., $W = u, B = B_y, E = E_z$) the components of the rotor of magnetic induction

$$\begin{aligned} \text{rot}_x B &= \frac{\partial B_z}{\partial y} - \frac{\partial B_y}{\partial z} = 0, \\ \text{rot}_y B &= \frac{\partial B_x}{\partial z} - \frac{\partial B_z}{\partial x} = 0, \\ \text{rot}_z B &= \frac{\partial B_y}{\partial x} - \frac{\partial B_x}{\partial y} = \frac{dB}{dx} \end{aligned}$$

and the component of the vector product

$$[\text{rot } B \times B]_x = (\text{rot}_y B) B_z - (\text{rot}_z B) B_y = -B \frac{dB}{dx} = -\frac{1}{2} \frac{dB^2}{dx}. \quad (145)$$

Substituting this expression into (144), we come to the following form of the equation of energy for a stream which is located in perpendicular (lattice-type) electromagnetic fields

$$I_{\kappa} = I_0 + \frac{AB^2}{4\pi^2 \mu_0 g p} - \frac{A v_H B}{4\pi^2 \mu_0 g p W} \frac{dB}{dx} = \text{const.} \quad (146)$$

If the gas possesses very high conductivity ($\sigma_R \rightarrow \infty, v_H \rightarrow 0$), the last term in equation (146) can be disregarded, and then the conditions of the retention of effective total enthalpy for a stream in lattice-type fields will be written as:

$$I_{\kappa} = I_0 + \frac{AB^2}{4\pi^2 \mu_0 g p} = \text{const.} \quad (146a)$$

The equation of magnetic induction (84) as applied to the unit stream is also substantially simplified.

For transverse electromagnetic fields ($B_x = B_z = E_x = E_y = v = w = \frac{\partial}{\partial y} = \frac{\partial}{\partial z} = 0$, $W = u$, $B = B_y$, $E = E_z$, $j = j_z$) in the case in question in equation (55) only one component of current density is retained

$$j_z = \sigma_R \left(E_z + \frac{1}{c} u B_y \right);$$

from the Maxwell equation (68a) for a stationary field ($\frac{\partial B}{\partial t} = 0$) it follows that

$$E = E_z = \text{const.}$$

and from the Maxwell equation (65), as it was already shown, we have

$$j_z = \frac{c}{4\pi\mu_0} \text{rot}_z B = \frac{c}{4\pi\mu_0} \frac{dB_y}{dx}.$$

From here we obtain the equation of induction for a stream in transverse lattice-type fields

$$u B_y = \frac{c^2}{4\pi\mu_0 \sigma_R} \frac{dB_y}{dx} + \text{const.} \quad (147)$$

where

$$\text{const} = -c E_z.$$

If the conductivity of the gas is very great ($\sigma_R \rightarrow \infty$), then the equation of magnetic induction for a unit stream which is located in a transverse magnetic field acquires the very simple form

$$u B_y = \text{const.} \quad (147a)$$

In the case of an inviscid noncompressible fluid ($\nu = 0$, $\rho = \text{const}$) it is possible instead of (90) to obtain another form of the equation of energy for a unit stream. We utilize for this purpose the equation of motion (83), which in projection on the direction of the stream ($W = u$, $v = w = 0$) for a transverse magnetic field ($B = B_y$, $B_x = B_z = 0$) takes the following form:

$$\rho u \frac{\partial u}{\partial x} = - \frac{\partial}{\partial x} \left(p + \frac{B^2}{8\pi\mu_B} \right). \quad (148)$$

Integrating (148), we obtain

$$p_0 = p + \rho \frac{u^2}{2} + \frac{B^2}{8\pi\mu_B} = \text{const} \quad (149)$$

or

$$p_0 = p + \frac{B^2}{8\pi\mu_B} = \text{const}. \quad (149a)$$

Equation (149) is the Bernoulli equation for a stream of an incompressible electro-conductive fluid which is located in a transverse magnetic field. The third term of this equation is called *magnetic pressure* ($p_m = B^2/8\pi\mu_B$). During summation of p_m with total pressure p_0 an effective total pressure p_{0c} is obtained which retains in this case a constant value along the length of the stream.

During the action of a longitudinal magnetic field ($B = B_x$, $B_y = B_z = 0$) on the stream the integration of equation (82a) leads to a Bernoulli equation of the usual (hydraulic) form

$$p + \rho \frac{u^2}{2} = p_0 = \text{const},$$

since in this case

$$- \frac{\partial}{\partial x} \left(\frac{B^2}{8\pi\mu_B} \right) + \frac{1}{4\pi\mu_B} B_x \frac{\partial B_x}{\partial x} = 0.$$

Let us compose an equation of momentum for a stream which is located in electromagnetic fields. In Chapter I the general form of the equation of momentum of a unit stream was obtained which was valid for all cases of motion:

$$P_x = \frac{\rho}{\epsilon} (u_1 - u_2)$$

The account of the effect of the magnetic field lies in the fact that the projection of the resultant of all forces P_x we divide into two parts:

$$P_x = P_{xp} + P_{xm}$$

where P_{xp} - the projection of the resultant of all hydrodynamic forces; P_{xm} - the projection of the electromagnetic volume of the force applied in the section of stream 1-2.

The projection of the electromagnetic force applied to a unit of volume according to (72),

$$f_x = \frac{1}{c} [J \times B]_x = \frac{1}{4\pi c} [\text{rot } B \times B]_x$$

Projection on the x-axis of the force which acts on volume element comprises

$$dP_{xm} = f_x F dx$$

Here F is the cross-sectional area of the stream, dx is the length of its elementary section (in the direction of the vector of velocity u).

The projection of the electromagnetic force which acts on the section of stream 1-2,

$$P_{xm} = \int_1^2 \frac{F}{4\pi c} [\text{rot } B \times B]_x dx$$

In the case of a transverse magnetic field this integral can be converted with the help of (145)

$$P_{em} = -\frac{1}{8\pi\mu_0} \int r dB^2. \quad (150)$$

The electromagnetic force applied to the final section of the elementary stream of constant section for a transverse magnetic field is equal to

$$P_{em} = \frac{F}{8\pi\mu_0} (B_1^2 - B_2^2). \quad (150a)$$

The force of hydrodynamic pressure in this case comprises

$$F_{sp} = i(\varphi_1 - \varphi_2)$$

Thus the equation of momentum for an elementary stream of constant section for a transverse magnetic field takes the following form:

$$P_{sp} + P_{em} = -\frac{\partial}{\partial x} (u_1 - u_2).$$

From here according to the equation of continuity ($G/g = \rho uF = \text{const}$) we have

$$P_1 - P_2 + \frac{\rho^2}{8\pi\mu_0} (B_1^2 - B_2^2) = \rho u_1 (u_1 - u_2) = \rho u_2^2 - \rho u_1^2. \quad (151)$$

Inserting into equation (151) the effective pressure equal to the sum of the hydrodynamic and magnetic pressures

$$p_e = p + p_m = p + \frac{\mu_0 H^2}{8\pi}, \quad (152)$$

we reduce the equation of momentum for a unit stream of constant section for a transverse magnetic field to the following simplest form:

$$p_0 + \rho u^2 = p_{00} + \rho u_0^2 \quad (153)$$

Sometimes it is convenient to present the equation of momentum for a stream of constant section for a transverse magnetic field in the following form:

$$\rho + \frac{B^2}{2\pi\mu_0} + \rho u^2 = \text{const.} \quad (154)$$

The equation of momentum (154) unlike the Bernoulli equation (149) is useful not only for noncompressible fluids, but also for gases, i.e., for media of variable density.

§ 10. Magnetogasdynamic Shock Waves and Weak Disturbances

If in a space filled with a gas of infinite conductivity, a wave of magnetic induction ab appears (Fig. 13.15), then, as it will be shown further, the speed of its propagation is higher in those places where the value of magnetic induction B is greater.

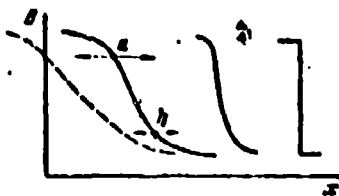


Fig. 13.15. The formation of a jump of condensation and smooth rarefaction wave (dotted line) in the field of magnetic induction.

Thus zone a at the "peak" of the wave is displaced more rapidly than zone b , located at the "foot" of the wave. This leads to the fact that in moving to the side of lesser field strength (to the right in Fig. 13.15), where this wave is propagated as a wave of condensation, it in the course of time acquires an ever steeper form, until it is converted into a jump of magnetic induction.

In the case of propagation to the side of greater field strength (to the left in Fig. 13.15) the wave ab is the wave of "rarefaction of magnetic field," whereupon as before the speed of its advance in zone a is greater than in zone b, which is why the rarefaction wave is gradually smoothed and weakened.

We will investigate the features of the condensation jump - the shock wave - of a magnetic field. In view of the complexity of the magnetogasdynamic wave theory we will be restricted to the simplest example - a normal magnetogasdynamic shock wave.

Let the front of the jump of magnetic induction B be arranged at right angles to the direction of gas flow (Fig. 13.16).

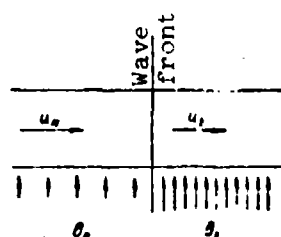


Fig. 13.16. Magnetogasdynamic normal shock wave.

Let us impart to the undisturbed flow of gas the speed u_H , equal in magnitude to the velocity of propagation of jump w_b , but opposite in sign:

$$u_H = -w_b$$

In this case the shock front will be fixed, and the flow of the undisturbed gas will accumulate on the plane of the front at a rate of u_H .

Let (Fig. 13.16) the magnetic displacement vector be perpendicular to the direction of flow $B = (0, B_y, 0)$, i.e., the wave front is a tangential rupture of the flow of magnetic induction. We will also consider that before and after the jump the values of

magnetic induction are constant ($B_H = \text{const}$, $B_1 = \text{const}$). Since the conductivity of the medium is infinite, then to the stream of the fluid the dependence (147a) found in § 8 is used:

$$u_H B_H = u_1 B_1 = \text{const.} \quad (155)$$

In other words, an intermittent increase in magnetic induction ($B_1 > B_H$) requires an intermittent decrease in the velocity of flow ($u_1 < u_H$).

In this case according to the equation of continuity a jump of gas density ($\rho_1 > \rho_H$) will also occur

$$\frac{\rho_1}{\rho_H} = \frac{u_H}{u_1} \quad (156)$$

and in accordance with the equation of momentum (151) the jump of effective pressure

$$p_{e1} - p_{eH} = \rho_H u_H (u_H - u_1) \quad (157)$$

Thus according to (155) and (156) induction in the jump should increase.

Thus the jump of magnetic induction in a gas flow, the secant of induction, will be necessarily combined with the shock wave, i.e., we are dealing with a magnetogasdynamic shock wave.

For the closing of the system of equations (155)-(157) let us add the condition of retention of effective total enthalpy (146a), which according to (155) and (156) we write in the form

$$t_e = 1 + \frac{A u^2}{2k} + \frac{A}{4\pi^2} \frac{u_H u_H}{\rho_H^2 B_H^2} = \text{const.} \quad (158)$$

and the equation of state

$$\frac{p_H}{\rho_H T_H} = \frac{p_1}{\rho_1 T_1} = \delta R. \quad (159)$$

Solving together the system of five equations (155)-(159), it is possible based on the assigned values of the velocity of propagation of a normal magnetogasdynamic wave ($w_B = -u_H$) and the variables of gas state and the magnetic field before the wave front (ρ_H, p_H, T_H, B_H) to find the values of the relative gas velocity (u_1) and the parameters of the gas and field (ρ_1, p_1, T_1, B_1) behind the wave front.

If the parameters of state of the undisturbed gas and the pressure increment in the jump are known, then it is not difficult to determine the velocity of propagation of a magnetogasdynamic wave.

From equations (157) and (156) we obtain

$$p_1 - p_H = u_H (\rho_1 - \rho_H) \frac{p_H}{p_1}, \quad (160)$$

from which it follows that the velocity of propagation of a shock magnetogasdynamic wave in a quiescent gas (w_B) or the velocity of flow equal to it in magnitude, which stops the counter wave (u_H), comprises

$$w_B = u_H = \frac{p_1 - p_H}{p_1 - p_H} \frac{p_1}{p_H}. \quad (160a)$$

From (160a) it also follows that

$$u_H u_1 = \frac{p_1 - p_H}{p_1 - p_H}. \quad (161)$$

Formulas (160a) and (161) differ from the corresponding formulas (5) and (10) of Chapter III for a usual shock wave only by the fact that in them the pressure (p) of the gas is replaced by effective pressure (p_c).

Let us present on the basis of (83) the effective pressure in the form of the sum of the hydrodynamic and magnetic pressures

$$p_e = p + p_m = p + \frac{B^2}{8\pi\mu_0}.$$

Then formulas (160a) and (161) take the form

$$w_1 = w_H = \frac{p_1 - p_H}{\rho_1 - \rho_H} \frac{\rho_1}{\rho_H} + \frac{B_1^2 - B_H^2}{8\pi\mu_0(\rho_1 - \rho_H)} \frac{\rho_1}{\rho_H}, \quad (162)$$

$$u_H w_1 = \frac{p_1 - p_H}{\rho_1 - \rho_H} + \frac{B_1^2 - B_H^2}{8\pi\mu_0(\rho_1 - \rho_H)}. \quad (163)$$

Magnetic induction behind the wave front is greater than in front of it ($B_1 > B_H$), therefore the magnetogasdynamic wave (162) is propagated more rapidly than the usual compression wave of the same intensity.

From the equations of magnetic induction (155) and continuity (156) we have

$$\frac{B_1}{\rho_1} = \frac{B_H}{\rho_H}. \quad (164)$$

Substituting this relation in (162), we come to the following expression for the velocity of a magnetogasdynamic shock wave:

$$w_1 = \frac{p_1 - p_H}{\rho_1 - \rho_H} \frac{\rho_1}{\rho_H} + \frac{B_H^2}{8\pi\mu_0\rho_H} \left(\frac{\rho_1}{\rho_H} + 1 \right) \frac{\rho_1}{\rho_H}. \quad (165)$$

In the extreme case of a very removable discontinuity ($p_1 \approx p_H$, $\rho_1 \approx \rho_H$, $B_1 \approx B_H$) we obtain the speed of its propagation in the direction perpendicular to the lines of magnetic field strength:

$$w_1 = c_1 = \frac{dp}{d\rho} + \frac{B^2}{4\pi\mu_0\rho} = k \frac{p}{\rho} + 2 \frac{p}{\rho}. \quad (166)$$

Here the first term of the right side is the square of the velocity of sound in a gas¹

$$a_0^2 = \frac{dP}{d\rho} = \frac{A}{\rho}, \quad (16'')$$

and the second term is the square of the velocity of propagation of Alfvén waves

$$b_H^2 = \frac{H_H^2}{4\pi\rho^2 H} = \frac{1}{2} \frac{A}{\rho}. \quad (16''')$$

The ratio of the velocity of the Alfvén wave to the sound velocity is equal to the Alfvén number introduced in [5] (see (14))

$$A = \frac{b_H}{a_0} = \frac{H_H}{\sqrt{4\pi\rho H}}. \quad (16'')$$

From (16')-(16'') we obtain

$$v = \frac{A}{\sqrt{2}} = \frac{1}{2} \sqrt{A^2}. \quad (17)$$

In magnetohydrodynamics it is proved that a weak Alfvén wave is propagated at a rate of b_H along the lines of force of the magnetic field ($b_H \parallel H$) in a gas of infinite conductivity ($\sigma_H = \infty$) and in a weak rotary wave (velocity component and magnetic induction, tangents to its plane, are turned without changing their value); the existence of such waves was discovered by Alfvén in 1942. In an Alfvén wave density and pressure do not change, and it has a finite velocity of propagation in a compressible liquid.

Thus the velocity of propagation of a weak magnetohydrodynamic wave (in infinite conductivity) is a direction perpendicular to the lines of force of induction, exceeding the speed of sound and comprises

¹Below it will be proved that in a gas of infinite conductivity an ideal adiabatic process is an isobaric process in which

$$c_{\perp} = \sqrt{a_H^2 + b_H^2}. \quad (171)$$

It is possible to show that along the lines of force of a magnetic field the weak magnetogasdynamic waves are propagated either at the speed of sound a_H or with an Alfven speed b_H .

From magnetogasdynamics it is known that in a general case the velocities of propagation of weak magnetogasdynamic waves, which are subdivided into rapid (c) and slow (c'), and also the velocity of propagation of Alfven wave (b) depend on angle θ between the selected direction and the magnetic induction vector B

$$\left. \begin{aligned} b &= b_H \cos \theta, \\ c &= b_H \sqrt{\frac{r+1 + \sqrt{(r+1)^2 - 4r \cos^2 \theta}}{2}}, \\ c' &= b_H \sqrt{\frac{r+1 - \sqrt{(r+1)^2 - 4r \cos^2 \theta}}{2}}. \end{aligned} \right\} \quad (172)$$

Here $r = a_H^2/b_H^2$.

In a particular case, when $\theta = 0$ (wave propagation along lines of force), we have

$$\begin{aligned} b &= b_H, & c &= c_1 = a_H, & c' &= c'_1 = b_H \quad (\text{with } r > 1), \\ b &= b_H, & c &= c_1 = b_H, & c' &= c'_1 = a_H \quad (\text{with } r < 1). \end{aligned}$$

In another special case $\theta = \pi/2$ (wave propagation in the direction of a normal to the lines of force) we have

$$b = 0, \quad c = c_{\perp} = \sqrt{a_H^2 + b_H^2}, \quad c' = c'_1 = 0 \quad (\text{with } r \geq 1).$$

Unlike the weak (acoustic) waves which are usual in gas dynamics, which are isotropic (they are propagated in all directions at the same velocity), magnetogasdynamic weak waves are anisotropic and, furthermore, are subdivided into rapid and slow.

Let us pass to the search for the basic relationships between the parameters of the gas and the field in a magnetogasdynamic shock wave.

From (155), (156), (168), and (169) we have

$$m = \frac{\rho_1}{\rho_H} = \frac{u_H}{u_1} = \frac{B_1}{B_H} = \frac{b_1^2}{b_H^2} = \frac{A_1^2}{A_H^2}. \quad (173)$$

If we designate the pressure ratio behind and before the shockwave front

$$n = \frac{p_1}{p_H}, \quad (174)$$

then the ratio of temperatures according to the equation of state can be presented in the form

$$\frac{T_1}{T_H} = \frac{n}{m}. \quad (175)$$

Utilizing known relationships $c_p - c_v = AR$, $c_p = kc_v$, expression (164) and the equation of continuity (156), we convert the equation of energy (146a) to the form

$$T = T_{0c} - \frac{k-1}{2kgR} u^2 - \frac{k-1}{kgR} \frac{B^2}{4\pi\mu_0}. \quad (176)$$

From the equation of state (159) and formula (176) we find the value of gas pressure

$$p = gRT_{0c} - \frac{k-1}{2k} \rho u^2 - \frac{k-1}{k} \frac{B^2}{4\pi\mu_0}. \quad (177)$$

From (177) we obtain the value of the pressure drop in the shock wave

$$p_1 - p_H = (p_1 - p_H) gRT_{0c} + \frac{k-1}{2k} u_H u_1 (\rho_1 - \rho_H) - \frac{k-1}{k} \frac{B_1^2 \rho_1^2 - \rho_H^2}{4\pi\mu_0 \rho_H^2}. \quad (178)$$

Here we take into consideration the constancy of the effective stagnation temperature ($T_{0c} = \text{idem}$) and the equalities following from the equation of induction (164) and the equation of continuity (156):

$$\left. \begin{aligned} \rho_H u_H - \rho_1 u_1 &= u_H u_1 (\epsilon_1 - \epsilon_H) \\ \rho_H u_H + \epsilon_1 u_1^2 &= u_H u_1 (\epsilon_1 + \epsilon_H) \\ B_1 - B_H &= B_H \frac{\epsilon_1 - \epsilon_H}{\epsilon_H} \\ B_1 + B_H &= B_H \frac{\epsilon_1 + \epsilon_H}{\epsilon_H} \end{aligned} \right\} \quad (179)$$

Substituting (163) and (173) into (178) and fulfilling the elementary conversions, we obtain the basic kinematic relationship for a natural magnetogasdynamic shock wave

$$u_H u_1 = \frac{2k}{k-1} gRT_{0c} + \frac{2-k}{k+1} \frac{B_H^2 (m+1)}{4\pi\mu_B \rho_H} \quad (180)$$

Here the first term of the right side is the square of the critical speed which corresponds to the effective stagnation temperature:

$$a_{sp,c} = \sqrt{\frac{2k}{k+1} gRT_{0c}} \quad (181)$$

In this case the distinction of (180) from kinematic relationship (15) of Chapter III for a usual shock wave amounts to the supplementary term which considers the influence of magnetic field.

Adding up the pressures before and behind the shock wave, we have from (177)

$$p_1 + p_H = (\epsilon_1 + \epsilon_H) gRT_{0c} - \frac{k-1}{2k} u_H u_1 (\rho_1 + \rho_H) - \frac{k-1}{k} \frac{B_H^2}{4\pi\mu_B} \frac{\epsilon_1 + \epsilon_H}{\rho_H}$$

Eliminating from here with the help of (163) the product of the velocities, we will obtain the basic dynamic relationship for a natural magnetogasdynamic shock wave

$$\frac{p_1 - p_H}{p_1 + p_H} = k \frac{p_1 + p_H}{p_1 + p_H} + \frac{B_1^2 (m-1)^2 (k-1)}{8\pi^2 p_H^2 (m+1)^2}, \quad (182)$$

which is distinguished from the similar relationship (17) of Chapter III (for a simple shock wave) by the additional ("magnetic") term in the right side.

In the particular case of removable discontinuity ($p_1 = p_H$, $\rho_1 = \rho_H$, $m = 1$) from (182) we have

$$\frac{dp}{d\rho} = k \frac{p}{\rho}, \text{ i.e., } \frac{p}{\rho} = \text{const.}$$

which proves the constancy of entropy in a weak magnetogasdynamic wave. After dividing all the terms of equation (182) by the value p_H/ρ_H and solving it relative to value p_1/ρ_H , we come to the equation of the shock magnetogasdynamic adiabatic curve

$$n = \frac{0m - 1 + q(m-1)^2}{0 - m}. \quad (183)$$

Here we accept the designations

$$m = \frac{p_1}{p_H}, \quad n = \frac{\rho_1}{\rho_H}, \quad q = \frac{B_1^2}{p_H}, \\ 0 = \frac{k+1}{k-1}.$$

In the absence of a magnetic field ($q = 0$) equation (183) coincides with equation (18) of Chapter III for a usual shock adiabatic curve. In the case of a very strong shock wave ($p_1 \rightarrow \infty$) we obtain from (183) the same extreme value of density

$$(\rho_1)_{\max} = \frac{k+1}{k-1} \rho_H,$$

as in a simple shock wave (see expression (19) of Chapter III). When $\rho_1 \rightarrow \rho_H$ we have $p_1 \rightarrow p_H$.

The degree of deviation of the magnetogasdynamic shock adiabetic curve from a simple shock adiabetic curve is shown in Fig. 13.17, where are plotted the curves $m(n)$ with the different values of relative magnetic pressure q for $k = 1.67$ (monatomic gas).

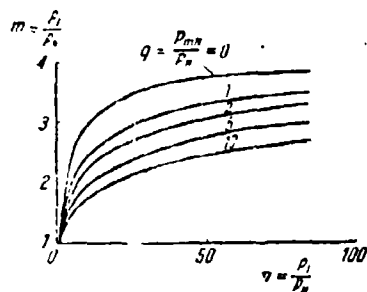


Fig. 13.17. The shock adiabetic curves of a magnetogasdynamic wave with the different values of the magnetic pressure parameter ($k = 5/3$).

With the help of (162) and (183) it is possible to express the Mach number which corresponds to the velocity of propagation of a magnetodynamic wave by the density ratios on its front

$$M_H = \frac{m \theta + 1 + q(\theta + 1)(m + 1) - 4m}{\theta - m}. \quad (184)$$

Dependences $M_H(m)$, calculated from formula (184) with $\theta = 4$ ($k = 1.67$), are plotted in Fig. 13.18.

It remains to determine the Mach number in a gas flow behind a magnetogasdynamic wave, for which we utilize expressions (156) and (175)

$$M_1 = \frac{u_1}{a_1} = \frac{u_1}{a_1} \frac{\rho_1}{\rho_1} \frac{T_1}{T_1} = \frac{M_H}{m}. \quad (185)$$

Curves $M_1(m)$ at different values of the parameter of magnetic pressure q are given in Fig. 13.19.

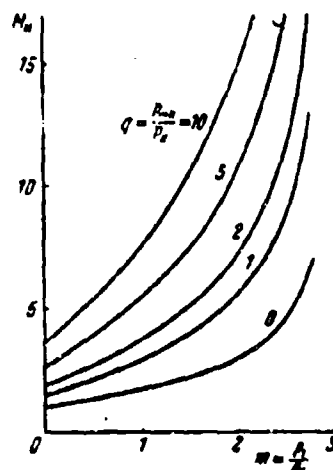


Fig. 13.18. The dependence of the velocity of a magnetogasdynamic shock wave on the compression ratio of gas with different values of the magnetic pressure parameter ($k = 5/3$).

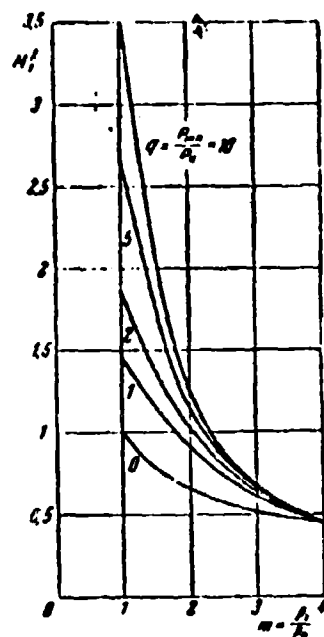


Fig. 13.19. The dependence of the velocity behind a magnetogasdynamic shock wave on the compression ratio of the gas with different values of the magnetic pressure parameter ($k = 5/3$).

With the degeneration of the magnetogasdynamic shock wave into a removable discontinuity ($m \rightarrow 1$, $n \rightarrow 1$) the speed of its propagation, as it was established above, proves to be greater than

the speed of sound; in this extreme case from (184) and (185) we obtain

$$M_{1n} = \frac{1}{k} \left(\frac{0+1}{0-1} + 2q \right) = 1 + \frac{2q}{k}, \quad M_{1n} = M_{1n}$$

In another limiting case - an infinitely strong magnetogas-dynamic wave ($m \rightarrow 0$, $n \rightarrow \infty$) - we have from (184), (185), and (183)

$$M_{1m} \rightarrow \infty, \quad M_{1m} \rightarrow \frac{k-1}{2k}.$$

§ 11. The Condition of Inversion of Effect During Gas Flow in an Electromagnetic Field

Let us examine a stationary one-dimensional flow ($W(x) = (u, 0, 0)$) of an inviscid and nonheat-conducting gas of finite conductivity in transverse lattice-type magnetic and electric fields.

Assuming that it is possible to disregard the induced magnetic field, let us assign the distribution of the cross-section averages of the values of electrical strength and magnetic induction along the length of a variable-area channel $E(x) = (0, E_y, 0)$, $B(x) = (0, 0, B_z)$. This makes it possible to solve the problem without drawing in the Maxwell equations.

Having differentiated the equation of flow rate

$$\rho u F = \text{const} = \frac{Q}{k}$$

in the direction of motion, we will obtain

$$\frac{1}{\rho} \frac{d\rho}{dx} + \frac{1}{u} \frac{du}{dx} + \frac{1}{F} \frac{dF}{dx} = 0. \quad (186)$$

Analogously from the equation of state for an ideal gas we have

$$\frac{dp}{dx} = GR \rho \frac{dT}{dx} + \frac{u^2}{h} \frac{d\rho}{dx}. \quad (187)$$

The equation of motion (82) for the one-dimensional flow of an inviscid and nonheat-conducting gas for transverse electromagnetic fields can be reduced to the form

$$\rho u \frac{du}{dx} + \frac{dp}{dx} = \sigma_R \left[E - \frac{uB}{c} \right] \frac{B}{c}. \quad (188)$$

The equation of energy of such a one-dimensional flow we obtain from (90) and (87)

$$\frac{1}{A} GR \rho \frac{dT}{dx} = \sigma_R \left[E - \frac{uB}{c} \right] E. \quad (189)$$

Taking into account that $1_0/A = 1/A + u^2/2g$, $AR = c_p - c_v$ and $c_p = kc_v$, the equation of energy (189) with $c_p = \text{const}$ takes the following form:

$$\frac{h}{k-1} GR \rho u \frac{dT}{dx} + \rho u \frac{du}{dx} = \sigma_R E \left[E - \frac{uB}{c} \right]. \quad (189a)$$

In these equations all parameters depend only on x , whereupon the velocity $u(x)$ is directed along the axis x , and the strengths of the magnetic and electric fields are perpendicular to each other and to the direction of motion $B_z = B(x)$, $E_y = E(x)$; we will consider the functions B_z and E_y , and also function $F(x)$, which describes a change in the cross-sectional area of channel, as assigned.

The system of equations (186)-(189) in general cannot be solved in an explicit form, but with its aid it is possible to determine how velocity derivatives and the Mach numbers depend on the basic parameters of the problem.

Eliminating from (187) and (189a) the gradient of temperature, we obtain

$$\frac{k}{k-1} \left(\frac{dp}{dx} - \frac{a^2}{k} \frac{dp}{dx} \right) + \rho u \frac{du}{dx} = \frac{e_R E}{u} \left[E - \frac{uB}{c} \right]. \quad (190)$$

Eliminating from (188) and (190) the pressure gradient, we have

$$-\frac{1}{k-1} \rho u \frac{du}{dx} = \frac{e_R}{u} \left[E - \frac{k}{k-1} \frac{B}{c} \right] \left[E - \frac{uB}{c} \right] + \frac{a^2}{k-1} \frac{dp}{dx}.$$

Substituting in this expression the gradient of density with the help of (186), we arrive at the expression

$$(M^2 - 1) \frac{1}{u} \frac{du}{dx} = \frac{1}{F} \frac{dF}{dx} - \frac{k}{\rho a^2} \frac{e_R B^2}{u c^2} \left(\frac{Ec}{B} - u \right) \left(\frac{Ec}{B} \frac{k-1}{k} - u \right), \quad (191)$$

which shows how the change in the cross-sectional area and the factor which reflects the nature of electromagnetic field (second term of the right side) influence the velocity change along the length of the channel.

If an electromagnetic field is absent, then equation (191) converts to the known relationship for a Laval nozzle (Chapter IV, (1)). If we add into the initial equations the terms which characterize the change in the gas flow rate, the work of friction, technical work, and heat supply from without, then by means of elementary conversions it is possible to convert equation (191) into a condition of inversion of the effect of an even more general form than condition (49) of Chapter V:

$$(M^2 - 1) \frac{1}{u} \frac{du}{dx} = \frac{1}{P} \frac{dP}{dx} - \frac{1}{Q} \frac{dQ}{dx} - \frac{R}{a^2} \frac{dL}{dx} - \frac{k-1}{A} \frac{R}{a^2} \frac{dQ_{\text{heat}}}{dx} - \frac{kR}{a^2} \frac{dL_{\text{fr}}}{dx} - \frac{k}{\rho a^2} \frac{e_R B^2}{u c^2} \left(\frac{Ec}{B} - u \right) \left(\frac{Ec}{B} \frac{k-1}{k} - u \right). \quad (192)$$

The term which considers the electromagnetic influence in equation (192) differs from all remaining terms of this expression by the fact that into it enter the values of the acting parameters, but not their derivatives, and, furthermore, its value depends on

the absolute values of velocity and pressure of the gas, and the sign is determined by the product of two differences, one of which is the difference between the gas velocity u and the drift velocity $W_d = Ec/B$, and the other - the difference between the gas velocity and a certain velocity $U_1 = \frac{Ec}{B} \frac{k-1}{k} = W_d \frac{k-1}{k}$.

Thus if we reject all effects except electromagnetic, i.e., if we examine the one-dimensional motion of an ideal gas in a heat-insulated channel of constant section in the presence of lattice-type electromagnetic fields, then the condition of inversion of effect for a velocity derivative will be written as

$$(M^2 - 1) \frac{du}{dx} = - \frac{\sigma_R B^2}{\rho c^2} \frac{k}{k-1} (u - U_1)(u - W_d) = - \frac{\sigma_R B^2}{\rho c^2} (u - U_1)(u - W_d) \quad (193)$$

Let us recall that during the flow of gas at a drift velocity (see § 5) the induced electric field is equal and oppositely superimposed, as a result of which the current does not go through the gas and there is no magnetohydrodynamic effect. As we see, with an invariable value of electromagnetic effect the sign of the velocity derivative changes to opposite upon transition from subsonic flow ($M < 1$) to supersonic ($M > 1$) and vice versa.

In the same way as in (193), it is possible to derive the condition of inversion of effect for the derived Mach number along the length of the channel. In the case $dF/dx \neq 0$ we have an expression similar to (191)

$$(M^2 - 1) \frac{1}{M \left(1 + \frac{k-1}{2} M^2\right)} \frac{dM}{dx} = \frac{1}{F} \frac{dF}{dx} - \frac{k}{\rho c^2} \frac{\sigma_R B^2}{k-1} \left(\frac{Ec}{B} - u \right) \left(\frac{Ec}{B} \frac{1 + kM^2}{k-1} - u \right). \quad (194)$$

For a channel of constant section ($dF/dx = 0$) we obtain

$$(M^2 - 1) \frac{1}{1 + \frac{k-1}{2} M^2} \frac{dM}{dx} = - \frac{k}{\rho c^2} \frac{\sigma_R B^2}{k-1} (u - W_d)(u - U_1) = - \frac{\sigma_R B^2}{\rho c^2} (u - W_d)(u - U_1). \quad (195)$$

where

$$U_1 = U_1 \frac{1 + \lambda M^2}{2 + (\lambda - 1) M^2} = W_A \frac{1 + \lambda M^2}{\lambda - 1 + \lambda M^2} \cdot \frac{1}{2}$$

Thus in the expression for dM/dx new characteristic velocity U_2 appears, the value of which depends on the Mach number.

With the help of (194) and (195) in Fig. 13.20 a diagram is constructed for possible systems of a one-dimensional gas flow in lattice-type electrical and magnetic fields. Along the axis of ordinates are plotted the values of velocity, and along the axis of abscissae - the Mach numbers.

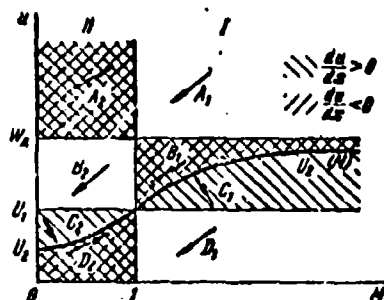


Fig. 13.20. The possible systems of one-dimensional flow in lattice-type electromagnetic fields.

Straight lines $u = U_1$, $u = W_A$, $M = 1$ and curve $U_2(M)$ separate the plane $(u; M)$ into areas

I. $M > 1$	II. $M < 1$
$A_1: W_A < u$	$A_2: W_A < u$
$B_1: U_1 < u < W_A$	$B_2: U_1 < u < W_A$
$C_1: U_1 < u < U_2$	$C_2: U_1 < u < U_2$
$D_1: u < U_1$	$D_2: u < U_1$

Let u and M be known in a certain cross section x . Then during displacement along the x -axis these parameters change so that in areas A_1 , B_2 and D_1 there is a displacement to the left

downwards, in areas A_2 , B, D_2 - to the right upward as indicated by the arrows, and in areas C_1 and C_2 - to the left upward.

From equation (194) it is clear that on lines $u = W_d$ and $u = U_1$ a smooth transfer is feasible through value $M = 1$ in the first point of the side of an increase of M , and in the second - a decrease.

In areas C_1 and C_2 there is acceleration of flow with a decrease in the Mach number; here the speed of sound grows more rapidly than the flow velocity.

The results obtained are easy to explain, if we recall that the effect of an electromagnetic field on a gas flow is reduced to the mechanical work of the electromagnetic force applied to a unit of volume,¹

$$-F \cdot W = -\frac{1}{c} W \cdot (J \times B)$$

and to the liberation of Joule heat taking into account of which the full input energy per unit volume

$$Q_H = E \cdot J.$$

In the one-dimensional case in question the relation of mechanical work to total energy

$$\Pi = \frac{\rho_R \left[\mu - \frac{uB}{c} \right] \frac{uB}{c}}{\rho_R \left[\mu - \frac{uB}{c} \right] \frac{u}{c}} = \frac{u}{W_s}. \quad (196)$$

The minus sign means that with $F > 0$ energy is imparted to the gas; above we always considered the work being accomplished by gas as positive.

If $u > W_A$, then the mechanical work of electromagnetic force exceeds the change in the total reserve of energy of the gas, i.e., mechanical energy partially converts to the energy of an electromagnetic field in the form of current, which can accomplish work in the external circuit of an MHD generator. If $u < W_A$, then the energy of the electromagnetic field is transferred to the gas in the form of mechanical work or heat (pump or accelerator).

In the first case the electromagnetic force is directed against the flow of the gas, and in the second - along the flow. In the second case with Π close to unity the effect of the field is expressed basically in the form of the work of electromagnetic forces, and with Π close to zero - basically in the form of heat supply.

With $u = U_1$, i.e., $\Pi = U_1/W_A$, the thermal and mechanical actions of the electromagnetic field are compensated for, as a result of which the gas velocity does not change ($du/dx = 0$), with $u = W_A$ both effects are equal to zero,¹ due to which also $du/dx = 0$. The feature of line $u = U_2$ lies in the fact that at the points of intersection with it of curves $u(M)$ the change in the value of the speed of sound is proportional to the change in the value of the gas velocity, by virtue of which the derivative of the Mach number along the length of the channel with $u = U_2$ is always equal to zero. Transfer through line $u = U_2$ is feasible on the diagram of Fig. 13.20 only vertically (with $M = \text{const}$).

§ 12. The Simplest Solutions of the Equations of a One-Dimensional Gas Flow in Lattice-Type Fields

The simplest solutions of the equation of one-dimensional flow of an ideal gas in lattice-type electrical and magnetic fields is

¹Such a system is obtained in the absence of Joule heat, but this is possible only in the absence of electric current and, consequently, also electromagnetic force.

obtained for a channel of constant width with $\tau = \text{const}$ and $E = \text{const}$; the last two conditions can be realized only at the low values of magnetic Reynolds number ($R_M \ll 1$), when the fields induced in the flow of gas are considerably weaker than superimposed fields.¹

After dividing equation (13) by equation (14) similarly, we find

$$\frac{d^2 u}{dx^2} = \frac{1}{1 + \frac{1}{2} \frac{M^2}{M^2}} \frac{d^2 u}{dx^2} \quad (137)$$

With $B = \text{const}$ and $E = \text{const}$ we have $\tau = \text{const}$ and $U_1 = \text{const}$; besides that in accordance with the definition specified in (135) we have

$$2 \frac{d^2 u}{dx^2} = \frac{1 + \frac{1}{2} \frac{M^2}{M^2}}{1 + \frac{1}{2} \frac{M^2}{M^2}} \frac{d^2 u}{dx^2} + \frac{\frac{1}{2} \frac{M^2}{M^2}}{1 + \frac{1}{2} \frac{M^2}{M^2}} \frac{d^2 u}{dx^2}$$

Substituting this expression in (137), we reduce the latter to the form

$$2 \left(\frac{u}{U_1} - 1 \right) \left(\frac{1}{M^2} + \frac{1}{2} \frac{M^2}{M^2} \right) \frac{d^2 u}{dx^2} - \frac{u}{U_1} \left(\frac{u}{U_1} - 1 \right) \frac{d^2 u}{dx^2} = \frac{1}{2} \frac{d^2 u}{dx^2} \quad (138)$$

It is not difficult to show that the left side of (138) is a differential of the product, therefore

$$d \left[\frac{u}{U_1} \left(\frac{u}{U_1} - 1 \right) \left(\frac{1}{M^2} + \frac{1}{2} \frac{M^2}{M^2} \right) \right] = \frac{1}{2} \frac{d^2 u}{dx^2} \frac{u}{U_1}$$

from which

$$\frac{1}{M^2} + \frac{1}{2} \frac{M^2}{M^2} = \frac{1}{2} \frac{d^2 u}{dx^2} \frac{u}{U_1} + \text{const} \quad (139)$$

¹Resler E. L., Zhurav V. K. *Mathematical models of gas flow*, translations and review of foreign literature, Vol. 1, No. 1, 1964.

The integration constant is selected according to some initial condition. For example, we accept $u = U_1$ with $M = 1$, then we will obtain $\text{const} = \dots$ we have

$$\frac{u}{U_1} = \frac{\frac{k+1}{2} M^2}{1 + \frac{k-1}{2} M^2} \quad \text{or} \quad M^2 - 1 = \frac{\frac{u}{U_1} - 1}{1 - \frac{k-1}{k+1} \frac{u}{U_1}}. \quad (200)$$

Now let us find the velocity change along the length of the channel. For this let us make use of the equation of continuity of flow

$$\rho u = \frac{Q}{gF} = \text{const} = m.$$

Substituting the value ρu in (193), we find

$$(M^2 - 1) \frac{du}{dx} = - \frac{\sigma_R B^2 h}{mc^2} \frac{KM^2}{u} (u - U_1)(u - W_1)$$

This expression with the help of (200) is reduced to the following form:

$$\frac{d \frac{u}{W_1}}{d \bar{x}} = \frac{2k}{k+1} \frac{\sigma_R B^2 h}{mc^2} \left(1 - \frac{u}{W_1}\right) = \frac{2k}{k+1} S_0 \left(1 - \frac{u}{W_1}\right). \quad (201)$$

where $\bar{x} = x/h$, h - the height of the channel, calculated along the normal to x , and $S_0 = \sigma_R B^2 h / mc^2$ - the parameter of magnetohydrodynamic interaction determined by relationship (97).

Integrating (201), we obtain the law of velocity change along the length of the channel

$$a = \frac{u}{W_1} = 1 - \frac{1}{k} e^{-\frac{\sigma_R B^2 h}{mc^2} \frac{2k}{k+1} \bar{x}} = 1 - \frac{1}{k} e^{-S_1 \bar{x}}, \quad (202)$$

where

$$S_1 = \frac{2k}{k+1} S_0.$$

As we see, $\bar{u} = 0$ is obtained with $x = -\ln k/S_1$, $\bar{u} = -1$ with $\bar{x} = -\infty$. For determining integration constant the length is counted off from the critical cross section, i.e., it is accepted that $x = 0$ with $M = 1$, where according to the condition $u = U_1 = W_1 \frac{k-1}{k}$.

Density change along the length of channel is found from the equation of continuity and dependence (202)

$$\frac{1}{\rho} = \frac{\rho_1}{\rho} = \frac{u}{u_1} = \frac{k}{k-1} \frac{u}{W_1} = \frac{k}{k-1} \left(1 - \frac{1}{k} e^{-S_1 \bar{x}}\right). \quad (203)$$

Here ρ_1 is gas density in the critical cross section of the channel.

The pressure gradient along the channel we find with the help of the equation of motion (188) and expressions (201) and (202)

$$\frac{dp}{d\bar{x}} = \frac{\gamma R B^2}{c^2} (W_1^2 - u) - m \frac{du}{d\bar{x}} = -\frac{k-1}{2k} m \frac{du}{d\bar{x}} = -\frac{U_1^2 R B^2}{c^2 (k+1)} e^{-S_1 \bar{x}}. \quad (204)$$

Integrating (204) we have

$$p = \frac{\rho_1 U_1^2}{2k} e^{-S_1 \bar{x}} + \text{const.}$$

In the critical cross section ($M = 1$, $u = a = U_1$, $\rho = \rho_1$, $p = p_1$), i.e., with $x = 0$,

$$p_1 = \frac{\rho_1 U_1^2}{2k} + \text{const.}$$

But, on the other hand, from the formula for the speed of sound follows

$$\rho_1 = \frac{\rho_1 U_1^2}{k} = \frac{\rho_1 a^2}{k},$$

therefore

$$\text{const} = \frac{\rho_1 U_1^2}{2k}.$$

Thus, the pressure change along the length of the channel

$$p = \frac{p_1}{\rho_1} = \frac{1}{2}(1 + e^{-2\bar{x}}) \quad (205)$$

With $\bar{u} = 0$ ($\bar{x} = -\ln k/S_1$) we have $\bar{p} = 1.2$, with $\bar{u} = 1$ ($\bar{x} = -\infty$) $\bar{p} = 0.5$.

Now with the help of (204) and (205) it is not difficult to find the temperature change along the channel, since from the equation of state

$$\bar{T} = \frac{T}{T_1} = \frac{p}{p_1} \frac{\rho_1}{\rho} \quad (206)$$

The electric current density in an arbitrary cross section of the channel

$$J = \sigma_R \left(E - \frac{uB}{c} \right) = \sigma_R E \left(1 - \frac{u}{W_A} \right) = \frac{\sigma_R E}{h} e^{-\bar{x}}.$$

Hence for the current density in the critical cross section ($x = 0$) we have

$$J_1 = \frac{\sigma_R E}{h}.$$

The dimensionless value of the current density

$$J = \frac{J}{J_1} = e^{-\bar{x}}. \quad (207)$$

The results of the calculation according to formulas (164) to (207) do not depend on the unit system, since the value $S = \sigma_p B^2 h / mc^2$ is dimensionless. The curves which show the value change of u , ρ , p , T depending on the dimensionless length $\bar{x} = x/h$, expressed in fractions of the height of the channel h , are given in Fig. 13.21; during the calculation of these dependences the following values of parameters were utilized

$$\sigma_R = 1 \text{ mho/cm} = c^2/10^9 \text{ CGSE unit}; k = 1.4; c = 3 \cdot 10^{10} \text{ cm/s};$$

$$T_1 = 2000^\circ\text{K}; p_1 = 1 \text{ atm(abs.)}; B_1 = 10^4 \text{ G}.$$

To these values correspond the values

$$\rho_1 = 1.67 \cdot 10^{-4} \text{ g/cm}^2; U_1 = a_1 = 9.4 \cdot 10^4 \text{ cm/s}; W_d = 32.1 \cdot 10^4 \text{ cm/s};$$

$$E = U_1 B/c = 0.032 \text{ CGSE unit}; j_1 = 0.206 \cdot 10^{11} \text{ CGSE unit} = 2.23 \text{ A/m}^2.$$

At channel height $h = 10 \text{ cm}$ the potential difference on its walls comprises $\Delta V = Eh = 94 \text{ volts}$, and the universal exponent

$$S_1 = \frac{\sigma_R B_1^2 h}{p_1 c^2 k + 1} = 0.075.$$

Figure 13.21 also gives the curves of the change along the length of the channel of the Mach number (with $k = 1.4$)

$$M = \frac{u}{a} = \frac{u}{a_1} \frac{a_1}{a} = \frac{k}{k-1} \frac{u}{W_d} \frac{1}{\gamma} = 3.5 \frac{a}{\gamma T} \quad (208)$$

and the relative value of total pressure

$$p = \frac{p_0}{p_{01}} = \frac{p_0}{p} \frac{p}{p_1} \frac{p_1}{p_{01}} = 0.528 (1 + 0.2 M^2)^{-3.5} p. \quad (209)$$

It goes without saying that the calculation carried out bears a conditional nature, since not all the conditions accepted during the solution of formula (202)-(209) can be realized in practice. Specifically the conductivity of the gas σ_R depends substantially on the temperature, which changes along the length of the channel. With variable values of the basic parameters it is possible to conduct the calculation by the numerical or graphic methods directly based on the differential equations (201) and (204) and the corresponding relationships for gas density, temperature, and electric current density.

Another form of a one-dimensional gas flow in lattice-type electromagnetic fields is obtained at a constant temperature, but

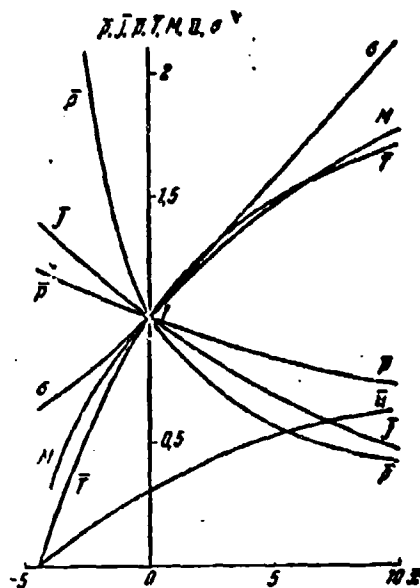


Fig. 13.21. Change of the basic parameters along the length of a flat channel of constant section with $E = E_y = \text{const}$; $B = B_z = \text{const}$; $\delta = \text{const}$; $k = 1.4$; $S_1 = \frac{\sigma_R B^2 h}{\rho_1 U_1^2 k + 1} = 0.075$.

a variable cross section of the channel. In this case the derivation of calculation formulas is based on the following initial equations:

the equation of continuity

$$\rho u F = \text{const} = \frac{Q}{g};$$

the equation of state

$$p = g R \rho T;$$

the equation of motion (188)

$$\rho u \frac{du}{dx} + \frac{dp}{dx} = \frac{1}{\epsilon} / B = \sigma_R \left[E - \frac{uB}{\epsilon} \right] \frac{B}{\epsilon};$$

the equation of energy (189a) which with $T = \text{const}$ takes the form

$$\mu u^2 \frac{du}{dx} = jE = \sigma_R E \left[E - \frac{uB}{c} \right]. \quad (210)$$

Substituting (210) into the equation of motion (188), we will obtain

$$u \frac{dp}{dx} = - \frac{j}{\sigma_R}. \quad (211)$$

Eliminating from (210) the density, we have

$$\frac{p}{gRT} u^2 \frac{du}{dx} = jE,$$

from which

$$p = gRTE \frac{j}{u^2 u'} = gRTE \xi, \quad (212)$$

where

$$u' = \frac{du}{dx}, \quad \xi = \frac{j}{u^2 u'}, \quad \xi' = \frac{d\xi}{dx}.$$

Hence during a constant strength of electric current ($E = \text{const}$) $dp/du = gRTE\xi'$. Substituting this expression in (211), we obtain $gRTE\xi' = -j^2/\sigma_R u = -\frac{j^2}{u^2 u'} \frac{u' u''}{\sigma_R}$ and therefore, $\sigma_R gRTE \xi' = -u''(u')^2$.

Integrating from $x = 0$ ($\xi = \xi_0$) up to the current value x , we have

$$\sigma_R gRTE \left(\frac{1}{\xi} - \frac{1}{\xi_0} \right) = \int_0^x u''(u')^2 dx. \quad (213)$$

Let us assign the exponential velocity distribution along the length of channel (with $E = \text{const}$ and $B = B(x)$)

$$u = bx^a, \quad u' = bax^{a-1}. \quad (214)$$

Substituting (214) in (213) after integration (with $n > 1/5$), we will obtain

$$\frac{1}{\xi} = \frac{b^5 n^5}{\epsilon_R g R T E} \frac{x^{5n-1}}{5n-1}. \quad (215)$$

Here it is taken into consideration that with $x = 0$, $u = 0$, $u' = 0$, i.e., with $j \neq 0$, $1/\xi_0 = 0$.

In the case $n = 1/5$ integral (213) gives a logarithmic function, which changes the form of all the calculation formulas. In the example in question the electric current density in the channel

$$j = en^5 u' = \frac{\epsilon_R g R T E}{b^5 n} \frac{5n-1}{x^{2n}} \quad (216)$$

and the magnetic field strength

$$B = \frac{E}{b x^n} \left[1 - \frac{g R T (5n-1)}{b^5 n x^{5n}} \right]. \quad (217)$$

The pressure we find from (212) and (215)

$$p = \frac{\epsilon_R (g R T E)^2}{b^5 n^2} \frac{5n-1}{x^{5n-1}}. \quad (218)$$

The cross-sectional area of the channel is found from the equation of continuity

$$F = \frac{Q b^5 n^5}{\epsilon_R g R T (g R T E)^2} \frac{x^{5n-1}}{5n-1}. \quad (219)$$

The Mach number according to (214) comprises

$$M = \frac{u}{a} = \frac{b x^n}{\sqrt{g R T E}}. \quad (220)$$

In the critical cross section ($x = x_1$) $M = 1$, therefore

$$b = \frac{\sqrt{g R T E}}{x_1^n}. \quad (221)$$

Substituting the value b into the formulas obtained, we finally have

$$\left. \begin{aligned} M &= \left(\frac{x}{x_1}\right)^n, \\ u &= \sqrt{k_g R T} \left(\frac{x}{x_1}\right)^n, \\ j &= \frac{a_R E^2 (5n-1)}{kn} \left(\frac{x}{x_1}\right)^{2n}, \\ B &= \frac{E}{\sqrt{k_g R T}} \left[\left(\frac{x}{x_1}\right)^n - \frac{5n-1}{kn} \left(\frac{x}{x_1}\right)^{2n} \right], \\ p &= \frac{a_R E^2 (5n-1) x_1}{n^2 k^2 \sqrt{k_g R T}} \left(\frac{x}{x_1}\right)^{5n-1}, \\ F &= \frac{G k^2 n^2}{a_R E^2 x_1} \frac{RT}{5n-1} \left(\frac{x}{x_1}\right)^{4n-1}. \end{aligned} \right\} \quad (222)$$

In the critical cross section ($x = x_1$):

$$\left. \begin{aligned} M_1 &= 1, \quad j_1 = \frac{a_R E^2 (5n-1)}{kn}, \\ u_1 &= \sqrt{k_g R T}, \\ B_1 &= \frac{E}{\sqrt{k_g R T}} \left[1 - \frac{5n-1}{kn} \right], \\ p_1 &= \frac{a_R E^2 x_1 (5n-1)}{n^2 k^2 \sqrt{k_g R T}}, \\ F_1 &= \frac{G k^2 n^2}{a_R E^2 x_1} \frac{RT}{5n-1}. \end{aligned} \right\} \quad (223)$$

The value of the abscissa of the critical cross section can be found from the rated value of pressure p in the critical cross section. In a dimensionless form the basic calculation formulas appear thus:

$$\left. \begin{aligned} M &= \left(\frac{x}{x_1}\right)^n = x^n, \\ j &= \frac{j}{j_1} = \frac{1}{M^2}, \\ B &= \frac{B}{B_1} = \frac{1 + knM - 5n}{M^2(1 + kn - 5n)}, \\ p &= \frac{p}{p_1} = \frac{p}{p_1} = \frac{1}{M^{5n-1}}, \\ F &= \frac{F}{F_1} = M^{4n-1}. \end{aligned} \right\} \quad (224)$$

From (224) it follows that with $n = 1/4$ the channel has a constant section.

Figure 13.22 depicts the curves $M(\bar{x})$, $j(\bar{x})$, $\bar{B}(\bar{x})$, $\bar{p}(\bar{x})$ and $\bar{F}(\bar{x})$ for the isothermal channel flow in question with $n = 1/6$ and $k = 1.4$. The curve of the change in the total pressure along the length of the channel was calculated according to formula (209) into which were substituted the values \bar{p} , found with the help of (224). Under the selected law of velocity change along the length of the channel ($n = 1/6$) the cross sectional area of the channel does not change very strongly. At large values n all parameters will change more noticeably.

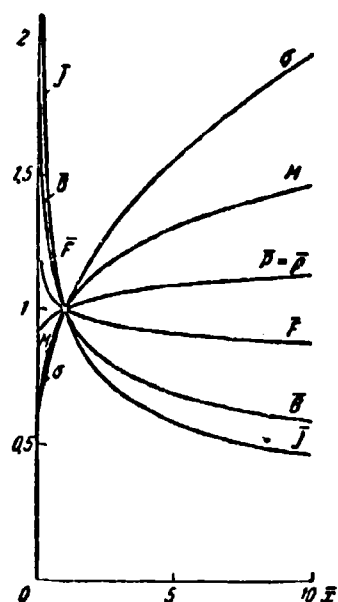


Fig. 13.22. Change in the parameters along the length of a channel with $E = E_y = \text{const}$; $\sigma_R = \text{const}$; $k = 1.4$; $T = \text{const}$; $n = 1/6$.

APPENDICES

Appendix I.

Table for calculating the supersonic gas flows
with a continuous increase in velocity
($k = 1.4$).

α	β	M	γ	P/P_0	ρ/ρ_0	T/T_0	α	ρ/ρ_0
0°00'	0°00'	1,000	1,000	0,528	0,634	0,833	0°00'	1
0°10'	13°08'	1,026	1,022	0,512	0,620	0,826	77°02'	1,027
0°20'	16°03'	1,039	1,032	0,504	0,613	0,822	74°15'	1,041
0°30'	18°24'	1,051	1,042	0,497	0,607	0,819	72°06'	1,051
0°40'	20°25'	1,062	1,051	0,490	0,601	0,816	70°15'	1,065
0°50'	22°06'	1,073	1,060	0,484	0,596	0,813	68°44'	1,077
1°00'	23°32'	1,083	1,067	0,479	0,591	0,810	67°28'	1,087
1°30'	27°06'	1,109	1,088	0,463	0,577	0,803	64°24'	1,108
2°00'	30°00'	1,133	1,107	0,450	0,565	0,796	62°00'	1,147
2°30'	32°33'	1,155	1,125	0,444	0,553	0,789	59°57'	1,176
3°00'	34°51'	1,178	1,142	0,424	0,542	0,783	58°08'	1,205
3°30'	37°00'	1,195	1,157	0,413	0,532	0,777	56°30'	1,234
4°00'	38°52'	1,219	1,172	0,402	0,522	0,771	55°08'	1,262
4°30'	40°39'	1,238	1,186	0,392	0,513	0,766	53°51'	1,290
5°	42°18'	1,257	1,200	0,383	0,504	0,760	52°12'	1,312
6°	45°24'	1,294	1,227	0,364	0,497	0,749	50°33'	1,372
7°	48°18'	1,331	1,253	0,346	0,468	0,738	48°42'	1,437
8°	51°00'	1,367	1,277	0,330	0,452	0,728	47°00'	1,498
9°	53°28'	1,401	1,300	0,314	0,437	0,718	45°32'	1,559
10°	55°50'	1,435	1,323	0,299	0,422	0,708	44°10'	1,626
11°	58°06'	1,469	1,345	0,285	0,408	0,698	42°51'	1,690
12°	60°20'	1,504	1,367	0,271	0,393	0,688	41°36'	1,772
13°	62°24'	1,530	1,388	0,258	0,380	0,679	40°36'	1,845
14°	64°25'	1,569	1,408	0,246	0,367	0,670	39°33'	1,923
15°	66°24'	1,603	1,428	0,234	0,354	0,660	38°38'	2,005
16°	68°24'	1,639	1,448	0,222	0,341	0,650	37°39'	2,094
17°	70°18'	1,673	1,467	0,211	0,329	0,641	36°42'	2,193
18°	72°06'	1,705	1,486	0,201	0,318	0,632	35°54'	2,291
19°	73°57'	1,741	1,505	0,190	0,306	0,622	35°03'	2,391

Appendix I (Cont'd).

ϕ	λ	M	σ	P/P_0	P/P_0	T/T_0	α	ρ/ρ_0
20°	73°42'	1.775	1.523	0.181	0.295	0.613	31°18'	2.500
21°	73°27'	1.809	1.542	0.171	0.284	0.599	31°33'	2.612
22°	73°12'	1.846	1.559	0.162	0.273	0.585	31°48'	2.735
23°	72°57'	1.880	1.576	0.154	0.263	0.570	32°03'	2.858
24°	72°30'	1.914	1.591	0.146	0.253	0.556	31°30'	2.993
25°	72°10'	1.951	1.610	0.138	0.243	0.540	30°50'	3.163
26°	71°48'	1.988	1.628	0.130	0.233	0.525	30°12'	3.319
27°	71°24'	2.028	1.644	0.123	0.224	0.509	29°33'	3.476
28°	70°58'	2.063	1.659	0.116	0.215	0.491	28°50'	3.647
29°	70°30'	2.099	1.673	0.1100	0.207	0.473	28°30'	3.820
30°	70°00'	2.130	1.691	0.1040	0.198	0.454	28°00'	4.018
31°	69°30'	2.173	1.706	0.0980	0.190	0.435	27°24'	4.256
32°	69°00'	2.209	1.722	0.0920	0.182	0.406	26°55'	4.436
33°	68°33'	2.245	1.737	0.0867	0.174	0.397	26°27'	4.710
34°	68°03'	2.285	1.752	0.0814	0.167	0.388	25°57'	4.955
35°	67°33'	2.327	1.767	0.0764	0.159	0.380	25°27'	5.236
36°	67°00'	2.366	1.782	0.0717	0.152	0.371	24°57'	5.521
37°	66°30'	2.411	1.797	0.0672	0.145	0.362	24°30'	5.741
38°	66°00'	2.454	1.810	0.0630	0.139	0.354	24°03'	6.166
39°	65°24'	2.498	1.824	0.0590	0.132	0.346	23°36'	6.472
40°	64°48'	2.539	1.838	0.0552	0.126	0.337	23°12'	6.919
41°	64°12'	2.581	1.852	0.0514	0.120	0.328	22°48'	7.362
42°	63°36'	2.624	1.865	0.0481	0.114	0.319	22°24'	7.798
43°	63°00'	2.670	1.878	0.0450	0.109	0.312	22°00'	8.260
44°	62°21'	2.717	1.891	0.0419	0.104	0.304	21°36'	8.710
45°	61°48'	2.765	1.905	0.0388	0.098	0.295	21°12'	9.184
46°	61°12'	2.816	1.918	0.0360	0.093	0.287	20°48'	9.954
47°	60°36'	2.869	1.930	0.0334	0.088	0.279	20°24'	10.57
48°	60°00'	2.910	1.943	0.0310	0.084	0.271	20°06'	11.20
49°	59°15'	2.959	1.955	0.0288	0.079	0.263	19°45'	11.97
50°	58°36'	3.010	1.967	0.0267	0.075	0.255	19°24'	12.94
51°	57°57'	3.064	1.978	0.0249	0.071	0.248	19°03'	13.62
52°	57°18'	3.119	1.990	0.0229	0.067	0.240	18°42'	14.72
53°	56°38'	3.174	2.002	0.0211	0.063	0.232	18°22'	15.78
54°	55°59'	3.236	2.014	0.0194	0.060	0.224	18°00'	16.90
55°	55°18'	3.289	2.025	0.0178	0.058	0.216	17°42'	18.62
56°	54°36'	3.344	2.036	0.0164	0.053	0.209	17°24'	19.49
57°	53°55'	3.404	2.047	0.0151	0.050	0.202	17°05'	20.89
58°	53°15'	3.470	2.058	0.0138	0.047	0.194	16°45'	22.49
59°	52°36'	3.542	2.069	0.0126	0.044	0.186	16°24'	24.38
60°	51°54'	3.606	2.080	0.0115	0.041	0.179	16°06'	26.30
61°	51°10'	3.666	2.090	0.0105	0.039	0.172	15°50'	28.32
62°	50°30'	3.742	2.100	$0.954 \cdot 10^{-2}$	0.036	0.165	15°30'	30.55
63°	50°48'	3.814	2.111	$0.869 \cdot 10^{-2}$	0.034	0.158	15°12'	33.89
64°	50°03'	3.876	2.121	$0.784 \cdot 10^{-2}$	0.031	0.150	14°57'	36.40

Appendix I (Cont'd).

θ'	θ	M	A	B/P_0	C/P_0	T/P_0	θ'	θ/P_0
65°	140°20'	3.919	2.130	$0.712 \cdot 10^{-2}$	0.029	0.244	14°40'	39.03
66°	141°38'	4.021	2.110	$0.645 \cdot 10^{-2}$	0.027	0.237	14°24'	43.15
67°	142°34'	4.124	2.150	$0.584 \cdot 10^{-2}$	0.025	0.239	14°02'	47.85
68°	144°12'	4.193	2.159	$0.525 \cdot 10^{-2}$	0.0235	0.223	13°48'	51.62
69°	145°27'	4.268	2.168	$0.474 \cdot 10^{-2}$	0.0219	0.217	13°33'	56.00
70°	146°42'	4.346	2.177	$0.426 \cdot 10^{-2}$	0.0203	0.210	13°18'	62.50
71°	147°57'	4.429	2.186	$0.380 \cdot 10^{-2}$	0.0187	0.204	13°03'	68.50
72°	149°12'	4.515	2.195	$0.339 \cdot 10^{-2}$	0.0172	0.197	12°48'	75.00
73°	150°30'	4.621	2.204	$0.311 \cdot 10^{-2}$	0.0158	0.190	12°30'	82.75
74°	151°42'	4.665	2.212	$0.270 \cdot 10^{-2}$	0.0146	0.184	12°18'	91.20
75°	153°00'	4.810	2.220	$0.241 \cdot 10^{-2}$	0.0135	0.179	12°00'	101.4
76°	154°15'	4.912	2.228	$0.214 \cdot 10^{-2}$	0.0124	0.173	11°45'	111.7
77°	155°30'	5.015	2.237	$0.186 \cdot 10^{-2}$	0.0112	0.166	11°30'	123.5
78°	156°45'	5.126	2.241	$0.165 \cdot 10^{-2}$	0.0103	0.160	11°15'	147.3
79°	158°00'	5.241	2.252	$0.145 \cdot 10^{-2}$	$0.040 \cdot 10^{-2}$	0.155	11°00'	154.8
80°	159°15'	5.362	2.260	$0.126 \cdot 10^{-2}$	$0.531 \cdot 10^{-2}$	0.149	10°45'	175.0
81°	160°30'	5.488	2.267	$0.112 \cdot 10^{-2}$	$0.780 \cdot 10^{-2}$	0.144	10°30'	196.0
82°	161°42'	5.593	2.274	$0.0971 \cdot 10^{-2}$	$0.705 \cdot 10^{-2}$	0.138	10°18'	219.8
83°	162°57'	5.735	2.282	$0.885 \cdot 10^{-2}$	$0.683 \cdot 10^{-2}$	0.132	10°00'	247.0
84°	164°12'	5.875	2.289	$0.722 \cdot 10^{-2}$	$0.570 \cdot 10^{-2}$	0.127	9°48'	279.0
85°	165°27'	6.028	2.295	$0.631 \cdot 10^{-2}$	$0.518 \cdot 10^{-2}$	0.122	9°33'	316.2
86°	166°42'	6.188	2.302	$0.545 \cdot 10^{-2}$	$0.466 \cdot 10^{-2}$	0.117	9°18'	361.0
87°	167°54'	6.321	2.309	$0.460 \cdot 10^{-2}$	$0.413 \cdot 10^{-2}$	0.111	9°00'	409.0
88°	169°09'	6.484	2.315	$0.388 \cdot 10^{-2}$	$0.373 \cdot 10^{-2}$	0.107	8°48'	460.0
89°	170°21'	6.649	2.321	$0.340 \cdot 10^{-2}$	$0.333 \cdot 10^{-2}$	0.102	8°33'	537.0
90°	171°36'	6.845	2.328	$0.285 \cdot 10^{-2}$	$0.294 \cdot 10^{-2}$	0.097	8°24'	631.0
91°	172°48'	7.013	2.331	$0.236 \cdot 10^{-2}$	$0.257 \cdot 10^{-2}$	0.092	8°12'	721.5
92°	174°09'	7.181	2.339	$0.197 \cdot 10^{-2}$	$0.226 \cdot 10^{-2}$	0.087	8°00'	811.2
93°	175°15'	7.343	2.345	$0.168 \cdot 10^{-2}$	$0.202 \cdot 10^{-2}$	0.083	7°45'	977.0
94°	176°27'	7.510	2.350	$0.140 \cdot 10^{-2}$	$0.176 \cdot 10^{-2}$	0.079	7°33'	1135
95°	177°40'	7.837	2.356	$0.114 \cdot 10^{-2}$	$0.153 \cdot 10^{-2}$	0.075	7°20'	1331
96°	178°54'	8.091	2.361	$0.954 \cdot 10^{-2}$	$0.131 \cdot 10^{-2}$	0.071	7°05'	1478
97°	179°06'	8.226	2.366	$0.778 \cdot 10^{-2}$	$0.116 \cdot 10^{-2}$	0.067	6°54'	1622
98°	181°21'	8.636	2.371	$0.628 \cdot 10^{-2}$	$0.096 \cdot 10^{-2}$	0.063	6°39'	2240
99°	182°34'	8.928	2.376	$0.502 \cdot 10^{-2}$	$0.849 \cdot 10^{-2}$	0.059	6°25'	2680
100°	184°48'	9.259	2.380	$0.403 \cdot 10^{-2}$	$0.726 \cdot 10^{-2}$	0.055	6°12'	3092
101°	185°00'	9.569	2.385	$0.324 \cdot 10^{-2}$	$0.617 \cdot 10^{-2}$	0.052	6°00'	3890
102°	186°12'	9.891	2.389	$0.257 \cdot 10^{-2}$	$0.526 \cdot 10^{-2}$	0.049	5°48'	4790
103°	187°24'	10.245	2.393	$0.202 \cdot 10^{-2}$	$0.444 \cdot 10^{-2}$	0.046	5°35'	6080
104°	188°36'	10.626	2.397	$0.156 \cdot 10^{-2}$	$0.368 \cdot 10^{-2}$	0.042	5°24'	7410
105°	189°48'	11.037	2.401	$0.118 \cdot 10^{-2}$	$0.302 \cdot 10^{-2}$	0.039	5°12'	9300
130°27'	220°27'	∞	2.419	0	0	0	0°00'	∞

Reproduced from
best available copy.

Appendix II. Table of gas-dynamic functions.

$k = 1.4$

M	ρ/ρ_0	p/p_0	T/T_0	A/A^*	τ/τ_0	λ/λ_0	μ/μ_0	ν/ν_0
0.00	1.0000	1.0000	1.0000	0.0000	0.0000	1.0000	1.0000	0.0000
0.01	1.0000	0.9999	0.9999	0.00158	0.00158	1.0000	0.9999	0.0001
0.02	0.9999	0.9998	0.9998	0.00315	0.00315	1.0000	0.9998	0.0004
0.03	0.9999	0.9997	0.9997	0.00473	0.00473	1.0000	0.9997	0.0009
0.04	0.9997	0.9990	0.9993	0.00631	0.00631	1.0000	0.9991	0.0015
0.05	0.9996	0.9986	0.9990	0.00788	0.00788	1.0015	0.9971	0.0022
0.06	0.9994	0.9979	0.9985	0.00945	0.00945	1.0021	0.9958	0.0030
0.07	0.9992	0.9971	0.9979	0.01102	0.01105	1.0028	0.9943	0.0039
0.08	0.9989	0.9963	0.9974	0.01259	0.01263	1.0038	0.9925	0.0049
0.09	0.9987	0.9953	0.9967	0.01415	0.01422	1.0047	0.9906	0.0060
0.10	0.9983	0.9942	0.9959	0.01571	0.01580	1.0058	0.9885	0.0071
0.11	0.9980	0.9929	0.9949	0.01726	0.01739	1.0070	0.9866	0.0083
0.12	0.9976	0.9916	0.9940	0.01882	0.01897	1.0083	0.9844	0.0096
0.13	0.9972	0.9901	0.9929	0.02036	0.02054	1.0100	0.9826	0.0109
0.14	0.9967	0.9886	0.9918	0.02190	0.02216	1.0113	0.9806	0.0123
0.15	0.9963	0.9870	0.9907	0.02344	0.02375	1.0129	0.9784	0.0137
0.16	0.9957	0.9851	0.9893	0.02497	0.02535	1.0147	0.9760	0.0151
0.17	0.9952	0.9832	0.9880	0.02649	0.02695	1.0165	0.9733	0.0166
0.18	0.9946	0.9812	0.9866	0.02801	0.02855	1.0185	0.9704	0.0180
0.19	0.9940	0.9791	0.9850	0.02952	0.03015	1.0204	0.9674	0.0195
0.20	0.9934	0.9768	0.9834	0.03102	0.03176	1.0227	0.9644	0.0210
0.21	0.9927	0.9745	0.9817	0.03252	0.03337	1.0250	0.9613	0.0225
0.22	0.9919	0.9720	0.9799	0.03401	0.03499	1.0274	0.9581	0.0240
0.23	0.9912	0.9695	0.9781	0.03549	0.03660	1.0298	0.9549	0.0255
0.24	0.9904	0.9668	0.9762	0.03696	0.03823	1.0315	0.9516	0.0270
0.25	0.9896	0.9640	0.9742	0.03842	0.03985	1.0335	0.9481	0.0285
0.26	0.9887	0.9611	0.9721	0.03987	0.04148	1.0358	0.9445	0.0300
0.27	0.9879	0.9581	0.9699	0.04131	0.04311	1.0386	0.9408	0.0315
0.28	0.9869	0.9550	0.9677	0.04274	0.04475	1.0415	0.9370	0.0330
0.29	0.9860	0.9518	0.9653	0.04416	0.04640	1.0445	0.9332	0.0345
0.30	0.9850	0.9486	0.9630	0.04557	0.04804	1.0476	0.9293	0.0360
0.31	0.9840	0.9453	0.9605	0.04697	0.04970	1.0508	0.9254	0.0375
0.32	0.9829	0.9419	0.9579	0.04835	0.05135	1.0539	0.9214	0.0390
0.33	0.9819	0.9384	0.9552	0.04972	0.05302	1.0573	0.9173	0.0405
0.34	0.9807	0.9349	0.9525	0.05109	0.05469	1.0606	0.9132	0.0420
0.35	0.9796	0.9313	0.9497	0.05243	0.05636	1.0641	0.9090	0.0435
0.36	0.9784	0.9276	0.9469	0.05377	0.05803	1.0676	0.9048	0.0450
0.37	0.9772	0.9238	0.9439	0.05509	0.05974	1.0712	0.9005	0.0465
0.38	0.9759	0.9199	0.9409	0.05640	0.06142	1.0748	0.8962	0.0480
0.39	0.9747	0.9161	0.9378	0.05769	0.06312	1.0785	0.8919	0.0495
0.40	0.9733	0.9122	0.9346	0.05897	0.06482	1.0822	0.8876	0.0510
0.41	0.9720	0.9083	0.9314	0.06024	0.06654	1.0860	0.8832	0.0525
0.42	0.9706	0.9043	0.9281	0.06149	0.06826	1.0898	0.8789	0.0540
0.43	0.9692	0.9002	0.9247	0.06272	0.06998	1.0937	0.8745	0.0555
0.44	0.9677	0.8961	0.9212	0.06394	0.07172	1.0976	0.8701	0.0570
0.45	0.9663	0.8918	0.9178	0.06515	0.07346	1.1016	0.8656	0.0585
0.46	0.9647	0.8874	0.9142	0.06633	0.07521	1.1056	0.8611	0.0600
0.47	0.9632	0.8830	0.9105	0.06750	0.07697	1.1116	0.8566	0.0615
0.48	0.9616	0.8785	0.9067	0.06865	0.07874	1.1156	0.8521	0.0630
0.49	0.9600	0.8740	0.9029	0.06979	0.08052	1.1197	0.8476	0.0645
0.50	0.9583	0.8695	0.8991	0.07091	0.08230	1.1239	0.8431	0.0660
0.51	0.9567	0.8650	0.8953	0.07201	0.08409	1.1279	0.8386	0.0675
0.52	0.9549	0.8604	0.8914	0.07309	0.08588	1.1320	0.8341	0.0690
0.53	0.9532	0.8558	0.8874	0.07416	0.08771	1.1362	0.8296	0.0705
0.54	0.9514	0.8511	0.8833	0.07520	0.08953	1.1403	0.8251	0.0720

Appendix II (Cont'd).

k = 1.4

A	B	C	D	E	F	G	H	I
0.55	0.04101	0.8314	0.8337	0.7023	0.9136	1.1445	0.7234	0.5032
0.56	0.04177	0.8287	0.8314	0.7024	0.9127	1.1436	0.7215	0.5021
0.57	0.04250	0.8260	0.8291	0.7025	0.9116	1.1428	0.7199	0.5010
0.58	0.04320	0.8172	0.8257	0.7026	0.9102	1.1420	0.7180	0.5000
0.59	0.04420	0.8112	0.8212	0.7025	0.9085	1.1410	0.6987	0.5019
0.60	0.04500	0.8053	0.8157	0.7023	1.0069	1.1401	0.6912	0.5039
0.61	0.04580	0.7982	0.8114	0.7024	1.0058	1.1391	0.6836	0.5050
0.62	0.04659	0.7932	0.8075	0.7025	1.0048	1.1381	0.6760	0.5061
0.63	0.04739	0.7870	0.8038	0.7026	1.0035	1.1372	0.6685	0.5071
0.64	0.04817	0.7808	0.8001	0.7025	1.0022	1.1362	0.6610	0.5082
0.65	0.04896	0.7745	0.8032	0.7023	1.0009	1.1352	0.6535	0.5093
0.66	0.04974	0.7681	0.8001	0.7024	0.9998	1.1343	0.6460	0.5104
0.67	0.05052	0.7617	0.8031	0.7025	0.9987	1.1333	0.6385	0.5115
0.68	0.05129	0.7553	0.8018	0.7026	0.9978	1.1324	0.6310	0.5126
0.69	0.05207	0.7488	0.8011	0.7025	0.9965	1.1314	0.6235	0.5137
0.70	0.05283	0.7422	0.8001	0.7023	0.9954	1.1304	0.6160	0.5148
0.71	0.05356	0.7356	0.8010	0.7024	0.9944	1.1294	0.6085	0.5159
0.72	0.05426	0.7289	0.7971	0.7025	0.9931	1.1284	0.6010	0.5170
0.73	0.05496	0.7221	0.7921	0.7026	0.9918	1.1274	0.5935	0.5181
0.74	0.05567	0.7154	0.7871	0.7025	0.9905	1.1264	0.5860	0.5192
0.75	0.05633	0.7086	0.7815	0.7023	0.9890	1.1254	0.5785	0.5203
0.76	0.05697	0.7017	0.7764	0.7024	0.9875	1.1244	0.5710	0.5214
0.77	0.05762	0.6948	0.7710	0.7025	0.9860	1.1234	0.5635	0.5225
0.78	0.05826	0.6878	0.7655	0.7026	0.9845	1.1224	0.5560	0.5236
0.79	0.05890	0.6808	0.7599	0.7025	0.9830	1.1214	0.5485	0.5247
0.80	0.05953	0.6738	0.7543	0.7023	0.9815	1.1204	0.5410	0.5258
0.81	0.06017	0.6668	0.7486	0.7024	0.9800	1.1194	0.5335	0.5269
0.82	0.06079	0.6597	0.7429	0.7025	0.9785	1.1184	0.5260	0.5280
0.83	0.06142	0.6525	0.7372	0.7026	0.9770	1.1174	0.5185	0.5291
0.84	0.06204	0.6454	0.7314	0.7025	0.9755	1.1164	0.5110	0.5302
0.85	0.06266	0.6382	0.7256	0.7023	0.9740	1.1154	0.5035	0.5313
0.86	0.06327	0.6310	0.7197	0.7024	0.9725	1.1144	0.4960	0.5324
0.87	0.06388	0.6238	0.7138	0.7025	0.9710	1.1134	0.4885	0.5335
0.88	0.06448	0.6165	0.7079	0.7026	0.9695	1.1124	0.4810	0.5346
0.89	0.06508	0.6092	0.7019	0.7025	0.9680	1.1114	0.4735	0.5357
0.90	0.06565	0.6019	0.6959	0.7023	0.9665	1.1104	0.4660	0.5368
0.91	0.06622	0.5946	0.6906	0.7024	0.9650	1.1094	0.4585	0.5379
0.92	0.06679	0.5873	0.6853	0.7025	0.9635	1.1084	0.4510	0.5390
0.93	0.06735	0.5800	0.6799	0.7026	0.9620	1.1074	0.4435	0.5401
0.94	0.06791	0.5726	0.6745	0.7025	0.9605	1.1064	0.4360	0.5412
0.95	0.06846	0.5653	0.6691	0.7023	0.9590	1.1054	0.4285	0.5423
0.96	0.06901	0.5579	0.6637	0.7024	0.9575	1.1044	0.4210	0.5434
0.97	0.06956	0.5505	0.6582	0.7025	0.9560	1.1034	0.4135	0.5445
0.98	0.07011	0.5431	0.6528	0.7026	0.9545	1.1024	0.4060	0.5456
0.99	0.07066	0.5357	0.6473	0.7025	0.9530	1.1014	0.3985	0.5467
1.00	0.07121	0.5283	0.6419	0.7023	0.9515	1.1004	0.3910	0.5478
1.01	0.07176	0.5209	0.6364	0.7024	0.9500	1.0994	0.3835	0.5489
1.02	0.07231	0.5135	0.6309	0.7025	0.9485	1.0984	0.3760	0.5500
1.03	0.07286	0.5061	0.6254	0.7026	0.9470	1.0974	0.3685	0.5511
1.04	0.07341	0.4987	0.6199	0.7025	0.9455	1.0964	0.3610	0.5522
1.05	0.07396	0.4913	0.6144	0.7023	0.9440	1.0954	0.3535	0.5533
1.06	0.07451	0.4839	0.6089	0.7024	0.9425	1.0944	0.3460	0.5544
1.07	0.07506	0.4765	0.6034	0.7025	0.9410	1.0934	0.3385	0.5555
1.08	0.07561	0.4691	0.5979	0.7026	0.9395	1.0924	0.3310	0.5566
1.09	0.07616	0.4617	0.5924	0.7025	0.9380	1.0914	0.3235	0.5577
1.10	0.07671	0.4543	0.5869	0.7023	0.9365	1.0904	0.3160	0.5588
1.11	0.07726	0.4469	0.5814	0.7024	0.9350	1.0894	0.3085	0.5599
1.12	0.07781	0.4395	0.5759	0.7025	0.9335	1.0884	0.3010	0.5610
1.13	0.07836	0.4321	0.5704	0.7026	0.9320	1.0874	0.2935	0.5621
1.14	0.07891	0.4247	0.5649	0.7025	0.9305	1.0864	0.2860	0.5632
1.15	0.07946	0.4173	0.5594	0.7023	0.9290	1.0854	0.2785	0.5643
1.16	0.07999	0.4100	0.5539	0.7024	0.9275	1.0844	0.2710	0.5654
1.17	0.08054	0.4026	0.5484	0.7025	0.9260	1.0834	0.2635	0.5665
1.18	0.08109	0.3952	0.5429	0.7026	0.9245	1.0824	0.2560	0.5676
1.19	0.08164	0.3878	0.5374	0.7025	0.9230	1.0814	0.2485	0.5687

Appendix II (Cont'd).

k = 1.4

A	B	C	D	E	F	G	H	I
1.20	0.7600	0.3827	0.5035	0.9331	2.4906	1.2286	0.2115	1.2566
1.21	0.7560	0.3757	0.4969	0.9184	2.5247	1.2211	0.2068	1.2708
1.22	0.7519	0.3687	0.4903	0.9035	2.5583	1.2200	0.2022	1.2843
1.23	0.7478	0.3617	0.4837	0.9384	2.5911	1.2151	0.2076	1.2971
1.24	0.7437	0.3548	0.4770	0.9331	2.6300	1.2105	0.2031	1.3126
1.25	0.7396	0.3479	0.4704	0.9275	2.6660	1.2054	0.2886	1.3288
1.26	0.7354	0.3411	0.4638	0.9217	2.7026	1.2000	0.2842	1.3413
1.27	0.7312	0.3343	0.4572	0.9159	2.7393	1.1946	0.2795	1.3558
1.28	0.7269	0.3275	0.4505	0.9096	2.7775	1.1887	0.2755	1.3705
1.29	0.7227	0.3208	0.4439	0.9033	2.8158	1.1820	0.2713	1.3853
1.30	0.7184	0.3142	0.4374	0.8969	2.8547	1.1765	0.2670	1.4002
1.31	0.7140	0.3075	0.4307	0.8901	2.8941	1.1699	0.2629	1.4153
1.32	0.7098	0.3010	0.4241	0.8831	2.9343	1.1632	0.2574	1.4305
1.33	0.7052	0.2945	0.4176	0.8761	2.9750	1.1562	0.2547	1.4458
1.34	0.7007	0.2880	0.4110	0.8688	3.0164	1.1490	0.2507	1.4613
1.35	0.6962	0.2816	0.4045	0.8614	3.0580	1.1417	0.2467	1.4769
1.36	0.6917	0.2753	0.3980	0.8538	3.1013	1.1341	0.2427	1.4927
1.37	0.6872	0.2690	0.3914	0.8462	3.1448	1.1261	0.2380	1.5087
1.38	0.6826	0.2628	0.3849	0.8389	3.1889	1.1180	0.2340	1.5248
1.39	0.6780	0.2566	0.3783	0.8320	3.2340	1.1098	0.2302	1.5410
1.40	0.6734	0.2505	0.3720	0.8246	3.2798	1.1012	0.2275	1.5575
1.41	0.6687	0.2445	0.3656	0.8171	3.3263	1.0924	0.2238	1.5741
1.42	0.6639	0.2385	0.3592	0.8096	3.3737	1.0835	0.2201	1.5909
1.43	0.6592	0.2326	0.3528	0.8023	3.4219	1.0742	0.2165	1.6078
1.44	0.6544	0.2267	0.3464	0.7969	3.4710	1.0648	0.2129	1.6250
1.45	0.6496	0.2209	0.3401	0.7778	3.5211	1.0551	0.2094	1.6423
1.46	0.6447	0.2152	0.3338	0.7687	3.5720	1.0453	0.2059	1.6598
1.47	0.6398	0.2095	0.3275	0.7593	3.6240	1.0351	0.2024	1.6776
1.48	0.6349	0.2040	0.3212	0.7499	3.6768	1.0249	0.1990	1.6955
1.49	0.6300	0.1985	0.3150	0.7404	3.7308	1.0144	0.1956	1.7137
1.50	0.6250	0.1930	0.3088	0.7307	3.7858	1.0037	0.1923	1.7321
1.51	0.6200	0.1876	0.3027	0.7209	3.8418	0.9927	0.1890	1.7506
1.52	0.6149	0.1824	0.2965	0.7110	3.8990	0.9816	0.1858	1.7694
1.53	0.6099	0.1771	0.2904	0.7009	3.9574	0.9703	0.1825	1.7883
1.54	0.6047	0.1720	0.2844	0.6909	4.0172	0.9590	0.1794	1.8078
1.55	0.5996	0.1669	0.2784	0.6807	4.0778	0.9472	0.1762	1.8273
1.56	0.5944	0.1619	0.2724	0.6703	4.1398	0.9353	0.1731	1.8471
1.57	0.5892	0.1570	0.2665	0.6599	4.2034	0.9233	0.1700	1.8672
1.58	0.5839	0.1522	0.2606	0.6494	4.2680	0.9111	0.1670	1.8875
1.59	0.5786	0.1474	0.2547	0.6389	4.3345	0.8988	0.1640	1.9081
1.60	0.5733	0.1427	0.2489	0.6282	4.4020	0.8861	0.1611	1.9290
1.61	0.5680	0.1381	0.2431	0.6175	4.4713	0.8734	0.1581	1.9501
1.62	0.5626	0.1336	0.2374	0.6067	4.5422	0.8604	0.1552	1.9716
1.63	0.5572	0.1291	0.2317	0.5958	4.6144	0.8474	0.1524	1.9931
1.64	0.5517	0.1248	0.2261	0.5850	4.6887	0.8343	0.1495	2.0155
1.65	0.5463	0.1205	0.2205	0.5740	4.7647	0.8210	0.1467	2.0380
1.66	0.5407	0.1163	0.2150	0.5630	4.8424	0.8075	0.1440	2.0607
1.67	0.5352	0.1121	0.2095	0.5520	4.9221	0.7939	0.1413	2.0839
1.68	0.5298	0.1081	0.2041	0.5409	5.0037	0.7802	0.1386	2.1073
1.69	0.5240	0.1041	0.1988	0.5298	5.0877	0.7664	0.1359	2.1313
1.70	0.5183	0.1003	0.1934	0.5187	5.1735	0.7524	0.1334	2.1555
1.71	0.5126	0.0965	0.1881	0.5075	5.2617	0.7383	0.1306	2.1802
1.72	0.5069	0.0928	0.1830	0.4965	5.3520	0.7243	0.1281	2.2053
1.73	0.5012	0.0891	0.1778	0.4852	5.4449	0.7100	0.1255	2.2308
1.74	0.4954	0.0856	0.1727	0.4741	5.5403	0.6957	0.1230	2.2567
1.75	0.4896	0.0821	0.1677	0.4630	5.6383	0.6813	0.1205	2.2831
1.76	0.4837	0.0787	0.1628	0.4520	5.7390	0.6669	0.1181	2.3100
1.77	0.4779	0.0754	0.1578	0.4407	5.8427	0.6523	0.1156	2.3374
1.78	0.4719	0.0722	0.1530	0.4298	5.9495	0.6376	0.1132	2.3653
1.79	0.4660	0.0691	0.1482	0.4185	6.0593	0.6232	0.1108	2.3937
1.80	0.4600	0.0660	0.1435	0.4075	6.1723	0.6085	0.1085	2.4227
1.81	0.4540	0.0630	0.1389	0.3965	6.2883	0.5938	0.1062	2.4523
1.82	0.4479	0.0602	0.1343	0.3855	6.4071	0.5791	0.1039	2.4824
1.83	0.4418	0.0573	0.1298	0.3746	6.5285	0.5644	0.1016	2.5132
1.84	0.4357	0.0546	0.1253	0.3638	6.6607	0.5497	0.0994	2.5449

Appendix II (Cont'd).

k = 1.4

1.85	0.1296	0.0379	0.1210	0.3530	6.7931	0.5319	0.0971	2.5766
1.86	0.1301	0.0381	0.1167	0.3423	6.9298	0.5292	0.0939	2.6061
1.87	0.1317	0.0389	0.1124	0.3316	7.0707	0.5255	0.0928	2.6329
1.88	0.1330	0.0395	0.1083	0.3211	7.2162	0.5209	0.0906	2.6772
1.89	0.1347	0.0412	0.1042	0.3105	7.3673	0.4762	0.0885	2.7123
1.90	0.1363	0.0399	0.1002	0.2992	7.5243	0.4617	0.0861	2.7481
1.91	0.13720	0.0477	0.0962	0.2898	7.6858	0.4472	0.0843	2.7849
1.92	0.13856	0.0456	0.0923	0.2797	7.8510	0.4327	0.0823	2.8225
1.93	0.1392	0.0446	0.0885	0.2695	8.0269	0.4183	0.0803	2.8612
1.94	0.13727	0.0416	0.0848	0.2596	8.2098	0.4041	0.0782	2.9007
1.95	0.13662	0.0297	0.0812	0.2497	8.3985	0.3899	0.0763	2.9414
1.96	0.13597	0.0279	0.0776	0.2400	8.5913	0.3758	0.0743	2.9831
1.97	0.13532	0.0262	0.0741	0.2304	8.7984	0.3618	0.0724	3.0261
1.98	0.13466	0.0245	0.0707	0.2209	9.0112	0.3480	0.0704	3.0701
1.99	0.13400	0.0229	0.0674	0.2116	9.2299	0.3343	0.0685	3.1155
2.00	0.13333	0.0214	0.0642	0.2024	9.464	0.3203	0.0668	3.1622
2.01	0.13267	0.0199	0.0610	0.1931	9.706	0.3074	0.0648	3.2104
2.02	0.13199	0.0185	0.0579	0.1845	9.961	0.2942	0.0630	3.2603
2.03	0.13132	0.0172	0.0549	0.1758	10.221	0.2811	0.0612	3.3113
2.04	0.13064	0.0159	0.0520	0.1672	10.502	0.2683	0.0594	3.3642
2.05	0.12996	0.0147	0.0491	0.1588	10.794	0.2556	0.0576	3.4190
2.06	0.12927	0.0136	0.0461	0.1507	11.102	0.2431	0.0558	3.4759
2.07	0.12859	0.0125	0.0437	0.1427	11.422	0.2309	0.0541	3.5343
2.08	0.12789	0.0115	0.0411	0.1348	11.762	0.2189	0.0524	3.5951
2.09	0.12720	0.0105	0.0386	0.1272	12.121	0.2070	0.0507	3.6583
2.10	0.12650	0.0090	0.0361	0.1198	12.500	0.1956	0.0490	3.7240
2.11	0.12580	0.0087	0.0348	0.1125	12.901	0.1843	0.0473	3.7922
2.12	0.12509	0.0079	0.0315	0.1055	13.326	0.1733	0.0457	3.8633
2.13	0.12439	0.0072	0.0291	0.0986	13.778	0.1626	0.0440	3.9376
2.14	0.12367	0.0065	0.0273	0.0921	14.259	0.1522	0.0424	4.0150
2.15	0.12296	0.0058	0.0253	0.0857	14.772	0.1420	0.0408	4.0961
2.16	0.12224	0.0052	0.0233	0.0795	15.319	0.1322	0.0393	4.1791
2.17	0.12152	0.0046	0.0215	0.0733	15.906	0.1226	0.0377	4.2702
2.18	0.12079	0.0041	0.0197	0.0678	16.537	0.1134	0.0361	4.3642
2.19	0.12006	0.0036	0.0180	0.0623	17.218	0.1045	0.0346	4.4633
2.20	0.11933	0.0032	0.0164	0.0570	17.949	0.0960	0.0331	4.5674
2.21	0.11860	0.0028	0.0149	0.0520	18.742	0.0878	0.0316	4.6758
2.22	0.11786	0.0024	0.0135	0.0472	19.607	0.0799	0.0301	4.7894
2.23	0.11712	0.0021	0.0121	0.0427	20.548	0.0724	0.0287	4.9080
2.24	0.11637	0.0018	0.0116	0.0408	22.953	0.0693	0.0253	5.0333
2.25	0.11563	0.00151	0.00966	0.0343	22.712	0.0585	0.0258	5.1938
2.26	0.11487	0.00127	0.00813	0.0299	23.958	0.0496	0.0256	5.3494
2.27	0.11412	0.00106	0.00740	0.0268	25.331	0.0461	0.0229	5.5147
2.28	0.11336	0.00087	0.00652	0.0234	26.893	0.0404	0.0216	5.6940
2.29	0.11260	0.00071	0.00564	0.0204	28.669	0.0352	0.0202	5.8891
2.30	0.11183	0.00057	0.00482	0.0175	30.658	0.0302	0.0189	6.1033
2.31	0.11106	0.00045	0.00407	0.0148	32.937	0.0258	0.0175	6.3399
2.32	0.11029	0.00035	0.00344	0.0124	35.551	0.0217	0.0161	6.6008
2.33	0.10952	0.00027	0.00280	0.0103	38.606	0.0180	0.0148	6.8865
2.34	0.10874	0.00020	0.00226	0.0083	42.233	0.0146	0.0135	7.2234
2.35	0.10796	0.00014	0.00170	0.0063	46.593	0.0111	0.0122	7.6033
2.36	0.10717	0.00010	0.00138	0.0051	51.914	0.0090	0.0109	8.0450
2.37	0.10638	0.00007	0.00103	0.0038	58.569	0.0068	0.0096	8.5619
2.38	0.10559	0.00004	0.00074	0.0028	67.144	0.0049	0.0084	9.1882
2.39	0.10480	0.00003	0.00050	0.0019	78.613	0.0034	0.0071	9.9624
2.40	0.10400	0.00002	0.00032	0.0012	94.703	0.0022	0.0059	10.957
2.41	0.10320	0.00001	0.00018	0.0007	118.94	0.0012	0.0047	12.406
2.42	0.10239	0.00001	0.00010	0.0003	150.65	0.0006	0.0033	14.287
2.43	0.10158	0.00001	0.00005	0.0001	242.16	0.0002	0.0023	17.681
2.44	0.10077	0.00001	0.00002	0.0000	499.16	0.0000	0.0011	25.367
2.449	0	0	0	0	∞	0	0	∞

Appendix II (Cont'd).

k = 1.33

0.00	1.0000	1.0000	1.0000	0.0000	0.0000	1.0000	1.0000	0.0000
0.01	1.0000	0.9999	0.9999	0.0159	0.0159	1.0000	1.0000	0.0000
0.02	0.9999	0.9998	0.9998	0.0318	0.0318	1.0000	0.9999	0.0000
0.03	0.9997	0.9995	0.9997	0.0476	0.0477	1.0000	0.9999	0.0000
0.04	0.9994	0.9991	0.9993	0.0635	0.0636	1.0000	0.9998	0.0000
0.05	0.9991	0.9986	0.9990	0.0793	0.0795	1.0015	0.9972	0.0463
0.06	0.9985	0.9980	0.9985	0.0952	0.0954	1.0021	0.9959	0.0556
0.07	0.9978	0.9972	0.9979	0.1110	0.1113	1.0028	0.9944	0.0649
0.08	0.9971	0.9964	0.9973	0.1267	0.1272	1.0037	0.9928	0.0742
0.09	0.9969	0.9954	0.9965	0.1425	0.1431	1.0046	0.9908	0.0834
0.10	0.9966	0.9944	0.9954	0.1582	0.1591	1.0057	0.9887	0.0927
0.11	0.9963	0.9932	0.9949	0.1738	0.1750	1.0069	0.9861	0.1020
0.12	0.9960	0.9918	0.9938	0.1894	0.1910	1.0081	0.9838	0.1113
0.13	0.9956	0.9911	0.9928	0.2052	0.2072	1.0096	0.9810	0.1206
0.14	0.9952	0.9889	0.9917	0.2209	0.2220	1.0111	0.9781	0.1299
0.15	0.9948	0.9872	0.9903	0.2366	0.2390	1.0126	0.9749	0.1392
0.16	0.9944	0.9854	0.9890	0.2514	0.2551	1.0143	0.9715	0.1485
0.17	0.9939	0.9836	0.9877	0.2667	0.2712	1.0162	0.9679	0.1578
0.18	0.9934	0.9816	0.9862	0.2820	0.2873	1.0181	0.9642	0.1672
0.19	0.9929	0.9796	0.9846	0.2972	0.3034	1.0202	0.9602	0.1765
0.20	0.9923	0.9774	0.9830	0.3123	0.3195	1.0223	0.9561	0.1858
0.21	0.9918	0.9751	0.9812	0.3273	0.3357	1.0245	0.9518	0.1952
0.22	0.9912	0.9728	0.9795	0.3423	0.3519	1.0269	0.9473	0.2045
0.23	0.9905	0.9702	0.9775	0.3571	0.3681	1.0292	0.9427	0.2139
0.24	0.9898	0.9675	0.9755	0.3719	0.3844	1.0317	0.9378	0.2233
0.25	0.9891	0.9648	0.9731	0.3866	0.4007	1.0343	0.9329	0.2327
0.26	0.9884	0.9619	0.9712	0.4011	0.4170	1.0369	0.9277	0.2420
0.27	0.9877	0.9590	0.9693	0.4156	0.4334	1.0395	0.9224	0.2515
0.28	0.9869	0.9560	0.9667	0.4300	0.4498	1.0425	0.9170	0.2609
0.29	0.9861	0.9529	0.9644	0.4443	0.4662	1.0453	0.9114	0.2703
0.30	0.9853	0.9496	0.9619	0.4584	0.4827	1.0483	0.9057	0.2797
0.31	0.9845	0.9463	0.9591	0.4724	0.4992	1.0516	0.8999	0.2892
0.32	0.9836	0.9428	0.9567	0.4863	0.5158	1.0549	0.8940	0.2986
0.33	0.9827	0.9393	0.9540	0.5001	0.5324	1.0579	0.8879	0.3081
0.34	0.9818	0.9358	0.9512	0.5137	0.5491	1.0612	0.8817	0.3176
0.35	0.9809	0.9319	0.9484	0.5273	0.5658	1.0643	0.8754	0.3271
0.36	0.9799	0.9281	0.9455	0.5407	0.5826	1.0680	0.8690	0.3366
0.37	0.9789	0.9241	0.9424	0.5539	0.5991	1.0714	0.8625	0.3462
0.38	0.9779	0.9201	0.9393	0.5670	0.6162	1.0750	0.8560	0.3557
0.39	0.9768	0.9159	0.9361	0.5799	0.6332	1.0783	0.8493	0.3653
0.40	0.9757	0.9118	0.9329	0.5928	0.6501	1.0822	0.8425	0.3749
0.41	0.9746	0.9075	0.9296	0.6055	0.6672	1.0859	0.8357	0.3845
0.42	0.9734	0.9030	0.9262	0.6179	0.6843	1.0895	0.8288	0.3941
0.43	0.9723	0.8985	0.9227	0.6303	0.7014	1.0934	0.8218	0.4037
0.44	0.9712	0.8940	0.9192	0.6425	0.7187	1.0972	0.8148	0.4134
0.45	0.9701	0.8893	0.9156	0.6545	0.7359	1.1010	0.8078	0.4231
0.46	0.9690	0.8850	0.9123	0.6666	0.7533	1.1053	0.8006	0.4328
0.47	0.9678	0.8797	0.9081	0.6786	0.7707	1.1098	0.7931	0.4424
0.48	0.9667	0.8749	0.9044	0.6896	0.7882	1.1148	0.7852	0.4522
0.49	0.9656	0.8699	0.9005	0.7009	0.8058	1.1197	0.7770	0.4619
0.50	0.9645	0.8648	0.8966	0.7121	0.8234	1.1247	0.7717	0.4717
0.51	0.9632	0.8596	0.8925	0.7233	0.8411	1.1297	0.7644	0.4815
0.52	0.9619	0.8544	0.8884	0.7343	0.8589	1.1347	0.7570	0.4913
0.53	0.9606	0.8491	0.8843	0.7443	0.8768	1.1397	0.7496	0.5011
0.54	0.9593	0.8436	0.8799	0.7546	0.8947	1.1447	0.7423	0.5110

Appendix II (Cont'd).

k = 1.33

A	B	C	D	E	F	G	H	I
0.55	0.9372	0.8382	0.8757	0.7651	0.9128	1.1406	0.7319	0.5208
0.56	0.9356	0.8327	0.8714	0.7752	0.9309	1.1447	0.7275	0.5208
0.57	0.9340	0.8271	0.8670	0.7850	0.9491	1.1487	0.7230	0.5107
0.58	0.9324	0.8214	0.8625	0.7946	0.9674	1.1526	0.7186	0.5206
0.59	0.9307	0.8156	0.8579	0.8040	0.9858	1.1563	0.7142	0.5006
0.60	0.9190	0.8098	0.8533	0.8133	1.0043	1.1603	0.6978	0.5706
0.61	0.9173	0.8040	0.8487	0.8224	1.0229	1.1643	0.6904	0.5807
0.62	0.9156	0.7980	0.8439	0.8312	1.0416	1.1684	0.6839	0.5907
0.63	0.9138	0.7921	0.8393	0.8399	1.0604	1.1724	0.6756	0.6008
0.64	0.9120	0.7860	0.8344	0.8483	1.0792	1.1762	0.6683	0.6109
0.65	0.9102	0.7798	0.8294	0.8564	1.0982	1.1799	0.6609	0.6211
0.66	0.9083	0.7737	0.8246	0.8645	1.1173	1.1838	0.6536	0.6313
0.67	0.9064	0.7674	0.8195	0.8722	1.1366	1.1874	0.6463	0.6413
0.68	0.9045	0.7612	0.8145	0.8798	1.1559	1.1911	0.6390	0.6517
0.69	0.9026	0.7548	0.8094	0.8871	1.1753	1.1947	0.6318	0.6620
0.70	0.9306	0.7483	0.8041	0.8941	1.1949	1.1981	0.6246	0.6723
0.71	0.9286	0.7419	0.7989	0.9011	1.2146	1.2017	0.6172	0.6826
0.72	0.9266	0.7354	0.7937	0.9077	1.2343	1.2051	0.6102	0.6930
0.73	0.9245	0.7289	0.7884	0.9143	1.2543	1.2086	0.6031	0.7034
0.74	0.9224	0.7223	0.7830	0.9204	1.2743	1.2118	0.5961	0.7139
0.75	0.9203	0.7157	0.7777	0.9265	1.2945	1.2151	0.5890	0.7243
0.76	0.9182	0.7090	0.7722	0.9322	1.3148	1.2182	0.5820	0.7348
0.77	0.9160	0.7023	0.7666	0.9377	1.3353	1.2212	0.5751	0.7454
0.78	0.9138	0.6955	0.7611	0.9430	1.3559	1.2241	0.5682	0.7561
0.79	0.9116	0.6887	0.7555	0.9481	1.3766	1.2270	0.5613	0.7666
0.80	0.9091	0.6819	0.7499	0.9529	1.3975	1.2298	0.5545	0.7772
0.81	0.9071	0.6749	0.7440	0.9575	1.4185	1.2321	0.5477	0.7880
0.82	0.9048	0.6678	0.7383	0.9618	1.4397	1.2349	0.5410	0.7987
0.83	0.9024	0.6607	0.7326	0.9660	1.4610	1.2374	0.5343	0.8095
0.84	0.9001	0.6535	0.7268	0.9698	1.4825	1.2397	0.5277	0.8203
0.85	0.8977	0.6462	0.7210	0.9735	1.5042	1.2419	0.5211	0.8312
0.86	0.8954	0.6389	0.7151	0.9769	1.5260	1.2440	0.5146	0.8421
0.87	0.8928	0.6316	0.7092	0.9802	1.5479	1.2461	0.5082	0.8531
0.88	0.8903	0.6243	0.7032	0.9839	1.5701	1.2478	0.5018	0.8641
0.89	0.8878	0.6169	0.6973	0.9859	1.5924	1.2497	0.4954	0.8751
0.90	0.8853	0.6094	0.6913	0.9883	1.6149	1.2512	0.4891	0.8862
0.91	0.8827	0.6018	0.6852	0.9901	1.6376	1.2525	0.4829	0.8974
0.92	0.8801	0.5942	0.6791	0.9915	1.6605	1.2539	0.4767	0.9086
0.93	0.8775	0.5866	0.6730	0.9934	1.6835	1.2552	0.4705	0.9198
0.94	0.8749	0.5791	0.6669	0.9957	1.7068	1.2561	0.4643	0.9311
0.95	0.8722	0.5713	0.6608	0.9972	1.7302	1.2572	0.4581	0.9424
0.96	0.8695	0.5635	0.6545	0.9981	1.7539	1.2577	0.4520	0.9538
0.97	0.8667	0.5559	0.6483	0.9989	1.7778	1.2583	0.4460	0.9653
0.98	0.8639	0.5481	0.6420	0.9995	1.8018	1.2586	0.4400	0.9768
0.99	0.8612	0.5403	0.6359	1.0000	1.8261	1.2591	0.4349	0.9884
1.00	0.8584	0.5324	0.6296	1.0000	1.8506	1.2591	0.4292	1.0000
1.01	0.8555	0.5245	0.6233	1.0000	1.8751	1.2590	0.4235	1.0117
1.02	0.8527	0.5166	0.6169	0.9995	1.9003	1.2587	0.4179	1.0234
1.03	0.8497	0.5088	0.6105	0.9989	1.9255	1.2583	0.4123	1.0352
1.04	0.8468	0.5010	0.6042	0.9981	1.9509	1.2576	0.4068	1.0471
1.05	0.8439	0.4931	0.5979	0.9972	1.9766	1.2570	0.4014	1.0590
1.06	0.8409	0.4853	0.5914	0.9958	2.0025	1.2559	0.3960	1.0710
1.07	0.8379	0.4774	0.5849	0.9941	2.0286	1.2548	0.3906	1.0830
1.08	0.8348	0.4695	0.5786	0.9920	2.0550	1.2534	0.3854	1.0951
1.09	0.8317	0.4617	0.5722	0.9907	2.0818	1.2520	0.3801	1.1073

Reproduced from
best available copy.

Appendix II (Cont'd).

k = 1.33

A	B	C	D	E	F	G	H	I
1.10	0.8286	0.4658	0.5658	0.9586	2.1087	1.2503	0.3750	1.1196
1.11	0.8255	0.4617	0.5593	0.9862	2.1360	1.2484	0.3698	1.1319
1.12	0.8223	0.4576	0.5528	0.9835	2.1635	1.2463	0.3648	1.1443
1.13	0.8192	0.4535	0.5463	0.9806	2.1913	1.2439	0.3598	1.1567
1.14	0.8159	0.4495	0.5399	0.9777	2.2194	1.2415	0.3548	1.1693
1.15	0.8127	0.4335	0.5334	0.9744	2.2478	1.2388	0.3499	1.1819
1.16	0.8094	0.4265	0.5269	0.9709	2.2765	1.2359	0.3451	1.1946
1.17	0.8061	0.4195	0.5205	0.9674	2.3055	1.2339	0.3403	1.2073
1.18	0.8028	0.4126	0.5140	0.9634	2.3349	1.2296	0.3356	1.2202
1.19	0.7994	0.4057	0.5075	0.9593	2.3646	1.2261	0.3309	1.2331
1.20	0.7961	0.3986	0.5007	0.9545	2.3940	1.2218	0.3263	1.2461
1.21	0.7926	0.3920	0.4946	0.9506	2.4249	1.2186	0.3217	1.2592
1.22	0.7892	0.3852	0.4881	0.9459	2.4556	1.2143	0.3172	1.2723
1.23	0.7857	0.3784	0.4816	0.9410	2.4867	1.2102	0.3127	1.2854
1.24	0.7822	0.3716	0.4751	0.9357	2.5181	1.2055	0.3083	1.2986
1.25	0.7787	0.3649	0.4686	0.9305	2.5500	1.2008	0.3039	1.3121
1.26	0.7752	0.3583	0.4622	0.9252	2.5821	1.1961	0.2995	1.3259
1.27	0.7716	0.3516	0.4557	0.9193	2.6147	1.1907	0.2953	1.3396
1.28	0.7680	0.3450	0.4493	0.9135	2.6477	1.1853	0.2911	1.3534
1.29	0.7643	0.3385	0.4429	0.9075	2.6811	1.1799	0.2869	1.3671
1.30	0.7606	0.3320	0.4365	0.9014	2.7149	1.1741	0.2828	1.3820
1.31	0.7570	0.3255	0.4300	0.8949	2.7492	1.1680	0.2787	1.3950
1.32	0.7532	0.3191	0.4236	0.8883	2.7838	1.1618	0.2747	1.4091
1.33	0.7495	0.3128	0.4173	0.8816	2.8190	1.1555	0.2707	1.4234
1.34	0.7457	0.3065	0.4110	0.8749	2.8545	1.1491	0.2667	1.4377
1.35	0.7419	0.3002	0.4046	0.8677	2.8905	1.1421	0.2629	1.4521
1.36	0.7380	0.2940	0.3984	0.8608	2.9271	1.1351	0.2590	1.4667
1.37	0.7342	0.2878	0.3920	0.8531	2.9642	1.1277	0.2552	1.4814
1.38	0.7303	0.2817	0.3857	0.8455	3.0017	1.1202	0.2515	1.4960
1.39	0.7264	0.2757	0.3796	0.8381	3.0398	1.1129	0.2477	1.5110
1.40	0.7224	0.2697	0.3733	0.8303	3.0784	1.1051	0.2441	1.5250
1.41	0.7184	0.2637	0.3671	0.8221	3.1176	1.0968	0.2404	1.5412
1.42	0.7144	0.2578	0.3609	0.8140	3.1573	1.0885	0.2368	1.5564
1.43	0.7104	0.2520	0.3548	0.8060	3.1977	1.0803	0.2334	1.5719
1.44	0.7063	0.2463	0.3487	0.7976	3.2386	1.0717	0.2298	1.5875
1.45	0.7022	0.2406	0.3426	0.7891	3.2802	1.0629	0.2263	1.6031
1.46	0.6981	0.2349	0.3365	0.7805	3.3222	1.0539	0.2229	1.6188
1.47	0.6940	0.2291	0.3305	0.7718	3.3649	1.0447	0.2195	1.6345
1.48	0.6898	0.2238	0.3245	0.7629	3.4083	1.0353	0.2162	1.6510
1.49	0.6856	0.2184	0.3186	0.7540	3.4524	1.0258	0.2129	1.6672
1.50	0.6813	0.2138	0.3126	0.7449	3.4972	1.0160	0.2097	1.6836
1.51	0.6771	0.2077	0.3067	0.7357	3.5426	1.0061	0.2064	1.7002
1.52	0.6728	0.2024	0.3009	0.7265	3.5890	0.9961	0.2032	1.7169
1.53	0.6685	0.1973	0.2951	0.7172	3.6358	0.9858	0.2001	1.7345
1.54	0.6641	0.1921	0.2893	0.7077	3.6836	0.9754	0.1970	1.7508
1.55	0.6597	0.1871	0.2836	0.6982	3.7321	0.9649	0.1939	1.7680
1.56	0.6553	0.1821	0.2779	0.6886	3.7813	0.9541	0.1909	1.7851
1.57	0.6509	0.1772	0.2722	0.6789	3.8316	0.9432	0.1879	1.8029
1.58	0.6464	0.1723	0.2666	0.6691	3.8825	0.9321	0.1849	1.8207
1.59	0.6420	0.1676	0.2610	0.6593	3.9345	0.9209	0.1820	1.8386
1.60	0.6374	0.1628	0.2554	0.6492	3.9874	0.9093	0.1791	1.8567
1.61	0.6329	0.1582	0.2500	0.6391	4.0410	0.8981	0.1762	1.8750
1.62	0.6283	0.1537	0.2446	0.6291	4.0957	0.8865	0.1734	1.8945
1.63	0.6237	0.1492	0.2392	0.6193	4.1514	0.8746	0.1706	1.9142
1.64	0.6191	0.1448	0.2338	0.6092	4.2080	0.8628	0.1678	1.9341

Appendix II (Cont'd).

k = 1.33

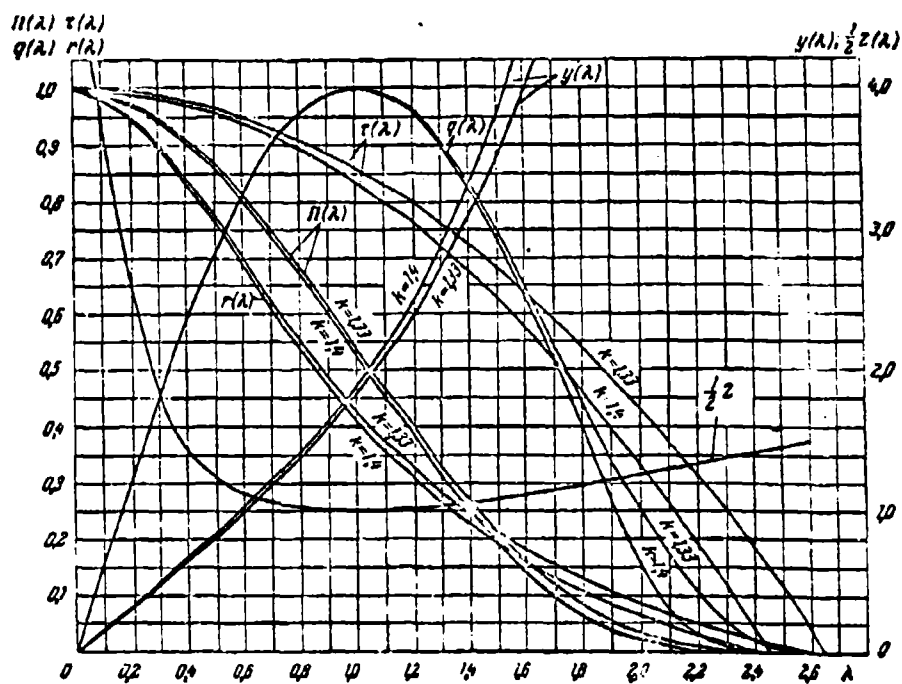
A	B	C	D	E	F	G	H	I
1.65	0.6144	0.1404	0.2266	0.5991	4.2659	0.8508	0.1651	1.9503
1.66	0.6097	0.1362	0.2233	0.5889	4.3250	0.8387	0.1623	1.9606
1.67	0.6050	0.1320	0.2181	0.5786	4.3849	0.8264	0.1597	1.9692
1.68	0.6003	0.1278	0.2130	0.5684	4.4458	0.8141	0.1570	2.0089
1.69	0.5955	0.1238	0.2079	0.5561	4.5082	0.8016	0.1544	2.0290
1.70	0.5907	0.1198	0.2029	0.5478	4.5718	0.7890	0.1519	2.0493
1.71	0.5859	0.1159	0.1979	0.5374	4.6362	0.7761	0.1493	2.0698
1.72	0.5810	0.1121	0.1929	0.5271	4.7027	0.7637	0.1468	2.0906
1.73	0.5761	0.1083	0.1881	0.5168	4.7703	0.7509	0.1443	2.1112
1.74	0.5712	0.1047	0.1833	0.5065	4.8399	0.7381	0.1418	2.1330
1.75	0.5663	0.1011	0.1785	0.4961	4.9090	0.7250	0.1394	2.1546
1.76	0.5613	0.0975	0.1738	0.4858	4.9808	0.7120	0.1370	2.1763
1.77	0.5563	0.0941	0.1691	0.4755	5.0543	0.6993	0.1346	2.1987
1.78	0.5513	0.0907	0.1645	0.4652	5.1291	0.6858	0.1323	2.2211
1.79	0.5462	0.0874	0.1620	0.4550	5.2057	0.6727	0.1299	2.2439
1.80	0.5411	0.0842	0.1555	0.4447	5.2839	0.6595	0.1276	2.2670
1.81	0.5360	0.0810	0.1511	0.4345	5.3642	0.6462	0.1254	2.2905
1.82	0.5309	0.0779	0.1468	0.4243	5.4459	0.6329	0.1231	2.3143
1.83	0.5257	0.0749	0.1425	0.4142	5.5297	0.6197	0.1209	2.3384
1.84	0.5205	0.0720	0.1383	0.4041	5.6153	0.6063	0.1187	2.3629
1.85	0.5153	0.0691	0.1341	0.3927	5.6835	0.5930	0.1165	2.3877
1.86	0.5100	0.0663	0.1300	0.3811	5.7928	0.5797	0.1144	2.4130
1.87	0.5047	0.0636	0.1260	0.3741	5.8850	0.5664	0.1122	2.4386
1.88	0.4994	0.0609	0.1220	0.3643	5.9795	0.5531	0.1101	2.4647
1.89	0.4941	0.0583	0.1181	0.3545	6.0764	0.5398	0.1081	2.4911
1.90	0.4887	0.0558	0.1142	0.3447	6.1757	0.5266	0.1060	2.5180
1.91	0.4833	0.0534	0.1105	0.3351	6.2779	0.5134	0.1040	2.5454
1.92	0.4779	0.0510	0.1067	0.3256	6.3820	0.5002	0.1020	2.5731
1.93	0.4724	0.0487	0.1031	0.3161	6.4899	0.4871	0.1000	2.6015
1.94	0.4670	0.0465	0.0995	0.3064	6.5949	0.4740	0.0980	2.6302
1.95	0.4615	0.0443	0.0960	0.2973	6.7128	0.4609	0.0961	2.6596
1.96	0.4559	0.0422	0.0925	0.2881	6.8289	0.4480	0.0942	2.6894
1.97	0.4504	0.0402	0.0892	0.2790	6.9487	0.4352	0.0923	2.7198
1.98	0.4448	0.0382	0.0858	0.2700	7.0720	0.4224	0.0904	2.7507
1.99	0.4391	0.0363	0.0826	0.2611	7.1983	0.4097	0.0885	2.7822
2.00	0.4335	0.0344	0.0794	0.2523	7.3288	0.3971	0.0867	2.8143
2.01	0.4278	0.0326	0.0763	0.2436	7.4635	0.3845	0.0849	2.8471
2.02	0.4221	0.0309	0.0733	0.2351	7.6020	0.3723	0.0831	2.8806
2.03	0.4164	0.0293	0.0703	0.2267	7.7448	0.3600	0.0813	2.9147
2.04	0.4108	0.0277	0.0674	0.2183	7.8923	0.3477	0.0795	2.9496
2.05	0.4048	0.0261	0.0645	0.2101	8.0444	0.3357	0.0778	2.9852
2.06	0.3990	0.0247	0.0618	0.2022	8.2016	0.3240	0.0761	3.0215
2.07	0.3931	0.0232	0.0591	0.1942	8.3639	0.3122	0.0744	3.0587
2.08	0.3873	0.0219	0.0564	0.1864	8.5323	0.3005	0.0727	3.0967
2.09	0.3814	0.0205	0.0539	0.1788	8.7059	0.2891	0.0710	3.1356
2.10	0.3754	0.0193	0.0514	0.1713	8.8854	0.2778	0.0694	3.1754
2.11	0.3695	0.0181	0.0489	0.1640	9.0725	0.2668	0.0678	3.2162
2.12	0.3635	0.0169	0.0466	0.1569	9.2652	0.2559	0.0662	3.2579
2.13	0.3574	0.0158	0.0443	0.1500	9.4629	0.2451	0.0646	3.3007
2.14	0.3514	0.0148	0.0420	0.1429	9.6737	0.2345	0.0630	3.3446
2.15	0.3453	0.0138	0.0399	0.1362	9.8903	0.2242	0.0614	3.3897
2.16	0.3392	0.0128	0.0378	0.1296	10.1116	0.2140	0.0599	3.4360
2.17	0.3331	0.0119	0.0357	0.1232	10.3319	0.2041	0.0583	3.4836
2.18	0.3269	0.0110	0.0338	0.1170	10.5592	0.1943	0.0568	3.5324
2.19	0.3207	0.0102	0.0319	0.1109	10.847	0.1847	0.0553	3.5828

Appendix II (Cont'd).

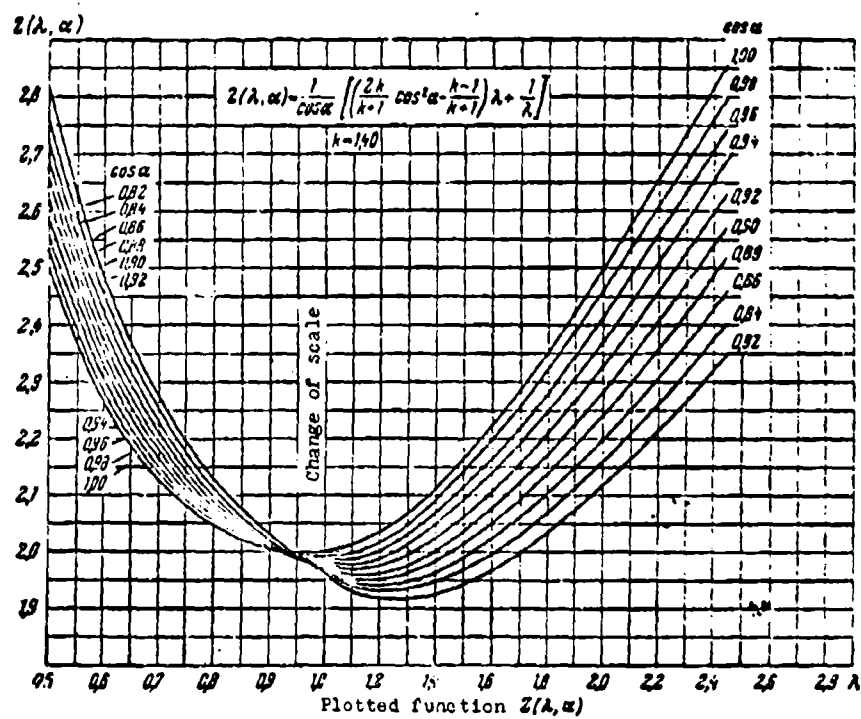
k = 1.33

220	0.3145	0.0091	0.0300	0.1050	11.111	0.1755	0.0539	3.6111
221	0.3083	0.0087	0.0282	0.0993	11.343	0.1661	0.0521	3.6577
222	0.3020	0.0080	0.0266	0.0937	11.678	0.1575	0.0509	3.7128
223	0.2957	0.0074	0.0249	0.0883	11.980	0.1488	0.0495	3.7995
224	0.2894	0.0068	0.0233	0.0830	12.207	0.1404	0.0481	3.8579
225	0.2830	0.00620	0.0218	0.0769	12.629	0.1323	0.0467	3.9555
226	0.2766	0.00560	0.0204	0.0731	12.973	0.1243	0.0453	3.9811
227	0.2702	0.00512	0.0190	0.0684	13.343	0.1167	0.0439	4.0458
228	0.2638	0.00465	0.0176	0.0635	13.732	0.1092	0.0426	4.1131
229	0.2573	0.00421	0.0163	0.0595	14.139	0.1021	0.0412	4.1828
230	0.2508	0.00379	0.0151	0.0553	14.568	0.0951	0.0399	4.2531
231	0.2443	0.00341	0.0140	0.0512	15.023	0.0885	0.0385	4.3244
232	0.2377	0.00306	0.0129	0.0474	15.505	0.0821	0.0372	4.4086
233	0.2311	0.00273	0.0118	0.0437	16.014	0.0759	0.0360	4.4943
234	0.2245	0.00243	0.0108	0.0402	16.557	0.0700	0.0347	4.5756
235	0.2179	0.00215	0.0099	0.0369	17.136	0.0644	0.0331	4.6647
236	0.2112	0.00190	0.0090	0.0337	17.751	0.0590	0.0321	4.7578
237	0.2045	0.00167	0.0081	0.0307	18.411	0.0539	0.0309	4.8557
238	0.1978	0.00146	0.0074	0.0278	19.118	0.0491	0.0297	4.9586
239	0.1910	0.00127	0.0066	0.0252	19.876	0.0445	0.0285	5.0665
240	0.1842	0.00109	0.0059	0.0226	20.696	0.0402	0.0272	5.1807
241	0.1774	0.00095	0.0053	0.0205	21.579	0.0364	0.0261	5.3011
242	0.1706	0.00080	0.0047	0.0181	22.536	0.0323	0.0249	5.4288
243	0.1637	0.00068	0.0041	0.0160	23.581	0.0287	0.0237	5.5645
244	0.1568	0.00057	0.0036	0.0141	24.719	0.0254	0.0225	5.7089
245	0.1499	0.00048	0.0032	0.0124	26.050	0.0223	0.0214	5.8631
246	0.1429	0.00039	0.0027	0.0108	27.345	0.0194	0.0203	6.0288
247	0.1359	0.00032	0.0024	0.0093	28.863	0.0168	0.0191	6.2067
248	0.1289	0.00026	0.0020	0.0079	30.556	0.0144	0.0180	6.3980
249	0.1219	0.00021	0.0017	0.0067	32.459	0.0122	0.0169	6.6079
250	0.1148	0.000163	0.001420	0.00503	34.587	0.01030	0.01580	6.8353
251	0.1077	0.000126	0.001169	0.00466	37.012	0.00853	0.01480	7.0851
252	0.1006	$9.55 \cdot 10^{-5}$	0.000949	0.00380	36.796	0.00698	0.01370	7.3614
253	0.0934	$7.10 \cdot 10^{-5}$	0.000759	0.00305	43.011	0.00562	0.01273	7.6681
254	0.0863	$5.14 \cdot 10^{-5}$	0.000596	0.00240	46.774	0.00444	0.01160	8.0125
255	0.0791	$3.62 \cdot 10^{-5}$	0.000457	0.00185	51.242	0.00343	0.01050	8.4028
256	0.0718	$2.49 \cdot 10^{-5}$	0.000342	0.00139	56.629	0.00258	0.00952	8.8506
257	0.0646	$1.60 \cdot 10^{-5}$	0.000248	0.00101	63.248	0.00188	0.00850	9.3716
258	0.0573	$9.86 \cdot 10^{-6}$	0.000172	0.00070	71.572	0.00132	0.00748	9.9892
259	0.0499	$5.68 \cdot 10^{-6}$	0.000114	0.00047	82.303	0.00088	0.00646	10.7357
260	0.0426	$2.99 \cdot 10^{-6}$	$7.02 \cdot 10^{-6}$	0.00029	96.998	0.00054	0.00543	11.6735
261	0.0352	$1.39 \cdot 10^{-6}$	$3.94 \cdot 10^{-6}$	0.00018	117.79	0.00031	0.00450	12.8884
262	0.0278	$5.36 \cdot 10^{-7}$	$1.93 \cdot 10^{-6}$	$8.02 \cdot 10^{-6}$	149.68	$0.152 \cdot 10^{-4}$	0.00353	14.5379
263	0.0201	$1.53 \cdot 10^{-7}$	$7.50 \cdot 10^{-7}$	$3.13 \cdot 10^{-6}$	205.17	$0.594 \cdot 10^{-4}$	0.00257	17.0777
264	0.0129	$2.43 \cdot 10^{-7}$	$1.88 \cdot 10^{-7}$	$7.82 \cdot 10^{-7}$	322.28	$0.150 \cdot 10^{-4}$	0.00162	21.5306
265	0.0054	$7.28 \cdot 10^{-8}$	$1.15 \cdot 10^{-7}$	$5.507 \cdot 10^{-8}$	770.12	$0.108 \cdot 10^{-4}$	0.00067	33.3991
2657	0	0	0	0	∞	0	0	50

Appendix III



Appendix IV



Appendix V. The table of units.

Name of value	Units				
	SI	technical	CGSM	CGSE	rauss
Time t.....	s	s	s	second (s)	s
Length l.....	meter (m) = 10^2	m	cm	centimeter (cm)	cm
Mass m.....	kilograms (kg) = 10^3	$\text{kgf} \cdot \text{s}^2 / \text{m} = 10^2$	g	gram (g)	g
Density ρ	$\text{kg} / \text{m}^3 = 10^3$	$\text{kgf} \cdot \text{s}^2 / \text{m}^4 = 10^{-5}$	g / cm^3	g / cm^3	g / cm^3
Force F.....	Newton (N) = 10^5	$\text{kgf} = 10^6$	dyne	dyne	dyne
Velocity W...	m/s	m/s	cm/s	cm/s	cm/s
Work A.....	joule (J) = $\text{Nm} = 10^7$	$\text{kgfm} = 10^8$	erg	erg	erg
Heat, Q.....	joule = 10^7	calorie = 427 $\text{kgfm} = 4200 \text{ J} = 4.2 \cdot 10^{10}$	erg	erg	erg
Power Q_m	Watt (W) = $\text{J/s} = 10^7$	$\text{kgfm/s} = 10^8$	erg/s	erg/s	erg/s
Electric charge q.....	coulomb (C) = $3 \cdot 10^9$	C	unit CGSM = $3 \cdot 10^{10}$	unit CGSE	unit CGSE

Appendix V (Cont'd).

Current strength I...	ampere (A) = $c/s = 3 \cdot 10^9$	A	unit CGSM = $3 \cdot 10^{10}$	unit CGSE	unit CGSE
Potential V..	volts (V) = $1/3 \cdot 10^{-2}$	V	unit CGSM = $1/3 \cdot 10^{-10}$	unit CGSE	unit CGSE
Electrical field strength E	$V/m = 1/3 \cdot 10^{-4}$	$V/cm = 1/3 \cdot 10^{-2}$	unit CGSM = $1/3 \cdot 10^{-10}$	unit CGSE	unit CGSE
Electric field induction D.....	unit CU = $12\pi \cdot 10^9$	$V/cm = 1/3 \cdot 10^{-2}$	unit CGSM = $3 \cdot 10^{10}$	unit CGSE	unit CGSE
Resistance R	ohm = $1/9 \cdot 10^{-11}$	ohm	unit CGSM = $1/9 \cdot 10^{-20}$	unit CGSE	unit CGSE
Conductivity σ_R	mho/m = $9 \cdot 10^9$	mho/cm = $9 \cdot 10^{11}$	unit CGSM = $1/9 \cdot 10^{-20}$	unit CGSE	unit CGSE
Capacitance C	farad = 9×10^{11}	farad	unit CGSM = $9 \cdot 10^{20}$	cm	cm
Dielectric constant of vacuum ϵ_0	$1/3.6\pi \cdot 10^{-14}$	1	unit CGSM = $9 \cdot 10^{20}$	1	1

Appendix V (Cont'd).

Strength of magnetic field H.....	$A/M = 3 \cdot 10^7$	$A/cm = 3 \cdot 10^9$	oersted = $3 \cdot 10^{10}$	unit CGSE	oersted
Flow of magnetic induction Φ	weber = $1/3 \cdot 10^{-2}$	weber = $1/3 \cdot 10^{-2}$	maxwell = $1/3 \cdot 10^{-10}$	unit CGSE	maxwell
Magnetic permeability of vacuum μ_{B_0}	$1/4\pi \cdot 10^7$	1	1	1	1
Magnetic induction B...	$\text{weber}/M^2 = 1/3 \cdot 10^{-6}$	$\text{weber}/cm^2 = 1/3 \cdot 10^{-2}$	gauss = $1/3 \cdot 10^{-10}$	unit CGSE	gauss
Coefficient of self-induction L...	henry = $\text{weber}/A = 1/9 \cdot 10^{-11}$	henry	unit CGSM = $1/9 \cdot 10^{-20}$	unit CGSE	unit CGSE

Note. The numerical values of units for which the dimension is not indicated pertain to the CGSE system of units.

Bibliography

1. Абрамович Г. Н., Теория турбулентных струй, Физматгиз, Москва, 1960.
2. Альтшуль А. Д. и Киселев Н. Г., Гидравлика и аэродинамика, Изд-во литературы по строительству, Москва, 1965.
3. Аржанников Н. С. и Сафедкова Г. С., Аэродинамика больших скоростей, «Высшая школа», Москва, 1968.
4. Баб-ин-и, Магнитная газодинамика и динамика плазмы, «Мир», Москва, 1964.
5. Борисенко А. Н., Газовая динамика двигателей, Оборонгиз, Москва, 1962.
6. Вулис Л. А., Термодинамика газовых потоков, Госэнергоиздат, Москва, 1950.
7. Вулис Л. А., Теория струй вязкой жидкости, «Наука», Москва, 1965.
8. Газодинамика разреженных газов, под ред. М. Девиса, Изд-во иностранной литературы, Москва, 1963.
9. Газовая динамика, Сборник переводов, Изд-во иностранной литературы, Москва, 1950.
10. Гаррис Л., Магнитно-гидродинамические течения в каналах, Изд-во иностранной литературы, Москва, 1963.
11. Герман Р., Сверхзвуковые входные диффузоры, Физматгиз, Москва, 1960.
12. Гинзбург И. П., Прикладная гидрогазодинамика, Изд-во ленинградского университета, Ленинград, 1958.
13. Гиро Ж., Основные вопросы теории гиперзвуковых течений, «Мир», Москва, 1963.
14. Депп М. Е., Техническая газодинамика, Госэнергоиздат, Москва, 1961.
15. Жуковский В. С., Техническая термодинамика, Гостехиздат, Москва, 1952.
16. Злур Р., Течения сжимаемой жидкости, Изд-во иностранной литературы, Москва, 1954.
17. Зельдович Я. Б., Теория ударных волн и введение в газодинамику, Изд-во АН СССР, Москва, 1916.
18. Идельчик И. Е., Гидравлические сопротивления, Госэнергоиздат, Москва, 1954.
19. Идельчик И. Е., Справочник по гидравлическим сопротивлениям, Госэнергоиздат, Москва, 1960.
20. Идельчик И. Е., Аэродинамика промышленных аппаратов, «Энергия», Москва, 1964.
21. Иноземцев Н. В., Авиационные газотурбинные двигатели, Оборонгиз, Москва, 1955.
22. Калитман Л. Е., Элементы магнитной газодинамики, Атомиздат, Москва, 1964.
23. Каулинг Г., Магнитная гидродинамика, Изд-во иностранной литературы, Москва, 1958.
24. Кочин Н. Е., Кибель Н. А. и Розе Н. В., Теоретическая гидромеханика, ч. I, II, Гостехиздат, Москва, 1955, 1956.
25. Куликовский А. Г. и Любимов Г. А., Магнитная гидродинамика, Физматгиз, Москва, 1962.
26. Ландау Л. Д. и Лифшиц Е. М., Механика сплошных сред, Гостехиздат, Москва, 1957.
27. Левинсон Я. И., Аэродинамика больших скоростей, Оборонгиз, Москва, 1950.
28. Липман Г. В. и Ролко А., Элементы газовой динамики, Изд-во иностранной литературы, Москва, 1960.
29. Лойцянский Л. Г., Механика жидкостей и газов, Гостехиздат, Москва, 1957.
30. Лойцянский Л. Г., Аэродинамика пограничного слоя, Гостехиздат, Ленинград, 1911.
31. Лойцянский Л. Г., Ламинарный пограничный слой, Физматгиз, Москва, 1962.
32. Магнитная гидродинамика, Тезисы симпозиума, Атомиздат, Москва, 1958.
33. Наттерсон Г. П., Молекулярное течение газов, Физматгиз, Москва, 1960.
34. Прикладная магнитная гидродинамика, Изд-во Академии наук Латвийской ССР, Рига, 1961.
35. Прикладная магнитная гидродинамика, Сборник переводов, «Мир», Москва, 1965.
36. Прандль Л., Гидроаэромеханика, Изд-во иностранной литературы, Москва, 1919.

37. Рахматуллин Х. А. и др., Газовая динамика, «Высшая школа», Москва, 1963.
38. Сопрежение состояние гидродинамики вязкой жидкости, под ред. С. Г. Галактикина, Изд-во иностранной литературы, Москва, 1918.
39. Сопрежение состояние аэродинамики больших скоростей, под ред. Р. Хуэрта, Изд-во иностранной литературы, Москва, 1933.
40. Седов Л. И., Методы подобия и размерности в механике, «Наука», Москва, 1967.
41. Седов Л. И., Плоские задачи гидродинамики и аэродинамики, «Наука», Москва, 1966.
42. Степанов Г. Ю., Гидромеханика решеток турбомашин, Физматгиз, Москва, 1962.
43. Степанов Г. Ю., Основы теории лопаточных машин комбинированных и газотурбинных двигателей, «Машиностроение», Москва, 1958.
44. Сыроватский С. И., Магнитная гидродинамика, Успехи физических наук, № 3, т. 62, 1957.
45. Фабрикант Н. Я., Аэродинамика, «Наука», Москва, 1963.
46. Ферри А., Аэродинамика сверхзвуковых скоростей, Гостехиздат, Москва, 1932.
47. Франк-Каменецкий Д. А., Лекции по физике плазмы, Атомиздат, Москва, 1964.
48. Франкль Ф. И., Христианович С. А. и Алексеева Р. Н., Основы газовой динамики, Труды ЦАГИ, вып. 364, Москва, 1938.
49. Хейл Э. Д. и Пробстни Р. Ф., Теория гиперзвуковых течений, Изд-во иностранной литературы, Москва, 1962.
50. Хинце Н. О., Турбулентность, Физматгиз, Москва, 1963.
51. Черныл Н. А., Основы газовой динамики, Гостехиздат, Москва, 1961.
52. Черныл Г. Г., Течение газа с большой сверхзвуковой скоростью, Физматгиз, Москва, 1939.
53. Шидловский В. П., Введение в динамику разреженного газа, «Наука», 1963.
54. Шерклф Д., Теория электромагнитного измерения раскола, «Мир», Москва, 1963.
55. Шлихтинг Г., Теория пограничного слоя, Изд-во иностранной литературы, Москва, 1938.